U.S. Department of Transportation
Federal Aviation Administration

DOT/FAA/CT-89/22

AIRCRAFT LIGHTNING PROTECTION

HANDBOOK

September 1989

FEDERAL AVIATION ADMINISTRATION
TECHNICAL CENTER

NOTICE

This document is disseminated under the sponsorship of the U. S. Department of Transportation in the interest of information exchange. The United States Government assumes no liability for the contents or use thereof.

The United States Government does not endorse products or manufacturers. Trade or manufacturers' names appear herein solely because they are considered essential to the objective of this report.

U.S. Department of Transportation
Federal Aviation Administration

Memorandum

COPY 1

Subject: **INFORMATION:** Lightning Protection Handbook

Date: [redacted]

From: Program Manager, ACD-230

Reply to Attn. of:

To:

Attached is a copy of the new Lightning Protection Handbook. This document has been 3 years in the writing, and the lightning community can well be proud of the effort Lightning Technologies, Inc. has put forth.

This handbook is a complete rewrite of the NASA RP 1008, which was published in 1976. The authors of the original document, F. A. Fisher and J. Anderson Plumer, have taken all their experience and research efforts of the last 15 years, and not only reorganized the book, but added additional sections, which address those subjects which are on the leading edge of technology.

It is intended that this document be one which can be revised, whether by changing technology, or by correcting errors. It would be greatly appreciated if the users would kindly suggest areas to be included in future revisions and correct errors to the current document.

I have been tasked to keep this document in the mainstream, keep the handbook updates, and all corrections current. My telephone contact at the FAA Technical Center, is (609) 484-4138, or FTS 482-4138.

We have taken the liberty to include suggested information for recommended changes and corrections. Please feel free to call me, or write to the following address: FAA Technical Center, ACD-230, Atlantic City International Airport, NJ 08405.

INFORMATION:
-Name, address, telephone
-Page, paragraph
-Revise from
-Change to
-Reason

Michael S. Glynn

Technical Report Documentation Page

1. Report No.	2. Government Accession No.	3. Recipient's Catalog No.
DOT/FAA/CT-89/22		

4. Title and Subtitle	5. Report Date
AIRCRAFT LIGHTNING PROTECTION HANDBOOK	September 1989
	6. Performing Organization Code
7. Author(s)	8. Performing Organization Report No.
F. A. Fisher and J. A. Plumer* R. A. Perala**	DOT/FAA/CT-89/22
9. Performing Organization Name and Address	10. Work Unit No. (TRAIS)
*Lightning Technologies Inc. 10 Downing Parkway Pittsfield, MA 01201	11. Contract or Grant No. DTFA03-86-C-00049
	13. Type of Report and Period Covered
12. Sponsoring Agency Name and Address U. S. Department of Transportation Federal Aviation Administration Technical Center Atlantic City International Airport, NJ 08405	Handbook
	14. Sponsoring Agency Code ACD-230

15. Supplementary Notes

** Electro Magnetic Applications Inc., Denver, Colorado 80226
Program Manager: Michael Glynn, FAA Technical Center

16. Abstract

This handbook will assist aircraft design, manufacturing, and certification organizations in protecting aircraft against the direct and indirect effects of lightning strikes, in compliance with Federal Aviation Regulations. It presents a comprehensive text to provide the essential information for the in-flight lightning protection of all types of fixed/rotary wing and powered lift aircraft of conventional, composite, and mixed construction and their electrical and fuel systems.

The handbook contains chapters on the natural phenomenon of lightning, the interaction between the aircraft and the electrically charged atmosphere, the mechanism of the lightning strike, and the interaction with the airframe, wiring, and fuel system. Further chapters cover details of designing for optimum protection; the physics behind the voltages, currents, and electromagnetic fields developed by the strike; and shielding techniques and damage analysis. The handbook ends with discussion of test and analytical techniques for determining the adequacy of a given protection scheme.

17. Key Words		18. Distribution Statement
Lightning Protection	Lightning Safety	Document is available to the public through the National Technical Information Service, Springfield, Virginia 22161
Fuel Vapor Ignition	Lightning Simulation	
Fuel System Safety	Aircraft Certification	
Atmospheric Electrical Hazards	Atmospheric Electromagnetism	
	Induced Currents & Voltages	
	Electromagnetic Shielding	

19. Security Classif. (of this report)	20. Security Classif. (of this page)	21. No. of Pages	22. Price
Unclassified	Unclassified	500	

Form DOT F 1700.7 (8-72) Reproduction of completed page authorized

CONTENTS

INTRODUCTION

This handbook will assist aircraft design and certification engineers in protecting aircraft against the direct and indirect effects of lightning strikes, in compliance with Federal Aviation Regulations pertaining to lightning protection. It is also intended to assist FAA certifying engineers in assessing the adequacy of proposed lightning protection designs. It will also be useful for designers of major subsystems, such as engines and electrical and avionics systems,

This is the second handbook of this type. The first such handbook, also entitled *Lightning Protection of Aircraft* by F.A. Fisher and J.A. Plumer, was published in 1976 by the National Aeronautics and Space Administration as *NASA RP–1008*. Since that book was published there have been major advances in protection techniques, standards and test practices, particularly in those dealing with the indirect electromagnetic effects of lightning.

This new handbook, which was commissioned by the FAA in 1986, was originally intended to be an updated version of *NASA RP–1008*, but as the project evolved, it became evident that additional topics, not included in the earlier book, should be incorporated and that much of the original material needed to be completely rewritten and expanded.

The book is organized along the same general lines as the earlier work, with the first half dealing with the *direct effects* (burning and blasting) of lightning and the second half dealing with the *indirect effects* (electromagnetic induction of voltages and currents) of lightning.

Among the new material found in this book are two chapters dealing with basic technologies and physical concepts. The first of these, Chapter 1 - *An Introduction to High Voltage Phenomena*, deals with the nature of high voltage electrical sparks and arcs and with related processes of electric charge formation, ionization, and spark propagation in air. All of these are factors that affect the way that lightning leaders attach to an aircraft and the way that the hot return stroke arc affects the surface to which it attaches. The material introduces practices and terms used for many years in the electric power industry, but which are not commonly studied by those dealing with aircraft. Those terms and practices have, however, affected the tests and practices used to evaluate the direct effects of lightning on aircraft.

The second, Chapter 9 - *Elementary Aspects of Indirect Effects*, reviews some of the electromagnetic phenomena that govern induction of voltages and currents by electromagnetic fields and introduces some of the terms and mathematical concepts encountered in analytic treatments of the indirect effects of lightning. The chapter is not intended as a complete review of electromagnetic theory, but some subjects occur so often in treatments of indirect effects that it seemed better to review them all at once, and in some detail, rather than introducing them piecemeal in subsequent chapters.

The user of this handbook is urged to study these two introductory chapters before proceeding with other sections of the book. The treatment of these topics begins on an elementary level and is aided by simple illustrations which should enable those with only a limited background in electricity to proceed to an adequate understanding of important principles.

Other topics not found in *NASA RP–1008* include a review of intra-cloud lightning phenomenology and the triggering of lightning flashes by aircraft (Chapters 3 and 10), the topic of considerable research during the years 1980-1987, a more thorough description of the procedural steps in lightning protection design and certification (Chapter 5), and a more complete treatment of protection design methods for advanced composite materials and structures (Chapter 6). This latter area received only brief treatment in NASA RP 1008, there being little practical experience with these materials at the time that book was published. Advanced composites have since become widely employed in fixed wing aircraft and rotorcraft, and efficient methods of protecting them from lightning damage have evolved. The new material on certification includes a discussion of the steps to be followed in reaching and verifying protection for flight critical electrical and avionic systems, such as full authority digital electronic controls, *FADEC*. These steps are presently being formalized in a new FAA regulation and advisory circular.

Finally, new material on indirect effects tests methods is presented, in Chapter 18. This is another area where considerable improvements have been made since publication of NASA RP 1008, though future improvements are expected to continue.

Elsewhere, the handbook is organized in a similar fashion to *NASA RP–1008*, with chapters on *Natural Lightning* (Chapter 2), *Aircraft Lightning Attachment Phenomena* (Chapter 3) and *Lightning Effects on Aircraft* (Chapter 4). Users should be familiar with these topics before proceeding with design and verification tasks.

Chapter 5, *The Certification Process* begins with a description of FAA airworthiness regulations pertaining to lightning, followed by a description of the standardized external lightning environment, the method of applying this environment to an aircraft, and the remaining steps in protection design and verification. Experience has shown that designs evolved

in this way have a high probability of success.

Methods of protection of airframes and fuel systems against physical damage and fuel ignition are described in Chapters 6 and 7, respectively. Fuel vapor ignition remains one of the most serious lightning hazards, and should be given careful attention in any design and certification program. Since much of an airframe contains fuel in direct contact with structural elements, the topics in Chapters 6 and 7 are closely related and should be studied together. As noted in these chapters, the electrical ignition sources and thresholds within aircraft structures are not easily identified or quantified by analyses methods, and so tests must play an important part in successful design and verification. This is true both for so-called "conventional" metal airframes and for advanced composite structures.

Chapters 8 through 17 focus on protection of electrical and avionic systems against indirect effects. As with all aspects of electromagnetic interference and control, the control of damage and interference from lightning becomes more and more critical as aircraft evolve. Most of the navigation and control functions aboard modern aircraft place a computer between the pilot and the control surfaces, often without mechanical backup. This makes it essential that the computer and control equipment be designed so as not to be damaged or unduly upset by lightning. Control of these indirect effects requires coordination between those who design the airframe and its interconnecting wiring, those who design avionic systems and those who oversee the certification process. Part of the overall control process requires the selection of transient design levels and establishment of suitable test standards and practices. This is an evolving area and there is still work to be done in ensuring that test requirements and practices are truly adequate and cost effective.

Chapter 8 introduces the subject of indirect effects and briefly discusses the subjects covered in more detail in later chapters. Chapter 9, as mentioned, covers a number of subjects common to the subsequent chapters. Chapter 10 covers the external electromagnetic field environment and Chapters 11 and 12 cover the way that these fields couple to the interior of the aircraft. These four chapters are the most analytically oriented of the book.

Chapter 13 discusses experimental methods of studying the interaction between the aircraft and the lighting flash. Chapter 14 discusses some of the practical problems of calculating the response of aircraft wiring to electromagnetic fields. Chapter 15 discusses shielding of aircraft wiring and emphasizes that some of the shielding and wiring practices in common use really provide little protection from the electromagnetic fields of lightning and may even accentuate problems. Chapter 16 discusses some of the policy matters relating to control of indirect effects, tasks that must be undertaken by those responsible for setting overall design practices. Principally these relate to shielding and grounding practices to be followed and to transient design level specifications to be imposed on vendors. These are not subjects that can be controlled by individual designers.

Chapter 17 discusses some aspects of circuit design, principally those relating to surge protective devices and methods of analyzing the damage effects of surge voltages and components on electronic devices.

Control of lightning indirect effects by analysis can only be carried so far; proof of resistance to indirect effects is most likely to come about by the conduct of tests on individual pieces of equipment and on interconnected systems. Chapter 18 presents an overview of verification test methods. It is intended to describe the approaches that can be applied for these tests and to acquaint the certification engineer with what to expect and what not to expect. Practices relating to testing are still evolving and the chapter discusses some areas where work is still needed and where present specifications may require testing that is either technically inadequate or excessively costly.

A few comments on personnel safety are in order. Lightning tests involve the generation and application of very high voltages and currents - far exceeding the levels employed in most electrical test laboratories. They also far exceed lethal levels and have proven fatal to inexperienced operators. Lightning tests to evaluate or verify either direct or indirect effects should be performed only by personnel experienced in this technology. This test methodology is beyond the scope of this handbook.

Acknowledgements

This handbook was commissioned by the Federal Aviation Administration Technical Center. Funds for its preparation were provided under contract DOT FAA DTFA03-86-C-00049 and by Lightning Technologies, Inc. Contributions to the chapters dealing with analytical modeling of aircraft lightning interaction processes, analysis methods for prediction of indirect effects, and the results of recent researches in intracloud lightning employing storm penetration aircraft were provided by Rodney A. Perala of Electro Magnetic Applications Inc., under subcontract to Lightning Technologies, Inc. Project manager for the FAA Technical Center was David M. Lawrence, and the project manager for Lightning Technologies, Inc. was Franklin A. Fisher.

Special gratitude is expressed to the following people for their contributions:

- David Lawrence of FAA Technical Center, who reviewed and proof read numerous versions of each chapter, offering valuable critique from a potential users standpoint, together with encouragement when the end seemed far away.
- Terence Rudolph of Electro Magnetic Applications, Inc. who contributed to the topics of aircraft lightning interaction, analytical modeling, and interpretation of intracloud lightning research.
- Edward Rupke of Lightning Technologies, Inc. who prepared many of the illustrations.
- Keith E. Crouch and John E. Pryzby of Lightning Technologies, Inc. who contributed to the chapters on protection against direct effects, including protection of advanced composite structure and fuel systems.
- Kenneth G. Wiles of Lightning Technologies, Inc. who contributed to the chapters on testing for the indirect effects of lightning.
- Kevin R. Bailey, Keith E. Crouch and Michael M. Dargi of Lightning Technologies, Inc. who assembled and positioned the manuscript.

Acronyms and Abbreviations

(This list includes abbreviations and groups of initials peculiar to the subject matter in addition to many standard acronyms)

AC	Advisory Circular
AEH	Atmospheric Electrical Hazards
AEHP	Atmospheric Electrical Hazards Program
ADF	Automatic Directional Finding
ANSI	American National Standards Institute
AE-4L	The Lightning Committee of the Society of Automotive Engineers
ATC	Air Traffic Control
AWG	American Wire Gauge
BIL	Basic Insulation Level
CW	Continuous Wave
CFC	Carbon Fiber Composite
DER	Designated Engineering Representative
DoD	Department of Defense
EFIE	Electrical Field Integral Equation
EFIS	Electronic Flight Instrumentation System
EMI	Electro-magnetic Interference
EMC	Electro-magnetic Compatibility
EMP	Electro-magnetic Pulse
ETDL	Equipment Transient Design Level
EUT	Equipment Under Test
FAA	Federal Aviation Administration
FADEC	Full Authority Digital Electronic Control
FAR	Federal Aviation Regulations
FW	Full Wave
GMT	Greenwich Mean Time
IEEE	Institute of Electrical and Electronic Engineers
IFR	Instrument Flight Rules
ITO	Indium-Tin Oxide
JAR	Joint Airworthiness Requirements
JSC	Johnson Space Center
LTRI	Lightning and Transients Research Institute
LTI	Lightning Technologies Inc.
LEMP	Lightning Electro-magnetic Pulse
LF-ADF	Low Frequency Automatic Direction Finding
LRU	Line Replaceable Unit
LTA	Lighting Transient Analysis

MFIE	Magnetic Field Integral Equation
MOV	Metal Oxide Varistor
NACA	National Advisory Committee for Auronautics
NASA	National Aeronautics and Space Administration
NATO	North Atlantic Treaty Organization
NEMP	Nuclear Electromagnetic Pulse
NLR	Non-linear Resistor
OAS	Overall Shield
RTCA	Radio Technical Commission for Aeronautics
RFI	Radio Frequency Interference
SAE	Society of Automotive Engineers
SE	Shielding Effectiveness
TCL	Transient Control Level
TG	Transient Generator
UHF	Ultra-high Frequncy
UTC	Universal Time Coordinated
VHF	Very High Frequency
2DFD	Two-dimensional Finite Difference
2DFD	Three-dimensional Finite Difference

Chapter 1

AN INTRODUCTION TO HIGH VOLTAGE PHENOMENA

1.1 Introduction

Lightning is a high voltage and high current phenomenon and those who would deal in protection against it should have some basic understanding of the physics involved. This chapter is intended to introduce the reader to the general physical nature of electrical sparks and arcs, and to provide some data on spark breakdown characteristics of various electrode configurations. Partly, the material is given to introduce the subject of lightning phenomena and partly to illustrate some of the factors that must be considered during tests to simulate the effects of lightning. An understanding of high voltage phenomena is also important when discussing when and where aircraft are struck by lightning and an understanding of high current arc phenomena is important when designing aircraft surfaces to withstand the effects of lightning.

The literature on high voltage phenomena is vast and no attempt will be made to give a comprehensive review. Most of the works are to be found in publications aimed at the electric power industry. Some specific works that deal with the subject will be cited, but since the following material is only a review, no attempt will be made to cite references for each point discussed. Some specific works that might be reviewed include [1.1] for a general review of the mechanism of breakdown through long air gaps, [1.2 - 1.4] for a very comprehensive review of recent investigations on the subject, [1.5] for a general review of gas discharge phenomena and [1.6] for a review of breakdown voltages of long air gaps.

1.2 Initial Ionization Effects

In the study of gas discharges, it is customary to divide the phenomena into two general types: those that are, and those that are not self sustaining. Complete breakdown of a gas, or the formation of a spark between two electrodes, is a transition from a non-self-sustaining discharge to one of several types of self-sustaining discharge. Usually it occurs with explosive suddenness. To illustrate some of the phenomena involved, consider Fig. 1.1, which shows how the current between two electrodes immersed in a gas depends on the voltage between the electrodes. In the space between the electrodes, there will be an electric field E of magnitude proportional to the applied voltage, the physical dimensions of the electrodes and the distance between them.

Under the influence of light and other radiation, such as X-rays, cosmic rays or radioactive decay, electrons will be emitted from the negative electrode, or cathode. Electrons may also be released in the gas by the radiation. At low levels of voltage, or electric field, all the electrons will drift towards the positive electrode, or anode, and be collected. For a considerable range of voltages, region 2 of Fig. 1.1, the current will remain constant, but the discharge will not be self-sustaining since the current will cease if the ionizing illumination of the cathode is removed.

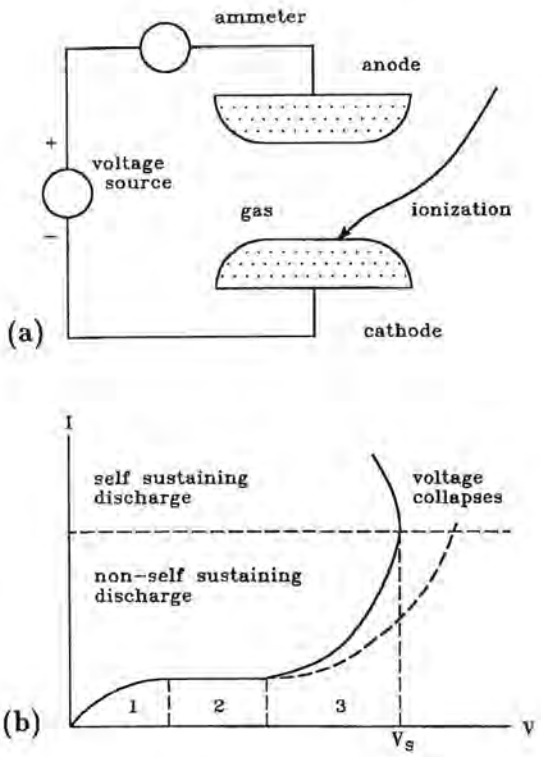

Fig. 1.1 Current-voltage relations in pre-spark regions.
(a) Electrode configuration
(b) V-I characteristics

If the voltage is increased into region 3 of Fig. 1.1, some of the electrons emitted from the cathode will collide with gas molecules with sufficient force that in some of these collisions an electron will be knocked from the molecule. Where there was one electron, there will now be two electrons plus one positively charged ion. Both electrons will then move under the influence of the field and will in turn strike more gas molecules and liberate still more electrons. The result is an electron avalanche. The total number of electrons produced by the acceleration of a group of electrons will be

$$N^- = n_0^- e^{\alpha d} \tag{1.1}$$

where N^- is the final number of electrons, n_o is the number of initial electrons and d is the distance traversed. The discharge will still not be self-sustaining since if the source of ionization is removed the current will cease.

The quantity α is called Thompson's first ionization coefficient and indicates the number of electrons produced by a single electron traveling a distance of 1 cm. It depends on the density of the gas and on the strength of the electric field. The electric field determines how much the electrons are accelerated and the gas density determines how far an electron may move before it collides with a gas molecule and liberates another electron. It follows that an electron avalanche will proceed faster in dense than in rarified gas. The molecules from which electrons are liberated will be left with a positive charge and will be accelerated in a direction opposite to the electrons, but their mass is much more than the mass of the electrons, so they move much more slowly.

If the voltage is increased into region 3 the current begins to depart from the simple exponential law of Eq. 1.1. Thompson ascribed the increased current to ionization resulting from the motion of the positively charged molecules, and considered the total current to have two components, one due to the motion of electrons, Eq. 1.1, and one due to the motion of the positively charged particles and governed by a similar relationship.

$$N^+ = n_0^+ e^{\beta d} \tag{1.2}$$

where N^+ is the final number of positively charged particles, n_0^+ is the initial number and d is the distance traversed.

The quantity β was designated Thompson's second ionization coefficient. It is now known that ionization by positive ions is insufficient to account for the increased current in region 3 of Fig. 1.1. Instead, the number of electrons is taken to be

$$N = \frac{n_0 e^{\alpha d}}{1 - \Gamma e^{\alpha d - 1}} \tag{1.3}$$

where the coefficient Γ is the *generalized secondary ionization coefficient*. Γ includes the α process considered by Thompson, but also other processes such as the action of positive ions, photons and metastable atoms at the cathode. Finally, at the sparking voltage V_s, the gap will break down and the voltage will collapse. A criterion for breakdown, or the achievement of a self-sustaining breakdown, would be that

$$\Gamma(e^{\alpha d - 1}) \geq 0. \tag{1.4}$$

If this criterion is met, the initial source of ionization could be removed and the current would continue to increase to a value limited only by the impedance of the external circuit.

Eqs. 1.3 and 1.4 include the effect of an attachment coefficient η since there are factors that act to capture electrons. The ionization and attachment coefficients are shown on Fig. 1.2. Below 25 kV/m the attachment coefficient is the larger, hence an avalanche cannot develop in a field less than 25 kV/m. This curve relates to standard sea level atmospheric conditions. Effects of non-standard conditions are discussed in §1.5.5.

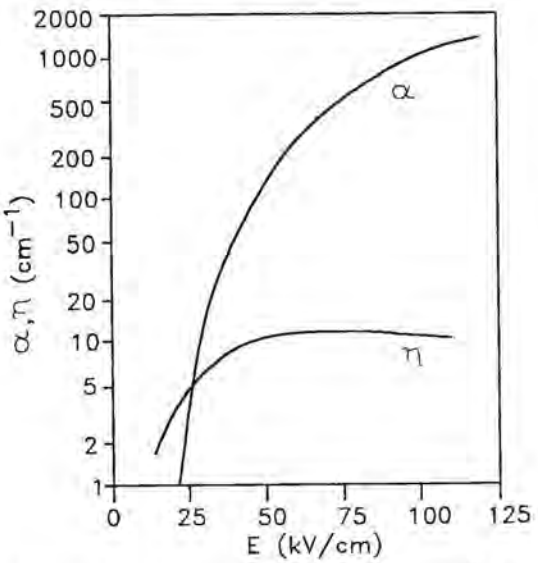

Fig. 1.2 Ionization and attachment coefficient.

1.3 Streamer Effects

The breakdown criterion of Eq. 1.4, though conceptually simple, is seldom used since the process is much more complicated. Breakdown is instead as-

cribed to the growth of a *streamer* that leads to ionization in the gas and is separate from any processes taking place at the electrodes. Whether the streamer leads to a complete breakdown between two electrodes, or is confined to the localized discharges called *corona* depends to a considerable extent on how the electric field is distributed across the entire gap. The localized *corona* discharge will be considered first. It occurs when only the region around the electrode is highly stressed; that is, exposed to a sufficiently high electric field, 25-30 kV/cm.

1.4 Corona

Corona, Fig. 1.3, is a glow discharge that forms around conductors when the surface voltage gradient (rate of change of voltage with distance normal to the surface of the electrode) exceeds a critical level, about 30 kV/cm in air at sea level atmospheric pressure. It can also form on grounded objects exposed to a high electric field from some remote source such as high voltage conductors or charged thunderstorm clouds. It also forms on the masts of ships and on the extremities of aircraft when they are charged by flying through clouds. Then the phenomenon is commonly called St. Elmo's fire, but the mechanism is the same as that observed on high voltage conductors. Corona is a localized discharge, but can be the precursor to complete breakdown, and can be a prolific source of interference in radio receivers.

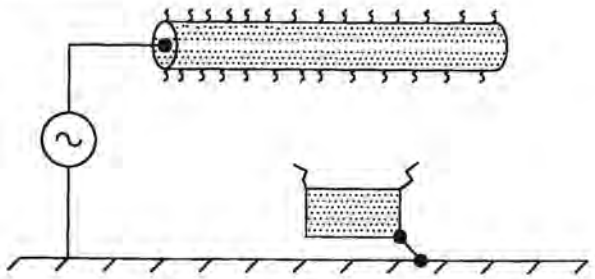

Fig. 1.3 Corona.

1.4.1 Negative Corona Processes

The negative corona process occurs when the electrode upon which the corona forms is subjected to a sufficiently large negative electric field, a negative field being defined as one in which an electron in the space around the electrode is forced away from the electrode, Fig. 1.4. A common situation involves the electrode being connected to the negative terminal of a power supply while the positive terminal is grounded. The negative electrode need not be directly connected to a power source however; the electric field may be created by induction from other charged electrodes. Consideration of where the other electrodes are located is rather academic since the important matter is the electric field in the immediate region of the conductor upon which corona is formed.

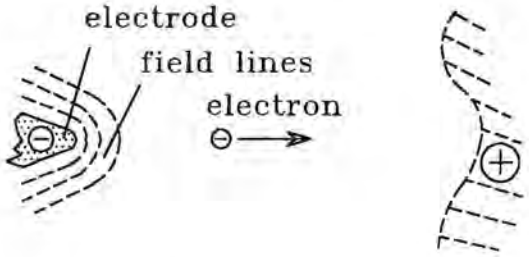

Fig. 1.4 Motion of an electron in a negative field.

Because of some initial ionization process, an electron is liberated in the gap. Under the influence of the electric field the electron is repelled away from the electrode. As it is repelled, it collides with the gas molecules and a flood of other electrons is triggered by the avalanche process described in §1.1. This leaves a cloud of mixed positive and negative charge, Fig. 1.5(a). The electric field forces the electrons away from the space where the avalanche is formed and so

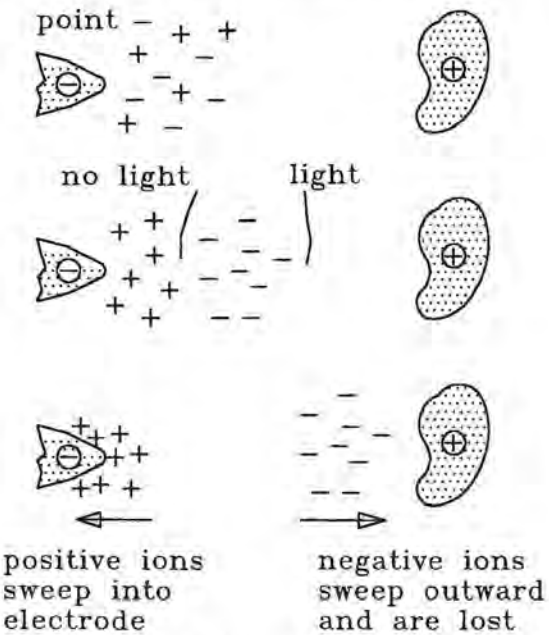

Fig. 1.5 Motion of ions for negative corona.

the slower and more immobile positive ions are left behind, as shown in Fig. 1.5(b). The electrons immediately attach to neutral ions, usually oxygen, and form negative ions.

The electric field in the gas depends on all the charge, the charge that is on the electrode and the charge that is in the space around the electrode. In the space beyond the positive ions the electric field is the sum of that produced by the negative charge on the electrode and the positive charge in the space adjacent to the electrode. The result is that the electric field in the space beyond the positive ions is reduced and the ionization process stops until the positive ions have been swept into the cathode and the negative ions have been moved away from the cathode and into the surrounding space, possibly being collected by the anode if it is nearby.

After the charges have been swept away, 1.5(c), the process may repeat, but if the electric field at the tip of the cloud of positive ions is not sufficient to cause further ionizing collisions the streamers will not extend further into the gap. This condition exists in divergent fields, those in which the stress is localized, such as the sharp pointed electrode of Fig. 1.6(a).

In a uniform field, such as that between the two flat electrodes shown on Fig. 1.6(b), whenever the electric field at the electrode reaches a critical gradient, the same critical gradient will exist all the way across the gap. As a result the corona will not remain localized, but will invariably grow and lead to complete breakdown.

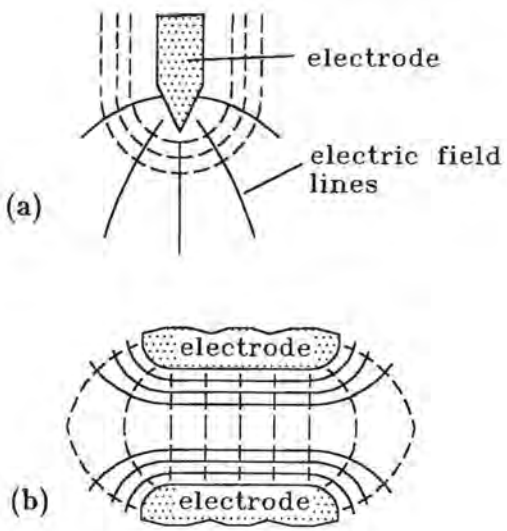

Fig. 1.6 Divergent (a) and uniform (b) electric fields.

The critical gradient at which corona is initiated is about 30 kV/cm at sea level conditions, though the gradient does depend somewhat on the physical size and shape of the electrodes. In a more rarified gas the critical gradient would be lower than 30 kV/cm, the governing factor being the density of the gas. Reference data relating density (pressure and temperature) to altitude is available in standard handbooks [1.7]. At an altitude of 10 000 ft. the critical gradient would be about 22 kV/m.

Corona is visible because light is emitted at the tip of the discharge as ions are bombarded and the collisions raise the impacted atoms to a higher energy state. Later, the excited atoms may revert to their normal lower energy state and as they do, the excess energy is radiated as electromagnetic waves, some of the radiation occurring in the visible band and appearing as light. The light ceases as soon as the bombardment stops and the charged ions are swept away. The charge itself is not visible. The visible light that is emitted is predominantly blue. It is also rich in ultraviolet and can be photographed much more readily through a quartz lens than a conventional glass lens.

The negative corona process may manifest itself as a train of individual pulses, called Trichel pulses after an early investigator of the phenomenon. It may also manifest itself as a pulseless glow or as negative streamers. Trichel streamers extend about 1 cm away from the electrode and each one produces a current pulse of amplitude varying from 1×10^{-8} A at point electrodes to 2×10^{-2} A at large electrodes.

The discharge propagates for up to 20 ns (20×10^{-9} sec) before being choked off by the space charge. Current rise times are between 25 and 50 ns, with half-value widths about twice that long. Because the pulses are short, they can lead to radio noise over a very wide band of frequencies. If the field strength increases, the rate at which the Trichel pulses are formed increases. The maximum frequency of the pulses has been reported as 2 kHz for an 8-mm sphere and 3 MHz for a 30 degree conical point.

After the Trichel pulses reach their maximum frequency, a pulseless glow forms around the electrode. Under these conditions the discharge current becomes essentially dc and ceases to emit radio noise. As the electric field is increased even further, negative streamers appear and extend out from the electrode several centimeters. The current consists of pulses superimposed on a quasi-steady state current with the rise times of the pulses being on the order of 0.5 μs (0.5×10^{-6} sec). The visual appearance of the corona pulses and the shape of the current pulses are sketched on Fig. 1.7.

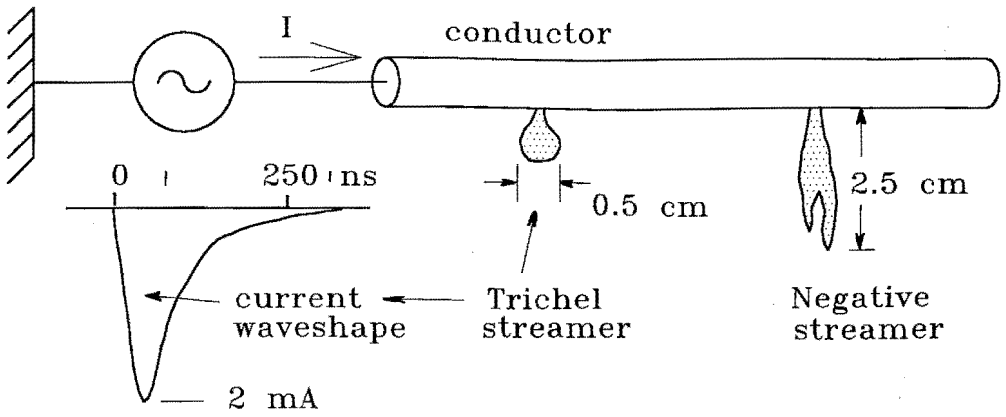

Fig. 1.7 Negative corona.

1.4.2 Positive Corona Processes

Positive corona occurs when the electric field at the surface of the electrode is positive, either because the electrode is energized with positive voltage or because it is grounded and in the electric field produced by an electrode energized with negative voltage. It has many of the same characteristics as negative corona, but the electrons and positive ions are accelerated in the opposite direction. The mechanism is illustrated on Fig. 1.8. The amplitude of the current pulses is generally much larger than occurs with negative corona, but the pulses do not occur with as high a repetition rate. The initial electron is drawn towards the positive electrode and the positive ions formed by collision are repelled away from the positive electrode. The field strength at the surface of the electrode diminishes and the discharge stops until the charged particles are swept from the space around the electrode. The electric field beyond the cloud of positive ions is enhanced because it responds both to the positive charge on the electrode and to the positive space charge. In this respect it is unlike the negative case where the positive space charge acts to lower the intensity of the field produced by the negative charge on the electrode. This enhanced field helps a positive streamer to propagate farther than would a negative streamer.

The positive coronas have three distinct forms; onset pulses, Hermstein's glow and positive streamers. Onset pulses appear as streamers in a stem with some branching, and a high repetition rate gives the corona a brushlike appearance. From an 8–mm sphere current amplitudes have been measured at 0.25 A. Mean rise time is 30 ns and mean decay time is about 100 ns.

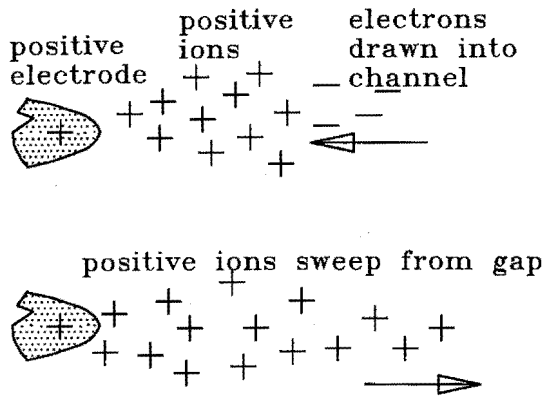

Fig. 1.8 Motion of ions for positive corona.

The maximum repetition rate is about 200 Hz for large electrodes and 2000 Hz for point electrodes. The somewhat longer rise and decay times might imply that the pulses produce less radio interference than negative corona pulses, but the higher amplitude of the current pulses makes the absolute interference levels higher.

As the voltage is increased the corona glow forms an ionizing layer (Hermstein's glow) and the discharge current consists of small ripples at a frequency of up to 2×10^6 Hz superimposed on a quasi–dc current. As the voltage is increased still further the streamers rapidly extend even further, the velocity of propagation being 20 to 2000 cm/μs.

Sketches of positive corona and the current waveshapes are shown on Fig. 1.9.

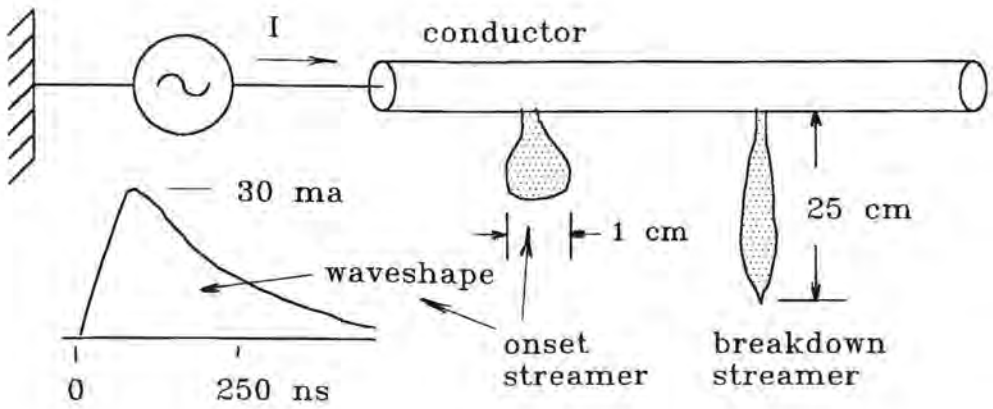

Fig. 1.9 Positive corona.

1.5 Breakdown Processes In Air Gaps

It is a common misconception that the breakdown strength of air is about 30 kV/cm or 3 MV/m. That figure is indeed about the electric field gradient at which corona will begin to form and it is the intrinsic breakdown strength of short air gaps contained between electrodes carefully contoured to eliminate any regions where the local electric field strength is greater than 30 kV/cm. Such electrodes are usually found only in laboratories. With practical gap geometries, and particularly with gap geometries greater than a few centimeters in extent, it is much more realistic to assume the average breakdown strength of air under lightning conditions to be about 5 kV/cm or 500 kV/m. With longer duration waveforms the average breakdown strength may be more on the order of 3 kV/cm. With short duration pulses the breakdown strength may be much more than 5 kV/cm, but such a condition usually means only that a developing breakdown has not had sufficient time to progress to final breakdown. With a large gap, such as found around an aircraft in flight, any place the macroscopic electric field has a gradient greater than 500 - 600 kV/m is a place where one can assume that a breakdown is in process or is about to be.

The following material will illustrate why the breakdown strength of air has this surprisingly (to some) low value. The section will discuss the conditions under which corona streamers can continue to grow until a gap is completely bridged. It will discuss the mechanism by which the streamers develop in a gap to which voltage is suddenly applied and show how it is different if voltage is gradually raised. It will also discuss conditions if the applied voltage has a decaying tail and explain both how front and tail times affect how fast the breakdown progresses and explain how this leads to a *volt–time* or *time–lag* effect.

The basic aim of the section will be to provide tutorial material with an emphasis on physical understanding of electrical arcs used in testing, of lightning phenomena and how lightning interacts with aircraft. It will deal only with air at near sea level atmospheric pressure and mainly with electrodes spaced so far apart that the field between them is far from uniform and in which the metal of the electrodes and the vapor from them can play no significant part in the breakdown process.

Also, the section will focus on the phenomena that occur when the electrodes are directly connected to a voltage source that supplies the energy necessary for the development of the arc and the electric field through which it propagates. On an aircraft the discharge may originate at the aircraft and the energy necessary for the development of the arc must be extracted from the pre-existing electrical field. There are some differences in the two processes and these differences are discussed in Chapter 3.

1.5.1 Types of Surge Voltage

When discussing the breakdown strength of air it is common practice to refer to lightning surges, switching surges and power frequency voltages. The terms

have their origin in the electric power field, to which most studies of breakdown strength of air gaps have been directed. For continuity, the terms will be retained here, though they are not particularly apt in relationship to aircraft.

Surges having front times measured in a few microseconds and decay times measured in a few tens of microseconds are commonly called lightning surges since surges induced on power lines by lightning have such waveshapes. Other mechanisms can, of course, also produce surges of such waveshapes.

Switching surges, as their name implies, arise on power lines through the operation of switches and circuit breakers. They are characterized by front times measured in tens and hundreds of microseconds and decay times measured in hundreds and thousands of microseconds. Such times are also involved as a lightning flash propagates towards or away from an aircraft.

Power frequency voltages primarily relate to 50 or 60 Hz energization of transmission lines and will be given only passing consideration in the following material.

Nuclear effects, NEMP, may lead to surges measured in tens of nanoseconds, but they are beyond the scope of the following material.

A distinction is also made between the terms *surge* and *impulse*. Accepted practice is to use *surge* to refer to a voltage produced at random by nature and *impulse* to refer to a voltage or current produced under controlled conditions in a laboratory. For even more precision the terms *lightning impulse* and *switching impulse* are used.

1.5.2 Waveform Definitions

Voltages and currents tend to have different waveshapes, both because of the nature of physical processes and because of the intrinsic behavior of testing machinery.

Voltage impulses: Voltage impulses used in high voltage testing and research most commonly have double exponential waveshapes, as illustrated on Fig. 1.10(a). They are described approximately by an equation of the form

$$E = E_0(e^{-\alpha t} - e^{-\beta t}). \qquad (1.5)$$

Double exponential waveshapes are used because they have the general characteristics of natural surges (fast front times and slower decay times) and can be produced by basically simple (though expensive) capacitor and resistor networks. Principles of such machines are described in §6.8. Double exponential waveforms are characterized by their peak amplitude, front time and decay time, definitions of front and tail time being given by industry standards [1.8]. The *virtual front time* is taken to be 1.25 times the time between the 30% and 90% points. For many purposes this virtual front time is a better characterization of the effects of the impulse than the time to actual peak because it also defines the effective rate of rise of the impulse. It is defined by the 30% and 90% points rather than the 10% and 90% used in electronic practice since the initial toe of the impulse is frequently distorted because of the characteristics of the impulse generator. The distortion is of little importance as regards the effect of the impulse, but can lead to controversy as to when the impulse reaches its 10% point. Decay time is usually taken to be the time to decay to 50% of the peak amplitude. It is seldom characterized by the time to decay to 37% (e–folding time), both because the 50% point is easier to determine and because the shape of the impulse below 50% is seldom of importance in studies of breakdown characteristics.

A waveshape commonly used in the electrical industry is a 1.2×50 μs wave, for which $\alpha = 1.46 \times 10^4$ and $\beta = 2.475 \times 10^6$, time being measured in seconds. The constants yield a wave with a 1.2 μs front as defined by industry standards, not the time to absolute peak voltage. Procedures for determining α, β, and E_0 in Eq. 1.5 are given in §9.10.1.

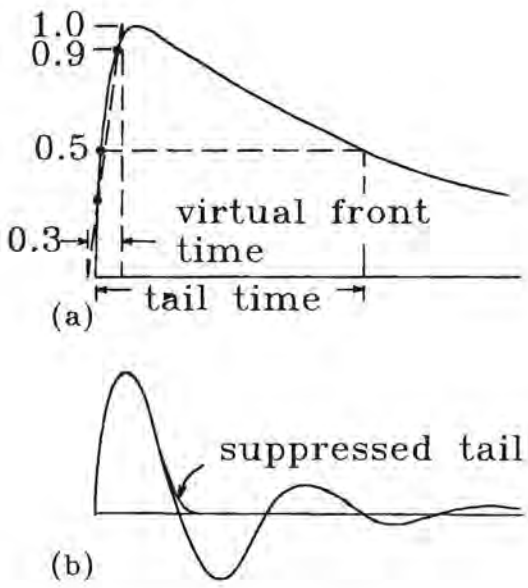

Fig. 1.10 Waveshapes for testing.
(a) Double exponential wave
(b) Suppressed oscillatory wave

A true double exponential wave can only be produced by a surge generator having one type of energy storage element, inductance or capacitance. If the generator has two types of energy storage element; that is, both inductance and capacitance, then a double exponential is only an approximation of the actual output waveshape. Capacitive surge generators optimized for high voltages usually have inductances sufficiently low that the output can be described quite well by a double exponential.

Current impulses: Current impulses used for evaluating low impedance surge protective devices often have waveshapes that cannot be described by double exponentials, mostly because the inductance of the generators used to produce the surges is not negligible. A common waveshape is shown on Fig. 1.10(b) and is described approximately as

$$I = I_0\ \epsilon^{-\alpha t} \sin(wt). \tag{1.6}$$

Frequently the nature of the device under test is such that only the first half cycle of the current is produced. A waveshape commonly used has an 8 μs front and a 20 μs tail. A wave having that particular ratio of front to tail time is not one that can be produced by a double exponential surge generator, though it is routinely produced by discharging an energy storage capacitor through an inductive circuit.

No special attempt should be made to relate the shape of surges used for testing insulation to the shape of the surges used for testing surge protective devices. The relationship has very little to do with the physical characteristics of lightning or of naturally occurring surges; it is mostly a historical matter reflecting the early development of the high voltage testing art and the incorporation of common practices into standards.

Also, one should not consider that these waveshapes necessarily represent the shapes of natural lightning currents or the voltages produced by lightning. They are intended to have the same general characteristics (fast fronts and longer tails) and have time scales typical of those produced by natural lightning, but they are only standardized waveshapes used for testing.

1.5.3 Volt–Time Curves

Repeated applications of voltage do not always produce the same pattern of flashover and if the voltage is barely sufficient to cause breakdown, some applications of voltage will cause breakdown and others will not. Breakdown is thus a statistical matter; if the voltage is low the probability of breakdown is low and if the voltage is high the probability is greater.

The breakdown voltage also depends strongly on waveshape. In general, long duration voltages will cause breakdown of a gap at lower levels than will be required if the voltage is of short duration. Short duration voltages may be sufficient to initiate the breakdown process and to produce intense ionization (and in the process draw large currents from the voltage source), but may not last long enough to cause a complete breakdown. Also, the current drawn by the developing breakdown may be so large that a considerable amount of the voltage initially applied to the gap will be lost in the impedance of the test circuit external to the gap. This loss of voltage may be sufficient to prevent the gap from breaking down.

Typical waveshapes that could be observed during breakdown testing with lightning impulse waves are shown on Fig. 1.11. In the figure the shape of the voltage actually developed across the gap is shown by the heavy line while the shape that the voltage would have if it were not interrupted by the breakdown of the gap is shown dotted. This latter is called the prospective voltage. Accepted terminology defines *full waves* (FW) as those that do not lead to break-

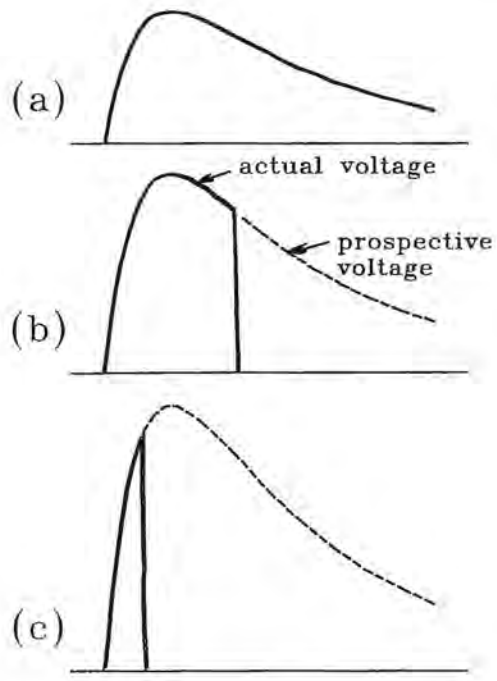

Fig. 1.11 Voltage waveshapes.
(a) Full wave
(b) Tail chopped wave
(c) Front chopped or steep front wave

down, *chopped waves* or *tail chopped waves* (CW) as those causing breakdown after the voltage has begun to decay and *steep front* (SF) or *front chopped waves* as those that cause breakdown before the wave reaches its peak prospective voltage.

If repeated applications of voltage are made, starting initially at a low level and then increasing, there can be found a level below which no breakdowns occur, the withstand (WS) level. At a somewhat higher level breakdowns will occur sometimes, but not always. If voltage is raised still further, a level is found where 50 percent of the impulses cause breakdown, the critical flashover (CFO) level. That peak voltage level is designated U50, from the German *Uberspannung* or overvoltage.

With short gaps, up to about 10 - 20 cm, the breakdowns will occur at the peak of the voltage wave, but with a sufficiently long gap the breakdowns will occur after the voltage has reached its peak and started to decay. If the voltage is raised still further breakdown occurs at earlier times, perhaps before the voltage has reached its peak prospective voltage. Connecting the breakdown points results in a *volt–time* or *time–lag* curve, Fig. 1.12. For breakdowns that occur after the voltage has begun to decay the point plotted is the maximum voltage and the time at which breakdown occurs. Fig. 1.13 shows volt–time curves measured on various lengths of transmission line insulators. Note that the critical flashover voltage is about 550 kV/m and that much higher voltages are required to produce breakdown at short times. This suggests that breakdown is a process that does not take place instantaneously. Research indicates that this is so.

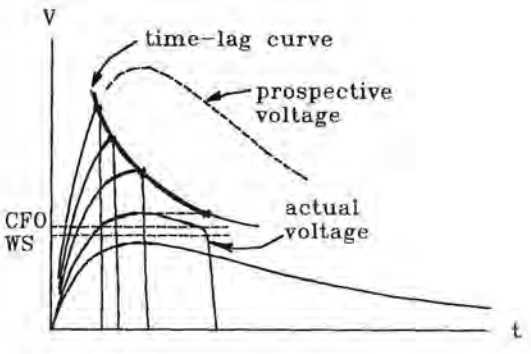

Fig. 1.12 Development of a volt–time or time–lag curve.

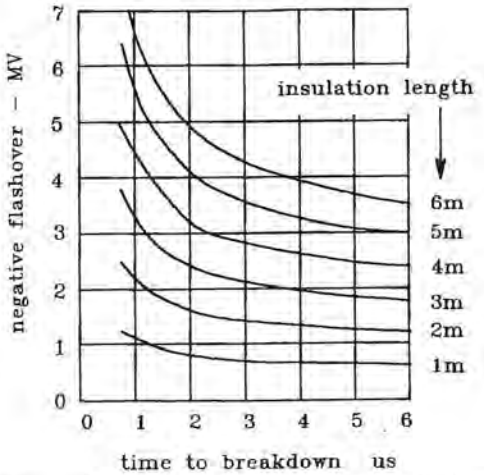

Fig. 1.13 Volt–time curves for transmission line insulators [1.6].

1.5.4 Streamer Development

When a long air gap (length greater than about 0.5 m) is stressed with a positive or negative impulse voltage and the flashover observed with a camera that is able to observe the stages of the breakdown process, it is found that there are several fairly distinct stages in the process. These are the formation of an initial corona, growth of a leader, and a final jump which culminates in the development of a highly conducting channel.

Initial corona: The initial burst of corona takes place from the energized electrode as soon as the electric field at the tip of the rod reaches about 30 kV/cm and usually this takes place before the applied voltage has reached its maximum value. The corona forms in a small fraction of a microsecond and propagates away from the electrode very rapidly, several meters per microsecond (m/μs). This corona discharge, however, does not go across the entire gap between the electrodes unless the electrodes are close together, perhaps 25 cm. If the voltage were to be removed the discharge would stop and there would be no breakdown.

Streamer: If the voltage is of sufficient magnitude and is maintained, a more intense and more localized discharge called a streamer develops out of this initial corona and works its way towards the grounded electrode in a manner very similar to that of lightning, as discussed in Chapter 2. Initially this leader propagates at several centimeters per microsecond (cm/μs), much slower than does the initial corona, and carries a current of about 100 A.

Leader voltage: The voltage drop along the leader is rather small, about 2 kV/cm, making the resistance on the order of 20 ohms per cm. The leader is thus sufficiently conductive that it acts as an extension of the rod and the result is that most of the applied voltage is impressed across the unbridged portion of the gap. As the leader progresses, the gradient across the unbridged portion of the gap increases and the leader progresses faster and carries more current.

Final jump: When the corona ahead of the leader contacts the plane a more conductive channel begins to grow through the leader and eventually bridges the entire gap. This is called the final jump. At this stage the entire gap is bridged by a highly conducting channel. As the channel carries more current it becomes hotter and more conductive, which allows it to carry more current and become hotter still. Eventually the current becomes limited by the external circuit and the voltage across the arc collapses.

Electrode configurations: The characteristics of a breakdown are influenced by the type of electrode, some common electrode configurations being shown on Fig. 1.14. The most easily studied geometry consists of an energized sphere or rod placed above a grounded plane, a sphere plane or rod plane configuration. Another common geometry consists of two rods, one energized and the other grounded. The breakdown process in such a rod–rod gap is more complicated than in a rod–plane gap since the breakdown develops simultaneously from each rod, one of which is energized positive and other negative. Sphere–sphere electrodes are used in studies of uniform fields and can be used as standard electrodes for measurement of voltage. When high voltage tests are made to determine the points at which lightning might attach to an aircraft, the geometry approximates that of a rod to plane configuration.

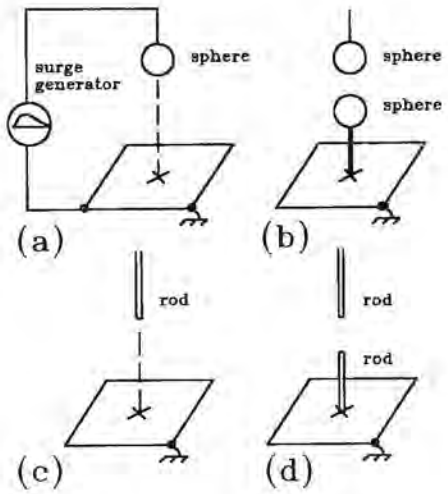

Fig. 1.14 Electrode configurations.
(a) Sphere to plane
(b) Sphere to sphere
(c) Rod to plane
(d) Rod to rod

Methods of observation: Early studies of breakdown phenomena focussed on the behavior of gaps exposed to lightning impulse voltages. One of the techniques used for the studies is shown on Fig. 1.15. The figure shows a test setup in which a positive polarity 3 MV (megavolts or 3×10^6 volts) impulse was applied to a rod–rod gap. A parallel rod–rod gap out of the field

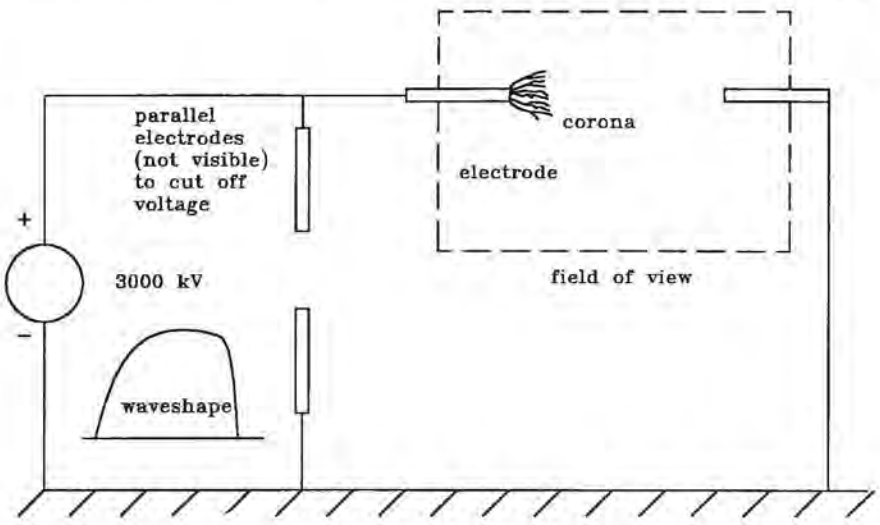

Fig. 1.15 Study of rod–rod breakdown.

of view of the camera was used to remove the voltage before the breakdown in the gap under study had progressed to completion. By adjusting the length of the parallel gap the phenomena in the gap under study could be observed at different stages in the development of the breakdown. A photograph of the early stages of breakdown, Fig. 1.16, shows a very extensive and diffuse set of tentacles extending from the impulsed electrode. This is the *first corona*. The photograph was taken through a quartz lens which passes more of the ultraviolet spectrum than does a conventional glass lens. A photograph taken with a glass lens would show very little of the diffuse corona.

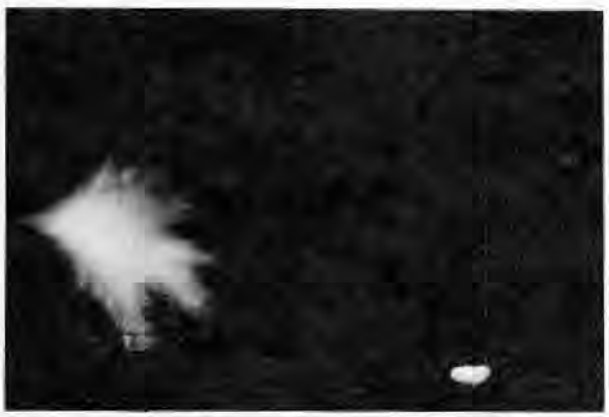

Fig. 1.16 Initial corona.

When the parallel gap was made longer and the discharge allowed to progress to a later stage, Fig. 1.17, one portion of this corona bridged the entire gap and a brighter and more conducting channel began to form around the lower (negative) electrode and progressed into the space bridged by the corona. This is called a *streamer*. Similar streamers develop at the upper (positive) electrode, but they are difficult to see through the corona. When the breakdown process was allowed to progress to completion the breakdown channel was as shown on Fig. 1.18. At the center of the gap can be seen the region where the downward and upward leaders joined. The direction of propagation of the leaders can be seen by the faint branches extending to the side of the main channel.

Streak camera: The technique of using a parallel gap to interrupt the developing breakdown is now seldom used; modern technique makes use of streak cameras. The basic principle of a streak camera is shown on Fig. 1.19. It basically consists of moving the lens

Fig. 1.17 Growth of a streamer.

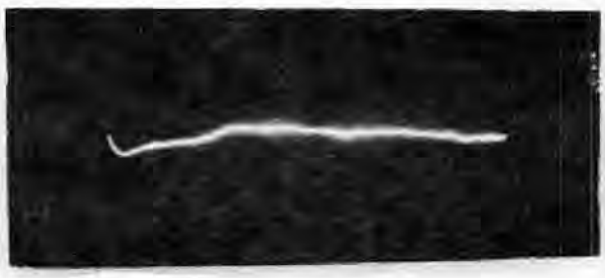

Fig. 1.18 Completed breakdown.

(mechanically or electronically) while the breakdown is in process. The result is that the image recorded on the film is spread out and displayed as a function of time. If the lens is moved in discrete steps (framing mode), Fig. 1.19(a), a developing breakdown can be photographed as a series of instantaneous snapshots. More commonly the lens is moved continuously (streak mode), Fig. 1.19(b), and the image is blurred. The luminous head of the leader photographs as a bright band gradually bridging the gap while other luminous processes show as a band behind the leader.

Boys camera: An early camera, called the Boys camera, after the inventor, moved the lens mechanically and has been widely used to study the breakdown processes in lightning. Modern devices achieve the same effect electronically. An optical image is formed on an electron emitting surface and the electrons from that surface are focussed with an electron lens (magnetic or electrical) onto a phosphorescent screen producing an image which can then be photographed with a con-

ventional camera. Generally an image intensifier section is used to amplify the image and make it possible to display phenomena that are only faintly luminous. The focused beam can be moved by deflection plates similar to those used in a cathode ray tube.

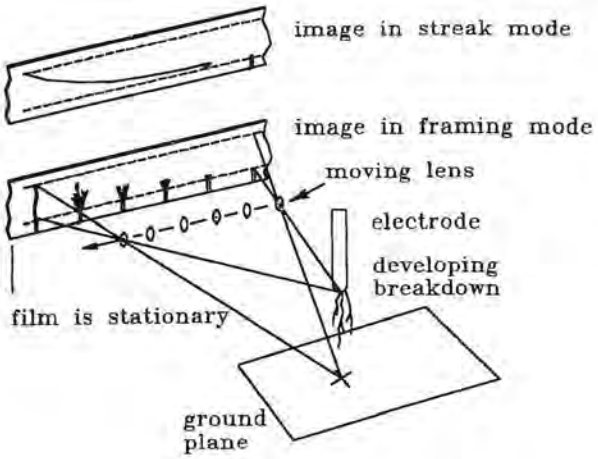

Fig. 1.19 Streak and framing cameras.

Switching impulses: Recent studies (from about 1965) have mostly focussed on the mechanism of breakdown when electrodes are exposed to switching impulses since it has been found that such impulses cause flashovers at much lower voltages than do lightning impulses. Positive impulses produce breakdown at lower voltage than negative impulses and have been the most studied. Also, the studies have focussed on the behaviour with voltages just sufficient to cause breakdown and have not dealt with the breakdown process when the gap is subjected to overvoltages. In this respect the studies have differed from early studies of breakdown with lightning voltages where the influence of excess voltage on the speed of breakdown has been important to design of insulation.

Fig. 1.20, adapted from Fig. 10 of [1.1] and from [1.9], shows sketches of what would be revealed when viewing, with a streak camera, the breakdown of a rod–plane gap when the rod is energized with positive polarity surges of the indicated waveshape. Photographs showing the phenomena in more detail appear in [1.1]. For some rates of rise of voltage the discharge proceeds fairly smoothly toward the ground electrode. If the rate of rise is lower the discharge becomes more discontinuous. In general, the corona propagates from the developing leader towards the ground plane, as evidenced by the slope of the image produced by the developing corona.

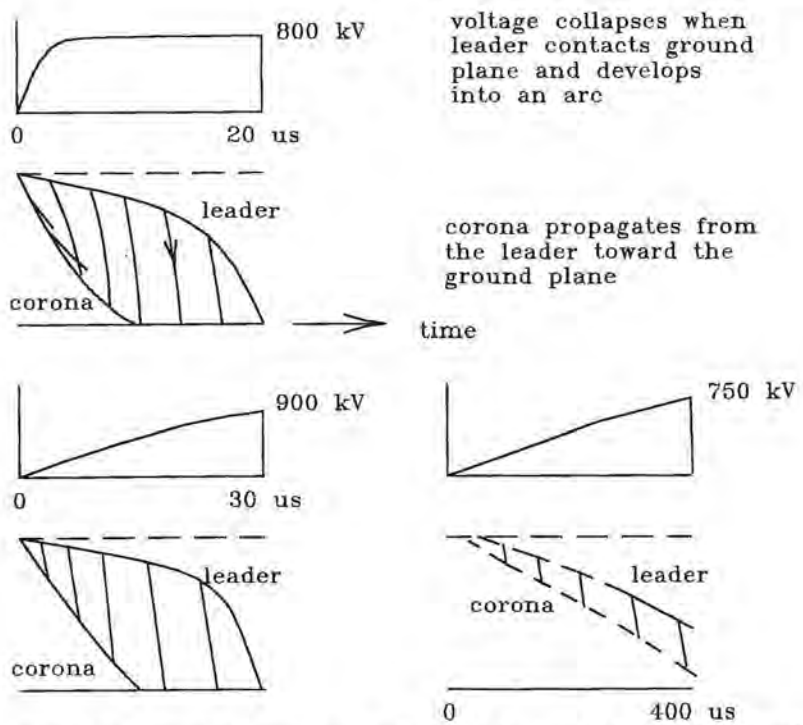

Fig. 1.20 Influence of wave–front on the development of the leader stroke. Adapted from [1.1] and [1.9].

With negative polarities the discharge is even more discontinuous. Discharges frequently take place in the air beyond the head of the leader and propagate both forwards toward the grounded electrode and backwards towards the advancing leader. The sketch of Fig. 1.21, adapted from Fig. 17 of [1.1] and from [1.10], shows the phenomenon. Note that the curvature of the image due to the corona is opposite to that of Fig. 1.20. With this geometry a leader also grows from the grounded rod towards the leader from the rod to which voltage is applied.

Studies also show that with switching impulse waves the critical breakdown voltage depends on the front time of the voltage, there being a front time that minimizes the breakdown voltage. This front time is in the range 200–600 microseconds, but it depends on the length of the gap, being longer for longer gaps.

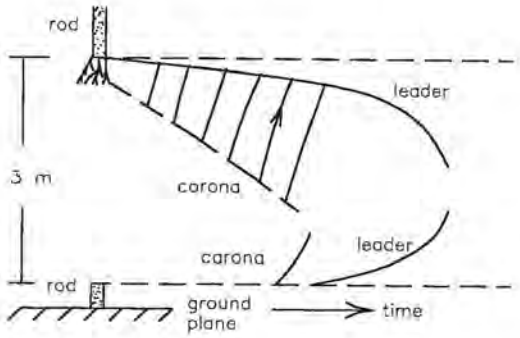

Fig. 1.21 Negative polarity sparkover of 3 meter gap rod to rod on plane gap. 1.5/1000 microsecond wave Adapted from [1.1] and [1.10].

The above is still a rather superficial description of the breakdown process and some more discussion is in order. Consider first the initial corona. The initial corona forms as soon as the electric field at the energized electrode reaches a critical gradient of 30-33 kV/cm and continues to propagate as long as the electric field is greater than about 25 kV/cm. If the gap is short or if the field in the gap is uniform the corona will bridge the gap and lead to complete breakdown.

More commonly the corona bridges only a portion of the gap, the extent of the corona depending on the distribution of electric field across the gap, as illustrated on Fig. 1.22. With a rod or pointed electrode the critical gradient will be reached at a lower voltage than if a more rounded electrode were used, but the highly stressed region around the electrode will be smaller with a rod electrode than with a rounded electrode. The result is that with a rod electrode the initial corona forms at a relatively low voltage, does not extend very far into the gap, and the initial velocity of the leader is relatively low.

Around a larger electrode with a more rounded tip the initial corona forms at a higher voltage, extends further into the gap and the initial velocity of the leader is greater. If the electrodes are sufficiently rounded, as with closely spaced spherical electrodes, the initial corona, when it forms, extends all the way to the other electrode and breakdown takes place in a fraction of a microsecond.

Streamer gradient: The rate at which the streamers extend themselves depends on the average gradient across the unbridged portion of the gap. As the leader works its way across the gap and places more voltage on the unbridged portion of the gap the average gradient across the unbridged portion of the gap increases with time and the velocity of the streamer increases. In general, the streamers will continue to propagate as long as the average gradient in the unbridged portion

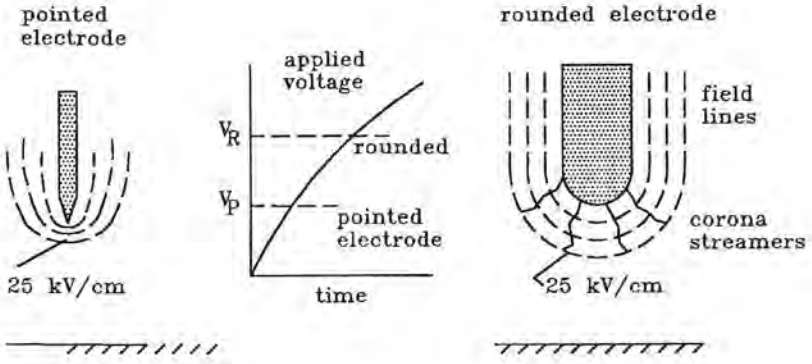

Fig. 1.22 Factors influencing initial corona.

is about 5 kV/cm or greater. If the gradient is greater than 5 kV/cm the streamers will propagate faster, but this requires injecting charge into the gap at a higher rate and hence more current is drawn from the source initiating the breakdown. Frequently the available current is limited and the streamers will propagate at a velocity such as to limit the gradient to about 5 kV/cm (500 kV/m). This critical gradient is basically what determines the minimum breakdown voltage of large air gaps, since the leader velocity determines how long the voltage must be maintained to cause breakdown. An average leader velocity of 10 cm/μs implies that a 50 cm gap would require voltage to be maintained for 5 μs before the flashover would be complete. If a higher voltage is applied to the gap the leader velocity may increase and the breakdown will grow to completion in a shorter time.

1.5.5 Effects of Gas Density and Humidity

The flashover voltage of air gaps depends on atmospheric conditions. Usually it is raised by an increase in air density or by an increase in humidity. An increase in air density (pressure and temperature both affect air density) decreases the mean free path of electrons and decreases the likelihood that they will be accelerated to a voltage sufficient to cause secondary emission. Water molecules tend to absorb electrons and thus decrease their chances to participate in the formation of electron avalanches.

For uniform field conditions and gap distances of a few centimeters the variation of breakdown voltage with pressure is governed by Pachen's Law, which states that the breakdown voltage depends on the product of gas pressure and gap length, as illustrated on Fig. 1.23. For most conditions breakdown strength decreases as pressure decreases, though there is a condition for minimum breakdown strength, below which breakdown strength increases. The data is not easily transferred to large and non- uniform gaps and for them the correction must be determined experimentally.

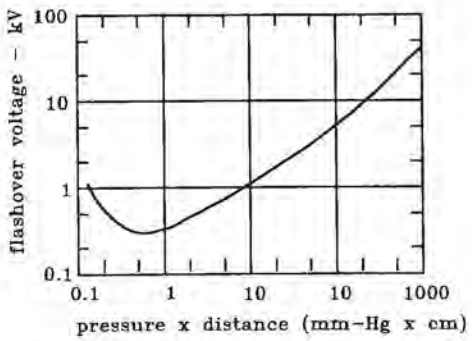

Fig. 1.23 Gap breakdown voltage [1.6].

Generally, published values of flashover voltage are corrected to standard conditions. In both Europe and the USA these are air pressure = 1013 mb., air temperature= 20° C and moisture content= 11 gm/cubic meter. In older US practice these were air pressure = 760 mm Hg, air temperature = 25° C and humidity = 15.5 mm Hg. Correction factors have been developed for both air density and humidity. A discussion of those correction factors is beyond the scope of this material, but they can be found in the literature [1.11 and 1.12].

1.6 Engineering Data on Breakdown

The following material provides some data on the breakdown voltage of various gap configurations. It is not intended to be a complete review of the available data; for that one is referred to the literature, some of which is cited in the following sections.

1.6.1 Sphere Gaps

Sphere gaps provide a uniform field condition as long as the spacing between the spheres is not too great – about half the sphere diameter. Breakdown depends mostly on the peak voltage, is not particularly affected by polarity or waveshape and is, for standard atmospheric conditions, about 30 kV/cm for small spacings. Fig. 1.24 shows sparkover voltage for spheres up to 25 cm diameter when energized with negative polarity lightning impulses. It is also valid for switching impulses and for peak values of alternating power frequency voltage. Sparkover with positive polarity is only slightly different. Sparkover voltages of larger spheres at larger spacings can be found in [1.13].

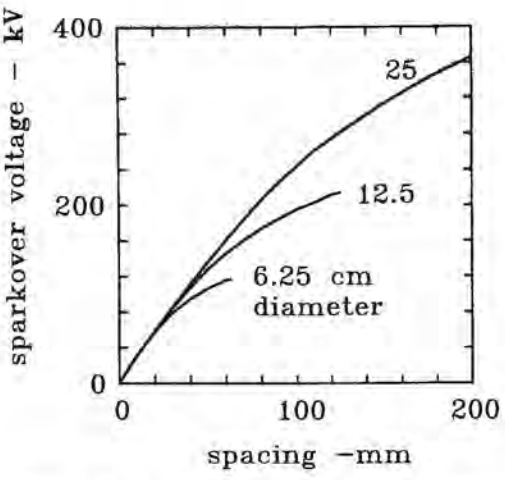

Fig. 1.24 Sparkover voltage of sphere gaps.

1.6.2 Rod Gaps

Sparkover voltage of rod–rod gaps exposed to lightning impulse voltages is given in Figs. 1.25 and 1.26. For long gaps the sparkover voltage is about 5.5 kV per centimeter of spacing. Positive polarity sparkover voltage of rod–rod and rod–plane gaps as a function of gap length and waveshape is given on Figs. 1.27 and 1.28. The data, from [1.14] is again given as average gradient. Note that the gradient falls as low as 3 kV/cm for certain waveshapes. Note also that the front time for minimum breakdown voltage increases with increasing gap length.

1.6.3 Sphere–Plane Gaps

Typical sparkover voltages with positive polarity switching voltage are shown on Fig. 1.29 [1.15].

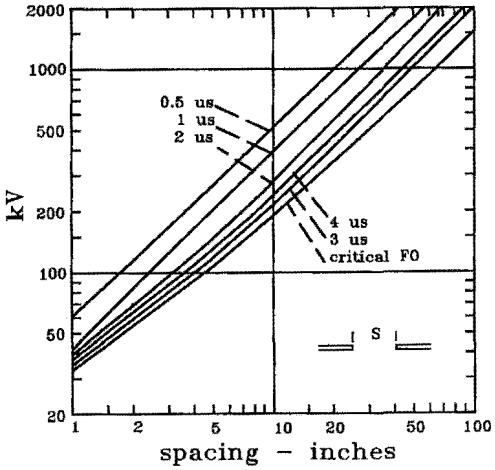

Fig. 1.25 Lightning impulse sparkover of rod to rod gaps – Positive polarity.

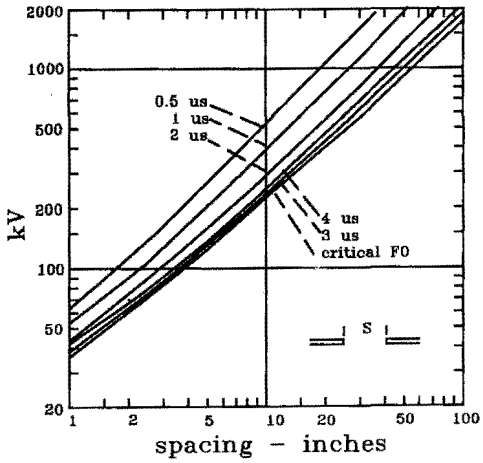

Fig. 1.26 Lightning impulse sparkover of rod to rod gaps – Negative polarity.

1.7 Gases Other Than Air

Some gasses, particularly sulphur hexaflouride, have better insulating properties than air, largely because they tend to absorb free electrons. They will not be discussed further since they are not germane to the protection of aircraft from lightning, other than their possible use in lightning simulators.

1.8 Properties of Arcs

An electrical arc is a self–sustaining discharge having a low voltage drop and capable of supporting large currents. Its characteristics depend on the materials of the electrodes from which the arc forms and the composition of the gas in which the arc burns. This discussion will deal only with arcs in air at atmospheric pressure.

In the context of aircraft and lightning protection, arcs form most commonly in response to an initial breakdown brought about by excessive voltage applied to the gap between two electrodes. In other situations, such as electrical switches and circuit breakers, they may also form between current carrying electrodes that are initially in contact and then separated.

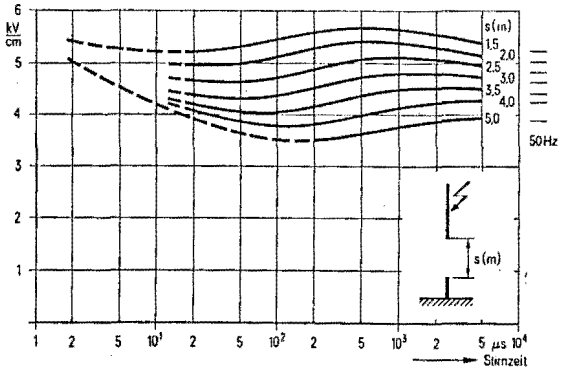

Fig. 1.27 Voltage gradient at sparkover. Rod–rod gaps, positive polarity [1.16]

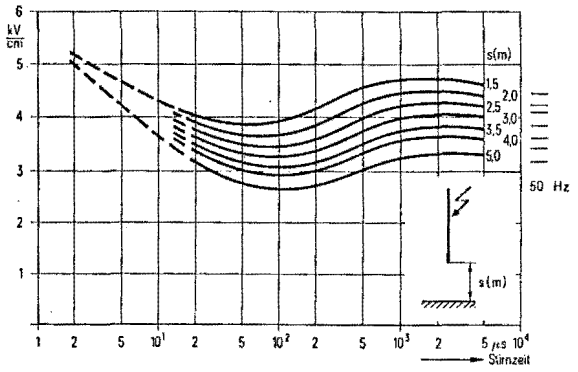

Fig. 1.28 Voltage gradient at sparkover. Rod–plane gaps, positive polarity [1.16]

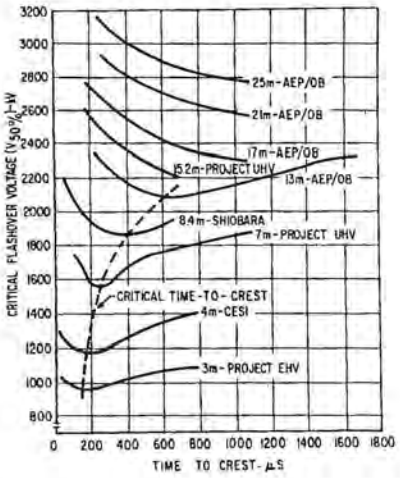

Fig. 1.29 Switching impulse sparkover of sphere to plane gaps. Positive polarity [1.6]

If the arc is initiated by a breakdown, prior to breakdown the voltage between the electrodes will be high and the current through the gap will be very low. Once the breakdown occurs there will be an ionized region in the gas between the electrodes and current will flow through that ionized region. If a plot is made of the distribution of potential between the electrodes, as shown on Fig. 1.30, it will be noted that part of the total voltage drop is concentrated at the cathode, part concentrated at the anode and that the rest is distributed along the column of the arc. The energy released in the three regions will be the product of the current and the voltage across that region.

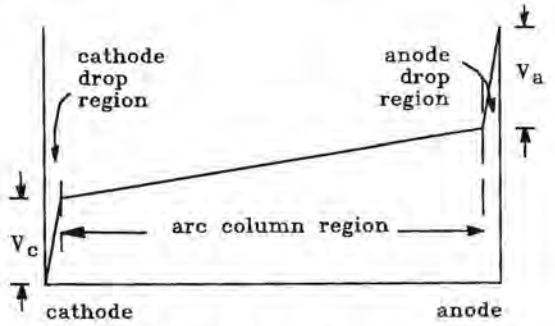

Fig. 1.30 Distribution of potential between electrodes.

Arc temperature: The energy released in the ionized region of a freely burning arc will, under most conditions, be sufficient to raise the temperature of the conducting path to between 5000° K. to 6000° K., sufficient to cause the arc to become such a good conductor that the current will be limited only by the impedance of the external circuit. If a very high current is built up very rapidly even higher temperatures will be reached, on the order of 20 000° K. in the conducting channel of a lightning flash.

Arc voltage: As the arc attains these temperatures the voltage across the arc channel will collapse from an initial value of about 5 kV/cm to a value on the order of 10 V/cm. The increase of temperature, and the collapse of voltage, is not instantaneous, but it can take place in a fraction of a microsecond. Development of a completely stable arc, though may take many seconds or minutes because the conditions at the electrodes also influence the development of the arc.

The cathode or negative electrode is the one that most affects the properties of an arc since it is at the cathode that the electrons transported through the arc are released. Before the arc forms, the cathode will be cold and electrons will be pulled from the cathode when the voltage gradient at the cathode surface approaches 30 kV/cm. After the arc forms the cathode will become heated in spots to its boiling temperature and the electrons will be pulled from the cathode by the electric field between the surface of the cathode and the adjacent column of ionized gas. For a freely burning arc this voltage drop will be on the order of 10 volts and will occur over a very short distance between the cathode and the arc channel, probably on the order of 5×10^{-5} cm. Before steady state conditions are reached it may be several times this value.

The energy released at the surface of the cathode is given by the product of gap current and cathode voltage drop and since the cathode drop region is very short, the energy released is readily transferred to the material from which the cathode is formed. Localized temperatures at the points from which the current emanates will always be high enough to cause local boiling at the surface of the electrode, on the order of 3400° K. for aluminum. Heating of an electrode is thus a very localized matter arising out of the cathode drop; it has little to do with the temperature of the column of gas adjacent to the electrode.

Current density: On average, the cathode current density will be on the order of 5000 A/cm^2 for iron or copper electrodes, at least for arc currents on the order of a few tens of amperes. It may be higher for higher arc currents. The electrons will not be emitted uniformly over the whole surface of the cathode however; they will be emitted from localized cathode spots. The current from any particular spot tends to be constant, and if the total current in the arc becomes too large to be supplied by one cathode spot, others will form.

The cathode spots will rapidly move about and if the arc is free to move there will be little damage to the surface of the cathode. Localized melting and boiling may occur, but the cathode spots will move away before the surface as a whole is noticeably damaged. Lightning flashes sweeping across the surface of bare aluminum surfaces of aircraft frequently produce only a mottled blemish on the surface. However, if the arc is constrained to stay in one point then the heating continues in that area and more intense damage may occur. Surface coatings, even a thin film of paint, may be enough to prevent the arc from moving freely.

Arc "resistance": Care should be taken in discussing the "resistance" of an arc; since it is a quantity that really only applies for a particular current and for steady state conditions. Arc voltage as a function of current is the more useful quantity. As regards aircraft, arc voltage is important in three main contexts; the amount of damage done to a surface contacted by an arc, the length of arc which may be swept across an insulating surface before the voltage becomes sufficient to puncture the insulation, and in the design of laboratory equipment with which to simulate lightning effects. All of these are discussed in more detail in later chapters.

An example of the voltage across an arc burning in air is shown on Fig. 1.31. In this particular case the voltage fluctuated with time as the high temperature carried the arc into the air and the arc length changed. Similar variations are noted if the conditions at the electrodes change, as during tests where the arc burns away the surface of the object under test.

Investigations of arc voltage with currents such as found in lightning flashes, several tens of thousands of amperes in the return stroke or several hundreds of amperes in the continuing current phase, have mostly been concerned with the performance of power circuit switching devices and are of limited value in analysis of effects of lightning on aircraft. Most investigations of the voltage across an arc in air, the condition of most importance regarding aircraft, were made many years ago with arc currents on the order of a few amperes or at most a few tens of amperes. They [1.16] show the total voltage across an arc of fixed length to decrease with current and be given approximately by an equation of the form

$$e_a = A + \frac{B}{i^n}. \tag{1.7}$$

The constant n seems to be a linear function of the absolute boiling temperature T of the anode,

$$n = 2.62 \times 10^{-4} T. \tag{1.8}$$

and ranges from about 0.5 to 1.5. For nitrogen at atmospheric pressure the constant A of Eq. 1.7 is about 51 and B about 84.

The characteristic curve relating arc voltage to arc current thus has the general shape shown in Fig. 1.32. Part of the voltage, on the order of 20 - 40 volts, is due to the cathode and anode drops and the rest is the voltage across the arc column. For long arcs in air, up to 50 cm, iron electrodes and for currents of a few amperes, the arc voltage is given by

$$e_a = A + (B + \frac{C}{i})x. \tag{1.9}$$

where x is the arc length in cm. and $A = 62$, $B = 11.4$ and $C = 32.6$. The quantity A would account for the effects at the electrodes and the vapor near the electrodes. The rest of the expression accounts for the arc in the air and suggests that the voltage along a freely burning arc would be on the order of 10 - 15 volts/cm. For higher currents Eq. 1.9 probably underestimates the arc voltage. Fig. 1.31 suggests the voltage would be about 25 volts/cm for arcs carrying several hundreds of amperes.

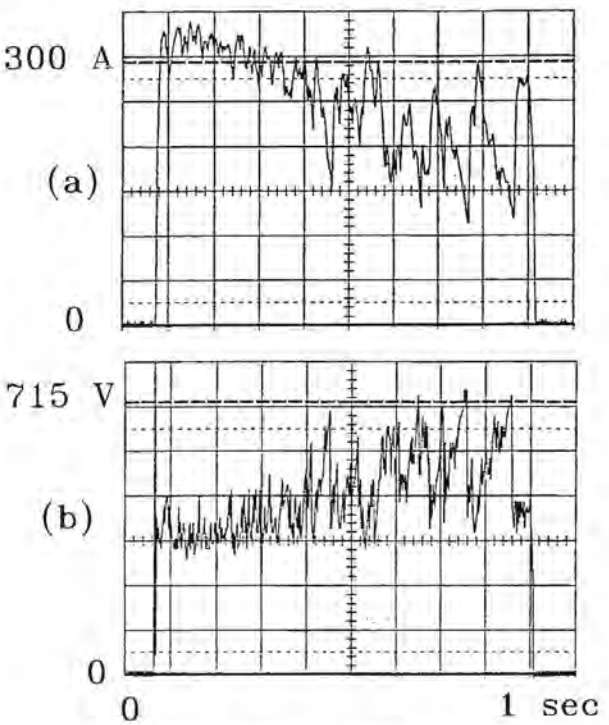

Fig. 1.31 Voltage and current of a 7 inch gap burning in air.
(a) Current
(b) Voltage

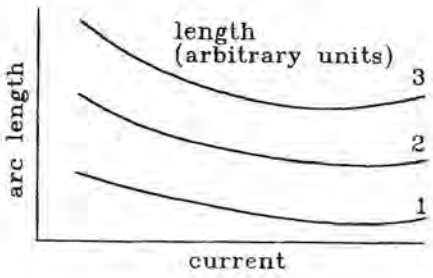

Fig. 1.32 Arc voltage vs. arc current.

The shape of the curve suggests that the diameter of the arc column expands as the current increases, thus lowering the resistance of the column. For currents on the order of a few amperes the cross sectional area of the arc expands faster than the arc current. With high currents the current density in the conducting channel reaches a limiting value and the cross sectional area expands about in proportion to the current in the arc. The result is that the arc voltage rises with current, but only slowly.

The arc voltage is a function of pressure, Fig. 1.33 [1.17] showing an example of measured data. Arcs in gases intentionally pressurized are not of concern as regards aircraft, but pressure on a confined arc will increase just due to the heating produced by the arc itself. The increased pressure results in an increased arc voltage which, for a constant arc current, increases the energy released into the arc column, which in turn causes a further increase in arc pressure. It is for this reason that a lightning arc flowing in a confined region, such as inside the wall of a house, can produce so much damage. The regenerative increase of arc voltage, arc energy and pressure continues increasing until the pressure is relieved by fracture of the containing structure.

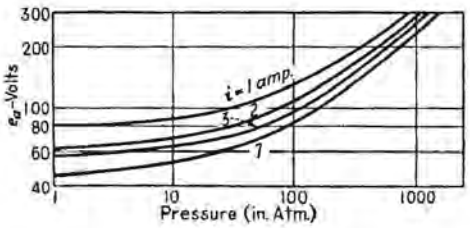

Fig. 1.33 Arc voltage vs. pressure [1.5].

References

1.1 T. E. Allibone, The Long Spark, *Lightning, Volume 1, Physics of Lightning, R. H. Golde – Editor*, Academic Press, London and New York, 1977, Chapter 7, pp. 231-280.

1.2 Les Renardieres Group, "Research on Long Air Gaps Discharges at les Renardieres, 1973 Results", *Electra, No. 35, July 1975*, pp. 49-156.

1.3 Les Renardieres Group, "Positive Discharges in Long Air Gaps at les Renardieres. 1975 Results and Conclusions",*Electra, No. 53, July 1975*, pp. 31-153.

1.4 Les Renardieres Group, "Negative Discharges in Long Air Gaps at les Renardieres", *Electra No. 74, January 1981*, pp. 67-216.

1.5 J. D. Cobine, *Gaseous Conductors*, Dover, New York, 1958

1.6 *Transmission Line Reference Book, 345 kV and Above*, Electric Power Research Institute, Palo Alto, Ca., 1982

1.7 *Reference Data for Engineers: Radio, Electronics, Computer, and Communications, Seventh Edition*, Howard W. Sams and Co., Indianapolis, Indiana, 1985, p. 48-4.

1.8 *IEEE Standard Techniques for High Voltage Testing, IEEE Std. 4-1978*, Institute of Electrical and Electronic Engineers, New York, 1978, pp. 47-55.

1.9 G. N. Aleksandrov et al, "Peculiarities of the Electric Breakdown of Extremely Long Air Gaps," *Dokl. Akad. Nauk SSSR*, Vol 183, 1968, p. 1048.

1.10 I. S. Stekolnikov, A. V. Shkilev, "The Development of a Long Spark and Lightning," *International Gas Discharge Conference, Montreux*, 1963, pp. 466-481.

1.11 *IEEE Std. 4-1978*, pp. 23-26.

1.12 *Transmission Line Reference Book*, pp. 528-530.

1.13 *IEEE Std. 4-1978*, pp. 107-121.

1.14 H. Dorsch, *Uberspannunen und Isolationsbemessung bei Drehstrom–Hochspannungslanlagen* ("Overvoltages and Insulation Measurements during Severe Current and High Voltage Discharges"), Siemens Ankiengesellschaft, Berlin and Munich, 1981.

1.15 *Transmission Line Reference Book*, p. 505.

1.16 Cobine, *Gaseous Conductors*, p. 299.

1.17 Cobine, *Gaseous Conductors*, p. 297.

Chapter 2

THE LIGHTNING ENVIRONMENT

2.1 Introduction

The lightning flash originates with the formation of electrical charge in the air or, more commonly, clouds. The most common producer of lightning is the cumulonimbus thundercloud. Lightning, however, can also occur during sandstorms, snowstorms, and in the clouds over erupting volcanos. Lightning has even been reported to occur in clear air, though this phenomenon is rare and is possibly a result of lightning originating in conventional clouds beyond the observers' field of vision. Lightning originating in sandstorms and volcanic eruptions is not of serious concern to aircraft, but lightning associated with snowstorms occurs often enough to present a problem, not because its nature is different from lightning associated with thunderstorms, but because it is apt to occur when it is unexpected. Pilots' reports on aircraft often state that they were struck "out of the blue"; that is, under conditions where a lightning stroke would not be expected. The circumstances of such reports are not always known, but they do suggest that there is still more to learn about the mechanism of the lightning flash.

The most common types of lightning are those involving the cloud and ground, called cloud–to–ground lightning, and lightning between charge centers within a cloud, called intracloud lightning. This latter is sometimes erroneously called intercloud or cloud–to–cloud lightning. True cloud–to–cloud lightning between isolated cloud centers is possible; however, what appears to be cloud–to–cloud lightning is often a spectacular manifestation of intracloud discharges. While aircraft may be involved with any of the three types of lightning, cloud–to–ground and intracloud lightning flashes are the most common types.

This chapter is mostly concerned with lightning flashes to ground and not with intracloud flashes or flashes to aircraft. There are several reasons for this emphasis, the major one being that most research on lightning has centered on cloud–to–ground lightning and most of our understanding of lightning comes from study of cloud–to–ground lightning. There have been several studies in recent years involving aircraft flown into storms in order to better study intracloud lightning. These studies have shed considerable light on the nature of intracloud lightning, and have shown that aircraft can trigger a lightning flash. The triggering mechanism and the nature of lightning flashes triggered by aircraft are discussed in Chapter 3.

Despite its importance to aircraft operation, there is simply much less information on the characteristics of intracloud lightning than on those of cloud–to–ground lightning. Intracloud lightning, unlike cloud–to–ground lightning, is largely hidden from direct observation and so is much more difficult to study. Conducting research on the characteristics of lightning is often a labor of love requiring both both extensive apparatus and extreme patience. Observing lightning from a fixed ground station is much easier and cheaper than observing lightning from a moving aircraft. Also, most of the funding for research on lightning has come, directly or indirectly, from those who are concerned with the effects of lightning on electric power transmission and distribution lines, which are affected only by cloud–to–ground strokes.

Cloud–to–ground strokes, though, are important for aircraft since aircraft are struck by cloud–to–ground lightning and there is considerable evidence that cloud–to–ground flashes are more severe than intracloud flashes. Most of the test specifications and test practices relating to aircraft and lightning have been derived, directly or indirectly, from studies of cloud to ground lightning. Finally, the ground facilities to support aircraft are only exposed to cloud–to–ground lightning. This handbook does not specifically deal with ground support facilities, but they obviously must be protected from lightning in order to fill their support role for flying aircraft.

To introduce the terms that will be discussed in the following sections consider a photograph of a typical cloud–to–ground lightning flash taken on a camera with a continuously moving film, Fig. 2.1(a), a Boys camera as discussed in §1.5.4. The image on the film would appear as shown on Fig. 2.1(b) and the current measured at ground level would appear as shown in Fig. 2.1(c). A *leader* starts at the cloud and works its way in steps toward the ground. When it nears ground an *upward streamer* forms upwards toward the descending leader. These are not very luminous and can seldom be seen by the naked eye.

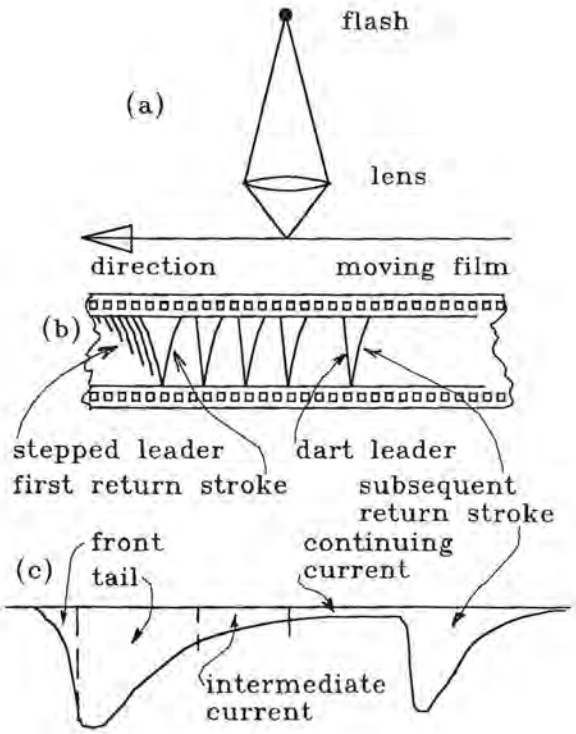

Fig. 2.1 Generalized nature of negative cloud–to–ground lightning.
(a) Orientation of lens and film in a Boys camera
(b) Image of a flash
(c) Major components

Eventually the two join and there occurs a very bright *first return stroke*. Later a *dart leader* starts at the cloud, progresses directly to ground and is followed by a *subsequent return stroke*. The pattern of dart leader – return stroke may repeat several times. The return strokes are characterized by four regions; a *front* lasting for a few microseconds or less, a *tail* lasting for times measured in tens of microseconds, an *intermediate current* lasting for a few milliseconds and a *continuing current* that may flow for up to a second or more. The intermediate current and continuing currents may not always occur and sometimes there may only be only one return stroke.

Each of these aspects of the flash will be discussed in the following sections. For a more complete discussion of the mechanism of the lightning discharge the reader is referred to the literature, of which [2.1 – 2.4] are probably the most most complete. Each of them contains extensive bibliographies and this chapter will not make any attempt to provide a complete review of the literature.

2.2 Generation of the Lightning Flash

The lightning flash originates with the generation of charge, after which the lightning flash develops by the streamer mechanism discussed in Chapter 1.

2.2.1 Generation of the Charge

The exact mechanism by which electrical charge develops in clouds is still a matter of dispute, but there is little doubt that the energy that produces lightning is provided by warm air rising upwards into a developing cloud. As the air rises it becomes cooler, and at the dew point, the excess water vapor condenses into water droplets, forming a cloud. When the air has risen high enough for the temperature to drop to -40°C, the water vapor will have frozen to ice. At lower elevations there will be many supercooled water drops that are not frozen, even though the temperature is lower than the freezing point. In this supercooled region, ice crystals and hailstones form.

According to one theory [2.5], the cloud becomes electrically charged by the following process. Some of the ice crystals which have formed coalesce into hailstones. These hailstones fall through the cloud gathering additional supercooled water droplets. As droplets freeze onto a hailstone, small splinters of ice chip off. Apparently, these splinters carry away a positive electrical charge, leaving the hailstone with a net negative charge. The vertical wind currents in the cloud carry the ice splinters into the upper part of the cloud, while the hailstone, being heavier, falls until it reaches warmer air, where some portion of it melts and the remainder continues to earth. Thus, the upper part of the cloud takes on a charge that is predominantly positive while the lower regions take on a charge that is predominantly negative.

Other theories [2.5 – 2.11] have been proposed to account for the electrification of the cloud. All of them are based on experimentally observed evidence that the charge in the top of the cloud is positive, while the lower portions of the clouds contain negative charge. Most of the early work on the distribution of charge in clouds was based on indirect evidence from the changes in electric field at ground level as lightning flashes take place. Such measurements can give ambiguous results, particularly if the electric field changes are observed at only one location, a matter discussed further in [2.3]. Direct measurement of charges by aircraft or instrumented balloons are more reliable. All the observations though, indicate that the top of the cloud does have a positive charge, that the middle regions of the cloud have negative charge and that there are also pockets of positive charge near the base of the

cloud. Some observations [2.12] suggest that the negative charge is distributed in a layer on the order of 1000 ft. thick, rather than being more or less evenly distributed through the lower portions of the cloud. Fig. 2.2 shows how the charge in a typical cloud might be distributed.

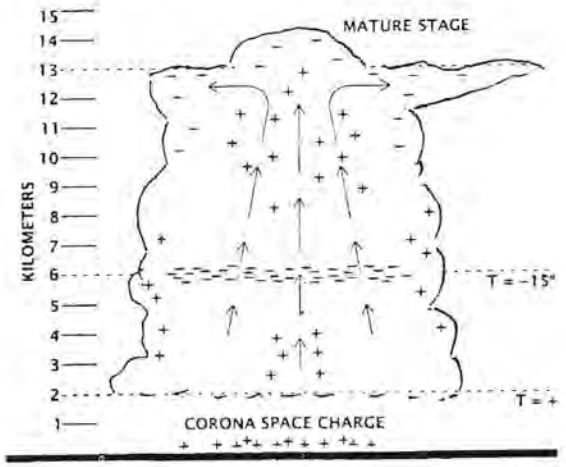

Fig. 2.2 Generalized diagram showing distribution of air currents and electrical charge in a typical cumulonimbus cloud [2.12].

The air currents and the electrical charges tend to be contained in localized cells and the cloud as a whole is composed of a number of cells. A typical cloud might have the cell structure shown in Fig. 2.3 [2.13]. The electrical charge contained within a cell might appear as shown in Fig. 2.4 [2.12]. The temperature at the main negative charge center will be about -5°C and at the auxiliary pocket of positive charge below it, about 0°C. The main positive charge center in the upper cloud will be about 15°C colder than its negative counterpart.

The lifetime of a typical cell is about 30 minutes. In its mature state the cell as a whole will have a potential, with respect to the earth, of 10^8 to 10^9 volts (V). It will have a total stored charge of several hundred coulombs (C) with potential differences between positive and negative charge pockets again on the order of 10^8 to 10^9 V. The cell as a whole will have a negative charge.

2.2.2 Electric Fields Produced by Charge

As the cloud passes over a point on the ground, an electrical charge is attracted into the ground under the cloud. The average electric field at the surface of the ground will change from its fair weather value of about 300 volts per meter (V/m) positive to as high as several

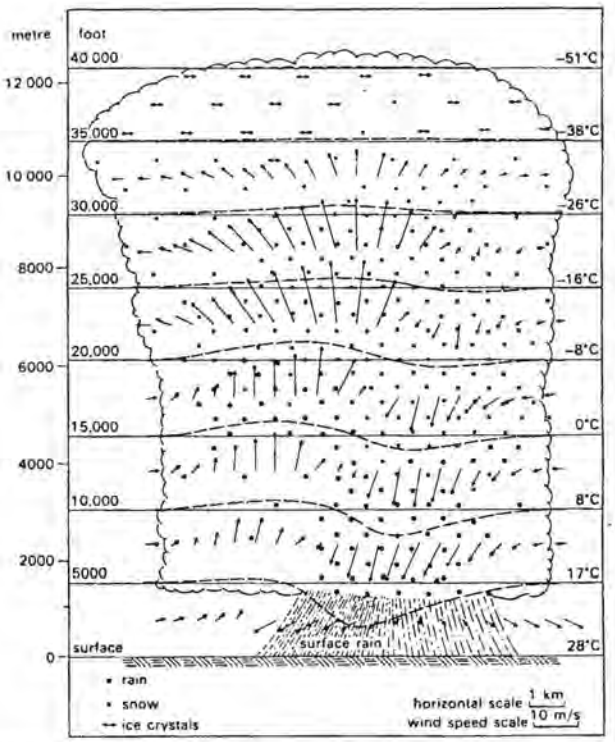

Fig. 2.3 An idealized cross section through a thunderstorm cell in its mature stage [2.13].

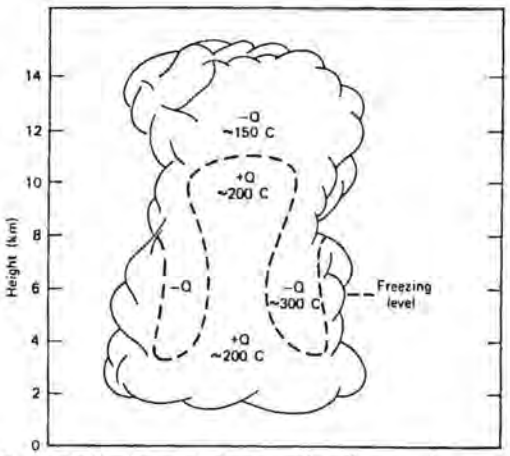

Fig. 2.4 Estimated charge distribution in a mature thundercloud [2.11].

thousand volts per meter. These polarity conventions are illustrated on Fig. 2.5. Generally, when a cloud is overhead, the field at ground level will be negative, but when a localized positive region is overhead, the field may be positive. The potential gradient will be concentrated around sharp protruding points on the ground and can exceed the breakdown strength of the air, which has a nominal value of 30 kV/cm at sea level conditions, and less at higher altitudes.

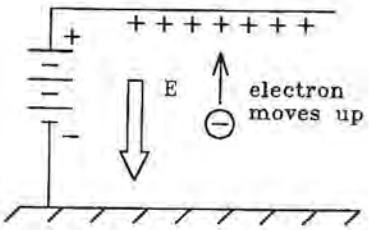

Fig. 2.5 Polarity considerations.

When the breakdown strength of the air is exceeded, current into the air increases sharply and a bluish electrical discharge called corona forms around a point. This discharge is the St. Elmo's fire discussed in Chapter 1. The magnitude of the current from a single discharge point may range from 1 or 2 microamperes (μA) to as high as 400 μA. This field induced corona is generally less intense than the corona observed on energized conductors and discussed in Chapter 1. The presence of St. Elmo's fire should be taken as signifying a dangerous condition to an exposed observer on the ground, such as a mountain climber on an exposed ridge. It is not necessarily an indicator that lightning is imminent, however, since it only reflects the state of the electric field at the ground surface, not at the base of the clouds where lightning usually originates.

Corona from grounded objects does not develop into a complete electrical arc or upwards lightning flash because the electric field is very localized and does not extend over a sufficient distance for streamers to propagate. An important reason for this is that the charges injected into the air by the corona accumulate and reduce the electric field strength at the ground surface. Because of this space charge, a developing breakdown in the air "sees" a much more uniform electrical surface than would a microscopic observer at ground level.

2.2.3 Development of the Leader

At some state in the electrification of the cloud, a discharge towards the earth takes place. It starts as a slow moving column of ionized air called the pilot streamer. After the pilot streamer has moved perhaps 30 to 50 m, a more intense discharge called the stepped leader takes place. This discharge lowers additional negative charge into the region around the pilot streamer, recharges it, so to speak, and allows it to continue for another 30 to 50 m, after which the cycle repeats. A discharge propagating in this manner is called a streamer discharge; its development was discussed in Chapter 1 and is illustrated further on Fig. 2.6.

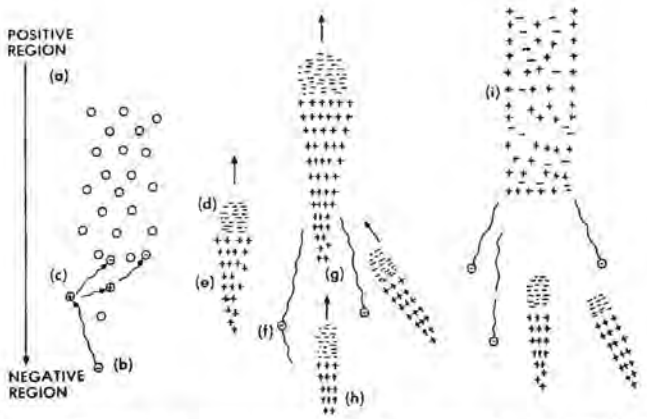

Fig. 2.6 Stages in the development of a leader.

If the initial development of the leader takes place in the charged cloud, the developing streamer branches and begins to collect charge from its surroundings. Because it collects charge in this way, the streamer may be viewed as connected to the cloud and at the same potential as the cloud. As the head of the leader moves farther into the un-ionized air, charge flows down from the charged regions of the cloud, along the partially conducting filament and toward the head of the leader, thus tending to keep all parts of the leader at a very high potential. The amount of charge, q_o, lowered into the leader will be on the order of 2 to 20 $\times 10^{-4}$ C/m of length. A leader 5 km long would then have stored within it a charge of 1 to 10 C.

The leader, as postulated by Wagner [2.14], appears as shown on Fig. 2.7. The head of the leader may have a larger diameter than the rest of the leader, though this is difficult to prove by photographs. The head of the leader is generally visible because of the optical radiation associated with the extension of the electron avalanches, but once the growth ceases, the radiation stops; consequently, the corona sheath surrounding the central conducting filament is not visible. Since the potential of the leader is very high, there will be a high radial electric field along the leader. This field will be high enough to exceed the breakdown strength of the air, and secondary streamers will branch out radially away from the central filament. The filaments will branch out radially until the field strength at the edge of the ionized region falls to about 30 kV/cm.

Diameter of the leader: It can be shown that the electric field strength at the edge of a cylinder containing a charge, q_0, per unit length is

$$Er = \frac{1.8 \times 10^{10} q_0}{r} \qquad (2.1)$$

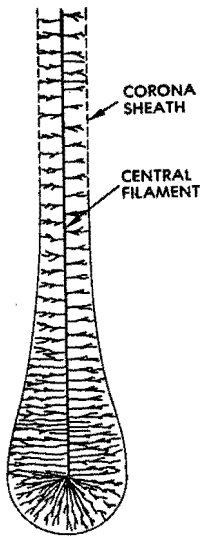

Fig. 2.7 The lightning leader as postulated by Wagner [2.14].

From this and the above breakdown strength of air, it can be deduced that the radius of the leader will be 1.2 to 12 m. At higher elevations the breakdown strength of air is less; hence the leader radius may be more.

Photographs of actual lightning leaders may be taken with a Boys camera, in which the film moves relative to the camera lens. Fig. 2.1 illustrated the principle and Fig. 2.8 [2.15] shows an example of such a photograph. The leader is seen originating at the top left hand corner of the picture and lengthening as time increases. The bright line at the right of the picture is produced by the return stroke as discussed in §2.2.5.

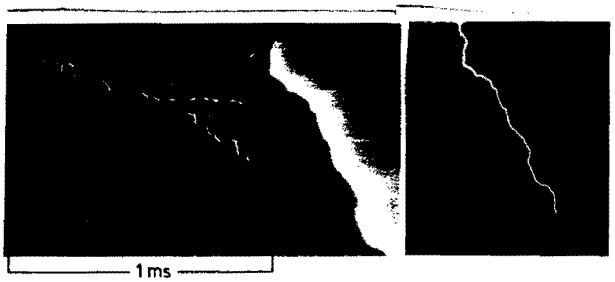

Fig. 2.8 Boys camera photograph of a lightning leader [2.15]

Leader velocity and current: From such photographs it has been learned that the leader advances at about 1 to 2 $\times$ 10^5 m/s, or 0.03% to 0.06% of the speed of light [2.16]. In order that a charge of 2 to 20 $\times$ 10^{-4} C be deposited by a leader advancing at the rate of 1×10^5 m/s requires the average current in the leader, i_l, to be 20 to 200 A. A current of this magnitude could be carried only in a highly conducting arc discharge, the assumed central conducting filament of the leader. Such an arc would have a diameter on the order of a few millimeters and an axial voltage gradient, g_l, of about 5×10^3 V/m. A leader 4 km long would then have a voltage drop along its length of 2×10^7V. The longitudinal resistance, R_l, of the conducting filament would then be in the range of 40 to 400 Ω per meter (Ω/m).

While of less importance as regards aircraft, it might be noted that leaders sometimes start at the ground and work their way toward the sky. This happens most frequently from tall buildings or towers, or from buildings or towers located atop hills. Generally, one can tell from the direction of the lightning flash branching whether the leader started at the cloud or at the ground: if the branching is downward, Fig. 2.9, the leader originated at the cloud; if the branching is upward, the leader originated at the ground.

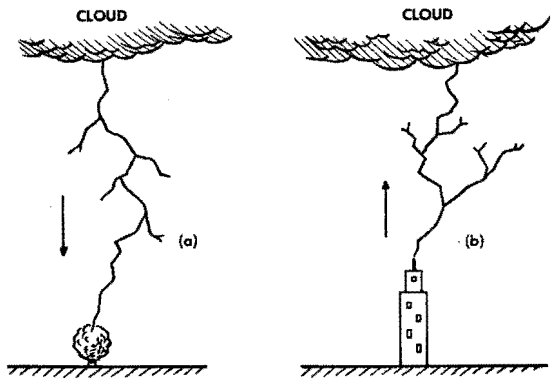

Fig. 2.9 Leader direction as determined from direction of branching.
(a) Downward branching leader starts at cloud
(b) Upward branching leader starts at ground

2.2.4 Transition from Leader to Return Stroke

As the negatively charged stepped leader approaches the ground, positive charge accumulates in the ground underneath it or, more accurately, negative charge is repelled away from the region under the leader. At some point the electric field strength around objects on the ground becomes sufficiently high that a streamer starts at the ground and works its way to-

ward the downward approaching leader. This seems to occur when the average voltage gradient between the leader and ground reaches about 5.5 kV/cm (550 kV/m). When the streamers meet, the conducting filament in the center of each streamer provides a low impedance path so that the charge stored in the head of the leader can flow easily to ground. As the current in the central filament increases from its initial amplitude of a few tens of amperes to higher values, the filament gets hotter, its diameter expands, its longitudinal gradient decreases, and it becomes an even better conductor, which in turn allows even more current to flow in the arc. As the charge in the lower part of the leader is neutralized, the heavily conducting arc reaches higher into the charged leader channel. The head of the region in which this neutralization takes place moves upwards at a rate of roughly 10^8 m/s (or one third the velocity of light) until it reaches the cloud. This heavily conducting region, called the return stroke, produces the intense flash normally associated with the lightning stroke.

Some stages in the development of the return stroke are shown in Fig. 2.10 [2.14]. Fig. 2.11 shows an oscillogram of an actual lightning current as measured at ground. The figure also shows the current associated with the subsequent return strokes discussed in §2.2.7.

The point at which the downward and upward going leaders meet can be recognized on photographs as a point where the channel seems to split. Fig. 2.12 [2.15, 2.16] shows an example observed on an actual lightning flash and Fig. 1.18 showed an example observed during laboratory testing. Another photograph of a junction is given in [2.17]. The point at which the downward leader first induces a leader from the ground effectively determines where on the ground the flash will ultimately terminate. The distance to the ground when the upward leader first initiates is called the striking distance and analysis of the striking distance is important as regards protection of grounded objects [2.17-2.19].

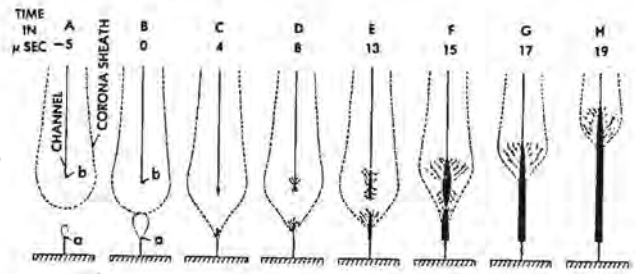

Fig. 2.10 Stages in the development of the return stroke [2.14].

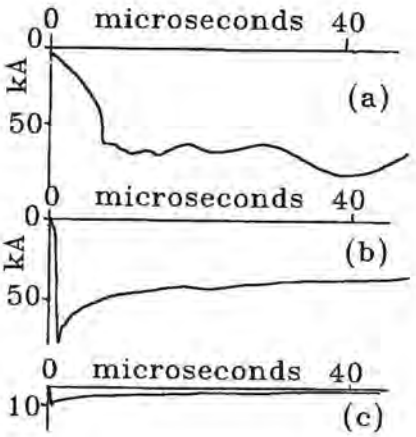

Fig. 2.11 Example of multiple stroke lightning current waveshapes [2.25].
(a) First stroke
(b) Second stroke
(c) Third stroke

Fig. 2.12 Junction of downward and upward streamers [2.18].

2.2.5 Further Development of the Initial Return Stroke

The high currents associated with lightning (10 kA to 200 kA) are produced as the return stroke drains

the charge left in the leader channel. The magnitude of the current is determined by the velocity with which this return stroke propagates, together with the amount of charge deposited in the leader channel. Let v be the velocity of the return stroke and q be the amount of charge deposited per unit length, dl, along the leader channel. Since

$$I = \frac{dq}{dt} \tag{2.2}$$

and

$$v = \frac{dl}{dt}, \tag{2.3}$$

it follows that

$$I = qv. \tag{2.4}$$

As a numerical example let

$$v = 10^8 \text{ m/s} \quad \text{and} \quad q = 10 \times 10^{-4} \text{ C/m}$$

Then

$$\begin{aligned} I &= 10 \times 10^{-4} \times 10^8 \\ &= 10 \times 10^4 \\ &= 100\ 000 \text{ A}. \end{aligned}$$

The velocity of the return stroke is not constant from one stroke to the next; it seems to vary with the magnitude of current that is ultimately developed. The relationship between current and velocity may be deduced either from theoretical concepts or experimentally. The relationship derived by Wagner [2.21] is shown in Fig. 2.13. Considerations of the return stroke velocity are primarily of importance in studying the time history of the electric field produced by the lightning flash. Measurements of electric field produced by remote lightning flashes have been used to estimate the peak current in those flashes.

There is evidence that the velocity decreases as the return stroke propagates up the channel and this would suggest that for a given flash the peak current at altitude would be less than the peak amplitude measured at ground level. The velocity may also affect the surge impedance of the lighting stroke, and thus the way that the stroke interacts with a metallic conductor like an aircraft.

Factors affecting velocity: The velocity of propagation of the return stroke is less than that of the speed of light for two basic reasons. The first reason involves the longitudinal resistance of the return stroke channel. Some of the factors associated with this longitudinal resistance are shown in Fig. 2.14. Central

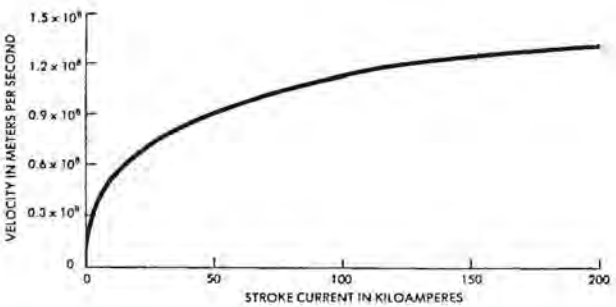

Fig. 2.13 Relation between stroke current and velocity of return stroke [2.21].

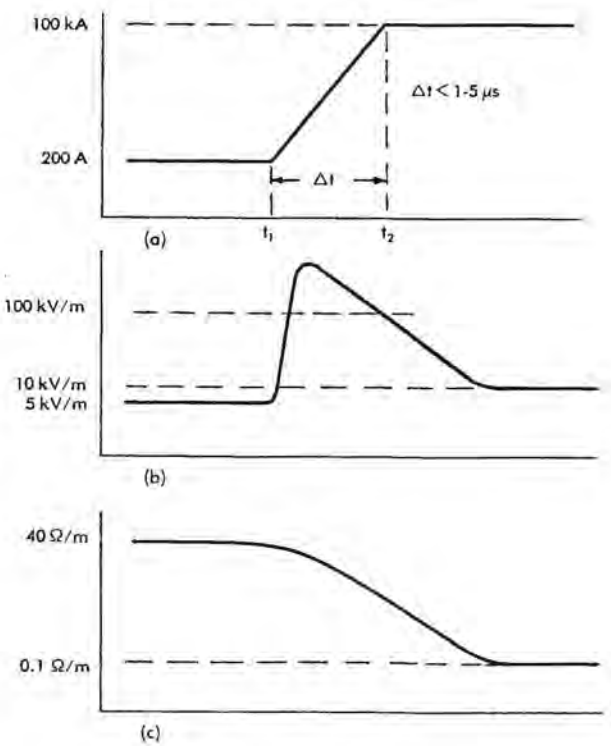

Fig. 2.14 Phenomena associated with passage of the return stroke.
(a) Current
(b) Longitudinal voltage
(c) Longitudinal resistance

to the phenomenon is the fact that the current in the lightning channel must increase fairly rapidly from the 200 A (approximately) current associated with the initial development of the leader to a current of perhaps 100 kA as the return stroke becomes fully developed.

It is a characteristic of an arc channel discharge that the current density remains fairly constant. If the current through the arc is increased, the arc channel expands in diameter. The channel cannot expand instantaneously however, since energy must be put into the channel to cause it to heat up sufficiently to force it to expand. Accordingly, if the current through the arc channel is increased suddenly by a large magnitude, as in Fig. 2.14(a), the longitudinal voltage gradient of the channel must suddenly increase.

Since the rate at which energy is injected into the channel is the product of the current and the longitudinal voltage gradient, the increased longitudinal voltage gradient may be taken as the mechanism forcing the arc channel to get hot enough to expand to the diameter required to carry the high currents.

It is not known what the maximum longitudinal voltage gradient would be in a lightning channel, but it is known from studies of arcs in laboratories that the gradient will fall to values on the order of 100 kV/m in a fraction of a microsecond. Presumably in a few microseconds, the channel diameter will have expanded to its final value, and the longitudinal voltage gradient will have decayed back toward values on the order of 5 to 10 kV/m. The longitudinal resistance, then, would fall from values on the order of 40 Ω/m to values on the order of a small fraction of an ohm per meter, in times on the order of a few microseconds.

This collapse of longitudinal resistance, however, is far from instantaneous. The initial resistance of the leader is high enough to retard the development of the upward going return stroke and hence reduce its velocity of propagation below that of the speed of light. Presumably, leaders which lead to the formation of high amplitude lightning currents either have a sufficiently low longitudinal resistance to begin with or the longitudinal resistance is reduced to low values sufficiently quickly by the high amplitude return strokes that the longitudinal resistance presents less of an obstacle for the upward going return stroke than it does for the flashes which involve lower peak currents.

There seems to have been little work that would substantiate the above estimates of longitudinal gradient, an unfortunate fact since the voltage along a conducting channel is of considerable importance to the question of swept strokes and dwell times, a subject discussed further in Chapter 3.

An additional factor that affects the velocity of the return stroke, and is the second reason that the velocity is less than the speed of light, is shown in Fig. 2.15. As explained earlier, the leader deposits in its wake a column of electrical charge with diameters on the order of several meters. At the center is a highly conducting core, which has a diameter of a few millimeters for the leader and which expands to a few centimeters during the passage of the return stroke. The inductance of this return stroke is determined by the diameter of the highly conductive central core, and the capacitance by the diameter of the column of electrical charge. The lightning stroke may then be modeled as shown in Fig. 2.15(b), in which a highly conductive central conductor is fastened onto a series of projecting spines, much like the backbone of a fish.

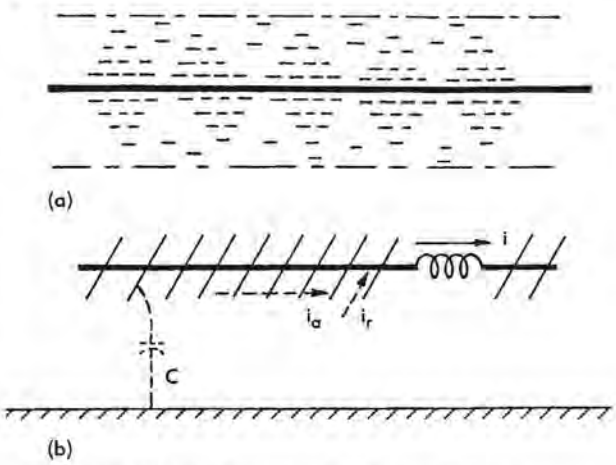

Fig. 2.15 Effect of corona cloud on velocity of propagation.
(a) Distributed charge surrounding a highly conductive central core.
(b) Highly conductive central conductor fastened onto a series of projecting splines.

A better analogy might be to view the lightning flash as a piece of tinsel rope for decorating a Christmas tree: a central piece of string is surrounded by a tube of fine filaments projecting radially away from the central core. In either case, the radial filaments can carry a radial current, i_r, but cannot carry an axial current, i_a. Accordingly, the lightning return stroke has both a high capacitance and a high inductance per unit of length. In this respect it differs from a solid conductor of large diameter which, while possessing a high capacitance per unit length, simultaneously possesses a low inductance per unit length. It follows that the surge impedance, governed by the ratio of inductance of capacitance, is high while the velocity of propagation, governed by the product of inductance and capacitance, is less than that of the speed of light.

Impedance of the flash: Wagner [2.21] concludes that the surge impedance of the lightning flash is of the order of 3000 ohms for return strokes of large ampli-

tude, say 100 kA. This large value is probably resistive and associated with the head of the return stroke as it collects the charge in the region through which the leader has passed and so is probably of most importance during the front of the return stroke current. After the charge has been collected and the current in the channel has attained its final value the longitudinal resistance will be quite small and the impedance will be determined primarily by the inductance and capacitance of the highly conductive lightning channel and more nearly the surge impedance (500 ohms) of a simple conductor in air and remote from a ground plane or other current return path.

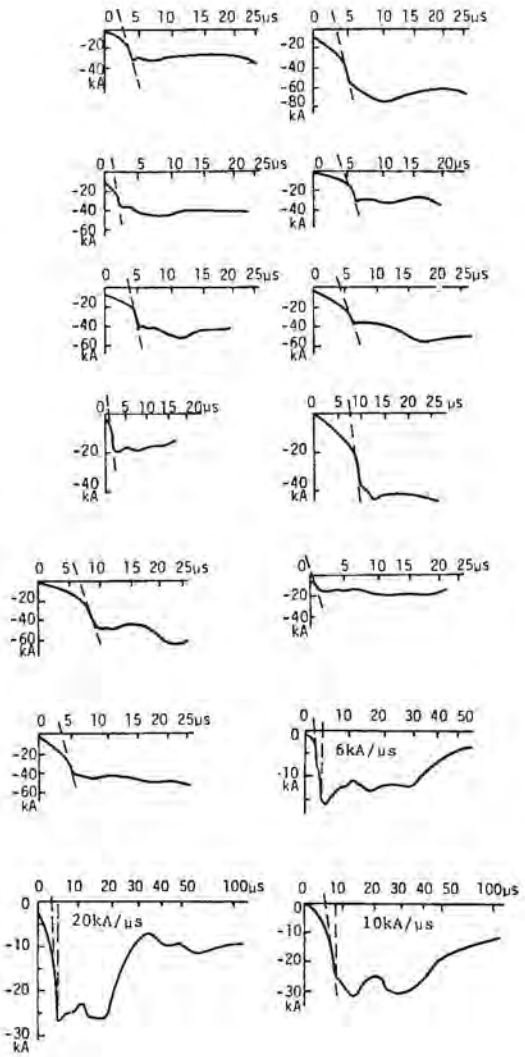

Fig. 2.16 Front waveshapes of lightning currents as measured by Berger [2.16].

Waveshapes of current: The waveshapes of lightning flash currents measured at ground level are reasonably well known, principally from the work of Berger [2.15, 2.16]. Typical waveshapes detailing the front of the initial return stroke are shown in Figs. 2.16 and 2.17 [2.22 and 2.23]. Fig. 2.17 shows the currents on two different time scales, one to indicate the shape of the front of the current and one to indicate the shape of the tail. In all cases, the current is seen to have a concave front, the current initially rising slowly, but then increasing to a maximum current rate of change just before crest amplitude is reached.

It may be speculated that the initial slowly changing portion of these current oscillograms (which, of course, were measured at ground level) represents the growth of an upward going leader from the lightning tower reaching upwards to contact the downward approaching lightning leader. It can also be speculated

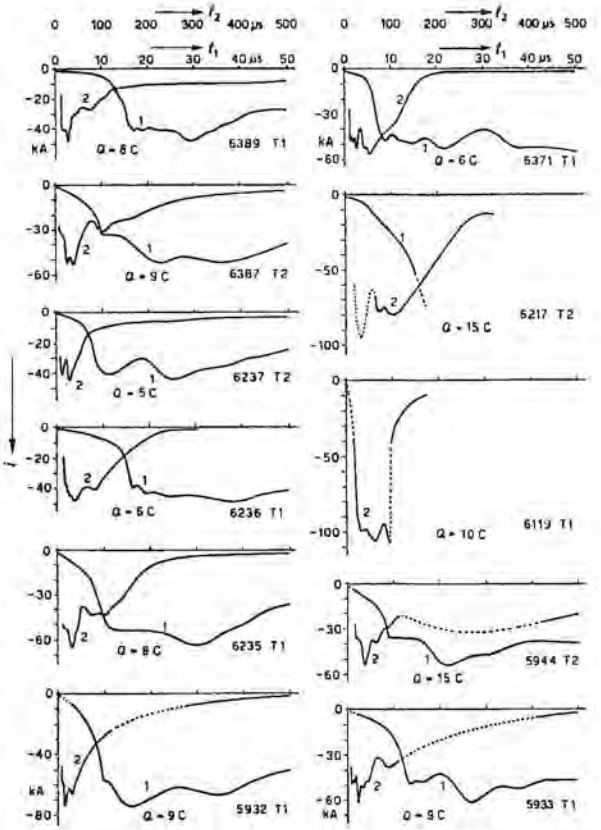

Fig. 2.17 Current oscillograms from single strokes of first downward strokes [2.16].
(a) Fast time scale $0 - 50$ μs
(b) Slow time scale $0 - 500$ μs

that the maximum rate of change of current, which occurs just before crest, is most representative of the rate at which the current can increase in the lightning channel as the return stroke passes one particular point in space. This is supported by the observation that subsequent strokes in a lightning flash, even measured at ground level, exhibit front times considerably faster than the rise time of the initial stroke in the flash. Subsequent strokes are discussed in §2.2.7.

The true front time of the leading edge of the return stroke as it passes a point remote from ground has probably never been measured. It seems appropriate, however, to assume that it will be faster than the leading edge of currents measured at ground level. Measurements with instrumented aircraft have recorded the front times of lightning currents, but many of the measurements have been of flashes presumed to have been triggered by the aircraft. Most of those flashes seem to have been more representative of intercloud flashes, than of cloud to ground flashes.

2.2.6 Further Development of the Lightning Flash

After the charge has been drained from the leader by the upwardly moving return stroke, the current measured at the ground decays, though at a rate slower than that at which the current rose to its peak. Oscillograms showing typical decay times were previously shown in Fig. 2.17. The figure displays the current on two different time scales, emphasizing the front and the tail. Some of the oscillograms showing the front are the same as those shown in Fig. 2.16.

As the return stroke approaches the cloud, it may encounter other branches of the leader, as shown in Fig. 2.18. As it passes these branches, the charge stored in them will feed into the developing lightning stroke and momentarily increase the current.

Eventually, the return stroke will reach the cloud. An understanding of the phenomena occurring within the cloud is hindered by not being able to see what takes place in the cloud, but some of the phenomena can be inferred from measurements of electrical radiation produced by the developing flash and from the usual behavior of the flash after the initial return stroke has passed. As the return stroke reaches into the cloud, it appears to encounter a much more heavily branched leader than it did in the air below the cloud. The return stroke can thus tap the charge diffused through a large volume of the cloud, rather than only the charge in the more localized leader. It would appear to be during this period that the intermediate current is developed.

As the discharge continues to spread through the cloud, for times on the order of fractions of a second, currents on the order of a few hundred amperes continue to flow in the lightning flash. These are referred to as continuing currents. As one may expect, there is no clear-cut demarcation between the tail of the return stroke and the intermediate current, or between the end of the intermediate current and the start of the continuing current.

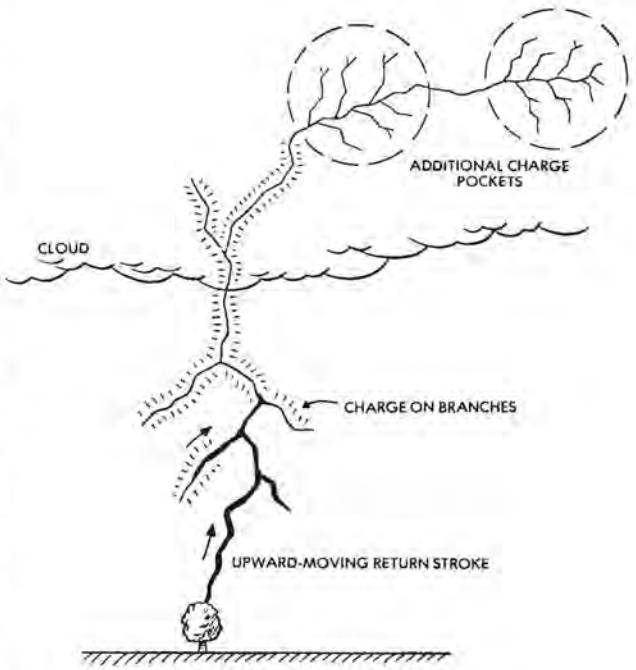

Fig. 2.18 Further development of the flash.

2.2.7. Subsequent Return Strokes

Usually the developing discharge within the cloud will eventually reach into a different cell of the cloud or, at any rate, into a region where there is another localized body of electrical charge.

At this stage there occurs what is called a restrike, Component F of Fig. 2.1(c). The restrike starts with additional charge being lowered from the cloud to form a new leader, or, more properly, to recharge the central portion of the old leader. Presumably, because of the residual ionization in the channel, this charging process occurs smoothly, not in the step-by-step process by which the initial leader penetrates into the virgin air. Accordingly, this is called a dart leader instead of a stepped leader. Unlike the initial stepped leader, the dart leader is seldom branched. When the dart leader reaches ground level, a return stroke again occurs. The amplitude of this return stroke is again high, since the

current comes from an intensely ionized region close to the ground. While the amplitude is usually not as high as that of the first return stroke, the current rises to crest more rapidly than does that of the initial return stroke, presumably because the upward leader from the ground does not have to propagate into virgin air.

An oscillogram of an actual subsequent return stroke was previously shown on Fig. 2.11. Anderson and Ericksson [2.24] averaged the results of many different recordings and derived the composite picture of the front of first and subsequent return strokes shown on Fig. 2.19.

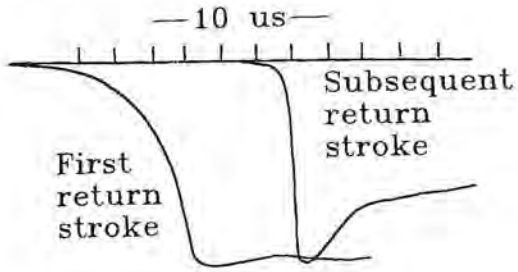

Fig. 2.19 Pictures of "averaged" first and subsequent return strokes. Adapted from [2.24].

2.2.8 Lightning Polarity and Direction

Most lightning flashes originate in the cloud and lower negative charge to earth. The question of direction of the lightning flash is sometimes confusing. With the intent of clarifying matters, the statement is sometimes made that lightning strikes upward and not downward. This is at least partially true; the return stroke that produces the high peak currents, thunder, and the highest intensity light, in fact does start near the ground and grows upward into the ionized channel previously established by the stepped leader, thus tapping the charge in the stepped leader. The stepped leader, nevertheless, originates at the cloud and lowers electrons into the leader channel, from whence they ultimately flow into the ground. The source of energy is in the cloud, and the lower amplitude and longer duration currents have their origin in the charge stored in the cloud. In terms of the engineering definition of current (positive to negative, opposite to the direction of electrons), these flashes result in the direction of current flow being from the earth to the cloud, but since the electrons flow into the earth this type is commonly called a negative polarity flash.

Flashes originating at the ground: When tall buildings or mountain tops are involved, the lightning flash often does originate at the ground; the stepped leader starts at ground level and propagates upwards into the cloud. Such flashes seem to be triggered by the high electric field concentrated around the top of the building or mountain. They may be recognized by the upward direction of branching, as mentioned earlier and shown in Fig. 2.9(b). Most commonly this type of flash is induced by a negatively charged cloud, or at least by a cloud having an excess of negative charge in its lower regions and the step leader carries positive charge upwards into the cloud. This type of flash starts off with a relatively low continuing current and lacks the original high current return stroke typical of flashes in which the leader originates at the cloud. Subsequent strokes, if they occur, will be similar to those found in flashes that originate at the cloud. Flashes of this nature can also be triggered artifically by launching from the ground a small rocket trailing a wire attached to the ground.

Positive flashes: Some flashes, perhaps 10% of the total, lower positive charge to the earth (or more accurately transport electrons from the earth to the cloud) and are accordingly called positive flashes. As with negative flashes they may either involve a leader that initially propagates from the cloud towards the earth, or they may involve a leader that initially propagates from the earth towards the cloud. A fraction of these positive flashes involve the highest peak currents and charge found associated with lightning. Examples of some of these strong positive flashes are shown in Fig. 2.20 [2.23]. They typically have only one high current stroke and lack the restrike phase generally noted on flashes of negative polarity. There is some evidence that lightning flashes that occur in the winter as a result of snow are of positive polarity and of exceptional severity. There is also some evidence that these very high amplitude positive flashes occur as a result of the air at the top of the cloud, the air that is known to contain positive charge, being transported close to the ground before the charge has a chance to flow off to the ionosphere.

2.3 Intracloud Flashes

Intracloud flashes occur between charge centers in the cloud. A distinguishing characteristic of intracloud flashes is that they seem to lack the intense return stroke phase typical of flashes to the ground, or at least that the electrical radiation associated with true intracloud discharges lacks the characteristics associated with the return stroke of cloud–to–ground flashes.

Discharges between charge centers take place during cloud–to–ground flashes as well, and, to an observer within an aircraft, it may be difficult to tell whether or not a flash to ground occurred.

With regard to aircraft the matter may be academic. Aircraft are struck underneath clouds by clear-cut cloud–to–ground flashes and also by flashes within clouds. Based on the damage observed, the peak current sometimes is very high. Whether the high current was associated with the upper end of a cloud–to–ground flash or with a true intracloud flash makes little difference.

In temperate regions about two–thirds of all lightning flashes are intracloud flashes. In tropical regions, where there is more lightning activity, the ratio is higher.

Aircraft may be able to trigger lightning by flying through a heavily charged region of a cloud. There is no consensus as to whether this takes place routinely, but triggering has definitely been observed with research aircraft that are flown into thunderstorms seeking to intercept lightning and measure its characteristics. The flashes that have been triggered seem to have more of the characteristics associated with intracloud lightning than with those associated with cloud–to–ground lightning. In particular the flashes that have been triggered have lacked a high amplitude return stroke. The question of triggered lightning is discussed further in Chapter 3.

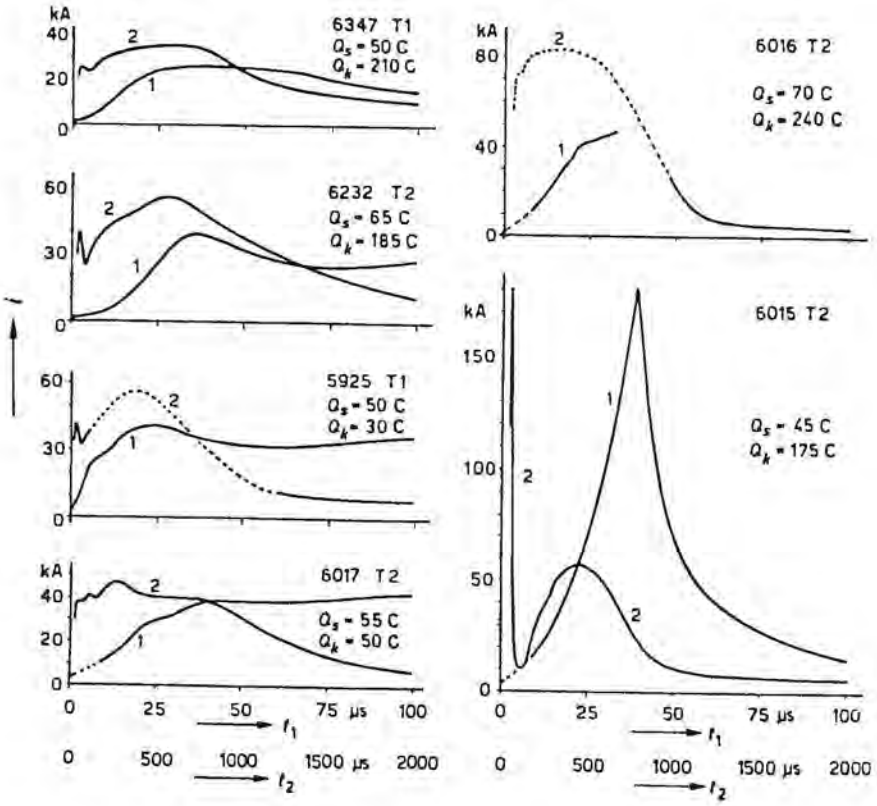

Fig. 2.20 Examples of strong positive strokes [2.16].
(a) Fast time scale $0 - 100$ μs
(b) Slow time scale $0 - 2000$ μs

Qs Electric charge (coulombs) within 2 μs from the origin
Qk Electric charge (coulombs) in the continuing current after 2 μs

2.4 Superstrokes

There is some evidence that there are sometimes lightning flashes that are much more powerful than those normally encountered, perhaps by one or two orders of magnitude. Some of the evidence is anecdotal and derived by examination of the damage caused by the lightning flash, such as conductors twisted by magnetic forces or glass shattered over wide areas. Other evidence comes from observations by satellites deployed to watch for evidence of nuclear explosions in the atmosphere. Little is known of these superstrokes other than that they are rare, but do exist. Those observed by satellites seem to be associated with the upper areas of clouds, but there is other evidence that winter storms in portions of Japan produce lightning flashes of exceptional severity. This probably has to do with proximity to the ocean and the fact that the freezing level in the clouds is quite low to the ground. Data on these superstrokes is practically non-existent and because of their evident rarity they are not presently considered in studies related to lightning protection of aircraft.

2.5 Statistical Information on Earth Flashes

Lightning flashes are quite variable from one to another. Peak currents, total duration, waveshapes, number of strokes in the flash, charge transferred, etc., may all vary over wide limits, and only in general terms can one find a correlation between different parameters. Data on the characteristics of lightning are best presented in statistical terms, the mode that will be used in the following sections.

One item that needs to be emphasized is that virtually all the data on lightning comes from measurements made at ground level, and these measurements are probably influenced by the growth of an upward leader. In recent years some measurements have been made of the amplitude and waveshape of lightning currents passing through aircraft. Most of the measurements that have been made were of strokes with lower peak currents and longer times to crest than those often observed at ground level. In part this may be explained by chance, but mostly it can be explained by the fact that most of the flashes were triggered by the aircraft and are more characteristic of intracloud flashes than of cloud-to-ground flashes. As noted earlier, intracloud flashes often lack the well-defined high-amplitude return stroke of cloud-to-ground flashes.

There are two main summaries of the characteristics of lightning; one made by Anderson and Erickson and one by Cianos and Pierce.

2.5.1 The Anderson and Ericksson Data

Anderson and Ericksson [2.24, 2.25] took measured waveshape data from a number of lightning strokes (principally those recorded by Berger on Mt. San Salvatore) and derived several sets of statistical data. Fig. 2.21 gives the key to the statistical data that follows in Figs. 2.22 through 2.29. The figures show data for both initial and subsequent strokes. As speculated in §2.2.5, the data on steepness just before the peak current is reached may best represent the rate of change of current to consider for aircraft.

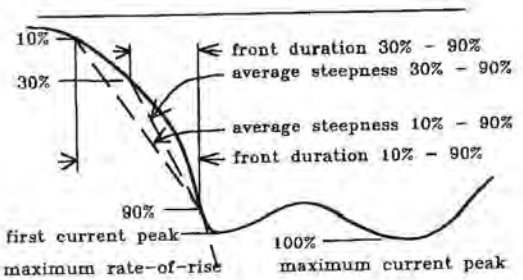

Fig. 2.21 Definition of waveform parameters. Adapted from [2.24].

2.5.2 The Cianos and Pierce Data

Cianos and Pierce [2.26] observed that many of the statistical characteristics of lightning were nearly linear when plotted as log-normal distributions; that is on a plot having a logarithmic ordinate and an abscissa of normal distribution. They then made a judgement as to the straight line that was the best fit to the experimentally observed data on such a plot. The figures that follow are reproduced from their report.

Peak currents: Fig. 2.30 shows data on the peak current amplitude in lightning strokes. The peak value of the current is related to the explosive, or blasting, effect of lightning. It is also related to the maximum voltage developed across ground resistance and hence to the risk of side flashes occurring in the vicinity of objects struck. It is also related to the maximum voltage developed across bonding resistance and hence to the possibility of sparking at structural interfaces. Regarding the damage that may be caused by lightning, this is one of the most important parameters. There are two curves shown, one for the first return strokes and one for subsequent strokes. The first return stroke is generally of the highest amplitude. For engineering analysis, Cianos and Pierce have determined that subsequent return strokes may be represented as half the amplitude of the first return stroke. Marked on the curves are the amplitudes corresponding to the 2, 10, 50, 90, and 98% probabilities.

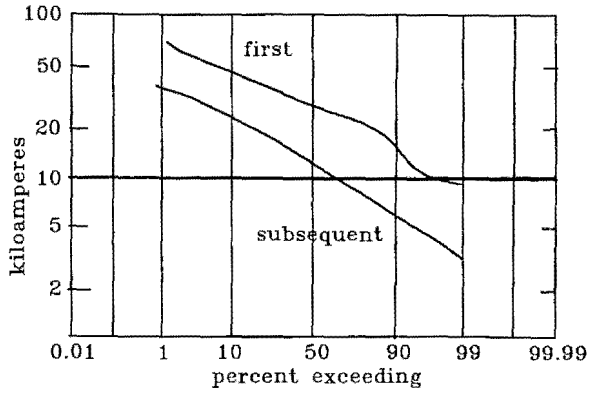

Fig. 2.22 Amplitude of first current peak.
Adapted from [2.24].

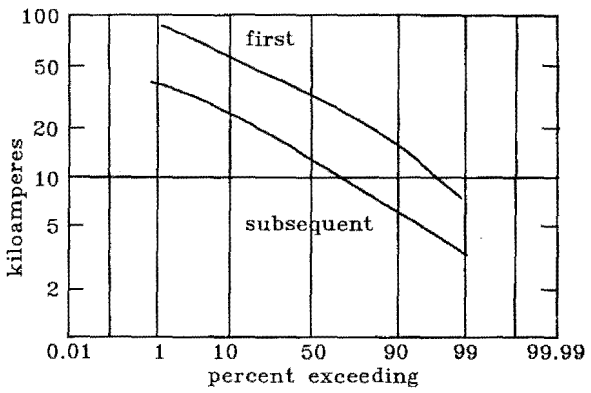

Fig. 2.23 Amplitude of maximum current peak.
Adapted from [2.24].

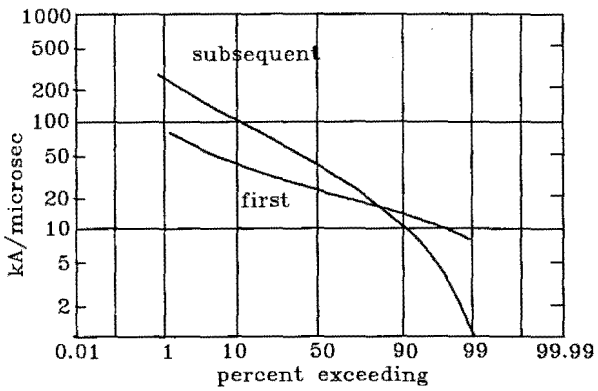

Fig. 2.24 Maximum rate–of–rise.
Adapted from [2.24].

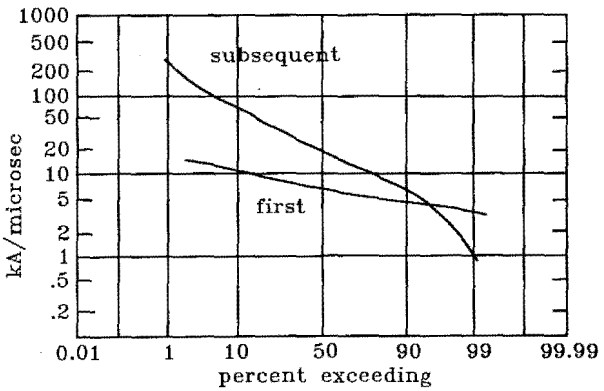

Fig. 2.25 Averages steepness 30%-90%.
Adapted from [2.24].

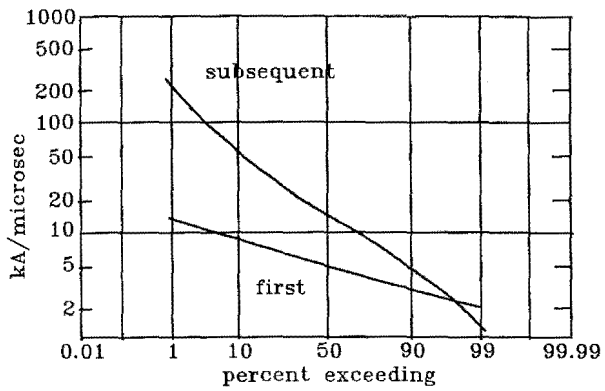

Fig. 2.26 Average steepness 10-90%.
Adapted from [2.24].

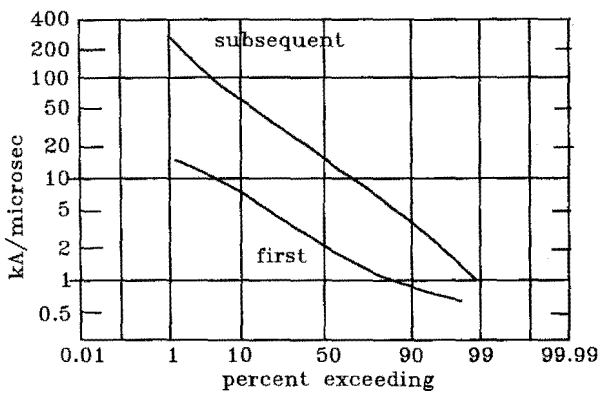

Fig. 2.27 Average steepness at 10%.
Adapted from [2.24].

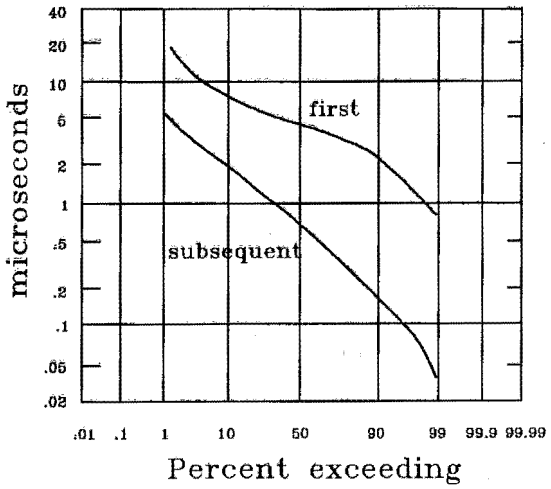

Fig. 2.28 Front duration 10-90%.
Adapted from [2.24].

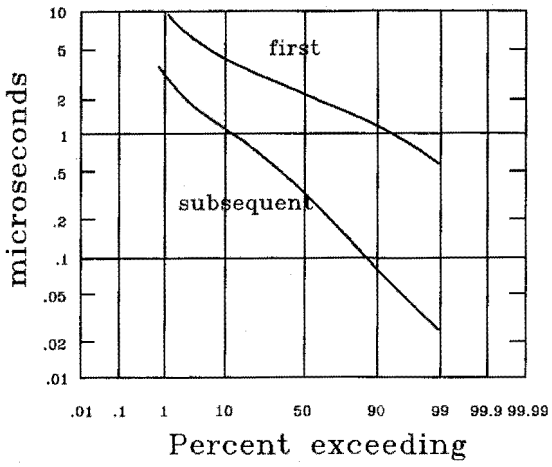

Fig. 2.29 Front duration 30-90%.
Adapted from [2.24].

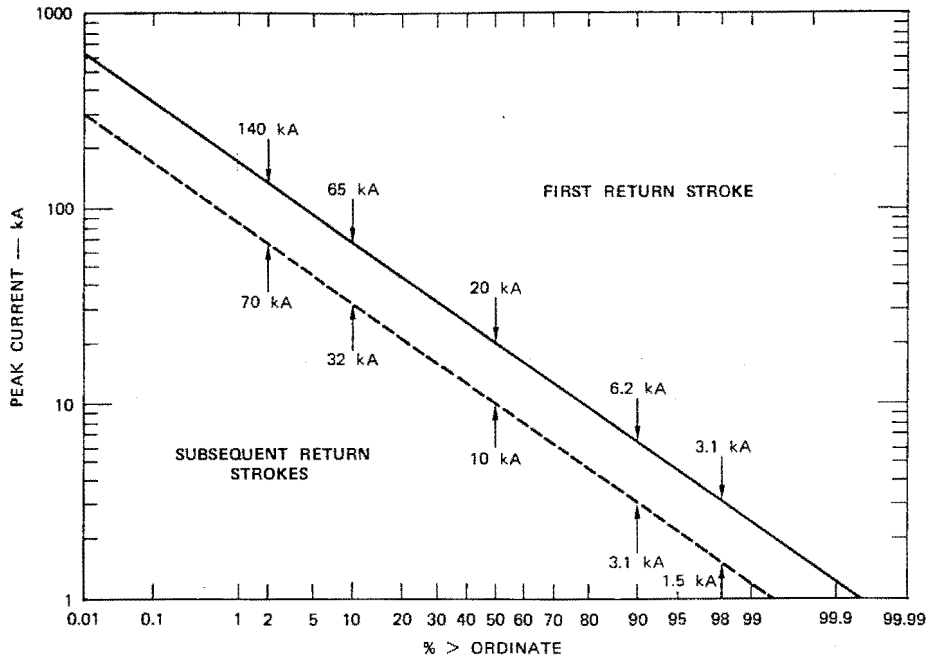

Fig. 2.30 Distribution of peak currents for first return stroke and subsequent strokes [2.26].

Rise time and rate of change: Fig. 2.31 gives a distribution of the time for the current to reach its peak amplitude. This time is subject to considerable interpretation for any particular lightning stroke, since there is seldom a clearly definable time at which the stroke starts. Lightning strokes typically have a concave front, starting out slowly and then rising faster as the current gets higher. Thus, the effective rate of rise of the lightning current is not directly obtained by dividing the peak current by the front time.

The best summary of the effective rates of rise is given on Fig. 2.32. The rate of rise of lightning current is an important factor in determining how much voltage is induced into electrical equipment, and in determining how many lightning conductors are needed and how they should be placed.

Flash duration: The duration of the stroke current affects the distance across which side flashes may develop, and affects how severely metal structures may be deformed by magnetic forces or the explosive liberation of energy. This distribution is shown in Fig. 2.33. The duration of the stroke, which is measured in tens of microseconds, should not be confused with the total duration of the lightning flash. The total duration of the flash, shown in Fig. 2.34, is frequently on the order of a second. The duration of the total flash is influenced by the number of return strokes in the flash (Fig. 2.35) and the time interval between strokes (Fig. 2.36).

Charge transfer: Fig. 2.37 gives information on the total charge transferred in the flash. Little of the charge is transferred by any one stroke. Instead, most of it is transferred by the continuing currents. The total charge transfer and the amplitude and duration of the continuing currents largely govern the thermal effects of lightning. Data on the characteristics of these continuing currents are shown in Fig. 2.38, 2.39, and 2.40.

2.6 Thunderstorm Frequency and Lightning Flash Density

One of the major factors to consider in determining the probability of lightning damage is the number of lightning flashes to earth in a given area and for a given time. Since precise quantitative data do not exist (except at a few specifically instrumented structures), a secondary measure, the frequency of thunderstorms, is used.

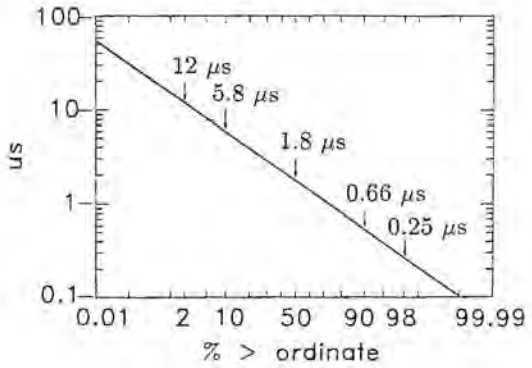

Fig. 2.31 Time to peak [2.26].

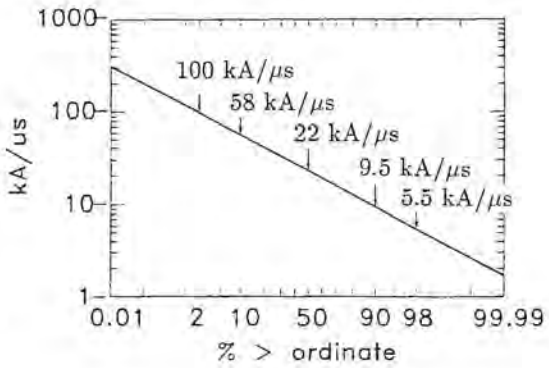

Fig. 2.32 Rates of rise [2.26].

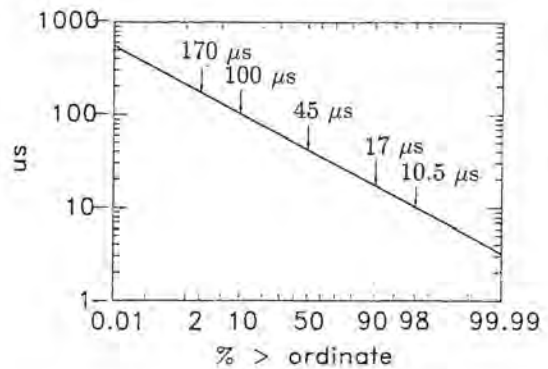

Fig. 2.33 Time to current half value [2.26].

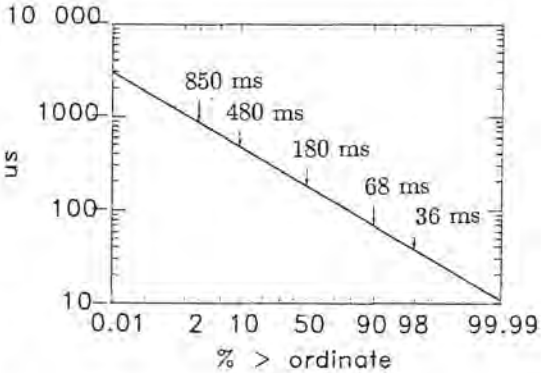

Fig. 2.34 Duration of flashes to earth [2.26].

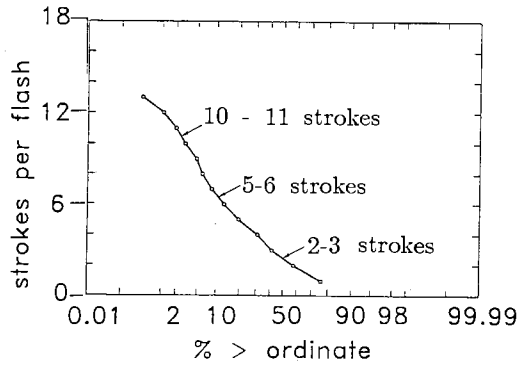

Fig. 2.35 Number of return strokes per flash [2.26].

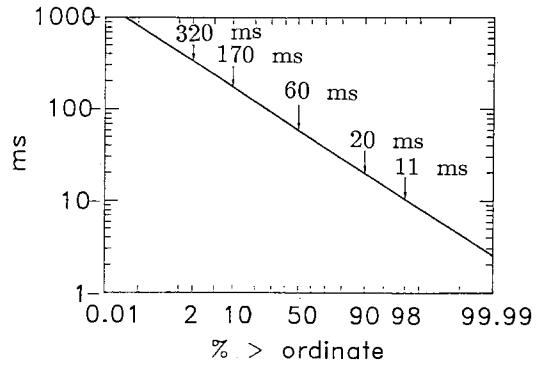

Fig. 2.36 Time interval between strokes [2.26].

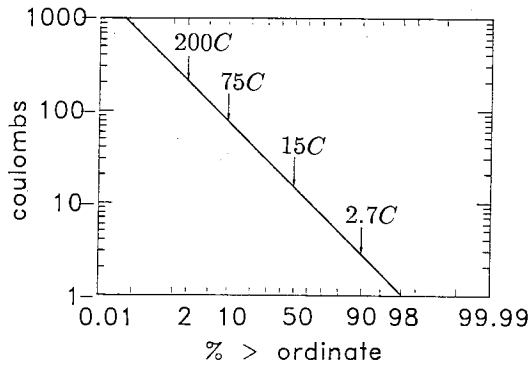

Fig. 2.37 Charge per flash [2.26].

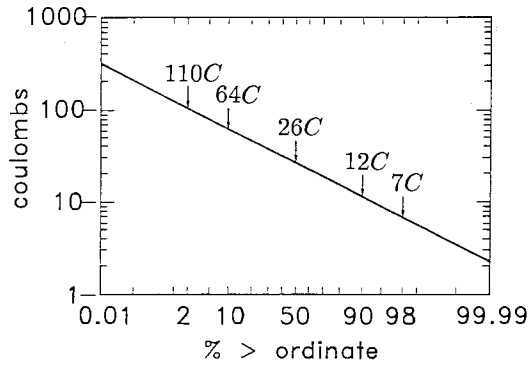

Fig. 2.38 Charge in continuing current [2.26].

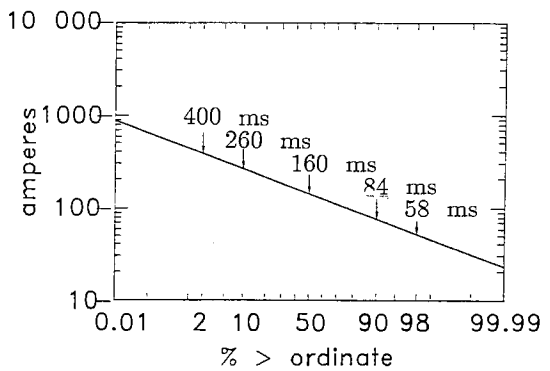

Fig. 2.39 Amplitude of continuing current [2.26].

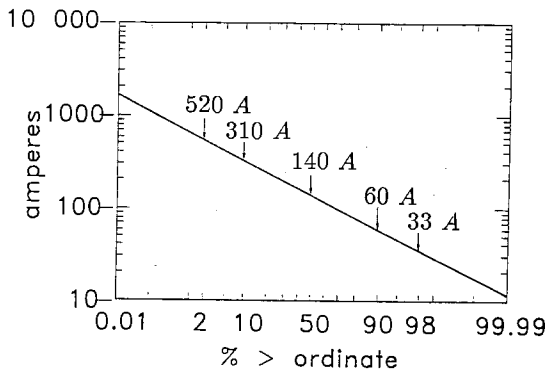

Fig. 2.40 Duration of continuing current [2.26].

Thunderstorm days: For many years, weather bureau stations have recorded thunderstorm days (the number of days per year on which thunder is heard). This index, called the isokeraunic level, is shown for the continental United States in Fig. 2.41 [2.28]. Similar data for the world as a whole is shown on Fig. 2.42 [2.29]. It should be noted that the information so collected is of limited value for several reasons. First of all, no distinction is made between cloud-to-cloud discharges and cloud-to-ground flashes. Also, there is no allowance for the duration of a storm. A storm lasting an hour would be counted as heavily as one lasting several hours.

A better indicator of lightning frequency would be thunderstorm hours per year. Some weather bureau records are now being made of thunderstorm hours, but not much data has been accumulated.

Flash density: Despite its limitations, the data on isokeraunic levels is broadly useful and can be correlated at least partially with lightning strokes to earth-based objects. Pierce [2.27] has summarized some of the available data and concludes that if there are 25 thunderstorm days per year that there will be about 4 flashes to earth per year per km^2. The ground flash rate is is not directly proportional to the isokeraunic level; it varies more as the square of the isokeraunic level. Anderson and Ericksson [2.24] also discuss the relationship between ground flash density and thunderstorm days.

The count of thunderstorm days includes both flashes between clouds and flashes to ground. There is some evidence that the proportion of flashes that go to ground is related to the geographical latitude of the point under study. This relation would exist because the proportion of flashes to ground depends partly on the average height of clouds, and this, in turn, depends on the type of storm formation. Pierce takes that factor into account in his discussion of the relationship between ground flash density and thunderstorm days.

Flash counters: A better measure of lightning frequency would be based on counts of actual lightning flashes, as opposed to counts of thunder. Instruments are available to make such counts.

One relatively simple type [2.30] detects the electric field changes produced by lightning and records on an electromechanical counter the number of times the field change exceeds a threshold value. By suitable choice of filters defining the frequencies to which the device is sensitive it can be made to respond to flashes within a certain range, generally on the order of 30 km. They can also be made to respond primarily to cloud to ground flashes and to reject field changes associated with cloud to cloud flashes. Networks of such instruments have been deployed in South Africa and parts of Europe, but no systematic use has been made of them in the USA.

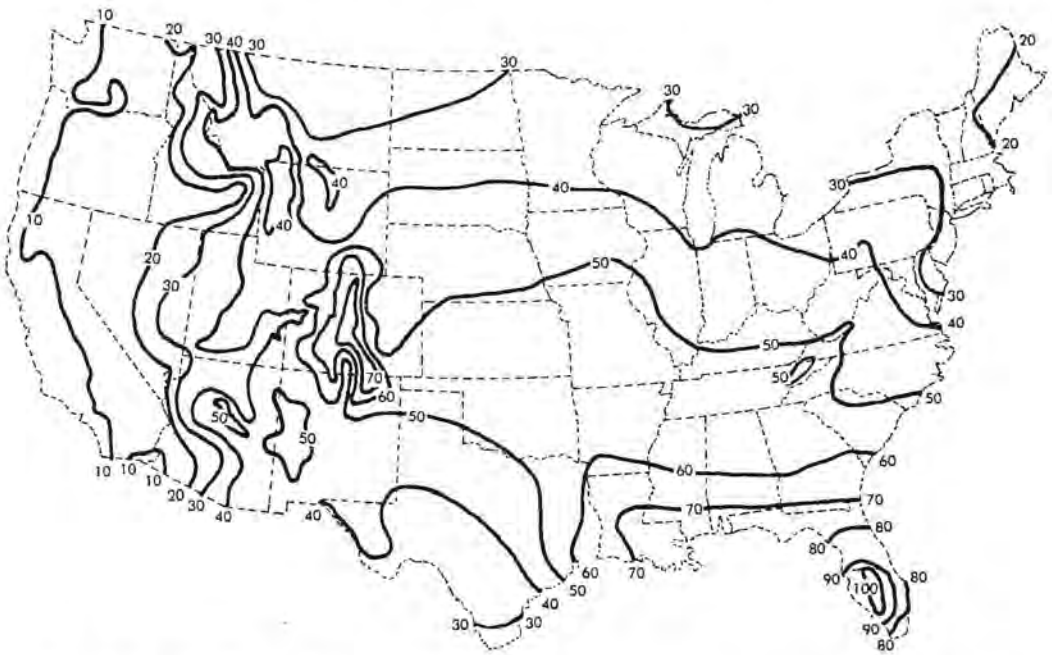

Fig. 2.41 Thunderstorm days (Isokeraunic Level) within the continental United States

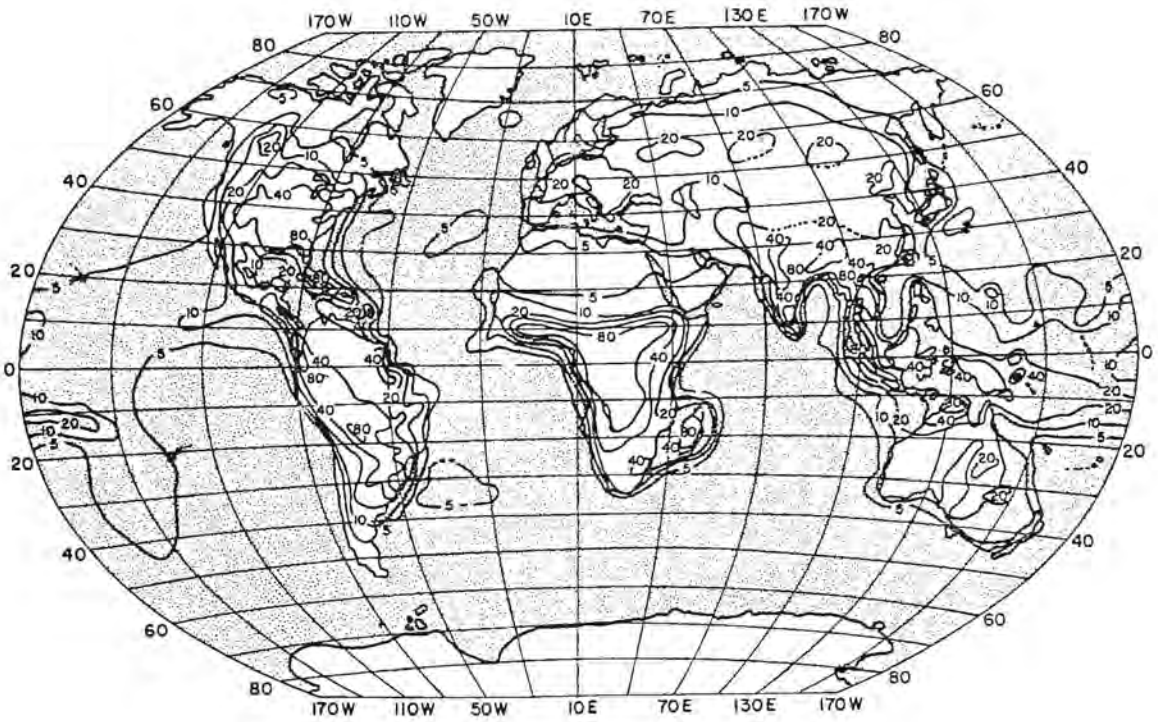

Fig. 2.42 Isokeraunic level of the world [2.29].

Lightning location: Another type of instrument [2.31 – 2.33] uses antennas to respond to both the electric and magnetic field changes produced by lightning, since by doing so one can determine the bearing of the lightning flash. Linking networks of such instruments allows the location of flashes to be calculated and plotted on a map, usually in near real time. The instruments can also be used to determine the waveshape and peak amplitude of the lightning strokes. Networks of such instruments are now to be found in several regions of the USA and in due course should provide much more accurate information on the frequency of lightning in various parts of the country.

Number of lightning flashes: The number of lightning flashes to any particular object depends strongly on the terrain upon which the object is situated. Objects on the crests of hills are more prone to be struck than are objects in valleys. All other things considered, however, the probability that a given object will be struck depends upon the area covered by that object. For objects flat upon the ground the strike interception area can be taken as directly equal to the area covered. If there is a protruding object on the ground, the stroke interception area depends upon the height of the object. With reasonable accuracy, it can be assumed that a structure of height h will intercept all flashes that would ordinarily strike the ground over a circle of radius $2h$. Fig. 2.43 illustrates the geometry.

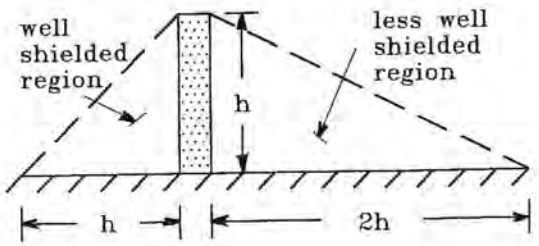

Fig. 2.43 Shielded areas.

It is not as easy to determine analytically how often aircraft in flight will be struck. Field experience seems to be the only reliable guide. Commercial aircraft in regularly scheduled service in the United States are struck about once per year, frequently while in takeoff, landing, or holding patterns, and usually while flying at less than 15 000 ft. altitude. Transport aircraft are seldom struck while at cruising altitudes and speeds, partly of course as a result of the

fact that storms usually can be, and are, avoided. Aircraft constrained to operate at low altitudes and along fixed corridors tend to be struck more often. Military aircraft tend to be struck less often than commercial aircraft, since they are flown in training flights, which are usually scheduled during good weather, much more often than in combat.

The question of how often aircraft encounter lightning is discussed further in Chapter 3.

2.7 Engineering Models of Lightning Flashes

Pierce in [2.26] gives several models of the current flowing in both typical and severe lightning flashes. These influenced the lightning models to which the Space Shuttle was designed, Fig. 2.44, [2.34] and it in turn strongly influenced the lightning models presently used for the certification of aircraft. These are discussed in subsequent chapters. All of these are idealized models for purposes of design and analysis. As such they duplicate the effects (usually worst case effects) of lightning, but the chance of any real lightning flash producing currents of this exact shape is usually zero. The models shown in [2.26] should not be used as specifications for purposes of testing since it may be very difficult and expensive for them to be produced in a testing laboratory. Waveforms to be used for specifications and testing are discussed in Chapter 5.

REFERENCES

2.1 *Lightning, Volume 1: Physics of Lightning*, R. H. Golde - Editor, Academic Press, London and New York, 1977. Volume 2 of the series deals with lightning protection.

2.2 M. A. Uman, *Lightning*, McGraw Hill, New York, 1969.

2.3 M. A. Uman, *The Lightning Discharge*, Vol. 39 in International Geophysics Series, Academic Press, 1987.

2.4 *The Earth's Electrical Environment*, National Academy Press, Washington, DC, 1986.

2.5 Sir Basil Schonland, "Lightning and the Long Electric Spark," *Advancement of Science 19*, November 1962, pp. 306-313.

2.6 C.T.R. Wilson, "Some Thunderstorm Problems," *Journal of the Franklin Institute.* Vol. 208, 1, July 1929, pp. 1-12.

2.7 C.T.R. Wilson, "Investigations on Lightning Discharges on the Electrical Field of Thunderstorms," *Proceedings of the Royal Society of London*, Series A, 221, 1920, pp. 73-115.

2.8 Sir George Simpson, "The Mechanism of a Thunderstorm," *Proceedings of the Royal Society of London*, Series A, 114, 1927, pp. 376-99.

2.9 E.A. Evans and K.B. McEachron, "The Thunderstorm," *General Electric Review*, September 1936, pp.413-25.

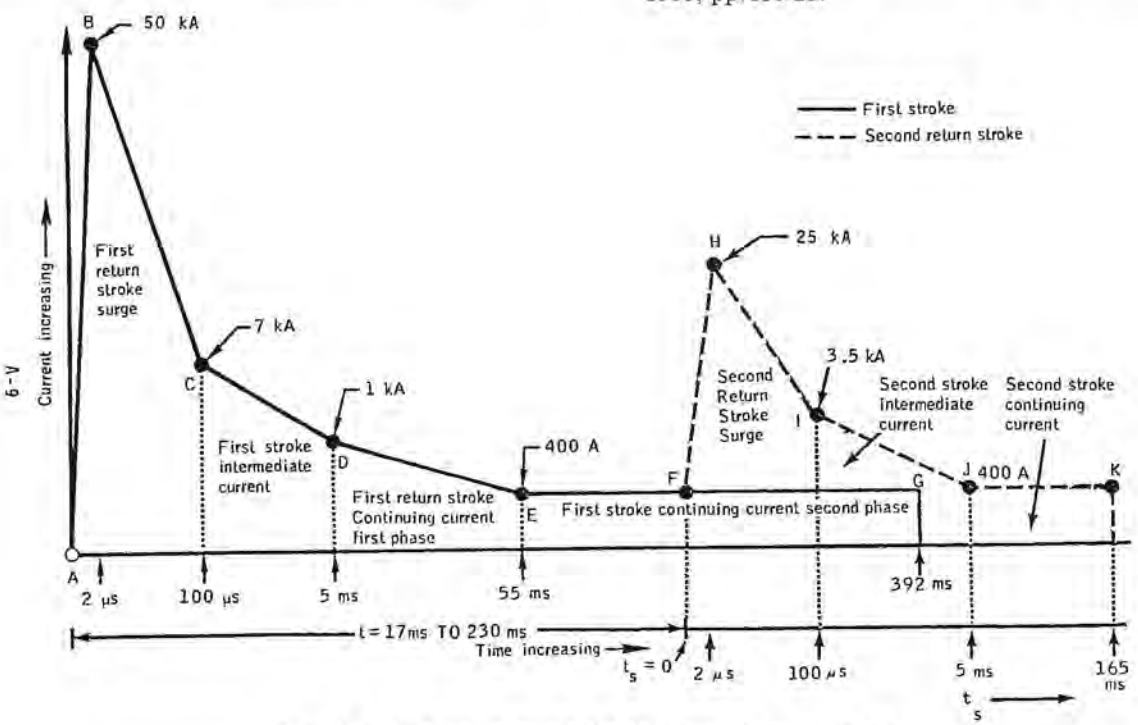

Fig. 2.44 Lightning model for the Space Shuttle [2.30].

2.10 G.C. Simpson, "Lightning," *Journal of the Institution of Electrical Engineers*, Vol 67,Nov. 1929, pp. 1269-82.

2.11 G.C. Simpson and F.J. Scrase, "The Distribution of Electricity in Thunderclouds," *Proceedings of the Royal Society of London*, Series A 161, 1937, pp. 3090-52.

2.12 E. R. Williams, "The Electrification of Thunderstorms,"*Scientific American*, Nov. 1988, pp. 88-99.

2.13 R.H. Golde, *Lightning Protection*, Edward Arnold, London, 1973.

2.14 C.F. Wagner and A.R. Hileman, "The Lightning Stroke II." *AIEE Transactions*, Vol 80, Part III, American Institute of Electrical Engineers, New York, New York (October 1961), pp. 622-42.

2.15 K. Berger and E. Vogelsanger, "Photographische Blitzuntersuchungen der Jahre 1955...1965 auf dem Monte San Salvatore," *Bulletin des Schweizerischen Elektrotechnischen Vereins*, 14 (July 9, 1966), pp. 599-620.

2.16 K. Berger, "Novel Observations on Lightning Discharges: Results of Research on Mount San Salvatore," *Journal of the Franklin Institute*, Vol. 283, 6, June 1967, pp. 478-525.

2.17 R. H. Golde, "The Lightning Conductor", *Journal of the Franklin Institute*, June 1967, p. 457.

2.18 R. H. Golde, "The Lightning Conductor",pp. 451-478.

2.19 J.L. Marshall, *Lightning Protection*, John Wiley and Sons, New York, 1973.

2.20 C.F. Wagner, "Lightning and Transmission Lines," *Journal of the Franklin Institute*, 283, 6 (June 1967): 558-594: 560, and C.F. Wagner, Stroke," *IEEE Transactions on Power Apparatus and Systems* Vol. 82, October 1963, pp. 609-17.

2.21 C.F. Wagner and A.R. Hileman, "Surge Impedance and its Application to the Lightning Stroke," *AIEE Transactions*, Vol. 80, Part 3, February 1962, pp. 1011-22.

2.22 Berger, "Novel Observations," op. cit., p. 492.

2.23 Berger, "Novel Observations," op.cit., p. 494.

2.24 R. B. Anderson and A. J. Ericksson, "Lightning Parameters for Engineering Applications," *ELEK 170, CIGRE Study Committee 33*, Suceava, Roumania, 25-29 June 1979 .

2.25 R. B. Anderson and A. J. Ericksson, "Lightning Parameters for Engineering Applications," *Electra*, Vol. 69, pp. 65-102.

2.26 N. Cianos and T. Pierce, A Ground–Lightning Environment for Engineering Use, *Technical Report 1*, prepared by the Stanford Research Institute for the McDonnell Douglas Astronautics Company, Huntington Beach, California, August, 1972.

2.27 Cianos and Pierce, p.124.

2.28 U.S. Department of Commerce, National Oceanic and Atmospheric Administration, Environmental Data Service, National Climatic Center, Asheville, North Carolina

2.29 D. W. Bodle et al, *Characterization of the Electrical Environment*, University of Toronto Press, Toronto, Ont., 1976, p. 14.

2.30 Anderson and Ericksson, *Electra* op. cit.

2.31 E. P. Krider, R. C. Noggle, and M. A. Uman, "A Gated Wideband Magnetic Direction Finder for Lightning Return Strokes", *J. Geophys. Res.*, Vol 82, 1976, pp. 951-960.

2.32 E. P. Krider, R. C. Noggle, A. E. Pifer, and D. L. Vance, "Lightning Direction Finding Systems for Forest Fire Detection", *Bull. Am. Meteorol. Soc.*, Vol 61, 1980, pp. 980-986.

2.33 R. E. Orville, R. B. Pyle, and R. W. Henderson, "An East Coast Lightning Detection Network", *IEEE Trans. Power Systems*, Vol PWRS-1, 1986, pp. 243-246.

2.34 *Space Shuttle Program Lightning Protection Criteria Document, JSC-07636, Revision A*, National Aeronautics and Space Administration, Lyndon B. Johnson Space Center, Houston, Texas (November 4, 1975), p. A-5.

Chapter 3

AIRCRAFT LIGHTNING ATTACHMENT PHENOMENA

3.1 Introduction

This chapter will deal with the circumstances under which aircraft are struck by lightning and the question of whether aircraft can trigger lightning or whether they just happen to be in the path of a naturally occurring flash. It also deals with how the lightning flash interacts with the aircraft surfaces and defines the lightning strike zones within which these surfaces fall. Methods for locating the zones on specific aircraft are discussed in Chapter 5.

Statistics on lightning strikes reported by aircraft pilots seem to indicate that no aircraft is likely to receive more than one or two lightning strikes in a year, but that some types of aircraft receive more strikes than others. Compared with exposure to other hazards, such as hail, birds and turbulence, which are also encountered during flight, the exposure of aircraft to lightning strikes seems relatively infrequent. Because of this, incorporation of lightning protective measures in the designs of some aircraft has been considered, by some, unnecessary. The question also arises: "If lightning strikes do in fact occur infrequently, can they be avoided altogether?" Because some types of aircraft seem to experience more than their "fair share" of lightning strikes, a related question also arises: "Why are some aircraft (seemingly) more susceptible than others?"

To answer these questions a considerable amount of research into the effects of such factors as aircraft size, engine exhaust, and microwave radar emissions on lightning strike formation have been undertaken over the years. Much of this research has been aimed at answering the question of whether or not an aircraft can in fact somehow produce its own lightning strike, or if it can trigger an impending flash from a nearby cloud. While some of the findings are inconclusive, others have provided definite answers to some of these questions. In this chapter we summarize what has been learned about the aircraft's influence on lightning strike occurrence and dispel some other misconceptions about this phenomenon. We also examine how other factors, such as flight and weather conditions, affect lightning strikes and conclude with why it is important that lightning protection be incorporated into all new aircraft designs.

The atmospheric and flight conditions prevailing when aircraft have been struck by lightning have been of interest since the beginning of powered flight because lightning and other thunderstorm effects, such as turbulence and icing, are to be avoided if possible. To learn about these conditions, various lightning strike incident reporting projects have been implemented. Beginning in 1938, the Subcommittee on Meteorological Problems of the National Advisory Committee for Aeronautics (NACA) prepared and distributed a sixteen page questionnaire to airlines and the Armed Forces [3.1]. Pilots filled out these questionnaires after each lightning strike incident and forwarded them to the NACA subcommittee for analysis. The questionnaire was evidently too long for widespread use, however, and was discontinued by 1950. Nevertheless, the program provided important data for the first time on the meteorological conditions prevailing when strikes occurred and the resulting effects on the aircraft.

Following that, programs were conducted by the Lightning and Transients Research Institute (LTRI) [3.2], the FAA [3.3] and Plumer and Hourihan of General Electric, together with five US commercial airlines [3.4]. This latter project is known as the Airlines Lightning Strike Reporting Project. Anderson and Kroninger of South Africa [3.5], Perry of the British Civil Aviation Authority [3.6], and Trunov of the USSR National Research Institute for Civil Aviation [3.7] have also conducted studies. More recent data from the Airlines Lightning Strike Reporting Project has been reported by Rasch et al of FAA and Lightning Technologies Inc. [3.8].

Strike incidence data, based largely on turbojet or turboprop aircraft, is usually summarized according to the following categories:

1. Altitude.
2. Flight path; that is, climbing, level flight, or descent.
3. Meteorological conditions.
4. Outside air temperature
5. Lightning strike effects on the aircraft

Altitude, flight path, meteorological conditions, and air temperature are topics discussed in this chapter. Lightning strike effects on aircraft will be discussed in the succeeding chapter.

3.2 Lightning Attachment Point Definitions

The lightning flash initially *attaches* to, or *enters*, the aircraft at one spot and exits from another. Usually these are extremities of the aircraft such as the nose or a wing tip. For convenience, these are called *initial entry* and *initial exit* points.

At any one time, current is flowing *into* one point and *out* of another. The "entry" point may be either an anode or a cathode; that is, a spot where electrons are either entering or exiting the aircraft. The visual evidence after the strike does not allow one to resolve the issue and usually no attempt is made. Instead, by convention, attachment spots at *forward* or *upper* locations have usually been called entry spots and those at *aft* or *lower* locations on the aircraft have been termed exit points.

Since the aircraft flies more than it's own length within the lifetime of most flashes, the entry point will change as the flash reattaches to other spots aft of the initial entry point. The exit portion may do the same if the initial exit spot is at a forward portion of the aircraft. Thus, for any one flash, there may be many "entry" or "exit" spots and the following definitions are used:

lightning attachment point: Any spot where the lightning flash attaches to the aircraft.

initial entry point: The spot where the lightning flash channel first "enters" the aircraft (usually an extremity).

final entry point: The spot where the lightning flash channel last "enters" the aircraft (usually a trailing edge).

initial exit point: The spot where the lightning flash channel first "exits" from the aircraft (usually an extremity).

final exit point: The spot where the lightning flash last "exits" from the aircraft (usually a trailing edge).

swept "flash" (or "strike") points: Spots where the flash channel reattaches between the *initial* and *final points*, usually associated with the *entry* part of the flash channel.

3.3 Circumstances Under Which Aircraft are Struck

The following paragraphs summarize the important findings from the transport aircraft data gathering projects noted previously and describe the flight and weather conditions under which lightning strikes are most common. Knowledge of these conditions may help pilots and minimize future lightning strike incidents, but such incidents can never be entirely avoided, unless by operating entirely in clear, "blue sky" conditions a long way from clouds.

3.3.1 Altitude and Flight Path

Fig. 3.1 shows the altitudes at which the reporting projects discussed above show aircraft are being struck, as compared with a typical cumulonimbus (thunder) cloud. The turbojet and turboprop data from the four summaries are in close agreement. For comparison, the data from the earlier piston aircraft survey of Newman [3.2] are also presented. Cruise altitudes of 10 -15 000 m (30 - 40 000 ft) for jet aircraft are considerably higher (15 km) than that of earlier piston aircraft, which flew at about 3 - 6000 m (10 - 20 000 ft); yet Fig. 3.1 shows the altitude distribution of lightning strike incidents to be nearly the same. This fact indicates (1) that there are more lightning flashes to be intercepted below about 6 km than above this altitude, and (2) that jet aircraft are being struck at lower than cruise altitudes: that is, during climb, descent, or hold operations. Flight regime data obtained from the jet projects shown in Fig. 3.2 [3.8] confirm this.

If the strike altitudes shown in Fig. 3.1 are compared with the electrical charge distribution in the typical thundercloud shown in this figure, it is evident that strikes which occur above about 3 km result from intracloud flashes between positive and negative charge centers in the cloud (or between adjacent clouds), whereas strikes below about 3 km probably result from cloud–to–ground flashes. Strike incidents occurring above 6 km occur less frequently because aircraft at these altitudes can more easily divert around thunderclouds than can aircraft at lower altitudes.

3.3.2 Synoptic Meteorological Conditions

Data discussed thus far might imply that an aircraft must be within or beneath a cloud to receive a strike and, since electrical charge separation is accompanied by precipitation, that most strikes would occur when the aircraft is within a cloud, or in or near regions of precipitation. Strike incident reports show that these conditions often do exist, but other lightning strikes occur to aircraft in a cloud when there is no evidence of precipitation nearby, and even to aircraft flying in clear air at a supposedly safe distance from a thundercloud. FAA and airline advisory procedures instruct pilots to circumvent thunderclouds or regions of precipitation evident either visibly or on radar, but strikes to aircraft flying 25 miles from the nearest radar returns or precipitation have been reported. Occasionally a report of a "bolt from the blue," with no clouds

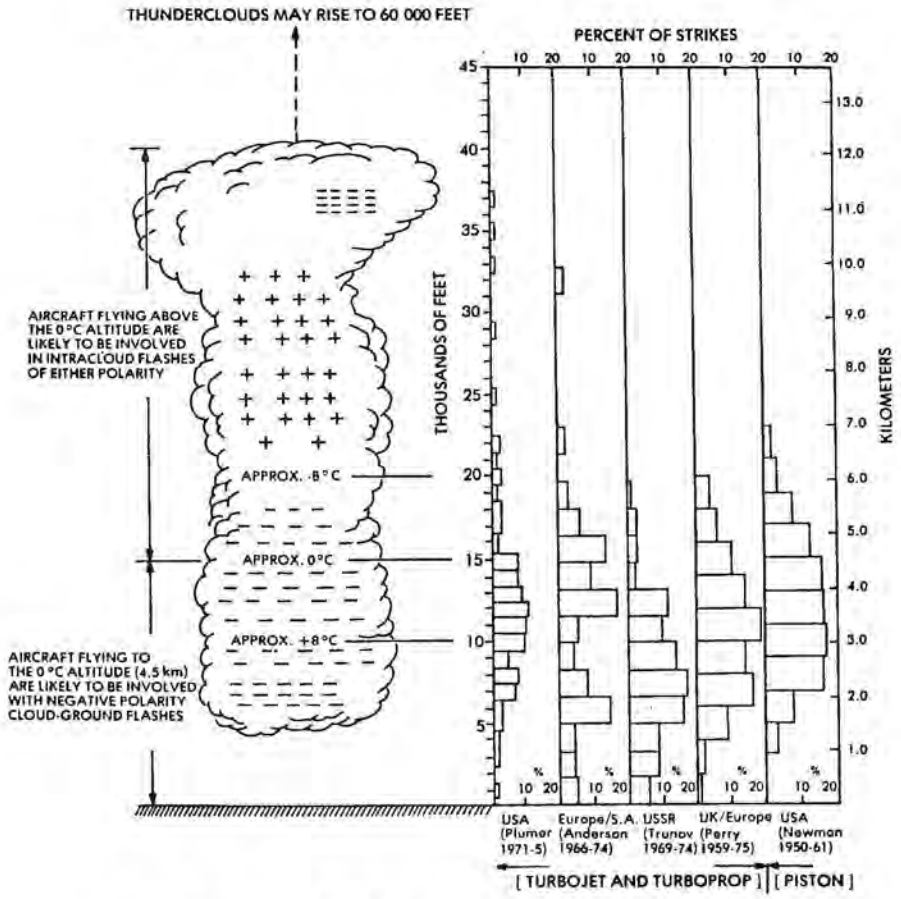

Fig. 3.1 Aircraft lightning strike incidents vs altitude.

anywhere around, is received. It is not certain that these reports are correct because it does not seem possible for electrical charge separation of the magnitude necessary to form a lightning flash to occur in clear air. In most well documented incidents, a cloud is present somewhere (i.e., within 25 miles) when the incident occurs.

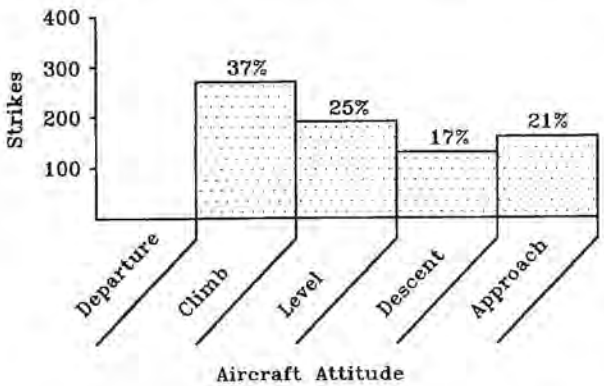

Fig. 3.2 Flight regime when struck.

Perhaps of most interest to aircraft operators are the area weather conditions which prevailed at the time of reported strikes. There is no universal data bank for this type of data, but several surveys have been conducted from time to time, including those of [3.2] through [3.8]. A survey involving a more limited number of strikes, but containing more weather information than the broad based surveys referenced above, is that of H.T. Harrison [3.9] of the synoptic meteorological conditions prevailing for 99 United air Lines lightning–strike incidents occurring between July 1963 and June 1964. Table 3.1 lists the synoptic type and the percentage of incidents (number of cases) occurring in each weather type. Examples of the most predominant synoptic conditions are presented in Fig. 3.3(a) through 3.3(d).

Harrison has drawn the conclusion that any condition which will cause precipitation may also be expected to cause electrical discharges (lightning), although he adds that no strikes were reported in the middle of warm front winter storms. Data from the Airlines Lightning Strike Reporting Project reported

by Rasch et al [3.8], and presented in Fig. 3.4, show that lightning strikes to aircraft in the United States and Europe occur most often during the spring and summer months, when thunderstorms are most prevalent

Table 3.1

Synoptic Types Involved With 99 Electrical Discharges July 1963 to June 1964

Synoptic Type	Percentage
Airmass instability	27
Stationary front	18
Cold front	17
Warm front	9
Squall line or instability line	9
Orographic	6
Cold LOW or filling LOW	5
Warm sector apex	3
Complex or intense LOW	3
Occluded front	1
Pacific surge	1

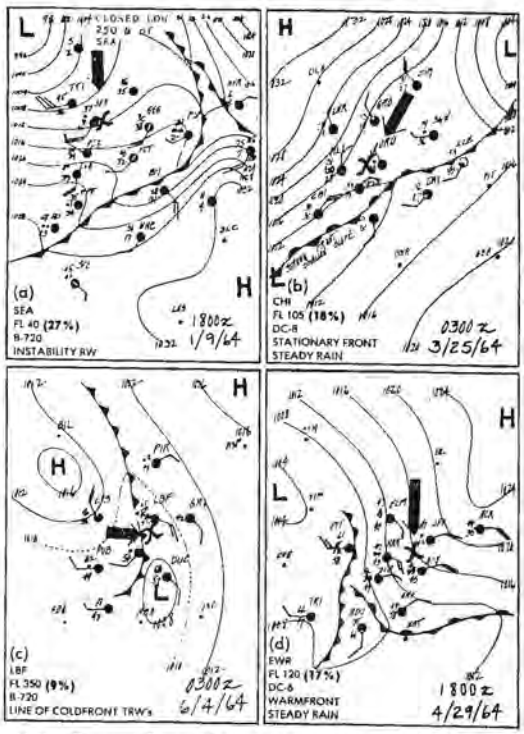

Fig. 3.3 Examples of most recent synoptic meteorological conditions when aircraft have been struck.

Tip of arrow indicates position of aircraft when struck.

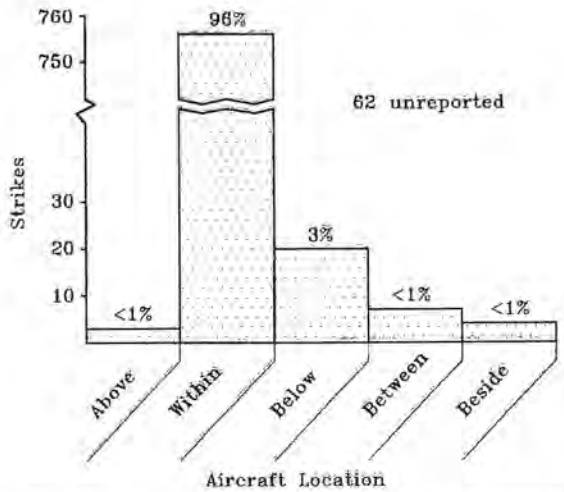

Fig. 3.4 Aircraft location with respect to clouds when lightning strikes have occurred.

It is also important to note that many strike incidents have been reported where no bona fide thunderstorms have been visually observed or reported. Harrison [3.9], for example, reports that United Air Lines flight crews reported 99 cases of static discharges or lightning strikes in flight during the period of his survey. Correlation of these incidents with weather conditions prevailing in the vicinity and in the general area at the time of strike gave the results shown in Table 3.2.

Table 3.2

Percentage of Strike Incidents vs Reported Thunderstorms

Thunderstorms reported in vicinity	33%
Thunderstorms reported in general area	24%
No thunderstorms reported	43%

3.3.3 Immediate Environment at Time of Stroke

Figs. 3.4, 3.5, and 3.6 show the immediate environment of the aircraft at the times of the 881 strikes reported in [3.8]. In over 80% of the strikes reported, each aircraft was within a cloud and was experiencing precipitation and some turbulence.

The incident reports above also show that most aircraft strikes have occurred when an aircraft is near the freezing level of 0° C. Fig. 3.7 [3.8] shows the distribution of lightning strikes to aircraft as a function of outside air temperature. Freezing temperatures (and below) are thought to be required for the electrical charge separation process to function. Of course, strikes to aircraft at temperatures higher than +10° C have occurred when the aircraft was close to (or on) the ground, where the ambient air temperature may be as high as about +25° C.

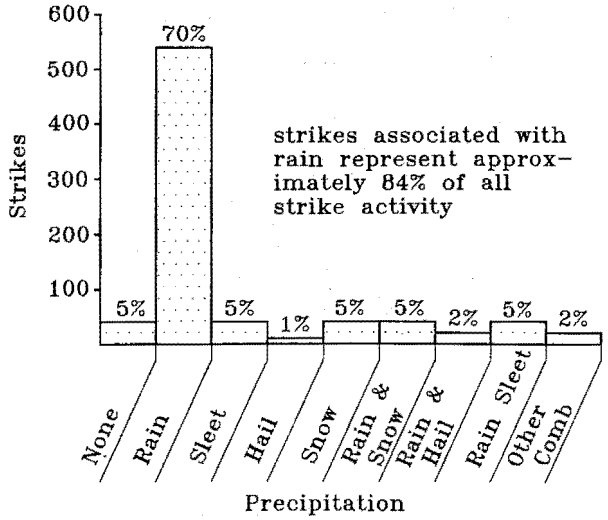

Fig. 3.5 Precipation at time of aircraft lightning strikes.

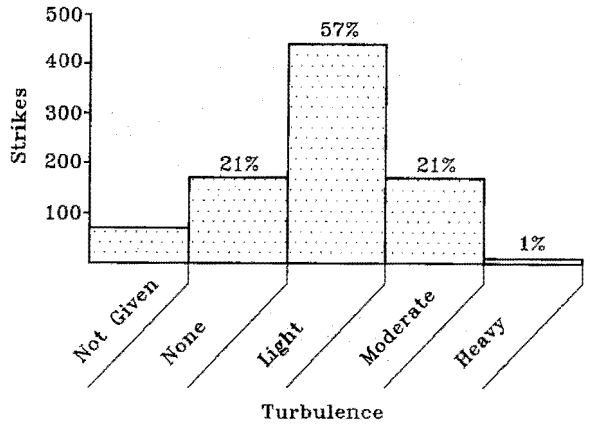

Fig. 3.6 Turbulence experienced when lightning strikes have occurred.

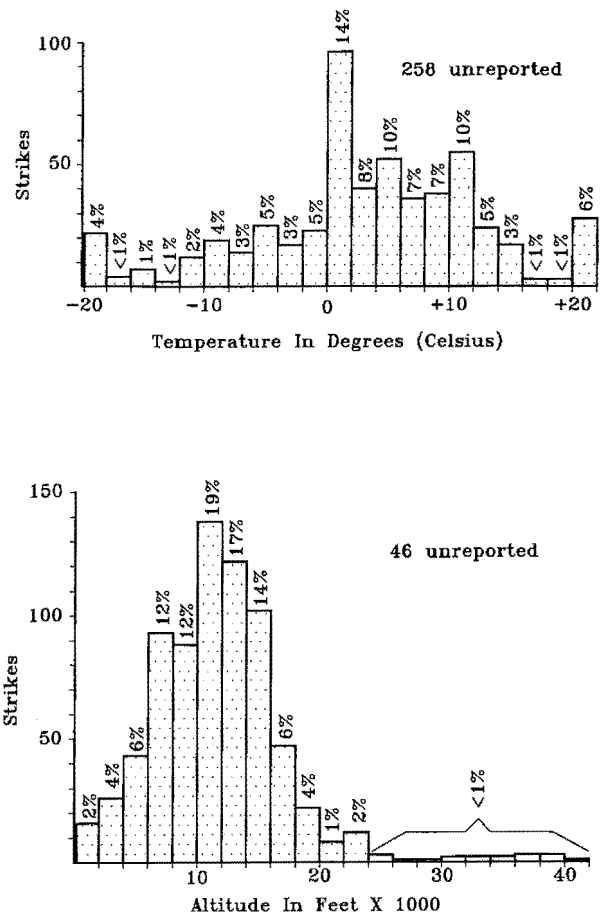

Fig. 3.7 Distribution of lightning strikes.
(a) With outside air temperature
(b) With altitude

3.3.4 Thunderstorm Avoidance

Clearly, whenever it is possible to avoid the severe environments which thunderstorms present, it is desirable to do so, for even if the aircraft is adequately protected against lightning effects, the turmoil caused by wind and precipitation in or near thunderstorms presents a serious hazard to safe flight. Consequently, the operating procedures of commercial airlines and those of other air carriers strongly advise against penetration of thunderstorms.

Thunderstorm indication: In attempts to avoid thunderstorm regions, pilots use three indicators:

1. Visual sighting of thunderclouds (cumulonimbus) in daytime and of lightning at night
2. Airborne radar patterns of precipitation areas
3. Airborne lightning strike indicators, which sense electromagnetic radiation from distant flashes and display their range and bearing on cathode ray tube displays in the cockpit.
4. Weather information, if available, relayed by Air Traffic Control (ATC) to aircrews together with instructions for thunderstorm avoidance.

Methods of avoidance: Methods of thunderstorm avoidance in common use are, in order of preference:

1. Circumnavigation of visible thunderclouds, ideally by 25 miles or more, but often by smaller distances due to traffic constraints.

2. Circumnavigation of areas of heavy precipitation indicated on airborne weather radar displays.

3. Flying over the tops of thunderclouds

The degree to which any of these measures is successful depends on the accuracy of the information received by the pilots.

Weather radar: Aside from visual observation, which has obvious limitations, the most common method of detecting thunderstorms is using airborne weather radar. Radar, however, cannot detect clouds themselves; it can detect only liquid droplets. Only the rain that may be present in the cloud will produce a radar echo and this allows occasional encounters with hail, and with lightning. A typical C–band airborne weather radar presentation of a thunderstorm (cumulonimbus) cloud with active precipitation and frequent lightning is shown in Fig. 3.8 [3.10]. The pictures were taken during a research project carried out by Beckwith of United Air Lines to determine the weather detection capability of airborne radar. The photographs shown were taken during a United Air Lines flight from Chicago to Denver on August 3, 1960. Fig. 3.8 shows the northern end of a line of severe thunderstorms, developed from a cold front in Illinois. A detour to the north was planned and successfully executed with the aid of this radar presentation. The flight remained in clear and generally smooth air while making the detour. The strong echos were easily detected with a slight upward tilt of the radar antenna to eliminate ground clutter.

Contour selection: It is possible to obtain more information regarding the intensity of a storm by use of the contour selection circuit provided on most radars. This feature provides a means of eliminating any reflected signal the intensity of which is above a certain level. Fig. 3.9 shows the same radar return as that in Fig. 3.8 one minute later with the contour feature employed.

The thin, distinct outlines which now appear in place of the original echo indicate a narrow boundary across which the intensity of rain varies from no rain (outside the white outline) to intense rain (inside the white outline). This change in return intensity is called the rain gradient; and the narrower the white outline of the return, the more abrupt, or steeper, is the gradient.

The amount of electric charge separation and lightning activity is known to be related to the degree of precipitation and vertical air currents (turbulence). Further, the severity of turbulence is also related to the temperature difference that exists between different masses of air. Thus, turbulence and electrical activity are likely to exist at well defined boundaries, such as those indicated by steep rain gradients on contoured radar. These boundaries derived from contour radar are often used in planning a detour.

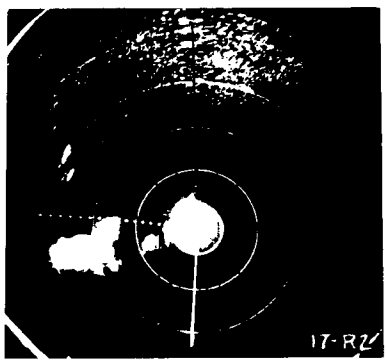

TIME: 0026Z
ALTITUDE: 28 000 FT.
RANGE MARKS: 10-MILE
ANT.: 1½° UP
HEADING: 255° TRUE
STRONG ECHOES HERE ARE THE N END OF A LINE OF THUNDERSTORMS WHICH WERE PRODUCING SEVERE WIND AND LIGHTNING DAMAGE BELOW. LESS THAN ONE HOUR EARLIER, HAILSTONES OF GOLF BALL SIZE WERE REPORTED IN THE AREA OF THE NEAREST LARGE

TIME: 0028Z
ALTITUDE: 28 000 FT.
SOUTH OF DUBUQUE, IOWA, LOOKING SE TO S AND W EDGE OF THUNDERSTORM LINE. THIS CUMULONIMBUS WAS BUILT TO AN ESTIMATED ALTITUDE OF 45 000 FEET. ECHO ON PHOTO 17-R2 CORRESPONDS TO THIS VISUAL.

Fig. 3.8 Radar presentation and subsequent photograph of a thunderstorm.
(a) Radar presentation
(b) Visual appearance of storm

Considering the variable nature of thunderstorms, and the limited information as to their whereabouts and severity available to pilots, it is not surprising that there are varying opinions as to what detour distance is adequate to avoid turbulence and lightning. Primarily, a pilot is advised to use distances commensurate with the specific capability of the radar used.

TIME: 0027Z
ALTITUDE: 28 000 FT.
RANGE MARKS: 10-MILE
ANT.: 1° UP
HEADING: 255° TRUE
CONTOUR: ON

Fig. 3.9 Same as Fig. 3.8(a), but with contour to show very steep rain gradient of each cell.

The specifications and policies of one of the major airlines [3.21] follow.

Specifications:

1. Wavelength - 3.2 cm (X band) through 5.6 cm (C band).
2. Antenna size - 30 cm (12 in) or larger (X band); 64 cm (25 in) or larger (C band).
3. Power (peak) - 10 kW (X band) or higher; 75 kW (C band) or higher

Policies:

1. When the temperature at flight level is 0°C or higher, avoid all echos exhibiting sharp gradients by 5 nautical miles.
2. When the temperature at flight level is less than 0°C, avoid all echoes exhibiting sharp gradients by 10 nautical miles.
3. When flying above 7000 m(23 000 feet) avoid all echoes, even though no sharp gradients are indicated, by 20 nautical miles.

Weather radar, however, is not a foolproof means of detecting and avoiding thunderstorms or other lightning strike conditions, because situations exist in which radar is not capable of distinguishing a thunderstorm return from the returns of ground or from ground clutter. Such a case is illustrated in Fig. 3.10 [3.11].

In this case, returns from the ground (ground clutter) obscured the return from the storm. However, if ground clutter does obscure a storm return and an aircraft is successful in avoiding all thunderstorms by the recommended distances of up to 25 miles, the severe turbulence associated with thunderstorms is usually also avoided. Nevertheless, lightning flashes may extend farther outward from the storm center than does turbulence and for this reason are not as easily avoided. Indeed, there are several reports each year of aircraft receiving strikes "in the clear" 25 or more miles from the nearest evident storm. That lightning flashes can propagate this distance is evident from ground photographs of very long, horizontal flashes.

TIME: 0153Z
ALTITUDE: 29 000 FT.
RANGE MARKS: 25-MILE
ANT.: 0°
HEADING: 060° TRUE. OVER ST. GEORGE, UTAH.
A THUNDERSTORM ECHO IS NOT DISTINGUISHABLE FROM TERRAIN AT THIS OR OTHER ANTENNA SETTINGS TO MATCH THE VISUAL SIGHTING AT 9:30 BEARING IN PHOTO 11-C2.

TIME: 0155Z
ALTITUDE: 29 000 FT.
DECAYING THUNDERSTORM BUILT TO ABOVE FLIGHT ALTITUDE FOR WHICH NO MATCHING ECHO WAS VISIBLE IN SCOPE PICTURE 11-R-3.

Fig. 3.10 Thunderstorms not distinguishable on radar scope.
(a) Radar presentation
(b) Visual appearance of storm

Color radar: Present airborne weather displays use colors to distinguish between different intensities of precipitation, which are defined in terms of dBz. The boundaries between bands of different color are the colors mentioned above. A typical color weather radar display is shown in in Fig. 3.11 [3.12].

A decaying thunderstorm, moreover, may not present a distinctive radar echo. Sometimes this type of storm becomes embedded in expanding anvils or cirrus clouds in such a way that it is not visible. In-flight measurements conducted by the Air Force and the Federal Aviation Administration, and reported by Fitzgerald [3.13], indicate that thunderstorms in their early stages of dissipation have sufficient charge to cause a few lightning discharges if a means of streamer initiation becomes available. An aircraft entering such a region may initiate, or trigger, such a flash. Thus, in normal IFR operations in regions where an active thundercloud is merged with decaying thunderclouds and other cloudy areas, diverting from the normal course to avoid the active cloud may take the flight through a decaying area, where a lightning strike is possible.

Lightning warning instruments: Attempts have been made from time to time to develop an airborne instrument capable of warning pilots of an impending lightning strike to the aircraft and providing information to the pilot for use in avoidance. Most such attempts have been based on the principle of detecting the ambient electric field which would exist when a lightning flash is imminent [3.14]. None of these field measurement instruments have been successfully tested in an aircraft, and because of the apparent wide variation of electric field intensities and other conditions which may precede a lightning strike to the aircraft, success seems remote. The situation is further complicated by the problems of field interpretation and translation into advisory information in sufficient time to aid the pilot in deciding on an avoidance maneuver.

There are instruments that locate and plot the locations of lightning flashes that are taking place, but that is a different story.

Perhaps the most effective warning of imminent strikes available to flight crews is that which is readily available–the buildup of static discharging and (at night) St. Elmo's Fire (corona). Static discharging causes interference (instability) in Low Frequency Automatic Direction Finding (LF–ADF) indicators, or audible "hash" in most communications receivers. St. Elmo's fire is visible at night as a bluish glow at aircraft extremities where the discharging is occurring.

Pilot responses to lightning strikes (which may also be called static discharges or electrical discharges) vary. Typical answers by pilots of one airline [3.9] to the question "Do you have any recommendations for avoiding electrical discharges?" were as follows:

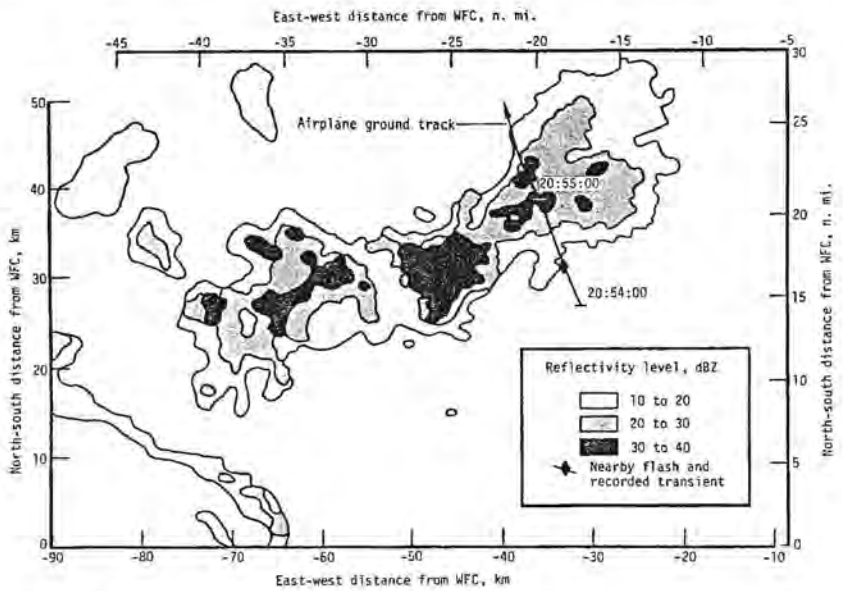

Fig. 3.11 Reflectivity contours at time of a strike near to the F–106B.
Flash 4, 20:54:21.9 GMT, July 22,1980.
Taken by NASA–Wallops SPANDAR radar at 20:56:51.5 GMT with a radar tilt angle = 0°C.

"From cruise speed, a reduction of 25% to 30% in airspeed will often allow the static buildup to stabilize at a lower maximum and dissipate rather than discharge. These build-ups are generally accompanied by a buzz-type static on VHF (very high frequency) and ADF (automatic direction finding) and a random swinging of the ADF needles though I have observed the ADF needles to hold a steady error of up to 90° as the static level stabilized at or near its peak, generally just prior to the discharge or beginning of dissipation."

"Climb or descend through the freezing level as quickly as possible."

"Avoid all precipitation. I know of no way to predict accurately where a discharge will occur."

"Slow down to minimum safe speed, change altitude to avoid temperature of −7°C (20° F) to 2°C (35° F)."

"Not without excessive detour, both route and altitude."

"The static discharges I have encountered have built up at a rate which would preclude any avoidance tactics (3 to 15 seconds)."

"No, I have never known when to expect this until just prior to the discharge."

"No, not in the modern jets. Once the static begins the discharge follows very quickly."

"All information received at the ... training center applicable to static discharges and their avoidance has been completely accurate and helpful."

"No, hang on!"

"Lead a clean life."

Thus, there is a wide divergence of pilot opinion regarding the best way to avoid lightning strikes. However, from this and many other sources, it is possible to list the symptoms most often present just prior to experiencing a lightning strike, and the actions (if any) which most pilots take to reduce the possibility of receiving a strike.

A lightning strike is imminent when a combination of some of the symptoms which follow is present.

Symptoms:

1. Flight through or in the vicinity of the following:

   Unstable air.

   Stationary front.

   Cold front.

   Warm front.

   Squall line.

2. Within a cloud.
3. Icy types of precipitation.
4. Air temperature near 0° C.
5. Progressive buildup of radio static.
6. St. Elmo's fire (when dark).
7. Experiencing turbulence.
8. Flying at altitudes between 1500 and 4500 m (5000 and 15 000 ft); most prevalent: 3350 m (11 000 ft).
9. Climbing or descending.

Actions:

1. Avoid areas of heavy precipitation.
2. Change altitude to avoid temperature near 0°C.
4. Turn up cockpit lights.
5. Have one pilot keep eyes downward.

Since air traffic congestion often precludes circumvention of precipitation and since diversion often poses hazards, avoidance, while desirable, is neither a dependable nor an adequate means of protecting the aircraft against lightning strikes. The aircraft, therefore, must be designed to safely withstand lightning strike effects.

3.3.5 Frequency of Occurrence

Commercial aircraft: The number of lightning strikes which actually occur, as related to flight hours for piston, turboprop, and pure jet aircraft, is tabulated in Table 3.3 based on the data of Newman [3.2] and Perry [3.6]. From this data it follows that an average of one strike can be expected for each 3000 hours of flight for any type of commercial transport aircraft.

Military and general aviation aircraft: Unlike commercial airlines, military and general aviation aircraft need not adhere to strict flight schedules or congested traffic patterns around metropolitan airports. The result is that these aircraft do not seem to experience as many strikes as do commercial aircraft, as is evident from Table 3.4, which shows U.S. Air Force experience for the years 1965 to 1969. USAF regulations, however, do not require that lightning strike incidents be documented by flight crews unless a substantial amount of damage is done to the aircraft. Thus, many strikes to USAF aircraft undoubtedly go unreported.

Table 3.3
Incidence of Reported Lightning Strikes to Commercial Aircraft

	Newman (1950 – 1961)		Perry (1959 – 1974)		TOTALS		
	Strikes	Hours	Strikes	Hours	Strikes	Hours	No. hours per strike
Piston	808	2 000 000	–	–	808	2 000 000	2475
Turboprop	109	415 000	280	876 000	389	1 291 000	3320
Pure Jet	41	427 000	480	1 314 000	521	1 741 000	3340
ALL	958	2 842 000	760	2 190 000	1718	5 032 000	2930

Table 3.4
Incidence of Reported Lightning Strikes to U.S. Air Force Aircraft

Aircraft type vs mean hours between lightning strikes						
	1965	1966	1967	1968	1969	Average per year
Bomber	55 500	48 000	47 900	73 000	28 000	50 480
Cargo	68 000	140 000	112 000	124 000	76 000	104 000
Fighter	141 000	105 000	112 000	65 000	73 000	99 200
Trainer	246 000	378 000	500 000	224 000	130 000	295 600

Statistics such as these, which apply to a broad category of aircraft and include data from a variety of different operators in varying geographic locations, may be misleading. For example, whereas Table 3.4 shows that there is an average of 99 000 flying hours between reportable lightning strikes to U.S. Air Force fighter–type aircraft, the strike experience in Europe is known to be about 10 times more frequent than strike experience in the U.S. and in most other parts of the world. Weinstock and Shaeffer [3.15] report 10.5 strikes per 10 000 hours for certain F–4 models flying in Europe, which rate is about 5 times greater than the world–wide exposure rate for these aircraft. A similar situation pertains to commercial aircraft operating in Europe, as indicated by Perry's summary of United Kingdom and European strike data [3.6], for example. This unusually high lightning–strike exposure seems to result both from the high level of lightning activity in Europe as compared with that in many other regions and from the political constraints placed on flight paths in this multinational region.

Trends affecting strike rate: There are several trends in commercial and general aviation which are likely to cause even greater exposure of aircraft everywhere to lightning strikes in the future:

1. Increases in the number of intermediate stops along former nonstop routes, resulting in more time in descent, hold and climb patterns at lower altitudes.

2. Increases in the number of aircraft and rotorcraft equipped for IFR flight.

3. Increasing use of radar and other navigation aids in general aviation aircraft, permitting IFR flight under adverse weather conditions.

These factors warrant continued diligence in the design and operation of aircraft with respect to the possible hazards lightning may present.

3.4 Aircraft Lightning Strike Mechanisms

In the following paragraphs the electrical conditions which produce lightning are described, together with the mechanisms of lightning strike attachment to an aircraft, While it is not possible to anticipate or avoid these conditions all of the time, it is important to understand the strike attachment process in order to properly assess the effects of lightning strikes on the aircraft.

3.4.1 Electric Field Effects

At the beginning of lightning flash formation, when a stepped–leader propagates outward from a cloud charge center, the ultimate destination of the flash, at an opposite charge center in the cloud or on the ground, has not yet been determined. The difference of potential which exists between the stepped leader and the opposite charge(s) establishes an electrostatic force field between them, represented by imaginary equipotential surfaces. They are shown as lines in the two dimensional drawing of Fig. 3.12. The field intensity, commonly expressed in kilovolts per meter, is greatest where equipotential surfaces are closest together. It is this field that is available to ionize air and form the conductive spark which is the leader. Because the direction of electrostatic force is normal to the equipotentials, and strongest where they are closest together, the leader is most likely to progress toward the most intense field regions.

If an aircraft happens to be in the neighborhood, it will assume the electrical potential of its location. Since the aircraft is a thick conductor and all of it is at this same potential, it will divert and compress adjacent equipotentials, thus increasing the electric field in-

tensity at its extremities, and especially between it and other charged objects, such as the advancing leader. If the aircraft is far away from the leader, its effect on the field near the leader is negligible; however, if the aircraft is within several tens or hundreds of meters from the leader, the increased field intensity in between may be sufficient to attract subsequent leader propagation toward the aircraft. As this happens, the intervening field will become even more intense, and the leader will advance more directly toward the aircraft.

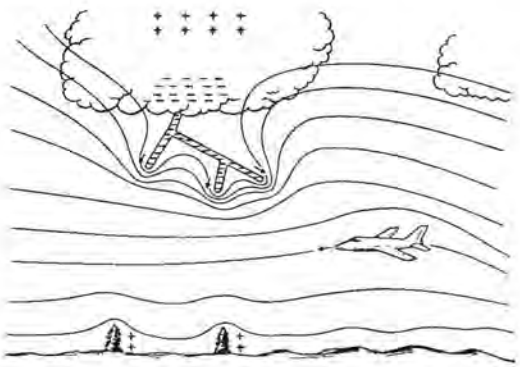

Fig. 3.12 Stepped leader approaching an aircraft.

The highest electric fields about the aircraft will occur around extremities, where the equipotential lines are compressed closest together, as shown in Fig. 3.13. Typically, these are the nose and wing and empennage tips, and also smaller protrusions, such as antennas or pitot probes. When the leader advances to the point where the field adjacent to an aircraft extremity is increased to about 30 kV/cm (at sea level pressure), the air will ionize and electrical sparks will form at the aircraft extremities, extending in the direction of the oncoming leader.

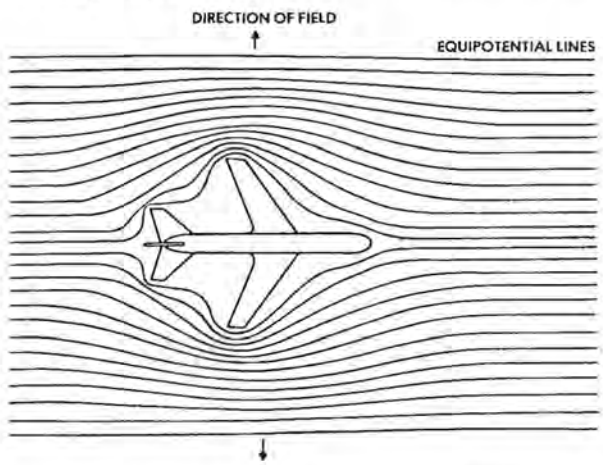

Fig. 3.13 Compression of electric field around an aircraft.

Several of these sparks, called streamers, usually occur nearly simultaneously from several extremities of the aircraft. These streamers will continue to propagate outward as long as the field remains above about 5 to 7 kV/cm. One of these streamers, called the junction leader, will meet the nearest branch of the advancing leader and form a continuous spark from the cloud charge center to the aircraft. Thus, when the aircraft is close enough to influence the direction of the leader propagation, it will very likely become attached to a branch of the leader system.

3.4.2 Charge stored on Aircraft

When the aircraft is attached to the leader, some charge (free electrons) will flow onto the aircraft, but the amount of charge which can be taken on is very small compared to what is available from the lightning flash. The charge will raise the aircraft to a high voltage and excessive charge will cause the electric field around the aircraft to become so high that intense corona streamers will form. These streamers will then carry away the excess charge.

If additional charge flows onto the aircraft, more profuse streaming will occur, and from extremities of larger radii of curvature. In fact, the maximum charge which can be on the aircraft probably exceeds by up to 100 times the streamer initiation value. However, statistics on natural lightning characteristics show that a typical leader contains about 1 to 10 coulombs (1-10 C), so there is still no room for any significant portion of this to accumulate on an aircraft. Thus, the aircraft merely becomes an extension of the path being taken by the leader on its way to an ultimate destination at a reservoir of opposite polarity charge.

Streamers may propagate onward from two or more extremities of the aircraft at the same time. If so, the incoming leader will have split, and the two (or more) branches will continue from the aircraft independently of each other until one or both of them reach their destination. This process of attachment and propagation onward from an aircraft is shown in Fig. 3.14.

When the leader has reached its destination and a continuous ionized channel between charge centers has been formed, recombination of electron and positive ions occurs back up the channel, and this forms the high-amplitude return stroke current. This stroke current and any subsequent stroke or continuing current components must flow through the aircraft, which is now part of the conducting path between charge centers, as shown in Fig. 3.15(a).

If another branch of the original leader reaches the ground before the branch which has involved the aircraft, the return stroke will follow the former, and all

other branches will die out, as shown in Fig. 3.15(b). No substantial currents will flow through the aircraft in such a case, and any damage to the aircraft will be slight. A still photograph of a downward-branching flash after completion of the main channel is shown in Fig. 3.16. Several dying branches are evident in the photograph.

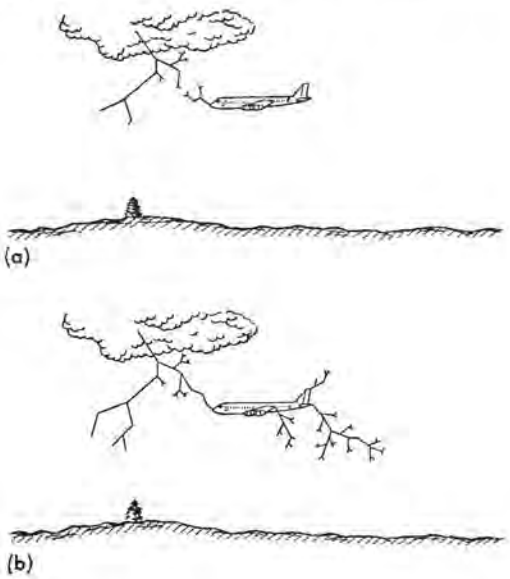

Fig. 3.14 Stepped leader attachment.
(a) Leader approaching aircraft
(b) Attachment and continued propagation

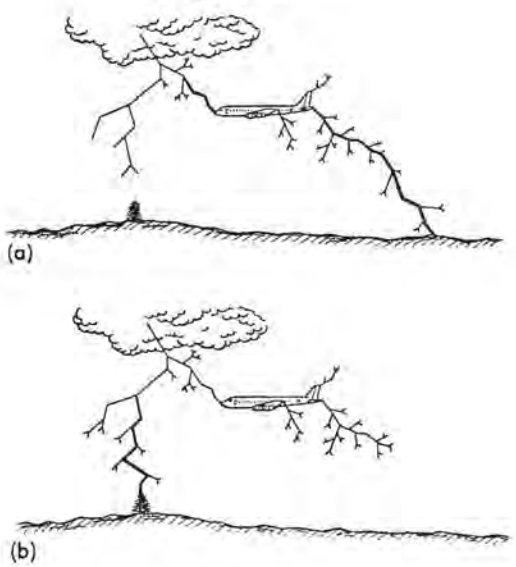

Fig. 3.15 Return stroke paths.
(a) Return stroke through aircraft
(b) No return stroke through aircraft

Fig. 3.16 Downward branching lightning flash.

3.4.3 Triggered Lightning Effects

A question often asked is "If an aircraft cannot produce a lightning flash from its own stored charge, can it trigger a natural one?" Stated another way the question might be "Would the lightning flash have occurred if the aircraft were not present?" A secondary question would be "Even if aircraft do trigger lightning, would there be an impact on the criteria to which aircraft must be designed?" The mechanism of aircraft triggering lightning is discussed in depth in Section 3.7, but some preliminary discussion is in order.

There is clear evidence that lightning flashes can be triggered by research aircraft that are intentionally flown into clouds to observe lightning phenomena, but it is not clear whether aircraft in normal service trigger lightning very often. The following factors suggest that most flashes which are encountered (by other than research aircraft) *are not* the result of the aircraft triggering the flash.

1. Aircraft often fly through electrified regions without being struck, even though lightning flashes are observed nearby.

2. The stepped leader must begin from a charge source capable of furnishing it with several coulombs of charge. Thus the potential (voltage) of this center, and the surrounding field intensity, would seem to be much greater than that about an aircraft, leaving the implication that, unless the aircraft is very close to the charge center, it can have little influence on the surrounding field or on the process of leader initiation.

3. Laboratory studies of breakdown in long air gaps, a mechanism similar to that of natural lightning, show that initial ionization always begins at one of the electrodes and not from an object suspended in the gap [3.16]. In those studies the object significantly influenced the voltage level at which breakdown began only if it was close enough to one electrode to influence the field about the electrode. Whether those studies were particularly representative of aircraft, however, is a subject still under debate.

4. Triggered lightning currents measured on research aircraft have generally been of lower amplitude than those of natural cloud–ground lightning measured at ground level. These current levels do *not* seem to be large enough to account for some of the physical damage observed on aircraft.

It *may* be that aircraft do not become involved in the formation of the lightning flash until after leader propagation has begun. If the leader happens to approach the aircraft, the field intensification produced by the presence of the aircraft becomes much more significant, and the leader may then be attracted to the aircraft.

There is some evidence [3.17] that jumbo (wide–body) aircraft do trigger their own flashes. If large–body aircraft are in fact triggering flashes, it is probably because their larger sizes make a more noticeable perturbation on the electric field near the cloud charge centers from which leaders begin.

The aircraft motion has little influence on the propagating leader because the aircraft is moving much slower, about 10^2 m/s, than the leader, which is advancing at 10^5 to 10^6 m/s. Thus, the aircraft appears stationary to the leader during the leader formation process.

Several other stimuli have been mentioned as possible causes of aircraft lightning strikes. These include engine exhaust and radiated electromagnetic energy, such as radar transmission.

Effect of engine exhaust: There has been speculation that the hot jet–engine exhaust gases may contain a sufficient number of ionized particles to attract or trigger a lightning flash to the aircraft. This speculation was heightened by the widely publicized launch of Apollo 12, which apparently triggered a lightning flash (or flashes) that twice struck the top of the vehicle; once when it had reached 1950 m (6400 ft) and again at 4270 m (14 000 ft). The flash(s) exited from the vehicle exhaust plume.

Studies by Nanevicz, Pierce, and Whitson [3.18] of this and other incidents in which a rocket was rapidly introduced into an intense electric field indicate that the exhaust plume does appear electrically conductive, making the rocket appear longer than its actual physical length.

An empirical study by Pierce [3.17] of documented strikes to tall grounded and airborne conductors concluded that there must also be a potential discontinuity between the conductor and the adjacent atmosphere of up to 10^6 V if the lightning leader is to be initiated from the conductor, and that the rapid discharge of hot ionized gas from the rocket engine may cause sufficient charge separation from the vehicle to increase its potential to 10^6 V or more with respect to its surroundings.

Shaeffer and Weinstock [3.15] have studied the conductivity of an aircraft jet–engine exhaust. In this case, ionized particles and free electrons in a jet exhaust originate in the combustion chamber as a result of chemical reactions taking place between the intake air and jet fuel. The ion concentration in a jet–engine exhaust has been measured by Fowler [3.19] to be between 5×10^6 and 3×10^7 particles per cubic centimeter (p/cm^3) and the free electron density deduced from this to be between 5×10^3 to $3 \times 10^5 p/cm^3$. The electron density in luminous rocket exhaust has been calculated by Pierce [3.20] to be 10^{12} p/cm^3, as has that in the tip of an advancing leader. Conversely, the free electron density in ambient air ranges from 100 to 10^3 p/cm^3. Evidently, then, the jet–engine exhaust is only slightly more ionized than the ambient air and much less so than the rocket exhaust, with the result that the jet exhaust would not be expected to have sufficient conductivity to initiate or attract a lightning leader. This conclusion is supported by aircraft lightning strike incident reports, which indicate that engine tail pipes are not often lightning attachment points unless they are already located at an aircraft extremity, where the electric field would be intense from geometrical conditions alone.

There is also no evidence to suggest that jet aircraft are struck more often than piston–engined aircraft. Overall, the ability of the jet aircraft to operate at higher altitudes and spend less time climbing and descending to airports has probably rendered the jet less susceptible than its piston engined predecessor to lightning strikes, which occur predominantly at low or intermediate altitudes.

Some records do exist of strikes to jet engines and in some cases these strikes have terminated inside the engine exhaust pipes, as illustrated in Fig. 3.17. These strikes are evidenced by spots of melted metal within

0.5 m (18 in) of the aft end of the pipe. Electronic engine instruments with sensors mounted on the engine have experienced damage from lightning indirect effects associated with strikes to the nacelles or tail pipes. Apparently, there is either sufficient ionization in the exhaust or the dielectric strength of the exhaust is sufficiently weakened as to divert a propagating leader into the exhaust channel, or to enable the formation of outward propagating streamers from the tail pipe, once the aircraft has been struck elsewhere by a leader.

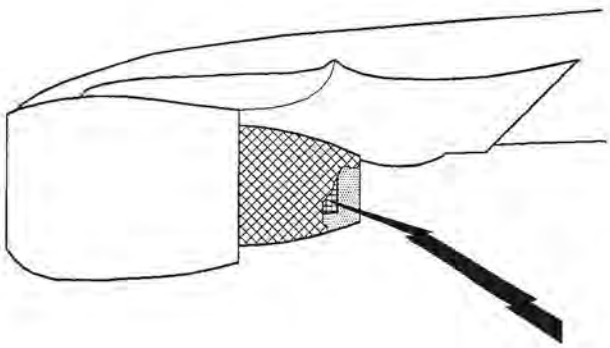

Fig. 3.17 Lightning flash terminating inside jet engine exhaust tail pipe.

While the engine exhaust may divert an existing leader, it seems improbable, however, that it could trigger a flash by itself, as can a rocket plume. Other strikes have terminated on the nacelles of wing and fuselage mounted engines, in the same manner as with other aircraft extremities.

Viewed another way, if the jet engine were leaving behind an ionized exhaust, it seems probable that an imbalance of charge on the aircraft would eventually result, even when flying in clear weather. As with P-static charging, this would change the aircraft potential with respect to its surroundings and cause static discharging and corona from sharp extremities, causing interference in radio equipment. It is well established that this does not happen.

Effects of Electromagnetic Radiation: It has been suggested that an aircraft's radar may trigger or divert lightning strikes. This question was also investigated by Schaeffer and Weinstock [3.15], who show that the transmitted power level of microwave radiation necessary to produce an electric field capable of ionizing air is about 6.7×10^6 watts (W), which is far greater than that available from aircraft radars.

Aircraft lightning strike incident reports also show no evidence of radar or other electromagnetic radiators having been involved in the lightning strike formation. There are cases in which radomes are punctured, but these clearly are the result of the electric field associated with the lightning strike causing breakdown of the plastic radome material, with the flash terminating on some airframe grounded object inside the radome or on the radar antenna itself. The punctures have occurred whether or not the radar set was operating. The addition of diverter strips to the outside of the radome usually prevents these punctures by enabling lightning flashes to attach directly to a diverter.

3.5 Swept Stroke Phenomena

After the aircraft has become part of a completed flash channel, the ensuing stroke and continuing currents which flow through the channel may persist for up to a second or more. Essentially, the channel remains in its original location, but the aircraft will move forward a significant distance during the life of the flash. Thus, whereas the initial entry and exit points are determined by the mechanisms previously described, there may be other lightning attachment points on the airframe that are determined by the motion of the aircraft through the relatively stationary flash channel. In the case of a fighter aircraft, for example, when a forward extremity such as the pitot boom becomes an initial attachment point, its surface moves through the lightning channel, and thus the channel appears to sweep back over the surface, as illustrated in Fig. 3.18. This occurrence is known as the swept stroke phenomenon. As the sweeping action occurs, the type of surface can cause the lightning channel to attach and dwell at various surface locations for different periods of time. This sweeping mechanism prevents the full energy of the lightning flash from being delivered to one spot on the aircraft surface, a phenomenon of particular importance as regards design and protection of fuel tanks.

If part of the surface, such as the radome, is nonmetallic, the flash may continue to dwell at the last metallic attachment point (aft end of the pitot boom) until another exposed metallic surface (the fuselage) has reached it; or the channel may puncture the nonmetallic surface and reattach to a metallic object beneath it (the radar dish). Whether puncture or surface flashover occurs depends on the amplitude and rate of rise of the voltage stress created along the channel, as well as the voltage withstand strength of the nonmetallic surface and any air gap separating it from the enclosed metallic objects. When the lightning arc has been swept back to one of the trailing edges, it may remain attached at that point for the remaining duration of the lightning flash. An initial attachment point at a

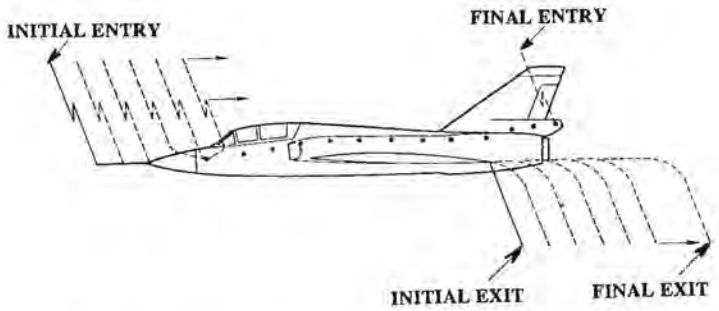

Fig. 3.18 Typical path of swept–flash attachment points.

trailing edge, of course, would not be subjected to any swept stroke action. Instead, the lightning channel is extended horizontally aft of the aircraft.

The aircraft does not usually fly out of, or away from, the channel. This is because the potential difference between charge centers (cloud and earth or another cloud) is sufficient to maintain a very long channel until the charges have neutralized each other and the flash dies.

3.6 Lightning Attachment Zones

Since there are some regions on the aircraft where lightning is unlikely to attach, and others which will be exposed to attachment for only a small portion of the total flash duration, it is appropriate to define the zones on the aircraft surface which will be exposed to different components of the flash and therefore receive different types and degrees of effects.

3.6.1 Zone Definitions

For purpose of protection design, the Federal Aviation Administration (FAA) has defined in its Advisory Circular *AC 20-53A* [3.21] the following zones:

Zone 1A: Initial attachment point with low possibility of lightning channel hang–on.

Zone 1B: Initial attachment point with high possibility of lightning channel hang–on.

Zone 2A: A swept–stroke zone with low possibility of lightning channel hang–on.

Zone 2B: A swept–stroke zone with high possibility of lightning channel hang–on.

Zone 3: Those portions of the airframe that lie within or between the other zones, which may carry substantial amounts of electrical current by conduction between areas of direct or swept stroke attachment points.

Zones are the means by which the external environment is applied to the aircraft. The locations of these zones on any aircraft are dependent on the aircraft's geometry, materials and operational factors, and often vary from one aircraft to another. Therefore, a determination must be made for each aircraft configuration.

Neither *AC 20-53A* nor any other airworthiness standards prescribe the actual locations of the zones on a particular aircraft since the locations of each zone are dependent upon the aircraft's geometry and operational factors, and may vary from one aircraft to another. Defining the zones is a subjective matter, not one amenable to exact analysis. Actual zones are usually established by the aircraft designer by reference to past inflight experience with aircraft of similar design or with the aid of lightning strike tests on scale models. Guidance for locations of strike zones on specific aircraft is given in Chapter 5, together with further discussion and examples of the factors affecting aircraft lightning attachments and zone locations.

3.7 Mechanism of Aircraft Triggered Lightning

Aircraft triggered lightning is defined as lightning which occurs because of the presence of an aircraft and would not otherwise occur. A frequent theme in pilots' reports of lightning strikes to aircraft is that the aircraft was struck before there was any evidence of lightning activity in the area, and a belief commonly expressed is that the aircraft triggered the lightning flash, rather than the aircraft just being an inadvertant bystander through which a naturally occurring lightning flash chose to pass.

Evidence has accumulated that aircraft can indeed trigger lightning and theories have been developed to explain the mechanism. It is well established that research aircraft intentionally flown into charged clouds have triggered flashes and that these flashes have originated at the aircraft. It is not as evident that aircraft flown under normal conditions and seek-

ing to avoid lightning often trigger lightning flashes. Possibly those aircraft are more often struck by a naturally propagating leader, as discussed in §3.4.3.

To some extent the matter may be academic since aircraft are struck by lightning and the measures taken to protect against lightning would be the same whether it were triggered by the aircraft or not.

The subject of aircraft triggered lightning first began to be seriously studied in the 1960's [3.22 - 3.26]. It was during this period that it was shown that lightning could be deliberately triggered by rockets with trailing wires [3.27]. Toward the end of the 1960's Apollo 12 was struck by what was deemed to be a triggered lightning flash and studies [3.28, 3.29] were undertaken to understand the conditions that could result in lightning being triggered by an aerospace vehicle.

In 1972, it was suggested [3.30] that necessary and sufficient conditions for triggering of lightning by any vehicle, including aircraft, were the existence of an ambient electric field of at least 10 kV/m, and that the vehicle span a potential difference of about one million volts. Also in 1972, an interesting study was published which concluded that aircraft could trigger lightning and that static charge on the aircraft was an important factor [3.31].

A good review of this subject and bibliography was published in 1982 [3.32]. Even up to this date, however, there was considerable uncertainty and debate regarding the possibility of aircraft triggered lightning. This was basically because there were no definitive measurements of aircraft triggered lightning and no physical models to explain it.

F–106B Research aircraft: In 1981 an F–106B aircraft, operated by the NASA Langley Research Center was outfitted as a research vehicle to be flown into clouds to collect data on the characteristics of lightning intercepted by aircraft. Starting in 1982 the UHF–band radar at the Wallops Flight Facility of the NASA Goddard Space Flight Center, was used to guide the F–106B through the upper regions of thunderstorms to increase the probability of the aircraft being struck by lightning [3.33].

Analysis of the radar echos showed that nearly every echo from a lightning strike to the F–106B started directly on top of the echo from the aircraft and propagated away from the aircraft. This certainly suggested that the lightning flashes were triggered by the aircraft and were not naturally occurring flashes. If they had been naturally occurring flashs intercepted by the aircraft, then an observer would have seen the echos start some distance from the aircraft and propagate toward the aircraft, finally blending with the echo from the aircraft at the time the strike was recorded by the aircraft. None of the lightning flashes showed this pattern. Many echos were seen from naturally occurring intracloud flashes, but none of them ever struck the F–106B.

In addition to the radar echos, analyses using three dimensional numerical models [3.33 - 3.36] have predicted currents to arise from triggering that are very similar to those observed on the vehicle. All of this evidence rather conclusively proves that the F–106B research aircraft has triggered lightning flashes.

There also has been other significant research into the mechanisms of triggered lightning. Work has been done on energy considerations [3.37 - 3.38], the role of positive corona streamers and precipitation particles [3.38 - 3.39], electrode velocity [3.42], and other topics [3.43 - 3.45]. Experimental studies have included a scale model Space Shuttle Orbiter vehicle [3.46] and an electrically floating cylinder [3.47].

Mechanism of triggering: Triggered lightning occurs because the local electric field induces charge on the extremities of the aircraft, this charge then producing an electric field sufficient to cause air breakdown at places on the aircraft, corona as discussed in Chapter 1 or St. Elmo's Fire, as discussed in Chapter 2. If the ambient electric field is sufficiently high, streamers then develop and propagate away from the aircraft.

The basic mechanism of propagation is similar to that described in Chapter 1 with one major difference. During breakdown of a gap subjected to an externally applied impulse, the energy required to establish the field into which the streamer propagates is produced by the externally applied impulse. The streamer may then continue to propagate by conducting charge along its channel and establishing a field at its tip sufficient to maintain propagation, the requisite field at the tip of the leader being on the order of 500 kV/m at sea level There does not have to be a pre–existing field since the charge to maintain the channel can come from the generator that applies the impulse to the electrode. Laboratory studies with switching impulse voltage, §1.5.1, of $\approx 5 \times 10^6$ volts peak have produced discharges propagating 30 – 60 meters (100 – 200 ft).

Lightning leaders propagate by a similar mechanism, drawing on the charge stored in the cloud.

With aircraft triggered lightning the difference is that the energy to maintain propagation must come from a pre–established field. Electrical charge stored on the aircraft may contribute to the initial breakdown, but can never be enough to maintain the discharge. A consequence that follows from this is that streamers must propagate away from the aircraft in both directions, one streamer being positive and one negative.

Requirements for triggering: For triggered lightning to form, the first requirement is that the static electric field in which the aircraft is immersed must be large enough and oriented properly so that the locally enhanced fields somewhere on the aircraft exceed the local air breakdown value. The largest enhancements of the field will be at sharp points or edges, particularly if those points and edges are oriented in the direction of the ambient field. An aircraft in flight has many such sharp points and sharp edges, such as propeller tips, wings and empennage tips. For distances of half a meter or so these locally enhanced fields are likely to be higher than the ambient field by a factor of ten or more. Hence, it is considerably more likely that initial air breakdown and formation of a lightning channel will occur in the presence of an aircraft than in its absence.

The second requirement for triggered lightning is that the electric field be sufficiently high, and high for a sufficient distance, that a streamer can form and propagate. Formation of corona is not sufficient; during thunderstorms corona forms on grounded objects all the time, but does not develop into streamers because the electric field into which the corona grows is not sufficiently high. The research discussed in Chapter 1, on streamer development from electrodes subjected to externally applied impulses, shows that the streamers will continue to propagate and develop into full fledged lightning leaders as long as the average electric field in the gap exceeds about 500 kV/m, at sea level. At flight altitudes, the ambient field sufficient to support continued streamer propagation is somewhat less due to lower air densities.

That research also shows that an average voltage gradient of 500 kV/m applied to an electrode gap will always lead to breakdown if the voltage is maintained long enough. 500 kV/m is the value at sea level; 250 kV/m could be expected to cause breakdown at 6000 m (20 000 ft) altitude. One conclusion from this is that an electric field of several hundred kV/m represents conditions that are just on the edge of breakdown. Another is that breakdown is almost certain to occur whenever the field achieves the requisite minimum level since in time there will be a local breakdown that will then be able to propagate. As a consequence all triggered lightning flashes should show similar properties.

In addition to the charge induced by an ambient electric field, an aircraft can also collect a net charge by various means, such as ejection of ionized particles in the exhaust of an engine or by interception of charged rain drops or ice crystals. Such a charge may significantly affect the occurrence of triggered lightning because it contributes to the local fields and can either suppress or enhance the initial breakdown and developing leaders.

3.7.1 Triggered Lightning Environment

The key factor in aircraft triggered lightning is the static electric field produced by thunderstorms. These fields have been measured by several researchers using aircraft, rockets, balloons, and parachuted sondes and show, Table 3.5, that the requisite fields of 250 - 500 kV/m can exist. Higher values have also been reported [3.48]. More recent observations [3.49 - 3.54] report values which are also consistent with Table 3.5. The review cited in Table 3.5 also contains an excellent bibliography on work related to electric fields.

Table 3.5

Thunderstorm Electric Fields Measured in Airborne Experiments

Investigator	Typical (V/m)	High Values Occasionally Observed	Measurement Type
Winn et al. (1974)	$5\text{-}8 \times 10^4$	2×10^5	Rockets
Winn et al. (1981)	-	1.4×10^5	Balloons
Rust, Kasemir	1.5×10^5	3.0×10^5	Aircraft
Kasemir and Perkins (1978)	1×10^5	2.8×10^5	Aircraft
Imyanitov et al. (1972)	1×10^5	2.5×10^5	Aircraft
Evans (1969)	-	2×10^5	Parachuted Sonde
Fitzgerald (1976)	$2\text{-}4 \times 10^5$	8×10^5	Aircraft

The simplified thunderstorm cell model [3.55] shown in Fig. 3.19 will be used to illustrate the conditions under which such such fields may be found. The illustration is based on information extracted from the NASA Langley Research Center Storm Hazards Research Program [3.56] using an F-106B research aircraft. The cell has a +40 Coulomb charge centered at 10 km (32 800 ft) above ground, a -40 Coulomb charge centered at 5 km (16 400 ft), and a +10 Coulomb charge centered at 2 km (6000 ft).

Calculation of the electric fields can be simplified by assuming point charges located in a vertical line with image charges in the ground. Contours of constant electric field from such an assemblage of charges are shown in Figs. 3.20 - 3.22. Because the calculations are based on point charges, the figures show an upper bound on the field. The actual charges are distributed. The field external to the charged region may be calculated correctly by assuming point charges, but for points inside the charged region, the actual field would be smaller than indicated on the figures.

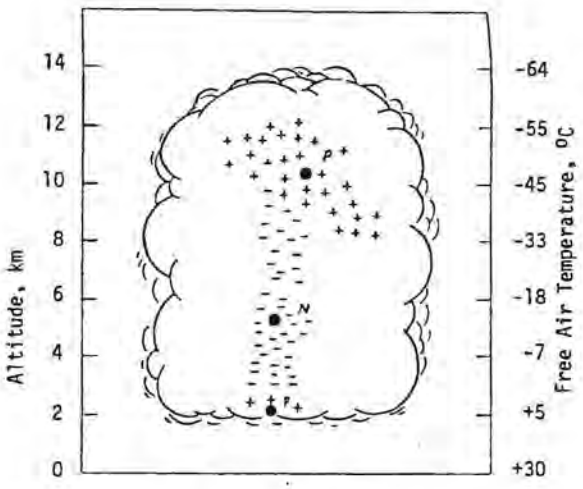

Fig. 3.19 Thunderstorm charge separation model.

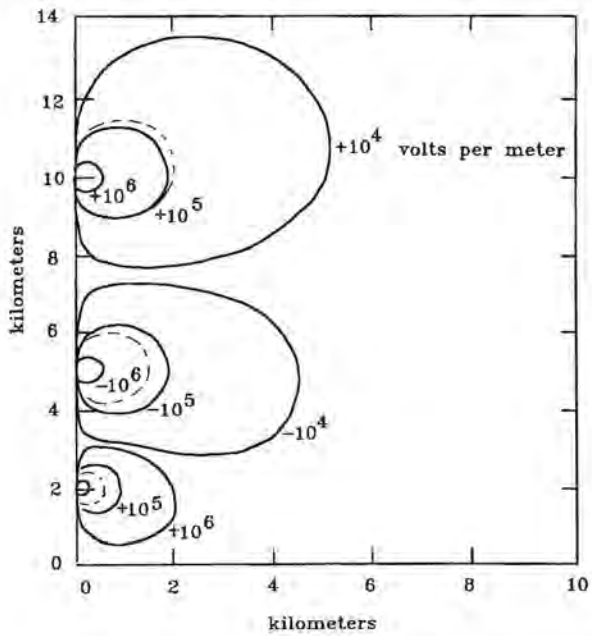

Fig. 3.20 Radial component of electric field.

Fig. 3.20 is the most interesting for the purposes of investigating triggered lightning on the F–106B. If the aircraft is in essentially level flight, the horizontal field will be the one most enhanced.

The triggered lightning response of the F–106B has been successfully modeled by the techniques to be described in Chapter 10. One part of this analysis is calculation of the degree to which the aircraft enhances the local electric field [3.57]. The calculations show that the horizontal fields at the nose of the aircraft are enhanced by a factor of about ten. Horizontal fields at the tips of the wings are enhanced by a factor of about seven. Which horizontal field is enhanced the most of course depends on which way the aircraft is oriented relative to the pre–existing electric field. Vertical fields at the tip of the vertical stabilizer are enhanced by a factor of about 3. Hence for level flight, vertical ambient fields are of much less importance than radial fields, unless the ambient vertical field level is several times larger than the radial field.

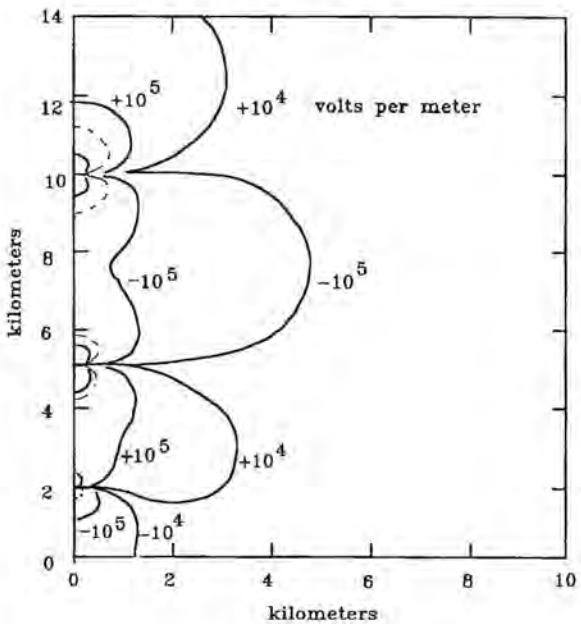

Fig. 3.21 Vertical component of electric field.

Lightning has the potential of being triggered at any point in space at which the enhanced field around the aircraft exceeds the minimum breakdown strength of the air. Since this breakdown strength depends on altitude, or more exactly air density, a field which causes triggered lightning at a high altitude ($\approx$ 10 km) may not do so at lower altitudes. Taking these factors into account, the dashed lines in Figs. 3.20 and 3.21 show the points in space at which an electric field of breakdown strength can be reached on the aircraft, assuming proper orientation. The calculations assume that the net aircraft charge is zero; if it were charged the dashed lines could extend further away from the charge centers. Fig. 3.22 shows the total magnitude of the field.

The dashed lines thus indicate the regions inside which the F–106B in level flight could trigger lightning. At high altitudes where the breakdown strength of air is low, triggering can occur up to two kilometers

from the charge center. At the very low altitudes (≈ 2 km) where the breakdown strength of air is greater the trigger region is only a few hundred meters across. In fact, because the charges are really extended and not point sources, it is possible that at these low altitudes triggering is not possible.

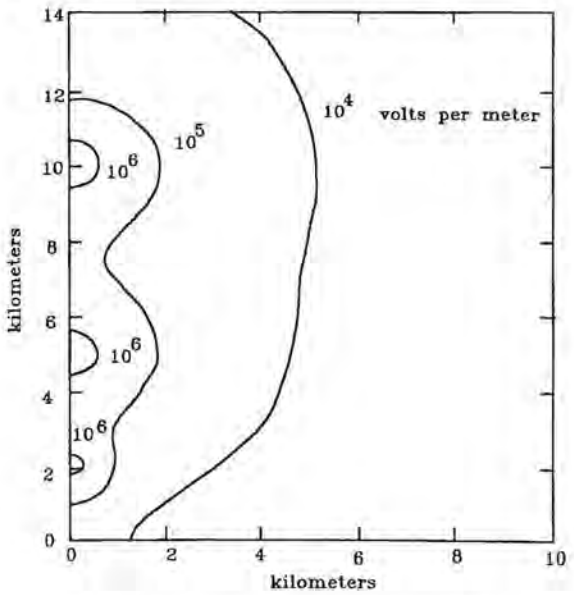

Fig. 3.22 Magnitude of total electric field.

3.7.2 The Response of Aircraft to Triggered Lightning

In elementary terms the response of an aircraft is illustrated on Fig. 3.23, which shows the F–106 aircraft flying directly toward a positive charge center. The aircraft, in response to the ambient field will become polarized; that is, electrons will be pulled from the aft end towards the nose. Thus it will accumulate a negative charge (surplus of electrons) at the nose and a positive charge (deficiency of the electrons) at the aft end, though the net charge on the aircraft will remain unchanged. The field strength at the surfaces of the aircraft will be the sum of that due to the incident electric field and the fields due to the induced charges, which is to say that the field will be enhanced by the presence of the aircraft. The electric field at the nose will point towards the fuselage and at the aft end will point away from the fuselage, the polarity of the fields being as defined in §2.2.2. For the orientation shown, the enhanced field will be largest at the nose of the aircraft.

As the aircraft flies towards the charged regions the electric fields at the surface of the aircraft will slowly increase; that is, become more negative at one end and more positive at the other end. Eventually the enhanced field at the nose will become large enough to cause a burst of corona, the electrons at the nose flowing off into the air ahead of the nose. This will reduce the field at the nose (make it less negative) and ultimately arrest the discharge.

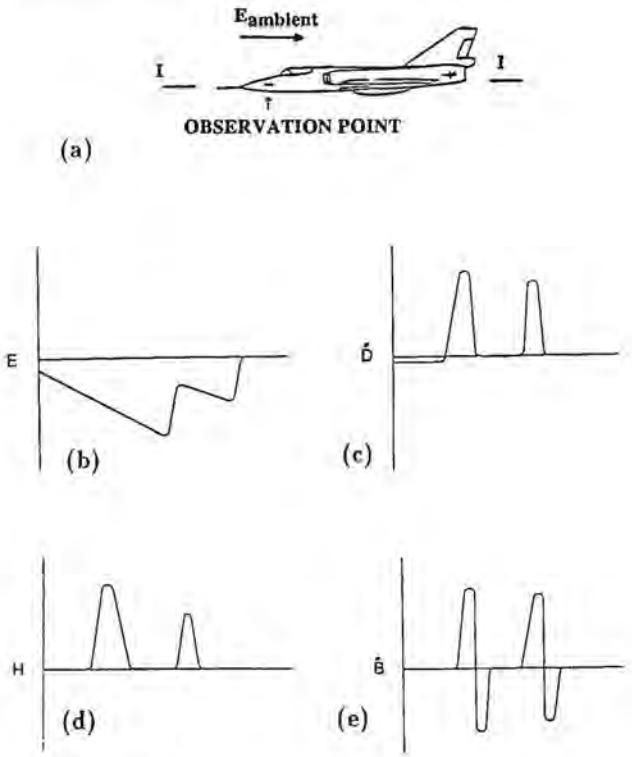

Fig. 3.23 Expected behaviour of triggered lightning for nose to tail oriented electric field.
(a) Observation point
(b) and (c) Electric field
(d) and (e) Magnetic field

The flow of electrons from the nose can equally well be viewed as a flow of positive charge from the air onto the aircraft, thus leaving the aircraft with a net positive charge. This additional positive charge will enhance the field at the aft end, eventually causing another breakdown there. That discharge may be viewed either as transferring positive charge into the air aft of the aircraft or as transferring negative charge from the air into the aircraft. Not every discharge at the nose will cause a simultaneous discharge at the aft end, but on balance all the negative charge transferred into the air at the nose will be balanced by charge transferred into the aircraft from a discharge at the aft end. The net result is a pulse of current flowing through the air-

craft, or more commonly two pulses of current, one charging the aircraft and another discharging it, the pulses being seperated by several tens or hundreds of nanoseconds. The shape of the pulses into and out of the aircraft will be different since the mechanisms will be somewhat different. One will have the characteristics of the negative discharges discussed in Chapter 1 and the other will have the characteristics of the positive discharges.

As the discharges extend into the air they will further enhance the electric field at their tips and, provided the ambient field is sufficient, will continue to grow. The two oppositely directed discharges thus act to transfer electrical charge out of one portion of the air and through the aircraft into another portion of the air.

Fig. 3.20 illustrated conditions such that a discharge would start at the nose and exit at the aft end, but other discharge paths are also possible, depending on the orientation of the aircraft relative to the electric field. On the F-106B most discharges (not all) involved the nose boom, but exit points on the wing tips and tail were common. On a larger aircraft one might expect discharges to start at points other than the nose.

Waveshape of current: The current flowing through the aircraft produces electromagnetic fields. For sensors located as indicated on Fig. 3.23, the electric and magnetic fields, and their derivatives, would have the indicated shapes. On the F- -106B only the D-dot and B-dot sensors had bandwidth sufficient to record the above phenomena; D-dot corresponding to the rate of change of electric field and B-dot corresponding to the rate of change of magnetic field. The plots are simplified to the extent of ignoring any behavior caused by the resonances of the aircraft.

Actual records could be expected to look like those in Fig. 3.23 only with respect to general features, but it is significant that both single pulses and double pulses are seen in the data measured on the aircraft. Fig. 3.24 shows examples [3.56]. The initial air breakdown takes place in a fraction of a microsecond and has a high frequency content sufficient to excite aircraft resonances and produce current waves that propagate back and forth between the extremities of the aircraft. These aircraft resonances are important in that they may enhance the coupling of electric and magnetic fields to the wires in the aircraft.

There are other facets of a triggered event which can last as long as a second [3.56]. For example, Fig. 3.25 shows for three different flashes the current flowing in the tip of the F-106B vertical fin. Each of the flashes produced a continuing current of average amplitude on the order of 80 amperes and lasting for about 0.3 seconds. Such magnitudes and duration are frequently found in the continuing current phase of flashes measured at ground level. The current, though, was not steady, it included many higher amplitude pulses superimposed on an underlying current. The recording channel with which the current of Fig. 3.25 was measured had a DC response that allowed the continuing current to be recorded faithfully, but the frequency response extended only to 400 Hz, insufficient to resolve the amplitude and waveshape of the individual pulses.

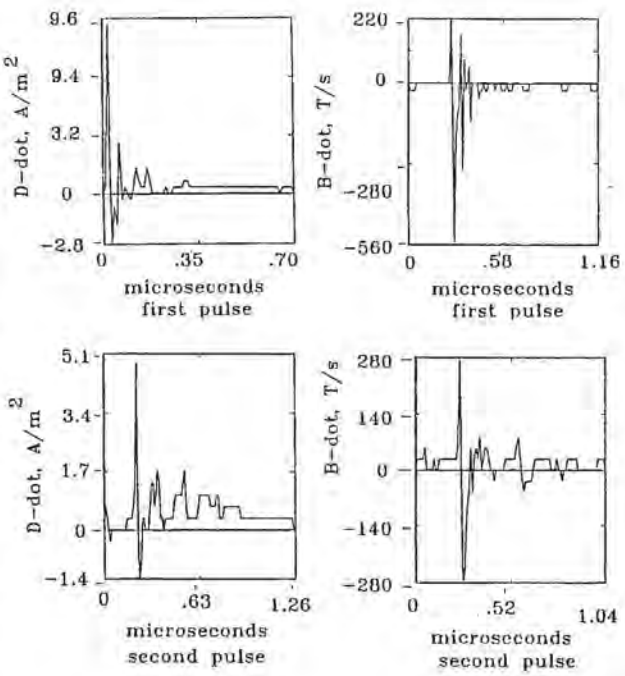

Fig. 3.24 Inflight D-dot and B-dot strike data.

Fig. 3.25 shows the character of another typical lightning flash, the figure showing the outputs from a number of different sensors as measured on a recorder with bandwidth 400 Hz to 100 kHz. Also shown is the fin current recorded with a dc to 400 Hz bandwidth. Each pulse of current is associated with a change of the electric field (D-dot) and a burst of light from the channel of the flash.

The fin current of Fig. 3.26 was also recorded with a digital transient recorder taking samples every 40 nanoseconds. Fig. 3.27 shows details of the first pulse of current from the fin, the time of triggering being indicated on Fig. 3.25. Pulses of current occur on average about every 50 μs. The highest amplitude pulse was 18 kA. Lightning currents of this nature are not noted at ground level.

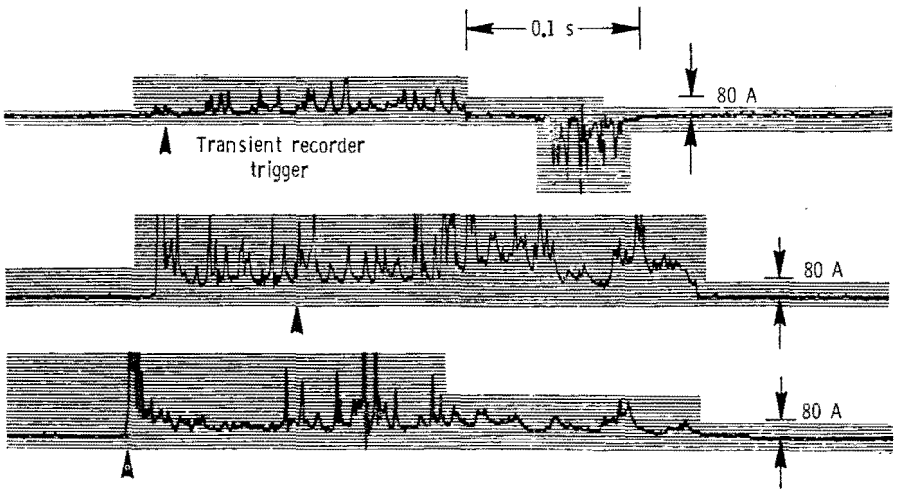

Fig. 3.25 Vertical fin currents.
Measuring bandwidth: DC to 400 kHz

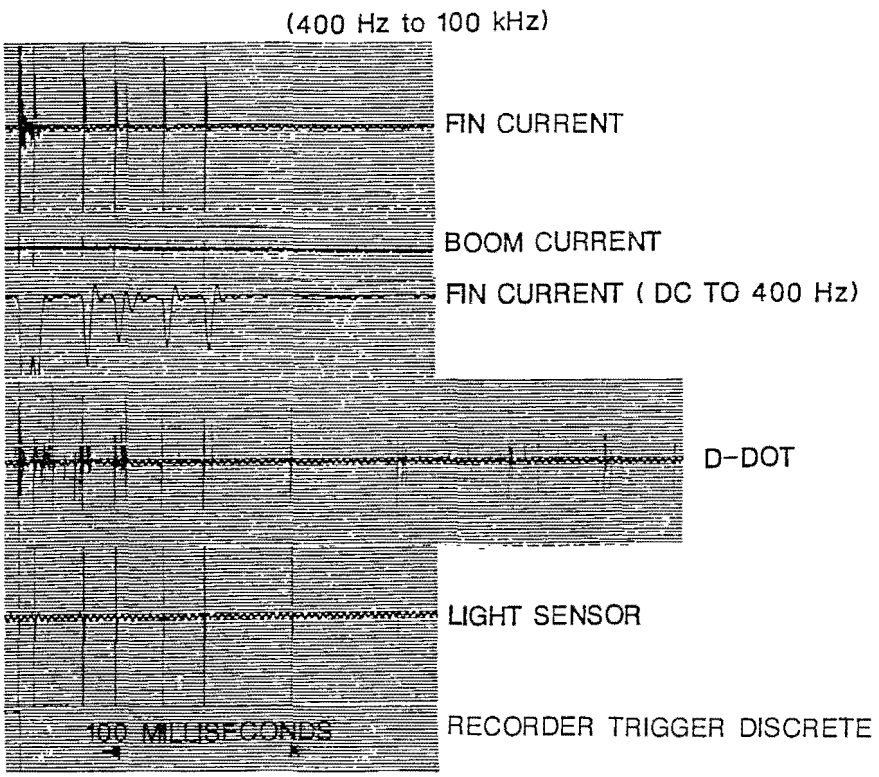

Fig. 3.26 Recordings made during the flash.

The measured current of Fig. 3.27 is of importance because it prompted the requirement for a *multiple burst* current test for indirect effects, as discussed further in Chapters 5 and 18.

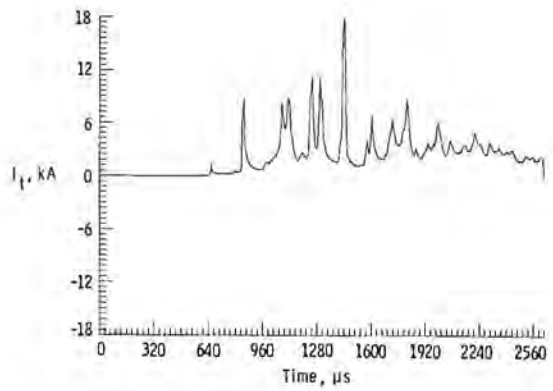

Fig. 3.27 Vertical fin current.

Rates of change: Rates of change of current and electric field are important quantities. The standardized lightning environment, discussed in Chapter 5, is largely based on measurements taken at ground level of cloud-to-ground lightning, but the measurements taken on the F–106B [3.56], provide some data on aircraft in flight and subjected to triggered lightning flashes. The data is summarized in Figs. 3.28 and 3.29. With 95% confidence the data suggest that the peak D-dot will exceed 48A/m^2 only 3.7 % of the time ($\pm$1%). With the same confidence the data suggest that the peak I-dot will exceed 250 kA/μs only 0.7 % of the time ($\pm$0.2%.

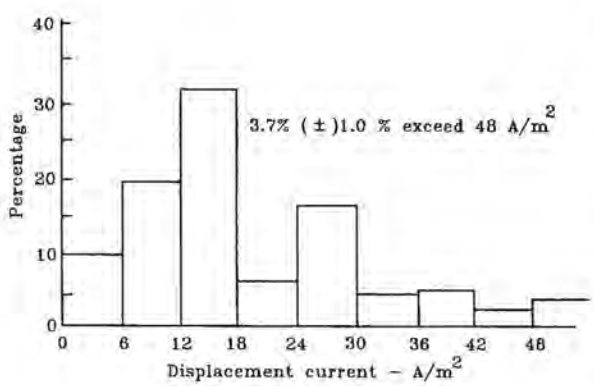

Fig. 3.28 D-dot measurements on the F–106B.

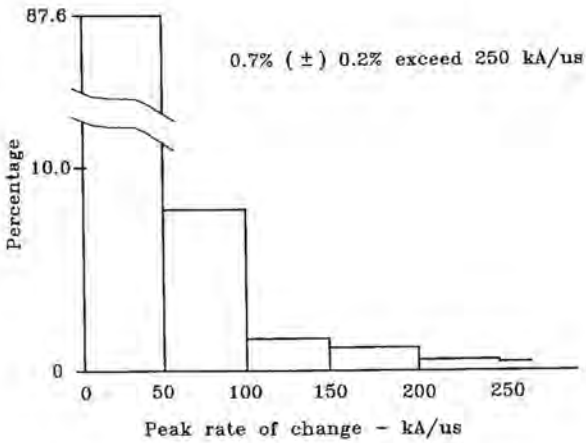

Fig. 3.29 I-dot measurements on the F–106B.

3.7.3 Calculation of Triggering Conditions

Calculation of the conditions that lead to lightning triggering conditions is accomplished by first computing the electric field gradients due to any net charge on the aircraft. The modeling techniques used for this are discussed further in Chapter 10. Then the fields on the aircraft caused by the static ambient thunderstorm fields can be added. The thunderstorm field magnitude which may enable triggering is that which causes the total field somewhere on the aircraft to exceed the corona level.

The location of this breakdown on the F–106B varied depending on the orientation of the field and the sign of the charge, but generally occurred in one of three places: the nose, one of the wing tips, or the tip of the vertical stabilizer. Occasionally two locations were involved, since a breakdown at one location might raise the local field at another location enough to cause a breakdown there also.

A number of calculations were made to illustrate the conditions under which the F–106B might trigger lightning, with results as summarized in Table 3.6. Calculations were made for several values of net charge on the aircraft. The maximum charge, Q_m, was taken to be 1.779 mC, the charge which by itself would cause corona to form on the aircraft. It should be noted that this aircraft had no static dischargers. If it had, they would probably have bled off charge and not allowed the aircraft to hold as much charge.

Along the upper row of the matrix in Table 3.6 is shown the orientation of the ambient electric field, the three orientations being along the principal coordinate axes of the aircraft; end to end along the the fuselage, wing to wing, and top to bottom. Both signs of field

Table 3.6

High and Low Altitude Triggering Fields For F106 vs Charge, Altitude and Orientation of Field

Aircraft Charge	Back to Front	Front to Back	Right to Left	Left to Right	Bottom to Top	Top to Bottom
0	190	190	280	280	470	470
	250	250	380	380	590	590
$+0.5Q_m$	107	200	200	200	300	600
	140	230	210	210	350	660
$-0.5Q_m$	273	150	200	160	640	300
	230	160	210	210	660	350
$+Q_m$	24	50	20	20	80	80
	34	60	40	40	120	160
$-Q_m$	24	15	20	20	80	80
	60	34	40	40	160	120

The top number is the high altitude field magnitude in kV/m. The bottom number refers to sea level.

are considered, because a negative corona air breakdown is different from a positive corona air breakdown.

In the leftmost column of each matrix is the net charge that was placed on the aircraft. Five charge values were used: no charge, $\pm 0.5\ Q_m$ and $\pm\ 1.0\ Q_m$.

The values in the interior of the matrix are the magnitudes of the thunderstorm electric field which would cause triggered lightning, or at least cause a burst of corona from the aircraft that has the potential of developing into a lightning channel. Note that, as expected, the field magnitudes are much less for the cases in which the aircraft has a pre–existing static charge of Q_m, because for those cases, the charge itself (by definition of Q_m) produces virtually all of the field necessary to produce breakdown.

A pre–existing charge on the aircraft, as from collisions with particles (triboelectric charging) is not sufficient to cause extended streamer propagation away from the aircraft and development into full fledged lightning leaders. As discussed earlier, there must be a pre–existing ambient field for leader *propagation* to occur. Pierce [3.17] suggests that requisite field strength is on the order of 10 kV/m. Thus aircraft charged or exposed to fields due only to triboelectric ("P–static") charging may develop corona and limited streamering at their extremities, but will not trigger lightning flashes, because there is not a pre–existing field into which the streamer can develop and extract the energy needed for further propagation.

A more intense ambient field is necessary to produce triggering if the charge on the aircraft is only half of Q_m. Field levels of the order 100 - 250 kV/m are needed to produce triggering if the field is oriented fore and aft along the aircraft. A somewhat stronger field is needed if the field is oriented wing to wing. Fields of these magnitudes are found in clouds and are consistent with the fields found necessary to cause breakdown in air gaps subjected to externally applied impulses.

Fields having magnitudes 300 - 600 kV/m would be necessary to cause triggering if the field were oriented top to bottom along an aircraft, with geometry similar to the F–106B. The fact that most flashes to the F–106 started at, or at least involved, the nose boom suggests that vertical fields of that magnitude are seldom encountered. Laboratory studies also suggest that fields of that magnitude are apt to lead to lightning flashes even without the intrusion of an aircraft.

The Effects of Aircraft Size and Shape on Trigger Conditions: Aircraft shape and aircraft size both affect the degree to which the fields at the surface of the aircraft are enhanced. The thunderstorm environment necessary for a triggered strike may be different for different types of aircraft; that is, for an identical thunderstorm environment, one aircraft may encounter a naturally occurring direct strike, while a second dif-

ferently shaped or sized aircraft will instead trigger a lightning flash. For this reason the study on the F–106 [3.56] included an investigation of the effects of aircraft size and shape. The aircraft studied were:

1. Half size F–106
2. Double size F–106
3. Normal size F–106, but delta wings replaced with more conventional straight wings
4. Normal size C–130
5. Normal size F–106

The first two aircraft cover a size range from approximately 10 m (35 ft) to 40 m (140 ft). Although the field enhancements around these two aircraft are, of course, the same, the effects of a given net charge on the aircraft are much different. The resonant characteristics of the aircraft would also be different.

The modified F–106 without the delta wing is meant to test the effect of the delta wing on field enhancements, resonant response, and charge storage properties. In particular, charge storage could be significantly affected, because the large flat delta wings increase the capacitance of the aircraft. This shape is typical, though somewhat larger, of some high performance general aviation aircraft.

The C–130 is representative of the shapes found in large transport category aircraft. It has more rounded contours, particularly at the nose.

The normal size F–106 is included for comparison purposes and determination of relationships with actual flight data.

For each aircraft, two different environments were used. In both, the net charge on the aircraft was fixed at -0.5 Q_m, where Q_m is the maximum charge which can be on the aircraft without causing corona to form at the extremities. Q_m is, of course diferent for each aircraft. Two orientations of the ambient field orientations were studied, one with the field oriented from nose to tail and the other oriented from top to bottom. For consistency, all computations were done for an altitude of 8300 m (27 000 ft) with an assumed relative air density of 0.5 and with a water vapor percentage of zero.

The results are summarized in Table 3.7. The field values, E_{mag} represent the minimum ambient field necessary to produce a triggered strike on the given aircraft model for the given orientation and Q_m. The labels NT and TB refer to nose to tail and top to bottom ambient field orientations, respectively.

Table 3.7

Trigger Conditions for Aircraft of Various Sizes and Shapes

Aircraft	Field Orientation	Q_m (mC)	E_{mag} (kV/m)
1/2 x F106	NT	0.49	100
	TB	0.49	250
2 x F106	NT	7.90	100
	TB	7.90	250
Straight Wing F106	NT	2.00	120
	TB	2.00	240
C130	NT	6.90	190
	TB	6.90	210
Normal F106	NT	1.79	130
	TB	1.79	310

NT = nose to tail
TB = top to bottom

Several items are apparent from Table 3.7. First, size is by far the dominant determining factor for Q_m. For aircraft with similar shapes, one would expect Q_m to scale in proportion to the surface area, that is, as the square of the length. This is seen to be true, as Q_m varies by a factor of about 16 between the half size and the double size F–106.

A second thing to notice is the effect of the delta wing. Q_m for the normal size F–106 with delta wing is 1.79 millicoulombs and is 2 millicoulombs without the delta wing. This is a somewhat surprising result, as one might expect the large surface area of the delta wing to hold a large amount of charge. However, the presence of the delta wing changes the static electrical characteristics of the aircraft considerably. Because of the delta wing at the rear of the aircraft, field enhancements are significantly larger around the nose. In fact, a nose to tail oriented field has an enhancement factor of 6.3 for the aircraft without the delta wing, and 7.2 for the aircraft with the delta wing. The same type of phenomenon occurs for a given net charge. That is, the charge arranges itself on the delta wing aircraft in such a way that it takes less charge to bring about corona formation.

Of importance also in Table 3.7 is the magnitude of the field required for a lightning strike on the C–130. For the nose–tail field direction, Q_m it is several times that required for the F–106. This is attributable to the bluntness of the nose of the C–130. In actual practice, the triggering field may differ by even more. The reason for this is that the C–130 is quite accurately represented near the nose by the model used for these calculations so its maximum enhancement should be

fairly accurate. However, the sharp nose boom on the F–106 is less accurately modeled, so actual enhancements on the F–106 are likely to be larger than the model predicts.

Hybrid lightning: A third type of strike to an aircraft is possible, which may be called a "hybrid" strike in that it is a combination of a triggered and natural event. A natural lightning leader channel might pass near the aircraft, but not near enough for the distortion in the electric field produced by the aircraft to alter the channel course. The lightning leader, being highly charged, creates in the space around it an intense electric field. The field at the aircraft might then be large enough to cause a triggered streamer from the aircraft. The streamer would then certainly propagate to the natural channel, becoming a branch of the natural leader. It is unclear whether a strike of this kind would be more characteristic of a natural strike or a triggered strike.

A simple calculation can be done to get some idea of how near a natural leader must be to the aircraft to cause a hybrid strike. For simplicity, the natural channel will be assumed to be vertical and have a uniform charge density per unit length. Also, steady state conditions will be assumed, a valid assumption since the lightning leader propagates so much slower than the velocity of light that no retardation effects need be considered. The electric field around an infinitely long line of charge Λ per unit length is radially directed and given by:

$$E_r = \frac{\Lambda}{2\pi\epsilon_0 r} \tag{3.1}$$

where

$$\epsilon_0 = 4\pi \times 10^{-7}\text{H/m}$$
$$r = \text{radius of the line of charge (m)}.$$

If one assumes an enhancement factor for the aircraft of about 10, which is typical around the nose of the F–106B aircraft, the distance at which triggering would occur is:

$$r_{\text{trig}} = \frac{\Lambda}{2\pi\epsilon_0(E_b/10)} \tag{3.2}$$

where E_b is the air breakdown field. A typical value for Λ is 5 coulombs over a 3 kilometer distance or 1.667×10^{-3} coulombs per meter. E_b varies with altitude, being about 3×10^6 V/m at sea level and about 1.5×10^6 V/m at 27 000 feet . Substituting these numbers into the above equations gives triggering distances of approximately 100 meters at sea level and twice that at 8000 m (27 000) feet altitude. This is a significantly greater distance than the distance at which the presence of the aircraft can directly alter the course of a natural lightning channel and hence a hybrid flash would appear much more likely to contact an aircraft than would a natural strike.

The region through which the passage of a natural lightning leader might be expected to initiate a leader from the aircraft can be called the capture cross section. A detailed study of the hybrid lightning process [3.57] has been done for the F–106. Fig. 3.30 shows the capture cross section as a function of altitude. The parameters for this calculation were zero net charge on the aircraft and a channel charge density of 1×10^{-3} C/m.

The capture cross section is also a function of aircraft net static charge. A summary of this variation is shown in Table 3.8. It is seen that the cross section is on the order of 10^4 square meters and increases with increasing altitude and charge.

The capture cross section can be combined with aircraft flight patterns and the flash rate density of a storm to obtain the expected probability of a strike to the aircraft. Calculations of this type have been done to try to enhance the probability of lightning attachment to the F–106B research aircraft [3.71].

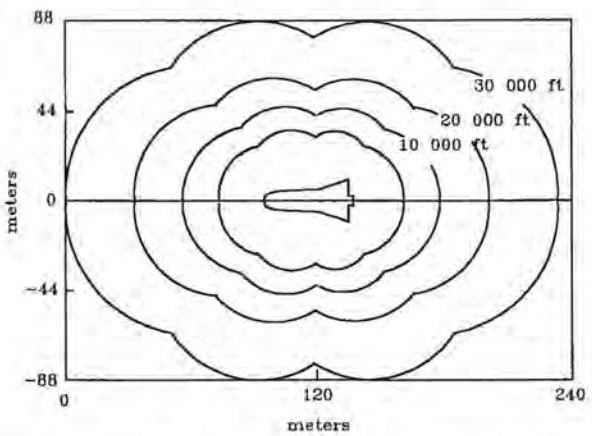

Fig. 3.30 Capture cross section vs altitude.

Table 3.8

Mean Capture Cross Section Area ($\times 10^4$ m^2) vs Altitude and Charge (μC) on the Aircraft

Altitude	$Q = 0$	$Q = -300$	$Q = -600$	$Q = -900$
Sea level	0.455	0.471	0.510	0.579
10 000 ft	0.830	0.878	1.012	1.273
20 000 ft	1.561	1.726	2.247	3.263

3.8 The Atlas Centaur 67 Incident

A significant lightning event occurred in March, 1987, when Atlas Centaur flight 67 was struck by lightning during launch, resulting in loss of the vehicle and payload [3.58 – 3.59]. It was determined that the rocket triggered the strike, evidently when the vehicle had achieved an altitude of about 3500 m (12 000 ft). The flash to the vehicle was not seen since the vehicle was in clouds, but a flash that continued to ground near the launch tower was seen at the same time, presumably a continuation of the flash to the vehicle. Evidence from ground based field mills and numerical analysis techniques indicate that the triggering field was on the order of 50 kV/m. Estimates of the lightning current amplitudes based on lightning location system data and analysis of the debris indicated that the current level was probably less than average. The lightning event induced transients in wiring to the flight computer, resulting in a change of a single word in the computer memory. That was sufficient to cause the vehicle to go off course and be destroyed.

This lightning event has created new interest in the lightning community and has had significant impact on launch rules.

REFERENCES

3.1 L. P. Harrison, "Lightning Discharge to Aircraft and Related Meteorological Conditions," *Technical Note 1001*, National Advisory Committee for Aeronautics, Washington, D.C. ,May 1946.

3.2 M. M. Newman and J. D. Robb, "Aircraft Protection from Atmospheric Electrical Hazards," *ASD Technical Report 61-493, or L and T Report 374*, Lightning and Transients Research Institute, Minneapolis, Minnesota, December 1961.

3.3 "Lightning Strike Survey Report for the Period of January 1965 through December of 1966," *Federal Aviation Agency Report of the Conference on Fire Safety Measures for Aircraft Fuel Systems. Appendix II.* Department of Transportation, Washington D.C., December 1967.

3.4 B. I. Hourihan, "Data from the Airlines Lightning Strike Reporting Project," June 1971 to November 1974, *Summary Report GPR-75-004*, High Voltage Laboratory, Electromagnetic Unit, Corporate Research and Development, General Electric Company, Pittsfield, Massachusetts, March 1975.

3.5 R. B. Anderson and H. Kroninger, "Lightning Phenomena in the Aerospace Environment: Part II, Lightning Strikes to Aircraft," *Proceedings of the 1975 Conference on Lightning and Static Electricity*, December 1975.

3.6 J. A. Plumer and B. L. Perry, "An Analysis of Lightning Strikes in Airline Operation in the USA and Europe," *Proceedings of the 1975 Conference of Lightning and Static Electricity*, December 1975.

3.7 O. K. Trunov, "Conditions of Lightning Strikes in Air Transports and Certain General Lightning Protection Requirements," *Proceedings of the 1975 Conference on Lightning and Static Electricity*, December 1975.

3.8 N. O. Rasch, M. S. Glynn and J. A. Plumer, "Lightning Interaction With Commercial Air Carrier Type Aircraft," *International Aerospace and Ground Conference on Lightning and Static Electricity*, Orlando, Florida, 26–28 June, 1984, paper 21.

3.9 H. T. Harrison, "UAL Turbojet Experience with Electrical Discharges", *UAL Meteorological Circular No. 57*, United Air Lines, Chicago, Illinois, January 1, 1965.

3.10 W. B. Beckwith, "The Use of Weather Radar in Turbojet Operations', *UAL Meteorological Circular No. 53*, United Air Lines, Denver, Colorado, April 1, 1965.

3.11 H. R. Hoffman and G. W. Peckham, "The Use of Airborne Weather Radar" , United Air Lines, Denver, Colorado, 1968, p. 12.

3.12 T. H. Rudolph et al., "Investigations Into the Triggered Lightning Response of the F106B Thunderstorm Research Aircraft," *NASA Contractor Report 3902*, June 1985.

3.13 D. R. Fitzgerald, "Probable Aircraft Triggering of Lightning in Certain Thunderstorms," *Monthly Weather Review*, December 1967, pp. 835-42.

3.14 G. A. M. Odam, "An Experimental Automatic Wide Range Instrument to Monitor the Electrostatic Field at the Surface of an Aircraft in Flight," *Technical Report 69218*, Royal Aircraft Establishment, Farnborough Hants, England, October 1961.

3.15 J. F. Shaeffer and G. L. Weinstock, "Aircraft Related Lightning Mechanisms", *Technical Report AFAL-TR-72-386*, prepared by the US Air Force Avionics Laboratory, Air Force systems Command, Wright-Patterson Air Force Base, Ohio, January 1973.

3.16 R. H. Golde, *Lightning Protection*, Edward Arnold, London, 1973.

3.17 E. T. Pierce, "Triggered Lightning and Some Unsuspected Lightning Hazards," *American Association for the Advancement of Science, 138 the Annual Meeting, 1971*, Stanford Research Institute, Menlo Park, California, January 1972.

3.18 J. E. Nanevicz, E. T. Pierce, and A. L. Whitson, " Atmospheric Electricity and the Apollo Series", *Note 18*, Stanford Research Institute, Menlo Park, California, June 1972.

3.19 R. T. Fowler, *Ion Collection by Electrostatic Probe in a Jet Exhaust*, graduate thesis, Air Force Institute of Technology, Wright-Patterson Air Force Base, Ohio, June 1970.

3.20 E. T. Pierce, "Atmospheric Electric and Meteorological Environment of Aircraft Incidents Involving Lightning Strikes", *Special Interim Report 1*, Stanford Research Institute, Menlo Park, California, October 1970.

3.21 "Protection of Aircraft Fuel Systems Against Lightning," *Federal Aviation Agency Advisory Circular AC 20-53*, Federal Aviation Administration, Department of Transportation, Washington, DC, October, 1967.

3.22 B. Vonnegut, "Electrical Behavior of an Aircraft in a Thunderstorm," Federal Aviation Admin., *Rep. FAA-ADS-36*, February 1965.

3.23 D. R. Fitzgerald, "Probable Aircraft Triggering of Lightning in Certain Thunderstorms," *Monthly Weather Review*, Vol. 95, p. 835, 1967.

3.24 B. J. Petterson, and W. R. Wood, "Measurements of Lightning Strikes to Aircraft," Final Report to Fed. Aviation Admin. under Contracts FA65WA1-94 and FA66NF-AP-12, January 1968.

3.25 W. E. Cobb and F. H. Holitza, "A Note on Lightning Strikes to Aircraft," *Monthly Weather Review*, Vol. 96,No. 11, Nov., 1968.

3.26 D. R. Fitzgerald, "Aircraft and Rocket Triggered Natural Lightning Discharges," *Lightning and Static Electricity Conference*, December 1968.

3.27 M. M. Newman, J. R. Stahmann, J. D. Robb, E. A. Lewis, S. G. Martin and S. V Zinn, "Triggered Lightning Strokes at Very Close Range," *J. Geophys. Res.*, Vol. 72, p. 4761, 1967.

3.28 R. Godfrey, E. R. Mathews, and J. A. McDivitt, "Analysis of Apollo 12 Lightning Incident," *NASA (MSC) Rep. 01540*, February 1970.

3.29 M. Brook, C. R. Holmes, and C. B. Moore, "Lightning and Rockets: Some Implications of the Apollo 12 Lightning Event," *Naval Research and Review*, April 1970.

3.30 E. T. Pierce, "Triggered Lightning and Its Application to Rockets and Aircraft," *1972 Lightning Conference Proceedings*, AFAL-TR-72-325.

3.31 J. F. Shaeffer, "Aircraft Initiation of Lightning," *1972 Lightning and Static Electricity Conf.*, pp 192-200, 12-15 December 1973.

3.32 D. W. Clifford, and H. W. Kasemir, "Triggered Lightning" *IEEE Trans. on Electromagnetic Compatibility*, Vol. EMC-24, No. 2, May 1983.

3.33 V. Mazur, B. D. Fisher, and J. C. Gerlach, "Conditions Conducive to Lightning Striking by an Aircraft in a Thunderstorm" *Proc. of the 8th Int. Aerospace and Ground Conf. on Lightning and Static Electricity*, Fort Worth, TX, DOT/FAA/CT-83-25, June 1983.

3.34 R. Rudolph, and R. A. Perala, "Linear and Nonlinear Interpretation of the Direct Strike Lightning Response of the NASA F-106 Thunderstorm Research Aircraft," *NASA CR-3746*, December 1983.

3.35 T. Rudolph, R. A. Perala, P. M. McKenna, and S. L. Parker, "Investigations into the Triggered Lightning Response of the F-106 Thunderstorm Research Aircraft," *NASA CR-3902*, June 1985.

3.36 T. H. Rudolph, R. A. Perala, C. C. Easterbrook and S. L. Parker, "Development and Application of Linear and Nonlinear Methods for Interpretation of Lightning Strikes to Inflight Aircraft," *NASA CR 3974*, 1986.

3.37 J. A. Bicknell, and R. W. Shelton, "The Energy Requirements of an Aircraft Triggered Discharge," *10th Int. Aerospace and Ground Conf.*, Paris, France, pp 217-221, 1985.

3.38 J. A. Bicknell, and R. W. Shelton, "Some Possible Energy Requirements of a Corona Triggered Lightning Stroke," *VIIth Int. Conf. on Atmos. Electricity*, Albany, NY, pp 438-440, June 3-8, 1984.

3.39 R. W. Shelton, and J. A. Bicknell, "Corona from Simulated Aircraft Surfaces and Their Contribution to the Triggered Discharge," *Int. Aerospace and Ground Conf. on Lightning and Static Electricity*, Dayton, Ohio, pp 28-1 - 28-9, June 24-26, 1986.

3.40 R. F. Griffiths, "The Initiation of Corona Discharges from Charged Ice Particles in a Strong Electric Field," *J. of Electrostatistics*, 1, 1975, 3-13.

3.41 T. H. Rudolph, et al., "Experimental and Analytical Studies of the Triggered Lightning environment of the F-106B," *EMA-87-R-37*, April 1987.

3.42 Y. Nagai, T. Koide and K. Kinoshita, "Relations of the Flashover Voltage Versus the Velocity of the Moving Electrode," Abstract, pp 23.1 - 23.8.

3.43 H. W. Kasemir, "Theoretical and Experimental Determination of Field, Charge and Current on an Aircraft Hit by Natural or Triggered Lightning," *Int. Aerospace and Ground Conf. on Lightning*

and Static Electricity, Orlando, FL, pp 2-1 2-10, June 24-26, 1984.

3.44 L. W. Parker, and H. W. Kasemir, "Predicted Aircraft Field Concentration Factors and their Relation to Triggered Lightning," *Int. Aerospace and Ground Conf. on Lightning and Static Electricity*, Dayton, Ohio, pp 9-1 - 9-18, June 24-26, 1986.

3.45 R. W. Ziolkowski, and J. B. Grant, "The Mathematical and Physical Scaling of Triggered Lightning" *Report No. DE84002480 UCID-19655*, Lawrence Livermore Laboratory, December 1983.

3.46 H. W. Kasemir, and F. Perkins, "Lightning Trigger Field of the Orbiter," *Report # CN 154148*, NOAA, Boulder, Co., October 1978.

3.47 G. Labaune, et al., "Experimental Study of the Interaction Between an Arc and an Electrically Floating Structure," *Int. Aerospace and Ground Conf. on Lightning and Static Electricity*, Dayton, Ohio, pp 27-1 - 27-9, June 24-26, 1986.

3.48 M. A. Uman, and E. P. Krider, "A Review of Natural Lightning: Experimental Data and Modeling," *IEEE Trans. on EMC*, Vol. EMC-24, No. 2, May 1983.

3.49 D. R. Fitzgerald, "Electric Field Structure of Large Thunderstorm Complexes in the Vicinity of Cape Canaveral," *Int. Conf. on Atmospheric Electricity*, June 3-8, 1984, Albany, N.Y., pp 260-263.

3.50 J. R. Gayet, "Location of Lightning Strokes on Aircraft in Storm Field with Measured Electrical, Microphysical and Dynamical Properties," *10th Int. Aerospace & Ground Conf. on Lightning and Static Electricity*, Paris, France, 1985.

3.51 Y. Goto, et al., "Electric Fields Produced by Winter Thunderstorms," *10th Int. Aerospace and Ground Conf. on Lightning and Static Electricity*, Paris, France, 1985.

3.52 Ishii, Masaru et al., "The Polarity of Ground Flashes and Possible Charge Structure in a Thundercloud," *VIIth Int. Conf. on Atmospheric Electricity*, Albany, New York, pp 339-343, June 3-8, 1984.

3.53 T. C. Marshall, W. D. Rust and W. P. Winn, "Screening Layers at the Surface of Thunderstorm Anvils," *VIIth Int. Conf. on Atmospheric Electricity*, Albany, New York, 3-8 June, 1984.

3.54 J. S. Schowalter, "Direct Lightning Strikes to Aircraft," *M.S. Thesis*, Air Force Institute of Technology, June, 1983.

3.55 D. J. Malan, *Physics of Lightning*, The English Universities Press Ltd., London, 1963.

3.56 F. L. Pitts, L. D. Lee, R. A. Perala and T. H. Rudolph, "New Results for Quantification of Lightning/Aircraft Electrodynamics," *J. of Electromagnetics*, Vol. 7, 1987, pp. 451-485.

3.57 R. S. Collier, T. Rudolph and R. A. Perala, "Enhancement of the Low Altitude Lightning Strike Capture Cross Section for an In-Flight Aircraft," *EMA Report EMA-86-R-35*, July 1986.

3.58 K. Crouch et al, "The Atlas Centaur 67 Incident," *Addendum to Proceedings of the 1988 International Aeropspace and Ground Conference on Lightning and Static Electricity*, Oklahoma City, OK., April 19 - 22, 1988.

3.59 R. A. Perala and T. H. Rudolph, "Triggering of Lightning by the Atlas Centaur Vehicle," *Proceedings of the 1988 International Aeropspace and Ground Conference on Lightning and Static Electricity*, Oklahoma City, OK., April 19 - 22, 1988.

3.60 *Report of Atlas/Centaur - 67/FLTSATCOM F-6 Investigation Board*, Vol 1. Final Report, National Aeronautics and Space Administration, Washington, DC., July 15, 1987.

CHAPTER 4

LIGHTNING EFFECTS ON AIRCRAFT

We had just taken off from Presque Isle, Maine, and had been in cruise power for 50 minutes, when a large thunderhead cumulus was observed directly on course. Lightning could be seen around the edges and inside the thunderhead. All cockpit lights were on and the instrument spotlight was full on, with the door open. I had just finished setting the power and fuel flows for each engine. As the ship approached the thunderhead, there was a noticeable drop in horsepower and the airplane lost from 180 MPH airspeed to 168 MPH, and continued to lose airspeed due to power loss as we approached the thunderhead...A few seconds before the lightning bolt hit the airplane all four engines were silent and the propellers were windmilling. Simultaneous with the flash of lightning, the engines surged with the original power. The lightning flash blinded the Captain and me so severely that we were unable to see for approximately eight minutes. I tried several times during this interval to read cockpit instruments but it was impossible. The First Officer was called from the rear to watch the cockpit. Of course, turbulent air currents inside the cumulus tossed the ship around to such an extent that, had the airplane not been on auto-pilot when the flash occurred and during the interval of blindness by the cockpit occupants, the ship could have easily gone completely out of control. The Captain and I discussed the reason for all four engines cutting simultaneously prior to the lightning flash and could not explain it, except for the possibility of a magnetic potential around the cumulus affecting the primary or secondary circuit of all eight magnetos at the same time.

First Officer N.A. Pierson's experience on a flight from Presque Isle, Maine, to the Santa Maria Islands on July 9, 1945 [4.1].

4.1 Introduction

It wasn't long after the beginning of powered flight that aircraft began being struck by lightning–sometimes with catastrophic results. Early wooden aircraft with metal control cables and guy wires were not capable of conducting lightning stroke currents of several thousand amperes or more. Wooden members and even the control cables exploded or caught fire. Even if severe structural damage did not occur, pilots were frequently shocked or burned by lightning currents entering their hands or feet via control pedals or the stick. Sometimes fuel tanks caught fire or exploded. These effects, coupled with the air turbulence and precipitation also associated with thunderstorms, quickly taught pilots to stay clear of stormy weather.

Early research: With the advent of all–metal aircraft, most of the catastrophic effects were eliminated, but thunderstorms continued to be treated with respect. Nonetheless, because a few bad accidents attributed to lightning strikes continued to happen, in 1938 the Subcommittee of Aircraft Safety, Weather and Lightning Experts was formed by the National Advisory Committee for Aeronautics (NACA) to study lightning effects on aircraft and determine what additional protective measures were needed. Dr. Karl B. McEachron, Director of Research at the General Electric High Voltage Laboratory, was a key member of this committee, and during its twelve year existence he performed the first man made lightning tests on aircraft parts. During and subsequent to this period, other organizations, such as the U.S. National Bureau of Standards, the University of Minnesota, and the Lightning and Transients Research Institute, also began to conduct research into lightning effects on aircraft.

Direct effects: For a long time the physical damage effects at the point of flash attachment to the aircraft were of primary concern. These included holes burned in metallic skins, puncturing or splintering of nonmetallic structures, and welding or roughening of moveable hinges and bearings. If the attachment point was a wing tip light or antenna, the possibility of conducting some of the lightning current directly into the aircraft's electrical circuits was also of concern. Today, these and other physical damage effects are called the *direct effects*. Since present day military and commercial aircraft fly IFR (Instrument Flight Rules) in many kinds of weather, protective measures against direct effects have been designed and incorporated into these aircraft so that hazardous consequences of lightning strikes are rare.

Indirect effects: In recent years it has become apparent that lightning strikes to aircraft may cause other effects, or *indirect effects*, to equipment located elsewhere in the aircraft. For example, the operation of instruments and navigation equipment has been interfered with, and circuit breakers have popped in electric power distribution systems when the aircraft has been struck by lightning. The causes of these indirect effects are the electromagnetic fields and the structural voltage rises associated with lightning currents in the aircraft. Even though metallic skins provide a high degree of electromagnetic shielding, some of these fields may penetrate through windows or seams and induce transient voltage surges in the aircraft's electrical wiring. The resistances of structural joints and nonmetallic structures permit voltages to occur between equipment locations in the aircraft. These surge voltages in turn may damage or upset electrical or electronic equipment.

Trends that increase potential hazard: To date, few aircraft accidents can be attributed positively to the indirect effects of lightning, but there are two trends in aircraft design which threaten to aggravate the problem unless specific protective methods are incorporated in system equipment designs. The first of these trends is the increasing use of miniaturized, solid state components in aircraft electronics and electric power systems. These devices are more efficient, lighter in weight, and far more functionally powerful than their vacuum tube or electromechanical predecessors, and they operate at much lower voltage and power levels. Thus, they are inherently more sensitive to overvoltage transients, such as those produced by the indirect effects of lightning.

The second trend is the increasing use of reinforced plastics and other nonconducting materials in place of aluminum skins, a practice that reduces the electromagnetic shielding previously furnished by the highly conductive aluminum skin. This reduced shielding may greatly increase the level of surges induced in wiring not protected by other means. Because electronic systems were being increasingly depended upon for safety of flight, the National Aeronautics and Space Administration, the Federal Aviation Aministration, and the Department of Defense initiated research programs, beginning in 1967, to learn how to measure or predict the levels of lightning induced voltages and how to protect against them. A considerable amount of research has been conducted since by government and industry organizations.

Since the indirect effects originate in the aircraft's electrical wiring, their consequences may show up anywhere within the aircraft, such as at equipment locations remote from the lightning flash attachments. The direct effects, on the other hand, occur most often at or near the points of lightning attachment or within structures or fuel tanks that lie within lightning current paths between strike entry or exit points. This comparison is illustrated in Fig. 4.1.

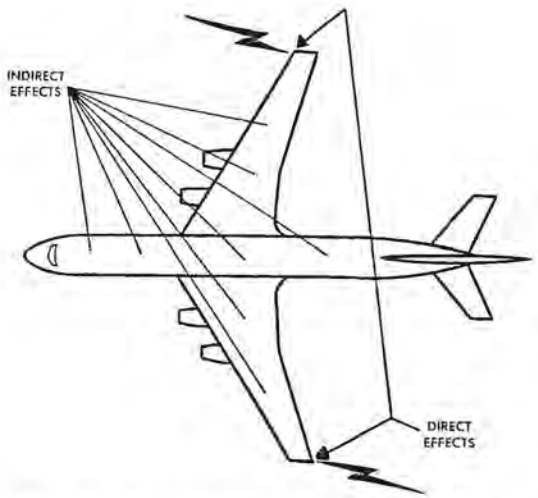

Fig. 4.1 Areas of direct and indirect effects.

Before discussing the techniques for protecting aircraft against either type of lightning effect, it is worthwhile to review some of the common examples of each which occur on today's aircraft. The purpose of this review is to remind the aircraft designer of areas needing particular attention and to alert pilots to what to expect when lightning strikes occur in flight. Detailed discussion of the causes of each effect, including the lightning flash characteristic most responsible and its quantitative relationship to damage severity, is deferred until protective measures are discussed, beginning with Chapter 6.

4.2 Direct Effects on Metal Structures

Metal structures include the outer skins of the aircraft together with internal metallic framework, such as spars, ribs, and bulkheads. Because lightning currents must flow between lightning entry and exit points on an aircraft and because these currents tend to spread out as they flow between attachment points, using the entire airframe as a conductor, the aluminum with which most of these structures are fabricated provides excellent electrical conductivity. As a result, the current density at any single point in the airframe is rarely sufficient to cause physical damage between entry and exit points. Only if there is a poor electrical bond (contact) between structural elements in the cur-

rent flow path is there likely to be physical damage. On the other hand, where the currents converge to the immediate vicinity of an entry or exit point, there may be a sufficient concentration of magnetic force and resistive heating to cause damage. Damage at these points is further compounded by the arc of the lightning channel, from which intense heat and blast forces emanate. Discussion of individual effects follows.

4.2.1 Pitting and Meltthrough

If a lightning channel touches a metal surface for a sufficient time, melting of the metal will occur at the point of attachment. Common evidences of this are the successive pit marks often seen along a fuselage or empennage, as shown in Fig. 4.2 [4.2] or the holes burned in the trailing edges of wings or empennage tips, as shown in Fig. 4.3 [4.3]. Most holes are melted in skins of 1 mm (0.040") thick, or less, except at trailing edges, where the lightning channel may hang on for a longer time and enable holes to be burned through much thicker pieces. Since a relatively large amount of time is needed for melting to occur, the continuing currents are the lightning flash components most conducive to pitting and meltthrough. Meltthrough of skins is usually not a safety–of–flight problem unless this occurs in an integral fuel tank skin.

Fig. 4.2 Successive pit marks extending aft from leading edge of vertical stabilizer.

4.2.2 Magnetic Force

Metal skins or structures may also be deformed as a result of the intense magnetic fields which accompany concentrated lightning currents near attachment points. It is well known that parallel wires with current traveling in the same direction are mutually attracted to each other. If the structure near an attachment point is viewed electrically as being made up of a large number of parallel conductors converging to this attachment point, then as lightning current flows from the point, forces occur which tend to draw these conductors closer together. If a structure is not sufficiently rigid, pinching or crimping may occur, as shown in Fig. 4.4 [4.4]. The amount of damage created is proportional to the square of the lightning stroke current amplitudes and is directly proportional to the length of time during which this stroke current flows. Thus the high amplitudes of return stroke and intermediate stroke are the lightning flash components most responsible for magnetic force damage.

Fig. 4.3 Hole melted in trailing edge corner of ventral fin.

Fig. 4.4 Example of magnetic pinch effect at lightning attachment points.

Besides the main airframe, other parts which may be damaged by magnetic forces include bonding or diverter straps, pitot probes, or any other object which may conduct lightning stroke currents. Magnetic force damage is usually not, by itself, significant enough to require abortion of flight, and may not even be detected until the aircraft is on the ground. However, since overstress or severe bending of metals is involved, aircraft parts damaged by this phenomenon are not often repairable.

4.2.3 Pitting at Structural Interfaces

Wherever poor electrical contact exists between two mating surfaces, such as a control surface hinge or bearing across which lightning currents may flow, melting and pitting of these surfaces may occur. In one incident, for example, the jackscrew of an inboard trailing edge flap of a jet transport was so damaged by a lightning flash that the flap could not be extended past 15 degrees. Since this jackscrew is located on the inboard side of the flap, the flash must have reached it after sweeping along the fuselage from an earlier attachment point near the nose, as shown on Fig. 4.5. Instead of continuing to sweep aft along the fuselage, the flash apparently hung on to the jackscrew long enough to melt a spot on it. The event did not cause difficulties in landing the aircraft, and the damage, in fact, was not discovered until after the aircraft was on the ground. The damage was extensive enough that the jackscrew had to be replaced.

The jackscrew in this instance was not an initial attachment point and it became an attachment point only by being in the path of a swept flash. This incident illustrates the fact that the lightning channels may reach seemingly improbable locations on the surface of an aircraft, and that protection designers must look beyond the obvious lightning attachment points to find potential hazards.

A second illustration of pitting is the damage caused to the seals of the hydraulic jack operating the tail control surfaces of another jet transport aircraft. In this case the jack was shunted by a jumper of adequate cross section to carry lightning stroke currents but of excessive length, which caused most of the current to flow through the lower inductance path directly through the jack body and across the seals, resulting in leakage of hydraulic fluid.

4.2.4 Resistive Heating

Another direct effect is the resistive heating of conductors exposed to lightning currents. When the resistivity of a conductor is too high or its cross–sectional area too low for adequate current conductance, lightning currents in it may deposit appreciable energy in the conductor and cause an excessive temperature rise. Since the resistivity of most metals increases with temperature rise, a given current in a heated conductor will deposit more energy than it would in an unheated, less resistant conductor; this process in turn increases the conductor temperature still further. Most metal structural elements can tolerate lightning current without overheating, and copper wires of greater than 0.5 cm^2 cross–sectional area can conduct severe lightning currents without overheating. Methodology for determining temperature rises in conductors of specific material or cross–sectional size is presented in Chapter 6. A wire of 0.5 cm^2 cross–sectional area corresponds to an American Wire Guide (AWG) No. 8 copper wire, as might be used for AC or DC power feed conductors.

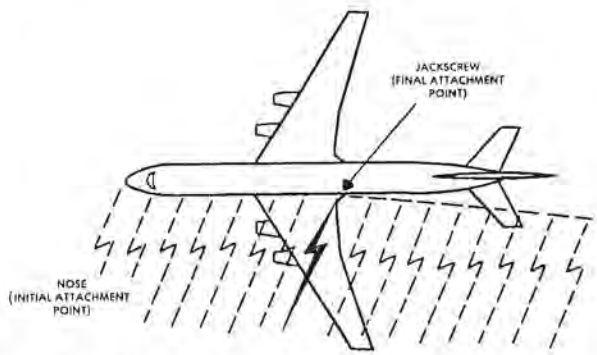

Fig. 4.5 Swept stroke attachment to inboard flap jackscrew.

Wire explosion: Resistive energy deposition is proportional to the action integral of the lightning current and for any conductor there is an action integral value at which the metal will melt and vaporize, as shown in Fig. 4.6. Small diameter wires, such as AWG 22 to 16, of the sizes commonly used to interconnect avionic equipment, or distribute AC power to small loads, will often melt or vaporize when subjected to full amplitude lightning currents.

Examples of the damage produced by explosive vaporization of conductors are shown in Figs. 4.7 and 4.8 [4.5, 4.6]. The damage is usually most severe when the exploding conductor is within an enclosure, such as the composite wing tips of Fig. 4.8, because then the explosion energy is contained until the pressure has built up to a level sufficient to rupture the container. Partly, the damage results because the chemical en-

ergy of combustion of the wire is released as it burns, and this adds to the energy deposited by the lightning current.

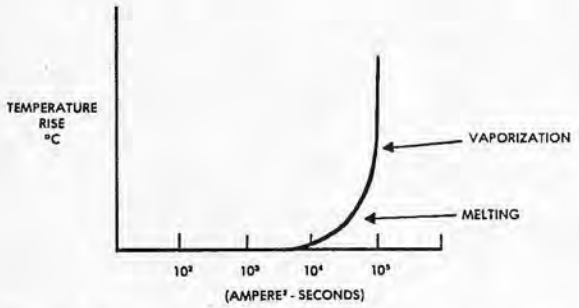

Fig. 4.6 (Ampere squared–seconds) vs temperature rise in a conductor.

Exposure of the wiring: In most cases, such wiring is installed within conducting airframes and so is not exposed to major amounts of the lightning current. Some exceptions occur, however, such as a wiring harness feeding a wingtip navigation light installed on a non–conductive, fiberglass wing tip that is not protected with protective coatings or other paths for lightning current. In such cases, lightning strikes to the navigation light vaporize and explode the wire harness, thus allowing the lightning current path to exist in plasma form within the wing tip. The accompanying shock wave can do extensive damage to the enclosing and adjacent structures, as illustrated in Fig. 4.7, which shows the remnants of a radome which enclosed a small diameter wiring harnesss feeding power to a pitot probe or heater.

Exploding wire harnesses are one of the most common and damaging lightning effects. They have, as far as is known, not had catastrophic consequences because these harnesses are usually found in secondary structures that are not flight critical. There is no reason, however, to allow these situations to persist because protection is easily applied, as will be described in Chapter 6. Such protection can also minimize the possibility of conducting lightning current surges into power distribution or avionic systems.

Fig. 4.7 Lightning damage to radome–probably as a result of exploding pitot tube ground wire.

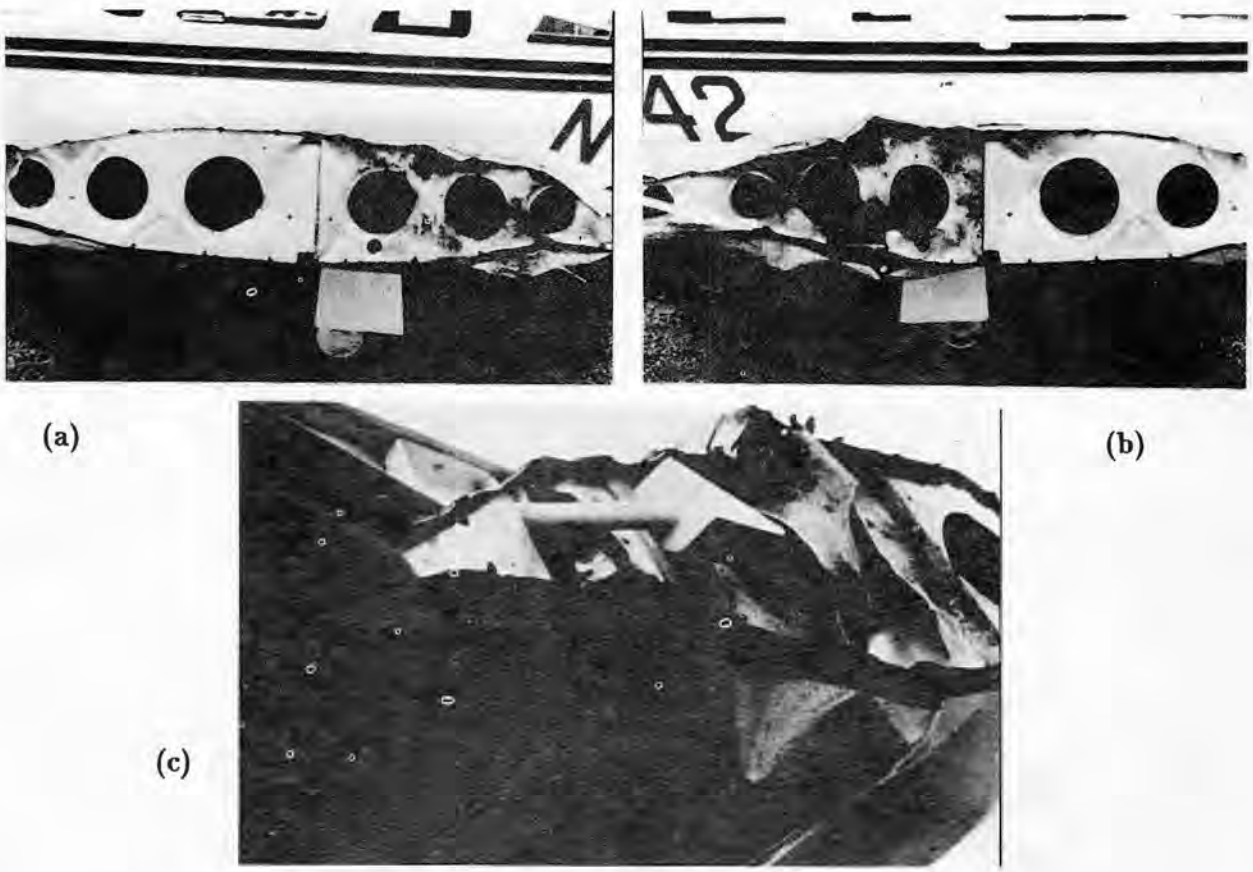

Fig. 4.8 Damaged wing tip structures due to exploding navigation light wire harnesses.
(a) Left wing tip, showing overpressure damage to aluminum outer wing
(b) right wing tip, showing similar overpressure damage to outer wing
(Note 1) Both fiberglass wingtips were destroyed by the strike in flight.
(Note 2) Flash entered at one wing tip and exited from the other.

4.2.5 Shock Wave and Overpressure

When a lightning stroke current flows in an ionized leader channel, as when the first return stroke occurs, a large amount of energy is delivered to the channel in 5 to 10 microseconds, causing the channel to expand with supersonic speed. Its temperature has been measured by spectroscope techniques to be 30 000 degrees K and the channel pressure (before expansion) about 10 atmospheres [4.7]. When the supersonic expansion is complete, the channel diameter is several centimeters and the channel pressure is in equilibrium with the surrounding air. Later, the channel continues to expand more slowly to the equilibrium situation of a stable arc. The cylindrical shock wave propagates radially outward from the center of the channel, and, if a hard surface is intercepted, the kinetic energy in the shock wave is transformed into a pressure rise over and above that in the shock wave itself. This results in a total overpressure of several times that in the free shock wave at the surface.

Depending on the distance of the channel from the aircraft surface, overpressures can range up to several hundred atmospheres at the surface, resulting in implosion type damage, such as that shown in Fig. 4.9 [4.8]. The lightning channel does not have to contact the damaged surface, but may simply be swept alongside it, as was evident in the case shown in Fig. 4.9. Apparently a return stroke or restrike occurred as the tip of the propeller passed just below the leading edge of the wing, positioning a cylindrical shock wave horizontally beneath the wing, as in Fig. 4.10. This hypothesis by Hacker [4.9] is supported by scorching of the paint on the imploded panels, an indication of a nearby heat source.

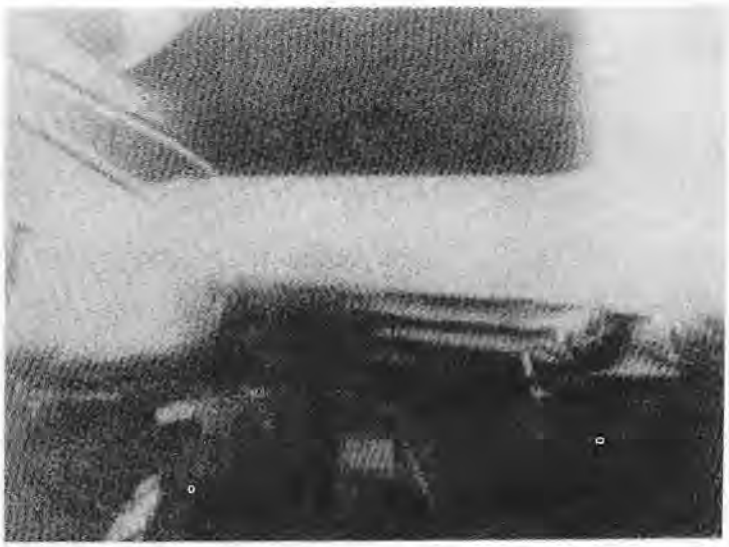

Fig. 4.9 Implosion damage from lightning flash overpressure. Flash swept aft beneath wing from propeller.

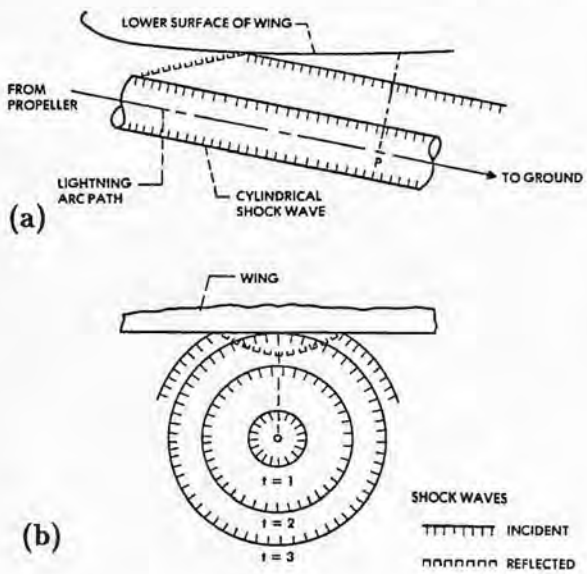

Fig. 4.10 Orientation of lightning path and shock wave with respect to lower side of aircraft wing shown in Fig. 4.9.
(a) Chordwise plane
(b) Fore–aft plane: perpendicular to lightning path at point P of part (a).

Other examples of shock wave implosion damage include cracked or shattered windshields and navigation light globes. Modern windshields, especially those aboard transport aircraft, are of laminated construction and evidently of sufficient strength to have avoided being completely broken by shockwaves and overpressures. Broken windshields resulting from a lightning strike, however, are considered a possible cause of the crash of at least one propeller driven aircraft [4.10].

4.3 Direct Effects on Nonmetallic Structures

Early aircraft of wood and fabric construction would probably have suffered more catastrophic damage from lightning strikes had it not been for the fact that these aircraft were rarely flown in weather conducive to lightning. The all–aluminum aircraft which followed were able to fly in or near adverse weather and receive strikes, but because aluminum is an excellent electrical conductor, severe or catastrophic damage from lightning was rare. There is a trend again, however, toward use of nonmetallic materials in aircraft construction. These include fiber reinforced plastics and polycarbonate resins, which offer improvement in cost and performance.

Non–conducting composites: Some of these materials have begun to replace aluminum in secondary structures, such as nose, wing and empennage tips, tail cones, wing–body fairings and control surfaces, and on several occasions the entire aircraft has been fabricated of fiber reinforced composites.

Often the nonmetallic material is used to cover a metallic object, such as a radar antenna. If this covering material is nonconducting, such as is the case with fiberglass, electric fields may penetrate it and initiate streamers from metallic objects inside. These streamers may puncture the nonmetallic material as they propagate outward to meet an oncoming lightning leader. This puncture begins as a pinhole, but, as soon as stroke currents and accompanying blast and shock waves follow, much more damage occurs.

An example of a puncture of a fiberglass honeycomb radome is shown on Fig. 4.11 [4.11]. In this case a streamer evidently propagated from the radar dish or some other conductive object inside the radome, puncturing the fiberglass–honeycomb wall and rubber erosion protection boot on its way to meet an oncoming lightning leader. Most of the visible damage was done by the ensuing stroke current.

Conductive composites: Plastics reinforced with carbon or boron fibers do have some electrical conductivity, and, because of this, their behavior with respect to lightning is considerably different from that of nonconductive materials. Carbon fiber composites (CFC) are employed extensively in secondary structural applications and occasionally in primary structures as well.

Boron reinforced composites were the subject of extensive development efforts in the 1970's, but failed to find applications in airframe design and, with a few exceptions, have disappeared from use.

To date, most CFC materials in lightning strike zones have been provided with suitable protection from lightning strike effects. Some in–flight lightning strikes have occurred, with superficial damage that has not become a flight safety hazard.

Simulated lightning tests which have been performed on CFC materials in the laboratory, however, have shown that unprotected composites may be damaged. The lightning damage is due to resistive heating of the carbon fibers, which vaporizes and ignites the binding resin and leaves the fibers in disarray, as shown in Fig. 4.12. Further damage results from the shock wave that accompanies the return stroke currents, and

Fig. 4.11 Puncture of a fiberglass–honeycomb radome.

this shock wave may crack thin CFC laminates. Unlike most aluminum alloys, which are ductile and will deform, but not break, CFC materials are stiff and may shatter. Fig. 4.13 shows the back sides of two test panels, one of aluminum and one of unprotected CFC, both of which had been subjected to the same simulated lightning test. The metal panel was only dented, but the CFC panel was badly broken.

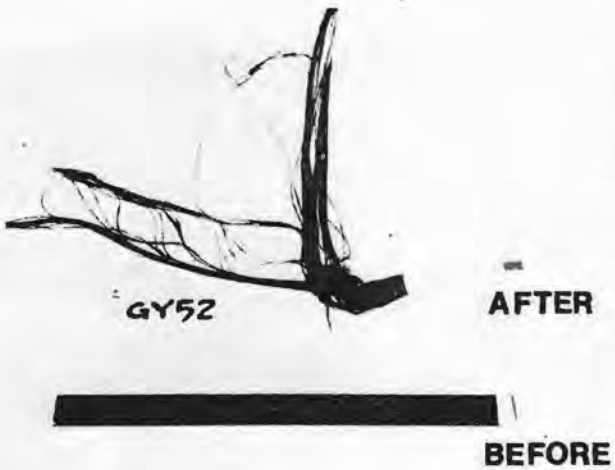

Fig. 4.12 Typical lightning stroke current damage to CFC skin material.

Other plastics: Transparent acrylics or polycarbonate resins are often utilized for canopies and windshields. These materials are usually found in *Zone 1* or *Zone 2* locations, where lightning flashes may attach or sweep by. Most of the polycarbonates are very good insulators, however, and so will successfully resist punctures by lightning or streamers. The electric field will penetrate them and induce streamers from conducting objects inside, but these streamers are not usually able to puncture a polycarbonate.

Fighter pilots beneath polycarbonate canopies have often reported electric shocks indicative of streamering off their helmets, but the current levels involved have not been harmful because the streamers have not come in direct contact with the lightning flash. Leaders approaching the outside of a canopy travel along its surface to reach a metallic skin, or those initially attached to a forward metal frame may be swept aft over a canopy until they reattach to an aft metallic point. Sometimes this occurrence will leave a scorched path across the canopy, as shown in Fig. 4.14 [4.12]. Scorches like this can usually be polished away.

Electric shock and flash blindness: While harmless to a canopy itself, flashes passing just outside frequently cause electric shock or flash blindness to the pilot. In at least one case shock or blindness to the pilot caused him to lose control of the aircraft at low altitude and resulted in a fatal accident.

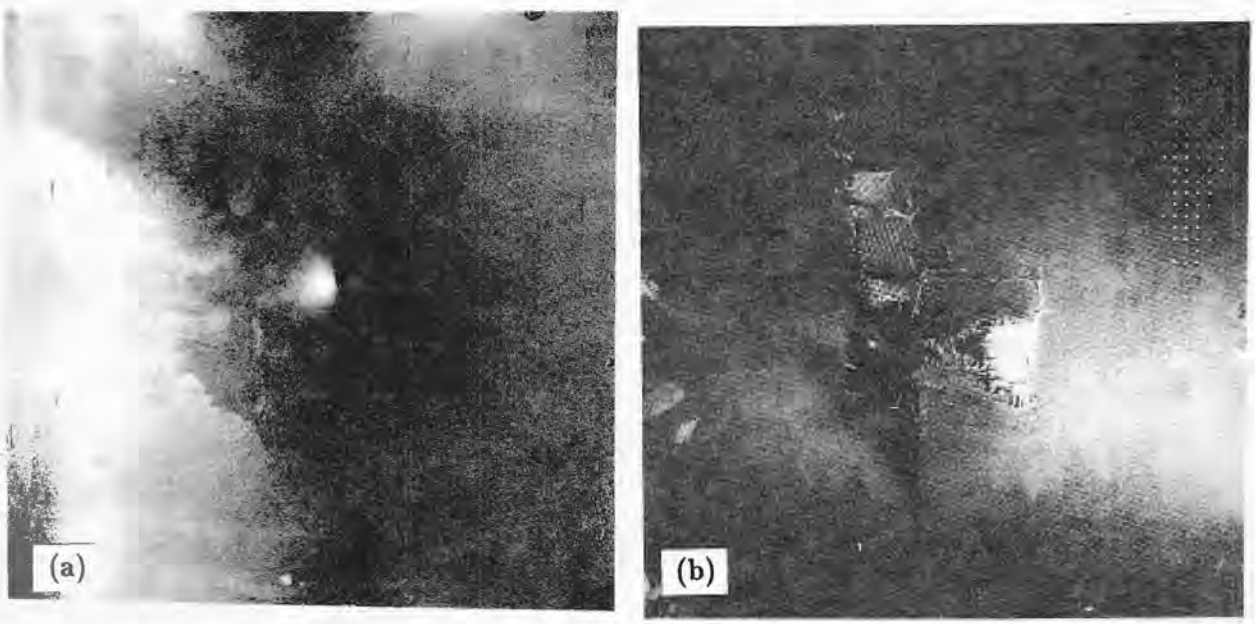

Fig. 4.13 Comparison of damage to different materials.
(a) Aluminum panel (b) CFC panel

Fig. 4.14 Evidence of lightning attachment to canopy fastener and scorching of canopy.

In addition to the direct effects described in the preceding paragraphs, replacement of metallic skins with nonmetallic materials removes the inherent protection against electromagnetic field penetration that is an important by–product of aluminum skins. Electrical wiring and electronic components enclosed inside nonmetallic skins are therefore likely to be much more susceptible to the indirect effects of lightning than those inside metallic skins unless specific measures are taken to reduce this susceptibility.

IR voltages: Airframes fabricated of CFC also have substantially more resistance than do aluminum airframes, and large potential differences, called *IR voltages* may arise between various locations in an airframe, contributing further to indirect effects on electrical and avionic systems. A further description of indirect effects is found in §4.7 and discussions of basic mechanisms are provided in Chapter 8.

4.4 Direct Effects on Fuel Systems

Aircraft fuel systems represent one of the most critical lightning hazards to flight safety. An electric arc conducting only one ampere or so of current is sufficient to ignite flammable hydrocarbon fuel vapor, yet lightning flashes inject may inject thousands of amperes of current into an aircraft.

There are several dozen civil and military aircraft accidents on record which have been attributed to lightning ignition of fuel. Examples are discussed in [4.13] and [4.14]. Although the exact source of ignition in each case remains obscure, the most likely possibility is that electrical arcing or sparking occurred at some structural joint or plumbing device not intentionally designed to conduct electric currents. Some accidents have been attributed to lightning ignition of fuel vapors exiting from vent outlets, but this has never been positively established.

In addition to the direct effects described above, there are several instances in which indirect effects have evidently accounted for ignition of fuel. Lightning induced voltages in aircraft electrical wiring are believed to have resulted in sparks, for example, across a capacitance type fuel probe or some other electrical object inside fuel tanks of several military aircraft, resulting in loss of external tanks in some cases and the entire aircraft in others. Capacitance type fuel

probes are designed to preclude such occurrences, and laboratory tests [4.15] have shown that the voltage required to spark a typical capacitance type probe is many times greater than that induced in fuel gauge circuits by lightning. However, other situations involving unenclosed circuits, such as externally mounted fuel tanks, exist wherein induced voltages may be much higher than those found in circuits completely enclosed by an airframe.

Outcome of research: The accidents referenced above prompted extensive research into the lightning effects on and protection of aircraft fuel systems. Improved bonding, lightning protected filler caps and access doors, active and passive vent flame suppression devices, flame retardant foams, and safer (i.e., less flammable) fuels are examples of developments which have resulted from this research. In addition, FAA airworthiness requirements now focus attention on lightning protection for aircraft fuel systems, as noted in Chapter 5. As a result of these safety measures, lightning strikes have presented fewer hazards to the fuel systems aboard modern transport aircraft than to those of older aircraft, and properly certified aircraft may expect to experience lightning strikes with no adverse effects on fuel systems. Continued changes in airframe designs and materials, however, make it mandatory that care and diligence in fuel system lightning protection not be relaxed in the future.

4.5 Direct Effects on Electrical Systems

If an externally mounted electrical apparatus, such as a navigation lamp or antenna, happens to be at a lightning attachment point, protective globes or fairings may shatter and permit some of the lightning current to enter associated electrical wiring directly.

In the case of a wing tip navigation light, for example, lightning may shatter the protective globe and light bulb. This may in turn allow the lightning channel to contact the bulb filament so that lightning currents may flow into the electrical wires running from the bulb to the power distribution bus. Even if only a fraction of the total lightning current enters the wires, they may be too small to conduct the thousands of amperes involved and thus will be melted or vaporized, as described in §4.2.

The accompanying voltage surge may cause breakdown of insulation or damage to other electrical equipment powered from the same source. At best, the initial component affected is disabled, and, at worst, enough other electrical apparatus is disabled along with it to impair flight safety. There are many examples of this effect, involving both military and civil aircraft. Externally mounted hardware most frequently involved includes navigation lights, antennas, windshield heaters, pitot probe heaters, and, in earlier days, the trailing long wire antennas that were deployed in flight for high frequency radio communications. The latter were quite susceptible to lightning strikes, and, since these wires were too thin to conduct the lightning currents, they were frequently burned away. The high frequency radio sets feeding these antennas were also frequently damaged, and cockpit fires were not uncommon.

Illustration of damage: Damage may be increased when an electrical assembly is mounted on nonmetallic portions of the airframe because some lightning current may have to use the assembly ground wire as a path to the main airframe, as described in §4.2. That the resulting damage can be extensive is exemplified by a strike to a small single engine aircraft with fiberglass wing tips which included fuel tanks, the type pictured in Fig. 4.15.

The details of this incident [4.15, 4.16] will illustrate several of the strike effects described in this section.

This aircraft, flying at about 900 m (3000 ft), was experiencing light rain and moderate turbulence when it was struck by lightning. The pilots had seen other lightning flashes in the vicinity before their aircraft was struck, and embedded thunderstorms had been forecast enroute, but there had been no cells visible on the air traffic control (ATC) radar being used to vector the aircraft, which had no weather radar of its own.

The strike entered one wing tip and exited from the other. It sounded to the pilot reporting like a rifle going off in the cabin, and the cabin immediately filled with smoke. Other effects follow.

1. The No.1 VHF communication set burned out.
2. Seventy five percent of the circuit breakers were tripped, of which only 50% could be reset later.
3. The left wing tip fuel tank quantity indicator was disabled.
4. The right main fuel tank quantity indicator was badly damaged
5. Several instrument lights were burned out.
6. The navigation light switch and all the lights were burned out.

The aircraft, nevertheless, was able to land at a nearby airport. Subsequent inspection showed extensive damage to the right and left wing tips and to their

electrical wiring. The attachment points and direct effects are pictured in Fig. 4.16(a) through (f) [4.16] and are represented by a diagram in Fig. 4.17.

Sequence of events: The evidence suggests that the flash included two or more strokes separated by a few milliseconds of continuing current. Assuming, for purposes of explanation, that the original lightning flash approached the right wing tip, the probable sequence of events was as follows: the initial point of attachment was the right wing tip navigation light housing, Fig.

The current exploded the sender unit ground wire but not the heavier filler cap ground braid, which was only frayed. Sparks undoubtedly occurred inside the fuel tank along the ground braid and between the filler cap and its receptacle, but the fuel–air mixture in the ullage of these half full tanks was probably too rich to support ignition.

4.16(a). Current from this stroke entered the housing ground wire and exploded both sections of it on the way to the right outboard metallic rib, as evidenced by the absence of these wires and the blackened interior shown in Fig. 4.16(b). Current continued through the airframe to the left outboard rib and out the sender unit ground wire to the sender unit, the base of which is shown in Fig. 4.16(c). From there, the current followed the filler gap ground braid and exited the aircraft at the filler cap, Fig. 4.16(d).

Blast forces from stroke No.1 at the right navigation light housing also shattered the lamp globe and bulb, as shown in Fig. 4.16(a). This shattering allowed a portion of the first stroke current to enter the right navigation light power wire, exploding it between the lamp and the outer rib, where the current jumped to the rib and continued through the rest of the airframe to the left sender unit ground wire.

Lightning current flowing in the navigation lamp power wire elevated its voltage to several thousand volts with respect to the airframe, a voltage high enough to break down the insulation at the outer rib feed through point, as shown in Fig. 4.17. Until breakdown occurred here, a few microseconds after the first stroke began, the wire was at sufficiently high voltage to break down the insulation to the neighboring sender wire. This breakdown occurred all along the wire inside the right wing. The portion of the current arcing into the sender wire caused a large voltage to build up across the right wing tip fuel gauge magnet inductance, to which this wire connects. This voltage in turn sparked over the gap between the gauge terminal and the nearest grounded housing wall, the arcing badly damaging the gauge unit. While the navigation light power wire was also exploded, it is probable that this did not occur until the second stroke.

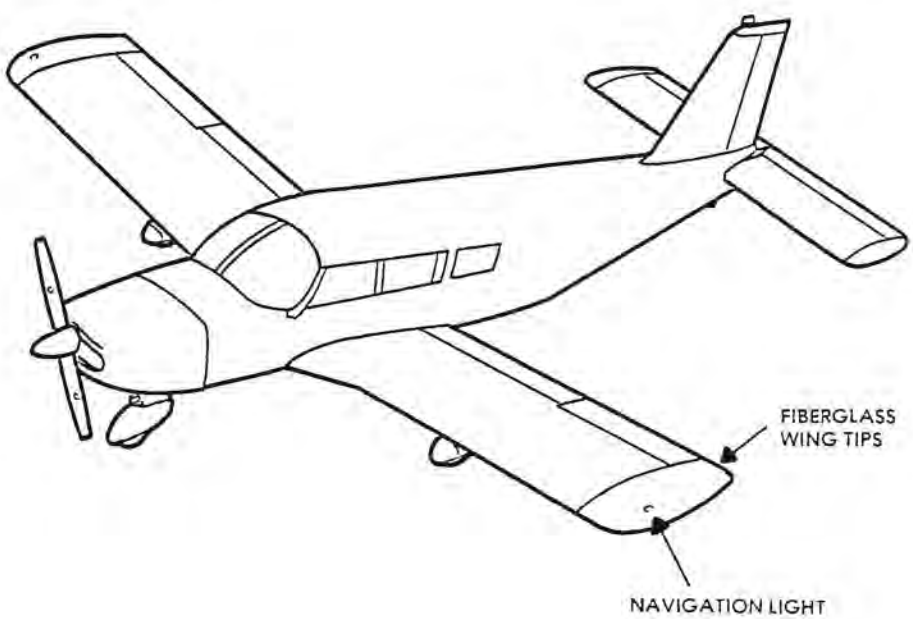

Fig. 4.15 General aviation aircraft with plastic wing tips.

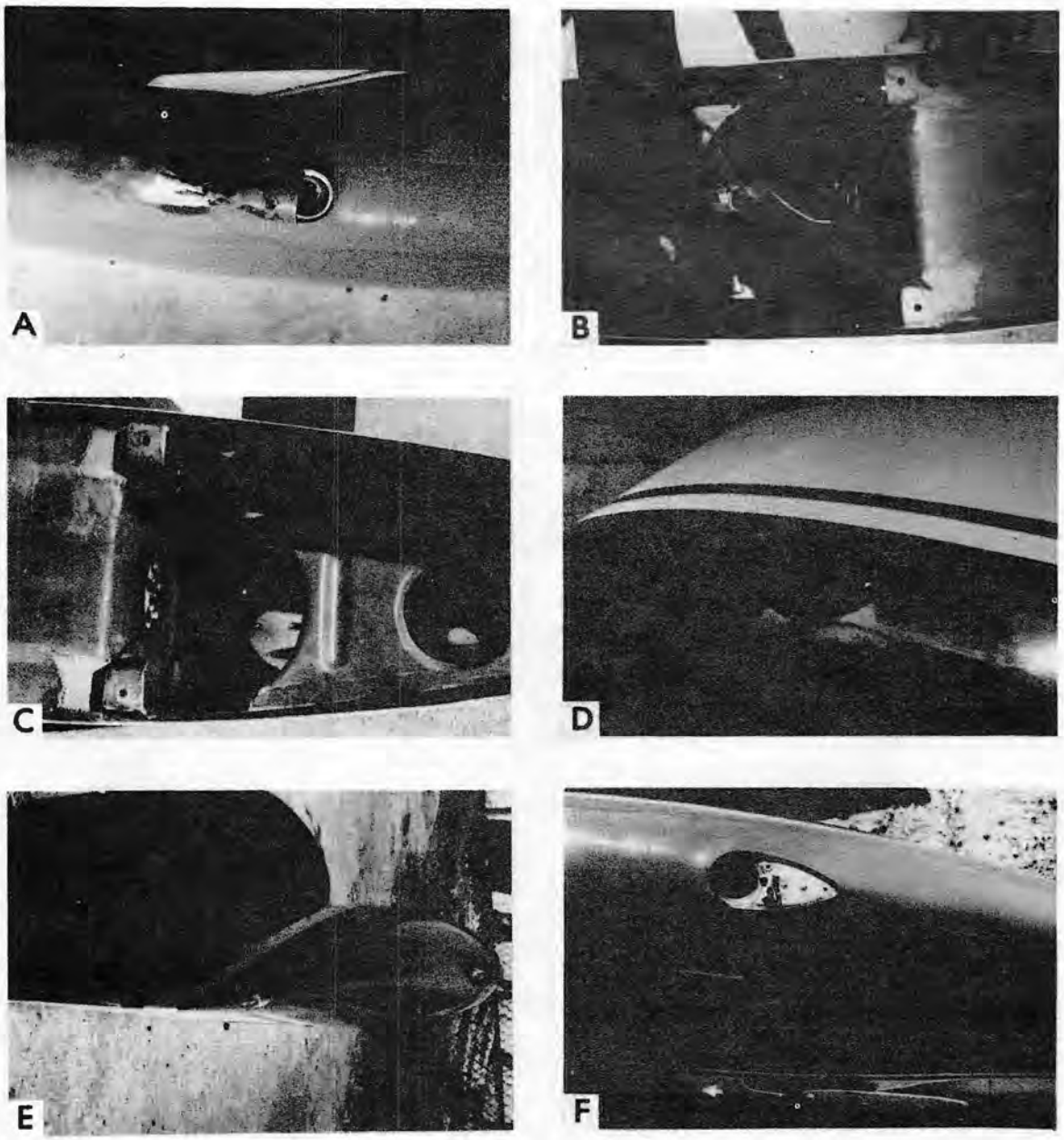

Fig. 4.16 Attachment points and direct effects on plastic wing tips.

Since the aircraft was moving forward, the entry and exit points of the second stroke were farther aft on both wing tips than the points of the first stroke. Since no other metallic components were present aft of the first stroke entry point on the right wing tip, the second stroke punctured a hole in the fiberglass trailing edge and contacted the metallic outboard rib, as shown in Fig. 4.16(e). As shown in Fig. 4.17, current from this stroke proceeded through the airframe to the left wing tip, where by this time the stroke had swept aft adjacent to the navigation lamp, shown in Fig. 4.16(f), from which point the stroke current exited. Current from stroke No.2 thus probably arced between the left outer rib to the navigation lamp power wire (the ground wire having been vaporized by the first stroke), which it followed to the lamp housing. The power wire was vaporized by the second stroke current flowing in it.

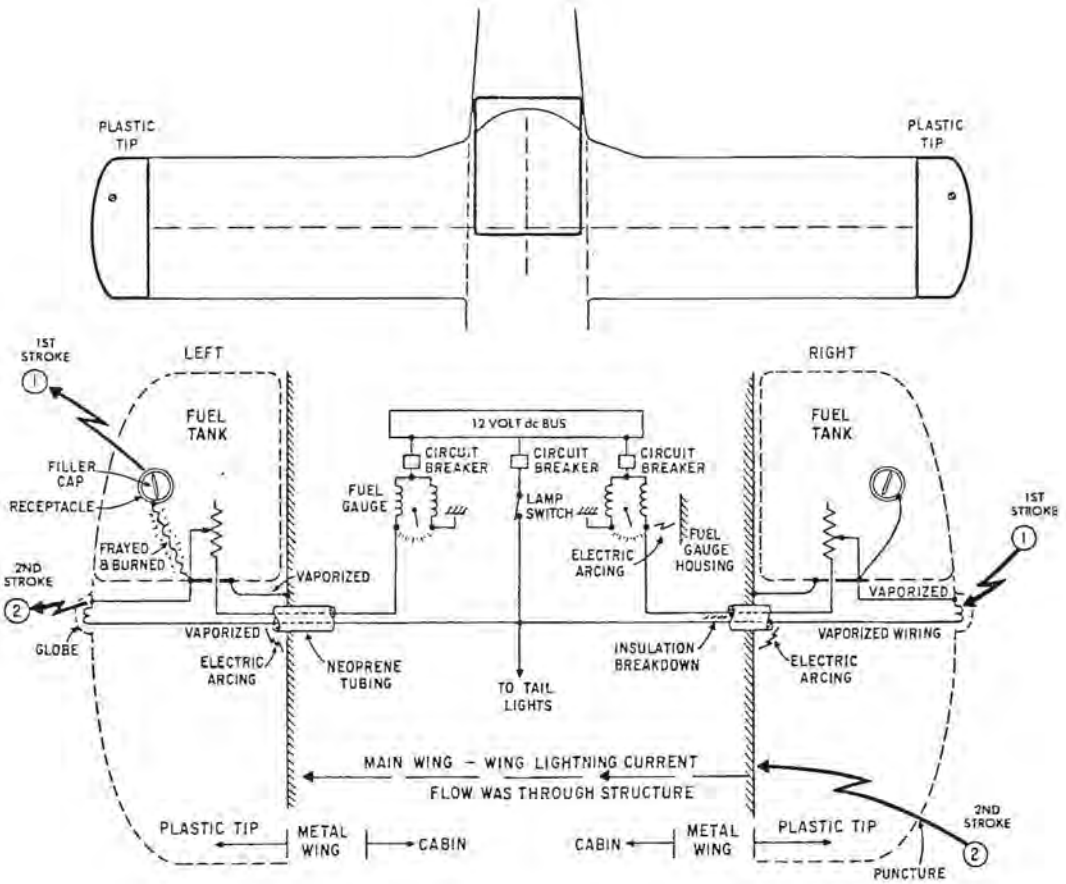

Fig. 4.17 Plastic wing tips and associated electric circuits and locations of lightning effects.

Both left and right navigation lamp power wires were connected together in the cabin and to both the 12 V dc bus and the tail light. The voltage and current surges which entered the lamp power wires inboard of the outer rib feedthroughs were also conducted to the tail light, burning it out, and to the 12 Vdc bus. The surge on the bus, of course, was immediately imposed on all of the other electrical equipment powered from this bus, or *all* of the electrical equipment in this aircraft. Arcing undoubtedly occurred in a number of components, causing circuit breakers to trip. Because circuit breakers, however, react much too slowly to prevent passage of a lightning surge, at least one piece of equipment (the No.1 VHF communication set) and several instrument lamps were burned out.

Similar incidents: There have been lots of similar incidents [4.17, 4.18], and together these have stimulated the design and verification measures [4.19] for general aviation aircraft with fiberglass components such as these wing tip fuel tanks. Many of these aircraft, however, are still flying without adequate protection.

The foregoing incident is an example of how a change in materials can increase the vulnerability not only of the airframe but also of other systems which previously had the inherent protection of conventional aluminum skins. The lightweight lamp and sender unit electrical wires were quite adequate for an installation in which a metal skin was available to carry away lightning currents, but they are woefully inadequate when used unmodified inside a plastic wing tip, where they become the only conducting path available to lightning currents trying to enter the main airframe.

4.6 Direct Effects on Propulsion Systems

With the exception of a few incidents of temporary malfunction similar to the incident reported in the introduction to this chapter, there have been no reports of adverse lightning effects on reciprocating en-

gines. Metal propellers and spinners have been struck frequently, of course, but effects have been limited to pitting of blades or burning of small holes in spinners, as shown in Figs. 4.18 and 4.19 [4.20, 4.21]. Lightning currents must flow through propeller blade and engine shaft bearings, but these are massive enough to carry these currents with no harmful effects. Wooden propellers, especially ones without metal leading edges, could probably undergo more damage, but these are seldom used on aircraft which fly in weather conditions where lightning strikes occur.

Turbine stalls: Reported lightning effects on turbojet engines show that these effects also are limited to temporary interference with engine operation. Flameouts, compressor stalls, and roll–backs (reduction in turbine rpm) have been reported after lightning strikes to aircraft with fuselage mounted engines. This type includes military aircraft with internally mounted engines and fuselage air intakes, or other military and civil aircraft with engines externally mounted on the fuselage.

There have been no attempts to duplicate engine flameouts or stall with simulated lightning in a ground test, and there has been no other qualitative analysis of the interference mechanism; however, it is generally believed that these events result from disruption of the inlet air by the shock wave associated with the lightning channel sweeping aft along a fuselage. This channel may indeed pass close in front of an engine intake, and if a restrike occurs, the accompanying shock wave is considered sufficient to disrupt engine operation. The steep temperature gradient may also be important. These effects have been reported as occurring more often on smaller military or business jet aircraft than on larger transport aircraft. Thus, smaller engines are probably more susceptible to disrupted inlet air than are their larger counterparts.

Operational aspects: In some cases a complete flameout of the engine results, while in others there is only a stall or roll–back. There is no case on record, however, in which a successful restart or recovery of the engine to full power was not made while still in flight. Perhaps because of this, together with the impracticality of a laboratory simulation, there has been little research into the problem. Nevertheless, operators of aircraft with engines or inlets close to the fuselage should anticipate possible loss of power in the event of a lightning strike and be prepared to take quick corrective action.

There have been only a few reports of lightning effects on wing mounted turbojet engines, since these are usually large engines in which the shock wave from a lightning flash is probably inadequate to noticably disrupt inlet air flow. There are no reports of power loss of turboprop engines as a result of lightning strikes.

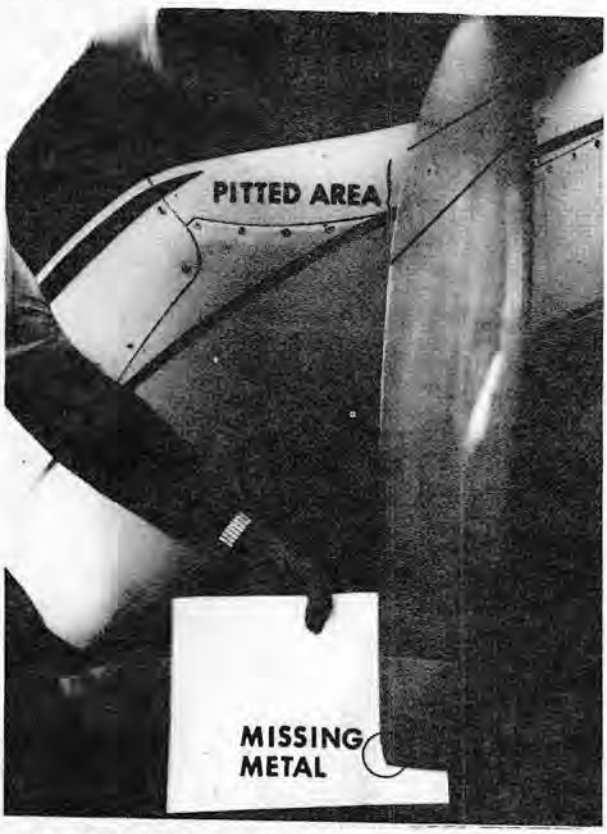

Fig. 4.18 Lightning strike damage to a propeller.

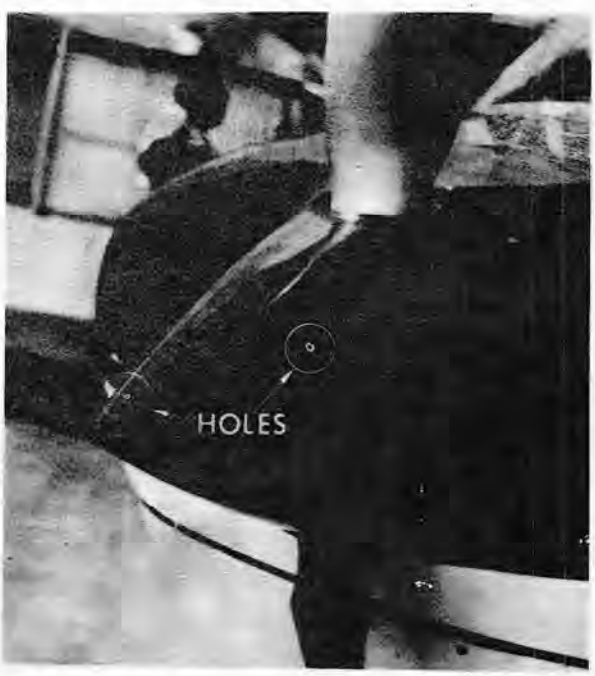

Fig. 4.19 Lightning strike damage to a spinner.

4.7 Indirect Effects

Even if the lightning flash does not directly contact the aircraft's electrical wiring, strikes to the airframe are capable of inducing voltage and current surges in this wiring.

Upset or damage of electrical equipment by these induced voltages is defined as an *indirect effect*. Indirect effects must be considered along with direct effects in assessing the vulnerability of aircraft electrical and electronics systems. Flight critical systems such as the full authority engine control system illustrated in Fig. 4.20 are potentially susceptible to indirect effects, and careful attention must be given to protection design and verification.

Reports: Until the advent of solid state electronics in aircraft, indirect effects from external environments such as lightning and precipitation static were not much of a problem and received relatively little attention. There is increasing evidence, however, of troublesome indirect effects. Incidents of upset or damage to avionic or electrical systems are showing up in airline lightning strike reports. Table 4.1 summarizes the reports of interference or outage of avionic or electrical equipment reported by a group of U.S. airlines for the period 1971 to 1984 [4.22].

Table 4.1 EVIDENCE OF INDIRECT EFFECTS IN COMMERCIAL AIRCRAFT (214 strikes)

	Interference	Outage
HF communication set	–	5
VHF communication set	27	3
VOR receiver	5	2
Compass (all types)	22	9
Marker beacon	–	2
Weather radar	3	2
Instrument landing system	6	–
Automatic direction finder	6	7
Radar altimeter	6	–
Fuel flow gauge	2	–
Fuel quantity gauge	–	1
Engine rpm gauges	–	4
Engine exhaust gas temperature	–	2
Static air temperature gauge	1	–
Windshield heater	–	2
Flight director computer	1	–
Navigation light	–	1
ac generator tripoff	(6 instances of tripoff)	
Autopilot	1	–

The incidents reported in Table 4.1 occurred in 20% of the total of 851 lightning strike incidents reported during the period. U.S. military aircraft have had similar experience. This experience is probably a result of the increasing sensitivity of miniaturized solid state electronics to transient voltages, a trend which necessarily would not have posed a problem in older, less sophisticated equipment. In any one incident, only a few electronic components are affected; others are not. Yet lightning induced voltages actually occur in all aircraft electric wiring at once. Thus it is evident that surges reach higher values in some circuits than in others or that some electronics are less tolerant of such surges than others.

Trends: While indirect effects have not historically been a major safety hazard, there are four trends in aircraft design and operations which could increase the potential problem. These include the following:

1. Increasing use of composite structures in place of aluminum.
2. Further miniaturization of solid state electronics
3. Greater dependence on electronics to perform flight critical functions
4. Greater congestion in terminal airways, requiring more frequent flight through adverse weather conditions at altitudes where lightning strikes frequently occur.

Consequences: One of the consequences of these trends is that protective measures which in older generation metal aircraft largely "come for free" must, in the future, be explicitly provided, usually with an adverse effect on aircraft weight and program cost.

Demarcation line: The demarkation line between direct and indirect effects may be somewhat arbitrary in some instances. An example might involve a lightning flash terminating on a wing tip navigation light. In this case, the burning or blasting damage to the light fixture would be considered a direct effect of the lightning. If the lightning flash were to contact the filament of the bulb and inject current into the wiring, electrical effects would be produced ranging from overvoltage breakdown of the insulation at the socket to tripping of remote circuit breakers or upset of equipment; effects of the resulting surge voltages on the power system. All of these effects will be considered indirect effects in this discussion, even though the initiating event was the direct injection of current into the filament.

Another hypothetical possibility would involve a lightning flash that passed close to but did not contact the aircraft. The changing electromagnetic field produced by that flash might upset electronic equipment. The circuit upsets produced by such a flash

would clearly be of an indirect nature, since there was no direct involvement of the aircraft with the lightning flash. Usually, however, the indirect effects of concern are produced by a flash that contacts the aircraft.

Mechanisms: The mechanism whereby lightning currents induce voltages in aircraft electrical circuits is illustrated in Fig. 4.20. As lightning current flows through an aircraft, strong magnetic fields which surround the conducting aircraft and change rapidly in accordance with the fast changing lightning stroke currents are produced. Some of this magnetic flux may leak inside the aircraft through apertures such as windows, composite fairings, seams, and joints.

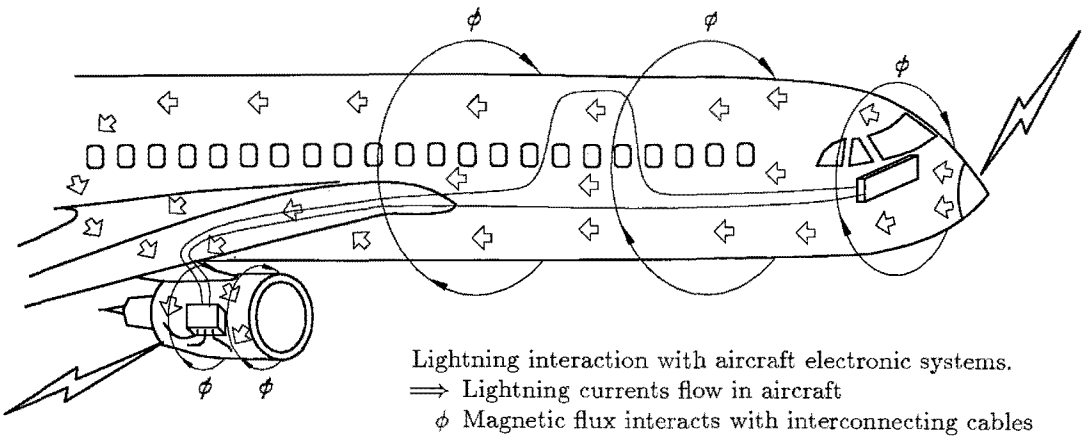

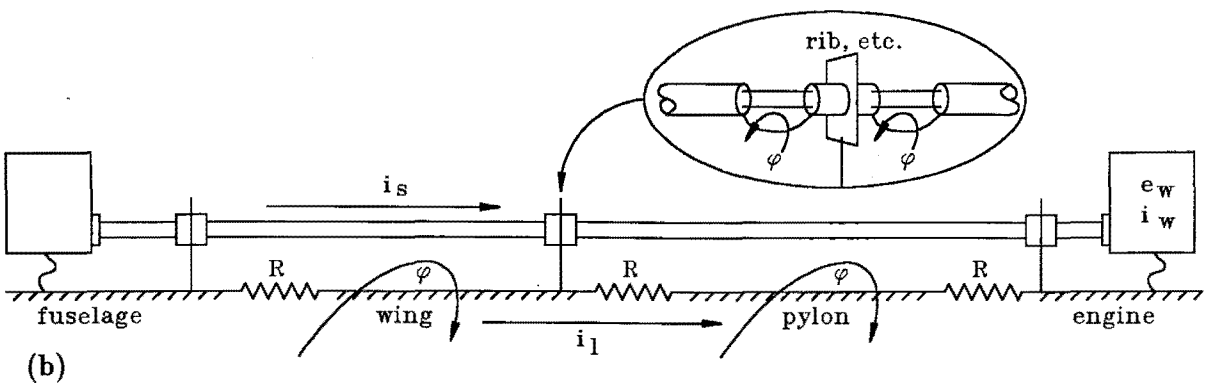

$$e_s = i_R + \frac{d\phi}{d\tau}$$

$$i_s = \frac{1}{L_s}\int e_s(\tau)d\tau$$

$$e_w = i_s R_s$$

$$i_w = \frac{1}{L_w}\int e_w(\tau)d\tau$$

where

$i_l =$ Lightning current in airframe
$R =$ Structural resistance of airframe
$\phi =$ Magnetic flux
$e_s =$ Shield external voltage
$i_s =$ Shield current
$e_w =$ Shielded wire voltage
$i_w =$ Shielded wire current (max)

Fig. 4.20 Magnetic flux penetration and induced voltages in electrical wiring.
(a) Installation (b) Mechanisms

Magnetically induced voltages: Other fields may arise inside the aircraft when lightning current diffuses to the inside surfaces of skins. In either case these internal fields pass through aircraft electrical circuits and induce voltages in them proportional to the rate of change of the magnetic field. These magnetically induced voltages may appear between both wires of a two–wire circuit, or between either wire and the airframe. The former are often referred to as *line–to–line* voltages and the latter as *common–mode* voltages.

Structural IR voltages: In addition to these induced voltages, there may be resistive voltage rises along the airframe as lightning current flows through it. These are called *structural IR voltages*. If any part of an aircraft circuit is connected anywhere to the airframe, these structural IR voltages may appear between circuit wires and the airframe, as shown in Fig. 4.20. For airframes made of highly conductive aluminum, these voltages are seldom significant except when the lightning current must flow through resistive joints or hinges. However, the resistance of steel or titanium is 10 times that of aluminum, and the resistance of most CFC structures is over a hundred times the resistance of comparable aluminum structures, so the structural IR voltages in aircraft fabricated of these materials may be much higher.

Other aspects of indirect effects: Magnetically induced and structural IR voltages occur simultaneously in nearly all wiring within an aircraft during a lightning strike, so the potential exists for multiple effects on avionic systems. For example, four channels of a quadruplex redundant digital flight control system might all be damaged at the same time, if protection against indirect effects is not incorporated. Safe operations of such systems in the lightning environment cannot be achieved by relying only on redundant systems.

Systems of concern: Systems of greatest concern regarding indirect effects include the following.

1. Full authority, digital engine control (FADEC) systems.
2. Full authority electronic flight control (Fly–by–wire) systems.
3. Supervisory control steps capable of initiating control inputs that could endanger flight safety.
4. Fully or highly integrated cockpit instruments and displays.
5. Electronic flight instrumentation (EFIS) systems.
6. Aircraft electric power control and distribution systems.
7. Electrical/avionic systems that include externally mounted apparatus, such as air data probes, heaters, actuators and antennas.

Relation to EMI and EMC: Indirect effects of lightning are part of the broad subject of electromagnetic interference *(EMI)* and control *(EMC)*. The *EMI* and *EMC* standards in industry wide use, however, do not deal with the indirect effects of lightning. Neither do aircraft industry performance standards, such as *DO-160* published by the Radio Technical Commission for Aeronautics (RTCA) [4.23]. Efforts are underway to add meaningful lightning indirect effects environments to the family of *EMI/EMC* standards, but significant differences exist between the two environments.

A major difference is that lightning induced transients are best characterized as a time domain phenomenon, while classical *EMI/EMC* concerns relate to the frequency domain. Susceptibility to excessive voltages or currents and susceptibility to narrow band interference or emission are not the same thing and protection against one does not necessarily imply protection against the other.

Coordination of standards: Coordinated standards are unlikely in the near future. Therefore, separate and dedicated efforts and protection criteria must be applied to achieve successful protection of flight critical/essential systems against lightning indirect effects. Design of protective measures against indirect effects is treated in Chapters 8 through 18.

REFERENCES

4.1 Answer to questionnaire Effects of Electrical Phenomena upon Airplanes in Flight, National Advisory Committee for Aeronautics, Washington, D.C. (July 7, 1945).

4.2 U.S. Air Force photograph.

4.3 National Aeronautics and Space Administration photograph.

4.4 National Aeronautics and Space Administration photograph.

4.5 U.S. Air Force photograph.

4.6 U.S. National Safety Board photograph.

4.7 M.A. Uman, *Lightning*, McGraw-Hill, New York, 1969, p.230.

4.8 Paul T. Hacker, "Lightning Damage to a General Aviation Aircraft–Description and Analysis", *NASA TN-7775*, National Aeronautics and Space Administration, Lewis Research Center, Cleveland, Ohio (September 1974).

4.9 Hacker, "Lightning Damage".

4.10 *Report of the Investigation of an Accident Involving Aircraft of U.S. Registry, NC 21798, Which Occurred near Lovettsville, Virginia, on August 31, 1940*, Civil Aeronautics Board, Washington, D.C.(1941).

4.11 United Airlines Photograph.

4.12 General Electric Company photograph.

4.13 *Aircraft Accident Report: Boeing 707-121, N709-PA, Pan American World Airways, Inc., near Elkton, Maryland, December 8, 1963*, File No. 1-0015, Civil Aeronautics Board, Washington, D.C. (February 25, 1965).

4.14 *Aircraft Accident Report: TWA Lockheed 1649A near Milan, Italy*, File No. 1-0045, Civil Aeronautics Board, Washington, D.C. (November 1960). English translation of report by Italian Board of Inquiry.

4.15 J. A. Plumer, "Lightning Induced Voltages in Electrical Circuits Associated with Aircraft Fuel Systems," *Report of Second Conference on Fuel System Fire Safety*, 6 and 7 May 1970, Federal Aviation Administration, Washington, D.C. (1970), pp.171-92.

4.16 General Electric Company photographs.

4.17 Don Flagg, "Night Flight," *Aero Magazine*, January/February 1972, pp. 18-21.

4.18 Page Shamberger, "Learning About Flying the Hard Way," Air Progress, February 1971, p. 64.

4.19 J. A. Plumer, "Guidelines for Lightning Protection of General Aviation Aircraft", *FAA–RD-73-98*, Federal Aviation Administration, Washington, D.C. (October 1973).

4.20 National Aeronautics and Space Administration photograph.

4.21 National Aeronautics and Space Administration photograph.

4.22 N. O. Rasch, M. S. Glynn and J. A. Plumer, "Lightning Interaction With Commercial Air Carrier Type Aircraft," *International Aerospace and Ground Conference on Lightning and Static Electricity*, Orlando, Florida, 26 -28 June, 1984.

4.23 *Environmental Conditions and Test Procedures for Airborne Equipment*, DO-160B, Radio Technical Commission for Aeronautics, 20 July 1984.

Chapter 5

THE CERTIFICATION PROCESS

5.1 Introduction

The purpose of this chapter is to describe the aircraft lightning protection requirements set forth by the Federal Aviation Administration (FAA) and other agencies, and to discuss the several steps that can be taken by applicants to comply with these requirements. Where applicable, the role of the FAA certifying engineer or designated representative is discussed in addition to the activities of the aircraft design engineers and certification managers.

The material in this chapter includes descriptions of performance requirements, standards, specifications and procedural steps. It does not include design data or methodology, which are the subject of the succeeding chapters. It is recommended that those responsible for design and certification be familiar with the material in this chapter before proceeding with a lightning design program, as the success and efficiency of an overall design depends considerably on the steps followed to achieve the design.

Aircraft lightning protection requirements and related standards have improved substantially in the past decade, to the point where they now address nearly all of the potential lightning hazards and incorporate the known aspects of the lightning environment. Before this, the aircraft protection requirements [5.1] focussed on one or two potential hazards, such as fuel tanks and access panels or antennas and other external" points of entry" while ignoring other areas such as internal arc and spark sources or indirect effects on electrical and avionic systems.

The requirements and standards are also being updated periodically to reflect improved understanding of the natural lightning environment and the emergence of new aircraft design technologies, such as electronic control systems and advanced composite airframes. This progress appears well positioned to adapt to future trends as well, via on–going technology review and standards writing activities among industry and regulatory agency groups.

The lightning protection design and certification process has been aided by a proliferation of technical literature on aircraft lightning interaction mechanisms, protection techniques and verification methods. Much of this material is summarized in this chapter and frequent references to important sources of additional information are provided.

5.2 FAA Lightning Protection Regulations

Since lightning represents a possible safety hazard whose consequences may extend to loss of the aircraft, and the lives of those aboard, the fundamental goal of aircraft lightning protection is to prevent catastrophic accidents, and to enable the aircraft to continue flying safely and be able to land at a suitable airport.

FAR's and AC's: Lightning protection requirements have therefore been included in the collection of Federal Aviation Regulations (FAR's) and Advisory Circulars (AC's) aimed at ensuring that the above goal is met for all except experimental and certain acrobatic aircraft. These regulations deal with the aircraft as a whole, and more specifically with the fuel system and other flight critical and essential systems. Specific regulations for each category of aircraft and rotorcraft are listed in Table 5.1 and reproduced in the following pages. As with most of the other US Federal Airworthiness Regulations, they state a performance requirement, but do not include guidelines for compliance or specific technical design requirements. In this manner the FAR's allow the designer a maximum amount of flexibility. Emphasis is placed by the FAA on verification and compliance with the FAR's, in this case by demonstrating, often by test, that the designs do in fact provide the necessary protection.

Lightning protection requirements are included in the FAR's for Transport Category Aircraft (Part 25), Normal, Utility and Acrobatic Aircraft (Part 23), which are herafter referred to as "General Aviation" aircraft and for both categories of rotorcraft (Parts 27 and 29), though some differences in applicable paragraph numbering and wording exist. Descriptions follow. It will be noted that the lightning protection regulations are functional requirements that are comparatively brief. The intensity of the lightning environment, the frequency of lightning strike occurences and locations where strikes enter or exit the aircraft are not provided in the protection regulations.

The lightning environment for design and certification purposes is presented in FAA Advisory Circulars [5.2, 5.3], along with definitions of lightning strike zones and guidance for locating them on specific aircraft. It is also discussed in §5.5.

Table 5.1 - Federal Aviation Regulations Pertaining to Lightning Protection

	Vehicle Type and Regulations			
	Aircraft			Rotorcraft
	General Aviation	Transport	Normal	Transport
Airframe	23.867	25.581	27.610	29.610
Fuel System	23.954	25.954	27.954	29.954
Other Systems	23.1309	25.1309	27.1309D	27.1309H

5.2.1 Protection of the Airframe

The basic lightning protection regulation for airframes is the same for all vehicle categories, and appears in the FAR's as:

LIGHTNING PROTECTION

§ 25.581 Lightning protection.

(a) The airplane must be protected against catastrophic effects from lightning.

(b) For metallic components, compliance with paragraph (a) of this section may be shown by—

(1) Bonding the components properly to the airframe; or

(2) Designing the components so that a strike will not endanger the airplane.

(c) For nonmetallic components, compliance with paragraph (a) of this section may be shown by—

(1) Designing the components to minimize the effect of a strike; or

(2) Incorporating acceptable means of diverting the resulting electrical current so as not to endanger the airplane.

Identical regulations are found in the FAR's dealing with General Aviation (Part 23) and Rotorcraft (Parts 27 and 29). These regulations state that compliance can be shown either by **bonding** components to the airframe or by **designing** components so that a strike will not endanger the airframe. In this context the term "bonding" refers to electrical connections among components, sufficient to withstand lightning currents.

At the time this basic regulation was formulated it was widely believed that hazardous lightning effects were limited to the external structure or to components directly exposed to lightning strikes and that protection from these effects could be achieved by ensuring that they were adequately bonded to the main airframe. Examples were flight control surfaces, air data probes, empennage tips and other components located at extremities of the aircraft where lightning strikes most frequently occur. Adequate bonding would prevent damage to the hinges, fasteners and other means of attaching these components to the airframe.

Bonding resistance: Unfortunately, this emphasis on bonding has led some designers to conclude that bonding, by itself, will provide adequate lightning protection for an aircraft and that little else need be done. To them, a lightning protected aircraft has meant a "bonded" aircraft. Verification of this "bonded" status has, in turn, been signified by attainment of a specified electrical resistance among the "bonded" components. The industry has adapted various bonding resistance limits for this purpose, among them the US military specification *MIL-B-5087B* [5.1], which requires that components subject to lightning currents be interconnected with a "bonding" resistance not exceeding 2.5 milliohms. This is achieved by allowing metal–to–metal contact among parts and verified by a dc resistance measurement.

Criteria like the 2.5 milliohm bonding specification have taken on an importance all of their own, to the neglect of the real purpose of design, which is to prevent hazardous lightning effects. Whereas electrical continuity among metal parts of an aircraft is important, there are many other features of a successful protection design that are of equal or greater importance.

Effects within the aircraft: The focus of *FAR 25.581* on the bonding and externally mounted components has perhaps led designers to give much less attention to lightning effects occurring within the airframe, either directly from current flow among internal structural members or indirectly, from changing magnetic and electric fields interacting with electrical systems. These indirect effects have been the cause of several catastrophic accidents, brought about by electrical arcing among fuel tank components and by burnout of flight essential electronic components. More de-

tailed discussions of these effects and related protection methods are found in the succeeding chapters.

The emphasis of *FAR 25.581* on the external and bonding aspects of lightning protection does not, of course, excuse the designer from actively identifying and addressing **all** potentially hazardous direct and indirect lightning effects. The first sentence of *FAR 25.581* is the important general requirement:

> *The airframe must be protected against catastrophic effects of lightning.*

5.2.2 Protection of the Fuel System

The emphasis of *FAR 25.581* on the external aspects of lightning protection, and the occurrence of several catastrophic accidents directly attributed to lightning-related ignition sources within fuel tanks, led to the addition of *FAR 25.594*, which focuses specific attention on aircraft fuel systems, as follows:

> **§ 25.954 Fuel system lightning protection.**
>
> The fuel system must be designed and arranged to prevent the ignition of fuel vapor within the system by—
>
> (a) Direct lightning strikes to areas having a high probability of stroke attachment;
>
> (b) Swept lightning strokes to areas where swept strokes are highly probable; and
>
> (c) Corona and streamering at fuel vent outlets.

Identical wording is found in the regulations for General Aviation Aircraft (Part 23) and Rotorcraft (Parts 27 and 29), shown in Table 5.1. Again the emphasis is on prevention of fuel vapor ignition sources due to the lightning strike attachment to exterior surfaces of the aircraft, but the first sentence states the important requirement:

> *The fuel system must be designed and arranged to prevent the ignition of fuel vapor*
> ...

FAR 25.594 thereby addresses one of the most important potential lightning hazards to an aircraft. Acceptable means of compliance with this regulation are described in a companion *Advisory Circular* (AC) [5.2].

5.2.3 Protection of Other Systems

No FAR's deal specifically with lightning protection of other systems, such as the flight control, propulsion, electrical and avionic systems. However, the general safety regulations for equipment, systems and installations aboard the aircraft, stated in *FAR 25.1309*, require protection against hazards resulting from any foreseeable operating condition, one of which is a lightning strike, as follows:

> **§ 25.1309 Equipment systems and installations.**
>
> (a) The equipment, systems, and installations whose functioning is required by this subchapter, must be designed to ensure that they perform their intended functions under any foreseeable operating condition.
>
> (b) The airplane systems and associated components, considered separately and in relation to other systems, must be designed so that—
>
> (1) The occurrence of any failure condition which would prevent the continued safe flight and landing of the airplane is extremely improbable, and
>
> (2) The occurrence of any other failure conditions which would result in injury to the occupants, or reduce the capability of the airplane or the ability of the crew to cope with adverse operating conditions is improbable.
>
> (c) Warning information must be provided to alert the crew to unsafe system operating conditions, and to enable them to take appropriate corrective action. Systems, controls, and associated monitoring and warning means must be designed so that crew errors that would create additional hazards are improbable.
>
> (d) Compliance with the requirements of paragraphs (b) and (c) of this section must be shown by analysis, and where necessary, by appropriate ground, flight, or flight simulator tests. The analysis must consider—
>
> (1) Possible modes of failure, including malfunctions and damage from external sources.
>
> (2) The probability of multiple failures and undetected failures.
>
> (3) The resulting effects on the airplane and occupants, considering the stage of flight and operating conditions, and
>
> (4) The crew warning cues, corrective action required, and the capability of detecting faults.
>
> (e) Each installation whose functioning is required by this subchapter, and that requires a power supply, is an "essential load" on the power supply. The power sources and the system must be able to supply the following power loads in probable operating combinations and for probable durations:
>
> (1) Loads connected to the system with the system functioning normally.
>
> (2) Essential loads, after failure of any one prime mover, power converter, or energy storage device.

(3) Essential loads after failure of —

(i) Any one engine on two- or three-engine airplanes; and

(ii) Any two engines on four- or more- engine airplanes.

(4) Essential loads for which an alternate source of power is required by this chapter, after any failure or malfunction in any one power supply system, distribution system, or other utilization system.

(f) In determining compliance with subparagraphs (e) (2) and (3) of this section, the power loads may be assumed to be reduced under a monitoring procedure consistent with safety in the kinds of operation authorized. Loads not required in controlled flight need not be considered for the two-engine-inoperative condition on airplanes with four or more engines.

(g) In showing compliance with paragraphs (a) and (b) of this section with regard to the electrical system and equipment design and installation, critical environmental conditions must be considered. For electrical generation, distribution, and utilization equipment required by or used in complying with this chapter, except equipment covered by Technical Standard Orders containing environmental test procedures, the ability to provide continuous, safe service under foreseeable environmental conditions may be shown by environmental tests, design analysis, or reference to previous comparable service experience on other aircraft.

Since *FAR 25.1309* makes no specific mention of lightning as a "foreseeable operating condition," this regulation has sometimes not been applied with respect to lightning protection. The occurrence of lightning strikes to aircraft is, however, today a widely recognized "operating condition", so the regulation is indeed applicable. The important language is found in paragraphs (a) through (d) and (g). The requirements of paragraphs (e) and (f) deal more specifically with propulsion system failures.

Multiple hazards: *FAR 25.1309* introduces the requirement for protection against any system failure that would prevent the "continued safe flight and landing" of the aircraft and that a failure condition must be made "extremely improbable". Likewise, the occurrence of other conditions which would "reduce the capability of the airplane or the ability of the crew to cope with adverse operating conditons" must be made improbable. This part of the regulation is very important vis à vis lightning, which is a condition which may occur along with other adverse environmental conditions, such as icing, precipitation, turbulence. Taken together with the possible effects of lightning on flight essential systems such as propulsion, electric power, airframe, flight control and navigation systems, all of which must perform satisfactorily, there may be multiple effects which may increase pilot work load and reduce the ability of the airplane or crew to continue safe flight.

The focus of this regulation on protection against multiple environments and hazards is perhaps its most important aspect.

Probability of occurrence: The requirements of *FAR 25.1309* are discussed further in an Advisory Circular [5.3] which defines "highly improbable" as no more than once in 1 000 000 000 (10^9) flight hours. The figure is more frequently expressed as a "10^{-9} probability of occurrence," or 10^{-9} events per hour.

Calculation of numerical probabilities of occurrence of a certain lightning hazard, or of the failure of a specific protection design, has rarely been attemped because of the difficulty of assigning numerical factors to a large number of possible lightning environment parameters and modes of interaction between lightning and the aircraft. A simple multiplication of probabilities, such as lightning current exceeding a tolerance level, or of lightning striking a particularly vulnerable location, or of fuel vapor being in a flammable condition can, if a sufficient number of factors is included, yield a very low probability of occurrence of a certain hazard. It can also lead, sometimes, to a conclusion that the 10^{-9} requirement has been met, and that there is no need to consider protection.

Such an approach is misleading and should **not** be accepted as evidence of compliance with the *FAR 25.1309* requirement of adequate protection of flight critical or flight essential systems!

General aviation and rotorcraft: The requirements of *FAR 25.1309* are not mirrored in the other Federal Aviation Requirements which address general aviation aircraft and rotorcraft. *FAR 23.1309*, reproduced below, is narrower in scope than *FAR 25.1309* and thus does not address "any foreseeable operating conditions" and cannot be considered a lightning protection requirement.

§ 23.1309 Equipment, systems, and installations.

(a) Each item of equipment, when performing its intended function, may not adversely affect—

(1) The response, operation, or accuracy of any equipment essential to safe operation; or

(2) The response, operation, or accuracy of any other equipment unless there is a means to inform the pilot of the effect.

(b) The equipment, systems, and installa-

tions of a multiengine airplane must be designed to prevent hazards to the airplane in the event of a probable malfunction or failure.

(c) The equipment, systems, and installations of a single-engine airplane must be designed to minimize hazards to the airplane in the event of a probable malfunction or failure.

5.2.4 Other FAA Requirements

Recognizing the increasing role of electronic controls in operation of the aircraft, the FAA initiated a rule–making project to add a FAR dealing specifically with lightning protection of flight critical and flight essential electrical and avionic systems and equipment. When adopted, this regulation will require that these systems and equipment continue to perform their intended functions; that is, remain operational, following an in–flight lightning strike. The requirement will thus further strengthen and apply the requirements of *FAR 25.1309* to lightning protection. It is anticipated that this regulation will first appear in Part 25 and shortly afterwards appear in modified form for the other categories of airplanes and rotorcraft.

Users of this handbook should ascertain the status of these new regulations and become familiar with their use and applicability. Methodology for compliance with these new regulations will be presented in a companion FAA Advisory Circular, which has been published in draft form by SAE Committee AE4L [5.4]. The guidelines in that reference have already been utilized for certification of full authority electronic flight and engine control systems.

The steps which may be followed to comply with the new regulation are described in [5.4] and repeated in §5.6 of this handbook.

5.3 Other Aircraft Lightning Protection Requirements

The US Department of Defense (DOD) has promulgated requirements for lightning protection of military aircraft and rotorcraft. The basic requirements document is *DOD Standard 1795* [5.5], which states the functional lightning protection requirements for "aerospace vehicles" purchased by DOD agencies, such as US Air Force, US Army and US Navy. The term "aerospace vehicle" refers to fixed wing aircraft, rotorcraft and missile "systems", as well as to major systems such as engines, external fuel tanks and weapons.

DOD Standard 1795: *DOD Standard 1795* was implemented in 1986, following many years of reliance upon *MIL-B-5087B* [5.1], which focused primarily on electrical bonding and which has been proven to be inadequate for lightning protection. DOD aircraft designed after 1986 are subject to the requirements of *DOD STD 1795*, which are more comprehensive than those of *MIL-B-5087B*.

Military Standard 1757: The lightning environment for design and verification test purposes of DOD aircraft is defined in *US Military Standard 1757* [5.6]. It incorporates the same lightning environment as defined in [5.2] and [5.4] for civil aircraft.

Certain DOD aircraft are subject to the FAA FAR's as well as to the DOD requirements. These include military transport and cargo aircraft which occasionally operate from civil airports and fly extended distances along civilian airways. Often these are airframes that have previously been certified in accordance with the FAA FAR's. Examples include the USAF KC-10A (DC-10), KC-135 (B-707) and RC-12 (Beech King Air, Model 200).

Fighters and bombers: Fighter and bomber type aircraft generally do not have to meet the FAA certification requirements.

Foreign aircraft and JAR's: Aircraft of non–US manufacture are usually certified by appropriate agencies of the country of origin, although these aircraft must also meet US FAR's if they are to be operated in the USA. The converse is true for US manufactured aircraft which are to operate in other countries. Compliance with the various requirements is facilitated by bilateral agreements among nations, and by use of Joint Airworthiness Requirements (JAR's), mutually agreed upon by participating nations.

The lightning protection requirements are similar in all sets of regulations, although the applicability and degree of enforcement has varied somewhat. There is a high degree of cooperation among aircraft lightning protection specialists worldwide and further progress in international standardization of lightning protection requirements and standards is likely to occur.

5.4 Summary of FAA Lightning Protection Requirements

The basic requirement is that:

the aircraft must be protected against catastrophic effects of lightning,

as stated in *FAR 25.581* and the companion documents. This applies to the airframe, plus all of the systems and components necessary to allow the aircraft to continue safe flight and landing, as stated in *FAR 25.1309*.

Other existing and proposed regulations focus attention on systems of specific importance, including

fuel (*FAR 25.954*) and other flight essential systems (*FAR 25.1309*). A forthcoming new regulation and accompanying advisory circular [5.4] will place further emphasis on protection of electrical and avionic systems. The absence of a regulation pertaining to a specific system does not, of course, mean that such a system does not need to be addressed, since all parts of the aircraft fall under the basic protection requirement.

The FAR's state only the functional requirements, and in the most general and broad terms. Translation of these terms to specific technical design goals is left to the manufacturer of the aircraft or system, with review and approval authority vested in the FAA or its Designated Engineering Representatives (DER's). The lightning environment for protection design and certification purposes is described in §5.5 and the steps necessary to complete the lightning protection and certification tasks are described in §5.6.

5.5 The Lightning Environment for Design and Verification

Before describing the specified lightning environment for aircraft, some discussion is in order as to how it evolved.

5.5.1 Early Lightning Standards

The first industry to experience lightning problems, and to establish the need for standardization of a lightning environment for design and test purposes, was the electric utility industry. Shortly after overhead power transmission and distribution lines became widespread, it was apparent that lightning would be a severe problem. Power transformers, generators, motors and switching devices experienced damage from voltage and current surges due to lightning strikes to the power lines. Research programs to quantify natural lightning electrical characteristics were initiated by utility companies and equipment manufacturers such as General Electric Company and Westinghouse Electric Company.

Shortly thereafter, standards emerged which defined lightning surge voltage and current levels to be withstood by power system apparatus. Extensive laboratory test facilities were constructed to enable equipment to be tested to verify ability to tolerate these standards. As power transmission voltages increased and associated equipment became more sophisticated, improvements were necessary in lightning protection technology and the need for better information on the natural lightning environment continued. As a result, an extensive amount of research into lightning phenomenology and its effects on electric power systems and apparatus was carried out during the period 1920 to 1960.

Insulation coordination: This research led to a comprehensive philosophy, called insulation coordination, dealing with the lightning protection of electric power equipment. It incorporates standardized voltage levels to which equipment is designed, standardized levels and procedures for proof tests on apparatus and standards on the performance of protective equipment, such as lightning and surge arresters. All equipment associated with electric power transmission and distribution facilities is designed, tested and protected in accordance with these industry wide lightning standards. The result is that whereas thousands of lightning strikes occur daily to electric utility systems, very few power outages are now attributable to lightning.

Early research on aircraft: Lightning standards for aircraft emerged at a later date. The Lovettsville, Virginia accident described in Chapter 4 prompted research into the possible effects of lightning on aircraft and several of the utility laboratories were called upon to provide test facilities and lightning expertise. During the next 15 years, several other accidents, involving ignition of fuel vapors, were thought to have resulted from lightning strikes. Additional research and testing programs were prompted by these accidents. Most of this work was conducted at the General Electric Company High Voltage Laboratory in Pittsfield, Massachusetts and the National Bureau of Standards High Voltage Laboratory near Gaithersburg, Maryland, under sponsorship of aircraft manufacturers, the Civil Aeronautics Board and the National Advisory Committee for Aeronautics (NACA), the predecessor of NASA.

Original airplane standards: The first airplane lightning protection design and test standards were published by the Federal Aviation Agency (FAA) in its *Advisory Circular 25-3* [5.7] and by the US Department of Defense (DOD) in military standard *MIL-B-5087* [5.1]. Both of these documents appeared in the mid 1950's. *AC 25-3*, reprinted somewhat later as *AC 20-53*, dealt exclusively with lightning protection of airplane fuel systems. *MIL-B-5087* dealt exclusively with provision of electrical bonding in airplane structures and apparatus. These were the areas of greatest concern at the time.

Defined lightning threat: *AC 20-53* and *MIL-B-5087* each defined the lightning threat as a 200 kiloampere (kA) peak current with a unidirectional waveshape, a rate-of-rise of 100 kA/μs and a decay time to 50% of peak amplitude of about 50μs. This represented a severe first return stroke in a cloud-to-earth flash. *AC 20-53* also defined an intermediate and continuing current component, but *MIL-B-5087* included only the return stroke in its defined environment.

Both documents required tests of critical components, such as fuel tank skins, access panels, filler caps, antenna installations, and other "points of entry" on the aircraft. No attention was given to the effects of currents conducted through interior structures or systems, or to indirect effects of lightning on electrical and avionics systems. These latter effects were not well understood during this period.

5.5.2 Experience With Early Aircraft Standards

Most of the early aircraft lightning protection design activities were focused on protection against the direct or physical damage effects of lightning, such as deformation of lightweight metallic structures, melting of holes through fuel tank skins, puncture of dielectric surfaces, such as radomes and canopies, and prevention of electrical arcing at structural interfaces in fuel tanks. The required testing was carried out by existing utility manufacturer laboratories, such as GE and Westinghouse, and by several small specialty organizations such as Lightning and Transients Research Institute. The stroke currents required by the specifications were produced by charged capacitor banks discharged through waveshaping impedances into the test specimens.

Unidirectional current waves: However, it was not possible to obtain the unidirectional waveshapes specified in *AC 20-53* and *MIL-B-5087* with the existing capacitor banks, even those available at the largest electrical equipment manufacturers' laboratories. The reason for this is that the specified unidirectional current requires an overdamped test circuit including an excessive amount of resistance. The resistance usually limits the peak current to amplitudes of 100 kA and below, with most of the energy originally stored in the capacitor bank being dissipated in the test circuit resistance, instead of the test specimen. The performance of test equipment, and some of the tradeoffs between generator size and waveshape, are discussed further in §6.8.

Oscillatory current waves: Since the specified overdamped waveform could not be readily produced, laboratories instead provided a damped sinusoid waveform. This required less circuit resistance and allowed the specified 200 kA peak current amplitude to be achieved. Unfortunately, the frequency and time duration of the damped sinusoid currents varied among laboratories, since the testing equipment had been built for purposes other than the testing of aircraft equipment. There being no standardized definition of a damped sinusoid test current, a wide variety of frequencies and time durations were utilized.

Three typical damped sinusoids, all with 200 kA peak amplitudes, are illustrated on Fig. 5.1. As illustrated in this figure, there is a significant difference in overall time duration and energy associated with each of the illustrated test currents. Clearly, the amount of damage that would be inflicted on a test specimen by current waveform $A1$ is much less than that inflicted by waveform $A2$ and greater than that of $A3$. This situation was a significant shortcoming in the early lightning test standards, and became especially apparent with the emergence of advanced composite structures, which are more sensitive to the effects of energy dissipation than were conventional aluminum structures. Standards now define the Action Integral of the current wave as well as the peak amplitude. Action Integral is discussed further in §5.5.3.

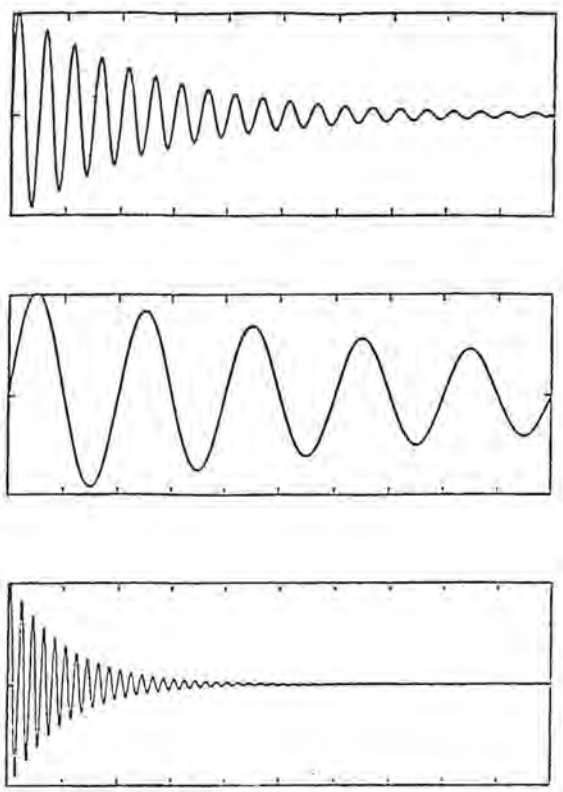

Fig. 5.1 Three typical damped sinusoid test currents prior to SAE standard.

Strike zones: An additional shortcoming in the early airplane lightning standards was the complete absence, in *MIL-B-5087*, or poor definition, in *AC 20-53*, of lightning strike zones. Strike zones are the means by which the lightning environment is applied to specific airplane surfaces and structures. The original

zone definitions did not distinguish between surfaces which were trailing edges and those which were leading edges or frontal surfaces, even though the duration of lightning attachment to these types of surfaces is significantly different. It is well known, for example, that lightning currents frequently melt holes in trailing edges where the flash may hang on for prolonged periods, whereas holes are infrequent in frontal or side surfaces of an aircraft.

Test methods and indirect effects: Finally, the early standards failed to define acceptable test methods, and did not address indirect effects on aircraft electrical and electronic systems. Lightning related accidents continued to occur, even to aircraft protected in accordance with *AC 20-53* and *MIL-B-5087*.

5.5.3 SAE Committee AE–4L (Lightning)

Recognizing the above deficiencies, the FAA and DOD in 1972 requested the Society of Automotive Engineers (SAE) committee on electromagnetic compatibility (SAE–AE–4) to form a subcommittee to develop improved aircraft lightning protection design and test standards. The new subcommittee included lightning phenomenologists and specialists in aircraft lightning protection design and testing. The committee was designated special task F and later given the permanent designation, AE–4L (lightning). This committee has functioned continuously since 1972 and has become the US focal point for development and standardization of aircraft lightning protection requirements.

A, B, C and D current components: The first task accomplished by the SAE lightning committee was to develop a standard lightning environment for design and test purposes, synthesized from the available natural lightning data. The result, which was first published in 1975 as a committee report entitled *Lightning Test Waveforms and Techniques for Aerospace Vehicles and Hardware* [5.8], included a standard severe lightning flash current waveform comprised of four current components, designated A, B, C and D and illustrated in Fig. 5.2, together with a set of test methods for utilizing the standardized currents. One of the important sources of natural lightning data drawn upon by the SAE Committee in formulating this standard was the compendium of world–wide cloud–to–earth lightning data published by Cianos and Pierce [5.9].

Component A represents the first return stroke of a cloud–to–earth flash and component D is a single subsequent stroke. Components B and C represent intermediate and continuing currents. The electrical parameters comprise a severe version (but not the most severe possible) of each of these important characteristics of cloud–to–earth lightning flashes. Very little data was available in the 1972–1975 time period on cloud–to–cloud or intra–cloud flashes, although these were generally believed to be less intense than the cloud–to–earth variety upon which the new standard was based.

Recognizing that the physical damage to aircraft structures, including arcing among structural joints in fuel tanks, was more dependent upon peak current amplitude and overall time duration than upon the actual waveform of stroke currents, and that generation of a unidirectional 200 kA first return stroke current was not likely to become feasible, the new specification allowed for application of either unidirectional or damped sinusoid currents as long as the peak amplitude, action integral and overall time duration were adhered to. Subsequent studies undertaken by the committee showed that physical damage is indeed related to these parameters, while not to the specific waveform.

Action integral: The *Action Integral, AI*, is the time integral of the current squared and represents the ability of the current to deposit energy in a resistive object. The expression for action integral is given by Eq. 5.1.

$$AI = \int_0^\infty i^2(t)dt \quad \mathrm{A^2s} \tag{5.1}$$

where

$i(t)$ = time varying lightning stroke current - A
t = time - s

Action integral, multiplied by specimen resistance (assumed constant), gives the energy dissipated in the specimen, as shown in Eq. 5.2.

$$W = AI \times R \tag{5.2}$$

where

W = energy - joules or watt-seconds
R = specimen or structure resistance - ohms

Electric field waveforms: The new SAE lightning environment also included several voltage waveforms intended to represent the electric field surrounding an aircraft immediately preceding lightning attachment. These waveforms, designated voltage waveforms A, B, C and D, are used in tests to evaluate possibilities of puncture of dielectric (non–conducting) materials such as radomes, windshields and canopies. Other tests were designed to evaluate fuel vapor ignition due to corona and streamers occurring near fuel vent outlets.

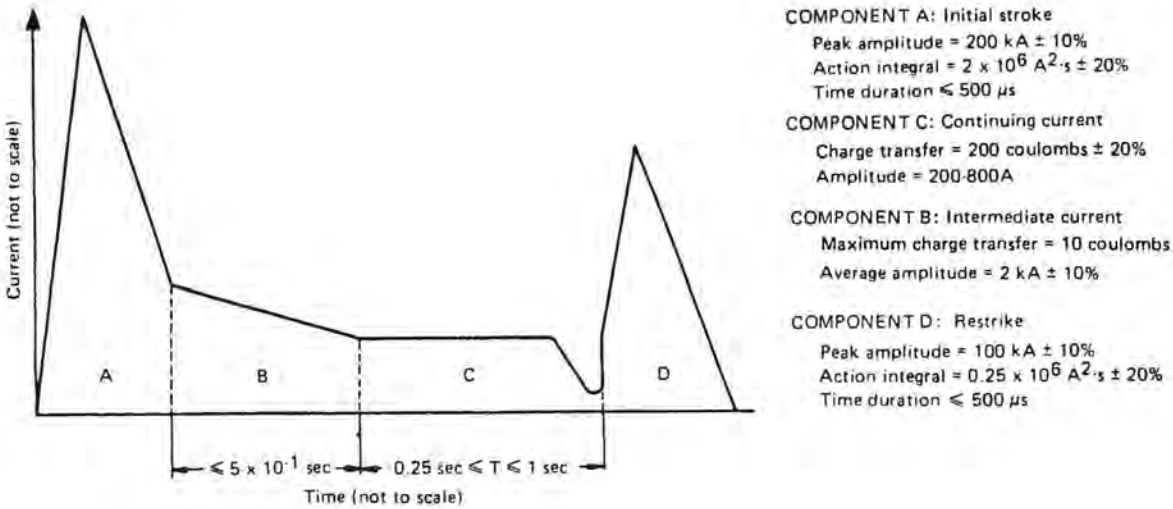

Fig. 5.2 SAE lightning flash current components.

SAE "Red book": The SAE committee report [5.8] rapidly became the US standard for aircraft design and certification testing. It quickly became known as the SAE "red book", after the color of its cover.

SAE "Blue book": Beginning in 1974, the SAE Committee had begun coordinating its work with similar lightning standardization activities taking place in the UK and Europe. An in-depth review of proposed standards was held at Culham Laboratory at Oxford, UK in 1975, resulting in changes and improvements in some details.

Following the US/UK/Europe deliberations of 1975, and a period of industry use and comment, the SAE Committee published in 1978 a slightly revised set of standards in its report entitled: *Lightning Test Waveforms and Techniques for Aerospace Vehicles and Hardware* [5.10]. This document superseded [5.8] and was given a blue cover. It soon became known as the "blue book" and continued as the US standard for aircraft protection design and certification testing, of both civil and military aircraft. Foreign certifying agencies have accepted this standard via bilateral agreements.

The SAE "red book" and "blue book" defined the lightning environment, strike zones, and test methods, but did not define lightning protection requirements or pass/fail criteria. These were left to individual contracts, in the case of military aircraft, and to FAA regulations applicable to civil aircraft.

The SAE and corresponding UK/Europe standards of the 1975-1978 era focused mostly on direct effects, as mechanisms of indirect effects and test methods for evaluating them were not yet fully understood or widely agreed upon by specialists. Research, development and standardization activities in these areas have continued in the US and Europe since 1975, with the result that there is today widespread agreement on methods to design and verify protection against indirect effects. Also, research has continued worldwide into other aspects of the natural lightning environment, such as characteristics of intra-cloud flashes and mechanisms of aircraft lightning interaction. Results of this research have begun to be incorporated into recent standards documents.

5.5.4 NASA Space Shuttle Lightning Criteria

The NASA Space Shuttle program was announced in 1970 and shortly thereafter NASA convened a panel of lightning phenomenologists and test specialists to formulate a standard lightning environment and other requirements for the Space Shuttle program. Concern regarding potential lightning hazards to the Shuttle was high due to the earlier NASA experience with a lightning strike to the Apollo 12 mission during launch, and to other lightning hazards experienced by earlier NASA and DOD vehicles and launch facilities. The result of this activity was publication in 1973 of the *Shuttle Lightning Criteria Document*, designated *JSC 07636* [5.11]. This document presented a lightning environment, vehicle protection requirements, and certain basic design guidelines for use by the Shuttle element contractors in meeting the protection requirements.

All of these deliberations and the publication of *JSC 07636* predated, and significantly influenced, the

activities of the SAE committee. Shortly thereafter, a companion document, *Shuttle Lightning Verification Document*, designated *JSC 20007*, was published [5.12]. This document set forth the requirement for verifying the adequacy of protection design. It described test waveforms and methods for evaluating adequacy of protection against direct and indirect effects, and also included certain analysis methods to be used for indirect effects evaluations. Some sections of *JSC 20007* had been included in the initial issue of *JSC 07636*.

Shuttle lightning environment: The lightning environment contained in *JSC 07636* was also based upon the known cloud–to–earth environment described by Cianos and Pierce in [5.9]. The Shuttle lightning environment differed somewhat from the later SAE standard in that several additional components were included in the idealized current waveform. The peak amplitude of the first return stroke (200 kA), total charge transfer and other key aspects were nearly the same.

The idealized waveform described in *JSC 07636* was intended for purposes of analysis and the intent was never to require that it be duplicated for tests, permissible test waveforms being described in *JSC 20007*. It was also described, for ease of analysis, by straight line segments between specified break points. Some have ascribed undue importance to the segments and breakpoints, even to the point of calling for test generators that produce straight line waveforms. Such was never the intent of the idealized waveform.

Because of the immediate need to translate lightning standards into hardware design features, emphasis in the NASA *Shuttle Lightning Criteria Document* was placed upon specific design guidelines. Less emphasis was placed on test methodology, as this technology area had not yet advanced to the point where standardized methods could be described.

TCL', and ETDL's: The Shuttle lightning criteria and verification documents were applied in design and verification of the major Shuttle elements (Orbiter, External Tank and Solid Rocket Boosters). These documents placed a major emphasis on protection against indirect effects, and required the establishment of Transient Control Levels (TCL's) and Equipment Transient Design Levels (ETDL's) for flight critical electrical and avionic systems. The TCL/ETDL concept, described in [5.13] and [5.14] is an attempt to provide a lightning protection philosophy for electronic equipment similar in concept to the insulation coordination philosophy used in the electric power industry.

This methodology is becoming more widely used in aircraft lightning protection design and certification programs and establishment of TCL's and ETDL's is one of the procedures called for in the forthcoming advisory circular on protection of electrical and electronic systems [5.4]. This procedure is the key to successful protection of these systems, and is discussed more fully in Chapter 15.

A large amount of testing and analyses were conducted during the design phase to establish transient levels expected to occur in inter–connecting wiring during a lightning strike to the vehicles and to verify that flight critical equipment could tolerate this environment.

This was the first time that such a comprehensive standard and set of specifications had been developed and applied to a major aerospace program and this standardization activity was largely successful. Basic protection requirements such as electromagnetic shielding of inter–connecting cables, electrical bonding of critical structures, isolation of certain flight critical circuits, separation of critical wiring types, and other features flowed into contractor design and quality control specifications from the Shuttle lightning criteria and verification documents.

5.5.5 Recent Standardization Activities

After a period of industry–wide experience in the late 1970's, DOD and FAA formally adopted the SAE lightning criteria in several standards and specifications pertaining to military and civil aircraft. In 1980, DOD issued *MIL-STD-1757* [5.6] which embodied the same lightning environment as published earlier in the SAE report *Lightning Test Waveforms and Techniques for Aerospace Vehicles and Hardware* [5.10]. The document also discussed tests and test methods. In 1983 *MIL-STD-1757* was reissued as revision A with an appendix which contained additional discussion of each test method. Shortly thereafter, in 1984, FAA issued a revised version of *AC 20-53*, designated Revision A [5.2] which also embodied the SAE lightning criteria. This advisory circular addresses lightning protection of aircraft fuel systems.

MIL-STD-1795: In 1986 DOD issued its new *MIL-STD-1795, Military Standard Lightning Protection of Aerospace Vehicles and Hardware* [5.5], which defines lightning protection requirements for military aircraft. This document supercedes the brief lightning requirements contained in *MIL-B-5087* referred to earlier. Also, it places equal emphasis on indirect and direct effects protection and incorporates double exponential descriptions of each of the lightning current components for use in evaluation of indirect effects.

In 1985, FAA announced the proposal to establish a new regulation requiring lightning protection for flight critical/essential electrical and avionic systems referred to in §5.3. Supporting this new regulation

will be a new advisory circular which will define the lightning environment and methodology to be used to verify compliance with the new regulation. SAE Committee AE–4L was tasked by FAA to draft the new advisory circular.

SAE "Orange book": The result of this activity has been published in the SAE Committee AE–4L report *Recommended Draft Advisory Circular: Protection of Aircraft Electrical/Electronic Systems Against the Indirect Effects of Lightning* [5.4]. This document, which is more commonly known as the "orange book", is now in wide use as a de facto standard for certification of flight critical or essential systems aboard transport category aircraft.

MIL-STD-1795 and the SAE "orange book" both embody the original SAE lightning current and voltage components which were derived from the cloud–to–earth lightning environment originally compiled by Cianos and Pierce. Subsequent reviews of this environment have been conducted by the SAE committee and UK/European standards organizations, and additional references compiling data obtained after the Cianos and Pierce publication have also become available. One such reference is that compiled by Anderson and Erickson [5.15]. Careful review of this data shows that the original Cianos and Pierce database is still representative of the cloud–to–earth lightning environment. Thus, no changes in this part of the lightning standards have been appropriate.

The advent of full authority control systems employing sensitive microelectronics began to focus attention on other aspects of the lightning environment including the characteristics of intra–cloud and cloud–to–cloud lightning strikes encountered by aircraft. Whereas the amplitude and action integrals of the currents in these strikes was believed to be less than those associated with cloud–to–earth flashes, other aspects, such as peak rates of change of current and multiplicity of pulses, were of concern, as was the need for better understanding of the locations of strike zones and the interaction of lightning flash channels with aircraft.

Research programs: For these reasons, several research programs were implemented, beginning in 1980, to study the intra–cloud and cloud–to–cloud lightning environment. In these programs, which were sponsored by NASA, the US Air Force, FAA, and the French government, aircraft were instrumented with devices capable of sensing and recording electrical parameters of in–flight lightning strikes. The results of these programs, which are reviewed in Chapter 3, have been widely published and several aspects of the intra–cloud lightning environment have been incorporated in the most recent aircraft lightning standards, such as *MIL-STD-1795* and the SAE "orange book".

Multiple burst environment: The most important of these is the "multiple burst" environment, comprised of a large number of comparatively low amplitude current pulses characterized by high rates–of–rise and short duration, and occurring randomly over the lifetime of the flash. Examples of typical intra–cloud lightning flash currents are presented in Chapter 3.

5.5.6 The Standardized Environment

The standardized lightning environment defined in [5.2] and [5.4] is in present use for aircraft design and certification purposes. This environment is a combination of individual waveforms which have been synthesized from the important characteristics of natural lightning flashes described in Chapters 2 and 3 for certification purposes. The waveforms of components A, B, C, and D are derived from cloud–to–ground lightning discharges. Component H represents additional characteristics of intracloud and cloud–to–cloud discharges.

There are five current component waveforms (A, B, C, D and H) that are applied as appropriate to the lightning strike zone(s) in which system is located. Together these components constitute the *external* lightning current environment. They are defined as follows:

Component A - Initial High Peak Current: Component A has a peak amplitude of 200 kA, an action integral of 2×10^2 A^2·s and a double exponential waveform. This waveform, represents a first return stroke of 200 000 amperes at a rate–of–rise of 1×10^{11} A/s at $t = 0.5\mu$s. It has a peak rate of rise of 1.4×10^{11} A/s at $t = 0+$. This waveform is defined mathematically as

$$i(t) = I_0\left[\epsilon^{-\alpha t} - \epsilon^{-\beta t}\right] \tag{5.2}$$

where

$$I_0 = 218810 \text{ A}$$
$$\alpha = 11354 \text{ s}^{-1}$$
$$\beta = 647265 \text{ s}^{-1}$$
$$t = \text{ time s}$$

The waveform is shown in Fig. 5.3.

The constants in Eq. 5.3 are given to multi-digit precision only for dimensional consistency and it should not be inferred that the actual lightning environment is known to that precision, or that tests made to duplicate that environment must duplicate such precision or that such precision has any engineering value.

Component B - Intermediate Current: Component B has an average amplitude of 2 kA and a charge transfer of 10 coulombs. For analysis, a double exponential current waveform should be used. This waveform is again described mathematically as

$$i(t) = I_0\left[\epsilon^{-\alpha t} - \epsilon^{-\beta t}\right] \tag{5.4}$$

where

$$I_0 = 11300 \text{ A}$$
$$\alpha = 700 \text{ s}^{-1}$$
$$\beta = 2000 \text{ s}^{-1}$$
$$t = \text{ time s}$$

The waveform is also shown in Fig. 5.3.

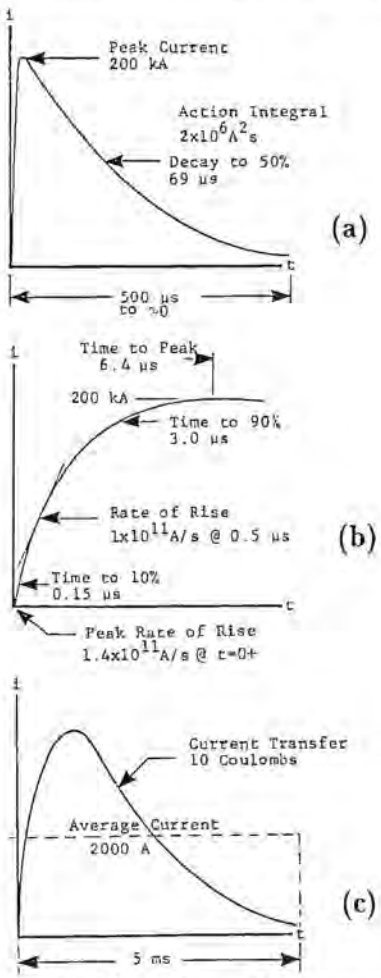

Fig. 5.3 Waveforms of current components A and B.
(a) Component A overall
(b) Component A front
(c) Component B

Component C - Continuing Current: Component C is a rectangular waveform delivering 200 coulombs of charge at a rate of between 200 A and 800 A, in a time period of between 0.25 s and 1 s. For analysis purposes, a rectangular waveform of 400 A for a period of 0.5 second should be utilized. This component transfers a charge of 200 coulombs. The primary purpose of this waveform is charge transfer. The waveform is shown in Fig. 5.4(a).

Component D - Restrike Current: Component D has a peak amplitude of 100 kA and an action integral of 0.25×10^6 A^2-s. This waveform represents a restrike of 100 000 amperes peak at a rate of rise of 1×10^{11} A/s at $t = 0.25$ s and a peak rate of rise of 1.4×10^{11} A/s at $t = 0^+$. The waveform is again defined mathematically as

$$i(t) = I_0\left[\epsilon^{-\alpha t} - \epsilon^{-\beta t}\right] \tag{5.5}$$

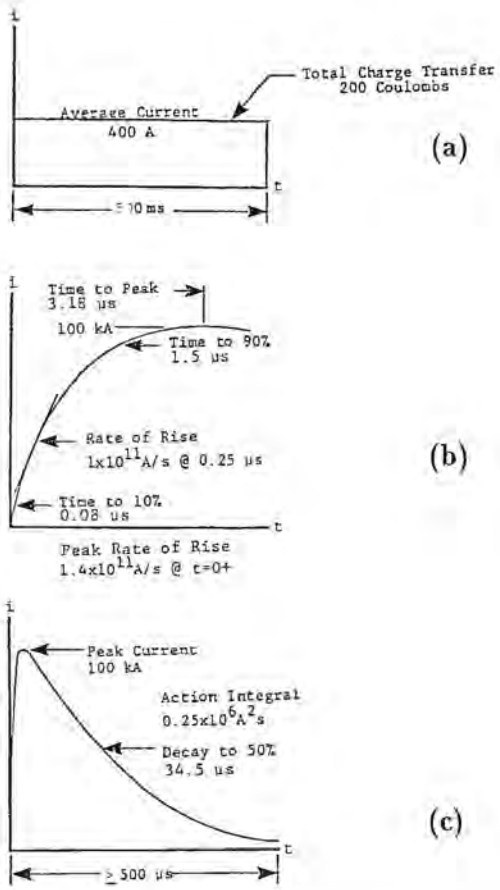

Fig. 5.4 Waveforms of current components B and D.
(a) Component C
(b) Component D overall
(c) Component D front

$$I_0 = 109405 \text{ A}$$
$$\alpha = 22708 \text{ s}^{-1}$$
$$\beta = 1294530 \text{ s}^{-1}$$
$$t = \text{ time s}$$

The current waveform is also shown in Fig. 5.4.

Component H - High rate of rise current: Component H has a peak current of 10 kA and a peak rate of rise of 2×10^{11} A/s at $t = 0^+$. The waveform is defined mathematically as

$$i(t) = I_0 \left[\epsilon^{-\alpha t} - \epsilon^{-\beta t}\right] \tag{5.6}$$

where

$$I_0 = 10572 \text{ A}$$
$$\alpha = 187191 \text{ s}^{-1}$$
$$\beta = 19105 \text{ s}^{-1}$$
$$t = \text{ time s}$$

The current waveform is shown in Fig. 5.6.

Application: Current components A, B, C, D and H together comprise the important characteristics of a severe natural lightning flash current although not all of the components may attach everywhere on the aircraft. Components A, B, D and H are described by double exponential expressions to provide the important waveshape characteristics such as rise and decay times, rate of rise, peak amplitude and charge transfer or action integral. Component C is a rectangular current pulse that transfers most of the charge in a lightning flash. The current components applicable to specific areas are shown in Table 5.2, which relates the current components to the lightning strike zones. Guidance for locating strike zones on a particular aircraft is presented in §5.6.1.

Table 5.2

Current Components Applicable in Various Zones

Zone	Current Waveforms					
	A	B	C	D	Multiple Stroke	Multiple Burst
1A	X	X			X	X
1B	X	X	X	X	X	X
2A		X		X	X	X
2B		X	X	X	X	X
3	X	X	X	X	X	X

A typical cloud-to-ground lightning flash contains more than one restrike, a severe version of which is represented by component D. In fact, flashes containing up to 24 strokes have been recorded. For protection against direct effects, it is adequate to consider only one return stroke or restrike (Component A or D) because this is assumed to occur anywhere within the appropriate strike zone ($1B$, $2A$ or $2B$). However, for evaluation of indirect effects it is necessary to consider the multiple-stroke nature of an actual lightning flash, because the succession of strokes may induce corresponding pulses in data transfer circuits (for example) causing upset or cumulative damage to sensitive systems or devices. For this purpose, the following multiple stroke flash has been defined, using as a basis the definitions of components A (first return stroke) and D (restrike).

Multiple stroke: The synthesized multiple stroke waveform is defined as an A current component followed by 23 randomly spaced restrikes of peak amplitude of 50 000 amperes each. This waveform is shown in Fig. 5.5. The 23 restrikes occur over a period of 2 sec according to the following constraints.

- The minimum time between subsequent strokes is 10 ms.
- The maximum time between subsequent strokes is 200 ms.

The restrikes have waveform parameters identical to the D current component with the exception that $I_0 = 54\ 703$ amperes. Because most of an airframe is located within zone 3 as well as one or more of the other zones, the multiple stroke environment is nearly always applicable. However, there may be special cases in zone 2 where the aircraft system or subsystem and its wiring is isolated from the effects of the initial A current component and is therefore not exposed to the A component current or fields. In these special cases, the multiple stroke still applies but the first current component can be reduced from a peak of 200 000 amperes to 100 000 amperes. The applicant should coordinate this reduction in multiple stroke environment with the FAA on a case by case basis.

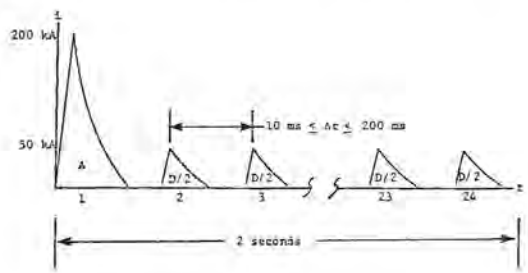

Fig. 5.5 Multiple stroke flash.

Multiple burst: The recommended waveform consists of repetitive component H waveforms in 24 sets of 20 pulses each, distributed over a period of up to two seconds, as shown in Fig. 5.6. The minimum time between individual component *H* pulses within a burst is 10 μs and the maximum is 50 μs. The 24 bursts are distributed over a period of 2 sec according to the following constraints:

- The minimum time between subsequent strokes is 10 ms.
- The maximum time between subsequent strokes is 200 ms.

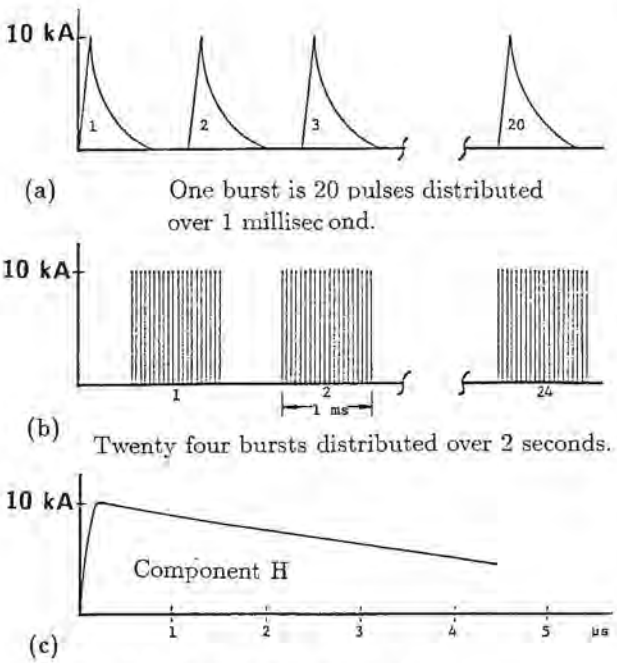

Fig. 5.6 Multiple burst waveform.
(a) Overall waveform
(b) Pattern of pulses in a burst
(c) Waveform of an individual pulse

Component H represents a high rate of rise pulse whose amplitude and time duration are much less than those of a return stroke. Such pulses have been found to occur randomly throughout a lightning flash, interspersed with the other current components. While not likely to cause physical damage to the aircraft or electronic components, the random and repetitive nature of these pulses may cause interference or upset to certain systems.

The multiple stroke and multiple burst environments are not intended to be applied to the full vehicle in a test. The multiple stroke and burst internal environment may be determined by testing using a single component to obtain the transfer function of interest, or to obtain the actual transient response level. The independent responses should then be repeated and spaced as described in Figs. 5.5 and 5.6 for upset assessment. It should then be shown by analysis or test that, by virtue of system design, architecture, hardware or software measures, there is sufficient immunity or recovery of the system from this environment.

A summary of the parameters of the idealized lightning current waveforms is given in Table 5.3.

Zone Application of Current Components: Current components *A*, *B*, *C*, *D* and *H* and the multiple-stroke and multiple burst waveforms may be utilized for analyses or test purposes, or for combinations thereof. The appropriate current component(s) for each zone of the aircraft are shown in Table 5.2. When the area of interest includes more than one zone, the protection assessment shall be performed utilizing the zone or zones with the most severe environment.

Zoning is used to determine the current path(s) through the aircraft and in locating the particular path(s) which represent(s) the most severe threat to the structure or system under investigation. For most applications, the airframe is located in *Zone 3* as well as one or more of the other zones (i.e. *Zone 1A*, *2A*, or *2B*). The current components from Table 5.5 are then applied together with the multiple stroke and multiple burst environments to assess the potential lightning effects on the aircraft structure or system, and verify adequacy of protection designs.

Test Waveforms: The idealized severe waveforms in Section 1 are appropriate for analysis, but they are sometimes difficult to apply to full scale components or vehicles in a test program. This is because it may become prohibitively costly to develop and operate simulators which can deliver the severe environments, especially to large vehicles such as transport aircraft. Therefore, the approach for testing will frequently involve the use of waveforms other than the idealized waveforms of Figs. 5.3 and 5.4. However, these alternate waveforms must have the property that test results can be readily extrapolated or scaled to those which would be obtained if the vehicle were tested with the idealized waveforms. Additional discussion of test waveforms and methods is found in Chapters 6, 7 and 18.

Table 5.3

Idealized Waveform Parameters

Parameter	Severe Stroke (Component A)	Intermediate Current (Component B)	Continuing Current (Component C)	Restrike (Component D)	Multiple Stroke half of (Component D)	Multiple Burst (Component H)
I_o (A)	218,810	11,300	400	109,405	54,703	10,572
$\alpha(s^{-1})$	11,354	700	NA	22,708	22,708	187,191
$\beta(s^{-1})$	647,265	2,000	NA	1,294,530	1,294,530	19,105,100
These equations produce the following characteristics:						
i_{peak}	200 kA	4,173 A	400 A	100 kA	50 kA	10 kA
(di/dt max) (A/s) at t = 0+ sec	1.4×10^{11}	NA	NA	1.4×10^{11}	0.7×10^{11}	2×10^{11}
di/dt (A/s)	1.0×10^{11} at t = 0.5 us	NA	NA	1.0×10^{11} at t = 0.25 us	0.5×10^{11} at t = 0.25 us	NA
Action Integral (A^2s)	2.0×10^6	NA	NA	0.25×10^6	0.0625×10^6	NA

5.6 Steps in Protection Design and Certification

Experience has shown that the most successful lightning protection design and certification programs have occurred when the work is conducted in a logical series of steps. In this case, success means achievement of a satisfactory protection design and compliance with the regulations, all with a minimum impact on overall weight and cost. The specific steps and order of occurrence may vary somewhat from one program to another, but most programs include the following basic steps.

Step a - Determine the lightning strike zones: Determine the aircraft surfaces, or zones, where lightning strike attachment to the aircraft is probable, and the portions of the airframe through which lightning currents must flow between these attachment points.

Step b - Establish the lightning environment: Establish the component(s) of the total lightning flash environment to be expected in each lightning strike zone. These are the currents that must be protected against.

Step c - Identify flight critical/essential components: Identify systems and components that might be vulnerable to interference or damage from either the direct effects (physical damage) or indirect effects (electromagnetic coupling) produced by lightning.

Step d - Establish protection criteria: Determine the systems and/or components that need to be protected, based on safety–of–flight, mission reliability or maintenance factors. Establish lightning protection pass–fail criteria for those items to be protected.

Step e - Design lightning protection: Design lightning protection measures for each of the systems and/or components in need of protection.

Step f - Verify protection adequacy: Verify the adequacy of the protection designs by similarity with previously proven designs, by simulated lightning tests or by acceptable analysis. When analysis is utilized, appropriate margins may be required to account for uncertainties in the analytical techniques. Developmental test data may be used for certification when properly documented and coordinated with the certification agency.

Variations in the above set of steps in use for design and certification of fuel systems and electrical and avionic systems are presented in [5.2] and [5.4], respectively. The steps to be followed for fuel and avionic systems are listed below:

Fuel systems [5.2]

a. Determine the lightning strike zones.

b. Establish the lightning environment.

c. Identify possible ignition sources.

d. Establish protection criteria.

e. Verify protection adequacy.

Electrical and avionics systems [5.4]

a. Determine the lightning strike zones.

b. Establish the external lightning environment for the zones.

c. Establish the internal environment.

d. Identify aircraft flight critical/essential systems, equipment and locations on or within the aircraft.

e. Establish Transient Control Levels (TCL) and Equipment Transient Design Levels (ETDL).

f. Verify design adequacy.

Further discussion of each of these steps follows.

5.6.1 Step a - Zone Location

The lightning strike zones are defined in the advisory circulars [5.2] and [5.4] and also in Chapter 3 of this handbook. The first step in a protection design and certification program is location of the zones on specific aircraft.

This section addresses some of the questions that have arisen recently concerning establishment of zone locations and boundaries. For example, an aircraft nose and a wing–mounted engine inlet have always been considered to be in *Zone 1A* (a direct strike zone with low probability of flash hang–on), but the possible rearward extent of this zone has not often been established. Whereas a lightning leader will almost always attach to the forward most extremity of a nose, continued movement of the aircraft may sweep the leader channel alongside the fuselage or nacelle for a finite distance prior to completion of the flash and arrival of the first return stroke (which is included in the *Zone 1A* environment).

Rearward extent of Zone 1: In the past, the rearward extent of *Zone 1A* has been of little interest because most fuselage and engine nacelle structures have had aluminum skins that easily withstand *Zone 1A* lightning currents. Replacement of aluminum skins with advanced composites, however, makes this aspect of lightning strike zone location take on much greater importance. Analysis shows that for some aircraft, *Zone 1A* may extend several meters aft of the initial leader attachment point, and some in–flight lightning strike incidents tend to confirm this. The altitude and speed of the aircraft are shown to be important factors in establishing zones, and in determining the probability of severe strikes within these zones.

Lateral extent of Zone 1: In earlier FAA zone definitions, now superseded by those of [5.2] and [5.4], the *Zone 1* regions included all surfaces of the aircraft that are located within 18 inches of the wing tip (measured parallel to the lateral axis of the aircraft) and other projections such as the nose, nacelle leading edges and tail. These earlier FAA definitions described *Zone 1* as being

> "··· within 18 inches of ···(the) trailing edge of the horizontal and vertical stabilizer, tail cone and any other protuberances"

but they did not apply the 18 inch criterion to surfaces behind *leading edges*. By custom, however, the first 18 inches aft of a leading edge or other forward–projecting object have also been considered to be within *Zone 1*.

Surfaces further aft of *Zone 1* areas, including

> "··· areas 18 inches laterally to each side of fore–aft lines passing through the *Zone 1* forward projection points of stroke attachment"

have traditionally been considered within *Zone 2*. Since a lightning flash may exist for one second or more, and most aircraft can travel more than their own length in this time, the *Zone 2* regions have usually been extended all the way aft along the fuselage or across the wing, as was done for the aircraft in Fig. 5.7.

The 18 inch lateral extensions of *Zone 1* and *2* account for the typical scatter of lightning attachment points in direct strike areas and the tortuosity of the flash channel as it sweeps along *Zone 2* surfaces. In–flight lightning strike experience has tended to confirm this judgment. Thus, in the example of Fig. 5.7, direct strike zones extend inboard 18 inches at the wing tips, and the swept stroke zones across the wings are 36 inches wider than the maximum width of the engine nacelles. The inboard 18 inches of each wing are also in Zone 2 due to their proximity to the fuselage.

The significance of either of the lightning strike zones is that skins, structures and other objects located in these zones must be designed to tolerate the effects of direct or swept lightning strike attachments. In Fig. 5.7, for example, the integral fuel tank skins aft of the nacelles were required to be thick enough to withstand swept lightning strike currents, whereas skins in *Zone 3* would perhaps not have to be this thick.

Swept stroke zones: Over the years, the terms *swept stroke* and *swept stroke Zone* have become synonymous with Zone 2, and the terms *direct strike* and *direct strike zone* have meant *Zone 1*, although this relationship has never been specifically stated in any FAA documents. This usage may be unfortunate, as will become evident.

Currents for each zone: The lightning currents to be expected in each zone are found in Table 5.3 and illustrated in Fig. 5.8. The shaded components apply in each zone indicated.

In Fig. 5.8 the *Zone 1* or *1A* areas at the nose and other leading edges were extended aft a distance

of 18 inches in accordance with traditional practice. Dielectric structures such as the radome, of course, were considered as being entirely within *Zone 1* even though their length is often longer than 18 inches, but in other cases the 18–inch criterion has been followed.

For conventional aluminum skins, the line of demarcation between *Zone 1A* and *2A* (or between *Zone 1* and *2* using the earlier definitions) is of little practical importance, because most aluminum skins can withstand even the first return stroke (SAE current component A) with little damage.

Composite structures: If the skin or structure aft of a leading edge attachment point is made of advanced composites, or other poorly conducting materials, the rearward extent of *Zone 1A* becomes of critical importance. Many carbon fiber composites can tolerate the effects produced by the *Zone 2A* currents without requiring additional protection, but the return (component A) designated for Zone 1 in the SAE criteria can deliver eight times more energy than the re–strike current (component D) included in the *Zone 2A* requirement, and the resulting damage can be extensive unless protective coatings or other methods have been applied.

Most protective measures add weight and increase cost. Thus, a decision regarding whether to apply protection or not, (or even whether or not a composite should be utilized in the first place), may depend directly on the designation of the lightning strike zones, and especially on a realistic determination of the rearward extent of *Zone 1A*.

The significance of the A and $\overline{B}$ designation can be seen in the currents specified for *Zones 1A* and *1B*. Due to the short hang–on time for an initial strike to a *Zone 1A* surface, only current components A and B, are applied, but all of the current components will be experienced by trailing edge surfaces in *Zone 1B*.

Arrival time of return stroke: Study of a number of instances of structural damage produced by in–flight lightning strikes indicates that in some cases the return stroke may not arrive until the lightning channel has swept considerably farther than 18 inches aft of the nose or other initial attachment point. This is because a finite period must elapse between the time the lightning leader initially attaches to a leading edge extremity and when the leader has reached its destination and the return stroke is initiated.

During this period the aircraft will have moved a certain distance and the leader channel will have been drawn aft alongside the structure, reattaching periodically to spots in its path. This situation is illustrated in Fig. 5.9

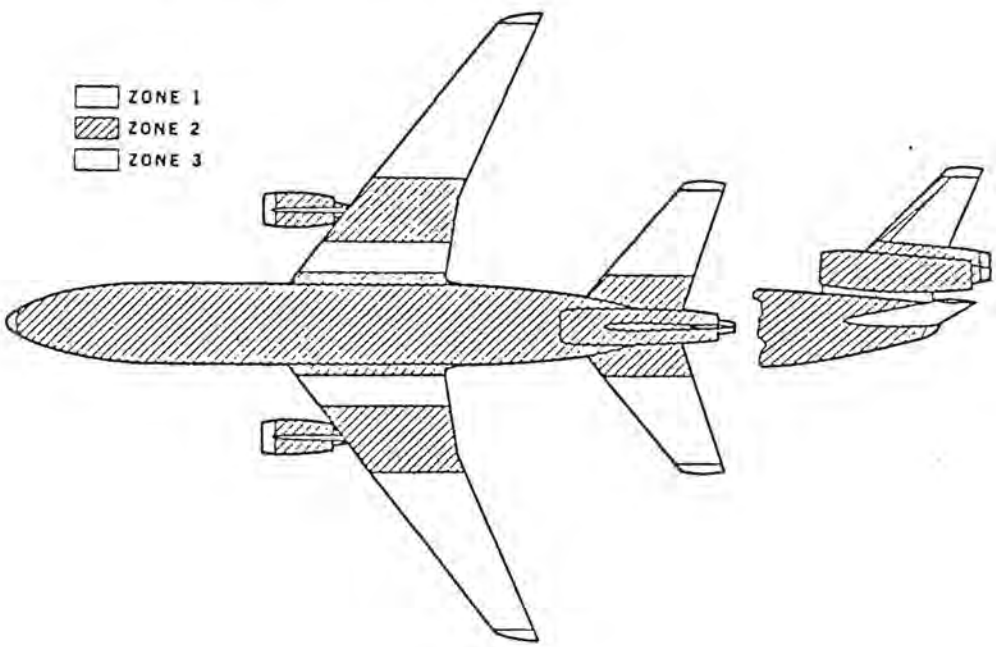

Fig. 5.7 Strike zones as determined from definitions given in FAA 20-53. (Now out of date.)

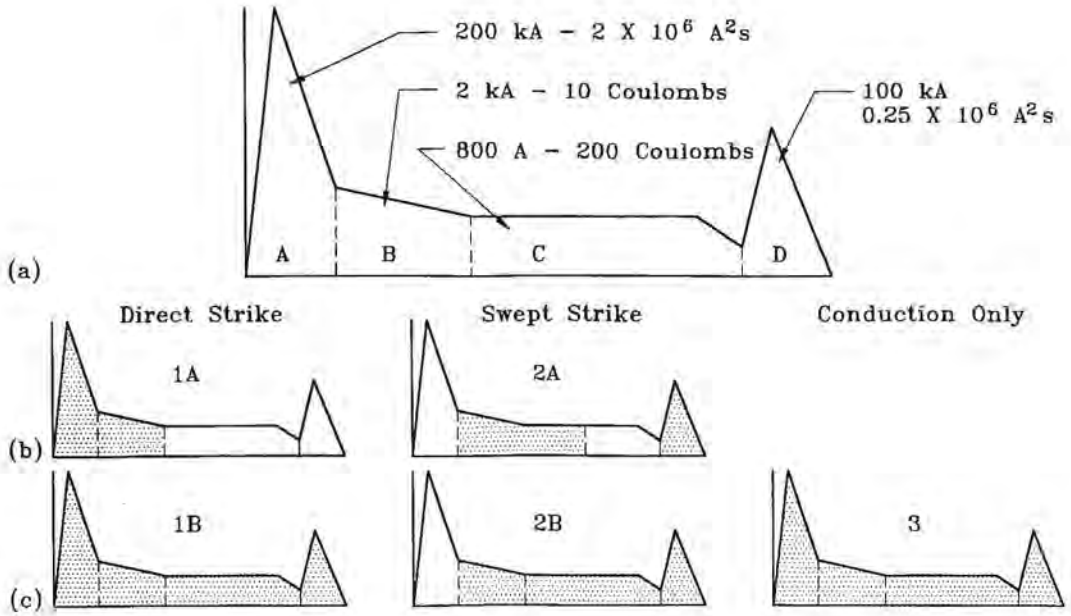

Fig. 5.8 Lightning current components required for each zone.
(a) Lightning current environment
(b) Low probability of hang–on
(c) High probability of hang–on
- Shaded areas represent the components required.
- The dip at the end of Component C signifies only that Component D may be applied separately from Component C.

As shown in Fig. 5.9, while flying at a velocity v_{ac} the aircraft travels a distance d during the time t over which the leader is continuing its propagation to earth. This time depends on the leader velocity v_l and the aircraft's altitude h. Thus, the distance traveled is related to the other parameters by:

$$d = h\frac{v_{ac}}{v_l} \tag{5.7}$$

The time at which the leader reaches the earth may be assumed to be the same as when the return stroke reaches the aircraft because, once initiated, the return stroke travels back up the channel much faster (about one third the speed of light) than the leader propagates toward ground.

A typical lightning leader travels at about 1.5×10^5 meters per second [5.16]. If this leader were to strike the nose of an aircraft traveling 134 m/s (300 miles per hour) at an altitude of 3 kilometers (10 000 ft), the aircraft would have moved about

$$d = \frac{(134 \text{ m/s})(3000 \text{ m})}{1.5 \times 10^5 \text{ m/s}} = 2.7 \text{ m} \tag{5.8}$$

by the time the return stroke arrived back at the aircraft.

Assuming that the leader channel may sweep aft and reattach to a spot, this same distance defines how far aft the *Zone 1A* region should extend.

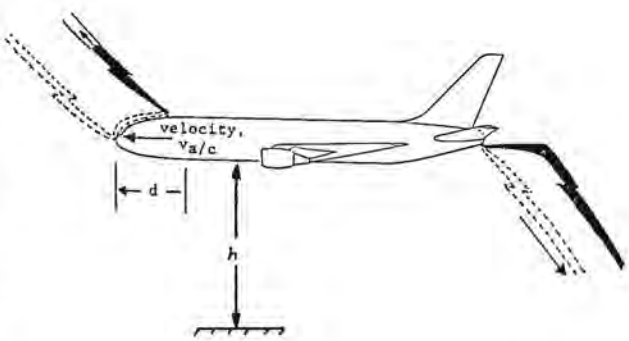

Fig. 5.9 Leader and return stroke attachment process.
h = altitude above ground
t = time for leader to reach ground
d = distance traveled between attachment of leader and arrival of returen stroke

The foregoing analyses are based on a cloud–to–ground lightning flash situation. A similar mechanism would probably exist for cloud–to–cloud discharges, but less is known about them than about cloud–to–ground discharges. Since cloud–to–ground flashes are generally believed to present the most serious environment, the analyses in this section will continue to represent the cloud–to–ground case.

Leader velocity: The velocity of a typical cloud–to–ground lightning leader has been determined by high speed photography and reported by many researchers as being about 1 or 1.5×10^5 m/s. Schonland, Malan and Collens [5.17], for example, reported in 1935 that the average velocities of 24 stepped leaders of negative polarity ranged from 1×10^5 to 13×10^5 m/s. Orville and Berger [5.18] measured a mean velocity of 2.5×10^5 m/s for an upward–progressing positive leader from a tower on Monte San Salvatore in 1965. Uman [5.19] reports a typical average stepped leader velocity as 1.5×10^5 m/s and more recently Fieux et al [5.20] have estimated leader velocities of the order of 0.2×10^5 to 1×10^5 m/s. Elsewhere in the literature one finds the values of 1×10^5 or 1.5×10^5 m/s quoted most widely. It is appropriate, therefore, to utilize velocities in this range for analyses of aircraft distance traveled in Eq. 5.7.

Distance traveled vs. flight conditions: From Fig. 5.9 it is evident that the distance d which the aircraft travels between the time of leader attachment and return stroke arrival is dependent on the aircraft velocity and altitude, in addition to the leader velocity. Fig. 5.10 shows the distances that may be traveled under the ranges of altitude and velocities throughout which most aircraft operate, as determined from Eq. 5.7.

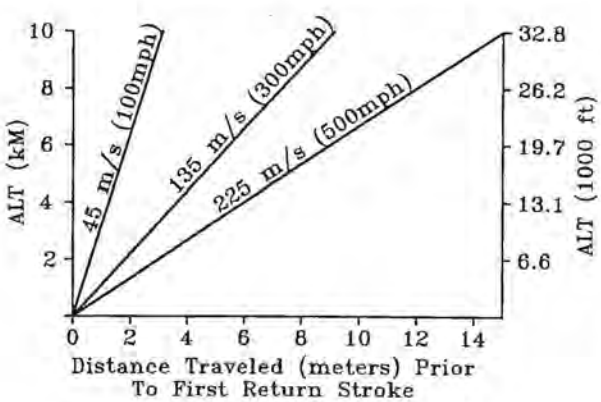

Fig. 5.10 Distance traveled prior to arrival of return stroke. Leader velocity = 1.5×10^5 m/s.

From Fig. 5.10 it may be seen that a turbojet aircraft cruising at 225 m/s (500 mph) airspeed at an altitude of 9 km (29 500 ft) would travel 13.5 m during the time it would take a lightning leader traveling 1.5×10^5 m/s to reach the earth and initiate the return stroke. This is more than the entire length of some small jet aircraft, and implies that surfaces along the entire length of such an aircraft may, at times, be exposed to the first return stroke of a lightning flash. Since the first return stroke is considered a part of the *Zone 1A* environment, surfaces of the aircraft that are exposed to the swept leader channel are within *Zone 1A*.

On the other hand, a propeller driven aircraft whose flight envelope extends only to a speed of 135 m/s (300 mph) and an altitude of 3 km (10 000 ft) would travel only 2.7 m before return–stroke arrival at these conditions. Aircraft surfaces aft of this distance would experience only the subsequent strokes, Component D, intermediate and continuing currents characteristic of *Zone 2A*.

Application considerations: Since many of today's general aviation, as well as transport and military aircraft are being designed to operate at high altitudes and speeds, a large portion of their surfaces aft of initial leader attachment points would, by the results of Figs. 5.9 and 5.10, be considered as within *Zone 1A*. This possibility was first recognized when the first "all composite" aircraft was being designed and was described in [5.21]. The significance of this has been academic for conventional aluminum structures because most aluminum skins can tolerate the lightning environment of *Zone 1A* about as well as the currents defined for *Zone 2A*.

Skins and structures made of advanced composites, however, are likely to suffer much greater damage from the first return stroke (Component A) defined for *Zone 1A* as compared with the subsequent stroke (Component D) defined for *Zone 2A* due to the higher action integral involved (2.0×10^6 $A^2 \cdot s$ as compared with 0.25×10^6 $A^2 \cdot s$).

External protection is often required for composites in *Zone 1A*, whereas it often is not needed for composites that only need to be designed to withstand the *Zone 2A* environment. Since some external protective measures entail weight and cost penalties, it is important to consider probability factors in establishing the rearward extent of *Zone 1A* on particular aircraft. In particular, there are several factors that combine to reduce the probability of experiencing a *Zone 1A* type stroke at the altitude and velocity extremes of the aircraft's flight envelope to an acceptable risk level, as follows:

Most strikes occur at lower altitudes: Experience shows that most lightning strikes occur when the aircraft is flying between 1.5 km (5000 ft) and 6 km (20 000 ft), as discussed in Chapter 3. This means also that the aircraft velocity is sometimes less than cruise, with the result that strikes in the upper and right–hand regions of Figs. 5.10 are less probable.

Most severe strikes occur at lower altitudes: Most strikes, though not all, that have inflicted severe damage to aircraft have also occurred at altitudes of 6 km or less, and many of these have been at altitudes below 3 km. In most of the cases of severe damage or loss of the aircraft the strike occurred at 3 km or below. These, of course, are the return strokes associated with the *Zone 1A* environment. In a few cases, severe damage has occurred at cruise altitudes of between 10 and 12 km.

It is logical that the most severe return strokes occur closest to the earth because these strokes result from discharge of the leader system. An aircraft attached to the lower "trunk" of a leader thus experiences more of the leader charge flow than does an aircraft in a leader closer to the cloud charge center, in which case most of the leader charge is below the aircraft.

Strikes at high altitudes may not be cloud–to–ground: The foregoing analysis is based on leader propagation between a cloud and the ground. It is probable that many of the strikes occurring at cruise altitudes above 6 km do not involve the ground, but propagate instead between upper level charge centers in or among the clouds. Less is known about the formation of these intracloud flashes, but it is probable that their leader propagation times are shorter than those of cloud–to–ground flashes originating at high altitudes. Again, this factor tends to reduce the probability of occurrences in the upper region of Fig. 5.10, but does not eliminate this possibility. Flashes originating in the upper reaches of the cloud have occasionally been observed to propagate all the way to ground.

Methodology for zone location: With the foregoing factors in mind, the following procedures can be used to locate the lightning strike zones on a specific aircraft.

1. All aircraft **extremities** such as the nose, wing and empennage tips, tail cone, wing–mounted nacelles and other significant projections should be considered within a direct strike zone because they are probable initial leader attachment points. Those that are forward extremities or leading edges should be considered in *Zone 1A*, and extremities that are trailing edges should be in *Zone 1B*, in accordance with the zone definitions.

   In–flight experience and laboratory tests of scale models of aircraft have shown that large, flat surfaces of some aircraft can also receive initial leader attachments. Examples are the top and bottom surfaces of wide–body transport aircraft and the upper surfaces of large, high wing, aircraft. These attachments are more likely to result from a propagating leader approaching the aircraft than from an aircraft triggered strike, and they are akin to the lightning strikes that are known to attach now and then to the flat roofs of large buildings.

   In such a case, the rearward extension of *Zone 1A* would begin from these "flat surface" attachments, rather than from an extremity or leading edge. The possibility of *Zone 1A* strikes to flat surfaces a significant distance aft of (or inboard from) an extremity has been acknowledged only recently and is explained by the compression of leader striking distance with aircraft geometry. One way of identifying susceptible surfaces includes rolling over the surface an imaginary sphere whose radius is the striking distance over the aircraft. The procedure is described more fully in [5.22].

2. Since all aircraft fly at some time at altitudes below 6 km (20 000 ft), the **minimum rearward extension** of *1A* zones on a particular aircraft should be determined from Fig. 5.10 or Eq. 5.7. The highest velocity at which the aircraft operates for an appreciable time within this altitude should be used. If the aircraft never reaches 6 km,, then its normal cruise altitude should be used instead. The leader velocity should be taken as 1.5×10^5 m/s.

   For most of today's aircraft, the above procedure will result in a rearward extension of *Zone 1A* of 4 - 6 m (13 - 20 ft).

3. For some aircraft that cruise extensively at higher altitudes and speeds a **further extension of zone 1A** may be appropriate, especially if the probability of a flight hazard due to a strike to an unprotected surface is high. Since the probability of severe strokes at the higher altitudes is lower, such further extension of *Zone 1A* may not otherwise be necessary. In other words, if the flight safety criticality of the surface is high, it should be considered as in *Zone 1A* and protected accordingly. If not, it may be designed in accordance

with the *Zone 2A* lightning environment, which may require less protection.

4. Since nearly all aircraft can travel more than their entire length in the one or two second lifetime of a lightning flash, the remainder of the surfaces aft of *Zone 1A* should be considered within *Zone 2A*. Trailing surfaces should be considered in *Zone 1B* or *2B*, depending on whether they were reached by an initial strike (*Zone 1B*) or a swept stroke (*Zone 2B*), in accordance with the definitions. Surfaces 0.5 m (18 in) to either side of those surfaces actually in the line of flight should also be considered within the same lightning strike zone, to account for small lateral movements of the sweeping channel.

5. Surfaces of the vehicle for which there is a low possibility of direct contact with the lightning arc channel and that are not within any of the above zones, but which lie between them, should be considered as within zone 3. **Structures** which lie between other zones are also within zone 3. Zone 3 areas may conduct all of the lightning currents that enter or exit from zones *1A* or *1B*.

Using the above guidelines, the lightning strike zones on the transport aircraft of Fig. 5.7 would be as shown on Fig. 5.11. In each case, the *Zone 1A* regions are extended aft at least 6m (20 ft) from the initial leader attachment point at the nose and wing-mounted inlets. Surfaces further aft are in *Zone 2A*, and trailing edges behind *Zone 2A* are in zone *2B*.

Overlapping zones: It must be remembered that surfaces within *Zone 1A* are also in *Zone 2A*, as in some cases the first return stroke may occur near the initial leader attachment point, as at a nose or engine inlet cowl, with subsequent strokes occurring within the rest of the *Zone 1A* areas. Protection designs should be based on the worst case zones.

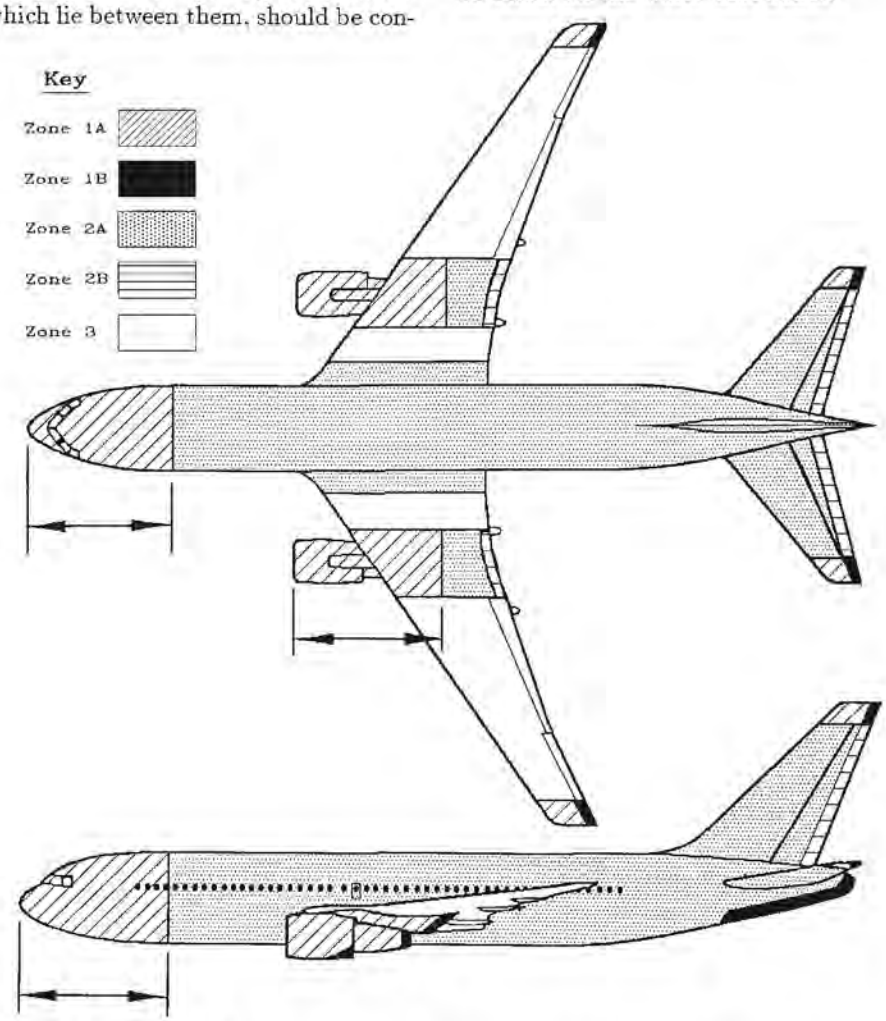

Fig.5.11 Strike zones showing rearward extension of *Zone 1A*.

Rotorcraft zones: Due to the fact that rotorcraft may be airborne with little or zero airspeed, the swept stroke phenomenon may not be applicable, and therefore attachment points at leading edges, frontal surfaces or any lower extremities may receive all components of the flash and be within *Zone 1B*. An example of lightning strike zones on a typical rotorcraft is shown in Fig. 5.12.

The zones on a typical twin turboprop aircraft are pictured on Fig. 5.13.

Once the lightning strike zones have been established they should be documented on a three–view drawing of the aircraft or rotorcraft, with boundaries identified by appropriate station numbers or other notation. It is usually appropriate for the applicant to review the zone drawings with cognizant FAA certifying engineers or Designated Engineering Representatives (DER's) to obtain concurrence, as the zones form the basis for certification of the designs that follow.

5.6.2 Step b - Establish the Lightning Environment

The external lightning environment is a consequence of the interaction of the lightning flash with the exterior of the aircraft. The environment is represented by the lightning current components at the aircraft surface. Application of the various current components to the strike zones is given in Table 5.3. These are the currents that must be protected against.

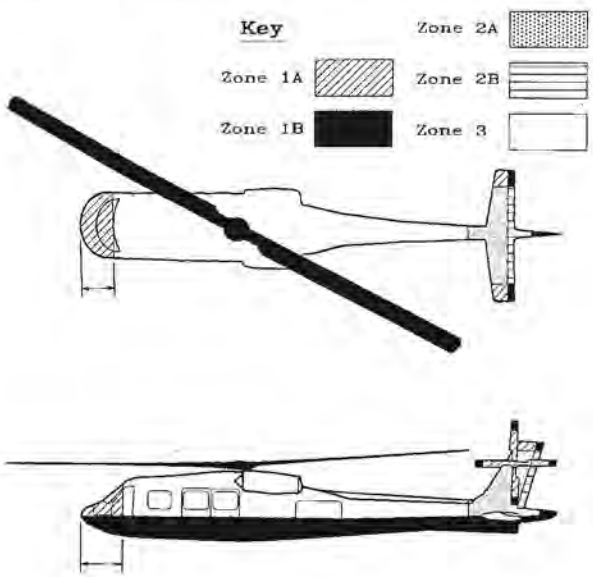

Fig. 5.12 Strike zones for helicopters.

Lightning current densities into skins and through the airframe are based on this environment. The internal lightning environment, which is produced by the external environment, is a result of current flow through the airframe and the penetration of electromagnetic fields. The fields and structural IR potentials give rise to indirect effects.

5.6.3 Step c - Identify Flight Critical/ Essential Systems and Components

Identify the aircraft systems and/or components that may be susceptible to direct and indirect effects of lightning, and whose proper operation is critical or essential to the safe flight of the aircraft.

Determine if any of these structures and systems could be damaged or upset by direct or indirect lightning effects.

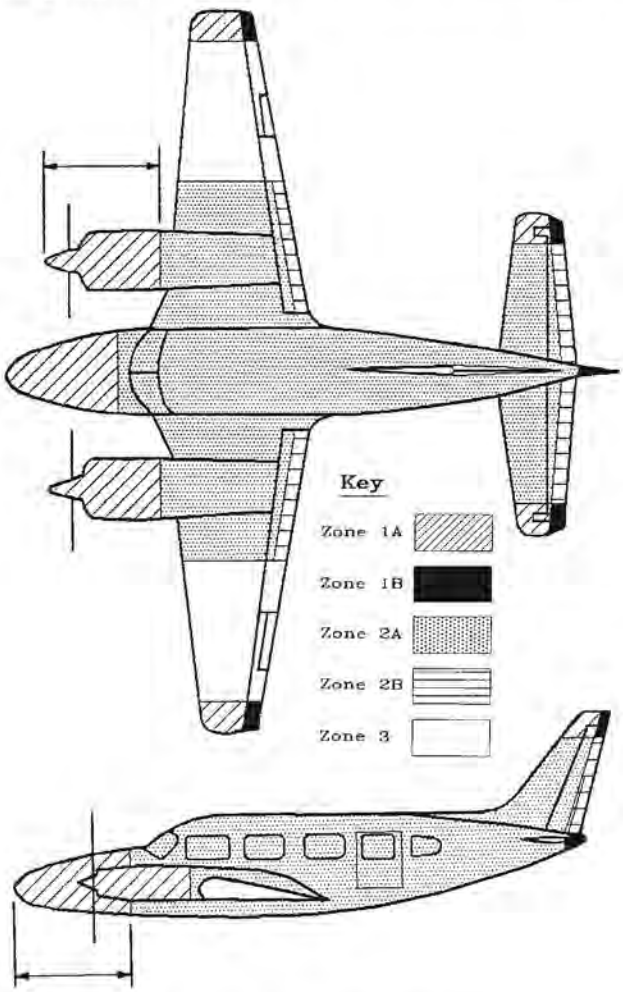

Fig. 5.13 Strike zones for a light twin turboprop aircraft.

5.6.4 Step d - Establish Protection Criteria

In this step, the specific criteria for each of the structures and systems in need of protection should be decided upon. For direct effects, this will include definition of the degree of physical damage that can be tolerated by flight critical/essential structures, and establishment of ignition free criteria for the fuel tanks. Further discussion of these topics is found in Chapters 6 and 7. For indirect effects protection, this will usually include establishment of Transient Control Levels (*TCL's*) for interconnecting wiring and Equipment Transient Design Levels (*ETDL's*) for electrical and electronic equipment.

Open circuit voltage and short circuit current: In most cases, these levels will be defined in terms of the open circuit voltage (e_{oc}) and the short circuit current (i_{sc}) appearing at wiring/equipment interfaces. The e_{oc} and i_{sc} will be related by the source impedances (i.e., loop impedance) of interconnecting wiring, and there may be different levels determined for different circuit functions or operating voltages. The relationship between transient control, equipment transient design and susceptibility levels is illustrated in Fig. 5.14. The *ETDL* is usually stated in the specifications for electrical/electronic equipment and constitutes an acceptance test level for this equipment.

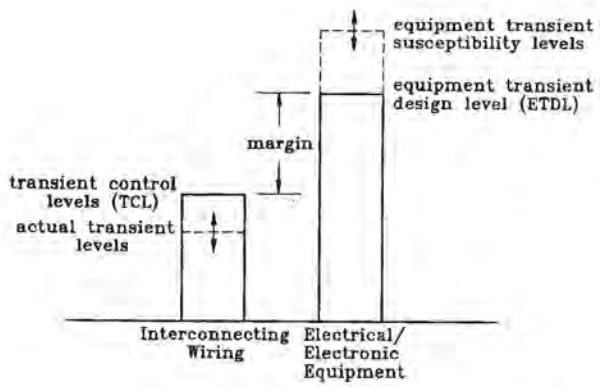

Fig. 5.14 Relationships between transient levels.

Since equipment transient design levels are typically represented by these standardized requirements, their use greatly simplifies protection evaluation. Normally, the transient control and design levels will be established by the airframe manufacturer or system integrator, who will compare the penalties of vehicle or interconnecting wiring protection with those of equipment hardening to establish the most efficient levels. Chapter 15 describes industry standards utilized for definition of *ETDL's* and *TCL's*. Further discussions of indirect effects protection are presented in Chapters 8 through 18.

5.6.5 Design Protection

In this step, specific design additions, changes or modifications are made to the flight critical/essential structures, systems and components to enable them to meet the protection criteria established in Step d. For direct effects, this will involve a large number of design techniques, ranging from solution of the basic structural material and manufacturing techniques to the addition of treatments or devices to improve electrical conductivity, arc or spark suppression, finishes, sealants and gaskets, application of lightning diverters, insulating structures and electrical bonding provisions and relocation of equipment. Further discussion of these methods is found in Chapters 6 and 7.

Protection against indirect effects involves application of electromagnetic shielding, provision of low impedance grounding surfaces, incorporation of surge suppressors and proper design of input and output circuits of electronic equipment. Further discussion of these methods is found in Chapters 8 though 17.

5.6.6 Step f - Verify Protection Adequacy

Verification of protection can be accomplished by analysis, similarity to previously proven designs or by test. Any of the three methods can be used, but similarity and analysis are normally considered first. Tests do need to be made, but they cannot be performed until hardware has been designed, built and made available for testing.

Analysis: Typical analyses used for verification of direct effects protection methods include calculation of conductor temperature rises due to current, based on conductor material, cross-sectional area and action integral of the lightning current, or calculation of magnetic forces effects which are dependent upon current amplitude and geometrical factors. These analyses are based on fundamental physical laws which can be described in mathematical terms.

Other analyses include comparison of present designs with earlier designs for which an empirical data base exists. In this case, extensions or extrapolations are utilized to relate the existing empirical data bases to the designs of interest.

Analysis can rarely be utilized to determine the behaviour of lightning currents in complex structures or components with multiple interfaces and current paths, especially when these interfaces have not been

designed to conduct electric currents. Therefore, testing must be used to evaluate lightning direct effects and verify protection design of such complex structures.

Similarity: Verification of direct effects protection by similarity means that current–carrying structures and joints must be shown to have equal or greater cross–sectional areas and interface surface areas than the designs to which they are similar, and that other design features are also sufficiently similar so as not to respond differently to other lightning effects such as shock waves and magnetic forces.

Demonstration of similarity includes comparisons of detailed design drawings, parts lists and installation details, combined with such analyses as are necessary to show that dissimilarities do not result in unforeseen hazards.

Examples of designs that can be verified by similarity are:

- Skins.
- Hinges and bearings.
- Landing gear.
- Flight control surfaces.
- Windshields.
- Joints, interfaces and couplings.

Test: Many subsystems or components will be verified by test. The environment will be determined by its physical location on the system and the lightning strike zones that are applicable. More than one zone may apply, that is, all components must conduct the lightning current away from the attachment point in addition to withstanding the thermal, blast and magnetic force effects of direct lightning attachment. Thus all subsystems or components must withstand the *Zone 3* environment in addition to the other zone requirements.

Lightning direct effects are usually limited to the near vicinity of the attachment point. In most structures, the current will diffuse radially away from the attachment point and as the current density decreases, the physical damage also decreases. This indicates that the specimen size for test can be small compared to the size of the total structure or component.

Methods for conducting direct effects verification tests are described in Chapter 6.

Verification of indirect effects protection: Indirect effects protection designs are usually verified by demonstrating that the induced transients appearing at the Line Replacable Unit (LRU) harness interfaces are less than the established *TCL's*, and that the equipment can tolerate the *ETDL's* at their interfaces.

Verification can again be accomplished by test, analysis or similarity to previously verified systems and equipment, or by combination of these methods. Further discussion of these methods is presented in Chapters 8 through 18. Appropriate margins will be required to account for uncertainties.

5.7 Certification plans

Experience has shown, particularly on aircraft employing major amounts of advanced composites or full authority electronic control systems that preparation and the submittal of a **certification plan** early in the program is desirable. FAA concurrence with this certification plan should also be obtained. This plan is beneficial to both the applicant and the FAA because it identifies and defines an acceptable resolution of the critical issues early in the certification process. As the process proceeds, analysis or test results may warrant modifications in protection design and/or verification methods. As necessary, when significant changes occur, the plan should be updated. The plan should include the following items:

Description of the system: There should be a description of the system, covering such things as its installation configuration, any unusual or unique features, the operational aspects being addressed, zone locations, lightning environment, protection design level(s) and approaches.

Description of the protection: There should be a description of the method of protection and the methods to be used to verify the effectiveness of the protection. Typically, the verification method includes a combination of analytical procedures and tests. If analytical procedures are used, the methodology for verification of these procedures should be described.

Pass/Fail Criteria: The pass/fail criteria should be identified and will apply to testing and analysis of lightning protection of fuel systems and electrical/electronic equipment and systems. The pass/fail criteria for an electronic system, for example, might include the following:

A. The equipment transient design level (ETDL).

B. The transient control level (TCL).

C. The margin between ETDL and TCL.

D. Interference with analog or digital data due to the

transients associated with multiple strokes and the multiple burst aspect of the external environment should not endanger safety of flight.

E. Flight safety should not be endangered by direct attachment of the lightning channel to exposed system components. Coverings, such as on fairings, skins and cowls, should normally prevent direct attachment of the lightning channel to underlying system components. However, if a direct lightning strike attachment to a system component can occur, a complete evaluation of both direct and indirect effects will be necessary.

Upset effects on system performance and flight safety should consider parameters such as time duration of upset, the effects of upset on the operation of the system, and the time of occurrence during the various flight modes of the aircraft.

5.8 Test Plans

When tests are to be a part of the certification process, plans for each test should be prepared which describe or include the following: purpose of the test; production or test article to be utilized; article configuration; test drawing, as required; method of installation that simulates the production installation; applicable lightning zone(s); lightning simulation method; test voltage or current waveforms to be used; diagnostic methods, pass/fail criteria, and the appropriate schedule(s) and location(s) of proposed test(s).

Some of the procedural steps that should be taken include the following:

A. Obtain FAA concurrence that the test plan is adequate.

B. Obtain FAA concurrence on details of part conformity of the test article and installation conformity of the test setup.

Part conformity and installation conformity should be judged from the viewpoint of similarity to the production parts and installation. Development parts and simulated installations are acceptable provided they can be shown to adequately represent the electrical and mechanical features of the production parts and installation for the specific lightning tests. Adequacy should be justified by the applicant and receive concurrence from the FAA.

Exploratory lightning tests are often conducted early in the development cycle, a process both recognized and encouraged. These development data may be considered for certification purposes provided the development parts and simulated installations meet the criteria stated above. If it is contemplated that results from development test results will become candidates for certification data, then adequate advance notice of this approach should be given to the FAA for review and acceptance.

C. Schedule FAA witnessing of the test(s).

D. Conduct testing.

E. Submit a final test report describing all results.

F. Obtain FAA approval of the report.

REFERENCES

5.1 *Bonding, Electrical and Lightning Protection, for Aerospace Systems*, US Military Specification MIL-B-5087B, 15 October 1964.

5.2 *Protection of Airplane Fuel Systems Against Fuel Vapor Ignition Due to Lightning*, FAA AC 20-53A, Federal Aviation Administration, Washington, D.C., 12 April 1985.

5.3 *System Design and Analysis*, FAA AC 20-1309, Federal Aviation Administration, Washington, D.C., June 21, 1988

5.4 *Recommended Draft Advisory Circular: Protection of Aircraft Electrical/Electronic Systems Against the Indirect Effects of Lightning*, Report of SAE Committee AE4-L, AE4L-87-3, 4 February 1987.

5.5 *Lightning Protection of Aerospace Vehicles and Hardware*, US DOD Standard 1795, 30 May 1986.

5.6 *Lightning Qualification Test Techniques for Aerospace Vehicles and Hardware*, US Military Standard MIL-STD-1757, 17 June 1980.

5.7 *Protection of Aircraft Fuels Systems Against Lightning*, US FAA Advisory Circular 25-3, Federal Aviation Administration, Washington, D.C., 10 November 1965.

5.8 *Lightning Test Waveforms and Techniques for Aerospace Vehicles and Hardware*, Report of SAE Committee AE–4, Special Task F, 5 May 1976.

5.9 N. Cianos and E. T. Pierce, *A Ground–Lightning Environment for Engineering Use*, Technical Report 1, Prepared by Stanford Research Institute for the McDonnell Douglas Astronautics Company, Huntington Beach, CA, August 1972.

5.10 *Lightning Test Waveforms and Techniques for Aerospace Vehicles and Hardware*, Report of SAE Committee AE–4L, 20 June 1978.

5.11 *Lightning Protection Criteria Document*, NSTS--07636, Lyndon B. Johnson Space Center, Rev. D. 16 July 1987.

5.12 *Space Shuttle Lightning Verification Document*, JSC 20007, Lyndon B. Johnson Space Center, February 1985.

5.13 F. D. Martzloff and F. A. Fisher, "Transient Control Level Philosophy and Implementation: I - The Reasoning Behind the Philosophy," *Second EMC Symposium*, Montreux, June 1977.

5.14 F. A. Fisher and F. D. Martzloff, "Transient Control Level Philosophy and Implementation: II - Techniques and Equipment for Making TCL Tests," *Second EMC Symposium*, Montreux, June 1977.

5.15 R. B. Anderson and A. J. Eriksson, *Lightning Parameters for Engineering Applications*, International Conference on Large High–Tension Electric Systems (CIGRE) Study Committee 33 Document 33-79 (SC)04 IWD.

5.16 F. A. Fisher and J. A. Plumer, *Lightning Protection of Aircraft*, NASA RP 1008, October 1977.

5.17 B. F. J. Schonland, D. J. Malan and H. Collens, "Progressive Lightning: II," *Proc. R. Soc. Lond.*, A 152, 1935, pp. 595-625.

5.18 R. E. Orville and K. Berger, "Spectroscopic and Electric Current Measurements of Lightning at the Monte San Salvatore Observatory in Lugano, Switzerland," *Proceedings of the Fifth International Conference on Atmospheric Electricity*, Garmish-Partenkirchen, Germany, 2-7 September 1974.

5.19 M. A. Uman, "Spark Simulation of Natural Lightning," *1972 Lightning and Static Electricity Conference*, 12-15 December 1972, pp. 5-13.

5.20 R. P. Fieux et al, "Research on Electrically Triggered Lightning in France," *IEEE Trans. on Power Apparatus and Systems*, Vol. PAS-97, No. 3, May/June 1978, pp. 725-733.

5.21 J. A. Plumer, "Further Thoughts on Lightning Strike Zones for Aircraft," Supplement to *Lightning Technology*, NASA Conference Publication 2128, FAA–RD–80–30.

5.22 C. C. R. Jones, "Zoning of Aircraft for Lightning Attachment and Current Transfer," *International Aerospace and Ground Conference on Lightning and Static Electricity*, Dayton, Ohio, June 24-26, 1986, pp.11-1 – 11-13.

Chapter 6

DIRECT EFFECTS PROTECTION

According to legend, protection of aircraft structures was important even to the ancient Greeks.

> *It was not easy, however, to escape from Crete, since Minos kept all his ships under military guard, and now offered a large reward for his apprehension. But Daedalus made a pair of wings for himself, and another for Icarus, the quill feathers of which were threaded together, but the smaller ones held in place by wax. Having tied on Icarus' pair for him, he said with tears in his eyes: "My son, be warned! Neither soar too high, lest the sun melt the wax; nor sweep too low, lest the feathers be wetted by the sea!" Then he slipped his arms into his own pair of wings and they flew off. "Follow me closely," he cried, "do not set your own course."*
>
> *As they sped away from the island in a north-easterly direction, flapping their wings, the fishermen, shepherds, and ploughmen who gazed upward mistook them for gods.*
>
> *They had left Naxos, Delos, and Paros behind them on the left hand, and were leaving Lebynthos and Colymne behind on the right, when Icarus disobeyed his father's instructions and began soaring towards the sun, rejoicing in the lift of his great sweeping wings. Presently, when Daedalus looked over his shoulder, he could no longer see Icarus; but scattered feathers floated on the waves below. The heat of the sun had melted the wax, and Icarus had fallen into the sea and drowned. Daedalus circled around, until the corpse rose to the surface, and then carried it to the nearby island now called Icaria, where he buried it.*
>
> Robert Graves, The Greek Myths I (Baltimore: Penguin Books, 1955):312-13.

6.1 Introduction

The materials from which an aircraft is made and the methods used to hold these materials together, forming the aircraft structure, are factors as important in protecting a modern aircraft from hazardous natural environments as they were for the mythical Icarus. Conventional aluminum airframes of riveted construction have, by virtue of their excellent electrical conductivity, rarely suffered critical structural damage from lightning strikes; and these structures have provided excellent protection for vulnerable systems, as well as for personnel, carried within. There are some important lightning problems that must be considered, such as protection of fuel systems and protection of avionic systems from indirect effects, but such protection has seldom had much of an impact on the basic aircraft structure.

But the day of all-metal aircraft is ending. Aircraft are being constructed using fiber-reinforced plastics which have desirable high strength and light weight, but these materials have much less electrical conductivity than aluminum. Some of these materials are being joined together with adhesives, which have essentially no conductivity. Whereas the designer of the all- metal structure needs to add little, if anything, to the design of the structure to achieve adequate lightning protection, the designers of nonmetallic structures must pay particular attention to the lightning environment, taking positive measures to provide conductive paths to ensure safety of flight.

This chapter reviews some basic lightning effects on metal structures, including metal objects common to all types of aircraft, objects such as bonding jumpers, hinges and light fixtures. It then reviews lightning effects on non-metallic materials such as fiberglass, aramid fiber and carbon fiber composites and concludes by discussing direct effects test techniques and practices appropriate for all categories of aircraft. The discussions will emphasize performance as it relates to the electrical effects of lightning.

6.2 Direct Effects on Metal Structures

The direct effects of lightning on metal structures were described in Chapter 4 and include the following:

1. Melting or burning at attachment points.
2. Resistive temperature rise.
3. Magnetic force effects.
4. Acoustic shock waves.
5. Arcing and sparking at bonds, hinges, and joints.
6. Ignition of vapors within fuel tanks.

This section will focus on protection against these ba-

sic effects since they pertain to aircraft of all types. Later sections will focus on the special problems presented by composite materials. Ignition of fuel vapors, though, is such an important subject that it is treated separately in Chapter 7.

6.2.1 Protection Against Melt–through

For conventional aluminum aircraft, melting at attachment points is mostly of concern as it relates to ignition of fuel vapors in integral fuel tanks, a subject treated at length in Chapter 7. This section on basic lightning effects will, arbitrarily, consider only the damage that lightning may produce on the skins of metal aircraft, such as the size of holes that might be melted. Whether melting of holes, or the creation of hot spots, might ignite fuel vapors, will be discussed in Chapter 7. Discussions as to the thickness of metal skins required to prevent such ignition will also be discussed in that chapter.

In most cases, the designer need be concerned only with prevention of holes in integral fuel tank skins, since small holes in other metal skins do not usually present a safety hazard. This section describes the factors that influence hole formation and methods that can be used to prevent melt–through of metal skins.

Important factors: Lightning usually produces very little damage where it attaches to a metal object, since relatively little energy is released at the attachment point. The energy released at that point is the product of the lightning current and the cathode or anode voltage drop at the end of the lightning channel, or the *arc root*. This drop is a few tens of volts, thus a 400 ampere continuing current releases power at the rate of 12 kW if the cathode (or anode) drop is 30 volts.

The lightning channel is an electrical arc, and it can be very hot (30 000°C), but only the root of the arc contacts the metal surface. Also, the arc is in air and any energy released is free to escape into the air.

Lightning current *can* produce spectacular damage when forced through a confined arc, a situation not normally encountered with aircraft. An exception to this general statement is covered in §6.2.2.

Assuming that the lightning channel is not confined, the damage produced at the point where lightning attaches to a metal object is largely controlled by how long the lightning channel remains attached to a particular point. If the channel sweeps swiftly across an unpainted aluminum skin, for example, the effect might be only to produce minor pitting of the surface. Usually, however, the channel is not completely free to move. Paint films on a metal surface in *Zones 1A* or *2A* will tend to keep the channel attached to individual spots along painted surfaces, thus allowing the metal skins to be melted at these spots. Fig. 6.1 shows an example of small pit marks left by a lightning flash sweeping across a metal surface.

At trailing edges, in *Zones 1B* or *2B*, the channel may remain attached for longer periods, melting away larger amounts of metal. This is usually not hazardous, and it is neither practical nor necessary to protect against holes in trailing edges.

Protection should be provided against any holes that would endanger safety of flight, but as a general rule holes may be permitted to occur anywhere on the aircraft as long as safety of flight is not impaired. The conditions under which safety of flight might be endangered from hole formation are:

1. When the hole is melted through the skin of a fuel tank or some other enclosure containing flammable materials.
2. When the hole causes depressurization of a pressurized enclosure.
3. When the hole sufficiently degrades the mechanical strength of a flight–critical component to cause failure.

There have been reports of holes melted in pressurized fuselages by swept strokes, but the holes are far too small (less than 0.1 cm dia) to cause depressurization problems. Since trailing edge areas are not pressurized, the larger holes melted by longer duration currents hanging on to trailing edges have not posed a depressurization problem, although the possibility of this event should be considered in any design that involves pressurization in trailing edge sections.

Melting and charge transfer: The relationship between lightning and the size of hole burned has been extensively studied. Basically, the studies have shown that the volume of metal melted away at a lightning attachment point is closely related to the charge carried into the point by the lightning flash and to the type of metal and its thickness. Most of the charge is delivered by intermediate and continuing current components of the flash. The volume of metal and the size of the hole are, of course, related by the thickness of the metal skin.

Hole size vs charge transfer: Quantitative relationships between electric arcs and typical aircraft skin metals were reported in 1949 by Hagenguth [6.1] who made laboratory measurements of the amount of continuing current necessary to melt holes of various sizes in various metals. He found a nearly linear relationship to exist between the amount of charge (Q) delivered to an arc attachment spot and the amount of

metal melted away from it. He found that the size of a hole melted in a metal sheet of a given thickness could be approximated by the following two empirical equations:

$$A = 0.93Q\ t^{-0.9} \quad \text{for } 0 < t < 0.8 \text{ mm} \qquad (6.1)$$

$$A = 0.81Q\ t^{-1.54} \quad \text{for } 0.8 < t < 4 \text{ mm} \qquad (6.2)$$

where

A = area of hole melted (square millimeters)
Q = charge (coulombs) delivered to the point by the arc
t = thickness of metal sheets (centimeters).

Hagenguth also reported that "the type of metal appears to have very little influence," but later investigations have contradicted this statement. Results of his laboratory tests are presented in Fig. 6.2.

Melt–through thresholds: Brick [6.2] and Oh and Schneider [6.3] made tests to determine the minimum amounts of charge and current required to melt through aluminum and titanium skins of various thicknesses, and thus the minimum lightning conditions that might produce ignition in integral fuel tanks. They also showed that the effects depended heavily on current amplitude as well as charge. Whereas Hagenguth had shown that over 22 C, when delivered by a current of 200 A, were necessary to melt through 2 mm (0.080 in) aluminum skins, Brick, Oh, and Schneider showed that only about 10 C, when delivered by about 500 A, was enough to melt completely through such a skin. In laboratory tests as little as 2 C, when delivered by about 130 A, melted a hole completely through 1 mm (0.040 in) of aluminum.

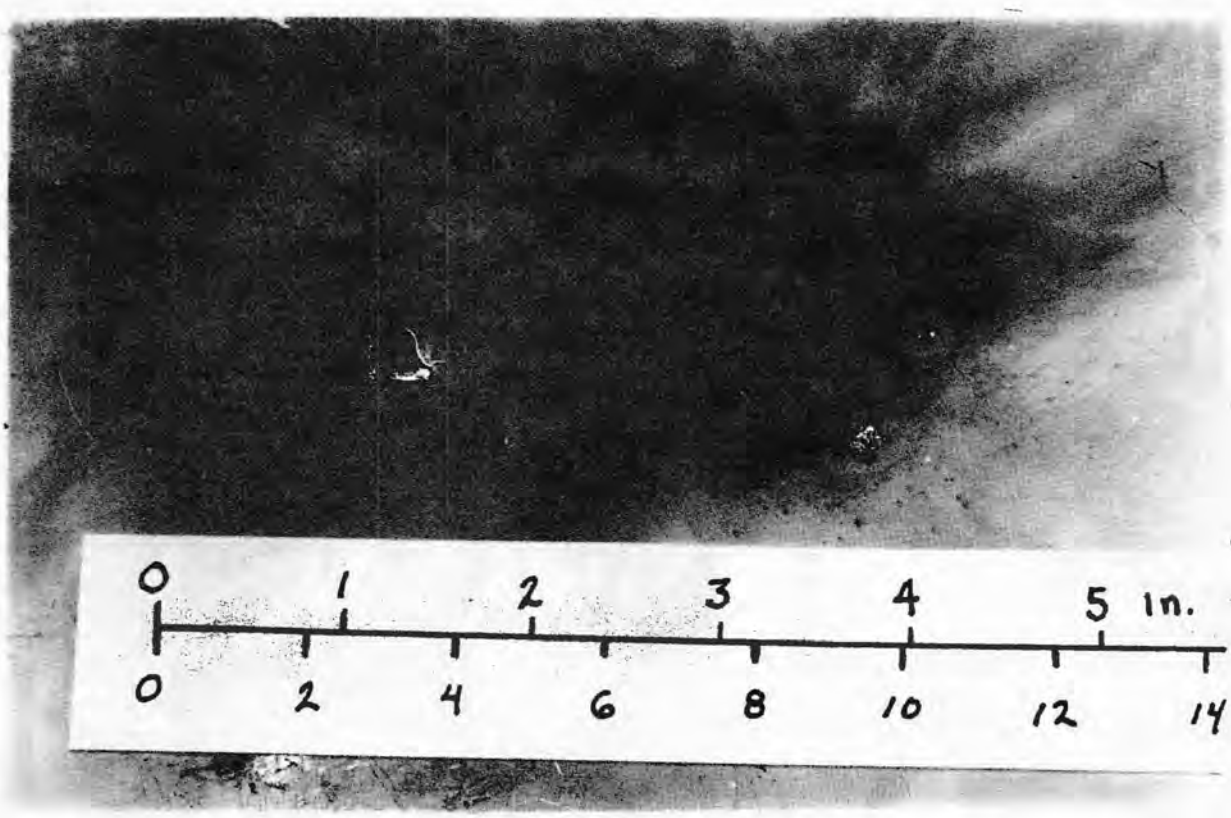

Fig. 6.1 Burn marks left on metal surface by simulated lightning flash.

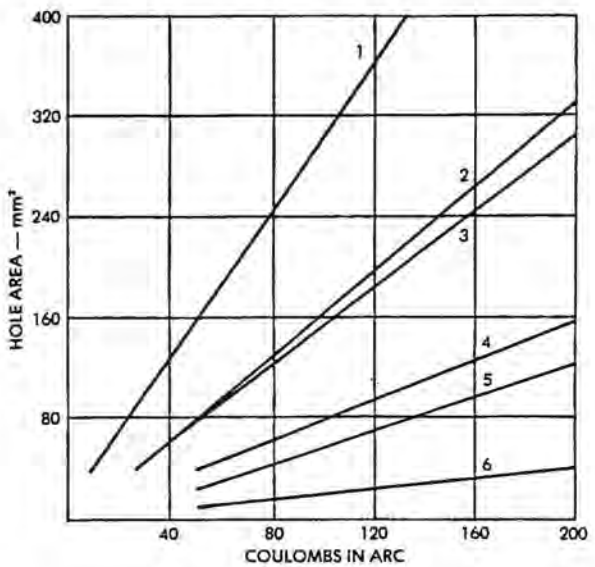

Fig. 6.2 Size of holes melted in metal sheets by arc currents ranging between 50 and 1000 A [6.1].
1. Stainless steel - 0.254 mm (0.010 in)
2. Galvanized iron - 0.381 mm (0.015 in)
3. Copper - 0.508 mm (0.020 in)
4. Stainless steel - 1.061 mm (0.040 in)
5. Aluminum - 1.295 mm (0.051 in)
6. Aluminum - 2.54 mm (0.010 in)

Oh and Schneider's melt–through thresholds for these and other skin thicknesses are shown in Fig. 6.3. The close proximity of their test electrode to the skins, 2.4 to 4.8 mm, might have restricted natural movement of the arc on the surface of the skin and been responsible for their low coulomb ignition thresholds. Such restrictions, however, should be assumed when the exterior surface is painted.

Additional data: Work by Kester, Gerstein, and Plumer [6.4] with an L–shaped electrode spaced 6.4 mm above the skin, permitting greater arc movement, showed that 20 C or more, when delivered at 130 A, are required to melt through a 1 mm aluminum skin. Their data is presented in Fig. 6.4. However, the magnetic interactions associated with currents in the L–shaped electrode might have forced unnatural movement of the arc, resulting in an optimistic result. Since movement of a natural lightning arc is neither restricted nor forced by any electrode, it is probable that the aluminum melt–through threshold data of Fig. 6.3 are conservative, while those of Fig. 6.4 might be optimistic.

Influence of paints: The electrical insulating properties of most paints tend to make the arc remain at one point and so would concentrate the heating effects on a smaller volume of metal, decreasing the amount of thermal energy required to melt completely through.

Influence of pressure: All the data on melt–through of metal surfaces discussed in the previous sections was taken on test panels in ambient conditions, that is, equal pressure on both sides of the panels. Many aircraft fuel systems, especially on fighters, maintain some pressure in the tank, to help pumping. Many other systems use ram air vent supplies and these also supply small amounts of pressure on the tank.

Pressure inside the tank on which burn–through tests are being made makes a big difference in the level at which a hole appears. A lightning arc may heat the surface to a point where metal is molten, but if there is no pressure, the surface tension prevents the molten metal from flowing away and leaving a hole. A very modest amount of pressure, however, suffices to push the molten metal away and leave a hold. Recent tests, not yet released for publication, showed that with a gauge pressure of 34.5 kPa (5 psig) holes could be burned in a 2.3 mm (0.090 in) aluminum skin by a 23 A.s discharge. With no pressure 66 A.s was required to produce an equivalent size hole.

This is a phenomenon that remains to be investigated more thoroughly.

Trailing edges: The structural integrity of a trailing edge closeout member or other load–carrying part may be degraded if a significant portion of metal is melted away by a lightning arc hanging on for a prolonged period of time. For design purposes, the charge transferred under the worst case lightning flash should be taken as 200 C, in accordance with *AC 20-53A* [6.5]. Estimates of the amount of metal to be melted away by 200 C of charge entering a lightning hang–on spot in *Zones 1B* or *2B* may be made from Figs. 6.2 - 6.4.

Protection methods: Some of the considerations governing protection of metal surfaces are illustrated in Fig. 6.5.

Protection by thickness: The most direct way to prevent melt–through of holes is to use aluminum skins sufficiently thick to withstand the lightning environment without complete melt-through. The specific thickness required depends on lightning flash dwell time. For unpainted aluminum skins, polished or anodized, where the dwell times usually do not exceed 5 ms, only current component *B* needs to be withstood. From Fig. 6.3, this requires a skin at least 1.5 mm (0.060 in) thick.

(a)

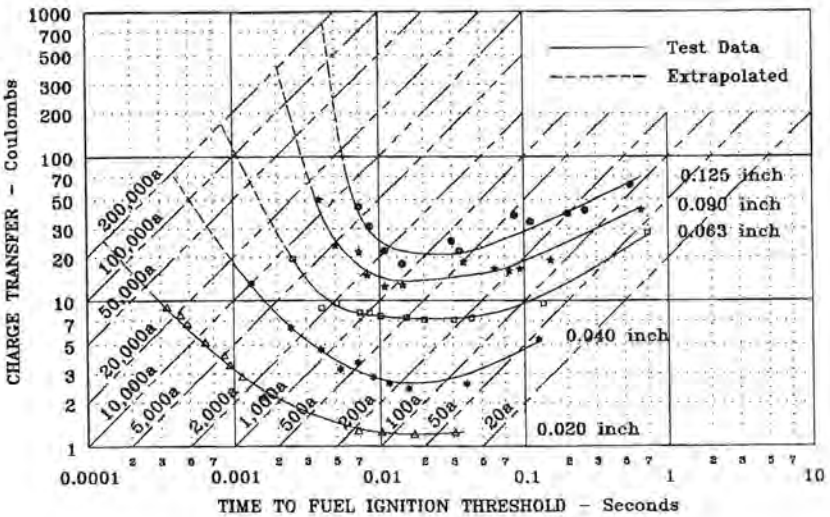

(b)

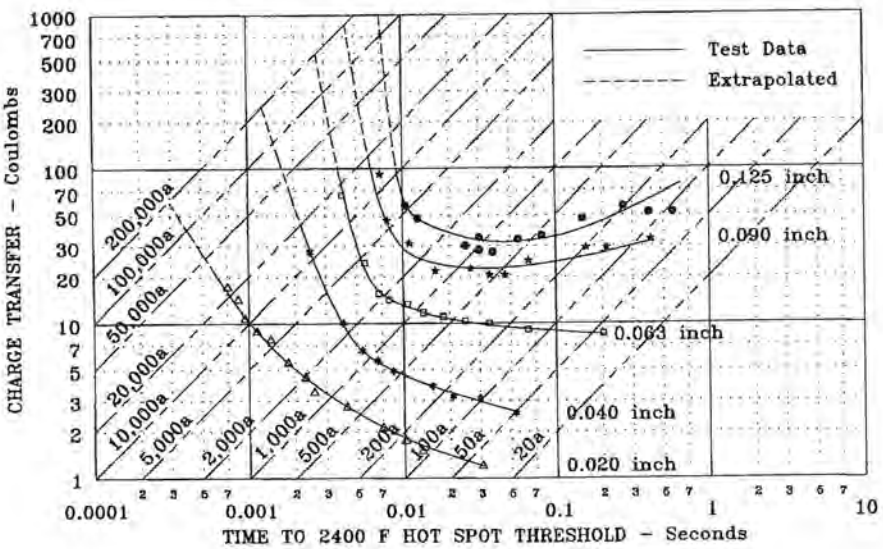

Fig. 6.3 Melt-through thresholds of metal skins.
(a) Aluminum skins - 2024 T3
(b) Titanium skins - 6AL 4V

For painted skins in *Zones 1A* or *2A*, dwell times should be asumed to be 20 ms for typical paint thicknesses not exceeding 0.25 mm (0.010 in) thick. This requires skin thickness of 2.0 - 3.0 mm (0.080 in - 0.120 in). This is the most common method of preventing holes in metal skins.

Protection by arc root dispersion: A second method of preventing melt–through involves treatment of the exterior surface with an electrically "bumpy" finish that promotes the arc root to divide into many paths and not to be concentrated at just one point. This approach is called *arc root dispersion*, is illustrated in

Fig. 6.5(b), and is applicable to CFC skins as well as metal ones. Fine wire screens and paint primers filled with chopped metal fibers have been effective in laboratory tests, though this method requires greater than average care and maintenance of the surface during the aircraft's life cycle. It is not presently in wide use.

Protection by multiple layers: A third method is to laminate thin metal skins with a non–conductive adhesive (most structural adhesives are non–conducting). Laboratory testing has shown that the melting activity is limited to the exterior ply of metal, with the inner ply remaining undamaged. The principle is illustrated in Fig. 6.5(c). The outer ply burns away, but in doing so separates from the inner ply and moves the arc root, where heat is released, away from the inner ply. Vaporization of the adhesive layer probably releases gasses which push the outer layer away. In effect, the outer layer is sacrificed to protect the inner ply.

As an example, an exterior ply of 0.5 mm (0.020 in) aluminum bonded to an inner ply of 0.75 mm (0.030 in) aluminum will sustain the same lightning environment as a single sheet of 2 mm (0.080 in) aluminum.

Since melting of holes in metal skins is so important to protection of fuel systems these studies are covered further in Chapter 7.

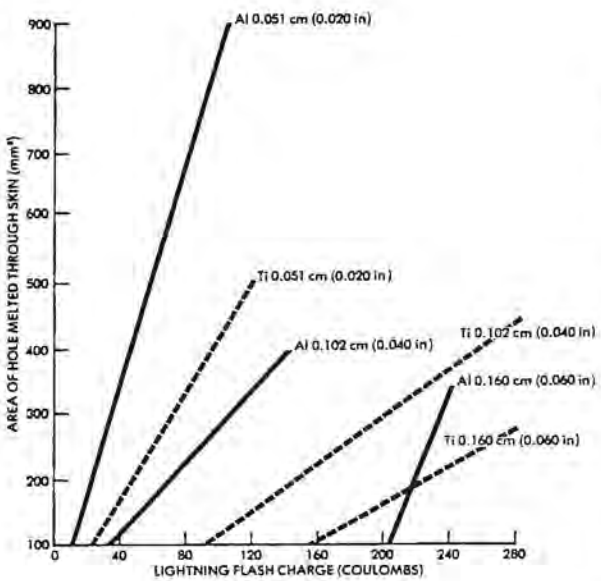

Fig. 6.4 Area of holes melted through aluminum and titanium skins.

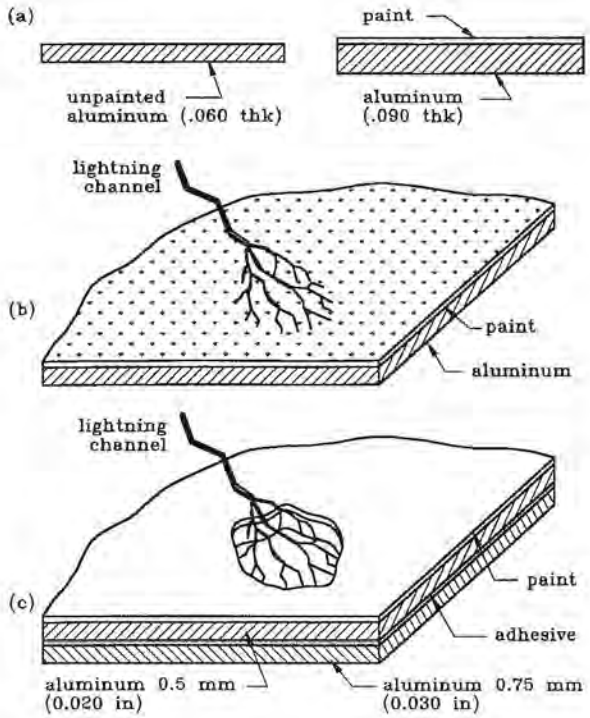

Fig. 6.5 Methods of protecting against melt–through.
(a) Increasing skin thickness
(b) Arc root dispersion
(c) Laminated skins

6.2.2 Resistive Heating

As current passes through the resistance of a metal conductor, it will generate heat. Resistive heating of metal skins by lightning current will never produce temperatures high enough to be of concern, because cross–sectional area will always be ample, but heating of conductors with small cross-sections can be sufficient, in some cases, to damage or destroy these conductors. Wiring harnesses and control cables are examples. A particularly important problem arises if a conductor is heated enough to melt it, because then the wire might literally explode and cause very severe damage.

Some of the factors that affect heating and melting of various metals are listed in Table 6.1.

Calculation of temperature rise: The temperature rise in a current–carrying conductor is:

$$\Delta T = \frac{0.2389\rho}{cDA^2}\int I^2 dt \qquad (6.3)$$

where

I = Amperes

t = seconds

c = specific heat - cal/g/degree C

D = density - g/cm^3

ρ = resistivity - ohm cm

A = cross–sectional area.

Temperature rise is directly proportional to the square of the lightning current and inversely proportional to the square of the cross–sectional area of the conductor. The equation is expressed in terms of unit length. Energy will be deposited uniformly along the length of the conductor, resulting in a uniform temperature rise along the length.

As it stands, however, Eq. 6.3 has two shortcomings:

1. It assumes there is no heat loss from radiation.
2. It assumes that resistance does not change with temperature.

Since little energy will be lost during the short duration of a lightning flash, the first shortcoming has a negligible effect on the accuracy of the predicted temperature rise. Resistance does depend on temperature, however, and, since resistance also affects the amount of electrical energy that can be deposited in the conductor, it is important to account for this dependency. This can be done by expressing resistivity as a function of temperature,

$$\rho = \rho_{20}[1 + \lambda \Delta T] \tag{6.4}$$

where

ρ_{20} = resistivity at 20°C

λ = temperature coefficient of resistivity.

Incorporating Eq. 6.4 into Eq. 6.3 gives:

$$\Delta T = \frac{0.2389\rho_{20}[1 + \lambda \Delta T]}{cDA^2} \int I^2 dt \tag{6.5}$$

Since everything but ΔT in Eq. 6.5 is a constant, it is most easily solved by combining the conductor dimensions, material properties and specified action integral into a constant, k, in the following expression:

$$\Delta T = k[1 + \lambda \Delta T] \tag{6.6}$$

$$\Delta T = \frac{k}{1 - \lambda k} \tag{6.7}$$

where k is given by the right side of Eq. 6.5.

Fig. 6.6 shows calculated temperature rises for various metals as functions of the action integral of the current. The data has been calculated from Eq. 6.5 and may be used for design purposes.

Physical and electrical properties needed in Eqs. 6.6 and 6.7 for common structural metals and electrical conductors are provided in Table 6.1. The melting points of these metals are also provided.

Table 6.1

Physical and Electrical Properties of Common Metals

	Aluminum	Copper	Titanium	Stainless Steel (304)	Magnesium	Silver
Resistivity Ω-cm	2.8×10^{-6}	1.72×10^{-6}	42×10^{-6}	72×10^{-6}	4.45×10^{-6}	1.59×10^{-6}
Temperature coefficient of resistance, λ (1/degree C)	0.00429	0.00393	0.0035	0.001	0.0165	0.0041
Thermal coefficient (1/degree C)	0.254×10^{-4}	0.164×10^{-4}	0.085×10^{-4}	0.120×10^{-4}	0.025×10^{-4}	0.019×10^{-4}
Specific heat cal/gm/degree C.	0.215	0.092	0.124	0.120	0.245	0.056
Density (g/cm^3)	2.70	8.89	4.51	7.90	1.74	10.49
Melting point (degree C)	660	1084	1670	1150	650	962

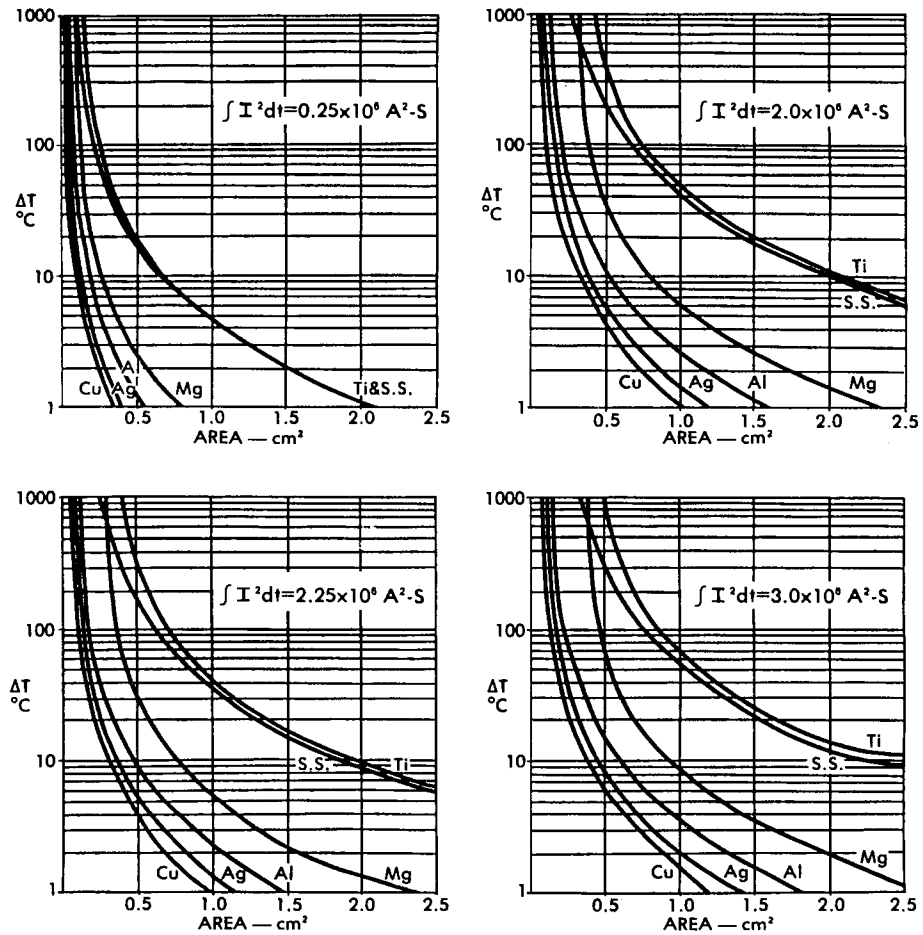

Fig. 6.6 Temperature rise as a result of electric current in conductors.

Because of their high amplitudes, the return stroke currents have the highest action integrals and will produce higher temperatures than the other components of the lightning flash. For design purposes, the action integrals associated with current waveform Components A and D, as specified in [6.5] and §5.5.6 should be used for determining temperature rise in conductors, depending on the lightning strike zone in which the particular conductor is located.

Example: The stroke current to be used for design purposes depends on the strike zone. Consider, for example, a case in which a navigation light is mounted on a plastic vertical fin cap and grounded to the airframe via two bond straps, as shown in Fig. 6.7. In this case, two parallel conductors are available to share the current, and the current in each will be divided by the number of conductors, but the action integral in each conductor will be reduced by the square of the number of conductors.

If this light is considered to be located in *Zone 1B*, its bond straps must be able to conduct the total flash current. If it is assumed that the lightning channel will not touch the bond straps, the design criterion for these straps is that together they must be able to carry safely current Components A and D, which have a total action integral of 2.25×10^6 A^2·s. One–half of the total current in each strap will produce only one–fourth of the total action integral, or about 0.56×10^6 A^2·s, in each strap.

If each strap is made of copper with a cross–sectional area of 0.1 cm^2 (0.015 in^2), the temperature rise produced by 0.56×10^6 A^2·s in a strap would be determined from Eq. 6.5, using the physical and electrical properties for copper given in Table 6.1. Solving first for k:

$$k = \frac{0.2389 \times 1.72 \times 10^{-6} \times 0.56 \times 10^{6}}{(0.092 \times 8.89 \times 0.1^{2})} = 25.6°C. \quad (6.8)$$

This would be the temperature rise if the resistivity remained constant, but the resistivity actually increases as temperature increases. Therefore, Eq. 6.5 must be used as follows to calculate the actual rise:

$$\Delta T = \frac{28.1}{1 - 0.00393 \times 28.1} = 31.6\ °C. \quad (6.9)$$

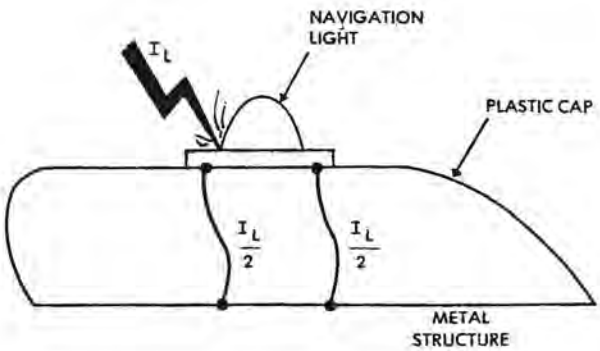

Fig. 6.7 Bond straps for navigation light.

A conductor with a 0.1 cm^2 cross-sectional area is about the same size as an AWG 15 wire. Since a 32 °C temperature rise would not damage the wire, two bonding straps or wires of this cross-sectional area could be utilized to conduct current Components A and D. If one of them were to work loose, however, all of the current would have to pass through the other one. If the total action integral were 2.25×10^6 $A^2 \cdot s$, the temperature rise would be just over 200 °C.

Consideration of temperature rise effects in conductors carrying lightning currents is most important where all, or a large fraction, of the stroke current will be carried in individual conductors. Examples include radome diverter bars, bonding straps (or jumpers), conduits or cable shields, ground wires passing through plastic radomes or wing tips, and certain hydraulic or control lines which might be exposed to lightning strike currents.

The temperature rises calculated must be added to the ambient temperature of the conductor to determine the final temperature. Calculated temperatures above several hundred degrees C will begin to diverge from the actual temperature because of physical property changes at higher temperatures. In most cases it is best to select conductor materials and cross sectional areas and cross-sectional areas so as to limit temperature rises to $100°C$, so that distortion, elongation and changes to temper of material will not occur.

If lightning current entering a conductive skin surface can be divided into multiple current filaments entering the skin at separate locations, the energy deposited in the resistance of the skin near each sopt will be reduced by the square of the number of current filaments from what it would be if all current were to enter the skin at a single point. The action integral associated with each filament of current would be

$$\int I^2 dt \text{ (each filament)} = \frac{\int I^2 dt \text{ (total)}}{N^2} \quad (6.10)$$

where N is the number of parallel filaments.

This implies that the damage to an airplane skin can be minimized by encouraging the splitting up of the lightning channel into many filaments as it enters a skin, a process known as arc root dispersion and which is discussed more fully in §6.5.1. The $1/N^2$ reduction implied by Eq. 6.10 is, of course, only true for heating and damage effects that are directly proportional to action integral, and there are other energy transfer mechanisms associated with electric arc attachment to conductive surfaces that are not dependent on, or at least directly related to action integral.

Nevertheless, tests have confirmed that thermal and shock wave damage to metal and CFC skins is greatly reduced when provisions are made to cause arc root dispersion.

Thermal Elongation: Most metals expand when their temperatures rise. This phenomenon will not be a problem for conductors which can deflect when expanded, but if the conductors are held rigidly in place large stresses may arise and the conductors may buckle. Examples would include a diverter strap, a ground conductor or the pitot probe air tube shown in Fig. 6.8.

By virtue of its location at the nose of the aircraft, the pitot probe will be in *Zone 1A* and provision must be made to conduct return stroke currents of 2×10^6 $A^2 \cdot s$ to the airframe. The air tubes, if made of metal, would have to have a large cross-section to carry the lightning current and withstand the resulting resistive heating, thermal elongation, and magnetic force effects of the lightning current, probably con-

siderably larger than needed just to transmit pitot–static air back to the flight instruments. It might be better, therefore, to fabricate the tubes of non–conducting plastic and provide a separate metal conductor to carry lightning current from the probe to the airframe. An AWG. No. 6 copper wire will suffice. A stranded conductor would be better than a solid one because it can flex a small amount because of temperature rise without the deflections presenting a problem.

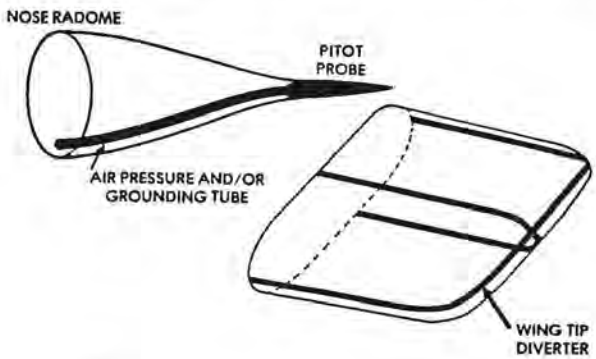

Fig. 6.8 Examples of rigidly held lightning current conductors.

Example of expected elongation: If the air tube in the radome of Fig. 6.8 were made of copper and had an outside diameter of 0.476 cm (3/16 in) and a wall thickness of 0.124 cm (0.049 in), it would have a cross–sectional area of 0.138 cm^2 (0.021 in^2). An action integral of 2×10^6 $A^2 \cdot s$ would raise the temperature of a conductor of this cross–sectional area by 67°C.

The amount of thermal expansion to be expected along any dimension of a part is dependent on the temperature rise and the thermal coefficient of linear expansion of the metal, according to the following relation:

$$\Delta L = L\alpha\Delta T \tag{6.11}$$

where α is the coefficient of expansion and L is the length of concern. Of course all dimensions of a homogeneous material will elongate proportionately and this may affect fittings and clamps. The most significant expansion, though, would be along the length of the conductor.

Based on the coefficient of linear expansion for copper given in Table 6.1, $0.164 \times 10^{-4}(1/°C)$, and on the assumption that the tube has a length, L, of 2 m when "cold," a 67°C temperature rise would cause an elongation of

$$\begin{aligned}\Delta L &= 2 \times 0.164 \times 10^{-4} \times 67 \\ &= 2.198 \times 10^{-3} \text{ m} = 2.2 \text{ mm}.\end{aligned} \tag{6.12}$$

This amount of expansion may be well within the limits established by normal environmental temperature cycling, but other situations might exist where the thermal expansion caused by lightning current could be a concern. Any conductor that might carry lightning current should be examined to see whether thermal elongation might be a problem.

Exploding Wires: A case in which an excessive temperature rise may occur is one in which lightning current is carried by only a single conductor, such as an undersized bond strap or a steel control cable. In these cases, the action integral of the lightning current and the resistance of the conductors may both be high enough to allow enough energy to be deposited in the conductor to raise its temperature to the melting or vaporization points. Since the resistance of most metal conductors increases with temperature, an even higher amount of energy will be deposited in the conductor as its temperature rises, and this, in turn, will increase the temperature even further. If the action integral is high enough, the conductor will melt and perhaps even explode. An explosion of a wire can cause severe damage since the chemical energy associated with combustion of the wire is added to the electrical energy produced by passage of the lightning current.

An example of damage to a radome that was probably the result of an exploding wire was shown in Fig. 4.7.

Another example was the unprotected composite wing tip design of Fig. 4.8, where the navigation light harness was the only conductor available to carry lightning current from the lamp assembly to the airframe. It exploded, destroying the wing tip. This could have been prevented by providing an alternate parallel path for the lightning current.

6.2.3 Magnetic Force Effects

As mentioned earlier, there are situations in which several conductors in parallel may carry lightning currents and, in such cases, each conductor will be acted upon by a magnetic force. One such case is shown in Fig. 6.9.

Based on Ampere's Law, the force per unit length on wire 2 is

$$\frac{dP_{1,2}}{dl_2} = \frac{2\mu I_1 I_2}{D} \tag{6.13}$$

where

$$\mu = 4\pi \times 10^{-7} \text{ A/m}$$
$$P_{1,2} = \text{force on conductors - N}$$

$l_{1,2}$ = length of conductors - m

D = distance between conductors - m

$I_{1,2}$ = current in conductors - A

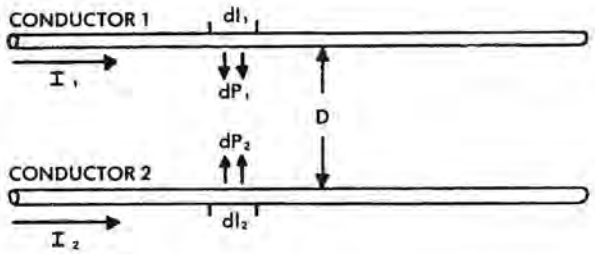

Fig. 6.9 Magnetic forces among parallel current-carrying conductors.

These forces act to pull the conductors together when the currents in them are in the same direction and act to push the conductors apart when the currents are in opposite directions. In either case, the magnetic forces are strongest when the conductors are close together. One such case would exist, for example, in a radome-mounted pitot system in which two metal air pressure tubes are needed to convey both static and pitot air pressure to the flight instruments. If these tubes were mounted 2 cm apart and half of the *Zone 1* lightning current (200 kA) were carried in each, the peak force in each conductor be:

$$\begin{aligned}\frac{dP_{1,2}}{dl_{1,2}} &= 2 \times 10^{-7} \times 100 \times 10^3 \times \\ &\qquad 100 \times 10^3 \times 2 \times 10^{-2} \\ &= 100,000 \text{ N/m of tube length} \\ &= 6,854 \text{ lb/ft of length} \qquad (6.14)\end{aligned}$$

This peak force, of course, will exist only at the instant when the lightning current is at its peak.

The inertia of the conductors will keep them from moving much during the short duration of the high amplitude stroke current, but energy will be stored in the conductors and they will continue to move after the current has passed. If both tubes are assumed to be of the size in the thermal calculation given previously, then the mass of each tube will be:

$$\begin{aligned}m &= DAl \\ &= 8.89 \text{ g/cm}^3 \times 0.138 \text{ cm}^2 \times 100 \text{ cm} \\ &= 122.7 \text{ g/m} \\ &= 0.1227 \text{ kg/m.} \qquad (6.15)\end{aligned}$$

Since

$$F = ma$$

and

$$a = \frac{10^5 \text{ N}}{0.1227 \text{ kg}} = 815 \times 10^3 \text{ m/s/s}$$

and the duration of the stroke is about 70 microseconds, the motion of the tubes will be

$$\begin{aligned}x &= 1/2\ at^2 \\ &= 1/2 \times 815 \times 10^3 \times (70 \times 10^{-6})^2 \\ &= 2 \text{ mm.} \qquad (6.16)\end{aligned}$$

The velocity will then be

$$\begin{aligned}v &= at \\ &= 815 \times 10^3 \times 70 \times 10^{-6} \\ &= 57.1 \text{ m/s,} \qquad (6.17)\end{aligned}$$

and the kinetic energy will be

$$\begin{aligned}E &= 1/2\ mv^2 \\ &= \frac{0.1227}{2} \times 57.1^2 \\ &= 200 \text{ joules.} \qquad (6.18)\end{aligned}$$

This energy will cause the tube to continue moving for some distance. The resulting deflection will depend on the degree of restraint provided by supports and the elasticity of the tube, but forces of the magnitude predicted by Eq. 6.14 have caused tubes to slam together, leaving permanent deformations, which can disrupt the air data system.

Effective transient force: Mathematical calculation of expected deformations from impulsive forces such as these is difficult, and such calculation is further complicated by unknown mechanical factors. James and Phillpott [6.6], however, have defined an effective transient force, P_t, which, if applied slowly but continuously, results in the same stress as that produced by the peak magnetic force, P_o, calculated by Eq. 6.14. This effective force, P_t, is a function of the natural angular frequency, ω, of the mechanical system being acted upon and of the electric current decay time constant, τ.

It is usually much easier to determine magnetic force effects by tests of candidate installations, rather than by calculations, and the results are more likely to be correct. A discussion of test methods is presented in §6.8.

Angular frequency: In most practical applications the natural angular frequency ω of the conductor will be between about 10^3 for heavy, flexible systems and 10^4 for light, stiff systems. James and Phillpott give relative values of P_t/P_o. These are shown in Table 6.2 for each of these frequencies and for three lightning current waveforms. The 200 kA and 1 kA currents represent a return stroke and continuing current of the same magnitude as those represented by Components *A* and *C* of *AC 20-53A*. However, the 50 kA intermediate current would deliver much more energy than would the 2 kA intermediate current, represented by Component *B*. A current pulse of 50 kA amplitude, and decaying in as long as 2 ms, would be found only in the most severe of positive polarity flashes. These occur very seldom. In any event, Table 6.2 shows that the 200 kA stroke current creates a much higher effective transient force, P_t, than does either of the other currents.

An example of how the table is used may be found in the case of the two parallel air pressure tubes 2 cm apart, for which a peak force P_o of 100 000 N/m of length was calculated. Assuming that these tubes have an angular frequency of 10^4, Table 6.2 shows that the effective transient force, P_t, would be

$$P_t = 0.45 P_o \tag{6.19}$$

or 45 000 N/m (3084 lb/ft) of length. This is the amount of force which should be used in performing mechanical response calculations or mechanical strength tests.

James and Phillpott conclude that:

(a) The continuing current phase of a lightning flash does not give rise to a high effective force because I^2, and therefore the peak magnitude force, is too low.

(b) If $\tau \ll 1/\omega$, as for relatively heavy flexible systems ($\omega = 10^3$), the effective force is roughly proportional to $I^2 t$. Thus, the fast and intermediate components give about the same effective force, even though the peak forces are very different.

(c) If $\tau \gg 1/\omega$, as for relatively light stiff systems ($\omega = 10^4$), the effective force equals twice the peak force, and is therefore proportional to I^2. For this doubling of the peak force to occur it is assumed that the current rise time is $\ll 1/\omega$.

(d) If $\tau \approx 1/\omega$, the effective force is 45% of the peak force for the case of the fast component, with $\omega = 10^4$. This alternative also gives the highest effective force because the high value of I^2 more than compensates for the effects of a small value of τ.

James and Phillpott also conclude that "the effect of magnetic forces on current–carrying components is influenced by a large number of parameters, but the contribution from the continuing current is negligible." Concurring with the authors of this book, they also conclude that future studies of or tests on components likely to be damaged by magnetic forces should be performed with simulated lightning currents having values of I and action integral similar to Components *A* or *D*, depending on the zone in which the installation is located.

Examples of magnetic damage: Secondary airframe structures and control surfaces sometimes become badly damaged by magnetic force effects. One example is the wing tip trailing edge shown in Figs. 4.4, in which the upper and lower surfaces of this wing were made respectively of 0.71 mm (0.028 in) and 0.80 mm (0.031 in) aluminum. Hacker ([6.7] has made a very interesting analysis of the magnetic forces acting upon

Table 6.2

Effective Transient Magnetic Force P_t

I (kA)	τ (ms)	Coulombs (C)	I^2t 10^6 (A^2-s)	P_o (Relative Units)	P_t/P_o		P_t (Relative Units)	
					$\omega = 10^3$	$\omega = 10^4$	$\omega = 10^3$	$\omega = 10^4$
200 (Stroke)	0.1	20	2.0	16.0	0.05	0.45	0.8	7.2
50 (Int)	2.0	100	2.5	1.0	0.75	1.73	0.75	1.73
1.0 (Cont)	200	200	0.1	0.0004	2.0	2.0	0.0008	0.0008

these surfaces and found, as illustrated in Fig. 6.10, that the directions of the calculated forces and the calculated damage, Fig. 6.10(c), correlate well with the actual damage pattern. Figs. 6.10(a) and (b) give details of the geometry on which the calculations were based.

Hacker calculated that a 100 kA stroke would have created 21 500 N/m (1476 lb/ft) on a 4 cm wide path across the skins. This amounts to 5.4×10^5 N/m^2, or 78 psi, an extremely high compressive pressure for a wing structure reportedly designed for a steady state loading of 1.7×10^3 N/m^3 (0.25 psi). The reader is referred to Hacker's report for a more thorough discussion of the procedure followed in making this analysis.

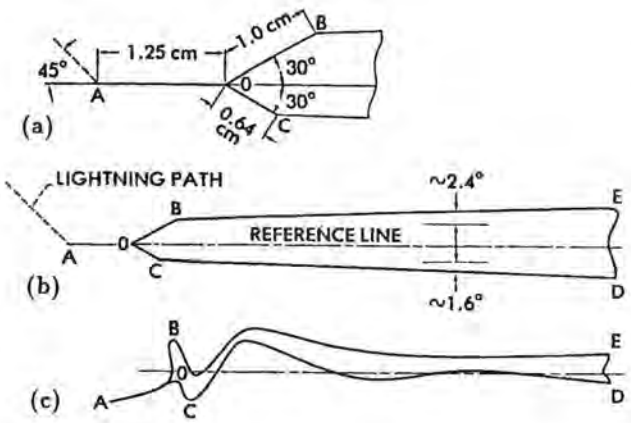

Fig. 6.10 Calculation of magnetic deformation.
(a) Geometry at tip
(b) Geometry of chord
(c) Calculated deformation

Repulsive Forces: The foregoing examples have illustrated the case in which the magnetic forces are attractive; that is, when the parallel currents are in the same direction. Cases exist, however, where currents in adjacent conductors, or in adjacent legs of the same conductor, are in opposite directions. When this happens, the magnetic force acts to separate the conductors, a fact that may create a problem.

An example is the force that a lightning channel sweeping alongside a radome as on metal ground conductors, such as a pitot heater grounding tube, fastened to the inside of the radome wall. This situation is illustrated in Fig. 6.11(a). The result is often severe damage to the grounding tube and radome wall, as the tube is ripped away from the wall.

This problem might be reduced by using segmented diverters. They might allow the flash to reattach sooner, minimizing magnetic force effects, as illustrated in Fig. 6.11(b).

Protection designs should be tested to verify adequacy, as magnetic force effects are not readily determined by analysis. Test specimens should be arranged to simulate the sweeping action of the lightning channel, by positioning the high current test electrode along the radome, as if it were a sweeping channel. Further discussion of these aspects of testing is presented in §6.8.

Magnetic forces on bond straps: Another common example of a situation in which the currents in opposite directions give rise to repulsive forces is the bent bond strap shown in Fig. 6.12(a). Even if the strap has a cross-sectional area sufficient to conduct the current, but forms a bend of more than about 45 degrees, it may break, as shown in Fig. 6.12(a), if it is subjected to major portions of the stroke current. Whenever possible, such straps should be installed with gentle bends, as in Fig. 6.12(b).

Another reason for keeping the bond strap as straight and short as possible is that the inductive voltage rise caused by lightning currents in a longer strap may be sufficient to spark over a direct, shorter path across the air gap. Some other "do's" and "don'ts" regarding the design of bond straps intended to carry lightning currents are presented in Fig. 6.13. The basic rules to follow are:

1. Use conductors with sufficient cross-sectional area to carry the intended lightning current action integral.
2. Keep bond straps as short as possible.
3. Avoid bends of more than 45 degrees, or other features that result in a reversal of the current direction.
4. Avoid all sharp turns.
5. If two or more parallel straps are used, separate them sufficiently (usually 30 cm or more) to minimize magnetic force effects.

The above rules should, of course, be followed for any light weight conductor, such as a metal air tube or hydraulic line that must carry lightning current. Flight critical installations should be tested to verify design adequacy.

Consequences of magnetic damage: Because of weight limitations, the strength and rigidity of some metallic components, such as wing tips, flaps, and

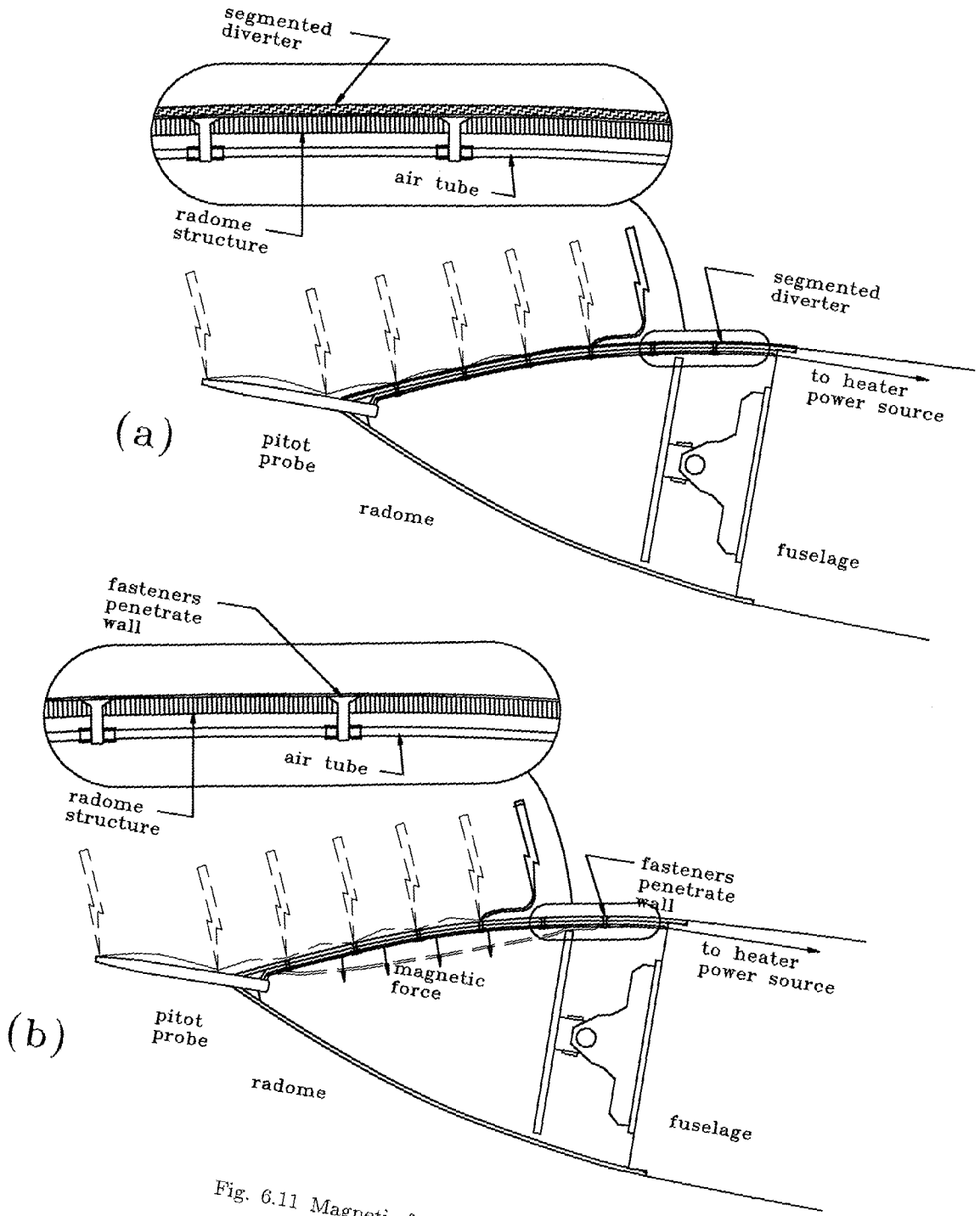

Fig. 6.11 Magnetic forces.
(a) External diverter
(b) Internal diverter

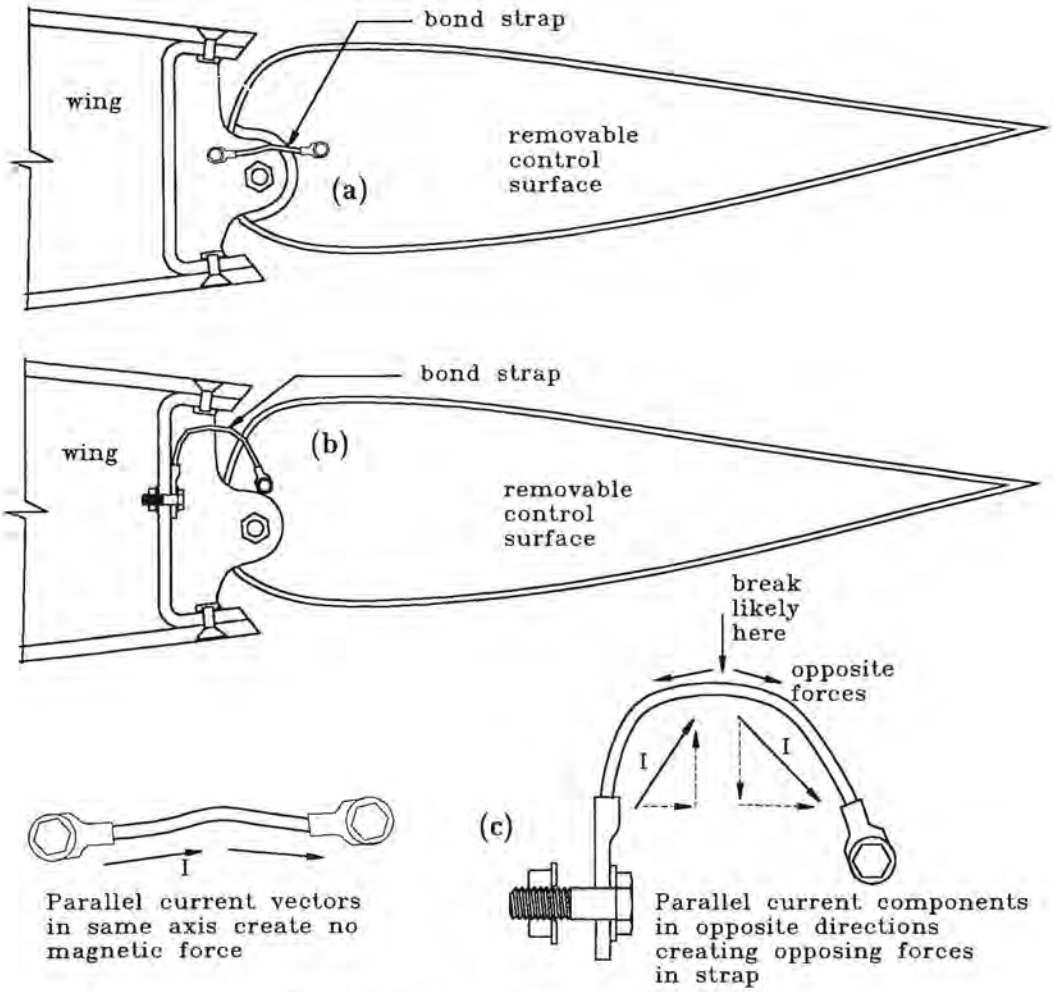

Fig. 6.12 Magnetic force on a bond strap.
(a) Straight strap - good
(b) Sharply bent strap - bad
(c) Origin of forces

ailerons, may not be sufficient to resist deformation as a result of the magnetic forces from lightning currents concentrated in these extremities. Such deformations will not normally impair safety of flight, but they may require repairs or replacement. Normally, only severe lightning currents cause this deformation. Reinforcement to prevent magnetic deformation of extremities must be justified on economics.

Since determination of magnetic force effects by mathematical analysis for all but the most elemental geometries is very difficult, laboratory tests may prove the most straightforward and economical way to determine whether or not magnetic force effects are likely to cause deformation of prospective structures.

6.2.3 Acoustic Shock Waves

A lightning return stroke supplies energy to its channel virtually instantaneously, after which a cylindrical pressure wave propagates away from the channel, initially at supersonic speed, perhaps 10 times the velocity of sound. Calculations by Hill [6.8] and summarized by Uman [6.9] for a 30 kA stroke, and shown in Fig. 6.14, suggest that the initial overpressure 1 cm away from the channel would be about 30 atmospheres and that 4 cm away it would be about 3 atmospheres. A summary of work on overpressures compiled by Uman and shown in Fig. 6.15 suggest that at distances of a few tens of cm the overpressure might

be about 0.05 atmospheres. The subject of pressure waves from high current arcs is discussed in considerable detail by Uman [6.9], who also gives a number of other references.

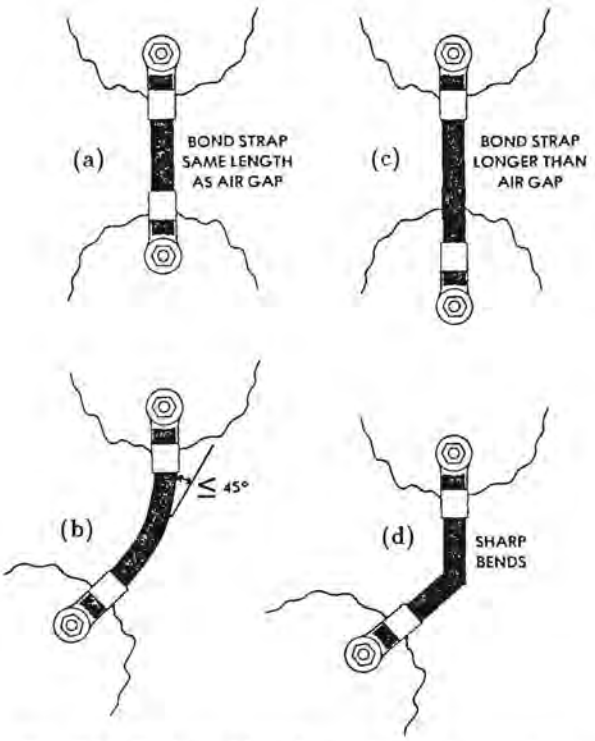

Fig. 6.13 Design of bonding straps, or jumpers.
(a), (b) Good
(c), (d) Bad

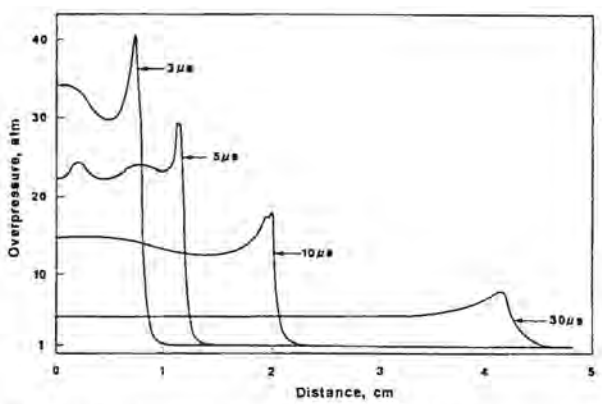

Fig. 6.14 Pressure vs. radius at four times following development of a 30 kA arc [6.14]. Double exponential waveshape with $\alpha = 3 \times 10^4$ sec^{-1} and $\beta = 3 \times 10^5$ sec^{-1}.

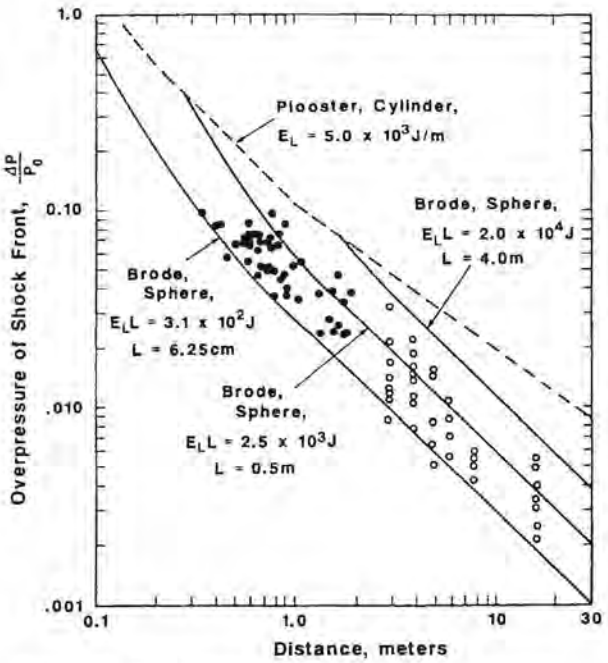

Fig. 6.15 Shock wave overpressure as a function of distance from a 4-m laboratory spark.

The acoustic pressure wave associated with a return stroke has cracked windshields and, in laboratory tests with simulated lightning arcs, has caused cracks in CFC skins up to 6 mm (0.236 in) thick. Whether cracking occurs or not is dependent on the stiffness and degree of reinforcement provided by frames and stiffeners.

Very stiff structures can be broken by the shock wave since they can not bend to absorb the shock, whereas more flexible or ductile unreinforced materials can deform without cracking or breaking. Lightning shock waves are sometimes overlooked by designers and laboratory test specialists who fail to account for or adequately evaluate these effects.

Laboratory testing: One area where acoustic waves must be considered is during laboratory testing where high currents are injected into a test sample from a metal electrode close to the item under test. Gap spacings between the electrode and the test surface are usually limited to between 2 and 5 cm by the voltage limitations of the test generators. An acoustic wave could be partially confined by the electrode and cause unnatural damage to the surface under test, as indicated in Fig. 6.16(a). To ensure that this does not happen, the end of the electrode is generally encased in a sphere of insulating material, as in Fig. 6.16(b). This forces the origin of the arc on the electrode to be at right angles to the surface under test. Shock

waves originating at the electrode, will not be directed toward the test surface and, since the surface of the insulated electrode nearest the test surface is spherical, shock waves originating at the surface under test will be dispersed and not reflected by the electrode.

Further discussion of testing considerations is found in §6.8.

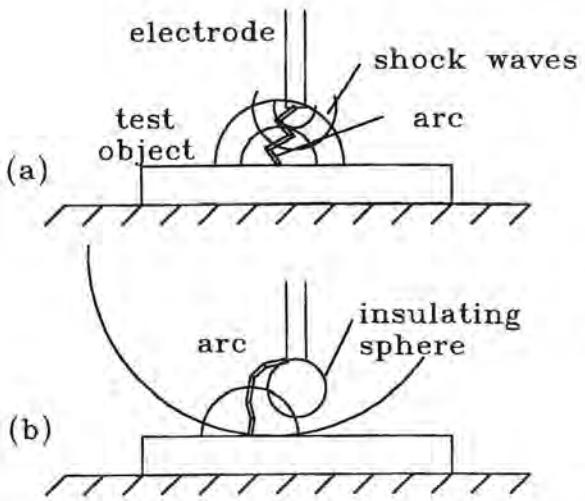

Fig. 6.16 Shock waves encountered during laboratory testing with high currents.
(a) Pressure waves confined by a metal electrode
(b) Insulating sphere to force arc from underneath electrode

6.2.4 Arcing across Bonds, Hinges, and Joints

Riveted joints: There is some conflict between the construction practices best for lightning protection and those best for control of corrosion. Ideally, for lightning protection, joints in metal structures should provide a metal–to–metal contact between the surfaces being joined. This would require that the joints be made before paints or sealers are applied. Control of corrosion, however, generally requires that metal surfaces be painted or sealed before the rivets are installed. Usually it also requires that the rivets and rivet holes be painted or sealed. Such films might provide an insulating surface, through which current must arc as it passes through the joint. In general, of course, arcing is undesirable.

In most applications, the insulating films associated with corrosion protective coatings have not resulted in major lightning arcing problems. Many times, the insulating films are broken during installation, providing a conductive path, though newer epoxy paints and sealants are much more resistant to mechanical puncture than the older paints. Also, the large number of fasteners required to meet mechanical requirements tends to ensure that many parallel conducting paths are established, thus greatly limiting the arc damage at any one fastener.

These observations, though, must be qualified since there are some situations where lightning current through a riveted joint might present some hazards. One would be if the space behind the riveted joint contained flammable fluids or flammable vapors. Any possibility of sparking should then be considered as presenting a hazard. Fuel tanks are the most common example of such a situation and because of the potential hazards are given special attention in Chapter 7.

Example: The riveted joint of Fig. 6.17 carried 200 kA without arcing or any other evidence of distress, but it should be noted that the current path was end–to–end, a pattern that did not give rise to any unbalanced magnetic forces. A different current path might give rise to magnetic forces that could, possibly, lead to mechanical failure of the rivets, a phenomenom having little to do with arcing. If the current pattern were known to be such that unbalanced magnetic forces might develop, it would be prudent to conduct high current tests on the joint.

Design guidelines: Most airframe structural interfaces are located in *Zone 3* and so will conduct some portions of lightning current when the aircraft encounters a lightning strike. Nearly all riveted or fastened interfaces of *primary* structure can tolerate lightning current without structural damage or other adverse effects. This holds true if the density of stroke currents is held to 5 kA or less per fastener or rivet. Since large numbers of rivets are utilized in most primary structures, current densities are nearly always below this guideline and no special features need to be added to the design for lightning protection purposes, except for the arc or spark suppression techniques to be described in Chapter 7 for structures that enclose fuel.

Exceptions: Some possible exceptions to this situation exist:

1. Secondary structures.
2. The primary structure of very small aircraft; those of gross weight less than about 1800 kg (4000 lbs),

and employing comparatively few fasteners. This includes small two place recreational and utility aircraft.

3. Primary structure utilizing adhesive bonds in place of rivets or fasteners.

Secondary structures: Secondary structures, such as wing tips, tail cones, wheel well doors and flight control surfaces often do not have enough fasteners to transfer lightning currents without significant damage to the fasteners and surrounding structural material. Sometimes this damage is due to magnetic forces and other effects, in addition to or besides arcing at the fasteners. In many cases this damage does not present a major hazard and nothing need be done to protect against it. Repairs can be made if the aircraft is actually struck by a lightning flash.

An example of such damage is illustrated in Fig. 6.18, which shows the aluminum vertical fin and cap of a small aircraft after an in–flight lightning strike described by the pilots as "very loud." The aluminum cap was joined to the fin with 16 removable fasteners. Intense arcing is evidenced by the dark soot. Arc pressure and magnetic forces deformed the surrounding structure. The damage is typical of what might be expected in this *Zone 1B* location, though the actual magnitude of the flash is of course unknown.

Small Aircraft: Some areas where lightning currents might be expected to flow through a small number of fasteners are shown in Fig. 6.19.

Adhesive bonds: Structural adhesives are being used more frequently to augment or replace rivets in structural joints. Such adhesives reduce manufacturing costs and leaks in fuel tanks, and provide more uniform distribution of mechanical loads. Nearly all of these adhesives, however, are electrical insulators and by virtue of their uniform application along joints, effectively insulate one part from another. This allows lightning and other electrical currents to spark through the adhesive at random locations inside or alongside a joint.

These situations are illustrated in Fig. 6.20. The sparking illustrated will occur anywhere that the adhesive is in a lightning current path, unless alternative paths are available through nearby fasteners in the same joint or parallel structural elements. If sufficiently intense, the expanding gasses from the sparks may damage or destroy the bond. Also, sparks at the bond edges may ignite fuel vapors if any are present.

In order to ensure uniform coating, some adhesives are carried by thin fiberglass cloths, rather than being brushed or sprayed on the parts to be joined. The carrier cloth forces a minimum separation of about 0.1 mm (0.005 in) between the parts, virtually guaranteeing that no electrical contact will exist between the bonded parts. Other adhesives are brushed or flowed on without carriers, but the adhesive layer itself is thick enough, 0.05 to 0.1 mm (0.002 - 0.005 in) to act as an insulator.

Fig. 6.17 Riveted joint that carried 200 kA.

Fig. 6.18 Lightning damage to a small aircraft.
(a) Rudder and cap after stroke
(b) Cap removed

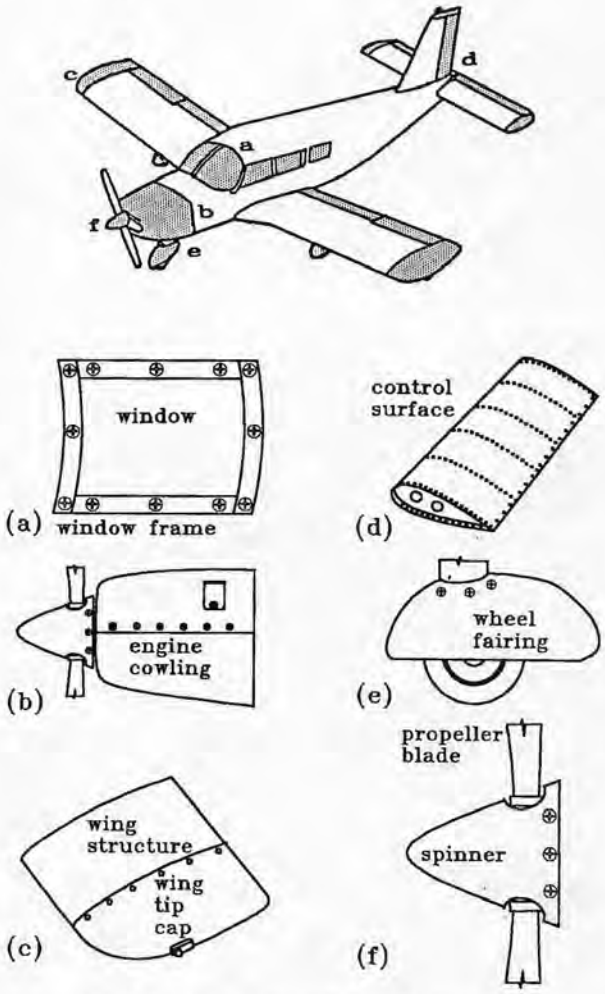

Fig. 6.19 Situations where lightning may cause damage.

Situations where adhesives interrupt the main lightning paths through structure are of greatest concern because then sparking is almost certain to occur. Of lesser concern, outside fuel tank structures at least, are designs employing adhesively bonded stiffeners or frames which are in parallel with electrically conductive skins or other members. In these latter situations the intensity of sparking across or through the bonds will be lower. Fig. 6.21 shows examples of each situation, along with guidelines for protection design.

Further discussions of lightning protection aspects of adhesive bonds, as applicable to CFC structures and fuel tanks are found in §6.5 and 7.11 respectively.

Hinges and bearings: If hinges or bearings are located where lightning currents might pass through them, such as on control surfaces in Zones $1B$ or $2B$, they must be able to safely conduct the currents without impairment of their function, such as pitting or welding of surfaces. Otherwise suitable means should be provided to carry the lightning current around the rotating surfaces. Tests and experience are the only real guides as to whether the hinge might be excessively damaged.

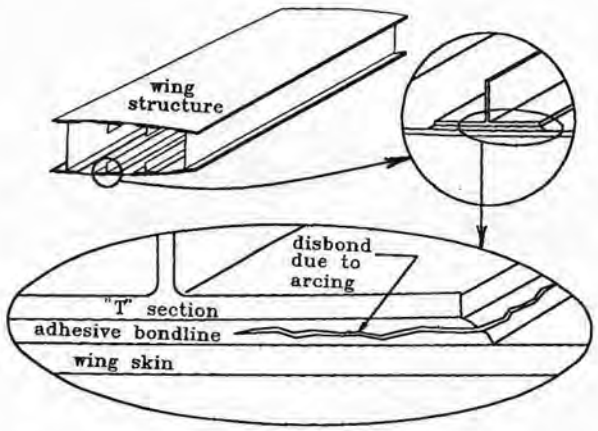

Fig. 6.20 Sparking at adhesive bonded joints.
(a) Typical situation
(b) Photograph of test specimen

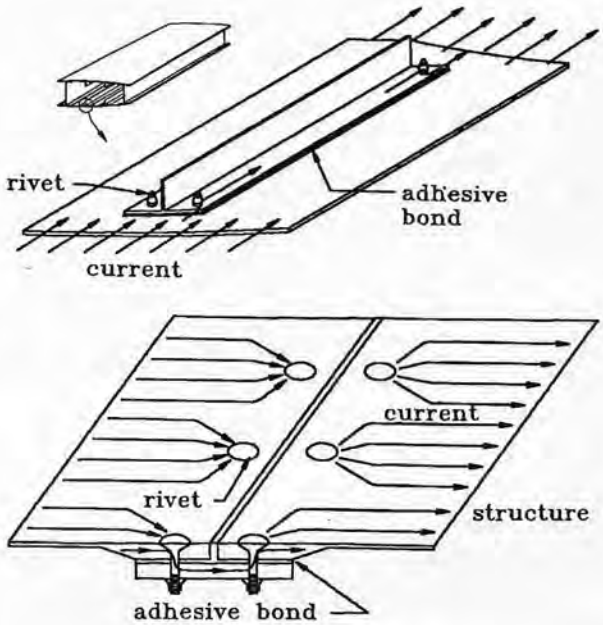

Fig. 6.21 Current carrying paths added to adhesively bonded joints.
(a) Stiffener
(b) Structural joint

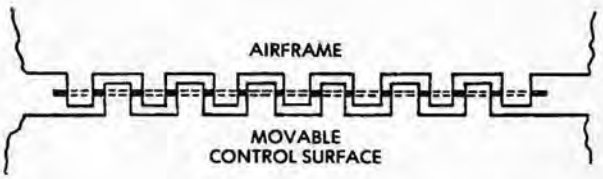

Fig. 6.22 Piano-type hinge.

Problems and considerations regarding rapidly rotating bearings of propulsion systems are discussed in §6.7, but for slowly rotating joints experience indicates that pitting and welding damage is only likely to occur when a hinge or bearing has a single point of contact through which most of the lightning current must pass. During laboratory testing, welding of poorly joined metal surfaces can occur, but the welding is seldom so severe that the joint cannot be broken apart by hand. Hinges with multiple points of mechanical contact, such as the piano hinge illustrated in Fig. 6.22, are able to safely conduct lightning currents with pitting or erosion so minor as not to present any real hazard.

Hinges and bearings for aircraft control surfaces are usually of such a size as to require no special protection. Lightning current could, conceivably, weld movable parts together, but the weld point would be small enough that the actuators could free the joint.

If tests were to indicate that excessive damage might occur, additional conductivity should be provided. The most effective way of providing this additional conductivity is to provide additional areas of contact in the hinge itself, or else to provide additional hinges.

Bonding jumpers on hinges: Flexible bonding straps or jumpers of the type shown in Fig. 6.12 have often been installed across hinges. In many cases, however, the jumpers do not really reduce the hinge current. The reason for this is that lightning current tends to follow the path of least inductance rather than the path of least resistance and the jumpers almost always involve longer and more inductive paths than do the paths directly through the hinges.

This has been demonstrated by Stahmann [6.10], who found that bonding jumpers make little or no difference in the amount of superficial pitting that occurs on typical piano-type hinges on control surfaces or landing gear doors, even when the dc resistance through the hinge was as high as several ohms. No binding or other adverse consequences were found to result from the pitting that occurred in Stahmann's tests of piano-type hinges and ball joints.

Bond straps across hinges are sometimes required to prevent the electromagnetic interference that arises when precipitation static charges must be conducted through hinges with loose or resistive contact. The low currents involved are sometimes unable to follow interrupted paths, with the result that minute sparking occurs. Bond straps are usually able to provide enough conductivity to reduce this sparking. If bond straps are applied for this purpose, the guidelines of Fig. 6.12 should be followed.

To be sure of the ability of a particular hinge design to safely conduct lightning currents, tests in which simulated lightning currents are conducted through a prototype hinge, should be performed. The test waveforms and current applicable for the zone in which the hinge is located should be used. If excessive pitting, binding, or welding of the hinge is found to occur, additional conductivity may be necessary.

6.2.5 Joint and Bonding Resistance

While not a lightning effect per se, some discussion on joint and bonding resistance is is order. The question of what constitutes "good" grounding and bonding has always been murky and is still one that evokes controversy. One of the documents widely cited in regard to bonding and lightning protection is US Military Standard *MIL-B-5087B* [6.11] on bonding and grounding. One approach to defining a "good" joint would be to invoke *MIL-B-5087* and adopt a position that any joint that meets its criteria is "good." That standard requires, for lightning, that

> *"The component must carry the lightning discharge without risk of damaging flight controls or producing sparking or voltages in excess of 500 volts."*

Such a voltage did not present much of a hazard to the electromechanical and vacuum tube components in use when *MIL-B-5087B* was formulated. For a 200 kA lightning discharge, the 500 volt criterion basically requires that the end-to-end resistance not be greater than 2.5 milliohms (2.5×10^{-3} ohms).

What is sometimes read into the standard is that for lightning purposes *all* joints must have a resistance of 2.5 milliohms or less. Combined with the term *sparking* in the standard, one can take 2.5 milliohms as the resistance necessary to prevent sparking. That does not appear to have been the intent of the standard.

Whatever may have been the intent of those who drafted *MIL-B-5087B*, the document has become so ingrained in engineering lore as to become an article of faith. In particular, a belief has developed that *any* joint that has a resistance of 2.5 milliohms *or less is*, by virtue of *MIL-B-5087B*, "good" and therefore satisfactory for all purposes, including lightning. A corollary of this belief (myth is a better term) is that designers need be concerned *only* with demonstrating that a joint have a resistance of 2.5 milliohms or less. A request for any further consideration of joints is sometimes taken to be unnecessary and unreasonable.

The facts of the matter are that dc resistance is a poor criterion to use for evaluating whether a joint is "good". The ability of a joint to carry high current without sparking or burning is really determined by contact size, treatment of mating surfaces, type and number of fasteners and the contact pressure on the mating surfaces. These happen also to be the factors that govern joint resistance, but that is not the same as saying that *resistance* is the proper measure of the ability of a joint to carry lightning current.

A desire to have a bonding resistance number that can be cited in quality control documents is understandable, but discussions in this book will not attempt to answer the question of what resistance might be a good measure of the quality of a joint, mostly because the authors feel that any number that might be cited would be misleading and probably inadequate. It is much better to rely on experience and the results of tests.

Many joints that have proven capable of carrying lightning current have demonstrated resistances much lower than 2.5 milliohms, but some joints have produced spark showers, even though the dc resistance was less than 2.5 millioms. An example is shown in Fig. 6.23. The cover plate shown had a resistance prior to test of 0.53 milliohms, by virtue of the bonding jumper shown, yet a test at 100 kA produced violent sparking. Whether 100 kA represents a reasonable current to expect on that particular plate, or whether the

observed sparking really represents a hazard, depends on the total current to be expected in the structure and the number of fasteners available to conduct this current.

At other times, there have been joints that had resistance much greater than 2.5 milliohms, yet would have been perfectly adequate for the particular application.

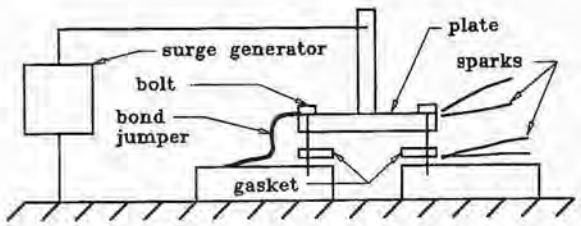

Fig. 6.23 Sparks from a test piece having a joint resistance of only 0.53 milliohms.
(a) Geometry
(b) Photograph during test

In summary, a joint resistance of 2.5 milliohms, or any other specific resistance, does not, of itself, prove that the joint is either suitable or not suitable for any particular application where lightning is involved. The adequacy of any joint or fastener configuration to safely carry lightning current must be determined by laboratory test at current levels representative of the full specifed lightning threat. No dc resistance criterion or analysis procedures exist that can reliably predict when arcing or the effects of arcing will occur at a particular joint.

6.3 Non–Conducting Composites

While lightning protection of metallic structures is mostly a matter of attention to detail and does not usually incur much cost or weight, lightning protection of non–metallic structures is another matter entirely. Lightning protection must be considered from the start and such protection may involve unexpected and unwelcome program costs or may involve added materials and weight. Radomes in particular must be given special attention to protect them from lightning. They are, of necessity, made from insulating material and because they are mounted on extremities of the aircraft they are natural targets for lightning.

There are several basic types of nonmetallic material used in aircraft structures; non–conducting composites, covered in this section, and electrically conductive composite materials, covered in §6.5 and §6.6. The non–conducting materials include fiber reinforced plastics, such as aramid fiber and fiberglass, and non–filled resins, such as polycarbonates and acrylics. Glass is also employed, particularly for windshields, as discussed in §6.4.

Non–conductive composites are employed in many secondary structures such as radomes, wing and empennage tips, fairings and fins, where medium strength is sufficient and complex shapes can be more readily molded than fabricated or where skins must be transparent to radio and radar waves. Polycarbonates, acrylics and glass are used for canopies and windshields where optical transparency is desired.

6.3.1 Damage Effects

Non–conductive composites are electrical insulators and cannot carry lightning current. When employed as an exterior skin, they are often punctured by a lightning flash that contacts some metal object beneath the skin. The high amplitude return stroke currents can then result in large holes and damage to these materials, as described in Chapter 4. Radomes not provided with lightning protection devices are subject to such puncture and an example of a radome destroyed by puncture was shown in Fig. 4.11.

Punctures of these composites can be prevented by installing conductors to intercept the lightning flashes and divert them to the surrounding metallic structure. Design of such conductors requires some understanding of the mechanism of puncture and this is reviewed in the following section.

6.3.2 Mechanism of Damage

Lightning produces damage to a non–conducting skin by two different mechanisms; by puncture or by surface flashover. Both are controlled by the strength of the local electric field.

Electric fields: The basic electrical breakdown process was reviewed in Chapter 1 and in Chapter 3 the mechanism of attachment to an aircraft was reviewed. As noted in those sections, high electric fields result in the formation of corona and streamers which propagate outward from the aircraft. Fig. 6.24 shows a sketch of the process. Whether the streamers from the aircraft are induced by the rapidly changing electric field of an approaching lightning leader or whether they grow in response to a quasi–static electric field is rather academic; the point is that the leaders do develop.

The surface conductivity of the composite, 10^{12} to 10^{14} ohms per square for materials used in fairings and 10^{6} ohms per square for materials used in radomes, is sufficient to yield relaxation times of 10-100 milliseconds. Relaxation time is a measure of how long it takes electrical charge to move off a surface.

What this means is that in response to a slowly changing external electric field, charges will migrate from neighboring conductive structures on to the non–conductive surface. These charges reduce the electric field intensity within and underneath the surface.

If the external electric field changes rapidly, however, as it does if it is produced by an approaching lightning leader, charge cannot move across the surface of the composite material fast enough to prevent electric fields from penetrating to the regions covered by the dielectric skin. If the internal electric field becomes high enough, electrical streamers will form on the internal metallic objects and will propagate outward and come into contact with the internal surface of the skin. There they will deposit electric charge, as shown in Fig. 6.24. A crude analogy is that the streamers spread electric charge around in the same way that a water hose would spread water around on the internal surface.

The electric charge will produce an electric field, Fig. 6.24(b), having one component directed tangentially along the inner surface and one component directed radially through the skin and out to the air.

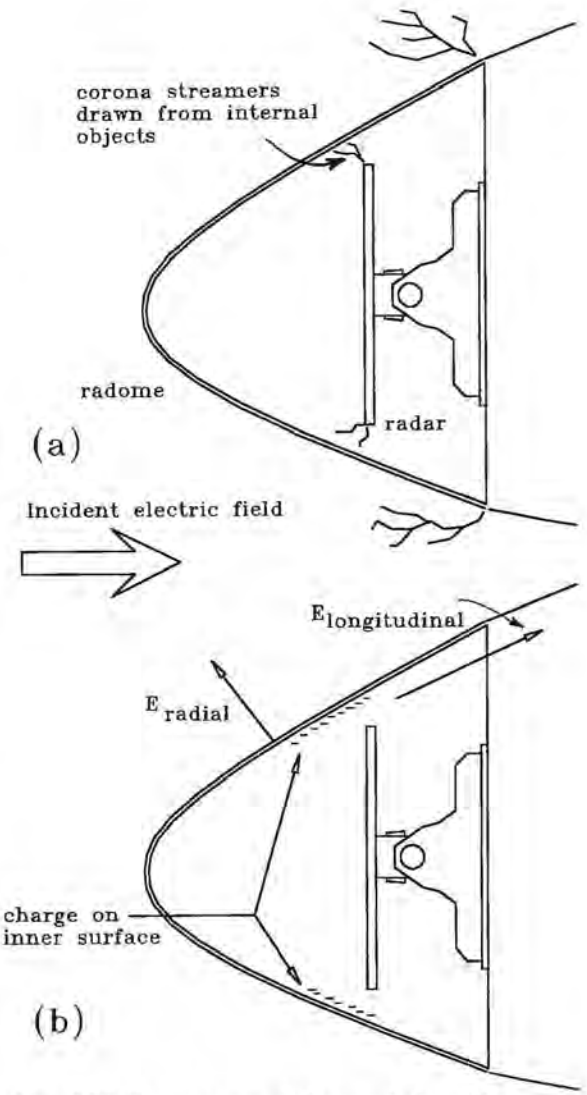

Fig. 6.24 Streamers and charges induced by an incident electric field.
(a) Internal and external streamers
(b) Charges and electric fields produced by internal streamers

Because the dielectric constant of the skin is higher than that of the air, the electric field in the composite skin material will be lower than the electric field in the air. What happens next involves some complex interactions between the development of the internal and external streamers and the dielectric strength of the materials involved.

External flashover: One possibility is that external streamers from adjacent metal structure may develop fast enough to suppress the internal streamers. A streamer develops from a metal surface when the elec-

tric field at that surface becomes sufficiently high. As the streamer propagates away from the surface the field at its tip remains high (which is why it propagates), but the streamer acts like a conductor and tends to reduce the electric field at points behind it, as shown in Fig. 6.25. This reduction robs any parallel streamers of the electric field they need to continue propagating. If the surface electric field is reduced enough, the other electric streamers will cease to grow and the external streamer that is furthest extended will, so to speak, win the race and provide the path for the lightning flash. An example of an external streamer intercepting an approaching leader is shown in Fig. 6.26.

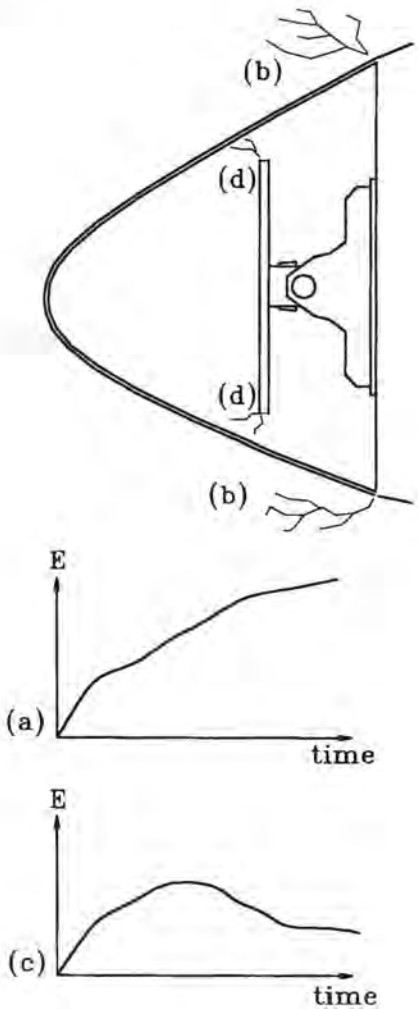

Fig. 6.25 Suppression of electric field by streamers.
(a) External electric field
(b) External streamers
(c) Suppressed internal electric field
(d) Suppressed internal streamers

Fig. 6.26 Simulated lightning attachment point tests of a nose radome.
Note intersection of approaching and induced streamers.

Puncture: The other situation, however, is that corona forms on the outer surface of the cover and propagates out into the air, as shown in Fig. 6.27. This deposits charge on the outer surface as well and eventually results in a radial electric field sufficiently high that the cover is punctured. Once puncture occurs, a spark is formed and current is free to pass through the skin material. If the main lightning path is to an adjacent metallic structure, the puncture may only produce a small pinhole in the skin, but if the main lightning current goes through the skin, the shock wave released frequently is enough to severely damage the skin. Damage produced by puncture of a radome was shown in Fig. 4.11.

Puncture is most likely to occur with a composite material because those materials have microscopic holes through which an electric discharge can easily propagate. The voltage required to puncture a given thickness of fiberglass or aramid fiber composite is, in fact, only slightly greater than that required to ionize a similar thickness of air. A measure of the ability of a non–conductive material to resist puncture is its dielectric strength. Homogeneous materials, such as acrylic and polycarbonate sheets, have very high dielectric strength and are more resistant to puncture.

The puncture voltage of some typical fiberglass skins used in radomes is shown in Table 6.3.

Unprotected radomes are most often punctured, partly because of the low dielectric strength of non-conductive composites and partly because the radar antenna must, of necessity, protrude beyond any surrounding metal structure. This, in turn, means that the electric field is concentrated around the metal structure of the radar and that electrical streamers can most easily form there. The mechanism of puncture is shown in Fig. 6.27.

Table 6.3

Impulse Breakdown Voltages of Typical Fiberglass Skin Materials

Skin Construction	Total Thickness	Breakdown Voltage
One fiberglass sheet	0.163 cm 0.064 in	21 kV
Two filament-wound fiberglass tape skins enclosing polyimide foam filler	1.27 cm 0.50 in	150 kV
Two fiberglass skins enclosing foam filler	0.99 cm 0.39 in	70 kV

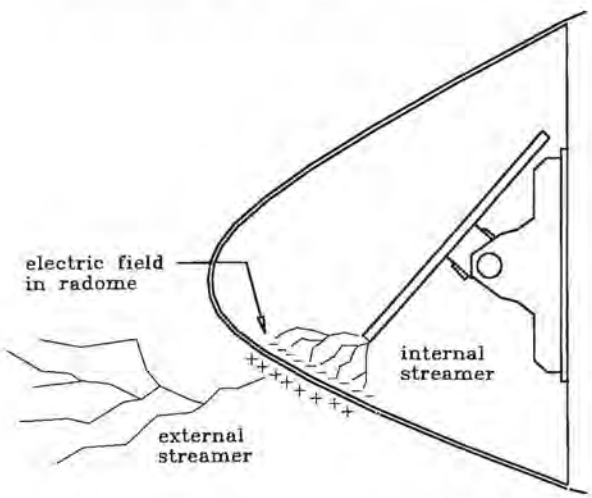

Fig. 6.27 Mechanism of puncture of a radome.

Protection of non-conductive composites: Whether or not a structure needs to be protected against lightning depends both on its function and the consequences of damage. If loss of the structure does not create a serious hazard, then protection may not be required. For example, the loss of a small tail cone or empennage tip may not endanger the aircraft and these can be left unprotected and repaired or replaced in the event of a lightning strike. The loss of a nose radome during IFR conditions, however, would probably not be acceptable since loss of the radome might also lead to the radar being disabled.

There are two basic ways of providing protection for non-conductive composites. One employs diverter strips or bars on the exterior surface to intercept lightning flashes, while allowing the skin to be transparent to electromagnetic waves. This is the approach used for protection of radomes and some antenna fairings. The other method is to apply an electrically conductive material over the exterior of the structure. This latter method provides the most effective lightning protection and should be employed whenever possible. It also provides improved protection of enclosed systems against indirect effects.

6.3.3 Protection With Diverters

There are two types of diverter: solid and segmented. If properly applied, either type significantly reduces the number of lightning related punctures (of a radome for example), but they are not 100% effective. Occasional punctures of protected radomes will still occur. Application of diverters will be discussed with particular emphasis on radomes, because that is where they are most commonly used, but the discussion is equally applicable to any insulating structure, such as wingtips made from non-conducting composites.

Solid diverters: Solid diverters are continuous metal bars placed on the outside of a skin to intercept a lightning flash and conduct the current to an adjacent metallic structure. They also provide some electrostatic shielding from the external electric field for objects under the skin, and thus they tend to inhibit the growth of streamers from these internal objects. Fig. 6.28 shows solid diverters mounted to the outside of a radome.

Solid diverters should be designed to conduct, without damage, the lightning current of the zone in which the part is located, typically 200 kA, 2×10^6 A^2s for diverters on a nose radome in *Zone 1A*. Solid diverters are usually made of aluminum, with a rectangular cross section sufficient to permit conduction of the current without excessive tmperature rise. For mechanical reasons, and to prevent holes for fasteners from unduly reducing the cross-sectional area, most diverters have cross-sectional areas of about 0.5 cm^2 (0.08 in^2, though some are larger. A common design is 3.2 mm (0.125 in) thick by 12.7 mm (0.50 in) wide, but thicknesses of up to 6.4 mm (0.25 in) have been used. The diverters are usually attached to the skin with screws spaced approximately 15 cm (6 in) apart. It is important that the diverters be securely fastened to the skin to prevent their loss due to rain erosion

and lightning magnetic force effects. In sandwich type skins with foam or honeycomb cores, the mounting fasteners are often surrounded by plastic inserts to prevent moisture from entering the cores.

If solid diverters are installed on the outside surface, they may cause some drag. This can be minimized by orienting the bars parallel to the airstream, by shaping the cross section of the bars aerodynamically, or by embedding the diverters into the external surfaces of the skins.

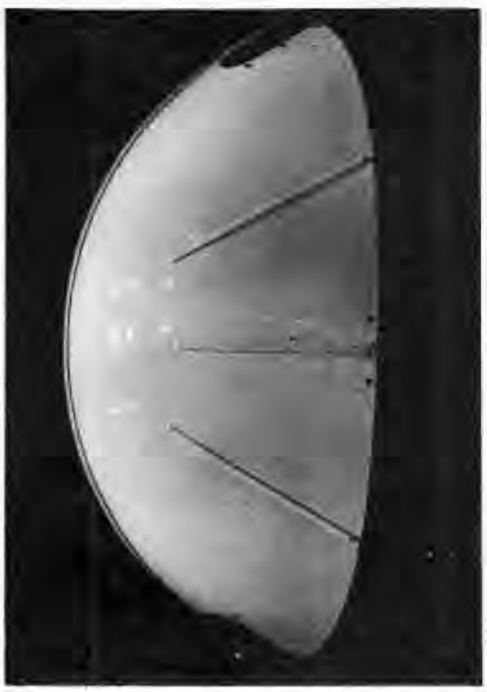

Fig. 6.28 Solid diverters on a radome.

Internal diverters: Embedding solid diverters into a composite skin creates tooling and manufacturing problems and may also degrade the strength of the skin because of stress concentrations along the required grooves. An alternative is to mount solid diverters on the inside surface, with metal fasteners, sometimes called *studs* protruding through the wall to serve as lightning attachment points, as shown in Fig. 6.29. Although this type of diverter installation may reduce the aerodynamic drag created by external mounting, it does not take advantage of the insulation capability of the dielectric wall, and internal side flashes can result. In addition, magnetic forces due to lightning flashes sweeping from one stud to the next may tear the diverter away from the skin.

In general, the thicker the wall, the farther apart may be the studs. In many cases, 30 cm (1 ft) is close enough, but each individual case must be evaluated by strike attachment tests. Appropriate test procedures are discussed in §6.8.

Foil strips: Thin foil strips, usually made of aluminum 0.008 to 0.040 cm (0.003 to 0.015 in) thick, have occasionally been used in the past, but these usually provide protection against only one flash since they may melt or vaporize. In such a case they leave an ionized channel through which subsequent currents in the same flash can travel. Protection is lost for later flashes. Also, the exploding strip may sometimes damage the adjacent composite material. For these reasons they are not recommended for certifiable designs and no further discussion of them will be provided.

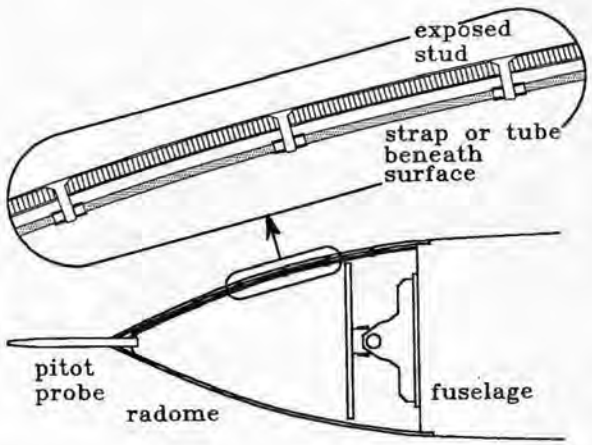

Fig. 6.29 Internal diverter strip with protruding studs.

Segmented diverters: Solid diverter bars tend to interfere with the beam from a radar antennna, and to overcome this, segmented diverters, also called "button strips," were developed [6.12 - 6.15]. These consist of a series of thin, conductive segments, or "buttons," interconnected by a resistive material, and fastened to a thin composite strip which can then be cemented to the surface to be protected. Typical strips [6.17] are shown in Fig. 6.30.

Segmented diverters do not provide a metal path to carry lightning current. Instead, they provide many small airgaps that ionize when a high electric field is applied. Since the small gaps are close together, the resulting ionization is nearly continuous and thus provides a conductive path for lightning leaders and flash

currents. The segmented diverters thus guide, rather than conduct, the flash across the protected surface. The structure and ionization process of segmented diverters are shown in Fig. 6.31.

Segmented diverters have been used on many radome systems. The field experience to date indicates that for most applications, they appear to be almost as effective as solid diverters.

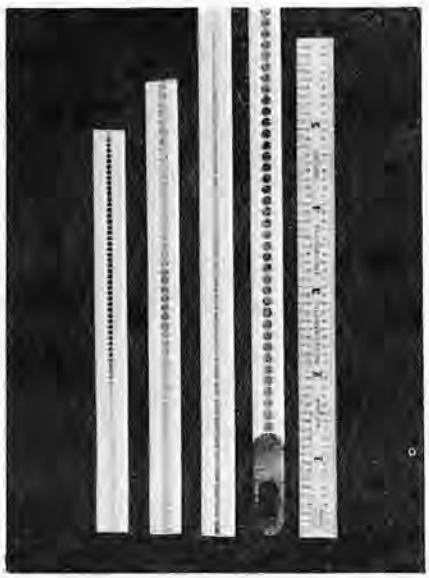

Fig. 6.30 Segmented diverters.

Ionization: In order for segmented diverters to ionize, there must be an electric field tangential to the length of the diverter. This is provided by the approaching lightning leader, or by intense ambient fields that precede an aircraft triggered strike.

Effect of internal conductors: Conductors beneath the structure being protected can affect the performance of segmented diverters. A conductor immediately beneath the strip will short out most of the tangential electric field and inhibit ionization of the diverter. Even if the diverter does ionize, there will be a voltage rise along it and that voltage may be sufficient to cause puncture to the internal conductor. This can also happen when tubes or antennas are placed on or near the inside surface of the radome. Positioning such conductors away from the skin will improve the situation.

Spacing between diverters: The maximum spacing between segmented diverters, and the minimum permissible spacing to underlying conductors, is dependent, among other things, upon the amount of voltage required to ionize the segmented strips. Ideally, the ionization voltage (electric field strength might be a better term) would be lower than that required to ionize a path along the bare surface of the radome and also much lower than that required to puncture the radome. Laboratory tests have shown the ionization levels of several strip designs to be 20 to 50 kV per meter. This is much less than the 500 to 700 kV per meter required to ionize the air across an insulating surface.

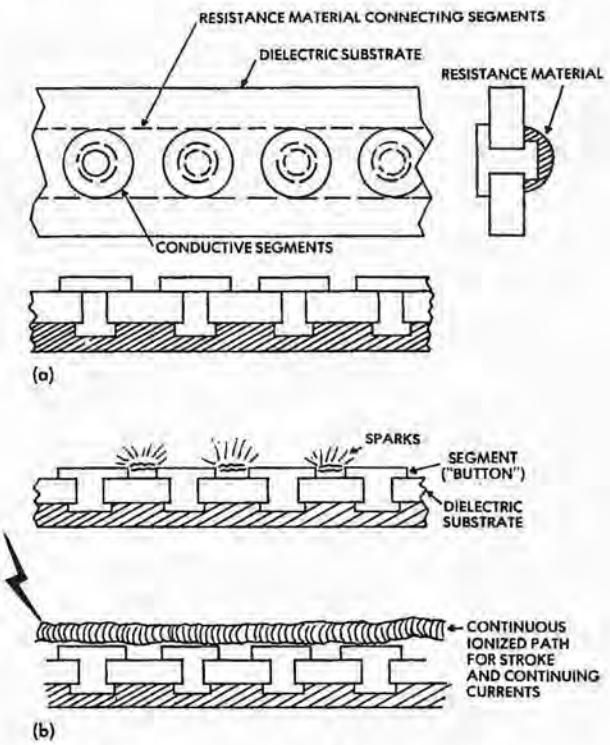

Fig. 6.31 Design and breakdown process in segmented diverters.
(a) Design
(b) Breakdown and conduction process

Breakdown voltage: Ionization of segmented diverters is a highly nonlinear process and the total voltage required to cause ionization, when applied end to end, may change very little as the length of the strip is varied. Ionization probably proceeds from the ends in a self propagating manner, similar to the propagating leaders discussed in Chapters 1 and 2. The test configuration, generator characteristics, measurement connections and gaps between the generator and the strip have been observed to significantly alter the test results and the conditions to cause ionization are not understood as well as one might like. Laboratory comparisons of various diverter designs may not be suffi-

cient to tell how the diverters will work in actual practice. Laboratory testing of complete non–conducting structures, such as radomes, including simulation of the conducting objects inside the radome, is the best way to evaluate any particular design.

Application of diverters: Proper application of either type of diverter involves being sure that there is never enough voltage to cause puncture through the insulating structure to the internal objects. Voltage can develop because of the resistance of the ionized channel along a segmented diverter or because of the inductance of a solid diverter. Diverters should be neither too far from the objects to be protected nor too close. Typical diverter spacings range from 30 cm (12 in) to 60 cm (24 in). Application guidelines are:

1. As much as possible, orient the diverters in a fore and aft direction, as shown in Fig. 6.32(a). This provides an opportunity for swept strokes to follow the diverter, rather than jumping across the insulating structure being protected.

2. Provide an adequate number of diverters and keep the current path as short as possible, although this might require some diverters to be oriented perpendicular to the line of flight.

3. Use enough diverters to be sure that any lightning strike will flash across the surface of the skin rather than puncturing the skin and striking the objects under the skin. Fig. 6.32(b) illustrates the point.

4. The spacing of either type of diverter depends on the dielectric strength of the skin material, the proximity of conducting objects behind the skin, and the length of the diverters. Typical spacings range from 30 cm (12 in) to 60 cm (24 in), but there are no "cook book" analytical tools with which to determine the necessary spacing for particular configurations. Selection of spacing is best done by test of actual structures with diverters applied in a "cut and try" process. Flat panel specimens of the non–conductive composite skin may be used for spacing tests; it is not necessary to have a complete sample of the object to be protected. A typical test setup is shown in Fig. 6.33.

5. Be sure that the current along the diverter does not produce enough inductive voltage rise to cause puncture to the internal objects, as illustrated in Fig. 6.34. The inductive voltage rise,

$$V = L\frac{di}{dt} \tag{6.20}$$

may be calculated by assuming L to be 1 μH/m for most diverters, and assuming dI/dt to be 100,000 A/μs (1×10^{11} A/s). This voltage rise must be compared with the puncture voltage of the composite skin and the air gap between the skin and conductive objects inside. If this is not known, the design can be verified by a high current test of a typical diverter installation.

6. Fasten the diverter strips or bars securely to the skin. Solid diverters are mechanically fastened about every 15 cm (6 in). Segmented diverters are adhesively bonded directly to the composite skin.

   At the aft end of either type of diverter, provide a suitable path to carry the lightning current to the conducting airframe structure. This can be via a single fastener or a fastener and spacer combination, as illustrated in Fig. 6.35. In either case the arrangement should be capable of conducting currents appropriate for the zone in which the diverters are located.

7. Provide an appropriate finish. This may be a paint on solid diverters, but the individual segments of segmented diverters must not be covered with primers or paints. If covered with paint, these diverters will not ionize and thus will not function.

8. The protection adequacy of a complete diverter arrangement should be verified by high voltage strike attachment tests to verify ability to intercept strikes and prevent puncture, and by high current tests to confirm adequacy of mechanical and electrical fastening and grounding designs. These tests must be conducted on full scale hardware duplicating that to be used in production.

The intent of Guideline 3 is to assure that enough diverters are used to prevent punctures resulting from initial srikes. Guideline 4 extends this criterion for swept strokes, and Guideline 5 is aimed at preventing punctures resulting from inductive voltages that arise when lightning currents flow through the diverter. Guideline 6 is aimed at assuring that the diverter remains physically attached and adequately bonded to the airframe when it is called upon to conduct or guide high currents.

In applying these guidelines it is helpful to know the voltage needed to puncture covers or to cause flashover across a surface. The voltage to puncture a particular nonmetallic skin is a function of the material type and thickness, as well as of layup patterns, core fillers, and surface treatments. Examples of skin

puncture voltages determined from 1000 kV/μs impulse tests were given in Table 6.3. The voltage required to produce a flashover through air or across an insulating surface is about 500 kV/m or 5 kV/cm, if the voltage is maintained for several microseconds, as it might be when a streamer first contacts the surface. If the voltage is of short duration, such as the inductive voltage produced by current along a diverter, then the required breakdown stress is higher, perhaps 10 kV/cm. The influence of gap length and duration of voltage was also discussed in §1.5.3 and §1.6.2.

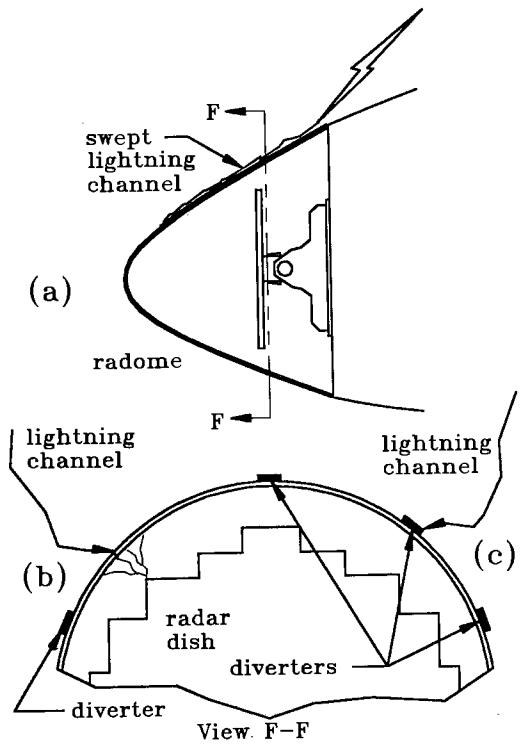

Fig. 6.32 Diverters on a radome.
(a) Fore and aft diverters to allow flash to sweep
(b) Excessive spacing of diverters allows puncture
(c) Proper spacing of diverters

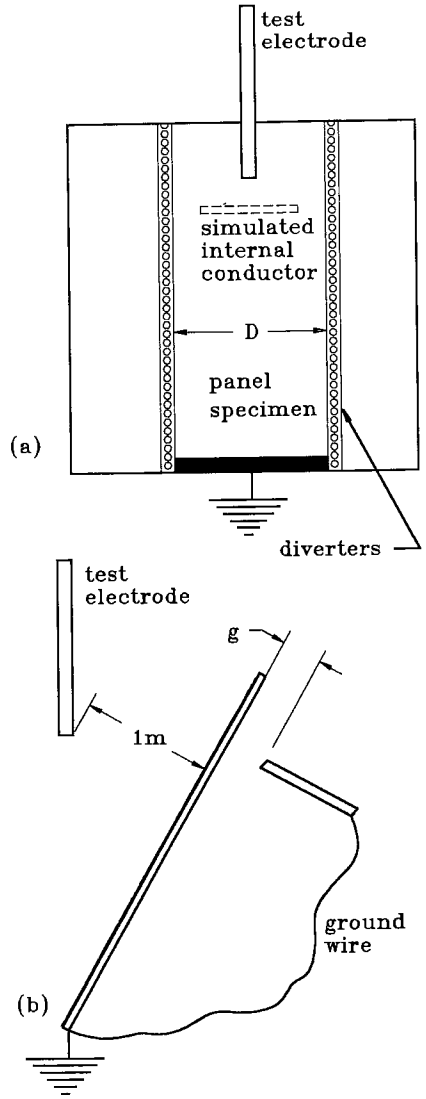

Fig. 6.33 Test of flat panel to determine diverter spacing.
(a) Front view
(b) Side view

Balancing spacing between diverters with the puncture strength of the surface being protected usually requires tests, the principles of which are shown in Figs. 6.33 and 6.36.

6.3.4 Protection With Conductive Coatings

Where electromagnetic transparency is not required, conductive materials can be applied to the surface to conduct lightning currents to the airframe. Materials include arc or flame sprayed metals, woven wire fabrics, solid metal foils, expanded metal foils, aluminized fiberglass, nickel plated aramid fiber and metal loaded paints. Some of these systems can also be used to protect CFC materials, as described in §6.5.

Arc or flame sprayed metals: These are solid metal coatings applied by spraying molten metal onto the surface to be protected. Thicknesses range from 0.1 to 0.2 mm (0.004 - 0.008 in) and the most common

metal is aluminum, though other metals have occasionally been used when corrosion is of major concern. The metal solidifies on the exterior surface of the composite, resulting in a hard, stiff and conductive layer which is capable of conducting *Zone 1A* or *1B* currents with very little damage. The sprayed metal can, and should, be painted, but the paint will intensify damage at strike attachment points. Sprayed coatings will have a somewhat rough finish and may require smoothing. This can be overcome by spraying the metal into a mold, after which the composite plies are laid in and cured. In this case the metal finish is smooth.

Advantages of the arc or flame-sprayed metals are very good protection for all strike zones and their ability to cover complex shapes that would be difficult to cover with wire meshes or foils. Disadvantages are cost, weight and difficulty of having the sprayed metal release from a mold.

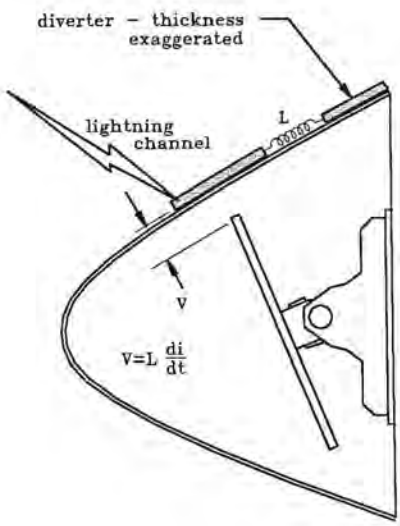

Fig. 6.34 Inductive voltage developed along a diverter.

Woven wire fabrics: Metallic fabrics woven from small diameter wires of aluminum or copper can provide very effective protection for non-conductive surfaces. Quinlivan, Kuo and Brick [6.18], and King [6.19] investigated woven wire fabrics and metal foils primarily as protection for carbon fiber composite (CFC) materials, but their findings apply to the protection of non-conductive composites as well. The metal fabrics most commonly applied are woven of aluminum wires spaced 40 to 80 per cm (100 or 200 per inch). Wire diameters range from 0.05 to 0.1 mm ((0.002 - 0.004 in). These fabrics are identical to filter screens commonly used in the chemical and water processing industries.

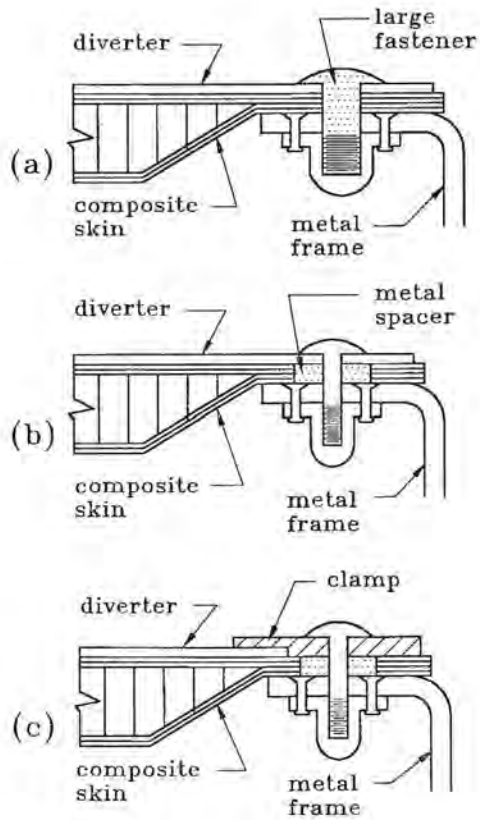

Fig. 6.35 Methods of grounding diverters.
(a) Single large diameter fastener
(b) Single small diameter fastener with conductive spacer
(c) Same as (b) with clamp over end of diverter

Woven wire fabrics do not drape well over surfaces with compound curves and this is especially true of tightly woven fabrics. They must be cut and lapped to fit. Wire fabrics can readily be co-cured in a composite laminate since the resin can flow around the individual wire strands. They can also be cemented onto a previously manufactured surface, though care should be taken not to let much of a film of adhesive build up atop the wires.

Advantages of wire fabrics include ability to co-cure with the composite laminate, very effective protection for all strike zones, flexibility and light weight, typically 0.15 - 0.2 kg/m^2 (0.03 - 0.04 lbs/ft^2). Part of their effectiveness comes because the roughness of the wire fabrics encourages arc root dispersion. They also provide protection against particle erosion.

A disadvantage is difficulty in draping over compound curves. This may require the fabrics to be cut into gores and lapped to fit.

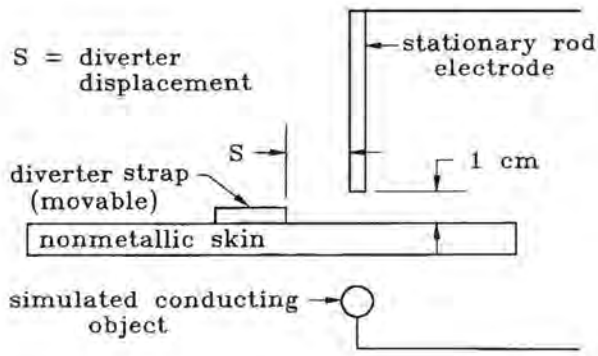

Fig. 6.36 Experimental determination of maximum diverter displacement distance.

Solid metal foil: Metal foil can be cemented over a non–conducting surface to provide a conducting layer. Metal foils of 0.025 mm (0.001 in) or greater provide lightning protection that is about the same as that provided by wire meshes. A substantial amount of foil this thick will be melted away at lightning attachment points, but the non–conductive material underneath will not generally suffer more than cosmetic damage. Partly, the protection is afforded because the foil separates from the surface being protected, moving the arc root away from the surface.

The amount of metal foil melted away by a strike is related to the intensity of the lightning current and to the thickness of the foil, but there are no significant differences in performance for the various types of metals. Most protection applications have used aluminum foil.

Manufacturing concerns have limited the application of metal foil as protection. Metal foil, like metal fabrics, will not drape smoothly over a compound curve. To prevent wrinkles it must be cut and spliced and this results in seams which might arc and delaminate, even at low current levels. The foil also has a smooth surface, which makes it hard to bond to the surface to be protected. Unbonded areas may allow the foil to become delaminated and they also can collect moisture, which can cause corrosion.

Because of these difficulties solid metal foils are rarely used to protect composite materials.

Expanded metal foils: These are fabricated by a milling process that perforates and stretches a solid metal foil. It has the appearance of a woven wire mesh, yet is fabricated of one piece of metal, and thus has better conductivity than metal fabrics which depend on contact between the wires to provide conductivity. Protection effectiveness is very good for all zones and about the same as woven wire meshes and flame sprayed metals.

Expanded foils are better than wire fabrics at draping over compound curves since they can be stretched somewhat. They can be bonded to composite laminates as well as wire fabrics and, like fabrics, tend to promote arc root dispersion. Thus, much less expanded foil will be burned away at a strike attachment point than would be the case for an equal thickness of solid foil.

Aluminized fiberglass: Glass fibers can be coated with aluminum and the result is a material with significant electrical conductivity. An individual fiber has a nominal resistance of 2 ohms/cm. The coated fibers and prepregs made from the fibers are available commercially. A virtue of the material is that the outer ply of a structure can be replaced by a ply made from the coated fibers.

Individual fibers can carry 50 A for 1μs, 5 A for 1 ms and 0.3 amperes continuously. They have this good capability for carrying currents of duration 1 μs to 1 ms because of the excellent thermal coupling between the aluminum and the glass. The glass provides a heat sink, enabling the aluminum coated fiber to carry twice the current that could be carried by the aluminum by itself.

At the point of lightning strike attachment, some volume of the aluminum will be explosively vaporized, the area affected depending on the magnitude of the strike and the amount of aluminum on the prepreg. If the coated fiberglass material is covered by fillers or paints, the expanding gasses will be contained and more of the explosive force will be directed into the material to be protected, the added amount of damage being related to the mass of covering material. Materials that might be applied over coated fiberglass include fillers, paints and other layers of fiberglass. Standard thicknesses of paint and primer, 5 to 7 mils, are usually not sufficient to cause any significant damage, but 10 mils of putty or a ply of fiberglass can result in damage to several layers of fiberglass below the aluminum coated fiberglass.

Increased damage caused by confinement of arc products is not a problem only with aluminized fiberglass; it occurs with any protective material. Confinement does, however, seem to promote more extensive damage to aluminized fiberglass than to either woven wire fabrics or expanded metal foils.

Metal loaded paints: Adding metal particles, such as copper or aluminum, to a paint results in a surface that has a certain amount of conductivity and has some ability to provide lightning protection, though the protection is marginal since the metal particles make only random contact with each other. As a result the coating has a much lower conductivity than an equivalent film of pure metal.

No practical thickness of paint is sufficient to provide metallic conduction of a full lightning current. Instead, the paint acts mostly to guide a flashover across the coated surface and the lightning current is then carried more in the resulting arc than in the coating of conductive paint.

Conducting paint films are least effective if there is some conducting object under the surface of the insulating surface being protected. In such a case, the arc voltage might be high enough to cause a puncture through the insulating surface to that object.

Conducting paint does have the virtue that it can be applied to an existing surface, even one of complex shape. Copper paints have been the most widely used. One of the most successful applications of copper loaded paints has been in the protection of helicopter rotor blades fabricated of non–conductive composites. A coating of conductive paint approximately 0.1 mm (0.003 - 0.005 in) applied under the finish coat of paint has been shown to prevent punctures of the blade skin. Paints have been less successful on blades with metal spars or embedded heater wires because sufficient voltage builds up along the conducting paint to puncture to the internal conductors. The mechanism is sketched on Fig. 6.37.

Conductive paints are the least desirable of lightning protection methods, partly because of this voltage buildup problem and also because they may erode away when exposed to intense rain or hail.

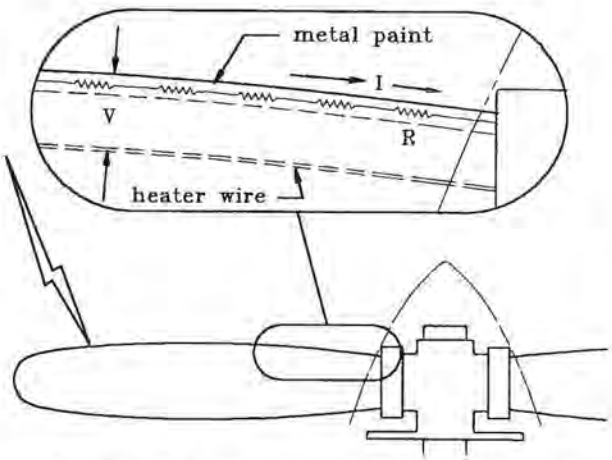

Fig. 6.37 Voltages developed along metal loaded paint.

6.4 Windshields, Canopies and Windows

Windshields, canopies, and side windows are often located in direct and/or swept stroke attachment regions, *Zones 1A* or *2A*. Lightning damage to windshields has not been frequent, but at least one accident in the 1930s has been attributed to such damage [6.20]. There are several aspects of windshield and canopy designs which could make them susceptible to damage and designers should verify that these conditions do not result in safety of flight hazards.

Windows and windshields are fabricated from glasses, acrylics, and polycarbonates, or some combination of these materials. These materials all have higher dielectric strengths than the non–conductive composites. Generally, conductive objects will not be positioned close to the inside surface and thus there will be little tendency for a lightning flash to puncture the windows.

Lightning punctures can occur to the electrical heating elements embedded in windshield laminates.

Electrically heated windshields: Electrical heating elements embedded within laminated windshields are used to clear icing and fogging. Typical configurations are shown in Fig. 6.38. Heating elements are either fine metal wires or metal films, powered from either 28 volt dc or 115 volt ac systems.

Since the wires are of small diameter and arranged in zig–zag patterns, an electric field directed through the glass is concentrated at those wires and can result in puncture of the glass ply and conduction of lightning currents directly into the heating elements and the power circuits. Electric fields can be produced either by an approaching lightning leader or by electrical charge that collects on the outside of the window as the aircraft flies through precipitation. Puncture should be less likely with metal films because they provide less tendency for the electric field to concentrate at points.

Other potential hazards that could result from puncture of the outer ply of the windshield are illustrated in Fig. 6.39. The first is the partially contained shock wave. This is always sufficient to shatter the exterior ply and sometimes sufficient to shatter the inner ply as well. If that happens, particles may be blown directly into the pilot's face.

Another potential hazard is direct conduction of very high surge currents into the aircraft's electric power distribution system, often after damaging the electrical loads powered from the same source.

Protection methods: One method of eliminating these problems is to de–ice the windshield with hot air instead of electrical heating elements. Removing the heating elements eliminates the most frequent cause of windshield puncture and eliminates the conducted surge problem.

The following approaches can be followed to reduce or eliminate the hazards if electrical heating elements are present.

1. Utilize a tough center ply of acrylic or polycarbonate resin. These materials are usually resiliant and tolerant of shock wave or impact damage.

   Some specifications require that windshield structures be able to survive the impact of a 2 kg (4 lb) bird at 200 knots. Such windshields have sometimes been capable of tolerating the effects of *Zone 1A* punctures through the outer ply.

   Since failure can result from tearing at the interface between the laminate and the frame, as well as by puncture of the laminate itself, this part of the design must also be considered from a lightning protection standpoint. Approaches that successfully tolerate reasonable bird strike requirements are also likely to meet lightning requirements.

2. Utilize a metal film heating element instead of fine embedded wires. The films are less conducive to puncture of the outer ply.

3. Employ surge suppression devices on power distribution circuits or busses feeding electrical windshield de-ice systems.

   Such devices should be rated to limit surge voltages to the system transient control level (TCL), as defined in Chapter 5, while safely conducting substantial currents to airframe ground. Fig. 6.40 shows where surge suppressors should be installed. Information on surge suppression devices is given in Chapter 17. Metal oxide varistor (MOV) type devices have proven capable of conducting 50 000 amperes and should be used for protection of windshield heater power feed and control circuits.

4. Since windshields, canopies and other windows are usually flight critical items, candidate designs should be tested. This is especially true of windshields since data bases relating to newer, high strength, light weight laminate designs do not exist. Appropriate test methods are described in §6.8.

The foregoing protection methods are applicable to bubble type canopies and side windows, as well as to frontal windshields, though windshields represent the most likely lightning related problem.

Canopies rarely employ de-ice elements and are fabricated most often of polycarbonate resins which have very high dielectric strengths. This is also true of side windows. Sometimes metal films are deposited on the interior of bubble type canopies to shield the pilot from strong electric fields that would otherwise cause electric shocks. These films have not promoted puncture of canopies fabricated of polycarbonate resins.

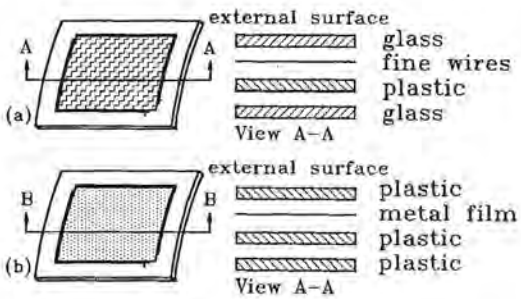

Fig. 6.38 Electrically heated windshields.
(a) Fine wires in glass/acrylic sandwich
(b) Metal film in acrylic or polycarbonate sandwich

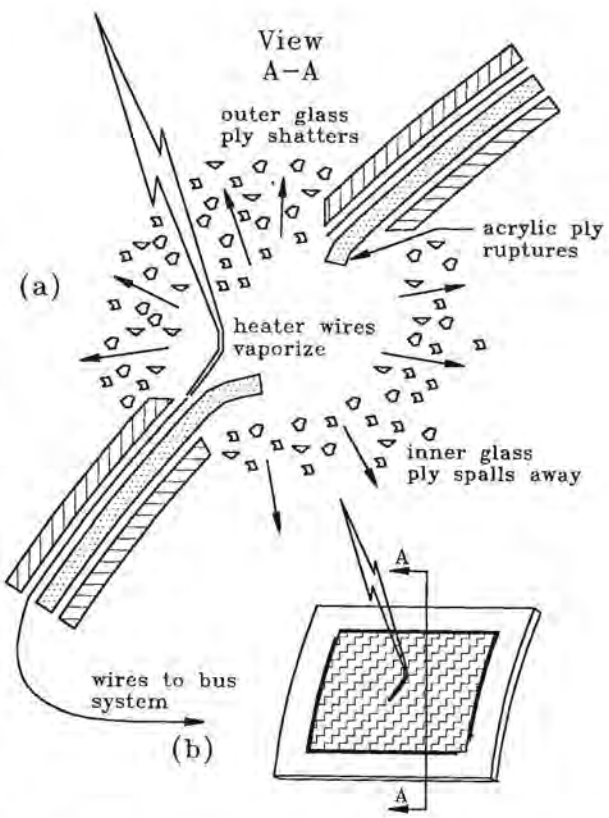

Fig. 6.39 Lightning damage to electrically heated windshield.
(a) Shock wave damage to laminate
(b) Surge current into power system

Anti–static coatings: Electrical charges that accumulate on frontal windshields and canopies can be bled away by electrically conducting surfaces. To remain optically transparent, these films must be very thin and their conductivity is not sufficient to conduct lightning currents.

The most common coating in present use is indium tin oxide (ITO) and it is preferred for its comparative durability against erosion.

Flash blindness: If a lightning strike occurs at night in front of a windshield the bright flash might temporarily blind the pilot, making it difficult or impossible to read instruments. The flash blindness may last for a minute or two and several accidents have resulted when the aircraft was on final approach to an airport or in IFR conditions.

No windshield treatment has been found to prevent this effect without impairing normal visibility. When there are two pilots, one of them should focus on the instruments and avoid looking out the windshield during conditions that might lead to a lightning strike. Cockpit instrument lights and display intensities should also be kept at maximum brightness.

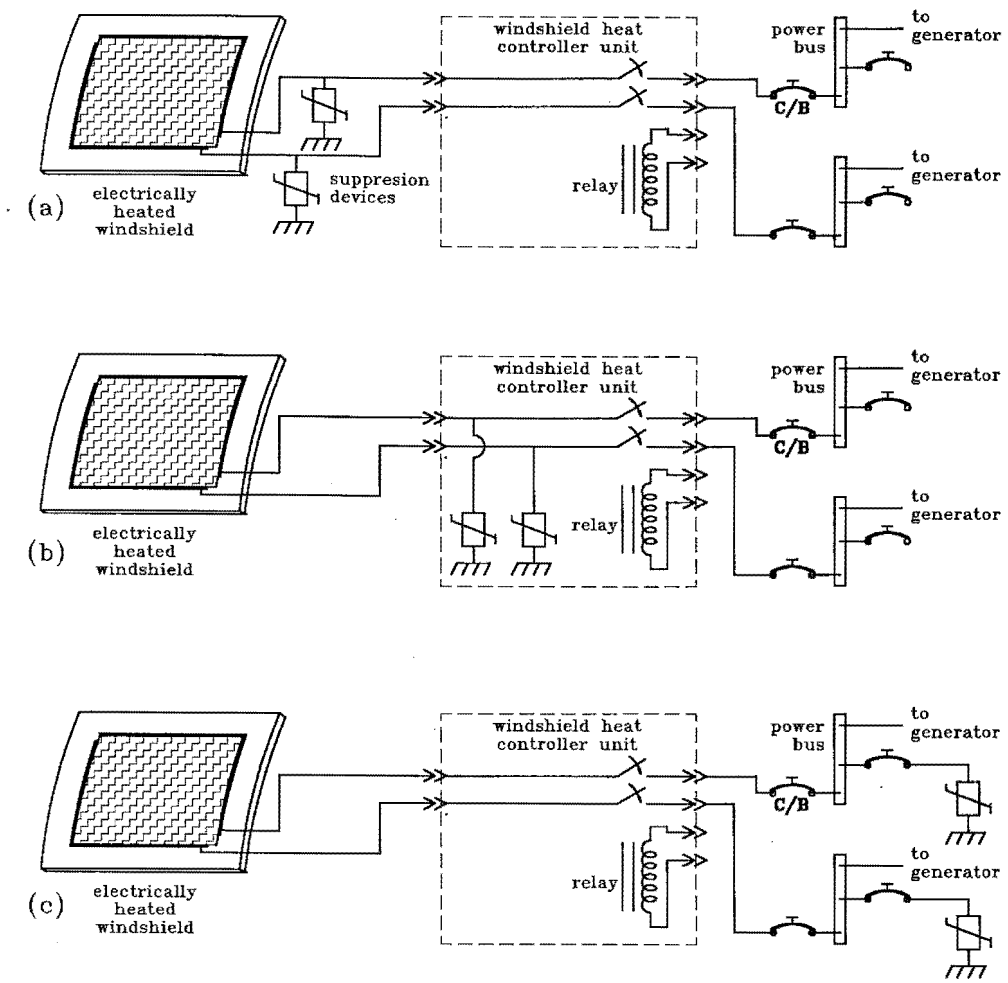

Fig. 6.40 Surge protection of windshield heater circuits.
(a) Diverter at windshield - Best
(b) Diverter in heat control unit - Intermediate
(c) Diverters on power supply bus - Least desirable

6.5 Electrically Conducting Composites

Electrically conductive composites include resins reinforced with various arrangements of carbon fibers or yarns, and other other resins reinforced with boron filaments. Carbon fiber composites (CFC), also known as graphite–epoxy composites, are by far the most common. Some boron composites are in use, but all of these were designed prior to 1980 because economic and structural advantages of CFC have precluded the use of boron in modern design. The protection designs described in this section will therefore deal with CFC, though a brief discussion of lightning effects on boron composites is included at the end of this section.

6.5.1 Protection of CFC Skins

As described in Chapter 4 and [6.21], lightning strikes may cause damage to CFC skins, including pyrolysis of resin and fracture of laminates due to shock wave effects. These effects occur at or near points of lightning attachment and are due primarily to stroke currents. Thus, they may occur in all zones, with the exception of Zone 3. The extent of this damage depends on the type and thickness of the CFC skins, the thickness of finishes and paints, and the intensity of the lightning strike. Experience has shown that surface damage is most closely related to action integral. Fig. 6.41 shows typical physical damage that may occur to an unprotected CFC skin in *Zone 1A*.

Design objectives: Most solid CFC laminates employed as aircraft skins have thicknesses ranging from 2 plies (0.5 mm, 0.02 in) to 20 plies (5 mm, 0.20 in). The thinner skins are used in sandwich constructions, and thicker laminates are employed as solid skins. Skins of any of these thicknesses can safely conduct lightning currents away from strike points; thus the protection design objectives are as follows:

1. Prevent hazardous damage (i.e. puncture, cracking) at strike attachment points in *Zones 1A*, *2A*, *1B* and *2B*.

2. Provide adequate lightning current paths among parts, so as to prevent damage at joints. In CFC fuel tanks, this objective must be accomplished without arcing or sparking which could ignite fuel vapors. Design methods for arc and spark suppression are discussed in Chapter 7.

3. Lightning direct effects protection designs for CFC must be coordinated with other electrical requirements, such as *EMI* control, power system grounding, and lightning indirect effects protection design.

Whether protection is required or not depends on the structural purpose of the CFC skin and the consequences of damage. If this damage represents a flight safety hazard, as may occur if a pressure hull is punctured or a control surface is delaminated, protection

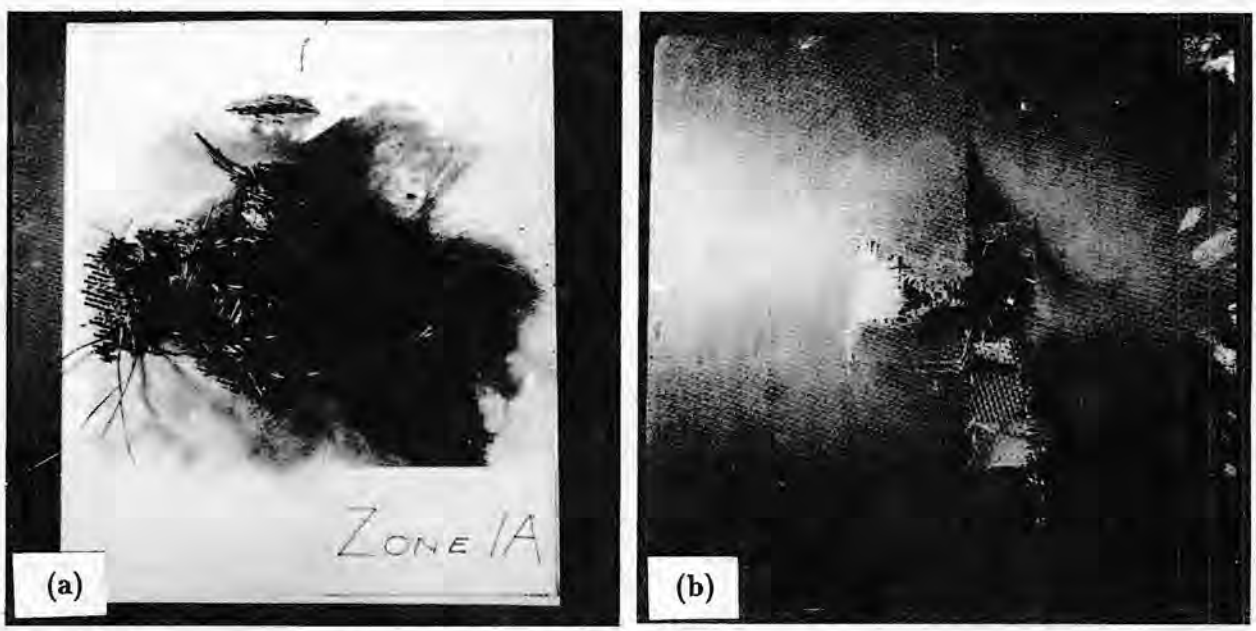

Fig. 6.41 Extent of damage to a CFC skin.
(a) Front side (b) Back side

must be applied to comply with the *FARs*. On the other hand, damage to some structures will not compromise safety and a decision is made not to protect.

Examples of CFC skins that usually do and do not require protection are as follows:

CFC skins that may need protection.

- o Fuselage pressure hulls.
- o Engine nacelles and pylons.
- o Flight control surfaces.
- o Leading edge devices.
- o Avionics bays.
- o Wing and empennage tips and activator housings.
- o Fuel tank skins.

CFC skins that may not need protection.

- o Tail cones.
- o Non–pressurized fuselage skins.
- o Wing–body fairings.
- o Ventral and dorsal fins.
- o Landing gear doors.

The nuisance factor associated with some of the non–protected items listed above may warrant protection, and as will be shown, effective protection can be provided with very little impact on cost and weight. Methods for protection of CFC skins and application considerations are discussed in the following sections.

The basic protection benefits provided, in varying degrees, by each of the following methods include: (1.) improved electrical conductivity, so that a portion of the lightning current flows in the protective layer and not in the CFC and (2.) arc root dispersion, so that lightning currents are caused to enter skins at a multiplicity of points over a wider area, as compared with a single point.

Woven wire fabrics: These are fabrics woven of fine metal wires, typically 0.05 - 0.1 mm (0.002 - 0.004 in) in diameter. Aluminum is the preferred metal, since it is light in weight and has low resistivity as compared with other metals. Plain and satin weave patterns with 40 to 80 wires per cm (100 - 200 wires per inch) are typical. One layer of this fabric is resin bonded to the exterior of the CFC laminate during the original cure process, so that the metal fabric is in direct contact with carbon fibers.

Some designers express concern regarding corrosion, and incorporate a thin barrier of fiberglass cloth between the metal fabric and the CFC. Accelerated salt–spray tests have shown that aluminum fabrics cured and encapsulated with resins and coated with paint do not corrode, though long term service experience is not yet available to confirm this. Other metals, such as tin and stainless steel, are more compatible with CFC and are sometimes preferred from a corrosion standpoint, but their lightning protection effectiveness is less than that of aluminum fabrics.

The woven metal fabrics provide both improved conductivity and arc root dispersion, and protective effectiveness is very good, even on thin (2 - 4 ply) CFC skins. The latter effect is due to the roughness of the woven surface, which encourages stress concentration and puncture at many points during the strike attachment process. Physical damage is normally limited to erosion of a small area of the mesh.

The weight penalty of woven wire fabrics is about 0.5 lb per m^2 (0.05 lb per ft^2). This protection of large surface areas implies a significant weight penalty. These fabrics should be laid up in the skin mold, together with any barrier ply and the CFC. The wire mesh must be the outermost ply of the laminate.

Expanded metal foils: These are fabricated of single sheets of foil, perforated and stretched to provide openings and an appearance similar to woven meshes. The expanded foils are typically 0.05 - 0.1 mm (0.002 - 0.004 in) thick, and have current conduction and protection effectiveness characteristics similar to those of woven wire meshes. They should be co–cured with the CFC laminate, using resin pre–impregnated CFC fabric to bond and encapsulate them.

Aluminum and copper foils provide the most effective lightning protection, and are typically used because they offer some electromagnetic shielding.

The weight penalty of expanded foils is somewhat greater (depending on specific thicknesses) than that of the wire meshes, but the foils provide somewhat better electromagnetic shielding than do the meshes, due to the better contact afforded with mechanical fasteners and hard metal surfaces. For this reason expanded foils are sometimes employed when protection against both direct and indirect effects is desired.

Metal coated CFC: CFC yarns and cloths are available with nickel electroplated or electrodeposited on them to increase conductivity of skins. The metal is typically several microns thick, but usually all fibers in a yarn or ply of cloth are coated and so a significant reduction in resistance is achieved, resulting in a coated CFC ply with one tenth the volume resistivity of an uncoated ply.

Coated CFC suffers some mechanical strength degradation as compared with uncoated material, so the coated ply can not always be counted as a structural ply and one additional layer of structural CFC may have to be furnished, thereby increasing weight.

As with the metal fabrics and foils, only one ply of coated material should be used, and it must be the outermost ply.

The lightning protection effectiveness of metal coated CFC is not as good as that of woven wire meshes and expanded foils, allowing some damage to the coated ply and one or two underlying plies.

Metal coated CFC is most often employed when the possibility of corrosion is of special concern, because the metal used (nickel) is compatible with CFC.

Interwoven wires: CFC fabric is available with small diameter metal wires woven along with the carbon yarns in each direction [6.22, 6.23]. Typical arrangements have from 3 to 9 wires per cm (8 to 24 wires per inch) of cloth, and the wires have diameters of 0.08 and 0.12 mm (0.003 to 0.005 in.). The periodic appearance of the wires at the fabric surface intensifies the electric field at a multiplicity of locations, sufficient to cause multiple punctures of paint layers and allow lightning currents to enter the CFC surface at many points, rather than at a single spot, thus achieving arc root dispersion.

A typical CFC laminate containing a ply with interwoven wires is illustrated in Fig. 6.42. This figure shows, in exaggerated form, the yarns in the top ply, which is to be the exterior ply and exposed to lightning strikes. The electric field intensifies where the wires appear at the surface, causing the multiple lightning attachment points.

Fig. 6.43 is a photograph of a typical unpainted CFC laminate, showing the interwoven wires.

Fig. 6.44 shows the behavior of a simulated lightning leader attaching to a painted CFC laminate with interwoven wires. Each of the current filaments attaches to a wire at the laminate surface, puncturing the paint. An individual attachment point on a wire is pictured in Fig. 6.45. The resin shown in this photograph has been punctured, exposing the wire, but the wire was not damaged because the test current, representative of a lightning leader, was small.

Full threat, return stroke currents enter a wider area of surface, as illustrated in Fig. 6.46, and usually vaporize the exposed portions of the wires, typically over a surface area 10 – 20 cm (4 – 8 in) in diameter. In most cases, this damage is limited to the outermost ply, which contains the wires. The exposed portions of the wires are vaporized, giving the surface a speckled appearance and often delaminating this ply from the other plies over a similar area. A four ply CFC skin panel 1.3 mm (0.051 in.) thick following a *Zone 1A* lightning test is shown in Fig. 6.47. The damage is limited to the outermost CFC ply.

The weight penalty of the interwoven wires is very small, being only 5% (or so) of the penalty associated with the woven wire fabrics or expanded metal foils described earlier. Also, the wires do not affect CFC strength and the interwoven wire ply is also a structural ply.

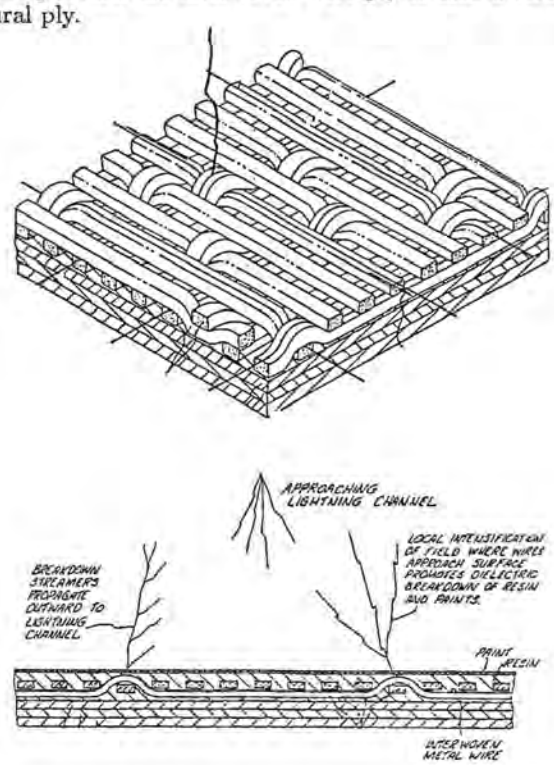

Fig. 6.42 CFC laminate with interwoven wires.

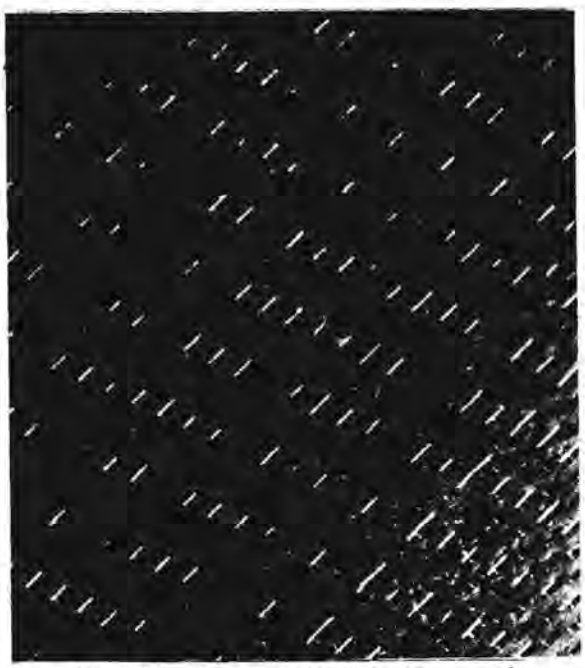

Fig. 6.43 Unpainted CFC laminate with interwoven wires.

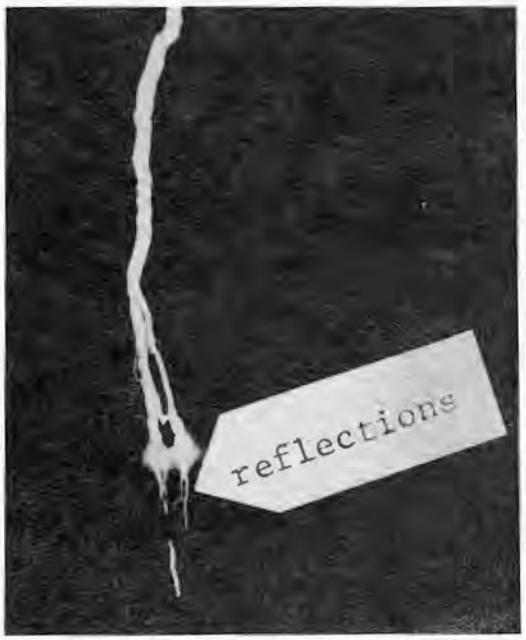

Fig. 6.44 Simulated lightning leader attaching to a painted CFC laminate containing interwoven wires.
- Each current filament attaches to a wire.

Fig. 6.45 Typical attachment spot on interwoven wire.
- 35X magnification

Fig. 6.46 Simulated lightning current entering a CFC laminate with interwoven wires.

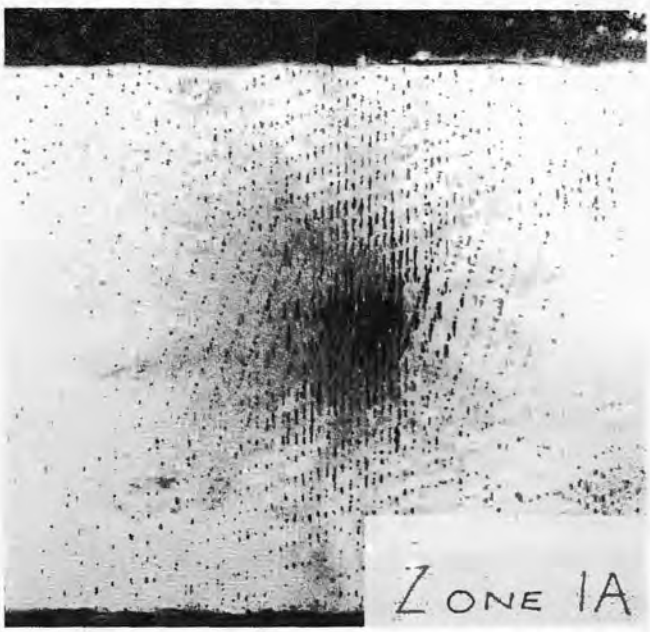

Fig. 6.47 Damage to protected graphite composite panel 1mm (0.040 in) thick.
Zone 1A flash, 190 kA, 1.24×10^6 $A^2 \cdot s$.

6.5.2 Protection of CFC Joints and Splices

In addition to damage at attachment points, lightning currents can also cause damage at the places where they flow from one piece of CFC to another, as at interfaces with adjoining skin panels or with substructure such as ribs and spars. Two basic methods of joining composites are in use:

Adhesive bonding: Adhesives are frequently used at structural joints and seams, either alone or in combination with mechanical fasteners. Since nearly all adhesives are electrical non-conductors, they present a barrier to current flow and force lightning currents to flow in fasteners and other places where CFC or other conductive parts of the structure come in contact. If no such paths exist, the adhesive must be made sufficiently conductive to permit current transfer.

Specific ways to provide electrical conductivity across adhesive joints are:

1. Doping of adhesive with electrically conductive particles.

2. Insertion of a conductive scrim into the bond.

Doped adhesives: Adhesives doped with some electrically conductive particles are commercially available, but the conductive particles are usually aluminum and their main purpose is thermal, rather then electrical conduction. Tests [6.24] have shown such adhesives to be capable of conducting up to about 100 A per cm^2 (645 A per in^2) of lightning stroke current without loss of mechanical strength. However, these adhesives are not as strong as non-conductive adhesives and so are not often found in primary structural applications. The use of aluminum particles in a CFC structure also raises concerns regarding possible corrosion.

Conductive scrim: Improvement of conductivity by insertion of a conductive scrim into the bond has proved successful in some applications. The scrim makes contact with each side of the joint, while allowing the adhesive to flow between yarns. Typical configurations are shown in Fig. 6.48. The most common scrim is a single loosely woven layer of carbon fiber cloth.

Galvanically compatible metal fabrics have also been used. In either case anticipated current densities must be kept low enough to preclude arcing at points of contact between the scrim and CFC parts within the bond. Such arcing would cause pressure buildup within the bond and possible disbonding.

Bolted and riveted joints: The other method of joining composite materials is with bolted joints, in which bolts, rivets, or other mechanical fasteners are employed to hold two members together. Metal fasteners are used since no other materials have been developed with sufficient strength.

Bolted or fastened joints offer electrically conductive paths, but the contact area between the fastener and the composite is usually limited to the surface under the fastener head and/or nut. There may be contact in the hole to the shank of the fastener, but it will be a loose contact at best and may not occur in all instances. This results in a relatively high current density at the fastener heads and nuts or collars, sometimes exceeding the level at which the composite will carry without damage.

To obtain better contact between the fasteners and the CFC, countersunk holes and beveled washers and fastener heads are used. Even so, tests have shown that significant arcing can take place around the fastener, especially when the lightning attachment point is near or at the fastener and fastener current densities are high. As discussed in Chapter 7, arcing at a fastener can be a concern when the fastener protrudes into a fuel tank.

Methods of eliminating this arcing or separating it from fuel vapors are described in Chapter 7. The loss of mechanical strength due to arcing at fasteners has not been of as great concern because a small amount of arcing will not significantly damage the CFC nor weaken the fasteners. The number of fasteners or rivets employed in most designs is usually sufficient to conduct most *Zone 3* lightning currents.

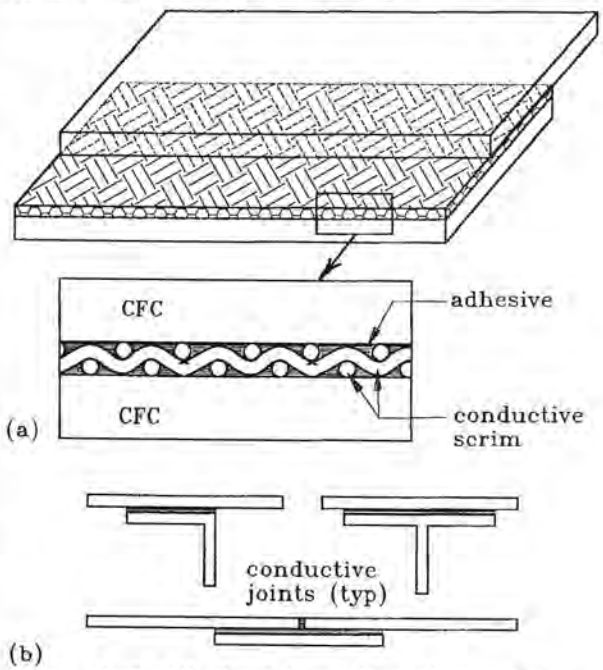

Fig. 6.48 Adhesive joint with conductive skrim.
(a) Basic concept
(b) Examples

Loss of strength at joints: Work has been done to evaluate the degree of strength loss caused by lightning currents in composite joints. Schneider, Hendricks, and Takashima [6.25] have studied the effects of lightning currents on typical bonded and bolted joints of graphite composites, and their preliminary findings show that bonded joints suffer more damage from lightning currents than do bolted joints. Other tests [6.26] have also been made on various joints, with similar results. The reader is referred to these sources for further information on the specific joints that researchers have evaluated and the results that they have obtained.

Candidate bond and joint designs should be tested with anticipated current densities to verify that these joints can tolerate the design level currents without loss of mechanical strength.

6.5.3 Application Considerations

Other aspects of lightning protection design for CFC skins include cloth or tape layup patterns, arrangement of ply seams, electrical bonding to fasteners and repair techniques. Brief discussions of each of these topics follow.

Layup patterns: Experience has shown that woven cloth fabrics are more tolerant of lightning strike effects than are laminates made of unidirectional tapes. The interweaving of carbon yarns in the woven cloth restricts damage propagation due to blast of shock wave effects, and the cloth plies also have more uniform electrical conductivity.

Unidirectional tapes, on the other hand, tend to unwind along the tape, causing damage for greater distances from the strike point than is the case for woven cloths. Also, electrical conductivity tends to be somewhat better in the direction of the tapes and less in perpendicular directions. This causes lightning currents, and damage, to penetrate deeper into a laminate to final conductive paths in all directions.

Tape laminates are also less capable of being protected with interwoven wires or metallized yarns, as the improved conductivity afforded by these methods is often achieved only in the direction of the conductive fibers.

If tapes must be utilized for strength purposes, it is sometimes possible to include cloth plies on the inner and outer surfaces of a laminate. This affords the opportunity to utilize cloth with interwoven wires, or metallized cloth for lightning protection purposes.

Ply seams: Seams are necessary in CFC cloth layups where the edges of pieces of cloth meet. As long as the seams of adjacent plies do not coincide, there will be adequate electrical conductivity throughout the laminate. Ply seams are usually simple butt joints, and electric currents flow through adjacent plies at such seams.

Seams in some lightning protective layers may need to be applied or bridged in some manner to allow current transfer and minimize arcing. Protective layers requiring splicing include wire meshes and expanded foils. Splices can be separate pieces of the mesh or foil, or overlaps. Two common designs are illustrated in Fig. 6.49. In either case, the amount of overlap necessary to transfer currents depends on the current density. Overlaps of 1 cm (0.5 in) have been found capable of transferring currents of 2.5 kA per cm (1 kA/in) across overlaps or splices without debonding or excessive arcing, when the adjoining pieces are co- cured along with the underlying laminate and in good contact with each other. Larger overlaps, of up to about 5 cm (2 in.) are usually necessary at joints exposed to higher current densities, as would exist at wing or empennage tips, or other structures in which lightning currents are high.

Splices and overlaps which are secondarily bonded with a layer of adhesive are not nearly as conductive as cocured splices because the adhesive separates conductive layers and promotes arcing. If secondary bonds must be used, adhesives should be non-supported and of minimum thickness. Vacuum bagging and curing should be conducted so as to encourage maximum metal-to-metal contact in the overlap or splice.

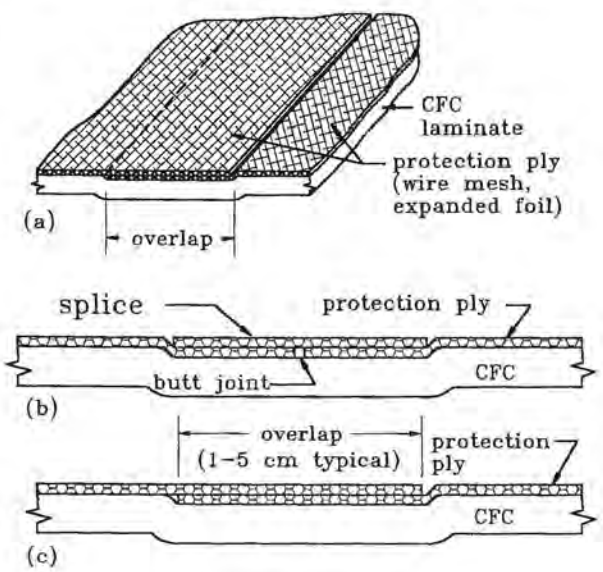

Fig. 6.49 Typical configurations of splices in protective plies.
(a) Concept
(b) Splice
(c) Overlap

Splices at manufacturing joints: Splices in protection layers that extend across manufacturing joints in large structures may need to have larger overlaps if they are to be the only means of transfering current across such a joint. Several joint designs are shown in Fig. 6.50. Most candidate joint designs should be tested to verify that current transfer occurs in the designated splice plies or plates and not in an alternate manner which would involve arcing and debonding which would degrade mechanical strength.

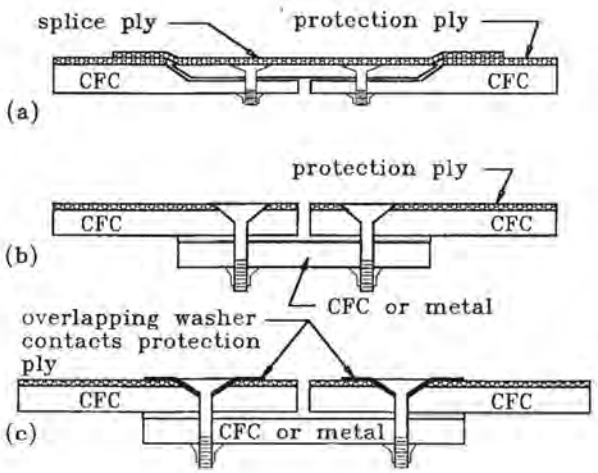

Fig. 6.50 Splices across manufacturing joint.
(a) Splice ply
(b) Splice plate
(c) Splice plate with overlapping washers

Seams in interwoven wire and metalized fabrics: Splices are not usually required in laminates protected with interwoven wires or metalized fabrics, because these methods depend on the bulk CFC laminate for conduction purposes, and serve mostly to minimize damage at lightning attachment spots. Protection ply overlaps and splices across seams are, therefore, not required. The edges of protection plies may be butted together and cocured with the rest of the laminate.

Electrical bonding to fasteners: It is frequently necessary to make contact between protection layers and metal fasteners, for transfer of current to adjoining parts or substructures. This can be done either by direct conduction between CFC laminate and the fastener in the hole, or by installing the fasteners in overlapping washers (sometimes called dimpled washers) or metal doubler plates. These concepts are shown in Fig. 6.51.

It is rarely possible to extend protection plies or layers into countersunk fastener holes, as the protection ply is (and should be) co-cured with the laminate and holes must be drilled afterwords. Good conductivity can be achieved if the fastener is drawn tightly into the countersunk hole and sealant barriers are minimized, so that the fastener head can be drawn tightly against the cross section of CFC in the hole, as shown in Fig. 6.51(a).

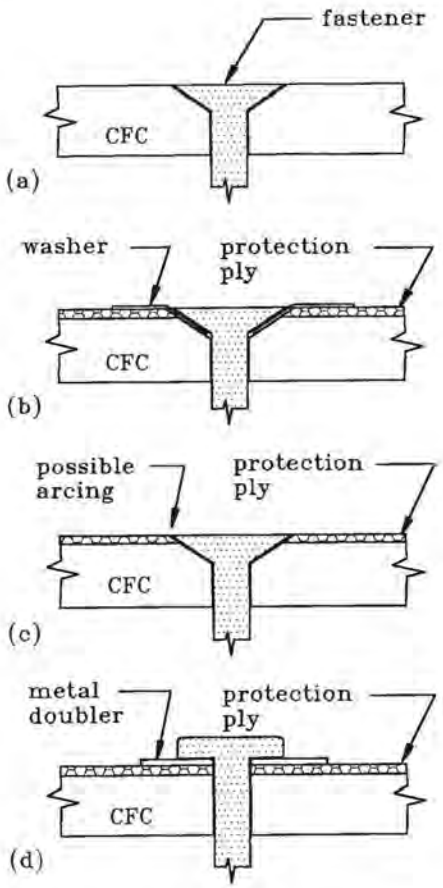

Fig. 6.51 Bonding to fasteners.
(a) Bonding in countersink
(b) Bonding with overlapping washer
(c) Bonding with protection ply and hole (allows arcing)
(d) Bonding with metal doubler

If a protection ply is shown, it can be electrically bonded to the fastener via overlapping washers or a metal doubler plate, as shown in Fig. 6.51(b) and 6.51(d). These methods afford the best bond between

protection layers and fasteners, which is necessary if the protection layer is also intended to afford electromagnetic shielding of on–board systems. A typical application is the avionics bay access door illustrated in Fig. 6.52. Good shielding requires that the protection ply be bonded to surrounding structure on all edges, as shown. This is accomplished by the removable fasteners on the edges by the piano–type hinge on the fourth edge.

6.6 Boron Structures

Boron materials were at one time under consideration for composite structures. Interest in them has waned and they are not likely to be considered in the future, but, for completeness, the research on such materials will be briefly reviewed here.

6.6.1 Lightning Effects on Boron Composites

Fassell, Penton, and Plumer [6.27] began the study of lightning effects on boron composites with a study of the degradation process in a single boron filament. These filaments are formed by deposition of boron on a 0.13 mm (0.0005 in) diameter tungsten filament called the substrate. The boron sheath, which provides the filament's strength, is about 1.3 mm (0.005 in) in diameter.

Mechanism of damage: The tungsten substrate is a resistive conductor, but the resistance of the boron is much greater by several orders of magnitude. Thus, electric currents entering a boron composite will tend to flow in the tungsten substrates instead of in the boron.

Tungsten has a positive temperature coefficient of resistivity, which means that, as its temperature rises, its resistivity increases as well, and it becomes even hotter as current flows. When temperature rise is calculated as a function of current action integral by Eq. 6.5, the temperature rise curve of Fig. 6.53 results. The quantity $\int I^2 dt$ is, of course, equal to the unit energy dissipation in the substrate (per ohm of resistance) and is dependent solely upon the electric current amplitude and pulse waveform.

Fig. 6.53 shows that very little temperature rise occurs as $\int I^2 dt$ is increased to 20×10^{-6} $A^2 \cdot s$. However, increases beyond this value cause moderate temperature increases, and increases beyond 100×10^{-6} $A^2 \cdot s$ result in extreme temperature rise. Fassell, Penton, and Plumer [6.27] injected currents beyond 100×10^{-6} $A^2 \cdot s$ into single filaments and found

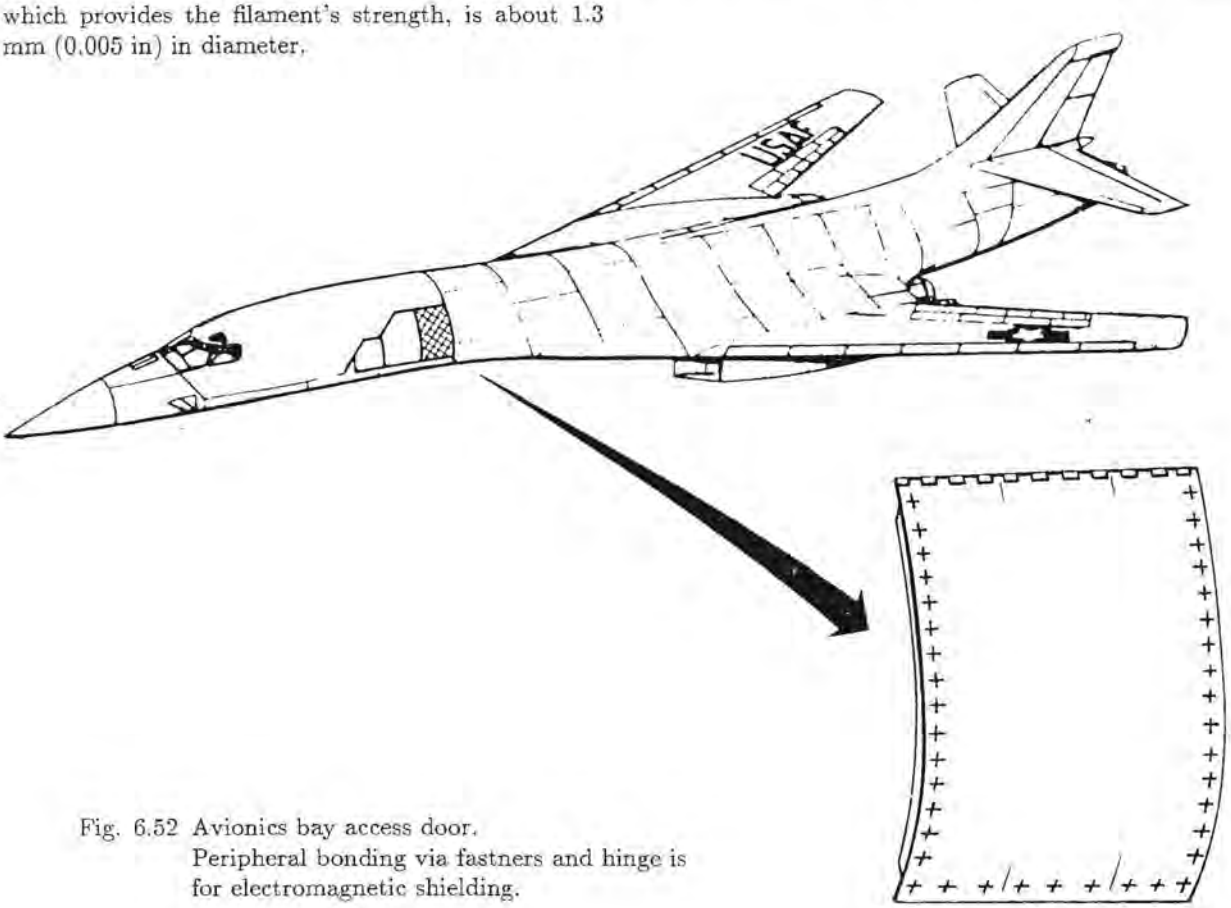

Fig. 6.52 Avionics bay access door.
Peripheral bonding via fastners and hinge is for electromagnetic shielding.

them to be severely cracked and to lose all mechanical strength. Correspondingly, filaments exposed to pulses with $\int I^2 dt$ values of 100×10^{-6} $A^2 \cdot s$ or less exhibited little or no evidence of degradation.

The mechanism of filament failure was found to be transverse and radial cracking of the boron sheath, presumably caused by excessive thermal expansion of the tungsten substrate. Examples of cracked filaments are shown in Fig. 6.54. Thus, the calculated temperature rise is a significant indication of filament failure onset. In comparison to natural lightning currents, it is noted that when distributed over several thousand filaments, a lightning stroke current of several thousand amperes may provide only 1 A of current per filament. If this current exists for 100 μs, it will indeed provide an $\int I^2 dt$ of 100×10^{-6} $A^2 \cdot s$ in a single filament. If this current exists for 20 μs, it will provide an $\int I^2 dt$ of 20×10^{-6} $A^2 \cdot s$ in a single filament, etc.

While the previous example illustrates the manner in which lightning currents may cause mechanical property degradation of boron composite materials, it also illustrates the relatively flat region in which increasing values of $\int I^2 dt$ do not result in corresponding increases in temperature rise. For protection design, this fact emphasizes the desirability of distributing lightning currents throughout as many filaments as possible.

To explain the process of current flow into the many boron filaments in a composite, Penton, Perry, and Lloyd [6.28] formulated an electrical model of two boron filaments in a resin matrix, as shown in Fig. 6.55. Each filament is made up of incremental portions of the tungsten substrate resistance. These researchers found that the filament–to–filament breakdown voltage is about 300 V and that the insulation breakdown at this level is represented by the back–to–back Zener diodes, which have a reverse conduction (Zener) voltage of 300V.

They found that a lightning current flowing in the outer filament would remain in this filament until the resistive voltage rise along it exceeds the boron and resin breakdown voltage, this being represented by the Zener diodes, at which point current enters the neighboring filament. In most cases this would be a filament in the next ply of the laminate. While some material strength degradation undoubtedly occurs from the breakdown of the resin and boron sheaths, the major loss of strength was found to be a result of temperature rise in the filaments and cracking of the boron sheaths along the entire length of the current flow.

When the filaments in an outer layer fail by transverse, or axial, cracking, the resistances of their tungsten substrates also increase (by cracking) and so does the voltage rise along this layer, until the breakdown level of the boron sheaths and resin between it and the next layer of filaments is reached. When this happens, the current enters this next layer of filaments, and the process continues. The depth of penetration, of course, depends on both the amplitude and duration of the lightning current and the number of filaments into which this current can distribute.

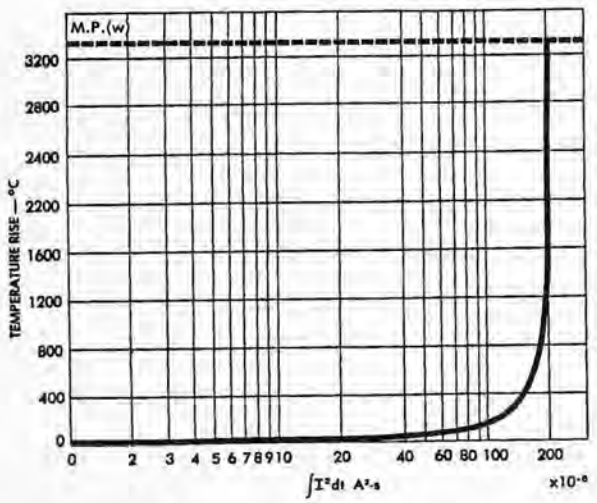

Fig. 6.53 Temperature rise of tungsten substrate of a boron filament.

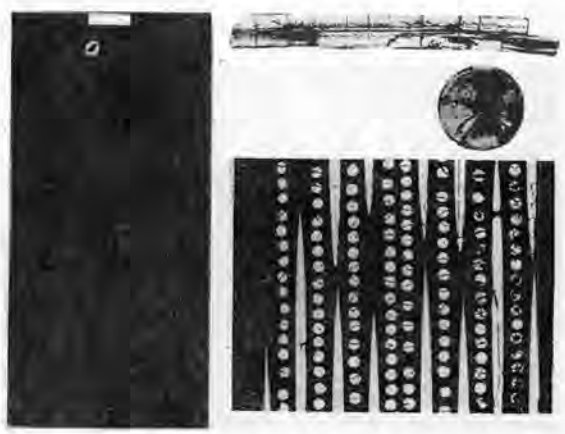

Fig. 6.54 Cracking of boron filaments due to excessive current.

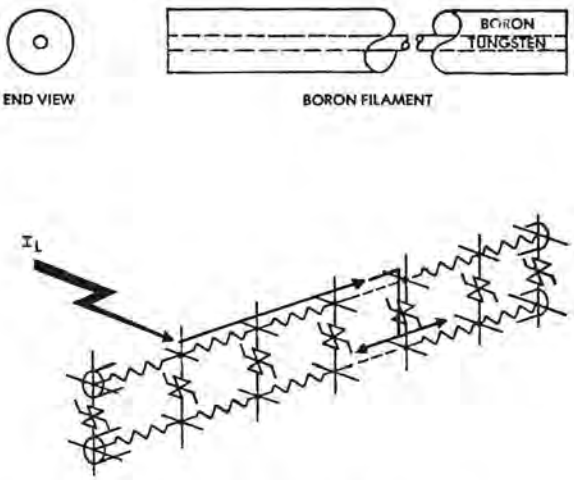

Fig. 6.55 Zener diode model of boron filaments within a laminate.

In addition to the current conduction effects just described, the high temperature and blast forces from the arc have been found to cause substantial damage to a boron composite at the point of attachment, just as with CFC structures. Holes blown in a boron composite material tend to be somewhat greater than would be expected in a CFC panel of similar thickness. Details of test results will not be reviewed further since boron materials are now seldom used.

6.6.2 Protection of Boron Composites

Boron composites can be protected by several of the same techniques previously described for non–conductive composites. The electrical behavior of boron is more like the non–conductive composites reinforced with aramid fiber and glass than CFC, so the woven wire mesh, expanded aluminum foil and arc or flame–sprayed metals are most appropriate. Interwoven wires and metal–coated boron filaments have not been evaluated for protection of boron composites and these methods are not as likely to be as successful as they are for protection of CFC.

If composites reinforced with boron or other less familiar materials are to be employed in the future, extensive testing will be necessary to define and quantify lightning effects and develop satisfactory protection methods.

6.7 Direct Effects on Propulsion Systems

Lightning attachment to an engine pod or nacelle can result in damage to the structure. Structural effects of this type are identical to those discussed previously for other exposed structure. The aircraft propulsion system does contain some unique functions which can be damaged by lightning direct effects. The new high efficiency engines contain numerous electronic monitors and controls which may be vulnerable to the indirect effects of lightning. Those effects are covered in Chapters 8 - 18. The effects discussed here are those related to propellers and rotors, gear boxes, and stalls of turbofan engines.

6.7.1 Propellers

Aircraft propellers are frequent targets for lightning strikes. The general location of propellers, front for traction or rear for pusher, probably accounts for their susceptibility to lightning strike attachment. Tractor blades are in a *Zone 1A* or *2A* location while pushers will be in *Zone 1B*. The high current component of lightning , due to its short duration, will affect only one blade. The duration of the intermediate current is of a short enough time that it will also involve only one of the blades, but the propeller does spin fast enough that the long duration continuing current will divide among all the blades.

A lightning flash to a metal propeller does little damage. It may produce minor pitting and erosion of metal at trailing edges, but not sufficient to require corrective action beyond filing down of rough spots.

Propellers of fiberglass are more vulnerable to lightning, especially if internal conducting parts are present. Then the flash can puncture to those internal conducting objects, causing delamination and eventually complete destruction. If the internal part has only a small cross–section it can explode and cause explosive shattering of the blade. Lightning current entering a heater wire, for example, could propagate elsewhere and cause problems, but that is an indirect effect treated in later chapters. Protection techniques are the same as for other dielectric structures as described in §6.3.5 and include conductive paints, diverters, and surface coatings. Often a metal leading edge rain erosion strip can be designed to safely intercept the lightning flash.

Dielectric blades will be subject to precipitation static problems and any antistatic system that is installed will be subject to lightning as well. The effects of lightning strikes to the antistatic system must be assessed to insure that no safety of flight hazards can occur. Graphite composite blades are less vulnerable to lightning than dielectric composites, but verification is mandatory due to the critical function of the blade. If protection is required, methods discussed in §6.5 can be applied.

6.7.2 Rotor Blades

In general, helicopter rotor blades or rotating wings are similar to propeller blades in their lightning performance. The main difference is the greater size of the rotor blades. The larger size often will involve greater complexity in terms of heater blankets for de-ice and tip lights. Such additional systems will usually require that protection be designed and applied to other than metal blades.

6.7.3 Gear Boxes

Lightning currents entering propellers or rotor blades must exit to the aircraft through the gears and bearings supporting the propeller or rotor shaft. The conduction of these currents through the bearings, which are supported on insulating lubricant films, will result in some pitting of the bearing surfaces. This does not appear to be a major problem since there do not appear to be any records of any catastrophic failures of bearings associated with lightning strikes. Engine manufacturers, however, have always recommended that gear boxes and bearings be disassembled and inspected after a strike. This usually results in replacement of the bearing since it is not possible to differentiate between arc pitting and wear. There does not appear to be any way of avoiding such pitting since lightning current will always go through the bearing.

There are no practical ways of diverting current away from the bearings.

Helicopter manufacturers generally do not recommend bearing inspections, but depend on gearbox chip counter circuits to indicate the conditions of bearings and gears.

6.7.4 Turbine Engines

Small turbine engines, especially those mounted on the fuselage, may experience turbine stall or roll-back during a lightning event. The phenomenon is thought to be caused by the lightning channel interrupting the air flow at the engine air inlet. Numerous cases of power loss have been reported [6.29] and in one particular instance both engines sustained a flame-out. Damage to the engine or nacelle is generally not observed. No protective measures are known, other than pilots being aware of the problem and practiced in restart procedures.

6.8 Direct Effects Testing

Lightning tests on aircraft are an attempt to duplicate the *effects* of lightning, not an attempt to duplicate lightning itself. The point is important because the exigencies of test equipment make it necessary to evaluate the high voltage effects of lightning separately from the high current effects. Test machinery is not available to duplicate the energy levels of lightning, that is, to produce currents of the magnitude involved in the lightning return stroke while simultaneously duplicating the high voltages of a developing lightning leader. High voltages can readily be developed and high currents can readily be developed, but not simultaneously by the same machines. Also, a focus on lightning effects, rather than lightning itself, makes it feasible to perform high current testing with waveshapes different from those produced by natural lightning.

These points will be elaborated upon in the following sections. Mostly the discussion will be that of Section 6.8.1, dealing with test machinery. That section will describe the methods of operation and factors governing performance, cost and tradeoffs of test machinery. Section 6.8.2 will discuss test standards and test procedures, including some discussion of the background of their development. That discussion will be brief because there are other documents that cover test standards and procedures in considerable depth.

6.8.1 Test Equipment

There are basically two types of test made on aircraft to evaluate direct effects: (a) high voltage discharge tests to help identify where lightning might attach, and to evaluate the efficacy of lightning diverters and (b) injection of high currents into objects to evaluate their resistance to the burning and blasting effects of the return strokes.

High voltage surge generators: High voltages of the magnitude, hundreds and thousands of kilovolts, associated with the lightning leader are commonly produced by slowly charging a group of capacitors in parallel and rapidly discharging them in series, "Marx" generators, after the inventor. They were originally developed for testing the degree to which the insulation of high voltage electric power transmission equipment could resist the high voltages produced by natural lightning striking power transmission lines. That remains their most common use today, a fact that has influenced standardized waveshapes, including the waveshapes used for evaluating lightning effects on aircraft.

Several configurations are possible for impulse generators, one of which is shown in Fig. 6.56. Each of the capacitors is initially charged to a voltage V through resistors, as shown in Fig. 6.56(a). Then, all the switches, S_1, S_2, S_3 $\cdots$ are closed simultaneously, thus connecting all the capacitors in series, as shown in Fig. 6.56(b), and allowing them to discharge through the external waveshaping circuit. Charging

voltage is typically 50 - 200 kV per stage. The particular circuit gives a negative going output voltage for a positive charging voltage, but other configurations can give positive output voltage.

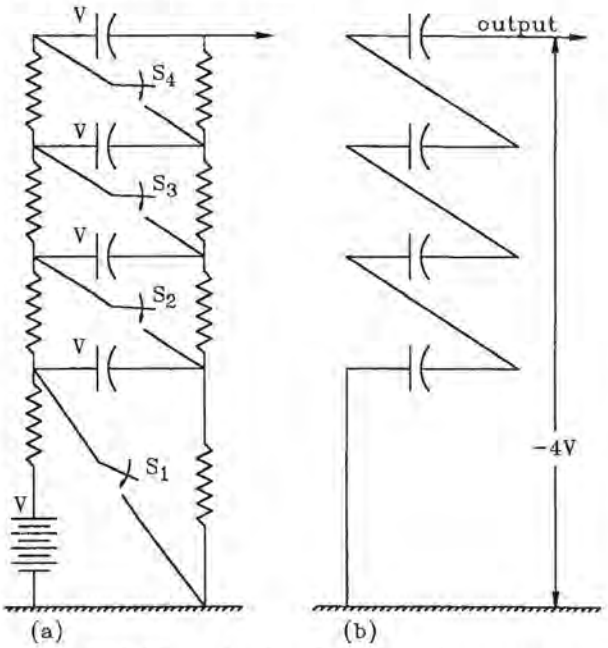

Fig. 6.56 Marx circuit voltage impulse generator.
(a) While charging
(b) After erection

In practice, the switches are spark gaps, usually spheres a few tens of centimeters diameter. Closure of S_1 connects C_1 and C_2 in series, which places $2V$ on C_2, which then sparks over placing C_1, C_2 and C_3 in series, placing $3V$ on S_4. The process, called erection, cascades until all capacitors are in series. Stray capacitance from the various stages to ground is essential to the initial development of the overvoltages required to close switches other than the one initially fired. For air insulated generators, erection takes place in about 10 ns, 10^{-8} seconds.

The initial switch closure can be effected by physically moving the spheres together enough to allow S_1 to breakdown by a dc overvoltage or by inducing breakdown by a pulse applied to a trigger electrode, a trigatron spark gap. A discussion of triggering mechanisms is beyond the scope of this volume, but can be found in the literature. Reference [6.30] gives a good introduction to the matter and also provides additional references to the vast literature on pulsed power surge technology.

Marx circuit voltage generators are usually rated in terms of their open circuit voltage capability because they are used for testing insulation and other high impedance devices. Operation into low impedance circuits is the exception, except in study of nuclear EMP effects, in which case compactness and speed of erection becomes important. Such generators are generally insulated with oil or insulating gases, such as sulfur hexafluoride, but the generators used during tests for lightning effects are most commonly air insulated.

Voltage generators are also rated in terms of their stored energy,

$$W = nC_g V_c^2 \text{ joules or watt-seconds.} \qquad (6.23)$$

A large machine for the electric power field might have an open circuit voltage of about 5 MV (5×10^6 V) and a stored energy of 250 kilojoules. 10 MV is about the highest voltage that has been used for air insulated machines. Testing for aircraft applications seldom calls for such voltages or stored energy. A 5 MV machine can produce discharges through 10 or more meters of air, but standardized test practices for determining attachment points on aircraft seldom call for gaps more than about 1 m in length.

After erection, the surge generator can be treated as a single capacitor of magnitude $C_g = C_{\text{stage}}/N$ charged to a voltage $V_g = NV_{\text{stage}}$. A common complete generator circuit, including waveshaping components, is shown in Fig. 6.57.

Disregarding the stray inductance of the circuit, it produces open circuit voltages of double exponential waveshape, as discussed in §1.5.2 and §9.10.1. Front time is controlled by the charging time constant of the series resistance R_s and the waveshaping capacitor C_l. Tail time is determined by how long it takes C_g and C_l to discharge through the resistors to ground, R_g and R_d. In practical circuits, R_d is frequently a resistive voltage divider to measure the output voltage and waveshape, though this can also be done by using the waveshaping capacitor C_l as the high voltage arm of a capacitive voltage divider. A discussion of measuring techniques is presented in [6.31]. Some circuits dispense with either R_g or R_d, but if a low resistance must be used to prevent the tail time from being too long, it is more efficient to use a high resistance voltage divider (R_s) and a low resistance for R_g.

Approximate values of the front and tail times are

$$T_{\text{front}} = 3R_s C_l \qquad (6.24)$$

$$T_{\text{tail}} = 0.7\left[\frac{R_g(R_s + R_d)}{R_g + R_s + R_d}\right] \qquad (6.25)$$

In the high voltage power field the waveshape most commonly produced has a front time of 1.2 μs

and a tail time of 50 μs, as defined in §1.5.2. Shorter front times can be produced, but the effects of stray inductance become more important, both to the performance of the generator and to calculation of the waveshape produced by a given set of circuit constants. Longer tail times can be produced, though the influence of the charging resistors must be taken into account. Efficient generation of short tail times requires the addition of inductance in series with the discharging resistors [6.32].

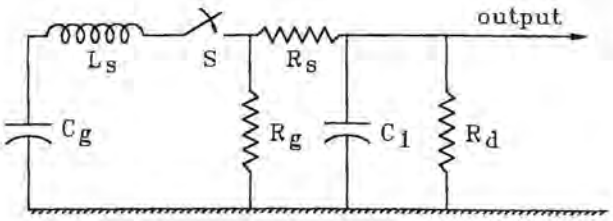

Fig. 6.57 Generator circuit including waveshaping elements.

Analytic expressions for the effects of these various factors are available, but it is more practical just to make numerical calculations using one of the many time domain circuit analysis programs. For the circuit of Fig. 6.58(a) the calculated open circuit voltage would be as given in Figs. 6.58(b) and (c). The front and tail times, as defined in [6.33] are 1.3 μs and 67 μs respectively. The circuit constants of Fig. 6.58(a) are typical of a small generator that might be used for testing of aircraft equipment.

Since the purpose of the generators is not to duplicate lightning, but only to duplicate the effects of high voltages produced by lightning, the ability to produce high currents serves no special purpose and is seldom attempted. High voltage generators are large and tend to have high inductance. Also, they are usually designed with internal series resistance to prevent oscillatory currents from flowing, since such currents lead to reversals of voltage on the capacitors, which may shorten their life. The circuit constants of Fig. 6.59(a) are fairly representative of an actual moderate size machine machine, particularly as regards the internal inductance and resistance. Figs. 6.59(b) and (c) show, for two different values of external series resistance, the short circuit current that would be obtained. The circuit dispenses with a load capacitor on the premise that a unidirectional current wave would be desired.

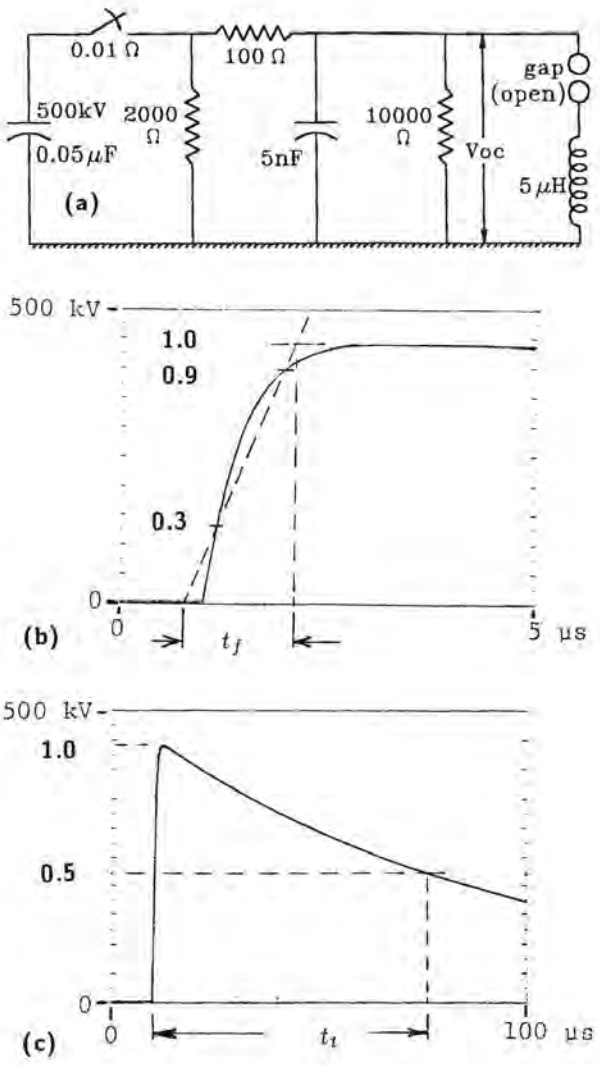

Fig. 6.58 Open circuit voltage waveshape.
(a) Representative circuit values
(b) Waveshape of front
(c) Waveshape of tail

High current generators: Direct effects testing for aircraft components more generally calls for the injection of high currents into a portion or sample of the aircraft structure. Injection into a complete aircraft is seldom either attempted or necessary. Most commonly, the current is injected into the item under test either through a small air gap a few cm. in length or sometimes by direct metallic connection.

Surge current generators, such as those required to produce the Component *A* and Component *D* currents specified [6.34] for testing of aircraft, employ many large capacitors in parallel, connections being

configured so as to minimize internal inductance, with Fig. 6.60 showing a representative configuration. The maximum peak current available from a capacitor bank depends on the circuit inductance, part of which is internal and somewhat under the control of the bank designer and part of which is associated with the test object and the connecting leads. This latter depends on the size of the test object and may be the inductance that limits peak current available from a particular generator. The external circuit inductance associated with large structures is largely the reason that high current tests on complete aircraft are seldom attempted.

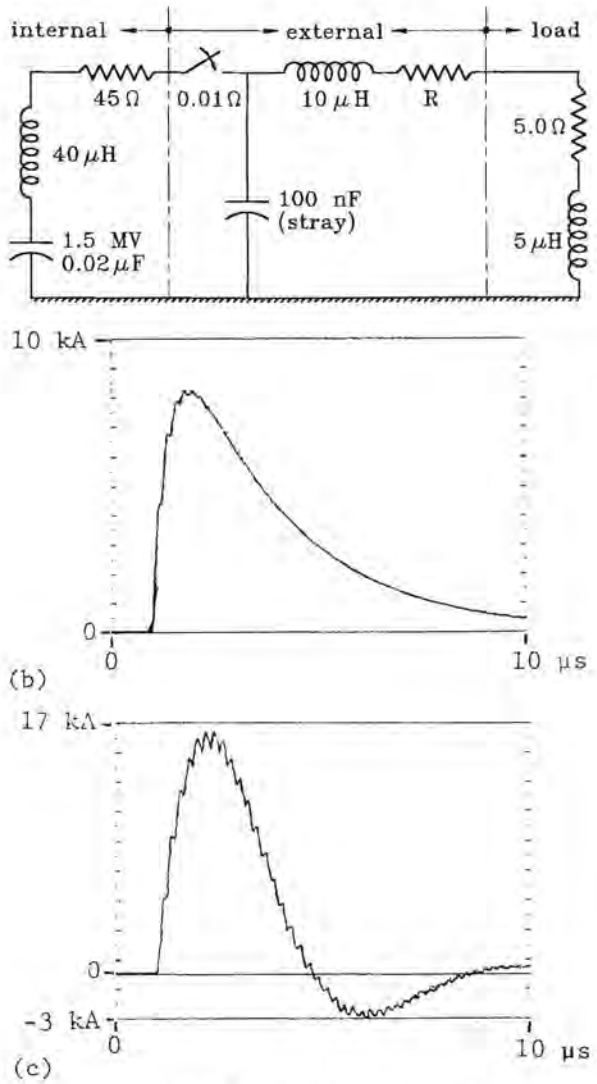

Fig. 6.59 Short circuit currents.
(a) Circuit
(b) $R = 100$ ohms
(c) $R = 1$ ohm

Since the external inductance is relatively large, the discharge switch can frequently be just a heavy duty sphere mechanically brought into contact with a metal plate. Generators optimized for minimum internal inductance should have more sophisticated switching devices, such as those discussed in [6.30]. For a given generator and load, peak current is varied by adjusting the charging voltage of the surge generator. Peak current may not vary directly with charging voltage because of the effects of arcing test pieces, but the non-linearities are small.

Surge generators are most commonly operated underdamped in order to obtain maximum current. Underdamped, by definition, means that the output current is oscillatory, unlike the unidirectional currents associated with natural lightning and the unidirectional voltage waves easily obtainable from generators optimized for production of high magnitude impulse voltages. It also means that the front time of the surge current inherently has a rather long front time. Attaining unidirectional current waves of very high amplitude with short front times is difficult. It can be done, but the machines become very large and expensive. For direct effects testing, development of fast front times is not essential since damage depends primarily on peak current and current duration, not the front time of current. The front time of the current is important for evaluating indirect effects, but that is a different matter.

With an undamped machine the maximum peak current is

$$I_{max} = \frac{V}{\sqrt{L/C}} \tag{6.26}$$

where

V = charging voltage
C = generator capacitance
L = circuit inductance.

The initial rate of change of current, at $T = 0$, is

$$\frac{dI}{dt} = \frac{V}{L} \tag{6.27}$$

and the frequency of oscillation is

$$f = \frac{1}{2\pi\sqrt{LC}} \tag{6.28}$$

Moderate damping does not have much effect on the above values.

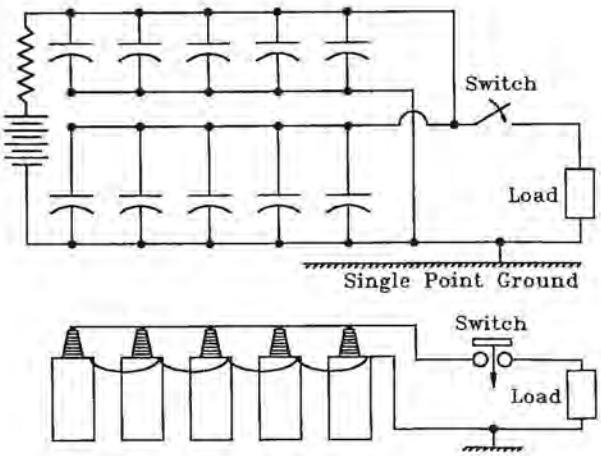

Fig. 6.60 High current surge generator.
(a) Circuit diagram
(c) Approximate dimensions

Unidirectional current waves: There are three ways to produce unidirectional current waves. The most straightforward is to use sufficient series resistance to damp the oscillations. Critical damping is obtained with a resistance of

$$R = 2\pi\sqrt{\frac{L}{C}} \tag{6.29}$$

Fig. 6.61 shows the effect on waveshape of the current from the indicated surge generator as resistance is increased. The greater the resistance, the faster the front time, but the less the peak current. Series resistance effectively brings about a unidirectional current wave by throwing away as heat most of the energy initially stored in the capacitor bank.

Another way is to use a series resistor that has a non–linear VI characteristic, such as afforded by the zinc–oxide blocks used in surge arresters. Such a block would have a low dynamic resistance and little effect on the current when the current is high, but as the current returns to zero and tends to reverse the dynamic impedance becomes high and rapidly absorbs energy, suppressing subsequent half cycles. Fig. 6.62(a) shows the connection and Fig. 6.62(b) illustrates the current waveshape.

The third way to obtain a unidirectional current wave is by "crowbarring", that is, to short the surge generator at the instant when current in the test piece is at a maximum [6.35, 6.36]. Ideally, all the energy stored on the capacitors would then have been transferred to external inductance, where it could be "trapped" by the crowbar switch. Prior to shorting, the current waveform is governed by the circuit capacitance and inductance. After shorting the current decays with a time constant governed by the load inductance and the external resistance. Crowbarring thus does nothing to improve the rise time of the current.

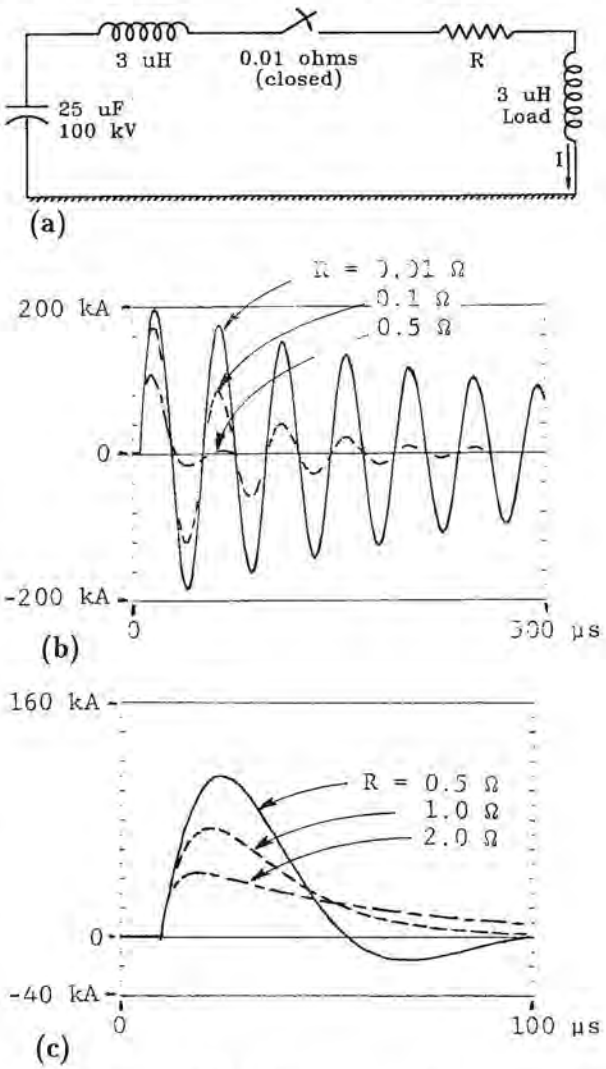

Fig. 6.61 Effect of damping resistance on waveshape.
(a) Circuit
(b) Underdamped circuits
(c) Overdamped circuits

Fig. 6.63(a) shows the principle and Figs. 6.63(b) and (c) illustrate the resulting waveshapes. The figure shows the generator to have some internal inductance, since it can never be completely eliminated.

Crowbarring greatly complicates the test circuit and is difficult to do successfully. If the surge generator were free of inductance, the voltage across the capacitors would be zero at the time of shorting, all

of the energy initially stored having been transferred to the inductance of the test piece. Since the switch must close at or near voltage zero, it is difficult to use a triggered spark gap for the job. Recourse is often had to switches using a solid dielectric that is mechanically ruptured by an explosive charge, techniques for which are discussed in [6.30]. The unavoidable internal inductance of the generator results in some of the circuit energy being trapped internal to the generator, giving rise to oscillatory currents in the storage capacitors. This tends to lower the life of the capacitors.

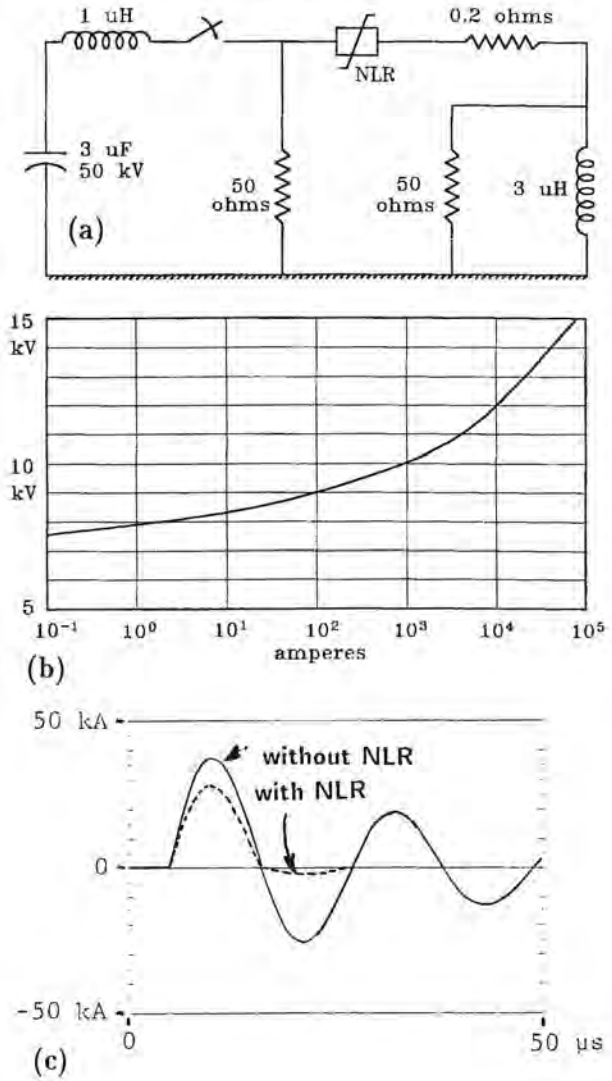

Fig. 6.62 Unidirectional wave produced by series non-linear resistor.
(a) Circuit
(b) VI characteristic of non-linear resistor
(c) Calculated output current

Compound circuits: One way to improve the front time of surge current generators is to use compound circuits. In the overdamped circuit of Fig. 6.64(a) a judicious choice of small parallel capacitors and series resistance can boost up the leading edge of the current, as shown in Fig. 6.64(b). Theoretically, almost any wave can be obtained by proper choice of parallel elements for the generator, though three parallel elements represents about the limit of practical usage. Choice of suitable peaking elements generally requires considerable numerical or physical experimentation since there is considerable interaction among the circuit elements.

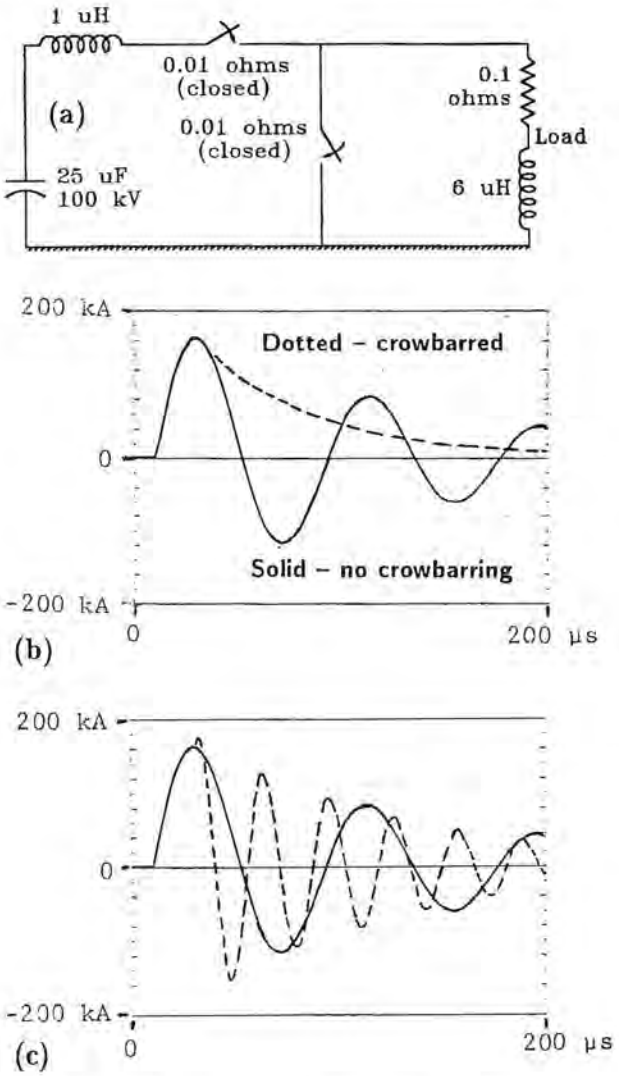

Fig. 6.63 Unidirectional wave produced by crowbarring.
(a) Circuit
(b) Calculated output current
(c) Current in capacitors

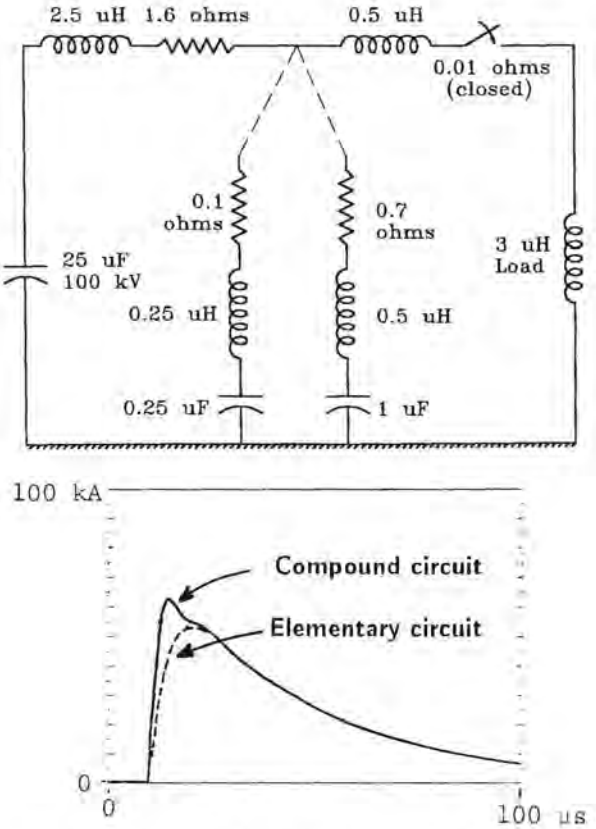

Fig. 6.64 Waveshape improvement by compound circuit.
(a) Circuit
(b) Calculated waveshapes

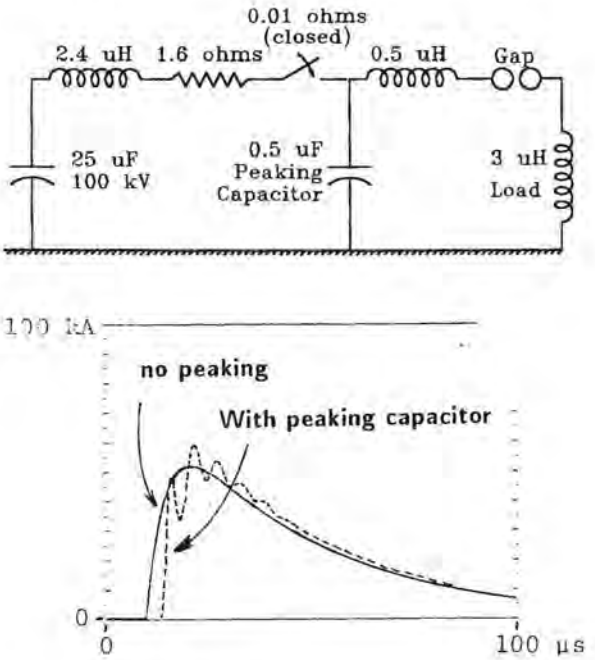

Fig. 6.65 Waveshape improvement by peaking capacitor.
(a) Circuit
(b) Calculated waveshapes

Peaking capacitors: Another compound circuit, Fig. 6.65(a) employs a low inductance peaking capacitor, C_p, which is rapidly charged when the main energy storage bank is discharged [6.37]. This is then discharged into the test piece when the auxiliary spark gap G_2 is fired. Fig. 6.65(b) shows calculated waveforms with and without the peaking capacitor, though the indicated circuit elements have not been optimized to give the best waveshape.

A virtue of the concept is that the peaking capacitor can be charged to a voltage higher than the charging voltage of the main energy storage bank, by virtue of the oscillation that takes place when the main switch is closed. Higher voltage on the peaking capacitor means that it can supply more initial current.

A peaking capacitor works best when its inductance and the inductance of the discharge path are small. Sometimes a parallel plate peaking capacitor can be used, the capacitor being formed from a mesh of wires held above a ground plane with the test object being underneath the overhead grid, though this is only practical for large outdoor generators. Numerical or physical experimentation may be necessary to determine the circuit elements that give optimum waveshape.

Rating of current generators: Current generators are most commonly rated in terms of their stored energy, their maximum current and the duration of the current they can deliver to a test piece. One measure of a surge current is its *Action Integral*, defined as

$$AI = \int_0^\infty I^2 dt \qquad (6.30)$$

If load resistance were constant, the action integral would define the energy delivered by the current,

$$W = AI \times R \qquad (6.31)$$

Action integral is a useful concept, but it is not, however, a perfect measure of the ability of a test current to cause damage or a perfect measure of the energy transferred from the generator into the test sample.

Ideally, current generators would be rated in terms of their ability to cause damage to a test piece. Also, ideally, current generators would be high voltage and high impedance devices capable of injecting a specified current into a load of any impedance. As

a practical matter, current generators are low impedance devices and the current delivered to the load does depend on the impedance of the load. Peak current is one measure of the ability to cause damage and duration of current flow is another, but they do not completely define the matter. The fact that the current is oscillatory indicates that energy is being transferred back and forth between the capacitance of the generator and the inductance of the entire circuit. A current that oscillates for a long time, and thus might have a large action integral, does not indicate that it is capable of causing extensive damage; it only indicates that energy is not being lost from the surge generator.

When the high current produces arcing in the object under test, the load resistance is not constant, but may increase with time as the current burns the surface of the object under test. When this happens, the increased resistance causes more energy to be deposited in the test sample, which is to say, causes energy to be transferred more efficiently from the generator into the test sample. The fact that energy has been extracted from the generator means that the degree of oscillation of the test current is reduced. An anomalous situation then arises, because the action integral of the current, which supposedly measures the damage producing ability of the current, is reduced *because* the current has produced damage to the object under test.

Intermediate currents: Intermediate currents, Component B of [6.34] can also be produced by capacitor banks. Capacitances are larger than those used to develop Component A currents, but charging voltage need not be as high.

Continuing currents: Continuing currents can be produced by a dc source, such as storage batteries connected in series, ac transformers feeding rectifiers or rotating machines. Storage batteries are probably the most straightforward and economical method.

Complete current circuit: Direct effects testing frequently requires that Component A, B and C currents be injected into a test piece. A typical circuit that allows this to be done is shown in Fig. 6.66. Closure of switch S_1 allows the Component A generator to discharge into the test piece, the frequency of oscillation being determined by the capacitance of the generator and the circuit inductance and the decrement being controlled by R_1. The resulting voltage across gaps G_1 and G_2 causes them to spark over and allows the Component B and C generators to discharge into the test piece. L_b and R_b are adjusted so that the Component B current is unidirectional and of the proper amplitude and duration. L_c and R_c adjust the amplitude of the continuing current, Component C, and prevent the Component A and B generators from discharging into the low impedance storage battery. The duration of the Component C current can be adjusted by opening switch S_2, closing switch S_3 or by blowing of fuse F. Currents are measured by pulse current transformers and resistive shunts, T_1, R_2 and R_3.

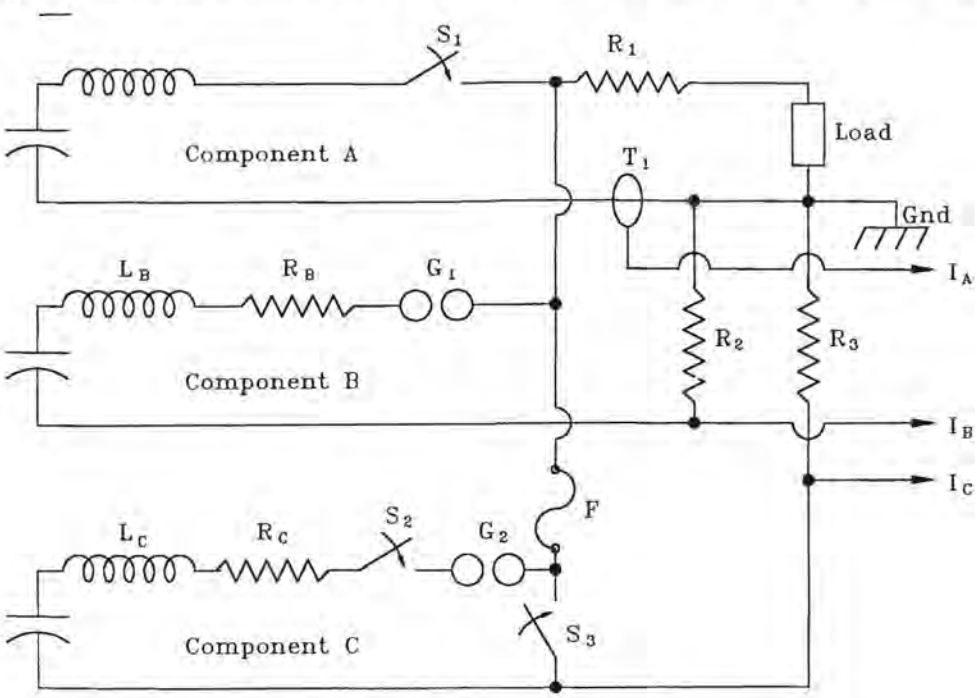

Fig. 6.66 Complete current generator.

In order to minimize interference to measuring equipment, a complete surge generator normally would have the low voltage side of all the component generators connected together at one point, as shown in Fig. 6.48.

6.8.2 Test Practices and Standards

Techniques and waveforms for direct effect lightning tests on aircraft have been codified by industry working groups and are presented in [6.34] and [6.38]. The documents present a general consensus of practice in both the USA and Europe. They have been influenced by test practices that were common in the electric power industry long before testing on aircraft was codified, and some discussion of those practices is useful in interpreting [6.33] and [6.38]. Power industry practice is codified in documents such as [6.33] and [6.39 - 9.41] and wherever possible aircraft testing practices have tended to follow those guidelines, deviating no more than necessary.

Voltage test waves: Impulse voltage test waves were developed in response to the observation that voltages induced on power transmission lines by lightning were generally unidirectional and tended to have front times of a few microseconds and decay times of a few tens of microseconds. Similar waveforms could be produced in the laboratory by simple, though expensive, surge generators such as the Marx circuit impulse generator. Generators that might produce other idealized waves, such as square, trapezoidal or triangular waves, would have been much complex.

Present practice is to define the standard lightning test wave as one having a 1.2×50 μs waveshape, that is, a front time of 1.2 μs and a decay time of 50 μs, the definitions being as given in §1.5.2. Front time is taken as the virtual front time of Fig. 1.10 because it is often more clearly defined than the actual time to crest. High voltage surge generators do not deliver mathematically pure double exponential waves; the wave is initially distorted by the firing of the spark gaps of the generator and the wave near crest may be distorted by non-linearities of the test piece. None of these have any practical effect on the response of insulation, but they can cause expensive controversy in interpretation.

Early practice, before about 1960, called for a 1.5×40 μs waveshape in the USA and Canada and a 1×50 μs waveshape in Europe. Tolerances on front and tail times were intentionally loose, however, and there was little practical difference between the two. International standardizing activities have led to a compromise and the present 1.2×50 μs wave is used worldwide. The wave, when not interrupted by breakdown of a gap or insulation, is called a Full Wave, as discussed in §1.5.3 and Fig. 1.11. It is carried over into aircraft testing as *Voltage Waveform B -Full Wave* in paragraph 3.2.1.2 of [6.34].

When measuring the performance of a spark gap it is usually found that the breakdown voltage depends on how rapidly the voltage is increased. Power industry practice has been to measure the breakdown voltage of protective spark gaps by applying voltage waves rising at the rate of 1000 kV/μs. Such a voltage can be produced by suitable adjustment of the charging voltage and circuit elements of standard Marx circuit impulse generators. The resulting voltage is called a Steep Front, SF, wave. It is carried into aircraft testing as *Voltage Waveform A – Basic Lightning Waveform* in paragraph 3.2.1.1 of [6.34].

Power industry practice also calls for evaluating the sparkover voltage of transmission line insulators when exposed to switching surges having front times of several tens or hundreds of microseconds. Such voltages can also be produced by Marx circuit impulse generators. Similar voltages are called for in aircraft testing as *Voltage Waveform D - Slow Front Model Tests* of paragraph 3.2.2.2 of [6.34].

Current test waves: Power industry testing of surge arresters calls for a 8×20 μs wave, as was discussed in §1.10. In the aircraft industry, similar test waves are used for evaluating surge arresters used in aircraft, but are not in use otherwise.

REFERENCES

6.1 J. H. Hagenguth, "Lightning Stroke Damage to Aircraft," *AIEE Transactions* 68, American Institute of Electrical Engineers, New York, 1949, pp. 9-11.

6.2 R. O. Brick, "A Method for Establishing Lightning Resistance and Skin Thickness Requirements for Aircraft," *1968 Lightning and Static Electricity Conference*, December 1968, pp. 295-317.

6.3 R. O. Brick, L. L. Oh and S. D. Schneider, "The Effects of Lightning Attachment Phenomena on Aircraft Design," *1970 Lightning and Static Electricity Conference*, December 1970, pp. 139-156.

6.4 F. L. Kester, J. A. Plumer and M. Gerstein, "A Study of Aircraft Fire Hazards Related to Natural Electrical Phenomena," *NASA CR1076*, June 1968.

6.5 *Protection of Airplane Fuel Systems Against Fuel Vapor Ignition Due to Lightning*, FAA AC 20-53A, Federal Aviation Administration, Washington, D.C., 12 April 1985.

6.6 J. Philpott, "Factors Affecting Puncture of Aluminum Alloy by Simulated Lightning," *Lightning and Static Electricity Conference Papers*, December 1972.

6.7 Paul T. Hacker, "Lightning Damage to a General Aviation Aircraft–Description and Analysis," *NASA TN D-7775*, National Aeronautics and Space Administration, Lewis Research Center, Cleveland, Ohio, September 1974, p.49.

6.8 R. D. Hill, "Channel Heating in Return Stroke Lightning," *J. Geophys. Res.*, Vol 76, 1971, pp 637–645.

6.9 M. A. Uman, *The Lightning Discharge*, International Geophysics Series, Volume 39, Academic Press, Orlando, 1987, pp. 293–303.

6.10 J. R. Stahmann, "Control Surfaces and Door Hinge Bonding Effectiveness in Modern Aircraft," *Proceedings of the 1972 Lightning and Static Electricity Conference*, 12-15 December 1972, pp. 327–34.

6.11 *Bonding, Electrical, and Lightning Protection for Aerospace Systems*, MIL–B-5087B (ASG), 15 October 1964.

6.12 M. P. Amason, G. J. Cassell, J. T. Kung, "Aircraft Applications of Segmented–Strip Lightning Protection Systems," *Proceedings of the 1975 Conference on Lightning and Static Electricity*, 14-17 April 1975, at Culham Laboratory, England

6.13 S. A. Moorefield, J. B. Stryon, and L. C. Hoots, "Manufacturing Methods for Advanced Radome Production," *Interim Technical Report 6*, prepared by the Brunswick Corporation for the Air Force Materials Laboratory, Air Force Systems Command, United States Air Force, Wright–Patterson Air Force Base, Ohio, November 1975, pp. 32-40.

6.14 Amason, Cassell, and Kung, "Aircraft Applications of Segmented–Strip Lightning Protection," p.9.

6.15 D. A. Conti and R. H. J. Cary, "Radome Protection Techniques," *Proceedings of the 1975 Conference on Lightning and Static Electricity*, 14-17 April 1975, at Culham Laboratory, England.

6.16 J. A. Plumer, "Guidelines for Lightning Protection of General Aviation Aircraft," *FAA–RD-73-98*, Federal Aviation Administration, Department of Transportation, Washington, D.C., October 1973, p.8.

6.17 Courtesy of Lightning Diversion Systems, Inc.

6.18 J. T. Quinlivan, C. J. Kuo, and R. O. Brick, "Coatings for Lightning Protection of Structural Reinforced Plastics," *AFML–TR-70-303 pt. I*, Air Force Materials Laboratory, Nonmetallic Materials Division, Air Force Systems Command, Wright–Patterson Air Force Base, Ohio, March 1971.

6.19 R. O. Brick, C. H. King, and J. T. Quinlivan, "Coatings for Protection of Structural Reinforced Plastics," *AFML–TR-70-303 Pt. II*, Air Force Materials Laboratory, Nonmetallic Materials Division, Elastomers and Coatings Branch, AFML/LNE, Wright–Patterson Air Force Base, Ohio, February 1972.

6.20 *Report on the Investigation of an Accident Involving Aircraft of U.S. Registry NC 21789, Which Occurred Lear Lovettsville, Virginia, on August 31, 1940*, Civil Aeronautics Board, Washington, D. C., 1941.

6.21 F. A. Fisher and W. M. Fassell, "Lightning Effects Relating to Aircraft, Part I – Lightning Effects on and Electromagnetic Shielding Properties of Boron and Graphite Reinforced Composite Materials," *AFAL–TR-72-5*, Air Force Avionics Laboratory, Air Force Systems Command, Wright–Patterson Air Force Base, Ohio, January 1972, p. 55.

6.22 Plumer - D. H. McClenahan and J. A. Plumer, "Protection of Advanced Composites Against the Direct Effects of Lightning Strikes," *International Aerospace Conference on Lightning and Static Electricity*, Vol. II, Oxford, 23 - 25 March, 1982, G3-1 – G3-9.

6.23 McClenahan et al. U.S. Patent Number 4,448,838, May 1984.

6.24 J. E. Pryzby and J. A. Plumer - "Lightning Protection Guidelines and Test Data for Adhesively Bonded Aircraft Structures," *NASA Contractor Report 3762*, Jan. 1984.

6.25 S. D. Schneider, C. L. Hendricks, and S. Takashima, "Vulnerability/Survivability of Composite Structures- Lightning Strike," *D6-42673-3*, prepared by the Boeing Commercial Airplane Company for the Air Force Flight Dynamics Laboratory, Aeronautical Systems Division, Wright–Patterson Air Force Base, Ohio, April 1976.

6.26 Pryzby and Plumer, "Lightning Protection Guidelines ... ", op. cit. Jan. 1984.

6.27 W. M. Fassell, A. P. Penton, J. A. Plumer, "The Susceptibility of Advanced Filament Organic Matrix Composites to Damage by Simulated Lightning Strikes," *Lighting and Static Electricity Conference*, 3-5 December 1968, pp. 530-69.

6.28 A. P. Penton, J. L. Perry, J. A. Plumer, *The Effects of High Intensity Electrical Currents on Advanced Composite Materials*, U-4866, prepared by the General Electric Company for the Naval Air Systems Command, Department of the Navy, Washington, D. C. 15 December 1970, pp. 2-30, 2-32.

6.29 D. Newton, *Severe Weather Flying*, McGraw–Hill, New York, 1983, p. 65.

6.30 I. M. Vitkovitsky, *High Power Switching*, Van Nostrand Reinhold, New York, 1987.

6.31 A. J. Schwab, *High–Voltage Measurement Techniques*, The M.I.T. Press, Cambridge, Mass., 1972.

6.32 A. Carrus, "An Inductance on the Marx Generator Tail Branch. New Technique for High Efficiency Laboratory Reproduction of Short Time to Half Value Lightning Impulses," *IEEE Transactions on PAS*, Vol 4, No. 1, January 1989, pp. 90-94.

6.33 "Standard Techniques for High Voltage Testing," *Institute of Electrical and Electronic Engineers*, IEEE Standard 4, 1978.

6.34 "Lightning Test Waveforms and Techniques for Aerospace Vehicles and Hardware," *Report of SAE Committee, AE4L*, 20 June 1978.

6.35 R. A. White, "Lightning Simulator Circuit Parameters and Performance for Severe–Threat, High–Action– Integral Testing," *International Aerospace and Ground Conference on Lightning and Static Electricity*, Orlando, FL, June 26-28, 1984, pp. 40-1 – 40-14.

6.36 M. J. Landry, W. P. Brigham, "UV Laser Triggering of Crowbars Used in the Sandia Lightning Simulator," *International Aerospace and Ground Conference on Lightning and Static Electricity*, Orlando, FL, June 26-28, 1984, pp. 46-1 – 46-13.

6.37 R. A. Perala et al, "The Use of a Distributed Peaking Capacitor and Marx Generator for Increasing Current Rise Rates and the Electric Field for Lightning Simulation," *International Aerospace and Ground Conference on Lightning and Static Electricity*, Orlando, FL, June 26-28, 1984, pp. 45-1 – 45-6.

6.38 *Lightning Qualification Test Techniques for Aerospace Vehicles and Hardware*, MIL–STD-1757A, 20 July 1983.

6.39 *High Voltage Test Techniques - Test Procedures*, IEC Publication 60-2, *International Electrotechnical Commission*, Paris, 1973.

6.40 *High Voltage Test Techniques - Measuring Devices*, IEC Publication 60-3, *International Electrotechnical Commission*, Paris, 1976.

6.41 *High Voltage Test Techniques - Measuring Devices Application Guide*, IEC Publication 60-4 *International Electrotechnical Commission*, Paris, 1977.

CHAPTER 7

FUEL SYSTEM PROTECTION

7.1 Introduction

The design of adequate lightning protection for aircraft fuel systems is one of the most important lightning protection tasks to be accomplished. Government airworthiness certification requirements stress fuel system safety because this system has been responsible for most lightning-related aircraft accidents.

Elements of the fuel system are typically spread throughout much of an aircraft and occupy a significant amount of its volume. They include the fuel tanks themselves, associated vent and transfer plumbing, and electrical controls and instrumentation. Careful attention must be paid to all of these elements if adequate protection is to be obtained.

The main objective of fuel system lightning protection is to keep ignition of fuel from destroying the aircraft during a strike. This goal is quite challenging because thousands of amperes of current must be transferred through the airframe when the aircraft is struck by lightning and a tiny spark of less than one ampere may release sufficient energy inside a fuel tank to ignite the fuel vapor and initiate an explosion.

Prevention of fuel ignition hazards from lightning must be accomplished by one or more of the following approaches:

1. **Containment:** Designing the structure to be capable of containing the resulting overpressure without rupture.
2. **Inerting:** Controlling the atmosphere in the fuel system to ensure that it cannot support combustion.
3. **Foaming:** Filling the fuel systems with a material that prevents a flame from propagating.
4. **Eliminating ignition sources:** Designing the structure so that lightning does not produce any ignition sources.

The following paragraphs discuss all of these methods of preventing fuel system hazards. Several important studies relating to fuels and the mechanism of ignition are reviewed and guidelines for effective protection of fuel systems are then presented.

Laboratory studies involving simulated lightning strikes to fuel tanks or portions of an airframe containing fuel tanks have demonstrated several possible ignition mechanisms. Investigations of the accidents involving fuel tank fires and explosion have raised other possibilities. Possible ignition sources can be divided into the following two broad categories, thermal and electrical.

Thermal ignition sources

1. Hot spots on the interior surfaces of metal or composite fuel tank skins, due to lightning attachment to exerior surfaces.
2. Hot parts, such as electrical wires, ground braids or tubes, raised to elevated temperatures by high densities of lightning currents on these parts.

For hot spots to ignite fuel vapor, their temperature must usually exceed 800°C or 1500° F for a period of one second or more. Some metals, such as aluminum, will melt through before the interior surface reaches the ignition point of the fuel.

Electrical ignition sources

1. Electrical *sparks* between conductive elements isolated from each other, due to potential differences arising from lightning currents in the airframe, or from changing magnetic fields.
2. Electrical *arcs*, the ejection of molten and/or burning material due to current passing between conductive elements in contact with each other when the current density exceeds the current carrying capability of the contact points.

Arcing and sparking within the fuel vapor space of a fuel tank is one of the primary concerns of the fuel tank protection designer. The distinction between arcing and sparking is worth reviewing. Arcing is the result of current through the interface between two conducting materials which are making limited electrical contact. Such a condition may exist at the interface of a fastener with structure, as at an access door, or between two structural components such as a spar and rib. A spark, on the other hand, is an electrical discharge resulting from a difference of potential across an air gap or along a dielectric material. This condition may exist, for example, when two structural elements are isolated from each other such as a spar and wing skin which are bonded together by an electrically non–conductive adhesive. Current through the tank may result in a difference of potential between these struc-

tures, causing a spark to jump across the bond line between the two. In most tank designs, sparks are less likely than arcs.

While the above mechanisms have been postulated as the probable cause of the in-flight fuel tank explosions associated with lightning strikes, the exact location or source of ignition has not been positively identified in any of these accidents. The amount of energy in an electrical spark required to cause ignition is so small that such a spark would leave little or no other evidence of itself, such as pitting of a metal surface. It may also be possible that ignition occurred outside the fuel system itself, for example, at a fuel vent outlet, and then propagated through vent pipes to the inside.

7.2 Fuel Flammability

Fuel cannot ignite until some of it has become vaporized and mixed in a combustible ratio with oxygen or air. The flammability of the vapor in a fuel tank varies according to the concentration of evaporated fuel in the available air. Reducing the fuel–to–air ratio below a definite minimum value produces a mixture that is too lean to burn. Likewise, if the fuel–to–air ratio is too high, the mixture will be too rich to burn. In between these extremes there is a range of mixtures that will burn.

When only equilibrium conditions are considered, the particular fuel–to–air ratio that can exist in a tank is determined by the temperature of the fuel and the altitude (pressure) of the aircraft. The temperature determines the vapor pressure, and thus the quantity of the fuel vapor, and the altitude determines the quantity of air. The combination of temperature and altitude determines whether the vapor in the ullage (the space from which fuel has been drained) of a fuel tank is either flammable or nonflammable.

Research concerning fuel vapors and their flammability characteristics has included laboratory investigations of fuel vapors that exist within laboratory type containers as well as those that exist during flight.

Nestor's study: Perhaps the most comprehensive laboratory work is that of Nestor [7.1], who paid particular attention to the behavior of fuels in aircraft tanks and flight environments. He found wide variations in the amount of fuel that can exist in the vaporized state as a result of a wide variety of temperatures, pressures, and motions that can exist in flight.

In addition to fuel already present as a vapor, the aircraft motion and vibration also causes the liquid fuel to be dispersed in the vapor space in the form of mists and spray. An ignition source might heat these droplets of fuel to a point where there is enough vapor present to support a flame, even if insufficient vapor has been released from the bulk fuel surface itself. The developing flame then vaporizes more fuel, which continues to feed and enlarge the flame. Temperature and altitude, however, are the primary characteristics related to flammability.

Types of fuel: Almost all aircraft with reciprocating engines use 100 octane aviation gasoline (AvGas). Turbine engine fuels, however, come in two broad categories based on their distillation temperature ranges; aviation kerosenes and wide–cut fuels. The aviation kerosenes include Jet A, Jet A-1, and JP-5. The wide–cut fuels, which have a higher percentage of volatile components, include Jet B and JP-4. Turbine powered commercial aircraft in the United States and in some foreign countries are fueled with aviation kerosenes. U.S.A.F. aircraft, and commercial transports in some other countries, have fueled with wide–cut fuels in the past. Th U.S.A.F. will convert to JP-8, starting with NATO and finishing in the U.S. in the mid 1990s. The U.S. Navy uses JP-5 for carrier operations because it has a high flash–point.

Flammability envelopes: The relationship of temperature and altitude to tank vapor flammability is illustrated by the flammability envelope. A typical flammability envelope is shown in Fig. 7.1 [7.2]. The flammability limits for aviation gasoline and the turbine fuels are presented in Fig. 7.2. [7.3] As shown in Fig. 7.2, the lean limit for the aviation kerosenes ranges from 40 to 60°C at sea level and the rich limit ranges from 85 to 105°C. For the wide–cut fuels, the lean and rich limits at sea level are about −30°C and 10°C, respectively. For aviation gasoline the lean limit is approximately −40°C and the rich limit about −5°C.

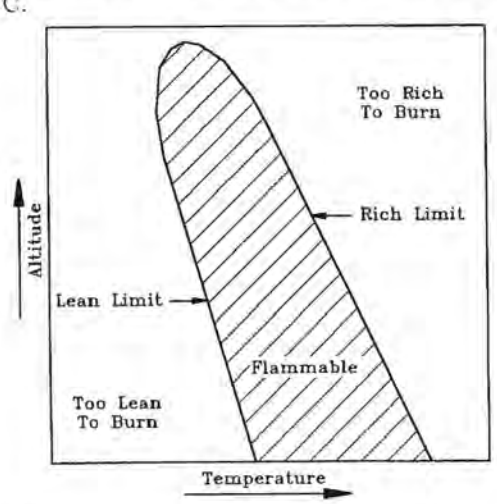

Fig. 7.1 Typical flammability envelope of an aircraft fuel.

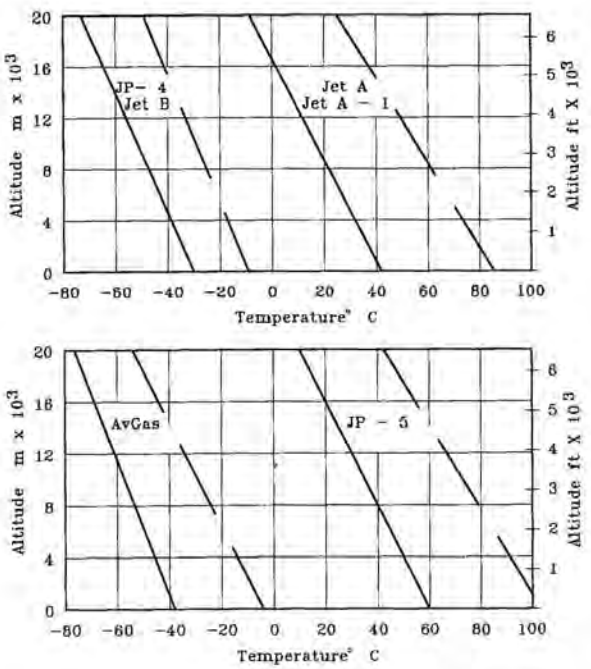

Fig. 7.2 Flammability limits for typical aircraft fuels as a function of altitude and temperature.

The volatility of each of the above fuels is related to the vapor pressure of the fuel. Fuels with higher vapor pressures, such as JP-4, will release sufficient vapor at lower temperatures to reach a flammable mixture, thus lowering the flammability envelope. Fuels with lower vapor pressures, such as JP-5, must be at a higher temperature to release sufficient vapor to form an ignitable mixture.

Mixing of fuels: There are important factors which may alter the flammability limits of the vapor inside an aircraft fuel tank from those shown in Fig. 7.2, however. One of these is the mixing of one type of fuel with another. Fig. 7.3 [7.4] shows, for example, the flammability limits determined by Nestor of a mixture comprised of 85% Jet A and 15% Jet B fuels. Such a mixture might have occurred if the aircraft had originally been fueled with Jet B and later refueled with Jet A. The flammability envelope of the resulting mixture in the tank would be lower than if the tanks had contained 100% Jet A fuel. As such, the lowered envelope encompasses the altitudes and temperatures where most lightning strikes to aircraft have occurred.

Agitation: Agitation is another way that the flammability envelopes might be altered from those shown in Fig. 7.2, for the latter are valid only when the mixture is stabilized. Agitation of fuel or spray from a pump or pressurized fuel line can extend the flammability envelopes of Figs. 7.2 and 7.3 to the left into the region of colder temperatures. Thus, even though Figs. 7.2 and 7.3 indicate that the vapor-air mixture in the tanks of an aircraft fueled with Jet A would be too lean to support combustion for the conditions under which most lightning strikes occur, there can be no assurance that this is always so, since agitation of the fuel may occur in flight.

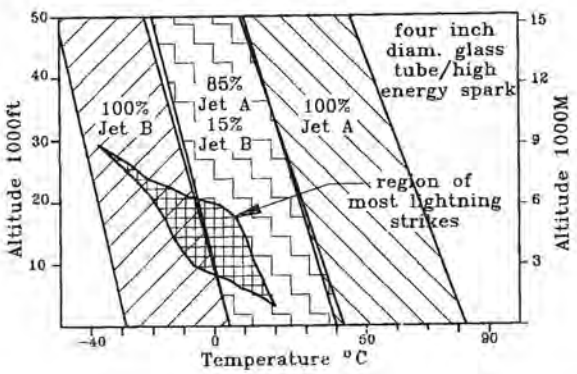

Fig. 7.3 Flammability envelope of the fuel blend 85% Jet A/15% Jet B, and altitude/temperature envelope enclosing most lightning strikes.

Inerting: A number of methods have been developed to inert the ullage in aircraft fuel tanks to keep flames from enlarging and spreading even if there were a source of ignition. These include filling the fuel tank ullage with non-flammable gases, such as nitrogen or carbon dioxide.

Extinguishing: Extinguishing involves detecting a flame and rapidly filling the tank with some gas (ie. halogen) that extinguishes the flame.

Foaming: The use of reticulated foams in fuel tanks to prevent the propagation of a flame front has been shown to be very successful in some applications. The foams add very little weight and displace less than 3% of the fuel in the tank. The foam cools and slows the spead of the flame causing it to die. Unfortunately, some of the foams generate static charges sufficient to ignite fuel vapors. Each time such an ignition occurs, some of the foam is lost. After many hours of flight, the foam will have burned away to the extent that it may no longer provide protection. A conductive foam has been developed (CSF-204 beige) which significantly reduces the tendency for internally generated sparks. Non-conductive foams (Type II yellow and Type IV, blue) both have been shown to generate internal static sparks [7.5].

Nitrogen inerting systems have been developed and flight tested on the USAF C-141 and C-135 aircraft [7.6] among others. Foaming and extinguishing systems have been incorporated in the design of several fighters to provide protection against fuel ignition due to enemy gunfire. None of these systems have been used on any of the commercial aircraft fleets because of potential cost and weight penalties.

Ignition thresholds: Lewis and Von Elbe [7.7], in studies made in the 1950's and 1960's for the US Bureau of Mines, found that the minimum ignition energy of most light hydrocarbon fuels (methane, propane, pentane, etc.) was 200 microjoules, a figure which is the basis for the present fuel system protection specifications and test procedures.

More recent investigations by Crouch [7.8] to determine minimum ignition thresholds of the hydrocarbon fuels commonly found in aircraft fuel tanks have shown that there is no specific energy level above which ignitions will always occur and below which they will never occur. In particular, it was found that the 200 microjoule criterion would not always cause an ignition. Test results showed that under optimum conditions, with the oxygen content at 20%, spark ignitions from an electrical spark dissipating 200 microjoules of energy occurred at a rate of between only 1 ignition in 1000 tests (0.1%) and 1 ignition in 10 000 tests (0.01%).

The test data, for a 1.2 stoichiometric mixture of propane with 20% oxygen, is plotted in the graph of Fig. 7.4(a). Tests were made with sparks of several energy levels. The horizontal line at each point represents the range of probability of ignition among the individual sparks at a given nominal level. Levels with no ignitions (0%) or all ignitions (100%) are shown as lines on the left (0%) and right (100%) margins which indicate the probability that would result if an additional test had resulted in an ignition or non-ignition. If a criterion of a 50% probability of ignition is used, then the required energy level is seen to be in the range of 700 to 800 microjoules.

The probability of ignition was also increased by raising the oxygen content of the mixture. Crouch found that a 200 microjoule spark would ignite a 30% oxygen mixture between 70% and 80% of the time as shown by the test data graph of Fig. 7.4(b).

Thus, it would appear that if a 200 microjoule criterion is required, tests must be conducted using an enriched oxygen mixture. If a standard 1.2 stoichiometric mixture is used, then sparks of less than 700 to 800 microjoules will not likely be detected.

Although a 700 to 800 microjoule level is 3.5 to 4 times the criterion presently in use, it is still extremely low compared to the thousands of joules that can be developed by a lightning strike. It is easy to see how even a small portion of this energy entering the fuel system can result in fuel ignition and a safety of flight hazard.

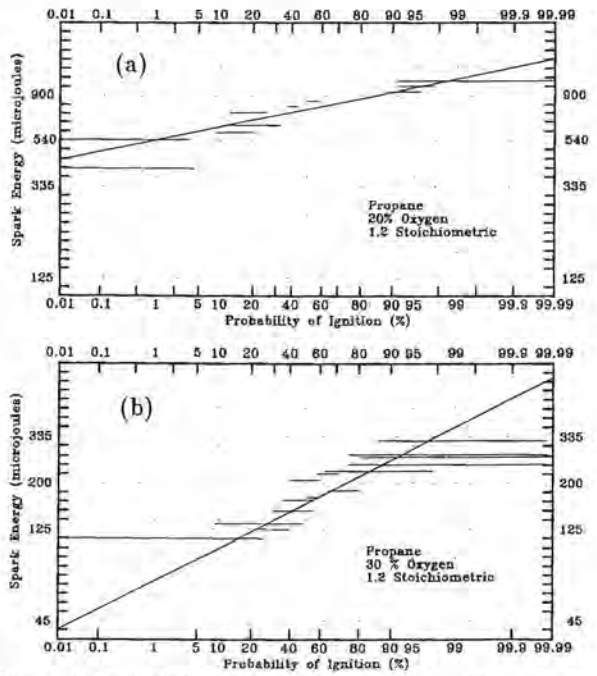

Fig. 7.4 Probability of ignition versus spark energy.
(a) Propane, 20% oxygen, 1.2 stoichiometric
(b) Propane, 30% oxygen, 1.2 stoichiometric

Current–time threshold: While the minimum energy concept helps greatly in evaluating the hazard from sparks, most lightning data are described analytically or experimentally in terms of current waveforms, rather in terms of energy. Attempts have been made to evaluate probability of ignition in terms of current. Fig. 7.5 presents one investigators [7.9] conclusions, but a review of that data indicates that it does not appear to be reliable and that evaluations in terms of current (magnitude and waveshape), rather than energy, are too simplistic to be useful.

The foregoing data illustrate the necessity of preventing *any* electrical arcs or sparks from occurring within an aircraft fuel tank, since even very small percentages of the total lightning current might produce incendiary arcs or sparks.

7.3 Vent Outlets

The temperature of a lightning channel far exceeds that required to ignite a flammable fuel–air mixture; therefore, any direct contact of the lightning flash with such a mixture must be considered an ignition source. Since fuel tank vents are the primary means

by which a flammable fuel vapor can be exposed to the outside of an aircraft, a considerable amount of research has been undertaken to evaluate the possibilities of lightning ignition of fuel vent vapors.

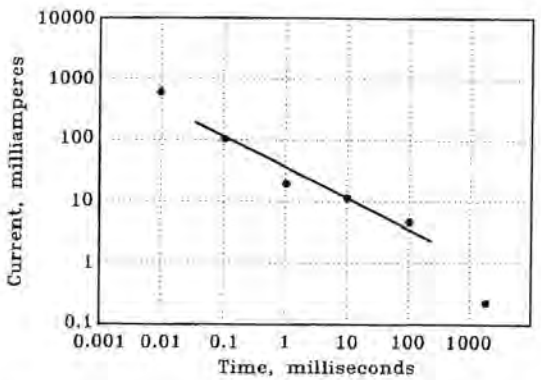

Fig. 7.5 Ignition current versus pulse duration.

7.3.1 Review of Basic Studies

Lockheed study: One of the first fuel vent studies was that of the Lockheed-California Company and the Lightning and Transients Research Institute in 1963 for the National Aeronautics and Space Administration [7.10]. In that program, fuel–air concentrations in the vicinity of aircraft vent outlets of several configurations were measured and mapped under various conditions of tank vapor fuel–air ratio and effluent velocity. The tests were performed in a wind tunnel producing an airflow of up to 100 knots. Mast vents discharged into wakes and into free air streams were tested, as well as flush vents discharging into boundary layers, as shown in Fig. 7.6 [7.11].

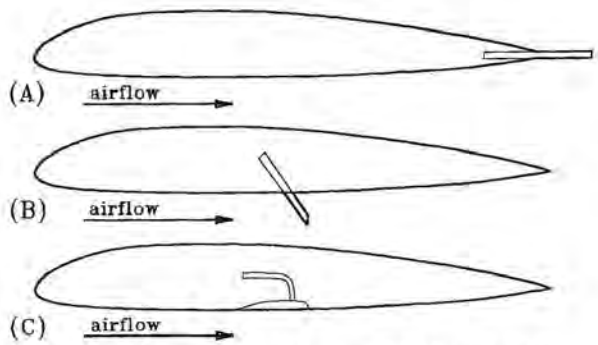

Fig. 7.6 Three general classes of fuel vent exits.
(a,b) Mast or extended outlets
(c) Flush vent outlet

The study showed that a vent discharging into a free air stream provides the greatest dilution of fuel vapor and thus has the smallest flammable region of the vent configurations tested, but it also showed that flammable mixtures could exist in the immediate vicinity of each type of vent outlet.

Dilution profiles: A typical mixture concentration profile of the area aft of a flush vent outlet is shown in Fig. 7.7. [7.12] Dilution of the original effluent by air to 30% or less of the initial concentration might well lean it out of the flammability envelope, depending on its original fuel–air concentration. Thus, dilution to a nonflammable mixture probably occurs at a distance of one vent diameter or more from the vent outlet. This finding suggests that a lightning strike or associated streamer must occur very near to the edge of a vent outlet for an ignition to occur.

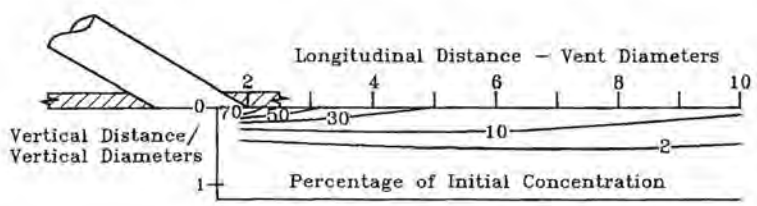

Fig. 7.7 Typical profile of vent effluent in air stream aft of a flush vent outlet.
- Profiles vary according to boundary layer thickness and velocities of effluent and air stream
- Boundary layer thickness = 0.50 vent diameters
- Vent exit velocity = 0.1× free stream velocity

Flame arresters: The above prediction was confirmed in the second part of the 1963 Lockheed–LTRI study [7.13]. During these tests, lightning strikes were applied to flush vent outlets from which flammable fuel–air mixtures were exiting into a 100 knot airstream. The tests were performed with and without flame arresters installed. These flame arresters, which were being evaluated as possible protective devices, consisted of a parallel bundle of small diameter metal tubes inserted into the vent line near the vent outlet, as pictured in Fig. 7.8(a). An alternate construction utilized a series of baffles extending into the fuel vapor flow, as shown in Fig. 7.8(b). The object in either case was for the tubes or baffles to cool the flame enough to extinguish it.

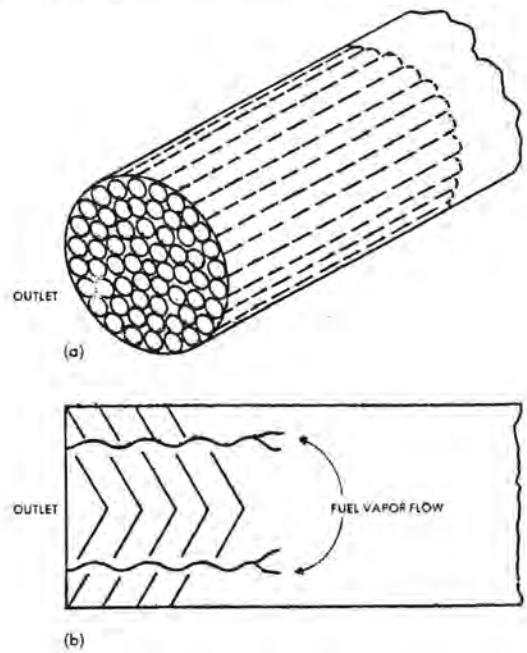

Fig. 7.8 Flame arrester configurations.
(a) Tubular construction
(b) Baffle construction

The test results showed that it was only possible to ignite the vent effluent in the 100 knot airflow when the lightning arc was delivered directly to the lip of the vent outlet. Arcs delivered to spots as close as 2.5 cm (1 in) away did not ignite the effluent. The results also showed that flames ignited by the strikes to the outlet could propagate inward through the flame arresters when they were installed near the vent outlet. While the flame arresters did extinguish some flames ignited at the outlet, they did not stop all such flames. Evidently the intense blast pressures of the lightning arc acted to force the flame through.

FAA/Atlantic Research studies: The crash of a Boeing 707 aircraft near Elkton, Maryland, on December 8, 1963, after being struck by lightning [7.14], prompted another investigation into the possibility of lightning initiated fuel tank vent fires. This investigation, sponsored by the FAA, was undertaken by Bolta and others of the Atlantic Research Corporation with the support of Newman and others of the Lightning and Transients Research Institute [7.15]. The work focused on the Boeing 707 wing tank and vent system, with the objective of determining the conditions under which ignition of fuel vent effluent allows flames to propagate back through the vent duct and surge tank and from there into the reserve tank. Another objective was the evaluation of various protective measures, including flame arresters and flame extinguishing systems.

Unlike the earlier Lockheed program, the vent was tested in still air, the rationale being that, if an ignitable effluent is assumed to be at the outlet, attachment of the lightning arc to the lip of the vent outlet is the governing factor in obtaining ignition. The ignitable mixture was a 1.15 stoichiometric mixture of propane and air.

Thermocouples were installed along the vent line to determine the time at which a flame passed by, thus enabling calculation of flame front velocities. The latter information was important because operation of an automatic extinguishing system under consideration depended on the elapse of sufficient time between the initial sensing of a flame at a vent outlet and the activation of an extinguisher in the surge tank located about 1 m (3.3 ft) down the vent line.

The simulated lightning tests confirmed that a strike must occur very close to the vent outlet for ignition to occur.

Flame velocities: Average flame velocities of up to 45 m/s were recorded between the vent outlet and the surge tank when simulated lightning strokes of 175 kA and 1.5×10^6 ampere^2 · seconds ($A^2 \cdot s$) were applied. These tests simulated a severe return stroke, such as might be experienced if the vent outlet were located in *Zone 1A* or *1B*.

Other tests were performed with the high current directed to the desired spot through a 10 cm (4 in) wide aluminum foil tape which exploded as the current passed through it. The resulting flames reached higher velocities (up to 126 m/s, 413 ft/s), but the exploding tape may have caused the higher flame speeds, creating conditions more severe than occur during a natural lightning strike attachment, where an arc alone is the ignition source.

When lower amplitude currents of 44 kA and only 0.001×10^6 $A^2 \cdot s$ were applied, ignitions still occurred,

but the highest average flame velocity was 17.4 m/s (57.1 ft/s), which indicates that the intensity of the lightning discharge is one of the factors that affects the flame velocity. The 44 kA current was described by Bolta as a "high-voltage" discharge [7.15] because it was applied with a Marx–type, high voltage generator. The ignitions occurred as soon as the 13 cm (5.1 in) or 30 cm (11.8 in) air gap between the discharge electrode and vent outlet broke down. The current level affects the velocity of the flame front, but the energy required to cause the ignition occurs at the very start of the current.

Flame arresters: Various flame arresters were tested, including ones fabricated from corrugated aluminum and stainless steel, a ceramic material, and various copper screens. None of them was capable of stopping a flame ignited by a simulated stroke current when installed near the outlet of the vent line. Arresters wound from corrugated stainless steel 1.27 cm (0.5 in) or 2.54 cm (1 in) deep did stop flames when installed about 1 m (3.3 ft) upstream from the vent outlet near the surge tank as shown in Fig. 7.9 [7.16], even when the flames traveled in the vent tube at an average speed as high as 122 m/s (400 ft/s), the highest measured. Other arresters made of screens and ceramics did not stop flames ignited by the simulated strokes.

A flame suppression system developed by Fenwal, Inc. [7.17] for industrial applications was also tested in this program. This system consisted of a fast acting sensor for detecting the presence of a flame and a set of canisters containing a quantity of liquid suppressing agent for release into the surge tank by an electric detonator. When the detector sensed the light of the flame, it sent a signal to the detonator, which dispersed the extinguishant into the tank within a few milliseconds, before the flame itself had reached the tank.

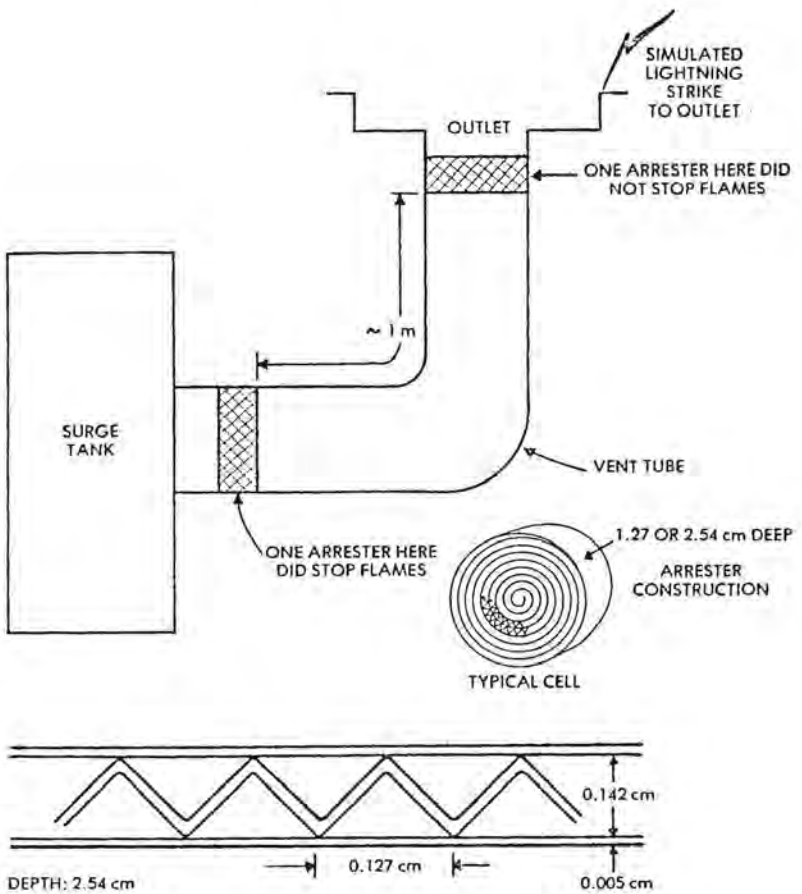

Fig. 7.9 Successful flame arrester installation in simulated vent tube of transport type

This system effectively suppressed those flames which traveled slowly enough, 30 m/s (100 ft/s) or less, to give the system time (18 ms) to react, but did not stop flames which had gone past the surge tank by the time the extinguishant was released. In the latter case, the extinguishant might still have extinguished the fire in the surge tank, but the flame front, on its way through interconnecting vent lines to the fuel tanks, would have passed out of the reach of the extinguishant.

The Atlantic Research–LTRI program also included an investigation of arc plasma propagation into the vent line, which was inconclusive because of instrumentation difficulties.

Effect of ice: The effect of ice formation on the preformance of a flame arrester was also considered [7.18], resulting in the conclusion that unacceptable icing would occur only when the worst combination of atmospheric and flight conditions existed. This conclusion was based on analysis only and should be verified by flight tests.

7.3.2 Airflow Velocity Effects

Lightning attachment to the lip of a vent outlet was assumed to be possible in the Atlantic Research–LTRI and Lockheed programs reviewed in the preceding paragraphs. No attempt, however, was made in either program to establish whether or not this phenomenon could occur to an aircraft in flight or, if it could, how often. Neither the Elkton B-707 aircraft [7.14], nor any other aircraft known to have been struck by lightning, has shown physical evidence of lightning attachment directly to a vent outlet. The outlet in the B–707, while located near the wing tip, is not located at the very tip of the wing where lightning attachments occur most often. It is therefore improbable that flush mounted vents, such as those on the B–707, will receive direct strikes.

The question then arises as to whether a lightning flash could sweep across the vent outlet from another point and ignite the effluent. Answers to this question were sought by Newman and others who undertook an experimental program [7.19] during 1966 and 1967. Simulated lightning strikes were delivered to a B–707 wing tip and vent assembly to learn more about these possibilities, as well as the degree to which air flowing past at realistic speeds would make ignition unlikely, even if an arc did attach to the outlet.

In earlier programs [7.10, 7.15], ignitions were obtained nearly 100% of the time when the vent outlets were in still air, but Newman found that ignition of a 1.5 stoichiometric propane–air mixture by a 48 kA, 0.009×10^6 $A^2 \cdot s$ direct strike occurred only once in 34 shots with a 90 knot (46 m/s, 150 ft/s) airflow over the outlet, and not at all during 200 shots in a 200 knot (100 m/s, 330 ft/s) airflow. When strokes of longer duration were swept across the vent outlet by the 90 knot windstream, the effluent was ignited 11 times out of 15 tests, but when the airflow was increased to 200 knots, only 2 ignitions occurred in 46 tests.

Nearly all of Newman's tests were performed under the most vulnerable effluent condition, which was found to be a 1.5 m/s (5 ft/s) flow out of the vent outlet such as might exist when an aircraft is climbing. Since more than half of all reported lightning strikes occur when the aircraft is either in level flight or descending and since most aircraft climb at well over 90 knots, the probability of an in–flight ignition from a direct strike to a vent outlet must be remote. Newman's investigation, however, showed that a flash sweeping across the vent outlet might have a greater chance (2 in 46) of igniting an effluent, even under climb conditions at the more realistic speed of 250 knots. This result demonstrates the importance of locating vent outlets away from both direct strike and swept flash zones on the aircraft.

7.3.3 Explosive Ignitions

In the program just described, Newman and his colleagues conducted a test [7.20] in which a strike to the vent outlet produced indications of unusually high flame velocities and severe deformation of the vent outlet, indicating much higher pressures than normal. They cite a similar case in another program in which flames traveling in excess of 300 m/s (1000 ft/s) were actually measured. The implication of these findings is serious because an arrester or surge tank protection system capable of extinguishing the lower velocity flames may not be able to stop flames traveling as fast as 300 m/s.

Kester's study: Kester and others [7.21] attempted to reproduce such speeds in a 14 cm (5.5 in) simulated vent tube, but did not measure flame velocities higher than 20 m/s (65 ft/s) in this system, even when severe, 180 kA, 1.0×10^6 $A^2 \cdot s$ strokes were applied. These velocities were comparable to those measured in the Atlantic Research–LTRI program of 1964.

Kester and his colleagues also reported one explosive ignition when a stroke of 195 kA was delivered to the vent outlet. It was found that the 195 kA stroke current had induced a voltage in instrument wiring sufficiently high to spark over the insulation around several pressure probes inside the vent line. The vent outlet and parts of the surge tank were badly deformed, even though they were made of 6.4 mm (0.25 in.) steel. Again, much higher than usual pressures were indicated.

The explosion in the Kester program serves as a warning that a similar consequence might conceivably result from multiple ignition sources in an actual fuel system unless, by means of design, care is taken to eliminate such situations.

Gillis' study: The question of whether or not these explosive ignitions could occur in actual fuel tank vent systems was of such importance that the Federal Aviation Administration undertook yet another study of flame propagation in vent systems. The work, conducted by Gillis [7.22], expanded upon earlier research by including the study of flame behavior in the long vent lines leading inboard from the surge tanks to the fuel tanks, which comprise a typical, complete, vent system [7.23]. Gillis did not use simulated lightning arcs for an ignition source but, instead, discharged 100 J of electrical energy into a spark plug at the vent outlet. This is much less energy than would be released by a lightning arc of the same length. Nevertheless, Gillis recorded flames [7.24] that had accelerated to 300 m/s (1000 ft/s) far inboard when the aircraft was in climb condition.

The total number of authentic tests performed by Gillis was 13, of which 11 resulted in flame velocities of 150 m/s (500 ft/s) or higher. The occurrence of such high speeds is perhaps best explained in Gillis' own words [7.25]:

> When an explosive gas is confined in a channel and ignited, the flow induced by the thermal expansion of the gas in the combustion wave is restricted by the channel wall. Consequently, the flow attains much higher velocities than under conditions of free expansion in an open flame and flame and flow commonly augment each other by a feedback mechanism as follows: stream turbulence, however slight it may be initially, produces a wrinkling of the combustion wave surface; the resulting increase of surface increases the amount of gas burning per unit time, namely, the flow of gas in the channel; this in turn produces more turbulence and hence, increased wrinkling of the wave, and so on, so that the progress of the combustion wave becomes nonsteady and self accelerating. In addition, the burning velocity increases as the unburned gas ahead of the flame is preheated and precompressed by the compression waves that are generated by the mass acceleration in the combustion wave. The compression wave is initially a comparatively weak pressure wave, which is overtaken and reinforced during its travel by numerous other pressure waves originating in the combustion zone. The coalescence of these pressure waves into a strong shock front in a configuration which is dead-ended can result in a reflection of the shock wave back toward the combustion zone. The effect of the passage of this reflected shock wave through the combustion wave is similar to the effect of a sudden release of pressure by a rupture of a diaphragm. A rarefaction wave propagates backward into the unburned gas and a jet of unburned gas develops which penetrates deeply into the burned gas. The shear between burned and unburned gas in this flow configuration produces extreme turbulence so that a sudden large increase in the burning rate occurs.

In three of the 13 tests mentioned above, localized pressures were developed of intensity sufficient to distort 1 to 1.5 m (3 to 5 ft) sections of the rectangular vent duct. A subsequent hydrostatic pressure test of a 1 m (3.3 ft) section of similar duct showed that a pressure of approximately 475 psig was required to produce similar distortion. This pressure exceeds the structural limitations of typical aircraft fuel tank and vent structures.

Gillis concluded that the surge tank located just inboard of the vent outlet was a factor contributing to the high flame speeds because, when a flame reaches it from the vent outlet, the pressure permitted to build up in it serves as a force to drive flames rapidly down the vent lines towards the fuel tanks. This creates turbulence in these ducts which further serves to accelerate flames down the ducts.

Gillis' work is perhaps the best demonstration to date that flames traveling at sonic velocities with damaging overpressures can occur in typical transport aircraft vent systems. Since flame arresters or surge tank protection systems reliably capable of stopping such flames are not yet available, the importance of preventing any source of ignition within or near the vent system is very clear.

7.3.4 Summary and Recommendations

Table 7.1 summarizes the ignition and flame velocity results for each of the research programs just discussed. While not all of the answers to lightning-related vent flame questions are in hand, a number of important conclusions and protection considerations can be drawn from the research.

1. Although there has been no positive evidence that a lightning strike has ever ignited a vent effluent on a transport type aircraft, there have been several in-flight explosions which occurred following strike attachments within a meter or so of vent outlets. This suggests, though it does not prove, that ignition of vent effluent has been the cause of some accidents.

2. For ignition to occur, a lightning type arc must attach directly to, or within a few centimeters of,

the edge of a vent outlet. Ignition may also occur from a flash which has swept back over a vent outlet from an initial attachment point elsewhere on the aircraft. This would indicate that it is desirable to locate vent outlets in areas not subject to direct or swept flash attachments. Guidance in locating direct attachment and swept flash zones has been provided in FAA *Advisory Circular AC-2053* [7.26] and its companion *User's Manual* [7.27]. Care must be taken when using this information since many of today's aircraft are of unusual geometries for which zone locations and boundaries are not easily defined. Further guidelines on location of zones is given in Chapter 5.

3. Flame arresters of the corrugated steel type shown in Fig. 7.9 have been the most effective in stopping flames. Flame arrester performance is most satisfactory when the arrestor is located some distance away from the vent outlet so that blast forces from the lightning arc will not propel flames through the arrester. The most successful location seems to be at the surge tank end of the vent outlet tube, as shown in Fig. 7.9. An arrester at this location will certainly reduce the possibility of flames entering the surge tank, although there is no assurance that the arrester will stop all flames at this location.

   An arrester located anywhere in the vent system is subject to having its passages becoming blocked by ice. This possibility should be evaluated, preferably by in–flight tests under the expected environmental conditions. Electrical deicing devices may have to be added to the vent system if icing is possible.

4. Surge tank protection systems, which are designed to sense flames originating at vent outlets and extinguish them before they reach fuel tanks, are available and should be considered if a vent outlet must be located in or adjacent to a *Zone 1* or 2 area. Since the elapsed time between sensing of the flame and dispersion of the extinguishant is several milliseconds, there is a possibility that flames traveling at sonic velocities will outrace the system . Thus, while an extingishing system will unquestionably improve overall safety, it must not be relied upon to provide absolute protection of the vent tubes.

5. Ninety–degree bends in the vent lines should be avoided because they expand the turbulence and surface area associated with propagating flames and thereby increase the velocity of propagation. Instead, straight or smoothly curved ducts should be used because they minimize the possibility of explosive flame propagation.

Table 7.1

Summary of Results of Simulated Lightning Strike Tests of Fuel Vent Systems

Program	Amplitude (kA)	Action Integral (10^6 A^2s)	Airstream Velocity (knots)	Attachment Point	Results
1963 Lockheed-LTRI	100	0.069	100 (50 m/s)	Lip of vent outlet	100% ignitions and flames propagating with and without flame arrester installed at vent outlet.
1964 Atlantic Research-LTRI (Bolta, et al)	175	1.5	0	Lip of vent outlet	100% ignitions and flame propagating up to 45 m/s, and at 126 m/s when ignited by an exploding foil. Flame arrester stopped these flames when installed 1 m upstream from outlet.
1964 Atlantic Research-LTRI (Bolta, et al)	44	0.001	0	Lip of vent outlet	100% ignitions and flames propagating up to 17.4 m/s (no arrester).
1966 LTRI (Newman, et al)	48	0.009	90 (46 m/s)	Lip of vent outlet	1 ignition and flame propagation out of 34 direct strokes to vent outlet (no arrester).
1966 LTRI (Newman, et al)	48	0.009	200 (100 m/s)	Lip of vent outlet	0 ignitions out of 200 direct strokes to vent outlet.
1966 LTRI (Newman, et al)	58	0.172	90 (45 m/s)	Swept access outlet	11 ignitions out of 15 swept strokes across the vent outlet.
1966 LTRI (Newman, et al)	58	0.172	200 (100 m/s)	Swept access outlet	2 ignitions out of 46 swept strokes across vent outlet.
1966 LTRI (Newman, et al)	58	0.172	250 (130 m/s)	Swept access outlet	No ignitions out of 2 swept strokes across vent outlet.
1966 Dynamic Science-GE (Kester, et al)	195	1.0	0	Lip of vent outlet	100% ignitions and flames propagating up to 20 m/s.
1969 Fenwal (Gillis)	100 J spark		0	Lip of vent outlet	11 ignitions and flame velocities over 150 m/s in. 13 authentic tests. Several at sonic velocity (300 m/s).

Strokes to lip vent outlets only. No ignitions were obtained from strokes away from vent outlet.

6. Location of the fuel vent outlet in an ascertained *Zone 3* area will provide the highest degree of protection of any of the methods described above. A recessed or flush outlet is highly preferred over a protruding tube outlet, because the latter could become a source of corona or streamering which might result in an attachment when the aircraft is flying in a strong electric field.

Flame arresters are utilized for other purposes besides lightning protection. One potential hazard that results from installation of flame arresters is arcing at the flexible vent tube couplings at either side of the arrester, due to lightning currents in the tube, as arresters are often in locations where they would share substantial amounts of lighting current with surrounding structure. Thus, proposed installation designs should be verified by test as free of ignition sources. Suitable test methods are described in §7.14.3.

7.4 Fuel Jettison and Drain Pipes

On some aircraft, provisions exist for dumping or jettisoning fuel overboard, often through a pipe extending into the airstream from a fuel tank, as shown in Fig. 7.10. A normally closed and electrically operated valve is installed in the pipe, so that it is unlikely a flame could travel past this valve into the fuel tank. Even if the pipe, which is filled with fuel, were struck by lightning while jettisoning fuel, it is unlikely that flames could propagate through the pipe into the tank.

A more likely hazard, if not prevented by design, is electrical arcs caused by lightning currents crossing a poor electrical bond between the pipe and the fuel tank wall, or at fasteners through bulkhead fittings, since the wall is frequently coated with electrically insulating, corrosion resistant paints or finishes. Electrical bonding jumpers installed across such joints may be adequate to equalize static charge differentials which sometimes occur in fuel systems, but these usually have too much inductance to prevent some lightning current from breaking down insulation and arcing or sparking at the interface between the pipe and tank wall.

The best way to avoid problems with bonding jumpers is not to rely on them, but instead to make the shortest physical path be the one to carry the current, as shown in Fig. 7.11. This may be done by making the faying surfaces of clean, uncoated metal and/or by providing bare metal-to-metal contact via the rivets or bolts, and by covering exposed interfaces with a tough resilient fuel tank sealant to contain arc products that may occur. Guidelines for the use of fuel tank sealant are found in §7.6.3 and §7.10.3.

If there is doubt about the adequacy of a particular electrical bond, the bond should be tested with simulated lightning currents to assure that sparking does not occur at the interface. The test currents and test practices should be those recommended in [7.26 and 7.28] for the particular lightning strike zone in which the jettison or drain pipe is located.

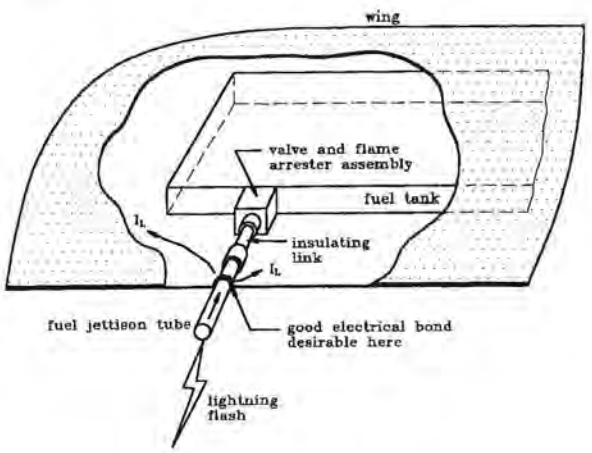

Fig. 7.10 Bonding at a fuel jettison pipe.

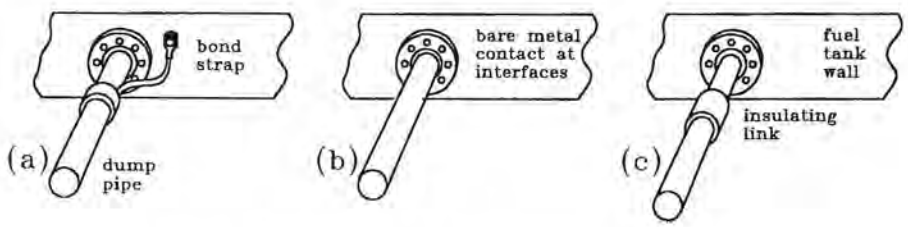

Fig. 7.11 Bonding of fuel dump pipes to fuel tanks.
(a) Bond strap
(b) Metal–metal contact
(c) Insulating link

Another solution to this problem is to break the current path to the fuel tank by inserting an electrically non–conductive section of tubing between points (a) and (b) in Fig. 7.10. This would force all of the current to exit at point (a) and thus eliminate the possibility of sparking at the fuel tank skin interface.

As an alternative, the whole fuel jettison pipe could be fabricated of a electrically non–conductive material which would eliminate it as a lightning attachment point altogether. Of course, other requirements such as non–flammability, crash–worthiness and durability must be satisfied by those non–conductive materials.

7.5 Burn Through and Hot Spots in Fuel Tank Skins

Integral tank skins are those in which fuel is in direct contact with the outside skin of the aircraft. Tanks of this type are commonly found in the wings of transport and some general aviation aircraft, and in the wings and fuselages of modern fighter aircraft. External fuel tanks of the type carried on pylons or wing tips are also of the integral type.

If integral tank skins are located in direct or swept lightning attachment zones, measures must be taken to ensure that a lightning flash does not melt through the skin or get the inside surface hot enough to ignite the fuel. Factors that must be taken into account include the type and thickness of the metal skin and how long a lightning flash might dwell at a particular spot.

For the aluminum skins in common use, a lightning arc will melt through the skin before getting the inside surface hot enough to ignite the fuel vapor. The melting temperature of aluminum ($\approx 500°C$), is lower than the ignition temperature of most hydrocarbon fuel vapors. Experiments by Crouch [7.29], using propane, pentane, and JP-4 fuels, showed that ignitions would not occur until the skin temperature reached 900°C. Thus, fuels within an aluminum integral tank would not be ignited unless a hole were burned completely through the skin and the fuel vapor exposed to the extremely high temperature of the lightning arc, upwards of 30 000°C.

On the other hand, the melting temperature of titanium is 1700°C and that of stainless steel is 1400°C. Both of these are higher than the fuel ignition temperature. While such a skin is more resistant to lightning melt through, it does not need to be melted completely through for ignition to occur.

The amount of lightning current required to erode or melt holes in metal aircraft skins has long been of interest, first, for the purpose of estimating how much lightning current actually was involved in the damage sustained by aircraft in flight, and second, for determining the minimum skin thickness required to prevent melt–through of an integral fuel tank skin.

7.5.1 Review of Basic Studies

Research on the size of holes that might be burned through metal skins of various thickness was previously discussed in Chapter 6. Knowing the size of holes that might be burned is important when considering protection of structures, but in relation to fuel, it more important to know the minimum amount of charge that can ignite the fuel, which for aluminum structures means knowing the amount of charge necessary to burn even the smallest hole in the tank.

Ignition thresholds of aluminum skins: The amount of charge and current required to melt through aluminum and titanium skins of various thicknesses causing fuel ignition was reported by Brick in 1968 [7.30] and by Oh and Schneider in 1972 [7.31] to depend heavily on current amplitude as well as charge. While earlier work had shown that over 22 C, when delivered by a current of 200 A, were necessary to burn through 2.06 mm (0.080 in) aluminum skins, the work of Brick, Oh, and Schneider showed that only about 10 C, when delivered by about 500 A, was enough to melt completely through the same thickness of aluminum skin. In their laboratory tests as little as 2 C, when delivered by about 130 A, melted a hole completely through 1.02 mm (0.040 in) of aluminum.

Oh and Schneider's melt–through thresholds for these and other skin thicknesses are shown in Fig. 7.12 [7.32]. The close proximity of their test electrode to the skins, 2.4 to 4.8 mm (0.1 to 0.2 in), may have restricted natural movement of the arc on the surface of the skin and caused all of the charge to enter the same spot, thus causing low coulomb ignition thresholds.

Work by Kester, Gerstein, and Plumer [7.36] with an L–shaped electrode spaced 6.4 mm (0.25 in) above the skin, permitted greater arc movement, and showed that 20 C or more, when delivered at 130 A, are required to melt through a 1.02 mm (0.040 in) aluminum skin. However, magnetic fields generated by currents parallel to the skin might have forced movement of the arc. Since a natural lightning arc is neither restricted nor forced by an electrode, it is probable that the true aluminum meltthrough threshold is between the two limits, at least for unpainted surfaces. On the other hand, the electrical insulating properties of most paints tend to make the arc remain at one point and so would concentrate the heating effects on a smaller volume of metal, decreasing the amount of thermal energy required to melt completely through.

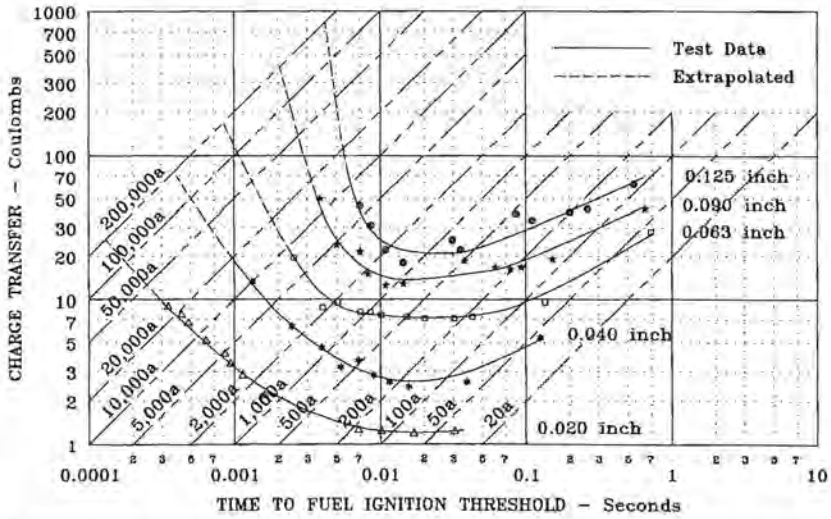

Fig. 7.12 Coulomb meltthrough and ignition threshold for aluminum skins (2024 T3).

Pressure effects: All the data reported on melt-through of fuel tank skins has been taken on test panels in ambient conditions, that is, equal pressure on both sides of the panels. Many aircraft fuel systems maintain some air pressure in the tanks. Fighter aircraft use pumps to supply pressure which is used to force fuel flow under extreme atitudes and manuvers. Most other aircraft fuel vent systems use ram air vent systems which provide some level pressure on the tank.

Pressure inside the tank on which burn–through tests are being made makes a big difference in the level at which a hole appears. A lightning arc may heat the surface to a point where metal is nearly molten, but if there is no pressure, the surface tension prevents the molten metal from flowing away and leaving a hole. A very modest amount of pressure, however, suffices to push the molten metal away and leave a hole. Recent tests, not yet released for publication, showed that with a gauge pressure of 34.5 kPa (5 psig) holes could be burned in a 2.3 mm (0.090 in) aluminum skin by a 23 C discharge. With no pressure, 66 C was required to produce a hole.

This problem has not yet been addressed in the requirements for testing fuel systems, and was not considered in the data presented above. This phenomenon remains to be investigated more thoroughly. It is not a factor that was considered in previous tests to determine burn–through thresholds.

Ignition thresholds of titanium skins: Oh and Schneider have similarly determined the coulomb ignition thresholds for titanium skin materials of various thicknesses, as shown in Fig. 7.13 [7.34]. They and other researchers have confirmed that, since the melting point of titanium is higher than the fuel ignition temperature, it is not necessary for a hole to be melted completely through for ignition to occur, but only that a hot spot be formed on the inside surface. The lower thermal conductivity of titanium prevents rapid heat transfer away from the arc attachment point and accounts for the generally lower coulomb ignition thresholds than those for aluminum.

Ignition thresholds for CFC skins: There are several mechanisms which may result in ignitions of fuel vapor beneath carbon fiber composite (CFC) skins. One of these, discussed in Chapter 6, is the punch through caused by ohmic heating of the CFC fibers resulting in pyrolosis of the resin, and the shock wave accompanying high peak currents, such as SAE Components *A* and *D*. These effects can punch comparatively large holes in CFC skins, producing large areas of contact between fuel vapors and the hot lightning arc. The other mechanisms include hot spot formation and fiber breakage.

There have been fewer temperature measurements made on interior CFC skins than on aluminum. Analytical studies by Lee and Su are described in [7.35]. Tests conducted by Schulte [7.36] on 0.125 inch thick aluminum and CFC panels showed that for the same applied test, temperatures of 100 to 150°C were reached on the interior surfaces of CFC panels while aluminum panels of the same thickness reached teperatures of 160 to 200°C. Panels of 0.25 inch thickness reached temperatures of 70 and 80°C respectivily. The major difference was noted in the time to reach peak temperature. The CFC panels responded 100 times slower

than the aluminum, taking seconds to reach peak temperature. Aluminum panels reached their peak temperatures in tens of milliseconds. A summary of the data is shown in Fig. 7.14 which relates the temperatures and the times for a given test applied.

Wahlgren [7.37] also investigated hot spot temperatures, but the temperatures obtained seemed to exceed those needed for pyrolosis and so may be suspect. Possibly there was only an error in translation of the paper.

The panels tested by Schulte [7.36] were comparatively thick, as might be found on inboard sections of transport or fighter type aircraft wings, and the tests used a *Zone 2A* environment, not the more damaging *Zone 1A* environment. This latter environment includes Component *A*, which has an action integral eight times greater than that of Component *D* found in *Zone 2A*. Thus, hot spot temperatures for CFC skins in *Zone 1A* might be higher than those recorded by Schulte.

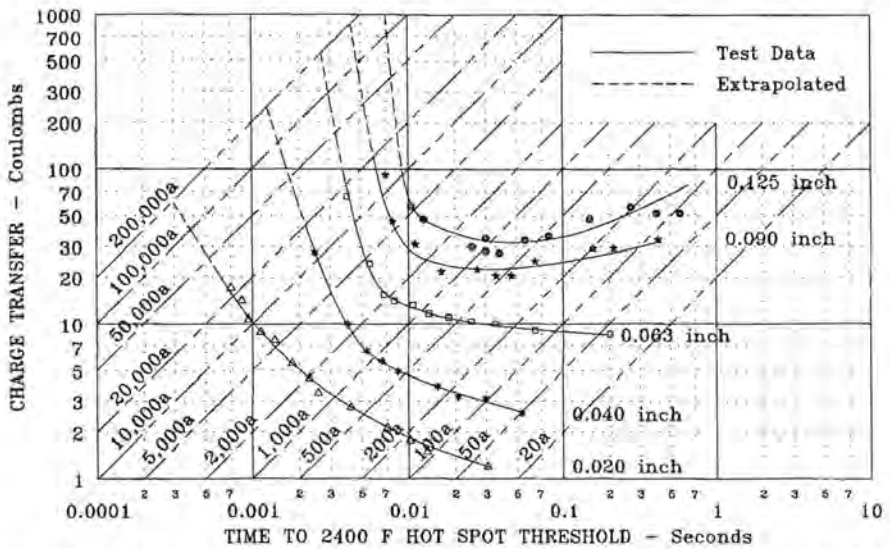

Fig. 7.13 Coulomb hot spot and ignition thresholds for titanium skins (6AL4V).

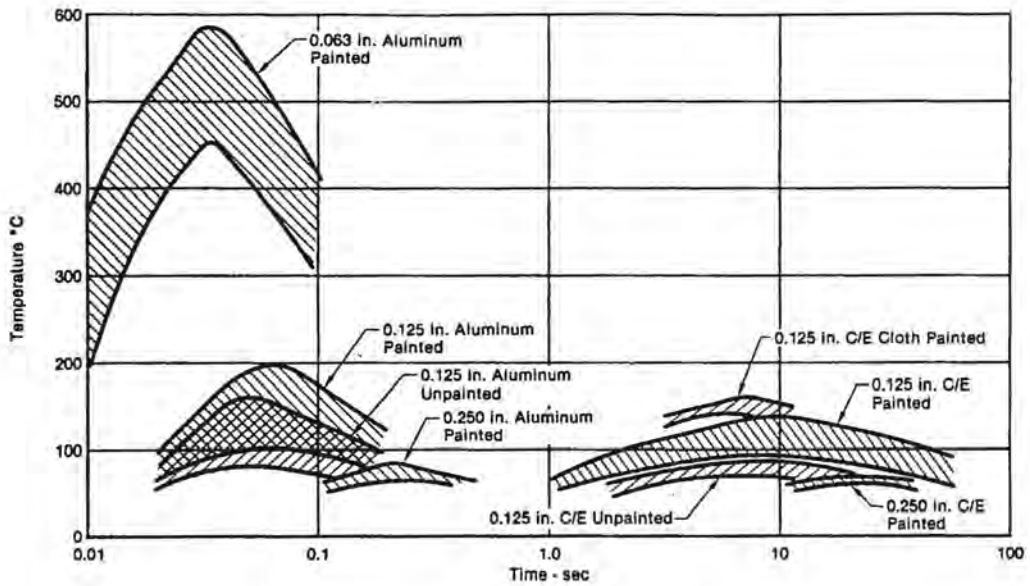

Fig. 7.14 Hot spot temperature versus time.

Hot spot data for thinner CFC skins has been obtained by Olsen et al [7.37] under a variety of conditions. They did not record inner surface hot spot temperatures, but instead recorded whether fuel vapor was ignited or not. A summary of their results, for CFC skins 1.0 mm (0.040 in) and 1.14 mm (0.045 in) thick is presented in Table 7.2. The authors noted that the ignitions may not have been been caused by hot spots per se, but by glowing hot fibers of graphite, either loose in the system or released by pyrolyzed resin.

The Olsen data show that paint aggravates lightning effects, allowing ignitions to occur following lower amounts of charge transfer. This is due to the current concentrating and blanketing effects of the paint. The Olsen data show that painted CFC skins can tolerate larger amounts of charge transfer by a factor of 2 or more than can alumninum skins of the same thickness. The data applies for *Zone 2B*, where the stroke current is Component *D*. Tests at *Zone 2A* levels did not result in any ignitions. In *Zone 2* the causative factor is continuing current charge transfer. In *Zone 1* the important factor will undoubtedly be the action integral of Component *A*. Tests on skins of this thickness using Component *A* usually result in a blast punch through and exposure of the combustible vapors to the arc plasma which results in an ignition. Unfortunately, very little test data employing this environment are available in the literature.

Designers thus need to know the lightning strike zones within which protective skins fall and the possible lightning arc dwell times, in order to assess the possibilities of fuel vapor ignition. For example, a dwell time not exceeding 5 ms, expected on most unpainted or thinly painted skins, would allow only 10 coulombs of charge to enter the skin, with no possibility of fuel vapor ignition beneath aluminum skins at least 1 mm (0.040 in) thick. However, a thick coat of paint, or combination of surface smoother and paint, would result in dwell times of up to 20 ms, and corresponding charge transfers of 16 coulombs, which approaches the ignition threshold of 22 coulombs reported in [7.31]. In such cases, candidate skin and surface finish combinations should be tested to verify that there is no possibility of igniting fuel vapor.

The Olsen tests, and most other test programs, were conducted at room temperature. The Schulte data showed that the airstream had a significant cooling effect on aluminum but a much smaller effect on CFC. Since the amount of cooling will vary widely with air temperatures existing from near sea level to flight altitudes, it is probably not possible to rely upon additional safety factors or design margins from this source. Ignition and hot spot data at room ambient conditions, 20°C (68°F) should be utilized for design purposes.

Dwell times: The data presented in the two preceeding sections can be used to determine the possibility of melt– through of metal skins or of hot spot formation of metal or CFC skins sufficient to cause ignition if the amplitude of the current in an attachment point and the amount of time a lightning arc dwells at that point, the dwell time, are known. The mechanism of swept strokes was discussed in §3.5 and illustrated in Fig. 7.15. A knowledge of dwell times in swept flash zones is of great importance because integral fuel tank skins are often found in these zones.

Early regulatory documents, such as FAA *Advisory Circular AC 20-53* [7.38], had specified that aluminum skins in lightning strike zones should be at least 2.0 mm (0.080 in.) thick to withstand melt–through. Initially, structural design demands also made it necessary to use skins at least 2.0 mm thick, and the lightning protection requirement presented no design penalties.

Table 7.2

Zone 2B Test Results for Ignition Thresholds

Test panel	Thickness (in)	Prepreg form	Ply orientation (deg)	Finish	Coulombs required for ignition
1-1	0.045	Tape	$[0/\pm45/90]_S$	Unpainted	50 to 60
1-2	0.045	Tape	$[0/\pm45/90]_S$	Painted	35 to 45
4-1	0.040	Fabric	$[0/90]_3$	Unpainted	37 to 40
4-2	0.040	Fabric	$[0/90]_3$	Painted	22 to 25
7-1	0.040	Fabric	$[\pm45]_3$	Unpainted	33
7-2	0.040	Fabric	$[\pm45]_3$	Painted	22 to 25
7-3	0.040	Fabric	$[\pm45]_3$	Painted	24 to 29
0.063 Al	Aluminum			Unpainted	6 to 9

In recent designs, thinner skins can meet the structural requirements and will permit a saving in weight and cost if the lightning protection requirement can be met with less than a 2.0 mm thick skin. To determine the actual skin thickness required to resist melt–through or hot spot formation, it is necessary to know the maximum possible dwell time for intended skin surface treatment. Dwell time information has been obtained from laboratory tests simulating the "sweeping" of the lightning flash channel over typical surfaces, and from study of natural lightning strikes to aircraft.

Brick, Oh and Schneider's work: Brick, Oh, and Schneider [7.39] studied dwell times of 400 A decaying arcs blown by the exhaust from a wind tunnel over aluminum and titanium skin panels with several surface treatments to see how long such an electrical arc might actually dwell at one point before reattaching to the next. Wind speeds of 67 m/s (150 mph) and 112 m/s (250 mph), representing approach speeds for typical aircraft, were utilized. The test current was representative of the continuing current portion of the lightning flash and delivered an average charge of about 0.2 coulombs per millisecond of dwell time.

The researchers reported that the arcs dwelled for 2 ms or less on uncoated surfaces of both metals, and for 4.8 ms on an anodized aluminum surface. These dwell times are within the time period of current Component B, 5 ms. The 2 ms dwell time would therefore have allowed a charge of 4 coulombs to enter a single spot, whereas the 4.8 ms dwell would have permitted nearly the entire charge of 10 coulombs of Component B to enter the spot. Of course, the actual charge entering the attachment point will be determined by the level of lightning current in the flash at that time. In testing, the current components are usually applied in order of their magnitude, the highest first followed by successively lower levels. In nature, the components can come in any order. To ensure that the worst case has been applied, various types of lightning current must be evaluated.

After dwelling at one point, the arc will reattach at a point farther aft on the aircraft as shown in Fig. 7.15. During the dwell times, the aircraft would be moving, and the distance covered would be:

$$D = vt_d \tag{7.1}$$

where

D = distance arc is drawn along surface (m)

v = aircraft velocity (m/s)

t_d = dwell time (s)

Thus, at velocities of 67 and 112 m/s, and with the dwell times of 2.0 and 4.8 ms reported by Brick, spacings between successive dwell points would be as given in Table 7.3.

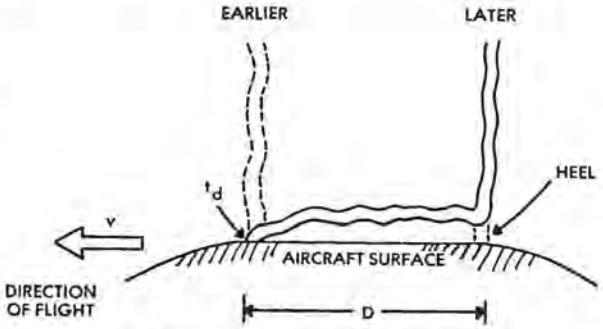

Fig. 7.15 Basic mechanism of swept–stroke reattachment.

Table 7.3

Typical Lightning Flash Dwell Times

Skin Material	Surface Finish	Dwell Time
Aluminum	Unpainted	≤ 2 ms
Aluminum	Anodized	≤ 5 ms
Aluminum	Painted	≤ 20 ms
CFC	Same as metal skins	

Actual dwell time for paint depends on paint thickness

As a lightning flash sweeps across a surface, the points at which the lightning arc remains attached are marked by burn spots. Spacings between burn spots are often found to be of the the order given in Table 7.4 and thus the dwell times predicted by the Brick tests are realistic.

The later work of Oh and Schneider [7.31] basically confirms these results for uniform airflow conditions, but shows that conditions which cause the airstream to leave the surface may force the arc to dwell longer at the last attachment point before the airflow is diverted. Oh and Schneider also demonstrated that higher aircraft velocities resulted in shorter arc dwell times, since the arc is stretched greater distances, allowing sufficient voltage to build up along its length to break down the insulation at its heel at an earlier time.

Validity of wind tunnel tests: The validity of the wind tunnel technique for simulating swept flash attachments along metal surfaces has been questioned because the airstream used to blow the arc along the

surface of the test object must, of necessity, move faster than the arc. Air speed is thus not a perfect indicator of how fast the arc moves. In addition, there will be cooling of the arc by the faster moving air. This, perhaps, allows the arc voltage to rise at a faster rate than would occur normally, and so might create a new attachment point sooner than had cooling not occurred. Also, the behavior of the upper terminus of the arc as it moves along the electrode probably has some effect on the behavior of its lower terminus at the test object.

A more realistic simulation would undoubtedly result if the test object, like an aircraft in flight, could be moved through a stationary arc. Plumer [7.41] attempted this by moving a wing tip fuel tank beneath a high–voltage electrode at a velocity of 15.5 m/s (35 mph), the fastest speed that could safely maintained in the test area. A flash was triggered when the approaching tank, carried atop a truck, sufficiently closed the airgap between the electrode and the ground.

Limitations of this technique were the low velocity and the low (4 ampere) test current amplitude. Subsequent in–flight lightning strikes to two fuel tanks of this type have confirmed the occurrence of the predicted attachment points and breakdown paths.

Despite the lower velocity and lower current amplitude, the arcs in Plumer's tests also dwelled for times of between 1 and 4 ms on unpainted aluminum surfaces, results closely parallel to those of the wind tunnel work. These parallel conclusions seem to indicate that the arcs in the wind tunnel tests may not have moved as fast as the wind itself, and, also, that current amplitude has relatively little to do with dwell time.

Effects of coatings: Robb, Stahmann, and Newman [7.42] have utilized the wind tunnel technique to determine arc dwell times on various painted or coated surfaces. Most of these coatings were electrically insulating and thus required that the arc be further lengthened to allow the greater voltage buildup necessary to puncture the insulation and form the next attachment point. Dwell times of up to 20 ms were recorded on painted surfaces. Times undoubtedly depended on the type and thickness of the paint, but precise records of those conditions were not kept as their importance had not yet been recognized.

More recent dwell time data has been obtained from the inflight experience of the NASA F–106B aircraft [7.43]. This plane was instrumented as part of the NASA–Langley Research Center Storm Hazards Program to study lightning parameters and effects on aircraft. Spacings between burn marks on surfaces of the aircraft showed that dwell times were less than 2 ms for unpainted skins and between 1 and 6 ms across the painted aluminum fuselage and wing surfaces. The dwell times were determined from the spacings between burn marks and the aircraft velocity, 182 m/s (409 mph), during the thunderstorm penetrations.

A tabulation of laboratory and in–flight strike data is shown in Table 7.4 for several surfaces commonly found in swept flash zones (*Zone 2A*).

The FAA User's Manual [7.26] for the updated *Advisory Circular AC-20-53A* [7.27], recognizes that the coatings and paints found on aircraft surfaces can affect dwell times. It recommends that proposed paints and finishes be compared with data bases such as those presented here to establish anticipated dwell times. New coatings for which little experience is available should be tested to establish dwell times and melt-through or hot spot ignition thresholds. Guidance for performing such tests is given in §4.2 of [7.28].

Once the expected dwell times have been established, it is then necessary to determine the amplitude of the current during these periods.

Table 7.4

Lightning Dwell Times on Typical Aircraft Surfaces in Zone 2A

	Aircraft Velocities		
Surface Type	15.5 m/s (35 mph)	58 m/s (130 mph)	103 m/s (230 mph)
Aluminum and titanium unpainted	1 to 4 ms	2.0 ms	1.0 ms
Aluminum anodized		4.8 ms	2.6 ms
Aluminum painted		up to 20 ms	up to 10 ms

Ways to reduce dwell time: The foregoing discussion makes clear the importance of lightning arc dwell time in establishing whether or not ignition resulting from a strike to a skin is likely to occur. Dwell time is perhaps the only lightning characteristic over which the integral fuel tank designer has any control. The objectives, of course, should be to minimize dwell time at any one spot and to spread the arc attachment among many different spots. A bare metal external finish will best achieve these aims, since most paints and other coatings act to concentrate the attachment at more widely separated points for correspondingly longer times than does a bare surface.

If paint must be used, lightning dwell times may be reduced by making the paint partially conductive. Robb and others [7.42] have demonstrated that aluminum powder is effective in increasing the conductivity of polyurethane paints, thereby increasing the ability of the arc to reattach to new points as the aircraft surface moves beneath the arc. Since no parametric data relating dwell time to amount of additive is available, it is advisable to make laboratory determinations of the degree of improvement afforded by particular combinations.

McClenahan and Plumer [7.44] have shown that small diameter metal wires intermingled with carbon yarns in CFC skins act to disperse the electric arc and reduce damage at attachment points. This effect, which has been termed *arc root dispersion* in §6.2.1, is due to intensification of the electric field and puncture of non–conductive finishes above the wires. The extent to which this treatment shortens swept flash dwell times has not been evaluated.

7.5.2 Current Amplitudes

The high amplitude return strokes of the lightning flash are too short in duration to deliver appreciable charge and cause significant melting of metal skin materials. Most of the charge in a flash is delivered by continuing currents of several hundred amperes and by intermediate currents of several kiloamperes. In analyses of swept stroke effects, emphasis should be placed on the intermediate and continuing currents, Components B and C, because these can deliver large amounts of charge.

There is, of course, a time dependency, as was shown in Fig. 7.13. Currents of 200 - 500 A will melt through at lower coulomb levels than either higher or lower currents. This is related to the current density in the arc channel. The density, A/m^2, is limited so at higher currents, the diameter of the arc channel expands. This can result in multiple arc roots which spread out the current, rather than leaving it concentrated at a single point. This reduces the damage. In practical terms, 300 amperes for 10 milliseconds will produce more damage that 3000 amperes for 1 millisecond, even though the charge transferred, 3 coulombs, is the same in either case.

For example, for design and tests of swept flash effects, §4.1.2.2 of [7.28] specifies that current components B, C, and D should be applied in *Zone 2A*, with D applied first, since it is a restrike current which would be expected to create a new dwell point. Components B and C are then applied for whatever dwell time is expected, or for 50 ms if the dwell time has not been determined from swept flash tests or is otherwise unknown. This current is shown in Fig. 7.16. If a dwell time of less than 5 ms is expected, an average current of 2 kA should be applied for the actual dwell time only. It should be noted that even though the standard specifies that testing be conducted in this manner, nature is not restricted to the test environment and can deliver currents in any sequence. If Component C applied for the entire dwell time is more severe than a combination of Component B and C, then that threat must be considered.

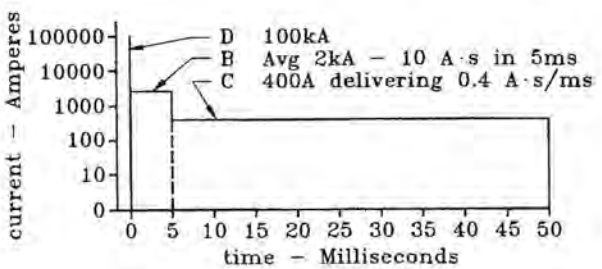

Fig. 7.16 Current and charge expected at a Zone 2A dwell point.
Drawn with straight lines only for purposes of explanation

The environment for *Zone 1A* includes current components A and B, but no portion of component C. Component A applies a higher action integral and more intense shock wave, which can puncture unprotected CFC and some thin metal skins, as described in Chapter 6. Meltthrough of metal skins, however, is due primarily to charge transfer from intermediate and continuing currents. Since many fuel tank skins are, in fact, within *Zones 1A* and *2A*, they should be designed to tolerate the most damaging components of each, that is, stroke current component A combined with components B and the portion of C that would be applicable in *Zone 2A*.

Fuel tank skins in *Zone 1B*, such as external tanks on rotorcraft, must tolerate all four current components, *A*, *B*, *C* and *D*, assumed to enter the skin at any spot in that zone. This will usually preclude use of integral skin tanks, unless such skins have multiple layers, as in sandwich construction.

The standard lightning environment described in [7.28] and Chapter 5 is based on the known aspects of cloud to earth flashes, as discussed in Chapter 2, combined with studies of in–flight damage reported by aircraft operators over the years. As such, these current amplitudes are a good representation of what to expect in a severe natural lightning flash. It is recognized, however, that more severe currents, like those which sometimes occur in a positive polarity, cloud–to–ground flash, could appear at *Zone 2A* dwell points. An example of such flashes, recorded by Berger [7.45], is shown in Fig. 7.17.

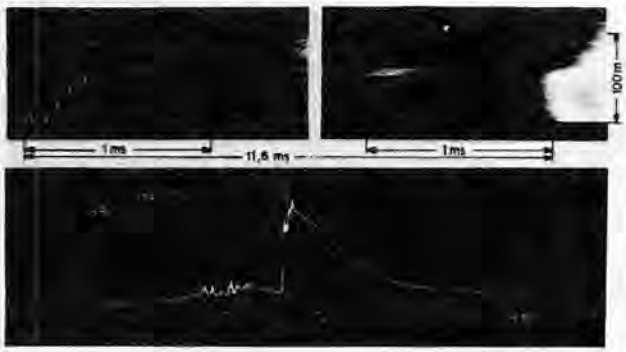

Fig. 7.17 Positive polarity flash with delayed starting time.

The current waveform measurement shown in that figure was made at an instrument tower on the ground, and the long, upward–moving leader which extended from this tower to the cloud base, accounted for the 11.5 ms delay which elapsed before the return stroke appeared at the ground. Not all of this delay would have occurred had the measurement been made on an aircraft in flight intercepting such a flash. Several milliseconds of delay still could have elapsed between initial leader attachment to a forward extremity of the aircraft and the occurrence of the return stroke over a fuel tank surface. The positive polarity return stroke could have delivered about 20 A·s (coulombs) to this attachment point during the 2 ms of time it would have dwelled there. According to the data of Fig. 7.13, melt–through of a 1.6 mm (0.063 in.) aluminum skin could be possible under these conditions.

There are reports of holes melted in 1.02 mm (0.040 in.) skins from in–flight strikes in *Zone 2A* areas, but holes in 1.6 mm aluminum have not been reported, a fact that demonstrates the apparent rarity of the high–energy positive polarity flash in *Zone 2A* areas. Present standards and test practices do not account for these flashes due to lack of evidence that they have struck aircraft in critical zones.

7.5.3 Required Skin Thicknesses

Assuming that current amplitude, charge and dwell time have been established, the graphs of Figs. 7.13 and 7.14 allow the designer to determine the thicknesses of aluminum or titanium skins required to ensure that the skin will not be melted through or overheated causing a hot spot by lightning.

Aluminum skins: As an example, assume that a bare aluminum skin is planned for an integral tank in *Zone 2A*. Further, assume that the aircraft will fly at velocities as low as 58 m/s (130 mph), which is typical for approach to landing.

From Table 7.3 the expected dwell time for this unpainted skin would be 2 ms. From Fig. 7.16, an average of 2 kA would flow into the dwell point during this period, delivering 4 A·s of charge. On Fig. 7.13 these parameters intersect at a point about half–way between the coulomb ignition threshold curves for 0.51 mm (0.020 in) and 1.02 mm (0.040 in) aluminum skins. This indicates that 0.81 mm (0.032 in) is the thinnest skin that should be considered. Since there would be little margin of safety if a skin of this thickness were actually used, it would be prudent to select a greater thickness, such as 1.02 mm (0.040 in) if at all possible.

Surface coatings, such as paint, will usually cause the dwell times to be longer than they would be on unpainted skins. The type and thickness of the coating both affect the dwell time. Generally, the thicker the coating, the longer the dwell time and the thicker the skin must be to avoid melt–through. Consider, for example, the longest dwell time, 20 ms, recorded by Robb, Stahmann, and Newman [7.42] for a painted surface. During this period the current of Fig. 7.17 would deliver 16 C. These parameters intersect at a point just above the 2.29 mm (0.090 in) curve in Fig. 7.13, indicating that even the 2.03 mm (0.080 in) thickness advised by some design guidelines would be insufficient to prevent ignition where certain paints are used. Therefore, if paints must be used, it is advisable to perform swept flash tests, or to refer to in–flight experience, if applicable, to establish the actual dwell time and, therefore, the required skin thickness necessary to prevent melt–through.

Titanium skins: By using the graph of Fig. 7.13, it is possible to determine titanium skin thicknesses in a

manner similar to that for determining aluminum skin thicknesses. The coulomb ignition threshold for titanium occurs when the back side of the skin reaches 900°C (1650°F), a temperature Crouch found sufficient to ignite a fuel-air vapor from hot spot formation [7.46]. Because titanium will not melt at this temperature, no hole will be formed before the ignition threshold is reached. No graphs of the type shown in Figs. 7.12 and 7.13 have been generated for other metals, since, with the exception of certain space vehicles, these materials seldom appear as integral tank skins.

Carbon fiber composite skins: The data of §6.5.1 can be utilized to select necessary CFC thicknesses and protective treatments to prevent punch through by stroke current effects, Components *A* or *D*. The data presented in §7.5.1 of this chapter indicates that incendiary hot spots are not possible. Ignition by hot filaments was found, but since the presence or absence of the fibers did not depend on the magnitude of the lightning current, no guidelines can be established regarding what is necessary to eliminate the hot filaments.

Fuel tanks and trailing edges: On trailing edges, lightning flashes tend to remain attached at one spot and can continue to burn long enough to melt through metal skins of almost any reasonable thickness. As an example, Fig. 7.13 shows that 200 coulombs, delivered in 1 second or less, as required by [7.28], would melt through aluminum skins up to 80 mm (0.313 in.) thick. A titanium skin 32 mm (0.125 in.) thick would not be melted by such a charge, but Fig. 7.13 shows that it would be heated to a temperature of 1320°C (2400°F) which exceeds that necessary for ignition.

Allowing fuel or fuel vapor to accumulate in trailing edges located in *Zones 1B* or *2B* is thus hazardous. Trailing edges of wings with integral fuel tanks are where the flaps and ailerons are located and fuel vapors are not likely to accumulate in such areas. With externally mounted fuel tanks or tip tanks, however, it is possible that fuel vapor could exist at a trailing edge. Protection must be provided by closing out and venting the aft-most volume of the tank, as shown in Fig. 7.18, so that if melt-through does occur, there will be no fuel vapor to be ignited.

Other ways to protect skins: Several other methods have been utilized successfully to prevent melt-through or incendiary hot spot formation in metal skins. These include the use of laminated skins and the application of thermal insulating materials to the interior surfaces of skins.

Laminated skins employ two or more sheets of metal adhesively bonded together. Tests have shown that the lightning flash melts away the exterior ply without melting into the interior ply. The ranges of metal ply and adhesive thicknesses that are satisfactory have not been fully evaluated so candidate configurations should be tested as appropriate for the applicable zones.

Thermal barriers have consisted of layers of polysulfide type fuel tank sealants. Such materials prevent hot arc products or hot spots from contacting fuel vapors. Again, candidate designs must be tested to verify effectiveness. Life cycle aspects such as durability and compatibility with fuels must also be considered to ensure continued airworthiness.

Bladder fuel tanks, which have been used extensively in older designs where it was not possible to adequately seal the skins, will also provide a barrier between the lightning melt-through or punch-through and the fuel vapor.

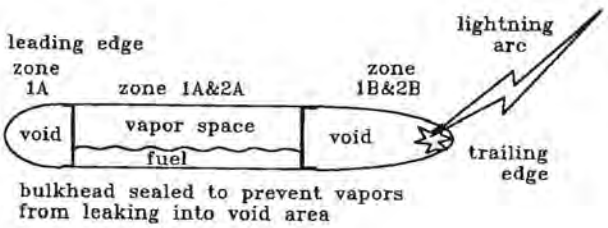

Fig. 7.18 Trailing edge construction to avoid fuel ignition from extended flash hang-on.

7.6 Effects of Current In Tank Structures

In the aircraft accidents that have been attributed to lightning and that occurred as a result of in-flight explosion of fuel, the exact cause of fuel ignition has remained obscure. Ignition at fuel vent outlets or by melt-through of integral tank skins has been suspected in several cases, but no conclusive evidence to this effect has ever been found. Another possibility is that lightning current passing through the fuel tank structure or fuel system components could have caused sparking or arcing in the tanks and ignited the fuel vapor. No conclusive evidence of this has been found either, but the marks left by a spark releasing a few millijoules of energy would be difficult to detect in any case.

Much attention has been given to keeping lightning currents out of the interior of the aircraft by providing conductive and tightly bonded skins. Still, current does exist on interior structural elements such as spars and ribs, and also on fuel and vent pipes. When-

ever current crosses joints and couplings, there exists the possibility of arcing or sparking. Since so little energy is needed to ignite fuel, the behavior of these internal currents is of great importance to fuel system safety.

Arcing can also occur, at some instances, when lightning currents in the skin encounter discontinuities, such as access doors and filler caps. Electrical wires in fuel tanks pose another potential sparking problem because high voltages could be produced by the high electromagnetic fields associated with lightning.

Fig. 7.19 shows the possible lightning current paths in a typical fuel tank and calls attention to the areas of greatest concern. In the following paragraphs each of these areas is discussed. Areas of concern for which little or no quantitative data is yet available will also be discussed.

7.6.1 Filler Caps

Problems: Filler caps must be fitted with gaskets and seals between the cap and its adapter in the tank. Most of these seals have little or no electrical conductivity. If a lightning flash contacts the filler cap there may be a spark across or through the seals. The spark may then generate sufficient pressure to blow plasma past the seal and into the fuel vapor space.

Newman, Robb, and Stahmann [7.47] were among the first to recognize this possibility and evaluate it in the laboratory. They demonstrated that direct strikes to filler caps of the design then in common use would cause profuse spark showers inside the tank. They applied simulated strikes, which ranged in energy from a very mild 35 kA, 0.006×10^6 $A^2 \cdot s$ stroke to a very severe 180 kA, 3×10^6 $A^2 \cdot s$ stroke, to typical fuel filler caps. Profuse sparking occurred under all conditions. When an ignitable fuel mixture was placed in the tanks, these spark showers readily produced ignition.

Newman and his colleagues did not report sparking or fuel ignition when the same filler caps were not struck directly but were only located in a tank skin through which lightning current was being conducted. Other literature does not report such sparking either, but the possibility of such an occurrence might still exist under some conditions.

Protection techniques: After observing the sparking from direct strikes to the original filler caps, Newman evaluated several design modifications to prevent this sparking. Fig. 7.20(a) shows where sparking can take place on the inside surfaces of an unprotected filler cap while Fig. 7.20(b) shows a design intended to prevent internal sparking.

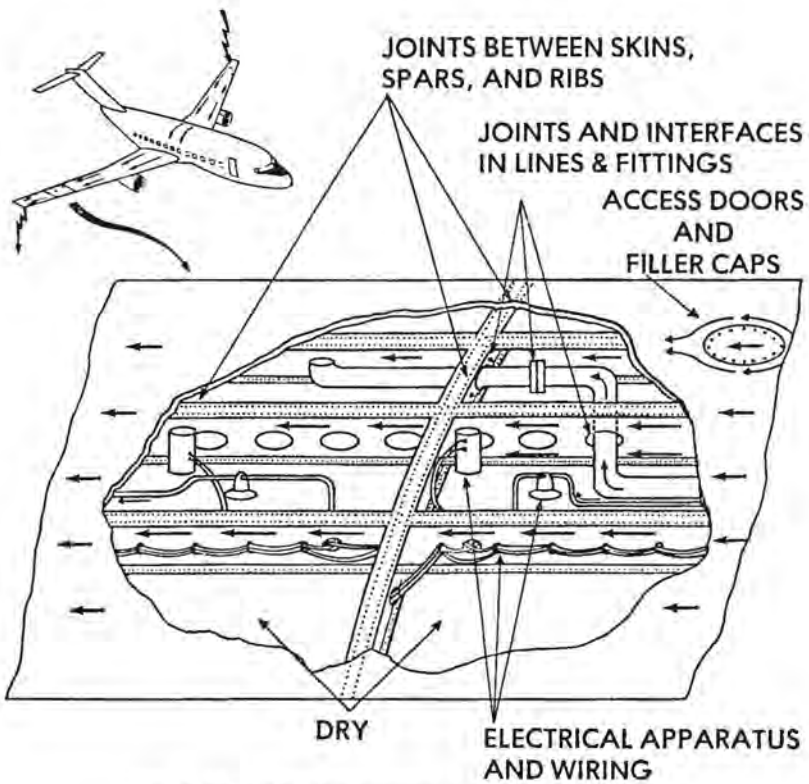

Fig. 7.19 Lightning current paths in a fuel tank and potential problem areas.

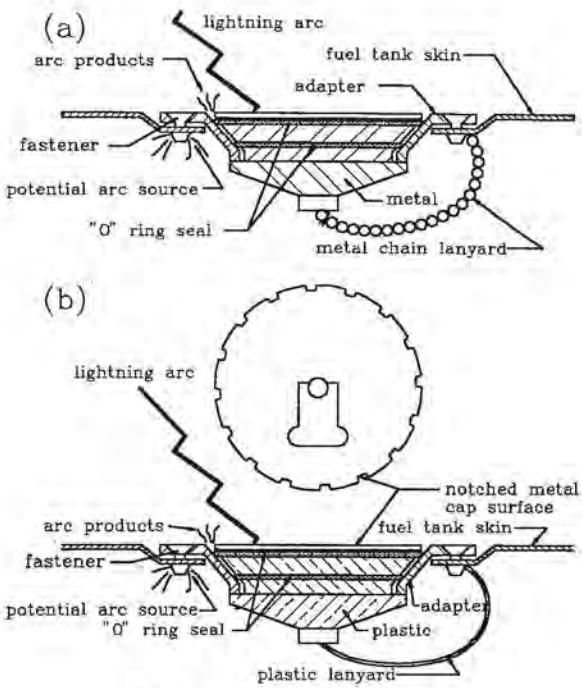

Fig. 7.20 Fuel filler cap designs.
(a) Unprotected
(b) Protected

A lightning protected cap typically uses a plastic insert so that there are no metallic faying surfaces across which sparking can occur. If a lanyard is required, it is made of plastic since one source of sparking on filler caps was found to be along the ball chain used to retain the cap.

Lightning protected caps are generally designed to be used in conjunction with mating adapters. An electrically non–conductive O–ring provides a seal between the plastic insert and the mating adapter to prevent fuel leaks. When a strike to the cap occurs, the resulting lightning currents arc from the cap to the adjacent adapter, since the O–ring seal prevents direct electrical contact between the two parts. The arcing creats a pressure buildup at the O–ring. If the pressure is too high, arc products could blow past the O–ring and into the fuel vapor. In order to minimize pressure buildup, a series of cutouts is made around the perimeter of the cap surface so that arc products can vent to the outside of the tank.

An alternative protection design replaces all the metal parts of the cap with plastic, thus preventing direct arc attachment and any arcing from taking place at the O–ring seal.

Lightning protected caps should always be used if there is any possibility that the cap may receive a lightning strike, i.e., if the cap must be located in direct or swept flash *Zones 1A*, *1B*, *2A*, or *2B*. At least one specification, *MIL-C-38373B*, has been written describing a lightning protected cap. If there is any doubt about the protection capability of the particular design, the cap should be tested with its mating adapter as described in [7.28]. The interface between the filler cap adapter and the surrounding tank skin can also arc and care must be taken to prevent such arcing from contacting fuel vapors. The methods employed are discussed in §7.10.3.

7.6.2 Access Doors

Problems: Access panels or doors are found in nearly all fuel tank designs to enable installation and maintenance of system hardware. Typical doors are shown in Fig. 7.21. Since they are frequently in the external skins, they are exposed to lightning strikes. Early tests showed that sparking could occur at access doors not specifically designed to tolerate lightning. Modification procedures [7.48] were developed which prevented sparking, even when the access doors were struck directly. Such modifications usually consist of some combination of the following features:

1. Avoidance of metal to metal contact between parts exposed to fuel vapor spaces.

2. Provision of adequate current conduction paths between door and adapter and between adapter and surrounding skin, away from fuel vapors. This is usually via the fasteners, which are separated from vapor areas by O–rings, gaskets or sealants.

3. Application of sealant to other potential arc or spark sources, so as to prevent contact with fuel vapors. Sealants are discussed in §7.6.3.

Protection techniques: Any design which allows the door installation to tolerate the applicable lightning environment while meeting other performance and structural requirements is acceptable and there are many design applications and approaches that have proven satisfactory. Some acceptable access door designs are shown in Figs. 7.22(a) through 7.22(d).

O–rings: Fig. 7.22(a) shows a common design in which an O–ring, fitted in a slot in the doubler, prevents arc products around the fastener from entering the fuel vapor space. Instead, the arc products escape to the outside. In addition, the access door riveted nut plate (dome nut), doubler fastener, and the fillets have been covered with polysulfide type fuel tank sealant to contain the arc products occurring at these locations, thus preventing them from contacting fuel vapor.

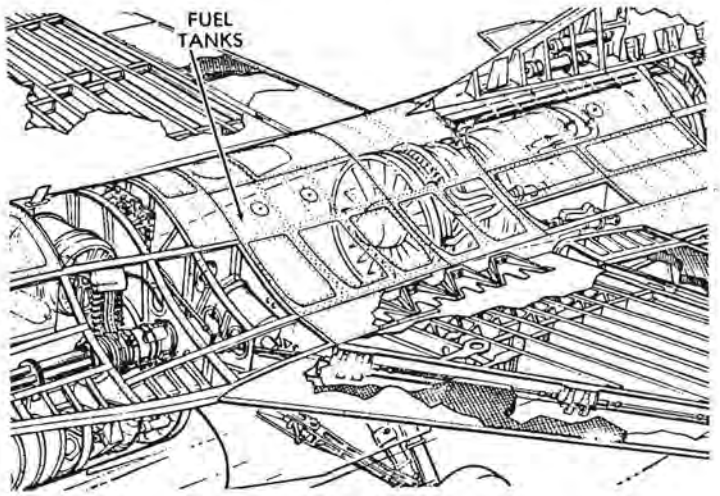

Fig. 7.21 Large access doors in Zone 2A over fuselage fuel tanks.

Integral nut ring: In example (b) of Fig. 7.22, the riveted nut plate has been replaced with an integral nut ring. This configuration, where the captive nut is installed inside a casting or the ring has a tapped hole, allows higher currents to be conducted than the riveted nut plates. Current entering the integral nut ring diffuses to several fasteners which share the current carried to the doubler and the skin. Fuel tank sealant is applied around the fillets, nut–ring–to–doubler fasteners and skin–to–doubler fasteners (if present) to prevent arc products from entering the vapor space from these interfaces.

Elimination of fasteners: Two additional designs are shown in Figs. 7.22(c) and (d) where the doublers of examples (a) and (b) have been removed. This eliminates the need for the skin–to–doubler fasteners of the previous examples thus removing them as potential ignition sources.

Preferred fastener locations: In Fig. 7.22(c), the access door fastener head is located in the door so that a strike to the door causes current to leave through the door fastener. This creates potential arc and spark sources at the fastener interfaces with the resultant arc products contained by the use of the O–ring seal and the polysulfide sealed riveted nut plate.

In Fig. 7.22(d), the fastener head is located in the skin rather than the access door. A strike to the fastener will let a majority of the current go directly into the skin thus decreasing the current density in the door–to–skin fastener. The decrease in fastener current density in turn minimizes the intensity of arcing at the fastener/door interface. The use of an integral nut ring will further reduce current density in the door–to–ring fasteners. Arc products which are formed are contained by the use of the O–ring seal as before.

Non–conductive doors: If the door, rather than a door fastener is struck, current density through any of the door fasteners will also be low since the current from the door to the skin will be divided among all of the door fasteners. Currents can be eliminated in the door altogether if the door is constructed of a non–conductive material such as chopped glass fiber reinforced composite. A lightning attachment to such a door will simply result in a surface flashover to the adjacent skin or fastener.

Alternative gasket approaches: Figs. 7.23(a) and (b) shows two access door gasket designs. Example (a) shows an O–ring which fits into the slot shown in the doubler and prevents arc products from entering the vapor space within the fuel tank. In Fig. 7.23(b), a flat gasket has been slotted as shown so that arc products occurring at the door–to–doubler (or door–to–skin) fasteners can be vented to the external surface away from the internal fuel/vapor space.

Other modifications: Other modifications in access door seal design have proven equally effective in preventing arcing. In some cases anodized clamp rings or insulating gaskets have been acceptable when sufficient metal–to–metal conductivity existed via the bolts or fasteners alone. The door for which the modification

described in [7.48] was developed, had only 23 fasteners, whereas other doors having over 40 fasteners have been found to resist arcing even if insulation finishes or paints such as anodizing or zinc chromate remained on the mating surfaces. The large number of fasteners available for conduction results in a low current density per fastener compared to a door with only 23 fasteners.

Guidelines for doors: Some guidelines to follow in designing a protected door include the following:

1. Provide as much electrical contact via screws or fasteners as possible and make the current paths through these fasteners as short as possible.
2. Isolate the fasteners from vapor areas with non-conductive gaskets or O-ring seals.
3. Thoroughly coat all fasteners with tank sealant.

The importance of eliminating ignition sources at access doors installations cannot be overemphasized, especially in cases where the access door is itself a large part of the aircraft skin and encloses fuel. Such a case is illustrated in the small fighter aircraft of Fig. 7.21, in which several large access doors cover a fuselage fuel tank. The doors cover a large area and will be exposed to lightning strikes sweeping aft from the nose. Doors of new design should be tested to be certain that protection is adequate.

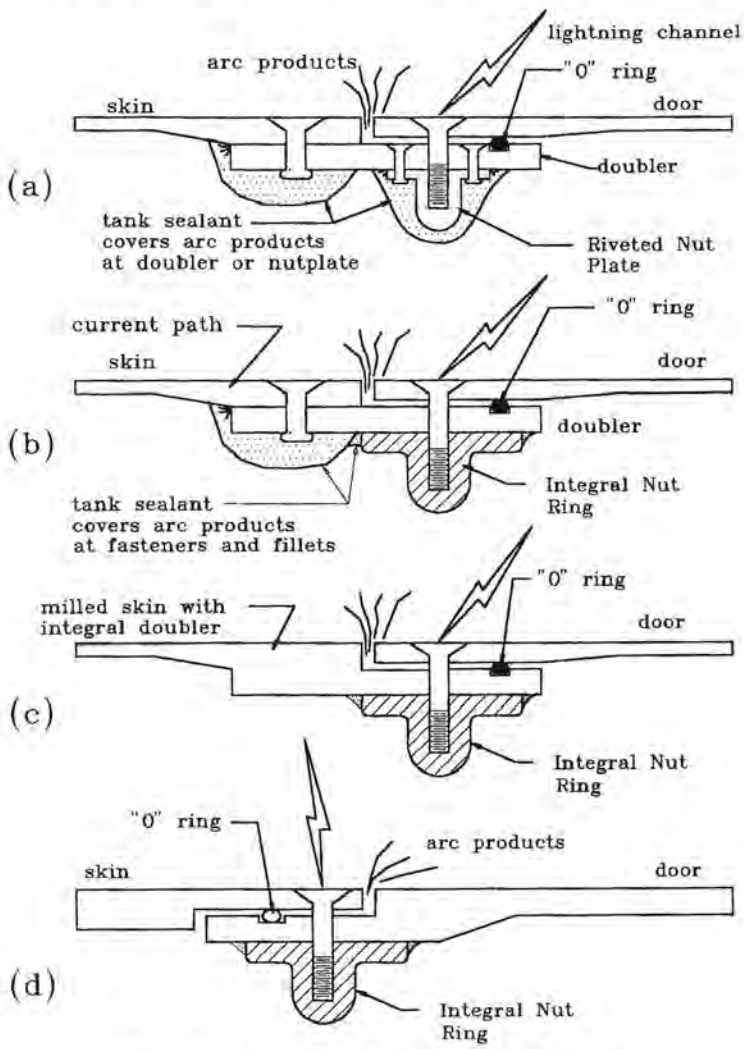

Fig. 7.22 Treatment of fasteners on access doors.
(a) O-ring
(b) Integral nut plate
(c) , (d) Elimination of doublers.

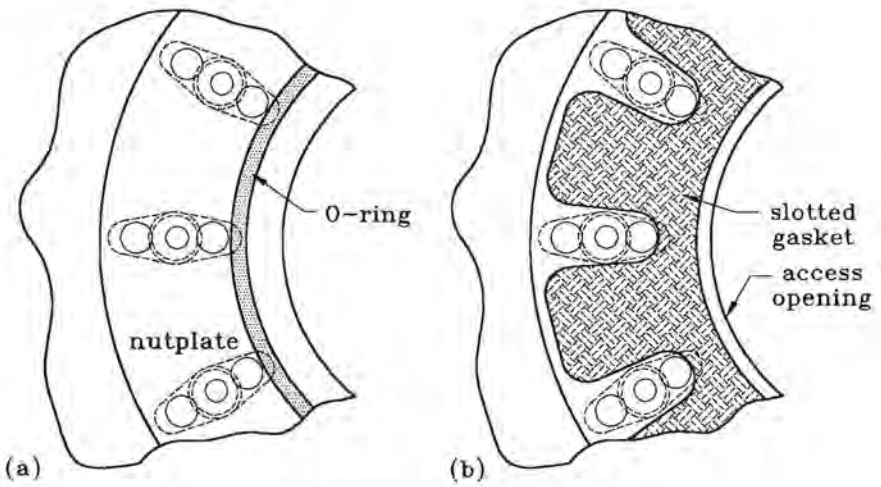

Fig. 7.23 Alternative gasket designs.
(a) Conventional ring gasket
(b) Ventilated gasket

Resistance measurements: Adequate electrical conductivity and protection cannot be verified just by measuring the dc resistance between the door and the surrounding airframe and seeing that it is below some arbitrary value, such as 2.5 milliohms. Shortcomings of resistance measurements were previously discussed in §6.2.5.

Verification of protection: The only way to be certain that a protection design is adequate is to perform lightning tests on production-like installations. Other factors, such as mating surface finishes and fastener torque or tightness play a role in protection effectiveness and these factors, with appropriate tolerances, should be accounted for in test planning and assessment of results.

The SAE report [7.28] describes tests appropriate for all zones.

7.6.3 Fuel Tank Sealant

In some situations it is not possible to prevent all sources of arcing around fasteners. In those cases the arc products must be prevented from contacting fuel vapors, often by coating the arc source with polysulfide type tank sealant. In addition to preventing fuel leaks, the sealant acts to contain the arcs and sparks which occur at these fasteners during a strike attachment and prevents contact of the arc products with the fuel vapor space. Typical areas requiring sealant protection include structural interfaces, fasteners which extend through the tank skin from the exterior surface, and internal fasteners and rivets which form part of the current path, especially if the structural members are of CFC material. A further discussion of sealant is given in §7.10.3.

Protection requires that sealant application be thorough and of sufficient thickness, with no voids, or thinly applied areas.

Advantages of sealant: The advantages of sealant include the following:

1. Sealants may already be applied to prevent leaks.

   Containment of arcs and sparks may only require that the sealant be applied more thickly or over a wider area.

2. Easily applied.

3. Can be applied to existing designs.

Disadvantages of sealant: The disadvantages of sealant include the following:

1. Application is operator dependent.

   The adequacy of the sealant application depends on the skill of the person applying the sealant, especially in areas of the tank which are difficult to access. In these areas, even a skilled operator may have difficulty in ensuring that sealant coverage is complete without voids or thin spots. Some areas may receive excessive sealant while others may receive too little to contain the more energetic arcs and sparks. Application also depends on how closely the operator adheres to sealant guidelines.

2. Sealant exacts a weight and cost penalty.

   While applying thick layers of sealant increases lightning protection, it also adds to the weight of the aircraft which increases costs through additional fuel consumption. Exact figures on the weight added as a result of lightning protection measures are difficult to determine since much of the sealant is normally applied to fasteners and interfaces in a fuel tank for prevention of fuel leaks. However, any additional sealant applied for lightning protection adds weight at a rate of $0.048 - 0.056$ lb/in^3.

3. Protection may deteriorate with age and constant "working" of the airframe.

   As the sealant ages it may deteriorate so that there may be areas within the tank where the sealant is no longer capable of containing the arcs and sparks which occur during lightning current flow. Some progress has been made in this area with improved sealants that remain pliable throughout the life of the aircraft.

7.7 Structural Joints

High–density patterns of rivets or fasteners, as commonly used to join fuel tank skins to stiffeners, ribs, and spars, should be capable of conducting 200 kA stroke currents even when nonconductive primers and sealants are present between the surfaces, as in Fig. 7.24. Short [7.49], for example, reports 200 kA stroke tests of skin–to–stringer joint samples fastened with double rows of taper–lock fasteners. The samples tested had 16 fasteners on each end of the joint, and no sparking was detected anywhere at the joint.

There is no hard–and–fast rule for the number of fasteners per joint which are necessary to avoid arcing, but a rough guideline of 5 kA per fastener, as discussed below, can give some indication of the number of fasteners which may be required to transfer lightning currents among structural elements without arcing. In general, it has been found that structural fastener configurations inside tanks and not exposed to direct strikes can tolerate *Zone 3* current densities without visible arcing and the need for overcoating with sealant. Fasteners exposed to exterior surfaces in *Zones 1* or *2*, however, must usually be protected and verified by test.

At areas of high current density, arcing usually occurs at the interfaces between the fastener and surrounding metal, as shown in Fig. 7.25, and the occurrence of such arcing depends on other physical characteristics, such as skin thickness, surface coatings, and fastener tightness. Tests in which simulated lightning currents are conducted through the joint should always be made on samples of joints involving new materials or designs to confirm protection adequacy.

Arc thresholds of fasteners in Zone 3 areas: Under a program sponsored by NASA [7.50], tests were performed to determine the spark threshold level of typical fasteners used in aircraft installations. For those tests, aluminum lap joint specimens were bonded with electrically non–conductive fuel tank sealant and were also fastened with a single rivet which had been "wet" installed with the same sealant. Currents were conducted directly into one end of the specimen and removed from the other end. All current was forced through the single fastener since the non–conductive sealant eliminated any direct electrical contact between the mating surfaces. No coatings of any kind were applied to the head of the fastener.

The tests indicated that the spark threshold current level of the fasteners was 5 kA. Thus, a door containing 40 fasteners could conduct nearly 200 kA without sparking if the current were distributed evenly among the fasteners. In most cases, however, the current will not divide uniformly, but will be concentrated in those fasteners closest to the point of attachment or exit.

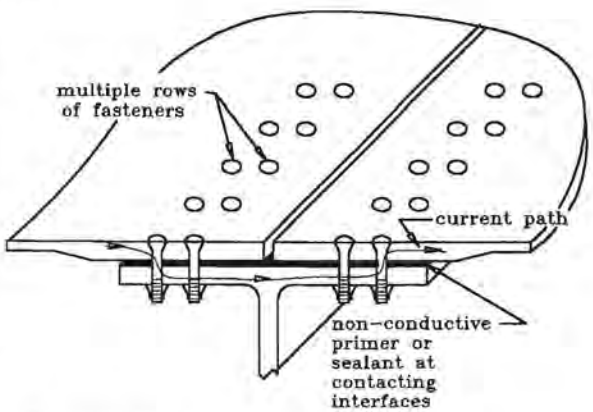

Fig. 7.24 Bonding through mechanical fasteners. Mating surfaces coated with non-conductive finishes and sealers.

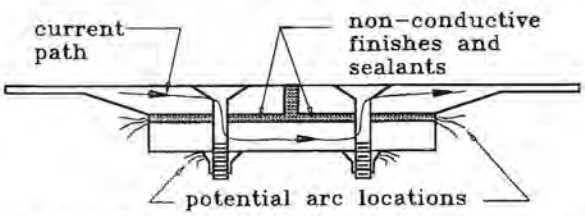

Fig. 7.25 Potential arc source locations at structural interfaces coated with non-conductive finishes and sealants.

Direct attachments: The preceeding discussion relates to joints located in *Zone 3* which must conduct only a portion of the lightning current. Joints located in other zones can be struck directly by the lightning arc. It is possible for the lightning arc to remain attached to a single fastener or rivet. If that happens, the arc can melt or otherwise damage the rivet and surrounding skin. If ignitable fuel vapors exist beneath such a joint , the joint may have to be larger than would be otherwise required.

Guidelines for joints: Some other guidelines which should be noted in designing integral tank joints are as follows:

1. Provide electrically conducting paths among the structural elements so that lightning currents can be conducted among elements without excessive arcing, and without having to spark across nonconducting adhesives or sealants. Often this will be via rivets or removable fasteners, which make metal to metal contact with joined parts. There must be sufficient areas of contact among all of the fasteners in the current path to avoid excessive arcing, damage to the fasteners or surrounding structural material.
2. Try not to put any insulating materials in places that would divert lightning current from straight and direct paths between entry and exit points on the aircraft. Voltages which may cause sparking will build up wherever diversions in these paths exist. The diversions through the fasteners and stringer of Fig. 7.24 are acceptable. More extended paths may not be.

3. Account for aging and mechanical stress which may cause reduced electrical conductivity. Continued flexing of structures under flight load conditions may eventually loosen a joint to the point where arcing could occur. To evaluate this possibility, perform simulated lightning tests on joint samples which have been previously subjected to fatigue or environmental tests.

4. Coat all joints thoroughly with fuel tank sealant to contain any arcs or sparks which may occur. A further discussion on sealing is found in §7.6.3.

5. Do not depend on resistance measurements to confirm the adequacy of lightning current conductivity in a joint. The inductance of the path plays an equally important part. Resistance measurements (ac or dc) may be useful as a production quality control tool, but they are not useful for establishing the adequacy of the lightning current path through the joint.

7.8 Connectors and Interfaces in Pipes and Couplings

Electrical plumbing lines within a fuel tank will usually conduct some of the aircraft lightning currents since they provide conducting paths in contact with conducting structures. The amount of current in plumbing depends on the resistance and inductance of current paths in plumbing as compared with surrounding structural paths. Currents in plumbing within metal aircraft may be small, a few tens or hundreds of amperes, but current in metal pipes inside nonconducting or CFC structures may be very high.

Problems: The current in these lines may cause sparking at pipe couplings where there is intermittent or poor electrical contact. Some pipe couplings, for example, are designed to permit relative motion between the mating ends of a pipe to relieve mechanical stresses caused by wing flexure and vibration and this precludes the tight metal to metal contact needed to carry current. Also, electrically insulating coatings such as anodized finishes are often applied to the pipe ends and couplings to control corrosion. Relative motion and vibration may wear this insulation away, providing unintentional and intermittent conductive paths, situations that lead to sparking. Therefore, particular attention should be given to the design of fuel system plumbing.

Lightning currents in plumbing: The mechanism by which lightning currents diffuse to the interior of an aircraft is discussed in Chapter 11. There it is pointed out that it can take many microseconds for lightning currents to become distributed through the aircraft because rapidly changing currents distribute primarily according to the inductance of the paths while slowly changing currents distribute according to resistance.

The high amplitude return stroke currents will not spread very deeply into interior structural elements or other interior conductors because they are of short duration, but will instead tend to remain in the metal skins. Still, there will be some current. During a NASA sponsored program [7.51] currents in the fuel lines within a fuel tank with adhesively bonded aluminum structural elements were measured. With a current of 88 kA injected into the wing, the current in a small diameter fuel line within the tank was 160 amperes.

The analytical procedures for determining how rapidly changing currents distribute, §11.4, are complex, but intermediate and continuing currents persist for times long enough for the distribution to be calculated on the basis of the dc resistances involved.

Assume that the leading and trailing edge sections of a wing are nonconductive or sufficiently isolated as to be unavailable for conduction and that the remaining wing box is comprised of skins and spars having the dimensions as shown in Fig. 7.26. The cross sectional area of the spars and skins forming this box is 135 cm^2 (21 in^2). The tank also contains an aluminum vent pipe electrically bonded to the structure at each end of the tank. This tube has an outside diameter of 10 cm (4 in), a wall thickness of 0.5 mm (0.02 in^2) , and a cross sectional area of 1.56 cm^2 (0.24 in^2).

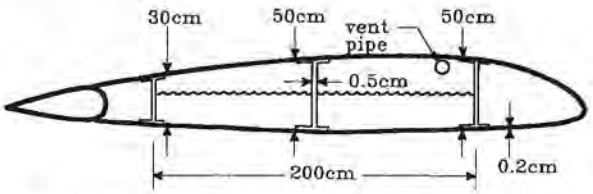

Fig. 7.26 Hypothetical wing box with integral fuel tank.

Assume an intermediate strike with an average amplitude of 2000 A for 5 ms, in accordance with Component *B* of [7.28]. The current in the pipe can be calculated as follows:

$$I_{pipe} \approx \left[\frac{1.56\ cm^2}{135\ cm^2}\right] \times 2000\ A = 23.1\ A \qquad (7.2)$$

Currents of this order of magnitude have produced arcs at movable, poorly conducting, interfaces in some couplings. More common examples of electric arc sources include motor commutators.

Bond straps: Electrical bond straps or jumpers are sometimes installed across poorly conducting pipe couplings, as shown in Fig. 7.27. These bond straps should not be relied upon to prevent sparking from lightning currents. Current is apt to divide in proportion to resistance which may be the result of a small contact area in the coupling. Some current in the coupling could lead to sparking even with the bond strap in place.

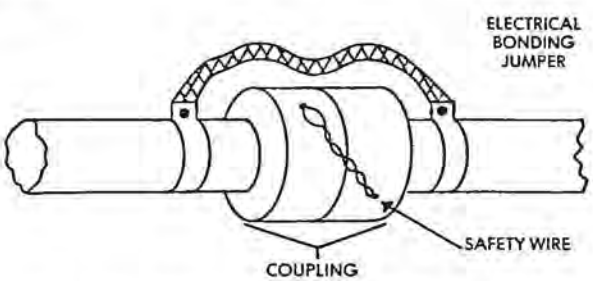

Fig. 7.27 Electrical bonding jumper across insulated coupling.

Conduction through couplings and interfaces: The extensive use of anodized coatings to provide noncorrosive mating surfaces in pipe couplings would seem to preclude arcing across the pipe interface, but relative motion between these surfaces can wear through the anodized coating, forming a conductive path. If there happens to be a large, bare metal–to–metal contact within the coupling, this could provide a spark free path. However, a slight change in the relative position of the mating surfaces, or introduction of dirt or residue might drastically change the electrical capability of a coupling. It is probable that the electrical capability of a typical pipe coupling changes many times during a flight as a result of relative motion caused by structural vibrations and flexing.

Some of the commercially available couplings and bulkhead fittings have been designed to conduct impulse currents up to 2500 amperes without sparking. These couplings should be adequate for use in most metal tanks where currents are of the order of a few hundred amperes or less.

Fuel tanks fabricated of CFC materials, however, are more highly resistive than aluminum. Currents on the exterior skin surface of such tanks will diffuse more rapidly to internal conductive plumbing and currents might greatly exceed 2500 amperes.

Guidelines for protection: In the absence of definitive data on the electrical conductivity of pipe couplings under in–service conditions, it is advisable to take the following approach:

1. Determine, by analysis or test, the fraction of lightning current expected in a particular pipe.
2. Inject this current into a sample of the coupling under simulated in–flight vibration and contamination conditions.
3. Perform this test in a darkened enclosure and observe whether any arcs or sparks occur. Repeat the test until a reliable result is established.

Non–conducting interfaces: One solution to the problem of arcs and sparks at couplings and plumbing interfaces with aircraft structure is to insert electrically non–conductive isolation links into these lines to eliminate them as current carrying paths. This solution, of course, requires additional couplings, which may add additional weight compared to the traditional all aluminum plumbing.

Another solution is to make the pipes of a non–conductive material. Various solid polymers or fiber reinforced resins may be used for this purpose. Some electrical conducting material must be provided in the interior linings of pipes transferring fuel however, to

prevent frictional charge accumulation. The resistivity of these materials should be on the order of 10^6 to 10^8 ohm–cm. This is sufficiently high to prevent lightning currents, but still adequate to dissipate static charges. Lower values would make the lines too conductive. One such system presently under development is a reformable duct system of electrically non–conductive thermoplastic fluoropolymer, reinforced with aramid fibers.

7.9 Electrical Wiring in Fuel Tanks

Problems: Lightning current in an aircraft may induce voltages in electrical wiring. If this wiring enters a fuel tank, the induced voltages may be high enough to cause a spark.

Electrical wires found inside fuel tanks are typically those used for capacitance–type fuel quantity probes or electric motors used to operate pumps or valves. If these wires are totally enclosed by metal skins and ribs or spars, the internal magnetic fields and induced voltages will be relatively low. Electrical devices, such as fuel quantity probes, and their installation hardware, have been intentionally designed to withstand comparatively high voltages without sparking. The fuel system designer, however, must be continually alert for changes in material or structural design that might permit excessive induced voltages to appear in fuel tank electrical circuits.

Sparkover characterics of small gaps: A number of measurements have been made of the voltages which lightning currents can induce in fuel probe wiring. Measurements have also been made of the voltages required to cause a spark to occur between the elements of typical capacitance–type fuel quantity probes. The sparkover voltages have usually been found to be much higher than those found to be induced in the wiring. As an example, Newman, Robb, and Stahmann [7.47] found that dc voltages of at least 3000 V were required to cause a spark to jump between the active and grounded cylinders of a capacitance–type fuel probe found in a KC-135 aircraft wing, and that even higher voltages were needed to spark over the other gaps in this probe. Plumer [7.51] ran a similar test using impulse voltages and found that 12 kV were required to cause a spark to jump between the inner and outer cylinders of a typical probe. Small gaps like this will withstand more impulse than dc voltage, and the impulse test more realistically represents an induced voltage.

Effects of air pressure: The tests reported above were made at ground level. At flight altitude, the same gap would break down at a lower voltage because of the lower air pressure. The amount of reduction to be expected in impulse sparkover voltage at various altitudes can be determined from the Paschen curve of Fig. 7.28 [7.52]. To use the figure, one would first determine the product of pressure and gap distance, pd. Pressure can be obtained from the chart of the figure. As an example, if it is desired to find the sparkover voltage of a 5 mm (0.2 in) gap at a 10 000 m (33 000 ft) altitude, the pressure at this altitude would first be found from the chart as 198.16 mm Hg. The product pd would then be 990.8 mm Hg. From Fig. 7.28, the gap would spark over at approximately 5500 V.

Ignition energy vs altitude: The ignition energy also rises as pressure drops and this effect tends to offset the reduction in sparkover voltage with pressure. Tests [7.8] have shown that 20 times as much spark energy is needed to cause ignition at 11 000 m (36 000 ft) as at sea level. The ignition threshold might rise to 4 - 10 millijoules, instead of 0.2 - 0.5 microjoules. Most induced voltages that are capable of producing a spark, however, can produce more than 10 joules, so one should not rely on the spark ignition threshold being sufficiently high to prevent problems.

Lightning strikes to aircraft have been reported at all flight levels through about 11 000 m (36 000 ft), although few occurances above 5000 m (16 000 ft) appear to have involved severe currents. Thus, it is probably sufficient to design and certify small air gaps at the SAE lightning environment at about 10 000 m (33 000 ft) without sparkover.

The sparkover voltages of Fig. 7.28 should be considered only approximate, since the curve relates to uniform field conditions, such as found in parallel plane electrodes. Other electrode configurations, such as a sharp point–to–plane, would spark at lower voltages, perhaps 25% less. It is best to actually measure the sparkover voltage of specific gaps, preferably using impulse voltages and the actual hardware, as electrode shapes and surface treatements also influence sparkover voltage. The tests can be made at ground level pressure and corrected approximately for altitude by multiplying ground test data by the percentage reduction in sparkover voltage of the same gap at flight altitude.

Guidelines for design: In practice, design of small airgaps should incorporate a margin of 100% over anticipated actual voltage levels, to account for mechanical installation tolerances, the effects of contaminants, and the statistical variations in small gap sparkover voltages themselves. Thus, a particular gap should be sized to withstand, at altitude, twice the anticipated actual voltage.

In some cases, particularly installations within CFC tanks, this will require unacceptably large clear-

ances between objects such as fuel quantity probes and adjacent structure. In such cases other means, such as coating adjacent surfaces with dielectric films, may be explored to enable smaller gaps to withstand twice the anticipated voltage. Designs like this must be given voltage withstand tests, as handbook type data does not exist to support specific designs.

It is particularly important that sufficient insulation be provided between the active elements and the airframe because the highest induced voltages usually appear between the wires and the airframe. These voltages may be IR voltages related to lightning currents in the structural resistance of the wing or they may magnetically induced voltages as illustrated in Fig. 7.29. Structural IR voltages may be only a few volts for a metal wing, but they may be several thousand volts in a composite wing.

Testing considerations: When determining the sparkover voltages of small gaps such as those at a fuel quantity probe, care must be taken to apply test voltages to all of the gaps which may exist, though this need not be done simultaneously. In most cases both the "high" and "low" elements of a quantity probe are insulated from "ground" (the airframe), but there is always a mounting bracket which brings the probe in proximity to the airframe. Fig. 7.30 is an illustration. Thus, the test should evaluate both the sparkover between the "high" and the "low" electrodes and the sparkover between the "low" electrode and the structure upon which the probe is mounted. Usually, the gaps to the mounting bracket or airframe will be larger than the others and require a higher voltage to cause sparkover, but these are also the gaps that experience the highest induced voltages.

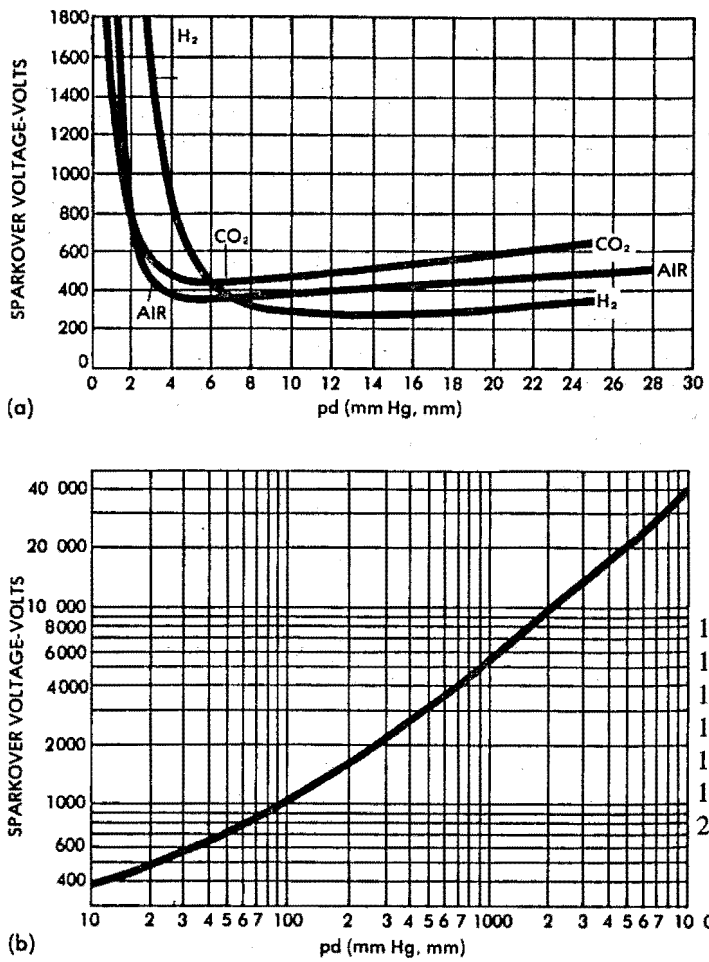

Altitude m	Pressure mm of Hg
0	760.00
500	715.99
1000	674.09
1500	634.18
2000	596.23
2500	560.11
3000	525.79
4000	462.26
5000	405.09
6000	353.77
7000	307.87
8000	266.89
9000	230.45
10 000	198.16
11 000	169.66
12 000	145.05
14 000	106.02
16 000	77.48
18 000	56.65
20 000	41.41

Fig. 7.28 Sparkover voltages and altitude pressures.

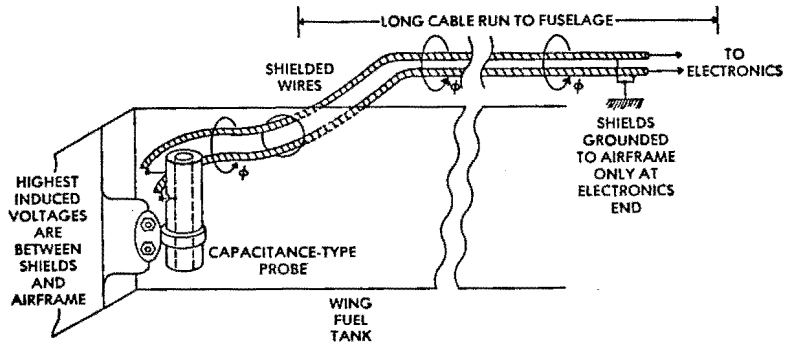

Fig. 7.29 Typical fuel probe wiring.

- Most magnetic flux and induced voltage appears between wire (or shield) and the airframe at probe end.
- Less flux and induced voltage exists between any two wires.
- Even less flux and voltage exists between a wire and its shield.
- Other voltages can occur between probe and airframe because of structural IR potentials.

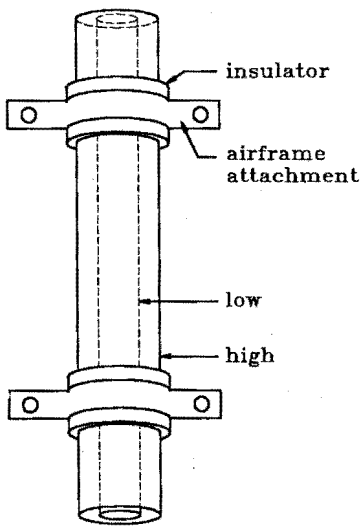

Fig. 7.30 Possible breakdown of gaps in capacitance–type probe.
1. High to low
2. High to airframe
3. Low to airframe

Contaminants that accumulate with time on the probe surfaces may act to reduce the sparkover voltage; therefore, it is wise to incorporate a factor of two when designing clearances necessary to tolerate the anticipated induced voltages expected in fuel tank wiring harnesses.

Fig. 7.29 illustrates that the proximity of the probe to the airframe structure on which it is mounted is very important in determining breakdown voltages to the airframe. Because of this, design of adequate insulation between the active elements of the probe and the airframe may not be entirely within the probe designer's control.

Shielding of fuel probe wires: The fuel probe wires are most closely referenced to the airframe at the electronics end, which is usually in the fuselage. If one or more of the wires are shielded, there can be a conflict between the grounding practices that are best for control of lightning induced voltages and those considered best for control of steady state electromagnetic interference, EMI.

Usually, because of EMI considerations and concern for "ground loops", only one end of the shield is grounded; most commonly at the end remote from the fuel sensor. Grounding the shield at both ends permits stray ac fields to induce circulating currents in the shield, and such currents may interfere with the operation of the fuel quantity electronics.

The conflict arises because a shield grounded at only one end does not act to reduce magnetically induced voltage between conductors and ground, though it may reduce voltages between conductors in the shield. The subject is treated at length in Chapter 15, but the gist of the matter is that a shield can reduce voltages between conductors and ground only if it is grounded at both ends and allowed to carry current. If a shield is ungrounded at one end, magnetically induced voltages can develop at that end between the conductors and ground. Thus, most shields found on fuel quantity probe wiring harnesses offer little or no protection from lightning induced effects.

Measurements of induced voltages: Newman, Robb, and Stahmann [7.53] measured about 11 V on the fuel quantity probe circuits routed inside a KC-135 wing fuel tank through which 50 kA strikes with 50 kA/μs rates of rise were being conducted. This voltage would extrapolate to a maximum of 44 V at a severe strike amplitude of 200 kA. Plumer [7.54] measured up to 4 V in a fuel probe circuit routed inside the tanks of an F-89J wing. The simulated lightning current in this case was 40 kA, with a rate of rise of 8 kA/μs. From these results he predicted that a 200 kA, 100 kA/μs lightning strike would induce 185 V in the same circuit.

These voltages are not sufficient to cause any sparking. These measurements were made on metal aircraft and similiar measurements on CFC structures would result in substantially higher levels.

Routing of wires: The routing of the fuel probe wires can have a lot to do with how much induced voltage appears at apparatus inside fuel tanks. A comprehensive discussion of shielding practices is given in Chapters 15, 16 and 17.

7.10 Elimination of Ignition Sources

The previous sections have described some of the more likely potential sources of ignition and have described ways to prevent them. In the following sections, some overall design approaches are discussed which can be followed to reduce or eliminate potential ignition sources. These approaches involve selection of basic structural materials, modifications in the airframe structural design, and methods to prevent contact between any remaining ignition sources and fuel vapors. Successful implementation of these measures requires the lightning protection specialist to work closely with airframe and structures designers and manufacturing technologists at a very early point in the design cycle. Structural design modifications to minimize lightning protection problems can result in substantial savings in weight and cost penalties due to lightning protection, but these benefits can not be obtained unless the designs are incorporated early in the design cycle. Structures designs must satisfy many requirements and some of the features that would alleviate potential lightning problems may not be compatible with these other requirements.

The following design approaches should be utilized, to the extent practical, to minimize potential ignition sources within aircraft fuel tanks.

1. Designing the fuel tank structure to minimize the number of joints, fasteners and other potential arc and spark sources in fuel vapor areas.
2. Providing adequate electrical conductivity between adjacent parts of structures.
3. Providing a barrier to separate remaining arc or spark products from the fuel vapor.
4. Design of fuel system components to interrupt potential current paths and withstand potential differences that may exist during lightning strikes to the airframe.

7.10.1 Tank Structures Design

As illustrated in the foregoing sections, most ignition sources are associated with structural joints and fasteners of various kinds. As much as possible, joints and fasteners should be eliminated in fuel vapor areas. If they cannot be eliminated, they should be designed so that they do not spark. If sparks cannot be completely eliminated, the fastener must be sealed so that the sparks do not contact the vapor. Several design approaches are possible.

Eliminating penetrating fasteners: Figs. 7.31 - 7.33 show how wing spars and ribs can be rearranged to eliminate penetrations of fasteners into the fuel tank. This approach may eliminate possible fuel leaks at the fasteners as well as eliminating ignition sources, though the possibility of leaks due to bowing of the closeout rib would have to be considered. Care must be given to ensuring that the edges of spars and the rib–to–skin interfaces do not present arc or spark sources themselves. This is usually done by use of electrically insulating, corrosion resistant finishes, as well as sealant materials between parts. Also, polysulfide type sealant is sometimes necessary at fillets and edges, as discussed in §7.6.3.

The approaches illustrated in Figs. 7.31 through 7.33 are applicable to CFC as well as to metal structures. Lightning currents in fasteners in CFC structures may be higher than those in aluminum structures because diffusion times in CFC are much shorter than in aluminum and more current will seek to flow in interior structural elements such as ribs and spars. Also, it is usually more difficult to make arc free electrical contact between CFC parts. Thus these design approaches may be more necessary in CFC airframes than for aluminum airframes.

Likewise, the lightning current densities in airframes of small size, general aviation aircraft and small rotorcraft, will be proportionally higher than the current densities in larger transport category vehicles exposed to the same total amount of lightning current. Design approaches such as shown in Figs. 7.31 through 7.33 can be followed to eliminate potential ignition sources in small integral tank structures.

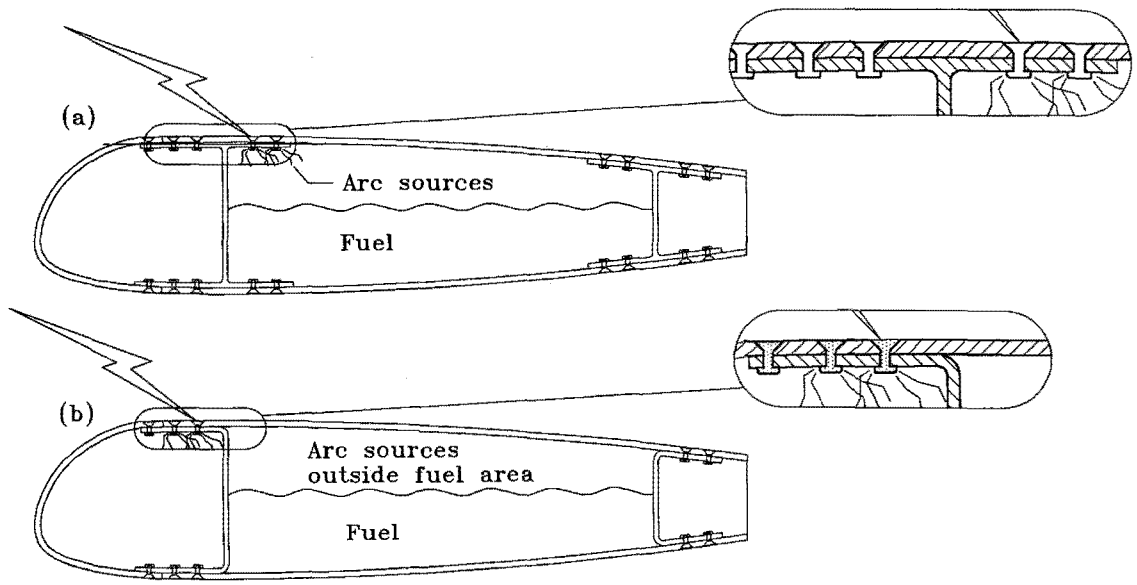

Fig. 7.31 Spar–skin interface design to reduce ignition sources.
(a) Conventional – fasteners in fuel area
(b) Improved – fasteners outside fuel area

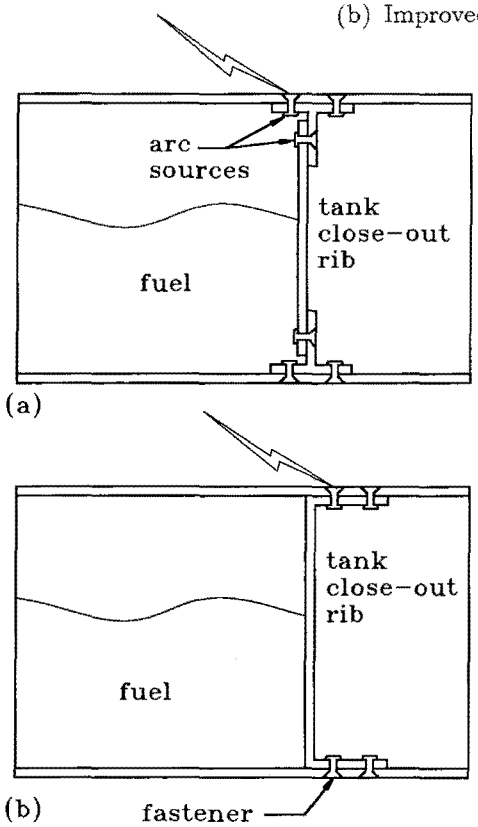

Fig. 7.32 Wing fuel tank closeout rib–skin interface design to reduce ignition sources.
(a) Conventional
(b) Improved

Co–curing of CFC tanks: The most radical way of eliminating fasteners and their associated problems is to build the tank as a single monolithic structure which is electrically conductive throughout. While this is not done at present, it is a technique that could be used to build CFC tanks. Fig. 7.34 illustrates the principle.

In Fig. 7.34(a) fasteners penetrate the tank. In Fig. 7.34(b) filament winding is used to achieve an entirely co–cured structure. Practical limitations may prevent this method from being utilized to build complete wings of large aircraft, but similar approaches may be useful for construction of various substructures.

Co–cured joints in CFC structures will eliminate potential arc and spark sources and provide the best possible electrical conductivity among structural sections. In these joints, the pre–impregnated resin is used to bond yarns and plies together without the need for additional adhesives. Practical difficulties arise in co–curing large structures, but great improvements in lightning protection of CFC structures can be achieved by co–curing of simple interfaces, such as between stiffeners and skins.

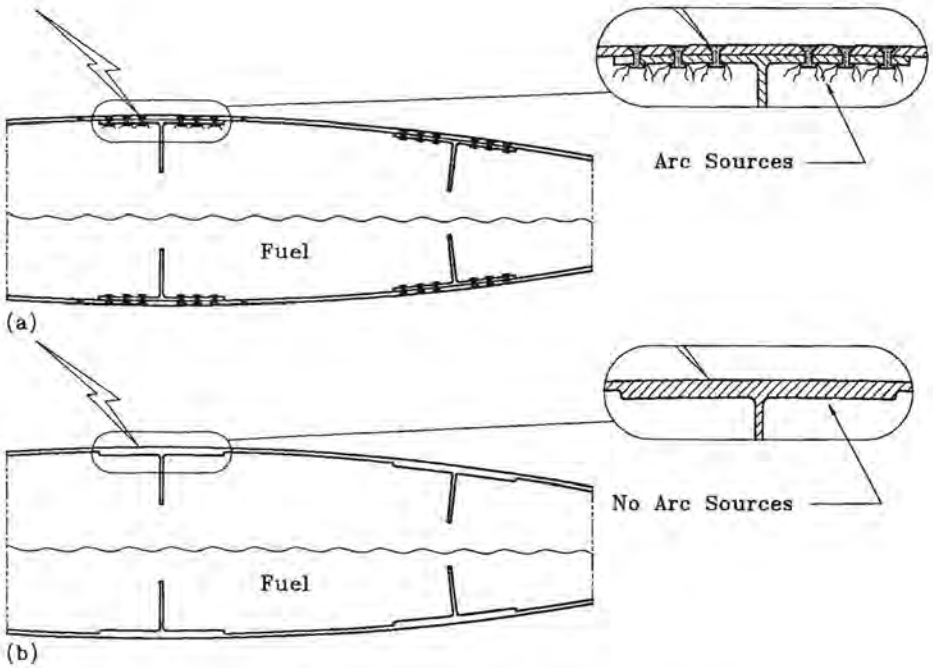

Fig. 7.33 Wing stiffener design to eliminate ignition sources
(a) Conventional – penetrating fasteners
(b) Improved –integral stiffeners

Non–conductive spars: Another method, shown in Fig. 7.35, illustrates the use of fiberglass or aramid fiber reinforced composites to fabricate spars within a wing fuel tank. In this case, lightning currents tend not to flow into fasteners because these bear against non–conducting interior surfaces and do not constitute current paths. Mechanical strength considerations may preclude use of other than CFC material for spars and ribs. If so, several other approaches can be used to interrupt current through fasteners. These are illustrated in Figs. 7.36 and 7.37.

Non–conductive shear ties: Fig. 7.36 illustrates the use of a non–conductive shear tie, sometimes called a clip or shear clip, to interrupt electric current paths between skin and interior structures which are conductive. This allows these elements to remain conductive, yet ensures that lightning currents remain in the tank skin and eliminates potential arc sources at fasteners.

Prevention of fastener sparks: If it is not possible to use a non–conducting shear tie, Fig. 7.37 illustrates a method of controlling internal sparking at the fastener. A non–conductive ply or multi–ply laminate is bonded to the interior surface of the clip. This prevents current from arcing from the fastener to the back of the shear tie at the surface.

The structural designs illustrated in Figs. 7.31 through 7.37 are examples of the kinds of approach that can be followed to eliminate potential fuel vapor ignition sources. These concepts avoid the "brute force" methods of extensive sealant overcoat that impose cost and weight penalties and concerns regarding life–cycle durability. Designers are encouraged to develop other approaches to achieve the same ends. Since success or failure depends on factors such as small dimensions, clearances and tightness whose performance cannot always be predicted, candidate designs should always be evaluated by simulated lightning tests.

When employing electrically insulating structural materials to interrupt lightning current, as illustrated in Figs. 7.36 and 7.37, it must be remembered that current paths must be provided between extremities, such as nose, tail, wing and empennage tips and control surfaces. Thus, non–conductive elements may be utilized within a CFC tank, but the tank skins, and often the main spars, must be fabricated of conductive materials capable of conducting lightning currents.

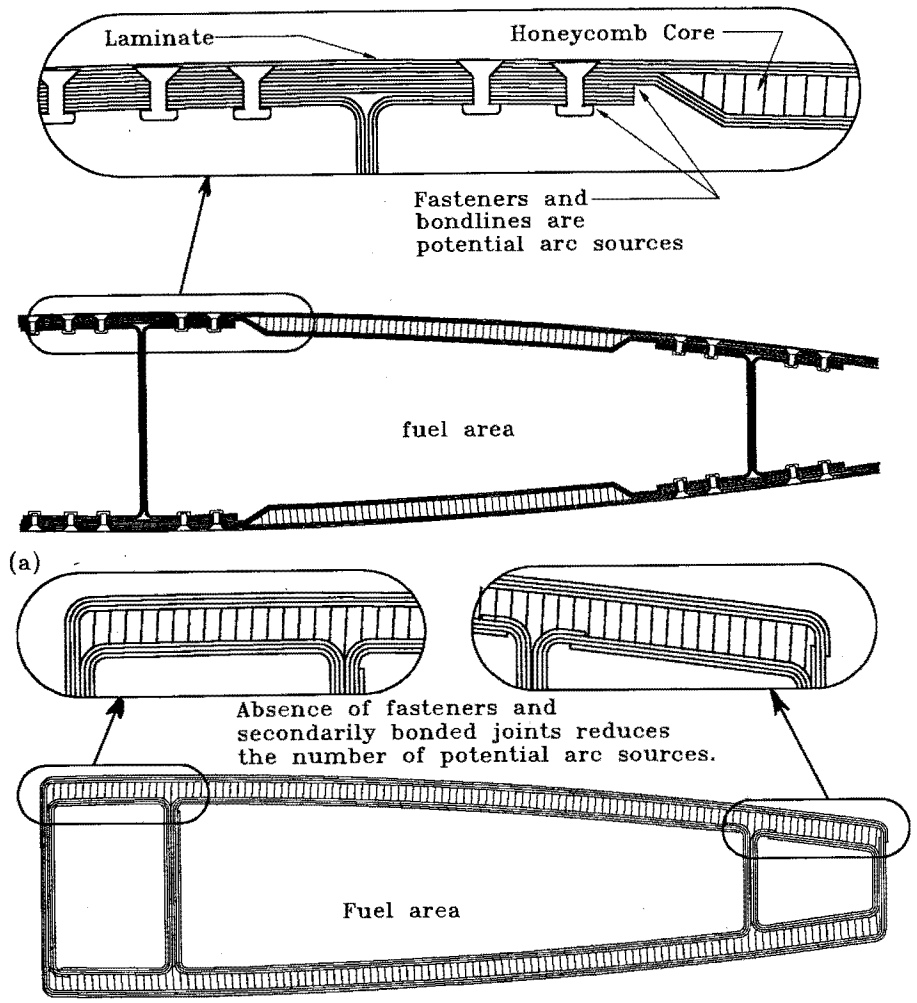

Fig. 7.34 Use of filament winding techniques to obtain co-cured, monolithic structure and eliminate fasteners.
(a) Conventional – penetrating fasteners
(b) Improved – fasteners eliminated

7.10.2 Provision of Adequate Electrical Contact

A primary means of current transfer between fuel tank structural elements is through fasteners. When current is conducted through them, arc products may be produced. These consist of plasmas of ionized air, vaporized and melted metals, and/or composite fiber–epoxy materials. Any of these arc products can be hot enough to ignite fuel vapors.

The basic mechanism is shown in Fig. 7.38. The lightning current is conducted from one part to another through the fastener, threaded nut, and washer. With lightning densities of hundreds or thousands of amperes per fastener, arcing will occur at the points of contact between fastener and fastened parts, as illustrated in Fig. 7.38. If the fastener could bear directly against bare metal, the arc threshold (amperes per fastener) could be increased. However, bare, uncoated parts are almost never tolerated within aircraft structures due to the possibility of corrosion.

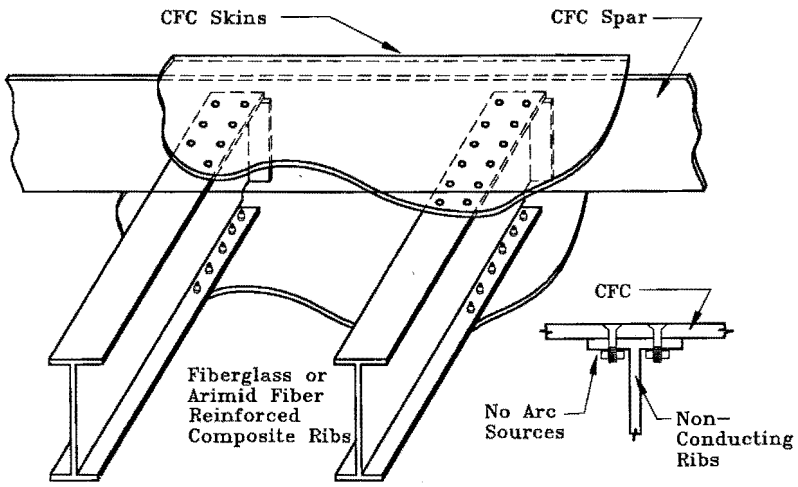

Fig. 7.35 Non–conducting ribs to eliminate arc and spark sources at fasteners.

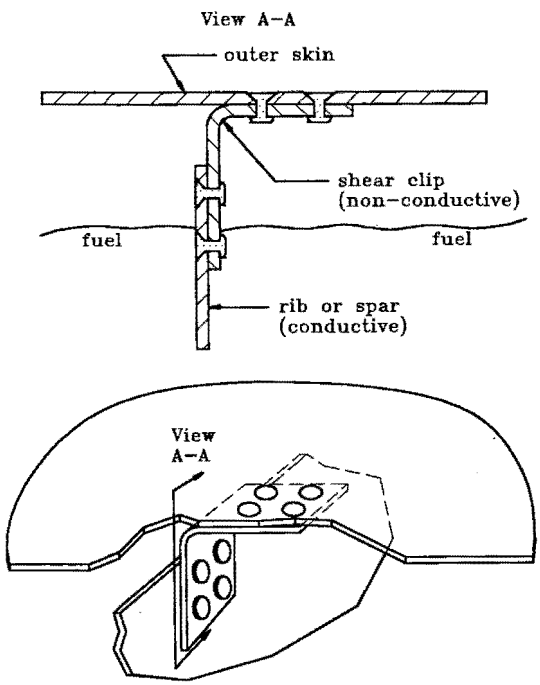

Fig. 7.36 Non–conducting shear clips to interrupt current paths.

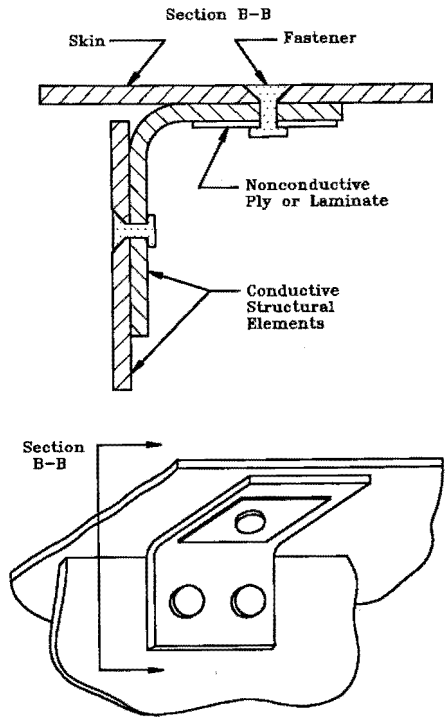

Fig. 7.37 Non–conducting ply or laminate.

Keeping current densities low: One method to minimize arcing at a fastener is to keep the current density in the fastener low. This may be accomplished by using fasteners as large as possible to maximize the contact area between the fastener and the joined surfaces, as is shown in Fig. 7.39. The upper drawing shows arcing occuring at the fastener interface with the parts due to small cross–sectional contact area. When the contact area is increased, as shown in the lower drawing, the current density through the fastener is reduced, which decreases the intensity of the arcing at the interfaces.

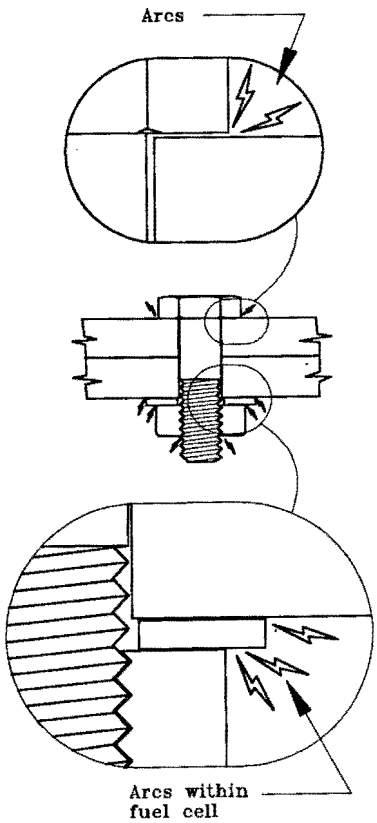

Fig. 7.38 Arcing and sparking at fastener interfaces.

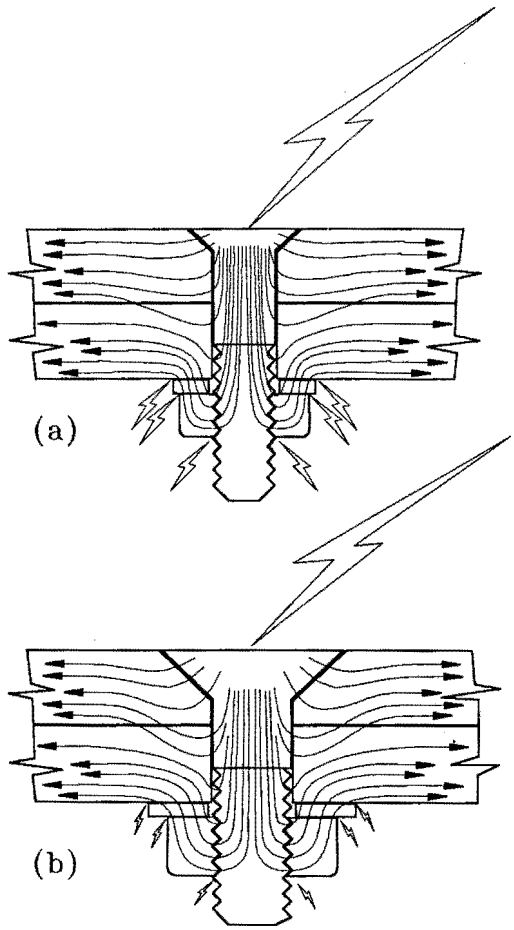

Fig. 7.39 Effect of fastener contact area on current density and arcing.
(a) Small area and high current density
(b) Large area and low current density

The intensity of arcs may also be reduced by allowing or encouraging the current to be shared among several fasteners. This concept is shown in Fig. 7.40. With a large number of fasteners in a current path, the current in any one fastener will be lower. Lightning currents do not divide evenly among all fasteners in most designs, since overall current densities diminish with distance away from lightning entry and exit points. Reliable analysis methods are not readily available to calculate the current distribution among fasteners. Gross estimates can be made by intuition, sufficient to design test specimens and establish appropriate current levels.

7.10.3 Arc Containment

As noted earlier, certain design methods can be employed to reduce the intensity of arcs at conductive interfaces. These methods may prevent ignitions at low to moderate current levels, but at higher levels the arc pressure buildup may be sufficient to blow arc products into the fuel vapor space. For this reason, it is generally necessary to employ a barrier between arc sources and fuel vapor areas.

Containment with tank sealant: The most common method of containment is the addition of a fuel tank sealant coating over the exterior surface of the fasteners. Advantages and disadvantages of sealant were previously discussed in §7.6.3. The basic principle is shown in Fig. 7.41. It must be emphasized that sealant does not eliminate the arcs which occur, but merely contains the resulting products so that they do not contact the flammable vapor space.

Protection increases as the thickness of the applied sealant is increased, though there is a practical limit to the amount of sealant which may be applied because of the weight which it adds to the aircraft and the cost of labor and material. The effectiveness of overcoating depends upon the skill of the operator. The fastener must be thoroughly coated and there must be no voids or thinly coated areas.

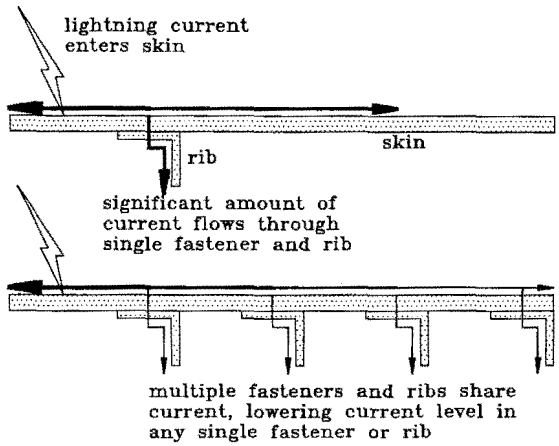

Fig. 7.40 Effect of multiple paths on current density.

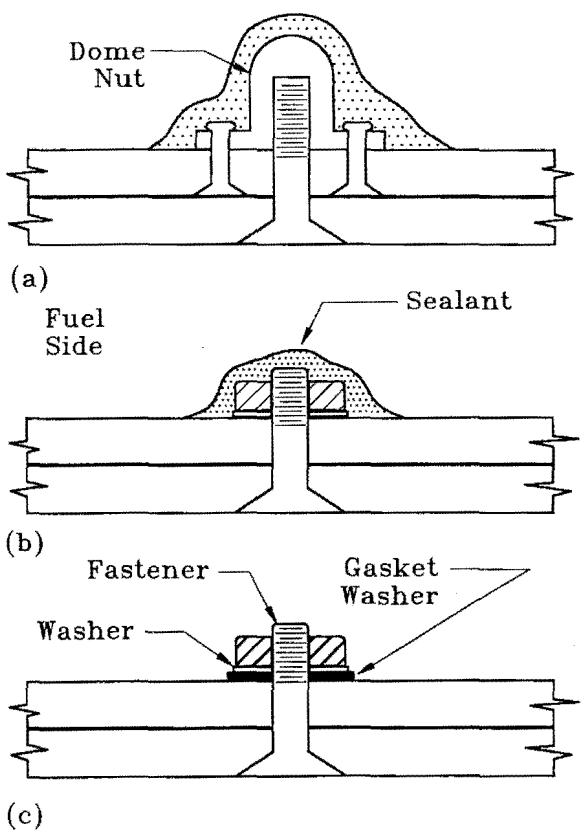

Fig. 7.41 Fastener sealing concepts.
(a) Dome nut
(v) Sealant over a fastener
(c) Washer under a fastener

Examples of acceptable and unacceptable sealant coverage for fasteners are shown in Fig. 7.42. Fig. 7.42(a) shows sealant applied at the sides of the fastener, but not of sufficient quantity to prevent arc pressure blowby through the sealant or at the interfaces between the sealant and the fastener. This is remedied, as shown in Fig. 7.42(b), by applying a coating thick enough to prevent arc product breakthrough. In addition, the sealant has been extended over the fastener head, thus eliminating the possibility of arc product blowby through the sealant at this location.

Containment with fasteners: Although arcing can take place at any point of contact between the fastener and the CFC structure, the most significant arcing takes place between the shaft of the fastener and the hole surface. Pressure then builds up in this area and can vent under the fastener nut or washer into the fuel tank vapor space since the faying surfaces in this area are very hard to manufacture smooth.

A method of containing these products is to use fasteners which provide a mechanical seal. Examples of this type of fastener are shown in Fig. 7.43. Each of these fasteners is fabricated with a gasket to contain the arc products which result from contact between the fastener and the structure. Arcing may occur between surfaces in close proximity, such as between the fastener housing and the skin surface as shown in the sketches, but electrically non-conductive primers or finishes on the skin surface may help prevent this problem. Typical installations should be tested to be certain.

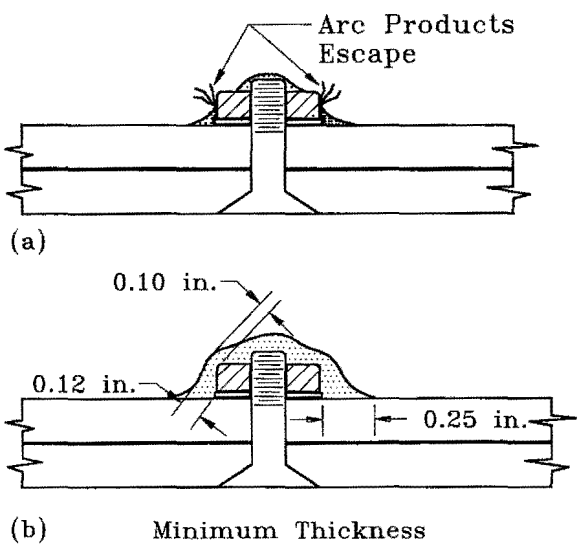

Fig. 7.42 Guidelines for overcoating of fasteners.
(a) Inadequate coverage
(b) Adequate coverage

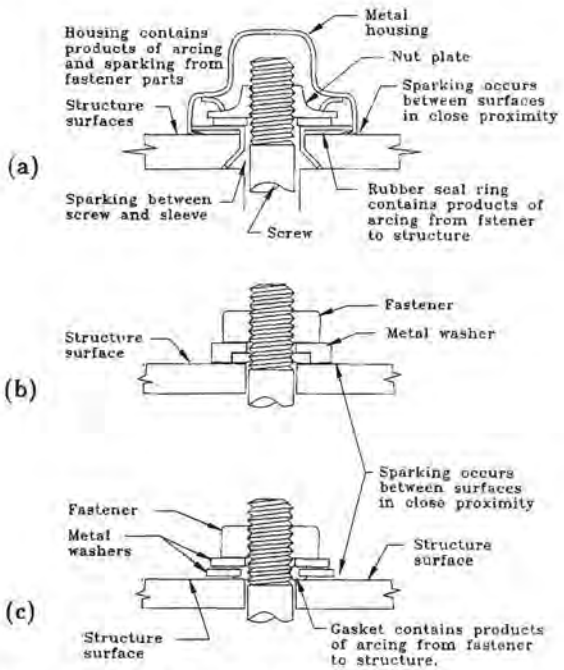

Fig. 7.43 Gasket sealed fasteners.
(a) Self sealing rivetless nut plate
(b) Gask–o–Seal washer
(c) NAS 1523 sealing washer

Arcing threshold levels of self-sealing rivetless nutplates, Fig. 7.43, are generally higher than similar nutplate fasteners with rivets, due to the combination of the rubber seal, which prevents blowby of arc products into the fuel vapor space, and the elimination of the rivets which are generally the source of arcing when currents of any appreciable amplitude are conducted through the nutplate fastener. While arcing threshold levels of typical fasteners have been shown to be approximately 5 kA, the levels achieved by rivetless nutplate fasteners have been three to four times this level.

Structural interfaces: Sealant coatings must also be applied to structural interfaces, at least in exterior skins where current densities are highest. In tanks fabricated of aluminum, coatings of electrically non–conductive corrosion finishes on interfacing parts can result in arcing between the parts due to the poor electrical contact. For CFC tanks, arcing can be caused by the non–conductive resins and adhesives used in the fabrication of structures. Arcing may occur due to insufficient electrical contact between elements and sparking may occur due to voltage potential differences between elements. Recommended fillet sealing dimensions are shown in Fig. 7.44. [7.55].

Spark and arc thresholds: The arc and spark threshold level of a particular aircraft design depends on several factors which include the following:

1. Type of skin material.
2. Skin thickness.
3. Thickness of primer and surface finishes.
4. Arc entry vs. conducted current entry.
5. Current amplitude.
6. Current division among structural elements.
7. Thoroughness of fuel tank sealant coverage.

The threshold levels at which arcs and sparks occur in a new aircraft design may be estimated by similarity with other designs for which a data base exists. However, the fuel tank designer should be careful when assuming that a new design is similar to a previous one. Any differences in materials, thicknesses, coatings, or number of fasteners will change the impedances and current paths within the tank, which can alter the threshold levels.

The current density in a particular set of fasteners can be estimated by mathematical techniques, but determination of structural current is not yet possible due to the complexity of current paths and the difficulty of describing them in electrical terms. Techniques for such estimates are described in Chapters 10 and 11. Since there is some uncertainty about the reliability of these calculations, it is best that designs be based on similarity or upon analysis supported by test data.

7.11 Plumbing and Composite tanks

The use of CFC materials, which are 1000 times more resistive than aluminum, subjects the internal components to higher electrical levels which might result in arcs or sparks that would not occur in aluminum.

The three areas in which CFC construction materials have increased the problems associated with fuel tank design are:

1. An increase in the possibility of sparks due to high voltage potential differences developed within the tank.
2. An increase in the possibility of arcs due to higher magnitude currents in internal plumbing and other hardware.
3. An increase in the induced voltage levels appearing on internal electrical wiring from reduced shielding effectiveness of the surrounding structure.

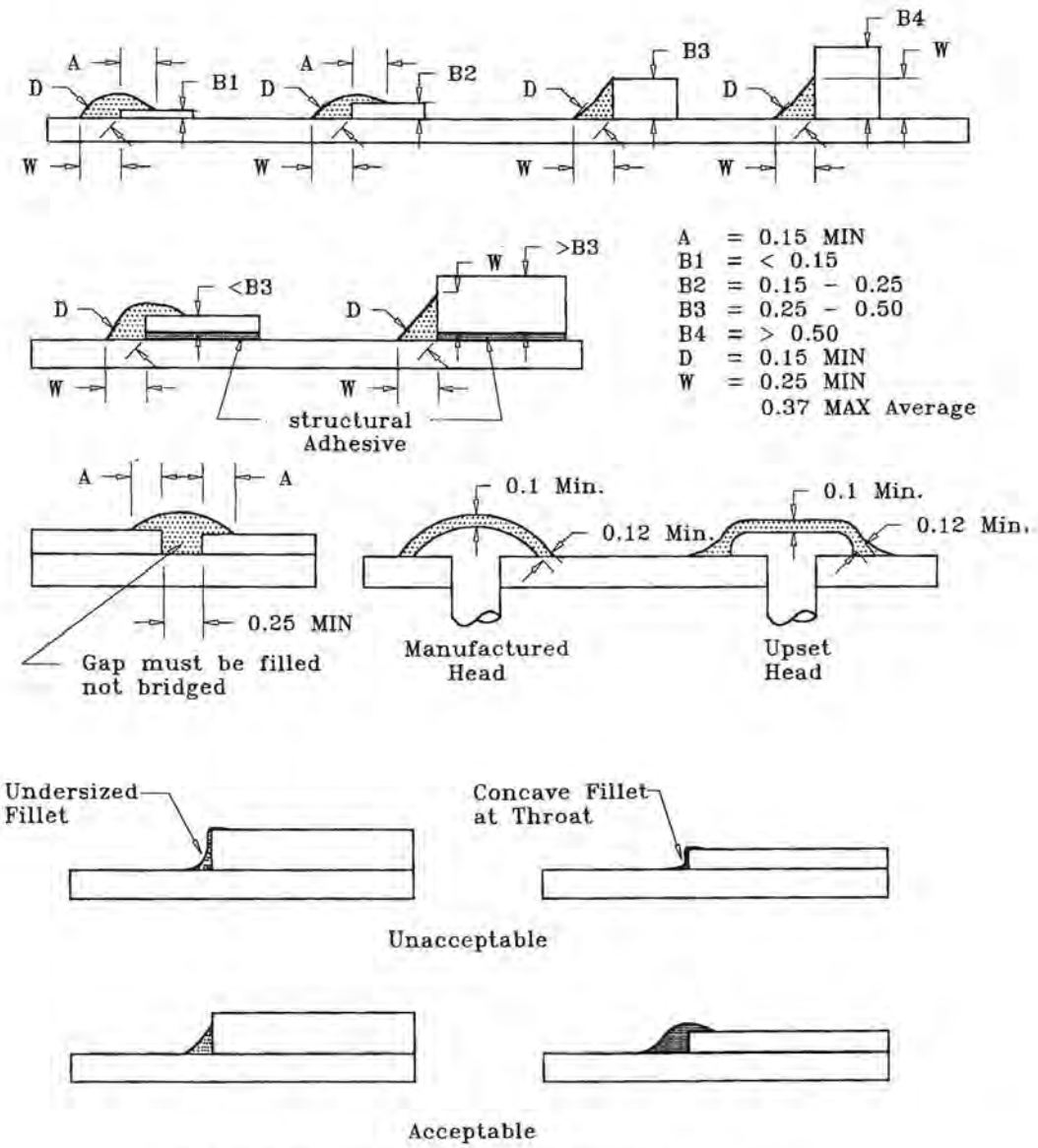

Fig. 7.44 Recommended fillet configurations.
(Based on less than 0.003 inch joint deflection)

IR Voltages: High voltages might be developed within a resistive CFC fuel tank carrying lightning current. As an example, consider the CFC wing subjected to lightning tests during a NASA sponsored program to gather design data on adhesively bonded aircraft structures [7.56]. During this program, tests were conducted on a CFC wing whose length was approximately 6.1 m (20 feet) from wing tip to fuselage centerline. The resistance of this wing, determined during impulse current injection tests, was found to be approximately 25 milliohms. If a severe lightning strike of 200 kA were to strike the wing tip and be conducted to the wing root, the voltage rise along the wing would be

$$\begin{aligned} V &= IR \\ &= (200,000 \text{ Amps})(0.025 \text{ ohms}) \\ &= 5,000 \text{ volts} \end{aligned} \tag{7.6}$$

where V = Voltage along the wing
I = Peak amplitude of lightning current
R = Resistance of wing.

If there were a fuel quantity probe at the tip end and if it were referenced to instrumentation ground in the avionics bay, there would be 5000 volts between the probe and the skin. This voltage might cause a spark between the probe ends and adjacent top or bottom skins.

If the aircraft were at 30 000 feet when struck, then by calculations using the Paschen curve of Fig. 7.27, the air gap required to prevent sparkover would have to be at least 4.5 millimeters. If a safety factor of 2 were used, as recommended in §7.3.6, the air gap distance would have to be about 10 mm (0.4 in).

If fuel quantity measurement requirements make it impractical to provide this much clearance, the designer would need to provide insulation in some other way, such as adding a dielectric coating to the fuel quantity probe or bonding of one or more layers of dielectric material to the interior fuel tank skin adjacent to the quantity probe tip ends. Either method would minimize the possibility of a spark flashover. An actual probe specimen should still be tested to determine the actual sparkover voltage.

The problem of high IR voltages is not confined to the design of hardware installations. Potential differences can also develop between structural elements located along the lightning current path which are isolated from each other. This is the case in a wing tank in which the spars and ribs may be adhesively bonded to the wing skins with electrically non–conductive adhesives. The potential differences which can occur under such conditions can result in voltage sparkover of the adhesive bond line between the structural elements. This will happen most often in locations where no rivets or fasteners are used in either composite or metal structures although the potential is greater in composite structures due to the higher voltages which may develop.

Adhesive bond line voltages: Adhesive bond line voltages, recorded on two full scale wing structures during the NASA study mentioned previously [7.57], showed that voltages across adhesively bonded aluminum structural elements could reach 2.5 volts during conduction of 200 kA test currents. By contrast, voltages measured across adhesively bonded CFC elements were 200 volts for 190 kA test currents [7.58]. This voltage might be reduced by adding a few rivets at selected locations to lower the voltage potential difference between the elements. Alternatively, fuel tank sealant could be applied along joint interfaces to contain any sparks.

Increased currents: The second problem faced by the designer of CFC tanks is the magnitude of the currents through the fuel tank plumbing. A lightning strike to a wing tip, for example, will result in lightning current passing through the wing to an exit point located elsewhere on the aircraft. These currents will seek conductive paths which include the wing skin, spars, ribs, and internal fuel tank plumbing.

Initially, the current divides according to the inductance of all the elements and largely stays in the CFC. At later times currents divide according to resistance of the various current paths. The internal metal plumbing is more conductive than the CFC skin, so a large part of the current transfers to the plumbing. Since the current diffuses rapidly into the CFC, the waveshape of the current on the inside surfaces of CFC structures is thus about the same as it is on the external surfaces.

Typical current distributions in metal and CFC tanks are shown graphically in Fig. 7.45. The total lightning current entering the wing is shown in Fig. 7.45(a). The currents in metal plumbing or hardware can reach high levels, in some cases being a major portion of the total current. By comparison, currents will remain for a longer period of time in the skin of a metal wing and diffuse more slowly into internal metal conductors, never reaching high amplitudes.

Current distribution patterns: Current distribution patterns in a CFC wing structure were measured during a NASA study [7.59 and 7.60]. A 900 A current wave was injected into the base of a static discharger located at the wing tip with the amplitudes of the current in the skin, leading edge conduit, control cables, and hydraulic lines measured at four microseconds and 80 microseconds. Results are shown in Figs. 7.46 and 7.47. The figures show that during the initial portion of the strike, the skin conducted approximately 74% of the test current but this percentage decreased to 29% after 80 microseconds. At this latter time, a large portion of the current, which had been originally conducted by the skin, was now being conducted by the leading edge conduit, control cables, and hydraulic lines.

The higher peak amplitude currents conducted by fuel tank plumbing in a CFC tank present additional challenges for the designer. While plumbing in an aluminum tank may conduct currents of several amperes or even hundreds of amperes, plumbing within a CFC tank may be required to conduct currents of several thousand amperes. Couplings designed for plumbing of metal tanks can conduct up to 2500 amperes without sparking. This level is satisfactory for metal tank designs but is inadequate for the thousands of amperes which can occur within a CFC tank. Thus, the designer will need to consider alternatives such as electrically non–conductive isolation links located within the plumbing lines at appropriate locations or com-

plete replacement of metal fuel or vent lines by electrically non–conductive lines.

If electrically non–conductive lines are used, the material from which they are fabricated will need to be doped to provide a minimal level of electrical conductivity (high resistivity) for static charge dissipation. The resistivity of the material should be of the order of 10^6 ohm–centimeters. If this is not done, high speed refueling and rapid fuel transfer operations could build up static charges on these lines resulting in spark discharges within the tank.

Fuel and vent lines which conduct currents should be carefully designed at their interfaces with the structure to contain arc and spark products which may occur. The performance of these interfaces should be verified by tests performed at the maximum current level expected.

Induced voltages: The third problem faced by the fuel tank designer of a CFC tank is that of voltages induced on electrical wiring within the tank, such as those associated with the fuel quantity probes. As discussed in §7.7.5, induced voltages can appear between all of the incoming wires and the airframe. Since the shielding effectiveness of the CFC skin is lower than that of an aluminum skin, additional care must be taken by the designer to ensure that adequate gaps are maintained between the active electrodes of the fuel quantity probe and the airframe.

Magnetic field intensity: A comparison between the magnetic field intensities occurring within an aluminum wing and those occurring within a CFC wing was made during tests conducted for the previously mentioned NASA program [7.61]. The magnetic fields in the CFC wing were 3.0 to 3.7 times larger than in a comparable aluminum wing.

Direct arc attachment: The problems described above must be addressed during the design of both aluminum and CFC fuel tanks but are more difficult to solve for CFC tanks. In addition, the designer must also solve the problem of direct lightning arc attachment to the fuel tank external skin. The problem of a possible skin melt–through faced by the designer of a metal fuel tank becomes the problem of a skin puncture for the designer of a CFC tank.

The CFC material is composed of graphite yarns and epoxy resin. Since the melting point of graphite 2060°C (3735°F) is much higher than the temperature at which pyrolysis of resin occurs 160°C (315°F), attachment of the lightning arc damages the CFC by pyrolysis and, usually, ignition of the resin, which in turn causes gross delamination. Burning of the resin then leaves the entire composite in disarray; however, damage is generally limited to that which is visible at the attachment point.

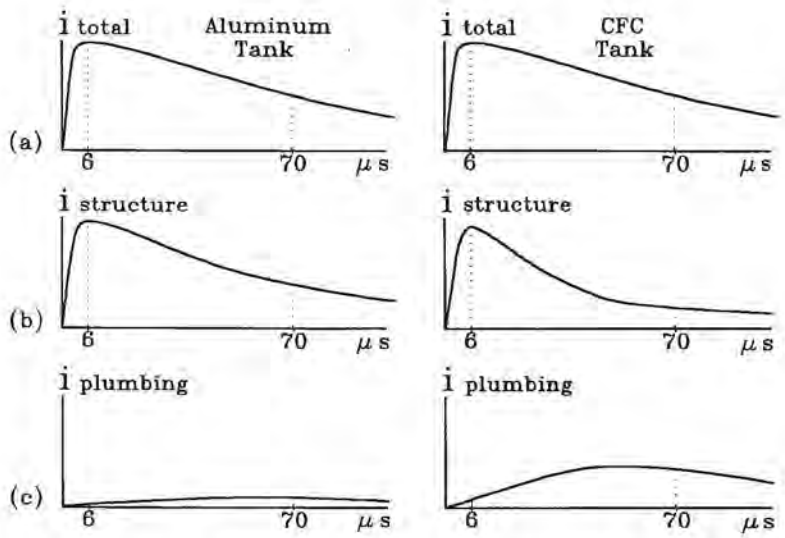

Fig. 7.45 Lightning currents in plumbing within aluminum and CFC tanks.
(a) Total current
(b) Current in structure
(c) Current in plumbing

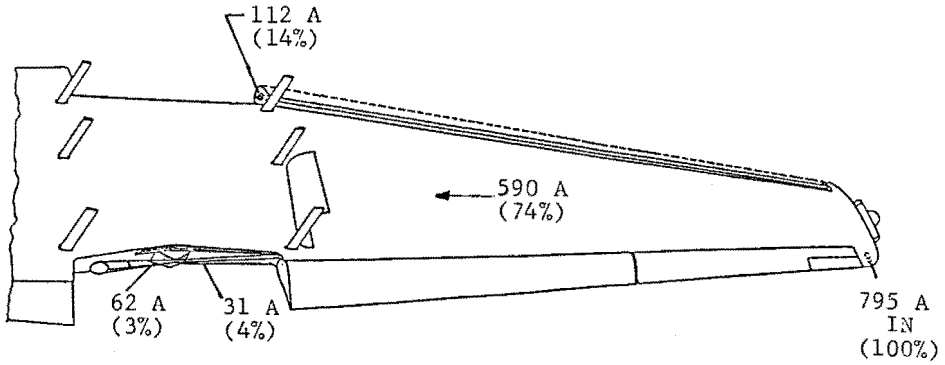

Fig. 7.46 Current distribution patterns in a CFC wing.
- T = 4 microseconds, 900 ampere current
- Strike to the static discharger.

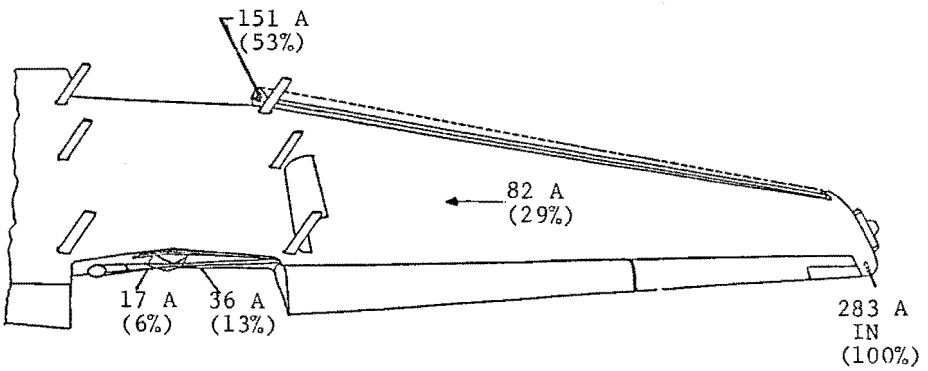

Fig. 7.47 Current distribution patterns in a CFC wing.
- T = 4 microseconds, 900 ampere current
- Strike to the static discharger.

Graphite epoxy skins 0.150 inches thick will generally be capable of sustaining a severe lightning strike without puncture or cracking. Thinner material, or the addition of primers and paints to the exterior surface, will lower the peak current amplitude and action integral which the skin can successfully sustain without creating a fuel ignition hazard. Lightning protection methods might need to be employed. These may include exterior surface protection consisting of flame or arc spray metals, woven wire mesh, metallized fabric or tape, or the use of thin wires woven into the outer ply fabric. The protection afforded by the method chosen should be verified by test. A complete discussion of the protection methods mentioned above is found in Chapter 6.

7.12 Non–Conductive Tanks

In some cases electrically non–conductive materials, such as fiberglass–reinforced plastics (FRP) are used instead of metals or conductive composites for skins of fuel tanks. For example, the light aircraft of Fig. 7.48 has FRP wing tips containing fuel tanks containing aviation gasoline. These tanks have suffered several in–flight explosions due to lightning strikes. The explosions are probably the result of these tanks being located in *Zones 1A* and *2A*.

A lightning arc that contacts an aluminum tank may melt through the skin, while one that attaches to a tank made of conductive composite may puncture the skin. For a tank fabricated of electrically non–conductive material, however, the lightning flash will either:

1. Puncture the skin and attach to an electrically conductive object inside the skin (tank), or

2. Divert around the non–conductive skin and attach to the adjacent conductive skin or to some other object.

If the arc remains on the exterior surface, it is not likely that the skin will be damaged such that a fuel

ignition occurs. The current is not being electrically conducted through the skin and the hot arc does not lie close enough to the the surface to burn through it. Usually all that happens is that the surface is slightly singed.

The punctures that do occur may be explained by the basic lightning attachment mechanism described in Chapters 3 and 6. Obviously, if a puncture occurs through an integral fuel tank wall, fuel is placed in direct contact with the lightning arc, and ignition is probable.

Even if a puncture does not occur, it is possible that, an internal streamer could ignite fuel by itself, though this has not been proven by test. Tests have shown that corona currents (glow discharge) are not capable of ignition. Protection against ignition therefore requires that two basic criteria be met:

1. Punctures must be prevented.
2. Internal streamers should be prevented.

These criteria are, of course, in addition to other requirements such as elimination of ignition sources from strikes to vent outlets or sparking across joints discussed elsewhere in this chapter.

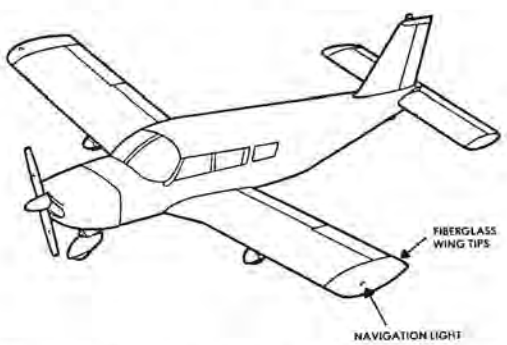

Fig. 7.48 General aviation aircraft with plastic wing tips

Prevention of puncture: Successful prevention of internal streamers is necessary to prevent skin punctures. Because streamers form most readily from sharp conducting edges and corners, the number of metal parts inside a electrically non-conductive fuel tank should be minimized whenever possible, and those that remain should be located as far from electrically non-conductive skins as possible and designed with smooth, rounded edges instead of sharp points. Puncture of electrically non-conductive skins can also be prevented through the use of several possible protection materials, as was discussed more thoroughly in Chapter 6. These include:

1. Flame or arc sprayed metals.

   These provide very effective protection with a weight penalty of approximately 0.5 kg/m^2 (0.1 lb/ft^2). Application is operator dependent.

2. Woven wire mesh.

   Typically, a mesh of aluminum wires, 47 to 79 wires per cm (120 to 200 per inch), is used. Weight penalty is approximately 0.25kg/m^2 (0.05 lb/ft^2). These work well on flat surfaces, but not on compound contour surfaces.

3. Metallized fibers.

   Metallized fibers of aramid resin or fiberglass are used for the surface layer. May be painted.

A more detailed discussion of the above protection methods is presented in Chapter 6.

7.13 Fuel System Checklist

A considerable amount of information on various aspects of fuel systems has been presented in the preceding paragraphs. With reference to these paragraphs, the following checklist is provided to summarize key points and to focus the designer's attention on the important aspects of fuel system lightning protection:

1. Are the fuel tanks located in *Zones 1* and *2*, where lightning strikes may directly contact their skins? (Chapter 5). If so,
   (a) What is the expected arc dwell time on these skins? (§7.6).
   (b) If the tank is of metal construction, are the skins thick enough to avoid melt–through? (§7.6).
   (c) If the tank is of conductive composite construction, is adequate protection provided to prevent puncture? (§7.8).
   (d) Can a lightning arc attach directly to an access door or filler cap? If so, can the lightning current be conducted into the surrounding skin without arcing inside the tank? (§7.7).
2. Are there "dry bay" areas into which fuel may leak from adjoining tanks or plumbing? If so, these are also subject to questions 1a, 1b, 1c, and 1d.
3 Are fuel vent outlets or jettison pipes located in direct strike zones (*Zones 1A* or *1B*) or swept

flash zones (*Zones 2A* or *2B*) where the lightning arc may attach or sweep close to the vent outlet? (Chapter 5, §7.4 and §7.5). If so,

(a) Is an effective flame arrester or surge tank protection system used? Has the effectiveness of this system been verified by test? (§7.4).

(b) Is the response time of the surge tank suppression system shorter than the possible flame propagation time from the sensor to the extinguisher? (§7.4).

(c) Is the system protected from false trips resulting from lightning–induced voltages in its electrical wiring or from the light of nearby flashes?

4 If electrically non–conductive skins are used, is adequate protection provided by protective surface materials? (§7.9).

5. Is the fuel tank structure capable of conducting Zone 3 lightning currents even if the tank itself is not located in a direct or swept flash zone? Has this been demonstrated by a test in which simulated lightning currents are conducted through a complete tank structure? (§7.7).

6. If a simulated lightning test of the complete tank assembly is not feasible, have all of its individual joints, access doors, filler caps, drains, vents, plumbing, and electrical systems been tested for their ability to conduct simulated lightning currents and found to be free of arcing? (§7.5 and §7.7).

7. Are electric circuits entering the fuel tanks protected against high induced voltages? (§7.7). Have they been routed away from other wiring, such as navigation lamp circuits, which may be susceptible?

8. Are clearances between exposed electrical parts or between any of them and the airframe sufficient to prevent the occurrence of sparks from induced voltages? (§7.7).

9. Have the electrical circuits inside the tank been adequately shielded so that excessive induced voltages will not occur? (§7.7).

10. Have applicable government airworthiness certification regulations, military standards, or other specifications pertaining to lightning protection been adhered to? (Chapter 5.)

7.14 Tests and Test Techniques for Fuel Systems

Some of the tests appropriate for fuel systems are discussed in the following sections.

7.14.1 Measurement of Electrical Continuity and Resistance

Previous discussions on fuel tank arcing have described the need for good electrical contact between mating structural elements and between fuel line plumbing and its interface with structural elements in order to minimize the possibility of arcing. For metal tanks, assurance of adequate electrical contact can be obtained by performing electrical bonding measurements between appropriate conducting elements. These measurements may be performed using a Kelvin bridge or equivalent.

The military specification on electrical bonding, *MIL-B-5087B* [7.62], specifies that for Class L bonding (lightning protection), voltages in excess of 500 volts shall not be produced during application of currents of 200 kA. This specification implies that the maximum bonding resistance should be 2.5 milliohms.

Bonding resistance measurements made on composite structures present difficulties not encountered in metal structures. While adequate electrical contact can be made between a metal structure and measurement leads by cleaning the contact surface of finishes and contaminants, the same is not true of parts constructed of CFC material. The epoxy in CFC material, of course, is an electrically non–conductive material integrally bound with the electrically conductive graphite yarns.

Surface resin, therefore, may prevent electrical contact from being made with the graphite yarns. A light sanding of the CFC surface may expose some of the graphite yarns resulting in intermittent or marginal contact with a flat–surfaced test probe. If a pointed probe is used, a reading will be obtained only if the probe point contacts one of the graphite strands. Since structural elements of CFC will be adhesively bonded in the majority of cases, the electrically non–conductive adhesive will cause the bond line resistance to be very high with the actual resistance depending on the degree to which contact is made across the bond line

To date no specific guidelines for composite bonding measurements have been included in *Mil-B-5087B*.

7.14.2 Tests on Individual Items

Federal Aviation Regulations parts 23, 25, 27, and 29 require that an aircraft fuel system be designed to

prevent the ignition of fuel vapor within the system. Tests are usually needed to verify that the possibility of a fuel tank explosion has been minimized. These tests can be performed on panel specimens representative of sections of the full scale fuel tank as well as on individual plumbing hardware items such as a fuel quantity probe or fuel line couplings. Once these tests have been performed and the lightning protection design proved, further tests on a full scale tank can be performed for certification. This may not be practical for all cases. Certification in these cases may be based on the results of the panel specimen and plumbing hardware tests as well as on analyses and similarity to previous designs.

Tests which may be performed on panel specimens or plumbing hardware include the following, with all tests performed in accordance [7.28].

Skin thickness: The exterior tank skin should be tested by high current direct attachment tests to verify that the skin thickness and/or protection design is sufficient to prevent melt–through of a metal skin or puncture of a CFC skin. All typical fillers, primers, and paints should be applied to the skin surface since their presence is a factor in the degree of damage which occurs. The dwell time of the test can be determined by analysis or by swept stroke tests.

Access doors: A typical access door configuration should be fabricated into a panel specimen and tested by high current arc attachment to determine if arcs or sparks occur on the interior side of the door. This may be accomplished by attaching the panel specimen to one end of a light–tight chamber, as shown in Fig. 7.49, with cameras located within the chamber at the opposite end. With the chamber sealed, the simulated lightning arc is discharged to the specimen surface during which time the camera shutters are open to record any arcs or sparks which may occur. Following the test, the shutters are closed, the film removed, developed and then examined for light spots that would indicate the possibility of arcs or sparks. It is helpful to use both Polaroid and 35 mm cameras, since the Polaroid pictures provide instant data and the 35 mm film can be processed after the test series is complete.

Arc entry tests should be applied to the center of the access door as well as to several door fasteners. These tests will show the adequacy of the access door–to–adapter gasket seal as well as the seals of the door fasteners/dome nuts to prevent arcs and sparks from entering the fuel vapor space. These specimens may also be tested with a flammable fuel/air mixture in the chamber but, should an ignition occur, it would be difficult to locate its source.

Vent outlets: Simulated strikes to a vent outlet should be performed to determine if fuel vapor ignition can occur, especially if the outlet is located in a direct strike attachment zone on the aircraft. This may be accomplished by striking a vent outlet structure which contains a flammable vapor mixture. If an ignition occurs, an investigation should be made to determine the cause of the ignition. Possible corrections should be investigated, such as incorporation of a flame arrestor in the design if one does not exist. If no ignition occurs, the vapor should be ignited manually, by a spark plug for example, to verify that a flammable vapor did exist during the test. The tests should be repeated several times to obtain additional information as to the expected probability of an ignition.

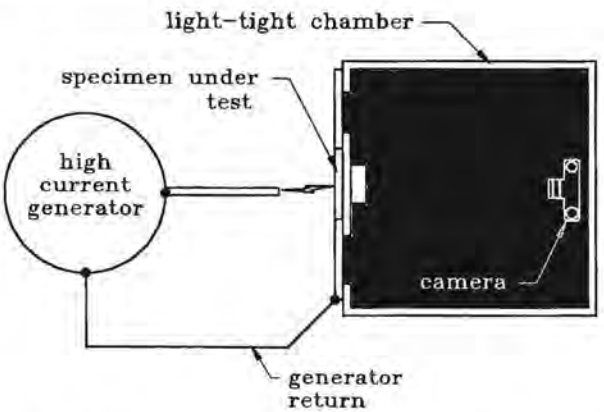

Fig. 7.49 A light-tight chamber for fuel tank component and skin arc and spark tests.

Drain valves: A typical drain valve/skin interface panel should be fabricated and tested. These tests may consist of the flammable vapor technique in which a successful test result is the absence of fuel ignition or by the light–tight chamber technique in which the absence of visible light on the Polaroid and 35mm films indicates the lack of an ignition source.

Fuel filler caps: A panel should be fabricated which includes the fuel filler cap, its mating adapter, and the adjacent fuel tank skin. All gaskets and sealants associated with the filler cap and its adapter should be present. The cap may be tested with a flammable vapor; however, the photographic technique is used more often since it is difficult to determine the exact cause of a failure when a flammable vapor ignition has occurred. The test involves striking the cap directly by high current arc entry.

Fuel line couplings: As mentioned previously, some fuel line couplings can conduct currents without arcing or sparking at current levels of less than 2500 am-

peres. For a tank constructed of CFC, there is a high probability that this limit will be exceeded so that alternatives, such as isolation links or electrically nonconductive fuel and vent lines should be considered. If the expected current levels in the plumbing are low, as in a metal tank for example, it may be desirable to evaluate the arc threshold level of the couplings to compare with the currents which are expected. The arc threshold level may be determined by inserting the coupling into the light-tight chamber described previously. Initial test current amplitudes should be lower than the expected arc threshold level of the coupling with subsequent tests performed at increasing current amplitudes until arcs are detected. Several coupling samples should be tested to obtain a range of spark threshold levels.

Fuel quantity probes: Capacitance type fuel quantity probes, as described in §7.9, may become fuel ignition hazards if the voltage potential difference developed between them and the adjacent interior tank skin surface is high enough to result in an air gap flashover. This condition is most likely to occur in a fuel tank constructed of CFC because of the high IR voltages which can develop along the skin during a lightning strike. It is advisable to perform voltage flashover tests on a typical fuel quantity probe since the curves shown in Fig. 7.27 can only be considered approximate.

The probe to be tested should be positioned adjacent to a simulated fuel tank skin surface so that the test setup accurately represents actual fuel tank probe to skin air gap dimensions. Voltage impulses, such as the 1.2×50 μs voltage waveform B of [7.28] and MIL-STD-1757A [7.63], should be applied by direct connection to the probe with the simulated tank skin connected to test circuit ground. Initial peak voltage levels applied to the probe should be lower than the expected flashover level, with subsequent tests performed at increasingly higher levels until voltage breakdown results in an air gap flashover. The voltage flashover level determined by these tests must be adjusted for the air pressure level at cruising altitude.

7.14.3 Full Scale Tests on Tanks

Once tests have been completed on the hardware and panel specimens described above, the fuel tank should be ready for full scale tests to verify portions of the design which cannot be obtained from the panel and hardware tests. These include measurement of adhesive bond line voltages, current amplitudes in plumbing and vent lines, voltage potential differences between fuel quantity probes and adjacent fuel tank skin, and evaluation of potential ignition sources at access doors, fuel filler caps, structural interfaces, fuel quantity probes, and couplings in fuel and vent lines.

Measurement of voltage and current on wiring: Measurements of voltages and currents induced in electrical wiring and plumbing located within the tank should be made. Test currents are conducted directly into a typical lightning attachment location, such as the wing tip. Current return wires are connected to a typical current exit point, such as the wing root area. Positioning of the return wires around the structure is important since the magnetic fields associated with them can affect the magnetic field environment within the tank. Ideally, the internal tank field environment should only be a function of the currents in the tank skin as occurs during strike attachment, in a natural lightning environment. Return wire influence can be minimized by positioning the wires in a radial array around the aircraft structure, as discussed in Chapter 13.

Measurement of current on plumbing: If possible, measurements should also be made of currents in fuel and vent lines for comparison with the spark threshold levels determined during fuel and vent line hardware tests and also for comparison with analyses of the current levels expected in these tanks.

Measurement of voltage on fuel probes: Voltage differences between fuel quantity probes and the adjacent interior skin surfaces can be measured and compared to the voltage breakdown levels determined during tests on the probes. Measurements at five fuel probe locations within the NASA CFC wing showed voltages ranging from 1200 volts at the wing root probe to 3200 volts for the wing tip probe when currents of 190 kA were conducted through the wing.

Tests to determine ignition sources: Ignition source tests should be performed on a full scale wing to determine whether couplings, access doors, fuel filler caps and adapters, structural interfaces, or fuel quantity probes located within the tank will be the source of fuel ignitions. Although tests will most likely have been performed on individual fuel tank elements to determine arc and spark threshold levels, it is also recommended that ignition source tests also be performed on a full scale fuel tank. Current densities in materials and current amplitudes in structural elements are difficult to analyze for a complex full scale structure and the numerous paths that can exist in a tank can result in the existence of several locations where arcs or sparks could occur. Full scale tank tests can also verify the adequacy of the sealant application which is usually an important part of the lightning protection design. A more detailed discussion of procedures for

arc and spark source detection tests is given in §7.14.4.

Measurement of adhesive bond line voltage: Adhesive bond line voltages should be as low as possible, with a maximum upper limit of 500 volts as specified by *MIL-B-5087B*. It may be desirable to measure bond line voltages when the opportunity arises, but the tests should be viewed as an attempt to gain engineering data, and not as an attempt to verify a design. The only way to know if bond line voltages can result in arcs or sparks is to conduct full level tests on the wing.

7.14.4 Detection of Internal Arcs and Sparks

The most important tests to performed on a full size tank involve the detection of potential arc and spark sources within the tank. Areas of concern include access doors, fuel filler caps and their adapters, drain valves, couplings in fuel and vent lines, fuel quantity probes, and interfaces between electrically conductive elements.

Many tests will be required because of the numerous areas which need to be checked, with each of them performed at the applicable severe lightning threat current level. In order to minimize damage to the test article, the majority of the tests should be performed by directing the test currents into the test specimen at a typical attachment point, such as the wing tip area for a wet wing tank. Arc attachment tests must also be made to a wing skin area, wing tip, fuel filler cap, vent and drain valves, access doors (to the center of the door as well as to several door fasteners), and exterior skin fasteners which extend to the interior of the tank.

Detection of arcs and sparks may be performed by two methods: through the use of a flammable vapor mixture or by the photographic technique.

Flammable vapor tests: This test involves placing a flammable vapor in the tank and seeing if any test on the tank ignites the vapor. The method is more suitable for testing structures of small volume than it is for most full size fuel tanks. If the volume of the tank interior is small enough, it may be desirable to perform the tests with a flammable vapor such as a 1.2 stoichiometric mixture of propane and air. Suitable precautions should be taken, such as the use of blow out panels, to preclude explosion of the structure. The fuel/air mixture technique is useful if the tank contains numerous interfaces and an intricate plumbing arrangement such that a camera would not be able to view all of the areas of concern during the tests.

Advantages and disadvantages: Advantages of the fuel vapor ignition technique include the ability to evaluate tanks of complex construction or tanks with tightly spaced interiors, and the ability to evaluate tanks constructed partially or completely of translucent material. Disadvantages include the dangers inherent in working with flammable vapors which include hazards to personnel as well as possible damage to the test article, the inability to pinpoint the cause of an ignition should one occur, and the need for large volumes of fuel for tests on large tanks.

Sensitivity of fuel vapor ignition tests: The 200 microjoule minimum ignition level criterion is based on the Bureau of Mines work by Lewis and Von Elbe and others. However, their work was to determine minimum ignition characteristics and contained no information on conditions, procedures, or statistics related to the ignitions. Tests by Crouch [7.68] showed that the probability of a 200 microjoule ignition under optimum conditions was of the order of 1 in 1000 to 1 in 10,000. Thus the 200 microjoule criterion may be too severe and a 500 to 600 microjoule level, which occurred between 1 and 10 percent of the time, may be more realistic.

An alternative would be to use an oxygen rich mixture (30% oxygen) to detect 200 microjoule sparks. Crouch found that this ratio would result in ignitions 70-80% of the time. Whether the photographic or fuel vapor ignition technique is used during a test program will depend on the type of information test personnel wish to obtain and the physical configuration of the specimen to be tested.

Photographic detection: The photographic technique is the preferred method for full scale testing. Information on ignition source testing using the photographic method of detection is described in §4.1.3 of [7.28] and §5.0 of [7.63]. These documents state that the visible light emitted from a source of ignition can be detected on photographic film having a light sensitivity rating of ASA 3000 when used in conjunction with a camera whose lens is set to an aperture of f/4.7.

Advantages and disadvantages: The advantages of the photographic method are that it is safe, able to pinpoint the source of an arc or spark, can be used to test both large and small tanks as well as fuel system components, and that it requires a minimum amount of equipment. Disadvantages include the inability of cameras to view all areas of a tank due to tank complexity and space constraints, the marginal ability of the camera/film combination to detect 200 microjoule sparks, the possible confusion of dust on the photograph as a minute spark, and the inability to detect arcs and sparks when all or part of the material of

which the test article is constructed is translucent. Translucence has become a greater problem in recent years as more and more aircraft parts and structural elements are manufactured of plastics or composite materials.

Film and cameras: Several small cameras (35mm or Polaroid) are located within the tank to view as much of the tank interior as possible for each test. The cameras are loaded with black and white or color film having an equivalent sensitivity rating of ASA 3000 and f/4.7. This can be accomplished using faster films and higher f/stops or vice versa.

Color film has some advantages over black and white film. Different light sources might produce different colors on the film. The light from a spark source might record as blue or white, while the light transmitted through translucent interior tank walls may show dull red or yellow. This could help test personnel determine the nature of the light source. An example of a photograph showing light from an ignition source in a fuel tank is shown in Fig. 7.50.

Fig. 7.50 Photograph obtained during full scale fuel tank test.
Existence of light on the photograph indicates that an ignition source may be present.

Test procedure: In order to minimize the number of strikes applied to the fuel tank under test and also be able to view all the potential arc and spark sources which may exist, it will be necessary to use as many cameras as practical for each test. The procedures are as follows:

1. Position each camera to view an area of the tank considered to contain a potential arc or spark source. The cameras should be held in position through the use of an electrically non-conductive material, such as styrofoam, which can be placed between the cameras and the tank structure. This material will also electrically isolate the cameras from the tank, minimizing the possibility of arcing between the cameras and the tank.
2. Illuminate the tank interior and take a photograph with each of the cameras. This procedure will provide background photographs which show the tank areas as viewed by each of the cameras. If arcs or sparks are recorded during the tests, these background photographs will be helpful in determining their locations.
3. Set each camera lens at the appropriate aperture to satisfy the lens aperture/film speed requirements stated in the test documents.
4. Seal each area in which a camera is located so that it is light-tight.
5. Open and lock the shutter of each of the cameras to keep the lenses open.
6. Discharge the high current generator into the tank.
7. Close the camera shutters.
8. Recock the camera shutters and repeat steps 1-7 for the required number of tests.

Several tests may be performed before removing the film from the cameras. Indications of light on the photographs should be investigated since they could represent possible ignition sources. If it is determined that a light source is the result of an arc or spark, corrective measures can be taken, if possible, and the test repeated to determine if the corrective action has eliminated the light source.

Sensitivity of photographic detection: Questions have been raised about the reliability of the photographic method of testing and the 200 microjoule spark level criterion for fuel vapor tests.

The photographic method of arc and spark detection, developed in the late 1950's or early 1960's, grew out of a need to avoid the dangers of explosive testing. Initially the sparks were observed manually, but volunteers were not always available to sit in the test chamber with the test piece. Polaroid photography was employed to replace the observer. At that time, Polaroid camera lenses had a maximum aperture of f/4.7 and the film had a light sensitivity rating of ASA 3000. No data had been gathered to correlate spark energy with recorded light intensity, but the f/4.7 lens

aperture and ASA 3000 film speed combination was capable of detecting the light seen by the obsever.

Recent investigations by Crouch and Robb [7.67] have shown that a 200 microjoule spark is marginally detectable at distances of three feet with the f/4.7 lens aperture/Polaroid film combination described above. For a 35mm camera/film system, the 200 microjoule spark can be detected at camera–to–spark distances up to nine feet.

Pass/Fail criteria: Generally, a failure has been taken to be the presence of light on the test film(s) when photography is employed, or an ignition when a flammable vapor is used. Neither method gives a quantitative assessment of the margin by which the test specimen passed or failed. The test results do not give any indication whether a slight or major modification to the test article is needed for it to pass. Further investigations, such as the work being done by Crouch for the Naval Air Development Center [7.70], may provide the information needed to perfect fuel system test techniques.

REFERENCES

7.1 L. J. Nestor, "Investigation of Turbine Fuel Flammability Within Aircraft Fuel Tanks", *Final Report DS-67-7*, Aeronautical Engine Department, Naval Air Propulsion Test Center, July 1967.

7.2 Adapted from Nestor, "Investigation of Turbine Fuel Flammability", ibid, p. 8.

7.3 Redrawn from Coordinating Research Council, Handbook of Aviation Fuel Properties, *CRC Report No. 530*, Second Printing May 1984, p. 72.

7.4 Adapted from Nestor, "Investigation of Turbine Fuel Flammability", op cit, p. 23.

7.5 A. R. Bigelow, M. P. Hebert, H. Jibilian, "Electrostatic Field Measurements in a Foam Filled C–130 Fuel Tank During Fuel Sloshing," *International Aerospace and Ground Conference on Lightning and Static Electricty*, Dayton, OH, June 23-26, 1986, pp. 47-1 - 47-6.

7.6 W. Q. Brookley, "SAF C-141 and C-135 Fuel Tank Nitrogen Inerting Tests," *Report of the Second Conference on Fuel System Fire Safety*, 6 and 7 May 1970, Federal Aviation Administration, 1970, p. 75.

7.7 Von Elbe, G., Lewis, B., et al., "Ignition of Explosive Gas Mixtures by Electric Sparks", *Third Symposium on Combustion & Flame & Explosion Phenomena*, Baltimore: Williams & Wilkins Co., 1949.

7.8 K. E. Crouch, "Aircraft Fuel System Lightning Protection Design and Qualification Test Procedures Development Investigation of Fuel Ignition Sources", *NADC-86100-20*, August 1986, Naval Air Development Center.

7.9 M. M. Newman and J. D. Robb, "Investigations of Minimum Corona Type Currents for Ignition of Fuel Vapor," *NASA Technical Note D-440*, June, 1960.

7.10 "Investigations of Mechanisms of Potential Aircraft Fuel Tank Vent Fires and Explosions Caused by Atmospheric Electricity," *Final Report under Contract No. NA Sr-59*, prepared by the Lockheed–California Company, for the National Aeronautics and Space Administration, May 31, 1963.

7.11 Redrawn from "Investigations of Mechanisms of Potential Aircraft Fuel Tank Vent Fires," ibid, p. 84.

7.12 Redrawn from "Investigations of Mechanisms of Potential Aircraft Fuel Tank Vent Fires,"op cit, p. 90.

7.13 Redrawn from "Investigations of Mechanisms of Potential Aircraft Fuel Tank Vent Fires", p. 123.

7.14 Civil Aeronautics Board Aircraft Accident Report, Boeing 707-121, N709PA, Pan American World Airways, Inc., near Elkton, Maryland, December 8, 1963, File No. 1-0015, adopted February 25, 1965.

7.15 C. C. Bolta, R. Friedman, G. M. Griner, M. Markels, Jr., M. W. Tobriner, and G. von Elbe, "Lightning Protection Measures for Aircraft Fuel Systems, Phase II," *Technical Report ADS-18*, prepared by the Atlantic Research Corporation with the Lightning and Transients Research Institute for the Federal Aviation Agency, May 1964.

7.16 Based on Bolta et al, "Lightning Protection Measures", ibid, pp. 22 and B-3.

7.17 Bolta et al, "Lightning Protection Measures", excerpted from *Proposal No. PS-139*, Fenwal, Inc., Ashland, Massachusetts , pp. 70-79 and C-1 to C-3, January 23, 1964.

7.18 Bolta et al, "Lightning Protection Measures", ibid, pp. 116-149.

7.19 M. M. Newman, J.R. Stahmann, and J. D. Robb, "Airflow Velocity Effects on Lightning Ignition of Aircraft Fuel Vent Efflux", *FAA Final Report DS-67-9*, prepared by the Lightning and Transients Research Institute, with Consultant Staff Cooperation of the Atlantic Research Corporation, for the Federal Aviation Administration, July 1967.

7.20 Newman, Stahmann, and Robb, "Airflow Velocity Effects", ibid, pp. 10-20.

7.21 Redrawn from F. L. Kester, M. Gerstein, and J. A. Plumer, "A Study of Aircraft Fire Hazards Related to Natural Electrical Phenomena",*NASA CR-1076*, prepared by Dynamic Science for the

National Aeronautics and Space Administration, Department of Transportation, June 1968, p. 75.

7.22 J. P. Gillis, "Study of Flame Propagation through Aircraft Vent Systems", *Final Report NA-69-32*, prepared by Fenwal, Inc., Walter Kidde and Co., for the National Aviation Facilities Experimental Center, Federal Aviation Administration, May 1969.

7.23 Redrawn from Gillis, "Study of Flame Propagation", ibid, pp. 21, 22.

7.24 Gillis, "Study of Flame Propagation", ibid, p. 23.

7.25 Gillis, "Study of Flame Propagation", ibid, p. 35.

7.26 Federal Aviation Administration, *Advisory Circular AC 20-53A*, "Protection of Airplane Fuel Systems Against Fuel Vapor Ignition Due to Lightning", April 12, 1985.

7.27 Federal Aviation Administration, *User's Manual for AC-20-53A*, "Protection of Airplane Fuel Systems Against Fuel Vapor Due to Lightning", October 1984

7.28 Society of Automotive Engineers, Warrendale, Pennsylvania,"Lightning Test Waveforms and Techniques for Aerospace Vehicles and Hardware", 20 June 1978.

7.29 Crouch, "Aircraft Fuel System Lightning Protection", op cit, pp 6-6 to 6-9.

7.30 R. O. Brick, "A Method for Establishing Lightning–Resistance/Skin–Thickness Requirements for Aircraft," *Lightning and Static Electricity Conference*, 3-5 December 1968, pp. 295-317.

7.31 L. L. Oh and S. D. Schneider, "Lightning Strike Performance of Thin Metal Skin," *Proceedings of the 1975 Conference on Lightning and Static Electricity*, 14-17 April 1975, at Culham Laboratory, England.

7.32 Redrawn from L. Oh and S. Schneider, "Lightning Strike Performance," op cit, p. 12.

7.33 Kester, Gerstein, and Plumer, "A Study of Aircraft Fire Hazards ," op cit, p. 39.

7.34 Redrawn from L. Oh and S. Schneider, "Lightning Strike Performance," p.12.

7.35 T. S. Lee, W. Y. Su, "Transient Spark–Arc Hotspot Heating on Metallic and Reinforced Composite Skins," *International Aerospace and Ground Conference on Lightning and Static Electricty*, Orlando, FL, June 26-28, 1984, pp. 27-1 - 27-9.

7.36 E. H. Schulte, W. T. Walker, "Rear Surface Temperature Measurement of Aircraft Materials Subjected to Zone 2A Lightning Strikes," *International Aerospace and Ground Conference on Lightning and Static Electricty*, Orlando, FL, June 26-28, 1984, pp. 31-1 - 31-12.

7.37 K. G. Lovstrand, B. Olsson, B. Wahlgren and L. Anderson, "Lightning Test of a CFC Wing Skin," *International Aerospace and Ground Conference on Lightning and Static Electricity*, Orlando, FL, June 26-28, 1984, pp. 30-1 - 30-9.

7.38 G. Olsen, R. Force, and J. Lauba, "Ignition Hazard Study of Advanced Composite Fuel Tank," *Report D180-25598-1*, Boeing Military Airplance Co. Seattle, WA, May, 1980.

7.39 *Protection of Aircraft Fuel Systems Against Lightning*, Federal Aviation Administration, Advisory Circular AC 20-53, October 1967.

7.40 R. O. Brick, L. L. Oh, and S. D. Schneider, "The Effects of Lightning Attachment Phenomena on Aircraft Design," *1970 Lightning and Static Electricity Conference*, 9-11 December, pp. 139-156.

7.41 J. A. Plumer, "Lightning Effects on General Aviation Aircraft," *FAA-RD-73-99*, Federal Aviation Administration, October 1973, pp. 21-44.

7.42 J. D. Robb, J. R. Stahmann, and M. M. Newman, "Recent Developments in Lightning Protection for Aircraft and Helicopters," *1970 Lightning and Static Electricity Conference*, pp. 25-35.

7.43 B. D. Fisher, G. L. Keyser, Jr., P. L. Deal, "Lightning Attachment Patterns and Flight Conditions for Storm Hazards, 1980," *NASA Technical Paper 2087*, December, 1982.

7.44 D. H. McClenahan and J. A. Plumer, "Protection of Advanced Composites Against the Direct Effects of Lightning Strikes," *International Aerospace Conference on Lightning and Static Electricity*, Vol. II, Oxford, 23 - 25 March, 1982, G3-1 – G3-9.

7.45 K. Berger, "Development and Properties of Positive Lightning Flashes at Mount S. Salvatore with a Short View to the Problem of Aviation Protection," *Proceedings of the 1975 Conference on Lightning and Static Electricity*, 14-17 April 1975, at Culham Laboratory, England, p.7.

7.46 Crouch, "Aircraft Fuel System Lightning Protection", op cit, pp. 6-6 to 6-9.

7.47 M. M. Newman, J. D. Robb, and J. R. Stahmann, "Lightning Protection Measures for Aircraft Fuel Systems–Phase I," *FAA ADS-17*, prepared by the Lightning and Transients Institute for the Federal Aviation Agency, May 1964, pp. 22-44.

7.48 J.D. Robb, E.L. Hill, M.M. Newman, and J.R. Stahmann, "Lightning Hazards to Aircraft Fuel Tanks," *Technical Note 4362*, National Advisory Committee for Aeronautics, Washington, D.C. September 1958, pp. 12-14.

7.49 L. E. Short, "Electrical Bonding of Advanced Airplane Structures," *Lightning and Static Electricity Conference*, 3-5 December 1968, pp. 425-

441:433.

7.50 J.E. Pryzby and J.A. Plumer, "Lightning Protection Guidelines and Test Data for Adhesively Bonded Aircraft Structures," *NASA Contractor Report 3762*, pp. 33-35, January 1984.

7.51 J. A. Plumer, "Lightning–Induced Voltages in Electrical Circuits Associated with Aircraft Fuel Systems," *Report of Second Conference on Fuel System Fire Safety*, 6 and 7 May 1970, Flight Standards Service, Engineering and Manufacturing Division, Federal Aviation Administration, Washington, D.C. (1970), pp. 171-191.

7.52 J. D. Cobine, *Gaseous Conductors: Theory and Engineering Application* New York: Dover Publications, 1958, p. 164.

7.53 Newman, Robb, and Stahmann, "Lightning Protection Measures," op cit, p.15, 21-44.

7.54 Plumer, "Lightning Induced Voltages," op cit, pp. 176-178, 187-191.

7.55 Mahoney, J.W., Bush, C.A., and Dickerson, E.O., "Aircraft Integral Fuel Tank Design Handbook," Report *AFFDL-TR-79-3047*, Air Force Flight Dynamics Laboratory, pp. 3-11.

7.56 J.E. Pryzby and J.A. Plumer, "Lightning Protection Guidelines ", op cit p. 133.

7.57 Pryzby,"Lightning Protection Guidelines," ibid, p. 107

7.58 Pryzby, "Lightning Protection Guidelines," ibid, p. 165.

7.59 Pryzby, "Lightning Protection Guidelines," ibid, p. 142.

7.60 Pryzby, "Lightning Protection Guidelines," ibid, p. 143.

7.61 Pryzby, "Lightning Protection Guidelines," ibid, pp. 167-169.

7.62 *Bonding, Electrical, and Lightning Protection, for Aerospace Systems*, MIL-B-5087B, , 31 August 1970.

7.63 *Lightning Qualification Test Techniques for Aerospace Vehicles and Hardware*, MIL-STD-1757A, 20 July 1983.

7.64 Pryzby, "Lightning Protection Guidelines," op cit, p. 66

7.65 Pryzby, "Lightning Protection Guidelines," ibid, p. 147

7.66 Pryzby, "Lightning Protection Guidelines," ibid, p. 154

7.67 Pryzby, "Lightning Protection Guidelines," ibid, pp. 27-33

7.68 Crouch, "Aircraft Fuel System Lightning Protection Design", op cit, pp. 3-18 to 3-28.

7.69 Crouch, "Aircraft Fuel System Lightning Protection Design," op cit, p. 5.

7.70 K. E. Crouch, Work in progress, not yet reported.

CHAPTER 8

INTRODUCTION TO INDIRECT EFFECTS

8.1 Introduction

The previous chapters have dealt with the *direct effects* of lightning, but the remaining chapters will deal with *indirect effects*. The term *indirect effects* of lightning refers to the damage to or malfunction of electrical equipment that results from lightning flashes. These effects may range from tripped circuit breakers to computer upset, to physical damage of input or output circuits of electronic equipment. There may be other indirect effects of lightning flashes that pertain to aircraft safety, such as flash blindness of the crew or acoustic shock waves. These effects, however, are not treated in this chapter. Included in this definition and discussed here are the voltages and currents induced by lightning on the electrical wiring of the aircraft, irrespective of whether or not such voltages and currents cause damage or upset of electrical equipment.

This chapter is intended as an introduction to the chapters that follow. In it will be explained, briefly, some of the electrical phenomena involved along with a discussion of the program steps that must be taken to deal successfully with the indirect effects. Some of the measurements that have been made on aircraft to determine the nature of indirect effects will also be reviewed. Most of the subjects that will be discussed here will be discussed in more detail in later chapters.

8.2 Industry Activities

Some overview of industry activities is worthwhile because this volume can review only a small fraction of the material available on the indirect effects of lightning. The discussions in this and the following chapters will cite various references, but certain groups of documents are particularly important for further attention.

EMI/EMC: Many of the practices involved in the control of lightning indirect effects are the same as those involved in classical electromagnetic interference and electromagnetic compatibility and generally one can say that the practices that are good for control of lightning indirect effects, grounding, bonding and shielding are also good for control of *EMI/EMC* problems. This is not to say that they are the same and certainly not to say that attention to control of *EMI/EMC* problems will prevent problems of lightning. Some of the practices and mythology that have developed in fact impede solution of lightning problems. The classical EMI practice of grounding wire shields at only one end is perhaps the most important, a subject discussed in Chapter 16.

Speaking very broadly, analytical tools and test techniques developed for *EMI/EMC* are not particularly applicable to lightning indirect effect problems, principally because lightning is a time domain phenomenon and most *EMI/EMC* activities deal with the frequency domain. Practices related to narrow band RF emission and absorption may not adequately deal with time domain voltages and currents of magnitude sufficient to burn out electrical components.

NEMP: Nuclear electromagnetic pulse, *NEMP*, activities have had a great influence on lightning indirect effects, partly because that activity has been well funded and partly because *NEMP* is a time domain phenomenon, as is lightning. Virtually all of the analytical work on indirect effects has been influenced by the work done in the field of *NEMP*. Most computer codes of use for lightning analyses in aircraft were originally developed for *NEMP* and most of the analytical analyses dealing with coupling through apertures were refined and disseminated in connection with *NEMP*. Perhaps the best single summary of that analytical work is [8.1]. It contains numerous references to the most important of the original works.

Test techniques developed for *NEMP* have also influenced those for lightning. This is particularly true of bench tests in which current and voltage are injected into electronic equipment and the interconnecting wiring. Some of the test levels and waveshapes that appear in purchase specifications regarding lightning are virtually the same as those developed for *NEMP*.

All of the work related to voltage and current levels necessary to damage semiconductors (Wunsch analyses) have also come from the *NEMP* community. Some of that work is reviewed in Chapter 17

AEHP: A comprehensive review of work dealing with lightning indirect effects was conducted the Atmospheric Electricity Hazard Program organized by the US Air Force with Boeing Military Airplane Company as the prime contractor. In that program reviews were conducted of the lightning environment and the

threat presented to aircraft, protection concepts were reviewed and protection specifications were prepared for two testbed aircraft, an F-14A fighter aircraft and a YUH-61 helicopter. The program did not fund any research activities. Instead, it collected materials developed under other programs, sponsored various workshops to review the material and assembled them into a five part series of reports [8.2 - 8.6], each of which should be studied by the readers of this volume.

The AEH program dealt mostly with indirect effects of lightning, direct effects having been excluded from its charter. Direct effects were understood to be important and readers of the reports were cautioned to be aware of the necessity of dealing with direct effects. A limited review of direct effects was made [8.7], but no attempt was made to develop engineering data relating to direct effects.

SAE Committee activities: A group that has been charged with reviewing lightning design and test practices and with developing standards and advisory documents is the Society of Automotive Engineers (SAE) Committee AE4L. Members of this committee have included representatives from all areas of the US aircraft industry; manufacturers, the military, certifying agencies and test laboratories. It has also included representatives from the European counterparts of the US aircraft industry; this with the aim of coordinating US and European activities and promoting agreement between various certifying agencies.

Part of the SAE charter has been to draft documents that are ultimately issued as FAA Advisory Circulars and military standards. One such document [8.8] has previously been cited in connection with direct effects. Other documents include [8.9] and [8.10]. Much of the material from the SAE activities has been incorporated into a Military Standard [8.11].

FAA and NASA research: Both FAA and NASA have funded research oriented toward indirect effects. As examples, NASA funded the initial development [8.12] of the Lightning Transient Analysis (LTA) test technique to determine voltages and currents induced on aircraft wiring by lightning. The FAA has sponsored tests [8.13] to compare results using several test techniques, including the LTA technique.

8.3 Steps in a Control Program

Control of the indirect effects generally requires subjecting portions of the aircraft electrical and electronic systems to controlled tests in the laboratory. The control cannot be done only by analysis or by reliance on field experience, any more than control of other *EMI/EMC* problems can be controlled only by analysis; the aircraft systems and the aircraft interactions are too complex for that. One of the tasks that must be done is determining appropriate levels at which to conduct tests of the aircraft equipment, these being called equipment transient design levels (ETDLs). Electronic equipment in an aircraft is exposed to only a portion of the energy of the lightning flash, not its full effects. Analyzing how the lightning energy divides (and how it is manifested) can be called a *flowdown* process, though the term is not universally recognized.

The problem of analysis and control of indirect effects is a complex one, but, fortunately, analysis can be divided into several stages. These stages are illustrated in Fig. 8.1. The overall task is to determine how the lightning current, I_L, leads to voltages and currents on the internal wiring. The individual tasks in a program to control the indirect effects of lightning can be divided as follows:

1. Determine the amplitude and waveform of the current and electromagnetic fields external to the aircraft.

2. Determine the structural IR voltages and the internal electromagnetic fields.

3. Determine the response of the wiring of the aircraft to those voltages and fields; that is, determine the voltages and currents induced on the wiring.

4. Determine the response of electrical equipment to the voltages and currents; that is, identify circuits susceptible to either upset or damage.

5. Design and incorporate protective measures.

6. Conduct laboratory tests to prove immunity.

Organization of subsequent chapters: Broadly speaking, item 1 above is discussed in Chapter 10, item 2 in Chapters 11 and 12, items 3 and 4 in Chapters 13 and 14, item 5 in Chapters 15 and 16 and item 6 in Chapter 18. The various steps in the process, reduced to the form of a flow chart, are shown in Fig. 8.2. The section numbers on the figure refer to the AEHP design guide [8.14].

Background material: There are a number of miscellaneous points regarding electrical and mathematical concepts involved in analysis of indirect effects and these are reviewed and consolidated in Chapter 9, rather than being introduced piecemeal in later chapters. Some of the points discussed in Chapter 9, particularly the mathematical operations, are included for general reference since they are encountered in analytical works dealing with electromagnetic phenomena. Not all of them are explicitly used in the chapters that follow.

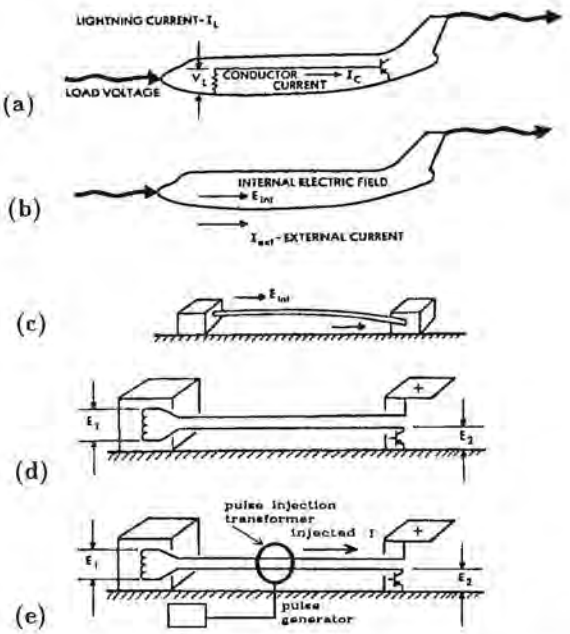

Fig. 8.1 Steps in controlling indirect effects.
(a) Determining the external environment
(b) Determining the internal environment
(c) Determining the response of cables
(d) Determining the response of terminal equipment
(e) Conducting verification tests

Loose coupling: The stages in the analysis can be separated because the aircraft and the wiring in it are only loosely coupled; meaning only that lightning affects the electrical wiring, but that the exact response of the wiring has no practical reverse effect on the amplitude or waveshape of the lightning current. There are situations where this may not be completely true and these are discussed in Chapter 10.

Status of standards and specifications: The arts of analysis and control of indirect effects are still evolving. Accordingly, the analytical procedures to be described are not as simple or as well developed as might be desired. Test practices, test procedures and test specifications likewise are still evolving. One result of this is that specifications for design and test are frequently incomplete, or stated in such a way as to force unnecessary or overly expensive design and test practices. Some of them neglect important aspects of lightning interactions with a result that systems may be put into practice without real lightning problems having been addressed. Some examples of these will be given in later chapters, along with discussions of good and bad points of typical standards and specifications.

8.4 Lightning vs Nuclear EMP

The art of analysis of lightning interactions has been influenced by research into *NEMP* and protective measures and test techniques have likewise been influenced by *NEMP*. Lightning and *NEMP* have certain similarities in their effects, but there are differences as well. Many of the practices that might be adopted for control of *NEMP* effects would also be good for control of lightning indirect effects (and *visa versa*) but it should not be assumed that the practices are the same. Certainly it should not be assumed that a design proven satisfactory for one phenomenon would necessarily be satisfactory for the other phenomenon. Some of the similarities and differences are discussed below and in the literature [8.1, 8.2].

NEMP: Ideally, *NEMP* can be considered as a phenomenon to which an aircraft will never actually be subjected.

If it should occur, it would consist of a single electromagnetic field pulse, or possibly several pulses if reflections are counted. The pulses would be of short duration (about 1 microsecond), would propagate in free space and would engulf an aircraft that is also in free space. When the pulses contact the aircraft they will be partially reflected and scattered with the result that there will be a certain electromagnetic field developed at the surface of the aircraft. These surface electromagnetic fields will be associated with currents on the aircraft and the currents would probably propagate back and forth, at a frequency determined by the size of the aircraft structure.

The surface currents, however, would be best thought of as a response to the electromagnetic field; that is, the field is produced first and it is the forcing function that causes the surface currents. It is logical, therefore, to base *NEMP* analyses on the response of the aircraft to electromagnetic fields. The most important response involves how much of the external field couples to the interior of the aircraft, a subject that is naturally addressed in terms of shielding effectiveness of the aircraft.

Lightning: Lightning to an aircraft is also a rare event, but does in fact occur sufficiently often that it should be regarded as something that sooner or later is almost certain to occur. It would differ from a *NEMP* event in that it is of longer duration (perhaps on the order of a second), involves many pulses in rapid succession, some of amplitude much higher than induced by *NEMP* and involves a direct contact between the

aircraft and the lightning arc. The currents on the surface of the aircraft may have an oscillatory component governed by the size of the aircraft, but the oscillation will also be influenced by the characteristics of the lightning channel.

The lightning current will produce electromagnetic fields at the surface of the aircraft, and also fields which propagate away from the aircraft. The forcing function, however, will be the current and the fields will be a consequence of that current. The concept of shielding effectiveness (ratio of field outside to field inside) is not a particularly helpful way to evaluate the response of the aircraft to the lightning current. It is more straightforward to base analyses of the effects of lightning on the concept of transfer impedance (ratio of internal voltage to external current), a subject discussed in Chapters 9 and 10.

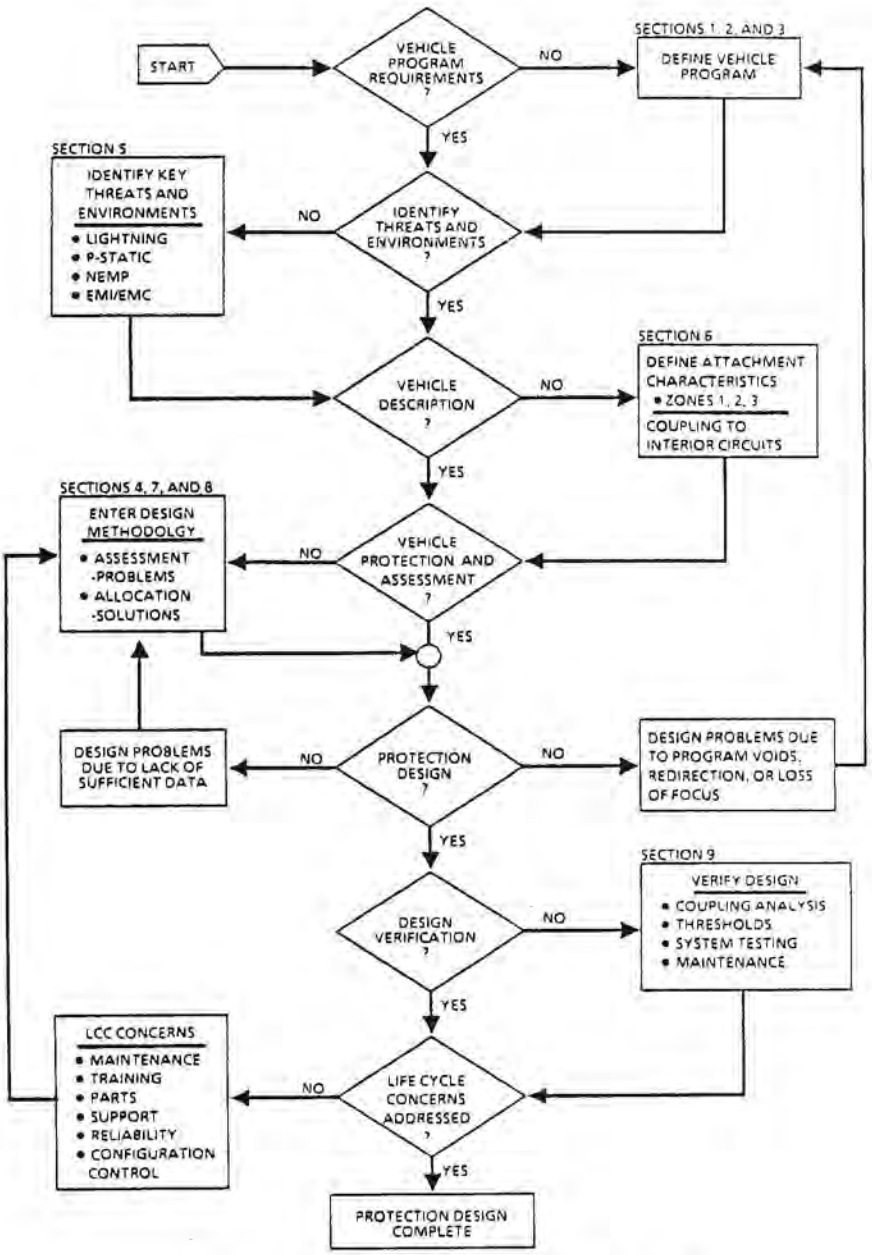

Fig. 8.2 Steps in the control of indirect effects (Flow chart form)

Coupling mechanisms: With *NEMP* the primary way that energy couples to the interior of the aircraft is through apertures. Aperture coupling is also important to lightning interactions, but coupling through resistive or diffusion mechanisms is also important, particularly for aircraft using large amounts of composite materials in their structure. These coupling mechanisms are illustrated in §8.5 and discussed in more detail in Chapters 11 and 12.

Frequency spectra: *NEMP* and lightning can also be compared according to their frequency spectra, Fig. 8.3 showing an example. Broadly speaking, *NEMP* involves more energy than lightning at high frequencies (50 MHz and above) while lightning contains more energy than *NEMP* at lower frequencies. The data of Fig. 8.3, should, however be viewed with caution since the frequency spectrum calculated for lightning is based on simplified waveforms that may not truly represent the multi–pulse nature of lightning. Research is indicating that there are portions of lightning currents that change with time more rapidly that previously assumed.

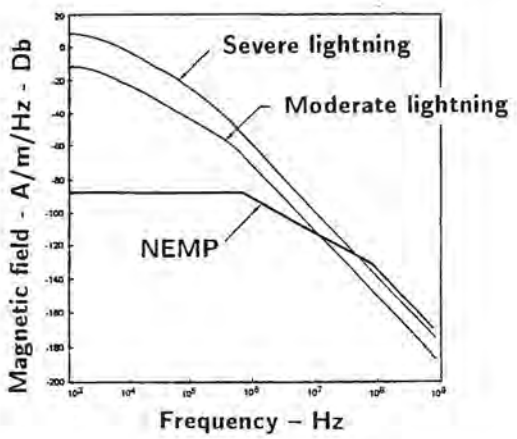

Fig. 8.3 Frequency spectra of lightning and *NEMP* (Range = 0.75 m)

8.5 Basic Coupling Mechanisms

A metal aircraft is often viewed as a Faraday screen, a concept from electrostatics which implies that the electrical environment inside the aircraft is separate and distinct from the environment outside. To some extent this is true; the lightning environment inside an aircraft is not nearly as harsh as is the external environment. There are, however, some important mechanisms by which electrical energy couples to the interior of the aircraft. The basic coupling methods are shown on Fig. 8.4. Subsequent chapters discuss the points in greater detail.

8.5.1 Resistive Voltage

The first of these relates to the electric field produced along the inner surface of the aircraft by the flow of current through resistance, or in elementary terms the resistive voltage rise caused by the passage of current. In some cases an easily identifiable resistance will be involved, though frequently the resistance will be of a distributed nature and probably frequency or time dependent.

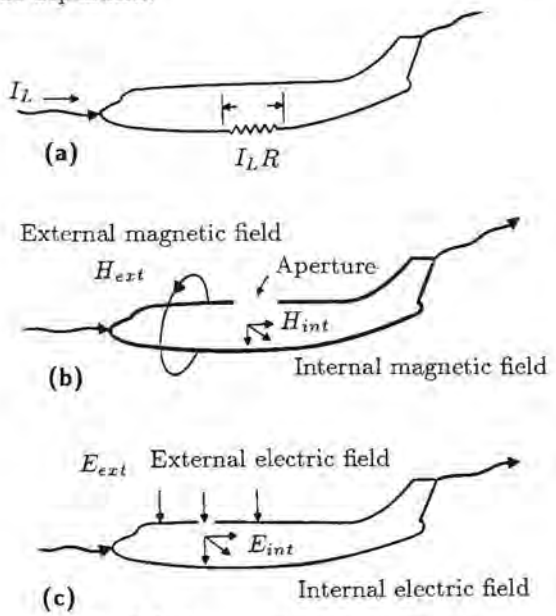

Fig. 8.4 Coupling mechanisms.
(a) Resistive
(b) Magnetic fields
(c) Electric fields

Voltage rise: The term *voltage rise* is preferable to *voltage drop* since the product of current and resistance acts as a source (akin to a battery as a voltage source) which is then applied to an external circuit, in this case the wiring of the aircraft.

Joint resistance: The most easily understood mechanism by which the passage of lightning current gives rise to voltages on aircraft electrical currents is that in which the current, flowing through joint resistances, produces a voltage by the elementary IR mechanism. Such a case is shown in Fig. 8.5. Here lightning is shown contacting a wing tip navigation light. The lightning current flowing through the resistance of the mechanical mounting structure of the lamp housing produces a voltage across that resistance. The voltage rise across the resistance will have the same waveform as that of the lightning current. The voltage at some remote point, however, may not have the same waveform, since the distributed inductance and capacitance

of the wire supplying power to the filament of the light will be set into oscillation by the suddenly developed voltage. The result is that at remote points there probably will be an oscillation superimposed upon the basic IR voltage.

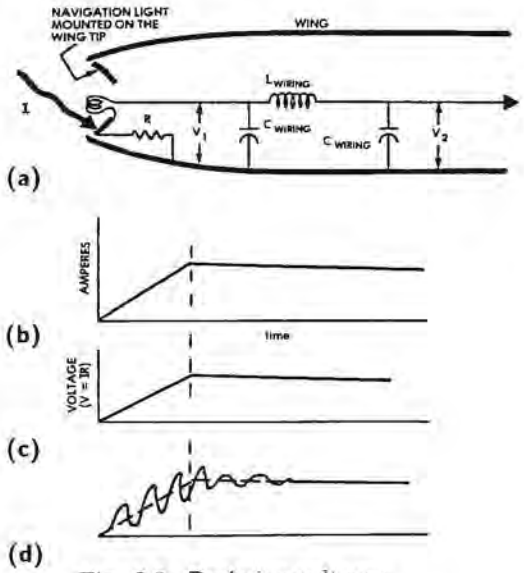

Fig. 8.5 Resistive voltages.
(a) Physical structure
(b) Current waveshape
(c) $V1$
(d) $V2$

Fig. 8.6 shows two other examples of cases in which resistive voltages might be encountered. The first would be at the pylons for mounting external stores, shown in Fig. 8.6(a). If lightning current were to contact such external stores, it would have to flow through the pylons to enter the aircraft. The pylons, not generally designed as current carrying members, and being points where the lightning current would be concentrated, might have a high voltage developed across them. Another example might be the structural bolts attaching a large segment of the airframe, such as the vertical stabilizer shown in Fig. 8.6(b).

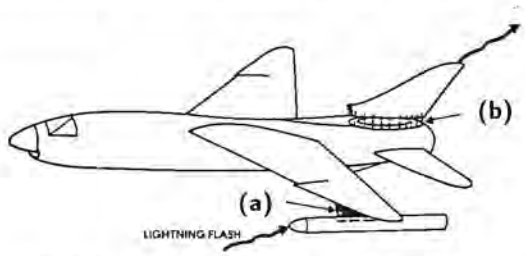

Fig. 8.6 Other examples of resistance.
(a) The pylons for external stores
(b) Joints in structural members

Effects of grounding: The effects of joint resistance on circuits are strongly influenced by the manner in which circuits are grounded, as shown in Fig. 8.7. Current flowing across the joint resistance, R, produces a driving voltage $V = IR$.

Since the circuit across which V_1 is measured employs the structure as a ground–return path, the circuit couples all of this voltage; thus V_1 would be high. A circuit employing a single–point ground does not include this resistive drop; hence V_2 would be low. The use of a single–point ground, however, does not eliminate the voltage, since in this latter case the voltage at the source end of the circuit, V_3, would be high.

Structural IR voltages are of particular concern in aircraft made from carbon fiber composite, CFC, materials because then the end to end resistance may be as much as 60 milliohms. A 200 kA current flowing through that resistance would produce 12 000 volts. Equipment located in the front of the aircraft and rferenced to a point in the rear would be subjected to that high voltage, either on the circuits or between the equipment and the local structure.

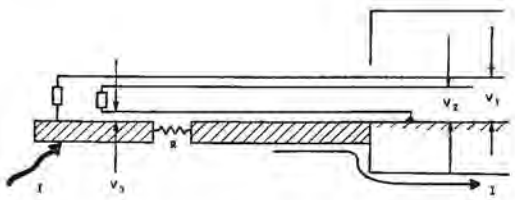

Fig. 8.7 Effects of grounding.
(a) Structural return, $V1 = IR$
(b) Single-point ground, $V2 =$ low
(c) Single-point ground, $V3 = IR$

Limitations: These elementary descriptions of joint resistance should not be relied upon to predict coupling into circuits extending throughout the entire aircraft. The more massive the joint and the lower the dc resistance, the greater will be the dependence of resistance on the waveform and frequency content of the lightning current, and the greater will be the proportionate effects of changing magnetic fields. While these effects will be discussed in more detail in other sections, one common oversimplification, shown in Fig. 8.8, should be pointed out here. If the total end–to–end resistance of the aircraft were 2.5 mΩ and a lightning current of 200 kA were flowing through the aircraft, the end–to–end voltage on any circuit could not be depended upon to be less than 500 V, the product of the lightning current and the dc resistance.

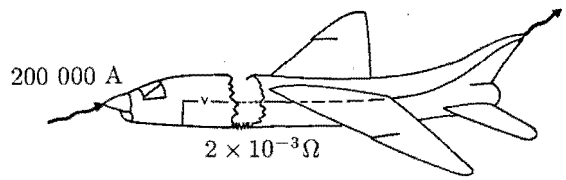

Fig. 8.8 An oversimplified model. Maximum voltage is not determined only by total end to end resistance.

8.5.2 Magnetically Induced Voltage

The second coupling mechanism, Fig. 8.9, involves magnetic fields in the interior volume of the aircraft.

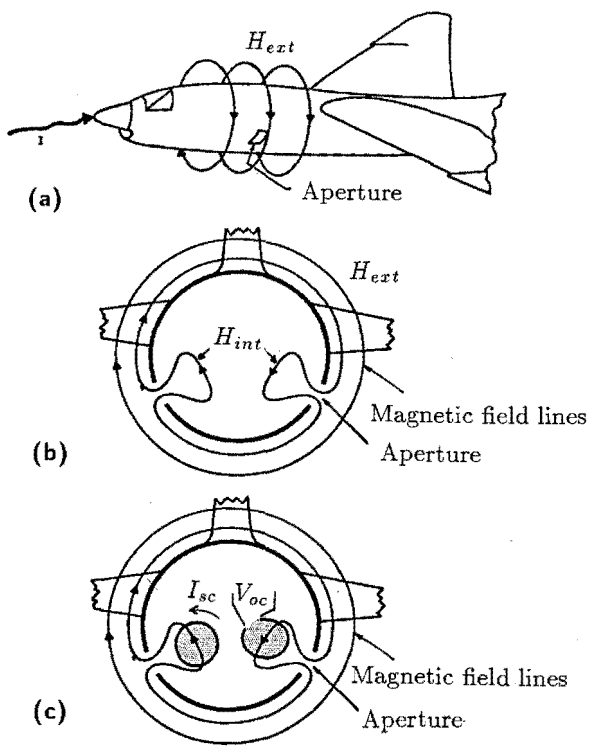

Fig. 8.9 Aperture-type magnetic field coupling.
(a) External field patterns
(b) Internal field patterns
(c) Induced voltages and currents

Aperture coupling: The most common and important type of magnetic field is that which passes from the exterior through apertures to the interior of the aircraft, as shown in Figs. 8.9(b). This is frequently called the aperture field. A changing magnetic field passing through a loop, Fig. 8.9(c), generates an open circuit voltage

$$V_{oc} = 4\pi \times 10^{-7} A \frac{dH}{dt} \tag{8.1}$$

or

$$V_{oc} = -\frac{d\phi}{dt} \tag{8.2}$$

where H is the magnetic field strength and ϕ is the total magnetic flux passing through the loop of area A.

The numerical relationships are discussed further in §9.7.4. The most important point is that the voltages are proportional to the *rate of change* of magnetic field, sometimes referred to as $\dot{H}$ or H dot.

Induced current: If the loop is short circuited, a current will be induced in the loop of magnitude

$$I_{sc} = \frac{1}{L} \int V_{oc}\, dt \tag{8.3}$$

where L is the self inductance of the loop. The current in the short circuited loop thus tends to have the same waveshape as the inducing magnetic field, unlike the voltage, which responds to the rate of change of magnetic field.

Diffusion coupling: There will also be magnetic fields produced by the diffusion of lightning currents to the inside surfaces of the aircraft skins. These are referred to loosely as the diffusion fields. The diffusion fields are also related to the frequency dependent properties of the resistively generated electric field. Because some of the concepts involved in the study of the diffusion fields are central to an understanding of other effects, particularly with respect to the response of shielded wires, they will be discussed (in Chapter 11) in detail before fields of other origins are considered.

Composite aircraft: Magnetic field effects will be more severe in composite aircraft than in metal aircraft. Fiberglass and aramid fiber reinforced plastics provide no magnetic shielding. Carbon fiber composites provide some shielding, but not nearly as much as provided by metal aircraft. Not only will the magnetic fields be higher, but they will rise to peak faster than in metal aircraft, this being a natural consequence of the high resistance of CFC materials. An effect of the increased magnetic fields is that much more of the total lightning current flows on internal metal objects in a CFC aircraft than flows in a comparable metal aircraft. Another way of phrasing this is that the re-

distribution time constants in a CFC aircraft are much faster than in a metal aircraft. The phenomena of redistribution is discussed further in Chapter 11.

8.5.3 Capacitively Generated Currents

The third type of coupling, Fig. 8.10, involves electric fields passing directly through apertures, such as windows or canopies, to the interior of the aircraft. The displacement current forced through a grounded object, Fig. 8.10(c) is

$$I_{sc} = 8.85 \times 10^{-12} A \frac{dE}{dt} \qquad (8.4)$$

where A is the area available to intercept displacement current E is the intensity of the electric field. If the current flows through an impedance it will, of course, produce an electrically induced voltage. Capacitively induced voltages and currents, which are discussed in §9.8.3, are proportional to the *rate of change* of electric field, frequently referred to as $\dot{E}$ or E dot.

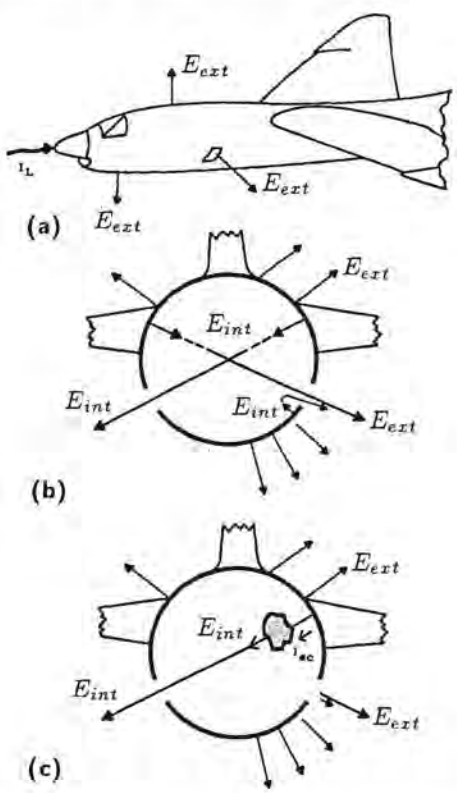

Fig. 8.10 Aperture-type electric field coupling.
(a) External field patterns
(b) Internal field patterns
(c) Induced current

In metal aircraft, electric field coupling is entirely through apertures, since virtually any thickness of metal provides extremely good shielding against electric fields. With composite aircraft this may or may not be the case.

8.6 Approaches to Determining the Response of Circuits

There are two basic methods of conducting a flow-down analysis, that is, determining how much voltage and current might be induced on aircraft wiring by lightning; numerical analysis and measurement.

Numerical analysis: Since an aircraft is a complex structure it is difficult to determine by analytical means the voltages and currents that might be induced on aircraft wiring by lightning. Some techniques are available for such analyses and they are reviewed in Chapters 10, 11 and 12. Most of them are based on techniques derived from the *NEMP* field, and in fact most of the advanced numerical and mathematical treatments of lightning interactions have their origins in the analytical studies funded by *NEMP* efforts. All of them require a considerable investment in computer resources and training of personnel. They are also limited in the degree to which they can predict the voltages and currents of actual aircraft wiring, as opposed to idealized and oversimplified geometries.

Numerical analysis, though, has the prime virtue that one can predict the general responses of an aircraft that has yet to be built. Also, using simplified and idealized geometries, one can predict the order of magnitude of voltage and current on circuits too complex to analyze precisely. Frequently, an order of magnitude estimate of the voltages and current induced by lightning is enough to enable one to make intelligent decisions regarding protective measures. In particular this is true if the primary purpose of the analysis is to give guidance for as to the levels at which to conduct laboratory proof tests.

Measurements: The other way of analyzing the response of an aircraft to lightning is to inject current into the aircraft and actually measure the resulting voltages and currents on wiring. Three basic approaches to such tests are as follows.

1. Inject continuous wave alternating currents into the aircraft and make frequency domain measurements of the response, relating the measured response to the response to lightning through Fourier analysis techniques.

2. Inject high level (full threat level) pulse currents into the aircraft and measure the response in the

time domain.

3. Inject low level (much less than full threat level) currents into the aircraft, measure the response in the time domain and extrapolate the results to full threat level.

These three techniques are discussed further in Chapter 13. The technique of injecting low level pulse currents into the aircraft is called the *Lightning Transient Analysis* (LTA) technique and is the one that has been used for most measurements of the response of aircraft electrical circuits. Full threat level tests are seldom made on aircraft; equipment for such tests is very expensive and at the limit of the state of the art and in any case can not be performed until the aircraft has been designed and built.

Sometimes of course, a designer does not have access to detailed analytical and experimental studies, or does not have the time or the funds to procure such studies. In recognition of this common problem Chapter 14 provides some very simplified tools with which to estimate the voltages and currents that might be induced on aircraft wiring. If the need is for guidance as to levels appropriate for conducting bench tests the tools may be sufficient for the job.

8.7 Examples of Induced Voltages Measured on Aircraft

There have been several sets of tests made on aircraft in which simulated lightning currents were injected into the aircraft and the resultant voltages and currents on the aircraft wiring measured. Space constraints preclude giving in this chapter a comprehensive summary of the test results, and the user is referred to the reports on the individual tests. A few examples of the measurements will be given in the following sections, primarily in order to illustrate the general nature of voltages and currents induced by lightning. Where appropriate, reference will be made to the subsequent chapters where the phenomena are discussed in further detail.

8.7.1 Wing from F-89J Aircraft

The first set of tests to be discussed [8.1] was one in which high lightning-like currents of amplitude up to 40 000 *A* were injected into one wing of an F-89J aircraft. During the test, represented in Fig. 8.11, the wing was fastened onto a screened instrument enclosure, which may be viewed as representing the fuselage of the aircraft. The current was injected into the wing or into the external wing tip tank, allowed to flow along the wing to the outer wall of the screened instrument enclosure, and then to ground. An example of one of the types of current injected into the wing is shown in Fig. 8.11(b).

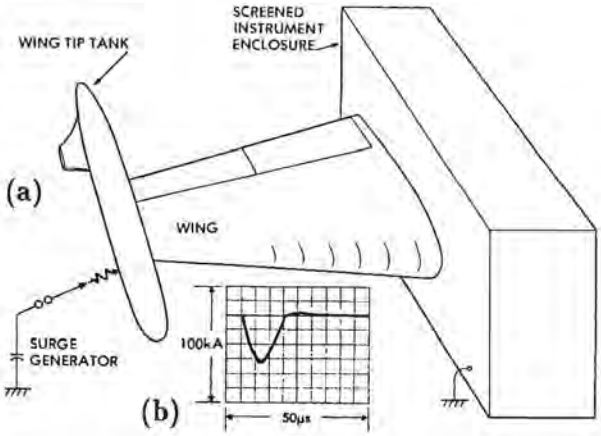

Fig. 8.11 High current injection tests on a wing from a fighter aircraft.
(a) Test arrangement
(b) Waveshape of injected current

In order to obtain maximum current, the surge generator was operated in a mode that essentially allowed the production of only one cycle of a damped oscillatory current, the technique having having involved a series non-linear resistor as previously discussed in §6.8.1. The surge current was, of course, unlike a typical lightning current, which would rise to crest rather fast and decay at a much slower rate. The shape of the current wave must be considered when observing the waveshape of some voltages that will be discussed. In particular, note that at about 20 μs there appears a major discontinuity in waveshape. This discontinuity in current waveshape is reflected in the induced voltages.

Within the wing there were a number of electrical circuits, such as those to navigation lights, fuel gauges, pumps, relays, and switches indicating position of flaps. Some of these ran in the leading edge of the wing and were well shielded from many electromagnetic effects, while others ran along the trailing edge between the main body of the wing and the wing flaps. These latter were the most exposed to the electromagnetic fields. All of the circuits were relatively simple and relatively independent of each other. They were not, as a rule, bundled together in one large cable bundle, a practice that provides maximum coupling from one circuit to another and makes analysis difficult.

The question of how location of wiring affects the lightning induced voltages is discussed in Chapter 16.

Position light circuit: The first circuit that will be discussed, shown in Fig. 8.12. was a circuit supplying power to a position light mounted on the external fuel tank. An electrical diagram of the circuit, shown in Fig. 8.12(b), shows that the circuit consisted of one wire supplying power to the filament of the position light with the return circuit for the light being through the wing structure. Accordingly, if the lightning current contacts the external tank, that circuit will be influenced by the resistance R_1 of the hangers fastening the tank to the wing, by R_2, the inherent resistance of the wing, and by magnetic flux arising from the flow of current.

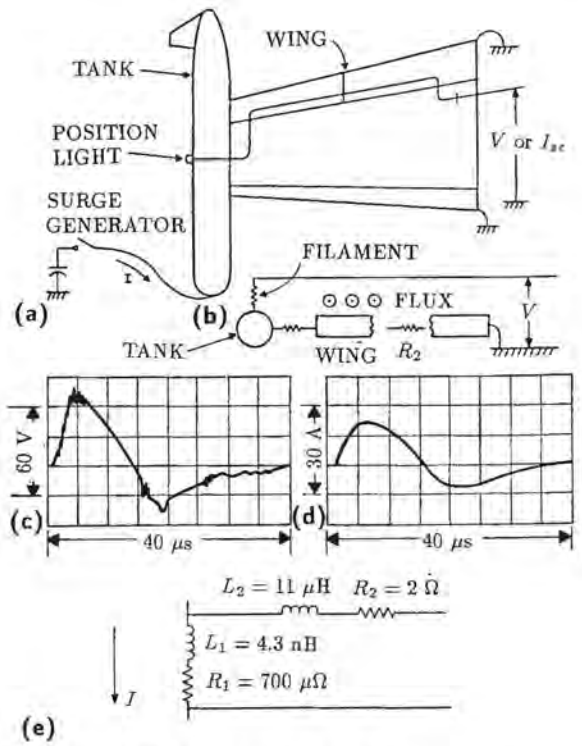

Fig. 8.12 A wing tip circuit.
(a) Circuit orientation
(b) Electrical details of circuit
(c) Open circuit voltage
(d) Short circuit current
(e) Equivalent circuit

Typical test results are given in Fig. 8.12(c) and 8.12(d). The open circuit voltage is seen to rise rapidly to its crest and to decay more rapidly than does the injected current shown in Fig. 8.11(b). This indicates that the open circuit voltage was responding primarily to magnetic flux.

When the conductor was shorted to ground at the instrument enclosure, the short circuit current rose to its crest in approximately the same length of time as did the injected current and displayed much the same waveshape as did the injected current.

Fig. 8.12(e) shows an approximate equivalent circuit that might be derived. L_1 and R_1 represent a transfer impedance between the current flowing in the wing and the voltage developed on the circuit. L_2 and R_2 represent the inherent inductance and resistance of the wires between the fuselage and the light. The transfer inductance and resistance are merely those values which, when operated upon by the external lightning current, produced the observed open circuit voltage. They do not necessarily represent any clearly definable resistance or inductance of the wing.

Pylon circuit: A different type of circuit is that shown in Fig. 8.13. In this circuit a conductor ran through the leading edge of the wing and terminated in an open circuit on a pylon mounted underneath a wing. In the electrical detail circuit shown in Fig. 8.13(b), it can be seen that this circuit would not respond to the voltage developed across the resistance between the tank and the wing. The circuit would respond in some measure to some fraction of the wing resistance and to some fraction of the magnetic field set up by the flow of current in the wing, but since the circuit was only capacitively coupled to the wing, the total coupling impedance should have been, and was, less than that of the circuit shown in Fig. 8.12.

The purpose of the conductor shown in Fig. 8.13 was to supply power to a relay and to explosive bolts in the pylon used to hold a weapon. In Fig. 8.13 the pylon was not installed, so there was no load on the conductor. Fig. 8.14 shows the results when that pylon was installed, when the conductor was connected to a relay with a return through the aircraft structure, and when the lightning flash was allowed to contact the pylon. The combination of a structural return path for the circuit and a lightning flash terminating upon the pylon and thus including the resistive drop across R_3, the resistance between the pylon and the wing, served to make the voltage much greater than it was when the conductor was open circuited. No attempt was made to completely analyze from which area the total amount of magnetic flux was coming or whether the flux ϕ_1, representing that in the pylon, or ϕ_2, representing that in the wing, was larger.

Antenna circuit: A third circuit, and one which illustrates the interaction between the lightning developed voltage and the circuit response is shown in Fig. 8.15. In this circuit a slot antenna excited by a grounded stub and fed from a length of 75Ω coaxial cable was installed in the leading edge of the wing. The shorted stub that excited the slot antenna was the predomi-

nant area intercepting the magnetic flux produced by the lightning current in the wing.

As in the three previous examples, the basic voltage developed in this antenna, and shown in Fig. 8.15(c) or 8.15(e) followed the same pattern as that shown for the other circuits. The rapid transition on the leading edge of the voltage, however, was capable of exciting an oscillation within the coaxial cable feeding the antenna. When the antenna circuit was terminated in a resistor matching the surge impedance of the cable, the higher frequency ringing oscillation disappeared, leaving only the underlying response of the antenna to the magnetic field surrounding the wing.

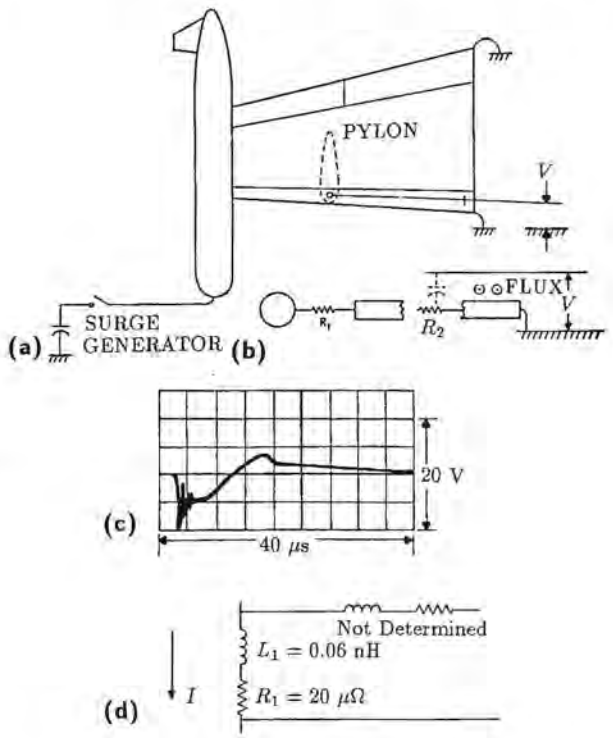

Fig. 8.13 A pylon circuit - open at pylon.
(a) Circuit orientation
(b) Electrical details of circuit
(c) Open circuit voltage
(d) Equivalent circuit

Significant conclusions: Several significant things were learned during this test series. The first was that the voltages induced in a typical circuit within the wing consisted of the sum of a magnetically induced component and a component proportional to the resistance of the current path. The location at which the lightning flash contacted the wing had an important effect on the magnitude of voltage developed on different circuits.

Nearly all the voltages and currents measured on the circuits could be explained in terms of a simple equivalent circuit, such as those shown in Fig. 8.16. One way to view these equivalent circuits is in terms of the self inductance of the wing, the self inductance of the circuit within the wing, and the mutual impedance between the wing and the internal conductor, as shown in Figs. 8.16(a) and (b). Some attempts at developing equivalent circuits have ignored the effects of mutual inductance, but it is not correct to do so.

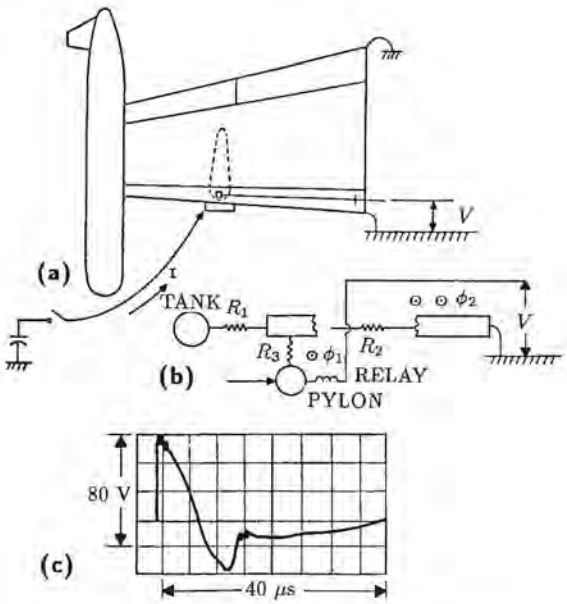

Fig. 8.14 A pylon circuit - loaded at pylon.
(a) Circuit orientation
(b) Electrical details of circuit
(c) Open circuit voltage

Another, and probably better, approach to viewing equivalent circuits is one based upon a transfer impedance, as shown in Fig. 8.16(c). In the approach based on self and mutual inductances the self inductance of the wing would be nearly equal to the mutual inductance between the wing and the internal conductor. The difference between the two would be equal to the transfer inductance in the latter approach. Since the values of the transfer impedance will be much smaller than the values representing the self impedance of the circuit, the latter approach leads to the more easily handled equivalent circuit. It is also compatible with the concept of mutual inductance or transfer impedance discussed for shielded cables in Chapter 13.

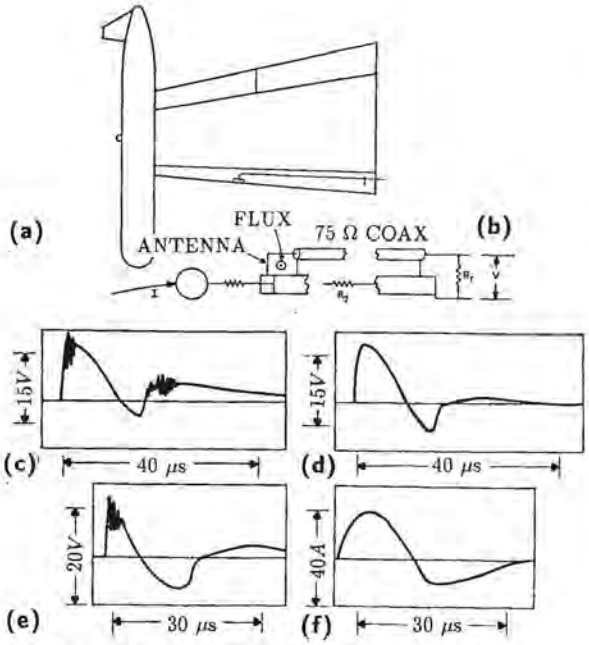

Fig. 8.15 An antenna circuit.
(a) Circuit orientation
(b) Electrical details of circuit
(c) Open circuit voltage - $R_T = \infty$
(d) Open circuit voltage - $R_T = 75\Omega$
(e) Open circuit voltage - $R_T = \infty$
(f) Short circuit current - $R_T = 0$

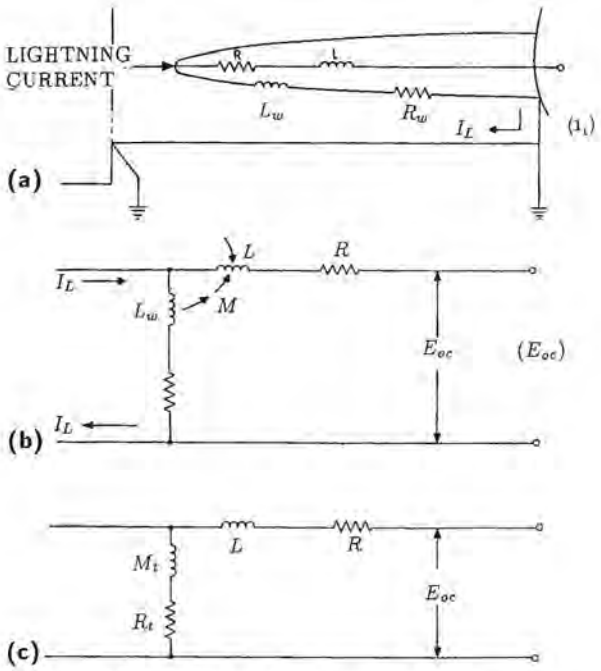

Fig. 8.16 Equivalent circuits.
(a) and (b) Circuits based on self and mutual inductances of the wing
(c) Circuit based on an equivalent transfer admittance: $Z = R_t + j\omega M_t$

There did not seem to be any easy way in which the magnitudes of the transfer impedance could be related to the physical geometry of the wing or to the location of the conductors within the wing. It was possible, however, to say that conductors located in the forward portion of the wing were better shielded, and consequently had lower transfer impedances, than those along the trailing edge. Likewise, it could be observed that circuits which did not have any electrical return through the wing structure had lower transfer impedances than those circuits which did have a return through the wing structure.

A significant point was that short circuit currents had waveshapes of longer duration than did open circuit voltages. This occurs because the impedance of conductors is primarily inductive, not resistive. Some of the specifications now being placed on proof testing for aircraft avionic systems do not recognize this inductive nature of wiring systems. Rather, by design or by oversight, they effectively treat the impedance as being resistive, a factor that complicates test procedures and may lead to improper interpretation of test results. This matter is discussed further in Chapter 18.

8.7.2 Digital Fly–By–Wire (DFBW)

The second set of measurements [8.16], about which some discussion will follow, was that made on an F-8 aircraft fitted with a fly–by–wire control system. The fly–by–wire controls, shown in Fig. 8.17, consisted of a primary digital system, a backup analog system, and a common set of power actuators operating the control surfaces. The major components of the control system were located in three locations: the cockpit, where sensors coupled to the control stick provided signals for the control systems; an area behind the cockpit, where there was located the digital computer; and a compartment behind and below the cockpit on the left side of the aircraft. This latter compartment was one that would normally have been occupied by guns. Accordingly, it will be referred to as the "gun bay", though in this research aircraft it was used to house the interface and control assemblies, not guns.

Several hydraulic actuators were located at each of the major surfaces. These were interconnected to the fly–by–wire control systems through wire bundles that ran under the wings. The control systems did not depend upon the aircraft structure as a return path; the system was considered to have a single–point

ground, and that single-point ground was located at a panel in the gun bay. By and large, none of the control wiring in the aircraft was shielded.

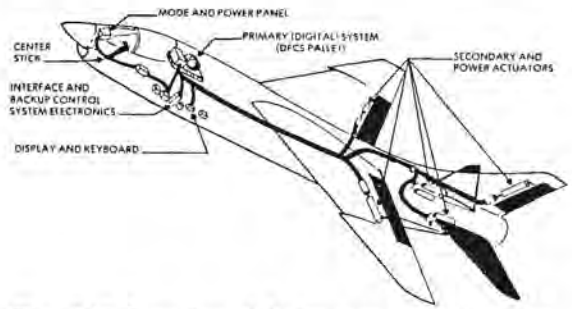

Fig. 8.17 Location of fly-by-wire control system hardware and wiring bundles in F-8 aircraft.

Test techniques: In contrast to the tests on the wing of the F-89J aircraft, in which high amplitude currents were injected into the wing from a high power surge generator, the tests on the complete F-8 aircraft were made using the lightning transient analysis technique described in §8.6 and Chapter 13. During the tests on the F-8, the injected current was on the order of 300 A. In the measurements that will be shown, the amplitudes refer to that injected current. To scale the results to what would be produced by a fairly common 30 kA lightning current the measured amplitudes should be multiplied by 100. To scale the results to the design level amplitude of 200 kA they should be multiplied by 666.

Several different current waveshapes were employed; the one to which most frequent reference will be made in this abbreviated set of test results is that described as the fast waveform, a current rising to crest in about 3 μs and decaying to half value in about 60 μs. These waveforms are shown in Fig. 8.18. The fast waveshape is the one most representative of that which is now recommended for such tests.

Fore and aft circuit: The first set of measurements to which reference will be made was that on a set of spare conductors running between an interface box in the gun bay and a disconnect panel located near the leading edge of the vertical stabilizer. The routing of the circuit is shown in Fig. 8.19(a) and the waveforms of the voltages are shown in Fig. 8.19(b). The voltage measured between the conductor and ground consisted of a high-amplitude oscillatory component and a lower amplitude, but longer duration component. This is the pattern that is most commonly noted on voltages induced by lightning currents.

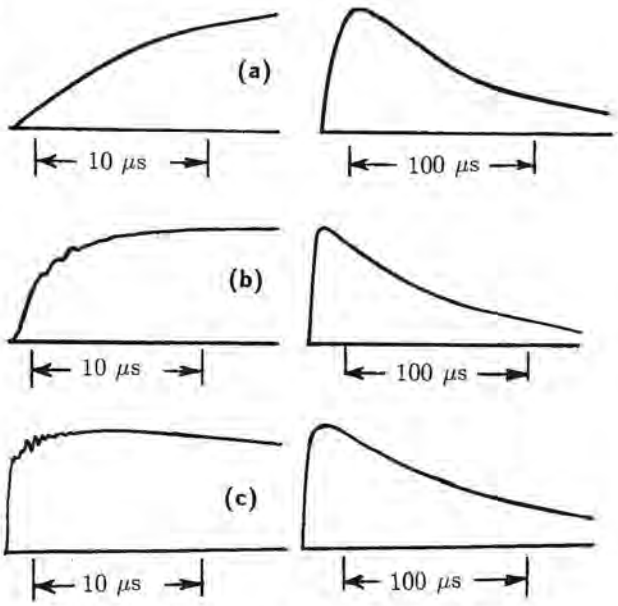

Fig. 8.18 Simulated lightning test waveforms.
(a) Slow wave
(b) Intermediate wave
(c) Fast wave

Voltages measured between conductors, shown in Fig. 8.19(c), were much smaller than the voltages measured between either of the conductors and the airframe. Such results would be expected on a well-balanced circuit. The voltages were, however, not zero, and one should not assume that voltages on twin conductor circuits will be low enough to eliminate problems.

The oscillatory component of voltage was excited by magnetic flux (and possibly electric fields) leaking inside the aircraft, while the longer duration component was produced by the flow of current through the structural resistance of the aircraft. Since the voltages induced by the leakage of magnetic flux were proportional to the rate of change of that flux, it follows that the oscillatory component would have been more pronounced for faster currents injected into the aircraft than it was for slower currents. This effect was noted, as indicated by the oscillograms.

Circuit to wing position indicator: The second set of measurements was made on a circuit running from the interface control unit and the gun bay to a wing position indicator switch located underneath the leading edge of the wing. The wing on the F-8 aircraft could be raised or lowered around a pivot point towards its rear in order to achieve a lower pitch angle during landing and takeoff and the purpose of the switch was to indicate the position of the wing.

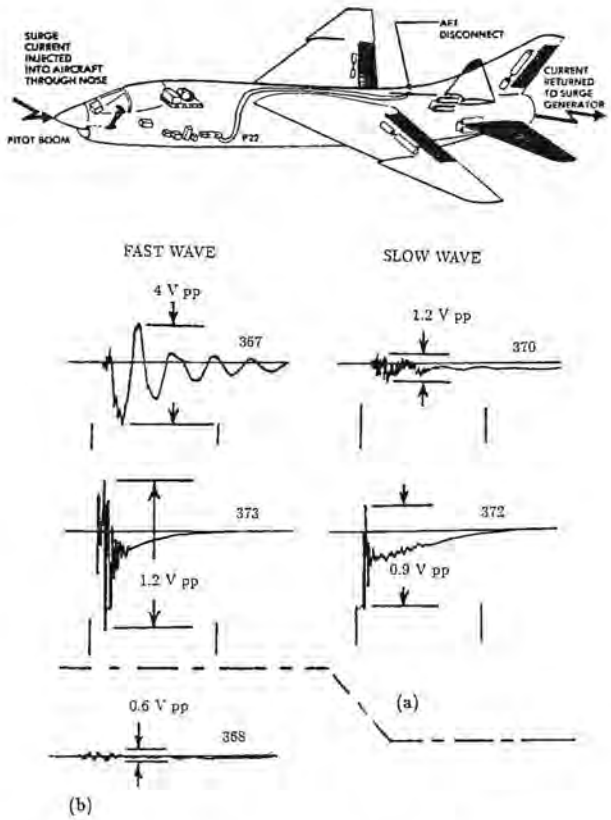

Fig. 8.19 Voltages on a fore and aft circuit
(a) Line to ground voltages (P22, Pin 24 to airframe).
(b) Line to line voltage (P22, Pin 24 - Pin 25).

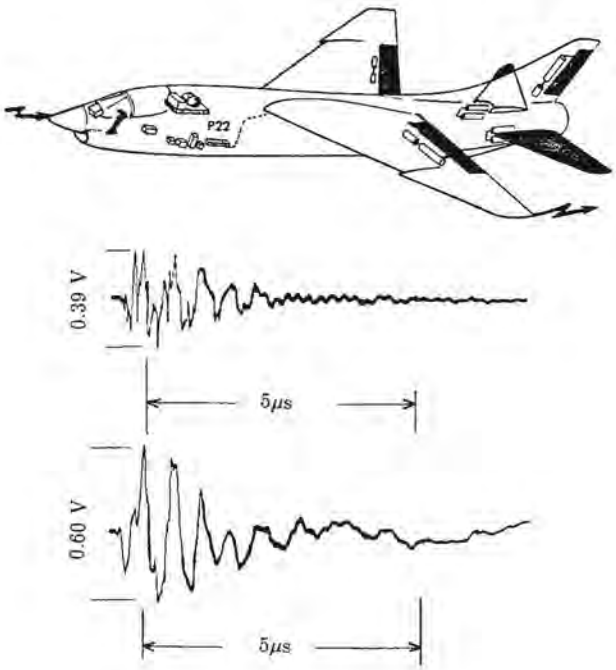

Fig. 8.20 Voltages induced in wing position indicator switch circuit at open plug P22.

The voltages induced on that switch circuit are shown in Fig. 8.20. The voltages measured from line to airframe were higher than those measured from line to line, but it is significant that the line to line voltages, while of a somewhat different waveshape, were not much lower than the line to ground voltages. The reason for this lay in the fact that the load impedances in the interface box in the gun bay were different from each other on the two sides of the circuit. One side connected to a power supply bus, while the other side probably connected to an emitter follower.

Another significant feature about these voltages was that they were again of an oscillatory nature. They were apparently excited by the leakage of magnetic flux inside the aircraft and were not excited by the rise in potential along the structural resistance of the aircraft.

Circuits to actuators: Figs. 8.21 and 8.22 show voltages measured on two different circuits going to actuators, one (Fig. 8.21) going to the left pitch actuator and the other (Fig. 8.22) going to the left roll actuator. In both cases the voltages displayed were the output of the driver amplifier used to control the servo valve in the actuator. Both of these were differential measurements, line–line voltage measurements. The significant feature about these measurements was, again, that the characteristic response was oscillatory and apparently excited by the leakage of magnetic flux inside the aircraft. There was some dependence of the voltage on the path of current followed through the aircraft, but the dependence was not large. Both lightning current paths produced about the same peak voltage of transient.

Bulk cable currents: On the F-8, as is typical of most aircraft, the control wires were laced together into fairly large bundles. The routing of some typical bundles in the gun bay housing the backup and interface electronic control boxes is shown in Fig. 8.23.

While it was not possible to measure the current on individual wires within these cable bundles because of limitations of measurement technique and because of the large number of wires within the bundles, it was possible to measure the total current flowing on the various bundles. This was done by clamping around the bundle a current transformer having a split core.

Typical results of these cable measurements are shown in Figs. 8.24 and 8.25. The bulk cable currents were also found to be oscillatory, just as were the voltages on conductors described earlier. Since the flight control wiring did not make use of multiple ground points within the aircraft, it follows that none of the currents in these cable bundles would exhibit any of the long time response characteristic of multiple–grounded conductors.

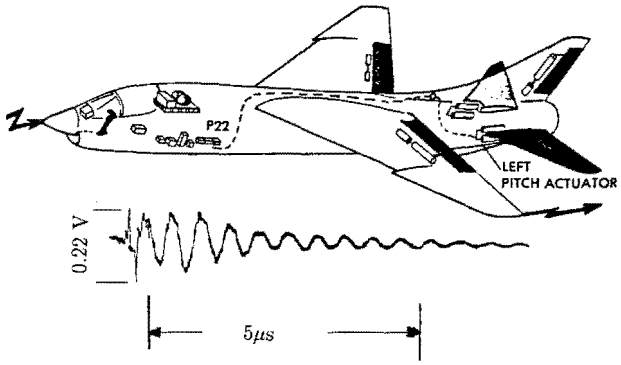

Fig. 8.21 Left pitch valve drive output (high to low) at plug P22.

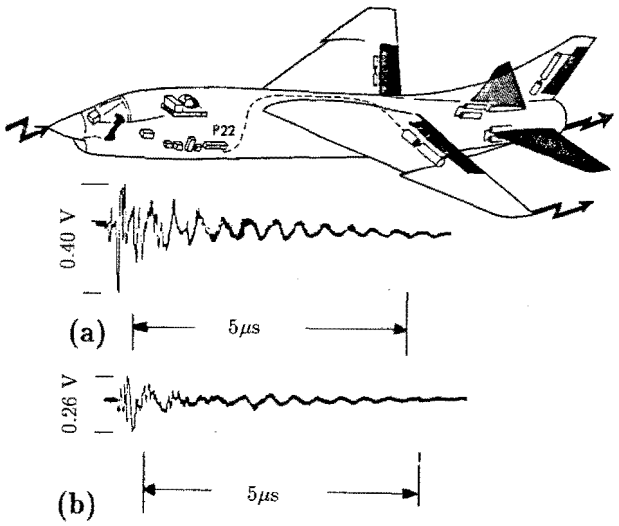

Fig. 8.22 Voltages induced in left roll valve drive output circuit (Pins 44-45) at open plug P22.

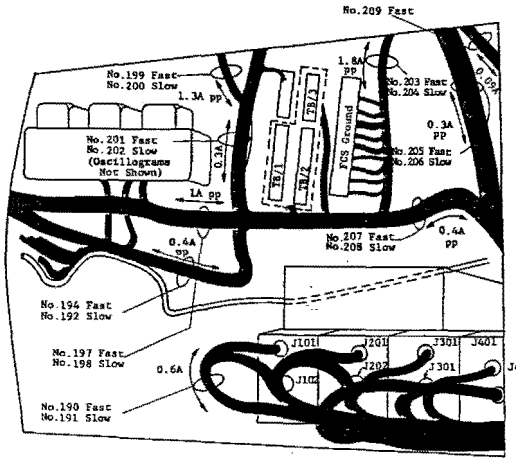

Fig. 8.23 Cable bundles within the gun bay.

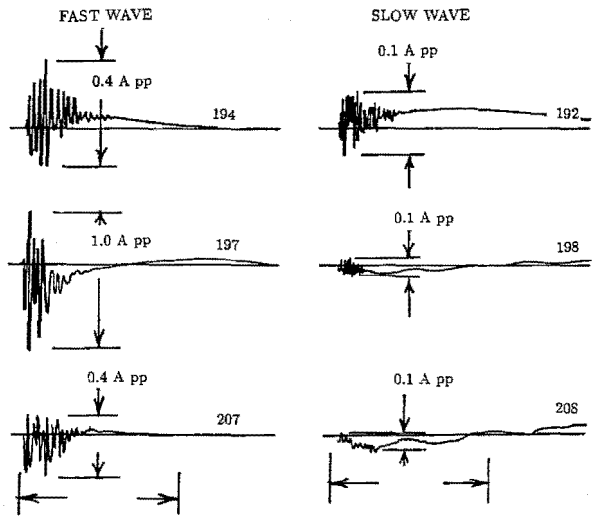

Fig. 8.24 Currents on cable bundles leading toward cockpit and left hand instrument panel.

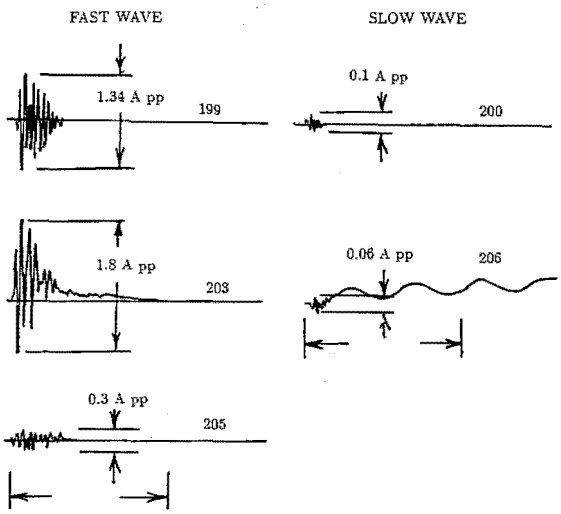

Fig. 8.25 Currents on cable bundles leading toward the area behind the cockpit.

Statistical distribution: Fig. 8.26 shows a statistical distribution of the peak amplitude of currents in all of the cable bundles upon which measurements were made. The distribution is shown for both the actual current amplitudes injected into the aircraft and in terms of what those currents would be if the results were scaled up to currents representative of actual lightning flashes. In terms of an average–amplitude lightning flash, 30 000 A, the total current on most cable bundles would have been on the order of 20 to 100 A.

Measurements of bulk cable current are important because one of the test practices now in common use for evaluating the effect of voltages and current induced by lightning involves coupling current onto a wiring assembly (usually through a transformer) and allowing the voltages and current on individual wires to develop as appropriate to the impedances of the circuits to which they connect. The technique of injecting current onto cables is discussed in Chapter 18.

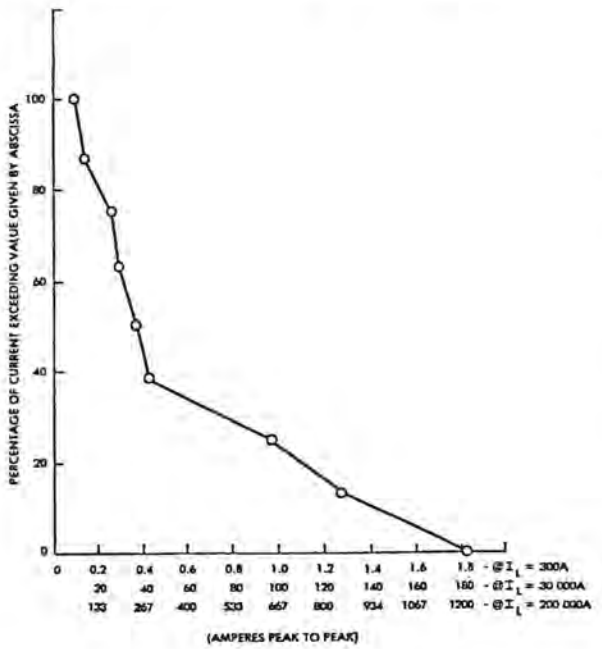

Fig. 8.26 Distribution of amplitudes of cable bundle currents (measured in left gun bay).

Magnetic fields: Measurements were made of the amplitude and waveshape of the magnetic field at a number of points in and around the aircraft. One location upon which attention was concentrated was the cockpit, since the cockpit is an inherently unshielded region and one in which many control wires would be subjected to changing magnetic fields.

The positions at which fields were measured, the peak amplitude of the fields, and the predominant orientation of the fields are shown in Fig. 8.27. The magnetic fields were measured with a probe which had a characteristic time constant of about 4 μs. When exposed to fields changing in times less than 4 μs, it would respond to the absolute magnitude of the field intensity, and, when exposed to fields changing in times longer than 4 μs, it would respond to the rate of change of the magnetic field.

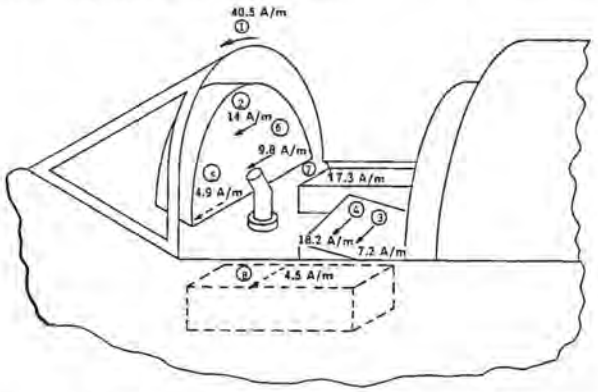

Fig. 8.27 Magnetic field measurements in the cockpit.

A few typical measurements of field waveshape are shown in Fig. 8.28. The most significant feature about these measurements is that there was no orientation of the magnetic field probe that resulted in a zero output, which indicated that the orientation of the magnetic field was not uniform with respect to time. The field produced at any one point was the sum of the field produced by the total flow of current through the aircraft and that produced by oscillatory current in the various structural members as the current in those structural members changed with time. When fields of high frequency are produced by oscillatory currents excited by an original transient field, the process is commonly called re–radiation.

Also, it was noticed that the waveshape of the magnetic field was quite oscillatory whenever the peak magnitude of the field was low. This is a pattern commonly found. It occurs because the low level magnetic fields found within partially shielded structures are due either to re–radiation produced by circulating currents or by coupling through apertures. As will be noted in Chapter 12, coupling through apertures is frequency dependent, high frequencies (or the high frequency portions of transient waveforms) being coupled more effectively than low frequencies.

Some measurements of the magnetic field within the gun bay housing the backup control system and the interface electronics package are shown in Fig. 8.29. Clearly, the magnetic field inside the gun bay com-

partment was of lower amplitude than that of the field external to the gun bay. The waveshapes of the fields are more difficult to understand. First of all, it must be kept in mind that the probe was responding to the rate of change in the magnetic field after about 4 μs and was responding to the field itself for times shorter than about 4 μs.

Accordingly, the oscillograms displaying the field inside the gun bay indicated that there was, first of all, a component of magnetic field that rose to its crest about as fast as did the outside field.

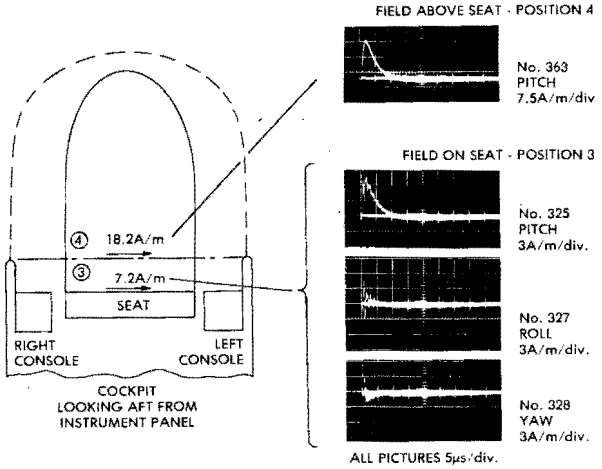

Fig. 8.28 Magnetic fields near pilot's seat.

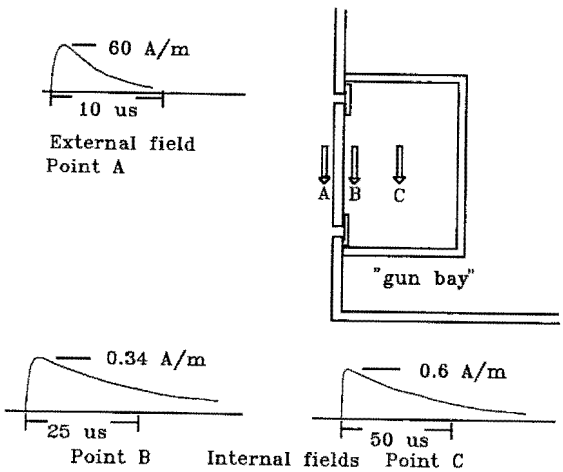

Fig. 8.29 Magnetic fields inside the gun bay.

From then on, the field continued to increase at a slower rate, the final value of the field not being indicated by the oscillograms. The fact that the field continued to rise, but at a slower rate, is in agreement with the behavior predicted in §11.3.5, Fig. 11.11 and §11.7, where it will be shown that the field should increase with a time constant characteristic of the internal inductance and resistance of the cavity in which the fields are measured.

Fields inside a battery compartment located aft of the gun bay are shown on Fig. 8.30. The measurements showed first some oscillatory magnetic field, followed by a field which rose to crest at a time much longer than the crest time or even the duration of the lightning current that was injected into the aircraft. Oscillogram No. 452 in Fig. 8.30 indicated the rate of change of field as falling to zero at about 400 μs. This would indicate that the field itself reached its crest value in about 400 μs.

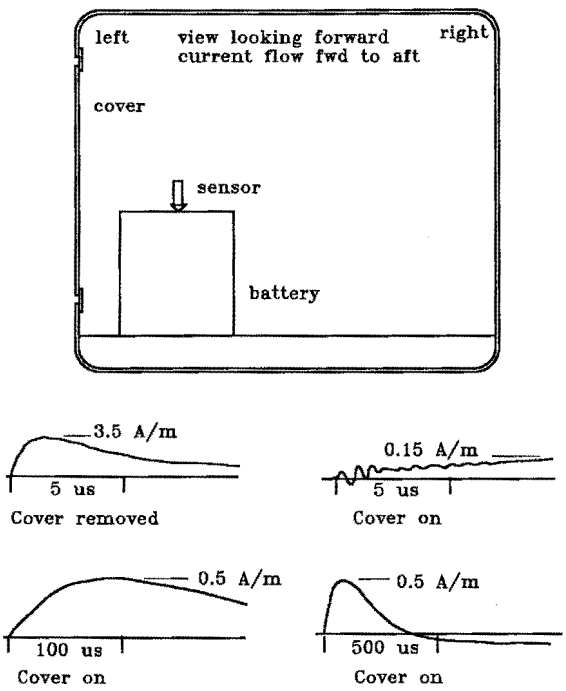

Fig. 8.30 Magnetic fields inside the battery compartment (probe time constant = 4μs).

The different nature of the response of the fields inside the gun bay and the battery compartment can be explained in terms of the types of covers and fasteners used on the two compartments. The cover over the battery compartment was held in place by fasteners spaced about every 3.8 cm., and hence made good contact to the rest of the airframe. The use of multiple fasteners resulted in many paths on which current could flow (minimum constriction of the current flow) and provided minimum resistance to the circulating current within the battery compartment.

The gun bay covers, on the other hand, since they were originally designed for ease of access, had far fewer fasteners. The fasteners in the gun bay, in fact, were spaced about every 30 cm. Accordingly, the cover on the gun bay provided a much greater constriction of current flow and a much greater resistance than did the cover on the battery compartment. Both of these factors were of a nature to allow the field within the gun bay to reach its peak value faster than did the field within the battery compartment. These points about the influence of fasteners are discussed further in §11.7 and Fig. 11.43.

It is practical to calculate, with reasonable accuracy, the magnetic and electric fields within an aircraft, given knowledge of the geometry of the aircraft. Numerical techniques for doing this are discussed in Chapters 10–12. From a knowledge of the strength of the magnetic and electric fields one can predict the order of magnitude of voltage and current induced on aircraft wiring. Simplified techniques for doing this are discussed in Chapter 14. The accuracy of the calculations may be questionable, but order of magnitude estimates may be sufficient.

Significant conclusions: Some significant points about the results of tests on this aircraft can be summarized here. The first was that the use of a single–point ground system most emphatically did not eliminate all transient voltage produced by the flow of lightning current through the structure of the aircraft.

The second was that the characteristic response of the wiring, both for voltage and for current, was a damped oscillation with a frequency in the range 1 to 5 MHz. The very abbreviated series of test results just presented does not indicate the fact clearly, but the frequency of oscillation depended considerably on the length of the circuit involved: the longer the physical length of the wires, the lower the oscillatory frequencies. This was not a clear–cut rule, since the response of any one circuit was greatly influenced by the high degree of coupling between all of the different circuits.

The third significant point is that the total current on any cable bundle was of the order of 20 to 100 A for an average lightning flash. This bulk cable current was again oscillatory with a frequency tending to correspond to the length of the cable bundle.

The fourth point was that the equipment bays in this aircraft, not being designed for electromagnetic shielding, allowed significant amounts of magnetic flux to develop within those bays. This is particularly true of those bays intended for ease of access. As a rule of thumb, it might be expected that on aircraft, the equipment bays housing electronic equipment might well be fitted with covers designed more with ease of access in mind than with magnetic shielding qualities in mind. It must thus be expected that those enclosures for which the electromagnetic shielding should in principle be the greatest may well be those enclosures having the poorest shielding.

Finally, the measurements of magnetic fields indicated that there will seldom be any clear–cut manner in which electrical wiring can be oriented so as to pick up the minimum value of magnetic field and hence have minimum induced voltages. One might best assume that the magnetic field at any point will always be oriented in the worst case. Also, one should assume that the internal magnetic fields will be more oscillatory than the external magnetic fields, this because of re–radiation and the frequency dependent transmission of energy through apertures.

No attempt was made to determine in this aircraft the degree to which any circuit voltages could be reduced by the use of shielded conductors. It was noted, however, that on those circuits in which a shield was used and in which the shield was grounded at more than one point, the current on that shield tended more to have the slower double exponential waveshape of the external lightning current than to have the high–frequency oscillatory current excited on all of the unshielded cable bundles.

8.7.3 Carbon Fiber Composite Aircraft

Voltages and currents induced in the wiring of aircraft using carbon fiber composite (CFC), or graphite/epoxy, materials for structural members are very different from those induced in aircraft made entirely from aluminum. In a metal aircraft the resistance of the structure is very low and the lightning current flows mostly on the metal surface. Only relatively small amounts flow on internal wiring and internal structures and in general the duration of current flow is no longer than that of the external lightning current. In a CFC aircraft the structure has a much higher resistance and a much larger fraction of the lightning current eventually flows on the internal wiring and internal structure. Initially the current may flow on the external structure, but at later times it transfers to the inside, a process called redistribution and which is

discussed further in §11.4.

The redistribution phenomenon also leads to the internal currents flowing for much longer times; longer even than the duration of the lightning current. The overall result is that indirect effects in a CFC aircraft can be more severe and harder to deal with than in a metal aircraft. Tests on a test bed fuselage for a CFC aircraft showed that by the time an external injected current had decayed to half value (82μs), 90% of the injected current was flowing on metal objects inside the fuselage.

Because CFC aircraft are relatively new, only a few test programs have been undertaken to measure the voltages and currents induced by lightning. A few examples of voltages and currents will be given here, mostly to illustrate the redistribution effects and to illustrate the time scale over which they take place. Since the source data is proprietary, the illustrations will not be as extensive as those in §8.7.1 and §8.7.2.

Aircraft structure: The general nature of the aircraft structure for which the following measurements were taken is shown in Fig. 8.31. The main shell of the aircraft was made from CFC laminates. In the nose of the aircraft was an avionic equipment bay built with aluminum shelves upon which the equipment was mounted. These shelves made good electrical contact with the CFC fuselage. In the main part of the fuselage were metal rails upon which seats were mounted and various electrical power wires and metal tubing.

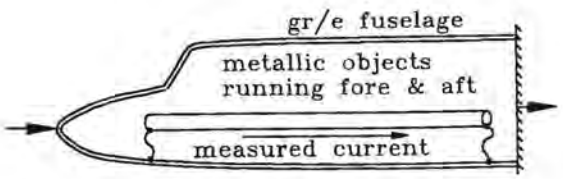

Fig. 8.31 General nature of CFC aircraft upon which tests were made.

Waveshape of injected current: The aircraft was tested by injecting current pulses into the nose and taking the current off the rear. The current, Fig. 8.32, had a double exponential waveshape with a time to peak of 6 μs and a decay to half value of 84 μs. Various peak amplitudes were used, ranging from 1 kA to 10 kA. Fig. 8.32 shows a current pulse with a peak of 1 kA. This waveform is nearly identical to current Component A.

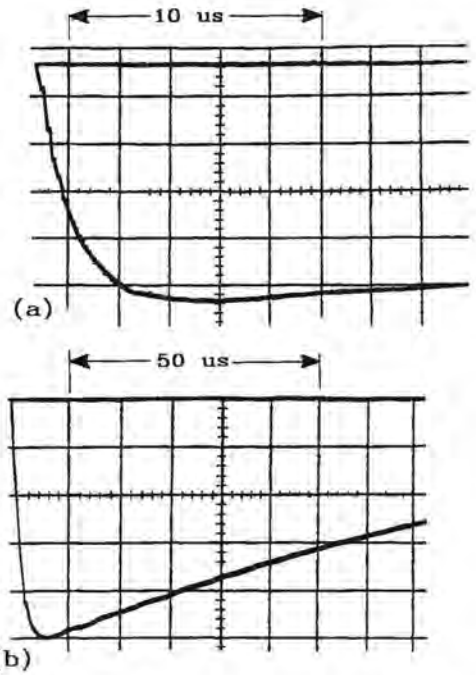

Fig. 8.32 Waveshape of current injected into CFC aircraft.
(a) Front of wave
(b) Tail of wave

Current on metal members: Current flowing on one of the metal tracks used to hold the seats is shown in Fig. 8.33(a) and current on an aluminum duct carrying air for heating is shown on Fig. 8.33(b). If the injected current were 200 kA, there would be 11 kA and 6.2 kA, respectively, on these members. These currents are much higher than would be encountered in a metal aircraft. They flow on these particular members because they are the ones that have a fairly low resistance. The currents themselves present no hazard to those objects since the current flows for only a short time, but allowance must be made to ensure that the current can flow without any sparking. The current is also seen to reach its peak long after the injected current has begun to decay. This is because the inductive time constant, $\tau = L/R$, is longer than the corresponding time constant of the fuselage of the aircraft.

Current on a power bus: Current on one of 28 V power return wires is shown on Fig. 8.34. If the current injected into the aircraft were 200 kA, there would be 2.04 kA flowing in this wire. This is also a current considerably higher than would flow in a comparable circuit on a metal aircraft. The current did not reach its peak until nearly 300 μs, by which time the injected

current would have decayed to nearly zero. This long time constant results from the low dc resistance of the copper power cable, and its relatively high inductance.

The tests showed that high voltages could be produced on power buses. The bus voltages can be clamped to levels that do not present a hazard to equipment on the bus, but currents similar to that on Fig. 8.34 would then flow through the protective devices. This question of current that can flow through protective devices, and the analyses that must be made to be sure that the devices are properly rated is discussed in Chapter 17.

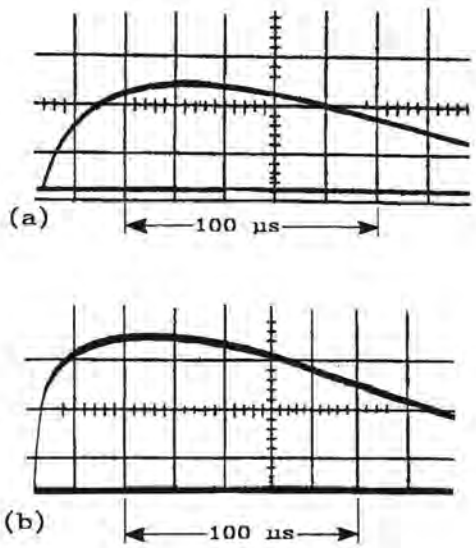

Fig. 8.33 Currents flowing through metal members
(a) Current on a seat rail
(b) Current on an air tube

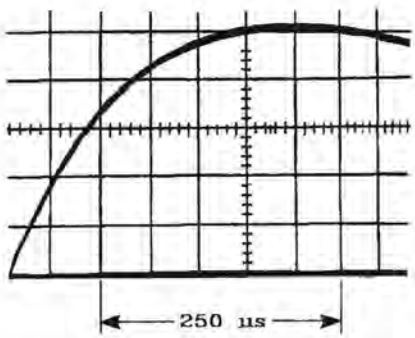

Fig. 8.34 Current flowing on a 28 V power return wire

Significant conclusions: The most important point shown by tests on CFC aircraft are that fairly large voltages can be developed on wiring and that fairly large currents can flow on metal objects inside the aircraft. Large currents also can flow through protective devices when they act to limit overvoltages, particularly if the protective devices are connected between line and aircraft structure. Stated another way, this means the surge impedance of the circuits in CFC aircraft may be very low.

REFERENCES

8.1 K. S. H. Lee, Editor, "EMP Interaction: Principles, Techniques and Reference Data (A Compleat Concatenation of Technology From The EMP Interaction Notes) EMP Interaction 2-1," *AFWL-TR-80-402*, Air Force Weapons Laboratory (NTMT), Albuquerque, NM, December 1980.

8.2 "Atmospheric Electricity Hazards Protection, Part I. Executive Summary," *AFWAL-TR-87-3025, Part I*, AFWAL, Wright-Patterson Air Force Base, OH, June 1987.

8.3 "Atmospheric Electricity Hazards Protection, Part II. Assessment, Test and Analysis - F-14A," *AFWAL-TR-87-3025, Part II*, AFWAL, Wright-Patterson Air Force Base, OH, June 1987.

8.4 "Atmospheric Electricity Hazards Protection, Part III. Assessment, Test And Analysis - ACAP Helicopter" *AFWAL-TR-87-3025, Part III*, AFWAL, Wright-Patterson Air Force Base, OH, June 1987.

8.5 "Atmospheric Electricity Hazards Protection, Part IV,. Design Guide for Air Vehicles," *AFWAL-TR-87-3025, Part IV*, AFWAL, Wright-Patterson Air Force Base, OH, June 1987.

8.6 "Atmospheric Electricity Hazards Protection, Part V. Qualification and Surveillance Tests and Analysis Procedures," *AFWAL-TR-87-3025, Part V*, AFWAL, Wright-Patterson Air Force Base, OH, June 1987.

8.7 G. O. Olson and M. M. Simpson, "Atmospheric Electricity Hazards Direct Effects Protection Evaluation," *D180-27423-43*, Flight Dynamics Laboratory, Wright Patterson Air Force Base, OH, September 1985.

8.8 "Lightning Test Waveforms and Techniques for Aerospace Vehicles and Hardware,", *Report of SAE Committee AE4L*, (the "Blue Book"), June 1978.

8.9 "Test Waveforms and Techniques for Assessing the Effects of Lightning Induced Transients," *Report of SAE Committee AE4L*, ("Yellow Book"), December 1981.

8.10 "Recommended Draft Advisory Circular, Protection of Aircraft Electrical/Electronic Systems against the Indirect Effects of Lighting," *Report of SAE Committee AE4L*, (the "Orange Book")

8.11 "Lightning Qualification Test Techniques for Aerospace Vehicles and Hardware," *MIL-STD-1757A*, 20 July 1983.

8.12 L. C. Walko, "A Test Technique for Measuring Lightning Induced Voltages on aircraft Electrical Circuits," NASA Contractor Report NASA CR-2348, National Aeronautics and Space Administration, February 1974.

8.13 W. W. Cooley, D. L. Shortess, "Lightning Simulation Test Technique Evaluation," *DOT/FAA/CT-87/38*, US Dept. of Transportation, Federal Aviation Administration, October 1988.

8.14 "Part IV. Design Guide," p. 4.9.

8.15 K. J. Lloyd, J. A. Plumer, and L. C. Walko, "Measurements and Analysis of Lightning–Induced Voltages in Aircraft Electrical Circuits," *NASA Contractor Report CR-1744*, February 1971.

8.16 J. A. Plumer, F. A. Fisher, and L. C. Walko, "Lightning Effects on the NASA F-8 Digital-Fly-By-Wire Airplane," *NASA Contractor Report CR-2524*, March 1975.

This page intentionally blank.

Chapter 9

ELEMENTARY ASPECTS OF INDIRECT EFFECTS

9.1 Introduction

For reference and to avoid repetition elsewhere, some concepts of electrical circuits and electromagnetic theory will be reviewed in this chapter. Mathematical operations are reviewed with particular attention to the use of imaginary or complex arguments. The concept of voltage as the line integral of electric field is reviewed since it is of fundamental importance in understanding how voltages are developed on wiring inside an aircraft struck by lightning. Magnetic field effects are treated in detail since there are some subtle points about flux linkages and inductance of conductors that are not always appreciated. A most important subject is that of §9.7.2, where it is pointed out that current flowing along a circular tube does not produce a magnetic field within the tube.

Capacitance effects are also treated, the most important points probably being those related to displacement currents induced by a changing electric field.

The discussions of internal and external surface current density, §9.9, should be reviewed carefully since they deal with why it is that conductors run along one path may be exposed to dangerous voltages as a result of lightning currents while conductors run along another path will experience only minor voltages. The discussions of how much voltage is induced in loops exposed to changing magnetic fields, §9.7.4, and how much current flows in objects exposed to a changing electric field, §9.8.4, are also of fundamental importance. Those discussions are presented in the classical frequency domain formulations. For analysis of lightning effects it is more useful to have formulations in the time domain. These are provided in Chapter 10.

9.2 Symbols and Units

In Chapters 9 - 18 dimensions will generally be given in SI units with English equivalents in parentheses. Symbols will generally be as follows with exceptions as noted in the text.

A = amperes
A = area - m^2
a = radius - m
C = Coulombs
C = capacitance - F
c = velocity of light - 3×10^8 m/s
D = time derivative of E - V/m/sec
E = electric field intensity - V/m
F = Farads
f = frequency - H_z
H = Henries
H = magnetic field intensity - A/m
I = current - A
j = current density - A/m^2
j = imaginary operator - $\sqrt{-1}$
L = inductance - H
l = length - m
m = meters
R = resistance - Ω
r = radius - m
S = Siemens (unit of conductivity)
s = seconds
t = time - s
V = Volts
V = voltage - V
v = velocity - m/s
γ = propagation constant
ϵ_0 = permittivity - F/m
η = wave impedance - ohms
μ = permeability - H/m
μ_0 = permeability of free space - H/m
μ_r = relative permeability
Ω = Ohms
ω = angular frequency - $2\pi f$
ρ = resistivity - $\Omega \cdot$ m
σ = conductivity - S

9.3 Mathematical Operations

Mathematical analysis of electromagnetic effects frequently involves functions with complex arguments. Some identities commonly encountered are the following. Others can be found in any mathematical handbook.

9.3.1 Complex Numbers

$$
\begin{aligned}
j &= \sqrt{-1} \\
1/j &= -j \\
\sqrt{j} &= (1+j)/\sqrt{2} \\
1/\sqrt{j} &= (1-j)/\sqrt{2} \\
\sqrt{2j} &= 1+j \\
1/\sqrt{2j} &= (1-j)/2 \\
(x+jy) &= r(\cos\phi + j\sin\phi) \\
e^{j\phi} &= \cos\phi + j\sin\phi \\
\text{whence } x+jy &= re^{j\phi} \\
\text{with } r &= \sqrt{x^2+y^2} \\
\phi &= \tan^{-1}(y/x) \\
e^{(1+j)\phi} &= e^{\phi}(\cos\phi + j\sin\phi) \\
\log(x+jy) &= \log r + j\phi \\
e^{-j\phi} &= \cos\phi - j\sin\phi \\
e^{-(1+j)\phi} &= e^{-\phi}(\cos\phi - j\sin\phi)
\end{aligned}
$$

9.3.2 Trigonometric and Hyperbolic Identities

$$
\begin{aligned}
\sinh^{-1}(x) &= \ln\left(x+\sqrt{x^2+1}\right) \quad -\infty < x < \infty \\
\cosh^{-1}(x) &= \ln\left(x+\sqrt{x^2-1}\right) \quad x \geq 1 \\
\tanh^{-1}(x) &= \frac{1}{2}\ln\left(\frac{1+x}{1-x}\right) \quad -1 < x < 1 \\
\coth^{-1}(x) &= \frac{1}{2}\ln\left(\frac{1+x}{1-x}\right) \quad x > 1 \text{ or } x < -1 \\
\sin(jx) &= j\sinh(x) \\
\cos(jx) &= \cosh(x) \\
\tan(jx) &= j\tanh(x) \\
\cot(jx) &= -j\coth(x) \\
\sinh(jx) &= j\sin(x) \\
\cosh(jx) &= \cos(x) \\
\tanh(jx) &= j\tan(x) \\
\coth(jx) &= -j\cot(x)
\end{aligned}
$$

9.3.3 Bessel and Hankel functions

Bessel and Hankel funtions are frequently encountered in analyses of circular objects, such as electrical conductors. Bessel functions are given by the following series, the arguments of which can be either real or complex. The most commonly encountered complex argument is that for $C\sqrt{\pi/2}$ or $(1+j)C$.

Functions of the first kind, orders zero and one

$$J_0(x) = 1 - \frac{x^2}{D(1)} + \frac{x^4}{D(2)} - \frac{x^6}{D(3)} \cdots \tag{9.1}$$

$$J_1(x) = \frac{x}{2} - \frac{x^3}{4D(1)} + \frac{x^5}{6D(2)} - \frac{x^7}{D(3)} \cdots \tag{9.2}$$

where
$$
\begin{aligned}
D(1) &= 2^2 \\
D(2) &= 2^2 \cdot 4^2 \\
D(3) &= 2^2 \cdot 4^2 \cdot 6^2 \text{ etc.}
\end{aligned} \tag{9.3}
$$

Functions of the second kind, orders zero and one

$$
\begin{aligned}
Y_0(x) = \frac{2}{\pi}&\left\{\ln(x) - \ln(2) + \gamma\right\}J_0(x) \\
&+ \frac{2}{\pi}\left\{\frac{x^2}{D(1)}\Phi(1) - \frac{x^4}{D(2)}\Phi(2)\right. \\
&\left. + \frac{x^6}{D(3)}\Phi(3) - \cdots\right\}
\end{aligned} \tag{9.4}
$$

$$
\begin{aligned}
Y_1(x) = \frac{2}{\pi}&\left\{\ln(x) - \ln(2) + \gamma\right\}J_1(x) - \frac{1}{\pi}\cdot\frac{2}{x} \\
&- \frac{1}{\pi}\left\{\frac{x}{2} - \frac{x^3}{4D(1)}[\Phi(1)+\Phi(2)]\right. \\
&\left. + \frac{x^5}{6D(2)}[\Phi(2)+\Phi(3)] - \cdots\right\}
\end{aligned} \tag{9.5}
$$

where
$$\gamma = 0.57722 \text{ Euler's constant} \tag{9.6}$$

$$\Phi(p) = 1 + 1/2 + 1/3 + \cdots 1/p \tag{9.7}$$

Modified functions of the first kind, orders zero and one

$$I_0(x) = 1 + \frac{x^2}{D(1)} + \frac{x^4}{D(2)} + \frac{x^6}{D(3)} \cdots \tag{9.8}$$

$$I_1(x) = \frac{x}{2} + \frac{x^3}{4D(1)} + \frac{x^5}{6D(2)} + \frac{x^7}{8D(3)} \cdots \tag{9.9}$$

Modified functions of the second kind, orders zero and one

$$
\begin{aligned}
K_0(x) &= -\left\{\ln(x) - \ln(2) + \gamma\right\}I_0(x) \\
K_1(x) &= \left\{\ln(x) - \ln(2) + \gamma\right\}I_1(x) + \frac{1}{x} \\
&\quad - \left\{\frac{2}{x} + \frac{x^3}{4D(1)}[\Phi(1)+\Phi(2)]\right. \\
&\quad \left. + \frac{x^5}{6D(2)}[\Phi(2)+\Phi(3)] + \cdots\right\}
\end{aligned} \tag{9.10}
$$

Hankel functions of the first kind, order n

$$H_n^{(1)}(x) = J_n(x) + jY_n(x) \tag{9.11}$$

Hankel functions of the second kind, order n

$$H_n^{(2)}(x) = J_n(x) - jY_n(x) \tag{9.12}$$

Calculation of functions: A computer routine for calculation of Bessel functions is discussed in §9.11.

9.4 Characteristics of Materials

9.4.1 Free Space

The permeability and permittivity of free space are defined as:

$$\mu_0 = 4\pi \times 10^{-7} \text{ H/m} \tag{9.13}$$

$$\epsilon_0 = 8.854 \times 10^{-12} \text{ F/m} \tag{9.14}$$

$$\epsilon_0 \approx \frac{10^{-9}}{36\pi} \text{ F/m}. \tag{9.15}$$

Three numerical quantities involving μ_0 and ϵ_0, taking ϵ_0 as defined by Eq. 9.15, are:

$$\eta_0 = \left[\frac{\mu_0}{\epsilon_0}\right]^{1/2} = 377 \tag{9.16}$$

$$\left[\frac{1}{\mu_0\epsilon_0}\right]^{1/2} = 3 \times 10^8 \text{ m/s} = (\text{velocity of light}) \tag{9.17}$$

$$\frac{1}{2\pi}\left[\frac{\mu_0}{\epsilon_0}\right]^{1/2} = 60. \tag{9.18}$$

Eq. 9.16 defines the wave impedance for plane waves propagating in free space:

$$\eta_0 = \text{E/H}. \tag{9.19}$$

Eq. 9.17 defines the velocity with which electromagnetic waves propagate in free space. Useful engineering approximations for this velocity are 0.3 m/ns or 1 ft/ns.

9.4.2 Other Materials

Any medium other than free space (or in practice any gas) will have a permeability $\mu = \mu_0\mu_r$ and permittivity $\epsilon = \epsilon_0\epsilon_r$ higher than given by Eqs. 9.13 and 9.14. The materials dealt with in analysis of lightning effects on aircraft will practically always be non-magnetic (aluminum, copper, composites etc.) and the relative permeability can be taken as unity, but the relative permittivity will be higher, typical values being given in Table 9.1.

Table 9.1

Relative Permittivity of Some Common Materials

Material	Relative Permittivity
Air	1.0
Glass	3.0
Mica	6.0
Oil	2.3
Paper	1.5 - 4.0
Polycarbonate	2.6
Polyethelene	2.3
Polystyrene	2.7
Porcelain	5.4
Quartz	5.0
Teflon	2.0

9.4.3 Resistivity of Materials

Resistivities (inverse of conductivity) of typical aircraft materials are given in Table 9.2. Metals are isotropic materials and the resistivity does not depend on the direction of current flow, but composite materials, because they are generally built up of plies bonded together with non-conductive resins, are non-isotropic and the resistivity may depend on the direction of current flow and the current density. Values given in Table 9.2 are average values.

Table 9.2

Resistivities of Typical Metals

Material	Resistivity ohm-meters	Conductivity as a fraction of that of copper	Resistivity relative to copper
copper	1.68×10^{-8}	1.0	1.0
aluminum	2.69×10^{-8}	0.62	1.6
magnesium	4.46×10^{-8}	0.38	2.65
nickel	10×10^{-8}	0.17	6
Monel	42×10^{-8}	0.04	25
stainless steel	70×10^{-8}	0.024	42
Inconel	100×10^{-8}	0.017	60
titanium	180×10^{-8}	0.009	107

Aluminum alloys range from 2.8 to 5.6×10^{-8} ohm-meters. Harder alloys generally have higher resistivities. Magnesium alloys containing aluminum and zinc range from 10 to 17×10^{-8} ohm-meters.

9.4.4 Good vs Bad Conductors

If a unit cube (all sides = 1 m) of material is bounded on opposite faces by electrodes, and a voltage is impressed on the electrodes there will be a current

through the material, partly because of resistive conduction and partly because of capacitive displacement.

For resistive conduction:

$$i = E\sigma \tag{9.20}$$

For capacitive conduction:

$$i = j\omega E\epsilon. \tag{9.21}$$

A good conductor is one in which resistive conduction current predominates ($\sigma \gg \omega\epsilon$) and a poor conductor or insulator is one in which capacitive displacement current predominates ($\omega\epsilon \gg \sigma$). The distinction may depend on frequency.

9.4.5 Skin Depth

If current is applied to the surface of a conducting material it will penetrate into the material and the depth at which the relative current density drops to $1/\epsilon$ is defined as the skin depth. Skin depth is a term that appears in the expressions for surface and transfer impedances of conductors, as discussed further in §9.9. It is:

$$\delta = \left[\frac{2}{\omega\mu\sigma}\right]^{1/2} \text{ m.} \tag{9.22}$$

A numerically useful expression is:

$$\delta = \frac{50}{\pi}\left[\frac{1}{\sigma f_{\text{kHz}}}\right]^{1/2} \text{ m.} \tag{9.23}$$

9.4.6 Propagation Constant

The propagation constant of a material or a conductor defines the velocity with which signals propagate and the rate at which they attenuate. For a material the propagation constant is:

$$\gamma = [j\omega\mu(\sigma + j\omega\epsilon)]^{1/2} \tag{9.24}$$

$$\gamma = (1+j)\left[\frac{\omega\mu(\sigma + j\omega\epsilon)}{2}\right]^{1/2} \tag{9.25}$$

Some notations use k for the propagation constant and define it as:

$$k = [\omega\mu(\sigma + j\omega\epsilon)]^{1/2}. \tag{9.26}$$

Using that notation, $k = j\gamma$, where γ is defined by Eq. 9.25.

In general, the propagation constant has real and imaginary parts:

$$\gamma = \alpha + j\beta. \tag{9.27}$$

where

$$\alpha = \omega\sqrt{\frac{\mu\epsilon}{2}\left(\sqrt{1+\left(\frac{\sigma}{\omega\epsilon}\right)^2} - 1\right)} \tag{9.28}$$

$$\beta = \omega\sqrt{\frac{\mu\epsilon}{2}\left(\sqrt{1+\left(\frac{\sigma}{\omega\epsilon}\right)^2} + 1\right)}. \tag{9.29}$$

The real part, α, defines the attenuation. Between two points l meters apart a signal, voltage or current, attenuates by αl nepers. The imaginary part, β, defines the phase shift. Between two points l meters apart a signal of angular frequency ω undergoes a phase shift of ωl radians. The phase constant is closely related to the velocity at which signals propagate:

$$v = \frac{\beta}{\omega}. \tag{9.30}$$

In a material having good conductivity the displacement current is negligible, thus:

$$\gamma = (1+j)\left[\frac{\omega\mu\sigma}{2}\right]^{1/2} \tag{9.31}$$

The quantity multiplying $(1+j)$ is the reciprocal of the skin depth, Eqs. 9.22. Thus:

$$\gamma = \frac{1+j}{\delta} \tag{9.32}$$

$$\gamma = \frac{\sqrt{2}}{\delta}\angle 45\,\text{deg}\,. \tag{9.33}$$

In a good conductor the attenuation and phase constants are equal; the phase angle is 45 degrees. It is this property that leads to the need to evaluate various functions with a complex argument of 45 degrees.

In an insulating material the conduction current is negligible, thus:

$$\gamma = j\omega(\mu\epsilon)^{1/2} \tag{9.34}$$

$$\gamma = \frac{j\omega}{v}. \tag{9.35}$$

where v is the velocity of propagation in the medium.

A conducting wire will also have a propagation constant,

$$\gamma = [ZY]^{1/2}. \tag{9.36}$$

where the series impedance per unit length is

$$Z = R + j\omega L \tag{9.37}$$

and the shunt admittance per unit length is

$$Y = G + j\omega C. \tag{9.38}$$

For a conducting wire in a homogeneous medium the two propagation constants will be equal at the surface of the conductor.

9.5 Geometric Mean Distances

Geometric mean distances and radii [9.1] are a mathematical concept of particular use when evaluating the impedance of conductors or groups of conductors. They will be introduced here as a mathematical device and the results used later when discussing internal impedance of conductors.

The geometric mean distance, GMD, from point P to the three points 1, 2 and 3 of Fig. 9.1 is defined as:

$$GMD = (S_1 S_2 S_3)^{1/3}. \tag{9.39}$$

If there were n points, the GMD would be

$$GMD = (S_1 S_2 S_3 \cdots S_n)^{1/n}. \tag{9.40}$$

A circle can be considered as an infinite number of points on a line, while an annulus or disk can be considered as an infinite number of points over an area. If all the points have equal weight, the GMD can be considered as an effective distance from the assembly of points to an external point. For circular geometries the GMD to an external point is the distance from the point to the center of the circle.

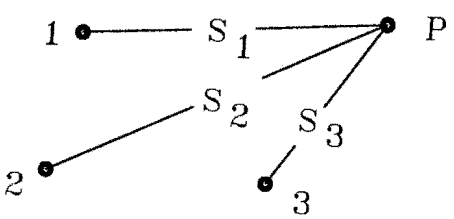

Fig. 9.1 Geometric mean distance.

The concept of GMD can also be extended to define the effective distance of all the points from each other. That distance is called the geometric mean radius, GMR. With regard to Fig. 9.2 the GMD is:

$$GMD = [(r_1 r_2 r_3 \cdots r_n)^{1/n} (S_{12} S_{13} S_{14} \cdots S_{1n})]^{1/n} \tag{9.41}$$

The GMR of some common geometries is given in Fig. 9.3.

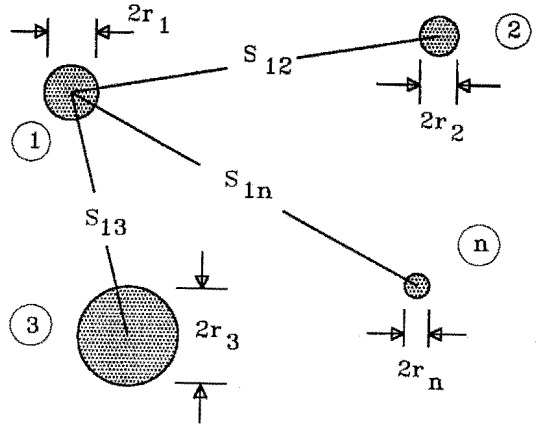

Fig. 9.2 Geometric mean radius of a group of conductors.

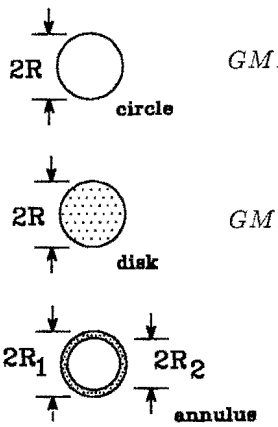

$GMR = R$

$GMR = R\ \ln(1/4) = 0.7788R$

$$GMR = \frac{R_1 \ln(R_1) - R_2 \ln(R_2)}{R_1^2 - R_2^2} - \frac{1}{2}$$

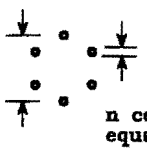

$GMR = [nrR^{(n-1)}]^{1/n}$

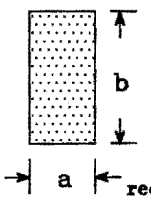

$GMR = 0.2235(a + b)$ – very nearly

Fig. 9.3 Geometric mean radii of some common geometries.

In the context of electrical conductors the points can be considered as the ends of current carrying filaments while the term "equal weight" implies that all the filaments carry equal current. In this context the GMR of an irregular shaped conductor, or of a group of conductors in parallel, is the effective radius. The concept is valuable since the self- inductance of any conductor is equal to the mutual inductance between two filaments separated by the GMR. That concept is discussed further in §9.7.3.

9.6 Voltage and Current Concepts

Experience shows that some concepts of electrical circuits are not as well understood as they might be, especially by those that are not specialists in the field of electromagnetic interactions. Some of the more important points are reviewed in the following sections.

9.6.1 Lumped Constant Elements

The relationships between voltage and current for lumped constant circuit elements are well known.

Resistance

$$i = E/R \tag{9.42}$$

Inductance

$$i = \frac{E}{j\omega L} \tag{9.43}$$

$$i = \frac{1}{L}\int E\, dt \tag{9.44}$$

$$E = L\, di/dt \tag{9.45}$$

Capacitance

$$i = j\omega C \tag{9.46}$$

$$i = C\, dE/dt \tag{9.47}$$

$$E = \frac{1}{C}\int i\, dt \tag{9.48}$$

9.6.2 Voltage as the Line Integral of Potential

The definition of voltage as the line integral of potential is less well appreciated. Voltage and potential are different concepts. A charged sphere, for example, Fig. 9.4, will establish a field E in the surrounding region. The potential of the sphere cannot be established independently; it can only be established by defining some separate point as a reference potential. Commonly "ground" is assigned a reference potential of zero and the potential of the sphere relative to a zero potential ground is found by integrating the field along the path S between the sphere and ground. Hypothetically the integration can be done by connecting a perfect voltmeter between the sphere and ground. The resulting deflection of the meter defines the voltage of the sphere, though for exactness, one should say that the meter indicates the voltage of the sphere relative to the ground.

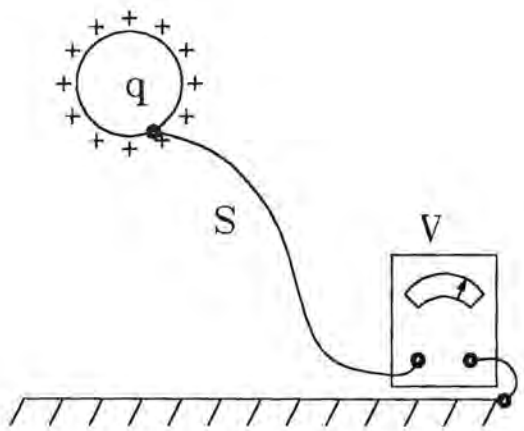

Fig. 9.4 Voltage as total difference of potential.

9.6.3 Importance of the Path of Integration

Does the voltage depend on the path of integration or upon the path taken by the leads connecting the voltmeter to the sphere and ground? This is not a trivial question; it is of fundamental importance for understanding how voltages develop in objects carrying current, such as an aircraft carrying lightning current.

DC and lumped constant elements: For dc conditions the answer is that the path taken by the measuring leads does not influence the voltage, but for ac or transient conditions this is true only if the measuring leads traverse a region free of electromagnetic fields. As a practical matter this situation is found only when measuring the voltage across lumped constant elements, those in which the electromagnetic field is entirely enclosed within the element.

As an example, the ac voltage developed across the winding of a transformer can be measured without regard to where one places the measuring leads because the magnetic field inducing the voltage in the windings is entirely (or nearly entirely) contained in the core of the transformer. The external magnetic field is negligible (ideally zero) and so not able to induce any voltage in the measuring leads.

Distributed circuits: With distributed circuits the role of the electromagnetic fields and their effect on the measuring leads is very important since the voltage does depend on the path taken by the measuring leads.

As an example, consider Fig. 9.5 where an alternating current is flowing through a metal cylinder. In an attempt to measure the voltage drop along the cylinder an experimenter has connected four voltmeters, and has observed that all four meters respond differently. They also respond different from the meter measuring the voltage of the power supply used to circulate the current.

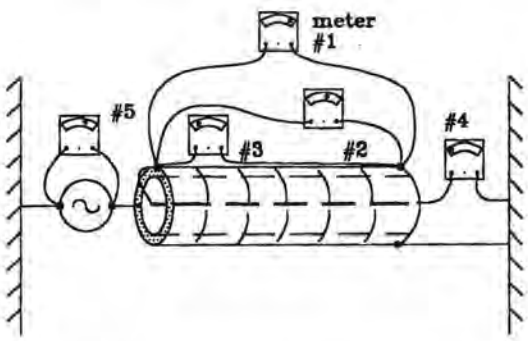

Fig. 9.5 Voltage as a function of path.

Which meter records the correct voltage or are any of them correct? The answer is that all of them respond correctly since there is no unique "voltage drop" associated with the pipe; each of the meters responds differently because for each situation the electric field is evaluated around a different path. The external voltmeters respond primarily to the magnetic field surrounding the cylinder. The leads connecting to meter 1 intercept more magnetic flux than do the leads connecting to meter 2 and consequently there is more voltage induced in the leads of meter 1 than meter 2. The amount of voltage induced in a loop exposed to a magnetic field is discussed in §9.7.4.

The leads for meter 3, which run flush with the surface of the cylinder intercept no magnetic flux. As a result, meter 3 responds only to the voltage produced by the current flowing through the resistance of the cylinder.

Meter 4 responds differently yet. Since there can be no magnetic field within the cylinder (see §9.7.2) there can be no voltage induced magnetically in the leads. The meter does, though, respond to the voltage produced by the flow of current through the resistance of the cylinder, but it still indicates a different voltage from meter 3. The reason is that meter 3 responds to the density of the current flowing on the outer surface of the cylinder while meter 4 responds to the density of the current flowing on the inner surface of the cylinder. The two are different, as discussed further in §9.6.4.

The concept of voltage as the line integral of electric field around a particular path is of great importance. Anomalies of voltage on circuit elements can generally be explained by careful attention to the path along which connecting wires are routed.

9.6.4 Internal vs External Impedances

Consider Fig. 9.6 which shows voltage applied to series circuits composed of a conductor, a return path and the gap between the two. The applied voltage V must be equal to the line integral of all the electric fields around the loop, that is, the sum of E_c, E_r and E_g where E_c is defined as the surface electric field of the conductor, E_r the surface electric field of the return path and E_g is the electric field of the gap or space between the conductor and the return path.

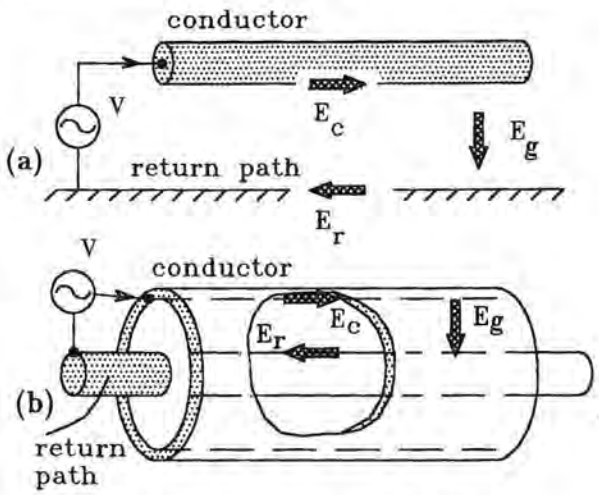

Fig. 9.6 Components of electric field.
(a) Conductor over a ground plane
(b) Coaxial conductors

In Fig. 9.6(a) E_c is best described as the external surface electric field with external return since the return path is external to the conductor. In Fig. 9.6(b) E_c is best described as the internal surface electric field with internal return.

The various electric fields can be related to the conductor current through impedances. On Fig. 9.7 are depicted the internal impedance of the conductor, the internal impedance of the return path and the external impedance of the conductor, or the impedance of the gap between the conductor and return path. The internal impedances of the conductor and return path are properties of the materials and the sizes of the conductors and can, in the frequency domain, be sep-

arated into real and imaginary components. The real part is a measure of resistance and the imaginary component is a measure of the internal inductance or the magnetic flux within the conductor. At dc the internal impedance of the conductor is just its resistance.

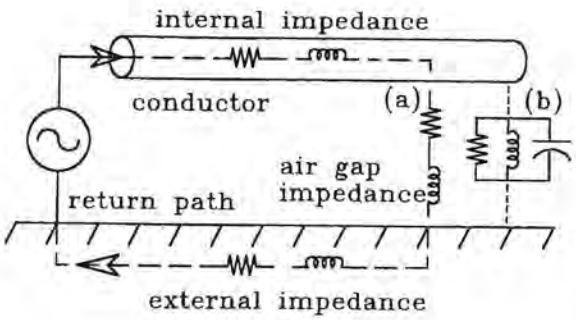

Fig. 9.7 Components of impedance.

The external impedance is a property of the space between the conductor and the return path, that is, of the size and shape of the conductor, the separation from the return path and of the material (insulation) between the two. With high frequencies the capacitance of the insulation must be included in the insulation impedance and it may also be more appropriate to treat the insulation losses as a shunt resistance. Fig. 9.7(a) shows the external impedance resolved into a series connection of resistance and inductance, while Fig. 9.7(b) shows it resolved into a set of parallel admittances.

Another circuit concept is that of transfer impedance. With a hollow conductor, Fig. 9.8, the electric field on the inner and outer surface will, in general not be the same. The transfer impedance of a conductor is the quantity that relates the conductor current to the electric field along the inner surface of the conductor; as opposed to the external impedance which relates the current to the electric field along the external surface.

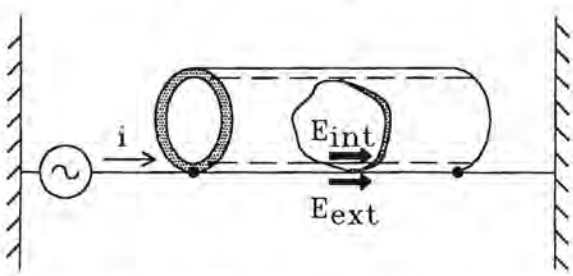

Fig. 9.8 Transfer impedance.

Evaluating these various impedances can be done just as a mathematical manipulation of equations, but it seems best to present some of the physical phenomena involved. This is done in the following three sections. Inductance and related magnetic field effects are covered in §9.7 and capacitance and related electric field effects are covered in §9.8. Both sections deal with subjects other than the impedance of conductors. Chapter 10 deals with mathematical formulations in the time domain of surface and transfer impedances.

9.7 Magnetic Field Effects

Magnetic field effects are probably the major reason why voltages are induced on aircraft wiring by lightning currents flowing on the aircraft. Situations where shielding proves to be ineffective are usually those where magnetic field effects have been overlooked. Capacitive effects are, of course, also of importance, but those are discussed in §9.8.

9.7.1 Field External to a Conductor

Infinite conductor: In the space around and external to a conductor of infinite length, Fig. 9.9, the magnetic field is:

$$H = \frac{I}{2\pi r} \text{ A/m.} \tag{9.49}$$

The return path of the current is assumed to be so far away that it does not contribute to the magnetic field.

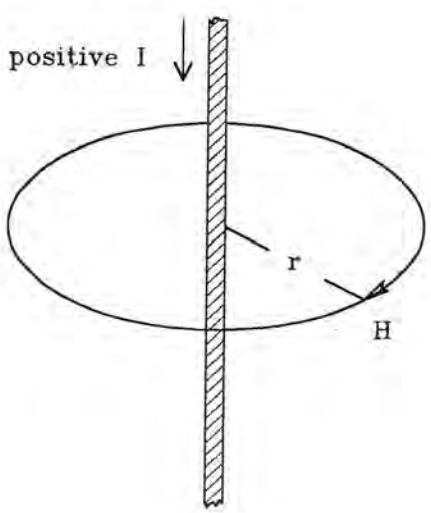

Fig. 9.9 Magnetic field of an infinite conductor.

Isolated filament: On an isolated filament or circular conductor carrying a current I over its entire length, Fig 9.10, the flux density at point P will be:

$$B = \mu H = 4\pi \times 10^{-7} \frac{I}{4\pi r}(\sin\alpha + \sin\beta) \text{ A/m.} \quad (9.50)$$

The return path for the current is assumed to be so far beyond r_3 that it does not influence the magnetic field.

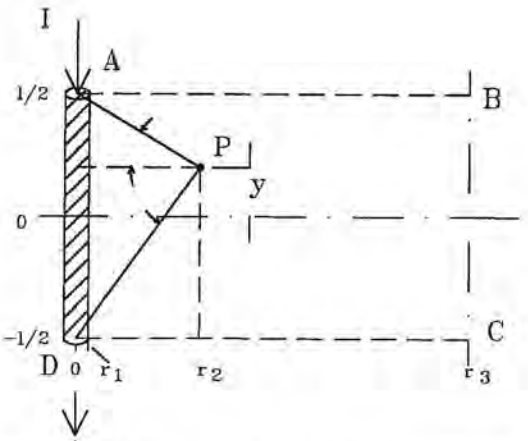

Fig. 9.10 Magnetic field of a finite conductor.

Dipole: For the limiting case of a short dipole, Fig. 9.11, the field is:

$$H = \frac{Il}{4\pi} \cdot \sin\alpha \text{ A/m} \quad (9.51)$$

The direction of the flux around a filament or a cylinder will be as given by the "right hand rule" illustrated on Fig. 9.9. For all high frequency conditions the magnetic flux lines will be parallel to the surface of conductors, even if the conductors are of irregular shape, and the magnitude of the field intensity, H, will be identically equal to the local surface current density measured in amperes/meter. For circular conductors the current density will be uniform and equal to the total current divided by the peripheral distance around the conductor. For conductors of irregular shape the current density will depend on the local radius of curvature, as discussed in considerably more detail in Chapter 10.

The magnetic field external to a current carrying tube is the same as though the current were concentrated on a filament at the center.

9.7.2 Fields Within Hollow Conductors

If there are several conductors the total field intensity is the sum of that produced by the individual conductors. With two conductors each carrying an equal current, Fig. 9.12, the fields will cancel at the midpoint. The fields at other points will not cancel, but their sum will be lower than in the space outside the conductors. With three equally spaced conductors carrying equal currents the fields will cancel at three places. With many conductors arranged in a circle and each conductor carrying an equal current, the field will cancel at many points within the circle.

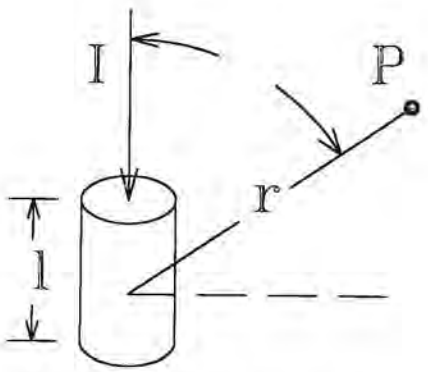

Fig. 9.11 Magnetic field of a dipole.

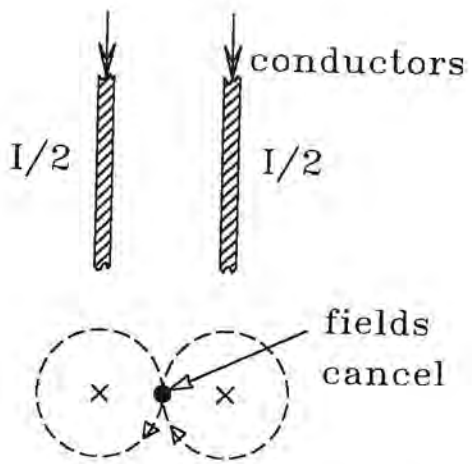

Fig. 9.12 Field between two conductors.

9.7.3 Inductance

The self-inductance of a conductor is defined as the ratio of magnetic flux surrounding a conductor to the current that establishes the flux while the mutual inductance between two conductors is defined as the ratio of the magnetic flux surrounding conductor 2 to the current in conductor 1.

$$L_{11} = \phi_1 / I_1 \tag{9.52}$$

$$L_{12} = \phi_{12} / I_1 \tag{9.53}$$

Isolated linear conductors: Determining the inductance of a conductor requires integrating the magnetic field intensity over an area to determine the total flux set up by current in the conductor. An elementary case is that of the isolated conductor of Fig. 9.10. in which the return path is assumed to be sufficiently far away that the magnetic field from the return path is negligible compared to that of the conductor under consideration. For dc conditions this implies that the return path is at infinity.

The self inductance is controlled by the flux in the area A-B-C-D. Integrating Eq. 9.51 first over the limits $-l/2$ and $l/2$ and then integrating that expression over the limits r_1 and r_3 gives:

$$\phi = 2 \times 10^{-7} Il \left[-\ln \left\{ \frac{l}{r} \left(1 + \sqrt{\left(\frac{r}{l}\right)^2 + 1} \right) \right\} + \sqrt{\left(\frac{r}{l}\right)^2 + 1} - \frac{r}{l} \right]_{r_1}^{r_3} \text{ webers} \tag{9.54}$$

from which the inductance can be determined using Eq. 9.52.

If there are two conductors, Fig. 9.13, the mutual inductance between conductors 1 and 2 is determined by the flux between the limits r_2 and r_3; that is, the flux in the shaded area.

The form of the equation is the same as that of Eq. 9.54; the limits being r_3 and r_2, rather than r_2 and r_1. Note that the radii of the conductors are not involved, only their locations. This implies that mutual inductance can be defined for filaments as well as conductors.

How one evaluates the flux, and thus the self or mutual inductance, depends on the relative values of r_2 and r_3.

Case 1 $l \gg r_3$**:** Under dc conditions the magnetic field extends to infinity and so Eq. 9.54 must be evaluated over the limits $r_3 = \infty$ and r_1. When $r_3 = \infty$, the sum of all the terms involving r_3 goes to zero and thus the self-inductance of conductor 1 becomes:

$$L_{11} = 2 \times 10^{-7} Il \left[\ln \left\{ \frac{l}{r_1} \left(1 + \sqrt{\left(\frac{r_1}{l}\right)^2 + 1} \right) \right\} - \sqrt{\left(\frac{r_1}{l}\right)^2 + 1} + \frac{r_1}{l} \right] \text{ H} \tag{9.55}$$

and the mutual inductance between conductors 1 and 2 is:

$$L_{12} = 2 \times 10^{-7} Il \left[-\ln \left\{ \frac{l}{r_2} \left(1 + \sqrt{\left(\frac{r_2}{l}\right)^2 + 1} \right) \right\} - \sqrt{\left(\frac{r_2}{l}\right)^2 + 1} + \frac{r_2}{l} \right] \text{ H.} \tag{9.56}$$

Case 2 $r_3 \gg l$**) and** $l \gg r_1$**:** For a long conductor under dc conditions the inductances are:

$$L_{11} = 2 \times 10^{-7} l \left[\ln \frac{2l}{r_1} - 1 \right] \text{ H/m} \tag{9.57}$$

$$L_{12} = 2 \times 10^{-7} l \left[\ln \frac{2l}{r_2} - 1 \right] \text{ H/m.} \tag{9.58}$$

Note that the inductances are not directly proportional to length.

Case 3 $l \gg r_3$**:** Where the two conductors are parallel and of equal length:

$$L_{11} = 2 \times 10^{-7} l \left[\ln \frac{r_3}{r_1} \right] \text{ H} \tag{9.59}$$

$$L_{12} = 2 \times 10^{-7} l \left[\ln \frac{r_3}{r_2} \right] \text{ H} \tag{9.60}$$

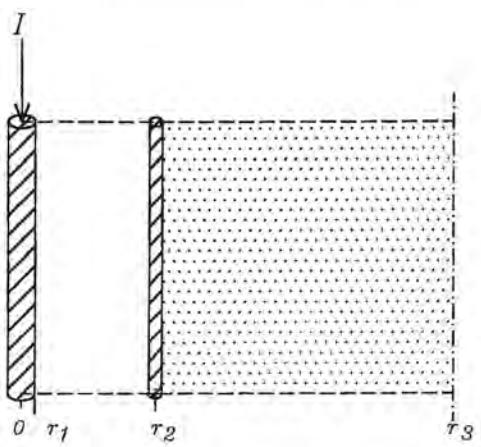

Fig. 9.13 Flux involved in mutual inductance.

The mutual inductance between two filaments of any arbitrary orientation is calculable and while the expressions are too long to include here they can be found in the literature [9.2, 9.3].

While the inductance of an isolated conductor is an important concept it must be used with care since an isolated conductor cannot actually carry current. Current can flow only if the conductor is part of a larger circuit and so the inductance of an isolated conductor should then be viewed as part of a larger problem, one in which the self and mutual inductances must be considered together.

All of these formulae give only the external or high frequency inductance. At low frequencies there will also be magnetic fields within the conductor, a subject treated in a later section.

Time dependence of inductance: Under transient conditions one must also consider the retardation effects associated with the finite velocity of propagation of an electromagnetic field, since if a current is suddenly applied to a conductor, the field will not initially extend to infinity. Instead it will propagate away from the conductor at the speed of light. The total amount of magnetic flux established in the space around the conductor will vary with time, becoming larger with time as the fields propagate farther from the conductor. The implication is that the inductance of a conductor will be less for short duration transients or high frequencies than it will be for long duration transients or low frequencies. In an engineering sense the effect is of more importance for long conductors than for short conductors. In $1\mu s$ a field will propagate 300 m. For a conductor one meter long 1 μs might be considered as "dc" conditions, but that would not be the case for a conductor 1000 meters long. For aircraft analyses frequency dependence of external inductance because of retardation effects would not normally be a factor to consider since the various conductors of necessity are close together.

Coaxial conductors: Most commonly inductance is evaluated for a "go-return" circuit. In a coaxial system the center conductor (the "go" conductor) is surrounded by a concentric "return"conductor, Fig. 9.14(a), and the inductance is found by evaluating the field intensity between the limits r_1 and r_2. The current flowing on the cylindrical return path does not need to be considered since it does not produce any internal magnetic field. Since in any practical situation the length is long compared to the diameter of both the inner and outer conductors the field may be evaluated from Eq. 9.59.

$$L_{11} = 2 \times 10^{-7} \ln\left[\frac{r_2}{r_1}\right] \text{ H/m} \qquad (9.61)$$

For all practical cases there are no end effects and the inductance is directly proportional to length.

If there were two conductors at a spacing S, both surrounded by a coaxial return path, Fig. 9.14(b) and the radius of the coaxial return path large compared to S, the mutual inductance would be:

$$L_{12} = 2 \times 10^{-7} \ln\left[\frac{2r_2}{S}\right] \text{ H/m.} \qquad (9.62)$$

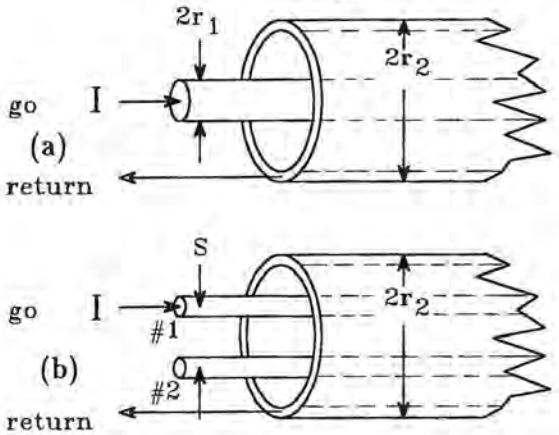

Fig. 9.14 Coaxial conductors.
(a) Single conductor
(b) Parallel conductors

Conductor pairs: Two parallel conductors can also be connected as a "go-return" pair. Two connections are possible, the connection in which current goes on one conductor and returns on the other, Fig. 9.15(a), being the most common geometry. The configuration of Fig. (9.15(b) is impractical for straight conductors since the magnetic field of the connecting leads would influence the result, but it is practical for conductors bent into a circle since that is the geometry of a helical coil.

The inductance of the pair involves four conductors; the two self inductances and the two mutual inductances:

$$L_T = (L_{11} + L_{12}) + (L_{22} + L_{21}). \qquad (9.63)$$

If the conductors are about the same diameter L_{12} and L_{21} are nearly equal, even if the conductors are fairly close together. Also, L_{11} and L_{22} will be equal if the diameters are the same. Thus:

$$L_T = 2(L_{11} + L_{12}) \qquad (9.64)$$

Evaluating the individual inductances in Eq. 9.63 gives:

$$L_T = 4 \times 10^{-7} l \left[\ln\left(\frac{2l}{r}\right) - 1 - \ln\left(\frac{2r_2}{S}\right) + 1\right] \text{ H} \qquad (9.65)$$

If the conductors are long compared to their spacing the d/l terms cancel and the inductance becomes directly proportional to length:

$$L_T = 4 \times 10^{-7} \ln\left[\frac{S}{r}\right] \text{ H/m.} \qquad (9.66)$$

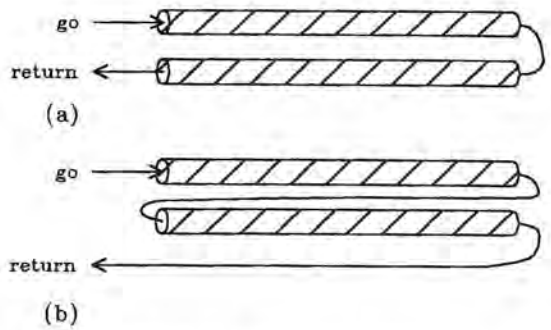

Fig. 9.15 Conductor pairs.
(a) Fields cancel
(b) Fields add

Conductors over a ground plane: If current flows along a conductor and returns through a perfectly conducting ground plane, Fig. 9.16, the current in the ground plane will be distributed, being most dense underneath the conductor and least dense at points far from the conductor. The effect is the same as though the return current were to flow on an image conductor underneath the ground plane. The self inductance of a conductor over a perfect ground plane can then be visualized as that of a conductor pair, the actual conductor and its image in the ground plane. Taking the individual inductances in Eqs. 9.63 and 9.64, and evaluating for the case where $l \gg h$ gives:

$$L = 2 \times 10^{-7} \ln\left[\frac{2h}{r}\right] \text{ H/m.} \qquad (9.67)$$

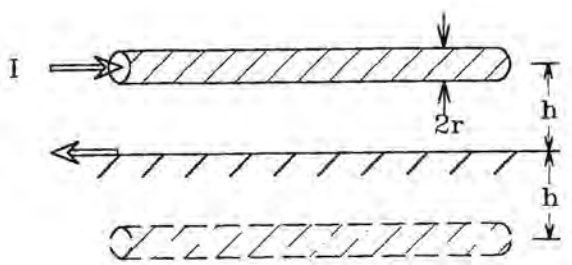

Fig. 9.16 Conductor over a ground plane.

Only one pair of inductances is involved; the image conductor does not actually carry current and the concept of a perfect ground plane implies that it has no internal inductance of its own.

The mutual inductance between two conductors, Fig. 9.17, is

$$L_{12} = 2 \times 10^{-7} \ln\left[\frac{D}{S}\right] \text{ H/m.} \qquad (9.68)$$

Ground planes that are not perfectly conducting surfaces are treated in §9.9.3.

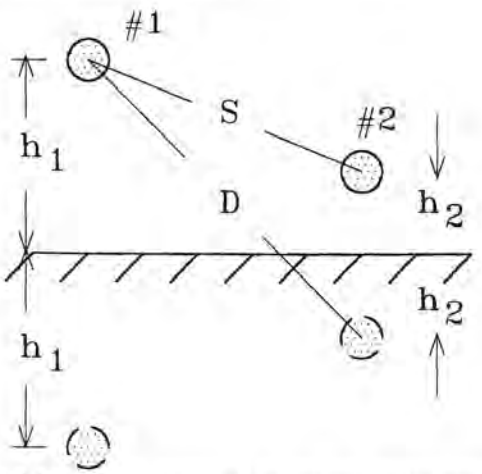

Fig. 9.17 Geometry involved in mutual inductance.

Proximity effects: The above formulations of inductance for conductor pairs and conductors over a ground plane are only approximations since they assume current to be uniformly distributed over the surface of the conductors. This is not the case if the conductors are close together. Exact formulations involve hyperbolic functions, the inductance of a conductor over a ground plane, for example being:

$$L_{11} = \frac{\mu_0}{2\pi} \cosh^{-1}\left[\frac{h}{r}\right], \text{ H/m} \qquad (9.69)$$

The hyperbolic function in Eq. 9.69 can also be written as:

$$L_{11} = \frac{\mu_0}{2\pi} \ln\left[\frac{h}{r} + \sqrt{\left(\frac{h}{r}\right)^2 + 1}\right] \text{ H/m.} \qquad (9.70)$$

Thus exact expressions for inductance can be written by substituting:

$$\frac{h}{r} + \sqrt{\left(\frac{h}{r}\right)^2 + 1} \quad \text{for} \quad \frac{2h}{r}. \qquad (9.71)$$

in Eq. 9.67.

Generally the error in ignoring proximity effects is small. Even when $h = d$, the simplified formula of Eq. 9.67 predicts an inductance only 5 % higher than predicted by the exact Eq. 9.70. These proximity effects do not arise on isolated or coaxial conductors.

Self-inductance in terms of GMR: Section 9.5 introduced the concept of geometric mean radius, GMR, and the GMR of some common geometries was given in Fig 9.3. The self inductance of any conductor can be evaluated by finding the mutual inductance between two filaments separated by the GMR of the conductor. As an example, consider a circular tubular conductor with a very thin wall. From Fig. 9.3 the GMR is equal to the physical radius. Substituting the GMR into Eq. 9.55 for the mutual inductance of two filaments gives the same formulation as Eq. 9.58 for the self inductance of a conductor of radius r.

This approach to formulating self-inductance is of most benefit for irregularly shaped conductors, Fig. 9.18. It also provides a way of evaluating the internal inductance of conductors, as discussed in the following section.

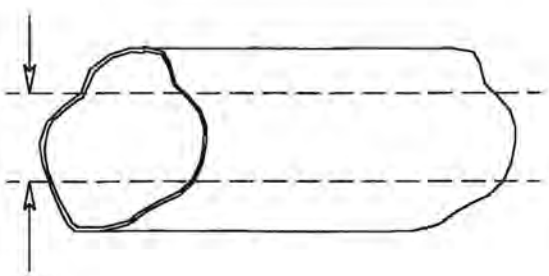

Fig. 9.18 Self inductance in terms of geometric mean radius.

Internal inductance of conductors: All of the formulations of §9.7.3 relate only to the fields external to the conductors, the formulations being valid for the high frequency case where skin effects confine current to the surface of conductors. At lower freqencies current penetrates into the conductors and a magnetic field is established within the conductor, Fig. 9.19. The maximum internal flux occurs with solid conductors and at dc where the current density is uniform. Under such conditions the flux density varies as the distance from the center. The total flux within the conductor and the internal inductance are found to be:

$$\phi = \frac{\mu_0 \mu_r}{8\pi} I \text{ webers} \qquad (9.72)$$

from which

$$L_{\text{int}} = \frac{\phi}{I} = \frac{\mu \times 10^{-7}}{2} = 0.05\ \mu\text{H/m}. \qquad (9.73)$$

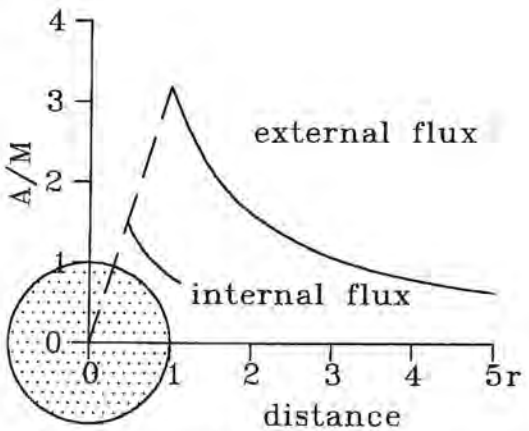

Fig. 9.19 Internal and external field density.

GMR as applied to internal inductance: An alternative approach to internal inductance involves the concept of geometric mean radius. In Fig. 9.1 the GMR of a disk of radius r was shown to be $\ln(1/4)\ r$ or $0.7788r$. Substituting this value into Eq. 9.58 for the mutual inductance of two filaments gives the total inductance of the conductor under dc conditions:

$$L_{11} = 2 \times 10^{-7} l \left[\ln \frac{2l}{r} - 1 + \frac{\mu_r}{4} \right] \text{ H/m}. \qquad (9.74)$$

The difference in inductance between the value given by Eq. 9.57 (treating only external inductance) and that of Eq. 9.74 is the internal inductance, or the inductance due to magnetic flux within the conductor. Numerically, for non-magnetic conductors, it is

$$L_{11} = \frac{2 \times 10^{-7}}{4} = 0.05\ \mu\text{H/m} \qquad (9.75)$$

While the internal inductance is generally small compared to the external inductance, it is intimately linked with the transient resistance of conductors. The transient resistance and internal inductance of conducting bodies is of such importance to how lightning currents penetrate into aircraft that the subject of internal impedance is discussed in much more detail in §9.9 and Chapter 10.

9.7.4 Practical equations for inductance

Equations have been developed for the inductance of almost any geometry, the best collection appearing in [9.4]. Equations for a few selected geometries are presented below. Inductances are in microhenries and dimensions are in centimeters.

Rectangle of round wire: The sides of the rectangle are a and b and the radius of the cross section is ρ.

$$L = 0.004\left[a\ln\frac{2a}{\rho} + b\ln\frac{2b}{\rho} + 2\sqrt{a^2+b^2} - a\sinh^{-1}\frac{a}{b} - b\sinh^{-1}\frac{b}{a} - 2(a+b) + \frac{\mu}{4}(a+b)\right] \quad (9.76)$$

For copper and other nonmagnetic materials, $\mu = 1$.

Regular polygons of round wire: The side of the polygon is s, and the radius of the cross section is ρ.

Equilateral triangle:

$$L = 0.006s\left[\ln\frac{s}{\rho} - 1.40456 + \frac{\mu}{4}\right] \quad (9.77)$$

Square:

$$L = 0.008s\left[\ln\frac{s}{\rho} - 0.77401 + \frac{\mu}{4}\right] \quad (9.78)$$

Pentagon:

$$L = 0.010s\left[\ln\frac{s}{\rho} - 0.40914 + \frac{\mu}{4}\right] \quad (9.79)$$

Hexagon:

$$L = 0.012s\left[\ln\frac{s}{\rho} - 0.15152 + \frac{\mu}{4}\right] \quad (9.80)$$

Octagon:

$$L = 0.016s\left[\ln\frac{s}{\rho} + 0.21198 + \frac{\mu}{4}\right] \quad (9.81)$$

One Turn of round wire

$$L = 0.004\pi r\left[\ln\frac{8r}{a} - 1.75\right] \quad (9.82)$$

Ring conductor

$$L = 0.004\pi r\left[\ln\frac{8r}{b} - 0.50\right] \quad (9.83)$$

Helical coil

$$L = \frac{2.54a^2n^2}{9a+10b} \text{ cm dimensions} \quad (9.84)$$

$$L = \frac{a^2n^2}{9a+10b} \text{ inch dimensions} \quad (9.85)$$

9.7.5 Magnetic Induction of Voltage and Current

Magnetically induced voltages and currents are probably the most common of the indirect effects of lightning.

Open circuit voltage: A changing magnetic field passing through a conducting loop, Fig. 9.20, induces a voltage:

$$e = -N\frac{d\phi}{dt}. \quad (9.86)$$

where N = number of turns and $\phi = \mu HA$, H being the field intensity and A being the loop area. The voltage appears across the gap and has a waveshape proportional to the derivative of the flux.

Short circuit current: If the loop is short circuited the voltage is impressed on the impedance of the loop and induces a circulating current:

$$I = \frac{1}{L}\int edt = -\frac{N\mu HA}{L}. \quad (9.87)$$

The waveshape of the current tends to be that of the incident magnetic field, unlike that of the open circuit voltage. The point is important; magnetically induced currents generally have longer front and fall times than do magnetically induced voltages.

Field penetration of a loop: If the loop has only inductance and no resistance the current will have the same shape as the incident magnetic field and will set up a magnetic field of its own, one that is of equal amplitude and opposite polarity to the incident field. As a consequence a magnetic field will not penetrate an ideal short circuited loop. If the loop has resistance, Fig. 9.20, the current will decay with a time constant proportional to L/R and the magnetic field will gradually penetrate the loop.

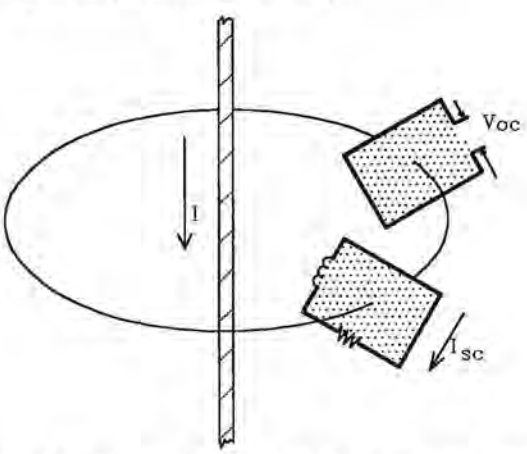

Fig. 9.20 Magnetic induction of voltage and current.

Field penetration of a surface: A conducting surface, Fig. 9.21, may be viewed as an assembly of conducting loops. A magnetic field line that attempts to penetrate the surface induces a circulating current (eddy current) that acts to oppose the penetrating field. The consequence is that under high frequency conditions a magnetic field incident on a surface can have only a tangential component. Any radial component is cancelled by an induced circulating current. Only as the circulating currents die away because of resistance will the magnetic field penetrate the surface. It is this property of eddy currents that allows nonmagnetic materials to provide substantial amounts of shielding against transient magnetic fields. That subject is explored more fully in Chapter 15.

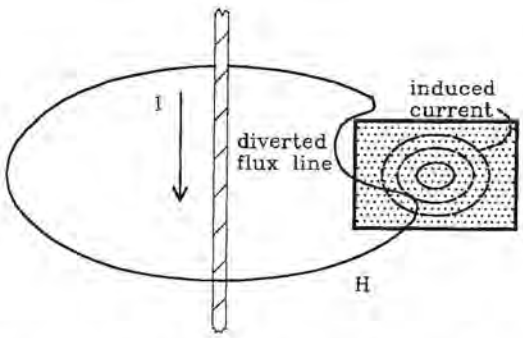

Fig. 9.21 Eddy currents in a conducting sheet.

9.8 Electric Field Effects

Changing electric fields also produce currents and voltages, particularly upon unshielded conductors.

9.8.1 Evaluation of Capacitance

Point charge: In the space around a charged point an electric field is established:

$$E = \frac{Q}{4\pi\epsilon_0 r^2} \text{ V/m.} \tag{9.88}$$

The field is directed radially away from the point.

Isolated sphere (in air): If the charge resides on a sphere of radius r the electric field outside the sphere will be as though all the charge were concentrated at its center. Integrating the electric field from the sphere to a remote point where the field is negligible (as at infinity) gives the total voltage difference between the sphere and that remote reference point:

$$V = \frac{Q}{4\pi\epsilon_0} \cdot \frac{1}{r} \text{ volts.} \tag{9.89}$$

Capacitance is defined as:

$$C = Q/V. \tag{9.91}$$

The capacitance of an isolated sphere is thus:

$$C = 4\pi\epsilon_0 r = \frac{10^{-9}}{9} r \text{ farads.} \tag{9.90}$$

The capacitance of an aircraft could be found by estimating the radius of an equivalent sphere. As an example, an aircraft having a surface area about the same as a sphere of 5 m radius would have a capacitance of about 556 pF.

Electric fields are different from magnetic fields in that an isolated object may have a charge and hence a finite capacitance, regardless of dimensions. Attempting to evaluate the inductance of an isolated conductor leads to conceptual and mathematical difficulties, as noted in §9.7.3, but no such problems arise with determining the capacitance of an isolated body.

Concentric Spheres: For concentric spheres, Fig. 9.22, the capacitance is found by integrating the electric field over the distance r_1 to r_2:

$$C = 4\pi\epsilon_0 \left[\frac{1}{r_1} - \frac{1}{r_2}\right] \text{ farads.} \tag{9.92}$$

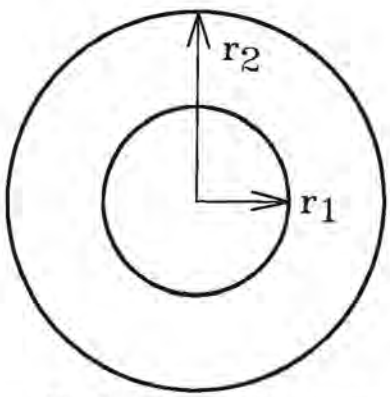

Fig. 9.22 Concentric spheres.

9.8.2 Sphere Over a Ground Plane

If the charged sphere is located over a ground plane there will be charge induced in the ground and the effect is as though there were a sphere of opposite charge below the ground, Fig. 9.23. The fields of the two charges combine to give the total electric field. At the ground plane the horizontal components cancel and the net electric field is oriented at right angles to the ground plane. Evaluating the electric field from the sphere to the ground plane gives the voltage between the sphere and the ground plane and hence the capacitance to ground.

$$C = \frac{10^{-9}}{9[1/r - 1/(r-2h)]} \text{ farads} \qquad (9.93)$$

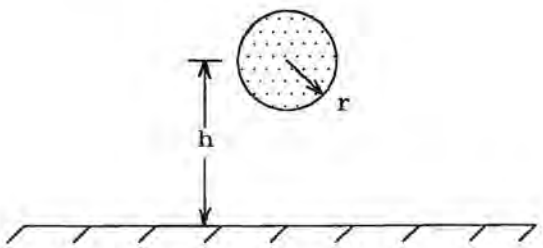

Fig. 9.23 Sphere over a ground plane

Isolated conductor: A charged conductor, Fig. 9.24, with q_0 coulombs per meter may be viewed as an assemblage of charged points. A rod of finite length, though, presents mathematical difficulties because the electric field intensity at the ends becomes infinite. This is overcome by approximating the rod as an ellipsoid having major and minor axes $2a$ and $2b$ with $c = \sqrt{a^2 - b^2}$. The capacitance is then:

$$C = 4\pi\epsilon a \frac{c/a}{\tanh^{-1}(c/a)} \text{ farads} \qquad (9.94)$$

or

$$C = \frac{222c}{\ln[(1-c/a)/(1+c/a)]} \text{ pF} \qquad (9.95)$$

Fig. 9.24 Isolated conductor.

Coaxial conductors: Evaluating the electric field as given by Eq. 9.95 between r_1 and r_2 gives the capacitance:

$$C = \frac{2\pi\epsilon_0\epsilon_r}{\ln(r_2/r_1)} \text{ farads/meter} \qquad (9.96)$$

or

$$C = \frac{55.56}{\ln(r_2/r_1)} \text{ pF/m} \qquad (9.97)$$

Conductor over a ground plane: The electric field is found by taking the vector sum of two fields; one due to the conductor and one due to its image in the ground plane. At the ground plane, Fig. 9.25, and for a conductor in air, the field is perpendicular to the ground plane and has a magnitude:

$$E = \frac{q_0}{\pi\epsilon_0} \cdot \frac{h}{h^2 + x^2} \text{ V/m.} \qquad (9.98)$$

The capacitance is:

$$C = \frac{2\pi\epsilon_0}{\ln(2h/r)} \text{ F/m.} \qquad (9.99)$$

Thus

$$C = \frac{55.6}{\ln(2h/r)} \text{ pF/m} \qquad (9.100)$$

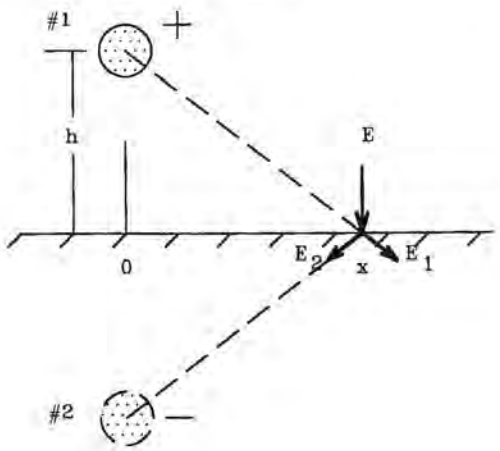

Fig. 9.25 Conductor over a ground plane.

9.8.3 Symmetry of Expressions for Inductance and Capacitance

The above expressions show a good deal of symmetry between the expressions for inductance and capacitance. This merely reflects the fact that the geometrical considerations that determine inductance also determine capacitance. In fact it can be shown that:

$$LC = \mu\epsilon. \qquad (9.101)$$

and that, if one knows one of the quantitites (inductance or capacitance) of a structure, one can determine the other. In fact, one can determine the inductance of a structure or set of conductors by measuring the capacitance. This holds true only for cases where the dielectric is homogeneous. In practical conductor systems using insulated conductors, the total dielectric space between conductors is not homogeneous.

9.8.4 Displacement Currents

If a capacitor is connected to a changing voltage the current that flows through the capacitor is proportional to the derivative of the voltage:

$$i = E\ j\omega C \text{ amperes} \tag{9.102}$$

or

$$i = C\ \frac{dE}{dt} \text{ amperes} \tag{9.103}$$

Similar displacement currents flow as a result of a changing electric field. Fig. 9.26, shows a surface exposed to a changing electric field, the field assumed to be oriented perpendicular to the surface. A portion of the surface has been isolated and connected to the rest of the surface through a conductor. The current through the conductor will be:

$$i = \epsilon_0 A \frac{d}{dt} E_a \text{ amperes.} \tag{9.104}$$

where

A = area of the surface - m^2
E_a = actual electric field intensity - V/m
E_u = undisturbed electric field intensity

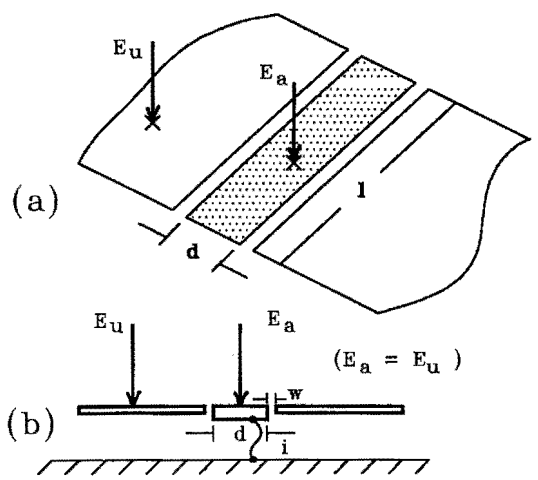

Fig. 9.26 A surface exposed to an electric field.
(a) Isometric view
(b) End view

For a surface flush with its surroundings, as in Fig. 9.26, the electric field impinging on the surface will be the same as the undisturbed field. If the isolated section is raised above the surrounding surface, Fig. 9.27, the electric field will be concentrated and the actual electric field intensity will be higher than the undisturbed electric field intensity E_u. Alternatively, one could say that the elevated plate has a capture area S larger than its physically projected area A. Effective areas for some typical geometries are given in Table 9.3 [9.5]. Displacement currents are also discussed in §14.4.3.

9.9 Surface and Transfer Impedances

In §9.6.2 it was observed that the voltage difference between two points is determined by summing the electric field between the points. §9.6.4 presented definitions of surface and transfer impedances and §9.7.3 presented some discussion of the internal impedance of conductors in terms of internal magnetic flux. This section will present mathematical expressions by which surface and transfer impedances may be calculated. The defining equations are here presented in the frequency domain and without discussion. Formulations in the time domain are given in Chapter 11. Some alternative formulations in the frequency domain are given in [9.6].

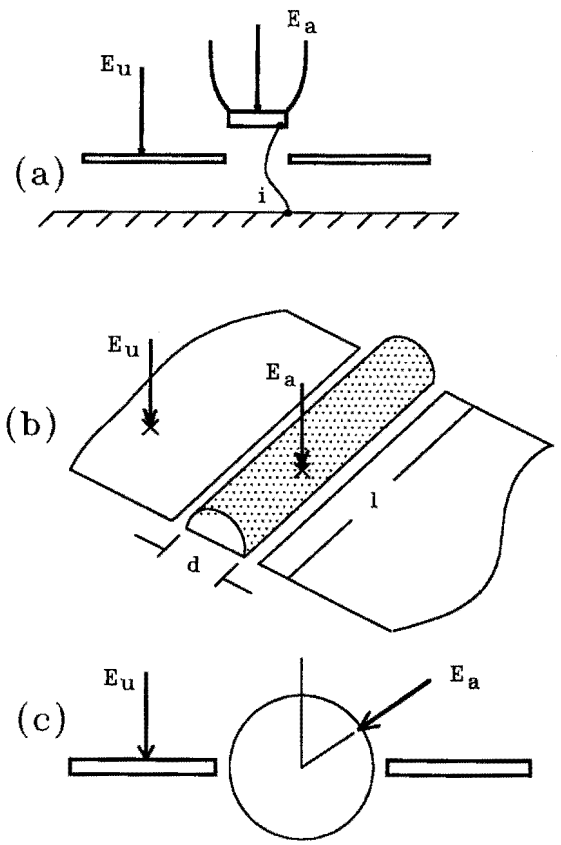

Fig. 9.27 Elevated surface.
(a) Flat surface
(b) Embedded hemicylinder
(c) End view

Table 9.3

Equivalent Area and Induced Short-circuit Current Equations for a Uniform Electric Field [9.5]

*Note: S is the equivalent area, I_{sc} is the induced short-circuit current.

$I_{sc} = j\omega\epsilon ES = ES/(3 \cdot 10^8)$, E in V/m S in m^2

Current induced on a sphere above ground

$$S = h\frac{4\pi}{\frac{1}{r} - \frac{1}{2H}} \text{ or } 4\pi h \text{ for } h \gg r \quad (1)$$

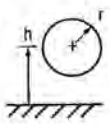

Hemisphere on the ground

$$S = 3\pi r^2 \quad (2)$$

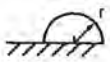

Cylinder above ground

$$S = \frac{2\pi h}{\ln\frac{2h}{r}}(l + 2r) \text{ where } h > 3r \quad (3)$$

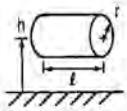

Half cylinder on the ground

$$S = 4r(l + 2r) \quad (4)$$

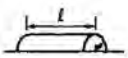

Rectangular solid, 45° shield angle approximation

$$S = AB + 2H(A + B) + \pi H^2 \quad (5)$$

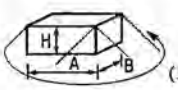

Rectangular solid, empirical

$$S = AB(1 + (1.4 + 5/(A/B)^{6/10})(0.1(H/B)^{1/2} + 0.78(H/B) + 0.07(H/B)^2 + 0.01((H/B)/(A/B))^3)) \quad (6)$$

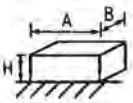

Rectangular flat plate, empirical

$$S = AB(1 + 8/(A/B)^{6/10})(.3(H/B)^{1/2} + 0.6(H/B) + 0.07(H/B)^2 + 0.0085((H/B)/(A/B))^3) \quad (7)$$

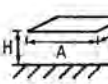

Vertical cylinder, I_{sc}

Error is less than 6% for $l/r > 6$

$$S = \frac{\pi l^2}{\ln\left[\left(\frac{l}{r}\right)\left(\frac{4h + l}{4h + 3l}\right)^{1/2}\right]} \quad (8)$$

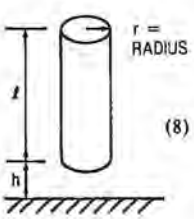

9.9.1 Tubular Conductors

Mathematically the simplest geometries are for coaxial tubular conductors.

Internal impedance with external return: In Fig. 9.28 current flows along a tubular conductor and returns through an external path, here taken as a coaxial cylinder so that the distribution of current on the surface of the tube is uniform. The analysis would be the same if the return path were a single conductor far away from the tube. A voltmeter is connected as shown with the leads flush with the surface (see §9.6.3) and so responds only to the voltage produced by the flow of current in the material of the tube. The ratio of voltage to current defines the internal impedance of the conductor with external return, Z_{ie}. The product of this impedance and the conductor current gives the surface electric field E_c previously shown on Fig. 9.6. The exact expression uses Bessel functions, as defined in §9.3.3.

$$Z_{ie} = \frac{\gamma}{2\pi b\sigma} \cdot \frac{I_0(\gamma b)K_1(\gamma a) + K_0(\gamma b)I_1(\gamma a)}{I_1(\gamma b)K_1(\gamma a) - I_1(\gamma a)K_1(\gamma b)} \quad (9.105)$$

The arguments of the function, σ, γ and δ, are the conductivity, propagation constant and skin depth as discussed in §9.4.6.

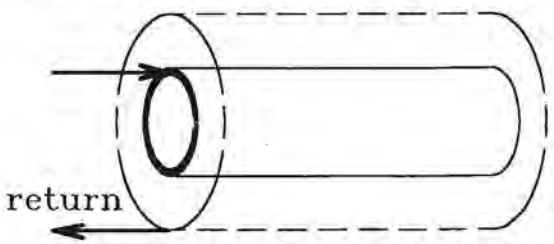

Fig. 9.28 Internal impedance with external return.

Approximations are good enough for most purposes, especially if the wall thickness is small compared to the radius of the tube, as is the case with most problems encountered during analysis of lightning effects or electromagnetic shielding.

$$Z_{ie} = \frac{1}{2\pi b\sigma}\gamma T \coth(\gamma T) \quad (T \ll a) \quad (9.106)$$

$$Z_{ie} = R_0 = \frac{1}{2\pi\sqrt{b\sigma T}} \quad (a \gg T \ll \delta) \quad (9.107)$$

$$z_{ie} = \frac{1 + j}{2\pi b\sigma\delta} \quad (\sigma \ll T) \quad (9.108)$$

Eq. 9.106 is the general case. Eq. 9.107 will be recognized as the dc resistance of a thin tube, and Eq. 9.108 is the high frequency case where the real and imaginary components of transfer impedance are equal.

Eq. 9.110 is the general case. Eq. 9.111 will be recognized as the dc resistance of a thin tube, and Eq. 9.112 is the high frequency case where the real and imaginary components of transfer impedance are equal.

As a numerical example, evaluate the internal impedance at 100 Hz and 10 kHz of an aluminum ($\sigma = 3.53 \times 10^7$ siemens) tube 2 cm diameter and a wall thickness of 2 mm ($a = 0.01$ m, $T = 0.002$ m, $b = 0.012$ m) .

The skin depth, Eq. 9.22, is 8.47×10^{-3} m (8.47mm) at 100 Hz and 8.47×10^{-4} m (0.847 mm) at 10kHz. At 100 Hz the skin depth is considerably greater than the wall thickness, implying that the current would be nearly uniformly distributed over the wall; dc conditions. The internal impedance of the tube is then just the dc resistance, 2.06×10^{-4} ohms/m. At 10 kHz the skin depth is only 0.847 mm, less than the wall thickness. The impedance would be $(1+j)4.54 \times 10^{-4}$ ohms/m.

Internal impedance with internal return: If the current returns on the inside of the tube, Fig 9.29 or Fig. 9.7, the impedance is Z_{ii}. The formulations are virtually identical with those for Z_{ie}, differing only in that a and b are reversed.

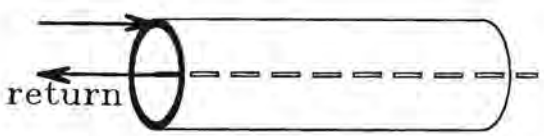

Fig. 9.29 Internal impedance with internal return.

Transfer impedance with external return: This is a measure of the field that leaks to the inner surface of the tube when current flows along the tube and returns through an external path, Fig. 9.8. The transferred field is that which would be measured by a voltmeter connected along the inner surface. The exact expression is again given in terms of Bessel functions, though simpler expressions are suitable for thin wall tubes.

$$Z_t = \frac{1}{2\pi ab\sigma} \cdot \frac{1}{I_1(\gamma b)K_1(\gamma a) - I_1(\gamma a)K_1(\gamma b)} \quad (9.109)$$

$$Z_t = \frac{1}{2\pi\sqrt{ab}\sigma T} \cdot \frac{\gamma T}{\sinh(\gamma T)} \quad (T \ll a) \quad (9.110)$$

$$Z_t = R = \frac{1}{2\pi\sqrt{ab}\sigma T} \quad (a \gg T \ll \sigma) \quad (9.111)$$

$$Z_t = \frac{1+j}{\pi\sqrt{ab}\sigma\delta} \cdot \exp[-(1+j)T/\delta] \quad (\delta \ll T \ll a) \quad (9.112)$$

$$Z_t = \frac{1+j}{\pi\sqrt{ab}\sigma\delta} \cdot [\cos(T/\delta) + \sin(T/\delta)] \quad (\delta \ll T \ll a) \quad (9.113)$$

For the same geometry discussed in §9.1.1 the transfer impedances are 8.47×10^{-3} ohms/m at 100 Hz (same as the internal impedance) and $(1+j)3.956 \times 10^{-4}$ ohms/m at 100 kHz.

Transfer impedance with internal return: This is a measure of the field that would leak to the outer surface of the tube if current flows on an internal conductor and returns along the inner surface of the tube. The defining equations are the same as those of §9.1.3 with a and b reversed.

9.9.2 Circular, but Solid Bodies

Two formulations are appropriate for solid conductors. Exact and simplified expressions are given in the following sections.

Internal impedance with external return: This is the same geometry discussed in §9.7.3 and the following equations provide one more formulation of the internal impedance.

$$Z_i = \frac{\gamma}{2\pi ab} \cdot \frac{I_0(\gamma a)}{I_1(\gamma a)} \quad (9.114)$$

$$Z_i = \frac{1}{\pi a^2 \sigma} \quad (\delta \gg a) \quad (9.115)$$

$$Z_i = \frac{1+j}{2\pi a\sigma\delta} \quad (\delta \ll a) \quad (9.116)$$

Internal impedance with internal return: This is the inverse of §9.9.2 and is a measure of the electric field along the surface of a hole through which is passed a current carrying conductor, Fig. 9.30.

$$Z_i = \frac{\gamma}{2\pi a\sigma} \cdot \frac{K_0(\gamma a)}{K_1(\gamma a)} \quad (9.117)$$

$$Z_i = \frac{\omega\mu}{8} + j\omega\frac{\mu}{2\pi}\ln\frac{\sqrt{2}\sigma}{\gamma a} \quad (\sigma \gg a) \quad (9.118)$$

$$(\gamma_0 = 1.781\cdots) \quad (9.119)$$

$$Z_i = \frac{1+j}{2\pi a\delta\sigma} \quad (\delta \ll a) \quad (9.120)$$

9.9.3 Flat Surfaces

Exact expressions for the impedance of flat surfaces are very complex and approximations are generally used.

Internal impedance of an infinite plate with external return: The geometry is shown on Fig. 9.30(b). One approach is to treat the surface as a hole of large diameter, as in Fig. 9.30(a).

$$Z_g = \frac{-j\gamma}{4\pi h\sigma} \cdot \frac{H_0^{(1)}(j\gamma 2h)}{H_1^{(1)}(j\gamma 2h)} \tag{9.121}$$

$$Z_g = \frac{1+j}{4\pi h\delta\sigma} \quad (\delta \ll 2h) \quad (\sigma \gg \omega\epsilon) \tag{9.122}$$

$$Z_g = \frac{\omega\mu}{8} + j\omega\frac{\mu}{2\pi}\ln\frac{\delta}{\sqrt{2}\gamma_0 h} \quad (\delta \gg 2h) \tag{9.123}$$

$$(\gamma_0 = 1.781\cdots) \tag{9.124}$$

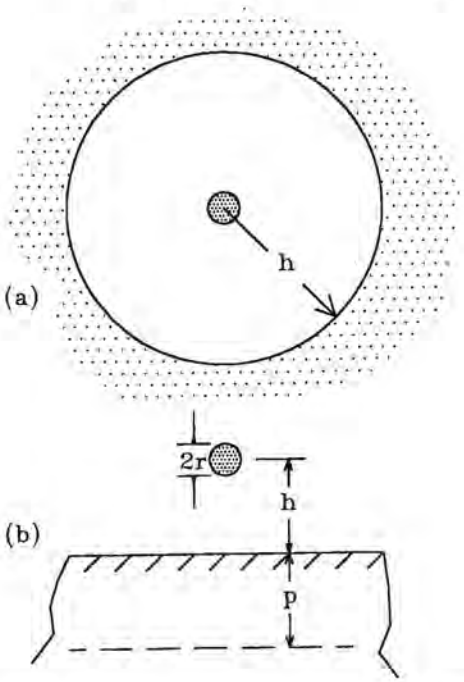

Fig. 9.30 Internal impedance of the return path.
(a) Conductor in a large hole
(b) Complex ground plane approach

In the electric power field this is the geometry that pertains to transmission line conductors above earth and the impedance is generally evaluated from Carson's equations, [9.7]. An alternative formulation, the "complex ground plane" is due to Deri, Semlyn et al, [9.8]. Since it is both simple and reasonably accurate it will be outlined here. Strictly speaking it applies only to infinitely thick ground planes, but it is also applicable to finite ground planes as long as the skin depth is small relative to the thickness of the plane.

The total series impedance of a conductor above an imperfectly conducting ground, or earth, is taken as:

$$Z_s = j\omega L = 2\pi f L \tag{9.125}$$

where

$$L = \frac{\mu_o}{2\pi}\ln\frac{2(h\ +\ p)}{r} \tag{9.126}$$

and

h = height of conductor above the ground surface
r = radius of the conductor
p = complex depth.

The complex depth, so called because it has both real and imaginary components, is:

$$p = (1-j)\frac{\sigma}{2} \tag{9.127}$$

where σ is the skin depth in the earth. Skin depth was covered in §9.4.5 and Eqs. 9.22 and 9.23 are as applicable to earth as to any other material. Frequently h is small compared to p and can be ignored.

Since $\log(a+jb) = \log C + j\phi$, C and ϕ being as discussed in §9.3.1, it can be shown that:

$$L = \frac{\mu_0}{2\pi}\left[\log(\sigma/r) - j\pi/4\right] \tag{9.128}$$

$$Z_s = 10^{-7}\left[\pi^2 f + 4f\ \ln(\sigma/r)\right] \tag{9.129}$$

Internal impedance of a thin sheet: The impedance consists of the impedance of the sheet (μ_2, ϵ_2) in parallel with the impedance of the medium in which the sheet is placed (μ_0, ϵ_0), hence the quantity χ that appears in the following equation:

$$Z_s = \frac{\gamma_m}{\sigma}\frac{\cosh(\gamma_m d) - \chi\sinh(\gamma_m d)}{\sinh(\gamma_m d) - \chi(\cosh(\gamma_m d) - 1)}. \tag{9.130}$$

where

$$\chi \equiv \frac{\mu_2}{\mu_0}\frac{\gamma_0}{\gamma_m} \tag{9.131}$$

$$\gamma_0^2 = -\omega^2\mu_0\epsilon_0 \tag{9.132}$$

$$\gamma_m^2 = j\omega\mu_2\ (\sigma + j\omega\epsilon_2) \tag{9.133}$$

For lightning interactions the medium is air, the impedance of which is far greater than the impedance

of the sheet, and $\chi \approx 0$. Thus, for the frequencies of interest in most lightning compatability analyses ($< 100\ MH_z$) and for most conducting materials, even the carbon fiber composite materials having conductivities of 8000 to 20 000 mho/m, χ is $\ll 1$ and the impedance can be taken as

$$Z_s = \frac{\gamma_m}{\sigma} \coth \gamma_m d \tag{9.134}$$

where

$$\gamma_m \approx (1+j)\left[\frac{\omega\mu\sigma)}{2}\right]^{1/2} \tag{9.135}$$

and σ = conductivity.

Transfer impedance of a flat sheet: In aircraft interactions this is of particular importance because it defines the resistive voltage produced by current flowing along the surface of a thin cylinder.

$$Z_t = \frac{(\gamma_m/\sigma)}{\sinh(\gamma_m d) - \chi(\cosh(\gamma_m d) - 1)} \tag{9.136}$$

The same considerations concerning the quantity χ apply here as for the internal impedance, and thus

$$Z_t = \frac{\gamma_m/\sigma}{\sin \gamma_m d} \tag{9.137}$$

9.10 Analytical Descriptions of Waveshapes

This section will discuss a few miscellaneous points about waveshapes used for test and analysis of indirect effects.

9.10.1 Difference of Two Exponentials

A waveform commonly used for analysis of both direct and indirect effects is the double exponential:

$$E = E_1(\epsilon^{-\alpha t} - \epsilon^{-\beta t}). \tag{9.138}$$

The constant β governs the rise of the wave while α governs the decay, but determining the values of these constants for a particular wave is not straightforward. The following describes the method of calculation given by Bewley [9.9], who also gives a graphical means of evaluating the constants in Eq. 9.138.

The peak amplitude is reached at the time t_1 when the derivative is zero.

$$\frac{dE}{dt} = 0 = E_1(-\alpha\epsilon^{-\alpha t_1} + \beta\epsilon^{-\beta t}), \tag{9.139}$$

from which

$$t_1 = \frac{\ln(\beta/\alpha)}{\beta - \alpha} = \frac{1}{\alpha}\frac{\ln(\beta/(\alpha)}{\beta/\alpha - 1)}. \tag{9.140}$$

The peak voltage is thus

$$E = E_1(\epsilon^{-\alpha t_1} - \epsilon^{-\alpha t_1(\beta/\alpha)}) \tag{9.141}$$

from which

$$\frac{E}{E_1} = (\epsilon^{-\alpha t_1} - \epsilon^{-\alpha t_1(\beta/\alpha)}). \tag{9.142}$$

The time t_2 at which the wave decays to half value on the tail is given by

$$\frac{1}{2}\frac{E}{E_1} = (\epsilon^{-\alpha t_1} - \epsilon^{-\alpha t_1(\beta/\alpha)(t_2/t_1))}. \tag{9.143}$$

Eq. 9.143 is transcendental, but may be solved in an iterative manner for the value of t_1/t_2 that satisfies the equality.

The procedure for evaluating the constants for a particular waveshape is thus:

1. From the known values of t_1 and t_2, solve by plotting or other method of approximation, for the value of β/α that satisfies Eq. 9.143.
2. Using that value, the known value of t_1, and Eq. 9.140, evaluate α and thence β.
3. From those values, the desired peak voltage E, and Eq. 9.142, evaluate E_1.

If t_2 were defined as the time to decay to 37%, the e-folding time, the value of 1/2 in Eq. 9.143 would be replaced by $1/2.718\cdots$.

A computer routine written in the BASIC language that performs the above operations is given in §9.11.

As an example, for a double exponential wave that reaches a peak of 1.0 in $1\mu s$ and decays to half value in $10\mu s$, $\alpha = 0.079237 \times 10^6$, $\beta = 4.001 \times 10^6$ and $E_1 = 1.1043$. Fig. 9.31 shows the waveshape.

The rise time (10% - 90%) of the wave would be $2.2/\beta$ and the time to decay to 10% would be $2.3/\alpha$.

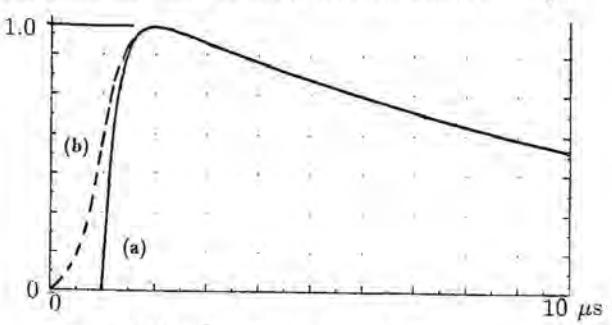

Fig. 9.31 Exponential waveforms.
(a) Double exponential
(b) Inverse exponential

9.10.2 Reciprocal of the Sum of Two Exponentials

A characteristic of the double exponential wave is that it has a discontinuity and its highest rate of change at $t = 0$. Discontinuous waves do not exist in nature and are sometimes undesirable for numerical simulation because they stimulate spurious responses. An alternative waveform [9.10] that avoids the discontinuity at $t = 0$, and thus deserves more attention, is

$$E = \frac{E}{\epsilon^{-\beta(t-t_0)} + \epsilon^{+\alpha(t-t_0)}} \qquad (9.144)$$

The rise time (10% - 90%) would be $4.4/\beta$ and the time to decay to 10% would be $t_0 + 2.3/\alpha$.

Using the same values of α, β andE_1 and for $t_0 = 10\ \mu$s as used in §0.10.1, the waveshape is as shown on Fig. 9.31.

9.10.3 Decaying Sinusoids

Transients induced by lightning frequently are oscillatory with a more or less exponential decay. An idealized decaying sinusoid is

$$E = E1 \sin(\omega t)\epsilon^{-\alpha t} \qquad (9.145)$$

where

$$\omega = 2\pi f \qquad (9.146)$$

$$\alpha = \pi f/Q \qquad (9.147)$$

The damping factor Q determines how fast the wave decays. Typical damping factors called for by specifications range from 6 to 24. Fig. 9.32 shows a 1 MHz oscillatory wave with a damping factor of 10.

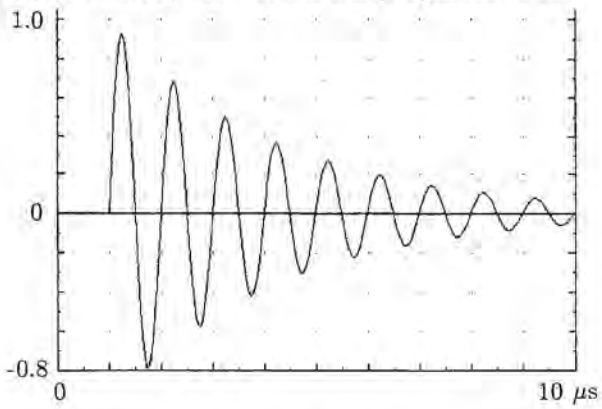

Fig. 9.32 Damped oscillatory wave.

9.11 Computer Routines

Two computer routines written in BASIC are given in Tables 9.4 and 9.5. BESSEL, on Table 9.3 can be used to find the values of the various Bessel functions discussed in §9.3.3. EXPON, on Table 9.5 can be used to find the constants for the double exponential wave described by Eq. 9.144. Sample outputs for BESSELL ($x = 0.3536 + j0.3536 = 0.5\angle 45°$) and EXPON are shown on Tables 9.6 and 9.7.

Table 9.4

BESSEL - A Program in BASIC for Calculation of Bessel and Hankel Functions of Complex Arguments (Partial)

```
1000 'A program for calculating Bessel Functions
1010 'of complex argument.
1020 'Written by F A Fisher
1030 '           Lightning Technologies Inc.
1040 '           10 Downing Parkway
1050 '           Pittsfield, MA 01201
1060 '           (413) 499-1015
1070 '           Program date January 7, 1989
1080 '
1090 DEFDBL A-H,J-Z
1100 DIM XR(20),XI(20)
1110 DIM D1(20),D2(20),P(21)
1120 PI= 3.1415926#:P2=2/PI:P3=1/PI
1130 D1(0)=1:D2(0)=1:P(0)=1:P(1)=1
1140 FOR I=1 TO 20  'calculate the D factors (1/D actually)
1150    D1(I)=D1(I-1)/((2*I)^2)
1160    D2(I)=D1(I)/(2*I+2)
1170 NEXT I
```

Table 9.4

BESSEL - A Program in BASIC for Calculation of Bessel and Hankel Functions of Complex Arguments (Continuation)

```
1180 FOR I=2 TO 21  'calculate the P factors
1190    P(I)=P(I-1)+1/I
1200 NEXT I
1210 '
1220 XR(0)=1:XI(0)=0
1230 '
1240 '
1250 INPUT "magnitude and phase of X ";XM,XP
1255 IF XM=1! THEN XM=1.0000001#
1260 IF XM=-99 THEN STOP ELSE 1280
1270 '
1280 V(3)=XM:V(4)=XP
1290 GOSUB 10430 'calculate real and imag parts of x
1300 XR=V(1):XI=V(2)
1310 J0=1:J2=0
1320 J1=V(1)/2:J3=V(2)/2
1330 Y0=0:Y2=0
1340 Y1=V(1)/2:Y3=V(2)/2
1350 I0=1:I2=0
1360 I1=V(1)/2:I3=V(2)/2
1370 K0=0:K2=0
1380 K1=V(1)/2:K3=V(2)/2
1390 N9=2
1400 GOSUB 10820 ' v^n9    calculate X^2
1410 X2=U(1):X3=U(2)
1420 FOR I=1 TO 20
1430    U(1)=XR(I-1):U(2)=XI(I-1)
1440    GOSUB 10280    'r tp p with u
1450    IF U(3)<1E+35 THEN 1490
1460    U(3)=1E+35
1470    GOSUB 10430   'p to r with v
1480    XR(I-1)=U(1):XI(I-1)=U(2)
1490    V(1)=X2:V(2)=X3
1500    W(1)=XR(I-1):W(2)=XI(I-1)
1510    GOSUB 10580  'v*w --x(i-1)*x^2 will be in u(1-5)
1520    XR(I)=U(1):XI(I)=U(2)
1530 NEXT I
1540 FOR I=1 TO 20
1550    N1(1)=D1(I)*XR(I)
1560    N1(2)=D1(I)*XI(I)
1570    W(1) =D2(I)*XR(I)
1580    W(2) =D2(I)*XI(I)
1590    V(1)=XR:V(2)=XI
1600    GOSUB 10580     'v*w
1610    N2(1)=U(1):N2(2)=U(2)
1620    IF N1(1)*N1(1)+N1(2)*N1(2)<1E-32 THEN 1870   'test for convergance
1630    IF N2(1)*N2(1)+N2(2)*N2(2)<1E-32 THEN 1870
1640    MM=(-1)^I
1650    J0=J0+MM*N1(1)                'real part of J0(x)
1660    J2=J2+MM*N1(2)                'imag part of J0(x)
1670    J1=J1+MM*N2(1)                'real part of J1(x)
1680    J3=J3+MM*N2(2)                'imag part of J1(x)
1690    Y0=Y0+MM*N1(1)*P(I)           'real part of Y0(x)
1700    Y2=Y2+MM*N1(2)*P(I)           'imag part of Y0(x)
1710    Y1=Y1+MM*N2(1)*(P(I)+P(I+1))  'real part of Y1(x)
1720    Y3=Y3+MM*N2(2)*(P(I)+P(I+1))  'imag part of Y1(x)
```

Table 9.4

BESSEL - A Program in BASIC for Calculation of Bessel and Hankel Functions of Complex Arguments

(Continuation)

```
1730    I0=I0+N1(1)                     'real part of I0(x)
1740    I2=I2+N1(2)                     'imag part of I0(x)
1750    I1=I1+N2(1)                     'real part of I1(x)
1760    I3=I3+N2(2)                     'imag part of I1(x)
1770    V(1)=I0:V(2)=I2
1780    W(1)=I1:W(2)=I3
1790    GOSUB 10700     'v/w
1800    I4=U(1)                         'real part of I0(x)/I1(x)
1810    I5=U(2)                         'imag part of I0(x)/I1(x)
1820    K0=K0+N1(1)*P(I)                'real part of K0(x)
1830    K2=K2+N1(2)*P(I)                'imag part of K0(x)
1840    K1=K1+N2(1)*(P(I)+P(I+1))       'real part of K1(x)
1850    K3=K3+N2(2)*(P(I)+P(I+1))       'imag part of K1(x)
1860 NEXT I
1870 V(1)=XR:V(2)=XI
1880 GOSUB 10180     'r to p with v
1890 GOSUB 10930     'log(v)
1900 F1(1)=P2*(U(1)-LOG(2)+.5772156)
1910 F1(2)=P2*U(2)
1920 V(1)=F1(1):V(2)=F1(2)
1930 W(1)=J0:W(2)=J2
1940 GOSUB 10580     'v*w
1950 F2(1)=U(1):F2(2)=U(2)
1960 W(1)=J1:W(2)=J3
1970 GOSUB 10580     'v*w
1980 V(1)=U(1):V(2)=U(2)
1990 U(1)=XR:U(2)=XI
2000 GOSUB 10640     '1/u
2010 W(1)=P2*U(1):W(2)=P2*U(2)
2020 GOSUB 10530     'v-w
2030 F3(1)=U(1):F3(2)=U(2)
2040 V(1)=XR:V(2)=XI
2050 GOSUB 10180     'r tp p with v
2060 GOSUB 10930     'log (v)
2070 F4(1)=U(1)-LOG(2)+.5772156
2080 F4(2)=U(2)
2090 V(1)=F4(1):V(2)=F4(2)
2100 W(1)=I0:W(2)=I2
2110 GOSUB 10580     'v*w
2120 F5(1)=-U(1):F5(2)=-U(2)
2130 W(1)=I1:W(2)=I3
2140 GOSUB 10580     'v*w
2150 V(1)=U(1):V(2)=U(2)
2160 U(1)=XR:U(2)=XI
2170 GOSUB 10640     '1/u
2180 W(1)=U(1):W(2)=U(2)
2190 GOSUB 10480     'v+w
2200 F6(1)=U(1):F6(2)=U(2)
2210 Y0=F2(1)-P2*Y0
2220 Y2=F2(2)-P2*Y2
2230 Y1=F3(1)-P3*Y1
2240 Y3=F3(2)-P3*Y3
2250 K0=F5(1)+K0
2260 K2=F5(2)+K2
2270 K1=F6(1)-K1/2
2280 K3=F6(2)-K3/2
```

Table 9.4

BESSEL - A Program in BASIC for Calculation of
Bessel and Hankel Functions of Complex Arguments
(Continuation)

```
2290 H0=J0-Y2                              'real part of H0-1(x)
2300 H1=J2+Y0                              'imag part of H0-1(x)
2310 V(1)=K0:V(2)=K2
2320 W(1)=K1:W(2)=K3
2330 GOSUB 10700      'v/w
2340 K4=U(1)                               'real part of K0(x)/K1(x)
2350 K5=U(2)                               'imag part of K0(x)/K1(x)
2360 H2=J1-Y3                              'real part of H1-1(x)
2370 H3=J3+Y1                              'imag part of H1-1(x)
2380 H4=J0+Y2                              'real part of H0-2(x)
2390 H5=J2-Y0                              'imag part of H0-2(x)
2400 H6=J1+Y3                              'real part of H1-2(x)
2410 H7=J3-Y1                              'imag part of H1-2(x)
2420 PRINT " Function         real          imaginary"
2430 PRINT
2440 F$="###.#####      ###.#####"
2450 PRINT " J0(x)          ";:PRINT USING F$;J0,J2
2460 PRINT " J1(x)          ";:PRINT USING F$;J1,J3
2470 PRINT " Y0(x)          ";:PRINT USING F$;Y0,Y2
2480 PRINT " Y1(x)          ";:PRINT USING F$;Y1,Y3
2490 PRINT " I0(x)          ";:PRINT USING F$;I0,I2
2500 PRINT " I1(x)          ";:PRINT USING F$;I1,I3
2510 PRINT " K0(x)          ";:PRINT USING F$;K0,K2
2520 PRINT " K1(x)          ";:PRINT USING F$;I1,K3
2530 PRINT " I0(X)/I1(X)    ";:PRINT USING F$;I4,I5
2540 PRINT " K0(X)/K1(X)    ";:PRINT USING F$;K4,K5
2550 PRINT " H0-1           ";:PRINT USING F$;H0,H1
2560 PRINT " H1-1           ";:PRINT USING F$;H2,H3
2570 PRINT " H0-2           ";:PRINT USING F$;H4,H5
2580 PRINT " H1-2           ";:PRINT USING F$;H6,H7
2590 PRINT
2600 PRINT
2610 INPUT "continue (Y/N)  ";A$
2620 IF A$ = "Y" OR A$ = "y" THEN 1250 ELSE STOP
2630 STOP
2640 '
2650 '
10000 '--------------- general purpose complex number routines
10170 'r to p with v   input is v(1) and v(2)
10180 U8 = ABS(V(1)):U9 = ABS(V(2))
10190 IF U8 => V9 THEN V(5) = ATN(U9/U8)
10200 IF U8 < U9  THEN V(5) = PI/2 - ATN(U8/U9)
10210 IF V(1) < 0 THEN V(4) = PI-V(5)
10220 IF V(2) < 0 THEN V(4) = -V(5)
10230 V(4) = V(5)*180/PI
10240 V(3) = SQR(V(1)*V(1) + V(2)*V(2))
10250 RETURN ' returns v(1) - v(5)
10260 '----------------------
10270 'r to p with u   input is u(1) and u(2)
10280 U8 = ABS(U(1)):U9 = ABS(U(2))
10290 IF U8 => U9 THEN U(5) = ATN(U9/U8)
10300 IF U8  < U9 THEN U(5) = PI/2 - ATN(U8/U9)
10310 IF U(1) < 0 THEN U(5) = PI-U(4)
10320 IF U(2) < 0 THEN U(5) = -U(5)
10330 U(4) = U(5)*180/PI
10340 U(3) = SQR(U(1)*U(1) + U(2)*U(2))
```

Table 9.4

BESSEL - A Program in BASIC for Calculation of Bessel and Hankel Functions of Complex Arguments (Continuation)

```
10350 RETURN 'returns u(1) - u(5)
10360 ' ----------------------
10370 'p to r with u  input is u(3) and u(4)
10380 U8 = COS(U(4)*PI/180):U9 = SIN(U(4)*PI/180)
10390 U(1) = U(3)*U8: U(2) = U(3)*U9
10400 RETURN  'returns u(1) - u(5)
10410 ' ------------------------
10420 'p to r with v   input is v(3) and v(4)
10430 U8 = COS(V(4)*PI/180):U9 = SIN(V(4)*PI/180)
10440 V(1) = V(3)*U8:V(2) = V(3)*U9
10450 RETURN 'returns v(1) - v(4)
10460 ' ----------------------
10470 ' v + w   needs v(1) and v(2) plus w(1) and w(2)
10480 U(1) = V(1) + W(1):U(2) = V(2) + W(2)
10490 GOSUB 10280
10500 RETURN  'returns u(1) - u(5)
10510 ' ----------------------
10520 ' v - w   needs v(1) and v(2) plus w(1) and w(2)
10530 U(1) = V(1) - W(1):U(2) = V(2) - W(2)
10540 GOSUB 10280
10550 RETURN  'returns u(1) - u(5)
10560 ' ----------------------
10570 '  v*w   needs v(1) and v(2) plus w(1) and w(2)
10580 U(1) = V(1)*W(1) - V(2)*W(2)
10590 U(2) = V(2)*W(1) + V(1)*W(2)
10600 GOSUB 10280
10610 RETURN  'returns u(1) - u(5)
10620 '-------------------------
10630 ' 1/u    needs u(1) and u(2)
10640 U8 = U(1)*U(1) + U(2)*U(2)
10650 U(1) = U(1)/U8:U(2) = -U(2)/U8
10660 GOSUB 10280
10670 RETURN  'returns u(1) - u(5)
10680 ' ------------------------
10690 ' v/w   needs v(1) and v(2) plus w(1) and w(2)
10700 U8 = W(1)*W(1) + W(2)*W(2)
10710 U(1) = (V(1)*W(1) + V(2)*W(2))/U8
10720 U(2) = (V(2)*W(1) - V(1)*W(2))/U8
10730 GOSUB 10280
10740 RETURN   'returns u(1) - u(5)
10750 '-------------------------
10760 ' reverse v and w   needs all parts of v and w
10770 FOR U8 = 1 TO 4:U9 = V(U8):V(U8) = W(U8)
10780 W(U8)=U9:NEXT U8
10790 RETURN  'returns all parts of v and w
10800 ' -------------------------
10810 ' v^(n9)
10820 U(3) = V(3)^N9:U(4) = V(4)*N9
10830 GOSUB 10380
10840 RETURN  'returns u(1) -u(4)
10850 ' -------------------------
10860 ' e (2.71828....)^v  needs v(1) and v(2)
10870 U8 = 2.7182918#^V(1)
10880 U(1) = U8*COS(V(2)):U(2) = U8*SIN(V(2))
10890 GOSUB 10280
10900 RETURN 'returns u(1) - u(5)
```

Table 9.4

BESSEL - A Program in BASIC for Calculation of Bessel and Hankel Functions of Complex Arguments (Conclusion)

```
10910 ' ---------------------------
10920 ' log(v)  needs v(1) and v(2)
10930 U(1) = LOG(V(3)):U(2) = V(4)*PI/180
10940 GOSUB 10280
10950 RETURN   'returns u(1) - u(5)
10960 ' ---------------------------
10970 ' v^w   needs v(1) and v(2) plus w(1) and w(2)
10980 GOSUB 10930
10990 V(1) = U(1):V(2) = U(2)
11000 GOSUB 10580
11010 V(1) = U(1):V(2) = U(2)
11020 GOSUB 10280
11030 RETURN   'returns u(1) - u(5)
```

Table 9.5

EXPON - A Program in BASIC For Evaluating Constants of Double Exponential Waves (Partial)

```
1000 INPUT "t1 and t2";T1,T2
1020 TOVERT = T2/T1
1040 FAC = .5  'find half amplitude point
1060 BOVOLD = 10*TOVERT
1080 BOVERA = BOVOLD
1100 GOSUB 1700   'find sum
1120 SUMOLD = SUM
1140 BOVERA = 5*TOVERT
1160 GOSUB 1700  'find sum
1180 '
1200 GOSUB 1580  'find new value for BOVERA
1220 BOVOLD = BOVERA
1240 SUMOLD = SUM
1260 BOVERA = BOVNEW
1280 '
1300 IF ABS(SUM)<.00001 THEN 1360 ELSE 1160
1320 '
1340 'print the answers
1360 ALPHA  = AT1/T1
1380 BETA   = BOVERA*ALPHA
1400 PRINT
1420 EOVERE = EXP(-AT1) - EXP(-A1)
1440 A$ = "\        \##.####^^^^  "
1460 PRINT USING A$;"alpha = ";ALPHA
1480 PRINT USING A$;"beta  = ";BETA
1500 PRINT USING A$;"E1/E = ";1/EOVERE
1520 PRINT
1540 STOP
1560 '
1580 'subroutine to find new BOVERA
1600 DELX   = BOVERA - BOVOLD
```

Table 9.5

EXPON - A Program in BASIC For Evaluating Constants of Double Exponential Waves (Conclusion)

```
1620 DELY   = SUM    - SUMOLD
1640 BOVNEW = BOVERA - DELX*SUM/DELY
1660 RETURN
1680 '
1700 'subroutine to find SUM
1720 AT1 = LOG(BOVERA)/(BOVERA-1)
1740 A1 = AT1*BOVERA
1760 A2 = A1*TOVERT
1780 A3 = AT1*TOVERT
1800 SUM = (EXP(-A3) - EXP(-A2))
1820 SUM = SUM - FAC*(EXP(-AT1) - EXP(-A1))
1840 RETURN
1860 END
```

Table 9.6

Calculation of Bessel and Hankel Functions for $X = 0.5\angle 45°$

Function	real	imaginary
J0(x)	0.99902	-0.06249
J1(x)	0.18224	0.17120
Y0(x)	-0.48333	0.57148
Y1(x)	-1.14039	0.85145
I0(x)	0.99902	0.06249
I1(x)	0.17120	0.18224
K0(x)	0.85591	-0.67158
K1(x)	0.17120	-1.52240
I0(X)/I1(X)	2.91772	-2.74097
K0(X)/K1(X)	0.56158	0.17445
H0-1	0.42754	-0.54582
H1-1	-0.66920	-0.96919
H0-2	1.57050	0.42083
H1-2	1.03369	1.31158

Table 9.7

Calculation of Constants for a Double Exponential Wave Having an Amplitude of 1.0 With Front and Tail Times of 1.0 and 10.0 Microseconds respectively

```
t1 and t2? 1e-6,10e-6

alpha =   79.2375E+03
beta  =   40.0102E+05
E1/E =     1.1043E+00
```

REFERENCES

9.1 F. W. Grover, *Inductance Calculations, Working Formulas and Tables*, Dover, New York, 1962 or D. Van Nostrand, New York, 1946, Chapter 3.

9.2 Grover, *Inductance Calculations*, Chapter 7.

9.3 F. A. Fisher, "Analysis and Calculations of Lightning Interactions with Aircraft Electrical Circuits", *AFFDL-TR- 78-106*, Air Force Flight Dynamics Laboratory, Wright Patterson Air Force Base, Ohio, 45433, pp. 196-201.

9.4 Grover, *Inductance Calculations*, Chapters 8, 13 and 16.

9.5 *Transmission Line Reference Book, 345 kV and Above/Second Edition*, Electric Power Research Institute, Palo Alto, CA, 1982.

9.6 E. R. Vance *Coupling to Shielded Cables*, Chapter 3, John Wiley and Sons, New York, 1978.

9.7 J. R. Carson, "Wave Propagation in Overhead Wires with Ground Return", *Bell Syst. Tech. J.*, Vol. 5, 1926, pp. 539-554, (Carson's equations are also discussed in almost any elementary textbook on electrical power theory.)

9.8 A. Deri, G. Tevan, A. Semlyn and A. Castanheira, "The Complex Ground Plane, a Simplified Model for Homogeneous and Multi-layer Earth Return", *IEEE Transactions on Power Apparatus and Systems*, Vol. PAS-100, No. 8, August 1981, 1981 pp. 3686 - 3693.

9.9 L.V. Bewley, *Traveling Waves on Transmission Systems*, Dover, New York, 1963 or John Wiley and Sons, New York, 1933 and 1951, pp. 24-26.

9.10 K. S. H. Lee, editor *EMP Interaction: Principles, Techniques and Reference Data*, AFWL EMP Interaction 2-1, 1980, pp. 298-300.

This page intentionally blank.

Chapter 10

THE EXTERNAL ELECTROMAGNETIC FIELD ENVIRONMENT

10.1 Introduction

In order to estimate the lightning induced transients in an aircraft, one must first determine the external electromagnetic fields. While they are not of prime concern, since the internal electromagnetic environment is what determines the voltages and currents induced on wiring, the internal environment is determined by the external environment and the degree to which it couples to the inside of the aircraft. Coupling mechanisms are discussed in Chapters 11 and 12.

The purpose of this chapter is to discuss the factors that affect the external environment and to outline methods of determining it. Elementary factors governing it will be discussed first, then various methods of calculation will be presented, ranging from simple approximations to the more complicated ones based on non-linear interactions of the aircraft and the lightning channel.

Detailed calculations are complex because the aircraft is a complex electromagnetic object. The geometry is complex, requiring three dimensional solutions. The materials are varied, consisting of highly conducting metals such as aluminum and copper, more resistive metals such as titanium, carbon fiber composites that are three orders of magnitude less conductive than metals, and insulators such as glass, Kevlar, fiberglass and plastic.

Finally, the lightning environment itself is complex. One of the more significant features is that it is both a high frequency and low frequency event. Time scales on the order of tens of nanoseconds must be resolved and some parts of the lightning environment may last on the order of one second. Also, different aspects of the lightning environment dominate at different times within the event. For example, during the attachment phase, the electric field and its rate of rise are of primary interest and at later times the current is of primary interest. For some times both are important. The interaction of the aircraft with the lightning channel is also a nonlinear phenomenon, some features of which are not yet well understood.

Fortunately, however, a mathematically rigorous treatment is not always required. One important simplification in the analysis procedure is that it can frequently be taken in stages since the inside and outside of the aircraft are only loosely coupled. What this means is that while the lightning may produce electromagnetic effects that couple to the inside of the aircraft, there is little need to study the reverse coupling; the voltages and currents induced on wiring will not affect the lightning. It is this separation of interaction effects that allows the internal response of the aircraft to be calculated by first determining the external electromagnetic fields without consideration of how they couple to the interior and then to apply the coupling factors to those fields to determine the internal environment. Some analysis procedures do calculate the external environment and the coupling simultaneously, but they can also be treated separately.

For many purposes approximate methods of analysis provide coupling estimates that are satisfactory for lightning protection purposes. The type of analytical method which one uses depends upon financial considerations, vehicle complexity, design requirements, available computational tools, and known susceptibility and criticality of electrical and electronic systems in the aircraft.

10.2 Elementary Effects Governing Magnetic Fields

In Chapter 9 it was shown that if a long conductor is carrying a current, I, and the return path is far removed, the field intensity at a distance, r, from the conductor, as shown in Fig. 10.1(a), is:

$$H = \frac{I}{2\pi r}. \tag{10.1}$$

If instead of a solid wire, the current is carried on a hollow tube of radius r_0, as shown in Fig. 10.1(b), the field intensity, H, at radius r is again:

$$H = \frac{I}{2\pi r}. \tag{10.2}$$

and at the surface of the tube, where $r = r_o$, the field intensity is:

$$H = \frac{I}{2\pi r_o}. \tag{10.3}$$

It follows that the field intensity at the surface of the tube is also equal to the total current divided by the circumference, P,

$$H = I/P. \tag{10.4}$$

Units of Field Intensity: In all the cases the units of field intensity are amperes per meter if the radii are measured in meters. H is, of course, the measure of magnetizing force per unit area. The density of the magnetic flux, measured in webers per meter^2, is

$$B = \mu H \tag{10.5}$$

where the permeability is, for air, $4\pi \times 10^{-7}$ H/m.

If the conductor is not cylindrical, as shown in Fig. 10.1(c), the field intensity at different points on the surface will be different. However, the average field intensity will still be equal to the total current divided by the circumference:

$$H_{\text{avg}} = I/P \tag{10.6}$$

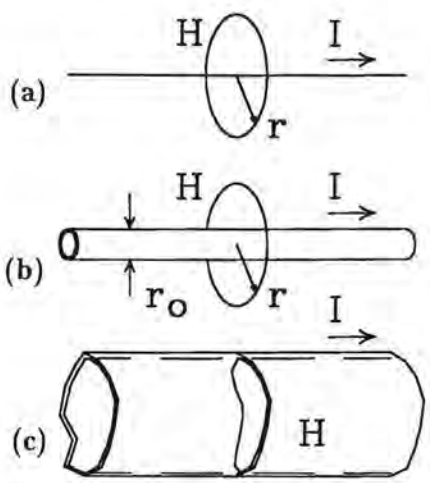

Fig. 10.1 Magnetic fields around current-carrying conductors.
(a) Current-carrying filament
(b) Tubular conductor
(c) Irregular conductor

Radius of curvature: The actual field intensity will be greater than average at points where the radius of curvature is less than average and it will be less than average at points where the radius of curvature is greater than average, as shown in Fig. 10.2. For example, the circumference of the fuselage of a typical fighter aircraft just forward of its wing is about 5.5 m. Assuming a lightning stroke current of 30 kA to flow through the fuselage, the average field intensity at the surface would be:

$$\begin{aligned} H_{\text{avg}} &= I/P \\ &= 30000/5.5 \\ &= 5455 \text{ A/m}. \end{aligned} \tag{10.7}$$

Since for that aircraft there are no points of very sharp radius, the field intensity around the fuselage would probably not vary greatly from the average value. If the fuselage cannot be approximated as a flattened cylinder, then the field intensity would have to be calculated by more sophisticated means.

The situation along a wing carrying lightning current is considerably different in that the leading and trailing edges have radii of curvature much less than the average. Field intensity along the leading and trailing edges would be quite high compared to the field intensity along the top and bottom surfaces, for example.

Fig. 10.3 shows, in general, how the magnetic field strengths would vary with position on an aircraft if a lightning flash enters through the nose pitot boom and leaves through the vertical stabilizer. The field intensity would be highest around the pitot boom, lowest around the midsection of the fuselage, and high again around the vertical stabilizer. In the vicinity of the nose equipment bays, the field would be of greater than average intensity. Since the field intensity is inversely proportional to the radius of curvature, it then follows that the field intensity outside the fuselage of a large transport aircraft would be considerably less than that outside the small fighter aircraft shown on Fig. 10.3.

Since both the average current density, J_{avg}, and the average field density, H_{avg}, are equal to the total current divided by the circumference, it follows that the tangential field intensity at the surface of a conducting object is equal to the current density at that point:

$$J_{\text{ave}} = H_{\text{ave}} = \frac{I}{P}. \tag{10.8}$$

This is in fact true, at least for transient currents. The relation is not true for dc currents or transients sufficiently slow that appreciable magnetic fields penetrate the skin.

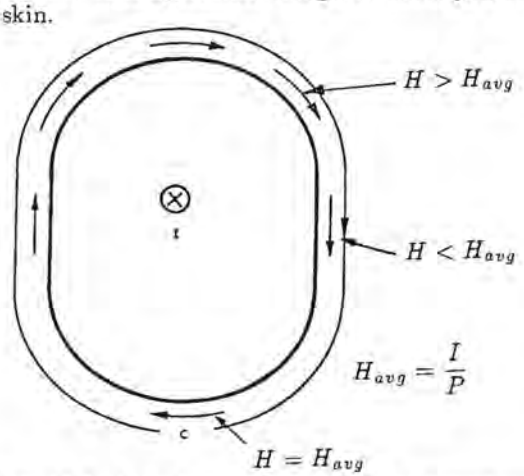

Fig. 10.2 Field intensity vs radius of curvature.

Orientation of magnetic field: The orientation of the H field vector is always at right angles to the direction of the current vector. While small gaps in the structure (Fig. 10.4) direct the current around the gap, the magnetic field is virtually unaffected, except directly on the surface and on a length scale that is small compared to the dimensions of the gap interrupting the current flow.

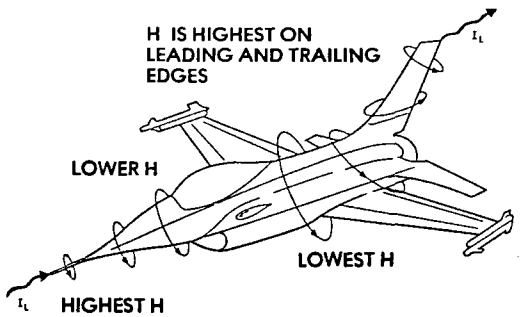

Fig. 10.3 Variation of magnetic field strength with aircraft radius of curvature.

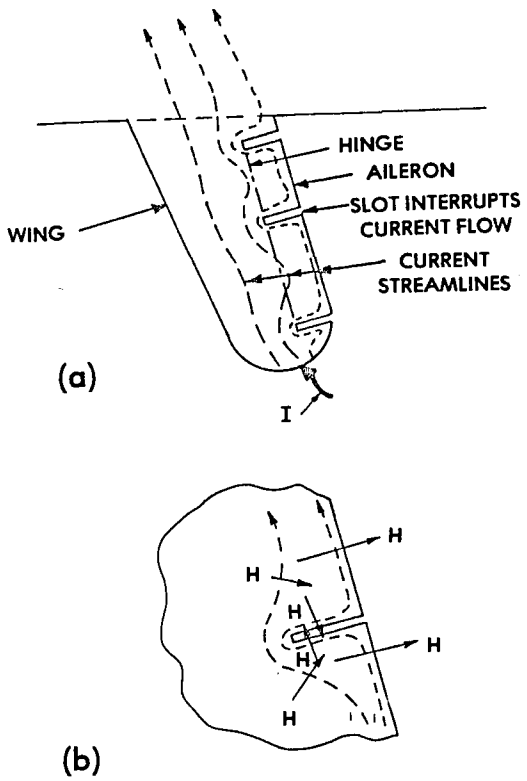

Fig. 10.4 Current flow and magnetic field around structural gaps.
(a) Current entering typical wing
(b) Resultant magnetic field virtually unaffected by slot interrupting flow of current

While Eq. 10.6 suffices to show the average current density, and thus the average intensity of the magnetic field, it does not show how the current is distributed over the surface. This distribution must be known since it affects both the resistive voltage rises inside a structure and the amounts of magnetic or electric field which penetrate through apertures.

Redistribution of current: Only for direct currents is the current density at the surface of a conductor determined by the dc resistance of the conductor. For most transient conditions the distribution is primarily controlled by magnetic effects. The magnetic distribution of current density can be calculated in simple geometries. Around the periphery of a cylinder, for example, the current density even for alternating currents is uniform, at least as long as the return path for that current is far removed from the cylinder – greater than ten times the diameter of the cylinder.

For anything other than a cylinder, the phenomenon of skin effect tends to force an alternating current to crowd toward the edges, making the current density and magnetic field intensity higher than average at places with a small radius of curvature (leading and trailing edges of a wing for example) and less than average at places with a large radius of curvature. With transients, the skin effect forces the current to initially concentrate at the edges in a manner that results in the magnetic field being tangential to the surface, as in Fig. 10.5(a). The current then gradually redistributes itself, with the distribution ultimately becoming controlled by the resistance of the structure. This resistive distribution leads to some of the magnetic field penetrating the surface, Fig. 10.5(b). The rate at which the current redistributes over the surface is governed by the ratio of inductance (a measure of magnetic fields) to resistance of the structure. It takes place faster for high resistance structures, such as those fabricated from graphite–epoxy, than it does for low resistance structures, such as those fabricated from aluminum. The time required for the current to redistribute from a pattern governed by magnetic field effects to one governed by resistive effects can be surprisingly long; hundreds or thousands of microseconds.

One geometry for which these effects can be calculated analytically is the elliptical cylinder shown in Fig. 10.6. Under high frequency conditions the current density or magnetic field intensity at the center $(X = 0, Y = \pm d/2)$, is:

$$H = \frac{I}{\pi b} \tag{10.9}$$

and at the edge $(X = \pm b/2, Y = 0)$

$$H = \frac{I}{\pi d}. \tag{10.10}$$

At intermediate points the magnetic field intensity or current density [10.1, 10.2] is:

$$H_{\text{surface}} = \frac{I}{\pi} \frac{1}{\sqrt{b^2 - (2x)^2\left[1 - d^2/b^2\right]}}. \qquad (10.11)$$

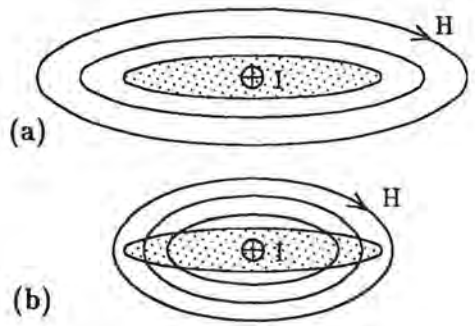

Fig. 10.5 Redistribution effects.
(a) Early time or high frequency
(b) Late time or low frequency

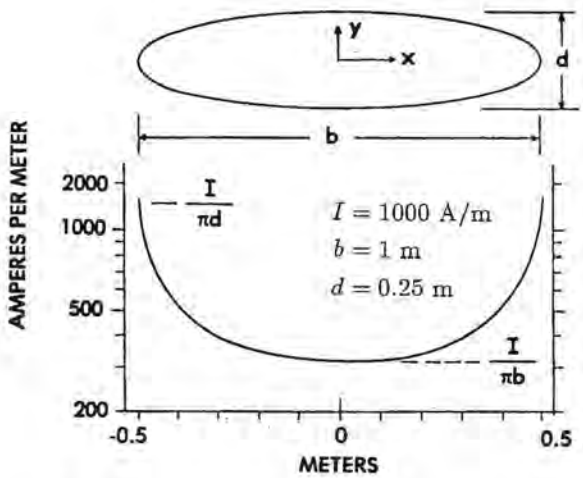

Fig. 10.6 Magnetic field intensity at the surface of an elliptical conductor.

This current distribution does not hold for dc currents where the current density over the surface is determined by the dc resistance. If the cylinder were of uniform thickness, the current density would in that case be uniform. The time span or frequency range over which a transition takes place between the uniform distribution of current governed by resistance and the nonuniform distribution governed by magnetic fields (Eq. 10.11) can be defined in terms of a factor K:

$$K = \sqrt{\frac{bd}{\delta}} \qquad (10.12)$$

where

b = width
d = depth
δ = skin depth

The classical skin depth is given by

$$\delta = \sqrt{\frac{2\rho}{\mu\omega}}, \qquad (10.13)$$

where

ρ = resistivity
μ = permeability
ω = angular frequency

and was further discussed in Chapter 9. For $K < 1$, the distribution of current is mostly controlled by resistance while for $K > 10$, the distribution is controlled by magnetic field effects. The skin depth and value of K for aluminum, as functions of frequency, are given in Table 10.1.

Table 10.1

Skin Depth as a Function of Frequency

Frequency	Skin depth	$\sqrt{bd/\delta}$
1 Hz	8.25×10^{-2} m	6.06
10 Hz	2.61×10^{-2} m	19.2
100 Hz	8.25×10^{-3} m	60.6
1000 Hz	2.61×10^{-3} m	192
10 000 Hz	8.25×10^{-3} m	606

As an example of the frequency range over which the transition takes place, consider an elliptic cylinder made from aluminum ($\rho = 2.69 \times 10^{-8}\ \Omega \cdot \text{m}$) with width $b = 1$m, depth $d = 0.25$m, and a wall thickness of 1 mm. Even at 10 Hz, $K = 19$, indicating that the current crowds to the edges of the ellipse and has a current density given by Equation 10.11. At 1 Hz, $K = 6$, about the point where resistive and magnetic effects have an equal effect on the current distribution. Thus, the frequency range over which the current density changes from its uniform dc value to the limiting ac distribution is perhaps 0.5 to 5 Hz. If a step function current were applied it would take nearly a second before the current became uniformly distributed over the surface. The manner in which the currents redistribute over the surface affects the voltages developed on internal circuits, in a manner to be described in Chapter 11.

With alternating currents applied, the surface current density remains distributed as given by Eq. 10.11 up to indefinitely high frequencies, probably until the width of the cylinder becomes on the order of a tenth of a wavelength. The current density through the wall thickness of the cylinder will vary with frequency, but it too remains constant until the skin depth becomes about the same as the wall thickness, 0 to approximately 3 kHz in this case.

In many cases the external current density may be determined with accuracy sufficient for practical purposes by approximating the surface under consideration by an ellipse or ellipses. If such an approximation does not give sufficient accuracy, there are other techniques that may be used. Some of these are discussed in §10.5.

10.3 Elementary Effects Governing Electric Fields

The electric field around a conducting surface is also of importance since a lightning flash produces rapidly changing electric fields which couple capacitively to the wiring in aircraft. The behavior of electric fields is in many ways similar to the behavior of magnetic fields, particularly in the way that electric charge crowds to the edges of conductors the same way current does. A static charge on the elliptic cylinder of Fig. 10.7(a), for example, would distribute itself in the manner shown, the density being given by equations of the same form as Eqs. 10.9 - 10.11. The electric field strength at the surface would be proportional to the charge density and directed at a right angle towards the surface, as contrasted to the magnetic field which would be tangential to the surface. The distribution of charge would not change with frequency; it would be the same for a DC static charge as it would be at high frequencies. Also, the distribution of charge would not be affected by the resistivity of the material, at least for DC conditions.

A conductor placed in an electric field will become polarized; that is, it will have electric charge induced on it by the field. As shown on Fig. 10.7(b), an electric field directed as shown will draw electrons to one side and leave a deficiency of electrons, or positive charge, on the other side. The electric field strength at the surface will thus be greater than the strength of the undisturbed electric field. For the symmetrical conditions shown on Fig. 10.7(b) the electric field strength will be equal at the two edges, though of opposite polarity. A static charge produced by some mechanism other than induction will add to the induced charge at one edge and subtract from it at the other edge, as shown on Fig. 10.7(c) making the electric field strengths unequal.

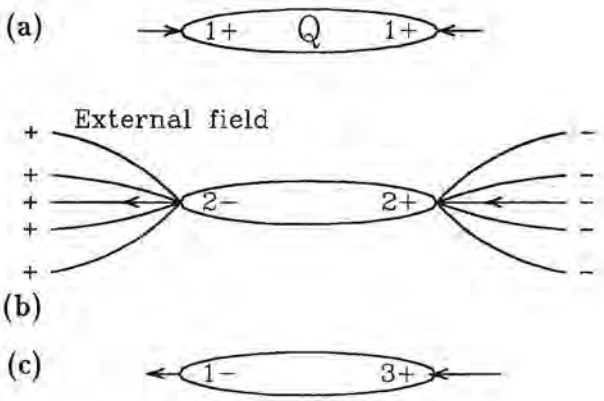

Fig. 10.7 Charge distribution.
(a) Due to a net charge
(b) Due to an external field
(c) Due to both factors

Since the field strength is proportional to the density of charge, the electric field strength will be greatest at points having a small radius of curvature, the nose boom of a fighter aircraft for example. If the electric field strength is sufficiently high there may be a breakdown in the air at that point, either corona as described in Chapter 1 or St. Elmo's Fire as described in Chapter 2. This breakdown may progress into triggered lightning as discussed in Chapter 3.

10.4 Combined Magnetic and Electric Fields

Under DC conditions, magnetic and electric fields can exist independently of each other (except for resistive E-fields) and one or the other or both may be present around a current carrying conductor. For transients and AC conditions, both will be present, and while for some conditions the effects of one or the other may be predominant, usually they must be considered together. They will both be present because a changing magnetic field gives rise to a changing electric field and visa versa, the relationship of course being given by Maxwell's Laws, as discussed in more detail in §10.6. The changing electric and magnetic fields will be oriented at right angles to each other and will propagate in a direction at right angles to the two. For example, a lightning current propagating along the conductor of Fig. 10.8 will produce magnetic and electric fields as indicated. The magnitudes of the E and H vectors will be given by the impedance Z of the surface over which they pass;

$$E/H = Z, \tag{10.14}$$

surface impedance having been discussed in Chapter 9. For the initial wave propagating over the surface of

a conductor in free space Z will be on the order of 377 ohms. When the wave reaches a discontinuity, such as the end of the surface or a point where one surface joins another surface of different size or orientation, a reflected wave will be generated and the total field will be given by the sum of the initial wave and the reflected wave. The reflected wave will also eventually reach a discontinuity and generate another travelling wave. The E and H field magnitudes of any of the wave components will be given by Eq. 10.14, but the total magnitude will be different. If current continues to flow long enough for steady state conditions to be approached, then the electric field associated with the flow of current will go toward zero.

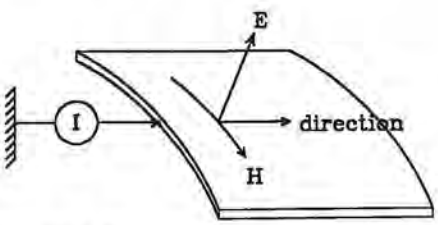

Fig. 10.8 Wave propagating over a surface.

The fields at a point to which a wave will propagate can be determined from the fields at the points previously traversed by the wave. Numerical techniques for doing this are given in §10.5 through §10.8. The phenomenon of waves propagating back and forth across the surface of the aircraft, or of aircraft resonances excited by an outside event, is discussed further in §10.10.

10.5 Methods of Evaluating Fields

There are a number of ways in which the electromagnetic field around a conductor may be evaluated. Three of the simpler methods will be discussed here, because they have both utility in their own right and because they illustrate some of the techniques used in the more powerful methods described in §10.6. Some of the results from the method to be described in §10.5.3 will also serve to illustrate the general nature of the way that external and internal fields are influenced by the shape of the aircraft.

10.5.1 Numerical Solution of Laplace's Equation

Analytically the solution of the field around a current carrying conductor may be determined by a solution of Laplace's equation:

$$\nabla^2 \phi = 0 \tag{10.15}$$

where $\phi =$ the potential.

In rectangular coordinates Laplace's equation becomes:

$$\frac{\partial^2 \phi}{\partial X^2} + \frac{\partial^2 \phi}{\partial Y^2} + \frac{\partial^2 \phi}{\partial Z^2} = 0. \tag{10.16}$$

For some geometries Laplace's equation can be solved analytically; an elliptical geometry is one of those cases. The equations defining the field distribution will not be presented here, but Fig. 10.9 shows an example of the field around an elliptical cylinder of infinite length. If the field is viewed as one due to current in the conductor, the equipotential lines depict the magnetic field lines, these being tangential to the conductor at its surface. If the field is viewed as one due to a static charge on the conductor, the lines directed into the conductor depict the electric field lines; the paths along which displacement currents flow.

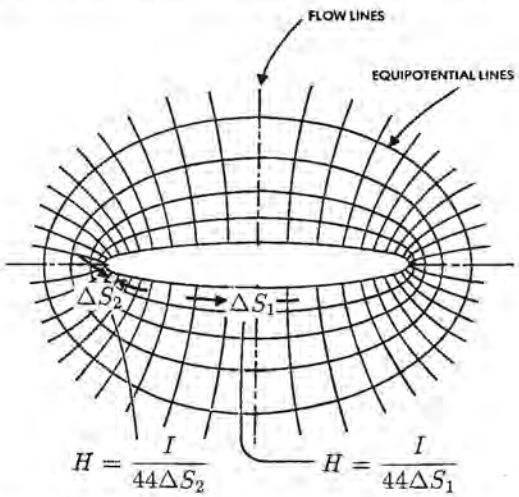

Fig. 10.9 The field around an elliptical conductor.

The return path for either the voltage maintaining the charge or the current is assumed to be sufficiently far away from the conductor that it does not influence the field around the indicated region.

The indicated flow lines divide the region into 44 sectors. At the surface of the conductor, the magnetic field strength is inversely proportional to the spacing between the flow lines. Since the average field strength around the surface is

$$H = I/P, \tag{10.17}$$

it follows that the field strength at the surface between any two flow lines is

$$H_{\text{surface}} = \frac{I}{44\Delta S}. \tag{10.18}$$

In only the simplest geometries is it possible to calculate the field analytically. Usually one must resort

to some numerical or graphical method of determining the field. Numerically, the field may be determined by a numerical solution of Laplace's equation. Fig. 10.10 shows a conductor at potential P surrounded by a return conductor, a circle in this case, at potential zero. To this geometry is fitted a rectangular grid, shown here as a very coarse grid.

Initially, all grid points that lie on the conductor would be assigned a potential P, and all the grid points that lie on the return path would be assigned a potential zero. Laplace's equation in two dimensions can be shown to be approximately:

$$\frac{\partial^2\phi}{\partial X^2} + \frac{\partial^2\phi}{\partial Y^2} \approx \frac{1}{k^2}[\phi_1 + \phi_2 + \phi_3 + \phi_4 - 4\phi_0] \quad (10.19)$$

From this it follows that Laplace's equation is satisfied if the numeric values at four points surrounding a central point have values that satisfy the equation

$$\phi_1 + \phi_2 + \phi_3 + \phi_4 - 4\phi_0 = 0 \quad (10.20)$$

A determination of the field around the conductor then involves assigning field values at all of the points between the conductor and its return path, and adjusting the value of these points until Eq.10.20 is satisfied everywhere within the grid. The literature [10.3, 10.4] indicates a number of the numerical techniques by which the potentials at the points may be adjusted to their final values. While the process is tedious, it is not completely impractical to do by hand, as discussed briefly in §10.5.2. Usually the process is done by computer routines that solve the field equations. In addition to tabulating the numerical values of the field at the grid points, frequently such computer routines allow one to plot the flow and equipotential lines.

Problem space and grid size: Fig. 10.10 illustrates two important aspects of numerical evaluation of electromagnetic fields. The first is that the solution can only take place in a defined problem space. For an isolated object such as an aircraft in flight, the problem space ideally should extend very far in all directions since, in theory, the field intensity at even the most remote point affects the field at the surface of the aircraft. The second is that the grid size affects the precision and detail with which the field may be calculated. Ideally the grid size should be much smaller than the dimensions of the aircraft around which the field is to be determined.

A small grid size and a large problem space would require an excessive amount of computer memory and an excessive amount of computer running time, particularly if calculations are desired in three dimensions. The problem is compounded for time domain solutions because the field must be calculated anew for each time step. Problem space, grid size and computer resources will usually limit solutions to less than the desired precision.

Frequently one is only interested in the field in the immediate vicinity of the aircraft. If so, the problem space, and the amount of computer memory needed, can be made relatively small by setting field magnitudes at the outer boundary of the problem to an approximation of their correct values, rather than zero, and concentrating the calculations on the field around the conductor under study. On the aircraft similar techniques can be used to concentrate the calculation on those portions of most interest.

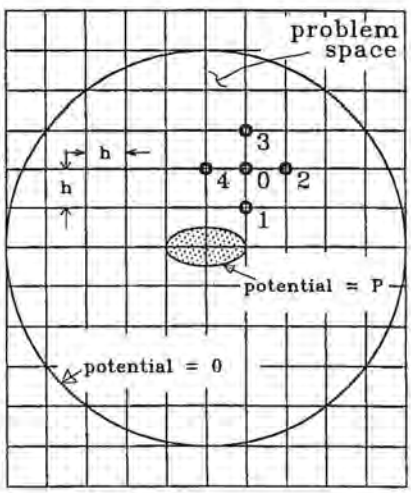

Fig. 10.10 A rectangular grid for evaluation of Laplace's equation.

Apertures: Any solution of Laplace's equation will also allow the pattern of low frequency coupling through an aperture to be calculated. Computer techniques are now commonly used for such solutions, but in the past electrolytic tank and resistive paper techniques were widely used. Hand mapping of the fields was also done and that technique is outlined in §10.5.2. Most computer routines deal either with two-dimensional problems or problems with rotational symmetry. In a two-dimensional case, the aperture would run the length of the conductor being studied. This is not necessarily a disadvantage, since some important geometries and apertures are basically two-dimensional. An important aperture is that which may exist behind the rear spar of a wing when the flaps have been extended. Since it is a convenient region to reach, wiring is often placed in this region. Electrically it is a poor place, since the aperture is near a region where the magnetic fields external to the wing are high. Another important set of apertures that may be approximated as a continuous opening is that formed by the windows in the fuselage of a transport aircraft.

Three dimensional objects: In principle, the field around three–dimensional objects may also be solved numerically by extending Eq. 10.19 to include eight points on a cube surrounding a central point. A solution of the field around a three–dimensional object not involving rotational symmetry requires large amounts of computer storage and running time if the calculations are to define the field satisfactorily in all three dimensions.

10.5.2 Hand Plotting of Fields

The fields around any geometry may also be determined graphically by a cut–and–try process in which flow lines and equipotential lines are drawn on the geometry and adjusted until repeated subdivision always yields small squares and the flow and equipotential lines intersect at all points at right angles. Cut–and–try field plotting, of which Fig. 10.11 is an imperfect example, may with care, patience, and liberal use of a soft pencil and eraser yield a field pattern of any desired accuracy.

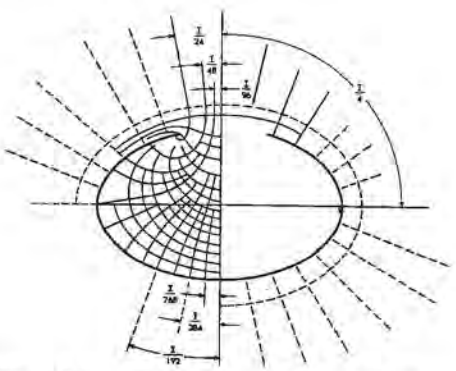

Fig. 10.11 Cut–and–try field plotting.

10.5.3 Calculation Using Wire Filaments

Another approach to determining current density, shown in Fig. 10.12, is based on the premise that a two–dimensional geometry can be represented as an array of parallel wires [10.5, 10.6]. If the current in each wire is known, the average current density along the surface defined by any two wires will be the average of the current on the two wires divided by the spacing between the wires.

If the wires are all of infinite length, so that no end effects need be considered, and are all connected together at their ends, the manner in which current divides among the wires may be calculated with the aid of a simple computer program the elements and equations of which are discussed below.

Self and mutual inductances: Let the location of the wires be defined in terms of the rectangular coordinates x_i and y_i, and let the radius of the conductors be r_1. The self–inductance per unit length of each wire is:

$$L = 2 \times 10^{-7} \ln\left[\frac{R}{r_1}\right] \qquad (10.21)$$

henries per meter. In this equation R is defined as the distance from the conductor, or from the group of conductors, to an arbitrary return path. The numerical accuracy of the current distribution to be calculated does not depend critically upon the value assigned to R, but it should be of the order of 10 to 20 times the greatest dimension of the structure being modeled. Between any two conductors, ij, there will be a mutual inductance

$$M_{ij} = 2 \times 10^{-7} \ln\left[\frac{R}{r_{ij}}\right] \qquad (10.22)$$

henries per meter. The spacing between conductors, r_{ij}, can be determined from the coordinates of the conductors.

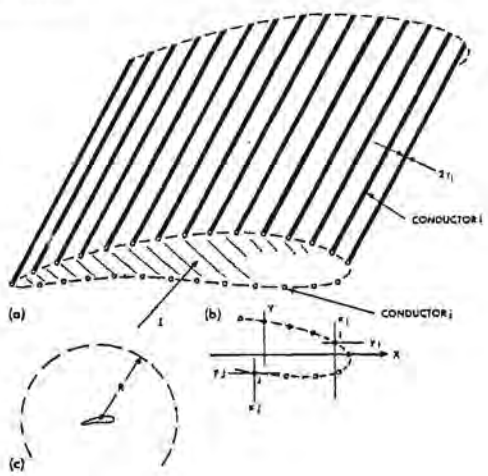

Fig. 10.12 A structure defined as an array of wires.
(a) The array
(b) Coordinates defining location
(c) Definition of the return path for current

Voltage in terms of current: If a group of conductors, each carrying a current, as in Fig. 10.13, is considered, and if the self– and mutual inductances of and between each conductor are known, the voltages across the self–inductance of each conductor will be, for angular frequency $\omega = 1$, as follows:

$$V_1 = \quad L_1\, i_1 - M_{12} i_2 - M_{13} i_3 + \cdots - M_{1n} i_n \qquad (10.23)$$

$$V_2 = -M_{21}i_1 + L_2\, i_2 - M_{23}i_3 + \cdots - M_{2n}i_n \tag{10.24}$$

$$V_3 = -M_{31}i_1 - M_{32}i_3 + L_3\, i_3 + \cdots - M_{3n}i_n \tag{10.25}$$

$$V_n = -M_{n1}i_2 - M_{n2}i_3 - M_{n1}i_n + \cdots + L_n\, i_n \tag{10.26}$$

Equations 10.23 through 10.26 may be placed in matrix notation as follows:

$$\begin{pmatrix} V_1 \\ V_2 \\ V_3 \\ \vdots \\ V_n \end{pmatrix} = \begin{pmatrix} +L_{11} & -M_{12} & -M_{13} & \cdots & -M_{1n} \\ -M_{21} & +L_{22} & -M_{23} & \cdots & -M_{2n} \\ -M_{31} & -M_{23} & +L_{33} & \cdots & -M_{3n} \\ \vdots & \vdots & & & \\ -M_{n1} & -M_{n2} & -M_{n3} & \cdots & +L_{nn} \end{pmatrix} \times \begin{pmatrix} i_1 \\ i_2 \\ i_3 \\ \vdots \\ i_n \end{pmatrix} \tag{10.27}$$

or, in more compact notation

$$|\, V \,| = |\, M \,| \times |\, i \,| \tag{10.28}$$

Current in terms of voltage: Premultiplying by the inverse of the M matrix, gives the following:

$$|\, M \,|^{-1} \times |\, V \,| = |\, M \,|^{-1} \times |\, M \,| \times |\, i \,| \tag{10.29}$$

$$|\, i \,| = |\, M \,|^{-1} \times |\, V \,| \tag{10.30}$$

$$\begin{pmatrix} i_1 \\ i_2 \\ i_3 \\ \vdots \\ i_n \end{pmatrix} = \begin{pmatrix} m_{11} & m_{12} & m_{13} & \cdots & m_{1n} \\ m_{21} & m_{22} & m_{23} & \cdots & m_{2n} \\ m_{31} & m_{32} & m_{33} & \cdots & m_{3n} \\ \vdots & \vdots & & & \\ m_{n1} & m_{n2} & m_{n3} & \cdots & m_{nn} \end{pmatrix} \times \begin{pmatrix} V_1 \\ V_2 \\ V_3 \\ \vdots \\ V_n \end{pmatrix} \tag{10.31}$$

where m_{11}, m_{12}, m_{13} are the elements of the inverse of the M matrix.

Current in each element: If all of the voltages are the same and equal to V, as is the case if all of the inductances are connected in parallel, the absolute current in each element is:

$$i_1 = (m_{11} + m_{12} + m_{13} \cdots + m_{1n})V \tag{10.32}$$

$$i_2 = (m_{12} + m_{21} + m_{23} \cdots + m_{2n})V \tag{10.33}$$

$$i_3 = (m_{31} + m_{32} + m_{33} \cdots + m_{3n})V \tag{10.34}$$

$$i_n = (m_{n1} + m_{n2} + m_{n3} \cdots + m_{nn})V \tag{10.35}$$

The total current that flows, which is proportional to the impressed voltage, is

$$i_r = (i_1 + i_2 + i_3 + \cdots i_n)V \tag{10.36}$$

The fraction of the total current that flows in each circuit is

$$I_1 = \frac{i_1}{i_r} \tag{10.37}$$

$$I_2 = \frac{i_2}{i_r} \tag{10.38}$$

$$I_3 = \frac{i_3}{i_r} \tag{10.39}$$

$$I_n = \frac{i_n}{i_r} \tag{10.40}$$

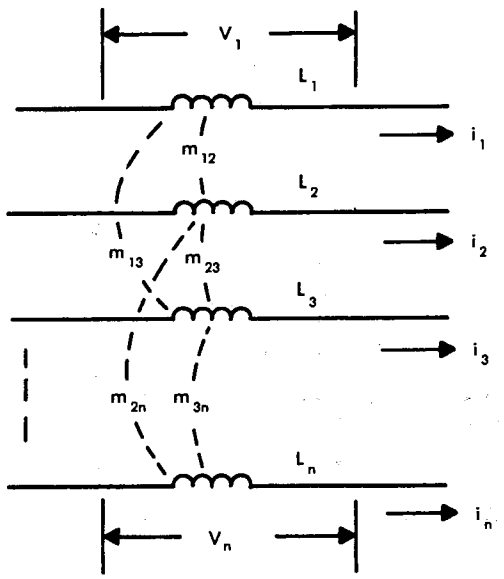

Fig. 10.13 Mutually coupled inductances.

10.5.4 Examples of External Magnetic Fields

The magnetic field within and around the cluster of wires can be determined by taking the proper summation of the magnetic field produced by each individual wire.

One computer program [10.7] which incorporates the above routines is MAGFLD. Some examples of calculations performed with it will now be described since they will serve to illustrate some of the points discussed in previous sections. The geometry chosen for analysis is the fuselage of the hypothetical aircraft shown in Fig. 10.14. The aircraft, whose airworthiness is not under discussion, has a fuselage of elliptical cross section, two meters along the major axis and one

meter along the minor axis. The fuselage is considered long enough that no end effects need to be considered. A lightning current of 1000 A is assumed to enter the nose and to exit through the rear of the fuselage. This elliptical fuselage is represented by 48 parallel conductors distributed in the manner shown in Fig. 10.15. Fig. 10.15 also shows the current density, or magnetic field strength, at the surface of the cylinder, both as determined from the program MAGFLD and analytically according to Eq. 10.11.

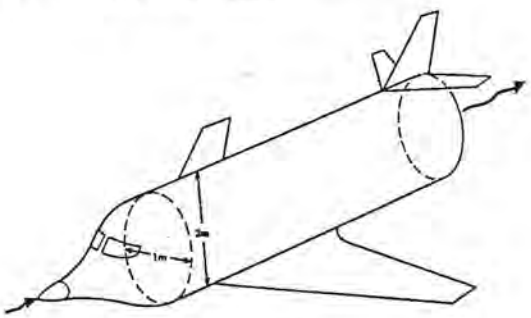

Fig. 10.14 A hypothetical fuselage to be modeled as a wire grid.

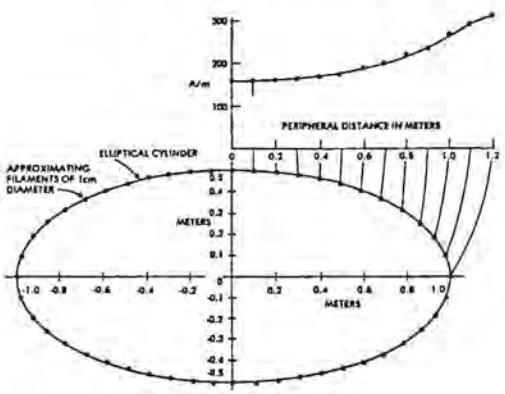

Fig. 10.15 Wire grid approximation of the elliptical fuselage.

Magnetic distribution of current: One quadrant of the elliptic cylinder is shown on Fig. 10.16. This figure shows the magnetic field strength both within and around the wire grid as calculated by MAGFLD. The orientation of the magnetic field is shown by the direction of the arrows, and the strength both by the length of the arrows and by the indicated contour lines. Note that the field lines external to the surface are tangential to the cylinder. The magnetic field strength inside the grid is much smaller than that outside, since on the inside the fields from each of the filaments tend to cancel, whereas outside the grid they tend to add. In Fig. 10.16 the fields inside the grid are largely the result of the finite number of wires defining the elliptic cylinder. If the cylinder were defined by more conductors, the fields inside would be smaller, vanishing if the number of wires were to become infinite.

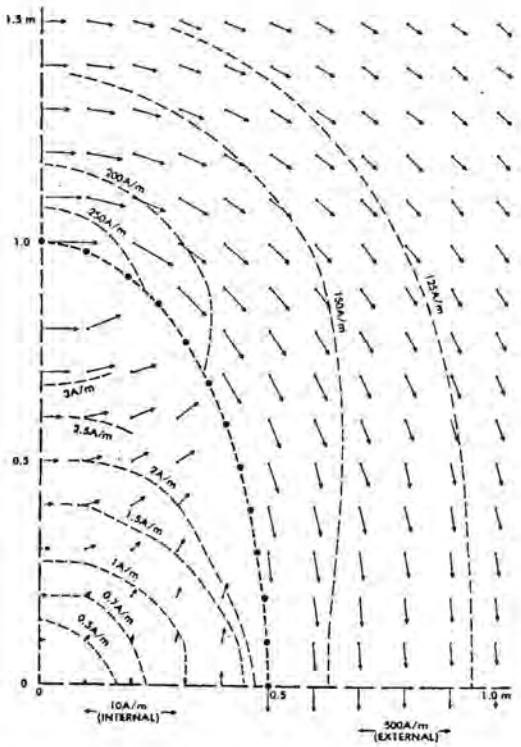

Fig. 10.16 Field with unequal current distribution.

Resistive distribution of current: Fig. 10.17 shows a similar plot with one important difference: the current was forced to be equal in each wire. The magnetic field pattern produced here would be that determined by the resistive current distribution, the pattern that represents the final stage after currents and current density have become uniform. The orientation of the field external to the grid shows only relatively slight differences from that in Fig. 10.16, but one important difference is that some of the field lines penetrate the surface and cause the increased field intensity in the interior of the grid.

Recessed cavity: A third example of field distribution, shown in Figs. 10.18 and 10.19, assumes that on each side of the fuselage there is a recessed cavity. Such a cavity would be an approximation of the equipment bays for electronic equipment frequently found on military aircraft. The figures again assume the current in each filament to be controlled by the magnetic distribution. The field patterns clearly show the field in the recessed cavity to be less than the field at other exterior points on the fuselage.

The degree to which the MAGFLD program can calculate the magnetic field in the space surrounding the aircraft fuselage, while interesting, may not be of great use for aircraft studies, since it is usually only the field intensity at the surface of the structure that is of interest. The program, however, is capable of calculating the field distribution in and around these simple geometries with sufficient accuracy for many purposes.

Redistribution: The filamentary method can be used to calculate redistribution effects by connecting in series with each of the inductors of Fig. 10.13 a resistor of the appropriate value. In the matrix operations of Eqs. 10.20 through 10.40 the values of L and M must be replaced by $R+j\omega L$ and $j\omega M$ and the matrix operations carried out with complex number routines, but the process is otherwise as indicated. Standard circuit analysis routines, such as SPICE, SCEPTRE, NET-II and ECAP can also be used to evaluate the current in each filament. Fourier transform techniques could then be used to evaluate the response as a function of time. Some of the circuit routines can, of course, evaluate the response directly as a function of time.

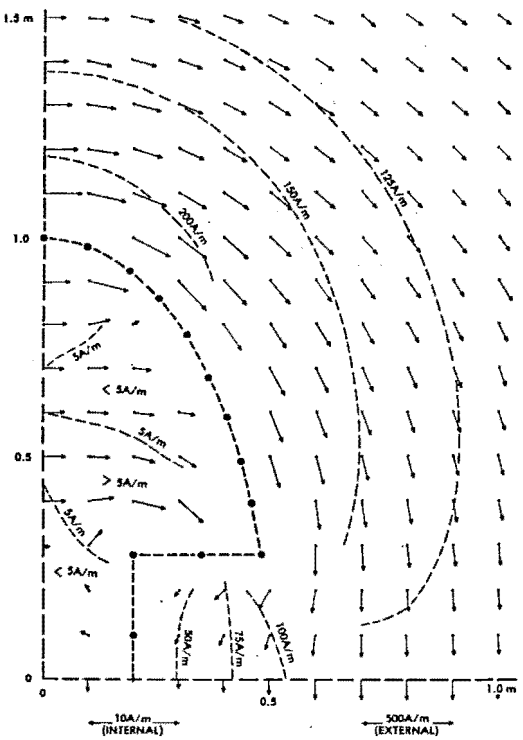

Fig. 10.18 Recessed bays.

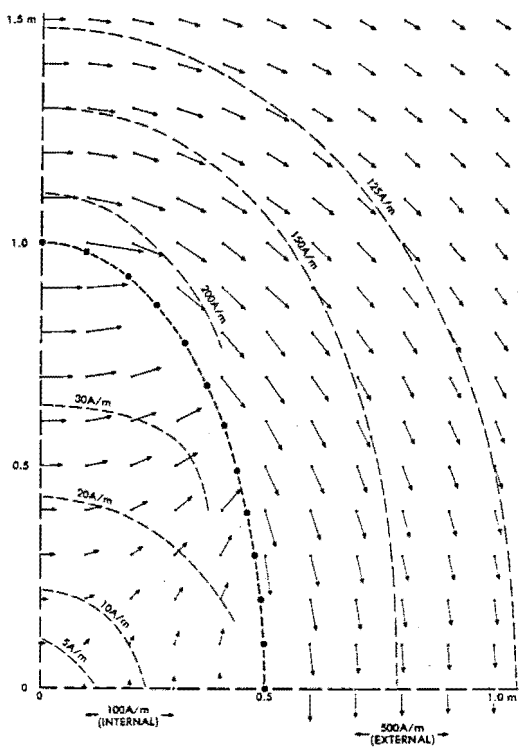

Fig. 10.17 Field with equal current distribution.

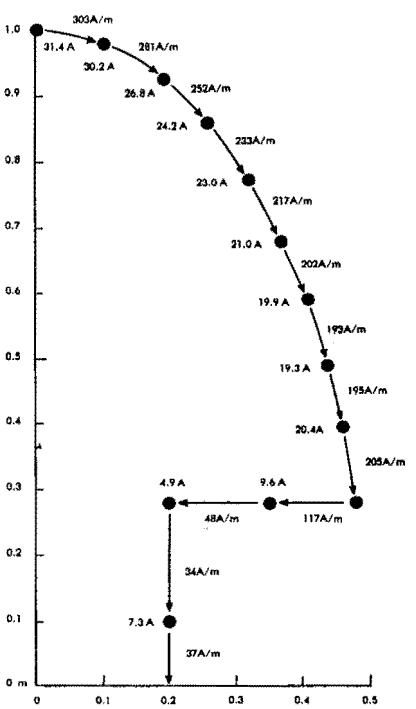

Fig. 10.19 Current distribution and magnetic field strength at the surface (one quadrant only shown).

Representation as charged strips: Rather than representing a surface as a group of filaments each carrying a current, one can represent the surface as a group of strips, each having a certain charge density. One then can, through matrix techniques [10.8, 10.9], calculate the charge density on each of the strips. Since current can be defined as the charge flowing past a point per unit time, the technique also gives the charge density. Fig. 10.20 shows a structure to which the technique was applied, point C representing a wire bundle in the trailing edge. The current distribution (for 1 ampere total current) is shown on Fig. 10.21. While the current densities at points C and D are too small to discern on the graph, they could have been obtained from a numerical printout of the computed results.

The technique can be used to determine the amount of current on the cable and also to determine the transmission properties of the cable; inductance and capacitance per unit length and surge impedance [10.10].

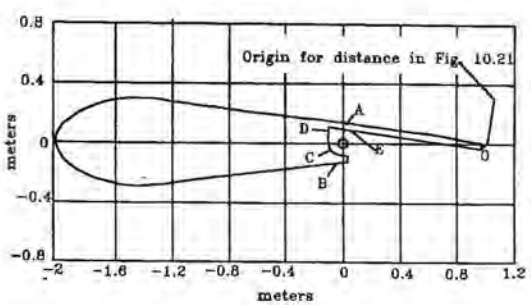

Fig. 10.20 A structure modeled with CAPCODE.

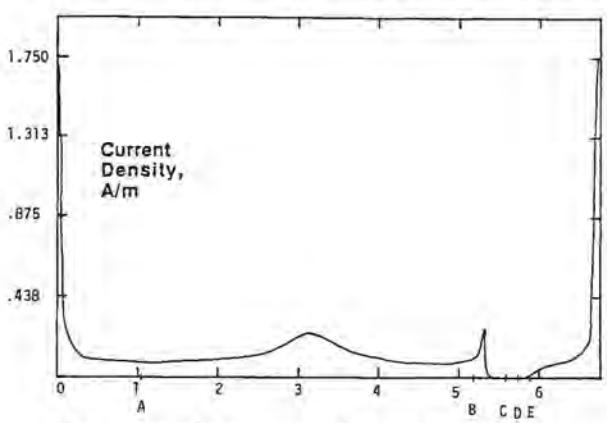

Fig. 10.21 Current distribution on airfoil for 1 ampere total current.

Calculation codes: The literature contains several references to techniques of representing a two dimensional (2D) surface by paralleled subsurfaces, among them being the programs CAPCODE [10.10], POTENT and INDCAL [10.11 - 10.14]. CAPCODE was used to calculate Fig. 10.10. Other programs use similar techniques to determine the capacitance and inductance matrices governing propagation along multiconductor cable bundles [10.15 - 10.17].

The technique of subdividing the surface into strips can also be used with the Method of Moments (MOM) [10.17] that has shown good accuracy when compared to analytic solutions and scale model tests.

One example of an application to which these 2D calculation techniques have been applied was calculation of the current that would flow through different struts if the U.S. Space Shuttle were to be struck by lightning [10.18].

10.6 Maxwell's Equations

The foundation of all lightning interaction problems is Maxwell's equations, given here in the time domain differential form:

$$\nabla \cdot E = \rho/\epsilon_0 \tag{10.41}$$

$$\nabla \cdot B = 0 \tag{10.42}$$

$$\nabla \times E = M_s - \frac{\partial B}{\partial t} \tag{10.43}$$

$$\nabla \times H = \sigma E + J_s + \frac{\partial D}{\partial t} \tag{10.44}$$

E, B, M_s and D are all vector quantities. Eq. 10.41 states that the number of lines of electric flux leaving a volume is equal to the amount of charge contained in that volume. Eq. 10.42 states that the number of lines of magnetic flux entering a volume is equal to the number leaving it. Eq. 10.43 states that a changing magnetic field gives rise to an electric field. Eq. 10.44 states that there are three sources of a magnetic field; conduction currents (σE), externally produced currents (J_s) and the displacement currents produced by a changing electric field. It should be noted that the externally produced magnetic current source M_s in Eq. 10.43 is a fictitious source inserted to provide symmetry to the equations. Physically, there is no such source, but including it in the equations provides a useful means of defining equivalent sources for certain scattering and interaction problems.

Starting premises: If one assumes that the lightning interaction problem begins with the injection of an external lightning current into the aircraft, then the source term for the interaction is J_s in Eq. 10.44. From a knowledge of J_s and the boundary conditions(that is, the aircraft geometry) electromagnetic fields can, in principle, be calculated everywhere.

Sometimes, however, the lightning interaction problem does not start with the injection of lightning current. In particular, this is true for analyses of trig-

gered lightning. For that, the source term is the current σE conducted into the air from the aircraft.

The starting point in this type of analysis could be knowledge of the way electrical charge is distributed, both on the aircraft and in the air surrounding the aircraft, because these suffice to calculate the electric field surrounding the aircraft. If all the charges are stationary then Eq. 10.41 collapses into Poisson's equation:

$$\nabla^2\phi = -\rho/\epsilon_0 \tag{10.45}$$

whence

$$E = -\nabla\phi \tag{10.46}$$

Generally, however, one does not try to calculate the electric field from any knowledge of the charges in the clouds; one simply makes an assumption as to what the electric field would be in the absence of the aircraft and calculates the response of the aircraft to that field, including, if necessary, the effects of any pre–existing charge on the aircraft. Calculations are made to determine the way electric charge is distributed on the aircraft. From these one can calculate the electric field strength at the surface of the aircraft and so calculate the current σE conducted into the air.

Air conductivity: The conductivity of the air is of course, nonlinear; poorly conducting until the electric field gets high enough to cause breakdown and very highly conducting as breakdown occurs. The result is that there is only a negligible current conducted into the air until breakdown occurs, but considerable current afterwards. That current then acts as a source of charge onto the aircraft, which affects the electric fields and may set in motion events that lead to a complete triggered lightning flash. Calculating the response of the aircraft to the current, though, is done in the same way as for a naturally occurring lightning flash.

Impinging fields: A third type of source is that involved when the electromagnetic field from a lightning channel, commonly designated Lightning Electromagnetic Pulse (LEMP), impinges upon the aircraft. Then the problem is to calculate the currents and charges induced on the vehicle by the incident LEMP. This is the classical electromagnetic scattering problem and requires special techniques to evaluate Maxwell's equations. One approach is to cast Maxwell's equations into an integral form [10.20], such as the electric field integral equation (EFIE) or the magnetic field integral equation (MFIE), whose frequency domain forms are given by:

EFIE

$$\hat{n} \times E_0(r,\omega) = \frac{1}{2\pi j\omega\epsilon_0}\hat{n} \times \int \{-\omega^2\mu_0\epsilon_0 J_s(r')\phi + (\nabla'\phi)[(\nabla' \cdot J_s(r)]\}da' \tag{10.47}$$

MFIE

$$J_s(r,\omega) = 2\hat{n} \times H_0(\omega) + \frac{\hat{n}}{2\pi} \times \int J_s(r'\omega \times \nabla')\phi)da' \tag{10.48}$$

where ϕ represents $\epsilon^{(jkR)/R}$.

In these equations, $E_0(r,\omega)$ and $H_0(r,\omega)$ are the incident electric and magnetic fields, R is the vector between the observation point (r) and the integration point (r') and J_s is the induced surface current density, which is the desired solution. The integration in Eqs. 10.47 and 10.48 is over the surface of the aircraft. Strictly speaking, these equations are only true for perfect conductors, but approaches have been developed to include lossy elements in integral equation formalisms.

Note that the integral equations have the unknown appearing in the integrand. The solutions are typically obtained by the Method of Moments (MOM) [10.21].

Another approach to solving the scattering problem is to invoke the equivalence principle [10.22]. In this approach the scattering object is completely surrounded by an imaginary closed surface. On this surface, one defines equivalent electric and magnetic current sources J_s and M_s for use in Maxwell's equations. These sources, called Huygen's sources, are tangential to the closed surface and are derived solely from the incident field which would exist in the absence of the scattering object. Therefore, if one knows the sources J_s and M_s, Maxwell's equations can be used to calculate the electromagnetic response everywhere in space, given the appropriate boundary conditions. This approach is commonly used to solve the scattering problem in the time domain finite difference method [10.23].

10.7 Survey of Interaction Models

In this section, available interaction models are surveyed. They fall into two important classes: finite difference solutions and integral equation solutions.

10.7.1 Time Domain Finite Difference Approaches

The term *time domain* implies that the response of a system is calculated as a function of time, as contrasted to the *frequency domain* in which the response is calculated as a function of frequency. All time domain solutions calculate the response of a system at specific time steps, using the response at a previous time step to calculate the response at the next time step.

Modeling and problem space: In the time domain the two Maxwell curl equations are:

$$\nabla \times E = M_s - \frac{\partial B}{\partial t} \tag{10.49}$$

$$\nabla \times H = \sigma E + J_s + \frac{\partial D}{\partial t} \tag{10.50}$$

Implementing a time domain solution of the equations in rectangular coordinates requires that each surface of the aircraft (or any other article) under study be modeled by an assemblage of three dimensional cells, as shown on Fig. 10.22.

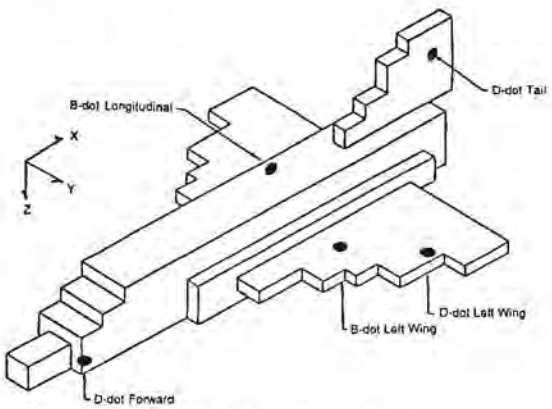

Fig. 10.22 Model of F-106 used in finite–difference code.

The size of the cells depends on the resolution desired in the time domain solution. A rule of thumb is that five cells are needed to resolve the wavelength of the highest frequency of interest. Therefore, if the desired resolution is up to 100 MHz, then the cell dimension would have to be about 2 foot (0.6 m) wide since the velocity with which electromagnetic waves propagate along the surface is about 1 ft/ns, or more precisely, 0.3 m/ns.

At any one time each cell contains information on the magnetic and electric fields. At the next instant of time the fields in each cell will have propagated to adjacent cells, in a manner depending on how the fields were distributed in those cells at the previous time step.

The analysis assumes that the way the fields in a particular cell propagate depends only on the fields in its immediate neighbors at the previous time step. This information suffices to allow the various partial derivatives in Maxwell's equations to be approximated by ratios of differences of two quantities, as suggested by Yee [10.24]. The procedure, which has been widely used in the NEMP community, will not be detailed here, but it is described in the literature [10.23, 10.25 - 10.27].

Information on the coordinates of each of the cells, along with information on the magnetic and electric field intensity in each of the cells must be stored in the computer (hand calculations are totally impractical) and the required memory locations provide one of the limitations on the degree to which the aircraft can be modeled. Doubling the resolution by halving the size of the cells raises the storage requirements by a factor of eight for 3D computations. Also, if the cell size is reduced by a factor of two, then the time step must be reduced by a factor of two. Therefore, in order to calculate the response of the more finely gridded problem space to the same final time as the original problem requires sixteen times as much computer time.

The time domain finite difference technique has had an extensive successful application to understanding the response of the F-106B and C-580 thunderstorm research aircraft to triggered lightning [10.28 - 10.37]. It has also been used to model the lightning response of helicopters [10.38], to model the response of aircraft in test facilities and to design lightning test facilities [10.39, 10.40]. Both two dimensional and three dimensional (2DFD) and 3DFD) approaches have been implemented.

Advantages: Because the approach is a straightforward solution of Maxwell's curl equations there are no *fundamental* approximations, though solution accuracy may be limited by the the degree to which the complex shape of an actual aircraft can be modeled as an assemblage of cells. The main limiting factor in analysis is the speed and memory of the computer used for the calculations and the cost of computer usage.

Other advantages of this approach are:

1. Nonlinearities can be modeled.
2. All three types of lightning sources described in §10.6 can be modeled.
3. Circuit and transmission line elements (linear and nonlinear) can be integrated and interfaced with 3DFD codes, thus allowing self–consistent interaction of lightning pulse generators and test fixtures with the aircraft being modeled.
4. It has considerable credibility in that it has been successfully compared to experimental data, both in the NEMP and lightning communities.
5. Complex three dimensional shapes can be modeled.

Disadvantages: One disadvantage of this approach is that the codes are complex and users need considerable skill. Another is that the codes may require sub-

stantial computer time and expense. Ongoing trends in computer speed and cost can be counted upon to reduce these problems.

Examples: Some examples of the use of this approach are given in §10.8 and §10.9, in which predictions of the response of the F-106B and C-580 thunderstorm research aircraft are compared to measured data. The predictions cover both linear and nonlinear (triggered lightning) modeling.

10.7.2 Integral Equation Approaches

There are at least three integral equation approaches which have been used for lightning interaction analysis. They all use the method of moments (MOM) and calculations are made only in the frequency domain. Determining the response to a lightning transient would require calculations to be made at many frequencies, after which the time domain response could be extracted by inverse Fourier transform techniques. Since making calculations at the large number of frequencies required for a meaningful transformation would be quite expensive, the methods have not been used much for lightning interaction problems. Also, because all the approaches assume linearity in their formulation, they cannot be used to solve nonlinear problems.

This is an inherent feature of all frequency domain analysis techniques, whatever the application, and is not peculiar to calculations of lightning interactions. A consequence of this is that none of them can be used to analyze initiation of triggered lightning. Lightning must be considered either as a discrete current source injected onto the aircraft at some point (and removed at one or more points elsewhere) or it must be assumed to be the source of an electromagnetic field that impinges on the aircraft.

WIRANT: The program WIRANT [10.41 - 10.43] is based on the electric field integral equation (EFIE) of §10.6. The aircraft is replaced by an approximately equivalent structure made of thin wire segments, as illustrated on Fig. 10.23. WIRANT is then used to determine the current on the individual wire segments. Those currents provide an approximation of the actual surface currents on the vehicle. Most commonly the procedure has been used to determine the response of a structure to an impinging electromagnetic field, but for lightning interactions the procedure can also be used to determine how current divides among the various wires if lightning current is injected at a particular point. Lossy materials can be included in the model. Results predicted by WIRANT have compared favorably with test data [10.44].

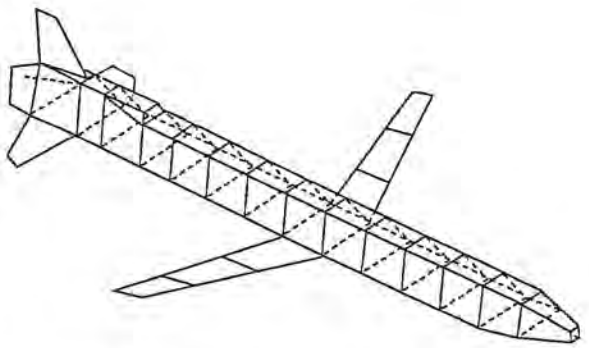

Fig. 10.23 Simple wire grid model of a cruise missile.

Triangular patch: The triangular patch method [10.44 -10.46] models the aircraft by an assemblage of triangular surfaces. The current at the center of each patch is then calculated using either the electric field integral equation (EFIE) or the magnetic field integral equation (MFIE), depending on the shape of the object being modeled. The MFIE can only be used for closed surfaces. A gridding of the F-18, showing the distribution of current at 1 MHz, is shown on Fig. 10.24. The method allows lossy materials to be modeled.

A virtue of a triangular grid is that it allows for fairly faithful modeling of complex shapes, and for this reason triangular grids are the ones most commonly used for field analysis in other disciplines. A drawback, though, is that the model can only be used for a steady state solution. The literature [10.44 - 10.46] shows several examples of the response at a fixed frequency, but no lightning transient responses have been published, perhaps because the cost of calculating the response at sufficient frequencies for a Fourier transform into the time domain has been excessive.

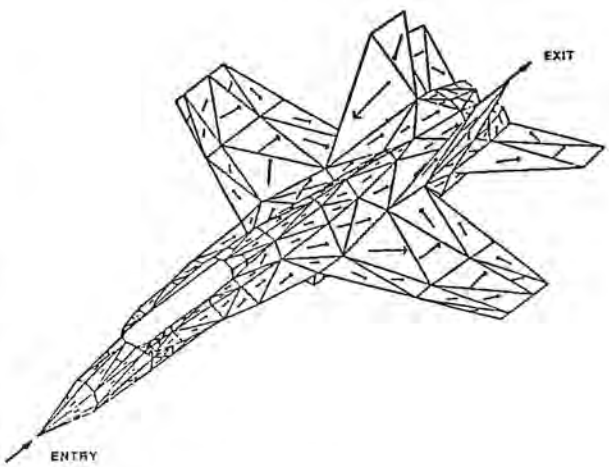

Fig. 10.24 Triangular patch model of an F-18.

GEMAX: The program GEMAX (General Electromagnetic Model for the Analysis of Complex Systems) uses a MOM integral equation solution for low frequencies and the geometrical theory of diffraction (GTD) for high frequencies [10.47 - 10.49]. For lightning interactions the frequencies are low enough that the integral equation approach is appropriate. The method has been used to study lightning coupling to a helicopter, the analyses being made in the frequency range 0.5 - 10 MHz. The lightning stroke was modeled as a conductor 20 times the length of the helicopter, though since a lightning channel is actually much longer, doing so may lead to resonant behaviour not truly appropriate for interaction with lightning. No lightning transient results have been published, again perhaps because computation at all the frequencies required for a Fourier transform is too expensive.

NEC: Another integral equation code which might be of some use for analysis of lightning effects is NEC [10.50 - 10.54], "Numerical Electromagnetic Code." The program is designed mainly for antenna and EMC work and no applications for lightning analyses seem to have been published.

None of these frequency domain approaches have been mated to techniques for determining the fields coupled to the interior of the aircraft or for determining the response of circuits inside the aircraft to such fields. They have only been used to determine the electromagnetic fields on the surface of the aircraft, after which the fields coupled into the aircraft have been analyzed as a separate task.

10.8 Application of Finite Difference Codes - Linear Modeling

This section will show examples of how the finite difference codes have been used to model two research aircraft; the F-106B operated by NASA's Langley Research Center [10.29, 10.30] and the CV-580 operated by Wright Patterson AFB and the FAA [10.31]. It will deal with linear modeling; that is the response of the aircraft to an assumed lightning stroke. §10.9 will give examples of how the codes have been used to predict the response to triggered lightning.

10.8.1 Modeling of the Aircraft

The way the F–106B was modeled as an assemblage of cells was previously shown on Fig. 10.22, that figure also showing the coordinate system and the location of several electromagnetic field sensors used on the aircraft. The large scale nature of the aircraft is well resolved, but it is clear that details, such as the nose boom, are not well resolved. This can cause difficulty when field distributions around such points are desired. In most cases, however, the model as shown is adequate to predict the response at the sensors of a given lightning event, partly because the sensors were intentionally placed on surfaces with a large radius of curvature, surfaces which are easily modeled.

Problem space: The problem space (see §10.5.1) into which the aircraft was placed was about twice the size of the aircraft itself and was divided into a grid one meter in X dimension (fore and aft) and one–half meter in the wing to wing and vertical dimensions Y and Z. The temporal resolution of the model was 1 nanosecond. The nominal frequency resolution of the mesh, assuming a minimum of five cells per wavelength, was thus approximately 60 MHz. The model was placed in the problem space in such a way that all tangential electric fields were zero at all times. This implies that the aircraft was perfectly conducting, with no significant apertures which would alter the field around the aircraft. This is a good approximation except for the immediate vicinity of the cockpit.

Representation of CV–580: The three dimensional finite difference representation of the CV–580 is shown in Fig. 10.25 [10.56]. Also shown are coordinate axes and the locations where the electromagnetic fields were calculated, these corresponding to the locations where field sensors were located on the actual aircraft. The angles $\theta$and ϕ are used to specify the direction of the ambient electric field for the nonlinear model discussed in §10.9. The spatial resolution of the model was one meter in all directions and the time step used was 1 nanosecond. The problem space used was of dimension 48 x 41 x 22 cells, putting the extremities of the aircraft eight cells away from the nearest boundary. This is about the minimum separation that allows a satisfactory simulation of the scattering problem.

10.8.2 Necessary Assumptions

There are a number of assumptions that must be made when using the linear transfer function technique. These are discussed individually below.

Lightning attachment locations: The places where the lightning attaches to the aircraft must be defined in advance since they constitute part of the initial conditions. Also, they cannot change with time since time dependent geometry is not consistent with the assumption of linearity. Any realistic condition requires that there be multiple channel attachments, but only one of these can act as a source injecting charge onto the aircraft, though there may be multiple channels to drain charge away. Having more than one source does not

violate linear constraints, but it does prevent the problem from having a single unique solution.

The linear technique can be used for either triggered or natural lightning; the distinction being that triggered lightning begins at the aircraft and moves away while natural lightning moves toward the aircraft. Typical geometries for each of these cases are shown in Fig. 10.26. The figure shows the channel attached to the nose of the aircraft, as often happened on the F–106B, but the analysis procedure allows attachment to any point on the aircraft.

The difference between Fig. 10.26(a) and Fig. 10.26(b) is the location of the current source. For calculations simulating natural lightning the source is located at the edge of the problem space, as far from the aircraft as possible, reflecting the fact that the initiation and driving forces for a natural lightning flash occur away from the aircraft and the lightning propagates towards it. For triggered lightning it is located near the point where the channel attaches to the aircraft, reflecting the fact that the flash originates at the aircraft and propagates away from the aircraft.

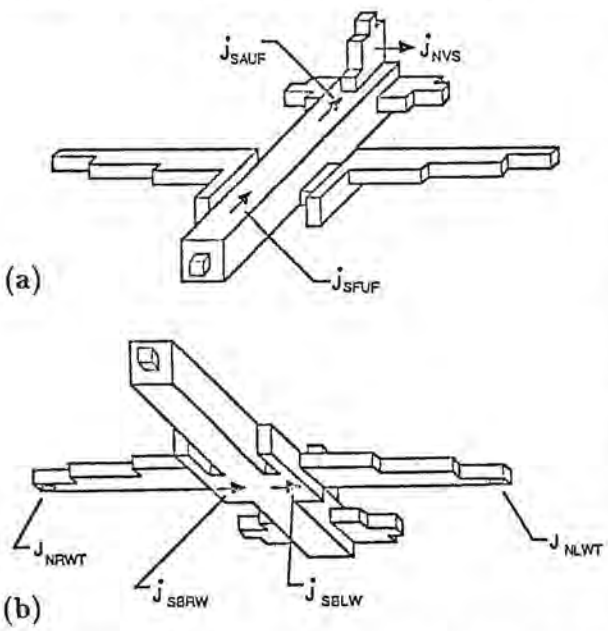

Fig. 10.25 3D finite difference model of CV-580 aircraft.
(a) Top view
(b) Bottom view

Formation times of multiple channels: While the routines can handle multiple exit channels, it is necessary to define in advance when they are to form; the formation times cannot be left as a matter to be calculated during the solution of the problem.

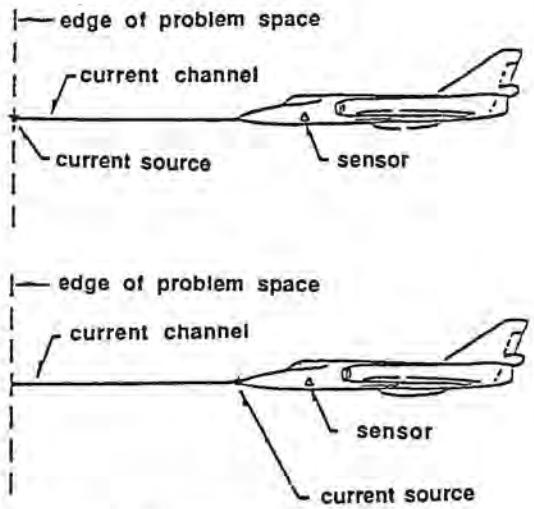

Fig. 10.26 Locations of current source used in computer code.
(a) Natural lightning
(b) Triggered lightning

Lightning channel geometry: The geometry of the lightning channels should be defined since there can be radiation from the channels that affects the response of the aircraft. This radiation, however, has much less of an impact on the response than does the current injected from the channel. Since the orientation of real channels cannot be determined in advance, it is generally satisfactory just to assume the lightning channels to be straight lines, as shown in Fig. 10.26.

Channel characteristics: The channel characteristics, the most important of which are impedance and velocity of propagation, must be defined since there are interactions between the aircraft and the channel and these depend on the channel impedance. Elementary aspects of this interaction were discussed in Chapter 8. The impedance and velocity of propagation are determined from the resistance and inductance and capacitance of the channel, per unit length, with the latter two being determined by the physical diameter of the channel, as discussed in Chapter 2.

The analysis technique allows the investigator to define any desired impedance characteristics of the channel, as long as those characteristics do not depend on the way the problem evolves. The impedance may vary with time, but the variation must be predicted in advance.

In an actual channel the impedance probably depends on the current that has flowed through the channel, but the linear analysis technique does not allow channel impedance to be defined as a function of current.

10.8.3 Transfer Functions

In the examples that follow, the shape of the lightning current injected into the aircraft was determined by using the finite difference code to see what current was necessary to produce a calculated field matching one of the fields measured on the aircraft. The injected current was then used to calculate the responses at the other points at which measurements had been made. The calculated fields were then compared to the measured fields to see the degree of correspondence.

Determining the appropriate shape of the lightning current involves the use of transfer functions. The transfer function, T.F., is a relationship in the frequency domain between a source function and a response function,

$$\mathcal{L}(\text{Output}) = T.F. \times \mathcal{L}(\text{Input})$$
$$\mathcal{L} \equiv \text{Laplace transform} \qquad (10.51)$$

and its use requires the system under study to be linear. This requirement is satisfied by a linear finite difference code, but is, of course, not satisfied in a real interaction between an aircraft and a lightning flash where the impedance of the lightning flash changes with time and with current. The justification for using transfer functions is that the nonlinearity in the real situation is mostly confined to the lightning channel itself. The responses of the aircraft are usually linear functions of the lightning current that flows onto the aircraft, at least to within the accuracy with which lightning interaction calculations can be made.

Transfer functions are determined by taking the Fourier transforms of the current source and the response waveforms:

$$T(\omega) = \frac{R(\omega)}{I(\omega)}. \qquad (10.52)$$

Here $T(\omega)$ is the transfer function in the frequency domain, $R(\omega)$ is the transform of the response waveform, and $I(\omega)$ is the Fourier transform of the current source waveform. A transfer function can be calculated (for given set of lightning channels) by assuming a current waveshape (time domain), making the calculations to determine the time domain response at a particular point and performing the transforms and calculations of Eq. 10.52. For the F-106 study the responses calculated were the rates of change of electric field at the locations where electric field sensors (D–dot sensors) were located on the aircraft. Several transfer functions were calculated, one for each location where there was a sensor of the electric field, all, of course, for the same geometry of the lightning flash. Because the model is linear the transfer functions are independent of the characteristics of the source.

Current from field waveshape: One way the transfer functions can be used is to calculate for each of the points where measurements were made the waveshape of the current that would have produced that response. If the lightning channels assumed for the calculations were those followed by the actual lightning flash, and if all of the responses of the aircraft upon which the calculated transfer functions were based were correct, then all of the calculated lightning current waveshapes would be the same. If not, then the calculations could be repeated until satisfactory performance was reached.

For this program a slightly different approach was used. The transfer function calculated for one point on the aircraft, and the response measured at that point, were used to calculate the lightning current flowing along the lightning channel assumed for the calculations. Then the responses calculated at all the measurement points were compared to the responses measured at those points. The degree to which the responses agree is a measure of the validity of the modeling technique.

10.8.4 Results of Calculations

Two examples of calculations based on measurements made during actual lightning strikes will be given. In each, the field waveshape measured at one location was used to calculate the most probable waveshape of the lightning current. That current was then used to calculate the field waveshape at other points. Measured and calculated field waveshapes were then compared.

F-106B: Results from the model for the F-106B are presented in Fig. 10.27. They pertain to a triggered lightning flash attaching to the nose with an exit streamer coming from the tip of the vertical stabilizer. The transfer function and measured waveshape used to derive the waveshape of the current were derived for the longitudinal magnetic field sensor (B–dot) located atop the fuselage, the waveshape at that sensor being shown on Fig. 10.27(a). The agreement between calculated and measured results only indicates that there were no numerical errors in the calculations.

Responses measured and calculated for the other points are shown in Figs. 10.27(b) - 10.27(e). The largest disagreement between measured and calculated responses is that for the tail, Fig. 10.27(e). After the calculations were done, it was discovered that the actual location of the sensor on the tail was considerably different from the location assumed for the model; in fact the calculations and measurements pertain to two different locations.

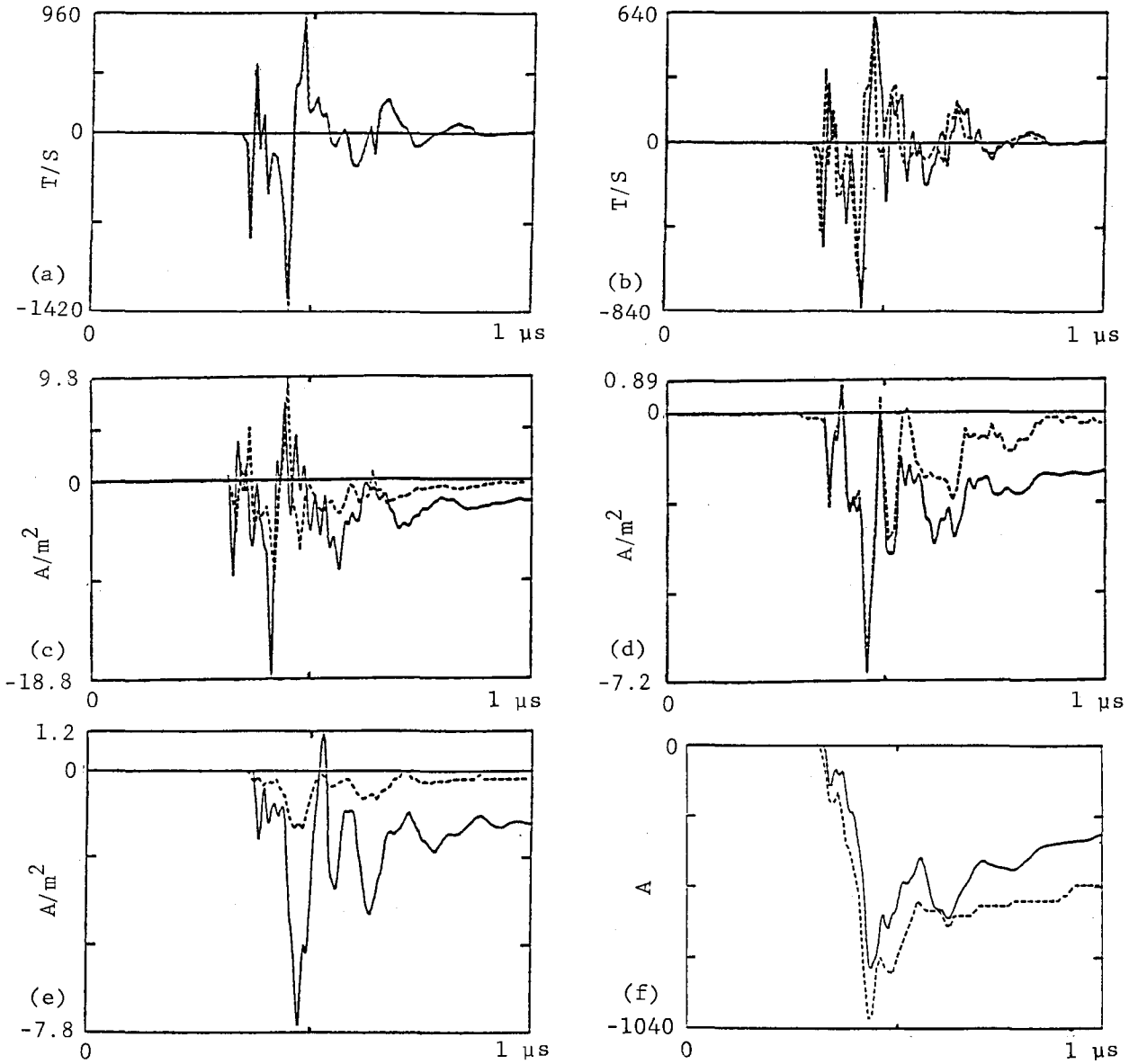

Fig. 10.27 Calculated and measured response to triggered lightning - F-106B.
(a) Longitudinal B–dot sensor (d) Left wing D–dot sensor
(b) Left wing B–dot sensor (e) Vertical fin D–dot sensor
(c) Forward D–dot sensor (f) Nose current

The waveshapes of the current calculated and measured as flowing into the nose boom of the F-106B are shown in Fig. 10.27(f).

CV-580: Similar results have been obtained with the CV-580 data. The situation illustrated here pertains to a strike that occurred on 5 September 1984 at 21:53:05 UTC (Coordinated Universal Time). This strike is known to have attached to the right wing [10.55]. For the calculations, the lightning channel was assumed to be vertical upward from the right wing tip. The current in the channel was determined using a transfer function based on a voltage source at the aircraft and the response measured for the electric field (D–dot) on the right wing. That response is shown on Fig. 10.28 and the agreement between measured and calculated results only indicates that calculations were numerically correct.

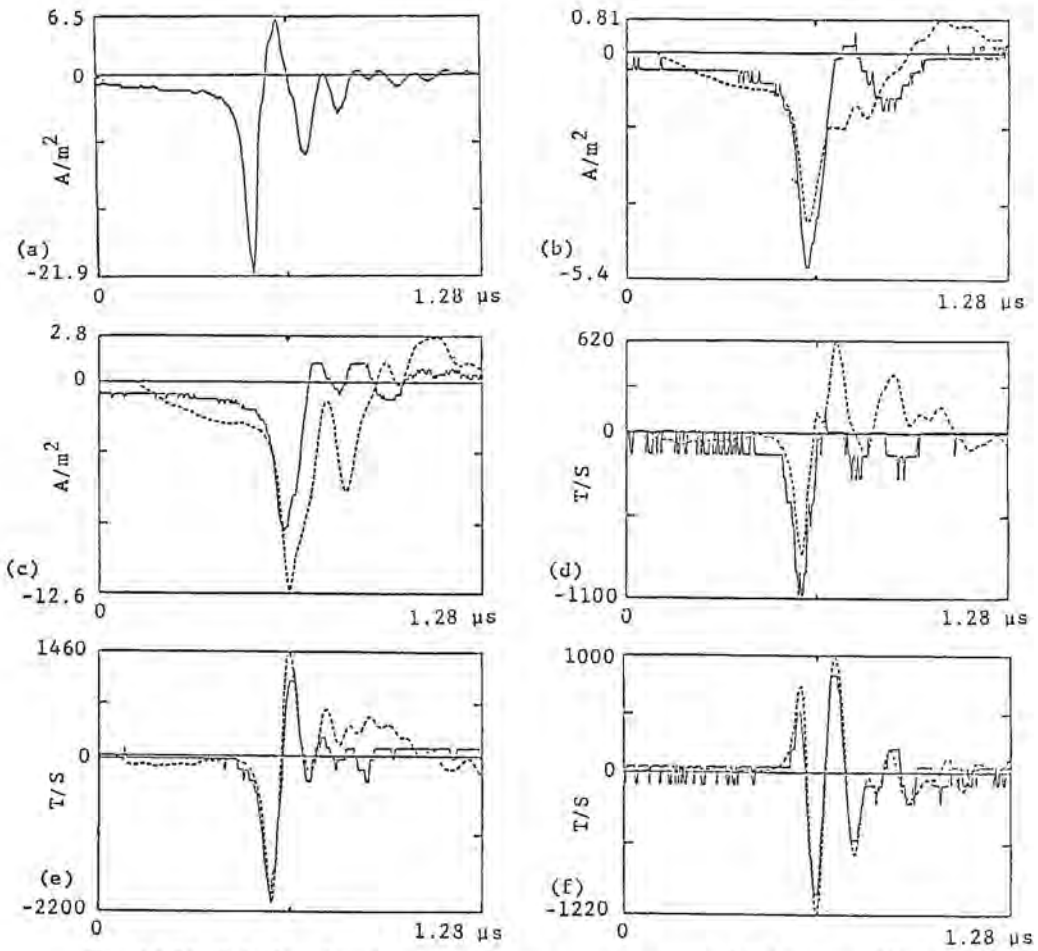

Fig. 10.28 Calculated and measured response to triggered lightning - CV-580.

(a) D–dot right wing sensor
(b) Vertical stabilizer D–dot sensor
(c) Left wing D–dot sensor
(d) Left wing B–dot sensor
(e) Right wing B–dot sensor
(f) Forward fuselage B–dot sensor
(g) Aft fuselage B–dot sensor

Measured - solid, Calculated - dotted

Responses for other points are shown in Figs. 10.28(a) - 10.28(f). The general agreement between measured (solid) and calculated (dashed) results is evidence that the simulation comes close to reproducing the effects of the real lightning flash.

The waveshape calculated for the current is shown in Fig. 10.29. The predicted lightning current has a peak amplitude of about 2 kA with a maximum rate of change of 20 kA/μs, values typical of the currents encountered during triggered lightning flashes.

10.9 Nonlinear Interaction Modeling

A description of triggered lightning was given in Chapter 3. Nonlinear modeling with time domain codes is a way of simulating the way corona forms around the aircraft and develops into a triggered lightning event. The currents involved can then be used to determine the response of the aircraft. Good comparisons between measured results and results from calculation give evidence that the numerical procedures used function properly and that the physical characteristics of the lightning flash are modeled reasonably correctly.

Calculation of triggered lightning phenomena is a very computer intensive process, for reasons described earlier. It has not been employed to calculate responses for the full duration of a triggered lightning event, but the model described here is applicable to at least the initial stage of triggered lightning.

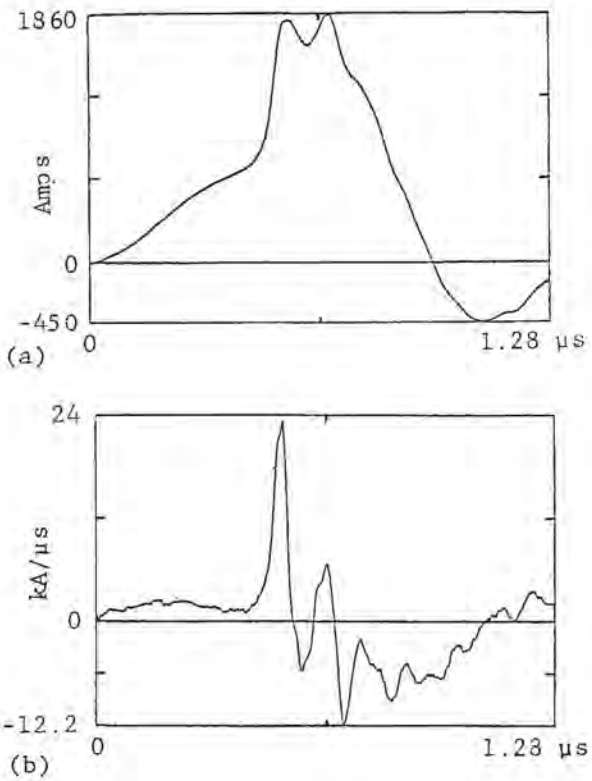

Fig. 10.29 Calculated injected current - CV-580.
(a) Current
(b) Rate of change of injected current

10.9.1 Air Conductivity

The details of the nonlinear model have been described elsewhere [10.29 - 10.31] and only a summary of the basic ideas is presented here. In this model, air conductivity, which can change by several orders of magnitude during air breakdown, is calculated and included in the finite difference equations. The subsequent flow of induced current during the breakdown constitutes the initial event of triggered lightning.

The calculation of the conductivity of air is based on a three species air chemistry model; electrons, positive ions and negative ions. The model calculates their densities by using continuity equations and the measured rates for various physical processes. These processes include electron avalanching, electron attachment to neutral molecules, recombination between electrons and positive ions and recombination between negative and positive ions. The conductivity of the air is determined by summing all the conducting particles:

$$\sigma = q(n_e\mu_e + n_-\mu_i + n_+\mu_i), \qquad (10.53)$$

where q is the electronic charge (1.6×10^{-19} coulombs, n_e n_-, and n_+ are the numbers of secondary electrons, negative ions and positive ions per cubic meter and μ_e and μ_i are the electron and ion mobilities in $m^2/volt \cdot sec$. The mobilities of positive and negative ions are assumed to be the same. The particle densities are calculated from the continuity equations:

$$\frac{\partial n_e}{\partial t} + \nabla \cdot (n_e v_e) + [\beta n_+ + \alpha_e - G] = Q(t) \quad (10.54)$$

$$\frac{\partial n_-}{\partial t} + \nabla \cdot (n_- v_-) + \delta n_+ n_- = \alpha_e n_e \quad (10.55)$$

$$\frac{\partial n_+}{\partial t} + \nabla \cdot (n_+ v_+) + \beta n_e n_+ + \delta n_+ n_- = Q(t) + G n_e \quad (10.56)$$

where α is the electron attachment rate (sec^{-1}), G is the electron avalanche rate (sec^{-1}), β is the electron–ion recombination coefficient ($m^3 sec^{-1}$), δ is the negative–positive ion recombination coefficient ($m^3 sec^{-1}$) and Q is the ambient ionization rate. These rate coefficients, as well as the electron and ion mobilities, are functions of the electric field intensity, the percentage of water vapor in the air, and the relative air density. The formulae for these coefficients were obtained by curve fitting to measured data, as discussed in [10.58]. For simplicity, the mobilities of the particles are used to calculate their velocities:

$$v_s = \pm \mu E. \qquad (10.57)$$

In the implementation of the model into the finite difference code, the conductivity of air is calculated for every spatial cell at the same time point as the magnetic field calculation; that is, the electric field from the previous time step is used to calculate the air conductivity which in turn is used to advance the electric field in time.

10.9.2 Steps in the Calculation Process

The first step is determining the static field distribution about the aircraft. This could be determined from calculation knowing the distribution of all the charges, both in the cloud and on the aircraft, or it can be determined just by assuming a given field. In any case it will be a static field since the rate at which the field builds up is very much slower than the rate at which the field collapses once air breakdown starts, build-up being measured in seconds, and breakdown being measured in nanoseconds.

Initial Conditions: For the calculation of the initial conditions, four basic electrostatic solutions are either computed or assumed. Three of these are to determine the electric field oriented along each of the coor-

dinate axes and the fourth is to determine the electric field produced by charge on the aircraft. These may be combined to give the total field. The basic solutions can be calculated by solving Poisson's equation, but with some slight modifications, the finite difference equations can also be used to yield the desired static solution. The latter approach is used here.

Input parameters: The input parameters for the nonlinear model are: the relative air density (a function of altitude), water vapor content of the ambient air, the ambient field, and the net charge on the aircraft. For nonlinear modeling, these parameters completely define the lightning environment.

To get a static solution for a given initial ambient field, equivalent sources on a Huygens' surface are used to obtain a field of one volt/meter along one of the coordinate axes. Numerically, the charges are assumed to appear instantaneously. This causes an oscillating response of the aircraft and so the code is run until a steady state is reached.

10.9.3 Examples of Calculations

If one can find a set of initial conditions that produce a response that matches measured data for a given lightning event, then there is reason to believe that the ambient environment assumed for the calculations was similar to the conditions that gave rise to the actual event. Because of the nonlinear character of the study method, it is not possible to make a simple scaling of calculated results to measured results and so come up with a better estimate of the initial conditions. One must just make a comparison between the response calculated for a specific set of conditions and the response produced by the actual event.

F-106B: Examples of comparisons for the F–106B are shown in Figs. 10.30 through 10.33. Of particular interest in the comparisons is the double pulse character shown in Figs. 10.30, 10.31 and 10.33. Thiscorresponds to an air breakdown at two different places, but at different times. This is the same type of phenomenon observed during actual triggered lightning events. The first pulse corresponds to the initial breakdown (usually at the nose boom) and the second pulse occurs elsewhere as charge flows onto the aircraft and raises the electric field strength elsewhere.

C-580: Results have also been obtained for the CV-580 response. A limited study [10.32] to define such an environment was done for the strike previously discussed in §10.8. It is known that this strike attached to the right wing and that it was most probably a triggered flash. With this information, the ambient field and the charge on the aircraft were adjusted so that breakdown occurred on the right wing. This required the ambient field to be oriented wing to wing.

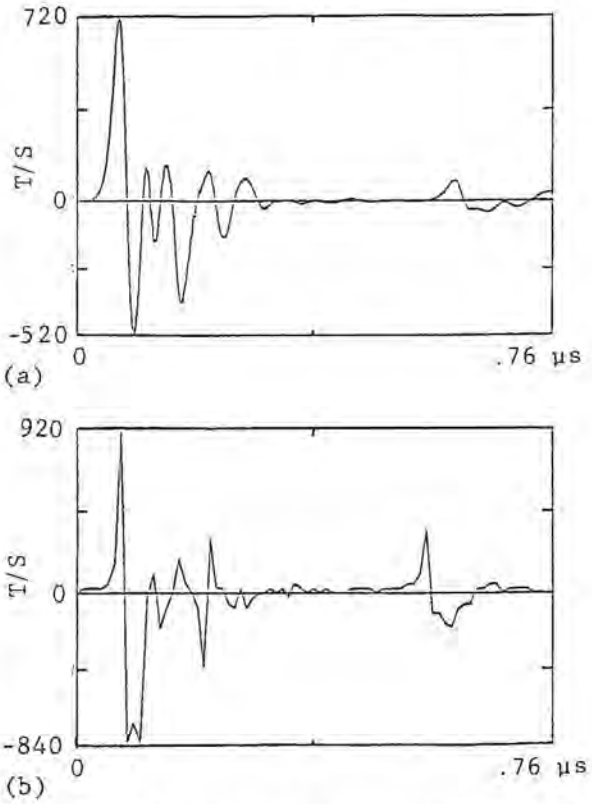

Fig. 10.30 Calculated and measured response of F-106B to triggered lightning longitudinal B–dot sensor.
(a) Calculated
- 2×10^5 V/m ambient electric field
- oriented nose to tail
- 1.35 mC net charge

(b) Measured - Flight 82-038, Run 7

Figs. 10.34 through 10.37 show calculated and measured results for the CV-580. These were calculated for an ambient field of 50 kV/m, net charge of 1.35μC on the aircraft and a relative air density of 0.5. The agreement is quite good, about the same quality as for the F-106B.

10.10 Aircraft resonances

Traveling Waves: Waves traveling on a conductor encounter a surge impedance given by the inductance and capacitance of the conductor,

$$Z = \sqrt{\frac{L}{C}}. \qquad (10.58)$$

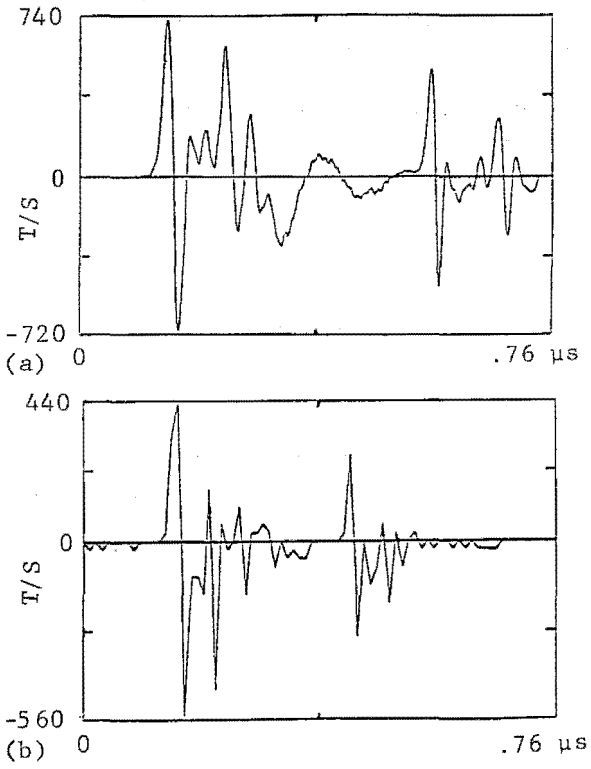

Fig. 10.31 Calculated and measured response of F-106B to triggered lightning.
- longitudinal B–dot sensor.
(a) Calculated
- 6.4×10^5 V/m ambient electric field
- oriented bottom to top
- -1.35 mC net charge
(b) Measured - Flight 82-038, Run 5

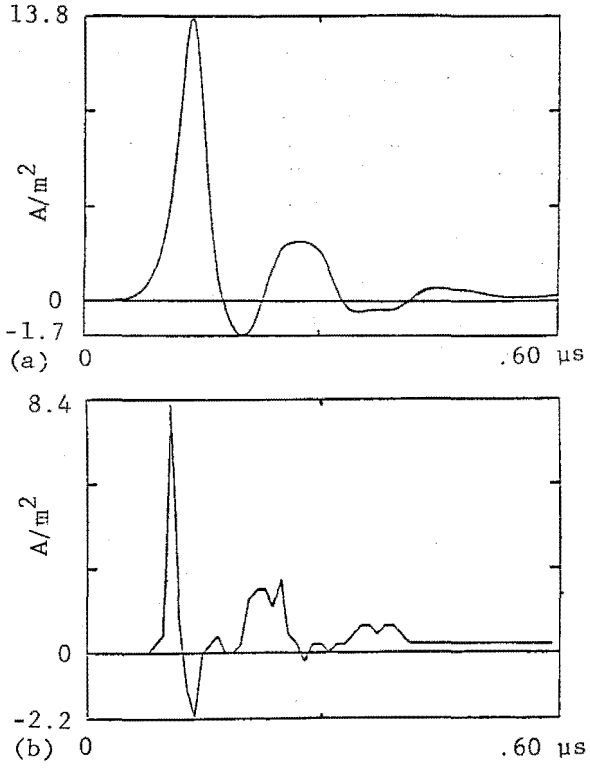

Fig. 10.32 Calculated and measured response of F-106B to triggered lightning.
- forward D-sensor.
(a) Calculated
- 1.99×10^5 V/m ambient electric field
- oriented nose to tail
- zero mC net charge
(b) Measured - Flight 82-024, Run 13

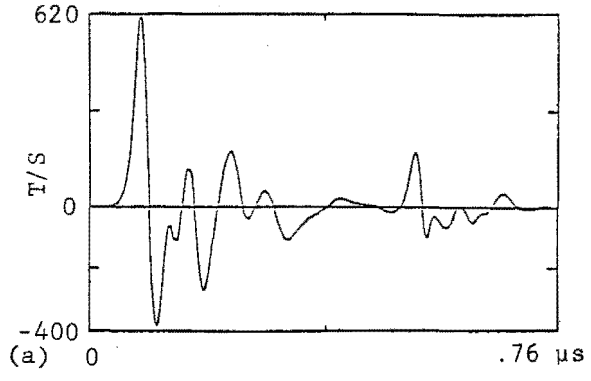

Fig. 10.33 Calculated and measured response of F-106B to triggered lightning.
- longitudinal B–dot sensor.
(a) Calculated
- 6.4×10^5 V/m ambient electric field
- oriented bottom to top
- 1.35 mC net charge
(b) Measured - Flight 82-038, Run 3

For a conductor in air the impedance will be in the range 300 - 500 ohms. If the wave encounters another conductor of different impedance part of the wave will be transmitted onto the other conductor and part will be reflected back along the conductor on which the incident wave was traveling. The magnitudes of the transmitted and incident waves are given by the relative surge impedances of the two conductors, the relevant equations being given on Fig. 10.38. If the wave on the second conductor encounters a third conductor there will be produced a second set of transmitted and reflected waves. The reflected waves on the second conductor travel back towards the source, again encounter a change in impedance and set up a third set of traveling waves. The process repeats until all the energy is radiated away or lost in the resistance of the conductor. The result is that an oscillatory wave is developed on the second conductor, the frequency of the oscillation being given by length of the second conductor, or more properly, by its electrical travel time. For a conductor in air, where the velocity of propagation is 3×10^8 m/s, the ringing frequency would be

$$f = \frac{3 \times 10^8}{2l} \tag{10.59}$$

where l is the length in meters.

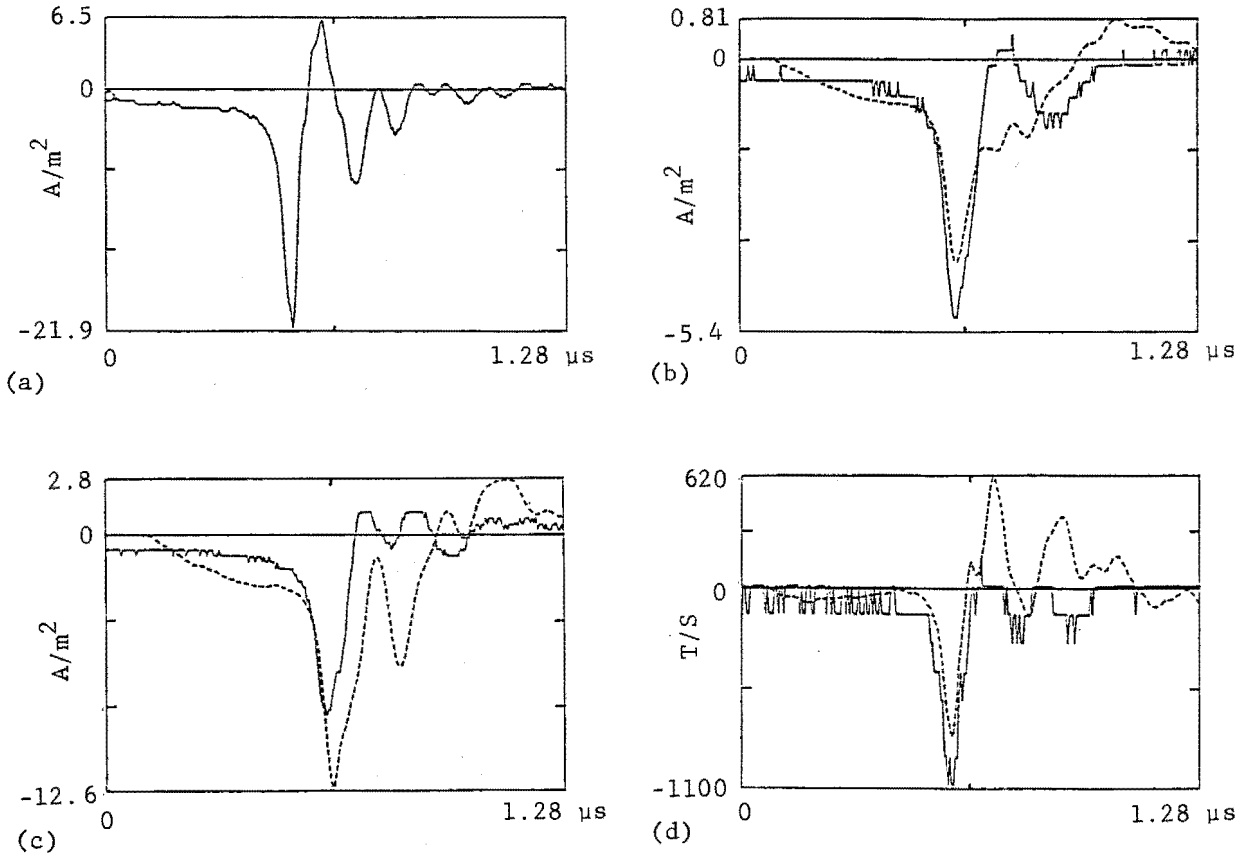

Fig. 10.34 Calculated and measured response of CV-580 to triggered lightning.
(a) Right wing D–dot sensor – calculated
(b) Right wing D–dot sensor – measured
(c) Left wing D–dot sensor – calculated
(d) Left wing D–dot sensor – measured

Measured - solid, Calculated - dotted

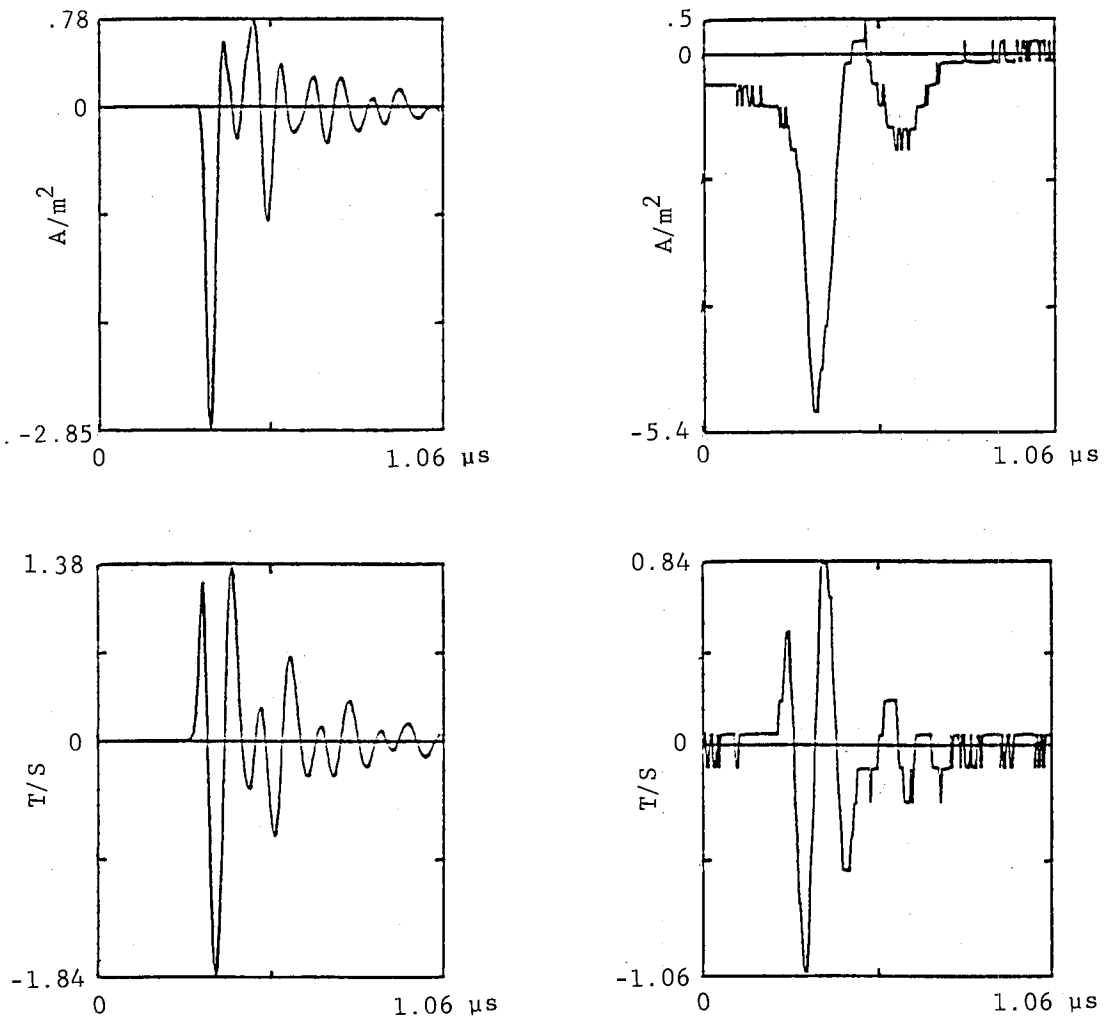

Fig. 10.35 Calculated and measured response of CV-580 to triggered lightning.
(a) Vertical stabilizer D–dot sensor – calculated
(b) Vertical stabilizer D–dot sensor – measured
(c) Forward fuselage B–dot sensor – calculated
(d) Forward fuselage B–dot sensor – measured

Influence of waveshape: The nature of the oscillation is also influenced by the shape of the incident wave. Fig. 10.39 shows the character of the waves for two different shapes of incident current, the geometry of the situation being shown on Fig. 10.39(a). There are two significant points about the figure; the first being that the input and output currents have different waveshapes and both are different from the current at the center of the second conductor. The second point is that the oscillation on the second conductor is more pronounced for the faster incident current. If the incident current had a sufficiently slow rise time the oscillations on the conductor would become insignificant. Although not illustrated, the nature of the oscillations is also influenced by the relative surge impedances of the conductors, the more nearly equal the impedances the less pronounced the oscillations.

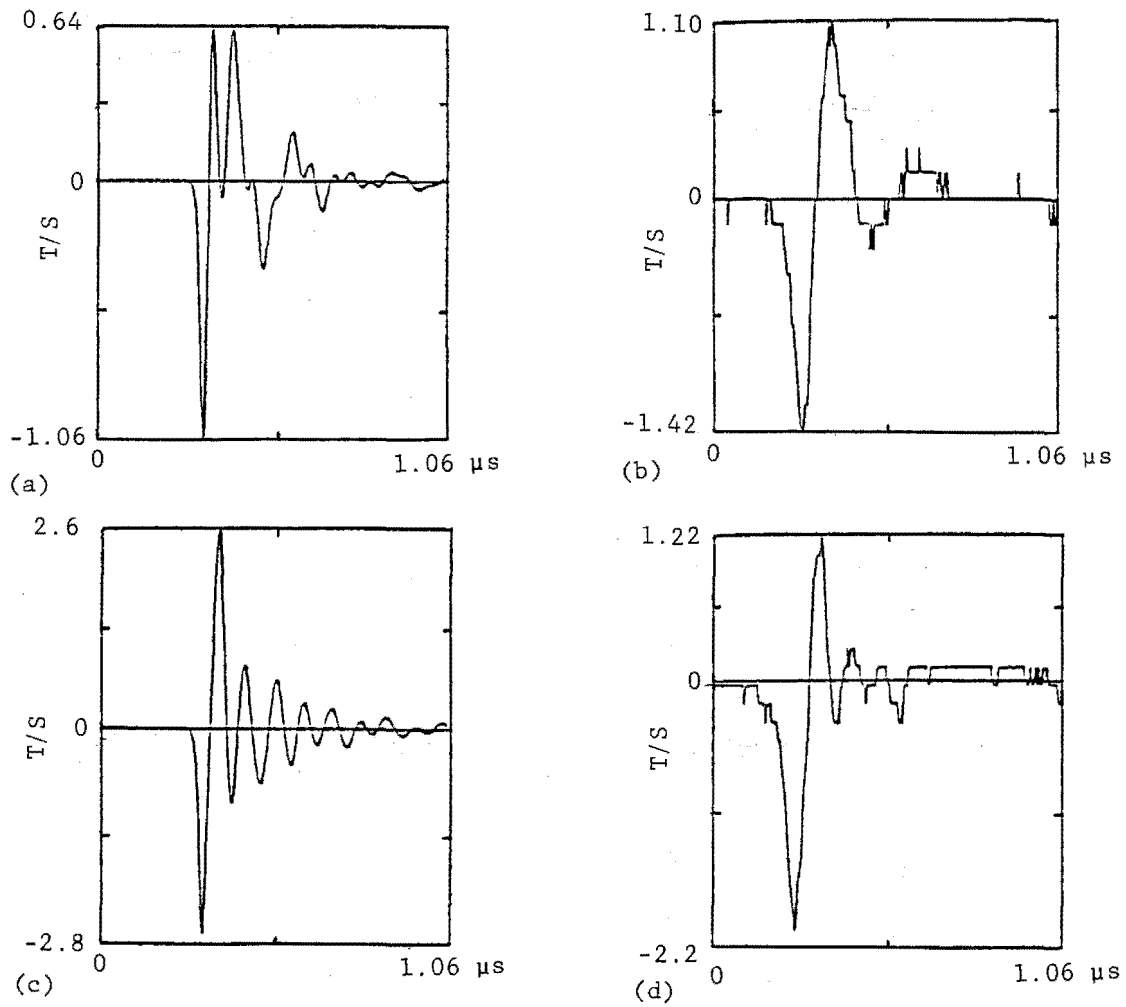

Fig. 10.36 Calculated and measured response of CV-580 to triggered lightning.
(a) Aft fuselage D–dot sensor – calculated
(b) Aft fuselage D–dot sensor – measured
(c) Right wing B–dot sensor – calculated
(d) Right wing B–dot sensor – measured

Lattice diagrams: The nature of the oscillations can be calculated graphically by the lattice diagrams described in the literature [10.57, 10.58] or by time domain computer routines capable of representing distributed constant transmission lines [10.59 and 10.60].

Oscillation modes on aircraft: Similar oscillations can be excited on aircraft, though the nature of the oscillations are more complex. One reason is that there are several modes of oscillation that can be excited, such as nose to tail and wing to wing. The modes are not independent of each other either. For example, a wave traveling nose to tail would have two components as shown on Fig. 10.40; one that propagated back and forth along the fuselage and one that crept along the wings. Speaking broadly though, the ringing frequencies will be given by the length of the path involved. An aircraft with a nose to tail length of 20 meters would have a ringing frequency about 5 Mhz. The actual ringing frequencies can be determined by test or can be calculated by the two and three dimensional time domain analytical techniques described in the preceeding sections.

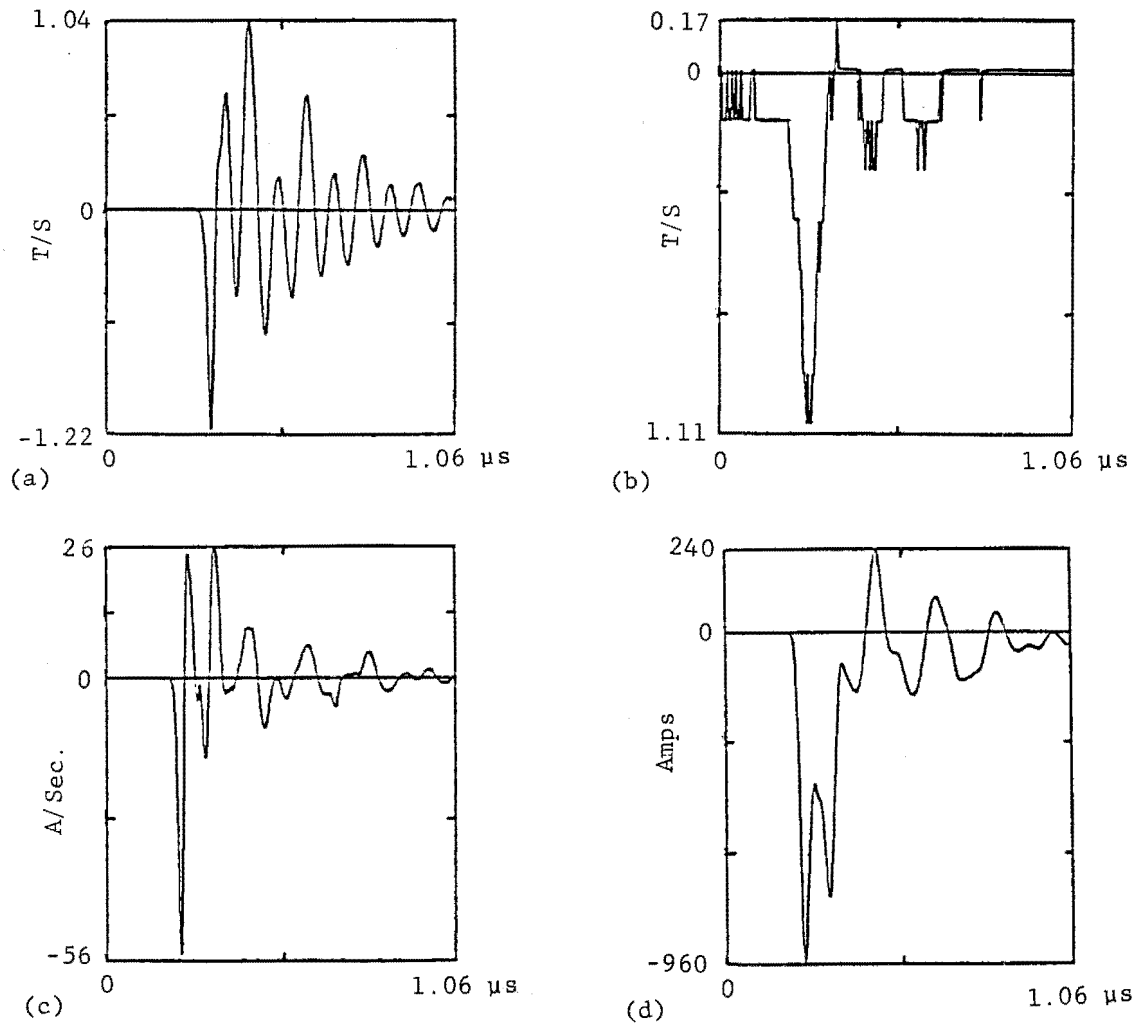

Fig. 10.37 Calculated and measured response of CV-580 to triggered lightning.
(a) Left wing B–dot sensor – calculated
(b) Left wing B–dot sensor – measured
(c) Right wing current – calculated
(d) Right wing rate of change of current – calculated

Significance of oscillations: Aircraft resonances are important in that they are one of the factors governing the ringing frequencies of the transients excited in aircraft wiring. If the aircraft ringing frequency happened to coincide with the ringing frequency of a wiring harness there would be the possibility of more efficient coupling of energy from the exterior of the aircraft to the internal wiring. The natural ringing frequency of the wiring harness, though is given more by the physical length of the harness than by the length of the aircraft. There is some correlation between the general nature of the aircraft ringing frequencies and the ringing frequencies of the transients typically induced on aircraft wiring; transients induced in small aircraft tend to ring at higher frequencies than do transients induced in large aircraft. Partly this would occur because wiring harnesses in small aircraft naturally tend to be shorter than wiring harnesses in large aircraft.

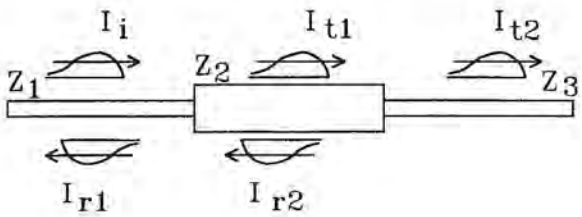

$$I_{t1} = I_1 \frac{2Z_2}{Z_1 + Z_2}$$

$$I_{r1} = I_1 \frac{Z_2 - Z_1}{Z_1 + Z_2}$$

$$I_{t2} = I_{t1} \frac{2Z_1}{Z_2 + Z_3}$$

$$I_{t1} = I_{t1} \frac{Z_3 - Z_2}{Z_2 + Z_3}$$

Fig. 10.38 Transmitted and reflected waves at a junction.

Resonances with NEMP: Considerable attention is given to aircraft resonance frequencies in NEMP studies, partly because of the fast risetime of EMP fields and also because the aircraft is isolated in space and the induced oscillations are damped only by resistance and by re–radiation from the aircraft.

Resonances with lightning: The nature and importance of aircraft oscillations is less clear in the case of lightning. Part of the reason is that the oscillations are damped by the attached conducting arc channel. Calculation of the effects is difficult because the impedance of the arc channel is not constant; it changes with time and with the amount of current flowing in the arc. An impedance of 3000 ohms, as used in Fig. 10.39 to illustrated traveling waves, might be representative of the period that a triggered lightning streamer is first developing from an aircraft, though perhaps not of the impedance of a fully developed lightning arc, as it would be during the passage of a return stroke current.

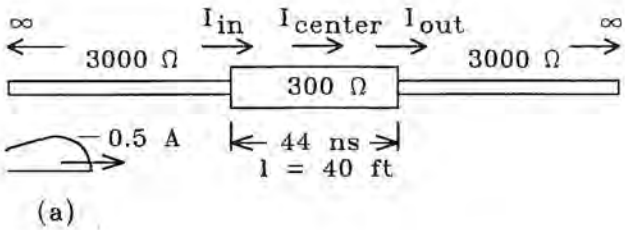

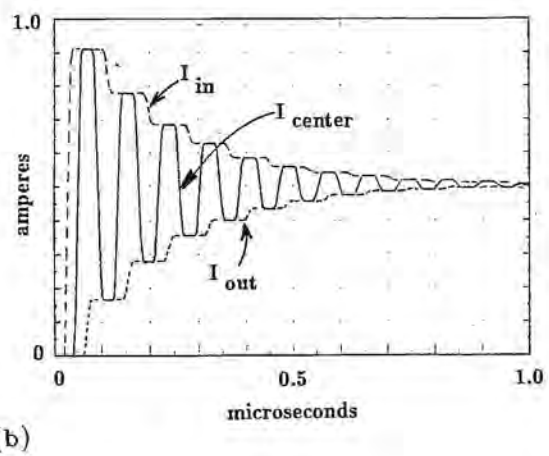

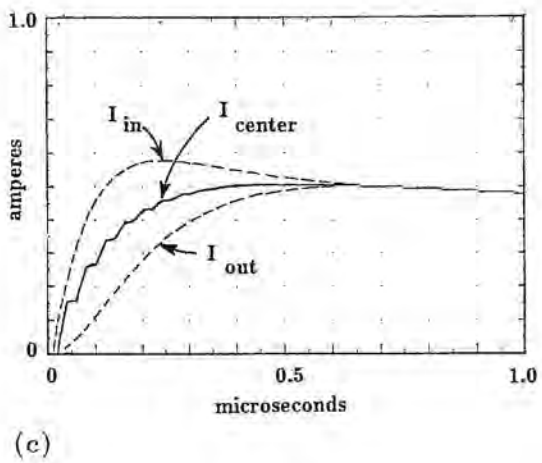

Fig. 10.39 Currents at various points on a conductor system.
(a) Geometry
(b) Waves excited by a 10 ns front time
(c) Waves excited by a 0.5 us front time

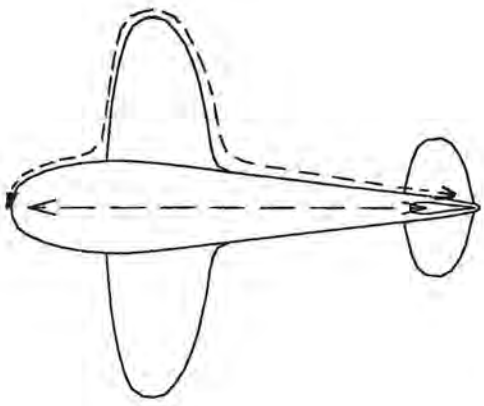

Fig. 10.40 Alternate paths for a nose–to–tail oscillation.

Significance of triggered lightning: Current pulses associated with the initial development of a triggered lightning flash are believed to have fast rise times. If so, and if the impedances shown on Fig. 10.39 are representive of the impedance of a developing lightning leader, then the oscillations shown might be representative of what would be produced by a triggered lightning flash.

In view of the uncertainties associated with the impedance of a lightning arc, it may be appropriate to view with caution calculations of the interaction of an aircraft with a lightning channel.

Resonances with LTA studies: One place where the oscillations associated with current waves traveling back and forth on an aircraft are important is during Lightning Transient Analysis (LTA) tests of an aircraft to determine, by measurement, the voltages induced on aircraft wiring. Interactions between the aircraft and the test circuit govern the waveshape of the current that can be injected into the aircraft. The oscillations are also such that the current on different portions of the aircraft may be different and also different from the current measured as being injected into the aircraft. The matter is discussed further in Chapter 13.

10.11 Composite Aircraft

The emphasis in the preceeding sections has been on metal aircraft which, as far as the external electromagnetic field distribution goes, can usually be accurately modeled as perfectly conducting. The distribution of current does change from an initial state governed by magnetic fields effect to a final distribution governed by resistance, but the time scale over which the redistribution takes place is long compared to the duration of lightning currents. The factors governing redistribution are discussed in more detail in Chapter 11. Some aircraft, however, can have significant amounts of carbon fiber composite (CFC) material, which are three orders of magnitude less conductive than aluminum. For structures which consist of a mixture of metal and composites, the redistribution takes place much more rapidly than on a metal aircraft and as a result the external current distribution and the internal coupling cannot be considered as distinct issues. Current penetrates to the interior of such aircraft on a time scale which is about the same as the duration of lightning currents. As a result, voltages coupled to internal circuits of CFC aircraft have higher magnitudes and have more of a resistive component than do voltages on metal aircraft.

The external current flow patterns and redistribution can be accounted for both in the simple 2D models discussed in §10.7.1 and in the more complex 3D models.

10.11.1 Implementation in 2D Cylindrical Models

Implementation of redistribution in the wire filament models discussed in §10.5.3 is rather straightforward. At sufficiently low frequencies, defined as occurring when the skin depth is on the order of the skin thickness, a filamentary model such as shown in Fig. 10.12 and 10.13 can account for the resistivity by inserting appropriate resistors in series with the inductors. The value of the resistor is that appropriate to the volume of the skin associated with each filament.

The resultant model would look like that of Fig. 10.13. Such circuits can be solved by a variety of network codes; examples being SPICE, SCEPTRE, ECAP and EMTP.

10.11.2 Implementation in 3D Models

Current redistribution can be included in both the finite difference time domain techniques and in the integral equation approaches.

The basic concepts of interest are the surface impedance, $Z_s(\omega)$ and the transfer impedance $Z_t(\omega)$. These are discussed in detail in Chapter 11.

The 3D time domain finite difference method requires a temporal representation. In Chapter 11, it is shown that $Z_s(\omega)$ becomes an infinite series of convolutions in the time domain. These can be implemented in the 3DFD code in a straightforward manner [10.26]. The number of terms required is not large and also decreases with time.

It is also possible to include $Z_s(\omega)$ in integral equation codes. For example, in a wire grid code, one can insert discrete equivalent impedances in the wires. These impedances are determined in such a way that the aggregate effect of the thin wire is to represent the actual surface impedance.

REFERENCES

10.1 V. Belevitch, "The Lateral Skin Effect in a Flat Conductor," *Philips Technical Review*, 32, 6/7/8/ (1971): 221-231.

10.2 H. Kaden, "Uber den Verlustwiderstand von Hochfrequenzleitern," (On the Resistance of High-Frequency Conductors), *Archiv fur Elektrotechnik*, 28 (1934): 818-25..

10.3 J. B. Scarborough, *Numerical Mathematical Analysis*, 6th ed.(Baltimore: Johns Hopkins University Press, 1966).

10.4 G. E. Forsythe and W. R. Wasow, *Finite–Difference Methods for Partial Differential Equations* (New York: John Wiley and Sons, 1960).

10.5 K. J. Maxwell, F. A. Fisher, J. A. Plumer, and P. R. Rogers, "Computer Programs for Prediction of Lightning Induced Voltages in Aircraft Electrical Circuits," *AFFDL-TR-75-36,Vol 1*, April 1975

10.6 F. A. Fisher, "Analysis and Calculations of Lightning Interactions with Aircraft Electrical Circuits," *AFFDL-TR-78-106*, August 1978

10.7 F. A. Fisher and J. A. Plumer, *Lightning Protection of Aircraft*, NASA Reference Publication # 1008, October 1977

10.8 F. J. Eriksen, T. H. Rudolph and R. A. Perala, "Atmospheric Electricity Hazards Analytical Model Development and Applications, Vol III, Electromagnetic Coupling Modeling of the Lightning/Aircraft Interaction Event," *EMA-81-R-21* and also *AFWAL-TR-81-3084*, August 1981.

10.9 R. A. Perala and R.J. Eriksen, "State-of-the-Art Methods for Computing the Electromagnetic Interaction of Lightning with Aircraft," presented and published in the *Proc. of the Lightning Technology Conf.* in Hampton VA, April 22-24, 1980. *NASA Conf. Publication 2128, FAA-RD-80-30, Lightning Technology.*

10.10 L. Licking, "Capacitance Analysis for Arbitrary Cylindrical Geometries: Application to Electromagnetic Coupling into Subsystems through Cables," *Sandia Laboratories, SC-RR-72 0299*, May 1972.

10.11 C. L. Thomas, "POTENT - A Package for the Computation of Electric and Magnetic Fields," *UKAEA Research Group, Culham Laboratory*, 1972.

10.12 C. L. Thomas, "POTENT - A Package for the Numerical Solution of Potential Problems in General Two Dimensional Regions," *UKAEA Research Group, CLM-P339*, Culham Laboratory, 1973.

10.13 B. J. C. Burrows, P. Pownall and C.A. Luther, "MTF (Aperture Flux) Effects in a Wing Model and the Development of 3D Prediction Techniques Based on POTENT (21D) Calculations," *Culham Lightning Studies Unit Memo No. 34*, December 1975.

10.14 B. J. Burroughs, "Electromagnetic Shielding Properties of Graphite Epoxy Panels to Lightning," *NADC-890237-20*, September 1980.

10.15 C. R. Paul, A. E. Feather, "Computation of the Transmission Line Inductance and Capacitance Matrices from the Generalized Capacitance Matrix," *IEEE Trans. on Electromagnetic Compatibility*, Vol. EMC-18, No. 4, November 1976.

10.16 J. C. Clements, C. R. Paul, and A. T. Adams, "Computation of the the Capacitance Matrix for Systems of Dielectric Coated Cylindrical Conductors," *IEEE Trans. on Electromagnetic Compatibility*, Vol. EMC-17, November 1975.

10.17 C. R. Paul, B. G. Melander, and D. H. Hall, "Lightning Current Redistribution," *Proceedings of the 1986 International Conference on Lightning and Static Electricity*, Dayton, Ohio, June 1986.

10.18 R. A. Perala and J. D. Robb, "The Experimental Verification of Circuit Modeling Techniques Used to Determine Lightning Current Distribution as Applied to the NASA Space Shutle Vehicle," *IEEE International Symposium on Electromagnetic Compatibility*, Seattle, WA. August 2-4, 1977.

10.19 T. H. McKenna, T. H. Rudolph, and R. A. Perala, "A Time Domain Representation of Surface and Transfer Impedances Useful for Analysis of Advanced Composite Aircraft," *Proceedings of the International Aerospace and Ground conference on Lightning and Static Electricity*, Orlando, FL. June 26-28, 1984.

10.20 R. A. Perala, T.H. Rudolph, and F. Eriksen, "Electromagnetic Interaction of Lightning with Aircraft," *IEEE Trans. on Electromagnetic Compatibility*, EMC-24, No. 2, May 1982.

10.21 R. F. Harrington, *Field Computation by Moment Methods*, New York, MacMillan, 1968.

10.22 R. F. Harrington, *Time Harmonic Electromagnetic Fields*, New York: McGraw Hill, 1961.

10.23 D. E. Merewether, and R. Fisher, "Finite Difference Solution of Maxwell's Equations for EMP Applications," *EMA-79-R-4*, April 22, 1980.

10.24 K. S. Yee, "Numerical Solution of Initial Boundary Value Problems Involving Maxwell's Equation in Isotropic Media," *IEEE Trans. Ant. & Propagat.*, AP-14, May 1966, pp. 302-307.

10.25 R. Holland, " THREDE: A Free–Field EMP Coupling and Scattering Code," *IEEE Trans. Nuc. Sci.*, Vol. NS-24, December 1977.

10.26 K. S.Kunz and K.M. Lee, "A Three–Dimensional Finite–Difference Solution of the External Re-

sponse of an Aircraft to a Complex Transient EM Environment: Part 1 - The Method and its Implementation," *IEEE Trans. on EMC*, Vol. EMC-20, No. 2, May 1978.

10.27 K. S. Kunz and K.M. Lee, "A Three–Dimensional Finite–Difference Solution of the External Response of an Aircraft to a Complex Transient EM Environment: Part II- Comparison of Predictions and Measurements," *IEEE Trans. on EMC*, Vol. EMC-20, No. 2, May 1978.

10.28 T. H. Rudolph and R. A. Perala, "Interpretation Methodolgy and Analysis of In–Flight Lightning Data," *EMA-82-R-21*, March 1982.

10.29 T. H. Rudolph and R.A. Perala, "Linear and Nonlinear Interpretation of the Direct Strike Lightning Response of the NASA F106B Thunderstorm Research Aircraft," *NASA Contractor Report 3746*, December 1983.

10.30 T. H. Rudolph and R. A. Perala, "Studies in Increasing the Probability that the NASA F-106B Thunderstorm Research Aircraft Will Be Struck by Lightning at Low Altitudes," *EMA-85-R-24*, February 1985.

10.31 T. H. Rudolph, R. A. Perala, P. M. McKenna and S. L. Parker, "Investigations Into the Triggered Lightning Response of the F106B Thunderstorm Research Aircraft," *NASA Contractor Report 3902*, June 1985.

10.32 P. H. Ng, T. H. Rudolph and R. A. Perala, "Linear and Nonlinear Interpretation of CV-580 Lightning Data," *EMA-86-R-36*, May 1986.

10.33 R. S. Collier, T. H. Rudolph, R. A. Perala, "Enhancement of the Low Altitude Lightning Strike Capture Cross Section for an In–flight Aircraft," *EMA-86-R-35*, July 1986.

10.34 T. H. Rudolph, R. A. Perala, C. C. Easterbrook and S. L. Parker, "Development and Application of Linear and Nonlinear Methods for Interpretation of Lightning strikes to In- -Flight Aircraft," *NASA Contractor Report 3974*, September 1986.

10.35 F. L. Pitts, G.B. Finelli, R.A. Perala and T.H. Rudolph, "F-106 Data Summary and Model Results Relative to Threat Criteria and Protection Design Analysis," *Proc. of the Int. Aerospace and Ground Conf. on Lightning and Static Electricity*, Dayton, Ohio, June 1986.

10.36 F. L. Pitts, L. D. Lee, R. A. Perala and T. H. Rudolph, "An Evaluation and Appraisal of the Direct Strike Lightning Threat to Aircraft: Estimation and Modeling of the Lightning/Aircraft Interaction Process," *Electromagnetics*, to be published.

10.37 C.C. Esterbrook, P.H. Ng, R.W. Haupt, R.A. Perala, and T. Rudolph, "Experimental and Analytic Studies of the Triggered Lightning Environment of the F106B," *EMA-87-R-37*, March 1987.

10.38 R. A. Perala and C.C. Esterbrook, "A Comparison of Lightning and Nuclear Electromagnetic Pulse Response of a Helicopter," presented at the *1984 Int. Conf. on Lightning and Static Electricity*, June 1984, and at the 1984 NEM Conf., July 1984.

10.39 R. A. Perala, T.H.Rudolph, P.M. McKenna and J.D. Robb, "The Use of a Distributed Peaking Capacitor and a Marx Generator for Increasing Rise–Rates and the Electric Field for Lightning Simulation," *Proc. of 9th Int. Aerospace and Ground Conf. on Lightning and Static Electricity, Orlando*, FL, 26-28 June 1984.

10.40 R. A. Perala, and J.D. Robb, "Measurements with Theoretical Analysis of a Full Scale NEMP Type Lightning Simulator for Aerospace Vehicles," published in the *1983 Proc, of the Int. Aerospace and Ground Conf. on Lightning and Static Electricity*.

10.41 W. L. Curtis, "Radar Cross Section of Arbitrarily Shaped Wires, *Boeing Company, Techn. Note 2-5453-30-55*, October 1967.

10.42 "Current and Charge Distributions on Aircraft," *Joint EMP Technical Meeting*, Kirtland AFB, September 1973.

10.43 D. F. Strawe, M. O'Byrne, and S. Sandberg, "Electromagnetic Coupling Analysis of a Learjet Aircraft," *Air Force Flight Dynamics Lab, AFFDL-TR-78-121*, Wright–Patterson AFB, OH, June 1978.

10.44 D. L. Sommer, "Atmospheric Electricity Hazards Balanced Protection Schemes," *AFWAL-TR-85-3053*, August 1984.

10.45 S. M. Rao, "Electromagnetic Scattering and Radiation of Arbitrarily Shaped Surfaces by Triangular Patch Modeling," *Ph.D. Thesis*, University of Mississippi, August 1980.

10.46 D. T. Auckland and J.A. Birken, "Electromagnetic Coupling Calculations on Three Triangular Patch Models of an F-14A Aircraft," *SRC TR81-1252,21* January 1982.

10.47 K. R. Siarkiewicz, "An Introduction to the General Electromagnetic Model for the Analysis of Complex Systems (GEMACS)," *RADC-TR-78-181*, September 1978, AD 060319.

10.48 K. R. Siarkiewicz, "EMACS - An Executive Summary," *Conference on Electromagnetic Compatibility*, 1985.

10.49 E. L. Coffey and J. L. Hebert, "Implementation of GEMACS for Lightning Interactions Analysis, presented at *Int. Aerospace & Ground Conf. on Lightning & Static Electricity*, Dayton, Ohio, 24-

26 June 1986.

10.50 G. J. Burke and A.J. Poggio, "Numerical Electromagnetic Code (NEC), Method of Meoments, Volume 1 - Program Description Theory," *Electromagnetic Pulse Interaction Note 363*, ed. by C.E. Baum, AFWL, Kirland AFB, NM, July 1977.

10.51 G. J. Burke, A.J. Poggio, J.C. Logan and J.W. Rockway, "Numerical Electromagnetic Code - A Program for Antenna System Analysis," *Third Symposium on Electromagnetic Compatibility*, Rotterdam, Holland, May 1979, p. 39.

10.52 G. J. Burke, A.J. Poggio, J.C. Logan and J.W. Rockway, "Numerical Electromagnetic Code (NEC), *Fourth Symposium on Electromagnetic Compatibility*, San Diego, CA October 1979, p. 46.

10.53 G. J. Burke and A.J. Poggio, "Numerical Electromagnetic Code (NEC) - Part 1, Part II, Part III," *Navelix Technical Document IL, ELEX 3041*, Naval Electronic Systems Command, San Diego, CA July 1977.

10.54 J. C. Logan, J. W. Rockway, "The Evolution of MININEC," *International Symposium on electromagnetic Compatibility*, IEEE 88CH2623-7, pp. 66-67.

10.55 P. L. Rustan and J.L. Hebert, "Lightning Measurements on an Aircraft Flying at Low Altitude," *Proc. of 2nd Int. Conf. on the Aviation Weather System, Montreal*, Canada, 19-21 June 1985.

10.56 J. S. Reazer and A.V. Serrano, "Spatial and Temporal Description of Strikes to the FAA CV-580 Aircraft," *Proc. of 1986 Int. Conf. on Lightning & Static Electricity*, Dayton, Ohio, June 1986.

10.57 P. L.Rustan and J.P. Moreau, "Aircraft lightning Attachment at Low Altitudes," *10th Int. Aerospace and Ground Conf. on Lightning and Static Electricity*, Paris, France, June 1985.

10.58 W. Radasky, "An Examination of the Adequacy of the Three Species Air Chemistry Treatment for the Prediction of Surface Burst EMP," *Defense Nuclear Agency, DNA 3880T*, December 1975.

10.59 L. V. Bewley, *Traveling Waves on Transmission Systems*, Dover, New York, 1963 or John Wiley and Sons, New York, 1933 and 1951, Chapter 4.

10.60 *Electrical Transmission and Distribution Reference Book*, Westinghouse Electric Corporation, East Pittsburg, Pa., 1950, Chapter 15.

10.61 H. W. Dommel, W. S. Meyer, "Computation of Electromagnetic Transients", *Proc. IEEE*, vol. 62, July 1974, pp. 983-993.

10.62 *Alternative Transients Program (ATP) Rule Book*, K. U. Lwuven EMTP Center, KARD. Mercierlaan 94, B-3030 Heverlee, Belgium or Tsuhuei Liu, 3179 Oak Tree Court, West Linn, Oregon, 97068

Chapter 11

THE INTERNAL FIELDS COUPLED BY DIFFUSION AND REDISTRIBUTION

11.1 Introduction

Lightning currents and electromagnetic fields on the outside of the aircraft couple to the inside through apertures and by the processes of diffusion and redistribution. Speaking in broad generalities, coupling through apertures, which is the subject of Chapter 12, is a high frequency mechanism, while coupling through diffusion and redistribution, the subjects of this chapter, are low frequency mechanisms. Diffusion refers to the process by which electric and magnetic fields penetrate through conducting materials. Redistribution refers to the process by which the overall pattern of current flow changes from an initial state where the distribution is controlled by magnetic fields to a final state where it is controlled by resistance. The factors that affect diffusion and redistribution on metal structures are the same factors that affect the electromagnetic shielding of such structures, though it might be better to say that diffusion and redistribution are the mechanisms by which electromagnetic shielding is obtained.

In the context of this document, diffusion primarily relates to the process by which electric fields build up on the inner surfaces of an aircraft in response to the external electric and magnetic fields produced by lightning. In the most elementary terms electric fields produced by diffusion can be thought of as those produced by passage of lightning current through the resistance of the aircraft, but a more thorough discussion can be made in terms of surface and transfer impedances, subjects that were introduced in Chapter 9.

Although these concepts apply to metal aircraft, they are especially significant for carbon fiber composite (CFC) aircraft; aircraft which are in reality a *mixture* of metal and CFC materials. This is because CFC materials have conductivities about three orders of magnitude less than that of aluminum. If lightning strikes such an aircraft, the early time (or high frequency) parts of the lightning current will distribute in the same manner as they would on an all metal aircraft. The late time (or low frequency) components, however, will distribute according to the resistance of the structural parts and there will be much more current on the inner structure of a CFC aircraft than there would be on a comparable all metal aircraft.

Another way of viewing the subject is that a CFC aircraft will be much less effective at providing electromagnetic shielding than an all metal aircraft. Magnetic field shielding that might be inherent to, and taken for granted, on an all metal aircraft may have to be intentionally provided on a CFC aircraft, usually with an unfavorable impact on program costs and weight.

In the sections that follow, internal and external electromagnetic fields are first discussed so as to differentiate somewhat between concepts used for lightning interactions and classical electromagnetic shielding problems. Concepts of circuit voltage are then discussed, first for a circular cylinder where only diffusion effects are encountered and then in terms of elliptical cylinders where redistribution effects must be considered. This portion will also include a discussion of the processes by which external current produces magnetic fields inside cavities, such as equipment bays. Redistribution effects are then illustrated for the more complex structures where recourse must be made to numerical analysis techniques.

11.2 Internal vs. External Fields

Fig. 11.1 shows a metal sheet which defines an interior volume. For these discussions the sheet can be considered either as flat and of infinite extent or closed and having a radius of curvature large compared to the thickness of the sheet. On the outside of the sheet an electromagnetic field is impressed, this being associated with a current flowing in the sheet. Some portion of the external electromagnetic field will penetrate through the sheet and couple to the interior volume defined by the sheet. Five regions important to the interaction problem can be defined: (a) the external region, (b) the external surface ($z = 0$), (c) the interior of the sheet, (d) the internal surface ($z = d$) and (e) the internal volume. Regions (a) and (b) are the main ones involved in the interaction between the sheet and any impinging electromagnetic field. Regions (b), (c) and (d) are involved in the way that the fields penetrate the sheet while regions d and e are involved in the way that fields build up in the interior volume.

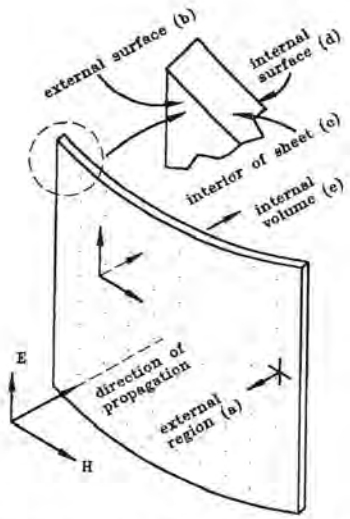

Fig. 11.1 A plane wave incident upon a shielding surface.

The penetration of fields to the interior is often discussed in terms of "shielding effectiveness", but there are two different ways that the external electromagnetic fields may be visualized. They can give rise to two very different measures of the "shielding effectiveness" of a structure.

11.2.1 Impinging Electromagnetic Field

In the most common treatment of electromagnetic shielding the field at the surface, region (b) above, is taken to be produced by some external source in region (a) that causes a field to propagate in a forward direction toward the surface. When the incident field arrives at the surface it is partially reflected and the reflected wave propagates back away from the surface. The sum of the incident and reflected waves, with proper regard for polarity, is what appears at the surface. If the sheet were a perfect conductor, the polarities of the incident and reflected waves would be such that the resultant magnetic field would be tangential to the surface and the resultant electric field would be normal to the surface.

The magnitude of the resultant field would depend on the shape of the conducting sheet and its orientation toward the incoming wave. With a flat conductor of infinite extent and oriented broadside to the incoming wave, the tangential magnetic field would be double that of the incoming field and the electric field would become zero. For other angles of incidence the magnetic field would be less than double and a radial electric field would be developed. For curved surfaces the fields that develop at the surface might be several times the magnitude of the incoming field.

Shielding effectiveness: For an impinging field, the "shielding effectiveness" is usually taken to be the ratio of the external impinging magnetic field to the internal magnetic field, expressed as

$$SE = 20 \log \left[\frac{H_e}{H_i} \right] \text{ dB.} \tag{11.1}$$

An effectiveness of shielding against electric fields could similarly be defined, though usually shielding against electric fields is an easier task than shielding against magnetic fields. The impinging magnetic or electric field is that which would exist in the absence of the sheet, and should not be confused with that which appears at the surface of the sheet.

The shielding effectiveness can be taken to have three components; one due to reflection at the surface, one due to transmission of the field through the sheet and one due to the way that the fields build up on the internal volume. As defined in Eq. 11.1, the "shielding effectiveness" is largely determined by how well the surface reflects the incident electromagnetic field.

11.2.2 Impinging Current

In many lightning interaction problems, however, the magnetic field at the surface is the result of injecting current into a structure and can be determined directly from the current density. The shielding effectiveness is best defined in terms of the magnetic field that appears at the surface.

$$SE = 20 \log \left[\frac{H_s}{H_i} \right] \text{ dB.} \tag{11.2}$$

This definition of shielding effectiveness treats only how the fields propagate through the sheet and how they couple to the interior volume. There will be an external field produced by the current, but any discussion of incident and reflected waves would be a roundabout way of determining the external field. Since the current is the independent variable which produces the external field there is no "surface reflection factor" to include in the shielding effectiveness. The result is that the "shielding effectiveness" has a lower value than in the case where the current is produced by an impinging field.

11.3 Diffusion Effects

The way that diffusion influences voltage on electrical circuits will first be illustrated for circular cylinders; partly because the effects are easiest to analyze and partly because cylindrical geometries are often encountered in lightning interaction problems.

11.3.1 DC Voltage on Circular Cylinders

Consider Fig. 11.2 in which a current, I, is entering a circular cylinder. The cylinder is considered long compared to other dimensions, so that there are no end effects, but short compared to the electrical wavelength of any of the frequency components of the current I. The return path for the current is not shown, but it is assumed to be sufficiently far away from the cylinder that there are no proximity effects. Also shown are two conductors, one external (1) and one internal (2) to the cylinder. These are connected to an end cap considered sufficiently massive that no electromagnetic fields penetrate the cap. At the other end of the cylinder are shown two voltages; V_1 measured from conductor 1 to the external surface of the cylinder, and V_2 measured from conductor 2 to the inner surface of the cylinder.

DC resistance: The cylinder will have a dc resistance

$$R = \frac{\rho \ell}{A} = \frac{\rho \ell}{2\pi r a}. \qquad (11.3)$$

where

ρ = resistivity
ℓ = length
A = cross sectional area
r = radius
a = thickness ($a \ll r$).

If the cylinder has the following dimensions and is made from aluminum of the indicated resistivity,

$\ell = 2$ m
$r = 15.7$ cm
$a = 0.381$ mm(0.015″)
$\rho = 2.69 \times 10^{-8}$ Ω·m

then the dc resistance, R, will be 1.43×10^{-4} ohms.

If the input current is 116 A (a value chosen because it was used in an experimental verification of the concepts), a voltage

$$e = IR = 116 \times 1.43 \times 10^{-4} = 0.0166\ V \qquad (11.4)$$

will be developed along the cylinder and this same voltage rise would be measured by a conductor external to the cylinder or by one internal to the cylinder.

Transient conditions: Until steady state conditions have been established, V_1 will not be equal to V_2, and neither of them will be equal to the steady state dc resistance voltage rise. Consider first voltage V_1, which can be considered as the line integral of potential (Chapter 9, §9.6.2) around the path $ABCD$ of Fig. 11.2. The voltage will have two components; a magnetically induced voltage due to the changing magnetic flux passing through the loop $ABCD$ and a voltage due to the surface impedance along the path CD. For dc, that surface impedance reduces to the dc resistance discussed above.

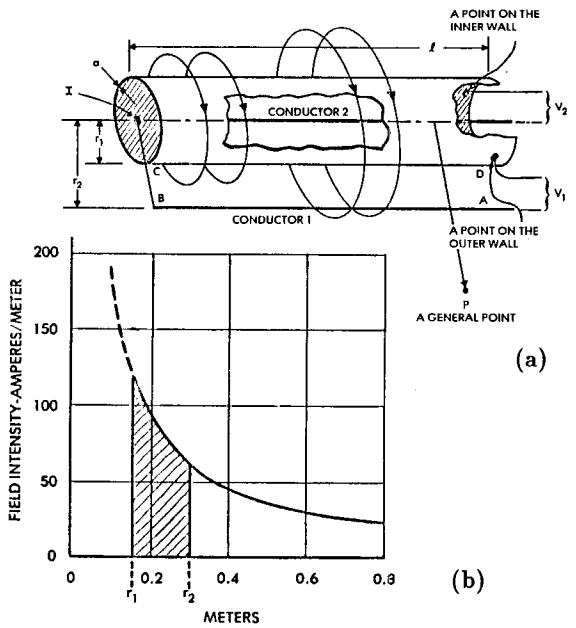

Fig. 11.2 Magnetic fields around a circular cylinder.
(a) Geometry
(b) Field intensity vs radius (for I = 116 A)

11.3.2 External Voltage on Circular Cylinders

External to the cylinder the flow of current sets up a magnetic field of intensity

$$H = \frac{I}{2\pi r} \qquad (11.5)$$

where

I = current
r = radius
H = field strength,

having a pattern as shown in Fig. 11.2(b). The magnetically induced component of V_1 will then be:

$$V_1 = \frac{d\phi}{dt} = \mu_o H \ell \log\left(\frac{r_2}{r_1}\right) \frac{dI}{dt}. \qquad (11.6)$$

while ϕ, the flux passing through the loop $ABCD$, is represented by the shaded area of Fig. 11.2(b). The flux, ϕ, would be measured in webers. Remembering that

$$\mu_o = 4\pi \times 10^{-7} \quad \text{A/m}, \tag{11.7}$$

V_1 becomes

$$V_1 = 2 \times 10^{-7} \ell \log \left(\frac{r_2}{r_1} \right) \frac{di}{dt}. \tag{11.8}$$

If r_2 is 31.4 cm and the indicated current of 116 A in Fig. 11.3 reaches crest in an equivalent time of 0.25 μs, V_1 will then reach an initial voltage of 129 V. As steady state conditions are reached and the external magnetic field ceases to change with time, V_1 will decay to its steady state value of 0.0166 V.

Influence of skin effect: This analysis ignores the skin effect, a phenomenon that causes the surface impedance to be higher for alternating currents or transients than it is for dc. Surface impedance will be discussed further in §11.3.4, but for external circuits the increased resistance resulting from skin effect will be of little consequence compared to the much larger voltage induced by the changing magnetic field.

Example of external conductors: While conductors external to a current carrying cylinder, such as an aircraft fuselage, are not common, they are not unknown. An example might be the cables on a missile or rocket that run between a control assembly in the nose and the engine controls at the tail. Of necessity, such cables must run, as shown in Fig. 11.4, external to the fuel and oxidizer tanks. If the cables are not in a shielded cable tunnel, they will be exposed to the external magnetic field.

Simplified expression: If the spacing between the wires and the surfaces of the vehicle is not large, Eq. 11.8 may be somewhat simplified, since the magnetic flux density does not vary greatly with distance away from the surface of the vehicle and may be considered uniform.

$$V_1 = \frac{2 \times 10^{-7} \ell d}{r} \cdot \frac{di}{dt}. \tag{11.9}$$

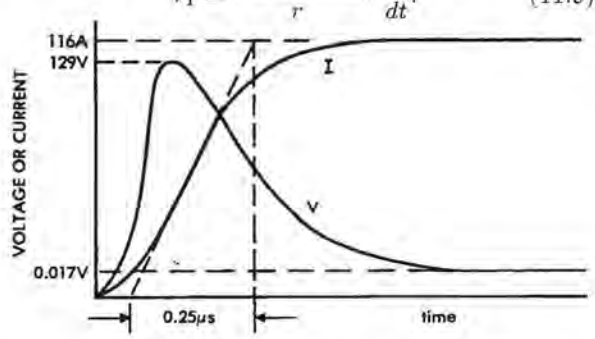

Fig. 11.3 External voltage (not to scale).

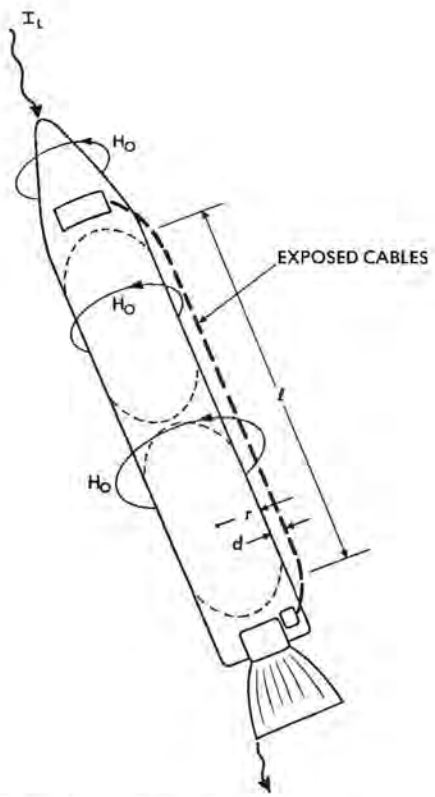

Fig. 11.4 Exposed cable antennas.

11.3.3 Internal Voltage on Circular Cylinders

Let us now consider the conditions internal to the cylinder. As with the external voltage, the voltage V_2 of Fig. 11.5 can be defined as the line integral of potential around a complete path; the path ABCD being the most appropriate. The voltage will again have two components, one due to the changing magnetic field passing through the loop $ABCD$ and one due to the flow of current around that path. Conditions inside the cylinder, however, will be very different from those on the outside.

First of all, the magnetic field internal to the inner surface of the cylinder will be zero, as explained in Chapter 9, §9.7.2. If there is no magnetic field, there will be no magnetically induced voltage. Any voltage will be due to the flow of current through the resistance of the various portions of the circuit. There will be no voltage along the path BC since we have assumed a perfect conductor for the end cap and there will be no resistive voltage along the path CD since we have assumed an open circuit between points A and D, which implies no current along CD. Any voltage must be due to the resistive rise along the path AB.

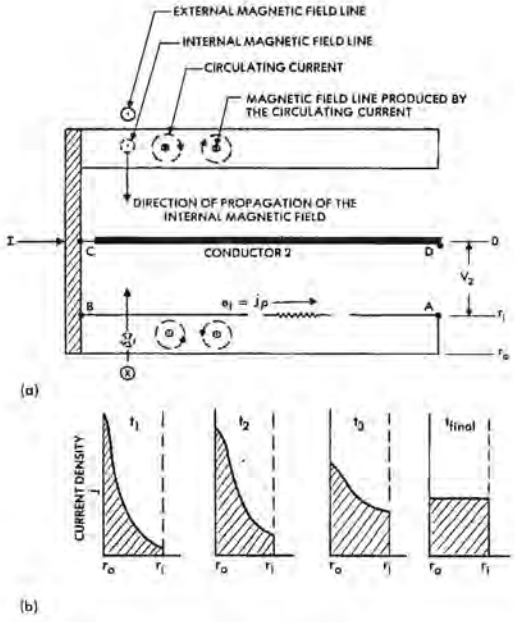

Fig. 11.5 Factors governing the internal voltage.
(a) Geometry and decaying eddy currents
(b) Current density at different times

Cause of skin effect: The voltage rise along the internal path AB of Fig. 11.5 will be completely different from the voltage rise along the path CD of Fig. 11.2. This is because the phenomenon of skin effect delays the buildup of current on the inner surface of the cylinder. The origin of the skin effect phenomenon is shown in Fig. 11.5. If a magnetic field line is assumed to be suddenly established internal to the wall of the conducting cylinder, there will be induced eddy currents circulating around that field line. These eddy currents will induce a magnetic field of their own of polarity opposite to that set up by the external magnetic field. Only as the eddy currents decay will the magnetic field penetrate the wall of the cylinder.

Further analysis of the resistively generated voltages requires a discussion of surface and transfer impedances.

11.3.4 Surface and Transfer Impedances

The surface impedance Z_s, is the ratio of the electric field on the external surface to the current density on the external surface, while the transfer impedance, Z_t, is the ratio of the electric field on the internal surface to the current density on the external surface. Formulations can be given in either the frequency or the time domain.

Frequency domain formulation: Exact expressions for surface and transfer impedance of a flat sheet were given in Chapter 9, but for most all cases of practical interest simplified expressions [11.3] are sufficiently accurate.

$$Z_s(\omega) = \frac{jk_m}{\sigma}\coth(jk_m d) \tag{11.10}$$

$$Z_t(\omega) = \frac{k_m/\sigma}{\sin(k_m d)} \tag{11.11}$$

where

$$k_m \approx \frac{1}{\sqrt{2}}(1-j)(\omega\mu_2\sigma)^{1/2} \tag{11.12}$$

and

d = thickness
σ = conductivity.

While Eqs. 11.10 and 11.11 can be readily evaluated in the frequency domain, it is sometimes helpful to use series formulations. This can be done by expressing the $\coth(x)$ and $\sin(x)$ functions by their series expansions.

$$\coth(x) = \frac{1}{x} + \sum_{n=1}^{\infty}\frac{1}{(n\pi)^2 + x^2} \tag{11.13}$$

$$\sin(x) = x\prod_{n=1}^{\infty}\left(1 - \frac{x^2}{n^2\pi^2}\right). \tag{11.14}$$

Substituting these expressions into Eqs. 11.10 and 11.11 gives

$$Z_s(\omega) = \frac{1}{\sigma d} + j\omega\left(\frac{2}{\sigma d}\right)\sum_{n=1}^{\infty}\frac{1}{\omega_n + j\omega} \tag{11.15}$$

$$Z_t(\omega) = \frac{2}{\sigma d}\sum_{n=1}^{\infty}\frac{(-1)^{n+1}}{(1 + j\omega/\omega_n)} \tag{11.16}$$

where

$$\omega_n = \left(\frac{n\pi}{d}\right)^2\frac{1}{\mu\sigma}. \tag{11.17}$$

These formulations [11.1] are applicable to flat sheets or to sheets having a radius of curvature large compared to the thickness of the sheet. For conditions where this is not so, applicable formulas are given in Chapter 9.

Variation with frequency: Figs. 11.6(a) and 11.6(b) show how these impedances vary with frequency. Fig. 11.6(a) relates to a carbon fiber composite (CFC) sheet 0.25 inches (6.35 mm) thick and having a resistivity 5×10^{-5} ohm-meters, a resistivity typical of CFC materials, while Fig. 11.6(b) relates to an aluminum sheet 0.05 inches (1.27 mm) thick and having a resistivity of ($\rho = 2.69 \times 10^{-8}$ ohm-meters)

Inspection of the equations and the figures show that at low frequencies both impedances reduce to a dc value

$$Z_s = Z_t = \frac{1}{\sigma d}. \tag{11.18}$$

This low frequency or dc value has the units of ohms, but is generally specified as "ohms per square", that is, the impedance between opposite sides of a square of any size.

At higher frequencies the surface impedance rises and the transfer resistance falls. In the limit, the surface impedance approaches the value

$$Z_s = \sqrt{\frac{j\omega\mu}{\sigma}}, \tag{11.19}$$

An alternative formulation is

$$Z_s = \frac{1+j}{\sigma\delta} \tag{11.20}$$

where the δ is the skin depth as defined in §9.4.5 by Eqs. 9.22 and 9.23.

The surface impedance thus approaches the intrinsic impedance of the material, has equal resistive and reactive components and has a magnitude that varies as the square root of frequency. The phenomenon is frequently referred to as the "skin effect."

Time domain formulation: $Z_s(\omega)$ and $Z_t(\omega)$ are defined in Eqs. 11.15 and 11.16 by the poles, ω_n, given by Eq. 11.17. The first order pole, given by

$$\omega_1 = \left(\frac{\pi}{d}\right)^2 \frac{1}{\mu\sigma}, \tag{11.21}$$

is used to define the diffusion or penetration time constant, τ, according to

$$\tau = \frac{1}{\omega_1} = \mu\sigma\left(\frac{d}{\pi}\right)^2. \tag{11.22}$$

The penetration time constant can also be given as

$$\tau = \frac{L}{\pi^2 R} \tag{11.23}$$

where R is the resistance of the surface and L is the internal inductance.

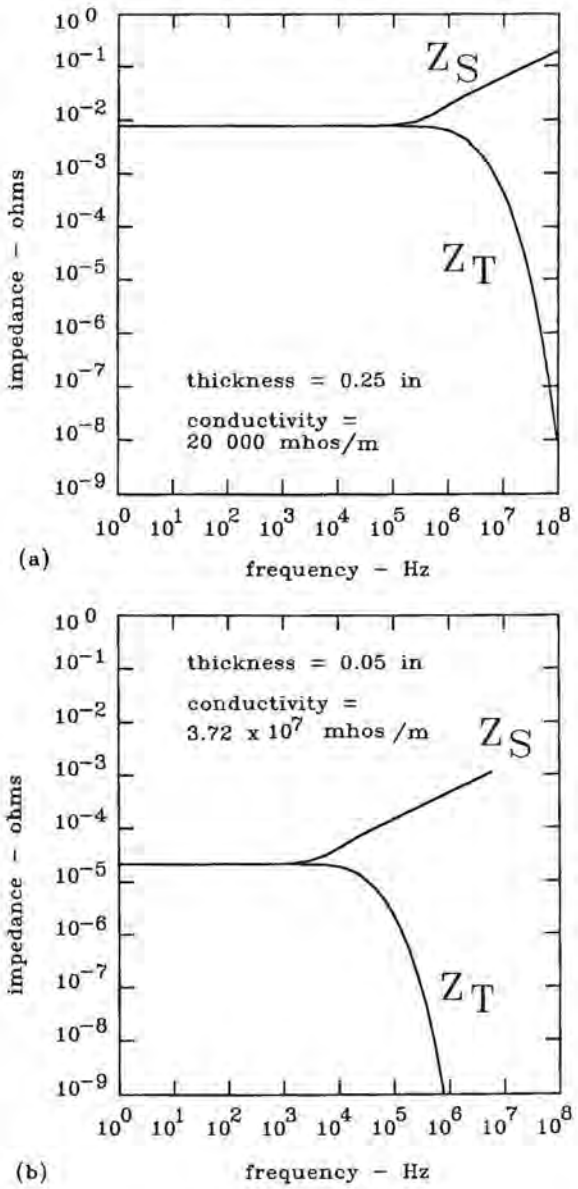

Fig. 11.6 Frequency dependence of surface and transfer impedance.
(a) CFC sheet
(b) Aluminum sheet

In response to a step function of injected current, I, the current density J at any point x in the sheet can then be given as [11.2]:

$$J(x) = I\left[1 + 2\sum_{n=1}^{\infty}(-1)^n\left(e^{n^2 t/\tau}\right)\cos\left(n\pi\frac{x}{d}\right)\right] \tag{11.24}$$

In Eq. 11.24 $x = 0$ at the inner surface and $x = d$ at the surface where current is injected. The current density at the surface where current is injected is given by evaluating Eq. 11.24 at $x = d$.

$$J_s = \sigma I\left[1+2\left(\epsilon^{-t/\tau}+\epsilon^{-4t/\tau}+\epsilon^{-9t/\tau}+\epsilon^{-16t/\tau}+\cdots\right)\right. \tag{11.25}$$

The current density at the other surface is given by evaluating Eq. 11.24 at $x = 0$.

$$Z_t(t) = \sigma I\left[1-2\left(\epsilon^{-t/\tau}-\epsilon^{-4t/\tau}-\epsilon^{-9t/\tau}-\epsilon^{-16t/\tau}-\cdots\right)\right] \tag{11.26}$$

In response to a step function applied current the current density along the inner surface builds up as shown on Fig. 11.7 and produces an incremental voltage which is the product of the current density and the resistivity of the surface. The voltage along the path AB is then given by integrating the incremental voltages. Since the voltage along the path AB is the only component of voltage V_1, it follows that V_1 will rise to the dc resistance following a path as shown on Fig. 11.7.

11.3.5 Characteristic Diffusion Response

This response curve is called a *diffusion-type response* and is characteristic of many types of situations involving the transmission on energy through a distributed medium. An example would be the transfer of heat into a block if a heat flux were suddenly applied to one face of the block. Another would be the transmission of electrical energy through an R/C or L/R ladder network. Fig. 11.8 shows examples, with Fig. 11.8(b) often being used as the best illustrative example of the phenomenon of skin effect.

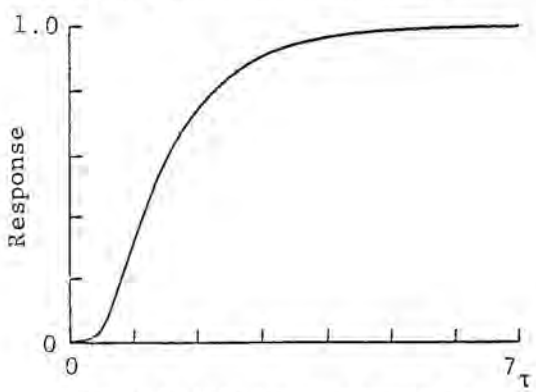

Fig. 11.7 Diffusion-type response to a step function.

Waveshape: Two important observations might be made about the shape of the response curve shown on Fig. 11.7. The first is that the response initially changes only slowly and thus has a zero first derivative, unlike a simple exponential response, which has a finite first derivative. The second is that the response approaches its final value much more slowly than does a simple exponential response. In three time constants (as defined by Eq. 11.23) the response has reached 90% of its final value, but the rise to the 99% point takes nearly 20 time constants. In contrast, an exponential response reaches 95% of its final value in three constants and reaches 99% in 4.65 time constants.

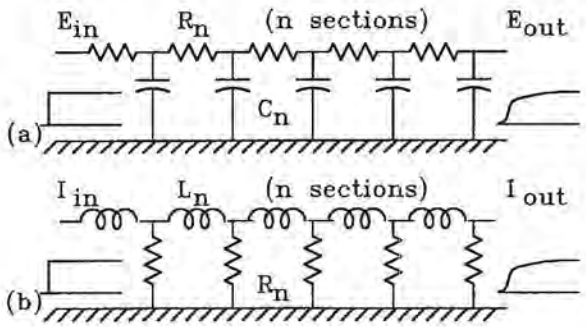

Fig. 11.8 Ladder networks displaying a diffusion-type response.
(a) R/C network
(b) L/R network

Influence of material: With respect to Eq. 11.22, it should be noted that the penetration time constant is directly proportional to the permeability of the material, inversely proportional to the resistivity of the material and directly proportional to the square of the thickness of the material. The relative permeability of structural materials used in aircraft is always very nearly unity, but thickness and resistivity can vary over wide ranges.

For reference, Eq. 11.21 is shown plotted in Fig. 11.9 as a function of material thickness and resistivity of the material. The resistivities of some typical metals were shown in §9.4.3. As an example, if we assume an aluminum alloy with a resistivity of 2.69×10^{-8} ohm-meters (twice that of copper) and a skin thickness of 1.016 mm (0.040 inches), the penetration time constant would be 3.9 μs. If a step function of current were established on the outside of such metal, it would take 11.7 μs for the current density on the other side to reach 90% of its final value. If the duration of the injected current pulse were short compared to 11.7 μs, the response would never reach the full IR voltage.

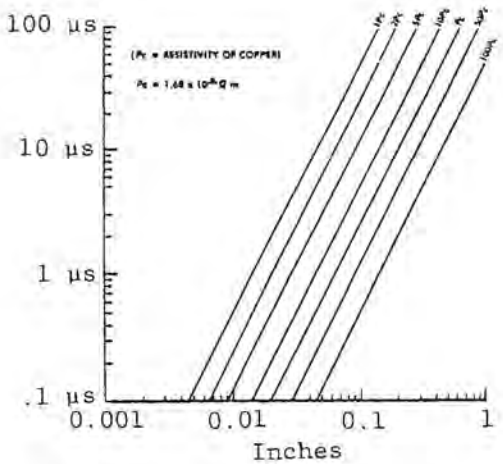

Fig. 11.9 Skin thickness vs penetration time constant.

Response to other waveforms: The response to other waveforms can be obtained by application of the convolution, or superposition, integral:

$$[f(t, I(t), \tau] = \frac{d}{dt}\int_0^t E(t-\tau)I(t)d\tau. \qquad (11.27)$$

Graphically, the elements of Eq. 11.27 are shown in Fig. 11.10. Just as an arbitrary waveform can be considered as the summation of a series of elementary step functions, the response to that arbitrary waveform can be considered as the summation of a series of step function responses. The process is described in many textbooks on circuit theory, such as [11.3]. The process, along with a computer routine for handling numerical data, was also described in [11.4]. Convolution assumes linear conditions, such as would prevail, for all practical purposes, in metals. CFC materials *might* be sufficiently nonlinear as to render convolution calculations suspect.

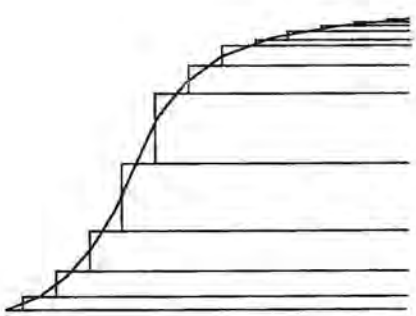

Fig. 11.10 A wave approximated as a superposition of step functions.

Equivalent circuits: The L/R network of Fig. 11.8(b) is a valuable way of representing diffusion effects because it can be directly solved with a variety of network analysis computer programs, most of which allow for driving functions other than step functions. The internal inductance of the surface is represented by n incremental inductors in series while the dc resistance is represented by $n+1$ incremental resistors in parallel.

As an example, consider the 2 meter long circular cylinder treated in §11.3.2. The exact internal inductance of such a cylinder is

$$L_i = \frac{\mu}{2\pi}\log\left[\frac{r_o}{r_i}\right] \text{ henries.} \qquad (11.28)$$

or, for non-magnetic materials such as aluminum

$$L_i = 2 \times 10^{-7}\log\left[\frac{r_o}{r_i}\right] \text{ henries.} \qquad (11.29)$$

An approximate expression applicable to thin tubes is

$$L_i = \frac{\mu l d}{2\pi r}. \qquad (11.30)$$

For a flat sheet of 1 meter width, length l and thickness d, the internal inductance would be simply

$$L_i = \mu l d. \qquad (11.31)$$

Using the dimensions given earlier, $r_i = 0.157$ m and $r_o = 0.157 + 0.000381$ m, $L_i = 9.695 \times 10^{-10}$ henries.

An equivalent circuit can be obtained by dividing this inductance into four equal parts, each 2.424×10^{-10} henries, as noted on Fig. 11.11. The incremental resistance on the figure is the 1.43×10^{-4} ohms calculated in §11.3.1 and divided into five sections.

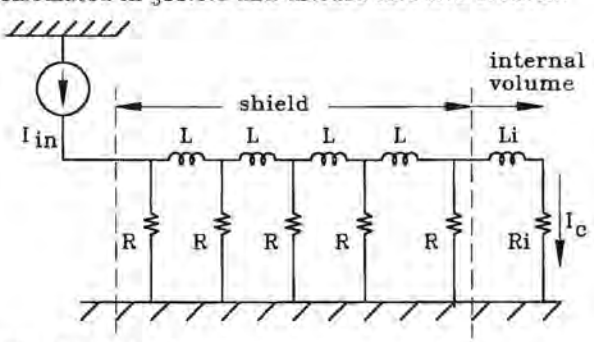

Fig. 11.11 Equivalent circuit representing propagation through a shield.
$L = 9.695 \times 10^{-4}$ Hy
$R = 2.860 \times 10^{-5}$ ohm
$L_i = 1 \times 10^{-6}$ Hy
$R_i = 1 \times 10^{-3}$ ohm

The response of the tube to two different waveshapes is shown on Fig. 11.12. The figure shows how the waveshape of the internal response may be almost independent of the waveshape of the external driving current, a situation that will occur if the duration of the external current is short compared to the pulse penetration time. The amplitude of the internal response will depend on the external driving current, but only on its impulse strength, or time integral.

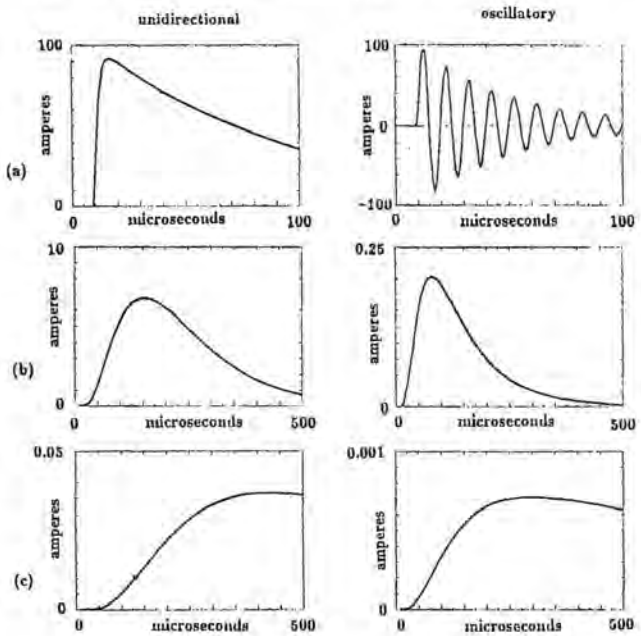

Fig. 11.12 Internal and external waveshapes.
(a) Input current – I_{in}
(b) Current on inner face – I_i
(c) Cavity current – I_c

Internal cavity impedance: The equivalent circuit can be extended by incorporating the internal impedance, R_i and L_i of the volume bounded by the shielding surface. In general, the internal impedance bounded by the surface will be dominated by the internal inductance, which leads to the observation that the internal current will be

$$I_i = \frac{1}{L_i} \int E_i \, dt. \tag{11.32}$$

The magnetic field will have the same shape as that predicted by Eq. 11.32, which is to say that the derivative of the internal magnetic field will have essentially the same shape as the voltage E_i shown on Fig. 11.12.

The question of internal impedance of cavities is discussed further in §11.7.

11.3.6 Plane Conducting Sheets

Thus far, attention has been focused on uniform current flow on plane sheets or on a circular cylinder. One might reasonably ask whether or not the concepts which have been discussed also apply to situations where the current flow is not uniform.

Such a situation is illustrated in Fig. 11.13, which shows a current entering a plane sheet of thickness d and homogeneous isotropic conductivity σ. This situation is of considerable practical importance, examples including a direct lightning strike on an aircraft fuel tank, to the conductive case of a rocket motor, or to an aircraft skin with internal nearby cables. The question of interest is the internal electric fields, perhaps to evaluate the possibility of fuel ignition or to evaluate the coupling to cables.

There are some significant differences between the situation of Fig. 11.13 and the previous examples, such as Fig. 11.1 (plane wave normally incident on a plane sheet) or Fig. 11.2 (uniform current flow on a cylinder). First, for Fig. 11.13, the current density is not uniform, in that the magnetic field on the outer surface of the sheet is given by

$$H = \frac{I}{2\pi r}. \tag{11.33}$$

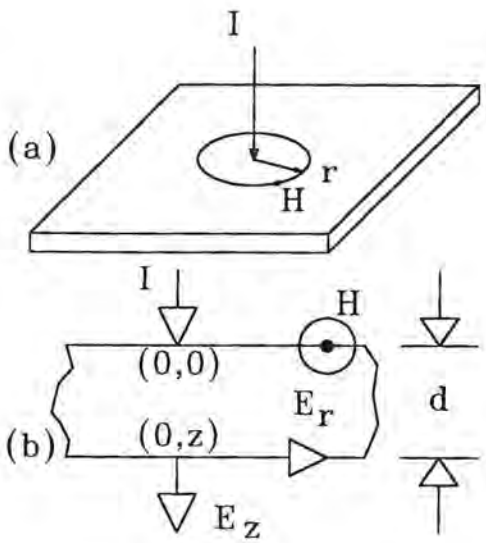

Fig. 11.13 Lightning strike to a plane conducting sheet.
(a) Oblique view
(b) 2DFD model used for the solution

The field lines would be circles centered around the injected current. The current density J would have the same amplitude as the field intensity, but the flow lines would be directed radially away from the point where the current was injected.

Second, there is a special concern about how to apply the concept of transfer impedance near the origin of Fig. 11.13(b). If diffusion effects are not considered, the radial voltage gradient E_r would be

$$E_r = \frac{I}{2\pi r} \cdot \frac{1}{\sigma d}, \tag{11.34}$$

which has a singularity at $r = 0$ where Eq. 11.25 would predict the current density to become infinite if the injected current were a step function. Physically this will not happen because the sheet has a finite thickness and because the current has a finite front time. Current spreads away from the injected point and the current density never becomes infinite. Still, the transfer impedance as defined in Eq. 11.11 cannot apply at or very near $r = 0$.

Unfortunately, the three dimensional problem in Fig. 11.13 does not have a known analytic solution and results cannot be expressed in a closed form. Numerical means must be employed.

2DFD numerical solution: A method that can be used to solve this problem is the two dimensional finite difference (2DFD) solution of Maxwell's equations, which has been mentioned in Chapter 10. The quantities used when solving the problem of Fig. 11.13 were:

- lightning channel radius a - 0.00635 m
- radial cell size - 0.0127 m
- axial cell size - 0.002 m
- time step - 2.0 $\times$ 10^{-11} sec.
- radial boundary at r - 0.3048 m
- axial boundary at z - 0.5232 m.

The lightning current waveform was assumed to be the modified step function shown in Fig. 11.14. Results are presented in Fig. 11.15 for two values of conductivity, $\sigma = 10^4$ mho/m and $\sigma = 10^3$ mho/m.

There are several interesting and significant features about Fig. 11.15. First of all, there is a signif-

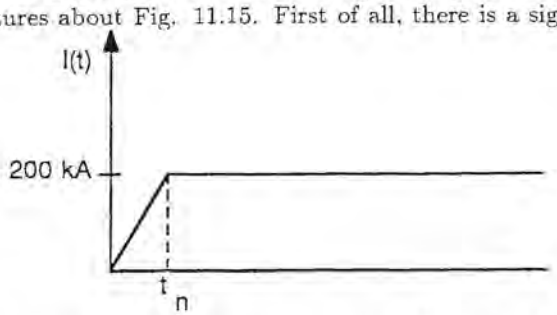

Fig. 11.14 Lightning current source for Fig. 11.13.

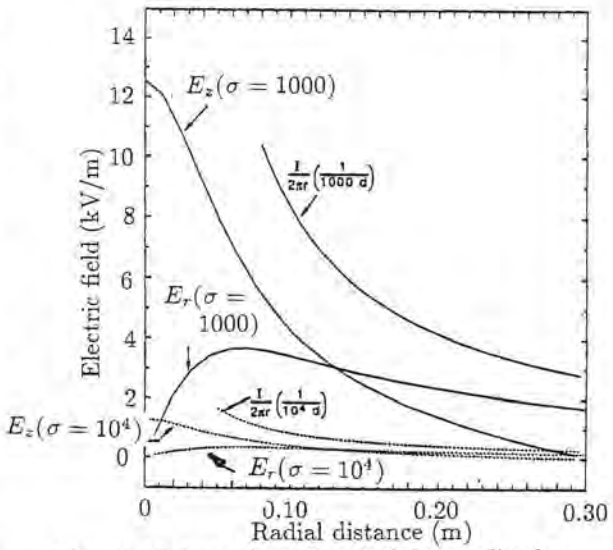

Fig. 11.15 Late time electric field amplitudes for Fig. 11.13.

icant normal electric field at $r = 0$, which decreases with increasing r. Its value, which is larger than the largest radial field, is not predicted by the uniform current flow assumptions implicit in Eqs. 11.11 or 11.16.

Second, there is a near zone effect with regard to the tangential electric field E_r near the origin. The radial field at the reverse side of the sheet is not highest at $r = 0$. Instead it is zero at $r = 0$ and increases to a maximum at some distance away, depending upon conductivity. Also, the radial field has a magnitude lower than predicted by Eq. 11.33, which is to say that the current density on the reverse side of the sheet is lower than it would be if diffusion effects were not operating. At late times and sufficiently far from the strike point the radial voltage gradient will be given by Eq. 11.33 and that distance can be taken as the end of the near field zone.

It should be noted that these curves scale directly with the conductivity σ, but not with the thickness d.

Although the time domain waveshapes are not shown here, they do have the diffusion waveshape shown on Fig. 11.7.

11.4 Redistribution

In many cases, analysis of lightning interactions must account for the phenomenon of redistribution, the process by which the division of current changes from an initial state governed mostly by inductive effects to one governed by resistive effects. An elementary example of redistribution can be illustrated by the RL circuit of Fig. 11.16, which also shows the waveform of the current in each of the two branches. A current pulse of short duration entering the network

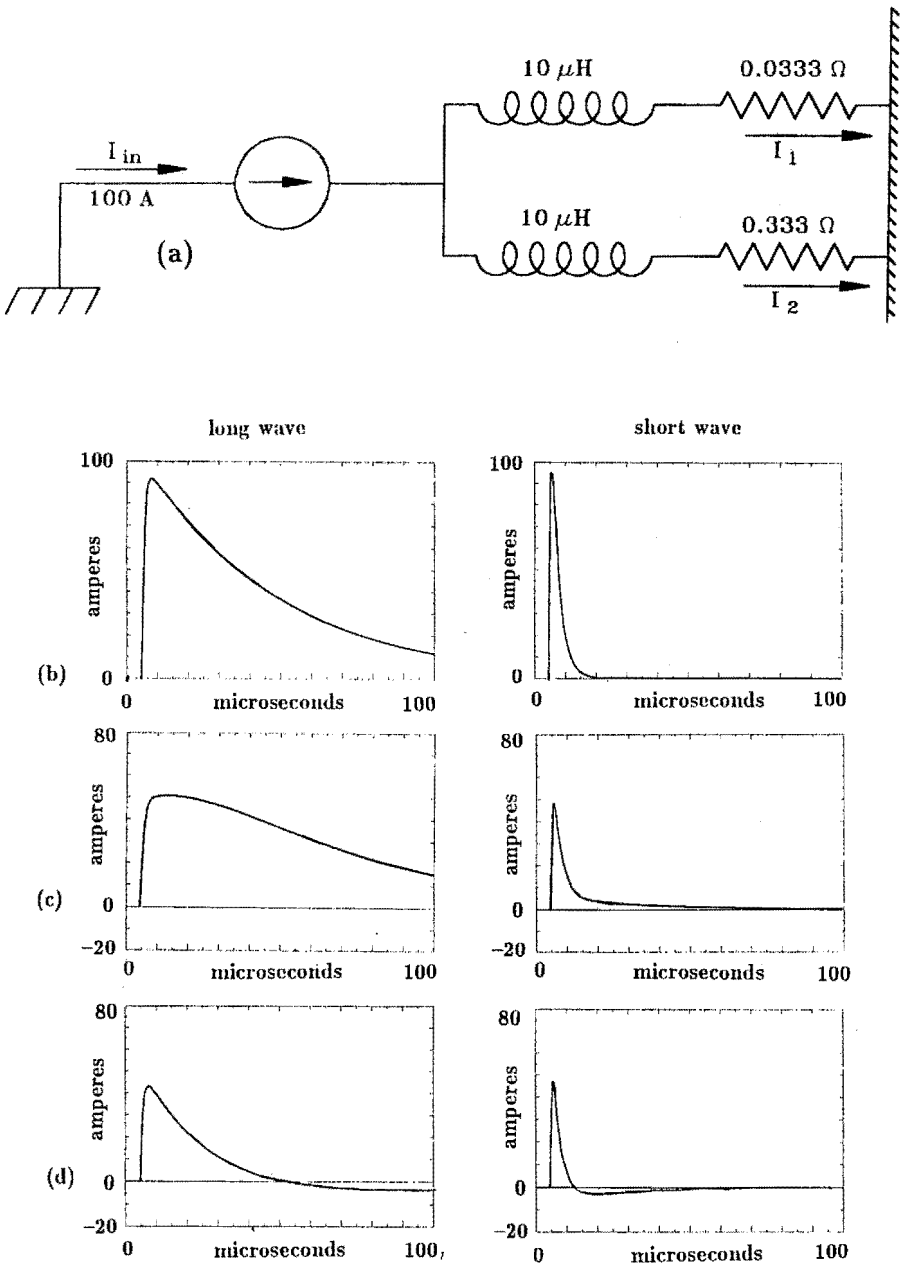

Fig. 11.16 Lumped constant circuit exhibiting redistribution effects.
(a) Circuit
(b) I_{in}
(c) I_1
(d) I_2

will divide between the two branches in proportion to the inductances, but a pulse with a long front and tail time will divide in proportion to the resistances. A pulse with a short front time and a long tail time will initially divide in proportion to the inductance, but then the distribution will change and ultimately become governed by the resistance.

Redistribution as a sum of components: One way of viewing the phenomenon is to consider the current in the two branches to be composed of the sum of two components: a steady state component governed by the resistances and a transient circulating current governed by the L/R time constants of the circuit. The transient circulating current will eventually die away as the energy injected into the circulating current is consumed by the resistance of the circuit. If the injected pulse has a finite duration, the circulating component of current will cause the current in the individual branches to last longer than the applied current. It will also cause the current in one of the branches to flow in a direction opposite to the polarity of the injected pulse.

Similar phenomena occur in aircraft structures. Usually they cannot be completely described in terms of circuits, though simple equivalent circuits, such as that of Fig. 11.11, can often help illustrate the phenomenon involved. In some cases internal magnetic fields develop of such a waveshape that it is difficult to distinguish between magnetically induced voltages and resistive voltages influenced by diffusion effects.

These redistribution phenomena will be discussed first for an elliptical cylinder and then illustrated for more complex structures in which the phenomena must be calculated by numerical means.

11.4.1 Elliptical Cylinders

Fig. 11.17 shows an elliptical cylinder into which a step-function current is injected. As in §11.3.1, the cylinder is assumed to be long enough that all end effects may be neglected, that it is short compared to the wavelengths of any frequency components of the injected current, and that the return path for the current is far enough removed that no proximity effects need be considered.

The instantaneous current in the cylinder will also be treated as composed of the sum of two components; a steady state component and a transient component where the transient component takes the form of a circulating eddy current. For the following section it should be kept in mind that the eddy currents described represent only the transient component of current and that the total current at any point or time is the sum of the two components.

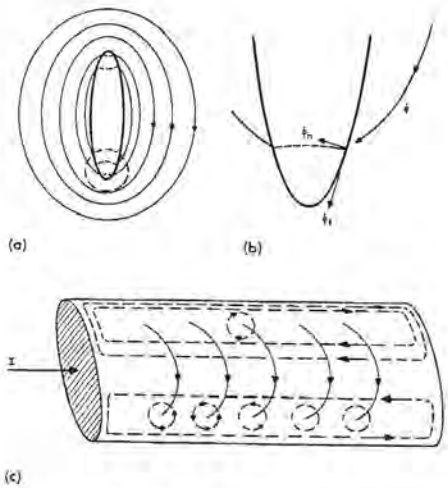

Fig. 11.17 Magnetic fields around an elliptical cylinder.
(a) Penetrating lines of flux
(b) Detail showing resolution into components
(c) Circulating currents induced by penetrating lines of flux

Steady state conditions: Under steady state dc conditions the current density along the wall of the cylinder will be governed by the dc resistance and, if uniform wall thickness is assumed, it will be uniform. The current in the cylinder will produce a magnetic field. Most of the field lines will completely encircle the cylinder, as shown in Fig. 11.17(a), but some, because of the uniform current density, will pass through the cylinder. The greater the eccentricity of the cylinder, the greater will be the number of lines of flux passing through the it.

Transient conditions: One such penetrating flux line is shown in Fig. 11.17(b). The vector defining that line may, at the point of entry, be resolved into two vector components, one, ϕ_n, normal to the surface, and another, ϕ_t, tangential to the surface. If the field line ϕ is suddenly established, it will induce a circulating, or eddy, current in the conducting sheet which it attempts to penetrate. The eddy current will produce a magnetic field of its own, and the intensity of the eddy current will be such that the magnetic field produced is exactly that required to cancel the normal component of the exterior field.

Circulating component: If, as shown in Fig. 11.17(c), a number of lines of magnetic flux attempt to penetrate the surface of the elliptical cylinder, the eddy currents produced by each line of flux combine to produce a circulating component of current. In an elliptical cylinder there will be four regions of circulating current, two on each of the two sides of the cylinder.

These circulating current components will be of such a nature as to increase the current density at the edges of the cylinder and to reduce it along the center. They also cancel any penetrating magnetic field, forcing the field around the cylinder to be entirely tangential to the surface, at least initially.

From the viewpoint of component currents, the circulating currents produce an internal magnetic field that initially has the same pattern as that produced by the dc current, but of opposite polarity, so as to initially reduce the internal magnetic field to zero.

Transition to DC conditions: The eddy currents cannot exist forever, since energy will be lost as the currents circulate through the resistance of the metal sheet. Accordingly, the current density at all points will vary with time, eventually becoming uniformly distributed in structures having uniform thickness and made of uniform resistivity materials. Fig. 11.18 shows the manner in which the current density will vary. As the circulating current shown in Fig. 11.18(c) decays to zero, the current at the edge will decay from its initial high value to the final resistively determined value, and the current at the center will increase from its initial low value. The current densities will change according to an essentially exponential pattern, though the transient increase in surface resistance produced by diffusion effects will prevent the circulating current from following a true exponential decay.

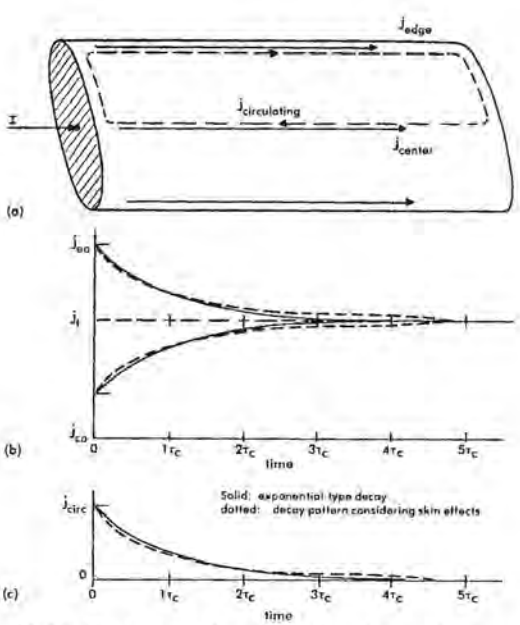

Fig. 11.18 Variation of current density with time.
(a) Current components defined
(b) Edge and center currents
(c) Circulating currents

Time constant: One expression giving the approximate magnitude of the redistribution time constant that has appeared in the literature [11.5] is:

$$\tau = \frac{\mu A a}{\pi P} \tag{11.35}$$

where

A = enclosed area of structure

P = peripheral distance around the structure.

The thickness of the wall, a, is assumed to be very small compared to other dimensions. For a rectangular box of sides height h and width d, Eg. 11.36 becomes

$$\tau = \frac{\mu h\, da}{2\rho(h+d)}. \tag{11.36}$$

These equations define the approximate redistribution times, but the actual time constants will depend on the geometry and will be somewhat different for different portions of a structure.

For an elliptical cylinder made from aluminum of thickness 0.0381 cm, having a major axis of 47 cm, a minor axis of 9.4 cm, and a perimeter of 98.7 cm (essentially a flattened version of the circular cylinder discussed in §11.2) the redistribution time constant predicted by Eq. 11.35 would be 745 μs. As will always be the case, the redistribution time constant will be much longer than the pulse penetration time constant.

11.4.2 Eddy Currents and the Internal Magnetic Field

As the circulating component of current dies out and the external lines of flux penetrate the walls of the cylinders, there will be set up an internal magnetic field oriented as shown in Fig. 11.19. In its latter stages the rate at which the internal field builds up will be dependent upon the rate at which the externally induced circulating currents die away, with a time constant about equal to the redistribution time constant.

The early time buildup of the magnetic field will depend on the rate at which the eddy currents build up along the inner surface. The eddy currents build up in response to the electric field on the inner surface, but are also governed by the inductance of the path through which they circulate, according to the elementary formula:

$$I = \frac{1}{L}\int_0^t E dt. \tag{11.37}$$

Since the internal surface voltages are retarded by the diffusion effect, it follows that the internal circulating currents, and hence the internal magnetic field, will build up even more slowly.

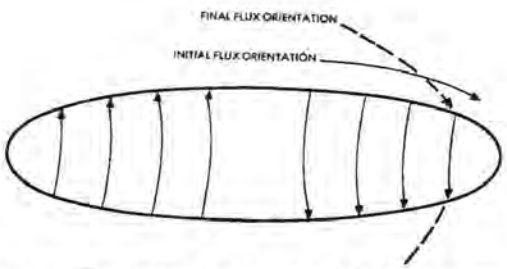

Fig. 11.19 The internal magnetic field that arises as a result of flux penetration.

11.4.3 Internal Loop Voltages

We are now in a position to evaluate the voltages on conductors contained in a cylinder of non-circular geometry. Fig. 11.20 shows an elliptical cylinder with two internal conductors, one adjacent to the surface and one in the center. Both are connected at one end to an end cap sufficiently massive that no voltage drops will appear along its inner surface. The other ends are open circuited. The usual assumptions about the length of the cylinder and the return path for the injected current apply. Voltages V_1 and V_2 are shown, both being measured between their respective conductors and a point on the inner wall of the cylinder. Fig. 11.20(b) shows that all of the internal flux will pass between conductor 2 and the inner wall of the cylinder, while only a small amount will pass between conductor 1 and the inner wall. Correspondingly, a large fraction of the internal flux passes through the plane defined by conductors 1 and 2.

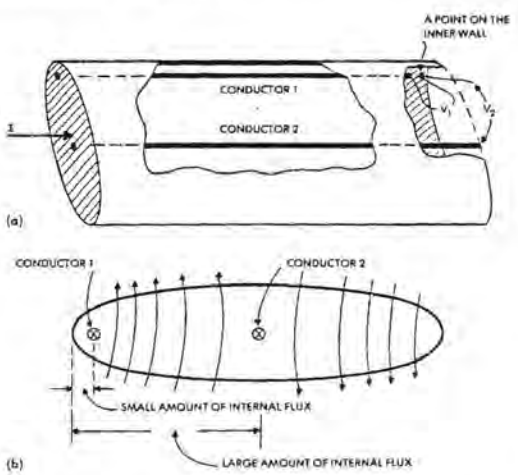

Fig. 11.20 Factors governing the internal voltage.
(a) The geometry
(b) Internal flux linkages

Voltage as line integral of potential: The voltage between any two points is defined again as the line integral of the potentials around a closed path. Figs. 11.21(a) and (b) show the simplest paths to consider. V_1 would be the sum of the potentials developed around the loop $ABCD$. If there is no current along conductor 1, the potential along path AB will be zero. The potential drop along the path $B - C$ will be zero because of the assumptions regarding the end cap. The potential along path CD will then be the voltage drop produced by the inner current density times the resistivity of the material along the path CD.

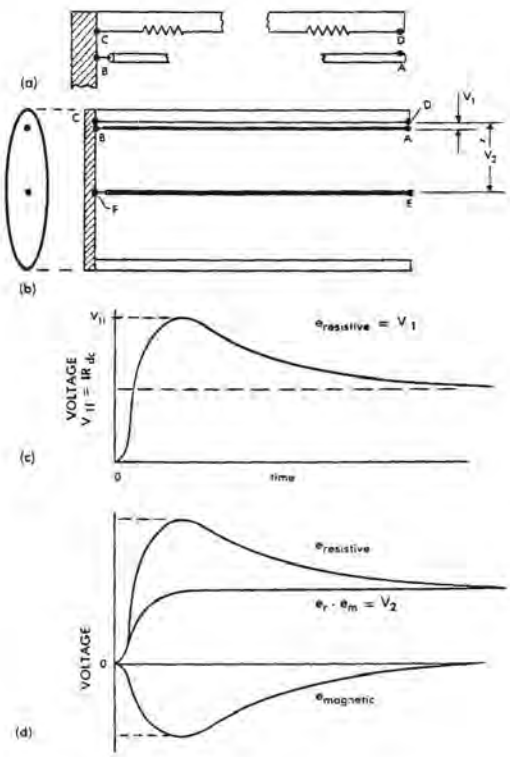

Fig. 11.21 The internal voltages.
(a) Detail of the edge surface
(b) Paths of integration
(c) Components of V_1
(d) Components of V_2

To these potentials must be added the voltage induced magnetically by the changing magnetic flux passing through the loop defined by the points A, B, C, and D. If the spacing of the conductor to the wall is made vanishingly small, so that $C - B$ and $D - A$ become zero, there will be no magnetic flux; hence the voltage V_1 between points A and D will be only the resistive voltage drop along the path CD.

As in the cylindrical geometry case, the voltage for a step function current injected into the exterior of the tube will build up according to the pattern shown in Fig. 11.7. Its magnitude will be greater than the dc resistance rise in the ratio by which the initial current density along the end of the ellipse exceeds the steady state current density.

V_2 will again be the sum of a resistive voltage rise and a magnetically induced voltage, this time along the path $EFDC$. The resistive component will be identical to the resistive component of V_1, the resistance rise along the path CD. For V_2, however, there will be a non-zero magnetic component of voltage produced by the passage of a finite amount of magnetic flux through the finite loop $EFDC$. The magnetically induced component of voltage will be given by

$$e_m = \frac{d\phi}{dt} = K\frac{d}{dt}(I_{\text{circ}}) \qquad (11.38)$$

where K is a proportionality constant relating the flux produced in the loop $EFDC$ to the internal current. In Eq. 11.32, however, it was shown that the internal current was proportional to the integral of the internal resistance rise. This leads to the rather unusual observation that the magnetically induced component of voltage has, initially at least, the same waveshape as the component of voltage produced by the flow of internal current through the resistance of the material.

The long term response of the magnetically induced voltage will be different from the resistively generated component, since, as steady state conditions are reached and the internal magnetic field reaches its final value, its rate of change will decrease to zero.

Influence of physical shape: The amount of the magnetically induced voltage will depend upon the location of the conductor and upon the degree to which the initial distribution of magnetic flux around the outside of the cylinder differs from the final distribution of magnetic flux. Since the difference between the initial and the final flux patterns is greater for cylinders of high eccentricity than it is for cylinders of low eccentricity, it follows that the flatter the cylinder, the greater will be the influence of the magnetic component.

11.4.5 Redistribution on a Rectangular Cylinder

Some situations are best studied by numerical means, an example being the rectangular coaxial transmission line of Fig. 11.22. It consists of a rectangular outer conductor, assumed here as perfectly conducting and only used to define the problem space, and a rectangular inner conductor made from a poorly conducting material. The driving source for the illustration is taken to be a 1 V/m axial electric field having the waveshape shown in Fig. 11.23. The current that ultimately results is given by the integral of the voltage and the inductance of the circuit.

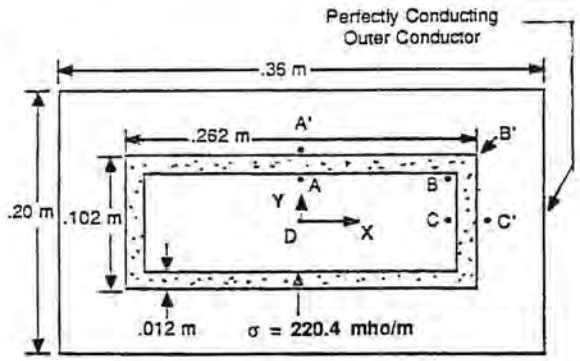

Fig. 11.22 Redistribution in a rectangular cylinder.

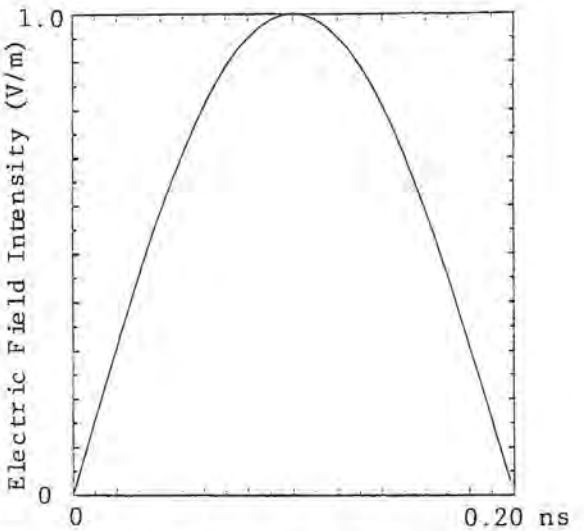

Fig. 11.23 Axial electric field used to drive current.

The problem was solved with the two-dimensional finite difference (2DFD) technique described earlier. The solution was based on a cell size in the x and y directions of 0.004 m and a time step of 9×10^{-12} sec. By Eqs. 11.23 and 11.35 the pulse penetration time would be 4.04 ns and the redistribution time constant would be 465 ns.

Fig. 11.24 shows the internal axial electric field at points A, B, C and D. Skin effects force the current on the center conductor to be highest at the corners (B) and lowest along the wider face (A), and this is reflected in the axial electric field being highest at point B and lowest at point A. After about one redistribution time constant, the currents and thus the internal electric fields, are nearly equal.

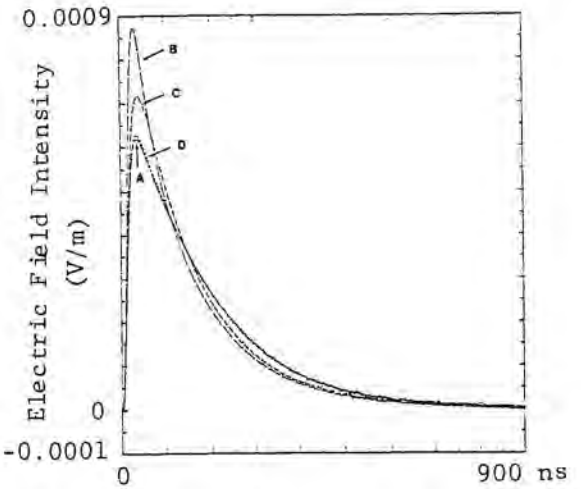

Fig. 11.24 Electric field variations at points indicated on Fig. 11.22.

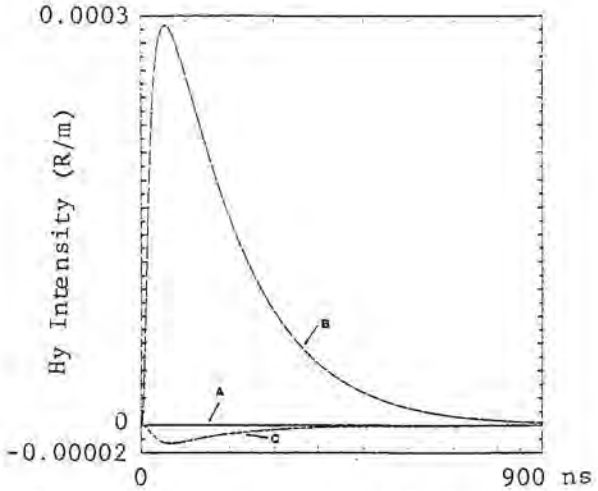

Fig. 11.25 Vertical component of magnetic field at points indicated on Fig. 11.22.

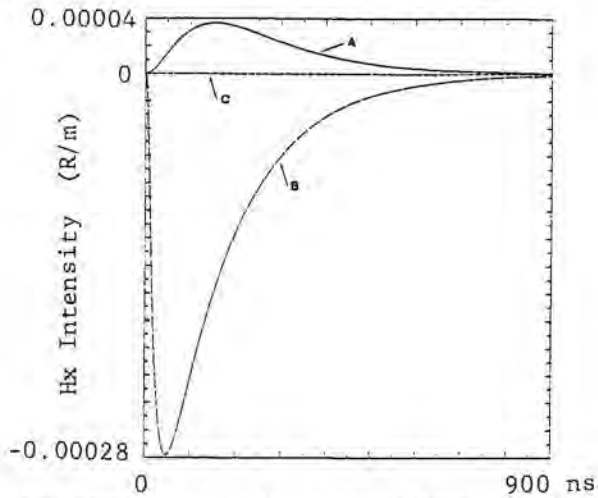

Fig. 11.26 Horizontal component of magnetic field at points indicated on Fig. 11.22.

An interesting feature of Fig. 11.24 is that the waveforms cross each other. This indicates that different time constants are dominant at different locations. This can be explained by noticing that, if the wall were discretized into a set of N filaments, the current in each filament would be of the form:

$$i_{\text{filament}} = \sum_{k=1}^{N} A_k e^{-t/\tau_k}. \qquad (11.39)$$

Therefore, each filament response contains the same time constants (related to the system poles) τ_k. However, the coefficient A_k (residue) depends upon location, so different time constants (or poles) dominate at different locations. It is clear that for the real system, there is actually a continuous spectrum of time constants (or poles) and coefficients (residues), which are only approximated by a discrete spectrum for any discretized analysis procedure such as a filamentary model or finite difference model.

Finally, at late time, the electric fields become uniform and equal to the product of total current and resistance per unit length.

The vertical and horizontal magnetic fields at points A, B and C are given in Figs. 11.25 and 11.26. The field is highest at the corners, showing the field lines to be penetrating the conductor. The fields peak at approximately the calculated redistribution time, but there is some variation depending on location.

11.4.6 Redistribution with Both Metal and Composite Materials

A so called "composite aircraft", which has large amounts of CFC material in its structure, is really a mixture of metal and CFC materials. The structures are sufficiently complex that there are no simple analytic formulas to estimate the redistribution time constants. Three dimensional solutions of Maxwell's equations can be used to solve this type of problem, but engineering estimates can frequently be obtained if one has sufficient physical insight.

Metal and CFC transmission line: A simple example of redistribution on a mixed metal/lossy structure will illustrate the principles involved. Fig. 11.27 shows another coaxial transmission line of which the outer conductor is assumed perfectly conducting and only used to bound the space in which the numerical solution takes place. The inner cylinder has a 20° sector made of metal (assumed perfectly conducting) and a 340°

sector made of a lossy material having a conductivity of 220.4 mho/m. The inner conductor is driven by an axial voltage having the same waveshape as shown in Fig. 11.23, but of 248 V/m, the field that produces a peak current of 1 ampere.

The solution of the problem used the 2DFD code with a cell having a thickness of 0.001 m in the lossy material and 0.01 m elsewhere. The angular width of the cell was 10° and the time step was 2.5 ps.

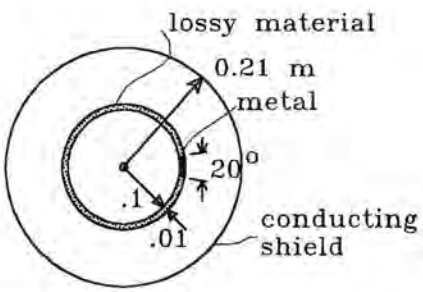

Fig. 11.27 Structure having both metal and CFC sectors.

Fig. 11.28 shows the current on the metal and the lossy portions of the conductor. Initially, most of the current flows on the lossy portion of the conductor, but eventually all the current flows on the metal portion. The redistribution time can be defined as the time when the currents on the two conductors are equal; 400 ns in this case. Because the metal conductors are assumed perfectly conducting, the current never decays to zero, even though the voltage pulse is of finite duration. If metal losses had been considered, the current would have eventually decayed to zero.

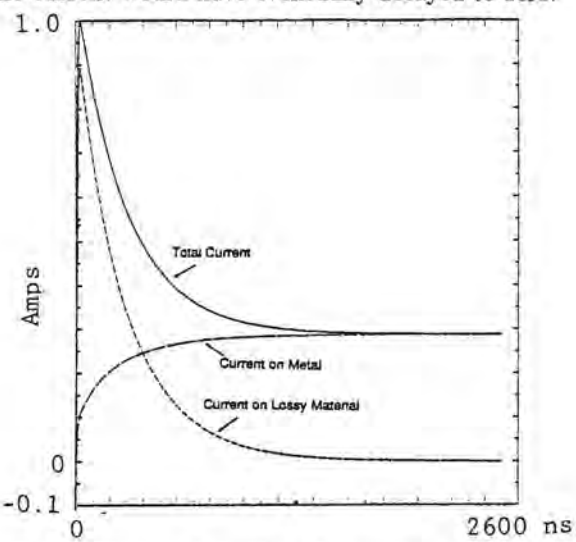

Fig. 11.28 Redistribution of current on structure shown in Fig. 11.27.

The magnetic and electric fields at $r = 0.05$ m and $\theta = 0°$ are shown in Figs. 11.29 and 11.30. The electric field initially increases because of diffusion, but then as redistribution occurs, it decays to zero. The magnetic field increases in amplitude and eventually approaches a steady state value determined by the current distribution on the center conductor and the inside surface of the outer conductor.

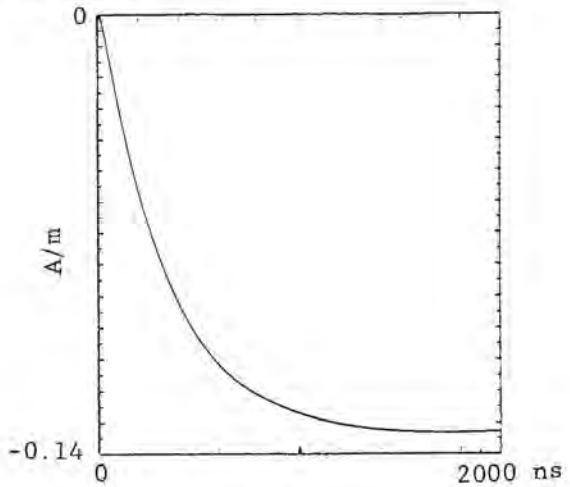

Fig. 11.29 Magnetic field at point indicated on Fig. 11.27.

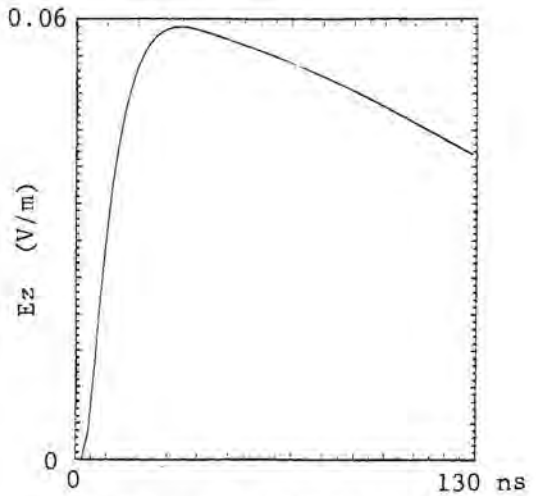

Fig. 11.30 Electric field at point indicated on Fig. 11.27.

11.5 Implementation of Diffusion and Redistribution in 3D Models

The two previous examples have illustrated how diffusion and redistribution problems can be solved with 2DFD models. They can also be incorporated into 3D models. The following sections will illustrate

how they are implemented and then illustrate the techniques as applied to an aircraft wing box incorporating both CFC and metal members.

Derivation of equations: With regard to the definition of $Z_s(\omega)$ in Eq. 11.10, one can form a decomposition of the series and then transform each term into the time domain. This results in an infinite sequence of ordinary differential equations in the time domain as follows:

$$E^0(\omega) = \frac{1}{\sigma d} J(\omega)$$

$$E^0(t) = \frac{1}{\sigma d} J(t)$$

$$E^1(\omega) = \frac{2}{\sigma d} \frac{j\omega}{\omega_1 + j\omega} J(\omega) <=>$$

$$\frac{d}{dt} E^1(t) + \omega_1 E^1(t) = \frac{2}{\sigma d} \frac{dJ(t)}{dt}$$

$$\cdot$$

$$\cdot$$

$$\cdot$$

$$E^n(\omega) = \frac{2}{\sigma d} \frac{j\omega}{\omega_n + j\omega} J(\omega) <=>$$

$$\frac{d}{dt} E^n(t) + \omega_n E^n(t) = \frac{2}{\sigma d} \frac{dJ(t)}{dt}. \qquad (11.40)$$

$J(\omega)$ and $J(t)$ are the frequency and time domain representations of the impressed current density. The solutions of these ordinary differential equations are analytic. The time domain electric field is then an infinite series of convolutions:

$$E(t) = \sum_{n=0}^{\infty} E^n(t)$$

$$= \frac{1}{\sigma d} \left[J(t) + 2 \sum_{n=1}^{\infty} \int_0^t dt' \epsilon^{-\omega_n (t-t')} \frac{dJ(t')}{dt'} \right]. \qquad (11.41)$$

With respect to the definition of $Z_t(\omega)$ in Eq. 11.16, one can follow the same procedure outlined above. The time domain electric field transmitted through the layer can also be written as an infinite series of convolutions:

$$E(t) =$$

$$\frac{1}{\sigma d} \left[J(t) + 2 \sum_{n=1}^{\infty} (-1)^n \int_0^t dt' \epsilon^{-\omega_n (t-t')} \dot{J}(t') \right] \qquad (11.42)$$

where once again $E^n(t=0) = 0 (n = 1, 2, \cdots \infty)$ and $J(t=0) = 0$.

Implementation in numerical codes: Implementation of the series expansions in Eqs. 11.41 and 11.42 in a time domain finite difference approximation solution requires back storage of the tangential components of the H fields in order to compute the external or internal coupling through the lossy material, at least at early times. At late times, both solutions converge to the dc resistance condition, $E(t) \approx J(t)/(\sigma d)$.

Depending on the bandwidth of the calculation, and the conductivity and thickness of the lossy material, the series expansion for the transfer impedance (Eq. 11.42) may converge with less than 20 terms at early time. The series expansion for the surface impedance (Eq. 11.41) requires approximately 200 terms to converge for calculations with 100 MHz bandwidths.

11.5.1 Redistribution on a Rectangular Box

As a demonstration of the technique described above, the results of external and internal electromagnetic coupling by lightning to a box, Fig. 11.31, are presented. The top, bottom, and two of the faces are assumed made of perfectly conducting metal and the other two faces are assumed made of graphite-epoxy composite with thickness 0.03 inch (0.762 mm) and conductivity 15 000 mho/m. Comparison calculations were also made for a box with all faces made of perfectly conducting metal. Into the top of the box was injected a current of 200 kA peak amplitude with a $\sin^2$ front rising to crest in 1 μs and decaying exponentially with a time constant of 50 μs. The current was removed from the opposite face. For the calculations, a grid size of 1 m in all directions and a time step of 1.75 ns were used.

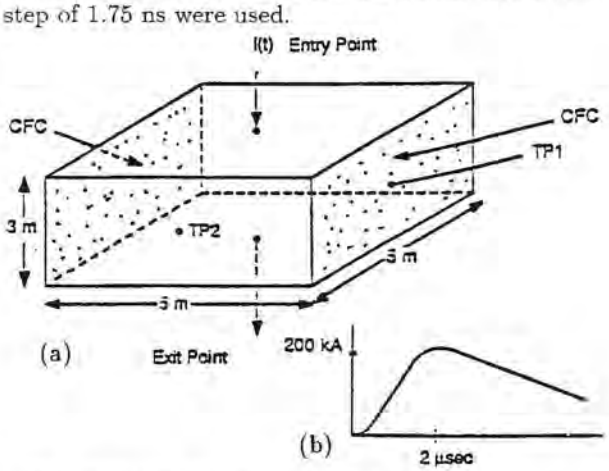

Fig. 11.31 Redistribution on a 3D object.
(a) Structure
(b) Waveshape of injected current

Fig. 11.32(a) shows the magnetic field (or current density) at the center of one of the faces formed from CFC, while Fig. 11.32(b) shows the field at one of the metal sides, the solid lines showing the waveforms for the box with CFC sides and the dashed line showing the waveforms for the box composed entirely of metal. At early times, the currents divide uniformly between the sides made of metal and CFC material, and the magnetic fields at the two surfaces are the same. For those early times the distribution of current is such that the internal magnetic fields are zero, as sketched on Fig. 11.33(a).

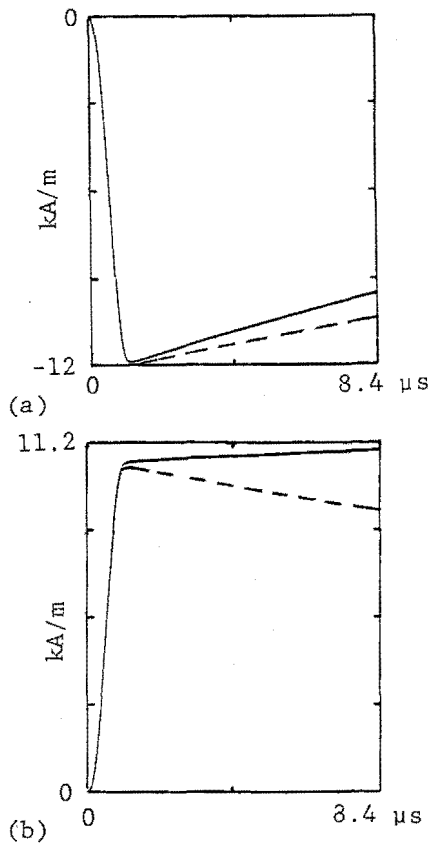

Fig. 11.32 Tangential H fields.
(a) Above a composite face
(b) Above a metal face

As time goes on, the current transfers from the CFC sides to the metal sides. As a result the magnetic field at the CFC side decreases while it rises (for the times indicated on the figures) on the metal sides. This is accompanied by a buildup of magnetic field on the inside of the box, as sketched on Fig. 11.33(b).

Fig. 11.34 shows the electric field along the CFC side. This, along with the internal magnetic fields, would act as a driver for conductors located inside the box.

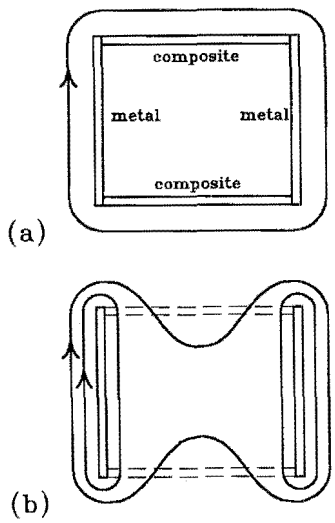

Fig. 11.33 Magnetic field patterns.
(a) Early time
(b) Late time

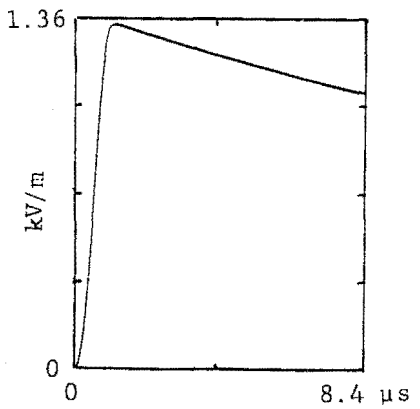

Fig. 11.34 Electrical H field above a composite face.

11.5.2 Redistribution On a Wing Box

So far, the examples which have been presented are for idealized geometries, but the numerical methods also work when applied to realistic configurations encountered in aircraft. An example is the aircraft wing box shown in Fig. 11.35, calculations and measurements for which were reported in [11.6].

Dimensions: The wing box was 2.6 m long, 0.7 m wide, and 0.1 m thick. The top and bottom skins, the side, the internal spars and one of the ribs were made of CFC. One rib, four strips and the ends of the box were made of aluminum. Thicknesses were as follows:

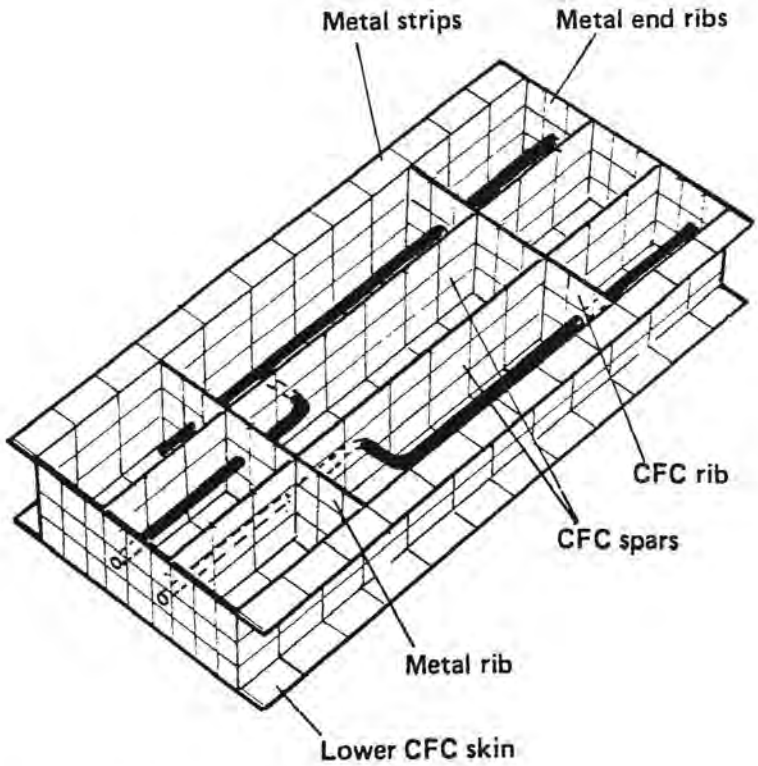

Fig. 11.35 Wing box analyzed with 3DFD technique.
Upper skin and details of installations omitted for clarity.

Top and bottom CFC skins	6 mm
CFC spars	2 mm
Aluminum spar	2 mm
CFC rib	2 mm.

The wing box included a fuel pipe, fuel pipe bell and cable conduit, these being numerically modeled as perfect conductors. The insulated fuel pipe couplings were modeled as gaps. The cable conduit was connected to the box at both ends and in the middle with bonding straps, assumed in the numerical model to be perfect conductors.

During tests, current was injected into one end of the wing box, the test geometry being as shown in Fig. 11.36. Voltages and currents were measured at the points shown in Figs. 11.37 and 11.38. Voltage and current probes were built into the test object when it was made, the current density in skin materials being measured by passing some of the skin material through Rogowski coils, a form of current transformer.

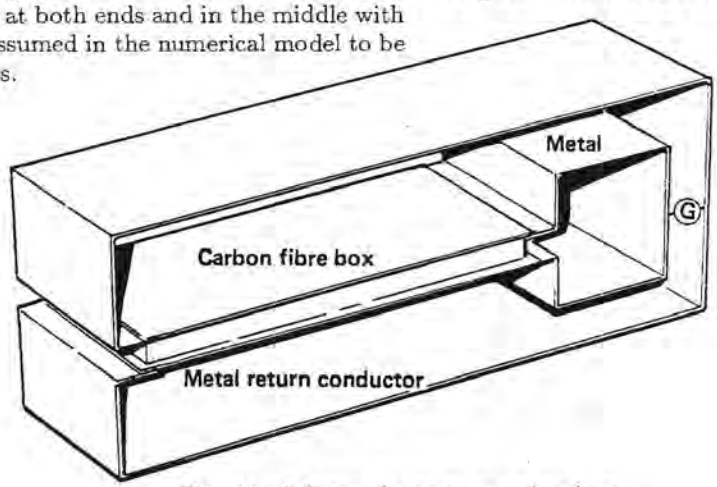

Fig. 11.36 Setup for tests on wing box.

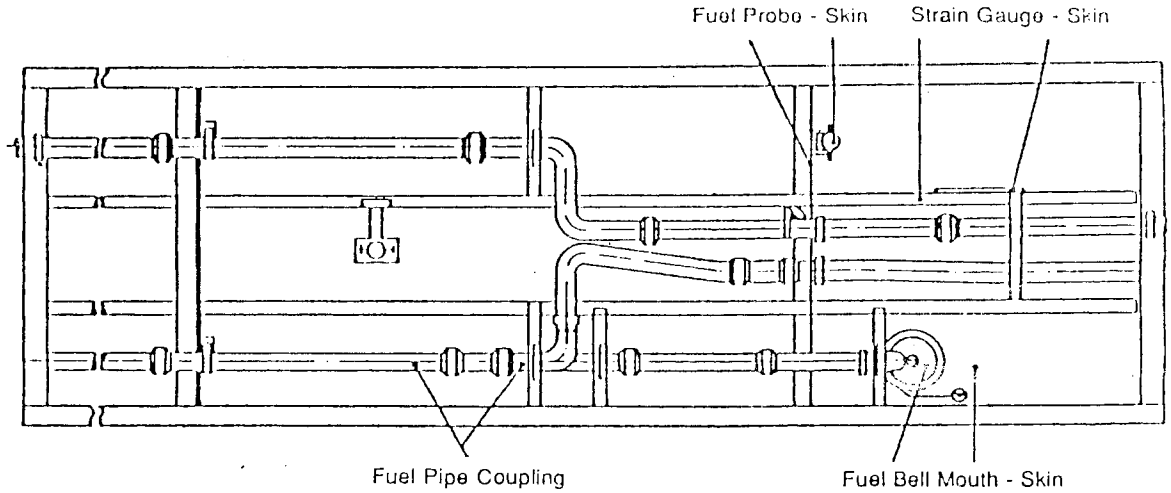

Fig. 11.37 Locations where voltages were measured.

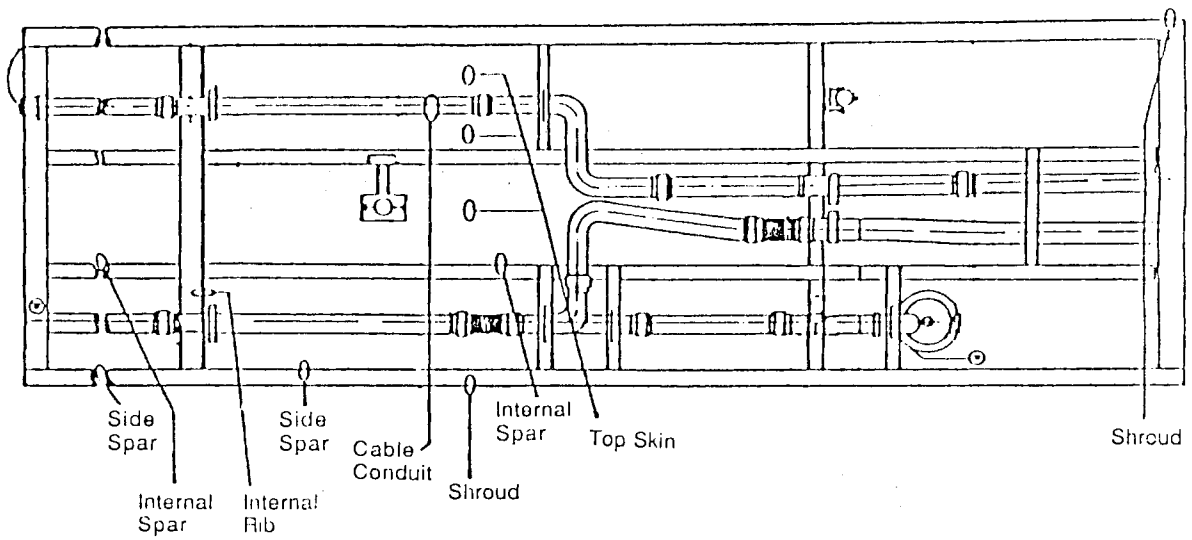

Fig. 11.38 Locations where currents were measured.

Test and analysis conditions: Analysis and tests were done for two different conditions:

Low level test: 400 A peak
0.25 μs rise time
1.0 μs decay time

High level test: 200 kA peak
10 μs rise time
150 μs decay time

The analysis was done with the 3DFD techniques described earlier. The CFC surface and transfer impedances were modeled by implementing Eqs. 11.41 and 11.42, though modified somewhat to conserve computer time. The time and space resolution for the two cases were:

Low level:
$\Delta x = 10$ cm
$\Delta y = 4$ cm
$\Delta z = 2.5$ cm
$\Delta t = 50$ ps
Volume = 60,680 cells
Number of time steps = 60,000
Simulated time = 3μs
Bandwidth = 700 MHz

High level:
$\Delta x = 20$ cm
$\Delta y = 7$ cm
$\Delta z = 4$ cm
$\Delta t = 100$ ps
Volume = 17,600 cells
Number of time steps = 30,000
Simulated time = 30μs
Bandwidth = 350 MHz

Results: Comparisons between numerical and experimental results are given in Tables 11.1 and 11.2. A comparison of the waveshapes for the fuel bell mouth skin voltage is given in Fig. 11.39.

The agreement between experimental and numerical results is quite good, especially in view of the complexity of the structure. Those who did the analysis and test note that the voltage and current measurements were very difficult to make, and that there is no reason to believe that the measurements were any more accurate than the analysis. In fact, the analytical results were extremely useful in justifying and explaining some of the test results which initially had been suspect.

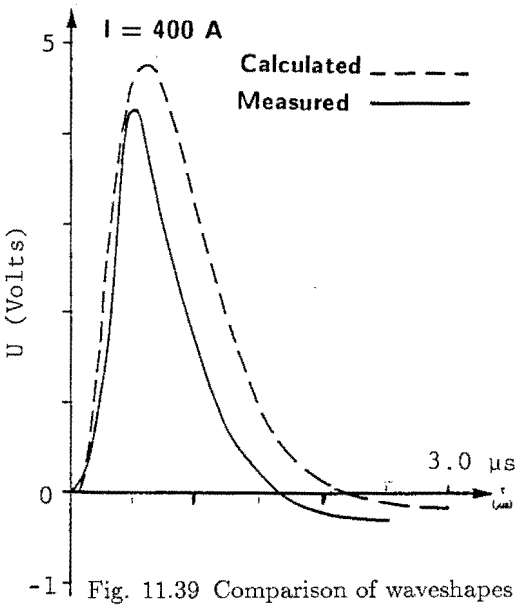

Fig. 11.39 Comparison of waveshapes at the bell mouth.

Table 11.1
Comparison of Analytical and Experimental Results for the Low Level Test

Test Point	Peak Values Analysis	Test
Fuel Probe - skin	5.5 V	4.0 V
Strain gauge - skin	6 V	5 V
Fuel bell mouth - skin	0.5 V	0.5 V
Fuel pipe coupling (insulated)	4.7V	4.5 V
Shroud current	21 A	20 A
Shroud current	23 A	27 A
CFC - skin current	7.5 A	7 A
skin current	6.5 A	6 A
skin current	6.5 A	6 A
Side spar	2 A	1.3 A
Side spar	2.4 A	1 A
Internal spar	0.7 A	1 A
Internal spar	0.7 A	1 A
Cable conduit	4 A	6 A

Table 11.2
Comparison of Analytical and Experimental Results for the High Level Test

Test Point	Peak Values Analysis	Test
Fuel probe - skin	720 V	670 V
Strain gauge - skin	850 V	720 V
Fuel bell mouth - skin	80 V	120 V
Fuel pipe coupling (insulated)	900 V	1030 V
Shroud current	30 kA	25 kA
Shroud current	30 kA	30 kA
Top-skin current (CFC)	1.9 kA	1.5 kA
Top-skin current (CFC)	1.6 kA	1.4 kA
Top-skin current (CFC)	1.9 kA	1.5 kA
Side spar, CFC	2.7 kA	0.65 kA
Side spar, CFC	1.1 kA	1.5 kA
Internal spar, CFC	750 A	600 A
Internal spar, CFC	750 A	600 A
Internal rib, CFC	320 A	150-250 A
Cable conduit	≥ 20 kA	18-23 kA

11.6 Diffusion and Redistribution on CFC Structures

Previous discussions in this chapter have been related to materials which are lossy, but isotropic. Carbon fiber composite, CFC, materials are, in general, anisotropic. CFC materials commonly used in aircraft construction typically have conductivities of $\approx 10^4$ mhos/m in directions tangential to the surface. The conductivity may vary according to the specific direction since the graphite strands may be woven in certain directions to increase physical strength in those directions, but the difference is seldom more than a factor of about two. In the direction normal to the surface, however, the conductivity may only be ≈ 50 mhos/m since the various layers of CFC material are insulated from each other by epoxy resin.

There have been many studies of CFC materials and their shielding properties [11.7 - 11.28]. The general conclusion of these studies is that for conditions of uniform current flow on CFC surfaces, the only conductivity which really matters is that tangential to the surface. This means that with the exception of the example in §11.3.6, the other examples apply to CFC structures only if one uses the conductivity tangential to the surfaces.

The example of §11.3.6 may not apply to anisotropic CFC materials, because in that example there was a significant conduction of current normal to the surface. The usual definitions of surface and transfer impedances (Eqs. 11.10 and 11.12) may also not apply, since they are based on current being able to flow normal to the surface. The reason the word "may" is used is that the conductivity in the direction normal to surface may depend on current density. For low level currents, the epoxy resin may insulate one surface from another, but for high level currents the voltage gradients may be high enough to cause internal sparking between layers. Such sparking would tend to increase the conductivity between layers, both during the time when lightning current is flowing and afterwards.

11.7 Fields Within Cavities

In §11.3.5 it was observed that the electric field developed along the inside of a shielding surface, in response to a current or magnetic field on the outside, excites a current around the cavity enclosed by the shielding surface. It frequently happens that in the fuselage of an aircraft there will be a cavity that is effectively exposed to the external field on only one face, either because the inner walls of the cavity are thick enough to provide more shielding from the other parts of the external field or because the cavity is much closer to one of the external surfaces than it is to any of the other external surfaces. A typical cavity would be a gun bay or an electronic equipment bay located along the fuselage of the aircraft and accessible through the access panels. For the moment the effects of the access panels will be ignored. The geometry is shown in Fig. 11.40(a).

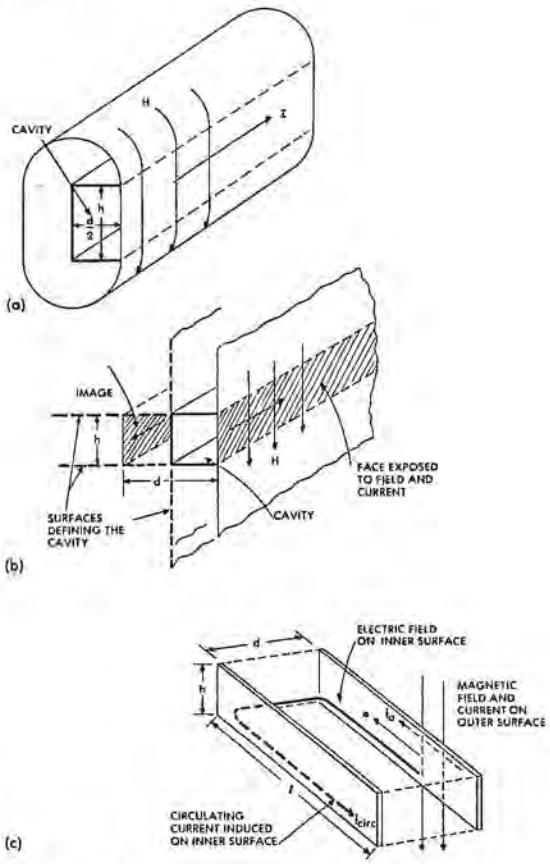

Fig. 11.40 A cavity exposed to a field on only one side.
(a) Cavity and field orientations
(b) An image in the reflecting surfaces defining the cavity
(c) Path defining the loop inductance

Internal current path: The cavity may be viewed as being formed from one face exposed to the external magnetic field and the current producing that field, and with its other faces formed by metal sheets, which, like the exposed surface, may be assumed to extend toward infinity. Mirrored in the reflecting surface defining the back of the cavity will be an image of the face

of the cavity exposed to the magnetic field. The image, Fig. 11.40(b), will be spaced at a distance D behind the face carrying the current, and in the image the reflection of the external current will be of opposite polarity. The electric field produced on the inner surface of the face exposed to the external current, shown in Fig. 11.40(c), will act to force a current, I_{circ}, around the interior of the circuit defining the cavity. The length of the loop involved will be the same as the length of the cavity, and the width will be twice the depth of the cavity. The internal voltage gradient will be proportional to the product of the inner current density and the resistivity of the face carrying the external current and, as described earlier, will exhibit the characteristic pulse penetration buildup described in Fig. 11.7.

Internal impedance: This voltage may be viewed as impressed across a loop or cavity inductance:

$$Z = R + j\omega \mathrm{L}. \qquad (11.43)$$

The resistance and inductance will both be governed by the effective characteristics of the loop defining the cavity. Typical current paths and their characteristic impedances are shown in Fig. 11.41. Some cavities may be viewed as being sufficiently long and narrow that they may be defined by parallel strips. Others are basically of rectangular or circular shape, or of some simple shape that may be approximated by an equivalent circular cylinder. The inductance and resistance of each configuration are shown. Each of the inductance equations [11.28] has a correction factor, log (k), F' or K, that relates to the shape of the enclosure. These correction factors are shown in Fig. 11.42.

Covers and fasteners: If the cavity is provided with a removable cover, and if this cover is in the external current flow or is exposed to the external magnetic field, the effects are as illustrated in Fig. 11.43. If the cover is assumed to be of the same material and thickness as the rest of the face upon which it is mounted, the principal effects relate to the resistance of the fasteners used to hold the cover in place. The covers will seldom make good electrical contact to the rest of the surface except at the fasteners themselves. Accordingly, the external current flowing in the face will be constricted in the vicinity of the fastener and pass from that face onto the cover through the fastener. The major effect of this constriction of current flow is to introduce a lumped resistance into the electrical circuit, although there is a certain amount of influence on the inductance of the circuit whenever the current is constricted.

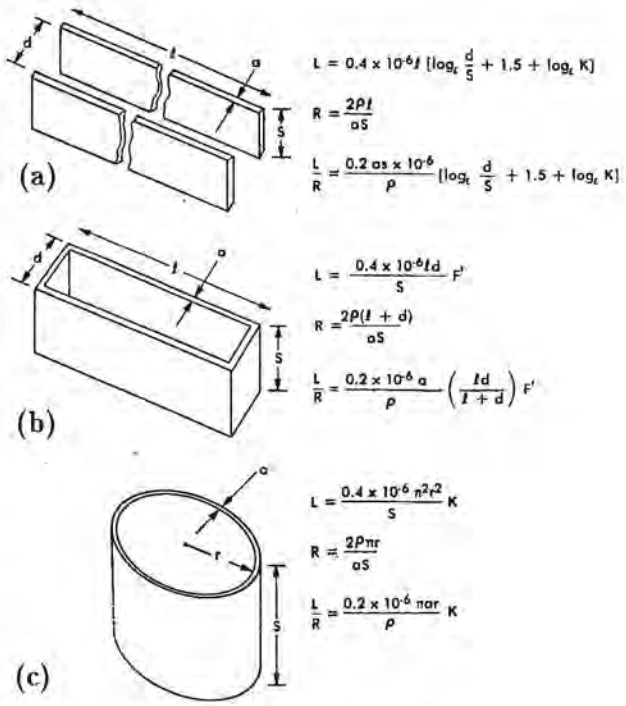

Fig. 11.41 Typical current paths and characteristic impedances.
(a) Long sheets
(b) Rectangular box
(c) Circular cylinder

It will be seen, then, that the greater the number of fasteners, the less the restriction of current flow and the less resistance inserted into the current path. The resistance introduced by the fasteners is important because it is frequently much higher than the intrinsic resistance of the metal surface and because the resistance is not subjected to the skin effects that retard the buildup of current density on the inner surface.

An equivalent circuit of the cavity including the effects of fasteners is shown in Fig. 11.44. R_f is the equivalent resistance of the fasteners. Circulated through this resistance is the undistorted current flowing in the exterior face of the fuselage. The sum of R_1 and R_2 is equal to the intrinsic resistance of the loop defining the cavity, the resistances being given by the equations in Fig. 11.41. The external current will develop a voltage across only a portion of this resistance, since it flows in only a portion of the loop. Letting R_1 be the resistance through which the external current flows, that resistance may be assumed to be subjected to the current as retarded by the pulse penetration time constant. The two voltages developed

across these resistances then circulate current across the entire loop. The rate at which the current builds up will then be the rate at which the magnetic field inside the cavity builds up.

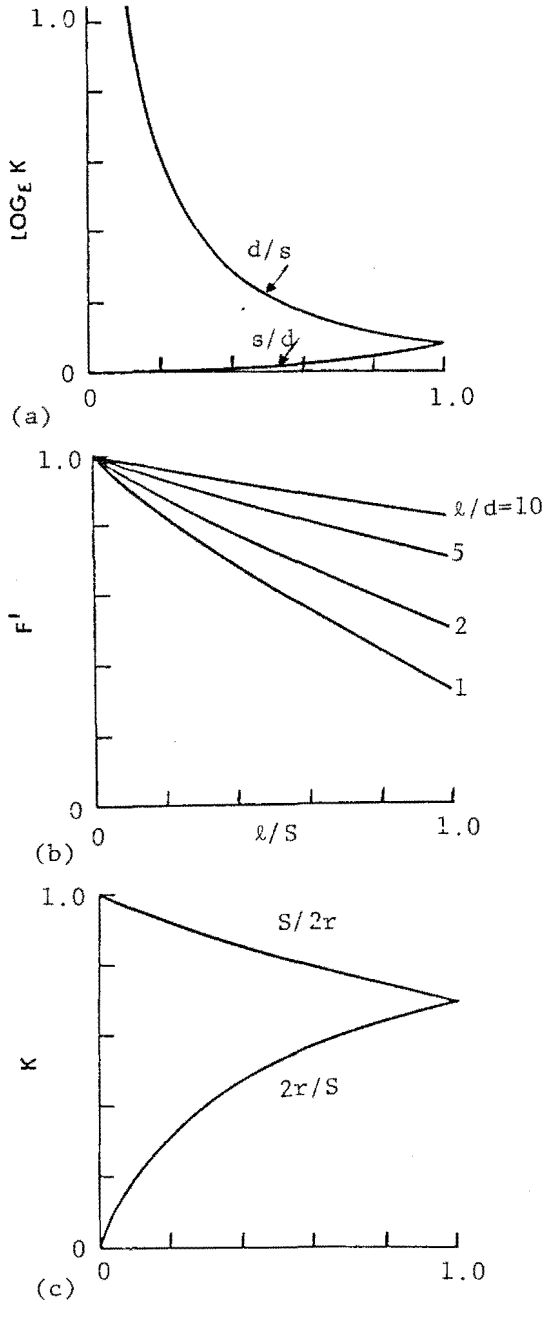

Fig. 11.42 Correction factors for inductance.
(a) Parallel strips
(b) Rectangular boxes
(c) Circular cylinders

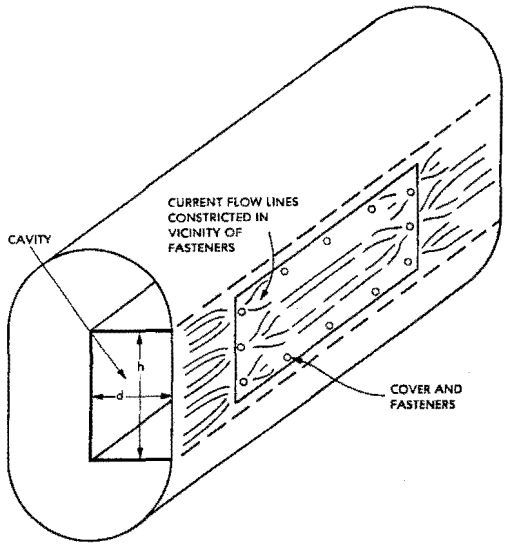

Fig. 11.43 Effects of covers and fasteners.

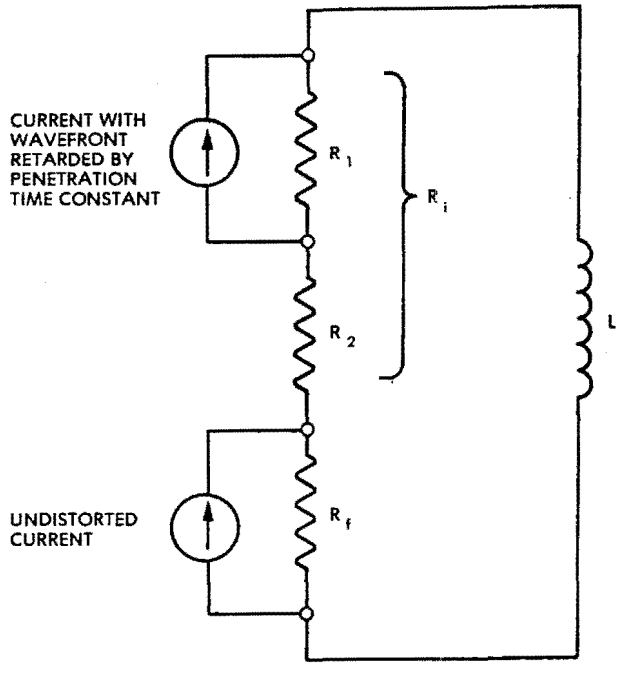

Fig. 11.44 Equivalent circuit governing buildup of magnetic field inside a cavity.

REFERENCES

11.1 P. M. McKenna, T. H. Rudolph, and R. A. Perala, "A Time Domain Representation of Surface and Transfer Impedances Useful for Analysis of Advanced Composite Aircraft," *"Proceedings of International Aerospace and Ground Conference on Lightning and Static Electricity,"* held in Orlando, FL, June 26-28, 1984.

11.2 B. J. C. Burroughs, "Induced Voltages, Measurement Techniques and Typical Values," *Lightning and Static Electricity Conference*, Oxford, England, 14-17 April, 1975, Session 4, Paper 6.

11.3 S. Goldman, *Transformation Calculus and Electrical Transients*, Prentice-Hall, Inc. Englewood Cliffs, NJ, 1949, 1955, pp. 112-120

11.4 F. A. Fisher, "Analysis and Calculations of Lightning Interactions With Aircraft Electrical Circuits", *Air Force Flight Dynamics Laboratory, AFFDL-TR-78-106*, August 1978, pp. 307-324

11.5 K. Khalaf-Allah, "Time Constant for Magnetic Field Diffusion into a Hollow Cylindrical Conductor," *UKAEA (United Kingdom Atomic Energy Authority) Research Group Report CL-1414*, Culham Laboratory, Abingdon, Oxfordshire, England. 1974.

11.6 B. I. Wahlgren and J. Rosen, "Finite Difference Analysis of External and Internal Lightning Response of the JAS39 CFC Wing," *Proceedings of 1988 International Aerospace & Ground Conference on Lightning & Static Electricity*, Norman, Oklahoma, April 1988.

11.7 R. A. Perala, et al., "Evaluation and Mitigation of Lightning and Microwave Hazards to the SRB Propellant." *EMA-87-R-63*, June 1987.

11.8 R. A. Perala, K. L. Lee and R. B. Cook, "EMP Coupling to a Composite Aircraft,"Presented and Published in the *Proceedings of the 1979 IEEE Int. Symp. on EMC."*

11.9 P. B. Papazian, et al."Transfer Impedance Measurements of the Space Shuttle Solid Rocket Motor Joints, Wire Meshes and a Carbon Graphite Motor Case." presented at *1988 International Aerospace & Ground Conference on Lightning & Static Electricity*, Oklahoma City, OK, April 19-22, 1988.

11.10 D. Strawe, and L. Piszker, "Interactions of Advanced Composites with Electromagnetic Pulse (EMP) Environment," *AFML-TR-75-141*, September 1975.

11.11 "Interim Report - Advanced Composite Aircraft Electromagnetic Design and Synthesis," *NAVAIR-518-1*, April 1980.

11.12 D. A. Bull, and G. A. Jackson, "Assessment of the Electromagnetic Screening Characteristics of Carbon Fibre Composite Materials," *IEEE Conference Proceedings*, No. 47, Vol. 1, pp. 1-198, 16-18th September 1980.

11.13 T. C. Holzschuch and W. J. Gajda, Jr., "DC Electrical Behavior of Graphite Fibers," *1977 IEEE Int. Symp. on EMC*, Seattle, Washington, August 2-4, 1977.

11.14 L. A. Scruggs and W. J. Gajda, Jr., "Low Frequency Conductivity of Unidirectional Graphite and Epoxy Composite Samples," *IEEE Int. Symposium on EMC*, Seattle, Washington, August 2-4, 1977.

11.15 J. T. Kung and M. P. Amason, "Electrical Conductive Characteristics of Graphite Composite Structures," *IEEE Int. Symposium on EMC*, Seattle, Washington, August 2-4, 1977.

11.16 T. S. Lee and J. D. Robb, "Ring Discharge on the Back surface of a Composite Skin with Ohmic Anisotropy in Response to Frontal High Current Injection," *10th Int. Aerospace & Ground Conference on Lightning and Static Electricity*," Paris, France, 1985.

11.17 W. F. Walker and R. E. Heintz, "Conductivity Measurements of Graphite and Epoxy Composite Laminates at UHF Frequencies," *IEEE Int. Symposium on EMC*, Seattle, Washington, August 2-4, 1977.

11.18 K. F. Casey, "Advanced Composite Materials and Electromagnetic Shielding." *IEEE Int. Symposium on EMC*, Seattle, Washington, August 2-4, 1977.

11.19 K. F. Casey, "Electromagnetic Penetration of a Composite Panel in a Perfectly Conducting Surface," *IEEE Int. Symposium on EMC*, September 8-10, 1988.

11.20 B. W. Smithers, "RF Resistivity of CarbonFibre Composite Materials." *Conf. on Electromagnetic Compatibility*, Vol. 1, pp. 1-198, Univ. of Southampton, UK, 16-18 September 1980.

11.21 J. L. Allen, "Electromagnetic Shielding Effectiveness for Isotropic and Anisotropic Materials," *RADC-TR-81-162*, Phase Report, June 1981.

11.22 F. A. Fisher and W. M. Fassell, "Lightning Effects Relating to Aircraft: Part 1 - Lightning Effects On and Electromagnetic Shielding Properties of Boron and Graphite Reinforced Composite Materials," *AFAL-TR-72-5*, January 1972.

11.23 K. F. Casey, "EMP Penetration through Advanced Composite Skin Panels," *AFWL Interaction Notes, Note 315*, December 1976.

11.24 K. F. Casey., "Electromagnetic Shielding by Advanced Composite Materials," *AFWL Interaction Notes - Note 341*, June 1977.

11.25 W. P. Geren, B. G. Melander and D. L. Hall, "Lightning Current Redistribution," Abstract presented at *1986 Lightning Conference* held at Dayton, Ohio.

11.26 B. J. C. Burrows and W. Walker, "Electromagnetic Shielding Properties of Graphite Epoxy Panels to Lightning," *Final Report No. NADC-80237-20*, Jan.-Sept. 1980.

11.27 "A Technology Plan for Electromagnetic Characteristics of Advanced Composites," *RADC-TR-76-206*, Phase Report, July 1976.

11.28 "Composite forward Fuselage Systems Integration," Vol. 1, *AFFDL-TR-78-110*, General Dynamics, September 1978.

11.29 F. W. Grover, *Inductance Calculations: Working Formulas and Tables*, New York: Dover, 1962.

Chapter 12

THE INTERNAL FIELDS COUPLED THROUGH APERTURES

12.1 Introduction

The most important mode by which electromagnetic energy couples to the interior of aircraft (metal aircraft at least) is through apertures. These are openings in the skin of an aircraft, examples of which include cockpits, wheel wells, bomb bays, seams, joints and covers on access panels. There are several reasons for the importance of aperture coupled fields. One is that apertures are effectively the only means through which external electric fields may penetrate to the interior of the aircraft. Another is that some apertures are quite large, windows being a prime example. Also, unlike fields coupled by diffusion through metal surfaces, the waveshape of the interior field is not retarded, but tends to be the same as that of the external electric and magnetic fields. The most important consequence of the coupled fields relates to the voltages induced by such fields. A field of given peak intensity is more apt to cause trouble if it rises to its peak quickly than if it is delayed and distorted. Small apertures, in fact, tend to accentuate the rate of change of the coupled fields; that is, they are more efficient at coupling high frequency components of the external electromagnetic field than at coupling low frequency components.

The subject of aperture coupling has been of considerable theoretical interest since the time of Lord Rayleigh [12.1]. Since literally hundreds of papers and articles have been written on the subject, no attempt will be made to give a complete review. Instead, this chapter will discuss the basic points of aperture coupling and make reference to the literature for additional details. Simple techniques will be given to estimate or bound responses. Also, numerical methods will be discussed which may be used to obtain more accurate results. For a more complete treatment of the mathematical aspects of aperture coupling, the reader is referred to some of the review articles that have appeared [12.2 – 12.5]. Ref. [12.2] is particularly recommended.

A distinction was made above between large and small apertures. One way to distinguish between large and small apertures is to relate the physical size of the aperture to the wavelength of the frequencies of interest. Since most of the energy in a lightning flash is contained in the frequencies below 50 MHz ($\lambda = 6$ m) it follows that most apertures on aircraft are small with respect to wavelength.

Another way to distinguish between large and small apertures is to relate them to the size of the aircraft. With a small aperture one may logically assume that the calculations of the external response of the aircraft (Chapter 10) and the calculations of how much energy propagates through an aperture may be treated separately. However, if the aperture is large with respect to the aircraft, then it will have an effect on the external response of the aircraft and the calculations of external and internal response must be done together. Examples of large apertures may include the windows in a cockpit or dielectric doors on a helicopter, or open bomb bay doors or wheel wells on a conventional aircraft.

12.2 Basic Concepts

Both electric and magnetic fields couple through apertures. For small apertures, it is convenient to determine this coupling in terms of the external electric and magnetic fields which would exist at the aperture location if the aperture were closed by a perfectly conducting surface. These fields are referred to as the short circuit fields, E_{sc} and H_{sc}, which, along with the geometry of the aperture are used to determine the magnitude of hypothetical electric and magnetic dipoles (equivalent antennas) which are placed just inside the shorted aperture. The process is shown in Figs. 12.1 and 12.2.

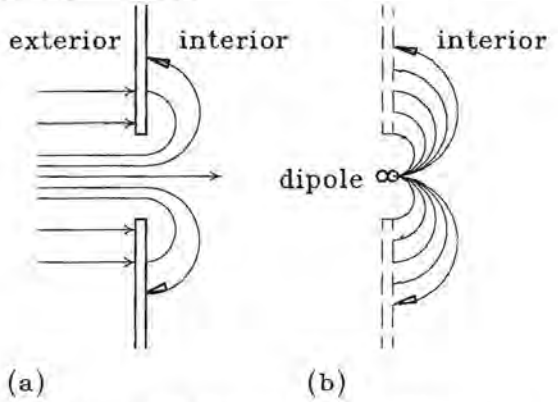

Fig. 12.1 Development of equivalent electric field dipole.
(a) Actual electric field
(b) Equivalent dipole

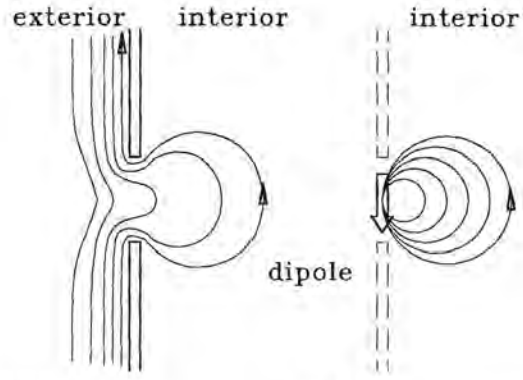

Fig. 12.2 Development of equivalent magnetic field dipole.
(a) Actual magnetic field
(b) Equivalent dipole

Analytically, the problem has two parts; first, to find the strength of the equivalent dipole and second, to evaluate the fields produced by those dipoles. For the analyses to follow, assume an electric and a magnetic field to exist on one side of an infinite conducting sheet containing an elliptical aperture; the geometry being as shown in Fig. 12.3. Because the surface is conducting, the electric field must be oriented at right angles to the surface, along the Z axis in this case. The magnetic field must be tangential to the surface. While it could be oriented in any direction in the x, y plane, it can be resolved into two components, one along the X axis and one along the Y axis. An elliptical aperture is considered because it is the most general of the elementary geometries. For this analysis the long axis of the ellipse will be taken to be along the X axis and the origin of the axes to be at the center of the ellipse.

From the reverse side of the sheet, Fig. 12.4, there is seen one equivalent electric field dipole, P, and two magnetic field dipoles, M_x and M_y, representing the x and y components of the tangential magnetic field. The amplitudes of these dipoles are:

$$M_x = 2\mu_0 \alpha_{mx} H_x \tag{12.1}$$

$$M_y = 2\mu_0 \alpha_{my} H_y \tag{12.2}$$

$$P = 2\epsilon_0 \alpha_{ez} E_z \tag{12.3}$$

where α_{mx}, α_{my} and α_{ez} are polarizability tensor elements whose magnitudes depend on the size and shape of the aperture. For the elliptical aperture, and following the treatment of Taylor [12.6, 12.7]:

$$\alpha_{mx} = \frac{\pi}{12} \frac{l_1^3 m}{K(m) - E(m)} \tag{12.4}$$

$$\alpha_{my} = \frac{\pi}{12} \frac{l_1^3 m(1-m)}{K(m) - E(m)} \tag{12.5}$$

$$\alpha_{ez} = \frac{\pi}{12} \frac{l_1^3 (1-m)}{E(m)} \tag{12.6}$$

where $m = 1-(l_2/l_1)^2$ and $K(m)$ and $E(m)$ are elliptic integrals of the first and second kind respectively.

Eqs. 12.4 - 12.6 may also be written as:

$$\alpha_{mx} = \alpha'_{mx} \times l_1^3 \tag{12.7}$$

$$\alpha_{my} = \alpha'_{my} \times l_1^3 \tag{12.8}$$

$$\alpha_{ez} = \alpha'_{ez} \times l_1^3 \tag{12.9}$$

where α'_{mx} α'_{my} and α'_{ez} are as given in Fig. 12.5.

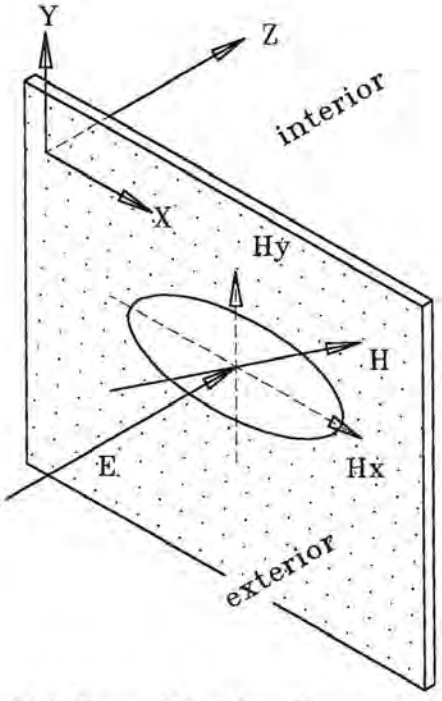

Fig. 12.3 External electric and magnetic fields impinging on an aperture.

Since the dipole strength is proportional to the cube of the length of the major axis of the aperture, it follows that large apertures will couple much more energy into an inner volume than will small apertures, the strength of the dipole increasing as the cube of the dimensions of the aperture while the area of the aperture increases only as the square of the dimensions.

Using the dipole along the X axis, M_x, as an example,the pattern of the magnetic fields in the interior region will be concentric closed loops lying in planes passed through the X axis, Fig. 12.6. At any point P, the total magnetic field can be represented as a vector normal to the radius vector r between the dipole and P and lying in the plane defined by point P and the X axis.

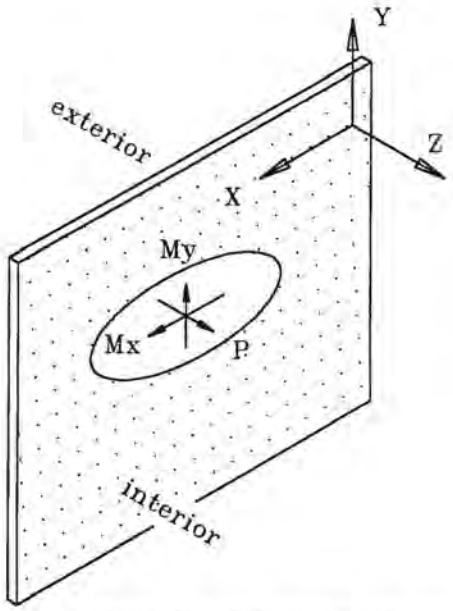

Fig. 12.4 Equivalent dipoles illuminating an interior volume.

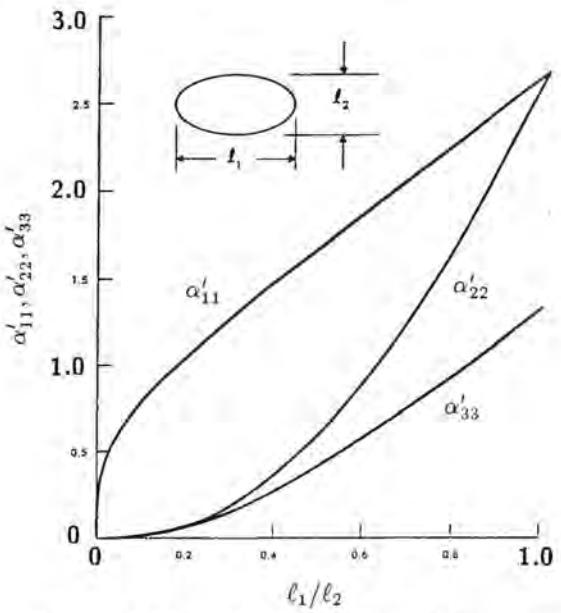

Fig. 12.5 Shape factors for elliptical apertures.

Likewise, the magnetic field due to the M_y dipole can be defined as a vector lying in the plane defined by P and the Yaxis.

The pattern of the electric field due to the P dipole will be concentric loops originating at the dipole and terminating on the plane containing the aperture.

The above describes the pattern of the static fields. If the fields change with time there will also

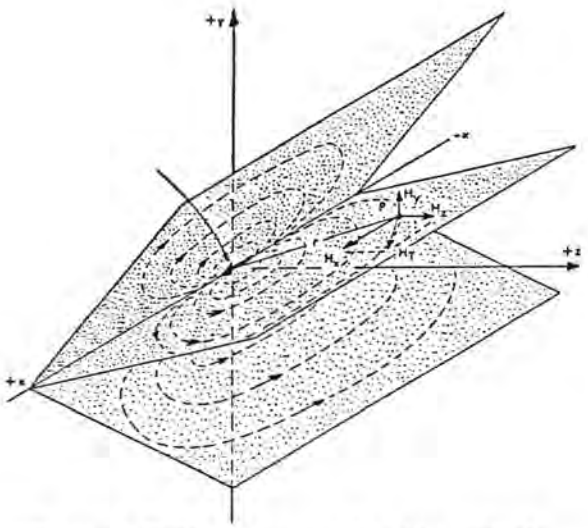

Fig. 12.6 Field patterns produced by a dipole lying along the X axis.

be magnetic fields produced by the changing electric fields and electric fields produced by the changing magnetic fields. In the frequency domain, and following the treatment in [12.8], the electric and magnetic fields can be described succinctly as

$$E_f = -\frac{1}{\epsilon_0}\nabla \times [P_f \times \nabla G_f] + j\omega\mu_0 M_f \times \nabla G_f \tag{12.10}$$

$$H_f = j\omega[P_f] \times \nabla\ G_f\ \nabla[M_f \times \nabla G_f], \tag{12.11}$$

where

$$G_f = e^{-\gamma r}/4\pi r \tag{12.12}$$

r = the distance to the point of observation

γ = propagation constant(§9.4.6) (12.13)

P_t = electric dipole

M_t = the total magnetic dipole (the sum of M_x and M_y)

∇ = vector differential operator.

P_f and M_f are vector quantities.

In the time domain, E and H are given by

$$E_t = \frac{1}{4\pi\epsilon_0}\nabla \times \left[\frac{1}{r^2}P_t \times u_z \times u_r\right] - \frac{\mu_0}{4\pi}\frac{1}{r^2}\dot{M}_t \times u_r \tag{12.14}$$

$$H_t = \frac{1}{4\pi\epsilon_0}\frac{1}{r^2}P)tu_z \times u_r + \frac{1}{4\pi}\nabla \times \left[\frac{1}{r^2}\dot{M}_t \times u_r\right], \tag{12.15}$$

where u_z is the unit vector perpendicular to the plane of the aperture, and the dot represents time differentiation. Note that the equations neglect the radiated far field components.

12.3 Apertures of Shape Other than Elliptical

If the aperture under consideration is not elliptical, a corresponding elliptical aperture can generally be specified, as shown in Fig. 12.7. The equivalent aperture would have the same area and the same eccentricity as those of the aperture under study.

Polarizabilities for many shapes have been determined numerically and analytically. Table 12.1 and Figs. 12.8 – 12.10 from [12.2] show examples.

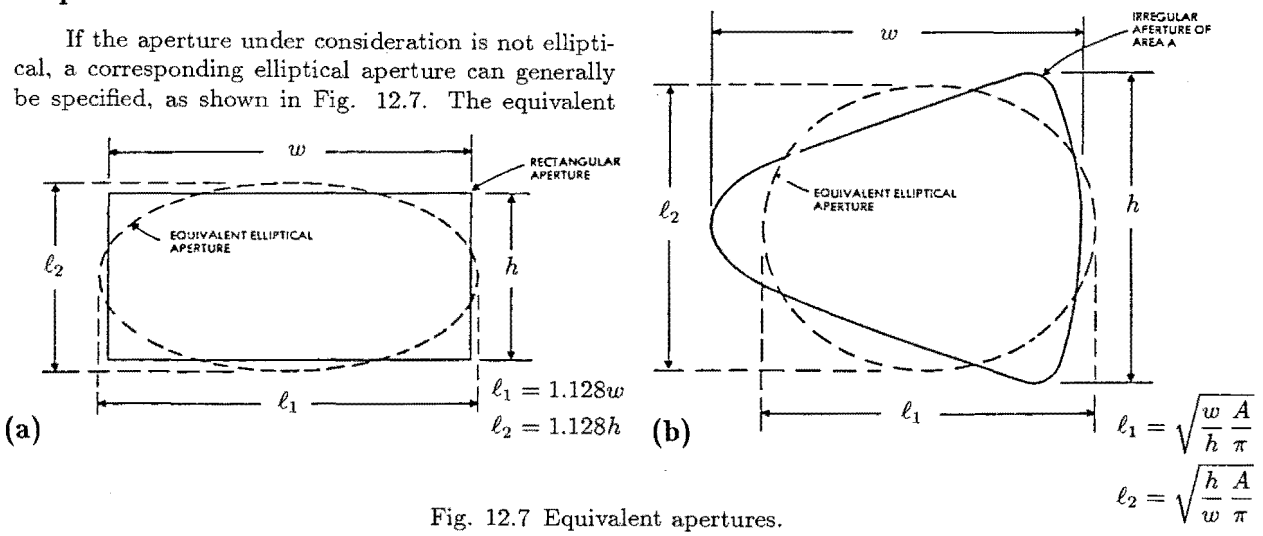

Fig. 12.7 Equivalent apertures.
(a) Rectangular aperture
(b) Irregular aperture

Table 12.1

Aperture Polarizabilities

Shape	$\alpha_{e,zz}$	$\alpha_{m,xx}$	$\alpha_{m,yy}$
Circle (d = Diameter)	$\frac{1}{12}d^3$	$\frac{1}{6}d^3$	$\frac{1}{6}d^3$
Ellipse*	$\frac{\pi}{24}\frac{w^2\ell}{E(m)}$	$\frac{\pi}{24}\frac{\ell^3 m}{K(m)-E(m)}$	$\frac{\pi}{24}\frac{\ell^3 m}{(\ell/w)^2E(m)-K(m)}$
Narrow Ellipse ($w \ll \ell$)	$\frac{\pi}{24}w^2\ell$	$\frac{\pi}{24}\frac{\ell^3}{\ln(4\ell/w)-1}$	$\frac{\pi}{24}w^2\ell$
Narrow Slit ($w \ll \ell$)	$\frac{\pi}{16}w^2\ell$	$\frac{\pi}{24}\frac{\ell^3}{\ln(4\ell/w)-1}$	$\frac{\pi}{16}w^2\ell$

* Ellipse eccentricity $e = \sqrt{1-(w/\ell)^2}$,

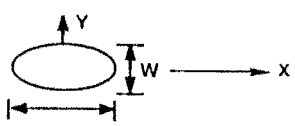

K and E are the complete elliptic integrals of the first and second kind, $m = e^2$.

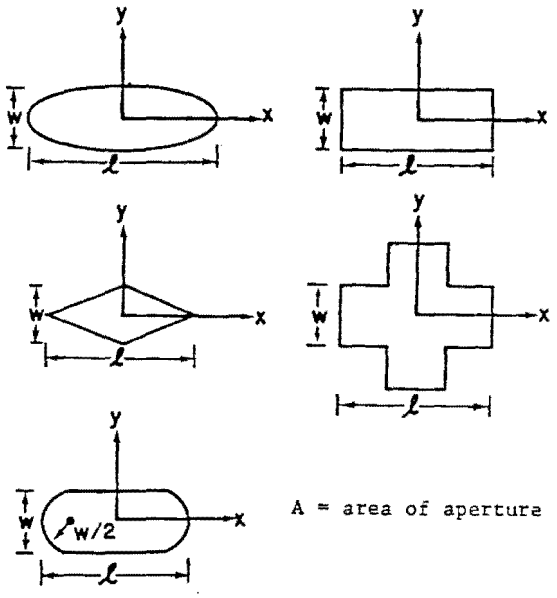

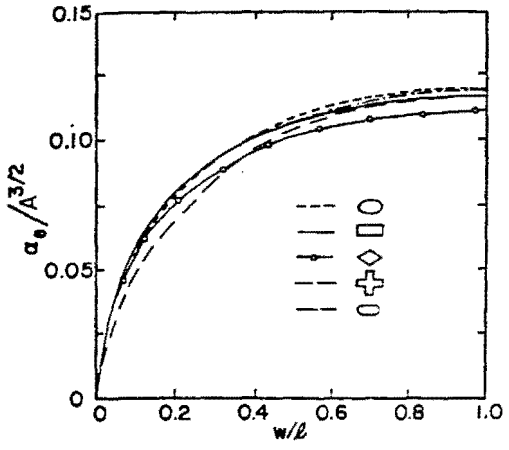

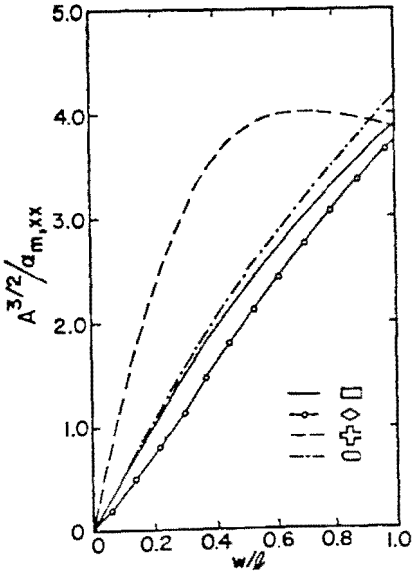

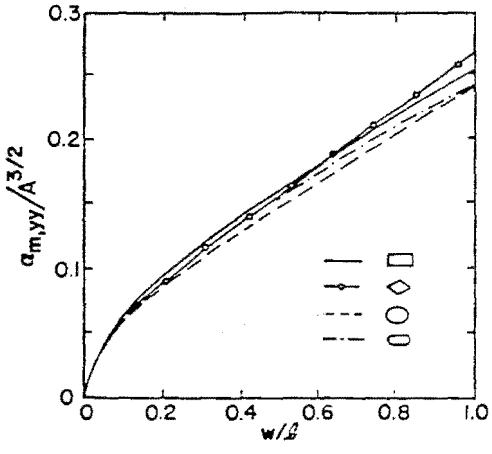

Fig. 12.8 Shape factors for various apertures.

(a) Shapes

(b) Normalized electric field polarizability

(c) Normalized magnetic field polarizability for X direction

(d) Normalized magnetic field polarizability for Y direction

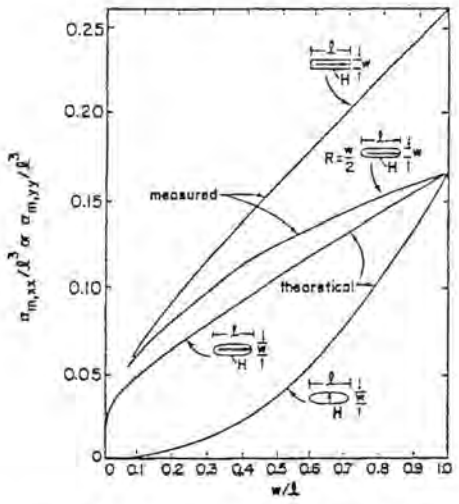

Fig. 12.9 Normalized magnetic (imaged) polarizabilities for elliptical, rectangular and rounded rectangular apertures.

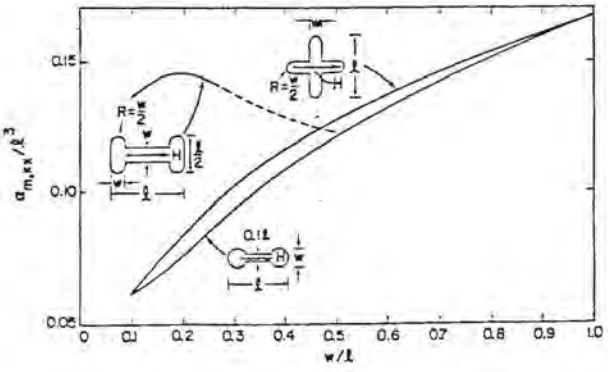

Fig. 12.10 Normalized magnetic (imaged) polarizabilities for three aperture shapes.

12.4 Treatment of Surface Containing the Aperture

Some formulations defining polarizability, and thus the strength of the dipoles, use a factor of 24 in the numerator, rather than the factor 12 used in Eqs. 12.4 – 12.6. Table 12.1 and Figs.12.8 – 12.10 are examples. This difference occurs because there are two different approaches to treating the dipoles. One is to consider the surface to be absent and the dipoles to be located in free space. The *location* of the surface containing the aperture is then used only to divide the exterior and interior regions; calculations being made only for the interior region. The other approach is to consider the surface containing the aperture to be present and acting as a reflecting surface with the dipole located just in front of the surface.

With the first approach, the strength of the dipoles would be as given by Eqs. 12.4 – 12.6, using the factor 12 in the numerator. With the second approach the strength of the dipoles would be half that given by Eqs. 12.4 – 12.6 (factor of 24),but calculations of field strength would have to consider the presence of the reflection in the surface of the dipoles; the effect of the reflection being to double the total field strength and restore the total dipole strength to that given by Eqs. 12.4 – 12.6. The two approaches give the same answer, but the second approach is the more physically correct, particularly when treating apertures defined by two or more surfaces, a subject considered in more detail in Section 12.6.

12.5 Fields Produced by the Dipoles

While Eqs. 12.10 and 12.11 or Eqs. 12.14 and 12.15 succinctly define the fields produced by the dipoles, they must be expanded in order to obtain numerical results.

12.5.1 Complete Formulation – Frequency Domain

The complete formulation [12.6, 12.7] of the fields produced by the dipoles (neglecting the far field radiation component) is, in the frequency domain:

From the magnetic dipole along the X axis:

$$E_{yx} = F1\left(-k_0 + j/r\right)\frac{z}{r} \tag{12.16}$$

$$E_{zx} = F1\left(-k_0 + j/r\right)\frac{y}{r} \tag{12.17}$$

$$H_{xx} = 2F1\left(j\frac{k_0}{r} + \frac{1}{r^2}\right)\frac{x^2}{r^2} - F1\left(j\frac{k_0}{r} + \frac{1}{r^2} - k_0^2\right)\frac{r^2 - x^2}{r^2} \tag{12.18}$$

$$H_{yx} = 2F1\left(j\frac{k_0}{r} + \frac{1}{r^2}\right)\frac{xy}{r^2} + F1\left(j\frac{k_0}{r} + \frac{1}{r^2} - k_0^2\right)\frac{xy}{r^2} \tag{12.19}$$

$$H_{zx} = 2F1\left(j\frac{k_0}{r} + \frac{1}{r^2}\right)\frac{xz}{r^2} - F1\left(j\frac{k_0}{r} + \frac{1}{r^2} - k_0^2\right)\frac{xz}{r^2} \tag{12.20}$$

where

$$F1 = \frac{M_x}{4\pi r}e^{jk_0 r} \tag{12.21}$$

$$k_0 = \frac{\omega}{3 \times 10^8}. \tag{12.22}$$

From the magnetic dipole along the Y axis:

$$E_{xy} = F2\left(-k_0 + j/r\right)\frac{z}{r} \tag{12.23}$$

$$E_{zy} = F2\left(-k_0 + j/r\right)\frac{x}{r} \tag{12.24}$$

$$H_{xy} = 2F2\left(j\frac{k_0}{r} + \frac{1}{r^2}\right)\frac{xy}{r^2} - F2\left(j\frac{k_0}{r} + \frac{1}{r^2} - k_0^2\right)\frac{xy}{r^2} \tag{12.25}$$

$$H_{yy} = 2F2\left(j\frac{k_0}{r} + \frac{1}{r^2}\right)\frac{y^2}{r^2} + F2\left(j\frac{k_0}{r} + \frac{1}{r^2} - k_0^2\right)\frac{r^2 - y^2}{r^2} \tag{12.26}$$

$$H_{zy} = 2F2\left(j\frac{k_0}{r} + \frac{1}{r^2}\right)\frac{yz}{r^2} - F2\left(j\frac{k_0}{r} + \frac{1}{r^2} - k_0^2\right)\frac{yz}{r^2} \tag{12.27}$$

where

$$F2 = \frac{M_y}{4\pi r}e^{jk_0 r}. \tag{12.28}$$

From the electric dipole along the Z axis:

$$E_{xz} = 2F3\left(j\frac{k_0}{r} + \frac{1}{r^2}\right)\frac{xz}{r^2} + F3\left(j\frac{k_0}{r} + \frac{1}{r^2} - k_0^2\right)\frac{xz}{r^2} \tag{12.29}$$

$$E_{yz} = 2F3\left(j\frac{k_0}{r} + \frac{1}{r^2}\right)\frac{yz}{r^2} + F3\left(j\frac{k_0}{r} + \frac{1}{r^2} - k_0^2\right)\frac{yz}{r^2} \tag{12.30}$$

$$E_{zz} = 2F3\left(j\frac{k_0}{r} + \frac{1}{r^2}\right)\frac{z^2}{r^2} - F3\left(j\frac{k_0}{r} + \frac{1}{r^2} - k_0^2\right)\frac{r^2 - z^2}{r^2} \tag{12.31}$$

$$H_{xz} = \eta_0 F3\left(k_0 + \frac{j}{r}\right)\frac{y}{r} \tag{12.32}$$

$$H_{yz} = \eta_0 F3\left(k_0 + \frac{j}{r}\right)\frac{x}{r} \tag{12.33}$$

where

$$F3 = \frac{P}{4\pi\epsilon_0 r}e^{jk_0 r} \tag{12.34}$$

$$\eta_0 f = \frac{\eta_0 k_0 P_0}{4\pi r}. \tag{12.35}$$

The x, y and z components of the total magnetic field strength at P would be the sum of the components produced by the dipoles lying along the X and Y axes:

$$H_x = H_{xx} + H_{xy} \tag{12.36}$$

$$H_y = H_{yx} + H_{yy} \tag{12.37}$$

$$H_z = H_{zx} + H_{zy}. \tag{12.38}$$

The total magnetic field at point P would be:

$$H_T = \sqrt{H_x^2 + H_y^2 + H_z^2}. \tag{12.39}$$

12.5.2 Low Frequency Approximation

At low frequencies, where the k_0 term is negligible, the equations are simplified.

From the magnetic dipole located along the X axis:

$$E_{xx} = 0 \tag{12.40}$$

$$E_{zx} = 0 \tag{12.41}$$

$$H_{xx} = \frac{M_x}{4\pi}\left[\frac{3x^2 - r^2}{r^5}\right] \tag{12.42}$$

$$H_{yx} = \frac{M_x}{4\pi}\left[\frac{3xy}{r^5}\right] \tag{12.43}$$

$$H_{zx} = \frac{M_x}{4\pi}\left[\frac{3xz}{r^5}\right]. \tag{12.44}$$

From the magnetic dipole located along the Y axis:

$$E_{xy} = 0 \tag{12.45}$$

$$E_{zy} = 0 \tag{12.46}$$

$$H_{xy} = \frac{M_y}{4\pi}\left[\frac{3xy}{r^5}\right] \tag{12.47}$$

$$H_{yy} = \frac{M_x}{4\pi}\left[\frac{3y^2 - r^2}{r^5}\right] \tag{12.48}$$

$$H_{zy} = \frac{M_x}{4\pi}\left[\frac{3yz}{r^5}\right]. \tag{12.49}$$

From the electric dipole located along the Z axis:

$$E_{xz} = \frac{P}{4\pi}\left[\frac{3xz}{r^5}\right] \tag{12.50}$$

$$E_{yz} = \frac{P}{4\pi}\left[\frac{3yz}{r^5}\right] \tag{12.51}$$

$$E_{zz} = \frac{P}{4\pi}\left[\frac{3z^2 - r^2}{r^5}\right] \tag{12.52}$$

$$H_{xz} = 0 \tag{12.53}$$

$$H_{yz} = 0 \tag{12.54}$$

$$H_{zz} = 0. \tag{12.55}$$

An example of an aperture–coupled field is shown in Fig. 12.11 in which the elliptical fuselage described in Section 10.5.4 has been approximated by two sheets of infinite size, one containing the aperture and another serving as the reflecting surface. The figure shows only the top half of the field pattern, the field in the bottom half being symmetrical with the top half. The aperture considered was 0.2 m high by 0.1 m wide, the long axis of the ellipse being oriented at right angles to the plane of the figure. The short circuit field strength (the field that would exist if the aperture were not there) was taken as 160 A/m, the field strength that would be produced by the aforementioned current of 1000 A flowing axially along the elliptical fuselage. The field strength that would exist at the aperture was 80 A/m, half of the short circuit field.

The field strength is seen to be inversely proportional to the cube of the distance from the aperture to the point in question. Accordingly, the aperture coupled fields will be localized in space near the aperture. Small apertures are thus less troublesome than large apertures, both because of the decreased magnetic field strength associated with the corresponding dipole and because of the lesser distance one must be removed from the aperture before the field strength becomes negligible compared to the field strength near the aperture.

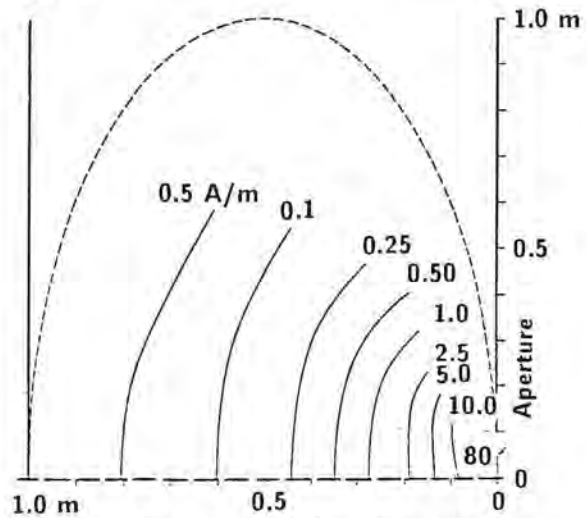

Fig. 12.11 Fields coupled through an aperture. Major axis oriented vertically (0.3 x 0.1 m aperture).

12.5.3 Limitations

The above formulation is valid only when the point at which the field is to be calculated is at a distance from the aperture that is large compared to the dimensions of the aperture. If an attempt is made to calculate the fields near the aperture the results will be too high, becoming infinite at zero distance from the plane of the aperture. Correction factors [12.9] may be applied to the above equations if the distance from the aperture is not large, Fig. 12.12 showing an example. Formulations of the problem can also be devised that are not based on the use of infinitesimal dipoles, but a simple rule of thumb is to recognize that the field at the plane of the aperture cannot be greater than half the magnitude of the short circuit field and simply to ignore numerical answers that are larger.

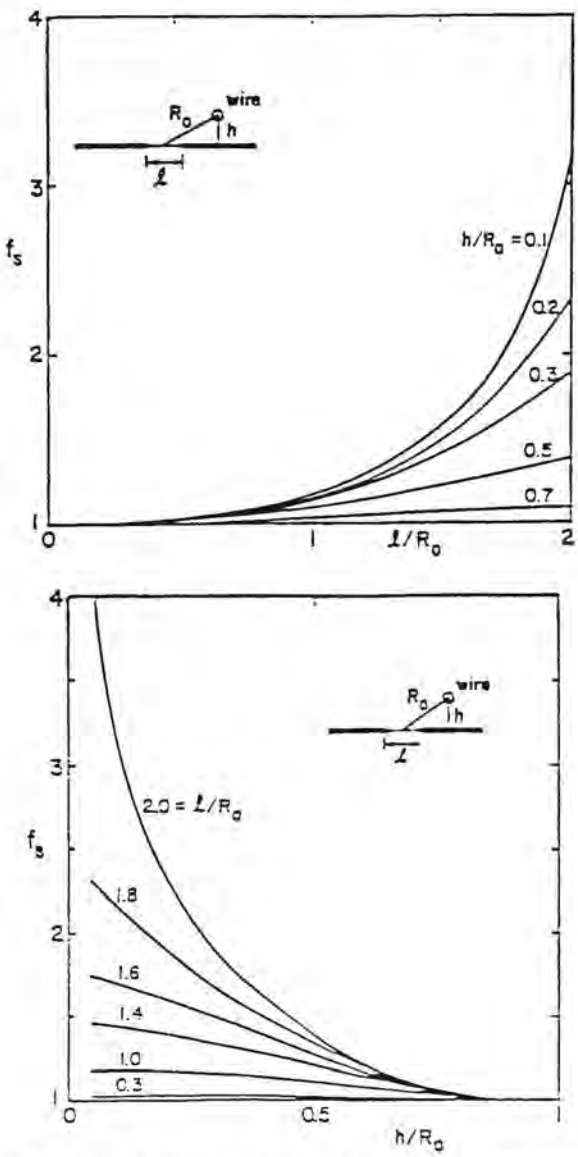

Fig. 12.12 Correction factors for a circular aperture.
(a) In terms of l/R_o
(b) In terms of h/R_0

12.6 Reflecting Surfaces

Frequently a calculation made to determine the effects of coupling through apertures needs to take into account the presence of reflecting surfaces. The simplest case, shown in Fig. 12.13, treats one reflecting surface of infinite extent and parallel to the surface containing the aperture. The total field at any point between the two surfaces is the sum of the fields produced by the infinite array of images of the original magnetic dipole. The field strength from each of the images would again be determined from Eqs. 12.16 through 12.55. Fortunately, in most cases only a few of the images need be considered because of the dependence of field strength on the cube of the distance to the point under consideration. The presence of reflecting surfaces will never cause the fields to be more than double the value due to the aperture by itself, an observation that may make calculating the effects of reflecting surfaces an unnecessary exercise.

In principle, additional reflecting surfaces could be included in the formulation to define completely an interior volume. Such reflecting surfaces are shown in Fig. 12.14.

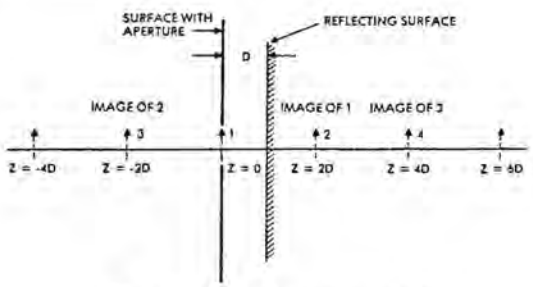

Fig. 12.13 Reflecting surface.

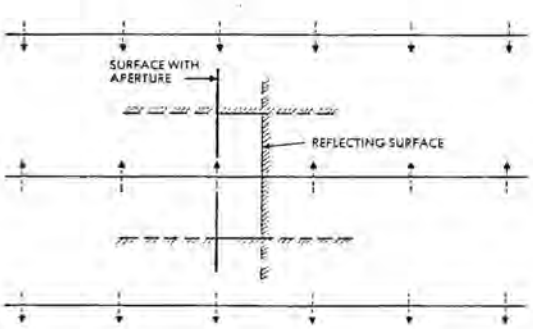

Fig. 12.14 Multiple reflecting surfaces.

12.7 Coupling From an Aperture to a Cable

If there is a cable in the space illuminated by the aperture, voltages and current will be induced into that cable. They can be determined by developing an equivalent circuit of the aperture, inserting that circuit into the cable and solving for the response of the cable. For this illustration, the aperture will be considered circular. The geometry of the situation is shown in Fig. 12.15. A cable having a characteristic surge impedance Z is located at height h above the surface containing the aperture and at a distance w from the aperture. The surge impedance is

$$Z = \sqrt{L/C} \tag{12.56}$$

$$\approx 60 \ln(2h/a). \tag{12.57}$$

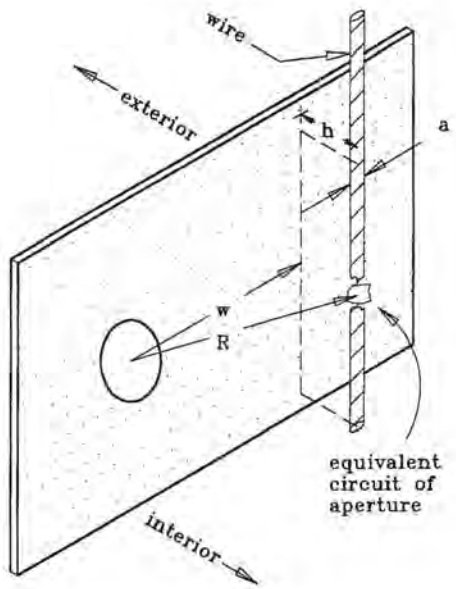

Fig. 12.15 Coupling from an aperture to a wire.

An equivalent circuit of the aperture is shown in Fig. 12.16. There are two aspects of the equivalent circuit that must be considered, the first being to determine the equivalent generators V_{eq} and I_{eq}. The second is to determine the effect that the aperture has on the inductance and capacitance of the cable. In an elementary geometry, the inductance, capacitance and surge impedance of the cable will be governed by the spacing between the cable and the adjacent ground plane, such as the conducting surface containing the aperture. In the region near the aperture the cable will, effectively, be farther from the ground plane, and so will have a somewhat larger inductance and a somewhat smaller capacitance. One could determine the pattern of the electromagnetic fields around the cable and so determine the localized inductance and capacitance, but it is easier to consider the cable to have a constant impedance and to account for these effects by

including an aperture inductance L_a and an aperture capacitance C_a in the equivalent circuit of the aperture. The capacitance is negative. Except for cables directly over the aperture, the aperture inductance and capacitance are usually small enough that they can be ignored.

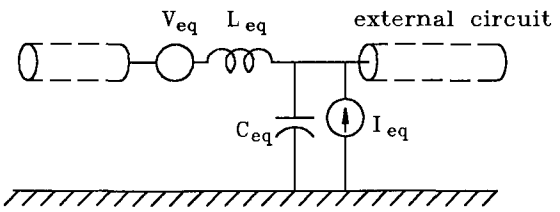

Fig. 12.16 Equivalent circuit of an aperture.

The approaches given in [12.9 – 12.12] provide an upper bound estimate to the equivalent generators and the inductance and capacitance due to the aperture.

$$V_{eq} = j\omega\mu_0 \left[\frac{h}{\pi R_0^2}\right] u_x \cdot \alpha_m \cdot H_{sc} \qquad (12.58)$$

$$I_{eq} = j\omega\epsilon_0 \left[\frac{h}{R_0^2}\right] \frac{\alpha_e Z_0}{Z_c} E_{sc} \qquad (12.59)$$

$$L_a = \mu_0 \alpha_m \left[\frac{h}{\pi R_0^2}\right]^2 \qquad (12.60)$$

$$C_a = -\mu_0 \left[\frac{\alpha_e}{Z_c^2}\right] \left[\frac{h}{\pi R_0^2}\right]^2. \qquad (12.61)$$

where $Z_0 = 377$ ohms, the impedance of free space.

It should be noted that these estimates are valid if the aperture is small with respect to wavelength, and if the distance to the cable is several times the length of the aperture. If the cable is too close to the aperture for Eqs. 12.58 – 12.61 to be valid, then correction factors, f_s, for the sources may be used [12.10]:

$$V_{eq} = f_s V_{eq-\text{small hole}} \qquad (12.62)$$

$$I_{eq} = f_s I_{eq-\text{small hole}}. \qquad (12.63)$$

Correction factors for a circular aperture were shown in Fig. 12.12.

The upper bound approach has been demonstrated experimentally [12.13]. A wire having a surge impedance of 240 ohms and terminated at each end in 240 ohms was placed adjacent to a circular aperture having a diameter of 0.1 m. A magnetic field having a short circuit current density as shown in Fig. 12.17 was established around the aperture and the voltage and current induced on the wire were measured. Measured (I_m) and calculated (I_c) values of current for various values of h and w (Fig. 12.17) are shown in Table 12.2. Also shown is the ratio of I_c/I_m. The table indicates that the calculated values are indeed upper bounds and that the ratio is much bigger where the wire is very close to the aperture.

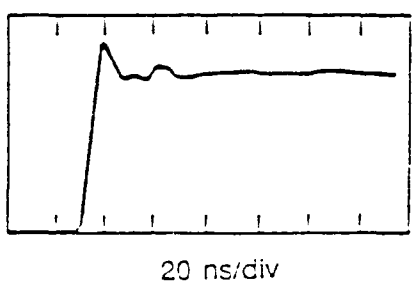

Fig. 12.17 Surface current density at aperture.

Table 12.2

Measured Currents and Calculated Upper Bounds For an Aperture Radius of 0.1 m and a 240 Ohm Transmission Line Terminated in 240 Ohms at Each End

h (m)	W (m)	$I_{measured}$ (ma)	$I_{calculated}$ (ma)	Ratio I_c/I_m
0.007	0	48	1400	29.2
0.050	0	22	197	8.9
0.100	0	13.2	98.5	7.6
0.007	0.23	0.3	1.3	4.3
0.100	0.23	2.8	15.6	5.6
0.200	0.23	3.8	21.2	5.6

It is also possible to derive less accurate (and more severe) upper bounds for the equivalent sources of Fig. 12.16, based on much simpler estimates. These are based on calculating the effective aperture inductance and capacitance, respectively. They can be derived by assuming that the aperture equivalent magnetic and electric dipole moments arise from a linear distribution of magnetic and electric currents on a dipole of finite length. The term "linear distribution" means that the current is maximum at the center of the dipole and falls off linearly to zero at the ends. The equivalent sources are:

$$V_{eq} \le L_a \cdot \frac{\partial J_{xsc}}{\partial t} \tag{12.64}$$

$$I_{eq} \le C_a \cdot \frac{\partial E_{zcc}}{\partial t} \tag{12.65}$$

$$L_a = \frac{2\mu_0 \alpha_{mxx}}{l_m} \tag{12.66}$$

$$C_a = \frac{2\epsilon_0 \alpha_{ezz}}{l_e} \tag{12.67}$$

Eq. 12.66 pertains to current flowing in the x direction and l_m is the length of the aperture in the y direction; that is, in the direction normal to the flow of current. A similar equation could be written for current flowing in the y direction with l_m pertaining to the length of the aperture in the x direction.

In Eq. 12.67, l is the smaller dimension defining the aperture, that is, l_2 in Fig. 12.5 or w in Table 12.1.

12.8 Slots

The coupling through slots, cracks, or other narrow gaps in the aircraft skin, may be analyzed by treating each as a slot antenna, as in Fig. 12.18. Since the slot antenna is the electromagnetic counterpart of the strip dipole, its characteristics can be found from the characteristics of the strip dipole. If the slot is short relative to the wavelength of the external field, the relevant equations [12.14] are as follows:

The fatness parameter for strip dipoles is given by

$$\Omega = 2 \ln \frac{8h}{w}, \tag{12.68}$$

For large fatness, the effective height of the slot or its complementary dipole is

$$h_{e(\text{slot})} = h_{e(\text{dipole})} = \frac{h}{2}. \tag{12.69}$$

Then the short–circuit current is

$$I_{sc} = 2h_e J_y. \tag{12.70}$$

The impedance of the strip dipole is capacitive and given by

$$C_{\text{dipole}} = \frac{h}{1.8 \times 10^{10}(\Omega - 3.39)} \text{ farads.} \tag{12.71}$$

for h in meters.

The impedance of the slot antenna is related to the impedance of the strip dipole by:

$$Z_{\text{slot}} = \frac{(60\pi\Omega)^2}{Z_{\text{dipole}}} \tag{12.72}$$

$$= \frac{(60\pi\Omega)^2}{1/(j\omega C_{\text{dipole}})} \tag{12.73}$$

$$= (60\pi\Omega)^2 j\omega C_{\text{dipole}}. \tag{12.74}$$

Hence, the impedance of the slot antenna is inductive.

To calculate the coupling to internal cables, one can use Z_{slot} in Eq. 12.74 as a transfer impedance and I_{sc} as one half of the current intercepted by the slot. Then, $V_{\text{int}} = Z_{\text{slot}} I_{\text{sc}}$ gives the internal voltage rise across the slot. This voltage rise is an upper bound and can be used a point source to drive internal cavities or cables.

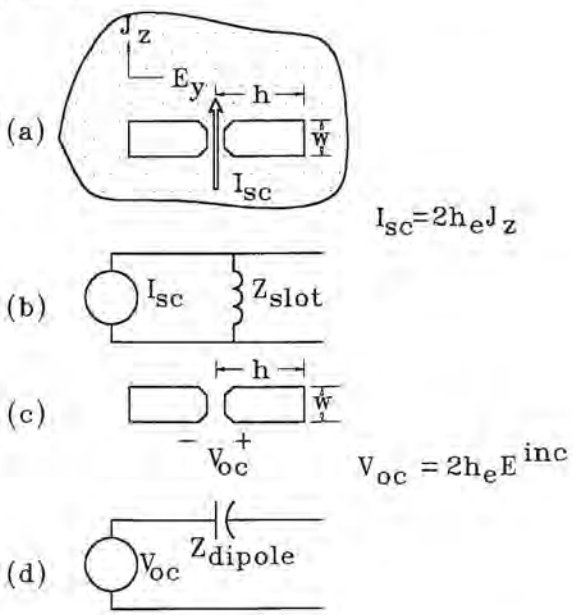

Fig. 12.18 Slot antenna.
(a) Slot in a conducting sheet
(b) Equivalent circuit
(c) Complementary strip dipole
(d) Equivalent circuit

12.9 Seams

On an aircraft, seams are formed when sections of skin are joined together by rivets or other fasteners. Other seams may be formed by wheel well or bomb bay

doors, in which case, long thin open slots are created. The coupling through such seams is on the borderline between the aperture coupling described in this chapter and the diffusion coupling described in Chapter 11.

Coupling into seams may be discussed in terms of Fig. 12.19, which shows a lightning current of density J_s flowing across the seam. The current, flowing through the transfer impedance of the seam creates a voltage rise on the interior surface. Transfer impedance typically has two components; a resistive component due to the flow of current through resistive films or through resistive fasteners and an inductive component due to leakage of magnetic fields. The resistive component generally predominates when overlapping metal surfaces are joined permanently with rivets or bolts. With surfaces that are easily separable, such as access panels providing entry to equipment bays, the inductive component may predominate. An impedance proportional to the square root of frequency is frequently observed if the faying surfaces make good metal–to–metal contact and the seam is fastened with multiple tightly fitting rivets [12.15]. Such an impedance is characteristic of the diffusion coupling mechanism discussed in Chapter 11.

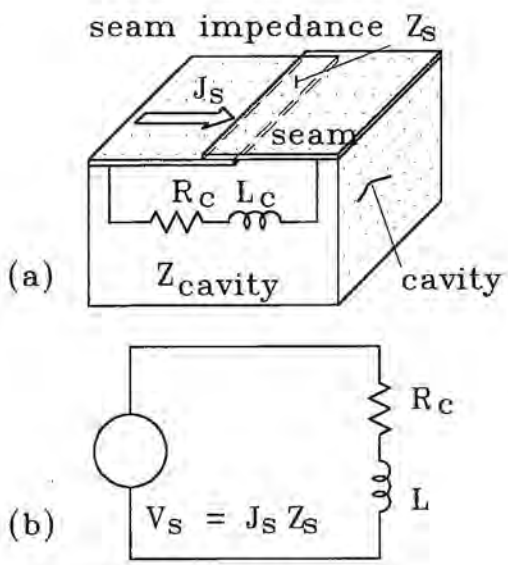

- RESISTIVE SEAM: $V_S = R_S J_S$
- INDUCTIVE SEAM: $V_S = L_S \frac{\partial J_S}{\partial t}$
- R_S = TRANSFER RESISTANCE
- L_S = TRANSFER INDUCTANCE

Transfer Impedance Z_t

- V_S ACTS AS A SOURCE WHICH DRIVES INTERIOR OF SHIELDED VOLUME

Fig. 12.19 Seams and joints.

Seam impedances have amplitudes in the range 10^{-6} to 1 $\Omega \cdot$ m, with typical values on the order of 10^{-3} $\Omega \cdot$ m. The lowest resistance is, of course, associated with the most tightly joined contacts.

12.10 Incorporation of Seam Impedances into Numerical Solutions

The concept of seam impedances can easily be used to calculate internal fields in cavities with the 3D finite difference technique. For example, for a seam with resistive and inductive components, the potential across the seam is:

$$E_t = \frac{(L\partial J_s/\partial t + R_s J_s)}{\Delta_s} \qquad (12.75)$$

where

E_t = transverse electric field in the joint
L = seam inductance
R = seam resistance
Δ_s = finite difference cell size

These values of E in the seam aperture create a boundary condition on electric fields which is used to solve Maxwell's finite difference equations. Because of the finite cell size needed in this type of code, the fields within one or two cells away from the aperture are not accurately modeled, but the fields further than that are accurately modeled. There are examples of comparisons of this method to experiment for nuclear electromagnetic pulse coupling to shelters, with excellent agreement [12.16 – 12.18].

12.11 Analysis of Complex Apertures

Classical methods (integral–equation techniques, small hole theory) of analyzing apertures are confounded by the presence of irregularly–shaped cavities which contain conductors. It appears that numerical techniques provide the best hope for solving realistic geometries. These techniques, such as the finite difference method, can solve irregular geometries. A possible limitation, however, is that, in order to resolve small geometrical features, small grid size and time steps must be used, which may place unreasonable demands on computer resources.

There are techniques, however, which can be used to solve the aircraft external interaction response with a large grid, and then use the large grid results to solve a small subset (e.g., an aperture) of the aircraft with a smaller grid which can resolve the geometrical details. Three approaches are presented here: a technique based on the equivalence principle; an approximate technique based on the uniqueness theorem; and a nested subgrid approach.

12.11.1 Equivalence Principle

The equivalence principle is discussed in [12.19]. Consider the generalized conducting body containing a cavity backed aperture, Fig. 12.20. Let S be the surface of the body, S_1 be the surface of the aperture, and V and V_1 be the volume of the body and the enclosed cavity, respectively. The field everywhere is broken into three components:

$$E = E^i + E^s + E^p \tag{12.76}$$
$$H = H^i + H^s + H^p \tag{12.77}$$

where E, H is the total field, E^i, H^i is the incident field produced by a distant source, E^s, H^s is the field scattered by the body with no aperture and no cavity present, and E^p, H^p is the "perturbed field" – the difference between the scattered field with and without the aperture and cavity present.

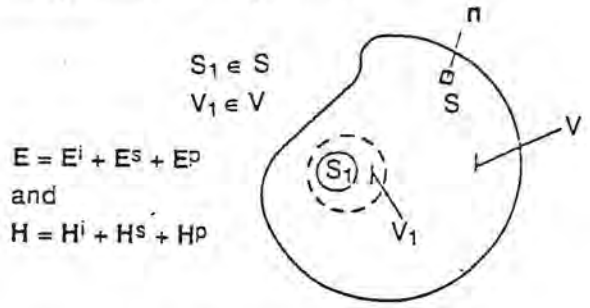

Fig. 12.20 Cavity backed aperture.

According to the equivalence theorem, the surface electric and magnetic current densities,

$$J_s = H \times n \tag{12.78}$$
$$M_s = n \times E, \tag{12.79}$$

if they are introduced in the surface S in place of the distant source, will produce the correct E, H field inside S, and zero field outside [12.20]. Here, the medium inside S is the medium of the body including the cavity behind the aperture.

Because the polarization and conduction currents that are responsible for the E^p, H^p components of the fields are contained within S, one can also define surface current densities:

$$J_s^p = n \times H^p \tag{12.80}$$
$$M_s^p = E^p \times n. \tag{12.81}$$

These produce the E^p, H^p component of the fields outside S with no field inside. If these two components are added together, the resultant current densities,

$$J_s' = J_s + J_s^p = (H - H^p) \times n \tag{12.82}$$
$$M_s' = M_s + M_s^p = n\,(E - E^p), \tag{12.83}$$

distributed over S, produce the correct total field inside S (E and H) and the perturbed field (E^p and H^p) outside S. Substituting Eqs. 12.80 and 12.81 into Eqs. 12.82 and 12.83 yields:

$$J_s' = (H^i + H^s) \times n \tag{12.84}$$
$$M_s' = n \times (E^i + E^s). \tag{12.85}$$

Considerable simplification in these formulas can be made; first, because $E^i + E^s = 0$ on a good conductor, and second, because J_s' impressed on the surface of the conductor produces no field (by application of the reciprocity theorem). Therefore the correct "total field" (E, H) inside the cavity and the correct "perturbed field" outside the body (E^p, H^p), are obtained by impressing a source current $J_s' = (H_{\tan,\,c}) \times n$ over the aperture S_1 in the body.

12.11.2 Uniqueness Theorem

Fig. 12.21 illustrates the uniqueness theorem. The approach is to first solve for the external interaction response of the aircraft with a large grid, all apertures being closed. Then, a region around the aperture is defined and the initial fields within the region R and the boundary fields (for all time) are stored. Next, a second problem is solved in which only the aperture and the region R are represented, but with a much finer grid size.

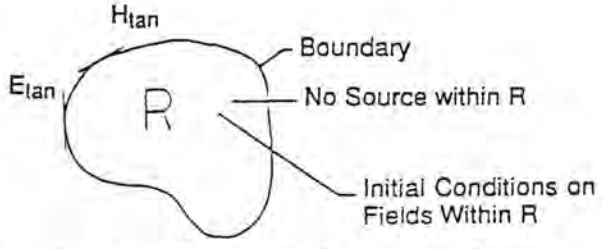

Fig. 12.21 Illustration of uniqueness theorem.

Advantages and disadvantages: The main advantage of this approach is that the solution does not require a radiation boundary (as does the equivalence principle approach) and this greatly eases the computer require-

ments. The disadvantage of the approach is that it is an approximation which assumes that the boundary fields do not not significantly depend on the presence or absence of the aperture. Considering the degree to which the external fields produced by lightning are truly known in the first place (as opposed to precisely calculated) this may not be much of a practical difficulty.

Steps in the process: The analytical procedure consists of three main steps. The first step is to short the aperture and solve for the fields external to the aircraft. This is done with a three–dimensional finite–difference code using a rather coarse gridding. At each step of the finite–difference code, the fields on a surface surrounding the eventual position of the aperture are stored. These stored fields are necessary to determine boundary conditions when the aperture is opened.

The second step is to shrink the gridding down to a size that is compatible with adequate modeling of the aperture. Hence it should be fine enough that several grid points fall within the now open aperture. The stored fields from step one serve as boundary conditions for the finer grid.

Shrinking the grid introduces two problems. The first is that the finer grid has more points on its boundary than the coarse grid that was stored, so it is necessary to interpolate for the additional points. Secondly, the finer gridding usually demands a smaller time step in the finite difference process; thus interpolation between stored time steps is necessary.

The third step in the analytic procedure is to again solve for the fields inside the cavity in a finite–difference fashion using the finer grid and the stored, interpolated boundary conditions. The uniqueness theorem implies that the internal fields are correct, assuming that the presence of the aperture does not significantly affect the boundary fields. This approximation should be valid if the boundary is kept far from the aperture.

Example: Calculations have been done employing the uniqueness theorem to solve for a cable response inside a C–130 aircraft struck by lightning [12.21]. The example presented here is for a cable in the cockpit. The code used to solve for the external fields is a three–dimensional finite difference code discussed in [12.21]. The boundary chosen for the example is shown in Fig. 12.22 and the cockpit window aperture is the hatched area in the figure. A three–dimensional finite difference code was used to solve for fields at various points inside the cockpit, and incorporated a cable bundle two inches in diameter running vertically in the cockpit 1.3 meters behind the window. Matching resistors were placed on the ends, and the voltage and current at the top end of the wire were calculated. The cable bundle was incorporated by standard finite difference thin wire techniques [12.20]. The example was run for three lightning–current waveshapes, all injected at the nose of the aircraft, exiting the tail, and of peak magnitude 53 kA. The three waveshapes had rise times of 30, 90, and 200 ns.

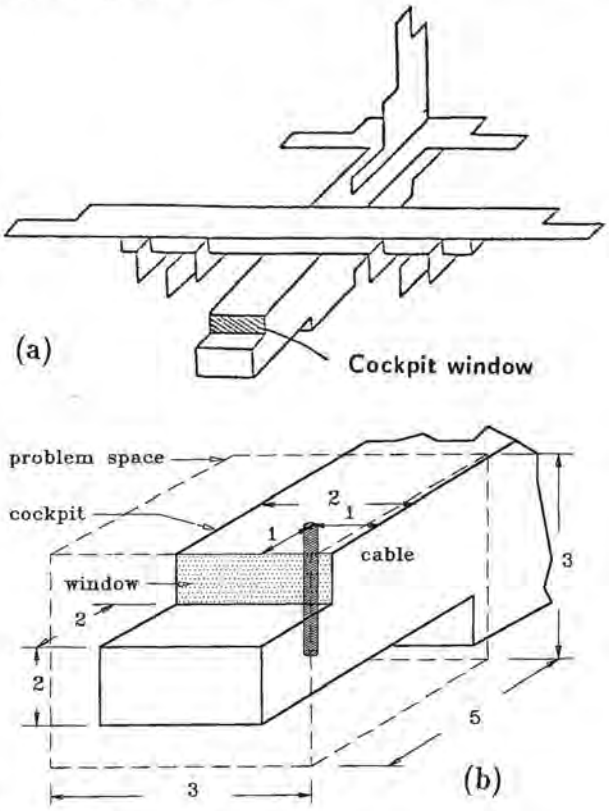

Fig. 12.22 Geometries to illustrate coupling into a cockpit.
(a) To determine external environment
(b) To determine coupling through window

It was expected that the largest response would be seen inside the cockpit for the 30 ns pulse because its high–frequency components should most easily penetrate the aperture. This proved to be the case. Fig. 12.23 shows the voltage at the top end of the wire while Fig. 12.24 shows the current. For clarity, only the responses to 30 ns and 90 ns currents are shown. Since the calculation assumed the wire to be terminated in its characteristic resistance, the voltage is quite high, sufficiently high in fact that an arc through nearly a foot of air could be expected were that voltage actually to be developed.

In real aircraft such arcs do not occur since any realistic cable bundle would have wires and shields that would form short circuits. The current shown on Fig.

12.24, however, is probably a realistic estimate of the current that would flow on such short circuits.

The voltage and current are oscillatory at frequencies that can be related to the dimensions of the cockpit. More than one frequency appears in the response since the cockpit cavity can exhibit several different modes of oscillation. Cavity oscillations are discussed further in Section 12.12.

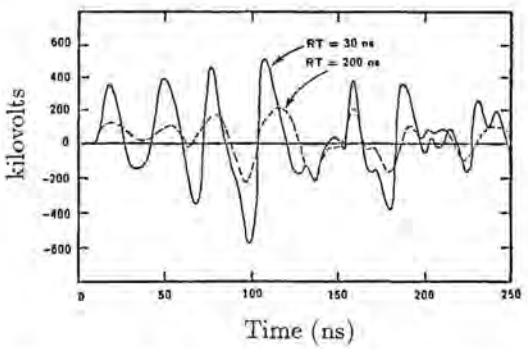

Fig. 12.23 Voltage on wire inside cockpit.

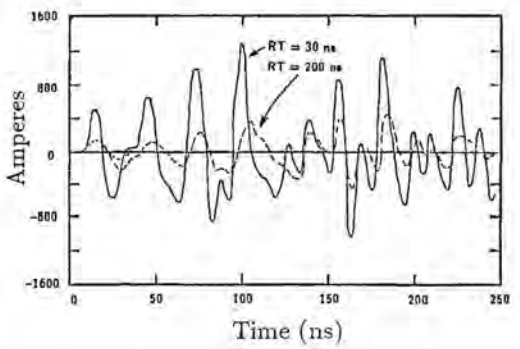

Fig. 12.24 Current on wire inside cockpit.

12.11.3 Nested Subgrids

A third way to solve these types of aperture is to use a nested subgrid approach. In this approach, the aperture is gridded with a finer mesh than the rest of the aircraft. This results in a coarsely gridded large problem space in which is "nested" a finer gridded volume. This nested volume resolves the fine features of the aperture and is solved simultaneously and self consistently with the larger volume. Thus, no inherent approximations to the physics are made. The approach is numerically difficult, because of the requirements of interpolating in time and space at the interface of the nested subgrid with the main program.

No application of this technique to apertures has been published in the open literature as far as is known, but it has been applied with good results to the resolution of fine structures on aircraft for the external coupling problem [12.22 – 12.24]. The concept is illustrated in Fig. 12.25 , which shows the finely gridded wing tip of a Learjet nested within the more coarsely gridded volume [12.22].

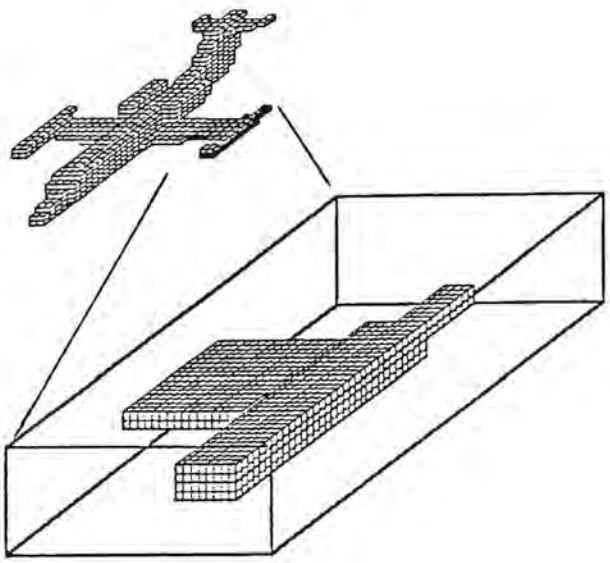

Fig. 12.25 Nested subgrid.

Brute force approach: It should also be noted that a "brute force" approach can be applied, in which the aperture, cavity, and aircraft are all solved in the same problem space with a small enough grid to resolve the aperture and cavity. This is feasible with sufficient computational resources and has been done for an aircraft cockpit [12.25]. The technique has been applied to an aperture in a cylinder and favorably compared to measured data [12.26].

3D corrections to 2D solution: Finally, one other approach to the cavity–backed aperture problem that has been used is to apply a three dimensional (3D) correction factor to a two–dimensional (2D) aperture [12.26]. In this approach, a cavity–backed aperture (e.g. a cockpit) can be modeled in two dimensions by a Laplace's equation method and a field distribution can be obtained. Measurements of 3D apertures with the same cross section dimensions (in 2D) can give a correction factor which relates the 3D–aperture excitation to the 2D–excitation. Thus, a family of curves can be developed and a solution for future apertures can be done in 2D along with application of a correction factor. This method could give a good approximation to the low–frequency or late–time solution, but cavity or aperture resonances would not be included.

12.12 Resonance Modes of Cavities

It is possible for an enclosed cavity to be resonant at a frequency that might be excited by electromagnetic fields penetrating an aperture. In the simple rectangular enclosure shown in Fig. 12.26, the simplest type of cavity resonance involves a plane wave bouncing off the four walls and arriving back at the starting point in phase with succeeding waves. This can only occur for certain characteristic frequencies. It is possible for the waves to arrive back at the starting point after making more than one bounce off each wall, and if there are more walls, there are an infinite number of reflection patterns for which a wave can return to the starting point in phase with succeeding waves. For rectangular enclosures, some of the simpler resonance modes are as shown in Fig. 12.27. The frequencies corresponding to such modes are given by

$$f(j,n,p) = \frac{c_0}{2}\sqrt{\frac{m^2}{a} + \frac{n^2}{b} + \frac{p^2}{c}} \qquad (12.86)$$

where m, n and p are integers identifying the resonance modes and $c_0 = 3 \times 10^8$ m/s, the velocity of light.

The magnitude of the integers m, n and p is equal to the number of repetitions of the magnetic field along the corresponding dimension.

As a numerical example, some of the characteristic resonance frequencies of a rectangular enclosure having dimensions $0.7 \times 1 \times 1.5$ m are given in Table 12.3.

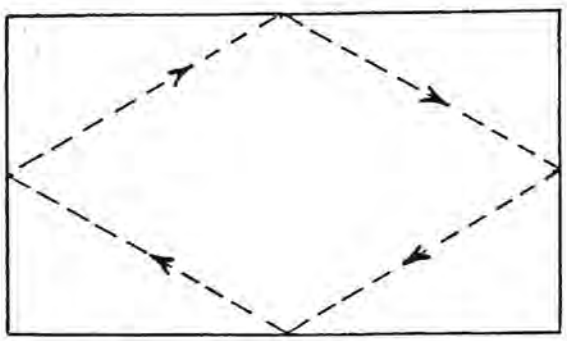

Fig. 12.26 An elementary mode of cavity resonance.

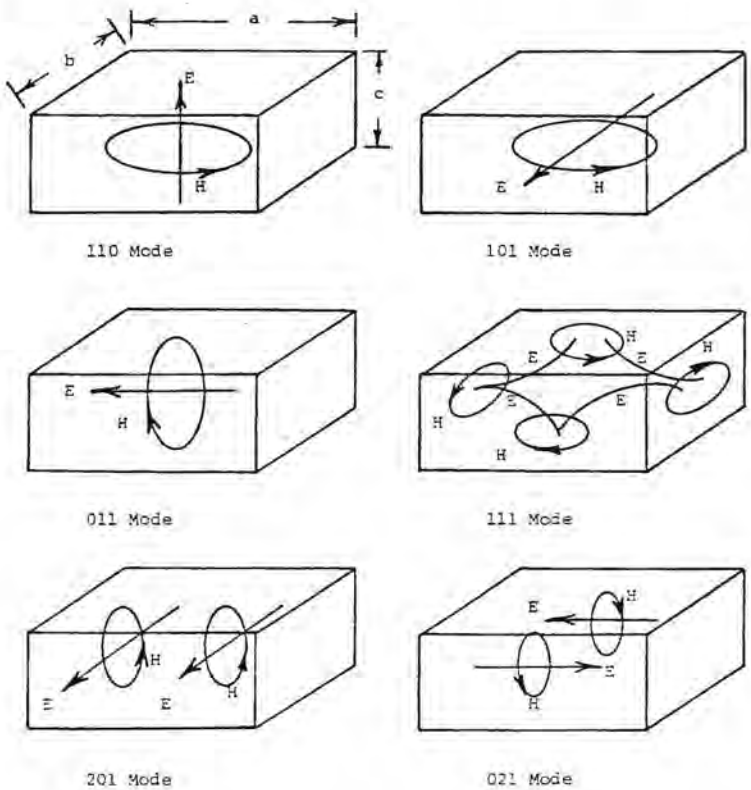

Fig. 12.27 Some resonance modes in a rectangular enclosure.

Table 12.3

Some Resonance Modes in a Rectangular Enclosure

(a = 1.5 m; b = 0.7 m; c = 1 m)

Mode	Frequency
110	236 Mhz
101	180
011	262
111	280
201	250
021	454

1. A study of the resonance modes or impedance of an empty cavity in an aircraft is probably a useless exercise. There are virtually no empty cavities, and if there were, there would be nothing in such a cavity to be damaged or to suffer interference.
2. Metal enclosures within such a cavity would tend to raise the resonant frequencies, while wires and connecting cables would tend to lower the resonant frequencies. In an actual aircraft, it is probable that the effects of connecting cables would prevail.
3. The principle value of knowing the resonance frequencies of an enclosure is in knowing the frequency above which one should not even attempt to make an interactions study using simple methods of analysis. As such, only the lowest frequency resonance mode is of interest. Note that this is not to say that the higher order resonance modes are not of importance.
4. Electrical energy oscillating in a cavity resonance mode will only appear if there is a source to excite that oscillation. Possibly the rapid field changes associated with triggered lightning and coupled through apertures could excite such oscillations, but excitation through diffusion coupling (Chapter 11) is most unlikely.
5. Enclosures that act as cavity resonators generallly have quite high Q factors; that is,they have low losses. If some transient electromagnetic condition excites a cavity oscillation, that oscillation may persist for much longer than the transient that excited the oscillation.
6. The frequencies associated with cavity resonances are apt to be of the same order as the frequencies associated with digital equipment located in the enclosures. Thus, one can speculate that a cavity resonance, if it occurs, might be more of a problem for digital electronics than it would be for analog electronics.

REFERENCES

12.1 Lord Rayleigh, "On the Incidence of Aerial and Electrical Waves on Small Obstacles in the Form of Ellipsoids or Elliptic Cylinders, on the Passage of Electric Waves Through a Circular Aperture in a Conducting Screen," *Phil. Mag.*, Vol. 44, pp. 28, 1897.

12.2 K.S.H. Lee, Editor, "EMP Interaction: Principles, Techniques, and Reference Data (A Compleat Concatenation of Technology from the EMP Interaction Notes)," *AFWL-TR-80-402*, December 1980.

12.3 D.E. Merewether, et al., "Electromagnetic Pulse Handbook for Missiles and Aircraft in Flight," *SC-N-710346, Sandia Laboratories*, Sept. 1972.

12.4 C.M. Butler, Y. Rahmat-Samii, and R. Mittra, "Electromagnetic Penetration Through Apertures in Conducting Surfaces," *IEEE Trans. Electromagnetic Compatibility*, Vol. EMC-20, No. 1, February 1978.

12.5 R.A. Perala, T.H. Rudolph, and F. Eriksen, "Electromagnetic Interaction of Lightning with Aircraft, "*IEEE Trans. on Electromagnetic Compatibility*," EMA-24, No. 2, May 1982.

12.6 C. D. Taylor, "Electromagnetic Pulse Penetration Through Small Apertures", *IEEE Transactions on Electromagnetic Capability*, Vol. EMC-15, No. 1, February 1973, pp. 17-26.

12.7 C. D. Taylor, "Electromagnetic Pulse Penetration Through Small Apertures", Interaction Note 74, *Electromagnetic Pulse Interaction Notes, 5*, March 1973.

12.8 K. S. Lee, "EMP Interaction: Principles, $\cdots$"pp. 435 - 441.

12.9 K. S. Lee, ibid, pp. 475 - 481.

12.10 William A. David, , "Bounding Signal Levels at Wire Terminations Behind Apertures,"*Interaction Notes, Note 384* February 1980.

12.11 K.F. Casey, "Low Frequency Electromagnetic Penetration of Loaded Apertures," *IEEE Trans. Electromagnetic Compatibility*, Vol. EMA-23, No. 4 (November 1981).

12.12 J. Hamm, W. Graf, and E.F. Vance, "Coupling of Natural Atmospheric Interference through Aper-

12.13 J.D. Kraus, "Antennas," McGraw-Hill, New York, 1950.

12.14 R.A. Perala, et al., "Evaluation and Mitigation of Lightning and Microwave Hazards to the Solid Rocket Booster Propellant," *EMA-87-R-63*, June 1987.

12.15 C.C. Easterbrook, et al., "Experimental and Analytic Studies of the Triggered Lightning Environment of the F106B," *EMA-87-R-37*, March 1987.

12.16 P.B. Papazian, et al., "Measurement of Seam Impedances of Tactical Shelters for Threat Level NEMP Simulation," *IEEE Int. Symp. on EMC*, San Diego, CA., September 16-18, 1986.

12.17 R.S. Collier, et al., "Correlation of MIL-STD-285 Measurements of Seam Transfer Impedance and EMP Shielding Effectiveness," *IEEE Int. Symp. on EMC*, San Diego, CA., September 16-18, 1986.

12.18 R.A. Perala, et al., "The Development and Demonstration of a NEMP Shielding Effectiveness Definition for Shielded Volumes," *EMA-86-R-10*, December 1985.

12.19 David E. Merewether and R. Fisher, "Finite- Difference Analysis of EM Fields Inside Complex Cavities Driven by large Apertures," *IEEE Trans. on Electromagnetic Compatibility*, Vol. EMC-24, No. 4, November 1982.

12.20 D.E. Merewether and R. Fisher, "Finite Difference Solution of Maxwell's Equation for EMP Applications," *EMA-79-R-4*, April 22, 1980.

12.21 F.J. Eriksen, T.H. Rudolph and R.A. Perala, "Atmospheric Electricity Hazards Analytical Model Development and Applications, Vol. III, Electromagnetic Coupling Modeling of the Lightning-Aircraft Interaction Event," *EMA-81-R-21*, August 1981.

12.22 G.J. Rigden, "Interference of Precipitation Static Discharge to Aircraft Navigational Systems," /sl 1988 Int. Aerospace & Ground Conference on Lightning and Static Electricity, Oklahoma City, OK, April 19-22, 1988.

12.23 G.J. Rigden, et al., "Interference of Precipitation Static Discharge to Aircraft Navigational Systems," *EMA-86-R-17*, June 1988.

12.24 Poh Ng, et al., "Application of Triggered Lightning Numerical models to the F106B and Extension to Other Aircraft," *EMA-88-R-17*, June 1988.

12.25 B.I. Wahgren, Saab-Scania, Linkoping, Sweden, Personal Communication.

12.26 Karl S. Kunz and H. Gerald Hudson, "Experimental Validation of Time-Domain Three-Dimensionall Finite-Difference Techniques for Predicting Interior Coupling Responses," *IEEE Trans. on Electromagnetic Compatibility*, Vol. EMC-28-No. 1, February 1988.

12.27 B.J.C. Burrows, "Induced Voltage Programme," *CLSU Memo No. 46*, Culham Laboratories, Nov. 1976.

Chapter 13

EXPERIMENTAL METHODS OF ANALYSIS

13.1 Introduction

Analytical techniques can seldom be relied on as the sole method of determining the voltages and currents to which aircraft wiring and avionic equipment would be subjected. Most aircraft design programs require some experimental analysis of the aircraft and its wiring, either as the primary methods of analysis or as backup to analytic studies. This chapter discusses some of the test methods available. It deals only with the response of the aircraft and its wiring. Testing of avionic equipment is discussed in Chapter 18.

There are several different approaches to testing of complete aircraft, each with advantages and disadvantages.

1. High level unidirectional pulses
2. High level oscillatory pulses
3. Intermediate level unidirectional pulses
4. Low level unidirectional pulses
6. Low level swept continuous wave (CW)

Techniques 1 through 5 are time domain techniques while the sixth is a frequency domain technique. High level time domain test procedures can be used as proof or verification tests; that is, *Go/No-Go* tests, to make an overall evaluation of the effectiveness of protective measures. Most commonly though, tests on complete vehicles are used only for analyzing the response of the aircraft and its wiring while verification tests of protective measures is done by bench level testing, as described in Chapter 18.

The following sections will discuss the various approaches to testing. The Lightning Transient Analysis (LTA) procedure will be discussed further in §13.4. Selection of the most appropriate method is challenging since it depends on the ultimate use of the data and the state of development of the air vehicle. A simulation technique that imposes all features of the lightning in a proper time sequence is desirable, but this may not be effective for subsystems or providing design data. It is especially important that the simulation technique provide data on the system, subsystem or component equipment or line replaceable unit (LRU) responses that can be extrapolated to the values that occur when the air vehicle is exposed to the real lightning environment.

This chapter will concentrate on techniques for performing low level pulse tests. Much of that discussion is, however, equally applicable for any of the test procedures.

13.2 Basic Assumptions

All of the experimental techniques are based to one degree or another on certain premises:

13.2.1 Defined Threat

A fundamental point, not always appreciated, is that lightning testing is done primarily in terms of a standardized lightning threat, one definable in documents, rather than in terms of what is most commonly produced by lightning. The standardized threat, presented in Chapter 5, is intended to represent a very severe lightning flash, though not necessarily the most severe conceivable. One of the aims of testing, therefore, should be to determine the response of the aircraft to the waveforms defined in that threat. Discussions as to whether those waveforms are truly representative of natural lightning is a topic to be addressed separately from that of how to perform tests related to the standardized threat. A test program may involve using or discussing other waveforms as well, but it should, as a minimum, deal with the waveforms of the defined threat.

13.2.2 Linearity

Another basic premise is that the response of an aircraft in flight to natural lightning can in fact be predicted by making tests at ground level. There is always some question as to whether this is actually so and some investigators, recognizing the complicated interactions of the electromagnetic fields surrounding an aircraft in flight during a lightning strike, refer to ground tests as "stimulations" rather than "simulations". The electromagnetic environment of an aircraft parked on a hangar floor is vastly different from that of one in flight.

Most test methods also assume linearity; that is, that the response of the aircraft to a low level test can reasonably be extrapolated to estimate the response to full threat lightning.

Resistive effects: Most of the test methods provide good simulation of the effects of resistance in the aircraft structure and the assumption of linearity is generally valid, even for aircraft using large amounts of CFC materials. Studies that have been made of the point [13.1, 13.2] have generally shown that predicted resistively coupled voltages, as predicted on an assumption of linearity, are if anything higher than any likely to be found in actual practice.

Magnetic field effects: The simulations also provide reasonable estimates of the magnetic field effects produced by lightning current. What this means is that the response produced by a low level pulse of current can be scaled linearly to give the response to a high level pulse of current, provided the waveforms of the currents are the same. The point is discussed further in §13.3.3.

Electric field effects: Whether any of the test methods provide good simulation of the electric field effects is less clear. Electric field coupling involves the strength of the electric field at the surface of the aircraft, but this can be influenced very greatly by the corona and streamers that appear around the aircraft when it is struck. Both of these are very non–linear phenomena. The corona and streamers limit the electric field at the surface and may limit the electric field coupling. Also, the circuits used for ground based aircraft tests probably do not give the same ratio of magnetic to electric field effects as is found in flight. This chapter will not attempt to address the question of whether electric field effects are correctly simulated; all it will do is alert the reader that there are questions about electric field coupling.

Some of the issues will be discussed in the following paragraphs, along with methods of obtaining an electromagnetic environment that is as representative as possible of that produced by natural lightning.

13.3 Time Domain Pulse Tests

All pulse testing basically involves charging capacitors and then discharging them through waveshaping elements into the aircraft. Differences between various techniques relate mostly to the energy levels of the surge generators and the techniques and degree of extrapolation needed to estimate full threat responses from tests made at less than full threat. Before discussing various approaches to testing, the basic response of an aircraft in a pulse test circuit will be discussed since that response is essentially the same whatever the test level.

13.3.1 Basic Test Circuit

As reduced to lumped constants, the basic pulse test circuit is shown in Fig. 13.1. Energy is stored in a capacitor, conducted into the aircraft and returned to the capacitor along a return circuit. Duration of current is controlled by the capacitance and series resistance while front time is controlled by resistance and series inductance, some of which may be intentionally added to the surge generator and some of which will be intrinsic to the aircraft and the return circuit. If single wires are used for the connections between the generator and the aircraft, the inductance of the circuit can be approximated as 1 μH/m or 0.3 μH/ft times the total distance around the circuit.

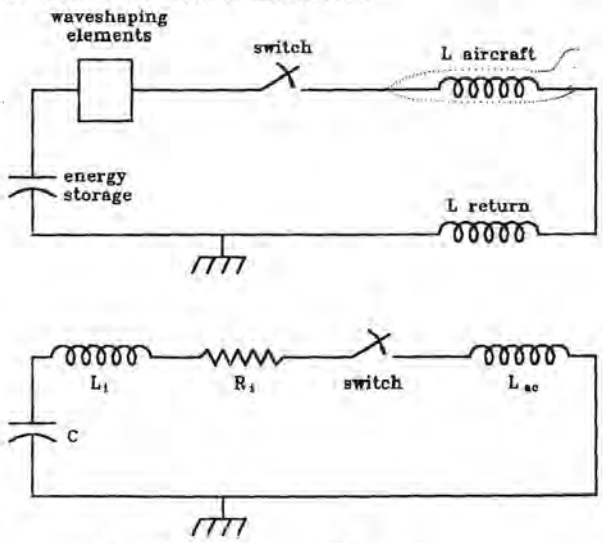

Fig. 13.1 Basic test circuit.
(a) Generic
(b) Practical test circuit

Coaxial return circuits: Using a single wire adjacent to the aircraft, Fig. 13.2(a), is not recommended as the way to return the current to the generator because the aircraft would respond to the magnetic fields produced by current in the return wire, as well as to the electric and magnetic fields produced by current in the aircraft. A coaxial geometry, with the aircraft as the center conductor and the return path as the outer conductor, Fig. 13.2(b). is better. As indicated in §9.7.2, current on a cylindrical conductor produces no magnetic field inside the conductor. In practice, the return circuit is formed from an array of wires surrounding the aircraft, as shown in Fig. 13.2(c), though sometimes metal sheets are used.

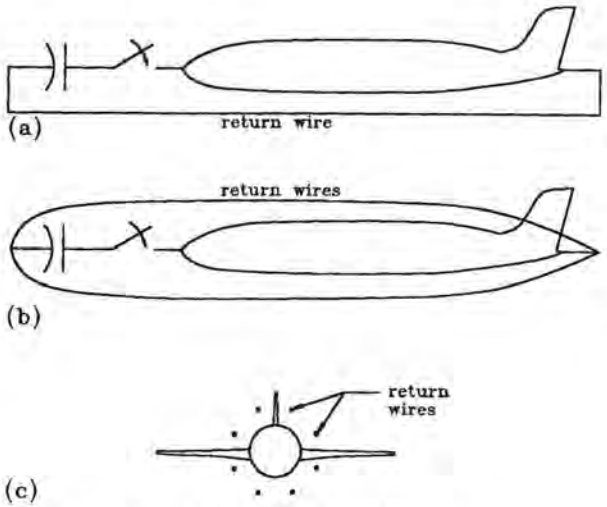

Fig. 13.2 Return circuits.
(a) Single wire - bad
(b) Coaxial wire - good
(c) End view

Diameter: In theory, the further the return grid is from the surface of the aircraft the better, but more spacing increases the impedance of the test circuit and adversely affects the ability to generate the desired currents through the aircraft. Best simulation would involve having the aircraft suspended with wheel well doors closed. Since this is seldom practical, the spacing to the wires cannot be more than the one or two meters that the wheels support the aircraft above the ground. Also, in theory, the more wires in the return path the better, but studies [13.2] have shown that about eight conductors arranged more or less uniformly around the aircraft are adequate.

Impedance: Inductance and surge impedance can be estimated by calculation. Treating the aircraft and the return circuit as coaxial cylinders of the dimensions shown on Fig. 13.3 gives an inductance of 0.18 μH/m or 2.7 μH for the indicated length. Inductance of an actual installation will be larger because the outer conductor is a cage of wires. For typical systems it runs about 0.5 μH/m, and is best determined by measurements on actual installations. One approach to measurement is to discharge a known capacitance into the circuit and observe the ringing frequency.

The surge impedance of the transmission line formed by the aircraft and return circuit of Fig. 13.3 calculates to be about 55 ohms, but for actual installations the impedance varies over the length of the aircraft since the aircraft geometry changes over its length. Typically it will be in the range of 75 to 125 ohms and is best evaluated by time domain reflectometry techniques.

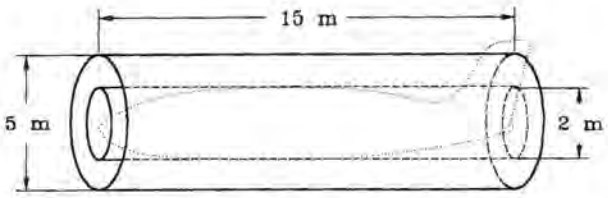

Fig. 13.3 Coaxial approximation of return circuit.

Lumped constant example: Fig. 13.4 shows typical waveshapes that might be expected when treating all elements as lumped constants. The generator circuit shown was one used in an actual test of an aircraft [13.3] and the waveshapes shown on Fig. 13.4(a) and (b) closely match those obtained in the actual test, as will be shown in Fig. 13.7. The inductance of the aircraft and its return circuit was not measured during the tests, but the 8 μH estimated by matching calculated and measured current waveshapes is typical of actual circuits. The intent of that particular test was to obtain a current having a front time of several microseconds and inductance of the aircraft was not critical since inductance was added to the generator to obtain the desired waveshape.

Lumped constant circuits are sufficient to estimate the peak current obtainable from a particular generator. For this circuit, and during the tests of [13.3], a current of 500 A was obtained with a generator charged to 25 kV. Obtaining a full threat current of 200 kiloamperes would have required a generator charged to 10 megavolts.

The circuit can be configured to obtain higher currents by reducing the series impedance, but doing so precludes obtaining the desired double exponential current wave. Reducing the series resistance increases the time at which the current reaches its peak. If the series resistance is reduced sufficiently the current becomes oscillatory. Fig. 13.4 shows the current waveshapes as series resistance is reduced.

13.3.2 Traveling Wave Effects

It is not really sufficient to analyze interactions between aircraft and surge generators using lumped constant circuit techniques since the aircraft structure is large enough that traveling wave effects must be considered. The aircraft and the return circuit form a short transmission line and when the switch in the generator is closed, a steep fronted voltage wave is injected into the aircraft. Associated with it will be a steep fronted current wave.

At the end of the transmission line formed by the aircraft and return conductors, reflected voltage and current waves are launched of polarity such that the

voltage wave at that point goes to zero and the current doubles. When the reflected waves return to the input end of the aircraft other reflected waves are generated. The waves combine to produce a current that increases in a series of jumps and a voltage that oscillates, as illustrated in Fig.13.5. On the figure the aircraft was treated as two transmission lines each of 20 ft length (6.1 m) and having surge impedances of 100 ohms and propagation velocities 80% that of the speed of light. The representation is overly simplified in that it makes no allowance for the non-uniform geometry of the aircraft, but it does illustrate the basic effects.

The first effect is that the current in the aircraft builds up not in an exponential manner, but in a series of steps as current propagates back and forth along the aircraft, reflecting at the discontinuites at the ends. The second is that the current is different at different points on the aircraft and the steps are least noted at the point of connection to the surge generator.

These traveling waves preclude developing current waves having exactly the shape of the idealized waves discussed in Chapter 5. They also influence the coupling of voltages and currents into the aircraft wiring.

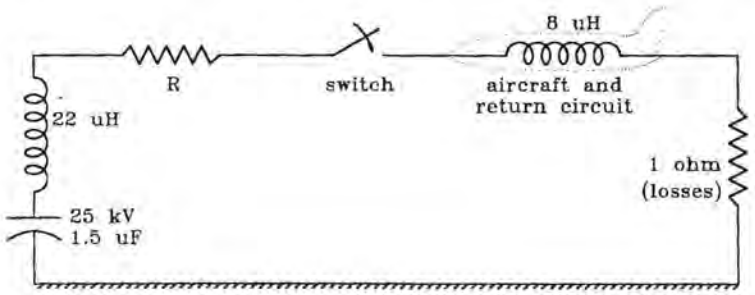

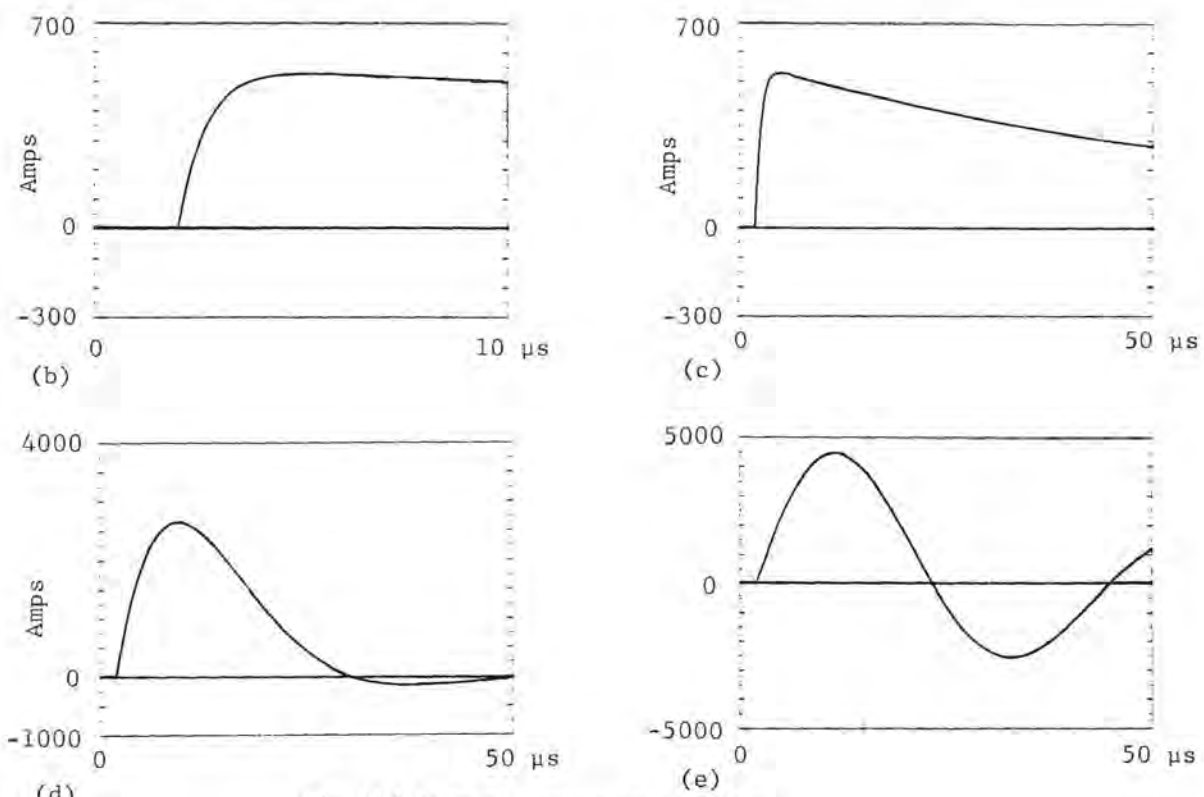

Fig. 13.4 Lumped constant representation.

(a) Circuit
(b) R = 45 ohms
(c) R = 45 ohms
(d) R = 5 ohms
(e) R = 0.5 ohms

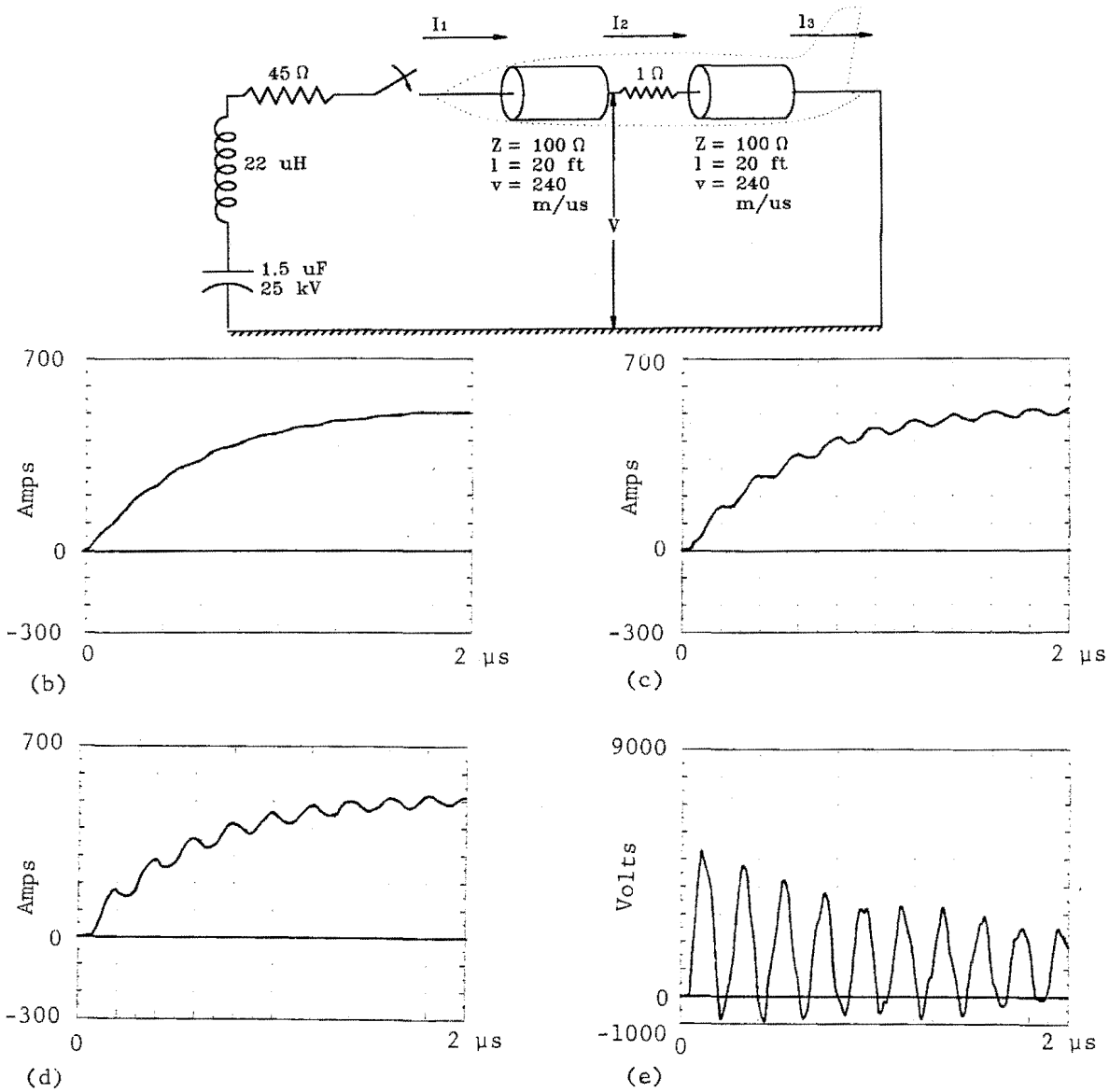

Fig. 13.5 Transmission line representation.
(a) Circuit
(b) I_1 (c) I_2
(d) I_3 (e) V

In the event of a real lightning event traveling waves may also be launched, particularly if it is a triggered lightning flash. The nature of the oscillations, though, is almost certainly different in nature than in the laboratory because the impedance of a lightning channel is different, and probably higher, than the impedance of a laboratory surge generator. Given that the intent of a laboratory test (one of them at least) is to duplicate, as closely as possible, the standardized lightning environment, these oscillations are undesirable and are best suppressed.

Detection of waves: These travelling waves on the aircraft are difficult to detect if the only measurement of current is that made at the input and exit points. Measuring the current at the midpoint of the aircraft is of course not feasible, though one could measure the magnetic field at the center and so estimate the

current. They can, though, be detected by measuring the voltage between the aircraft and ground or between the aircraft and the return conductors, preferably at the midpoint of the aircraft. Fig. 13.5(e) shows a calculation of the voltage.

Controlling traveling waves: These traveling waves can be controlled and a current wavefront with a relatively smooth double exponential front obtained by proper termination of the transmission line formed by the aircraft and the return circuit. One type of termination uses a resistor connected in shunt with the aircraft and another uses a resistor connected in series between the exit point on the aircraft and the return lines. Each is effective, as shown in Fig. 13.6. In actual practice neither is completely effective since the impedance of the aircraft is not uniform and actual resistors have inductance that degrade their performance.

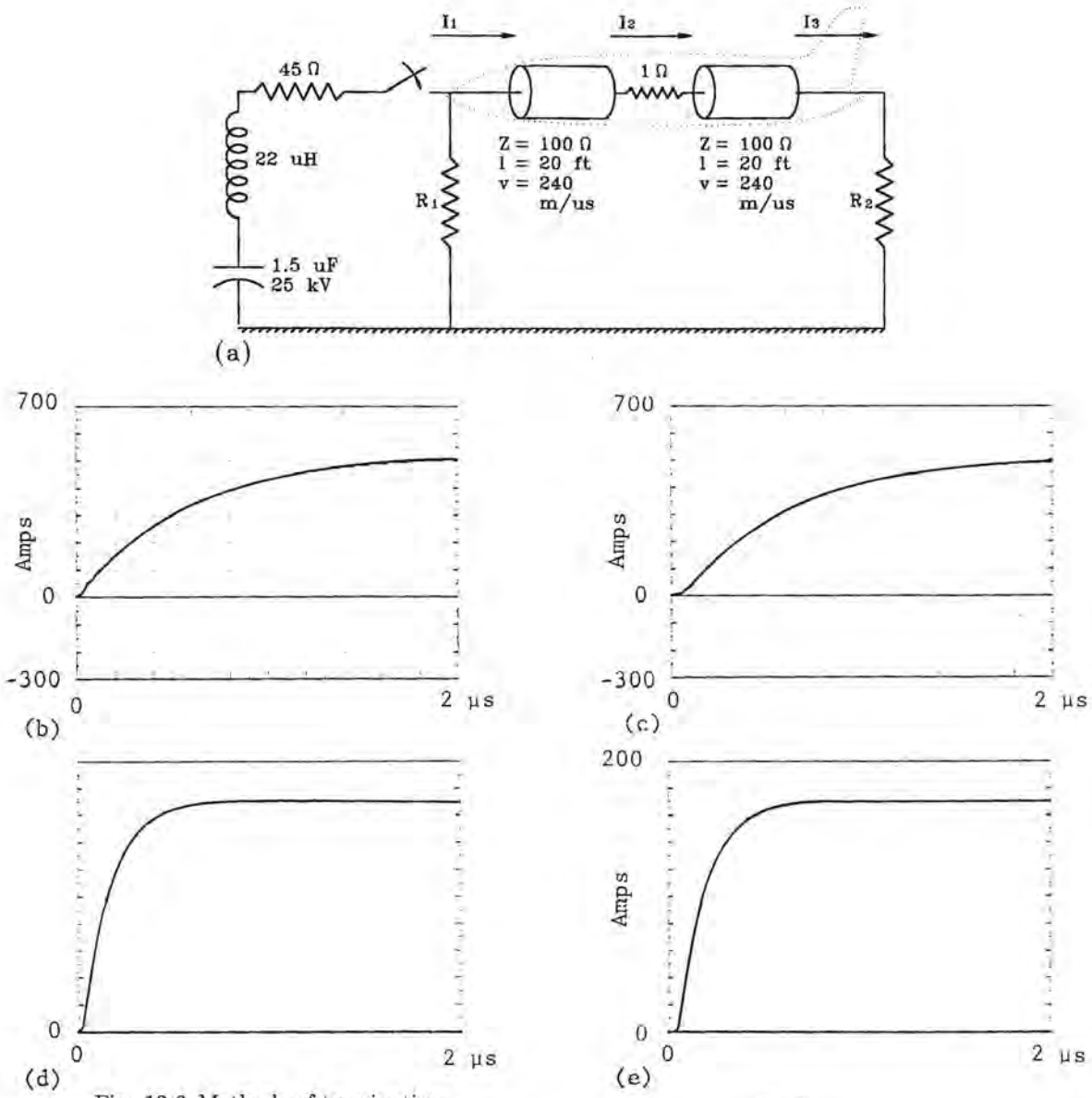

Fig. 13.6 Methods of termination.

(a) Circuit

(b) $I_1 - R_1 = 100\ \Omega,\ R_2 = 0\ \Omega$ (c) $I_1 - R_1 = 0\ \Omega,\ R_2 = 100\ \Omega$

(d) $I_2 - R_1 = 100\ \Omega,\ R_2 = 0\ \Omega$ (e) $I_2 - R_1 = 0\ \Omega,\ R_2 = 100\ \Omega$

One drawback to a series resistor is that it reduces the maximum current available from a given size surge generator. Another is that considerable voltage develops between the aircraft and the return circuit. For reasons of safety, it is preferable that the return circuit be grounded. Thus the aircraft potential rises and insulation under the wheels becomes necessary. Insulation capable of withstanding several hundred kV can be provided without undue difficulty, sufficient for tests at current levels up to several thousand amperes.

External oscillations on the return wires: Since the aircraft cannot be completely enclosed by a cylindrical return conductor, magnetic and electric fields will leak through the cage of return wires and couple to other conductors outside, such as steel in the hangar floor and walls. Energy coupled to these systems will cause a secondary set of traveling waves to propagate on the return wires, as well as the primary set propagating between the aircraft and the return wires. Reflections and refractions in the external systems will show up in the measurements made in the primary circuit.

These oscillations can be controlled by connecting both ends of the return conductors to building ground through resistors, RF and RR on Fig. 13.7. Values of 100 to 150 ohms are usually sufficient. The figure also shows the current waveshapes obtained in the actual test for which Fig. 13.4 showed calculations.

13.3.3 Scaling

The basic premise of pulse testing at other than full amplitude is that the aircraft system is linear and that results of measurements at low current levels can be scaled linearly to predict the response at full threat current level. As discussed in §13.2.2, aircraft are linear systems, at least as regards resistively and magnetically generated voltages. Some questions have arisen in the past as to what is the most important mode of interaction and whether scaling should be on the basis of relative amplitudes or relative rates of rise.

Simplistically, one might argue that the dominant mode of coupling is resistive and that only relative amplitudes of current are important. Equally simplistically one might argue that aperture coupling effects are of primary importance and that the induced voltages depend on rate of rise of current. On this premise, one would scale measurement results according to the rate of rise of the surge current.

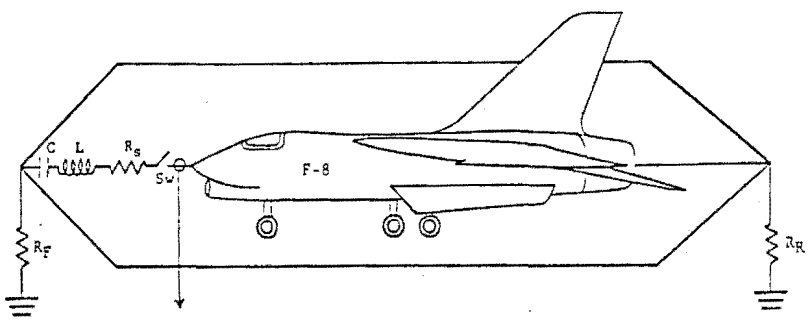

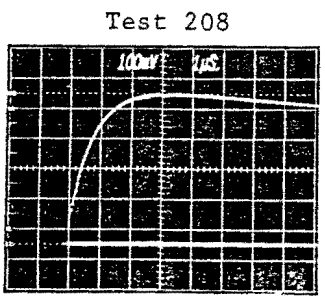

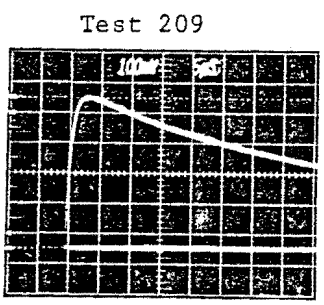

L = 18 μH
C = 1.5 μF
R_S = 45 Ω
E^S = 25 kV
R_f = 120 Ω
R_R = 130 Ω

Fig. 13.7 Termination resistors on the return lines.

Standardized threat: These two premises, combined with early visualizations of a standardized lightning threat, underlay early studies of lightning interactions using relatively high amplitude oscillatory currents. The standard lightning threat was taken to have an amplitude of 200 kA and also to be associated with a peak rate of change of current of 100 kA/μs. While amplitude and rate of change of current were not explicitely linked, the tacit understanding was that a standardized lightning threat, for indirect effects, could be represented as shown in Fig. 13.8.

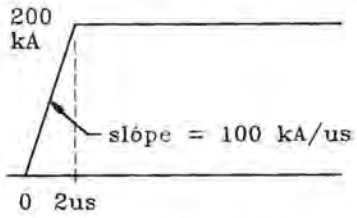

Fig. 13.8 An early view of the standardized environment.

Scaling by amplitude: Resistive effects were felt to depend primarily (or even entirely) on the amplitude of the lightning current. In such a case, any current that reached a peak amplitude of 200 kA would suffice to predict the resistively generated voltages in an aircraft. This, then was the justification for performing verification tests with high (preferably 200 kA) oscillatory current waves, even though the front time of such a wave was much longer than the 2 μs of Fig. 13.8. If the surge current, Fig. 13.9, had a peak amplitude less than 200 kA, then the results would be scaled by the amplitude of current.

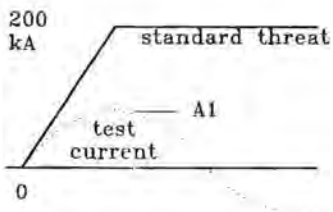

Fig. 13.9 Scaling by amplitude.

Scaling by rate-of-rise: Inductive effects were felt to depend primarily (or even entirely) on rate of change of current and that any current that had a high (preferably 100 kA/μs) rate of change would suffice to predict the inductively generated voltages. If the surge current, Fig. 13.10, had a lesser rate of change, the results would be scaled in proportion to the rate of change of current.

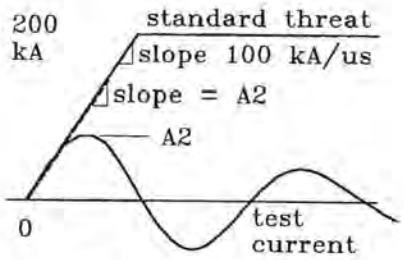

Fig. 13.10 Scaling by rate-of-rise.

Advantages: This approach to testing and scaling had some merit providing the test amplitudes approached that of the full threat. For resistively generated voltages it also had an advantage, real or supposed, that response voltages typically were obscured by high frequencies at early times, but not at later times. If the test current was oscillatory, the late time oscillatory response voltage could reasonably be considered "real" and the early time high frequency component could be considered "noise" in the measurement circuit.

Present thinking, however, is that much of the early time high frequency component of voltage also represents a "real" response voltage.

Disadvantages: The biggest objection to simplified scaling concepts is that the process was frequently pushed too far. In Fig. 13.11, there is no justification in using either waveform (b) or (c) as a predictor of the response to waveform (a).

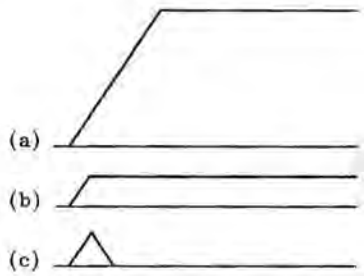

Fig. 13.11 Unjustifiable extrapolation.
(a) Full threat
(b) Front too short
(c) Duration too short

Constant waveshape: Scaling is most justifiable if the test current has the same waveshape as the standardized threat current, but has a lower amplitude, Fig. 13.12. Then questions related to scaling by amplitude or rate of change become moot since both amplitude and rate of change are related by the same scale factor,

$$K = \frac{200}{A_1} \qquad (13.1)$$

It is largely for this reason that the standardized lightning threat described in Chapter 5 is described in such detail.

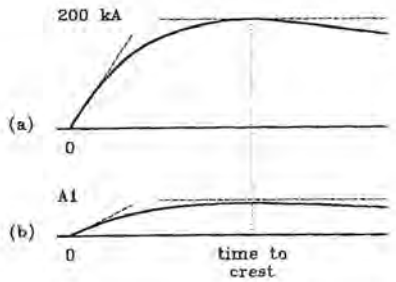

Fig. 13.12 Justifiable extrapolation.
(a) Full threat current
(b) Low amplitude test current

13.3.4 Approaches to Pulse Testing

There are several approaches to pulse testing:

Full threat verification tests: One approach to testing is to subject a complete aircraft, fully configured, with all systems operating, to a full threat lightning current and observe whether any harmful effects are noted. If treated as a *Go/No-Go* test, this approach has, in principle at least, the virtues of simplicity and requiring the least time for preparation, but is seldom used in practice because:

1. The cost and complexity of a simulator capable of generating 200 kA peak current with the required fast rise time is excessive.

2. The current and charge distributions on the aircraft while in the simulator will be different from those that exist while in flight.

3. Since the test program would not be aimed at gathering information on voltages and currents, there would be no information with which to correct problems should they be found.

4. There is no predictable method to update test results for aircraft modifications.

5. The perceived lightning threat may be changed in the future as more data becomes available.

6. There is a potential for damage to the test vehicle.

The major drawback to such tests is the cost and complexity of the test equipment. Equipment has been built to perform full threat tests, on small aircraft at least [13.4], but capacitor banks operating at more than 2 million volts are required. Because of the long duration of lightning currents, the energy required to be stored is many times that required for full threat nuclear electromagnetic pulse (NEMP) tests. Costs of facilities would be several million dollars.

Full threat analysis tests: Conceptually, it would be best to use full threat, or near full threat currents, during a measurement program to evaluate voltage and current at many points on the aircraft. Such tests are made during evaluations of NEMP effects, but the costs are quite high.

Full threat lightning analysis tests have seldom been made on aircraft, partly because of lack of test facilities. Even if test facilites were available, costs would be high since the tests would require a considerable amount of time to perform. Large energy storage banks require considerable time to charge, frequently need maintenance and safety requirements have to be quite stringent. Also, high current level test circuits are subject to the same constraints as lower level circuits in such things as size and impedance of return circuits and relationships between magnetic and electric field magnitudes.

High level oscillatory tests: As discussed in §6.8, unidirectional current waves are produced either by crowbarring, leading to circuit complexity, or by using enough circuit resistance to damp oscillations, leading to inefficient use of the energy stored in the surge generator. An alternative approach to testing, more widely used in the past than at present, is to accept oscillatory test currents when evaluating indirect effects, just as they are accepted during tests of direct effects. Oscillatory currents of high magnitude can be produced by simple capacitor banks, but the waveforms will be totally unlike those produced by natural lightning.

Accepted practice, in the past at least, has been to make tests using two different generators, each of which produces an underdamped oscillatory current. One generator, usually operated in a Marx configuration, is configured to oscillate at high frequency and provide a fast rate of rise while the other is configured to oscillate at low frequency and provide a long duration current. The high frequency waveform is intended primarily for evaluation of aperture effects and the low frequency waveform is intended for evaluation of resistive and diffusion effects.

Oscillatory currents had (and have) both advantages and disadvantages.

Advantages of the fast rate–of–change oscillatory wave:

1. Over a narrow band of frequencies it simulated one important aspect of indirect effects, the aperture coupling of electromagnetic fields

2. High amplitude was available from relatively low–energy surge generators since little energy is lost in waveshaping resistance.

3. It could be nearly a full threat test of the high frequency coupling effects.

Disadvantages:

1. It overemphasized (and deliberately so) one of the frequency components of lightning currents.

2. It underemphasized low–frequency coupling effects, particularly the effects of vehicle resistance and the diffusion penetration of magnetic fields.

3. It was potentially damaging to avionic equipment on the aircraft under test.

   Equipment susceptible to damage during a simulated lightning test could obviously be damaged by an actual lightning flash, but damage during development tests is undesirable.

The advantages and drawbacks of the fast current waveform are mirrored in reverse by the slow current waveform.

Advantages of the high amplitude oscillatory wave:

1. It simulates, over a narrow band of frequencies, the resistive coupling of electromagnetic effects.

2. High amplitude is available from relatively low–energy surge generators.

3. It can approach a full threat test of lower frequency resistive coupling effects, at least for lightning strokes of low to average amplitude.

Disadvantages:

1. It overemphasizes (and deliberately so) one of the component frequencies of lightning current.

2. It may not correctly simulate diffusion penetration of magnetic fields.

3. It does not constitute a full–threat test for the higher amplitude lightning flashes.

   Data obtained at low amplitudes requires extrapolation to give the effects that would be present at full lightning current amplitude.

4. It is potentially damaging to avionic equipment.

Moderate level pulse testing: A generator [13.5] capable of producing currents of 6 or 7 kA through an aircraft is sketched in Fig. 13.13. It is a two stage Marx circuit having an erected capacitance of 4 μF. The current waveform through a test bed aircraft is shown in Fig. 13.14, the test bed aircraft being described in [13.5]. Operating voltage when delivering the current pulse of Fig. 13.14 was apparently about 150 kV total. A similar generator of 20 μF erected capacitance, operated at 150 kV and a circuit resistance of 4 ohms would be capable of producing a peak current of 30 kA and similar waveform.

There are two advantages to performing aircraft tests with such levels. One is that when testing with moderate level generators (30 kA) the stress imposed on the aircraft is near that imposed by the lower amplitude natural lightning flashes. Another, and more important advantage, is that the amount of scaling or extrapolating to estimate full threat level responses is not great. Scaling to 200 kA from 6 kA tests involves an extrapolation of 33:1 while scaling to 200 kA from 30 kA tests involves an extrapolation of 6.7.

One drawback to testing with such machines is that they are not readily transportable to remote locations for tests on aircraft. Transport is possible, but involves disassembly and re–erection at the remote site. Another is that experience has shown that radiation from the spark gap switches in such machines tends to couple into the aircraft under test, and into the measuring instruments, and partially obscures the voltages and currents under observation. The larger the machine the more difficult it is to shield against or suppress this undesirable radiation.

Low level pulse testing: Many of the tests that have been done on aircraft have been done with surge currents of 200 - 1000 amperes. The practice of estimating aircraft response from tests with lower level unidirectional current pulses was initially described as the "Lightning Transient Analysis (*LTA*) Technique" and its development is traced in [13.2, 13.3 and 13.6 - 13.9]. Most commonly, tests have been performed

with currents on the order of 500 – 1000 amperes and using waveshapes as nearly like that of the standardized lightning environment as possible. Virtues of the technique are that test equipment can be transported in one package without the need to rebuild surge generators on site, and that a large amount of testing can be done in a short time, since the equipment is easy to operate. Another virtue is that the surge generator can be well shielded and incidental radiation from switching spark gaps can be well suppressed using small components in the package housing the energy storage capacitors. Finally, since all high voltage components can be contained in a shielded enclosure, exposure of operators to dangerously high voltages is minimized.

The main drawback to low voltage *LTA* pulse testing is that measured results must be extrapolated by large amounts. Extrapolating results from a test performed at 1 kA to a full threat current of 200 kA requires that results be extrapolated by a factor of 200.

Measurement techniques for *LTA* tests are described in §13.4. They are, of course applicable to tests made at higher current levels.

Shock-excited pulse: The pulse techniques described above have involved metallic connection of the surge generator to the aircraft and for the tests that have been made using those techniques the intent has generally been to assess the effects of resistively and magnetically generated voltages. These involve only the current injected into the aircraft. No attempt has been made to duplicate electric field levels at the surface of the aircraft. Generally, in fact, for reasons of safety the aircraft has been grounded and attempts made to minimize voltages between the aircraft and the return circuit, both of which have the effect of keeping the electric field intensity low.

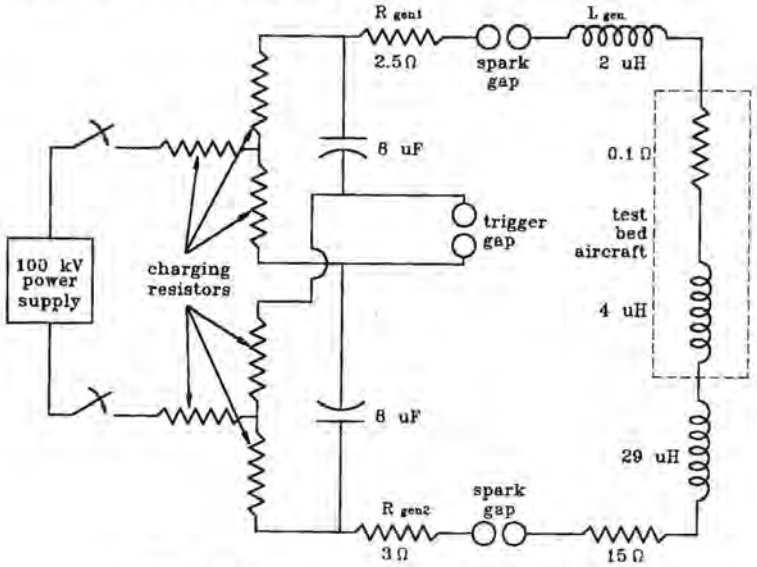

Fig. 13.13 Moderate level surge generator.

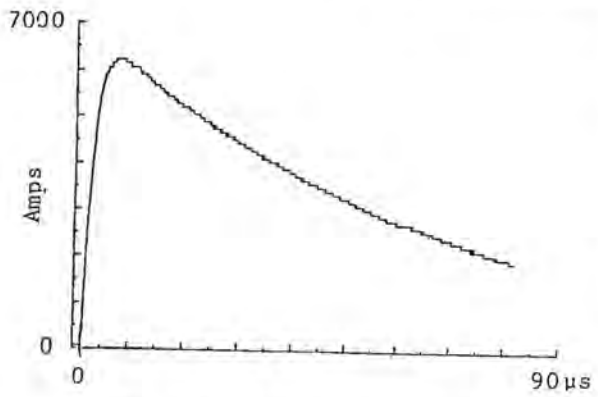

Fig. 13.14 Current waveform.

The fact that electric field coupling exists in addition to resistive and magnetic field coupling has been recognized, but the standardized lightning environment as it relates to indirect effects makes no recognition of electric field and imposes no specifications regarding it. Partly this is because the electric field effects have been felt to be of lesser consequence than other effects and partly because there is little firm knowledge on which to base specifications, should such specifications be desirable.

Questions surrounding some of the early full-vehicle tests led to the shock-excited test technique, Fig. 15, [13.10 - 13.11] in which the vehicle under test is insulated and excited at one point through an electrical arc. This suddenly raises the vehicle to a

high voltage relative to its surroundings and establishes a high electric field at the surface of the vehicle. A few microseconds later, a second arc will be established from the vehicle to ground, suddenly reducing the electric field back to zero and completing the circuit, allowing current to flow.

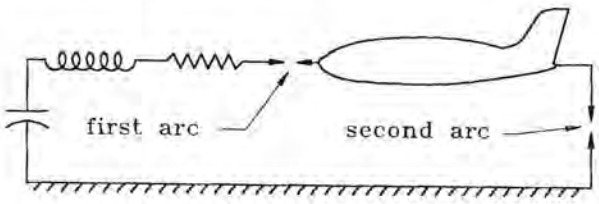

Fig. 13.15 Shock excited pulse technique.

These changes in electric field couple to the internal circuits, presumably in a manner similar to what exists in nature when the aircraft is struck. Testing probably should be done with a well shielded high voltage generator to minimize coupling from the spark gaps of the generator and should be done at voltages sufficiently high that corona forms and limits the electric field at the surface of the vehicle. Voltages in excess of 10^6 volts are probably required.

Some tests have shown that electric field coupling was the primary coupling method for high impedance signal circuits, as contrasted to low impedance circuits for which magnetic field coupling predominated. Electric field effects are not covered by the standardized lightning environment and there is as yet no clear consensus as to how they should be treated or what test techniques are best.

13.4 Conduct of LTA Tests

This section will discuss some of the objectives of *LTA* pulse tests and techniques for making satisfactory measurements. They are applicable whatever the current level at which the tests are made. The objectives are also applicable for tests made using the Swept CW technique discussed in §13.5.

13.4.1 Objectives

The main purpose of LTA tests, and of other types of full vehicle test described in the foregoing sections, is to determine the magnitudes of electrical transients actually appearing in aircraft interconnecting wiring. This data is necessary to verify that actual transients do not exceed the *transient control level* (TCL) established for specific systems and circuits and its collection is part of the certification process, as described in Chapter 5.

Open circuit voltages and short circuit current: The most important type of data to be collected is that on open circuit voltages and short circuit currents. There are two reasons for this:

1. They represent the maximum possible voltages and currents.

2. Equipment transient design levels (ETDLs) are defined in terms of open circuit voltage and short circuit currents appearing at the interfaces between wiring and equipment viewed looking into the wiring.

The open circuit voltage is the voltage appearing at the interface with the equipment disconnected. The short circuit current is the current flowing in a short between two wires, or between a wire and the airframe ground, also at the equipment interface.

The open circuit voltage and short circuit current suffice to define a Thevenin equivalent of the circuit. They also define the capabilites needed in a test generator used to evaluate the ability of the equipment to withstand equipment transient design levels. This latter process is the second part of the verification process described in Chapter 5. Methods for conducting equipment tests are described in Chapter 18.

Other measurements: Other measurements to be made during LTA tests include bulk cable currents, currents on shields of cables, magnetic fields within structures and structural IR voltages.

Test plans: Since it is never practical to measure transients in all wires of an aircraft, or even all wires of a flight critical system, measurements are usually made only on representative wires. The choice of which wires upon which to make measurements is made on the basis of wire routing, degree of shielding and circuit function, so as to be typical of other wires of similar description. The process of selection of circuits and wires to be measured is a very important part of the certification process, and together with selection of test conditions, that is, current entry and exit points, constitutes the *test plan*.

Proposed certification plans should be reviewed with certifying authorities for concurrence prior to the start of tests.

Establishment of TCLs and ETDLs: A second purpose of full vehicle tests is to obtain data from which TCLs and ETDLs can be established. This, of course, is only possible if a suitable airframe is available at an

early stage in the design cycle, when protection criteria are being established. Sometimes an earlier version of a derivative aircraft is available, with physical dimensions and materials of sufficient similarity to enable representative "ball park" transients to be measured in typical wire routes.

Occassionally, useful data can be obtained from tests of major subassemblies such as wing, fuselages or empennage sections. In these cases, test currents are circulated through the subassembly and measurements are made of transients induced in wires that have been installed in the subassembly specifically for test purposes.

13.4.2 Measurement Transducers

Lightning induced voltages are usually measured with oscilloscopes located inside the aircraft under test. These must be coupled to the points under measurement with voltage and current probes.

Where to make measurements: Ideally, one would measure the voltage induced on aircraft wiring at the semiconductor components in the "black boxes" at the ends of the wires, as in Fig. 13.16(a). This is seldom practical since it would disturb the circuit under test and because it is too susceptible to "noise". In practice the best one can do is to measure the voltage at the connector pins, Fig. 13.16(b). Sometimes one must make measurements on breakout boxes and cables, Fig. 13.16(c), but this is to be avoided if at all possible, since experience indicates that it is very difficult to avoid picking up excessive amount of noise on such breakout cables.

Open circuit and short circuit measurements: Frequently the objective of full vehicle tests is to study the intrinsic pickup on wiring harnesses, rather than how they interact with terminal devices. In such cases it is appropriate to disconnect the harnesses from the devices and to short one end of the conductors to ground. Open circuit voltage would then be measured between the other end and ground. Next, both ends of the harness would be grounded and the short circuit current measured.

High impedance voltage probes: Measurement of lightning induced voltages requires fairly sophisticated oscilloscopes These are quite large, compared to avionic "black boxes" and can seldom be placed as close to the devices under investigation as one would like. Furthermore, they are as much, or more, influenced by the electric and magnetic fields as are the aircraft "black boxes" This means that the oscilloscope must be shielded from the magnetic fields, which increases the space requirement even more.

If the oscilloscope can be placed close enough to the object under test, conventional high impedance voltage probes can be used to couple the signal to the oscilloscope. Probes with leads 2 - 3 m long are commercially available.

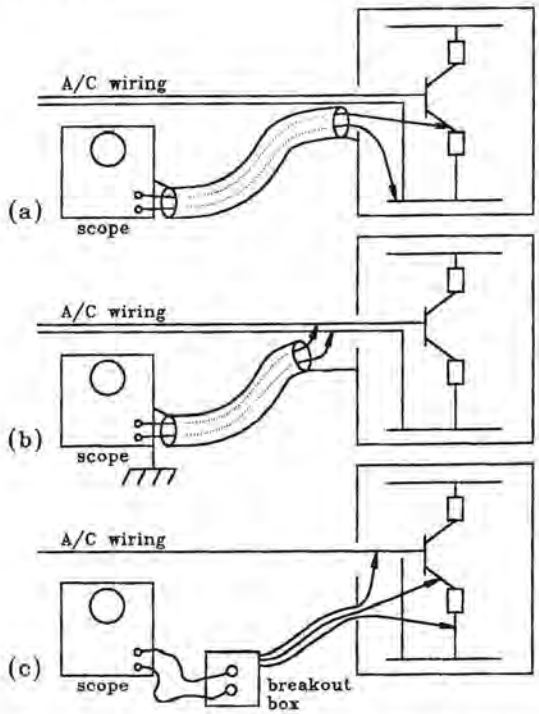

Fig. 13.16 Where measurements can be made.
(a) Ideal
(b) Sometimes practical
(c) To be avoided

Resistive probes: If the oscilloscope must be placed further away, then it must be coupled through low impedance coaxial cables. Connection through unterminated coaxial cables is only satisfactory for low impedance circuits and for low frequency measurements.

If higher frequencies are involved the cables must be terminated in 50 ohms, but then the circuit under test may be loaded excessively. Loading can be reduced by connecting a resistor in series with the measurement cable, but this has the drawback that the voltage delivered to the measurement oscilloscope is only a fraction of the original signal voltage and is more easily contaminated by noise pickup. The higher the resistance, the lower the loading, but the smaller the signal transmitted to the oscilloscope. If a 4950

ohm series resistor were used (total loading of 5000 ohms), only 1% of the signal reaches the oscilloscope. If the unloaded induced voltage signal were on the order of one volt, the signal to the scope would be 10 millivolts. Experience has shown that the background noise levels in the scope (thermal or "white noise") is on the order of 1 millivolt. This would be a signal to noise level of only 10:1, even without any margin for noise pickup on the measurement cables.

Active probes: Active probes may be required in some instances when small signals must be measured. Both single ended and differential probes are commercially available, but experience with some of them has indicated that their shielding may not be sufficient to eliminate problems of noise pickup. They must be checked to insure that the shielding is adequate. Active probes can also be custom made, Fig. 13.17. Both the probe and the power supply have to be well shielded.

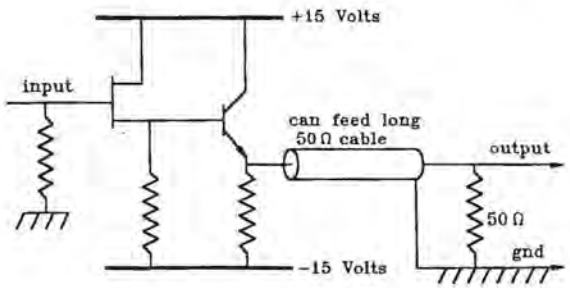

Fig. 13.17 Active probe.

Intrinsic pickup: If the task is only to measure the intrinsic pickup of an aircraft cable, and if some measurement error can be tolerated at short times, another approach is to use 50 ohm measurement cables and to install a short circuit at the far end of the aircraft cable under test. This forces the entire voltage induced into the aircraft cable to appear at the end connected to the measurement cable. Making the measurement without any series resistance allows the ultimate voltage to be recorded correctly, but the high frequency oscillations are not recorded correctly. Using a high series resistance allows the oscillations to be more faithfully reproduced, but of course reduces the level of the signal delivered to the oscilloscope.

Current measurements: Most current measurements are made using pulse current transformers that can be coupled through 50 ohm cable to the measuring oscilloscope. Spacing between the oscilloscope and the point under measurement is seldom a problem. Currents on individual wires and small bundles can be measured with clamp-on current probes, as in Fig. 13.18(a). Some clamp- on probes are available with large window openings through which large cable bundles may be passed. Other current transformers have solid cores that cannot be opened. Measurements require the conductor to be threaded through the transformer and then reconnected, generally feasible for cable bundles, provided the cable terminates in a removable connector. For single conductors such transformers may require the conductor to be cut and then respliced.

Sometimes it is feasible to improvise current transformers using toroidal or split cores. Construction details and circuits are shown in Fig. 13.18(b). The sensitivity of the transformer is

$$K = \frac{N}{R_e} \tag{13.2}$$

where R_e equals R paralleled by the 50 ohm input resistance of the measuring oscilloscope. Larger core size cross section, more turns on the secondary winding and smaller loading resistors all extend the low frequency response of the transformer. Improvised current transformers seldom have responses as good as commercially available transformers, but they may be sufficient for the task. Responses should be determined experimentally.

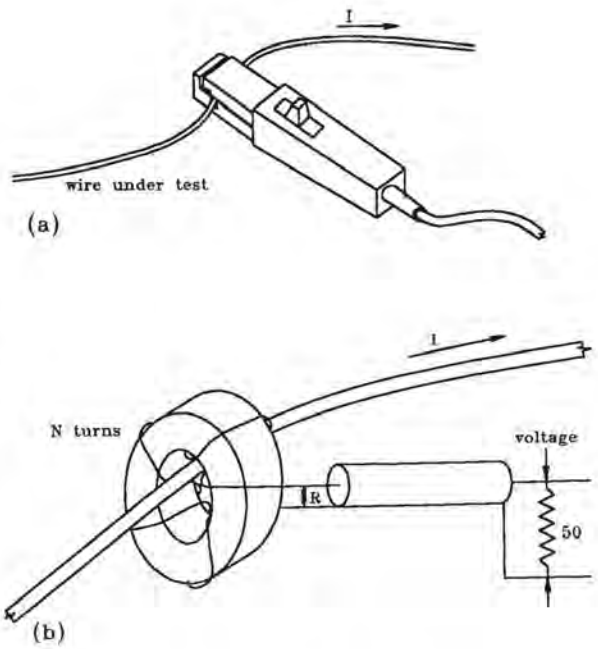

Fig. 13.18 Current transformers.
(a) Split core
(b) Solid core

Response of current transformers: Current transformers are limited both in their low and high frequency response, In the time domain they are characterized by droop at long times and roll-off and oscillations at short times. Particularly with measurements of short circuit current induced by resistive effects care must be taken that the response at low frequencies is adequate.

Power system and RFI transformers: Current transformers operate by passing the secondary current through a burden resistor to develop an output voltage. A high burden resistor provides high output voltage, but poor low frequency response, while a low burden resistor provides better low frequency response, but lower sensitivity. No transformer should be used without a burden resistor. Current transformers made for power frequency metering and relaying are not provided with a burden resistor and are not generally satisfactory for measurements, though if fitted with a non–inductive burden resistor may be. Response measurements would be necessary to prove the point. Current transformers made for *EMI/EMC* measurements are also usually not satisfactory since they are meant to be loaded with the 50 ohm input impedance of a measuring instrument and do not have satisfactory low frequency response.

13.4.3 Noise and Shielding

Noise is induced into the measurement system in several ways, as shown in Fig. 13.19. Electric and magnetic fields can impinge on the measuring oscilloscope and induce noise directly into the internal circuits. Experience indicates that the best way to avoid this problem is to install the oscilloscope in a shielded enclosure.

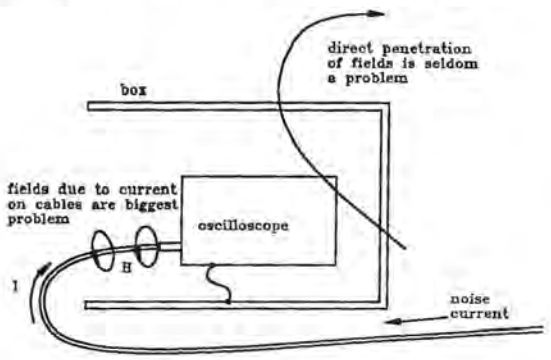

Fig. 13.19 Noise induced into measuring circuits.

A more common source of noise comes from current induced in the shields of the measurement cables. Such currents may be caused by differences in potential between the point of measurement and the oscilloscope, or they may be caused by electric and magnetic field induction into the measuring cable. As the currents flow through the resistance of the cable shield they produce a voltage drop which appears at the terminals of the cable. Minute amounts of magnetic and electric flux also leak through the holes in the shield and induce voltages. As the current on the cable flows through the connectors at the oscilloscope additional voltages are introduced. The way to eliminate these problems is to use well shielded measurement cables and to keep the noise currents out of the measurement cable and away from the oscilloscope, usually by using extra shielding or by using triaxial cables.

Shielding for oscilloscopes: The primary way to minimize noise problems during LTA tests is to shield the oscilloscope and the measuring leads. Some reference to such shielding has been made, but more discussion is in order since experience has shown a lot about which techniques are useful and which are not.

Fig. 13.20 shows more of how to shield the measuring oscilloscope and treat the leads carrying signals into the oscilloscope. There are two main concerns. The first is to prevent incoming leads from carrying noise current into the box and radiating electromagnetic noise directly into the oscilloscope. The box can shield against external electromagnetic fields, but not against fields produced by currents on the shields of the measuring cables. The other concern is to prevent current from flowing across connectors. Connectors (particularly BNC connectors) are a weak link; their resistances are relatively high and they are not particularly well shielded.

Shielding for measurement cables: The best way to avoid problems is to keep noise currents off the shields of the measuring cables. This can be done by fitting all incoming leads with an external braided shield and terminating this shield on the shielding box, not on the input connectors of the oscilloscope. Triaxial cable is good, but it is easy to slide woven copper braid over the top of ordinary coaxial cable.

The objective of the shield is to keep noise currents off the measuring cable and away from the oscilloscope, particularly the input connectors where the oscilloscope is most vulnerable to noise pickup. It is best to terminate the external shield on the rear of the box and as far from the input of the oscilloscope as possible. The inconvenience of having to reach into the back of the box to make connections is part of

the price of getting good shielding performance. It is preferable to bring the measurement cable (but not the external shield) through a hole in the box, Fig. 13.20(a), but a bulkhead connector for the signal carrying cable frequently is satisfactory, Fig. 13.20(b). If a bulkhead connector is used the overall shield should terminate on a shell around the connector, not on the connector itself, Fig. 13.20(c). Grounding the overall shield to the box through a pigtail, Fig. 13.20(d), should be avoided.

The overall shield on the measuring cable must be grounded at each end in order to protect against magnetic fields. Performance of shields is discussed more fully in Chapter 15.

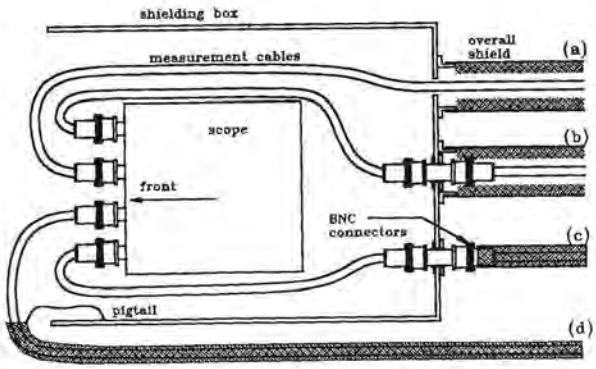

Fig. 13.20 How to bring cables into a shielding enclosure.
(a) Best
(b) Good
(c) Poor
(d) Worst

Differential measurements: Measurements with differential amplifiers are another way to minimize the effects of noise induction into measurement cables. Two signals are brought from the measurement point to a differential amplifier in the oscilloscope, one from the point under investigation and the other from a ground point adjacent to that point, as shown in Fig. 13.21. At the oscilloscope the two signals are subtracted. Since the same noise will be induced on both measurement cables (assuming they follow the same path, as they should), the result should be noise free.

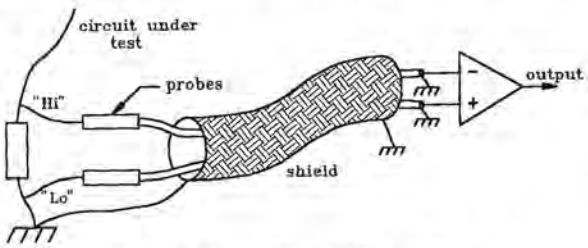

Fig. 13.21 Differential amplifiers.

Differential measurements are not a panacea and some words of caution are in order. Differential measurement systems are rated in terms of common mode rejection ratio, which is a measure of balance or the ability to subtract two identical noise signals and get zero output. Rejection ratios of 10,000:1 are commonly cited for differential pre-amplifiers. This means that if two identical 10 volt signals are applied to the input of the amplifier that no more than 1 millivolt will be displayed. This rejection ratio is usually only guaranteed for low frequencies. The ability to balance differential circuits becomes harder at higher frequencies and the common mode rejection may be much less at high frequencies. Also, if the common mode voltage is too high the amplifiers may saturate or be driven into a non-linear operation. No differential operation can be obtained under those conditions.

High common mode rejection ratios are only obtained in amplifiers specifically constructed for differential operation. Many oscilloscopes have a provision whereby one of two signals can be inverted and the results added. Such operation is not the same as is provided by an amplifier specifically configured for differential operation. The common mode voltage limit is reached at lower voltages and the common mode rejection ratio is seldom as good as obtained in true differential amplifiers. Still, the differential performance is perfectly adequate for most purposes.

Finally, the differential performance of the oscilloscope can be compromised if the external measurement probes are not well balanced. Considering all factors one should not normally count on the high frequency differential rejection ratio being better than about 100:1.

Trigger circuits: The measuring oscilloscope must be triggered to display the voltages resulting from discharging the *LTA* generator. There are several ways of doing so, as shown on Fig. 13.22. The preferred way is by taking a trigger signal from the *LTA* generator and carrying it to the oscilloscope along a coaxial cable, Fig. 13.22(a). If the trigger signal is to be carried into the aircraft, an isolating transformer, Fig. 13.22(b), must be connected in series with the trigger cable. Alternatively, Fig. 13.22(c), the trigger signal can be carried along a fiber optic link. The *LTA* generator may emit enough high frequency noise to allow one to trigger the measuring oscilloscopes from an electric field antenna, Fig. 13.22(d). This method of triggering has the virtue of simplicity, but may not provide as reliable or consistent triggering as the previous methods. Also, it may allow the oscilloscope to be triggered from other sources of electromagnetic interference.

With any of the techniques, delay may have to

be introduced in the circuit used to trigger the surge generator in order to compensate for the slow velocity of propagation in the trigger cable and to ensure that the oscilloscope is triggered before current builds up in the aircraft. Having a small amount of zero line available can greatly ease analysis of the recorded data.

Noise checks: Tests should be made to verify the effectiveness of the shielding on the measurement system. These are made by disconnecting the measurement leads from the aircraft wiring and discharging the surge generator. If no noise is picked up by the measuring system then one can have good confidence that the signal displayed on the oscilloscope truly represents the response of the aircraft wiring.

Digital oscilloscopes: Digital oscilloscopes are now to be preferred over analog oscilloscopes because the recorded signals can be retrieved for further processing. Digital oscilloscopes are subject to the same problems of noise pickup as analog oscilloscopes and should be shielded in the same way.

Measurements of lightning induced voltages and currents require that digital oscilloscopes have a wide bandwidth, on the order of 30 - 100 MHz. When reviewing the specifications of digital oscilloscopes care should be taken not to confuse the bandwidth of the analog input circuits with the bandwidth pertaining to sampled data. Accurate measurement of a 20 MHz oscillatory wave requires the wave to be sampled several times per cycle. Sampling 5 times per cycle would require the sampling rate to be 100 MHZ. Other discussions on requirements for digital measuring equipment are presented in [13.2].

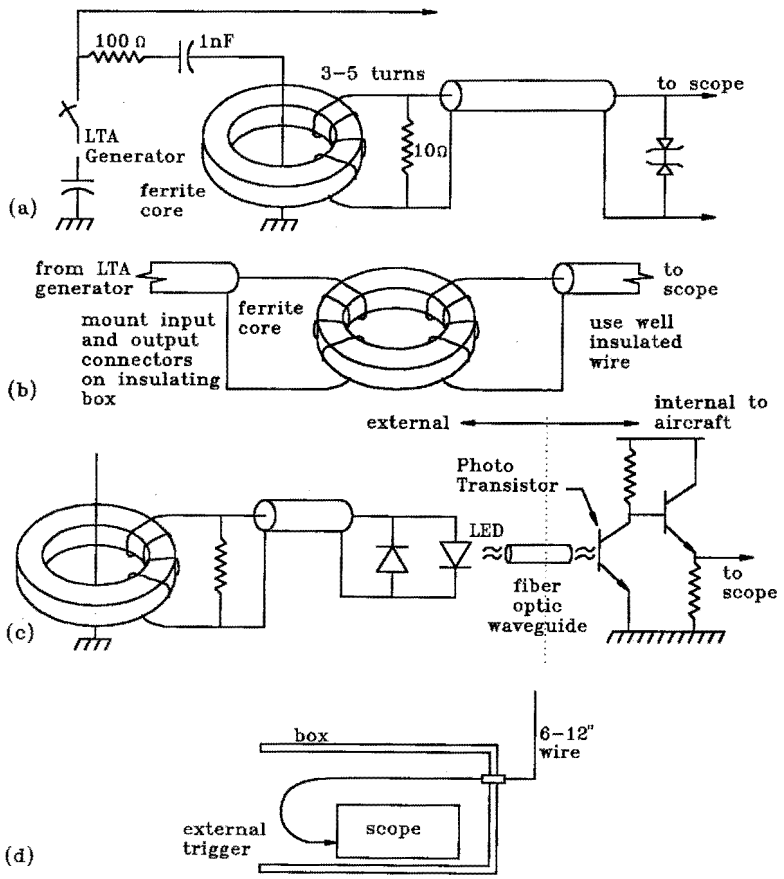

Fig. 13.22 Methods of triggering.
(a) Trigger transformer
(b) Isolation transformer
(c) Optical isolation
(d) Antenna triggering

Optical coupling: Some of the noise problems encountered during surge testing can be overcome by using optical links to couple the outputs from voltage and current probes to the measuring oscilloscope, but optical links have problems of their own. Analog, not digital, optical links are required, and the bandwidth of the optical link should be as wide as that of the measuring oscilloscope. Wide bandwidth optical links tend to have high noise levels and limited dynamic range. Sensitivity of the link is more prone to change than is the sensitivity of conventional hard wired links. Care must be taken not to overload the transmitters and the sensitivity of the link must be checked frequently.

13.5 Low-Level Swept Continuous Wave

This frequency domain technique involves exciting the aircraft with continuous waves rather than time domain pulses. Basically, the method utilizes a network analyzer to measure transfer functions, amplitude and phase, from the lightning attachment point to test points, voltage or current, within the aircraft. These transfer functions, if measured over a suitable wide frequency range, may then be multiplied by the frequency spectrum of a lightning pulse to determine the overall spectral response at the test point. Fourier transforms can then be taken to evaluate the time domain response.

Advantages and disadvantages of the swept CW technique are as follows:

Advantages

1. Standard low level oscillators and network analyzers may be used. These are commercially available and operate at levels sufficiently low that there are no safety problems, either to personnel or the aircraft.

2. Narrow band tuned measuring instruments can be used and these are more sensitive and less susceptible to interference than time domain instruments.

3. Aircraft and wiring system resonances are clearly displayed and quantified.

4. System responses may be quantified by tabular listings of amplitude and phase without need for developing equivalent circuits.

5. Many users are more used to working with frequency domain data than with time domain responses.

Disadvantages

1. No way to evaluate non-linearities in the aircraft response.

2. Scaling to full threat levels requires considerable mathematical manipulation.

13.6 Safety

Most simulated lightning testing, even though applied at reduced levels, involves the use and operation of high voltage equipment including capacitors and arcing switches. The electrical energies involved exceed the levels necessary to cause human fatalities and safety precautions must be taken and test procedures followed which ensure that during the test applications, personnel cannot accidentally come in contact with any electrically energized parts of the test circuit.

A secondary concern is the inherent danger of passing substantial currents through an aircraft fuselage containing fuel. This concern includes the problems associated with electrical arcing taking place in an area where fuel vapors may be present.

13.6.1 Personnel Safety

People actively involved with operating surge generators and measuring equipment may need to be physically close to or inside the aircraft during the test. This is particularly true for those operating measuring instruments. This can be done safely, but safety procedures must be developed and be well understood by all, both those involved in the tests and those who may be only casual bystanders.

Personnel familiarization: Prior to the start of active testing, all personnel working in the area, both those assigned to the test and those normally working in adjacent areas, should be assembled for a safety briefing and familiarization with the project. Written safety procedures are advisable.

Test area: The aircraft, test generators, waveshaping circuits, HV power supply, and capacitors will from time to time be energized to potentially dangerous voltages. A clearly defined test area should be fenced or roped off in such a manner as to preclude any person standing outside of the area from coming in contact with any of the above listed items or any other potentially hazardous point. No one should enter the test area without the permission of the test operator.

Safety ground point: A safety ground point should be established to which the facility ground, test circuit power supplies, low voltage side of the generator and safety grounding sticks can be connected. This ground point must be attached to the building structural steel, preferably in the floor. This point may also serve as an instrumentation ground reference point, though that is not its major function. The grounding stick can be in the form of a metal hook fastened to an insulating handle and connected to a flexible grounding wire. Another grounding hook should be provided for the surge generator.

Testing procedures: High voltage test equipment should be operated *only by qualified personnel* specifically designated to do so.

During a test, observers should not remain within the test area. Those who are working on the aircraft or assisting with the test should approach or enter the aircraft only when test equipment is de-energized and grounded. Both they and the test operator should have equal responsibility to ensure that equipment is de-energized and safety grounds connected.

Those who are operating the surge generator or operating measuring equipment should repair to their designated stations before the safety grounds are removed. Those operating measuring instruments may be in physical contact with the aircraft (in it or alongside it) during the test, but only if they are not simultaneously in contact with ground or the return wires.

With the exception of those operating measuring instruments, no one should contact the aircraft or return lines when a pulse from the surge generator is being applied.

Those who must have physical contact with the aircraft during tests have a special responsibility to ensure that they understand what type of contact is safe and what procedures are necessary to avoid unsafe contact.

Once the test area has been cleared of personnel, (with the exception of those operating measuring instruments) the test operator should enter, remove the grounding sticks, return to his station and perform the test. At the completion of a test or a series of tests, the operator should shut down the HV power supplies, enter the area and ground all potentially energized points before allowing any others to enter. The ground stick should be hung on the aircraft pitot boom or other current injection points between tests.

Operators of measuring instruments: When an oscilloscope is operated within the aircraft its case must be connected to the structure of the aircraft and it must be powered from an isolated power source; batteries and inverter or a well insulated isolation transformer. In such a case the oscilloscope can be operated perfectly safely by people within the aircraft. They may touch the framework of the aircraft or the measuring oscilloscope without regard for whether the aircraft is grounded or energized provided they not simultaneously touch any wire carrying external ground potential into the aircraft.

One lead that is likely to be brought into the aircraft is a coaxial cable carrying a trigger signal for the oscilloscope. Such a cable must be fitted with an isolating device so that neither the center conductor nor the cable shield provides direct current electrical continuity to external grounded objects. Methods of eliminating hazards from such sources are described in §13.4.3. In addition to possible safety hazards, externally connected leads brought into the aircraft are likely to carry undesirable electromagnetic interference onto the measuring oscilloscopes.

When an oscilloscope is operated adjacent to the aircraft, but not within the aircraft, it may still be operated safely, but safe operation requires more attention to the physical location of all apparatus. The case of the oscilloscope must again be connected to the aircraft and the oscilloscope must be powered from an isolated power source. Physically the oscilloscope will most likely have to be mounted on some sort of platform alongside the aircraft. This platform should be of an insulating material. Wooden stepladders or work platforms will provide sufficient insulation.

Personnel may still operate such equipment safely provided that satisfactory porcedures have been formulated and approved. As a minimum, such procedures should require the operator to stand on an insulating mat or be seated on an insulating chair set upon an insulating mat or platform. Barriers or insulating sheets should also be placed over the return wires.

13.6.2 Fuels Safety

Since the aircraft will usually be an operational aircraft, residual fuels may be present in the tanks, lines and vents. Since a fuel vapor mixture may be flammable, it is recommended that the tanks be drained of fuel and filled with dry nitrogen at positive pressure during the test period. As an alternative, the fuel tanks may be completely filled with fuel to eliminate as many vapor spaces as possible and the remaining spaces (such as fuel and vent lines) be filled with dry nitrogen at positive pressure so as to assure a non-flammable atmosphere during the test period.

Exposed electrical arcs: An attempt should be made to ensure that all switching arcs in the aircraft test circuit, including the switching gap in the surge generator, be restricted or enclosed. However, some tests may require or result in an exposed arc which could be an ignition source. Consequently, it will be very important for all personnel to be aware of and on the watch for fuel spills or fuel vapors in the test area. No test should be conducted with fuel leaks or spills in the area. Testing can resume only after the leaks or spills have been repaired and/or cleaned up. The source of any fuel vapors in the area must be identified and dealt with prior to proceeding with the tests.

REFERENCES

13.1 J. E. Pryzby and J. A. Plumer, "Lightning Protection Guidelines and Test Data for Adhesively Bonded Aircraft Structures," *NASA CR-3762*, NASA Langley Research Center, January, 1984.

13.2 K. E. Crouch, "Aircraft Lightning–Induced Voltage Test Technique Developments," *NASA CR 170403*, June 1983.

13.3 J. A. Plumer, F. A. Fisher and L. C. Walko. "Lightning Effects on the NASA F-8 Digital Fly-by–Wire Airplane," *NASA CR–2524*, 1975.

13.4 R. A. White, "Lightning Simulator Circuit Parameters and Performance for Severe–Threat, High Action Integral Testing," *International Aerospace and Ground Conference on Lightning and Static Electricity*, Orlando, FL, June 26-28, 1984, pp. 40-1 – 40-14.

13.5 W. W. Cooley, D. L. Shortess, "Lightning Simulation Test Technique Evaluation," *DOT/FAA/CT-87/38*, U.S. Dept. of Transportation, Federal Aviation Administration, October 1988.

13.6 L. C. Walko, "A Test Technique for Measuring Lightning–Induced Voltages on Aircraft Electrical Circuits," *NASA CR-2348*, NASA Lewis Research Center, February 1974.

13.7 L. J. Lloyd, J. A. Plumer and L. C. Walko, "Measurements and Analysis of Lightning–induced Voltages in Aircraft Electrical Circuits," *NASA CR–1744*, February, 1971.

13.8 J. A. Plumer, "Lightning Effects Relating to Aircraft, Part III–Measurements of Lightning – Induced Voltages in an F4H-1," *AFAL–TR–72–5, Part III*, Air Force Avionics Laboratory, Wright Patterson AFB, Ohio, March 1973.

13.9 J. A. Plumer, "YF–16 #1 Lightning Transient Analysis Test Report," *General Dynamics Report 16PR051*, 1975.

13.10 W. G. Butters, D. W. Clifford, K. P. Murphy, K. S. Zeisel and B. P. Zuhlman, "Assessment of Lightning Simulation Test Techniques," *Proceedings of IAGC on Lightning and Static Electricity*, March 1982.

13.11 D. W. Clifford, K. E. Crouch and E. H. Schulte, "Lightning Simulation Testing," *IEEE Transactions on Electromagnetic Compatability*, EMC-24, vol. 2, May 1982.

Chapter 14

RESPONSE OF AIRCRAFT WIRING

14.1 Introduction

Verifying that an aircraft will not be harmed by indirect effects is most likely to come about by performing bench tests in which voltages and currents are injected into the terminals and wiring of aircraft systems, tests such as described in Chapter 18. Specifications for such tests are often deficient in that they merely specify something like

> *Bench tests shall subject the equipment to the lightning environment specified in* ···

The referenced document then describes only the lightning environment to which the aircraft as a whole should be designed. Equipment inside the aircraft, of course, is not subjected to the full lightning threat, and it would not be meaningful to subject each individual box or cable to the 200 000 amperes peak current that might represent the external lightning threat.

Some sort of program is needed to estimate realistic levels at which tests should be conducted. Even if tests are not performed, some sort of program is needed to estimate levels to which equipment should be designed. If no estimates are made, either equipment must be designed and tested to arbitrarily chosen levels, or it will be designed or selected without any special regard for lightning indirect effects.

Some have called the process of determining voltages and currents on individual components a *flowdown* process, implying that it is one of determining how much of the external lightning environment "flows down" onto individual components. Ideally, the performance of flowdown calculations to determine the most likely voltages and currents on the wiring of an aircraft would be clearly identified as one of the necessary engineering tasks and would be allocated suitable staff, time and funding.

In principle, the voltages and currents on the aircraft wiring may be calculated from the geometry of the aircraft wiring and knowledge of the strength and orientation of the internal magnetic and electric fields, as discussed in Chapters 10, 11 and 12. Alternatively, they may be determined experimentally as discussed in Chapter 13. Since staff and funding are not always available to perform the necessary measurements and calculations, it is useful to have simplified techniques that at least let one determine the order of magnitude of the voltages and current induced by lightning effects.

This chapter undertakes to provide such techniques. The resulting estimates may not be very precise, but they can at least indicate the general magnitude and nature of the induced voltages and currents, and that may be sufficient for preliminary designs or tests.

The discussions to follow will treat both the open circuit voltage and the short circuit current induced on aircraft wiring. A knowledge of open circuit voltage is important because it represents the maximum voltage to which a circuit or electrical insulation might be exposed. Short circuit current is important because it represents the maximum current that might flow through an element designed to carry current, such as a protective spark gap or diode. The two factors together define the source impedance of the surge, a quantity needed in order to conduct rational bench testing of equipment.

The discussions will also provide an introduction to the art of modeling the response of electrical circuits to the voltages and currents induced by lightning.

14.2 Wire Impedances

Inductance and capacitance of conductors were treated in §9.7.3 and §9.8.1. For wires above a ground plane, Fig. 14.1, and using only air as insulation, simplified expressions for calculation are:

$$L = 0.2 \ln(4h/d) \ \mu\text{H/m} \tag{14.1}$$

$$C = \frac{55.56}{\ln(4h/d)} \ \text{pF/m} \tag{14.2}$$

where

$h =$ height above a ground plane
$d =$ conductor diameter

Inductance and capacitance may also be estimated from Figs. 14.2 and 14.3.

Inductance and capacitance also define the surge impedance of a conductor.

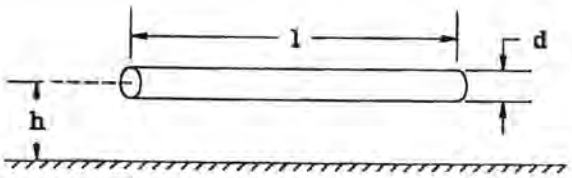

Fig. 14.1 Wire above a ground plane.

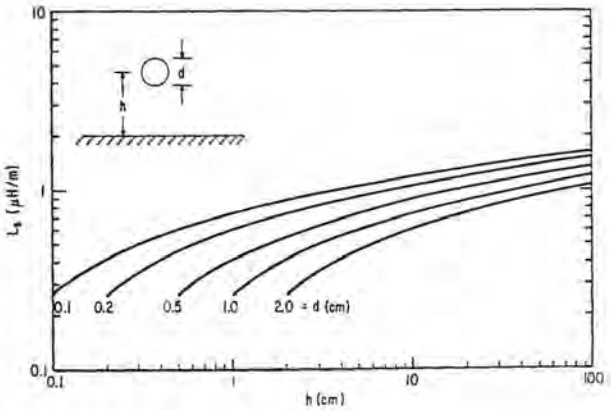

Fig. 14.2 Inductance of wires.

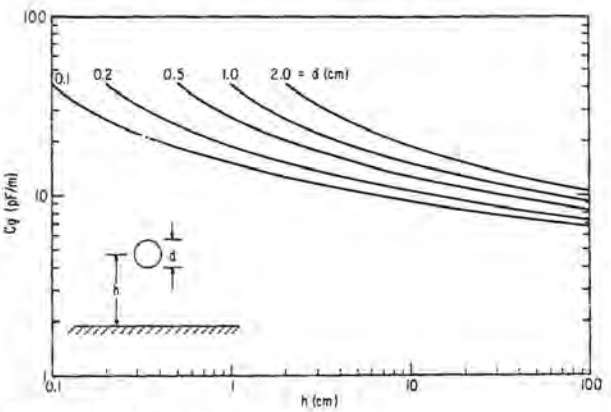

Fig. 14.3 Capacitance of wires.

$$Z = 60 \ln\left(\frac{4h}{d}\right) \text{ ohms} \qquad (14.3)$$

The velocity of propagation on such conductors is 300 m/μs, the speed of light.

14.3 Response Mechanisms - Short Wires

The response mechanisms will be reviewed first for conductors short enough that the response can be treated in terms of lumped constant elements. Many wiring systems in aircraft do not strictly qualify for this treatment, since they are long enough that they are better treated as transmission lines, but the lumped constant approach does illustrate the general nature of the response. Transmission line or distributed constant considerations are discussed further in §14.4.

14.3.1 Response to Resistive Voltage Rises

The elementary equivalent circuits are shown in Fig. 14.4. R_a represents the resistance of the aircraft, or more precisely the portion of the aircraft under consideration, while R_w and L_w represent the resistance and inductance of the wire. The most severe case involves conductors that are referenced to the airframe at one or more points. Power distribution systems are frequently so arranged. If the conductor is grounded at only one end, Fig. 14.4(a), the quantity of most interest is the open circuit voltage developed at the other end. If both ends of the wire are grounded, Fig. 14.4(b), the quantity of interest is the short circuit current.

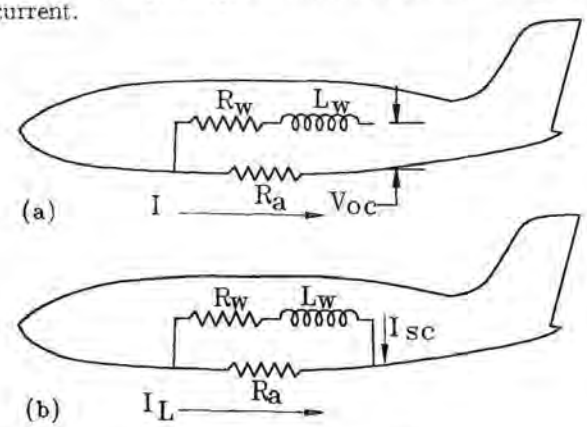

Fig. 14.4 Response to resistive voltage.
(a) V_{oc}
(b) I_{sc}

Open circuit voltage: A lightning current I_l produces an open circuit voltage

$$V_{oc} = I_l R_a. \qquad (14.4)$$

Wire routing or wire resistance will not affect the voltage.

Short circuit current: If the wire is connected to the airframe structure at each end, the current through the wire will depend on the resistance of the wire, its inductance and the waveshape of the lightning current. Such a connection may not appear to be a normal condition, but it does represent a limiting case if surge arresters are being employed to limit the voltage appearing between a conductor and the airframe. Assuming $R_a \ll R_w$, the wire current for lightning currents of long duration is

$$I_{sc} = I_l \frac{R_a}{R_w} \tag{14.5}$$

while for lightning current of short duration the wire current is

$$I_{sc} = \frac{1}{L_w} \int V_{oc} dt \tag{14.6}$$

where

I = amperes
L = self-inductance of wire or cable - H
V_{oc} = open circuit induced voltage - V
t = time - s

Multiple conductors: If there are several conductors in a bundle, all of the conductors will be subjected to the same open circuit voltage and short circuit current.

Wire shields: A shield on the wire, if it is grounded at only one end, Fig. 14.5(a), will not reduce the voltage or current to which the wire is subjected. If the shield is grounded at each end, as indicated in Fig. 14.5(b), it will reduce the voltage or current, but the degree of reduction will depend primarily on the resistance of the shield, as compared to the resistance of the aircraft and the resistance of the wire.

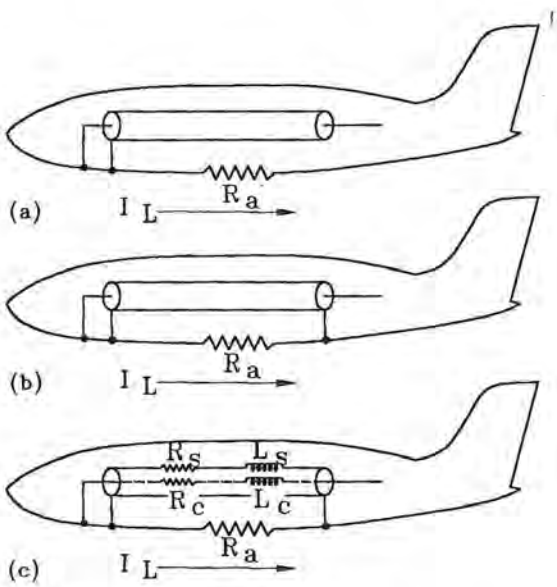

Fig. 14.5 Effects of a shield.
(a) Grounded at one end
(b) Grounded at both ends
(c) Equivalent circuit

Example: The geometry shown on Fig. 14.6(a) is somewhat representative of a conductor used for distribution of aircraft power. For the indicated lightning current, V_{oc} and I_{sc} are as shown on Fig. 14.6(d) and (e). The point of most importance is that the short circuit current is controlled more by the wire inductance than its resistance and reaches its peak long after the aircraft current has begun to decay.

Source impedance: Strictly speaking, source impedance would be found by taking the instantaneous values of voltage and current,

$$Z = \frac{V_{oc}}{I_{sc}} \tag{14.7}$$

and would be a quantity that was time or frequency dependent. Often however, the ratio of peak values of open circuit voltage and short circuit current is taken to be the source impedance and, for the above example, is 0.32 ohms. The quantity is a useful measure of the impedance of the circuit, but should be used with caution since it pertains only to the one waveshape of driving current.

The illustration of Fig. 14.6 is somewhat oversimplified, but it does illustrate the point that source impedance for resistively generated voltages is quite low, about the same as the resistance of the wire. This low source impedance is an important point that must be considered when applying surge protective devices, as discussed further in Chapter 16.

14.3.2 Response to Magnetic Fields

The simplest geometry to consider, Fig. 14.7(a), is that of a conductor placed adjacent to a metal surface and exposed to a uniform magnetic field oriented to produce maximum voltage in wiring. Single conductors are rarely found in an aircraft; more commonly conductors are part of a bundle of wires, or one of the wires in a multi-conductor cable. For the analyses to follow, the effects will be about the same for a single wire or for a group of wires comprising a cable or bundle. If the cable is fitted with a shield, the shield can be treated as just another conductor.

Open circuit voltage: The open circuit induced voltage between the wire and ground, or the common mode voltage of wires in a cable, will be

$$V_{oc} = \frac{d\phi}{dt} = \mu_o A \frac{dH}{dt} \tag{14.8}$$

where

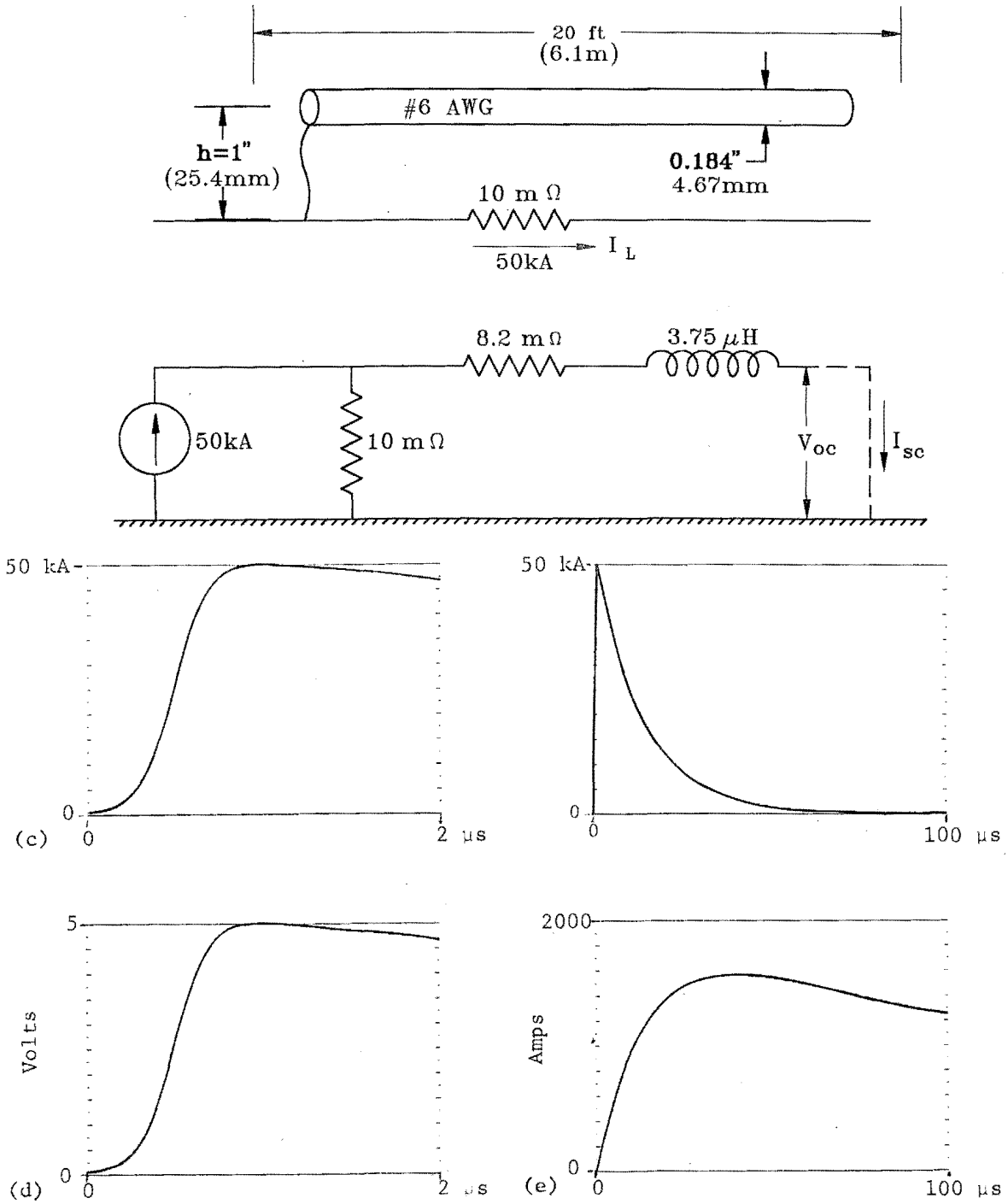

Fig. 14.6 Resistively coupled voltage.
(a) Geometry
(b) Equivalent circuit
(c) I_l (two time scales)
(d) V_{oc}
(e) I_{sc}

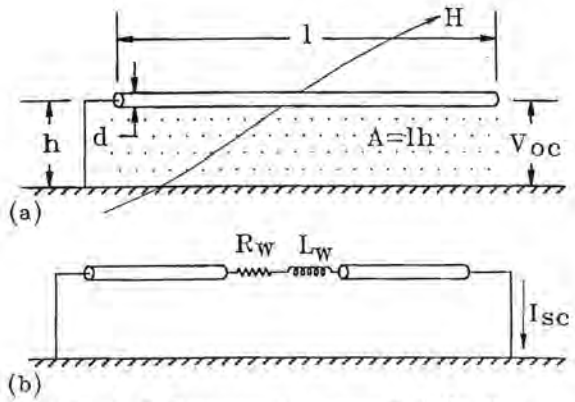

Fig. 14.7 Response to magnetic induction.
(a) V_{oc}
(b) I_{sc}

$A =$ area of the loop involved - m^2
$A = lh$ in Fig. 14.7
$\mu_o = 4\pi \times 10^{-7}$
$\phi =$ total flux linked - webers
$H =$ magnetic field intensity - A/m
$t =$ time - s

If l and h are measured in inches:

$$V_{oc} = 8.11 \times 10^{-10}\, lh \frac{dH}{dt} \qquad (14.9)$$

where

$l =$ length - in
$h =$ height above ground plane - in
$H =$ magnetic field intensity - A/m
$t =$ time - s

The induced voltage is thus proportional to the length of the wire, its height above ground and the strength of the magnetic field. Voltage can be reduced by keeping wires or cables close to the ground plane and by routing them along a path where the magnetic field strength is low. These points are discussed further in Chapter 15.

As will be discussed in Chapter 15, an elementary model for voltage induced in a wire consists of a voltage source placed at the center or one end of the wire, along with some representation of the loads at the two ends of the wire. The induced voltage then divides between the loads at the ends of the wire. The largest voltage appears across the load with highest impedance. For worst case analysis, one can consider one end of the wire to be grounded with the other end open circuited. All the voltage will then appear at the open circuit end of the wire.

Short circuit current: The maximum current is that which flows when both ends of the wire or cable are connected to the vehicle structure through a low or zero impedance, Fig. 14.7(b). The short circuit current is then mostly affected by the wire inductance and, treating only inductance, is

$$I_{sc} = \frac{1}{L} \int V_{oc} dt. \qquad (14.10)$$

where

$I_{sc} =$ amperes
$L =$ self-inductance of wire or cable - H
$V_{oc} =$ open circuit induced voltage - V
$t =$ time - s

The induced voltage, V_{oc}, that drives the current, is directly proportional to the cable height, but the cable inductance L that impedes the flow of current, is proportional to the logarithm of the cable height. Both V_{oc} and L are proportional to cable length. The result is that short circuit current is practically independent of the length of the cable and only moderately dependent on the height of the cable above ground.

An individual wire might have a low impedance load by being connected to a semiconductor, in which case the short circuit current might flow directly through the semiconductor and its bias source. If the circuit is intentionally designed to have a low input impedance, there may be no damage if the current is not too large. Maximum available short circuit current is an important point to consider when selecting surge protective devices.

Multiple wires: If a group of wires is involved, Fig. 14.8(a), the induced voltage so calculated is that existing between the entire group of conductors (comprising the bundle or cable) and the vehicle structure. Assuming equal load impedances, the voltages on each of the wires will be about the same and will not depend on the location of the wire within the bundle or cable.

Line-to-line voltages: Line-to-line voltages (also called differential or circuit voltages) will be less than line-to-ground voltages, generally by a factor of 10 to 200, or 20 to 46 dB, because individual conductors are usually close together and are often twisted, thus reducing the total loop area.

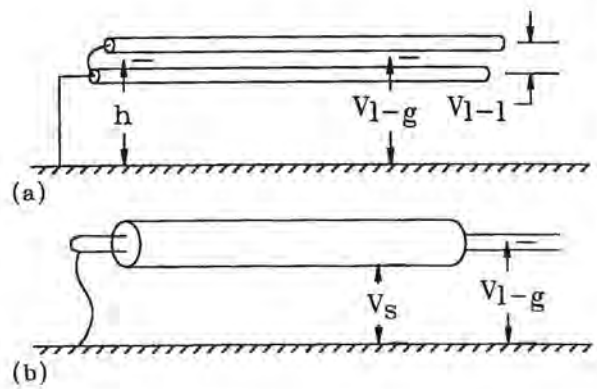

Fig. 14.8 Multiple conductors.
(a) Bundled conductors
(b) Shielded bundle

Determining the voltage between wires, or the dB difference between line–to–ground and line–to–line voltages in terms of wire locations, is beyond the capabilities of any elementary type of calculation. Modal analysis techniques are called for, but a discussion of that subject is beyond the scope of this book. Empirical estimates are often about the best that can be hoped for.

The actual magnitude of the circuit voltage is determined as much, or more, by the impedances of the circuits to which the wires connect as it is by the characteristics of the wire. Prudence might suggest not counting on line–to–line voltages being more than 20 dB less than line–to–ground voltages unless the circuits have been carefully designed to have balanced impedances at both ends of the cable.

Effect of a shield: If the wire is covered with a shield grounded at only one end, Fig. 14.8(b), the magnetically induced voltage from conductor to ground will not be much reduced, though the shield may reduce the voltage between conductors. The field will induce as much voltage between the end of the shield and ground as it does between the conductor and ground. A shield grounded at each end will reduce the voltage, but further discussion of the matter will be deferred to Chapter 16.

Orientation of the field: Eqs. 14.8 and 14.10 assume the magnetic field to be oriented at right angles to the plane of the wire loop. If the field were oriented differently the induced voltage would be less, but for simplified calculations such as these it is probably prudent to consider only worst case orientation of the field.

Example: Fig. 14.9(a) shows the same conductor as Fig. 14.6(a), but subjected to a changing magnetic field of the waveshape indicated in Fig. 14.9(c). In the equivalent circuit of Fig. 14.7(b) the voltage source would have a magnitude and waveshape as calculated by Eq. 14.9. For this elementary circuit the driving voltage would be the same as V_{oc}, Fig. 14.9(d), and its waveshape is that of the derivative of the magnetic field. The short circuit current, being proportional to the integral of the open circuit voltage, has nearly the same waveshape as the magnetic field driving the circuit.

Source impedance: The ratio of open circuit voltage to short circuit current for this circuit is 9.6 ohms, a value much higher than found for the resistively coupled example of Fig. 14.6. As in §14.3.1 the value of surge impedance applies only for a magnetic field having the indicated waveshape.

14.3.3 Response to Electric Fields

Equivalent circuits for objects exposed to an electric field are not as intuitively obvious as for conductors exposed to IR rises or to changing magnetic fields. They are best developed by discussing the short circuit current before discussing open circuit voltage.

Short circuit current: For conductors exposed to a changing magnetic field, the voltage and current can be eliminated, theoretically, by placing the conductors flush with the ground plane. For conductors exposed to a changing electric field this may not be so.

Fig. 14.10(a) (also shown in §9.8.3) shows a surface exposed to a changing electric field E_a, the field assumed to be oriented perpendicular to this surface. The changing electric field will produce a displacement current and if a portion of the surface is isolated and connected to the rest of the surface through a conductor, the current through that conductor will be

$$I_{sc} = K\epsilon_0 A\frac{dE_a}{dt} \qquad (14.11)$$

where K is unity for this geometry and

A = area of the surface - m^2
$\epsilon_0 = 8.854 \times 10^{-12}$ F/m
E_a = actual electric field - V/m
t = time - seconds
I_{sc} = short circuit current - amperes

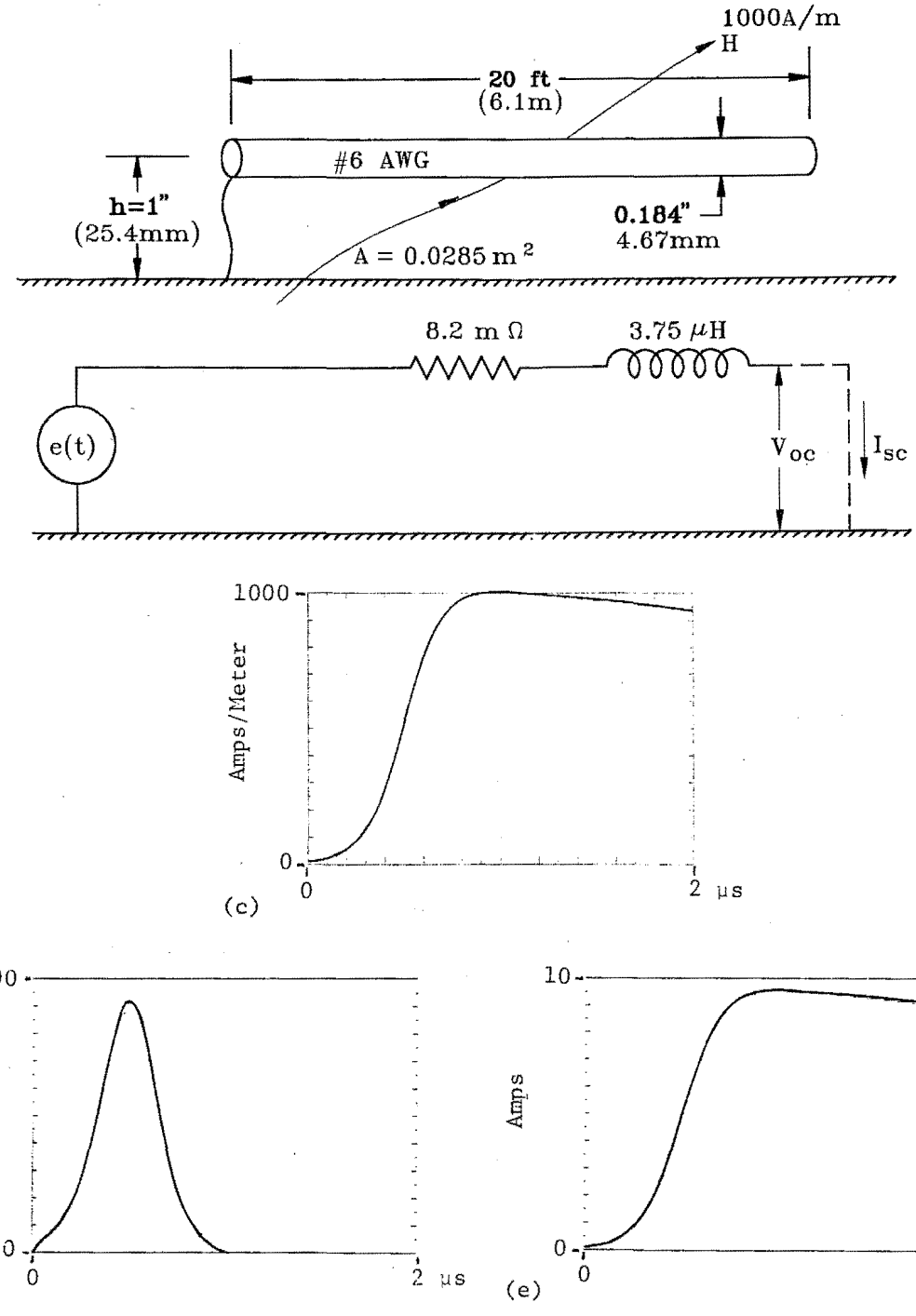

Fig. 14.9 Magnetically induced voltage.
(a) Geometry
(b) Equivalent circuit
(c) Magnetic field
(d) V_{oc}
(e) I_{sc}

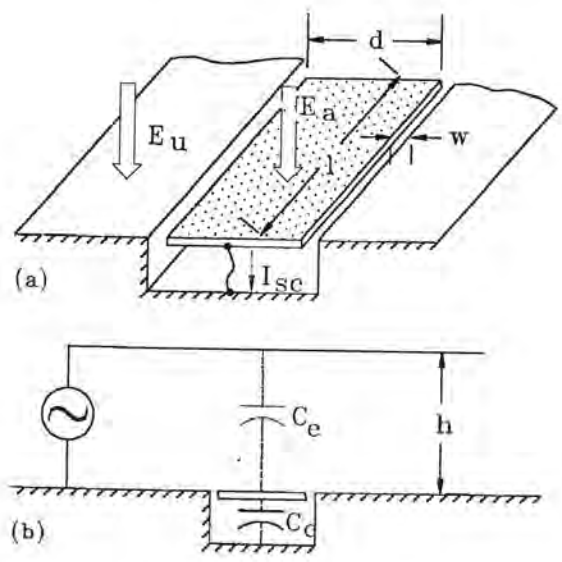

Fig. 14.10 Displacement currents.
(a) Geometry
(b) Equivalent circuit

The capacitance of the plate will depend on its geometry and that of the surroundings surfaces, and is a quantity that can be either calculated or measured. The capacitance will not affect the short circuit current, but it does affect the open circuit voltage, as will be discussed shortly.

An alternative view, more readily adapted to numerical circuit analysis, treats the problem in terms of the equivalent circuit shown in Fig. 14.10(b). It involves an equivalent capacitance C_h connected to a fictitious plate at a height h_e, the plate being energized from a fictitious voltage source V_e.

$$I_{sc} = C_h \frac{dV_e}{dt} \tag{14.12}$$

where

$$V_e = h_e E \tag{14.13}$$

$$C_h = \frac{\epsilon_0 l d}{h_e}. \tag{14.14}$$

Since h_e appears in both V_e and C_h, and thus in both numerator and denominator of Eq. 14.12, its value is immaterial and can be taken as unity.

The current depends on the intensity of the electric field E_a actually incident on the isolated section. If the isolated section were set flush with the rest of the surface, and the spacing w between the two sections were negligible, then the actual field E_a would be equal to the undisturbed field E_u.

If, as shown in Fig. 14.11, the surface is raised above the surrounding surface, the actual electric field intensity E_a would be greater than the undisturbed field E_u. Consequently, such a surface will intercept more displacement current. Calculating the current intercepted, or evaluating the factor K in Eq. 14.11, would require evaluating the electric field intensity at all points on the surface, either by cut-and-try field plotting or by one of the various 2D and 3D modeling techniques discussed in Chapters 10 - 12.

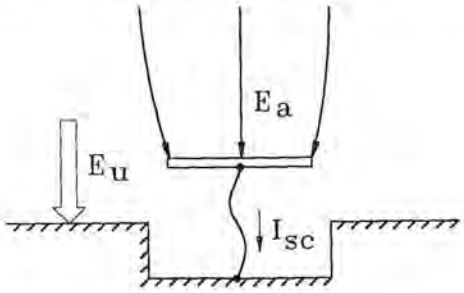

Fig. 14.11 Elevated surface.

A simple geometry for which K or E_a can be calculated is the hemicylinder shown in Fig. 14.12(a) and (b). For it

$$E_a = 2E_u \cos\phi. \tag{14.15}$$

Integrating this electric field over the surface of the hemicylinder shows that it will intercept twice the displacement current of a flush surface having the same projected area.

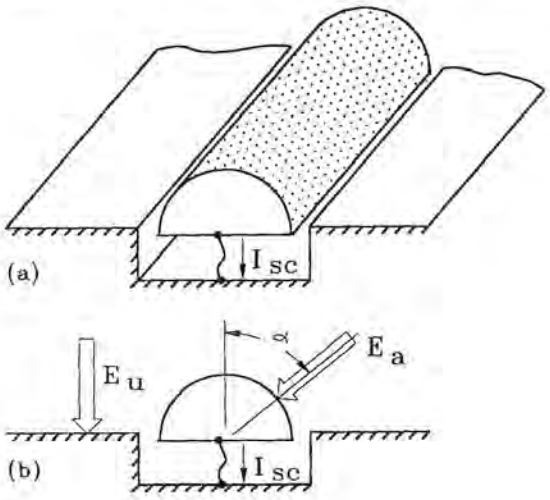

Fig. 14.12 Hemicylinder.
(a) Geometry
(b) End view

The factor K for the hemicylinder is thus 2. The current intercepted by several other geometries was shown on Table 9.5, and values of K for them could be calculated. Values of K for conductors above a ground plane can readily be calculated, as will be discussed shortly.

Open circuit voltage: Open circuit voltage is most easily obtained by integrating the displacement current in the known (by measurement or calculation) capacitance of the conductor.

$$V_{oc} = \frac{1}{C}\int I_{sc}dt. \tag{14.16}$$

Recognizing that I_{sc} is proportional to the rate of change of electric field, the open circuit voltage of the isolated plate of Fig. 14.10(b), for example, is

$$V_{oc} = \frac{\epsilon_0 l d}{C}E \tag{14.17}$$

where C is the capacitance of the plate.

Conductors above ground: For the case of an isolated conductor above ground, Fig. 14.13(a), the open circuit voltage would be

$$E_{oc} = hE_a. \tag{14.18}$$

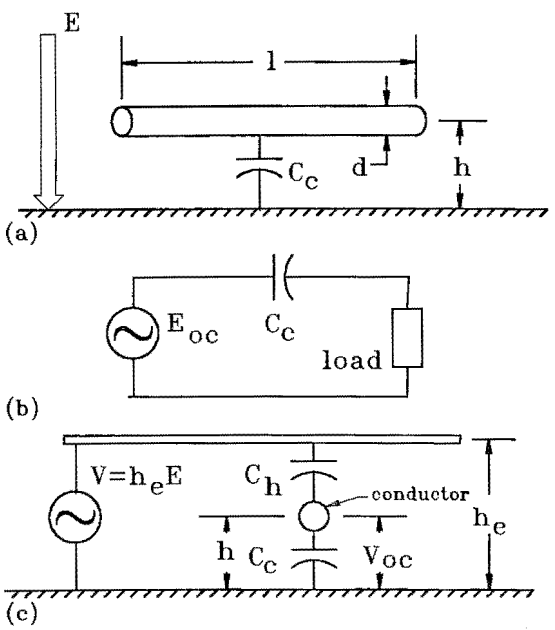

Fig. 14.13 Equivalent circuits for electric field coupling to elevated conductors.
(a) Geometry
(b) Equivalent in terms of V_{oc} and C_c
(c) Equivalent in terms of V and C_h

One equivalent circuit, Fig. 13(b), treats this open circuit voltage as being connected to a load through the capacitance of the conductor, the capacitance being as given by Eqs. 14.2 and 9.99. The short circuit current is then

$$I_{sc} = C_c\frac{dE_{oc}}{dt}. \tag{14.19}$$

Another equivalent circuit, Fig. 14.13(c), is more convenient for inclusion in circuit analysis programs. In place of an electric field, a fictitious surface at a height h_e is assumed, the surface being connected to a voltage $V_e = h_eE$. The open circuit voltage can then be defined in terms of the actual physical capacitance C_c and an equivalent coupling capacitance C_e:

$$V_{oc} = V_e\frac{C_h}{C_h + C_c}. \tag{14.20}$$

If $h < 1$, h_e may be taken as unity, in which case

$$C_h = C_2\left(\frac{h}{1-h}\right). \tag{14.21}$$

K factors: For isolated conductors the factor K as used in Eq. 14.11 can be calculated by equating short circuit currents as expressed by Eqs. 14.11 and 14.19.

$$K = \frac{h}{d}\cdot\frac{2\pi}{\ln(4h/d)} \tag{14.22}$$

K as a function of h/d is shown in Fig. 14.14.

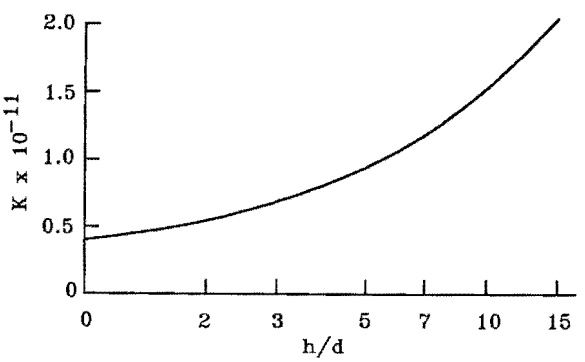

Fig. 14.14 Factor K for elevated conductors.

Example: Fig. 14.15(a) shows the conductor of Fig. 14.6 exposed to an electric field having the magnitude and shape given by Fig. 14.15(c). The equivalent circuit of Fig. 14.13(b) was derived as shown in Fig. 14.13(c) and Eq. 14.21, with h_e taken as unity. The open circuit voltage and short circuit current would then be as shown in Figs. 14.15(d) and (e).

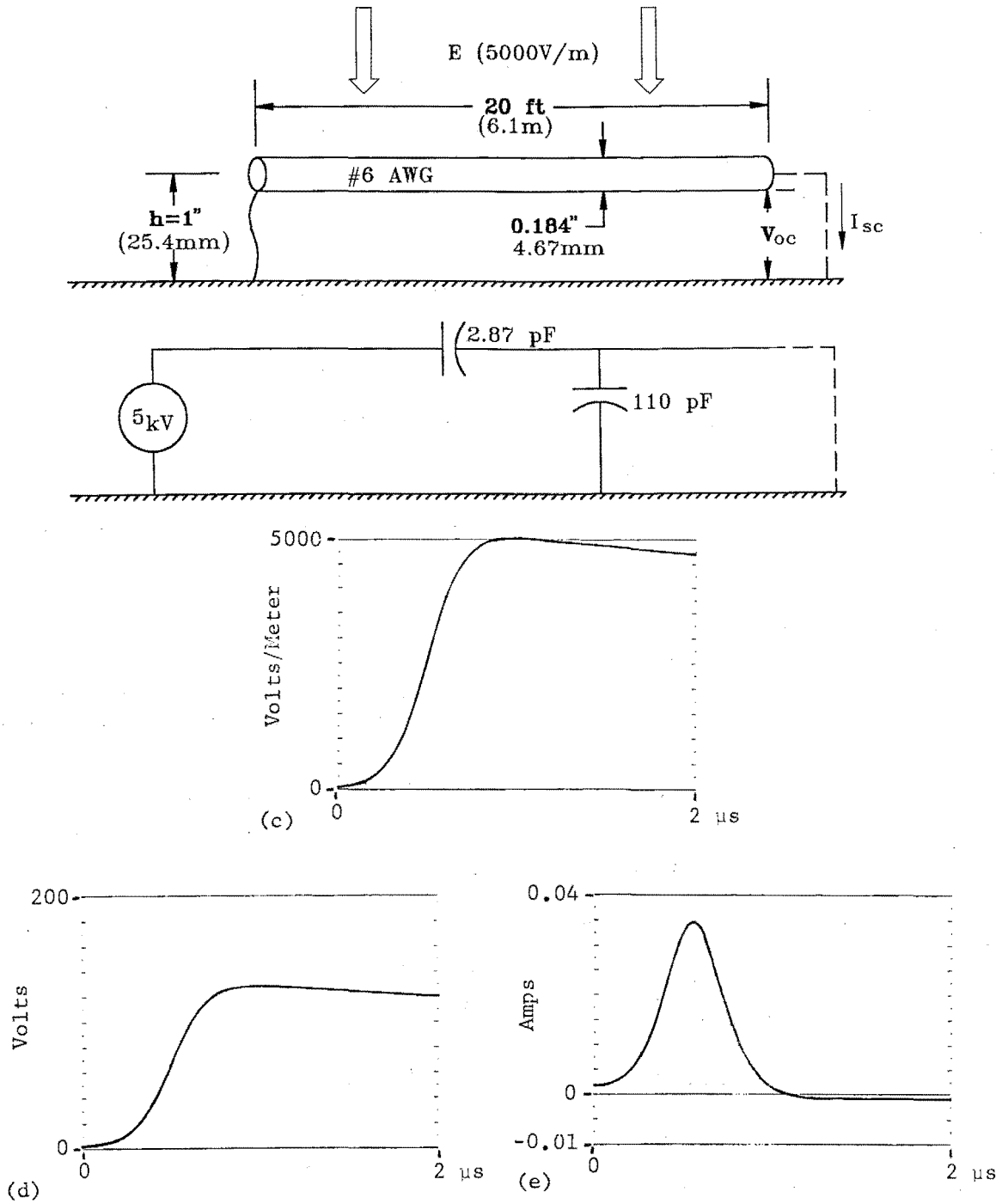

Fig. 14.15 Capacitively induced voltage.
(a) Geometry
(b) Equivalent circuit
(c) Electric field
(d) V_{oc}
(e) I_{sc}

Source impedance: The source impedance, defined by the ratio of the peak voltage and current, is 3681 ohms, a number much higher than for an equivalent conductor exposed to IR voltage rises or a magnetic field, though again it pertains only to one particular waveshape. This high value of source impedance partially explains why it is easier to provide effective shielding against electric fields than against magnetic fields or resistively generated voltages.

Multiple conductors: If there are multiple conductors in a bundle, the displacement currents will be intercepted primarily by the outer conductors and consequently location of a conductor in a bundle does make a difference as regards the capacitively coupled currents, unlike the situation with resistively or magnetically induced currents.

Effect of a shield: Since displacement currents are intercepted by the outermost conductor, a shield will reduce capacitively coupled currents, even if it is grounded at only one end. This assumes the shield to be sufficiently short that its impedance is negligible; an assumption generally made in discussions of shielding practices, though often unstated.

14.4 Transmission Line Effects

Conductors always have associated with them some distributed capacitance and inductance, the values of which are determined by the size of the conductors and the distance of the conductors from adjacent ground planes and other conductors. When these are considered, the effect of changing electric and magnetic fields is to produce oscillatory voltages and currents.

Example: Fig. 14.16 shows an example, the wire of Fig. 14.9 being treated as a transmission line of 185 ohms surge impedance, Eq. 14.3, with the induced voltage, Fig. 14.16(c) being connected at the center. The calculations pertain to a magnetic field with a faster rate of rise than was used on Fig. 14.9. The distributed nature of the wire gives rise to traveling waves or oscillations that persist longer than the induced voltage. The more rapid the rate of change of field, the more pronounced will be the oscillations. Losses reduce the oscillations and may eliminate them entirely, at least as calculated for simple circuits.

The oscillations are not noted on the short circuit current since it responds to the integral of the induced voltage. For the circuit of Fig. 14.16, source impedance was 62 ohms, several times higher than for the situation illustrated in Fig. 14.9. The difference in impedance is mostly due to the difference in waveshape of the magnetic field.

Complex oscillations: When the internal magnetic field is of complex waveshape, as is the usual case, and not the idealized inverse exponential function shown in the preceding figures, the resulting open circuit voltage may be of a very complex nature. A few examples were shown in Chapter 8. While the maximum voltage may be difficult to predict, given the complex nature of the superimposed oscillations, the amplitude of the envelope can at least be approximated using the elementary techniques described above.

Frequency: The frequency of the superimposed oscillations tends to be inversely proportional to the conductor length. Conductors, such as shields, grounded at one end tend to ring as quarter-wave dipoles. For example, a conductor 10 m long tends to ring at 7.5 MHz. Even this simple relationship is difficult to apply, since one conductor is seldom free of the influence of adjacent conductors. Capacitance and inductance at the ends of the conductors make the oscillatory frequencies lower and may result in oscillations being excited in a complete circuit when they would not be excited if only the distributed inductance and capacitance of the conductors were involved.

Aircraft wiring is usually grouped into bundles, the bundles usually containing both short and long conductors. The assembly, even if exposed to a magnetic field of simple waveshape, will oscillate in a complex manner. Generally there will be one dominant frequency with several other frequencies, usually higher, superimposed. Each will have its own characteristic decrement. About the only reliable generalization is that the bundles associated with large aircraft will be longer than the bundles associated with small aircraft and will generally oscillate at lower frequencies. On fighter aircraft, measurements of induced voltages have shown the characteristic frequencies to be in the range 1 to 10 MHz.

Currents measured on bundles of conductors also tend to be oscillatory, like the voltages, as long as the conductors are part of a wiring group employing a single-point ground concept. Currents on conductors contained in a shield grounded at each end tend not to be oscillatory, but to follow the underlying shape of the internal magnetic field.

14.5 Magnetic Field Zones

From the discussions of the preceeding chapters it can be seen that the task of mapping the electromagnetic fields inside a vehicle and making detailed flowdown calculations to determine the voltage or current on all circuits and cables could be a formidable task. A possible solution to the flowdown problem lies in rec-

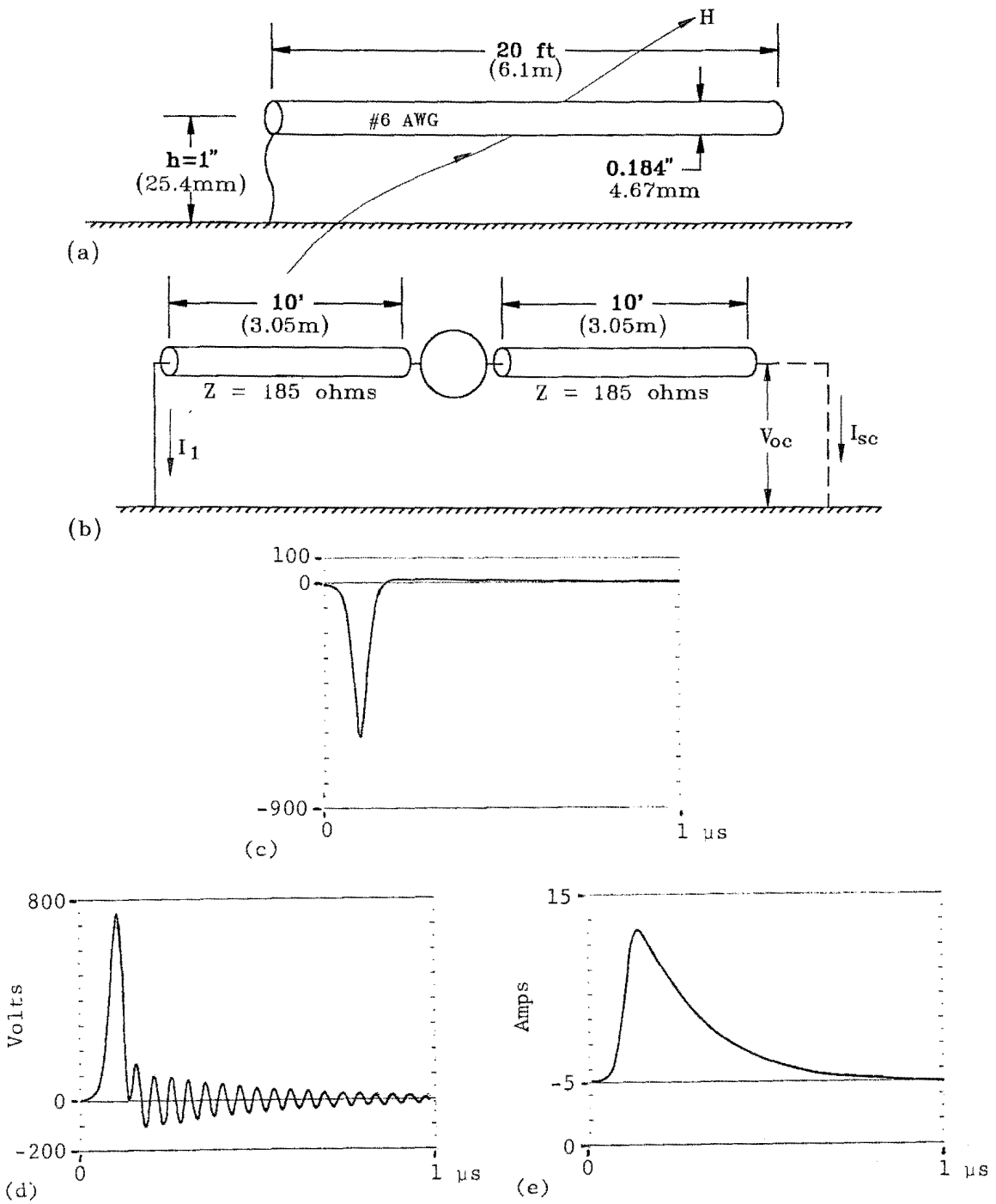

Fig. 14.16 Traveling wave effects.
(a) Geometry
(b) Equivalent circuit
(c) Induced voltage
(d) V_{oc}
(e) I_{sc}

ognizing that aircraft, or at least aircraft within a particular category, tend to possess characteristic zones, though the zones to be discussed should not be confused with the lightning strike zones discussed in the chapters dealing with direct effects of lightning.

As an example of a magnetic field zone, consider the cockpit of a fighter aircraft. It can be regarded as a magnetically open region exposed primarily to aperture–coupled magnetic fields. Within reasonable limits, all fighter aircraft probably have approximately the same magnetic field in the cockpit.

Another type of equipment zone characteristic of fighters would be equipment bays located in the forward section and behind the radome. All such equipment bays tend to be alike, the differences, perhaps, relating mostly to the type of fasteners used to hold the covers in place. The structure within a wing provides a type of magnetic field fundamentally different from either the cockpit or the forward equipment bays.

Accordingly, it would seem possible to divide an aircraft into a relatively small number of typical zones, to assign a ruling or characteristic magnetic field intensity to those zones, and to provide rather simplified tables or nomograms listing the characteristic transient likely to be induced in wiring of a given length.

This concept of dividing an aircraft structure into different magnetic field zones and assigning a ruling magnetic field strength to each zone, while imperfectly formulated at present, is fundamentally no different from the civil engineering practice of designing a structure to withstand a standard (generally worst case) wind loading. While the wind loading may differ widely at different points on the structure, the task of calculating the wind loading on each and every structural member would probably be sufficiently expensive that it would offset the savings that one might realize by tailoring each structural member to its own specific wind loading.

14.5.1 Zones as Applied to the Space Shuttle

This concept of dividing an aircraft into shielding zones was first used on the Space Shuttle [14.1]. The zones so defined are shown in Fig. 14.17. The electromagnetic fields assigned to each of these zones were initially estimated by a group of engineers knowledgeable about lightning interactions. These magnetic fields were then refined during the course of an extensive analytical investigation.

The magnetic field amplitudes assigned to each of these zones, based on the analytical study, are given in Table 14.1. The fields were divided into two components, an A–component referring to fields coupled through apertures and a B–component referring to fields coupled by diffusion through metal surfaces. The A–component of the field would tend to have the same rapidly changing waveshape as the external magnetic field, while the B– component would have a much slower waveshape.

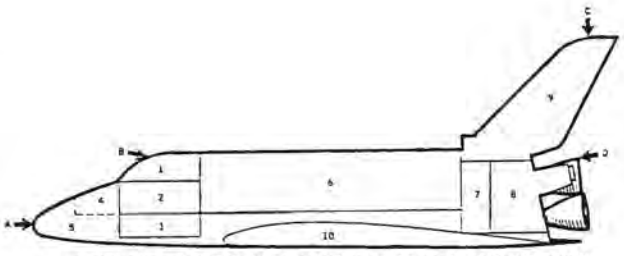

Fig. 14.17 Shielded zones within the *Orbiter* vehicle.

Table 14.1
Magnetic Fields in Different Zones of the Space Shuttle Orbiter

Zone	Aperture Fields A-component (A/m)	Diffusion Fields B-component (A/m)
1	1200	800
2	60	200
3	0	200
4	50	150
5	50	100
6	280	300*
		150**
7	50	570
8	200	680
9	200	3700
10	65	300

*Payload
**No payload

In the Space Shuttle study the waveforms of the different components were taken to be as shown on Figure 11.14. In each case the field intensity was based on a worst case 200 kA lightning current passing through the Orbiter vehicle. The field amplitudes of Table 14.1 were the maximum amplitudes calculated for any of the possible lightning current entry or exit points. While no particular claim for accuracy can be made about any individual point within the Orbiter, the field amplitudes at least seem reasonable.

14.5.2 Calculation of Voltage and Current

If the assumptions are made that there is a ruling field for a particular zone and that the magnetic fields have linearly changing waveshapes (constant rates of change), then it is possible to derive some simplified relationships between the magnetic field and the resulting induced voltages and currents. The principles were reviewed in §14.2. As applied to the Space Shuttle, additional assumptions were:

1. The conductor was of length l, diameter d, and spaced a height h above a ground plane.

2. The magnetic field was oriented to produce maximum voltages in the conductor.

3. One end of the conductor was grounded.

4. The magnetic fields were of the shape shown in Fig. 14.18. The figures and tables that follow would have to be recalculated if the fields had different waveshapes.

These are also the assumptions made in §14.2.

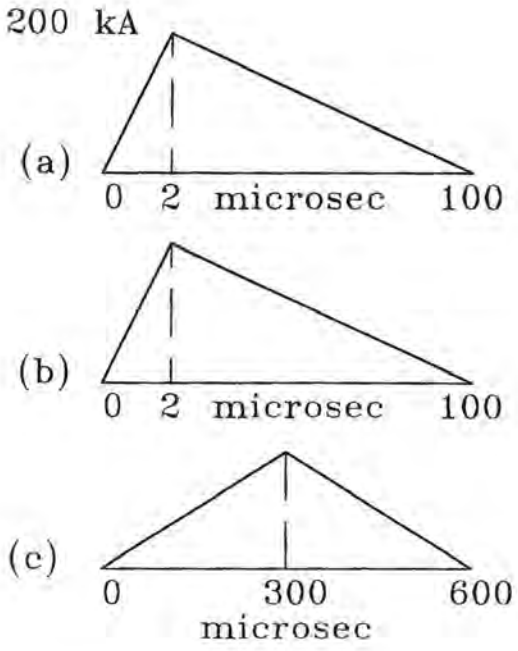

Fig. 14.18 Waveforms used for *Orbiter* analysis.
(a) Lightning current
(b) Aperture–coupled field, A–component
(c) Diffusion–coupled field, B–component

Open circuit voltage: The open circuit voltage was assumed to be developed only by the aperture coupled magnetic fields, all of which were assumed to rise linearly to their peak in two microseconds. Then:

$$V_{oc} = K_1 l h H \tag{14.23}$$

where

$K_1 = 0.63$ if l and h are in meters
$K_1 = 0.63 \times 10^{-4}$ if l and h are in centimeters
$K_1 = 0.41 \times 10^{-3}$ if l and h are in inches

In all cases H is expressed in amperes per meter. The waveshape of the open circuit voltages would be proportional to the derivative of the H field, and hence is likely to be oscillatory.

Short circuit current: Short circuit current was assumed to be governed by the diffusion–coupled magnetic field and, for conductors grounded at each end was

$$I_{sc} = K_2 h H \tag{14.24}$$

where K_2 was given by either Fig. 14.19 or 14.20, according to the units used for measurement of the conductor. Since current was governed by the dimensions of the conductor, or more exactly by its inductance, K was not a constant, but depended on the ratio h/d, as well as the rise and fall times of the magnetic field.

Conductor length does not influence short circuit current. The waveshape of the short circuit current tends to be the same as that of the incident magnetic field.

The height, h, of the cable bundle above a ground plane is difficult to specify because the ground plane is seldom purely a plane surface and because cable bundles are frequently strapped directly to a supporting structure. For purposes of analysis it was assumed:

1. That height h was measured to the nearest substantial metallic structural member.

2. That if the cable bundle was laid directly on that member, h equaled one–half the cable diameter.

3. That if the cable bundle was elevated above the metallic structural member, h equaled the clear height above the member plus one-half the cable diameter. If the cable height differed along its length, an average height was used.

Based on Eqs. 14.23 and 14.24, Fig. 14.18, and Table 14.1, the voltages and currents on typical wiring in the Space Shuttle Orbiter were calculated. The results are shown on Table 14.2 [14.1].

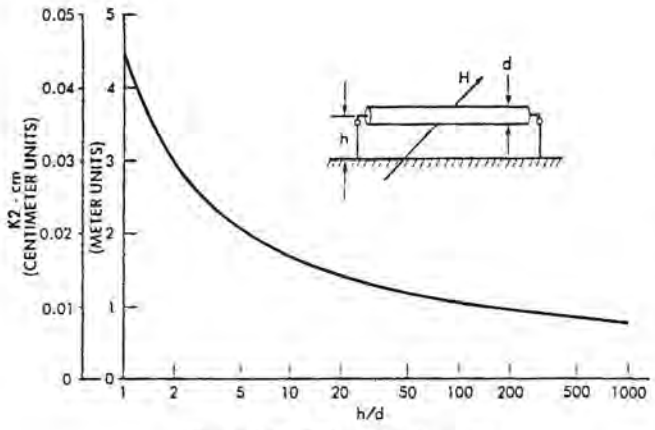

Fig. 14.19 K2 - metric units.

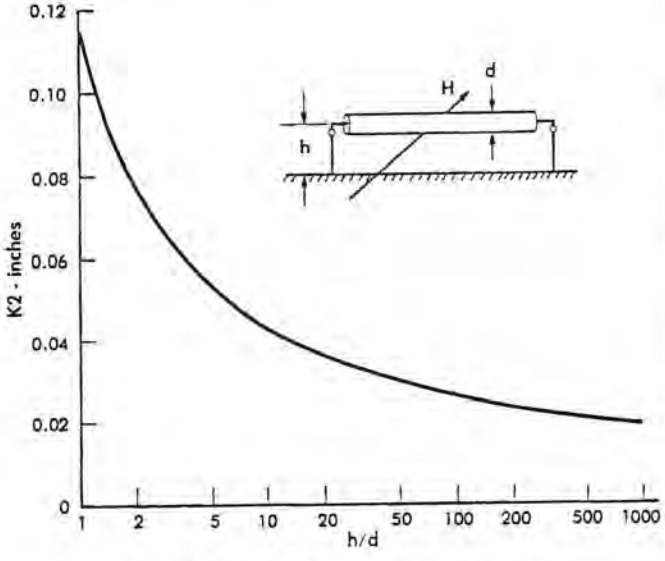

Fig. 14.20 K2 - inch units.

Screening calculations: Analyses of the nature illustrated were made for wiring on the Space Shuttle Orbiter and used for preliminary screening of all critical circuits [14.2]. For each conductor an estimate was made of the expected open circuit voltage and short circuit current and then an analysis was made to see if the electrical and electronic components to which that circuit connected could reasonably be expected to withstand those voltages and currents. Part of the process involved estimating the margin between what the equipment could reasonably withstand and the voltages and currents estimated by these simple techniques. For those relatively few circuits where there was a problem, or where the margin was not enough for comfort, more refined calculations were made and, if necessary, circuits were modified.

Table 14.2
Open Circuit Voltage and Short Circuit Cable Current in the Various Zones of the Space Shuttle

Zone	h = 1 in. Voltage (volts)	(0.0259 m) Current (amperes)	h = 2 in. Voltage (volts)	(0.0508 m) Current (amperes)	h = 5 in. Voltage (volts)	(0.1270 m) Current (amperes)	h = 10 in. Voltage (volts)	(0.254 m) Current (amperes)
1	76.90	133.3	153.8	184.9	384.6	321.8	769.1	521.1
2	3.92	7.10	7.84	9.42	19.59	16.39	39.18	26.54
3	0.085	0.154	0.170	0.204	0.425	0.356	0.850	0.576
4	3.25	5.89	6.51	7.82	16.27	13.62	32.54	22.05
5	3.23	5.85	6.46	7.76	16.14	13.51	32.29	21.87
6	17.99	32.59	35.99	43.26	89.96	75.28	179.9	121.9
7	3.43	6.21	6.87	8.26	17.16	14.36	34.33	23.26
8	13.05	23.64	26.11	31.38	65.27	54.62	130.5	88.44
9	14.33	25.96	28.66	34.45	71.65	59.96	143.3	97.09
10	4.27	7.74	8.55	10.28	21.37	17.88	42.75	28.96

*All values based on cable length of 157.48 inches (4 m) and diameter of 1 inch (0.0254 m). For other lengths, scale the voltage proportionately.

14.6 Modeling

This section will provide some further discussion of the art of modeling circuit response, either by hand calculations or with the aid of numerical circuit analysis routines. All of the discussion will deal with time domain modeling, though the equivalent circuits to be developed can equally well be solved with the aid of frequency domain circuit analysis programs.

Frequency domain modeling has some advantages, particularly in that frequency dependent losses of conductors can be more readily modeled than in time domain programs and that characteristic frequencies of circuits are readily revealed. Disadvantages of frequency domain modeling are that it is not readily adapted to analysis of non–linear surge protective devices and that conversion to the time domain requires time consuming Fourier transforms. Further discussion of the relative merits of time domain vs frequency domain modeling is, however, beyond the scope of this introductory treatment.

14.6.1 Steps in the Modeling Process

Some of the steps involved in modeling the response of a circuit are the following.

1. Break the aircraft geometry into manageable sections, such the magnetic field zones discussed above.

2. Simplify the cable geometry by determining average cable diameters and average heights relative to the surrounding ground structure.

3. Determine the ruling electric and magnetic fields for the zones discussed in Step 1.

4. Determine the voltages and currents developed by the fields. These will be used to drive the equivalent circuits.

5. Develop equivalent circuits of cable sections.

6. Identify end impedances, perhaps limited to opens and shorts.

7. Develop complete equivalent circuits.

8. Calculate response.

14.6.2 Example of Modeling

The above steps will be illustrated for the hypothetical aircraft of Fig. 14.21. It should be viewed only as illustrating the steps in the modeling process, and not as a representation of an actual circuit in any realistic aircraft.

The illustrations will assume that the aim is to develop an equivalent circuit that can be solved with a time domain circuit analysis program that accepts a description of the circuit in terms of its nodes and branches. Several programs that do so are ECAP, SPICE and EMTP, principles of which are described in the literature [14.3 - 14.7]. The illustrations that follow were performed using a program [14.8] based on the principles described in [14.5].

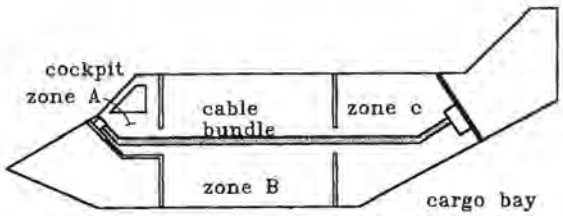

Fig. 14.21 Hypothetical aircraft.

Breaking into sections: For this illustration the aircraft will be assumed divided into the three indicated zones. A cable runs from the cockpit to the cargo bay, with no intermediate branches.

Cable geometry: The cable geometry, heights and distances from ground planes, will be assumed to be as shown in Figs. 14.22 - 14.24.

E and H fields: The electric and magnetic fields in the different zones will be assumed to be as shown in Figs. 14.25 - 14.27. The figures also show the currents and voltages that would be developed in the various cable sections by those fields. To simplify the illustrations to follow, only the magnetically induced voltages shown in Figs. 14.26 and 14.27 will be considered.

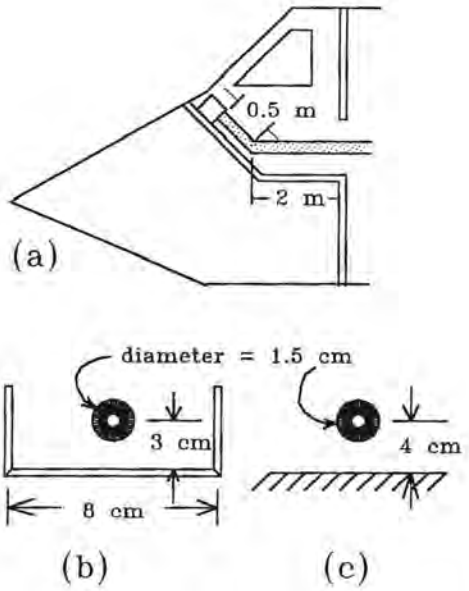

Fig. 14.22 Cable in zone A.
(a) Lengths
(b) Position for run A
(c) Position for run B

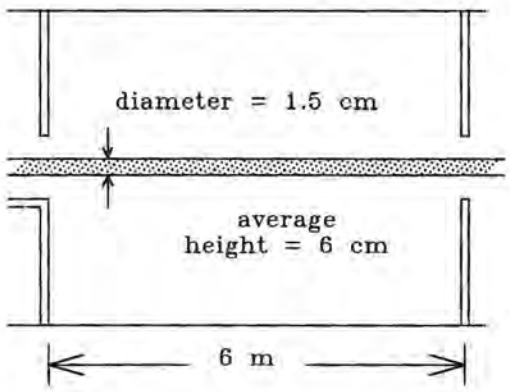

Fig. 14.23 Cable in zone B.

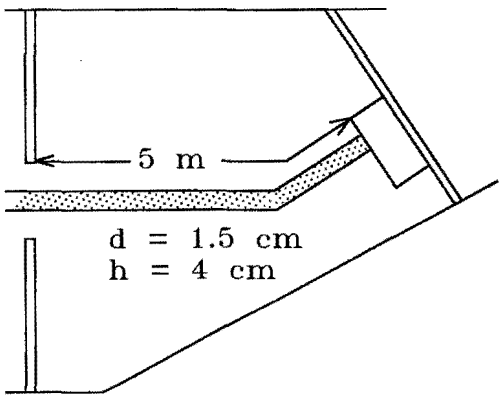

Fig. 14.24 Cable in zone C.

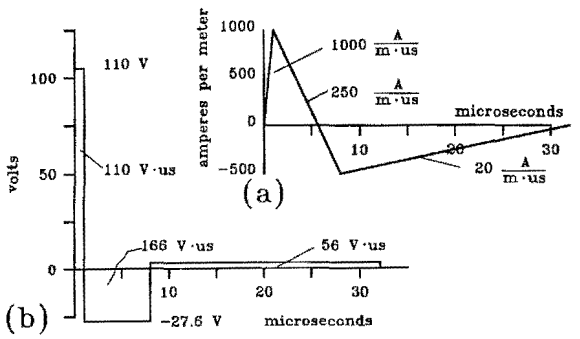

Fig. 14.26 Magnetic field effects in zone B.
(a) Magnetic field
(b) Induced voltage

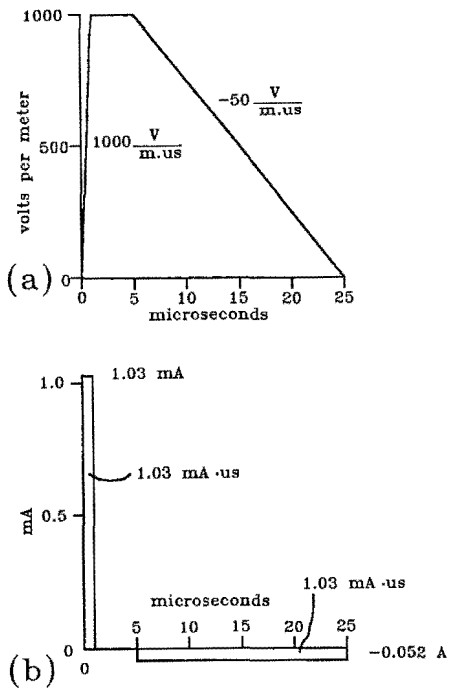

Fig. 14.25 Electric field effects in zone A.
(a) Electric field
(b) Injected current

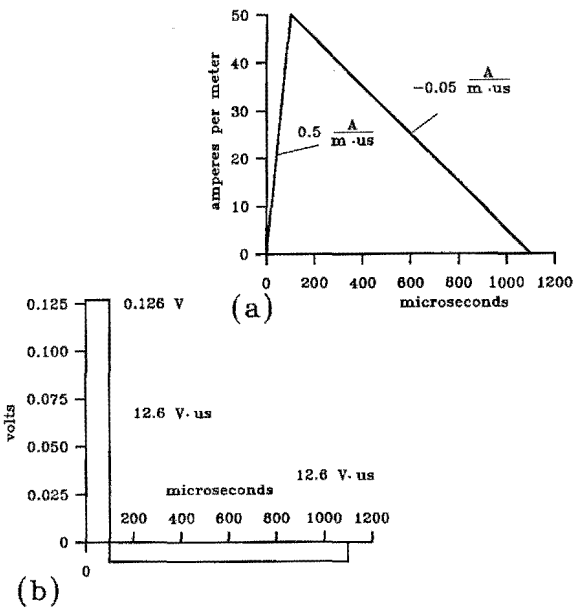

Fig. 14.27 Magnetic field effects in zone C.
(a) Magnetic field
(b) Induced voltage

The magnetically induced voltages will be taken as independent voltage sources having trapezoidal waveforms with front and fall times of 10 ns and having starting times and durations as indicated on the figures. Most circuit analysis programs require that voltage sources be described as being in series with a branch of some sort, rather than existing independently. For these illustrations they will be taken as being in series with 1 ohm resistors, though they could equally well have been in series with one of the inductors comprising a lumped parameter representation of a transmission line.

The electrically induced currents could be taken as a current source in shunt with some branch, though some circuit analysis programs allow a current source to be connected directly to a node. The circuits that follow show such a connection, but the electrically induced currents in Zone A were not included in the simulations since they were fairly small. Further discussion of methods of treating sources, including the use of dependent sources to treat coupling between circuits, is given in [14.9].

Equivalents of cable sections: If the circuit solution program to be used allows it, the simplest representation of a conductor treats it as a transmission line having a certain surge impedance and velocity of propagation. If not, a conductor should be represented as a ladder network of series inductors and shunt capacitors. For these analyses, the cable sections were treated as two inductors in series with the shunt capacitance distributed 1/6 at each end and 2/3 at the junction of the two inductors. The appropriate voltage sources for the cable sections were connected between the two inductors. The appropriate impedances for the various sections of cable were as indicated in Figs. 14.28 - 14.31.

The number of lumps into which a distributed transmission is broken depends on the accuracy desired of the solution. Use of more lumps gives greater accuracy (broader frequency range of validity), but incurs greater computation time. Discussion of the merits of various modeling alternatives is beyond the scope of this section. The illustrations that follow, however, show little significant difference between the response as calculated by the rather crude lumped constant approach and the more refined transmission line approach.

Any discussion of the merits of different modeling approaches must, of course, recognize that the wiring system of any real aircraft is probably too complex to model with complete precision whichever approach is used.

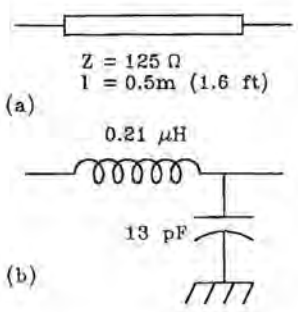

Fig. 14.28 Equivalent impedance for run A in zone A.
(a) Transmission line
(b) Lumped constant

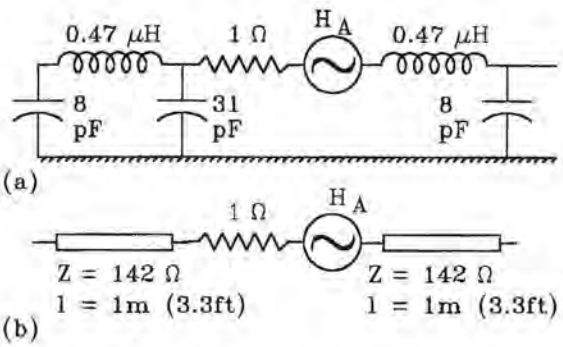

Fig. 14.29 Equivalent impedance for run B in zone A.
(a) Transmission line
(b) Lumped constant

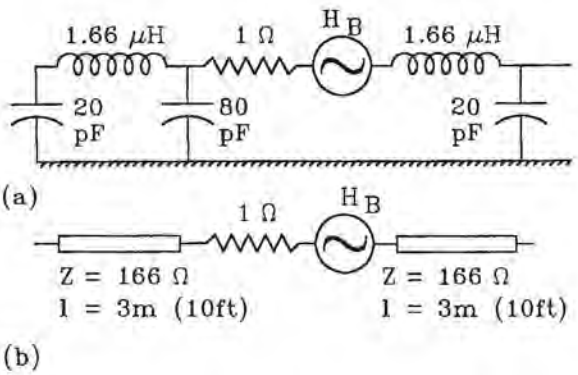

Fig. 14.30 Equivalent impedance for run C in zone B.
(a) Transmission line
(b) Lumped constant

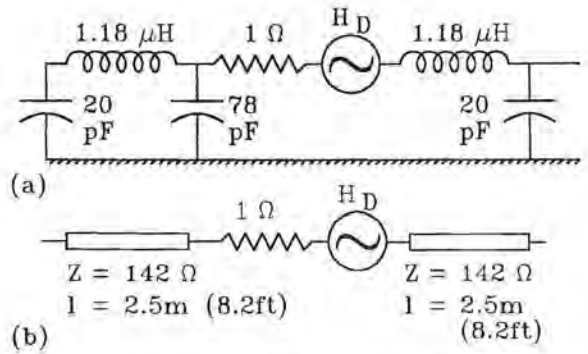

Fig. 14.31 Equivalent impedance for run D in zone C.
(a) Transmission line
(b) Lumped constant

End impedances: For these illustrations the cable will be assumed to be grounded through a low impedance (1 ohm) in the cockpit and in the cargo bay to be connected to ground through a 500 pF capacitor shunted by a resistor, 100 kilohms for calculation of open circuit voltage and 1 ohm for calculation of short circuit capacitance. In any actual calculation the terminal impedances would have to be determined by inspection of the circuit, perhaps supplemented by measurements of stray capacitance.

Complete equivalent circuits: Two representations of the complete circuit are shown; Fig. 14.32 showing a representation based on transmission lines and Fig. 14.33 showing one based on lumped constants. Each of them shows four equivalent sources, but only H_A and H_B were used in the calculations, E_A and H_C being of small magnitude and, perhaps, not greatly affecting the response of the circuit.

Calculated response: Figs. 14.32 and 14.33 also show the magnitude and waveshape of the current calculated to exist at the grounded end in the cockpit and the voltage calculated to exist at the open end in the cargo bay. Each of the responses is oscillatory, as is generally the case for real circuits in actual aircraft, where the response is excited by changing electric and magnetic fields. The current at the grounded end shows higher frequency components superimposed on a lower frequency fundamental oscillation. At the open end in the cargo bay the higher frequency oscillations are filtered out by the 500 pF shunt capacitor.

Voltages and currents at intermediate points will tend not to have high frequency components filtered out by terminal capacitance. Fig. 14.34, as an example, shows the voltage at the junction of cable runs C and D.

Fig. 14.35 shows the short circuit current calculated when the cable is grounded through a low impedance, 1 ohm, at the end in the cargo bay. As predicted by elementary theory, the current is less oscillatory than the open circuit voltage.

Discussion: The above calculations were made with the program described in [14.8] and using a 16 bit desktop computer running at 8 MHz clock speed. Solution time for 1000 to 5000 time steps was a few minutes. No attempt has been made to compare solution time or accuracy with other circuit analysis programs on other computer systems.

The calculations show no significant differences between the results made using transmission line or lumped constant representations.

14.6.3 Extensions and Limitations of Modeling

The above equivalent circuits are probably of about the minimum degree of complexity that should be used if the results of calculations are to have actual utility. More sophisticated modeling should include provision for losses in the circuit, for coupling between different cable systems and conductors, and for treatment of multi-mode propagation between conductors in a cable bundle.

Losses: In the circuits of Figs. 14.32 and 14.33 no attempt was made to model the losses of the circuit, losses that reduce the degree to which the circuits oscillate. A first order approximation to these losses could be made by including series resistance in the circuit, either by invoking the resistive option provided by [14.5] and [14.8] for transmission lines or by including lumped resistances in series with the inductors of Fig. 14.33. Losses in actual circuits are very frequency dependent and difficult to incorporate in circuit analysis programs, though considerable work has been done on methods of doing so [14.10 - 14.12].

Circuit–to–circuit coupling: Many problems of coupling between circuits can probably be done by modeling mutual impedance and mutual capacitance between circuits. Some of the considerations in calculating the coupling are given in [14.9]. Almost all circuit analysis programs include mutual inductors as an allowable circuit element. Some of them include provision for coupled transmission lines.

Multi–mode propagation: Realistic calculation of voltages and currents on closely coupled conductors requires recognition that waves between conductors generally propagate at speeds slower than waves prop-

agating between the conductors and ground. In particular this is true for waves propagating inside shielded conductors, where the analysis problem might involve determining the currents propagating on the outside of a shield and from that determining the voltages and currents induced on the conductors inside the shield. Multi-mode propagation is discussed in the literature [14.13 - 14.16] and is, to some degree, available in circuit analysis programs [14.17, 14.18]. Treatment of the effects greatly complicates calculations and probably should be considered at the edge of the modeling art.

Some discussions of equivalent circuits for shielded conductors are given in Chapter 16. Those circuits can be used with dependent current sources to provide some degree of modeling of the coupling into shielded circuits.

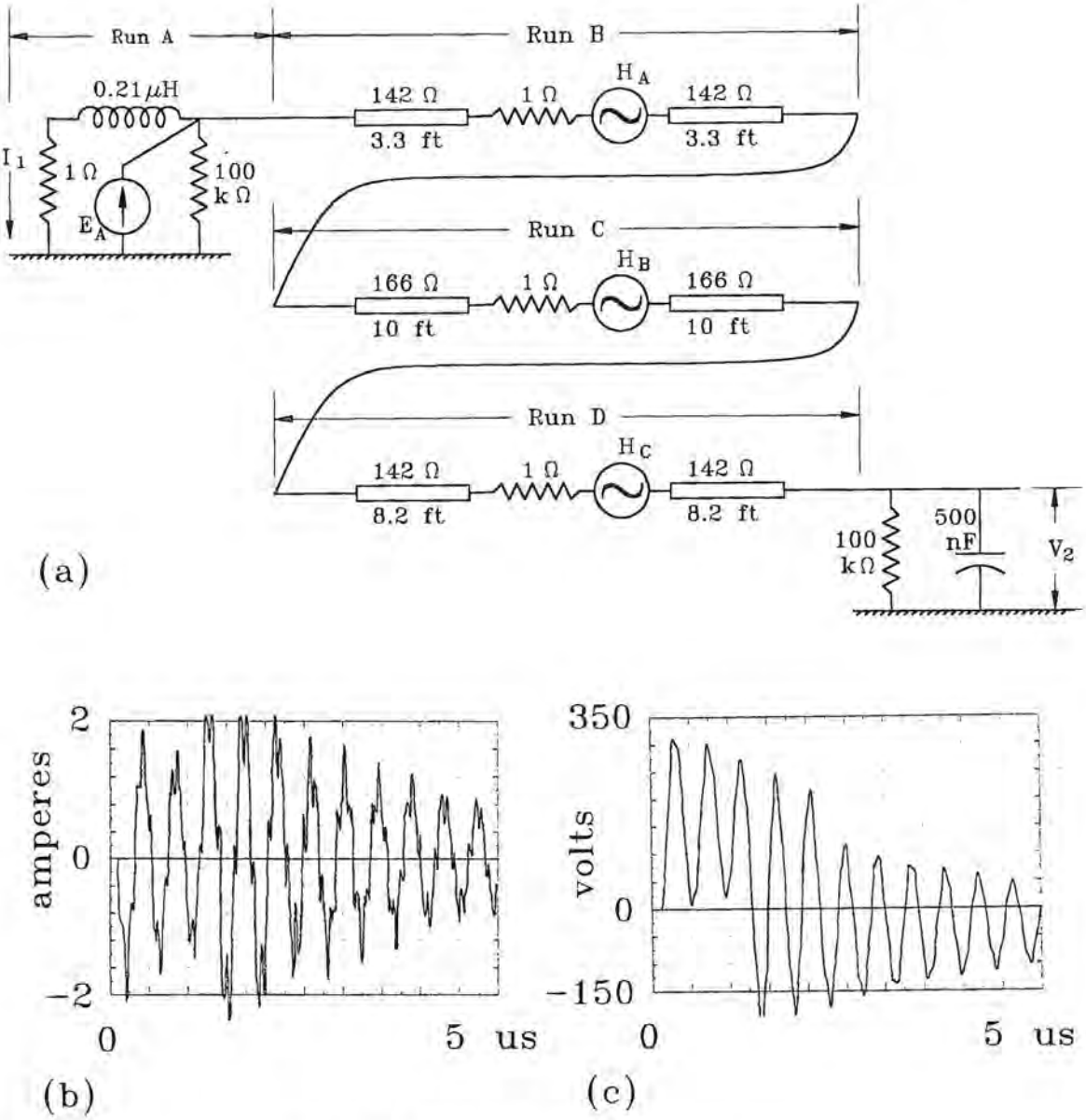

Fig. 14.32 Circuit modeled as transmission lines.
(a) Equivalent circuit
(b) I_1 – cockpit
(c) V_2 – cargo bay

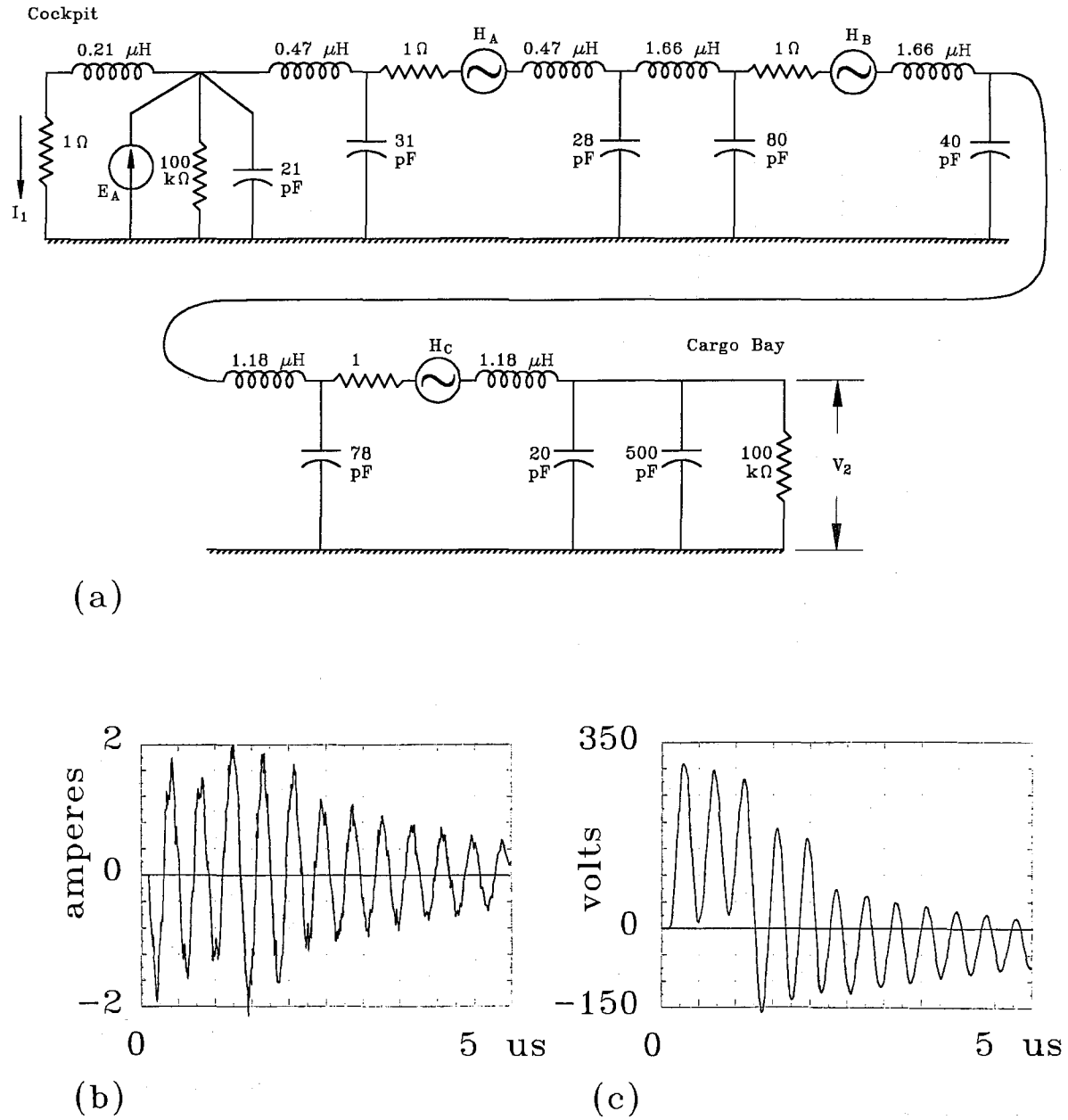

Fig. 14.33 Circuit modeled as lumped constants.
(a) Equivalent circuit
(b) I_1 – cockpit
(c) V_2 – cargo bay

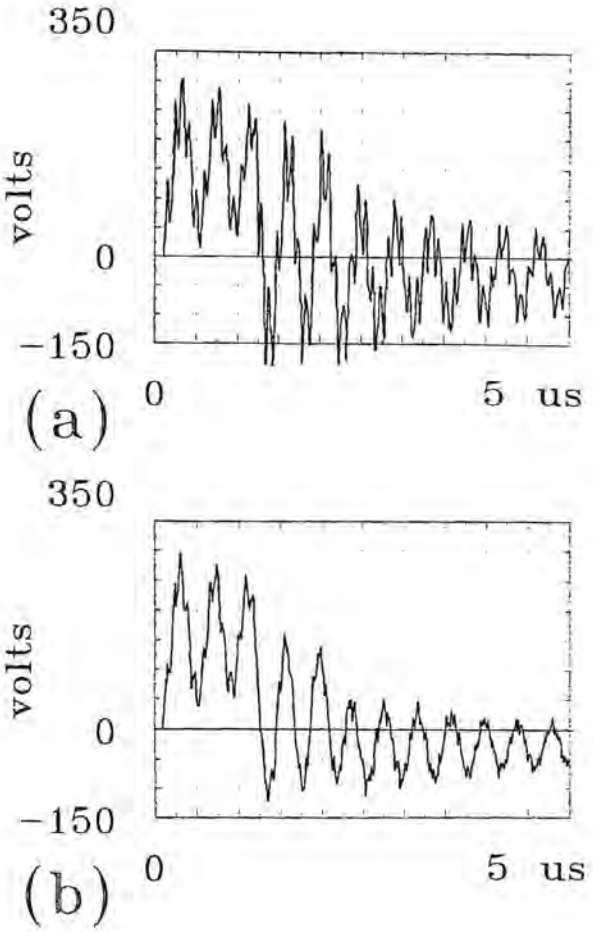

Fig. 14.34 Voltage at junction of cable runs C and D.
(a) Transmission line modeling
(b) Lumped constant modeling

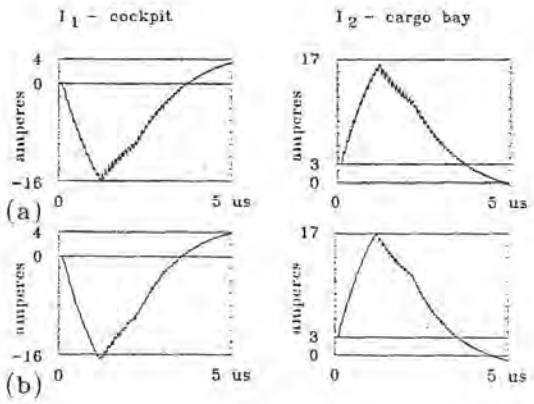

Fig. 14.35 Short circuit currents.
(a) Transmission line modeling
(b) Lumped constant modeling

REFERENCES

14.1 *Space Shuttle Program Lightning Protection Criteria Document*, JSC-07636, Revision A, National Aeronautics and Space Administration, Lyndon B. Johnson Space Center, Houston, Texas (November 4, 1975) p. F-6.

14.2 M. S. Amsbary, G. R. Read and B. L. Giffin, "Lightning Protection Design of the Space Shuttle," *Workshop on Grounding and Lightning Protection*, U.S. Department of Transportation and Florida Institute of Technology, Melbourne, Florida, 6-8 March, 1979.

14.3 F. H. Branin, Jr., "Computer Methods of Network Analysis," *Proc. IEEE*, vol 55, November 1967, pp 1787-1801.

14.4 L. O. Chua, Pen-Min Lin, *Computer Aided Analysis of Electronic Circuits*, Prentice-Hall, Englewood Cliffs, NJ

14.5 H. Dommel, "Digital Computer Solution of Electromagnetic Transients in Single and Multiphase Networks," *IEEE Trans. on Power Apparatus and Systems*, vol PAS-88, April, 1969, pp 388-399.

14.6 H. Dommel, W. S. Meyer, "Computation of Electromagnetic Transients," *Proc. IEEE*, vol 62, July 1974, pp 983-993.

14.7 *Alternative Transients Program (ATP) Rule Book*, K. U. Lwuven EMTP Center, KARD. Mercier-laan 94, B-3030 Heverlee, Belgium or Tsu-huei Liu, 3179 Oak Grove Court, West Linn, Oregon, 97086.

14.8 F. A. Fisher, "Trancalc", Unpublished, Lightning Technologies Inc., 10 Downing Parkway, Pittsfield, MA, 01201.

14.9 F. A. Fisher, *Analysis and Calculation of Lightning Interactions with Aircraft Electrical Circuits*, AFFDL-TR-78-106, Aug. 1978, Air Force Flight Dynamics Laboratory, Wright Patterson Air Force Base, Ohio, 45433.

14.10 A. Semlyn, A. Dabuleanu, "Fast and Accurate Switching Transient Calculations on Transmission Lines With Ground Return Using Recursive Calculations," *IEEE Trans. on Power Apparatus and Systems*, vol PAS-94, March/April 1975, pp 561-571.

14.11 A. Semlyen, A. Roth, "Calculation of Exponential Propagation Step Responses - Accurately for Three Base Frequencies," *IEEE Trans. on Power Apparatus and Systems*, vol PAS-96, March/April 1977, pp 667-673.

14.12 A. Semlyn, M. H. Abdel-Rahman, "Transmission Line Modeling by Rational Transfer Functions," *IEEE Trans. on Power Apparatus and Systems*, vol PAS-101, September 1982,pp 3576-3583.

14.13 D. E. Hedman, "Propagation on Overhead Transmission Lines, I - Theory of Modal Analysis," *IEEE Trans. on Power Apparatus and Systems*, March 1965, pp 200-205.

14.14 L. M. Wedepohl, "Application of Matrix Methods to the Solution of Travelling-wave Phenomena in Polyphase Systems," *Proc. IEE*, vol 110, December 1963.

14.15 T. K. Liu, "Coupling and Propagation in Multiconductor Transmission Lines," *International Conference on Electromagnetic Compatibility*, May 19-21, 1987, San Diego, CA, pp T21.12-14.

14.16 R. F. Harrington, "Time-Domain Response of Multiconductor Transmission Lines,"

14.17 A. R. Djordevic, R. F. Harrington, T. K. Sarkar, M. B. Bazdar, *Matrix Parameters of Multiconductor Transmission Lines*, Artech House Books, Norwood, MA. 1988.

14.18 A. R. Djordevic, R. F. Harrington, T. K. Sarkar, M. B. Bazdar, *Time Domain Response of Multiconductor Transmission Lines*, Artech House Books, Norwood, MA. 1988.

This page intentionally blank.

Chapter 15

SHIELDING

15.1 Introduction

If electronic equipment is to be operated in a region where there are changing electromagnetic fields, and if experience or analysis indicates that the currents and voltages induced by those fields may be harmful, the most straightforward approach toward achieving transient compatibility is through shielding, both of interconnecting wiring and of electronic equipment. Frequently the electronic equipment will be inherently shielded by enclosures, though there are practices that can defeat the inherent shielding of metal enclosures and there are non–metallic enclosures that offer little shielding. Discussions that follow will comment on shielding provided by enclosures, but they will treat mostly with shields on conductors.

15.2 Shielding Effectiveness

The degree to which a cable shield reduces the voltage induced on a conductor depends on the construction of the shield, solid tubular, braided, tape wound, diameter, thickness, material resistivity etc. All of these are factors that affect the resistance of the shield. Braided shields for cables are almost universely made from copper, but solid shields, such as conduits and enclosures are most commonly made from aluminum. Aluminum has the virtue of light weight, but copper has the virtue of solderability and resistance to cold flow at pressure points. Magnetic materials, such as iron and steel, can provide more shielding effectiveness than either copper or aluminum, but are seldom either needed or used in aircraft.

The above factors also affect the transfer impedance and how the noise current flowing on the shield of the cable is related to the noise signals coupled onto the signal conductors. The concept of transfer impedance was previously discussed in §9.6.4 and §9.9, the quantity of most interest for this discussion being the transfer impedance with external return, discussed in §9.9.1. Transfer impedance of cable shields will also be discussed in §15.6. The noise voltages are also affected by the way that the shield and conductors are connected to ground and loads. The effects of these connections, discussed in §15.3, are often of more importance than the construction of the shield.

In this chapter, transfer impedances are discussed in §15.6 while the more important connection effects are discussed in §15.3. The ultimate aim of the discussion is to develop equivalent circuits relating the voltage on conductors to the magnitude of the interfering current. Section 15.7 provides tabular data on the transfer impedance of various types of cable.

In *steady state* or *frequency domain* analyses of radio frequency interference (RFI), shields are generally rated in terms of their *shielding effectiveness* (SE) a quantity generally relating the voltages or currents on conductors with and without a shield, the definition of shielding effectiveness being

$$SE = 20 \log \left[\frac{\text{voltage (or current) without shield}}{\text{voltage (or current) with shield}} \right]. \tag{15.1}$$

When discussing *transient* or *time domain* analyses, the above definition of SE may not be the most valuable concept because shields not only reduce the amplitude of interfering voltages and currents, but change their waveshape as well. The SE does not account for the changes of amplitude. It is better to keep all analyses in the time domain and to discuss shielding in terms of *transfer impedances*, the approach that will be taken in the bulk of the material to follow.

15.3 Cable Grounding Effects

In aircraft, shielded conductors are most commonly used to control low–level and low–frequency interference signals. How to ground shields is often a controversial matter, with one school recommending that shields be grounded at only one end and another school recommending they be grounded at both ends.

Single point grounding: The aim of the *single point* ground concept is to minimize the flow of noise current on shields and so minimize the voltage rise along the shields. The assumptions, often unstated, are that the shields are short and that their function is to intercept low frequency electric field displacement currents and keep those currents from flowing on high impedance circuits. "Short" implies that the shield must be a small fraction of the wavelength of the interfering signal, perhaps $L/20$. With 30 kHz, as an example, the wavelength is 10 km and any shield on an aircraft would be "short".

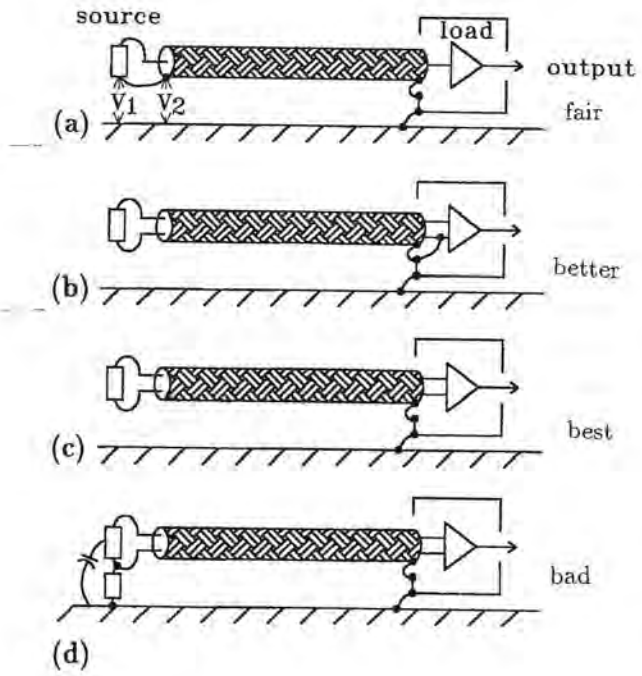

Fig. 15.1 Single point ground on shield.
(a) Shield used as a conductor
(b) Unbalanced two wire transmission
(c) Balanced transmission and reception
(d) Loaded source

The single point ground concept is most applicable in a situation such as that of Fig. 15.1(a) in which a *source* feeds a *load* in a grounded enclosure. If the source is physically and electrically ungrounded, any noise voltage that might exist between the source and ground, V_1, or between the source end of the shield and ground, V_2, does not couple to the interior of the shield and is of no consequence.

Noise currents on the shield are most objectionable if the shield is used as return for the source, Fig. 15.1(a), since any shield voltage is directly added to the signal from the source. Shield voltages are of lesser concern if two–wire transmission, Fig. 15.1(b), is used, since the shield voltages couple then only through the capacitance between the shield and the signal conductors. Shield voltages are of least concern if true balanced transmission is used, with the output taken from a differential amplifier, Fig. 15.1(c).

If the source is coupled to ground through an impedance, Fig. 15.1(d), the single point ground concept is degraded, regardless of the type of transmission, since this does allow some of the voltage on the source or the ungrounded end of the shield to couple to conductors and the load. An impedance often unrecognized is that provided by the stray capacitance to ground of the source. With rapidly changing electromagnetic fields the effects of such capacitance can be of more importance than the performance of the shield.

Multiple point grounding: In an aircraft subjected to the rapidly changing electromagnetic fields associated with lightning, interference frequencies can extend higher than 30 MHz ($L = 10$ m) and a shield 1 m long would begin to be "not short". Under such conditions, shields grounded at only one end may not be effective, and in some cases the shields may act as antennas and can make the surge voltages even larger than they would be if the conductors were not shielded in the first place. In such cases a *multiple–point* ground concept is more appropriate. That concept aims to ensure that noise currents *do* flow on shields, an aim directly opposite to that of the *single–point* ground concept.

Illustration of grounding effects: Some of these connection effects have been illustrated by a series of tests [15.1] made on a 5 m long length of RG–58/U coaxial cable. The cable was placed adjacent to a metal ground plane and a magnetic field passed between the cable and the ground plane to generate "interference". During the tests, measurements could be made of the common–mode voltage between the center conductor and ground at each end of the cable or of the current flowing in the shield of the cable. The magnetic field was not a distributed field but was confined to the core of a pulse injection transformer in the manner shown in Chapter 18. The "interference" was thus magnetically induced, the induced voltages being proportional to the rate of change of magnetic flux. In actual practice interference can also be induced by electric field coupling and with high frequencies one will never exist without the other. In the illustrations to follow the ultimate conclusions that are illustrated would apply equally well to interference induced by electric fields.

Unshielded conductor: Figs. 15.2 and 15.3 show conditions on an unshielded conductor, or one in which the shield is not used.

Balanced loads: In Fig. 15.2 the conductor has equal (open) load impedances at the two ends. The changing magnetic field induces a total voltage of 64 volts. How that voltage divides depends on the impedances at the end of the conductor. Since the impedances are equal, half of the voltage appears at each end of the conductor and the voltages are of opposite polarity, as would be produced if the conductor were considered to have an equivalent voltage generator at its center, Fig. 15.2(d).

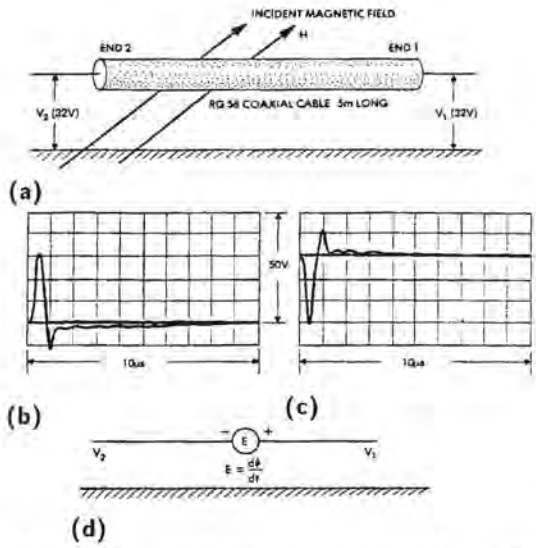

Fig. 15.2 Shield not grounded at either end
(a) Test conditions
(b) V1
(c) V2
(d) Equivalent circuit

Unbalanced loads: Fig. 15.3 shows conditions if the load impedances at the ends are unbalanced by the addition of a 50 ohm resistor at one end. The voltage at the loaded end is reduced, but since the total voltage induced around the loop remains unchanged, the voltage is just shifted to the end with the highest impedance. With reference to the equivalent circuit of Fig. 15.3(c), the fact that there is any voltage at V_2 implies the existence of some capacitive loading as well as the desired resistance load; otherwise there would be no voltage across V_2.

Shield grounded at one end: Adding a shield, but grounding the shield at only one end, Figs. 15.4 and 15.5, lowers the voltage at the end where the shield is grounded, but raises it at the other end. The phenomenon can be explained by the equivalent circuit of Fig. 15.4(c). The changing magnetic field induces a voltage between the ends of the shield and since one end of the shield is grounded, all the voltage must appear between the open end of the shield and ground. The conductor is exposed to the same field and the same voltage will be developed between the ends of the conductor as between the ends of the shield.

How this voltage divides depends on both the grounding of the shield and the load impedances on the conductor. With unloaded conductors, Fig. 15.4, the voltage at end 2 is reduced by the capacitance between the conductor and the grounded end of the shield, but the excess voltage just appears at the other end. With a loaded conductor, Fig. 15.5, the division of voltage is primarily governed by the load impedances and connecting the shield makes practically no difference in the voltage.

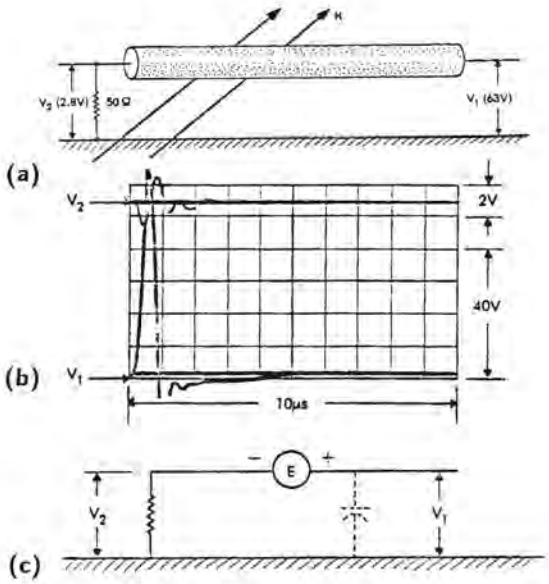

Fig. 15.3 Unequal load impedances.
(a) Test conditions
(b) Voltages
(c) Equivalent circuits

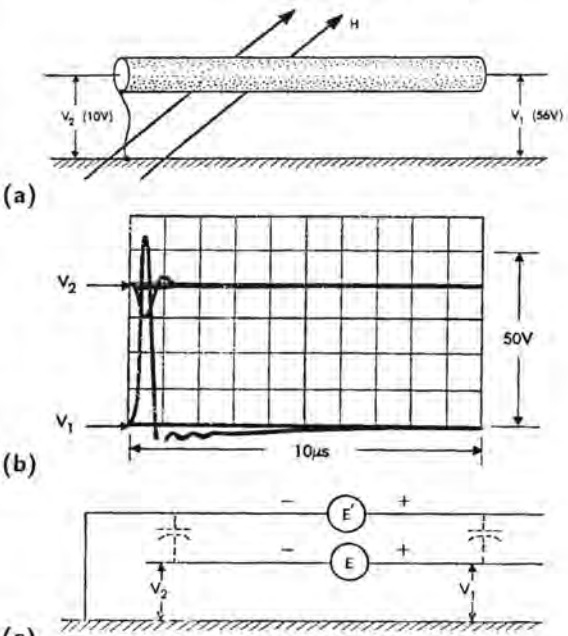

Fig. 15.4 Shield grounded at one end
(a) Test conditions
(b) Voltages
(c) Equivalent circuit

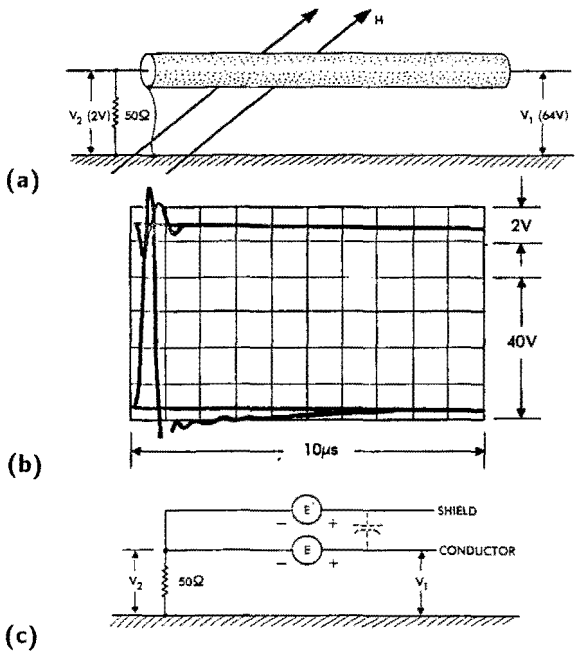

Fig. 15.5 Shield grounded at one end.
(a) Test conditions
(b) Voltages
(c) Equivalent circuits

Shield grounded at both ends: Grounding the shield at both ends and allowing it to carry current, as shown in Figs. 15.6 through 15.8, produces an entirely different response. The induced voltages are not only reduced in amplitude, but their waveshape is changed. If the shield is grounded at both ends, the voltage induced by the changing magnetic field appears across the inductance of the shield–ground plane loop. The result is a current through the shield, Fig. 15.6, one having a shape like that of the magnetic field.

$$E' = \frac{d\phi}{dt} = \mu A \frac{dH}{dt} \tag{15.2}$$

$$I = \frac{1}{L_s} \int E' dt = \frac{\mu A}{L} H \tag{15.3}$$

where

E' = voltage induced between ends of the shield
I = current on the shield
L = self–inductance of the shield

How shield current reduces voltage: This shield current reduces the voltage induced between the signal conductor and ground, as shown in Fig. 15.7. The reduction in voltage can be viewed equally well from two different viewpoints.

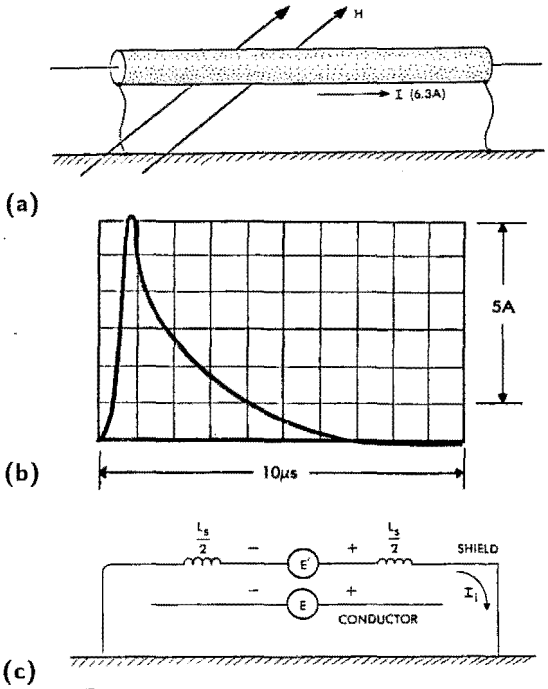

Fig. 15.6 Shield grounded at both ends.
(a) Test conditions
(b) Shield current
(c) Equivalent circuit

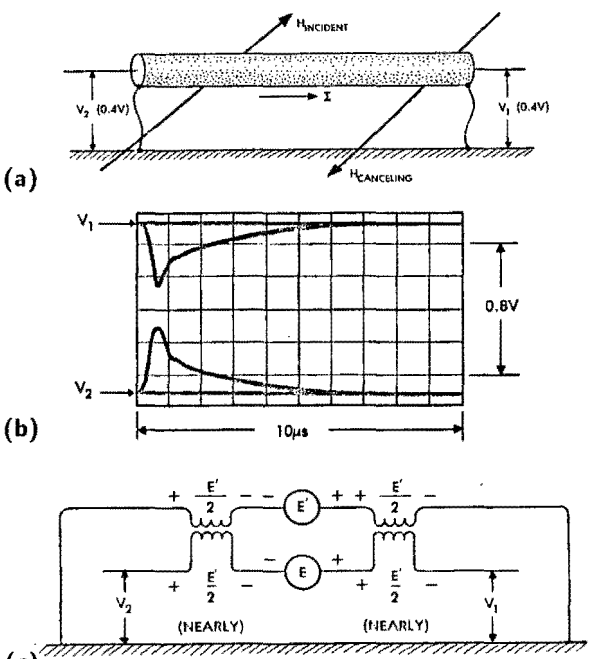

Fig. 15.7 Shield grounded at both ends.
(a) Test conditions
(b) Conductor voltages
(c) Equivalent circuit

Cancellation of incident field: The first is that the shield current produces a magnetic field that tends to cancel the incident field, Fig. 15.7(a). From this viewpoint the voltages between the signal conductor and ground depend on the difference between the incident and the cancelling fields.

Transformer coupling: Alternatively, the reduction in voltage can be viewed as the effect of the mutual inductive coupling between the shield and the signal conductor. This latter approach is illustrated by the equivalent circuit of Fig. 15.7(c). The shield is considered as the primary of a transformer and the conductor as the secondary. Since the shield is grounded at both ends, all the voltage developed on the shield appears across the primaries of the transformers. The mutual coupling between the shield and the signal conductor is very nearly unity since there is only a small (ideally zero) magnetic field internal to the shield and so the voltage induced in the secondary, or signal conductor, side of the equivalent transformer is about equal to the voltage originally induced in the shield. The voltage appearing between the ends of the conductor is the sum of that induced in the conductor and that coupled through the transformer from the shield. Accordingly, the voltages appearing at the ends of the conductor are lower than they would be if the shield could not carry current.

Transfer impedance: The transformer equivalent circuit of Fig. 15.7(c) is not well suited to numerical calculation since it requires that the self and mutual inductances be evaluated with high precision. The transfer impedance of Fig. 15.8 is better since it involves only the resistance of the shield and calculation of the magnetic flux that leaks through the shield and so does not equally link both conductors. This flux can be reduced to an equivalent transfer inductance L_{12}. The voltage induced on the conductor then depends on the shield current, R and L_{12}. How the voltage distributes depends on the loads at the end of the cable. In Fig. 15.8 most of the voltage develops on the open end.

15.4 Multiple Conductors in Cable Shields

If there are multiple conductors in the cable, each conductor will be exposed to the same amount of flux and will have induced in it an equal voltage. This holds true whether the conductor is located adjacent to the shield or in the center of the bundle of conductors comprising the core. Stated another way, position of the wire within the shield has little effect on the magnetically induced voltage. Accordingly, the voltage between any pair of conductors in the core will be small.

Present analytical tools do not seem of sufficient accuracy to predict with any assurance the magnitude of line–to–line voltages; they are best determined by actual measurement. Line–to–line voltages are much more strongly influenced by load impedances to which the conductors are connected than by the position of the conductors within an overall shield.

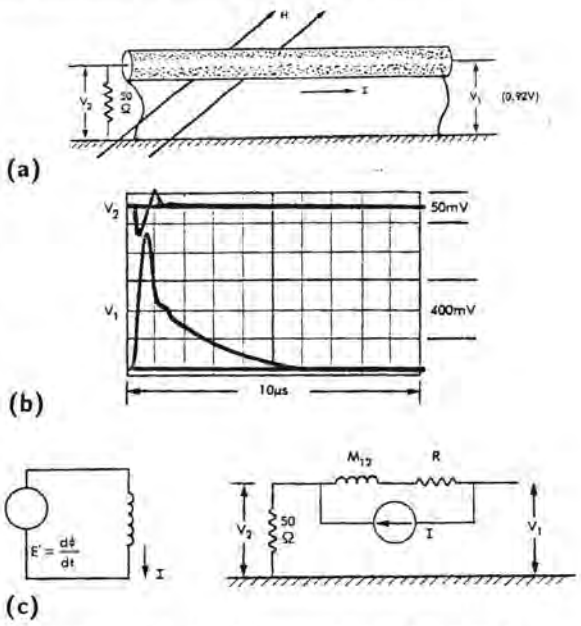

Fig. 15.8 Shield grounded at both ends
(a) Test conditions
(b) Conductor voltages
(c) Equivalent circuit

15.5 Multiple Shields on Cables

One very common situation involving multiple conductors is a configuration in which a shielded conductor is itself contained in an overall shield. Fig. 15.9 shows such a condition and shows some of the factors that must be considered when predicting the response of this two–cable network. They are the noise currents on the outer shield, the internal field of the outer shield, the current induced on the inner shield, the internal field of the inner shield and the coupling from the inner shield to the signal conductor. The internal field of the outer shield is the product of the noise current and the transfer impedance of the outer shield.

Inner shield grounded at only one end: If the inner shield is ungrounded at the right–hand end (switch S of Fig. 15.9(b) open), the internal field of the outer shield, $E_{\text{i-os}}$, produces a voltage difference, $V_{\text{is-os}}$, at the right- hand end of the cable. Neglecting the distributed capacitance between the inner and outer

shields, the noise current on the inner shield, I_{is}, will be zero. The total voltage to which the conductor is exposed is also $V_{is\text{-}os}$. Under such conditions the inner shield will not provide much reduction of the noise voltage.

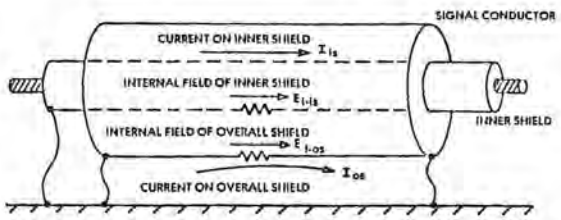

(a)

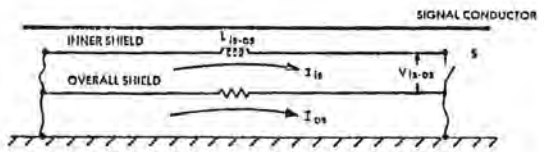

(b)

Fig. 15.9 Double shielded cable.
(a) Current and field polarities
(b) Current on inner shield and forced through $L_{is\text{-}os}$.

Inner shield grounded at both ends: If the inner shield is connected to the outer shield at both ends (switch S closed), the noise current will be shared by the inner and outer shields, but the conductor will respond only to the field along the inner surface of the inner shield. Initially all the current will be confined to the outer shield and under dc conditions the currents will be divided according to the resistance of the shields, but in between there will be a transient region where the division of current will be determined primarily by the inductance between the inner and outer shields.

Treatment as component currents: One way to visualize the phenomenon is to consider the current to have two components, the total noise current impressed from an outside source and a component circulating between the inner and outer shields. From this viewpoint the current on the inner shield will be equal to the circulating component while the current on the outer shield will be the sum of the two components. The voltage that drives the current on the inner shield will be that produced by the flow of current through the transfer impedance of the outer shield. This voltage, when impressed on the impedance between the inner and outer shields determines the current on the inner shield. For well shielded cables this impedance is predominantly inductive. The waveshape of the current on the inner shield, I_{is}, is then proportional to the time integral of the voltage developed along the inner surface of the outer shield. The current on the inner shield thus typically has a slower rise time and a longer duration than does the field along the inner surface of the outer shield. This current, I_{is}, on the internal shield then produces an electric field along the surface of the inner shield, $E_{i\text{-}is}$. The conductor responds primarily to the electric field along the inner shield.

Example of multiple shielding: It will be apparent that there are a number of combinations of shield connections and termination impedances which are possible, all of them affecting the overall response of the cable system. Some of these effects have been demonstrated during an extension of the tests described in Figs. 15.2 through 15.7. The piece of RG-58/U coaxial cable used for those tests was modified by pulling over the outer jacket another length of flexible copper braid, forming a triaxial cable. Triaxial cable is of course commercially available.

The test connections and results are shown on Fig. 15.10. The equivalent circuit has three separate components; separate in the sense that each, for all practical purposes, may be treated independently. The first part of the circuit determines the voltage induced along the inner surface of the outer shield. This is governed by the outer current flowing through the transfer impedance (see §15.4) of the outer shield, R_1 and M_1.

In the second stage of the problem, this inner shield voltage is impressed across the inductance existing between the inner and outer shields in order to determine the current flowing on the inner shield.

In the third stage, the current on the inner shield is passed through the transfer impedance of the inner shield, R_2 and M_2. The product of current and transfer impedance gives the voltages that appear between line and ground on the central signal conductor. The amplitudes and shapes of these voltages, shown in Fig. 15.10(c), are much less than those developed on the singly shielded conductor, Fig. 15.7.

15.6 Transfer Impedance of Cable Shields

The equivalent circuit of Fig. 15.7 is one which depicts, through the use of transformers, the self inductances of both the conductor and the shield and the mutual inductance between the two. Self and mutual inductances must be known with great precision if results are to be calculated accurately, a requirement that can be relaxed is the circuit is split into two parts, as in Fig. 15.8. One part of the circuit relates the magnetic field to the current flowing on the shield and another relates the current on the shield to the

voltage developed on the conductor through the use of a *transfer impedance*, L_{12} and R, the values of which depend upon the type of shield.

Transfer inductance vs. mutual inductance: The transfer inductance L_{12} should not be confused with the mutual inductance M_{12} between the shield and the conductor. For the two conductor system that was described in §9.7.3 and Fig. 9.13, mutual inductance is controlled by the magnetic flux in the shaded area between r_2 and r_3 while transfer inductance would be governed by the magnetic flux between r_1 and r_2.

Handbook data on shielded conductors often uses the term M_{12} for transfer inductance, but the usage is unfortunate.

If the resistance of the shield were zero and if the mutual inductance between the shield and the signal conductor were equal to the self-inductance, that is, unity coupling, the flow of current on the shield of the cable would not cause any voltage to be developed between the shield and the signal conductor. This section of the report will now discuss the factors that prevent the coupling between shield and signal conductor from being perfect.

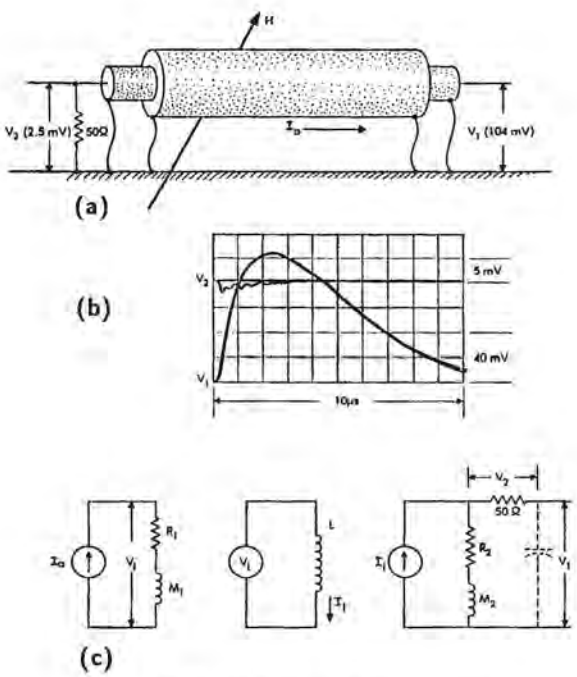

Fig. 15.10 Multiple-shielded cable.
(a) Test conditions
(b) Conductor voltages
(c) Equivalent circuits

Thin tubular Shields: Consider first a tubular shield with no openings, Fig. 15.11. An external noise current flowing through the resistance of the shield produces an electric field on the internal surface of the shield. The internal and external electric fields will be equal and since there are no openings through which a magnetic field can leak the transfer inductance term L_{12} of Eq. 15.4 will be zero.

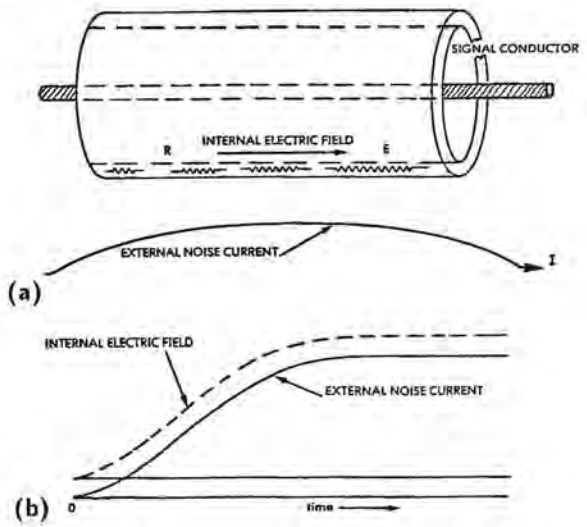

Fig. 15.11 Coupling resulting from resistance effects
(a) Current and field polarities
(b) Current and field waveshapes

The transfer impedance of a tubular shield was previously discussed in §9.9.1 and Eqs. 9.113 - 9.118. For thin tubes and low frequencies the transfer impedance is just the dc resistance of the shield;

$$R_o = \frac{1}{2\pi r \sigma a}. \tag{15.4}$$

where

r = radius of the shield
a = wall thickness
σ = conductivity of the shield

The waveshape of the internal electric field will be the same as that of the external noise current.

Eq. 15.3 would hold at any frequency for which the skin depth δ is large compared to the thickness of the shield. Skin depth was discussed in §9.4.5 and a numerically convenient expression shown to be

$$\delta = \frac{\pi}{50}\sqrt{\frac{1}{\sigma f_{\text{kHz}}}} \text{ meters.} \tag{15.5}$$

In the time domain the shield may also be considered "thin" if the pulse penetration time, §11.3.4, Eq. 11.23, is small compared to the rise time and duration of the interfering noise currents.

Thick tubular shields: If the shield is not thin, Fig. 15.12, the internal electric field depends upon the product of the resistivity of the shield material and the density of the current on the internal surface of the shield. As discussed in §11.3.3, this internal current density, J_i, will not, in general, be the same as the density of the current on the external surface of the cylinder. Because of the phenomenon of skin effect, the current density on the inner surface of the shield will rise more slowly than does the external noise current. The rate at which the current density on the inner surface increases will be directly proportional to the permeability of the shield material and to the square of the wall thickness and inversely proportional to the resistivity of the wall material. Cables with solid-wall shields and cable trays of solid metal with tightly fitting covers will typically exhibit this type of behavior.

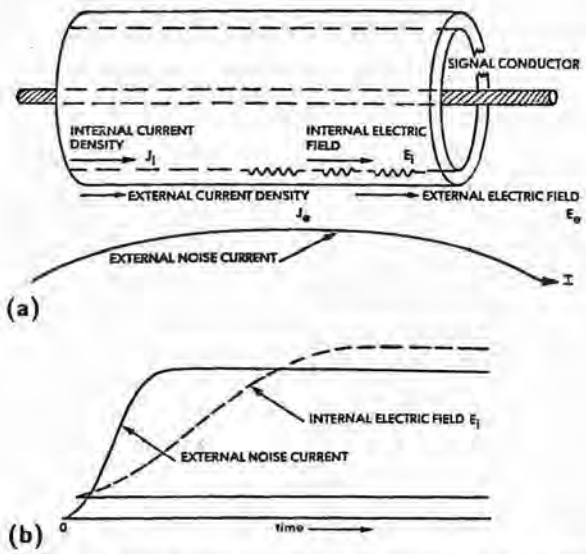

Fig. 15.12 Coupling via diffusion through a solid wall.
(a) current and field polarities
(b) Current and field waveshapes

The maximum transfer impedance is found at dc and decreases with frequency. For all practical purposes, the transfer impedance can be taken as that of Eqs. 9.116 and 9.117, or as expressed in [15.7],

$$Z = \frac{1}{2\pi r \sigma t} \times \frac{(1+j)t/\delta}{\sinh(1+j)t/\delta}. \qquad (15.6)$$

The above expressions assume that the wall thickness is small compared to the radius of the tube and that the radius is small compared to the smallest wavelength of interest. It is also assumed that the shield is made from a good conductor so that the displacement current in the shield material is negligible compared to the conduction current. Such is the case for any practical metal shield.

The time domain response was previously given in §11.3.4 and §11.3.5. In response to a step-function current the internal electric field will increase according to the pulse penetration time constant predicted by Eq.11.23 and shown in Fig. 11.8. An equivalent circuit applicable to both frequency and time domains is a ladder network of two or more terms, as shown in Figs. 11.8 and 11.11.

Braided Shields: Braided shields, Fig. 15.13, do not provide a perfect conducting cylinder since they have a number of small holes, Fig. 15.14, which permit leakage of electric and magnetic fields. The weaving of the braided-wire shield is described in terms of the number of bands of wires (carriers) that make up the shield, the number of wires in each carrier (ends) and the number of carrier crossings per unit length (picks). These characteristics, along with the radius of the shield, define the volume of metal in the shield, the optical coverage and the weave angle. A large volume of metal implies low resistance and good shielding, but also a large weight, which is a drawback for aircraft.

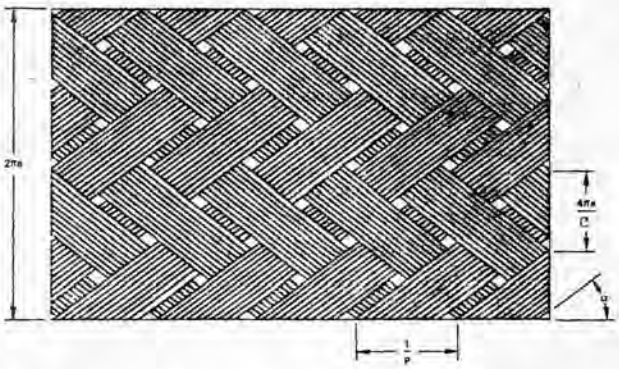

Fig. 15.13 Pattern of a braided shield [15.3].

Optical coverage and weave angle: The optical coverage of a shield is a measure of the number of holes in the shield, the higher the optical coverage the smaller the area of the holes and the better the shielding. The holes between the individual bundles of wire forming the shield can be approximated as a group of diamonds, the size and orientation of which depend upon the weave angle. If the weave angle is small the long

axis of the triangles is oriented along the shield, as at end A of the cable shown in Fig. 15.14(a) and if the weave angle is great the long axis of the hole is oriented circumferentially to the cable, as at end B of the cable. Other things being equal, a shield with a small weave angle provides better shielding performance than one with a large weave angle.

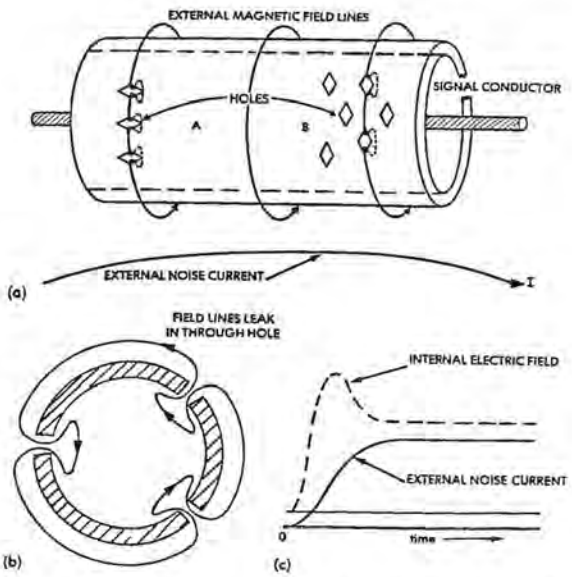

Fig. 15.14 Coupling via magnetic leakage through holes.
(a) Current and field polarities
(b) Field leakage through holes: end view
(c) Current and field waveshapes

Mechanism of magnetic field leakage: The external noise current produces a circumferential magnetic field around the outside of the shield and, as a first approximation, one may visualize the external magnetic field lines looping in and out of the holes in the braided shield. There will be more leakage in holes with their long axes oriented circumferentially to the end of the shield (end B of the cable, large weave angle) than there will be if the long axes of the holes are oriented along the shield, (end A of the cable, small weave angle). Viewed from the end of the cable, as in Fig. 15.14(b), the field that leaks into the cables produces a net magnetic field circumferentially around the inside surface of the shield.

This magnetic field produces an internal electric field of an amplitude dependent upon the degree of leakage into the shield and upon the rate of change of the external noise current. The total internal electric field is proportional to the resistance of the cable shield, to the rate of change of external noise current, and to the number of holes in the cable.

Impedance vs frequency: Some examples, from [15.3 – 15.6], of the variation of transfer impedance with frequency for various degrees of shielding are shown in Fig. 15.15.

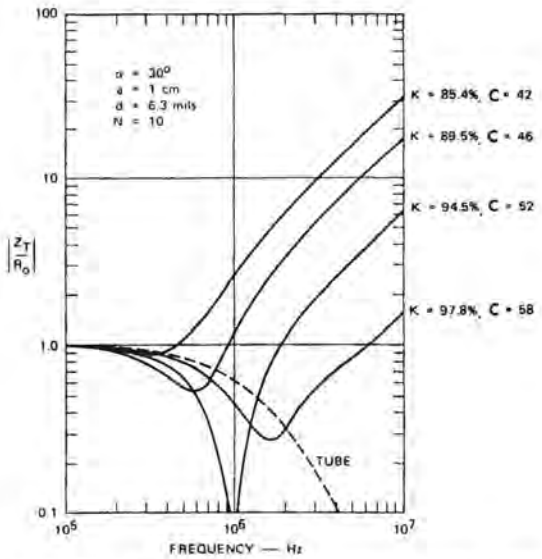

Fig. 15.15 Transfer impedance of a braided-wire shield [15.3].
k = Percent coverage
C = Number of carriers

Equivalent circuit: An equivalent circuit is shown on Fig. 15.16. The resistance can frequently be taken as the dc resistance of the shield, though with some shields the effective resistance will be less because of skin effects. The transfer inductance L_{12} will be on the order of 0.5 nH/m for small diameter cables with a small weave angle and several nH/m for large diameter cables with a large weave angle.

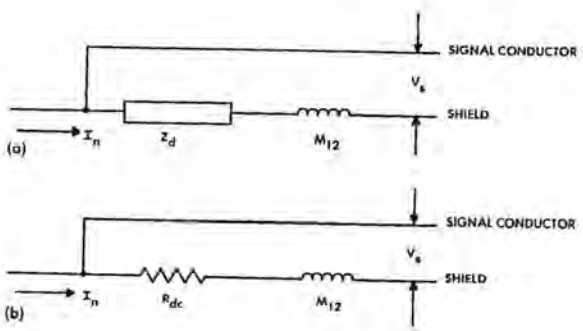

Fig. 15.16 Equivalent circuits.
(a) Transfer impedance
(b) Transfer impedance simplified

Calculation of shield performance: Vance [15.6] gives equations relating resistance and transfer inductance to the construction of the shield. Fig. 15.17 shows one example of how transfer inductance depends on weave angle. In the frequency domain the transfer impedance is generally dominated by the resistance below about 1 MHz and by the transfer inductance at higher frequencies. The reference to mutual capacitance will be discussed shortly under electric field shielding.

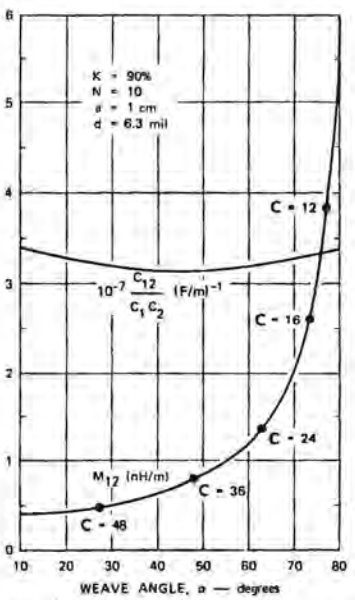

Fig. 15.17 Mutual inductance and mutual capacitance vs weave angle [15.3].

Flexibility vs. weave angle: Shielding effectiveness can be improved by making the shield more dense, but that reduces the flexibility of the shield. Small diameter shields can be made with a small weave angle, but on large diameter cables the weave angle must be large to maintain flexibility.

Overlapping layers of braid: An alternative construction involves two overlapping layers of braid, Fig. 15.18. Using two similar layers of braid will reduce the resistance by a factor of two (and double the weight of the shield), but can reduce the transfer inductance by a much greater factor, frequently to levels below 0.1 nH/m. Resistance can be calculated, but transfer inductance is best measured.

Porpoising: Sometimes cables exhibit a phenomenon, shown in Figs. 15.19(a) and (b), in which a change in external noise current induces an internal electric field of the opposite polarity. This is due to a phenomenon called *porpoising*. It occurs because braid wires loop back and forth between the inner and outer surfaces of the shield, carrying current to the inner surface by conduction rather than by diffusion. As shown in Fig. 15.19(c), wires carring axial current on the inside surface of the shield produce a magnetic field oriented oppositely to that which leaks in through holes. Measurements in the frequency domain would not show the effect unless they also included a measurement of phase as well as of magnitude. As a practical matter, porpoising is a phenomenon likely to be found only on poorly shielded cables.

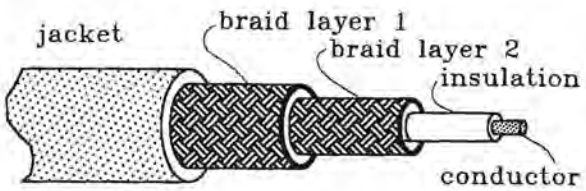

Fig. 15.18 Doubly shielded cable.

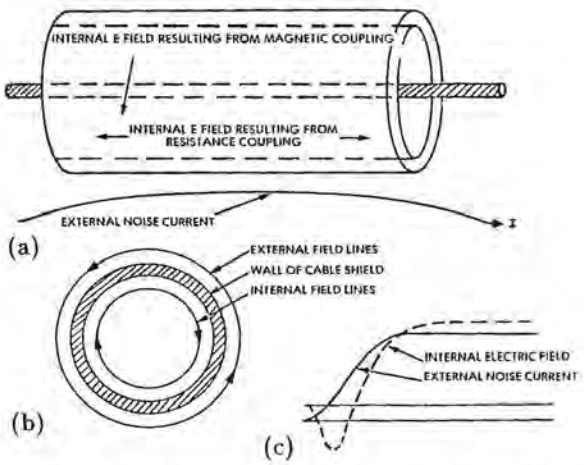

Fig. 15.19 Magnetic coupling giving effect of a negative coupling inductance.
(a) Current and field polarities
(b) Direction of field
(c) Current and field waveshpaes

Electric field leakage: Another source of coupling is via capacitive leakage through the holes in the shield, as shown in Fig. 15.20. If the shielded cable is subjected to an external and changing electric field, dielectric flux will pass through the holes in the cable from the external source and onto the signal conductor. The flow of these dielectric, or displacement, currents

through the external load impedances produces a voltage between the signal conductor and the shield. An alternate source of coupling, shown in Fig. 15.20(b), involves the voltage on the shield itself. Noise currents flowing through the external impedance of the shield may, if the shield is not perfectly grounded, produce a voltage between the shield and any external ground structure.

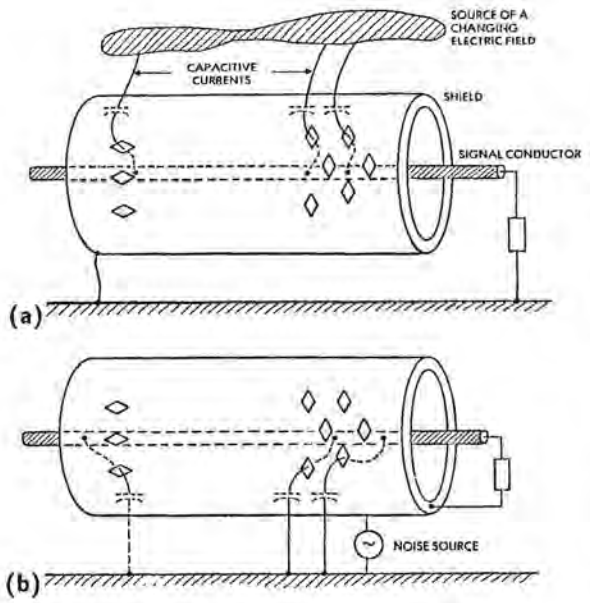

Fig. 15.20 Coupling via capacitive leakage through holes.
(a) From an external source
(b) From voltage on the shield

Leakage due to shield voltage: External impedances between the signal conductor and the shield, as well as the inherent capacitance between the shield and the signal conductor, force the signal conductor to assume nearly the same potential as the shield. Because the signal conductor is then at a potential different from the surrounding ground, dielectric flux can pass from the signal conductor through the holes in the shield and to ground, the dielectric currents again giving rise to a voltage between the signal conductor and the shield.

Equivalent circuit for capacitive leakage: An equivalent circuit for capacitive leakage, Fig. 15.21, is simply a transfer capacitance, C_{12}, (or transfer admittance, $j\omega C_{12}$, in the frequency domain). It depends on the total area of the holes in the shield and on the capacitances between the shield and the conductor, C_{12}, and the shield and the ground return path, C_2. The transfer capacitance is not very sensitive to weave angle, as was shown in Fig. 15.17.

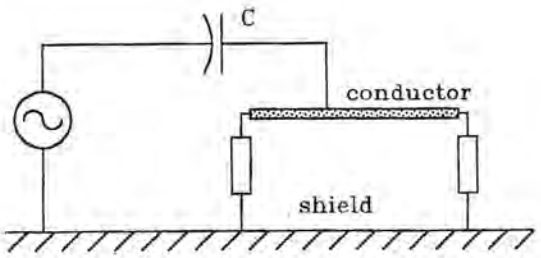

Fig. 15.21 Equivalent circuit for capacitive leakage.

Determination of leakage capacitance: Vance [15.6] also gives expressions relating transfer capacitance to shield construction. Some cables use a layer of metal foil, or a layer of metallized Mylar under the braid to improve the optical coverage and to reduce the transfer admittance. The transfer properties of such shields are best determined by measurement.

Relative order of importance: In most cases the effects of magnetic leakage are probably more important than the effects of capacitive leakage.

Tape wound shields: Tape–wound shields, as shown in Fig. 15.22, are often used where flexibility of the shielded cable is required. The shield may be formed either from a narrow metal sheet spiraled around the core or from a carrier of fine wires, again spiraled around a core. Flexible armor and flexible conduit, which is normally used primarily for mechanical protection, may also be analyzed as tape–wound shields. The tape–wound, or spiral–wound, shield is a rather poor shield for preventing coupling of current from the shield onto the internal conductor because the shield tends to behave as a solenoid wound about the internal conductors. There is thus a rather large transfer coupling term relating the internal voltage to the shield current. This is particularly true if the tape is wound without any overlap because in this case the entire cable current is forced to spiral around the core.

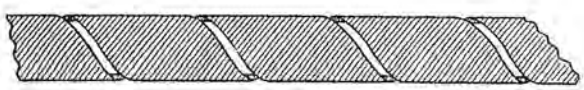

Fig. 15.22 Tape–wound shield.

Vance [15.6] analyzes a 1 cm radius cable wound with 0.25 mm thick, 1 cm wide copper tape, the tape applied without an overlap. The dimensions of the cable are thus similar to those of the braided–wire shield used for the calculations of Fig. 15.17. The transfer

inductance of the tape–wound shield was calculated as 3.9 μH/m, of the order 10^4 greater than the mutual inductance obtained for a braided–wire shield.

Cable trays: Cable trays are most often used for mechanical protection of wires, but if viewed as shields, they may also provide electrical protection. The characteristics of a cable tray that make for good electrical protection are the same as those of any other shield:

1. It must be able to carry current along its axis.
2. It should be of low–resistance material.
3. It should completely surround the conductors, implying that the tray should be fitted with a conducting cover, making good electrical contact along its entire length.
4. It should have a minimum number of openings through which magnetic fields may leak.
5. It should have as few joints as possible, and such joints should be made in such a manner as to provide minimum resistance and leakage of magnetic fields.

The transfer characteristics of the tray by itself would be about the same as those of the solid tubular shields discussed previously. This comparison assumes the tray to be of solid metal and fitted with a well sealed cover. Since covers never form perfect seals, the pulse penetration time constant would probably not be as long as predicted by Eq. 11.24. Even with an imperfect cover, the transfer impedance Z_T would not be greater than the dc resistance.

Trays are most commonly built in short sections and joined by splices or transition sections. Such sections frequently provide for thermal expansion and contraction and are, at any rate, seldom designed either to provide good electrical continuity or to protect against magnetic leakage. When joints are considered, the transfer characteristic of the tray is frequently found to depend almost entirely on the treatment of the joints. Leakage at joints can be reduced by covering them with flexible tape or metal braid. The transfer characteristics can seldom be determined by calculation; they must be determined experimentally.

Conduits: Conduits in aircraft work are most commonly used only for mechanical protection of wires and should not be relied upon for electromagnetic field shielding unless it has been verified that the conduit is electrically continuous and grounded at each end. More commonly, conduits are mounted in rubber insulated mounting brackets and so are not grounded.

15.7 Transfer Characteristics of Actual Cables

The transfer impedance of a shielded cable is not a factor commonly specified either by the manufacturer or by procurement specifications. Even among cables of the same nominal type, this transfer impedance may vary considerably between the cables supplied by different manufacturers. The most straightforward method of determining the transfer characteristic of a shielded cable, particularly if the cable involves multiple shields and multiple load impedances on conductors within the shield, is to make actual measurements of the conductor voltages that are produced by currents which are circulated through the shield. The techniques by which transient currents may be injected into the shields of cables through coupling transformers are described in Chapter 18.

If actual measurements of coupling effects are not available, the transfer characteristics of many cables can be estimated from other published literature. One such summary giving the parameters of coaxial cable shields is shown in Table 15.1 [15.9].

15.8 Connectors

Transfer impedance: The transfer impedance of a cable connector or splice can be represented by

$$Z_T = R_o + j\omega L_{12} \tag{15.7}$$

where R_o is the resistance measured across the connector and L_{12} is a transfer inductance between the external shield circuit and the internal conductors of the cable. The value of Z_T is usually not calculable, but it can be measured by passing current through a cable sample containing the connector and measuring the open circuit voltage induced on conductors inside the shield. Some typical values of R_o and L_{12} have been measured on cable connectors and are listed in Table 15.2.

The transfer impedance of a connector is a lumped element in the cable circuit, in contrast to the distributed nature of the transfer impedance of the cable shield. The effect of leakage through the connector can thus be represented by a discrete voltage source

$$V = IZ_T \tag{15.8}$$

where I is the shield current.

Transfer admittance: Because most connectors that would be used for shielded cables have essentially 100% optical coverage, their transfer admittance is usually negligible. In addition, most bulkhead or panel–mounting connectors are located at points where the

shield voltage is a minimum, so that excitation of the internal conductors by the transfer admittance is small, even if the transfer admittance itself is not small.

15.9 Ground Connections for Shields

The transfer parameters of Table 15.2 refer only to the properties of the connector itself. Additional transfer impedances may be produced by the manner in which the cable shield is connected to the connector or by the manner in which the cable connector is mounted to a bulkhead. Even slight inattention to detail may introduce into the circuit transfer impedances far greater than the impedance of the connector or possibly far greater than that of the rest of the cable shield.

Pigtail grounding: A common treatment of a shield at a connector is to insulate the shield with tape and connect it to the back shell through a pigtail. Such treatment is shown in Fig. 15.23(a). Equally common practice is to insulate a panel connector from a panel with an insulating block and to ground the panel connector either to the panel through a pigtail or, more commonly, to an internal ground bus. A very common treatment of a shield at a connector, shown in Fig. 15.23(c), is for the shield to be connected to one of the connector pins and grounded internally through a pigtail, either to the panel or to an internal ground bus.

Grounding to remote point: Sometimes shields are not connected at all to the panel on which the connector is mounted, but instead are connected to some remote "system ground" point, Fig. 15.23(c). Such practice should always be avoided because it introduces enough impedance to completely destroy the effectiveness of the shield. Such a practice reflects a misunderstanding of the role of "ground" connections.

Calculation of effects: The coupling introduced by any of these configurations can be studied in terms of the self-impedance of the conductor used for the pigtail and the mutual inductance between a portion of the pigtail and the conductors in the connector. The flow of current through the self-inductance of the pigtail produces a voltage

$$V = j\omega L \tag{15.9}$$

This voltage, less that induced in the mutual inductance between the pigtail and the conductors in the connector, will add directly to that produced by the flow of current along the shield.

The self-inductance of conductors was discussed in §9.7.3. There, Eqs. 9.57 and 9.75, the inductance of a straight conductor of non-magnetic material was shown to be

$$L = 2 \times 10^{-7} l \left[\ln \frac{2l}{r} - \frac{3}{4} \right], \tag{15.10}$$

where l = length and r = radius of the wire. The inductance of a typical pigtail will not be significantly different even if it is not straight.

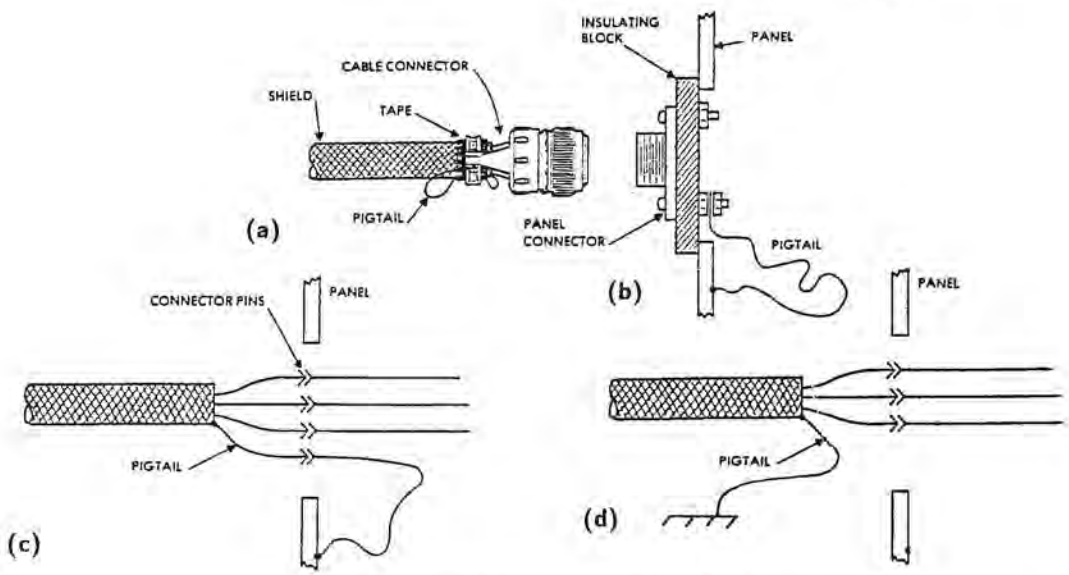

Fig. 15.23 Common treatment of shields at connectors.
(a) Pigtail connection to a backshell
(b) Pigtail grounding to a panel connector
(c) Shield carried on a connector pin
(d) Shield grounded to remote point

The mutual inductance between the two conductors is

$$M = 2lQ \text{ nH/cm} \qquad (15.11)$$

where the factor Q, shown in Fig. 15.24, is a function of the ratio of the length l of conductors to their spacing d. If $d < l$, then

$$M = 2l \left[\ln \frac{2l}{d} - 1 + \frac{d}{l} - \frac{d^2}{2l} + \frac{d^3}{4l} \cdots\right] \qquad (15.12)$$

Mutual inductance so defined should not be confused with the transfer inductance referred to in §15.6. Transfer inductance is $L_t = L_{\text{self}} - M$ and is a quantity that one would normally want to be small. Thus one would normally want the mutual inductance, Eq. 15.212, between two conductors to be large.

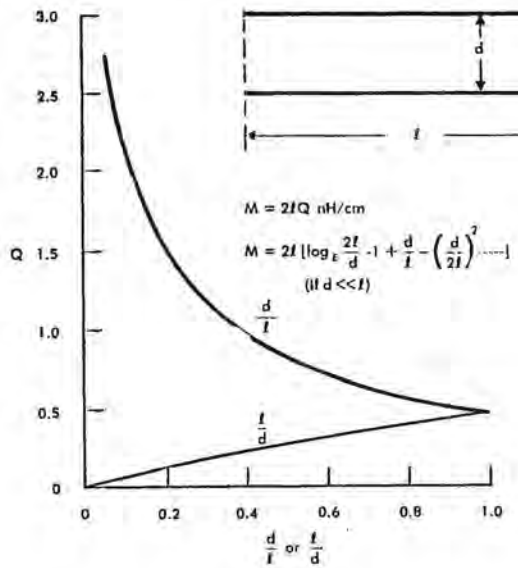

Fig. 15.24 Mutual inductance.

Numerical example: A numerical example will illustrate the problems associated with pigtail grounds. Assume a shield is carried, as in Fig. 15.23(c), through a panel on a pigtail and a set of connector pins. Assume the total length of the pigtail–pin combination to be 7 cm, the spacing between the pigtail and a signal conductor to be, on the average, 0.05 cm, and the pigtail to be made from number 22 AWG wire having a radius of 0.0323 cm. The self-inductance of the pigtail would then be 74.5 nH, the mutual inductance between the two would be 65.0 nH, and the difference, the factor equivalent to the transfer inductance for the shielded cable, would be 9.5 nH.

A rather mediocre shielded braid would have an inductance on the order of 1 nH/m, and a large diameter, tightly woven braid might have an inductance on the order of 0.25 nH/m. The amount of voltage injected into a signal circuit by the current flowing through this one relatively short pigtail, then, would be as much as that coupled onto the signal conductor by 10 to 40 m of cable shield braid.

Measured example: This point may be illustrated by Fig. 15.25, an extension of the test series previously discussed in reference to Figs. 15.2 through 15.8. One end of the cable was grounded through a 33–inch length of wire, while the other end was connected to the ground plane directly. Voltage $V1$ was increased from 0.4 V (Fig. 15.7) to 15.5 V solely because of the inductive rise in the ground lead.

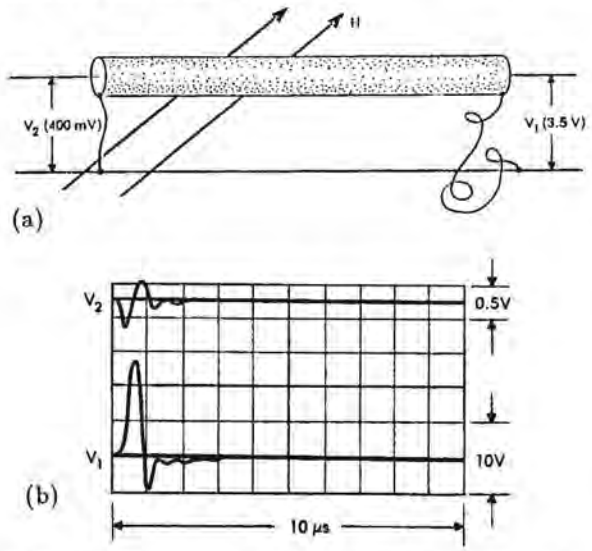

Fig. 15.25 Effects of inductance in a ground lead.
(a) Circuit
(b) Voltage

Drawbacks to pigtail grounding: There are two fundamental drawbacks to pigtail grounding. The first, shown in Fig. 15.33(a), is that the shield current, being constricted to a path of small diameter, sets up a more intense magnetic field at the surface of the conductor than it would if the conductor were larger. A more intense magnetic field of itself would not really be harmful if all the flux so set up would link the signal conductors as well, because then the mutual inductance would also be high, and the difference, $L - M$, would be low. If the shield current is confined to a small diameter path, the field intensity rapidly falls off with distance away from the conductor, and hence the mutual inductance will always be smaller than the self–inductance.

Peripheral grounding: The best type of connector (as regards transfer impedance) is one in which the shield currents are carried concentrically to the conductors

in the shield, Fig. 15.26(b). This can be done with grounding fingers of the type commonly used for single conductor coaxial connectors such as the type N series. Such connectors introduce much less voltage into the conductors for the following reasons:

1. The length of the path through which the shield current must flow is shorter.

2. The field intensity external to the shield is reduced by virtue of the inherently larger diameter of the path upon which the current flows.

3. The field intensity inside the shield is low, nearly zero.

The shorter, and larger diameter, current path implies less self–inductance. The absence of magnetic flux within the shield implies that the signal conductors are exposed to as much flux as is the shield: the transfer inductance is nil.

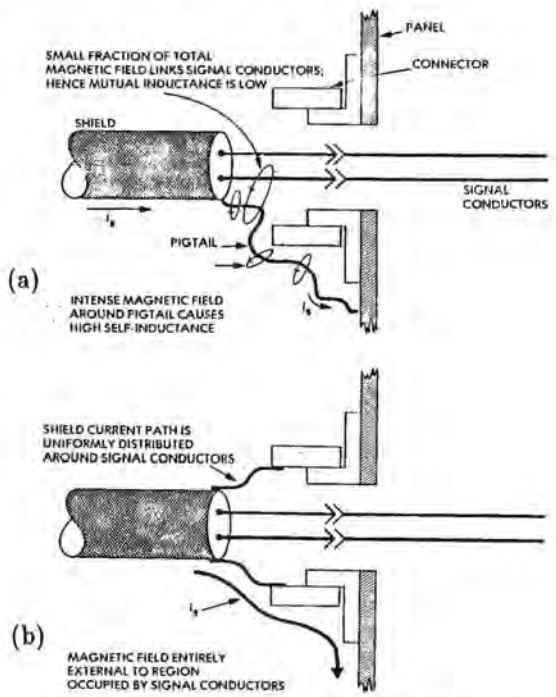

Fig. 15.26 Grounding of shields.
(a) Pigtails
(b) 360° peripheral

15.10 Shielding of Enclosures

Shielding performance of enclosures is usually discussed in terms of the the frequency domain, with shielding effectiveness related to materials, thicknesses, gaskets and openings. Discussions of these effects are given in many sources and will not be repeated here. What will be discussed (in qualititive terms only, not quantitative) is the response to time domain magnetic fields. Some of the material duplicates some of the more rigorous discussions of Chapters 11 and 12, but is repeated here for completeness.

Origin of magnetic shielding by non–magnetic materials: A magnetic field line that attempts to penetrate a conducting sheet, Fig. 15.27(a), induces circulating currents that induce an opposing magnetic field. The result is that a transient magnetic field initially goes around the sheet, Fig. 15.27(b), and only as time progresses will a portion of the field penetrate the sheet. This effect takes place even if the sheet is a non–magnetic material such as aluminum.

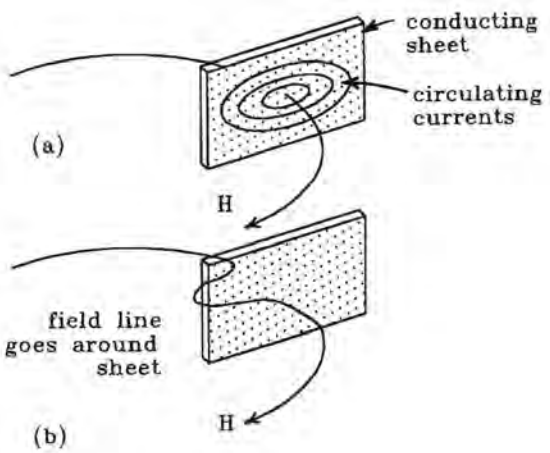

Fig. 15.27 Magnetic field intersecting a conducting sheet.
(a) Penetrating flux
(b) Tangential flux

Response of an enclosure: If a metal box is exposed to the field, Fig. 15.28, current that flows around the box is induced. In cross–section the field patterns will be as shown in Fig. 15.29. As time progresses, the field will penetrate the box, starting at the corners and eventually passing directly through.

Internal current: In response to a step function magnetic field the induced current density on the inside surface of the box will have the diffusion waveshape discussed in §11.3.5 and illustrated in Fig. 15.30(d). The current density, multiplied by the resistivity of the

metal, gives the internal voltage rise. The sum of all the internal voltages, Fig. 15.31(a), impressed across the internal inductance of the box, Fig. 15.31(b), drives an internal circulating current, which in turn produces the net internal magnetic field.

Injected current: Exposure to a magnetic field is not the only way to develop a current on the surface of the box. More commonly, the current will have been induced on a cable shield and carried to a termination point on the box, from which it distributes over the box, as illustrated in Fig. 15.32.

Factors that degrade shielding: One factor that degrades the shielding of the box is illustrated in Fig. 15.33. Covers will always present a higher impedance path than will undisturbed metal. Circulating current, flowing through the cover and joint resistance, produces a resistive voltage that is not retarded by diffusion effects.

Another factor is apertures, illustrated in Fig. 15.34. External magnetic fields loop in and out of the apertures, producing a net internal magnetic field. Apertures with their long direction oriented in line with the magnetic field result in more net internal flux than do apertures oriented crosswise to the field.

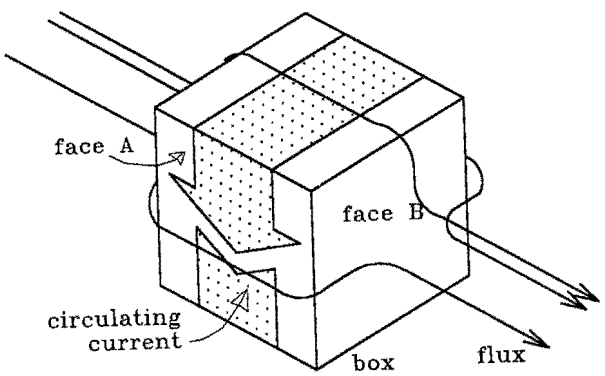

Fig. 15.28 Circulating current induced by a changing magnetic field.

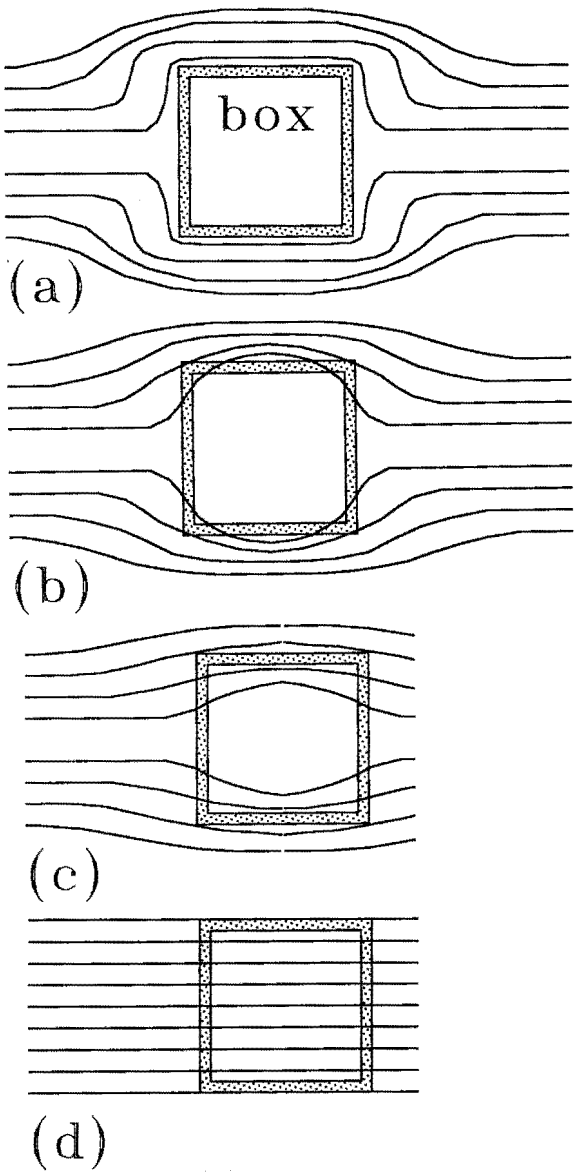

Fig. 15.29 Paths of the magnetic field.
(a) Initial conditions
(b) Later time
(c) Still later time
(d) Final conditions

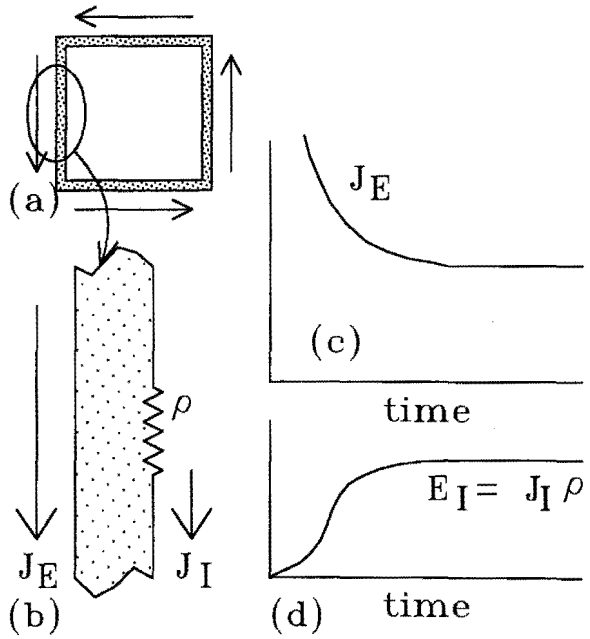

Fig 15.30 Current densities
(a) Cross–section of face B
(b) Detail
(c) External current density
(d) Internal electric field

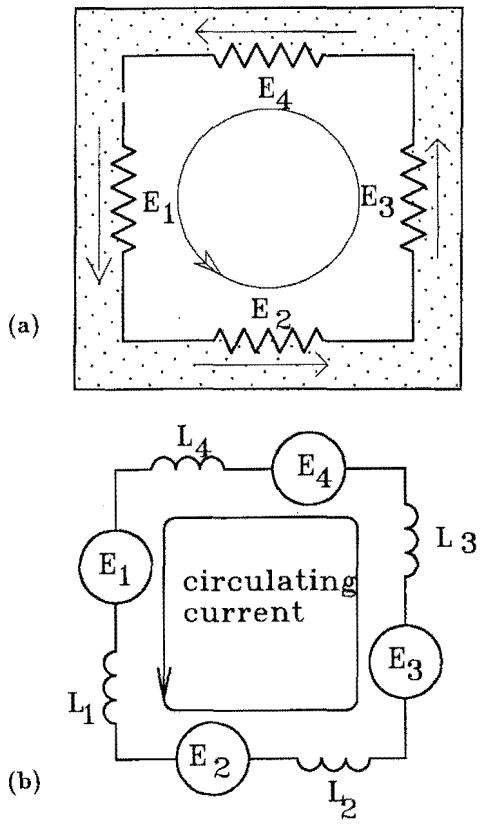

Fig 15.31 The internal circulating current.
(a) Physical
(b) Equivalent circuit

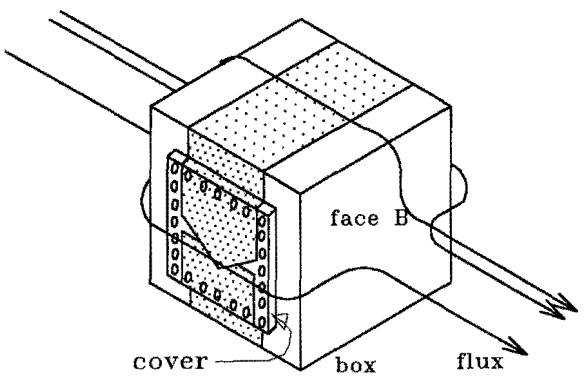

Fig 15.32 Direct injection of current.

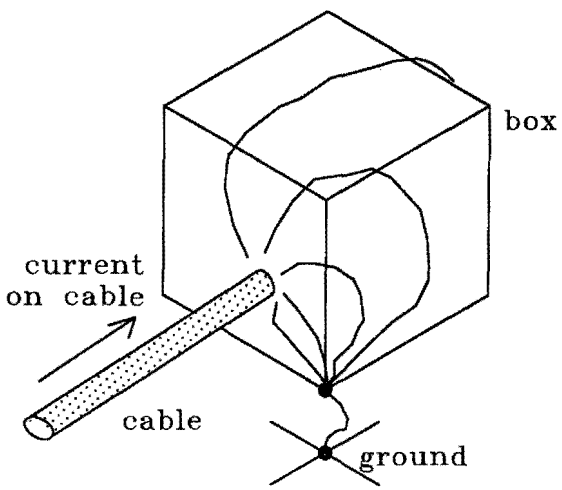

Fig 15.33 Interference with circulating current.

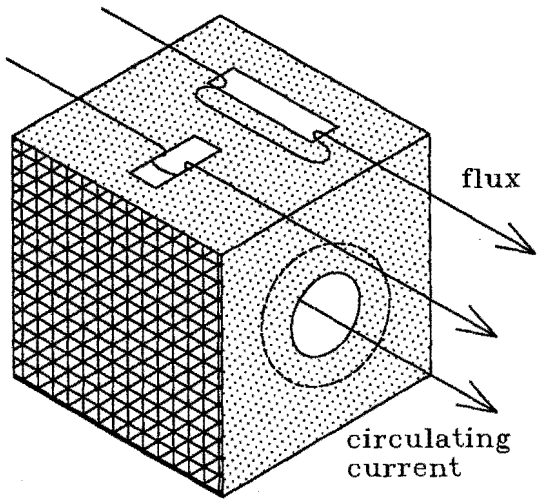

Fig 15.34 Leakage through apertures.

Table 15.1 Coaxial-cable Shield Parameters [15.9], (partial).

Cable Type (RG-)		Strand Diameter d (inches)	Outside Diameter (inch)	Carriers, C	Ends, N	Picks, P (inch^{-1})	Weave Angle,α (degrees)	Fill, F	Coverage, K (%)	Weight per Foot (lbs)	Stranding Factor	DC Resistance, R_o (mΩ/m)	Leakage Inductance, M_{12}(nH/m)	Leakage Capacitance C_{12}/C_1C_2(m/F)
6	I	0.0063	0.189	16	9	5.90	25.0	0.790	95.61	0.019	1.54	6.6	0.42	2.9×10^7
6	AI	0.0063	0.189	24	6	8.80	24.9	0.790	95.58	0.019	1.54	6.6	0.28	1.9
6	O	0.0063	0.214	16	9	8.79	37.7	0.886	96.23	0.022	1.98	7.5	0.36	1.9
6	AO	0.0063	0.214	24	6	13.00	37.6	0.885	96.18	0.022	1.98	7.5	0.25	1.3
11		0.0071	0.292	24	8	6.50	27.5	0.799	95.96	0.033	1.59	4.0	0.25	1.6
22	I	0.0063	0.291	24	8	9.10	35.9	0.763	95.27	0.028	1.95	5.5	0.34	1.9
22	O	0.0063	0.316	24	8	12.00	45.9	0.842	97.50	0.033	2.45	6.4	0.14	0.6
23	I	0.0063	0.394	24	9	10.50	48.2	0.799	95.95	0.039	2.82	5.9	0.29	1.2
25	I	0.0063	0.298	16	13	5.00	31.4	0.786	95.44	0.029	1.74	4.8	0.46	2.8
25	AI	0.0063	0.298	24	9	6.00	26.0	0.776	94.98	0.029	1.60	4.4	0.34	2.3
25	O	0.0063	0.355	16	15	5.00	35.8	0.887	96.29	0.036	1.88	4.4	0.35	1.9
25	AO	0.0063	0.355	24	11	5.00	25.7	0.799	95.96	0.035	1.54	3.7	0.25	1.6
35		0.0071	0.470	24	10	9.00	48.8	0.850	97.74	0.056	2.71	4.3	0.12	0.5
58		0.0050	0.120	12	9	7.70	27.7	0.746	93.57	0.089	1.71	14.2	1.0	6.6
58	A	0.0050	0.120	16	7	10.30	27.7	0.775	94.92	0.018	1.65	13.7	0.53	3.5
59		0.0063	0.150	16	7	8.20	27.6	0.780	95.14	0.015	1.63	8.6	0.49	3.2
59	A	0.0063	0.150	24	5	12.30	27.6	0.835	97.29	0.016	1.53	8.1	0.14	0.9
62		0.0063	0.151	16	7	8.20	27.8	0.776	94.98	0.015	1.65	8.7	0.52	3.4
62	A	0.0063	0.151	24	5	12.30	27.8	0.831	97.15	0.016	1.54	8.1	0.15	1.0
63		0.0071	0.295	16	12	4.30	27.6	0.792	95.66	0.033	1.61	4.0	0.42	2.7
63	A	0.0071	0.295	24	8	6.50	27.8	0.793	95.71	0.033	1.61	4.0	0.27	1.8

A – Alternate
A1 – First alternate
A2 – Second alternate

I – Inner
O – Outer
S – Shield (insulated from braid)

• Braid actually consists of flat tape conductors. Strand diameter and ends are estimated for the equivalent cross-sectional area of the tape conductor; therefore, F, K, and straning factor are approximate.

Table 15.1 Coaxial-cable Shield Parameters (continuation).

Cable Type (RG-)		Strand Diameter d (inches)	Outside Diameter (inch)	Carriers, C	Ends, N	Picks, P ($inch^{-1}$)	Weave Angle, α (degrees)	Fill, F	Coverage, K (%)	Weight per Foot (lbs)	Stranding Factor	DC Resistance, R_o ($m\Omega/m$)	Leakage Inductance M_{12} (nH/m)	Leakage Capacitance C_{12}/C_1C_2 (m/F)
65		0.0071	0.295	24	8	6.50	27.8	0.793	95.71	0.033	1.61	4.0	0.27	1.8
108		0.0050	0.164	16	6	10.80	36.4	0.546	79.36	0.009	2.83	17.6	4.6	25.0
114		0.0063	0.295	24	8	7.00	29.4	0.718	92.07	0.020	1.83	5.1	0.70	4.4
119	I	0.0071	0.337	24	10	5.40	26.4	0.862	98.10	0.041	1.45	3.1	0.08	0.5
119	O	0.0063	0.367	24	8	10.60	46.5	0.737	93.06	0.033	2.86	6.5	0.65	2.8
122		0.0050	0.099	16	6	12.90	28.9	0.801	96.02	0.008	1.63	16.2	0.37	2.4
122	A	0.0050	0.099	24	5	12.20	19.2	0.928	99.48	0.010	1.21	12.0	0.01	0.08
130		0.0100	0.487	24	8	6.30	39.9	0.786	95.41	0.076	2.16	2.3	0.33	1.7
142	I	0.0050	0.121	16	7	11.50	30.6	0.791	95.61	0.010	1.71	14.1	0.43	2.7
142	O	0.0050	0.141	16	7	14.50	40.7	0.778	95.09	0.011	2.23	16.0	0.55	2.8
144		0.0063	0.290	24	8	9.20	36.1	0.787	95.47	0.029	1.95	5.5	0.32	1.7
156	I	0.0063	0.290	24	8	11.20	41.6	0.851	97.77	0.031	2.10	6.0	0.11	0.55
156	O	0.0070	0.333	24	8	9.20	39.9	0.803	96.13	0.034	2.11	4.7	0.26	1.3
156	S	0.0063	0.413	24	8	14.00	57.3	0.838	97.38	0.043	4.10	8.3	0.17	0.51
157	I	0.0063	0.465	24	9	12.80	58.0	0.856	97.92	0.049	4.16	7.5	0.12	0.36
157	O	0.0070	0.500	24	10	7.30	44.5	0.729	92.67	0.046	2.69	4.1	0.70	3.1
157	S	0.0063	0.580	24	9	13.50	64.5	0.848	97.70	0.060	6.35	9.2	0.16	0.34
174		0.0040	0.063	16	4	16.30	24.4	0.630	86.33	0.003	1.91	36.5	2.3	15.8
179		0.0040	0.066	16	5	12.00	19.2	0.729	92.65	0.004	1.54	28.1	0.88	6.6
181	I	0.0063	0.215	24	7	8.80	27.7	0.836	97.30	0.023	1.53	5.7	0.14	0.9
181	O	0.0100	0.490	24	8	7.00	43.1	0.820	96.76	0.080	2.28	2.4	0.20	0.95
189	I	0.0100	0.635	48	7	6.00	27.2	0.918	99.33	0.114	1.38	1.1	0.008	0.06
189	O	0.0100	0.680	48	6	7.00	32.7	0.778	95.07	0.104	1.81	1.4	0.17	1.0
192	I	0.0100	1.725	48	11	5.87	53.3	0.806	96.22	0.265	3.47	1.1	0.14	0.49
192	O	0.0095	1.780	48	11	5.95	54.5	0.764	94.43	0.182	3.88	1.1	0.25	0.85
192	S	0.0100	1.890	48	11	6.03	56.4	0.796	95.84	0.289	4.11	1.2	0.17	0.53
193	I	0.0100	1.725	48	11	4.15	43.5	0.664	88.68	0.220	2.86	0.89	0.66	3.1
193	O	0.0095	1.780	48	11	5.50	52.3	0.726	92.50	0.225	3.69	1.2	0.39	1.4
193	S	0.0100	1.890	48	9	7.70	62.6	0.781	95.20	0.284	6.83	1.7	0.23	0.54

Table 15.1 Coaxial-cable Shield Parameters (continuation).

Cable Type (RG-)		Strand Diameter d (inches)	Outside Diameter (inch)	Carriers, C	Ends, N	Picks, P ($inch^{-1}$)	Weave Angle, α (degrees)	Fill, F	Coverage K (%)	Weight per Foot (lbs)	Stranding Factor	DC Resistance, R_o ($m\Omega/m$)	Leakage Inductance M_{12} (nH/m)	Leakage Capacitance C_{12}/C_1C_2 (m/F)
194	I	0.0100	1.725	48	11	4.15	43.5	0.664	88.68	0.220	2.86	0.89	0.66	3.1
194	O	0.0095	1.780	48	11	5.50	52.3	0.726	92.50	0.225	3.69	1.2	0.11	0.38
210		0.0063	0.151	16	7	8.20	27.8	0.776	94.98	0.015	1.65	8.7	0.52	3.4
210	A	0.0063	0.151	24	5	12.30	27.8	0.831	97.15	0.016	1.54	8.1	0.15	0.96
211		0.0080	0.625	36	10	5.60	32.1	0.844	97.56	0.082	1.65	1.7	0.09	0.48
211	A	0.0080	0.625	48	8	5.60	25.2	0.843	97.53	0.082	1.45	1.5	0.06	0.40
212	I	0.0063	0.189	16	9	5.90	25.0	0.790	95.61	0.019	1.54	6.6	0.42	2.9
212	AI	0.0063	0.189	24	6	8.80	24.9	0.790	95.58	0.019	1.54	6.6	0.28	1.9
212	O	0.0063	0.214	16	9	8.70	37.7	0.806	96.23	0.022	1.98	7.5	0.36	1.9
212	AO	0.0063	0.214	24	6	13.00	37.6	0.805	96.18	0.022	1.98	7.5	0.25	1.3
213		0.0071	0.292	24	8	6.50	27.5	0.799	95.96	0.033	1.59	4.0	0.25	1.6
214	I	0.0063	0.292	24	6	16.60	52.9	0.786	95.44	0.029	3.50	9.9	0.37	1.3
214	O	0.0063	0.317	24	7	15.40	53.0	0.850	97.75	0.034	3.25	8.5	0.13	0.45
217	I	0.0071	0.380	24	10	5.40	29.1	0.788	95.49	0.042	1.66	3.2	0.30	1.9
217	O	0.0071	0.405	24	8	10.60	49.3	0.794	95.75	0.045	2.96	5.4	0.32	1.3
218		0.0100	0.690	24	14	3.10	30.0	0.869	98.29	0.118	1.53	1.2	0.07	0.44
218	A1	0.0100	0.690	36	9	4.00	26.4	0.811	96.41	0.110	1.54	1.2	0.14	0.92
218	A2	0.0100	0.690	48	7	5.60	27.5	0.849	97.72	0.115	1.50	1.1	0.05	0.35
220		0.0100	0.925	36	12	3.50	30.0	0.840	97.44	0.151	1.59	0.91	0.09	0.53
220	A	0.0100	0.925	48	9	4.20	27.5	0.820	96.76	0.148	1.55	0.89	0.09	0.59
222	I	0.0063	0.189	16	9	5.90	25.0	0.790	95.61	0.019	1.54	6.6	0.42	2.9
222	AI	0.0063	0.189	24	6	8.80	24.9	0.790	95.58	0.019	1.54	6.6	0.28	1.9
222	O	0.0063	0.214	16	9	8.70	37.7	0.806	96.23	0.022	1.98	7.5	0.36	1.9
222	AO	0.0063	0.214	24	6	13.00	37.6	0.805	96.18	0.022	1.98	7.5	0.25	1.3
223	I	0.0050	0.120	12	9	9.00	31.5	0.775	94.95	0.010	1.77	14.8	0.72	4.4
223	AI	0.0050	0.120	16	7	11.50	30.4	0.795	95.80	0.010	1.69	15.5	0.43	2.3
223	O	0.0050	0.140	12	9	10.00	38.1	0.729	92.63	0.010	2.22	16.0	1.3	7.0
223	AO	0.0050	0.140	16	7	15.00	41.5	0.793	95.71	0.011	2.25	16.2	0.45	2.2
225	I	0.0063	0.290	24	6	16.60	52.7	0.788	95.52	0.029	3.46	9.8	0.36	1.3

Table 15.1 Coaxial-cable Shield Parameters (conclusion).

Cable Type (RG-)		Strand Diameter d (inches)	Outside Diameter (inch)	Carriers, C	Ends, N	Picks, P ($inch^{-1}$)	Weave Angle, α (degrees)	Fill, F	Coverage, K (%)	Weight per Foot (lbs)	Stranding Factor	DC Resistance, R_o (mΩ/m)	Leakage Inductance M_{12} (nH/m)	Leakage Capacitance C_{12}/C_1C_2 (m/F)
225	O	0.0063	0.315	24	7	15.40	52.9	0.852	97.80	0.033	3.22	8.5	0.12	0.44
226	I	0.0063	0.375	24	10	10.50	46.8	0.907	99.14	0.042	2.35	5.2	0.03	0.12
226	O	0.0063	0.400	24	8	10.50	48.6	0.706	91.33	0.035	3.24	6.6	0.92	3.7
301		0.0050	0.190	16	10	8.00	32.1	0.752	93.84	0.014	1.86	10.0	0.73	4.4
302		0.0050	0.151	16	7	11.50	36.0	0.684	90.04	0.010	2.23	15.0	1.5	8.4
303		0.0050	0.121	16	7	11.50	30.6	0.791	95.61	0.010	1.71	14.1	0.43	2.7
304	I	0.0063	0.190	24	5	14.50	37.6	0.749	93.71	0.213	2.12	9.0	0.52	2.8
304	O	0.0063	0.215	24	6	11.50	34.4	0.769	94.57	0.021	1.91	7.2	0.40	2.3
316		0.0040	0.063	16	5	4.50	7.2	0.723	92.32	0.004	1.41	26.8	0.88	7.7
326	I*	0.0035	0.550	24	27	6.46	43.3	0.890	98.80	0.042	2.12	5.9	0.05	0.22
326	O*	0.0035	0.566	24	27	6.46	44.1	0.877	98.49	0.043	2.21	6.0	0.06	0.30
328	I	0.0100	1.085	48	9	5.50	38.5	0.795	95.80	0.167	2.05	1.0	0.14	0.75
328	O	0.0070	1.125	48	12	6.70	45.0	0.796	95.85	0.111	2.51	1.7	0.15	0.66
328	S	0.0100	1.225	48	9	5.60	42.4	0.748	93.63	0.177	2.45	1.1	0.28	1.3
329	I	0.0100	0.390	24	7	5.90	32.3	0.772	94.80	0.060	1.82	2.4	0.38	2.3
329	O	0.0070	0.430	24	9	9.20	46.9	0.794	95.74	0.043	2.70	4.7	0.31	1.3
391		0.0063	0.307	24	7	16.30	53.8	0.891	98.82	0.034	3.21	8.1	0.05	0.17

Table 15.2 Transfer Impedance of Typical Cable Connectors [15.10].

Connector	Identification	R_o (ohms)	M_{12} (H)
Multipin Aerospace connectors (Threaded)	Burndy NA5-15863	0.0033	5.7×10^{-11}
	Deutch 38068-10-5PN	0.15	2.5×10^{-11}
	Deutch 38068-18-31SN	0.005	1.6×10^{-10}
	Deutch 38060-22-55SN	0.023	1.1×10^{-10}
	Deutch 38068-14-7SN	0.046	5.0×10^{-11}
	Deutch 38060-14-7SN	0.10	8.2×10^{-11}
	Deutch 38060-14-7SN	0.023	6.7×10^{-11}
	Deutch 38068-12-12SN	0.0033	3.0×10^{-11}
	Deutch 38068-12-12SN	0.012	1.3×10^{-11}
	Deutch 38068-12-12SN	0.012	1.3×10^{-11}
	Deutch 38060-12-12SN	<0.001	2.5×10^{-12}
	Deutch 38068-12-12SN	0.014	3.5×10^{-11}
	AMP	0.0067	1.6×10^{-11}
	AMP	0.0067	1.5×10^{-11}
	AMP	0.0033	1.9×10^{-11}
Type N	UG 21B/U-UG58A/U	*	*
Type BNC (Bayonet)	UG 88C/U-UG1094/U	0.002	$4\text{-}8 \times 10^{-11}$
Anodized	MS 24266R-22B-55	5×10^4	$\omega M < R_o$ @ 20 MHz
Open shell	MS 3126-22-55	0.5-1	$\omega M < R_o$ @ 20 MHz
Split shell	MS 3100-165-1P MS 3106A-	0.001	$\approx 20 \times 10^{-11}$

*Too small to measure in presence of 4 inches of copper tube used to mount connector.

REFERENCES

15.1 F.A. Fisher, "Effects of a Changing Magnetic Field on Shielded Conductors," *Lightning Protection Note 75-2*, Internal General Electric Memorandum, High Voltage Laboratory, Corporate Research and Development, General Electric Company, Pittsfield, Massachusetts, June 2, 1975.

15.2 F. A. Fisher, "A Way to Evaluate the Effects of a Changing Magnetic Field on Shielded Conductors," *IEEE Symposium on EMC*, Seattle, WA., August 2–4, 1977, pp. 60-65. and also *77CRD158*, General Electric Co., Corporate Research and Development Center, Schenectady, NY, 1977.

15.3 E. F. Vance, H. Chang, "Shielding Effectiveness of Braided Wire Shields," *Stanford Research Technical Memorandum 16*, November 1971.

15.4 E. F. Vance, "Comparison of Electric and Magnetic Coupling Through Braided-Wire Shields," *Stanford Research Technical Memorandum 18*, February 1972.

15.5 E. F. Vance, "Coupling to Cables," *DNA Handbook Revision*, Chapter 11, Stanford Research Institute, Menlo Park, California, December 1974.

15.6 E. F. Vance, *Coupling to Shielded Cables*, John Wiley and Sons, New York, 1978.

15.7 S.A. Shelkunoff, "Electromagnetic Theory of Coaxial Transmission Lines and Cylindrical Shields," *Bell System Technical Journal*, 13, 1934, pp. 532-79.

15.9 Vance, pp. 1-133 to 11-136.

15.10 Vance, pp. 11-166.

Chapter 16

DESIGN TO MINIMIZE INDIRECT EFFECTS

16.1 Introduction

This chapter covers some of the ways that indirect effects can be controlled, focusing mostly on matters that involve the aircraft as a whole, such as locations for equipment and types of wiring. Phrased another way, the chapter deals primarily with matters of basic policy regarding protection against lightning and with basic matters of systems integration.

Some of the policy steps involved in controlling indirect effects are:

1. Specify the requirements.
2. Choose the best locations for equipment.
3. Choose the best locations for wiring.
4. Choose good wiring and grounding practices.
5. Coordinate actual transients with specifications.
6. Explicitly require that equipment withstand transients.
7. Require that transient performance be verified by test.

These points are discussed in the following sections. The goals for design in §16.2 may seem self evident, but are frequently not followed. Location of equipment, §16.3, and locations for wiring, §16.4, discuss general good practice. Section 16.5 discusses shielding of interconnecting wiring and brings up the perennial controversy of single vs. multiple point grounding of shields, a subject that was covered in detail in Chapter 15. Determining the transient levels was the subject of Chapters 9 –14. Design of equipment is discussed further in Chapter 17 and verification testing is discussed in Chapter 18.

The transient control level concept is becoming more widely used for aircraft, but since it is still fairly new, it is explained in some detail, including a discussion of its historical development.

16.2 Requirements and Goals

The minimum requirements regarding indirect effects are probably:

1. Indirect effects should not cause physical damage.
2. Indirect effects should not cause interference that presents an imminent hazard to the safety of the vehicle or its crew, or interference that presents a severe risk of preventing the completion of aircraft's mission.

Other interference, though undesirable, might be tolerated. For example, indirect effects that cause warning lights to appear might be considered acceptable whereas indirect effects that lead to the tripping of circuit breakers might be unacceptable, even if it were possible to reset the circuit breakers. Interference that leads to the scrambling of one channel of a redundant digital control system is probably acceptable, but interference that causes computers to shut down is unacceptable, particularly if the computers are shut down in a disorderly manner which results in the internally stored programs being scrambled.

Some general premises that go along with these goals might be:

1. It is more productive to design electronic equipment so that it can accept lightning induced transients on input and output leads than it is to initiate a retrofit program to provide protection to an existing system.
2. It is more practical to design an electronic system around the capabilities of existing and proven protective devices or techniques than it is to develop and retrofit new and improved protective techniques to an electronic system designed without consideration of the transients that might be produced by lightning.
3. Trade–offs must be made between the cost of providing electronic equipment capable of withstanding lightning induced transients and the cost of shielding equipment and interconnecting wiring from the electromagnetic effects of lightning.
4. Designers should take as much advantage as possible of the inherent shielding that aircraft structures are capable of supplying and should avoid

placing equipment and wiring in locations that are most exposed to the electromagnetic fields produced by lightning.

These may all seem obvious, but experience indicates that they are often overlooked.

16.3 Location of Electronic Equipment

Because of other constraints the designer may not have much choice in the matter, but it is often possible to make improvements in the resistance to indirect effects by locating electronic equipment in regions where the electromagnetic fields produced by lightning current are lowest and by avoiding the placement of equipment in the region where the electromagnetic fields are highest. For example, since the most important type of coupling from the outside electromagnetic environment to the inside of the aircraft is through apertures, it follows that equipment should be located as far from major apertures as possible.

Further, since access doors with their imperfectly conducting covers are a major source of electromagnetic leakage, it follows that equipment should be located as far from such access doors as possible. In practice this may be more easily said than done, however, because frequently the purpose of access doors is to provide ready access to electronic equipment.

One main goal should be to locate electronic equipment toward the center of the aircraft structure rather than at the extremities, since the electromagnetic fields tend to cancel toward the center of any structure.

Another main goal should be to locate electronic equipment away from the outer skin of the vehicle; particularly away from the nose of the aircraft, where the radius of curvature of a prime current carrying path is smallest. Furthermore, if possible, electronic equipment should be located in shielded compartments.

Shelves and ground planes: One important factor that is under the designers control is the type of shelf upon which electronic equipment is to be located. The matter is of particular importance for aircraft using large amounts of composite material for the structure. These shelves will be called upon to provide ground planes or reference surfaces for electronic equipment and thus it is essential that they be highly conductive and be well bonded to the aircraft structure. They should either be made of metal or, if made from composite materials, they should be covered with a sheet of aluminum well bonded to the aircraft structure.

16.4 Location of Wiring

Designers have somewhat more control over the routing of wiring used to interconnect equipment than over the location of the equipment itself. Wiring should be located away from apertures and away from regions where the radius of curvature of structural members or the outer skin is smallest. Moreover, wiring should be located as close to a ground plane or structural member as possible. If the structural member is shaped or can be shaped to provide a trough into which the wiring may be placed, the member will provide more inherent shielding than it will if the wiring is placed on the edge of the member. Some examples of typical structural members and the best places for bundles of wiring are shown in Fig. 16.1. In each case the structural member is assumed to be carrying current along its axis.

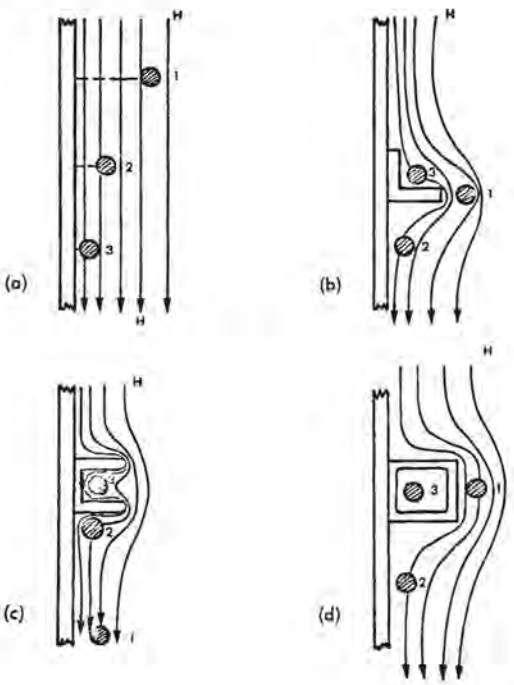

Fig. 16.1 Flux linkages vs conductor position.
(a) Conductors over a plane
(b) Conductors near an angle
(c) Conductors near a channel
(d) Conductors near a box
In each case pictured
Conductor 1 - highest flux linkages: worst
Conductor 2 - intermediate linkages: better
Conductor 3 - lowest linkages: best

Some basic principles to follow are:

1. The closer a conductor is placed to a metallic ground plane, the less is the flux that can pass between that conductor and the ground plane.

2. Magnetic fields are concentrated around protruding structural members and diverge in inside corners. Hence, conductors located atop protruding members will intercept more magnetic flux than conductors placed in corners, where the field intensity is weaker.

3. Fields will be weaker on the interior of a U–shaped member than they will be on the edges of that member.

4. Fields will be lowest inside a closed member.

Some examples of cable routing are shown on Fig. 16.2.

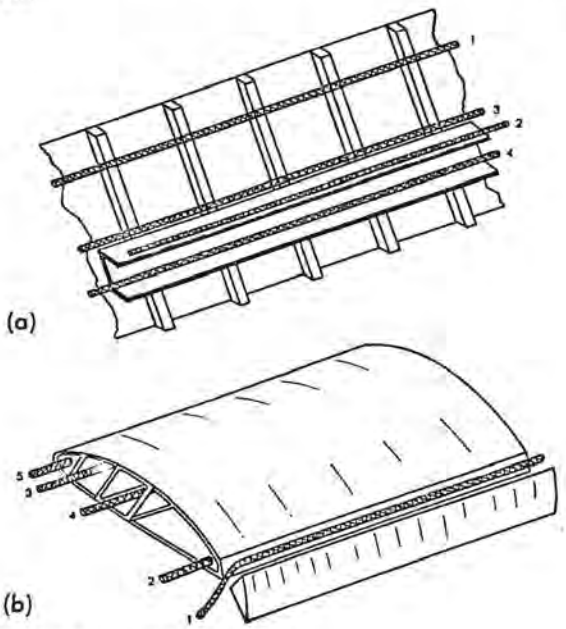

Fig. 16.2 Conductor routing.
(a) A fuselage structure
(b) A wing structure
In each case pictured
Conductor 1 - highest flux linkages: worst
Conductor 4 - lowest flux linkages: best

Stiffeners: Along the interior of a structure, a cable clamped to stiffeners, as at position 1, will effectively be spaced away from the metal skin by the height of the stiffeners. A conductor along the outside edge of the U–shaped member, as shown by conductor 2 in Fig. 16.2(a), may or may not be better placed than conductor 1: effectiveness depends on how closely the conductor is attached to the side of the U–shaped member. Conductor 3, placed along the edge where the U–shaped member is attached to the stiffeners, would probably be in a lower field environment than would either conductor 1 or conductor 2. Conductor 4, located on the interior of the U–channel, would be in the lowest field region and hence in the most effective position. Similar considerations apply to conductors located in structures like wings or stabilizers.

Trailing edges: A conductor located along the outside trailing edge of the wing, as shown by conductor 1 in Fig. 16.2(b), will pick up much more flux than will any conductor located on the inside, probably by several orders of magnitude. Hence conductor 2, located on the inside of the trailing edge, would be better placed. Conductors 3 and 4, in that order, would be in the regions of lowest magnetic flux. A conductor that could be run inside a major structural member, as shown by conductor 4, will be exposed to a minimum amount of magnetic flux. Conductor 5, located at the leading edge of the wing, would be in a well shielded region if the leading edge of the wing were metal, but it would be in a high field region and therefore vulnerable if the leading edge were a nonmetallic covering. However, even if the covering were metallic, conductor 5 would not be in as protected a region as either conductor 3 or conductor 4, because of the tight radius of the leading edge.

Windshield posts: Windshield posts, shown in Fig. 16.3, tend to concentrate the current flowing on the exterior surface of the vehicle, particularly if a flash is swept back, contacting the windshield post directly or the eyebrow region above the windshield. Since the current is concentrated, the magnetic field intensity inside the crew compartment tends to be very high. The situation is aggravated by the fact that the windshields, unlike other regions where the field might have to diffuse through the metal surfaces, act as large apertures and so allow the internal magnetic flux to build to its peak values very rapidly.

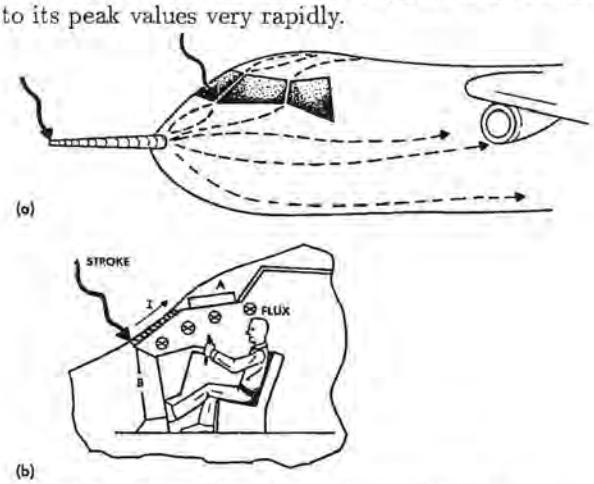

Fig. 16.3 Current flow along windshield posts.
(a) External current flow
(b) Internal magnetic fields

Instruments and wiring on the control panels are thus in a region of inherently high magnetic field strength. Conductors that run from overhead control panels (position A) to other instruments (position B) are often run along the windshield center posts. They are thus in a region of the most concentrated magnetic fields likely to be found on an aircraft, and accordingly they may have induced in them the highest voltages.

16.5 Wiring and Grounding Practices

Practices should be chosen with forethought, properly illustrated and implemented, and not be left to develop by chance. The design office should make sure that everyone knows what the design practices are and all designs should be checked to ensure that they follow practices good for resistance to lightning effects.

16.5.1 Basic Grounding Practices

Proper grounding of equipment is necessary if indirect effects are to be controlled, but there are many factors to be considered. Best practice for one aspect often conflicts with best practice for other aspects. There is no single point on an aircraft that can be called "Ground" and compatibility problems are not resolved just by making a wire connection to an "equipotential ground plane." The closest approximation to an equipotential surface will be found on the inner surface of a shielding enclosure or the inner surface of a properly terminated wire shield, places where the *density* of lightning induced noise currents is low.

Some basic considerations are as follows:

Aircraft structure as a return path: Lightning current flowing through the structure of an aircraft produces voltage rises which can couple to internal circuits. Historically, experience has shown that the structure of metal aircraft can be used successfully as a return circuit for power distribution, but aircraft structure should never be used as a return path for signal or control circuits. Aircraft using large amounts of composite materials for the structure should use separate dedicated return wires for power circuits.

Single point grounding: Single point grounding, Fig. 16.4, prevents the low frequency component of the voltage rises from coupling to circuits and should be used where possible. It does though, subject equipment to high common mode voltages. It is most easily implemented for simple electromechanical devices, such as motors, servos, solenoids, potentiometers, lights and switches. All of these are devices that can withstand several hundreds or possibly a few thousands of volts between the internal circuits and the case or frame of the device.

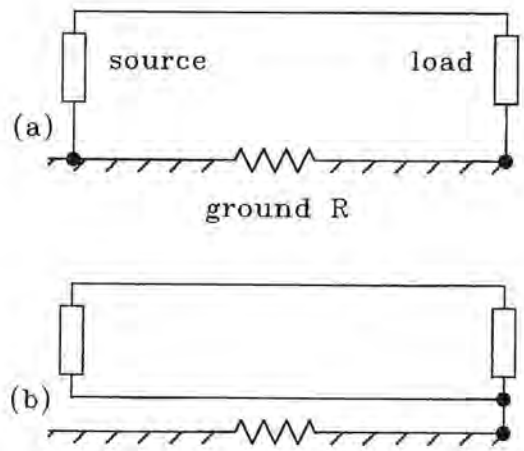

Fig. 16.4 Single point grounding.
(a) Coupling of structural IR voltage
(b) Elimination of structural IR voltage

Problems with single point grounding: While the single point ground concept avoids coupling of structural voltage rises, it does have problems, particularly in regards to low level electronic circuits.

1. It does not eliminate the high frequency component of voltage rises.

2. It eliminates the low frequency component of voltage rises only by subjecting equipment to a common mode voltage. The common mode voltages may be excessive for electronic equipment.

3. Long ground leads may be involved. These leads have impedance, resistance and inductance, and lightning current flowing through these leads produces dangerous voltages.

When investigations have been made of lightning induced damage to electronic equipment it is frequently found that a single point ground concept has been carried to extremes, or that it was applied without recognition of the common mode voltage problems that are entailed. For electronic circuits a multipoint ground concept is generally to be preferred.

Multiple point grounding: Shielding against electromagnetic effects requires multipoint grounding. Multipoint grounding, Fig. 16.5, requires that each LRU case be the single point reference for all internal circuitry. Each circuit or signal type is multipoint grounded to local reference planes and then each of these reference planes is terminated to the chassis. The chassis is then terminated to the nearest airframe ground plane.

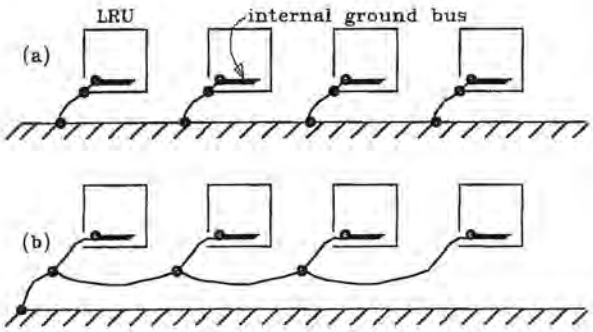

Fig. 16.5 Multiple point grounding.
(a) Good
(b) Bad

Multipoint grounding is sometimes objected to on the basis that it creates "ground loops" or that it may subject input and output circuits to high voltages. These are valid points, but generally it is easier to deal with the residual problems associated with multipoint grounding than with those associated with single point grounding.

16.5.2 Shielding of Interconnecting Wiring

In order to make an electronic system immune to the effects of lightning, it is almost always necessary to make judicious use of shielding on interconnecting wiring and to provide proper grounding of these shields. Factors governing the performance of cable shields were discussed in detail in Chapter 15, but will be reviewed here. Fig. 16.6 shows some of the basic considerations.

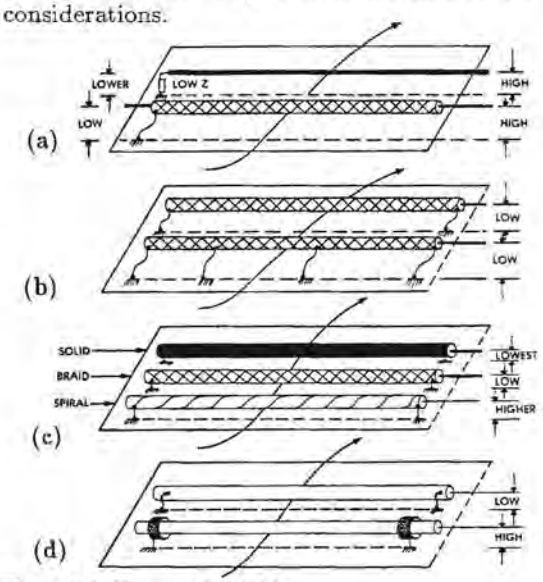

Fig. 16.6 Types of shield.
(a) Unshielded vs shielded
(b) Multiple-grounded
(c) Solid vs braid vs spiral wrapped
(d) Conduits

Unshielded conductors: In Fig. 16.6(a) an unshielded conductor, being exposed to the full magnetic field inside the structure, will have high voltages developed across the high impedance terminations.

Types of shield: Of the different types of shield, shown in Fig. 16.6(c), the solid shield inherently provides better shielding than does a braided shield, and a spiral wrapped shield can be far inferior to a braided shield in performance. In severe environments braided shields using two overlapping courses of braid may give shielding performance approaching that of a solid walled shield.

Conduits: Conduits, shown in Fig. 16.6(d), should not be relied upon for protection against indirect effects since they may or may not provide electromagnetic shielding.

Conduits in aircraft tend to be used more for mechanical protection than for electrical protection of conductors. Only if the conduit is electrically connected to the aircraft structure will it be able to carry current and thus provide shielding for the conductors within. Conduits for mechanical protection frequently are physically mounted in clamps that use rubber gaskets to prevent mechanical vibration and wear. Such clamps, of course, insulate the conduit and prevent it from having any magnetic shielding capability.

Clearly, nonmetallic conduits will not provide electromagnetic shielding.

16.5.3 Grounding of Shields

Shield grounded at one end: The presence of a shield grounded at only one end will not significantly affect the magnitude of the voltage induced by changing magnetic fields, although a shield may protect against changing electric fields. While a shield may keep the voltage at the grounded end low, it will allow the common mode voltage on the signal conductors to be high at the unshielded end.

Shield grounded at both ends: Shielding against magnetic fields requires the shield to be grounded at both ends, as shown in Fig. 16.6(b), in order that it may carry a circulating current. It is the circulating current that cancels the magnetic fields that produce common mode voltages.

Control of lightning indirect effects almost always requires that interconnecting wiring be provided with an overall shield and that the shield be grounded at each end. This does raise conflicts that must (and can) be resolved.

Multiple ground points: There is some virtue in staggering the spacing between multiple ground points on a cable shield, since it is theoretically possible that uniform grounding can lead to troublesome standing waves if the shield is illuminated by a sustained frequency interference source. Also, the cable may be exposed to a significant amount of magnetic field over only a small portion of its total length. If the shield is multiple-grounded, the circulating currents will tend to flow along only one portion of the cable whereas, if it is grounded at only the two ends, current is constrained to flow the entire length of the cable.

Possible conflicts: The requirement that a shield intended for protection against lightning effects must be grounded at both ends raises the perennial controversy about single-point versus multiple-point grounding of circuits. For many reasons, usually legitimate, low level circuits need to be shielded against low frequency interference. Most commonly, and usually legitimately, the shields intended for such low frequency interference protection are grounded at only one end.

A fundamental concept often overlooked, however, is that the physical length of such shields must be short compared to the wavelength of the interfering signals. Lightning produced interference, however, is usually broad band and includes significant amounts of energy at quite high frequencies, frequencies higher than those the typical low frequency shields are intended to handle.

Resolution of conflict: The conflict between the practices best for shielding against high frequency, lightning produced interference and those for shielding against everyday, low frequency interference is usually too great for both sets of requirements to be met by use of only one shield system.

Most commonly both sets of requirements can be met only by having one shield system to protect against low frequency interference and a second shield system to protect against lightning-generated interference. The lightning shield can usually consist of an overall braided shield on a group of conductors with this overall shield being grounded to the aircraft structure at least at the ends. Within the overall shield may be placed whatever types of circuit are needed.

Frequently these circuits will have a shielded conductor of their own. In a coordinated shielded system the designers of individual circuits should have the option of grounding such inner shields as their own requirements dictate, but they should not have the power of dictating the treatment of the overall shield. Such an overall shield (OAS) is shown in Fig. 16.7.

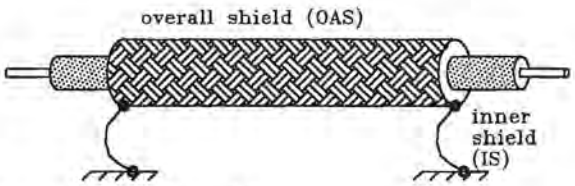

Fig. 16.7 Overall shield.

16.5.4 Ground Connections for Shields

The method of grounding an overall shield can have a great impact on its effectiveness in protecting against lightning generated interference. Figs. 16.8(a) through 16.8(e) show several methods of grounding such a shield when that shield is placed over a group of conductors being brought into an equipment case.

360 degree grounding: For best performance the OAS should be terminated on the back shell of a connector specifically designed for such termination. The shield should make a 360 degree circumferential connection to the back shell of the connector and the connector shell itself should be designed to have low dc resistance to its mating panel connector.

Most commonly, such low resistance mating requires the use of grounding fingers within the connector shell. Connectors without such grounding fingers frequently have high resistance between the mating shells, since the shells are frequently coated with an insulating coating to reduce problems of corrosion. The shell of the panel connector should also provide a 360 degree peripheral connection to the metal equipment case. Providing such a connection frequently requires that paint or other coatings on the case of the equipment be removed and the bare metal exposed.

Pigtail grounding: In the absence of a 360 degree connector, an external pigtail is often used for grounding the OAS, as shown in Fig. 16.8(b). Such pigtails are definitely inferior to the 360 degree connector because they force an interfering current on the shield to be concentrated through the pigtail, and hence provide a much greater degree of magnetic coupling to the core conductors than does the distributed flow on a properly designed connector back shell. If such a pigtail is used, it should be as short as possible and should terminate on the outside of the equipment case. A pigtail of only a very few inches in length may introduce more leakage from the shield onto the inner conductors than does a several foot section of the shield itself.

Grounding to a remote point: Cable shields should be grounded to the case upon which the connector is mounted and should not be grounded to a remote "low noise" ground point, as shown in Fig. 16.8(c)

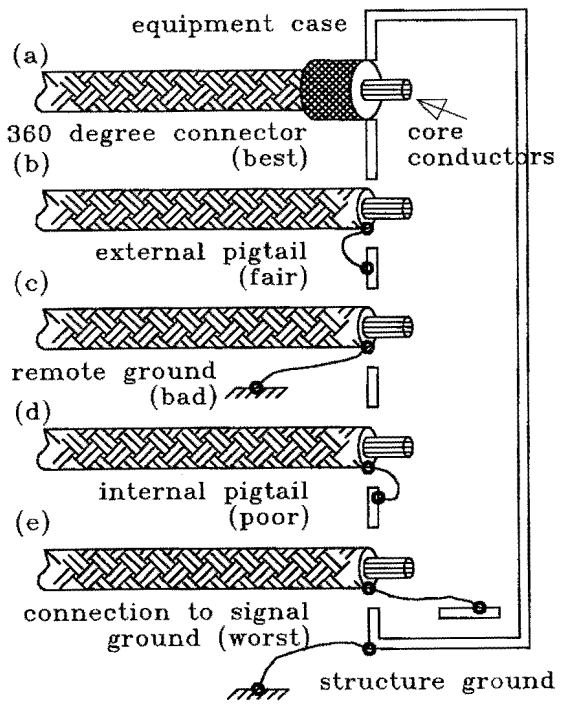

Fig. 16.8 Types of grounding for shields.

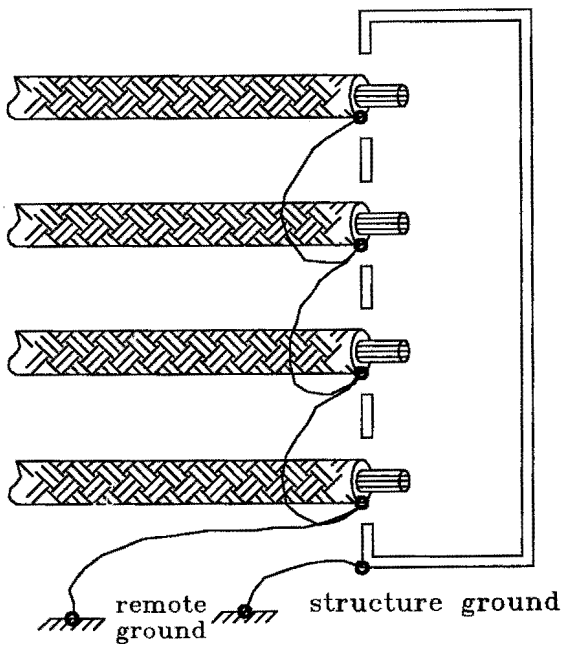

Fig. 16.9 Daisy chain grounding.

Grounding to an inside surface: Grounding an overall shield to the inside surface of an equipment case through a pigtail and a set of contacts in the connector is less effective than the use of an external pigtail, partly because the length of the pigtail is inherently longer and partly because it brings currents directly to the inside of the case. Such grounding of an overall shield should be avoided wherever possible and, in particular, must be avoided whenever the overall shield runs through a region where it will intercept a significant amount of energy from the external electromagnetic field.

Grounding to signal bus: In no case should an overall shield be connected to a signal ground bus.

Daisy chain grounding: Daisy chain grounding of cable shields, illustrated in Fig. 16.9, should never be used. It constrains current intercepted by all the shields to flow through a common path and so provides the greatest potential to defeat the purpose of the shields.

16.6 Coordination Between Transients and Specifications

Section 5.7 discussed *pass/fail* criteria in terms of *Transient Control Levels* and *Equipment Transient Design Levels, TCLs and ETDLs* while [16.1] suggests possible levels. The following material discusses the concepts in more detail.

Alternatives regarding transients: Three possible approaches to dealing with lightning induced transients are:

1. Designers of aircraft equipment ("black boxes") might be considered to have the responsibility to provide equipment that will withstand the transients that might be developed in the aircraft, whatever those transients might be.
2. Designers of aircraft wiring might be considered to have the responsibility for ensuring that transients never exceed the capabilities of terminal equipment, whatever that might be.
3. Design efforts might be coordinated so that designers of equipment would guarantee that their equipment could withstand transients of one level and designers of wiring systems would guarantee that the transients would never exceed another, and lower, level.

Transient coordination represents the third of the approaches.

16.6.1 Evolution of Transient Standards for Aircraft

Transient control level standards now coming into use for aircraft have evolved from several sources; aircraft, military and industrial.

Basic Insulation Levels: The transient control level philosophy was originally inspired by the Basic Insulation Level, BIL, or transient coordination philosophy used in the electric power field for many years [16.2]. It developed in recognition that power equipment, such as transformers would always be subjected to surges produced by lightning and that the magnitude of the surges could be known only in statistical terms. Experience had shown, however, that these surges were capable of destroying equipment and that equipment would have to be protected by surge arresters. It was also taken as axiomatic that the insulation built into equipment would have to be coordinated with the abilities of the arresters. Also, it was taken as axiomatic that it would be preferable to have standard ratings of surge arresters, coordinated to the limited number of standard ratings of operating voltages.

The transient coordination system that evolved [16.3] provided for a limited number of insulation levels, such as a 150 kV BIL level for 23 kV equipment and 550 kV BIL for 115 kV equipment. Equipment designed to operate at 115 kV was provided with insulation sufficient to withstand a 550 kV impulse and this was verified by test on each and every major piece of equipment before it was shipped.

The 550 kV represented only the level to which the designer knew the equipment would be tested in the factory and was never taken as representing the level of surges to which the equipment would be subjected in the field. All the designer needed was assurance that protective equipment was available and would be used to ensure that naturally occuring surges would be less than 550 kV by a suitable margin.

The essential elements of the BIL system thus consisted of:

1. Availability of equipment to control natural transients.
2. Standards covering equipment and practices for performing tests.
3. A limited number of standard voltage test levels.
4. Standard current test levels for surge protective devices.
5. Standard waveshapes, capable of being produced by equipment in many laboratories.
6. Agreement to perform the tests using the standard test levels and to make changes in levels only after it was agreed that improved protective equipment was commercially available.

The BIL system has been in place for many years, is recognized world wide and has resulted in electrical power equipment that is very seldom damaged by the effects of lightning.

ANSI Surge Withstand Capability Test (SWC) : Another specification that influenced development of the TCL philosophy was the ANSI (SWC) Surge Withstand Capability Test [16.4, 16.5]. The test was intended for simulation of the transients found in high voltage electrical substations when circuit breakers and disconnect switches were operated. Tests had shown that equipment in such substations might be exposed to oscillatory transient voltages of several kV in magnitude. To some extent the specification was applied to equipment of types other than those for which it was originally intended, largely because it was a specification in existence and recognized by standardizing agencies.

The document called for open circuit voltages of between 2.5 and 3 kV, with the oscillatory frequency being from 1.0 to 1.5 MHz. Decrement was specified by requiring that the envelope decay to 50% in no less than 6 μs ,though this implies a lower loss test circuit than might be found in practice. The voltage range specified was reasonable for apparatus in high voltage substations, but might be high for electronic equipment located in shielded locations.

The original intent of the test was that the specified voltages would be applied directly to the terminals of apparatus to verify that the equipment would not be damaged. Experience has shown that it is sometimes difficult to inject such voltages into circuits by transformer coupling.

The document recognized the importance of short circuit capability in that it called for a 150 ohm source impedance. The document also provided construction details of a surge generator to produce the specified wave. The recommended test generator circuit was somewhat uncontrolled, using an untriggered spark gap firing virtually at random at the crest of an ac charging voltage, though the waveform itself does not imply any particular generator test circuit.

Transients in residential wiring: Martzloff and Howell [16.6] proposed a transient voltage test with a frequency of 100 kHz and a voltage range of 0 to 8 kV. The wave was intended for the duplication of transients found in residential circuits on 120 V ac lines, for which measurements showed that transients were commonly oscillatory with frequencies measured in a few hundred kHz. The damping was specified such that the ratio of successive half-cycles should be greater than 0.6. This might be somewhat high, particularly is the transient is to be coupled into equipment through transformers.

No specification was made about the magnitude or waveshape of the short circuit current. Martzloff and Howell show a test circuit capable of injecting the transient onto 120 V ac lines where, since the output impedance of the circuit is basically 150 resistive, the shape of the short circuit current would be about the same as that of the open circuit voltage.

This waveform and this test circuit have been widely accepted in some fields. One example is in relation to ground fault interrupters [16.7].

NEMP: Test practices for simulation of NEMP effects were being developed about the time the TCL philosophy was evolving. Particularly valuable was the practice of injecting transients into conductors using transformer coupling. The waveshapes in use were most commonly oscillatory with frequencies of several MHz.

NASA Space Shuttle: The present TCL philosophy was first proposed in [16.8] and later presented in [16.9].

At one stage in the development of the *Space Shuttle Criteria Document*, there was an allowance made for two basically unidirectional transient test waves. While those test waves had some deficiencies and have been largely superseded, discussion of them is still appropriate, since that discussion will illustrate some of the problems inherent in waveform specifications.

Waveshapes for aperture effects: The first of these specifications dealt with a transient rising to crest in 2 μs and decaying to zero in 100 μs. The intent of this test wave was to duplicate in some manner the effects produced by magnetic flux leaking through apertures.

The specification gave only straight line representations of the waves, it being understood that actual test waves would have more complex waveshapes. Unfortunately, some groups misunderstood the intent of the specification and attempted to design, at great expense, pulse generators that produced triangular waves.

The *Shuttle* specification on waveforms permitted a backswing, a feature characteristic of transformer-coupled surges. The backswing amplitude was required to be less than 25% of the initial amplitude, but the duration of the backswing was left uncontrolled. The test waveform was not intended to be interpreted as requiring a backswing. An overdamped wave was perfectly satisfactory.

If an overdamped waveform was used, there would be no clearly defined time to zero. In such cases the decay time was intended to be taken as one-half the indicated value (50 μs instead of 100 μs) and measured to the time at which the wave had decayed to 50% of its initial amplitude. The waveform was thus similar to the standard ANSI test waveform derived for tests on high-voltage apparatus. The front time of 2 μs reflected the 2 μs front time of the basic lightning design current. The transients themselves were specified as having amplitudes of 50 V open circuit and 10 A short circuit.

The second specification was for a long-duration transient representing the effects produced by magnetic flux diffusing through the walls of cavities. Such flux would have rise and decay times much longer than those of the lightning current. The specification called for a short circuit current of 5 A and an open circuit voltage of 0.5 V, both taking 300 μs to reach crest and another 300 μs for decay to zero. The specification of equal times to crest and from crest back to zero is incompatible with the response of real physical elements. In practice, any waveform with a rise time of 300 μs would have a decay time longer than 600 μs.

One common deficiency of the above specification was that it did not clearly distinguish between transient voltages and transient currents, and did not satisfactorily account for the effects of transient source impedance. Both the short circuit current and open circuit voltage had the same waveshape. In practice the open circuit voltage would be of a duration shorter than that of the short circuit current.

Original TCL proposals: In the paper in which the concept of transient control levels was first presented [16.10], Fisher and Martzloff proposed a test wave that was primarily unidirectional. The open circuit voltage was characterized by a fast rise to crest and then a decay to zero in 5 μs, or greater. To allow for transformer coupling of the transient, a backswing was allowed after the transient had decayed to zero. The character of the backswing was not specified–only that its amplitude should be less than 50% of the initial amplitude.

The rationale behind this voltage waveform concept included the following aspects:

1. It should be in some measure proportional to the derivative of the magnetic field produced by a lightning current.
2. The duration of the transient should be long enough that possible failures of semiconductors would not be strongly affected by the waveshape of the transient, since, with transients of duration shorter than about a microsecond, the failure levels of semiconductors are strongly affected by waveshape.
3. The duration of the transient should be roughly comparable to the (then existing) duration of clock cycles in digital equipment.

4. The transient should include a rapidly changing phase to excite inductively coupled circuit elements.

5. The transient should be one that could be produced by and coupled to equipment by relatively simple test equipment.

Directly associated with the open circuit voltage transient was a short circuit current transient. The short circuit current was that current which would flow from a source the internal impedance of which could be represented as 50 Ω in parallel with 50 μH, Fig. 16.10(a). The test waves taken together as a set were thus more consistent than were those relating to the *Space Shuttle*. Amplitudes of neither current nor voltage were specified, since the test levels would be part of transient control level specification.

In answer to response from readers and users of the original Fisher and Martzloff paper [16.10] on the transient control level philosophy, Crouch, Fisher, and Martzloff [16.11] proposed a test wave somewhat different from the original one. The revised voltage wave, shown in Fig. 16.10(b), emphasized the oscillatory nature of the wave, rather than deemphasizing it, as did the original test wave. The front time was raised to 0.5 μs, the course of the wave after crest being defined in terms of its oscillatory frequency of 100 kHz and the decrement specified by requiring that the ratio of successive half-cycles be greater than 0.6. The voltage wave thus became nearly identical with that proposed by Martzloff and Howell.

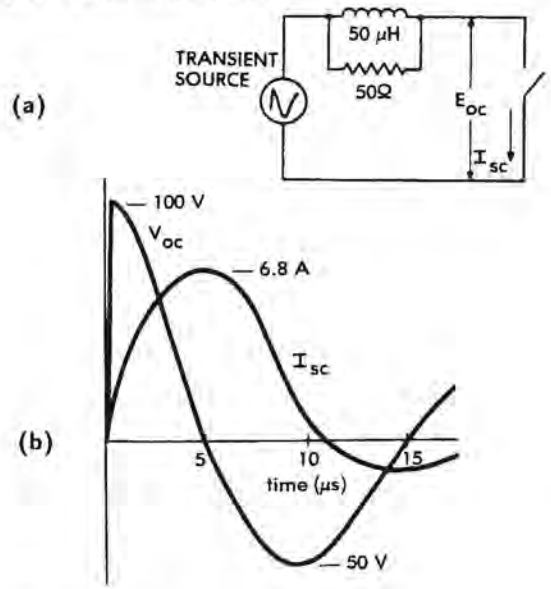

Fig. 16.10 Original TCL proposals.
(a) Source impedance
(b) Voltage and current

These papers seem to have been the first to explicitly deal with the question of source impedance in transient specifications.

16.6.2 Transient Control Level Philosophy

The TCL philosophy [16.12, 16.13] follows the basic concepts of the BIL approach to transient coordination in that targets or specifications relative to transients should be assigned both to those who design electronic equipment ("black boxes") and those who design wiring to interconnect those black boxes, rather than having things develop by chance. The levels would be assigned by a transient coordinator (Program Office) and tests would be performed to verify that the goals had been met; tests on equipment to verify that it can withstand the transients and tests on the aircraft to verify that the specified levels had not been exceeded.

The TCL philosophy is illustrated in Fig. 16.11.

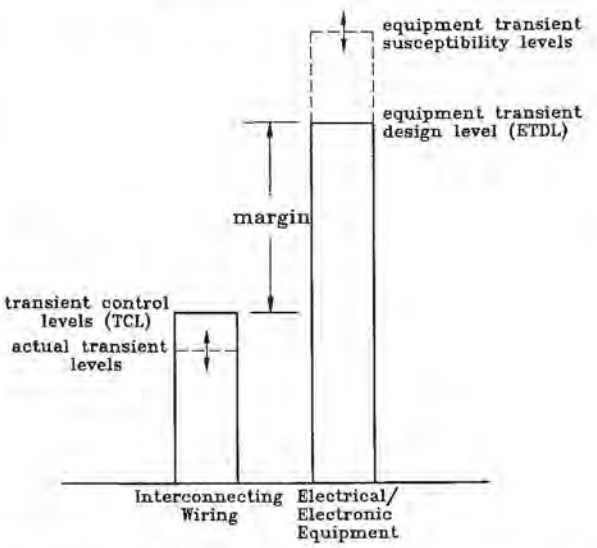

Fig. 16.11 The transient coordination philosophy.

It encompasses the following:

Actual transient level: Ensuring that the actual transient level produced by lightning (or any other source of transient) will be less than that associated with the transient control level number assigned to the cable designer. The cable designer's job would be to analyze the electromagnetic threat that lightning would present and to use whatever techniques of circuit routing or shielding would be necessary to ensure that the actual transients produced by lightning did not exceed the values specified for that particular type of circuit.

Equipment transient design level: The ETDL controlling the type of circuit or circuit protection techniques used, and assigned to the avionics designer, would be higher than the transient control level by a margin reflecting how important it was that lightning did not in fact interfere with the piece of equipment under design. A margin is necessary because any single lightning flash might produce an actual transient level higher than the assigned transient control level, which would have been derived for a predicted average in spite of the cable designer's good intentions. Prediction of actual transient levels is an imperfect art.

Vulnerability and susceptibility levels: The job of the avionics designer would be to ensure that the vulnerability and susceptibility levels of the equipment to be supplied would be higher than the assigned transient design level. The vulnerability level is that level of the transient which, if applied to the input or output circuit under question, would cause the equipment to be permanently damaged. The susceptibility level is defined as that level of transient that would result in interference with or malfunction of the equipment. The vulnerability level by definition, then, would have to be at least as high as the susceptibility level.

Ways of setting levels: Some fundamental points about the setting of levels are:

1. Levels must be compatible with the existing state of the art of providing protection by shielding and grounding of interconnecting wiring.

2. The levels must be compatible with the performance of existing surge protective devices. The minimum level of voltage to which protective devices can clamp surges is frequently several times the normal operating voltage of the system being protected.

There are several ways in which the levels might be set. In the first, the system integrator would set the desired transient level, then set the required margin, which in turn would set the transient control level. Whatever the rationale by which the system integrator sets the transient design level, that level would become a part of the purchase specifications and would, presumably, not be subject to variation by the vendor of the avionics.

As an alternative, the avionics designer might determine by suitable testing the vulnerability and susceptibility levels of his equipment and provide a guarantee as to the level of transients that his equipment could withstand. That level would then be the transient design level. After the system integrator had set the desired safety margin, the appropriate transient control level for the cable designer would have been established. One approach to the setting of margins appears in [16.8].

Open circuit voltage and short circuit current: The magnitude that would be assigned to the transient design level probably should be expressed in terms of the maximum voltage appropriate to a high impedance circuit (open circuit voltage) or the maximum current appropriate to a low impedance circuit (short circuit current).

Test levels: In order for the TCL philosophy to have most impact, there should be a limited number of levels. One set of levels that has been proposed [16.12] is shown in Table 16.1. With each level there was associated an open circuit voltage and a short circuit current; the two being related by the transient source impedance shown in Fig. 16.10 [16.12].

Table 16.1 Possible Transient Control Levels

Level Number	Open Circuit Voltage Level (volts)	Short Circuit Current Level (amperes)
1	60	2.2
2	150	5.4
3	300	11.
4	600	22
5	1500	54
6	3000	110
7	6000	220

Source impedance: If impedance is not defined in transient specifications there is the risk of a specification being worded so as to require that a specified voltage be developed regardless of the character or impedance of the object under test. A specification that can be taken, rightly or wrongly, as requiring that a test voltage of 1000 volts must be developed across a spark gap that flashes over at 500 volts and shorts an input surge to ground is clearly deficient. Likewise, a specification that can be read as requiring that a specified current be developed, regardless of impedance, is deficient.

Transient test specifications for aircraft and electronic equipment usually avoid such problems by defining both open circuit voltage and short circuit current. The intent is that if a circuit has a high impedance it is appropriate to define the voltage that should be developed and if the circuit is low impedance it is appropriate to define the maximum surge current.

If only voltage is defined, and not current, situations can arise in which design and test effort is totally wasted. An example might be for designers to place impedance in series with a spark gap so that, by brute force and the flow of enormous current, a specified voltage can be developed across a protected circuit. Such an effort would be totally contrary to the purpose of using a spark gap in the first place.

Implementation of the TCL Philosophy: The TCL philosophy is still evolving, but is becoming engrained in transient design of aircraft work. FAA requirements proposed, though not yet formally adopted [16.1], include requirements for TCL testing.

Levels appropriate for aircraft: Levels that have been suggested for aircraft use are shown in Tables 16.2 and 16.3. Table 16.2 relates to tests using single transients while Table 16.3 relates to tests using bursts of transients.

Table 16.2

Suggested ETDL Voltage and Current Levels

Level	Waveforms			
	2	3	4	5
	Vp/Ip	Vp/Ip	Vp/Ip	Vp/Ip
1	50/10	100/4	50/10	N/A
2	125/25	250/10	125/25	N/A
3	300/60	600/24	300/60	300/100
4	750/150	1500/60	750/150	750/1000
5	1600/320	3200/128	1600/320	1600/3000 to 20,000

V_p is the peak open circuit voltage in volts.

I_p is the peak test limit current in amperes.

Waveforms: The waveforms of voltage and current actually coupled to the internal structure and wiring of an aircraft are complex and depend on both the coupling mechanism and the type of circuit. The TCL philosophy recognizes, however, that they can be separated into several distinct categories and that their impedance depends on the coupling mechanism. The waveforms specified in FAA and evolving international standards [16.1 and 16.13] are shown in Fig. 16.12.

Waveform 1 is a double exponential, unipolar current waveform similar in shape to the defined lightning return stroke current (Component A). This waveform represents that portion of the lightning current that would flow in internal conductors, such as cable shields and conduits. Within certain structures this waveform will slow down and take on the appearance of current Waveform 5, described below.

Table 16.3

Suggested Multiple Burst Test Levels

Level	Waveform 3	
	Vpeak	Ipeak
2	125	5
3	300	12
4	750	30
5	1600	64

Vp = Peak Open Circuit Voltage
Ip = Peak Short Circuit Current

Waveform 2 is a double exponential derivative voltage waveform and is the classic open circuit response to the magnetic field produced in and around the aircraft during a lightning flash. This waveform is similar to the derivative of the lightning stroke current (Component A) and has a time to zero crossing equal to the time to peak of current Component A. Waveform 2 predominates in unshielded circuits with high impedance loads where magnetic field coupling is the major contributor.

Derivative voltage waveshapes can also appear in some shielded circuits, but the time to zero crossing will be controlled by the time to peak of the shield current, not the external lightning current. The short circuit current related to this voltage waveform will be similar to Waveform 1, or to the waveform of the related shield current.

Waveform 3 is a damped sinusoidal voltage waveform and is one of the responses to the lightning stroke currents, Components A and D. It is the only response to the multiple burst current, Component H. The predominant frequencies are often associated with the natural resonances of the aircraft, but may also be associated with resonances of aircraft apertures, aircraft wiring, shield terminations (pigtails) or circuit interfaces.

The defined frequencies for this waveform lie in the range of 1 to 50 MHz. Short circuit currents are typically related to this voltage waveform by the surge impedance of the aircraft circuit.

Waveform 4 is a double exponential, unipolar voltage waveform and represents the potential differ-

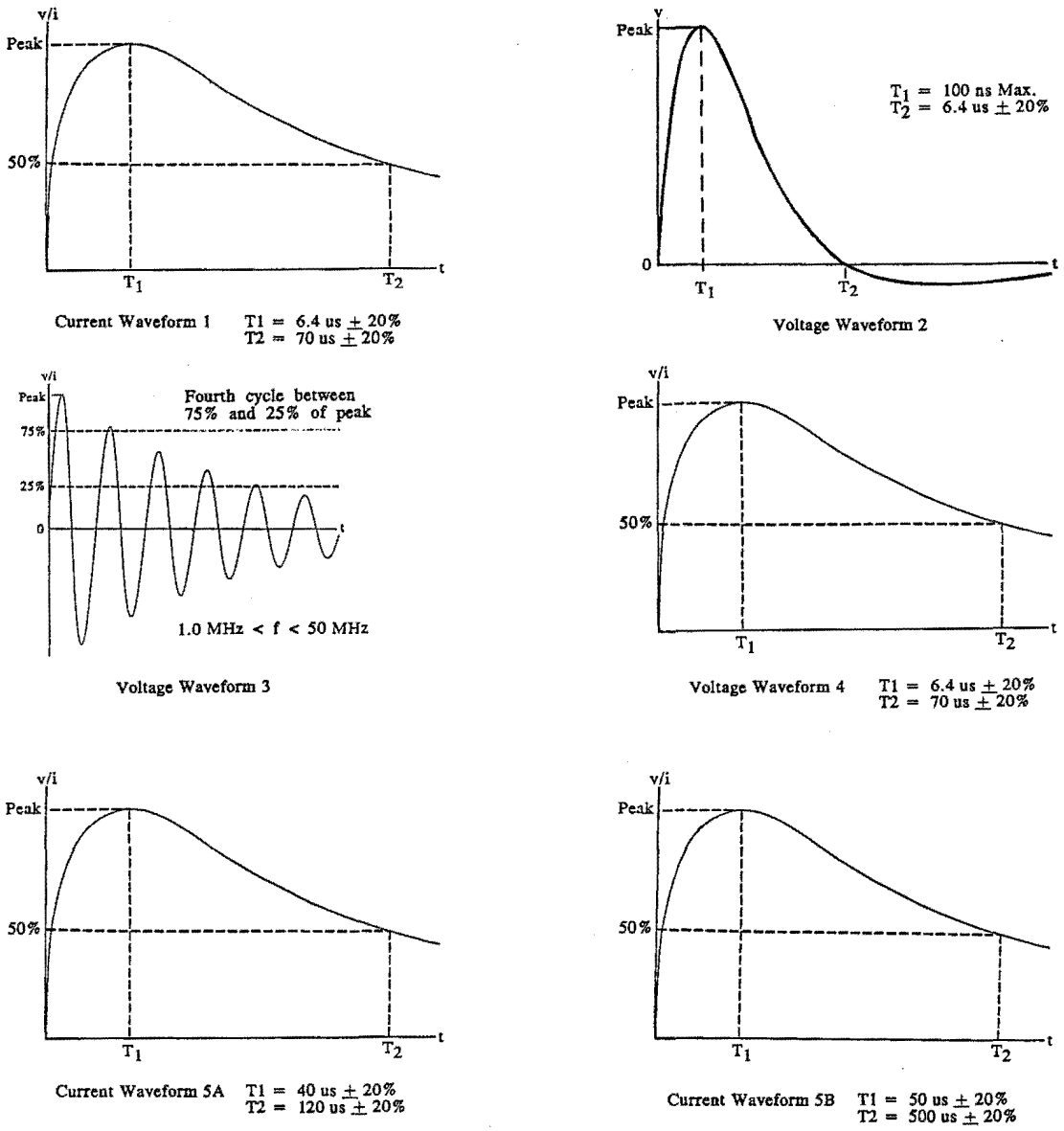

Fig. 16.12 Waveshapes for aircraft.

ences that can appear between interconnected equipment ground references when lightning current flows through the intervening resistance of the airframe structure. This waveform has the same waveshape as the lightning stroke current, Component A, and predominates in high resistance airframe structures where circuits use the airframe as return.

Waveform 4 is also typical of voltages that appear in shielded conductors because of current flowing through the shield resistance. The short circuit current related to this voltage waveform is Waveform 1. However, as the line-to-ground impedances of a conductor and its loads approach a short circuit, the conductor inductance and diffusion and redistribution currents tend to produce the longer duration current Waveform 5.

Waveform 5 is a long duration, double exponential, unipolar current waveform of the type found on most low impedance conductors within an airframe and results from the diffusion and redistribution of currents through shield boundaries formed by the surrounding airframe structure, shields and nearby conductors. This waveform is particularly prevalent when the airframe is constructed primarily of carbon fiber

composite (CFC). Because of their long duration, the distribution of these currents among the various airframe conductors are primarily controlled by the resistance of the conductors, rather than by their inductance.

The source impedance associated with Waveform 5 will tend to approach the dc resistance of the structure or shield across which the driving voltage is developed and may be as low as a few milliohms. Aside from the high energy content, the major concern in airframe wiring with this current waveform is that the accompanying voltages are sometimes insufficient to activate suppression devices and allow the current to be diverted away from paths where it may cause damage.

Waveform 5A is typical of the currents developed in low impedance conductors ($\ll$ 5 ohms) such as shields, power wires or other circuits with suppression devices at both ends. Current amplitudes associated with Waveform 5A will tend to be low to non-existent inside of an all metallic fuselage, but could be quite high on equipment with interfaces subject to a direct lightning strike, such as lights, antennas, and various pressure and temperature probes.

Waveform 5B occurs in much the same manner as Waveform 5A, but is observed more often in conductors within CFC structures because of the higher currents that result from resistive sharing with the structure. Current amplitudes associated with Waveform 5B will tend to be very high in CFC structures. Amplitudes may be hundreds of amperes in smaller gauge conductors, such as power and low impedance signal wires, and thousands of amperes in the larger gauge conductors, such as shields and power buses.

Multiple stroke waveforms: Simultation of the effects of the multiple stroke lightning currents defined in §5.5.6 involves applying one of the internal airframe waveforms to the operating system under test. Each pulse of the multiple stroke flash is represented by the selected internal waveform, which is scaled to represent the peak amplitude induced by the appropriate lightning components A and D/2. In some situations, more than one of the internal waveforms may be required to satisfy the system design requirements for multiple stroke.

Multiple burst waveforms: Practices regarding simulation of the effects of the multiple burst lightning currents defined in §5.5.6 are still evolving. The trend is toward using the damped oscillatory waveform 3, but no consensus has yet developed as to what frequencies, levels and rate of application are appropriate.

Categories of equipment for various levels: What transient test level is appropriate for various types of equipment is a task for the system integrator to decide. Guidance is offered in [16.1 and 16.13].

Level 1 (I): This level would be appropriate for equipment and interconnecting wiring installed entirely in a well protected environment, such as an avionics bay enclosed in an all–metal aircraft.

Level 2 (J): This level would be appropriate where the equipment and interconnecting wiring are in a partially protected environment, such as an avionics bay enclosed in an aircraft composed principally of metal.

Level 3 (K): This level would be appropriate for equipment and interconnecting wiring installed in a moderately exposed environment, such as the cockpit or flight deck of an aircraft composed principally of metal.

Levels 4 and 5 (L and M): These levels pertain to equipment and interconnecting wiring in severe electromagnetic environments, such as aircraft of which large portions are fabricated with composite material and where no special shielding measures have been taken.

Other waveforms: The TCL waveforms discussed in [16.1 and 16.13] are not the only ones currently called for in specifications. Some of them call for damped sine waves as shown on Fig. 16.12, Waveform 3, the waveforms being defined as

$$E = E_0 \left[\epsilon^{-(\pi f t/Q)} \sin(2\pi t) \right] \qquad (16.1)$$

Frequencies range from 1 MHz to 50 MHz (or more). Source impedance is generally specified as 100 ohms resistive.

These specifications call for specific damping factors, such as $Q = 6$ or $Q = 24$, damping factors not necessarily consistent with those defined in FAA and related documents. Figs. 16.13(a) and (b) show waves with those damping factors.

16.7 Common Problems in Specifications

Since transient specifications and techniques for controlling transients are still evolving there are situations where specifications are poorly worded or improperly applied.

A common error is to call for tests to be made on equipment within the aircraft at levels that are only appropriate for equipment located on the outside of the aircraft and exposed directly to a lightning flash. Most commonly this situation arises through misappli-

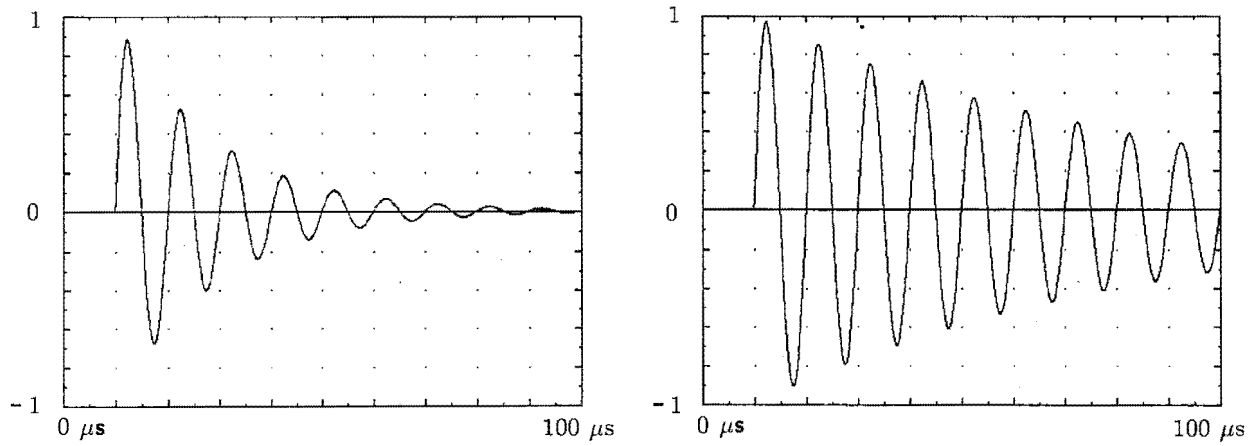

Fig. 16.13 Damped oscillatory waves.
($E_0 = 1, f = 100Khz$)
(a) $Q = 6$
(b) $Q = 24$

cation of *Test Method TO5* of *MIL-STD-1757A*[16.14]. The test method is titled *Indirect Effects - External Electrical Hardware.*

The test method calls for current Component E to be applied in order to check for magnetically induced effects, Component E being defined in [16.14] as a "fast rate of rise stroke test for full sized hardware". The specified waveform has a peak amplitude of 50 kA and a rate of rise of at least 25 kA/μs. The test method also calls for application of the high current waveforms specified in test method *TO2* for evaluation of direct effects. Those are the waveforms that have a peak amplitude of 200 kA and are intended to duplicate the effects of a lightning flash that directly contacts the exterior of the aircraft.

The references to **External Hardware** and to **full sized hardware** should be emphasized. Equipment on the inside of an aircraft is not exposed to such currents. There is no justification for performing such tests on (for example) a small metal box deep inside the structure of the aircraft and whose only function is to mount several electrical connectors and provide a way to distribute wires in several cables.

REFERENCES

16.1 *Protection of Aircraft Electrical/Electronic Systems Against the Indirect Effects of Lightning*, Report of SAE Committee AE4L, Revision A, October 1988.

16.2 A. C. Monteith, H. R. Vaughan and A. A. Johnson, "Chapter 18 – Insulation Coordination," *Electrical Transmission and Distribution Reference Book*, Westinghouse Electric Corp., East Pittsburg, PA, 1950.

16.3 *Standard Basic Impulse Insulation Levels, A Report of the Joint Committee of Insulation*, AIEE, EEI and NEMA Publication No. H-8 or NEMA Publication No. 109, *AIEE Transactions*, 1941.

16.4 ANSI C37.90a–1974 (IEEE Std 472–1974), "Guide for Surge Withstand Capability."

16.5 IEEE Static Relay Surge Protection Working Group, "Interim Report Static Relay Surge Protection," *IEEE Conference Paper C-72 033-4.*

16.6 F. D. Martzloff and E. K Howell, "Hi–Voltage Impulse Tester," *75 CRD 039*, Corporate Research and Development Center, General Electric Company, Schenectady, NY, March 1975.

16.7 *Proposed Requirements for Surge Tests on Ground Fault Circuit Interrupters*, Underwriters Laboratories Inc. Melville NY, July 1975.

16.8 *Space Shuttle Lightning Criteria Document*, JSC-07636, Revision A, NASA, Johnson Space Center, Houston, TX, November 4, 1975.

16.9 M. S. Amsbary, G. R. Read and B. L Giffin, "Lightning Protection Design of the Space Shuttle," *Workshop on Grounding and Lightning Protection*, Florida Institute of Technology and Federal Aviation Administration, Melbourne, FL, 6-8 March 1979.

16.10 F. D. Martzloff, F. A. Fisher, "Transient Control Level Philosophy and Implementation: I - The Reasoning Behind the Philosophy, II - Techniques and Equipment for Making TCL Tests," Second EMC Symposium, Montreux, June 1977.

16.11 K. E. Crouch, F. A. Fisher, F. D. Martzloff, "Transient Control Levels: A Better Way to Voltage Ratings in Power Converter Applications," *76CRD154*, Corporate Research and Development Center, General Electric Company, Schenectady, NY, July 1976.

16.12 F. A. Fisher, F. D. Martzloff, "Transient Control Levels: A Proposal for Insulation Coordination in Low–Voltage Systems," *IEEE Transactions on Power Apparatus and Systems*, PAS-95, No. 1, pp. 120-129, Jan/Feb. 1976.

16.13 "Environmental Conditions and Test Procedures for Airborne Equipment," Proposal for EUROCAE DO 160 C, Eurocae meeting 6 April, 1989.

16.14 *Lightning Qualification Test Techniques for Aerospace Vehicles and Hardware*, MIL–STD-1757A, 20 July 1983.

Chapter 17

CIRCUIT DESIGN

17.1 Introduction

This chapter deals on a circuit level with some of the factors involved in minimizing damage and upset of avionic equipment and will offer, where possible, examples of good and bad practice. Two subjects are treated in detail; surge protective devices and component damage analysis.

In general, practices good for control of lightning indirect effects and for control of steady state electromagnetic interference (EMI/EMC) are similar and what is good for one is good for the other. There are conflicts, however, some more apparent than real, and it does not necessarily follow that a design proven to be satisfactory for control of steady state EMI, or that meets other standards for EMC will be satisfactory for control of lightning indirect effects.

17.2 Signal Transmission

Most problems involving indirect effects originate with the coupling of lightning energy into the wiring of the aircraft with direct induction into the cases of LRUs running a far distant second. Proper choices about signal transmission help eliminate such problems. Basic considerations about circuit design and signal transmission are shown in Figs. 17.1 – 17.7.

Aircraft as a signal return: First, as shown on Fig. 17.1, signal circuits should avoid the use of the aircraft structure as a return path. If the structure is used as a return path, the resistively generated voltage rises will be included in the path between transmitting and receiving devices.

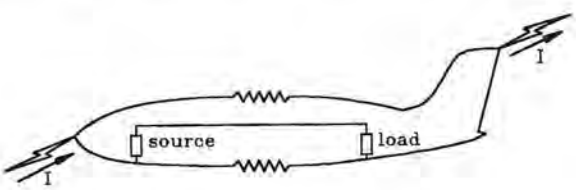

Fig. 17.1 Structural IR voltage.

Power circuits frequently use the airframe as a return path. With metal aircraft, experience has shown this to be generally satisfactory, but provisions should still be taken to ensure that lightning induced voltages on the power circuits are controlled within acceptable limits, possibly with the aid of voltage limiting devices, as discussed in §17.4.

On aircraft fabricated with poorly conducting composite materials, power return through the airframe should be avoided. A separate return wire should be used.

Single ended transmission: If single ended transmission over a shielded wire is used, with the shield used as a return path, Fig. 17.2, any noise current flowing in the shield will produce a voltage that adds to the signal voltage. Having the shield grounded at each end allows noise currents to flow and it is for this reason that wire shields are often grounded at only one end. Lightning current in the structure of the aircraft would be one source of noise current and could result in large voltages being coupled into the signal circuit in the event of a lightning flash.

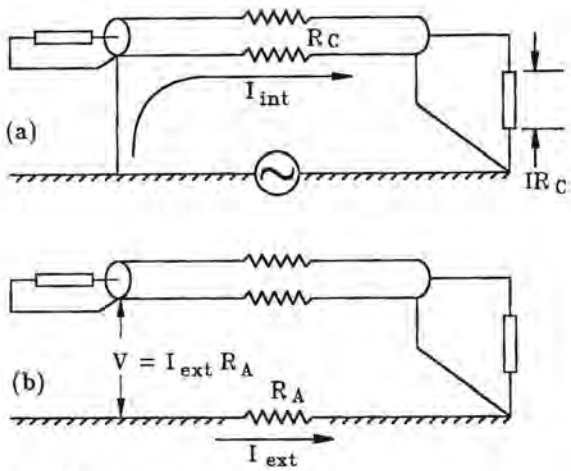

Fig. 17.2 Single ended transmission.
(a) Generation of error voltage
(b) Generation of common mode voltage

Grounding the shield at only one end, however, does not solve all the lightning problems because excessive voltage can still appear between the ungrounded end of the shield and the adjacent ground

system. Grounding at both ends removes the voltages to ground, but allows noise currents to flow in the shield and allows circuit voltages to develop. Which represents the greater hazard, common mode voltages or circuit voltages, depends on the circumstances of individual cases.

Two ways to resolve the dilemma are shown in Fig. 17.3. One way is to limit the voltage on the ungrounded end with a surge protective device, leaving the shield, in effect grounded at only one end for normal operation and grounded at both ends when lightning current flows. This does subject the circuit to temporary error voltages when lightning current flows, but the risk of permanent damage from high common mode voltages is reduced.

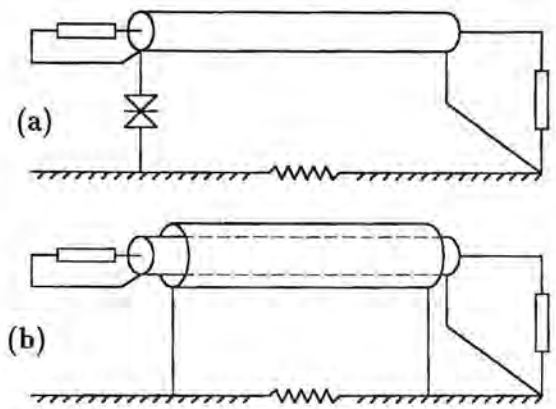

Fig. 17.3 Elimination of common mode voltage.
(a) Surge suppression device
(b) Overall shield

A better method of minimizing error voltages is to cover the signal shield with an overall shield grounded at each end. This minimizes both circuit and common mode voltages. It also separates the functions of providing for lightning protection and providing for noise free transmission under normal circumstances. The overall shield must, of course, be grounded at both ends.

Twisted pairs: Signal transmission over a twisted–pair circuit with signal grounds isolated from the aircraft structure, Fig. 17.4, tends to couple lower voltages because the resistive rise in the shield is not in the signal path. It must not be forgotten, however, that the use of twisted-pair transmission lines does not eliminate the common–mode voltage to which electronic systems may be subjected. That voltage is minimized only by grounding the shield at both ends.

Differential transmission and reception: Differential transmission and reception devices, used along with twisted pair wires, as shown in Fig. 17.5, allow the shield to be grounded at both ends since residual noise voltages produced by current in the shield is rejected.

Junctions with semiconductors: In general it is preferable that wiring interconnecting two different pieces of electronic equipment not interface directly with the junctions of semiconductors, as shown in Figs. 17.6(a).

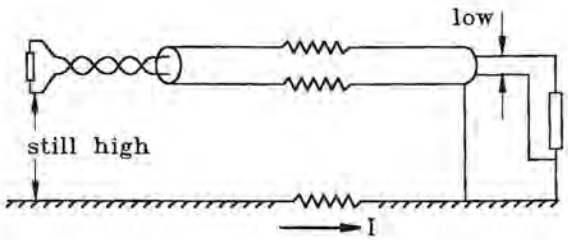

Fig. 17.4 Twisted pair transmission.

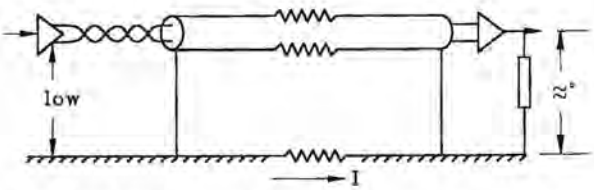

Fig. 17.5 Differential transmission and reception.

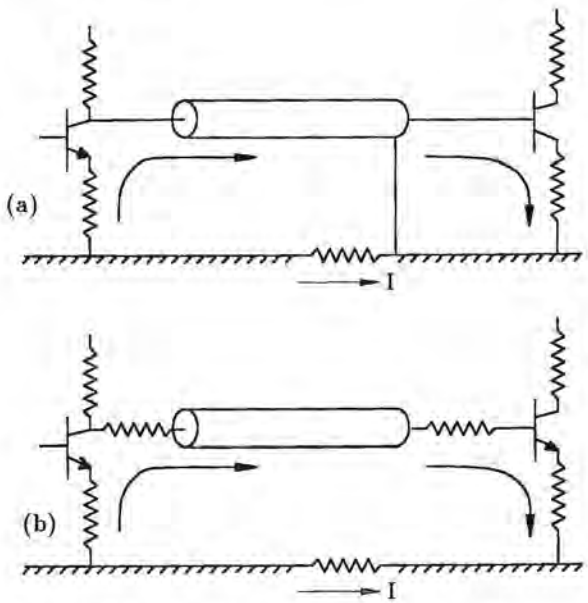

Fig. 17.6 Connection to semiconductor junctions.
(a) Direct connection - bad
(b) Current limiting resistor - good

Resistance in series with semiconductors: Where possible, resistors should be used to limit the surge current into semiconductor junctions from input and output wires. Even modest amounts of resistance connected between the junctions and the interfacing wires, shown in Fig. 17.6(b), can greatly improve the ability of semiconductors to resist the transient voltages and currents. Section 17.5 on component damage mechanisms gives examples of the degree of improvement that may be obtained through the use of series resistors. Resistors should be as large physically as possible. Half–watt resistors are better than quarter–watt.

Transmission through balanced transmission lines and transformers, coupled with input protection for semiconductors, probably provides the greatest amount of protection against the transients induced on control wiring.

DC coupling: Where possible, coupling that can pass dc should be avoided. AC transmission through isolation transformers offers one means of avoiding dc coupling paths and isolation via optical isolators is another. Optical isolation is particularly appropriate for digital circuits, but optically isolated operational amplifiers are available where analog signals must be transmitted.

DC coupling paths in power supply circuits can employ DC–DC converters using an intermediate isolation transformer.

Fiber optic transmission: Fiber optic transmission lines do not intercept lightning induced voltages or currents, but transmitting and receiving equipment at the ends could be susceptible to interference or damage.

17.3 Circuit Bandwidth

One of the most important considerations in the control of lightning–related interference through proper circuit design lies in the fundamental observation that a device with a broad bandwidth can intercept more noise energy than can a narrow bandwidth device. Some of the considerations that derive from this observation are shown in Fig. 17.7. The noise produced by lightning has a broad frequency spectrum. Considering for the moment only the spectrum of the lightning current, the observation is frequently made that most of the energy associated with the lightning current is contained in the low-frequency region, below 10 or 20 kHz.

Before any sense of security is derived from that observation, it should be remembered that equipment is damaged or caused to malfunction in accordance with the total amount of energy intercepted. In a lightning flash there may be plenty of energy left in the megahertz and multimegahertz region to cause interference. The energy that is available for damage or interference may well be concentrated in certain frequency bands by the characteristic response of the aircraft or the wiring within the aircraft.

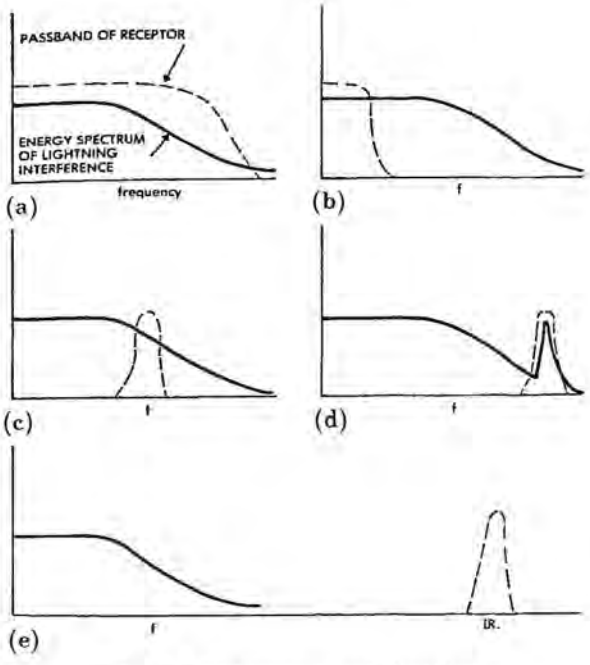

Fig. 17.7 Frequency considerations.

Without reference to any specific frequency regions, however, the energy spectrum of the lightning generated interference on electrical wiring within an aircraft will still be a broad spectrum. A receptor with a broad pass band, shown in Fig. 17.7(a), will inherently collect more energy than will a receptor with narrow pass band, shown in Fig. 17.7(b). The narrower the pass band, the better. In this respect analog circuits have an inherent advantage over digital circuits, since a narrow–pass band digital circuit is almost a contradiction in terms. If possible, circuits should not have a pass band that includes dc, shown in Fig. 17.7(c), because, when dc is excluded, the circuits will inherently be able to reject more of the energy associated with the flow of current through resistance of the structure.

Typical oscillatory frequencies: The studies of types of interference produced in aircraft by the flow of lightning current have shown that the lightning energy excites oscillatory frequencies on aircraft wiring, particularly if the wiring is based on a single–point ground concept. Those characteristic frequencies have tended to be in the range of several hundred kilohertz to a

few megahertz. If at all possible, the pass bands of electronic equipment should not include these frequencies, as does the hypothetical pass band shown on Fig. 17.7(d). Higher or lower pass bands would inherently be better than the one shown. As an extreme example, shown in Fig. 17.7(e), fiber optic signal transmission operating in the infrared region avoids the frequency spectrum associated with lightning–generated interference almost completely.

17.4 Protective Devices

Circuit protective devices can sometimes be used to limit the amount of electrical energy that a wire can couple into a piece of electronic equipment. While one can seldom eliminate *interference* through the use of the circuit protective devices, circuit protective devices judiciously used can virtually eliminate *physical damage to* electronic devices. *Judicious use* usually means that protective devices must be incorporated into a piece of equipment at the time it is built, not added after trouble has been experienced.

Basic types of protector: There are two basic types of overvoltage or transient protection device; switching devices and non-linear devices, having V–I characteristics as indicated on Fig. 17.8.

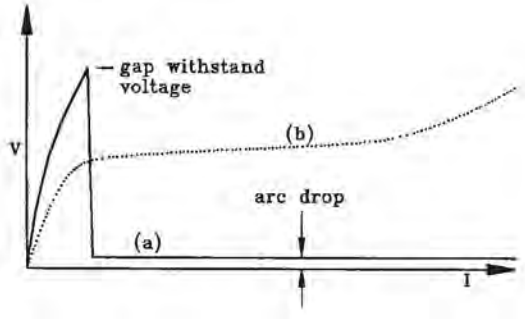

Fig. 17.8 V–I characteristics of protective devices.
(a) Switching device
(b) Non–linear resistor

Switching devices: Switching devices, Fig. 17.8(a), conduct essentially no current until the voltage across them reaches a critical value, at which time the voltage collapses to nearly zero and current is controlled by the external circuit. Examples are spark gaps and controlled rectifiers.

The instantaneous power dissipated in a transient protective device is the product of the surge current flowing through the device and the voltage across the device. Thus, even though the surge current through a conducting spark gap may be high, the power dissipated in the gap will be small.

Spark gaps and other switching devices do not control surges by absorbing the energy of the surge. Primarily they operate by reflecting surge energy back towards its source, where it may be dissipated in the resistance of the conductors.

Non–linear devices: Non–linear devices have V–I characteristics as shown in Fig. 17.8(b). They conduct very little current at low voltage levels, but once conduction begins, the voltage across the device remains fairly constant. Examples include Zener type surge suppression diodes and metal oxide varistors, MOV's. Because the voltage does not collapse to zero, energy is released in the device and the rating of the device will be governed by the amount of energy, the thermal mass and the allowable temperature rise of the device. Non–linear devices control surges partly by turning electrical energy into heat and partly by reflecting it back towards its source.

For a given surge-power handling capability, a spark gap will thus be smaller physically than a surge suppression diode or varistor device.

Recovery characteristics: Another fundamental difference between switching devices (spark gaps) and non–switching devices (surge suppression diodes or varistors) relates to their recovery characteristics after the surge has passed. If a line is protected by a spark gap and if that line is connected to a source of energy (a power bus, for example), that energy source must be disconnected from the line before the spark gap can switch back from its low–impedance conducting state to its high-impedance nonconducting state. Generally this requires opening a circuit breaker on the line. A surge suppression diode or varistor effectively ceases to conduct as soon as the voltage returns to its normal value. Operation of remote circuit breakers is not required.

Circuit interrupters: There are also devices which, on sensing an overvoltage, interrupt the power flow to the load. If this interruption is accomplished by electromechanical means, they should not be considered transient protection devices because they are inherently slow to respond. None of them will be discussed in this section.

Reflection of energy: All types of overvoltage protection devices inherently operate by reflecting a portion of the surge energy to its source and by diverting the rest into another path, all with the intention of dissipating the surge energy into the resistance of the ground and interconnecting leads. The alternative to reflecting the energy is to absorb the surge energy in an unprotected load. Reflection and diversion of the surge energy are not without their hazards:

1. The reflected energy can possibly appear on other unprotected circuits.

2. Multiple reflections may cause the transient to last longer than it would otherwise.

3. The spectral density of the energy in the surge may be changed, either high or low frequencies being enhanced. Interference problems on other circuits may well be increased even though the risk of damage to the protected circuit is reduced.

Locations for protective devices: Most commonly the appropriate type of transient protective device to be used depends on the amount of surge energy to be dealt with. Generally, this energy decreases the further away one gets from the stroke. The surge energy to be expected can also be related crudely to the normal operating power of the circuit involved. One would normally expect lower surge levels on low–voltage signal circuits than on medium–power control circuits, and even lower levels than those on main power distribution buses. Thus, one might logically use surge suppression diodes on individual circuit boards, varistors on terminal boards, and spark gaps on leads running to prime entry and exit points.

Circuit protective devices that are suitable for aircraft applications and are commercially available include gas–filled spark gaps, specially fabricated Zener diodes, and varistors. Each type has both advantages and disadvantages.

17.4.1 Spark Gaps

Incidental spark gaps: Sometimes spark gaps are incidental to the construction of some other device, terminal boards and connectors being examples. Whenever the voltage on the terminals becomes sufficiently high there will be a spark across or through the dielectric and the voltage on connected devices will be limited. Generally such sparkover is unplanned and undesirable, particularly if it causes puncture and permanent failure of solid dielectric, but the existence of such incidental spark gaps should be recognized. Sparkover across the surface of a dielectric might be allowable and sometimes can be made to provide perfectly acceptable surge protection at minimal extra cost.

Intentional spark gaps: Usually, though, spark gaps are composed of two metal electrodes separated by a dielectric, held at a fixed distance from each other and sealed in a container. Electrodes may be spherical, but in sophisticated devices they are not. Not all spark gaps use metal elecrtodes and not all are sealed. Telephone circuits, for example, are often protected by gaps using carbon electrodes. Outline sketches of spark gaps are shown in Fig. 17.9.

Electron avalanche: Conduction through a spark gap occurs because of an electron avalanche process, as discussed in Chapter 1. Dielectric composition, gas density and electrode geometry all affect sparkover voltage and the speed with which the avalanche develops. Sparkover voltage depends on the waveshape of voltage; a surge voltage with a fast rate of change will cause sparkover at a higher voltage than would a more slowly rising wave. A low pressure gap (low gas density more exactly) will sparkover at a lower voltage than will a similar high pressure gap, but the avalanche will develop more slowly, and the dependence of sparkover voltage on waveshape will be greater.

The dependence of sparkover voltage on rate of change of voltage partly relates to how long it takes, on average, for a free electron to appear and start the avalanche process. Commercially available spark gaps frequently contain minute amounts of tritium or other radioactive elements to reduce the dependence of sparkover voltage on voltage waveshape.

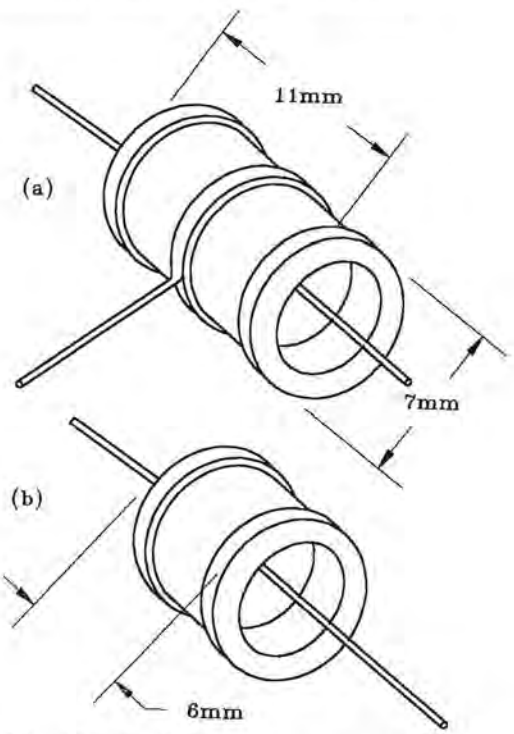

Fig. 17.9 Outline sketches of spark gaps.

Sparkover voltage: Impulse sparkover voltages for gaps with metal electrodes operating in air at standard atmospheric pressure will seldom be less than 1 – 2 kV, even with very small spacing between the electrodes. For commercial spark gaps, curves, such as

Fig. 17.10, are generally supplied to relate sparkover voltage to rate of change of voltage. Catalog specification sheets generally cite the sparkover voltage for very slowly changing voltages. Rated sparkover voltages for small gaps range upwards from a minimum of about 100 volts. Sparkover voltages for rapidly changing voltages may be substantially higher.

Normally, one should not consider spark gaps as the primary means for control of surges unless the equipment to be protected can withstand several hundreds of volts.

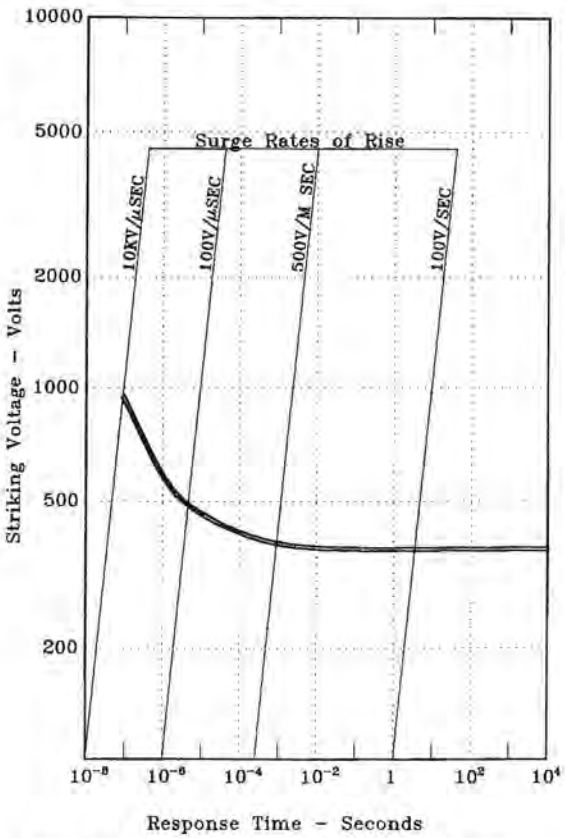

Fig. 17.10 Volt–time curve of a spark gap.

Recovery: Once a gap has sparked over, the current in the gap will be governed by the impedance of the circuit and the normal operating voltage. Current will continue to flow as long as the circuit is energized at a voltage greater than a few tens of volts. Gaps used for industrial machinery and commercial power systems can be made self–extinguishing for applied voltages up to about 100 V by using magnetic fields to blow and cool the arc, but they are not applicable for aircraft use.

Current rating: Small spark gaps generally can carry peak currents of several thousand amperes for surges lasting a few tens of microseconds and several hundreds of amperes for surges lasting a few milliseconds. Catalog sheets do not always clearly state the duration of surge current for which the specified peak current applies, but for aircraft protection the matter is of little importance since amost any gap can carry all the surge current likely to appear on internal aircraft wiring.

Spark gaps intended primarily for telephone circuits may be called upon to carry power system current for some period of time if the wires have come into contact with power lines. The allowable current, and its duration, are commonly specified by a curve, of which Fig. 17.11 is an example. Some gap assemblies are provided with thermal links which cause the circuit to be permanently shorted if current flows for an excessively long time. Such thermal links are not likely to be of value in aircraft applications.

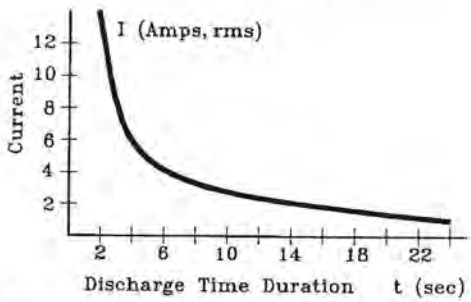

Fig. 17.11 Allowable ampere–time curve for a spark gap.

Residual voltages: Until such time as a spark gap ionizes, it has no effect on circuit voltage. Some residual surge voltage, Fig. 17.12, may be passed onto the rest of the circuit. Should this residual surge voltage be a problem it can often be suppressed with metal oxide or zener diode devices.

Fig. 17.12 Residual voltage.

Sometimes spark gaps are applied to a pair of conductors, as in Fig. 17.13(a). Ideally, in response to a common mode surge, the two spark gaps should ionize at the same time. If separate spark gaps are used, one of them may ionize before the other, resulting in a high voltage between the conductors, as in Fig. 17.13(b). To minimize this problem, three–electrode spark gaps are available. Sparkover of one half results in ioniza-

tion that spreads into the other half, simultaneously shorting the two conductors together and to ground.

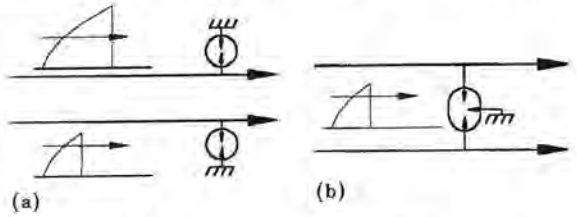

Fig. 17.13 Spark gaps on a conductor pair.
(a) Two separate gaps give high common mode voltage
(b) Three terminal gap

Application considerations: Spark gaps, and any other voltage limiting device for that matter, must be rated to withstand the normal maximum voltage expected on the circuit being protected. Provision must also be made to de–energize the circuit and allow them to regain their insulating properties. On power circuits, this is most commonly done with fuses that are blown or circuit breakers that are tripped by the system current that flows once the gap has been caused to spark.

For protection of semiconductors and electronic circuit boards, spark gaps may not be the most effective type of protective device. In particular, it is not advisable to place them directly on circuit boards in close proximity to sensitive semiconductors since they spark over at relatively high voltages and upon sparkover may be called upon to carry high currents. The further these high currrents can be kept away from the sensitive equipment the better.

Spark gaps might best be considered as the first line of defense against high energy surges, placed well away from the most sensitive equipment, and used in conjunction with devices that have lower voltage clamping levels, but less ability to carry high surge currents.

Failure mode: Most commonly, failure of a spark gap, either because of excessive surge current or because of excessive power system current following sparkover, will either shatter the case or burn away the connecting leads, causing the gap to fail open circuit.

Advantages of spark gaps:

1. Simple and reliable.

2. Low voltage drop during the conducting state, typically 10 to 20 V.

3. Large power-handling capability. Gas–filled gaps have the highest peak current handling capabilities of any transient protection device, and almost any gap can handle the maximum surge currents induced by lightning.

4. High impedance and low capacitance. The low shunt capacitance and leakage current characteristics of gas–filled spark gaps minimize insertion problems for operating frequencies below 1 GHz.

5. Bilateral operation, having the same characteristics on either polarity.

Disadvantages:

1. Relatively high sparkover voltage.

2. Power system follow current must be extinguished by removing the voltage (circuit breaker of fuse) or by inserting resistance rapidly into the circuit by an additional element, such as a zinc oxide varistor.

3. May have a large dependence of sparkover voltage on the waveshape of the voltage.

4. Reflect more energy than they absorb.

5. Rapid change of voltage on sparkover may excite circuit ringing.

17.4.2 Non–Linear Resistors

Non–linear resistors, or varistors, may be characterized by the expression

$$I = KV^N \tag{17.1}$$

where N and K are device constants dependent on the varistor material.

Varistors may be constructed of silicon carbide, selenium, or metal oxide, usually zinc oxide. This section will concentrate on metal oxide varistors, MOVs, [17.1] since in recent years they have almost completely supplanted the other materials. Zener diode type protectors can be considered as another of the non– linear resistors since their volt–ampere characteristics also follow Eq. 17.1, but since their fabrication is much different from MOVs, they will be treated separately in §17.4.3.

Formulation: Metal oxide varistors are formed from zinc oxide grains, Fig. 17.14, which, when pressed together and sintered into ceramic parts, act as though there were non–linear semiconductor junctions at the

grain boundaries. The volt–ampere characteristics of a finished part depends on the size of the grains and the number in series, which for a given formulation of the bulk material, implies that the voltage clamping level becomes directly proportional to the thickness of the finished part. Current handling capability depends on how many grains are in parallel, or for a finished part, on its area. The volt–ampere characteristic of MOVs thus derive from a bulk effect, which accounts for their large power handling capability.

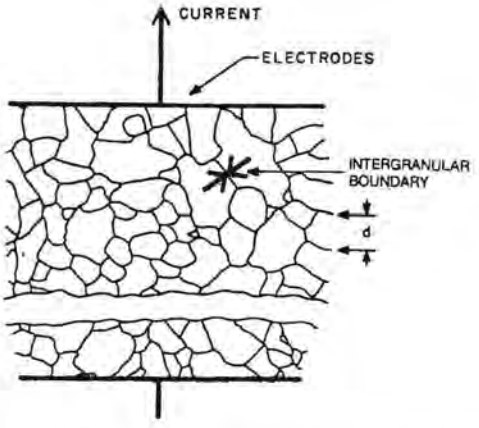

Fig. 17.14 Intergranular structure of MOV [17.1]. d is the average grain size.

Volt–ampere characteristic: The volt–ampere characteristic of a typical MOV device is shown in Fig. 17.15 and an equivalent circuit in Fig. 17.16. The V–I characteristic has three regions: very low current levels where capacitance C and leakage resistance R_{off} dominate, very high current regions where bulk resistance R_{on} becomes important and the intermediate region of normal operation.

Leakage region: At low current levels the leakage resistance is high enough, on the order of 10^9 ohms, that leakage current is often insignificant for circuits energized with dc. Leakage resistance is strongly dependent on temperature, as shown in Fig. 17.17. For high voltage applications where MOV materials are enclosed in porcelain shells and exposed to intense solar heating, leakage resistance may result in enough additional heat and temperature rise to lead to thermal runaway, but such problems are not likely in aircraft applications.

For circuits energized with ac, the effects of leakage resistance are overshadowed by the effects of parallel capacitance. Capacitance of MOV devices is fairly high, on the order of 1 - -10 nF for typical devices, nearly constant with frequency up to 100 kHz and little affected by temperature. Capacitance is not usually a problem for circuits operating at power frequencies and may even be valuable in that it helps shunt high frequency noise currents to ground. Its effects must be considered on circuits operating at high frequencies or reacting to rapidly changing pulses.

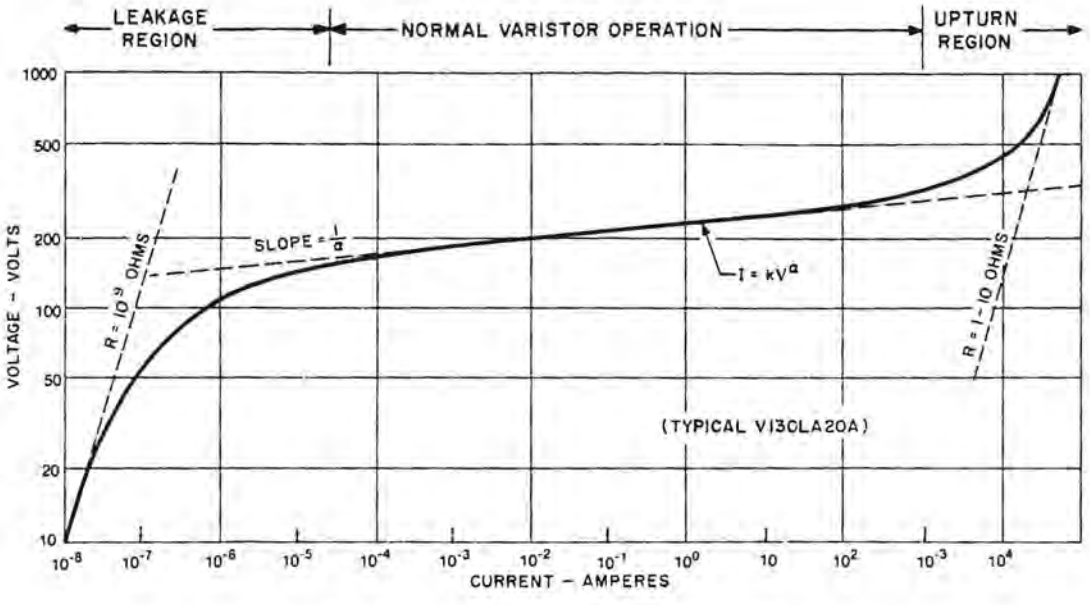

Fig. 17.15 V–I characteristic of MOV [17.1].

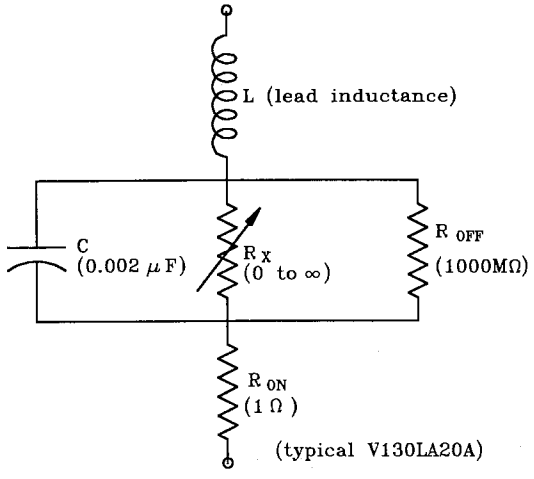

Fig. 17.16 Equivalent circuit of MOV [17.1]

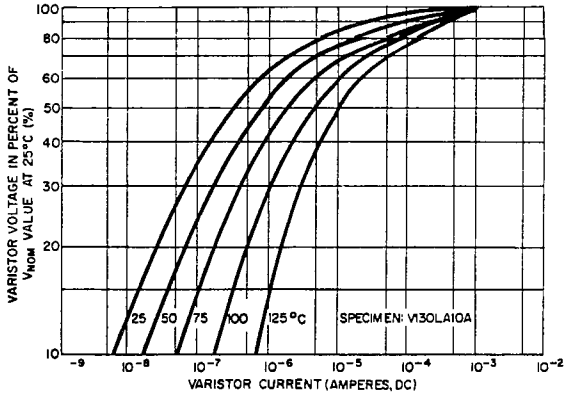

Fig. 17.17 Leakage current vs. temperature [17.1].

The capacitance of any particular MOV device may be measured with conventional bridges, providing only that the bridge voltage is not high enough to cause non–linear conduction.

Normal varistor region: In this region current is dominated by the non–linear resistor R_x having the characteristic

$$I = KV^{\alpha} \tag{17.2}$$

The exponent α is on the order of 20 – 50, implying that changing current by four orders of magnitude will result in a 25% change (or less) of voltage.

Upturn region: At high current levels, several hundreds to several thousands of amperes, bulk resistance becomes important and limits the varistor performance. Operation in this region should be avoided, either by limiting the surge current with series resistance, by using larger MOV packages or by operating MOV devices in parallel.

Waveshape dependence: Varistor performance is best discussed by treating surge *current* as the independent variable. Varistors are sometimes denigrated as having poor pulse response, or being subject to *overshoot*; that is, having excessive clamping voltage in response to rapidly changing surge currents. If a half–sinusoidal pulse of current, Fig. 17.18, is passed through a varistor, the voltage developed will be practically rectangular. A faster rising sinusoidal pulse will also produce a rectangular pulse voltage, but one of somewhat higher magnitude. The difference in voltage for slowly rising current pulses, > 10 μs, and for rapidly rising rising pulses, ≈ 0.5 μs, is seldom more than 10 – 20%. It is most noticable for large disks of MOV material than for small disks.

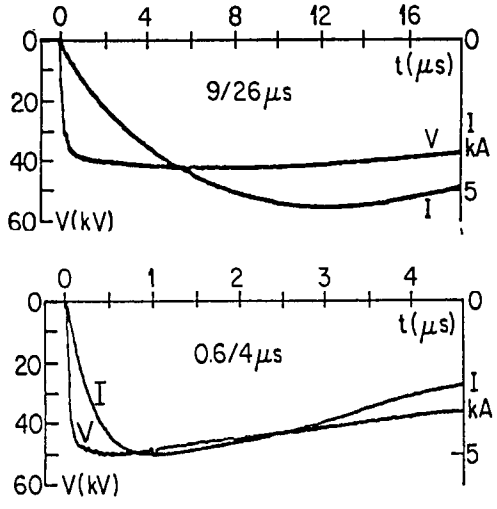

Fig. 17.18 Time dependence of MOV.
(a) Slowly changing current
(b) Rapidly changing current
Adapted from [17.3]

Studies of large MOV disks, such as are used in power transmission systems [17.2, 17.3], have shown the overshoot to be largely a matter of diffusion of current into the varistor material. Studies of small disks, such as those used for protection of low voltage equipment [17.1] have shown the time dependence of voltage to be only a few tens of percent, even for surge currents having fronts of a few nanoseconds.

The fact that surge currents of moderate steepness result in rapidly changing MOV voltages should be recognized in circuit design. Circuit oscillations resulting from the rapid change in voltage may give rise to unexpected interference problems.

Lead effects: Most instances of alleged overshoot of MOV protectors are usually due to lead inductance effects and are not really intrinsic to the varistor material. When applying MOVs, or any other surge protective device, care should be taken to keep short any leads through which high or rapidly changing currents might flow. Voltage developed across the inductance of such leads adds to the voltage developed across the varistor material. As an example, Fig. 17.19 shows two installations of MOV devices such as might be used on a 115 VAC power circuit, one using the minimum practical lead length and one with leads about 15 cm (6 in) long, along with the voltages developed by half sinusoidal current waves. For a current wave with a 10 μs front time the voltage is about the same with the two lead lengths, but for a current with a 0.5 μs front the voltage was nearly double with the longer leads.

Excessive lead length is a problem irrespective of the type of protector. Leads should always be kept as short as possible and, wherever practical, surge arresters should be treated as three terminal devices. Fig. 17.20 shows examples of good and bad practice.

Rating of MOVs: The several factors that are involved in the rating of a MOV device will be illustrated using as an example the General Electric V130LA series device, characteristics of which are shown in Tables 17.1 and 17.2 [17.1]. Similar devices are available from other vendors and the illustration should not be taken an endorsement of any particular brand of device. Application of MOVs should be based on manufacturers catalog data.

Device size: The most common packaging configuration for MOV devices is a disk with wire leads. The column listing the device size refers to the diameter of the disk. Thickness depends on the voltage rating of the device and will be given in outline drawings, but not in tables of specifications. Larger diameter disks have greater current carrying capability than smaller disks.

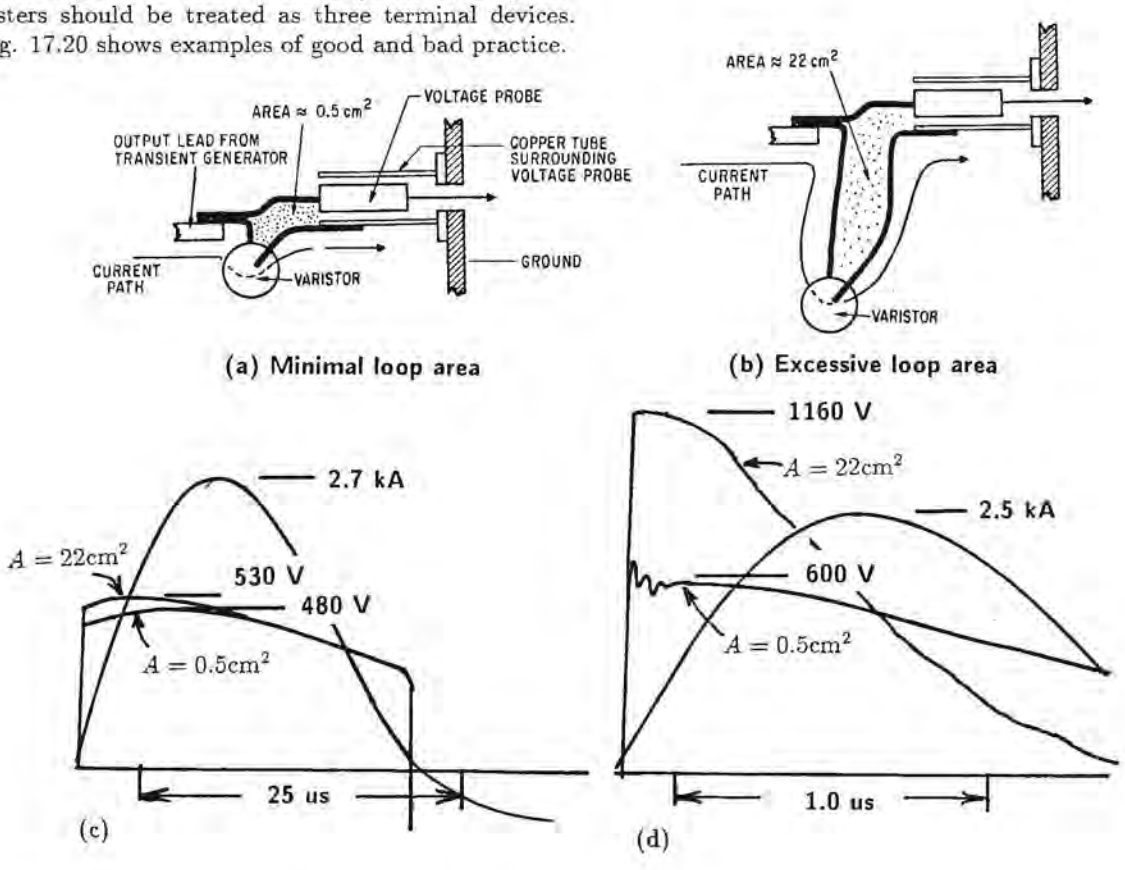

Fig. 17.19 Lead effects [17.1].
(a) Short leads (c) Current rise of 8 μs
(b) Long leads (d) Current rise of 0.5 μs

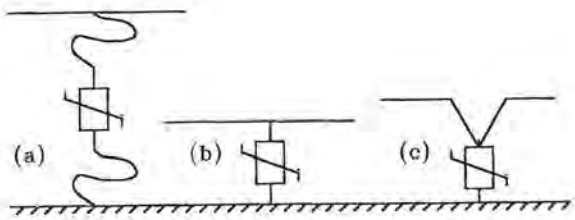

Fig. 17.20 Connections to MOV.
(a) Bad – long leads
(b) Better – short leads
(c) Best – three terminal connections

Table 17.1

Maximum Ratings for Typical 130 V Metal Oxide Varistors [17.1]

Model Number	Model Size Disc Dia. (mm)	Device Marking	Maximum Ratings (85°C)			
			Continuous		Transient	
			RMS Voltage	DC Voltage	Energy (10/1000μs)	Peak Current (8/20μs)
			$V_{m(ac)}$	$V_{m(dc)}$	W_{tm}	I_{tm}
			Volts	Volts	Joules	Amps
V130LA1	7	1301	130	175	11	1200
V130LA2	7	1302	130	175	11	1200
V130LA5	10	1305	130	175	20	2500
V130LA10A	14	130L10	130	175	38	4500
V130LA20A	20	130L20	130	175	70	6500
V130LA20B	20	130L20B	130	175	70	6500

Table 17.2

Specifications for Typical 130 V Metal Oxide Varistors [17.1]

Model Number	Characteristics (25°C)					
	Varistor Voltage @ 1mA DC Test Current			Maximum Clamping Voltage V_C @ Test Current (8/20μs)		Typical Capacitance
	Min.	$V_{N(dc)}$	Max.	V_C	I_p	f = 1 MHz
	Volts	Volts	Volts	Volts	Amps	Picofarads
V130LA1	184	200	255	390	10	180
V130LA2	184	200	228	340	10	180
V130LA5	184	200	228	340	25	450
V130LA10A	184	200	228	340	50	1000
V130LA20A	184	200	228	340	100	1900
V130LA20B	184	200	220	325	100	1900

Maximum continuous voltage: A fundamental consideration in the application of any surge protective device is that it not conduct excessively under normal operating conditions since the heat produced by continuous conduction is likely to destroy the device. Conduction must not take place even under the normally allowed excursions of operating voltage. As an example, some aircraft power systems operate at a nominal dc voltage of 28 volts, but if a regulator were to fail, voltage on the bus could go as high as 80 volts. A MOV on such a circuit would have to either be rated higher than 80 volts or would have to be fitted with a fuse or circuit breaker to disconnect it from the bus.

The V130LA devices are rated as capable of continuously withstanding 130 V-rms (184 V peak) or 175 V-dc without excessive conduction. Such a device would most likely be used on a nominal 115 V-rms ac power system. Lower voltage ratings would not be appropriate because operating voltage on a power system may temporarily be significantly higher than nominal.

RMS vs peak or dc voltage: Because MOV devices are frequently used on ac power systems, the reference to rms quantities should be noted. Other protective devices, notably zener diode based devices, are more commonly used on electronic systems and are usually rated for a nominal dc or peak ac voltage.

Transients: Two different types of maximum pulse rating are commonly supplied; the allowable energy and the maximum peak current. Peak current is defined for a surge having an 8×20 μs waveshape, a surge of the type generally used for testing of ac power equipment, as discussed in §1.5.2. The maximum allowable energy rating, on the other hand, is defined for the longer 10×1000 μs waveshape commonly used for testing of telecommunications equipment, as discussed in [17.4].

Since clamping voltage is relatively independent of surge current, instantaneous power is the product of surge current and clamping voltage. A rectangular surge current of 100 amperes, passing through a varistor clamping to 340 volts, would deliver a power of 34 000 watts. If the device were rated to withstand 70 joules (watt-seconds) then the surge could flow for 2.06 milliseconds. MOV specification sheets provide curves relating voltage and current. More precise estimates of surge energy dissipated could be made by relating instantaneous surge current to surge voltage and numerically integrating the result.

Voltage at 1 mA: Varistor voltage is commonly specified at 1 mA test current, partly because a leakage current of 1 mA is seldom cause for concern and partly because it is a convenient and easily measurable reference point for V-I curves.

Maximum clamping voltage: Catalog data commonly cites the maximum clamping voltage at a surge current appropriate to the size of the device. For more com-

plete information on V–I charactistics, curves similar to Fig. 17.15 are supplied.

Large, high energy MOV devices used for ac power systems are often rated in terms of the clamping voltage when carrying 10 000 amperes, and such devices are now becoming available for aircraft use.

MOVs in series: MOV devices of the same cross sectional area may be connected in series with no problems. They need not have the same thickness or voltage rating.

MOVs in parallel: When high energy surges must be suppressed, MOVs are sometimes connected in parallel, but care must be taken to match the V–I characteristics, as shown in Fig. 17.21. If not, one device may carry most of the surge current, defeating the purpose of using devices in parallel. Exact matching may not be necessary since by the time current becomes high enough to require parallel devices, the bulk resistance may dominate the performance and force current sharing. Use of one larger diameter disk, however, is preferable to using several small disks in parallel.

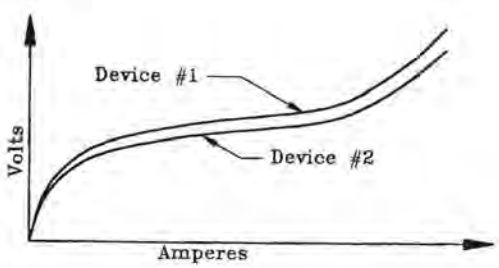

Fig. 17.21 Parallel operation of MOVs.

Wear–out: Specifications for MOV devices sometimes specify a maximum allowable number of surges of specific amplitude. This is sometimes taken as indicating that MOVs become "worn out", loose their non–linear properties and are no longer capable of protecting against surges. *This is not so.* The factor that may change after many surges is the leakage current at operating voltage. It may increase, but the MOV still retains its non–linear characteristic and its ability to protect against surges.

Turn–on voltage: Sometimes the V–I characteristics are presented on linear plots and discussions made about the "knee" of the curve or the voltage at which the MOV "turns on." Such discussions are misleading since the so– called "knee" is an artifact of the scale used for plotting current. The current is an exponential function of voltage and plotting the same function to a different current scale would indicate a different "knee." Also, discussions of "turn–on" imply a switching mechanism by which the mechanism of conduction changes from one state to another. There is no more a "switching" mechanism for an MOV device than there is for a semiconductor diode.

Failure mode: In response to a massive surge current MOV disks may shatter and fail open circuit. More commonly, they are caused to fail by excessive continuous voltage and current that fuses the disk and causes it to fail shorted. Sometimes the heat is sufficient to melt the solder holding the leads to the MOV disk and the device fails open circuit. Whether fail–open or fail–short is the preferred mode depends on the designer's preferences and requirements.

Advantages of metal oxide-based varistors:

1. Bilateral devices.
2. Small size.
3. Easily mounted. One common configuration is very similar in appearance to a disk ceramic capacitor.
4. Self-extinguishing. When applied voltage drops below the voltage for which the device is rated, they conduct very little current.
5. Inherently fast response time.
6. High power-handling capability. The current and energy handling capability is second only to certain types of spark gap. MOVs gives a higher ratio of energy absorbed to energy reflected than do conventional spark gaps. Moreover, the energy is absorbed throughout the bulk of the material and is not concentrated in a narrow P–N junction.

Disadvantages:

1. High capacitance.
2. Not too suitable for operating voltages below about 10 volts. Minimum clamping voltages are on the order of 30 volts.

17.4.3 Zener–Type Diodes

This category includes all single–junction semiconductor devices such as rectifiers, in addition to the Zener type diodes. While other semiconductor devices,

such as PNPN devices and bipolar transistors, may have application as surge arresters, they will not be covered here.

Zener diodes are basically polarized devices which exhibit an avalanche breakdown when the applied voltage in the reverse bias direction exceeds the device's specified breakdown, or Zener voltage of the device. Diodes intended for regulation of voltage can be used to suppress surge voltages, but diodes specially fabricated for surge suppression are better. These have bigger silicon junctions and more massive end caps to better dissipate heat. Some surge suppression diodes are intended only for protection against surges of one polarity and act as conventional forward biased diodes in the other direction. Others are intended for dual polarity and are effectively two diodes connected back–to–back.

The voltage across the diode does not switch to a low value when conducting, but remains at the Zener voltage. This characteristic accounts for their ability to cease conduction when the voltage falls below the Zener level, but it has a disadvantage thermally. During conduction, the power absorbed by the diode is the product of the current through the diode and the voltage across the diode. The power absorbed for constant current, thus, is directly proportional to the diode voltage.

Partially offsetting this disadvantage, however, is the phenomenon that surge energy absorbed in the diode is energy that cannot be reflected back into the system to cause trouble elsewhere.

Depletion layer: In diodes, the voltage drop takes place across the narrow depletion layer and the mass available for absorption of energy is thus very small. Heat must be conducted into the metal end caps and then dissipated through the leads of the diode. Energy handling capability of diodes is thus intrinsically less than that of spark gaps and metal oxide varistors. As a result, diode networks will not be the preferable protective device where extremely high transient current or energy is predicted. For most lightning hardening applications in aircraft, this is not a serious limitation, since the induced surge current levels are in the 1 to 100 A range at those locations where surge suppression diodes are most likely to be used.

Ratings of Zener–type diodes: Ratings of Zener–type protective devices follow a pattern similar to that discussed for metal oxide devices. The discussion that follows will be illustrated by reference to General Semiconductor diodes [17.5]. Table 17.3 refers to a line of 1500 watt bipolar devices in a DO–13 hermetically sealed package. Similar devices are available from other sources and, as with metal oxide varistors, the discussion should not be taken as an endorsement of any one product. For purposes of design, the manufacturers literature should be consulted.

Reverse standoff voltage: This specifies the voltage below which leakage current is negligible and thus corresponds to the leakage region discussed for metal oxide devices. One difference is that the quantity cited is a dc voltage, unlike MOV devices that would most likely be rated in terms of V-rms for sinewave excitation.

Breakdown voltage: This is the voltage developed in response to a test current, usually 1 mA dc, as is common with MOV devices.

Clamping voltage and peak pulse current: The allowable surges for protective diodes and MOVs are stated somewhat differently. Diodes are specified in terms of a clamping voltage at a specified current, the product of V_{cc} and I_{pp} yielding the *instantaneous peak power* of 1500 watts for which the devices are rated. MOVs are rated in terms of *total deposited energy*. For both protective diodes and MOVs the specified current wave has the 10×1000 μs waveshape specified in [17.4].

Instantaneous powers higher than 1500 watts may be dissipated if the duration of the surge current is less than 1 ms. Other product lines have higher power ratings.

When conducting, the voltage and current of a protective diode are related in the same manner as with MOVs;

$$I = kV^{\alpha} \tag{17.3}$$

The exponent α for protective diodes is in the range 100 – 500, higher than the comparable figure for MOVs. The clamping voltage for protective diodes is thus more nearly constant with surge current than for MOVs.

Capacitance: Surge suppression diodes have a high capacitance, several hundred pF to several nF, values on the same order as MOVs of comparable current and energy ratings.

Speed of response: Since the non–linear action of protective diodes takes place in the very thin depletion region, there is little dependence of clamped voltage on waveshape of surge current. Theoretical response times of 1 - 5 picoseconds ($1 - 5 \times 10^{-12}$ seconds) have been cited, but such times have little meaning since the performance of protective diodes is governed by inductance of leads just as with MOVs. Excessive lead length degrades the performance of any protective device.

Table 17.3 Specifications for Typical Protective Diodes [17.5]

JEDEC TYPE NUMBER	REVERSE STAND-OFF VOLTAGE (Note 1) V_R VOLTS	BREAKDOWN VOLTAGE BV @ VOLTS	I_T mA	MAXIMUM CLAMPING VOLTAGE @I_{PP} (1 mSEC) V_C VOLTS	MAXIMUM REVERSE LEAKAGE @V_R I_R μA	MAXIMUM PEAK PULSE CURRENT (Note 2) I_{PP} A
1N6036	5.5	6.75 - 8.25	10	11.7	1000	128.0
†1N6036A	6.0	7.13 - 7.88	10	11.3	1000	132.0
1N6037	6.5	7.38 - 9.02	10	12.5	500	120.0
†1N6037A	7.0	7.79 - 8.61	10	12.1	500	124.0
1N6038	7.0	8.19 - 10.00	10	13.8	200	109.0
†1N6038A	7.5	8.65 - 9.55	10	13.4	200	112.0
1N6039	8.0	9.00 - 11.00	1	15.0	50	100.0
†1N6039A	8.5	9.50 - 10.50	1	14.5	50	103.0
1N6040	8.5	9.90 - 12.10	1	16.2	10	93.0
†1N6040A	9.0	10.50 - 11.60	1	15.6	10	96.0
1N6041	9.0	10.80 - 13.20	1	17.3	5	87.0
†1N6041A	10.0	11.40 - 12.60	1	16.7	5	90.0
1N6042	10.0	11.70 - 14.30	1	19.0	5	79.0
†1N6042A	11.0	12.40 - 13.70	1	18.2	5	82.0
1N6043	11.0	13.50 - 16.50	1	22.0	5	68.0
†1N6043A	12.0	14.30 - 15.80	1	21.2	5	71.0
1N6044	12.0	14.40 - 17.60	1	23.5	5	64.0
†1N6044A	13.0	15.20 - 16.80	1	22.5	5	67.0
1N6045	14.0	16.20 - 19.80	1	26.5	5	56.5
†1N6045A	15.0	17.10 - 18.90	1	25.2	5	59.5
1N6046	16.0	18.00 - 22.00	1	29.1	5	51.5
†1N6046A	17.0	19.00 - 21.00	1	27.7	5	54.0
1N6047	17.0	19.80 - 24.20	1	31.9	5	47.0
†1N6047A	18.0	20.90 - 23.10	1	30.6	5	49.0
1N6048	19.0	21.60 - 26.40	1	34.7	5	43.0
†1N6048A	20.0	22.80 - 25.20	1	33.2	5	45.0
1N6049	21.0	24.30 - 29.70	1	39.1	5	38.5
†1N6049A	22.0	25.70 - 28.40	1	37.5	5	40.0

Series and parallel connection of diodes: Protective diodes may be placed in series with no problems. Diodes in parallel must be carefully matched for voltage, just as with MOVs.

Failure mode: Most commonly, excessive surge energy causes the semiconducting junction to melt and the device to fail shorted.

Advantages of Zener–type diodes:

1. Small size.
2. Easily mounted.
3. Low clamping voltage.
4. Low dynamic impedance when conducting.
5. Self–extinguishing. When applied voltage drops below the Zener level, they cease conduction.
6. Low volt-time turnup, or impulse ratio.

Disadvantages:

1. Not intrinsically bilateral. To protect against both polarities, two diodes in series back-to-back configuration are necessary. Bipolar packages are available.
2. High junction capacitance may cause significant signal loss at operating frequencies above 1 MHz. Special diode assemblies may extend the useful frequency to approximately 50 MHz.
3. They do not switch state between a conducting and a non–conducting mode.
4. Lower energy capabilities than spark gaps.
5. Not available for voltage below about 5 V.

6. Not normally available for voltages above a few hundred volts.

17.4.4 Forward-Conducting Diodes

In a forward-conducting state, a diode conducts little current below about 0.3 V for germanium and 0.6 V for silicon. They can, as a result, be placed directly across a low-voltage line and afford substantial protection. Diodes can be connected in series for higher voltage circuits. Diodes in parallel back-to-back would be needed for bipolar protection.

Advantages of forward-conducting diodes:

1. Small size.
2. Not costly.
3. Provide protection at very low-voltage levels.
4. Excellent surge-current ratings.

Disadvantages:

1. Not bilateral. For protection of both polarities, two diodes in parallel must be used. Some vendors supply bipolar diodes for protection purposes.
2. Conduction may occur on normal signals with attendant signal-clipping and frequency multiplication effects. Diodes must be used in series to raise voltage levels.
3. High capacitance.

17.4.5 Reverse Biased Diodes

Reverse biased diodes, as shown in Fig. 17.22, offer excellent protection for signal circuits. Under normal operation the diodes are reverse biased and effectively disconnected from the circuit, but whenever the voltage on the signal line exceeds the power supply voltage the diodes become forward biased and allow the surge to be conducted into the capacitors. Since no circuit will operate correctly for normal signals exceeding the supply voltage for the input semiconductor circuits, the supply voltage for the protective diodes is automatically of the correct level.

The reverse biased diodes have very low capacitance and the circuit is thus well adapted to protection of high frequency circuits for which the capacitance of MOVs and Zener type surge protective diodes presents problems. When called upon to provide protection, the diodes operate forward biased and even small signal diodes can carry very large surge currents. Some CMOS devices have similar diodes built in, but they are only intended to guard against static electricity and should not be relied on to offer protection against surges.

Resistors may be used to prevent excessive surge energy from being conducted into the circuit power supply and surge protective diodes can be used to bypass excessive surge energy to ground should the surge charge the capacitors to an excessive voltage.

Advantages of reverse biased diodes:

1. Low capacitance.
2. Excellent surge handling capability.

Disadvantages:

1. Must be included in initial design of circuit.
2. Seldom practical to add to existing circuit boards.

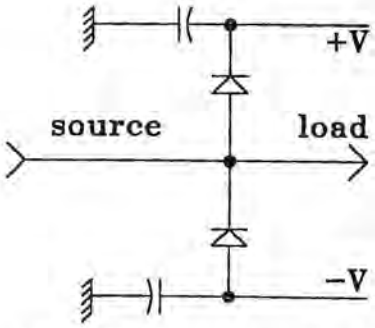

Fig. 17.22 Reverse biased diodes.

17.4.6 Hybrid Protection

Frequently a spark gap and a MOV, or a MOV and a surge protecting diode, are used together to provide added protection, as shown in Fig. 17.23. The higher energy device is connected close to the point where the surge may enter the system and the lower energy device is connected close to the more sensitive components. The principal is that the high energy device provides the primary protection and diverts the major portion of the surge energy while the lower energy device provides protection for the residual transients.

Isolation of devices: Protective devices cannot be operated directly in parallel since the device with the lowest clamping voltage would carry all the surge current. Impedance between the two is needed to limit

the surge current in the lower energy device and allow voltage to develop that initiates conduction in the high energy device.

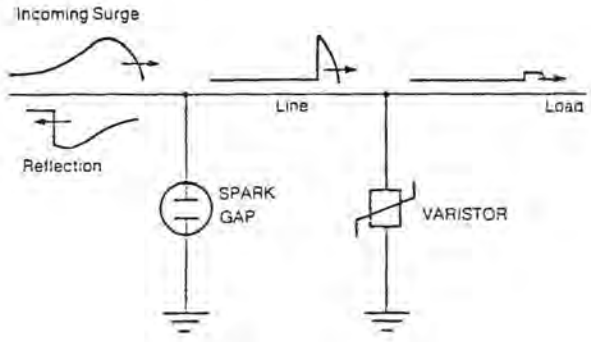

Fig. 17.23 Paralleled protectors physically separated.

Physical separation: Best protection is obtained if the two surge protectors are physically separated a considerable distance. For example, large MOVs or spark gaps should be located near exposed electrical apparatus such as lights and air data probe heaters, and smaller MOVs or diodes installed closer to solid state power controllers or other electronic equipment so that the interconnecting wires can provide the requisite impedance between high and low energy devices. Physical separation also minimizes problems of inductive voltage drop in grounding connectors.

Resistive or inductive isolation: Physical separation is not always possible in aircraft applications and additional resistance or inductance may be needed, as shown in Fig. 17.24. Inductance may be appropriate for power circuits, but has the disadvantage that slowly changing surge currents may still pass into the low energy protector without ever developing enough voltage to cause conduction through the high energy protector. Resistors are preferable because the current through the low energy protector can be controlled irrespective of the surge waveshape.

Commercial availability: Hybrid protectors are commercially available that have high and low energy protective devices incorporated into a single package.

17.4.7 Surge Protecting Connectors

At least two lines of activity have been pursued with the aim of incorporating surge protective devices directly in electrical connections. One approach [17.6] incorporated spark gaps between the connector pins and the connector shell. A high dielectric material, rutile, was used to stimulate internal flashover and to achieve a protective level of about 1100 to 1300 V with an impulse ratio nearly unity, even with voltage rates of change at 10 kV/μs. This design withstood extremely large currents (100 to 250 kA). The work on this device was performed at Sandia Laboratories and supported by the U.S. Atomic Energy Commission.

Another line of approach uses zinc oxide varistor material to hold the pins in a connector. This work was being done by General Electric Company for the U. S. Army Harry Diamond Laboratories.

Protective connectors are available commercially.

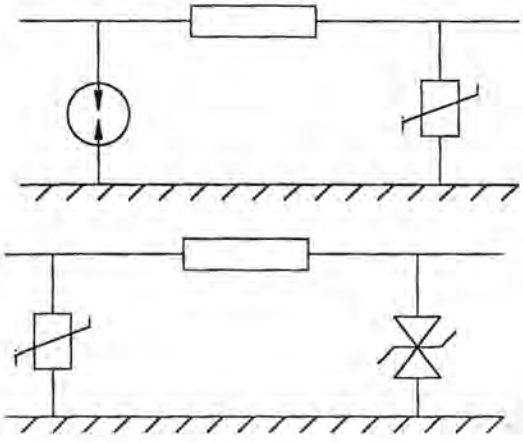

Fig. 17.24 Hybrid protectors.
(a) Sparkgap and MOV
(b) MOV and diode

17.5 Damage Analysis – Semiconductors

The energy coupled into a system by lightning induces large current pulses into the cabling and wiring of the system and resulting voltage pulses across loads. Determining whether or not these voltages and currents cause upset or damage to active or passive components requires a knowledge of the failure thresholds of devices. These failure thresholds have been investigated extensively during studies of nuclear electromagnetic pulse (NEMP) effects on electronic equipment. The following sections will discuss some of how damage analysis is performed.

Where vulnerability or failure involves thermal considerations one difference between NEMP and lightning analyses must be noted. NEMP vulnerability assessments are mostly made for a single pulse, but lightning subjects equipment to a series of closely spaced pulses.

Semiconductor electronic components are generally more vulnerable under pulse conditions than are non-semiconductor components. This discussion of

this section will be limited to semiconductors. Capacitors and some other components are discussed in §17.6 and §17.7.

17.5.1 Theoretical Models

Theoretical models have been developed which relate significant changes in the properties of a semiconductor PN junction to high temperatures generated in the junction region during application of a high voltage pulse. Theoretical models based on thermal analysis of the junction region yield a mathematical relation between junction temperature and power dissipation in the junction region. This relation can be used to define a constant characterizing the operation in a given time domain of each device.

17.5.2 Empirical Models

In addition to the theoretical correlations just described, the experimental data have been used in the development of empirical relations which are obtained from two models of semiconductor junction device–the junction capacitance model and the thermal resistance model. These models provide a framework from which the power failure threshold of an untested device can be estimated from the quantities listed in a data sheet description prepared by the manufacturer for a diode or a transistor.

17.5.3 Limitations

The assumptions made about junction heating and transfer of heat in the derivation of the models limit their applicability to the region of pulse durations of approximately 0.1 to 20 μs. For longer times appreciable heat transfer may take place away from the function area during the pulse input. For short pulses the power levels are so high (1 to 10 kW) that very large currents flow; consequently, the joule heating in the bulk material is appreciable. The transition behavior between these three regions of pulse duration (regions that will be more precisely described later in this section) is not well defined and may vary from one device type to another. Examination of available data indicates the transition region generally occurs between 100 ns and 1 μs.

Still another limitation is fundamental to the work summarized in this section: it applies only to junction burnout. Other modes of device failure, such as metallization burnout and internal arcing, are not treated. Based on the results obtained in studies of junction burnout, it would seem that other effects, such as metallization burnout, occur at higher power input levels than those input levels sufficient to damage the junction.

17.5.4 Failure Mechanisms–Semiconductors

The two principal breakdown modes for semiconductor PN junctions are the following:

1. Surface damage around the junction as a result of arcing.
2. Internal damage to the junction region as a result of elevated temperature.

Surface damage refers to the establishment of a high–leakage path around the junction which effectively eliminates any junction action. The junction itself is not necessarily destroyed, since, if it were possible to etch the conducting material away from the surface, the device might be able to return to its normal operating state. This is not practical, of course, in an operational semiconductor. It is equally likely that the formation of any surface leakage path would be the result of excessive heat development in the bulk of the material, and this would typically be an irreversible phenomenon.

It is very difficult to predict theoretically the conditions which will lead to surface damage because they depend upon many variables, such as the geometrical design and the details of the crystal structure of the surface. The theoretical prediction of surface arcing under pulse conditions is not practical [17.7]. It should be cautioned that surface damage, in the general case, may occur in devices at power levels which are orders of magnitude below those sustainable by devices in which *bulk damage* occurs [17.8].

Bulk damage, which results in permanent change in the characteristic electrical parameters of the junction, indicates some physical change in the structure of the semiconductor crystal in the region of the junction. The most significant change is melting of the junction as a result of high temperatures. Other types of change may involve the impurity concentrations, the formulation of alloys of the crystal materials, or a large increase in the number of lattice imperfections, either crystal dislocations or point defects.

Example: The simplest structure to analyze is a diode. Consider Fig. 17.25. In this diode a current is assumed to flow as a result of some outside stimulus and, in doing so, to produce a voltage across the diode. This voltage may be the forward bias voltage (0.5 to 1.5 V), or it may be the reverse breakdown voltage if the outside stimulus has biased the diode in the reverse direction. Assume that I is a square wave and that V is not a function of time, as it might be if V depended upon the junction temperature. The instantaneous power dissipated in the diode is then also a

square pulse of magnitude

$$P = IV \tag{17.4}$$

and the total energy produced is

$$W = \int_0^t P\,dt = IVt \tag{17.5}$$

Assume that the power level is sufficient that the device fails at the end of the pulse. Both experimental and theoretical analyses indicate that the power required to cause failure depends on pulse width: the narrower the pulse, the greater the power required to cause failure. Over a broad range of times, typically between 0.1 μs and 100 μs, the power required to cause failure is inversely proportional to the square root of time. For very short pulse durations the power required to cause failure is inversely proportional to time, and for very long pulse durations the power required to cause failure is a constant. These relations may be expressed by the following equations:

$$Pt = C \quad t < T_0 \tag{17.6}$$

$$Pt^{1/2} = K \quad T_0 < t < 100\ \mu s \tag{17.7}$$

$$P = \text{Constant} \quad t > 100\ \mu s \tag{17.8}$$

where T_0 generally lies between 10 ns and 1 μs. Fig. 17.26 shows an example for a 10 W diode. The most important region is the center region, where

$$P = Kt^{-1/2} \tag{17.9}$$

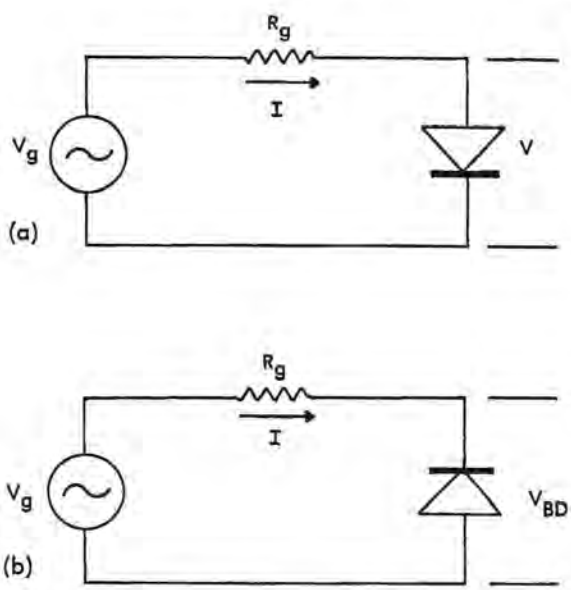

Fig. 17.25 Voltage and current through a diode junction [17.9].
(a) Forward bias case
(b) Reverse bias case, $V_g > V_{BD}$

Effects of bias: Junctions are less susceptible to burnout when operated with forward bias: first, because the power produced by a given current is lower when flowing through the low forward bias voltage than when developed across the higher reverse bias breakdown voltage, V_{BD}, and, second, because the current is more uniformly distributed across the junction in the forward direction. Accordingly, it requires more power in the forward direction to cause failure. An example is shown in Fig. 17.27. The 2N2222 transistor is a 0.5 W NPN silicon high- speed switch.

17.5.5 Damage Constants

From curves, such as those of Figs. 17.26 and 17.27, the value of a damage constant, K (or C), can be determined and tabulated for a range of devices. The appropriate threshold damage curve can then be reproduced as desired from a single damage characterization number, the damage constant K. It is convenient to express K in kW·$\mu s^{0.5}$, since the value of K in these units then becomes numerically equal to the power necessary for failure, dissipated by a square pulse of 1 μs duration.

If this point is located on a log–log graph, as shown in Fig. 17.26, then a curve of slope, -0.5, drawn through this point reconstructs the curve fit to the data for a particular device, and the power for failure at other pulse durations can be read directly from such a graph. Ideally, the K factor should be known for both the forward bias and the reverse bias conditions. Generally, only the K factor for the reverse bias condition is known. This limitation gives conservative answers, since K for the reverse bias condition is almost always lower than is K for the forward bias condition.

The magnitude of the damage constant depends upon the type of junction under consideration: broadly speaking, it is larger for large junctions and smaller for small junctions. Figs. 17.28 and 17.29 show the range of the damage constant for typical diodes and transistors.

17.5.6 Experimental Determination of K Factor

Experimentally the K factor is determined by injecting power pulses into the semiconductor junction, starting at low levels and increasing the levels until either failure or significant degradation of the junction occurs. Devices would normally be pulsed in both the forward and reverse directions.

The K factors and breakdown voltages for some representative semiconductors are given in Table 17.4 and 17.5. The tables are intended only to show the

type of data available and are not complete. More complete, and more up to date, data is available to qualified users. In the case of transistors, the K factor listed generally refers to the base–emitter junction, since this is generally the junction most susceptible to burnout. In all the cases the K factor refers to the reverse bias direction.

17.5.7 K Factor as Determined from Junction Area

If the K factor is not measured, it may be estimated [17.12, 17.13] by one or more of three methods. The most accurate of the indirect methods involves a knowledge of the area of the junction. If the area is known, the K factor may be estimated from the following relations:

$$\text{Diodes} - K = 0.56A \tag{17.10}$$

$$\text{Transistors} - K = 0.47A \tag{17.11}$$

K in kW · μs

A in cm^2

For transistors, the junction area to be used is that of the base–emitter region. This is generally the weaker junction (lower breakdown voltage), and it is that for which the experimental average value for K was obtained.

This method is of course limited by the availability of information on junction area, but where such information is available, the method yields damage constants accurate to within a factor of two. For planar devices, the junction area can often be measured directly on the silicon chip

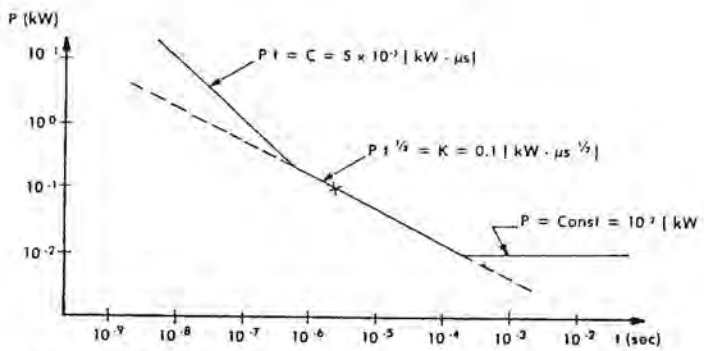

Fig. 17.26 Time dependence of pulse power failure [17.9]. Threshold for a 10 W diode

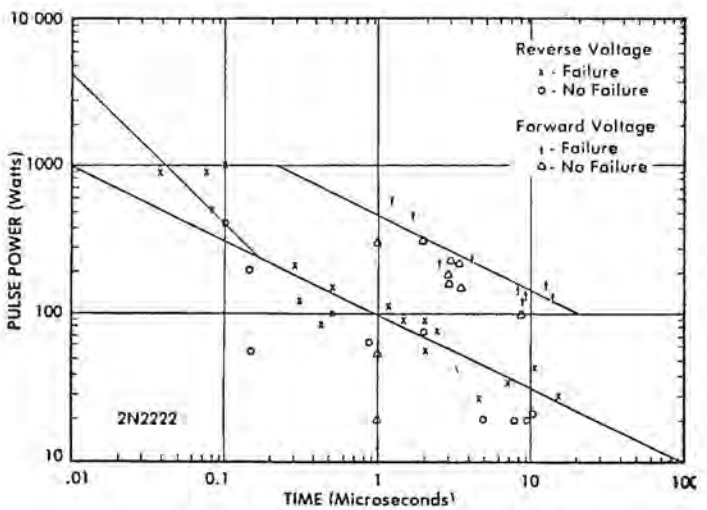

Fig. 17.27 Time dependence of pulse power failure [17.10]. 2N2222 transistor

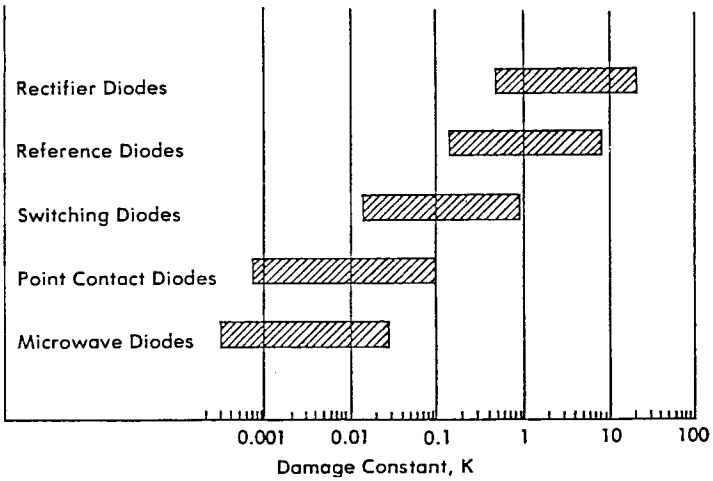

Fig. 17.28 Range of pulse power damage constants for representative diodes [17.11].

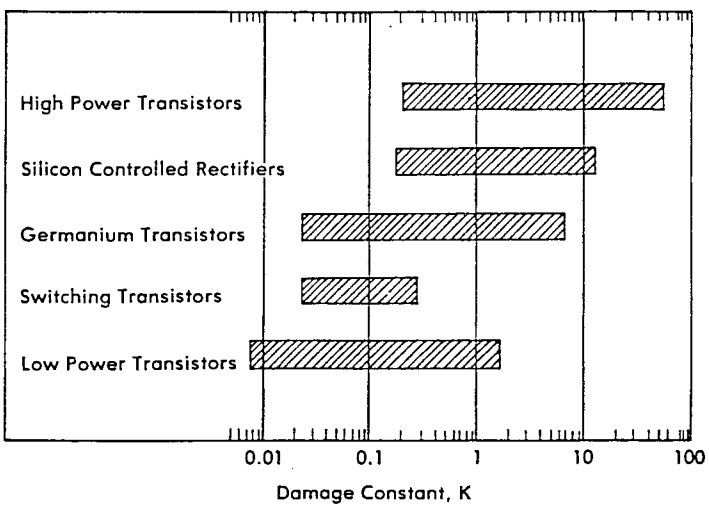

Fig. 17.29 Range of pulse power damage constants for representative transistors [17.12].

17.5.8 K Factor as Determined from Junction Capacitance

The next most reliable method of determining the damage constant is from a knowledge of the capacitance C_j and breakdown voltage V_{BD} of the junction. For silicon diodes and all silicon transistors except planar and mesa devices, the relation is

$$K = 4.97 \times 10^{-3} C_j V_{BD}^{0.57} \qquad (17.12)$$

For silicon planar and mesa transistors the relation is

$$K = 1.66 \times 10^{-4} C_j V_{BD}^{0.992} \qquad (17.13)$$

For a base–emitter junction, the capacitance used should be taken at a reverse bias of approximately 1 V. For a collector–base junction or diode junction, the value should be taken at the reverse bias of approximately 5 to 10 V.

Table 17.4 Typical Diode Damage Data [17.11, 17.26 - 17.28]

Device Number	K	V_{BD}
IN483, A	.3	70.
IN483, B	.3	80.
IN484A	.45	130.
IN484B	.3	130.
IN485	.3	180.
IN486, B	.29	225.
IN487, Z	.3	300.
IN488	.3	380.
IN536	1.	50.
IN537	.51	100.
IN538, M	1.	200.
IN539	1.	300.
IN540	.93	400.
IN547	12.1	600.
IN560	.625	800.
IN561	.625	1000.
IN562	1.8	800.
IN619	.36	10.
IN622	.347	150.
IN625	.164	30.
IN625A	.045	20.
IN643	.44	200.
IN643A	.1	200.
IN645	2.8	225.
IN646	2.29	300.

Device Number	K	V_{BD}
IN3157	.625	8.4
IN3189	10.	200.
IN3190	4.1	600.
IN3560	.038	.475
IN3561	.038	.475
IN3582A	.35	11.7
IN3600	.18	50.
IN3821	1.947	3.3
IN3828A	1.95	6.2
IN3893	6.41	400.
IN3976	132.	200.
IN4241	33.84	6.
IN4245	2.4	200.
IN4249	2.4	1000.
IN4312	.116	150.
IN4370A	.625	2.4
IN4816	6.8	50.
IN4817	6.8	100.
IN4820	10.	400.
IN4823	.208	100V
IN4989	14.33	200.
AM2	1.4	50.
D4330	.001	
FD300	.18	125.
SG22	.23	
SLD10EC		10,000.

17.5.9 K Factor as Determined from Thermal Resistance

The third, and least reliable, way of estimating the damage constant is from a knowledge of the thermal resistance of the junction, either the thermal resistance from junction to case (Θ_{jc}) or from junction to ambient (Θ_{ja}). For silicon diodes and all silicon transistors except planar and mesa devices, empirical relations are:

$$K = 707\Theta_{jc}^{-1.93} \quad (\Theta_{jc} > 10.0) \qquad (17.14)$$

$$K = 4.11 \times 10^4 \Theta_{ja}^{-1.7} \qquad (17.15)$$

For silicon planar and mesa transistors the relations are

$$K = 707\Theta_{jc}^{-1.93} \quad (\Theta_{jc} > 10.0) \qquad (17.16)$$

$$K = 2.74 \times 10^5 \Theta_{ja}^{-2.55} \qquad (17.17)$$

Normally Θ_{jc} and Θ_{ja} are not given in the transistor data sheets but, rather, must be calculated from the maximum operating junction temperature, (T_{jmax}), the total power dissipation (P_d), case temperature (T_c), and ambient temperature (T_{amb}).

$$\Theta_{jc} = (T_{jmax} - T_c)/P_d \qquad (17.18)$$

$$\Theta_{ja} = (T_{jmax} - T_{amb} \qquad (17.19)$$

Generally, at least one of these thermal resistances can be determined from the manufacturer's data sheet.

The accuracy of the damage constant as determined from either the junction capacitance or the junc-

tion thermal resistance is somewhat limited. Table 17.6 gives some estimate of the accuracy within which the damage constant can be calculated.

17.5.10 Oscillatory Waveforms

Eq. 17.9 is based on the assumption that the applied voltage, current, and power waves are rectangular in shape. Actual transients are very seldom rectangular, but it is possible to derive equivalent rectangular pulses for more common types of transient.

One such type of transient typically encountered is the damped oscillatory wave. Based on multiple pulse studies by Wunsch and others [17.15 and 17.16], it can be assumed that device damage will occur, if at all, during the first cycle of the damped sine wave. Therefore, the lower amplitude cycles may be neglected.

Two cases may be considered, one in which one of the half cycles of the transient does not exceed the reverse breakdown voltage of the junction, Fig. 17.30, and one in which the reverse breakdown voltage is exceeded, Fig. 17.31. In either case, one of the half cycles will bias the junction in a forward direction.

Reverse breakdown not exceeded: Treating first the case in which the reverse breakdown voltage is not exceeded, Fig. 17.30, the rectangular wave of the same peak amplitude, V_0, and producing the same probability of damage as the sine wave, has a duration τ_p, where

$$\tau_p = \frac{\tau_s}{5} \tag{17.20}$$

of the sine wave.

Table 17.5 Typical Transistor Damage Data [17.11, 17.26 - 17.28]

Device Number	K	BV EBO	BV CBO	BV CEO
2N43,A	.28	5.	45.	30.
2N117	.15	1.	45.	45.
2N118	.15	1.	45.	45.
2N128	.017	10.	10.	4.5
2N158	.499	30.	60.	60.
2N176	.46		40.	30.
2N189	.17		25.	25.
2N190	.58		25.	25.
2N243	.05	1.	60.	60.
2N244	.05	1.	60.	60.
2N263	.38	1.	45.	30.
2N264	.36		45.	30.
2N274	.0076	.5	35.	40.
2N279A	.047		45.	30.
2N297A	.499	40.	60.	40.
2N329,A	.21	20.	50.	30.
2N332	.45	1.	45.	30.
2N333	.32	1.	45.	30.
2N335, A	.55	1.	45.	45.
		(4.-2N335A)		
2N336	.55	1.	45.	30.
2N337	.12	1.	45.	30.
2N338	.12	1.	45.	30.
2N339	2.	1.	55.	55.
2N341	1.	1.	125.	85.

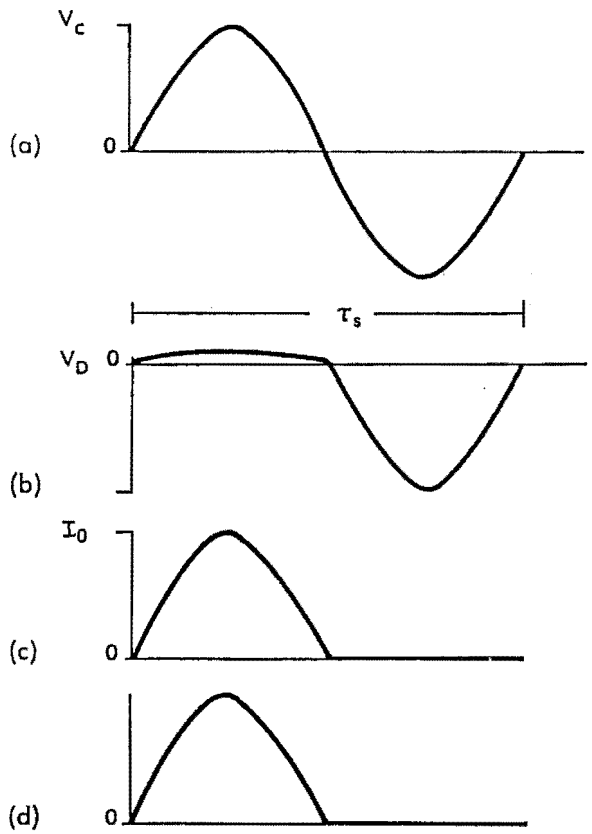

Fig. 17.30 Device waveforms for $V_g < V_{BD}$ [17.17].
(a) Generator voltage
(b) Diode voltage
(c) Junction current
(d) Junction power

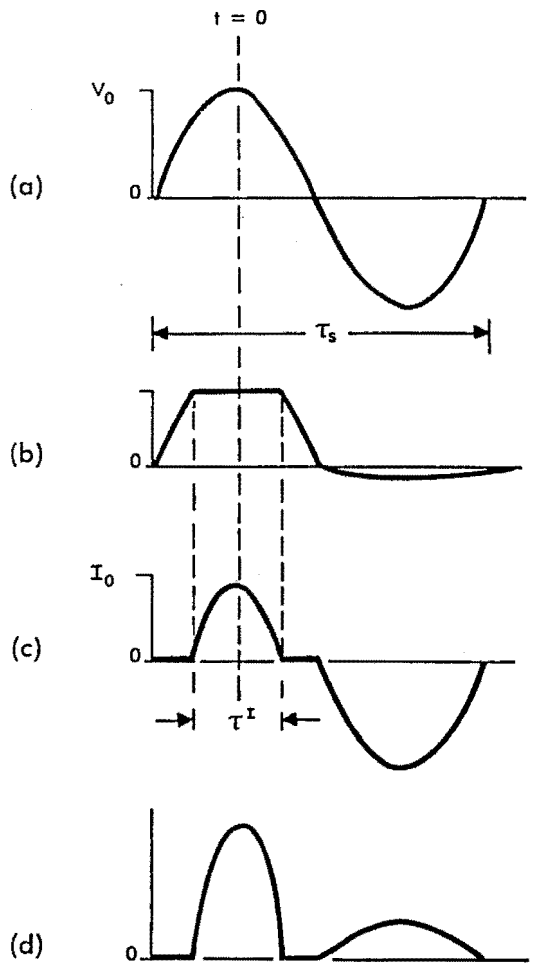

Fig. 17.31 Device waveforms for $V_g > V_{BD}$ [17.18].
(a) Generator voltage
(b) Diode voltage
(c) Junction current
(d) Junction power

Reverse breakdown exceeded: If the transient does exceed the reverse breakdown voltage, Fig. 17.31, the duration of the equivalent transient depends upon the fraction of the time that the oscillatory transient does exceed the reverse breakdown voltage. The duration of the equivalent rectangular wave is given by the expression

$$\tau_p = \frac{1 - (V_{BD}/V_0)^2}{\pi \cos^{-1}\left(V_{BD}/V_0\right)} \tau_s \qquad (17.21)$$

This expression is shown plotted in Figs. 17.32 and 17.33. For oscillatory transients whose initial amplitude considerably exceeds the reverse breakdown voltage of the junction, Eq. 17.15 approaches a limiting value of 0.2, and thus becomes identical with the forward bias case, Eq. 17.14.

Integrated circuits: A limited amount of data relating voltage and current durations to the breakdown of integrated circuits is shown in Figs. 17.34, 17.35, and 17.36 show the results of measurements on SN55107 line receivers, SN55109 line drivers, and CD4050 AE hex buffers.

17.6 Failure Mechanisms–Capacitors

Capacitors fail by a mechanism different from that of semiconductors. The mechanism of capacitor failure depends upon the type of dielectric.

Solid dielectrics: Capacitors with solid dielectrics, paper, Mylar, or ceramics, will, when subjected to non-repetitive transients, either fail by puncture of the dielectric or not fail at all. Typically, a capacitor can withstand short-duration transient voltages several times greater than the dc rating of the insulation.

The pulse–breakdown rating of the dielectric, however, is not a constant ratio to the dc voltage rating, nor is it normally part of any manufacturer's specification. Accordingly, it is safest to consider that such a capacitor is in danger of failure if the pulse voltage exceeds the dc rating of the capacitor.

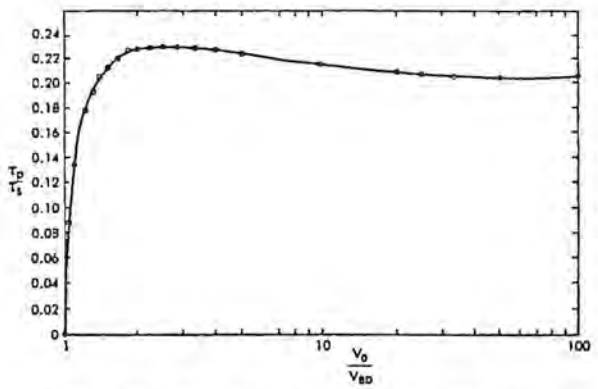

Fig. 17.32 Plot of τ_p/τ_s versus V_0/V_{BD} [17.19].

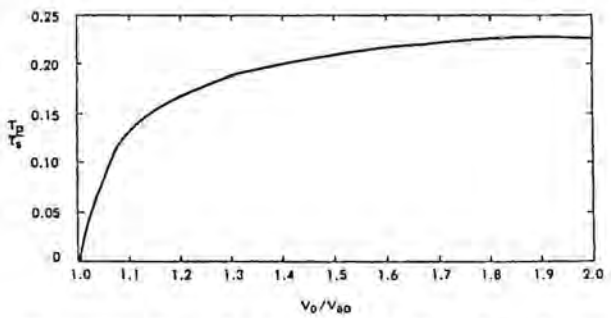

Fig. 17.33 Plot of τ_p/τ_s versus V_0/V_{BD} for values of V_0/V_{BD} less than 2 [17.20].

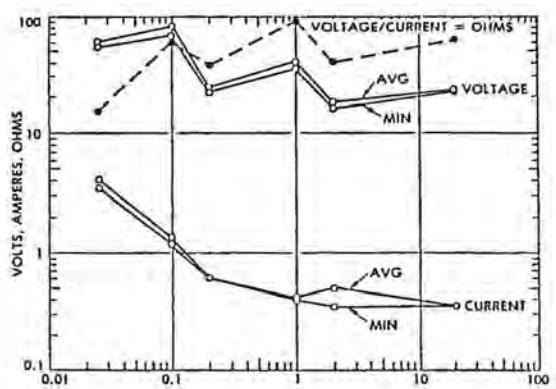

Fig. 17.34 Damage thresholds of SN 55107 line receivers [17.21]

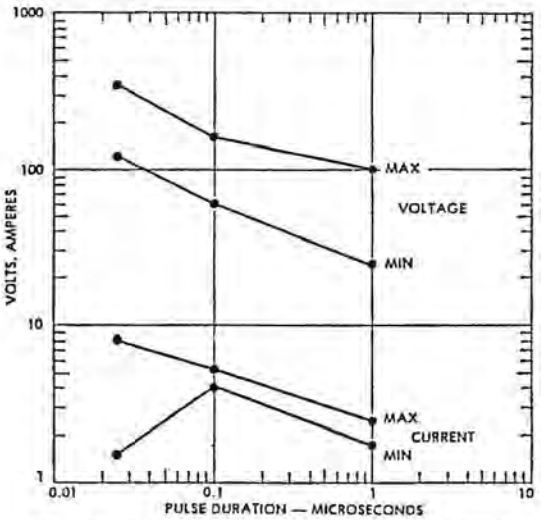

Fig. 17.35 Damage thresholds of SN 55109 line drivers [17.22].

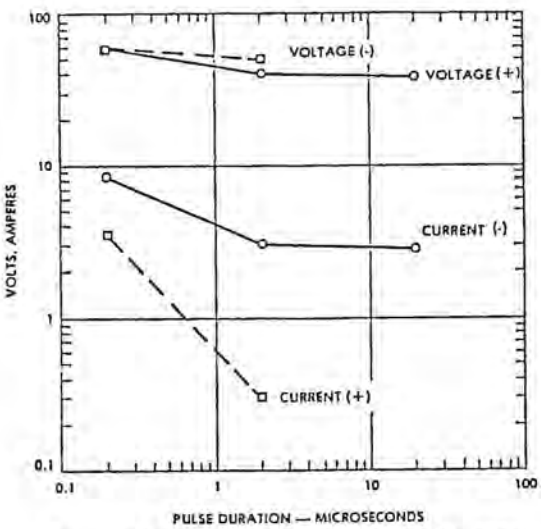

Fig. 17.36 Damage thresholds of CD 4050 AE hex buffers [17.23].

Electrolytic capacitors: Electrolytic capacitors, on the other hand, do not experience abrupt failure when exposed to short–duration transients. If the voltage across the capacitor exceeds the voltage used to form the dielectric film, the dielectric film begins to conduct. After the pulse has disappeared, the dielectric returns to nearly its normal state. During the transient period the dielectric film can carry substantial transient current without permanent or catastrophic degradation.

Transients, however, may lead to increased leakage currents. An example of data that is available re-

lates to a series of tests made on tantalum electrolytic capacitors of value 0.47 μF, 0.047 μF, and 0.0047 μF with a dc voltage rating of 350 V [17.24]. The data indicate that failure (defined as a substantial increase in the leakage current at voltages of less than 350 V) can generally be associated with the time during which internal conduction occurs. For these components, conduction was initiated at 3 to 4 times the voltage rating. Leakage current increased continuously with time of conduction, from initial values of a few nanoamperes through milliamperes.

The value of the capacitance determines how quickly the voltage across the capacitor reaches the breakdown voltage range, 90 to 140 V, which then relates to the time of conduction and the extent of damage. Fig. 17.37 shows the data for the nine 0.0047 μF capacitors tested. For a particular pulse duration of 5 μs, an increase in leakage current is expected; for pulse voltages of 100 to 150 V and for pulses of 150 to 200 V, an increase in leakage current to milliamperes is possible. It is cautioned that this behavior may not be readily extended to capacitors of different materials or construction. The capacitor data remains insufficient to draw general conclusions as to system implications at this time.

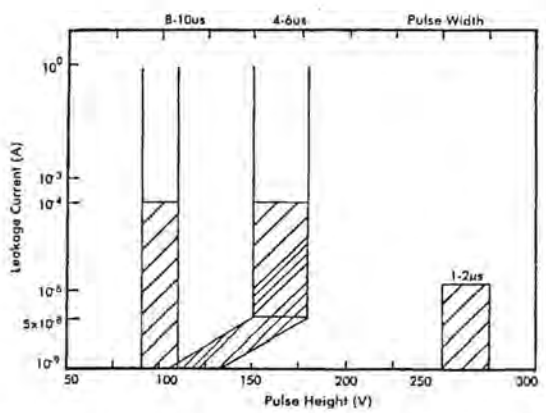

Fig. 17.37 Pulse test data for 0.0047 μF tantalum electrolytic capacitors [17.25].

17.7 Failure Mechanisms–Other Components

A limited amount of pulse test data is available for various non-semiconductor electronic circuit components. These data were mostly obtained by testing with a square-wave pulse input of 1 to 10 μs duration and up to 1 kV peak. As would be expected, not all such components are invulnerable to pulses of this shape. The test results for several kinds of component are presented in Table 17.7. The test conditions consisted of an 8 μs, 1 kV pulse applied 10 times to each device. In the case of multiterminal components, several pairs of terminals were tested in this manner.

Table 17.6 Accuracy of K Factors Determined by Indirect Methods [17.14]

Device Number	K	BV EBO	BV CBO	BV CEO	Reference Source
T1487	4.5	6.	80.	60.	SP
TIXM101	.01	.3	15.	7.	SP
SW3042	.1	--	--		DX

SP – SAP-1 Computer listing from *SAP-1 Computer Code Manual*, U.S. Air Force Weapons Laboratory, 1972.

DX – Experimental data from DASA (Defense Atomic Support Agency) *Handbook* [17.9].

	Conditions	Accuracy
K_{amb}	$50 < \theta_{ja} < 200$	Factor of 2
	$200 < \theta_{ja} < 500$	Factor of 10
	$\theta_{ja} > 500$	Factor of 30
K_{case}		Factor of 3
K_{cj}	$V_{bd} < 10$	Factor of 30
	$10 < V_{bd} < 200$	Factor of 10
	$200 < V_{bd} < 2000$	Factor of 2

K_{amb} = K as determined from θ_{ja}
K_{case} = K as determined from θ_{jc}
K_{cj} = K as determined from junction capacitance

17.8 Examples of Use of Damage Constants

Some examples follow of how the preceding material may be used to determine whether or not a given transient will cause damage to semiconductors.

Relay: The first circuit chosen for analysis, Fig. 17.38, is a simple remote-controlled relay. Across the terminals of the relay coil there is a diode which would be exposed to the same transients as those to which the coil is exposed. The analysis approach that will be taken is first to calculate the current level that would cause the diode to fail and then to see whether or not the transient voltage source could supply that current. It will be assumed that the oscillatory pulse is a transient of 1 MHz frequency or 1 μs period. At this frequency the inductive reactance of the relay coil would be sufficiently large that the relay could be neglected.

The current required to cause failure at time, t, would be

$$I_f = \frac{P_f}{V_{BD}} = \frac{Kt^{-1/2}}{V_{BD}} \qquad (17.22)$$

For a 1N540 diode, the reverse breakdown voltage, V_{BD}, is 400 V and the damage constant, K, is 0.93 (See Table 17.4). If a 200 ns pulse is used to approximate a 1 MHz damped sine wave, the failure current for the diode would be

$$I_F = \frac{0.93\ (2 \times 10^{-7})^{-1/2}}{400} = 5.2A \qquad (17.23)$$

Assume now that the impedance of the source from which the voltage transient generated is 10 ohms. The voltage required to produce a current of 5.2 A through the diode would be

$$V_{\text{Transient}} = V_{BD} + I_{\text{Transient}} R_{\text{Source}} \qquad (17.24)$$
$$V_{\text{Transient}} = 452V$$

Therefore, a single 452 V pulse, 200 ns wide or a 1 MHz damped sine wave having a peak amplitude of 452 V would cause the diode to fail.

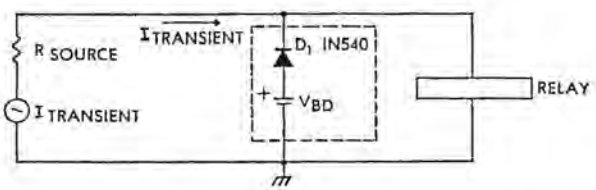

Fig. 17.38 Simple remote-controlled relay [17.27].

Phase splitter: The second circuit chosen for analysis is the simple phase-splitter amplifier shown in Fig. 17.39. The first step in determining the input current required for damage is to simplify the circuit. Again assume that the voltage source producing the transient is a damped sine wave of 1 MHz frequency. At such a frequency the reactances of capacitors C_1 and C_2 will be so small that they may be neglected. Likewise the 12V power supply line can be considered to be at ground potential.

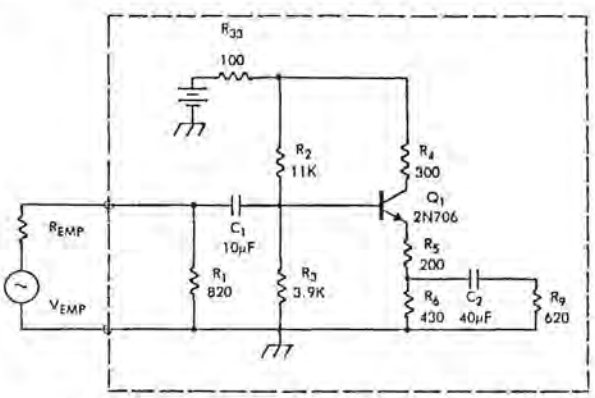

Fig. 17.39 Phase-splitter circuit [17.28].

The resultant circuit after simplification is shown in Fig. 17.40. The circuit can be further simplified by determining the equivalent resistances for the base and collector circuits. The base–emitter junction and the base-collector junction can also be replaced by their diode equivalents to represent operation in the breakdown regions. This simplified circuit is shown in Fig. 17.410. Also shown in the figure are the breakdown voltages and damage constants for the 2N706B. Note that for this transistor a damage constant for the collector–base junction is available, though not listed in Table 17.5.

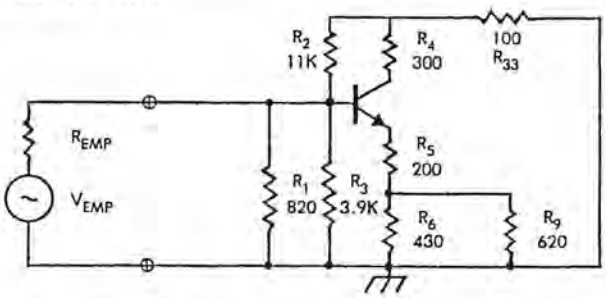

Fig. 17.40 Simplified phase-splitter circuit [17.29].

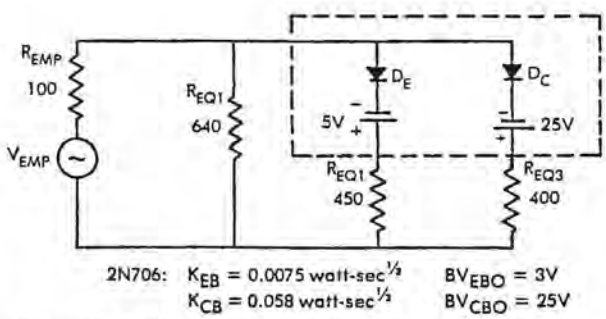

Fig. 17.41 Further simplification of phase-splitter circuit [17.30].

The circuit is now simplified to the point where it lends itself easily to hand analysis. The next step is to determine which junction will fail and what the failure mode is. The passive components are generally able to withstand higher energies for short-duration pulses than can transistors. Therefore, the transistor is the element to consider for damage. Failure is also assumed to occur in the reverse biased direction.

Using the Wunsch damage model ($P = Kt^{-1/2}$), a calculation is made to see whether the emitter–base junction or the collector– base junction would fail first.

$$P_{EB} = K_{EB} t^{-1/2} = 17W \qquad (17.25)$$
$$P_{CB} = K_{CB} t^{-}1/2 = 130W \qquad (17.26)$$

This calculation shows that the emitter-base junction is the more susceptible. The current required to fail the emitter-base junction would be:

$$I_{jF} = \frac{P_{EB}}{V_{BD}} = 3.4A \tag{17.27}$$

The voltage from the base to ground is

$$V_{BASE} = BV_{EBO} + I_{jF}R_{EQ2} = 1.5kV. \tag{17.28}$$

The current through the collector–base junction is

$$I_{CD} = \frac{V_{BASE} - BV_{CBO}}{R_{EQ3}} = 3.7A \tag{17.29}$$

The power dissipated in the collector–base junction is

$$P_{CB} = BV_{CBO}I_{CB} = 93W \tag{17.30}$$

which is below its failure–threshold power.

The total current into the circuit is then

$$I_{\text{transient}} = IjF + I_{CB} + \frac{V_{\text{base}}}{R_{eq1}} \tag{17.31}$$

and the $I_{\text{Transient}}$ voltage required to cause failure is

$$V_{\text{Transient}} = V_{\text{BASE}} + I_{\text{Transient}}R_{\text{Source}} = 2.5kV \tag{17.32}$$

Therefore (assuming a 100 ohm source impedance) a 2.5 kV pulse, 200 ns wide, will cause the transistor to fail.

Table 17.7 Damage Test Results for Non–semiconductors [17.26]

Device Type	Manufacturer	Manufacturer's Part Number	Properties	Test Results
Capacitor	Cornell-Dublier	C100K	10 pF	No change in capacity or leakage resistance
Capacitor	Cornell-Dublier	CK62 Series	4700 pF, 500 Vdc	
Capacitor	Sprague	96P Series	1 μF, 200 Vdc	
Capacitor	WES CAP	KF223KM	0.022 μF, 600 Vdc	
Coil	Collins	240-2524-00	220 μH	No change in inductance or resistance
Coil	Collins	542-0916-002	2 μH 10^3 Hz	
Filter	Bundy	21-0526-00	Notch 400 and 1200 Hz	No change in frequency response
Filter	Varo	954-0429-400	Bandpass 400 Hz	
Potentiometer	Computer Insts.	M18-178105	400 Ω	No changes
Potentiometer	Ohmite	51927-1	250 Ω	
Potentiometer	Ohmite	51927-3	25 Ω	
Relay	Babcock	RP11573-G2	Armature	Resistance increase: 625 Ω > 629 Ω
Relay*	C. P. Clare	A5245-1	Armature	Resistance increase: 418 Ω > 425 Ω
Relay	Hathaway	63862	Magnetic Reed	Resistance increase: 2.5%
Relay	Potter Brumfield	FLB4002	Magnetic Latching	Resistance decrease: <1%
Relay	Struthers Dunn	FC6-365	Armature	No changes
Transformer	Dektronics	D78Z222	Audio Frequency	No change in resistance or voltages, no arcing during pulse
Transformer	Dektronics	D78Z225	Power, Isolation	
Transformer	Freed	667-0386-00	Audio Frequency	
Transformer	Varo	950-1622-200	Power, Isolation	
Transformer	Varo	999-0197-200	Power, Isolation, Stepdown	
Vacuum Tube		6BX7	Med μ Twin	No change in characteristics Transconductance decrease, 35%
Vacuum Tube		5876	UHF High μ	
Vacuum Tube		6BC4	Med μ Twin	

*Arcing present continually for 700 V pulses.

REFERENCES

17.1 *Transient Voltage Suppression Manual, Fifth Edition*, Semiconductor Business Division, General Electric Company, Electronics Park, Syracuse, New York (1987).

17.2 W. Schmidt et al, "Behaviour of MO-Surge Arrester Blocks to Fast Transients," *IEEE Trans. on Power Delivery*, vol. 4, No. 1, January 1989, pp. 292-300.

17.3 C. Dang, T. M. Parnell, P. J. Price, "The Response of Metal Oxide Surge Arresters to Steep Fronted Current Impulses," *IEEE Trans. on Power Delivery*, Vol. PWRD-1, No. 1, January, 1986, pp. 157-163.

17.4 *Specification PE-60*, Rural Electrification Administration, Washington, D.C.

17.5 General Semiconductor Industries, Tempe, AZ.

17.6 J. A. Cooper and L. J. Allen, "The Lightning Arrester Connector: A New Concept in System Electrical Protection," *IEEE International Electromagnetic Compatibility Symposium Record*, IEEE 72CH0638-EMC, Institute of Electronic and Electrical Engineers, New York, New York (1972).

17.7 R.L. Davies and R.E. Gentry, "Control of Electric Field at the Surface on PN Junctions," *IEEE Transactions on Electron Devices*, ED-11, Institute of Electronic and Electrical Engineers, New York, New York (July 1964): pp.313-323.

17.8 H. S. Velorie and M.P. Prince, "High-Voltage Conductivity-Modulated Silicon Rectifier," *Bell System Technical Journal*, July 1957, pp. 975-1004.

17.9 *DNA EMP (Electromagnetic Pulse) Handbook, Vol. 2, Section 13: Analysis and Testing* , DNA 2114 H-2, Defense Nuclear Agency, Washington, D.C. (November 1971).

17.10 DNA EMP Handbook, *ibid.* ,p. 13-34.

17.11 DNA EMP Handbook, *op. cit.*, p. 13-53.

17.12 *EMP Susceptibility Threshold Handbook, (Appendix D)*, prepared by the Boeing Company for the U.S. Air Force Weapons Laboratory, Kirtland Air Force Base, Albuquerque, New Mexico (July 21, 1972).

17.13 *EC-135 Pretest EMP Analysis, I*, BDM/A-701-705, prepared by Braddock, Dunn and McDonald, Inc., for the Air Force Special Weapons Center, Albuquerque, New Mexico (March 1971).

17.14 DNA EMP Handbook, *ibid.* ,p. 13-47.

17.15 J. B. Singletary and D.C., "BDM Final Report, Semiconductor Damage Study, Phase II," Report BDM/A-66-70-TR, prepared by Braddock, Dunn and McDonald, Inc., for the U.S.Army Mobility Equipment Research and Development Center, Fort Belvoir, Virginia (April 1969).

17.16 D.C. Wunsch and L. Marzitelli, "BDM Final Report, Semiconductor and Non-semiconductor Damage Study, I," Report BDM-375-69-F-0168, prepared by Braddock, Dunn and McDonald, Inc., for the U..S. Army Mobility Equipment Research and Development Center, Fort Belvoir, Virginia (April 1969).

17.17 EMP Susceptibility Threshold Handbook, *op. cit.*, p. 212.

17.18 EMP Susceptibility Threshold Handbook, *op. cit.*, p.2

17.19 EMP Susceptibility Threshold Handbook, *op. cit.*, p. 223.

17.20 EMP Susceptibility Threshold Handbook, *op. cit.*, p. 224.

17.21 E. Keuren, R. Hendrickson, and R. Magyarics, "Circuit Failure Due to Transient-Induced Stresses," *First Symposium on Electromagnetic Compatibility*, Montreux, Switzerland, May 20-22, 1975, IEEE EMC Conference Record 75 CH10124, Institute of Electronic and Electrical Engineers, New York, New York (1975), pp. 500-505.

17.22 Keuren, Hendrickson, and Magyarics, "Circuit Failure," *ibid.* , p. 504.

17.23 Keuren, Hendrickson, and Magyarics, "Circuit Failure."*op. cit.*,

17.24 DNA EMP Handbook, *op. cit.*, pp. 13-19 to 13-101.

17.25 DNA EMP Handbook, *op. cit.*, p. 13-101.

17.26 DNA EMP Handbook, *op. cit.*, p. 13-100.

17.27 EMP Susceptibility Threshold Handbook, *op. cit.*, p. 144.

17.28 EMP Susceptibility Threshold Handbook, *op. cit.*, p. 146.

17.29 EMP Susceptibility Threshold Handbook, *op. cit.*, p. 148.

17.30 EMP Susceptibility Threshold Handbook, *op. cit.*, p. 148.

17.31 *Electromagnetic Susceptibility of Semiconductor Components*, AFWL-TR-74-280, Air Force Weapons Laboratory, Kirtland Air Force Base, Albuquerque, New Mexico (1974).

17.32 B. D. Faraudo and L. C. Martin, "Review of Factors for Application in Component Damage Analysis,"Protection Engineering and Management Note PEM-52, Lawrence Livermore Laboratory, University of California, Livermore, California, (September 1976).

17.33 D.M. Tasca, "Theoretical and Experimental Studies of Semiconductor Device Degradation Due

to High Power Electrical Transients," 735D4289, Corporate Research and Development, General Electric Company, Schenectady, New York (December 1973).

17.34 *Determination of Upset and Damage Circuit Thresholds*, PREMPT Program TN-25, the Boeing Company, Seattle, Washington (September 15, 1975).

Chapter 18

TEST TECHNIQUES FOR EVALUATION OF INDIRECT EFFECTS

18.1 Introduction

The purpose of this section is to discuss some of the existing test techniques for evaluation of indirect effects on electrical and electronic equipment, and to suggest possible avenues of improvement in some of these test techniques. Tests that might be performed on individual circuit elements are described, but most of the material will deal with tests that might be made upon individual pieces of electronic equipment or upon interconnected electronic subsystems.

Test techniques are still evolving and complete standardization has not yet been achieved. Practices discussed in standards and specifications may not yet address all the necessary aspects of lightning indirect effects and interactions. Ambiguities and conflicts between standards and specifications abound. Often, purchase specifications refer to inappropriate standards and call for tests that have little technical justification and may result in excessively costly test programs.

Some test equipment is available commercially, but most testing involves equipment fabricated in individual testing laboratories. Standards and guides do not yet exist that give specific construction details for test equipment and as a result different laboratories may employ quite different equipment to perform the same general type of test.

18.2 Types of Test

The various types of test that might be performed on aircraft electronic systems are described, in general terms, in the following material. Details on conducting some of these tests are discussed in later sections.

18.2.1 Pin Injection of Transients

Direct injection of transients into the input and output terminals of devices, Fig. 18.1, is an appropriate way of determining whether the equipment will be *damaged* by transients, but is generally not an appropriate method of testing for circuit upset since the low impedance transient generator may adversly load the circuits under test. Furthermore, verification of individual circuit and component damage tolerance to the specified test level becomes less certain due to the multiple current paths in interconnected circuits. The most common type of test, Fig. 18.1(a), involves common mode injection of transients, but differential injection, Fig. 18.1(b) can also be done.

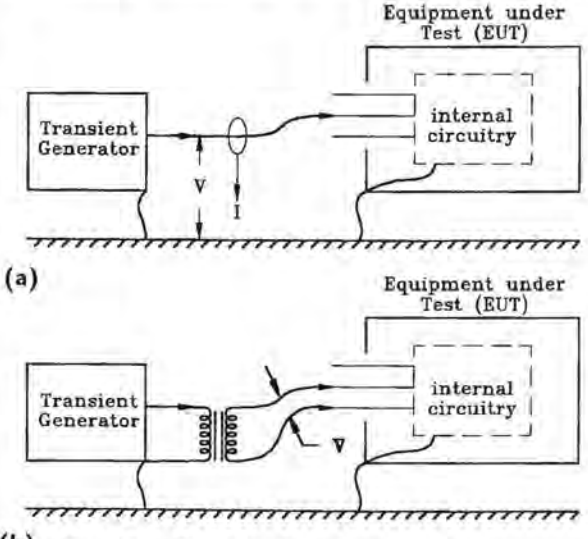

Fig. 18.1 Pin injection tests.
(a) Common mode injection
(b) Differential injection

Tests may involve injection of specified voltages or specified currents, though care must be taken in specifications to avoid wording that can be interpreted as requiring a specified voltage to be developed across a lead that is shorted to ground or requiring a specified current to flow into a lead that presents an open circuit or high impedance. Such erroneous specifications can be avoided by specifying the transient in terms of its open circuit voltage, and its short circuit current, as discussed in §18.5, or in terms of equivalent generator source impedance.

Techniques for pin injection test are discussed further in §18.5.

18.2.3 Transformer Injection

Transformer injection might logically be considered as a simulation of magnetic field effects, but it is useful whenever transient tests must be done on an interconnected system, whatever might be the source

of the transient on the actual system. Such a situation occurs when a system must be evaluated for upset. The test technique, Fig. 18.2, involves a pulse–injection transformer and a suitable pulse generator. Current from the pulse generator is passed through a primary winding on a magnetic core and sets up a magnetic field in that core. If the core is placed around a cable interconnecting two pieces of electronic equipment, the concentrated magnetic field contained in that core induces current or voltage in the interconnecting wiring in a manner very similar to that produced by distributed magnetic flux from an external lightning source.

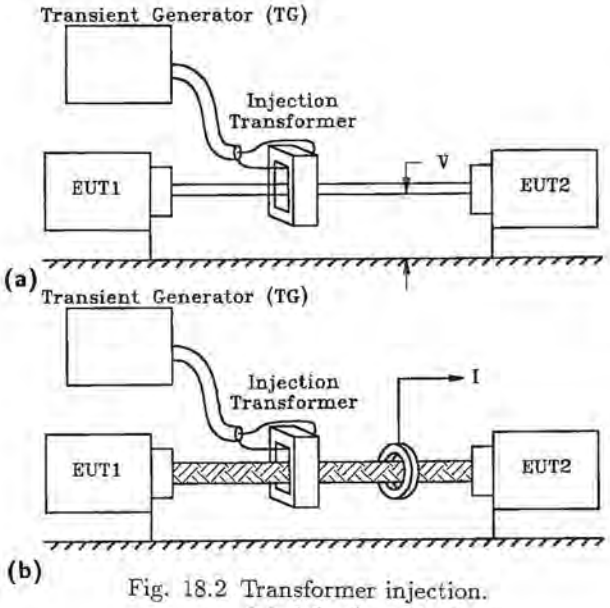

Fig. 18.2 Transformer injection.
(a) Injection of voltage
(b) Injection of current

Tests may involve injection of voltages and currents into unshielded cables, Fig. 18.2(a), or injection of currents into the shields of cables, Fig. 18.2(b). Some tests involve injection of transients into several cables simultaneously, Fig. 18.3. Tests may either be done either at levels appropriate to check for system upset or at higher levels to check for system damage. When injecting current into several cables of an interconnected system there may be problems of how to control the division of current among the various cables. Some of these problems are discussed in §18.7.1, but there are not yet standardized procedures for dealing with interconnected systems.

Procedures for conducting transformer injection tests are discussed further in §18.6.

Transformers work best for injection of current. Injection of voltage transients may be hampered by distortion caused by saturation of the transformer. Factors affecting the performance of injection transformers are discussed in §18.3.

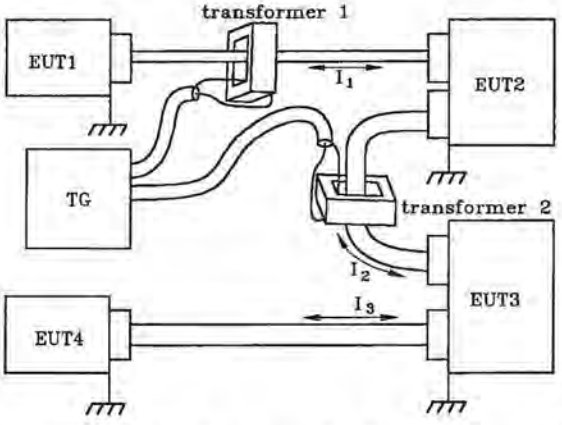

Fig. 18.3 Injection into several cables simultaneously.

18.2.3 Capacitive Injection

For injection of high frequency voltages and currents, capacitive injection, shown in Fig. 18.4, can be considered as a simulation of electric field effects. Discrete capacitors, Fig. 18.4(a), are appropriate for injection into individual conductors. Where connection of a discrete capacitor might upset the circuit, an alternative would be to use a distributed capacitor, Fig. 18.4(b). The distributed capacitor is also appropriate for injection into a group of conductors. Tests may be done either to check for system upset or to check for system damage.

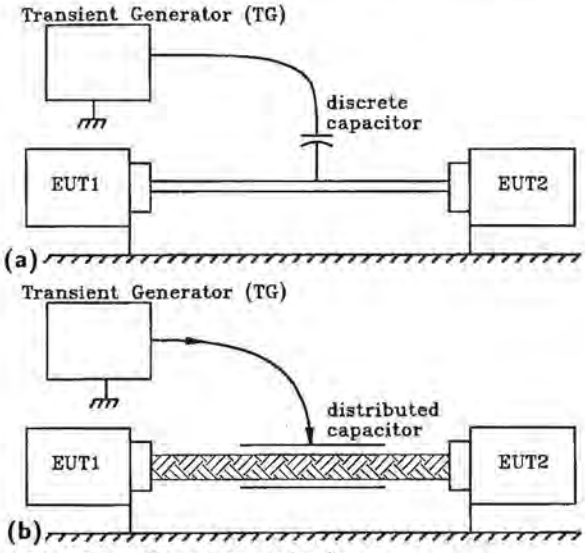

Fig. 18.4 Capacitive injection.
(a) Discrete coupling capacitors
(b) Distributed coupling capacitance

Capacitive injection is frequently used for evaluation of NEMP effects, but has not yet become widely used for evaluation of lightning effects.

18.2.4 Ground Circuit Injection

This might be considered a simulation of the effects of voltage rises that occur in portions of the aircraft when lightning current flows through the aircraft. The technique, illustrated in Fig. 18.5, involves applying a voltage to the case of the EUT and allowing the transient voltages and currents to distribute among the various interconnecting leads. Leads from the EUT that are normally grounded in the vicinity of the EUT are connected to the EUT for the test.

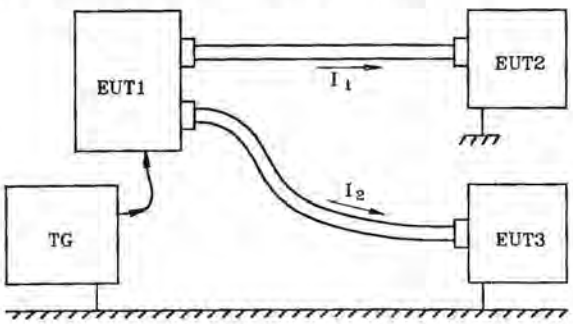

Fig. 18.5 Ground circuit injection.

The ground injection test is one that is generally made on a functioning system, either to check for upset or to check for damage. Test procedures are discussed further in §18.7.

18.2.5 Field immersion tests

Most lightning transient problems arise because of energy being coupled into interconnecting wires. For assessing this interaction the injection tests described above are appropriate. They do not, however, directly check for leakage of electromagnetic fields into the cases housing electronic equipment. These leakage effects can be checked by immersing a case in an electromagnetic field simulator, the elements of the test being shown in Fig. 18.6. Checking for electric field effects, Fig. 18.6(a), involves placing the case between two plates to which a voltage is applied of magnitude sufficient to develop the required electric field. Checking for magnetic field effects, Fig. 18.6(b), requires circulating around the case a current sufficient to generate the required magnetic field.

Some tests require that electric and magnetic fields be developed simultaneously, often with the ratio $E/H = 377$ ohms associated with a wave propagating in free space. Such tests can be made with strip line test cells, as sketched in Fig. 18.7. Test cells can be made large enough to hold several pieces of equipment, along with the necessary interconnecting cables.

Strip line test cells are most appropriate for evaluating coupling to items in free space and are not widely used to evaluate lightning indirect effects inside aircraft, where E/H is, in general, not 377 ohms

Field immersion techniques are discussed briefly in §18.8.

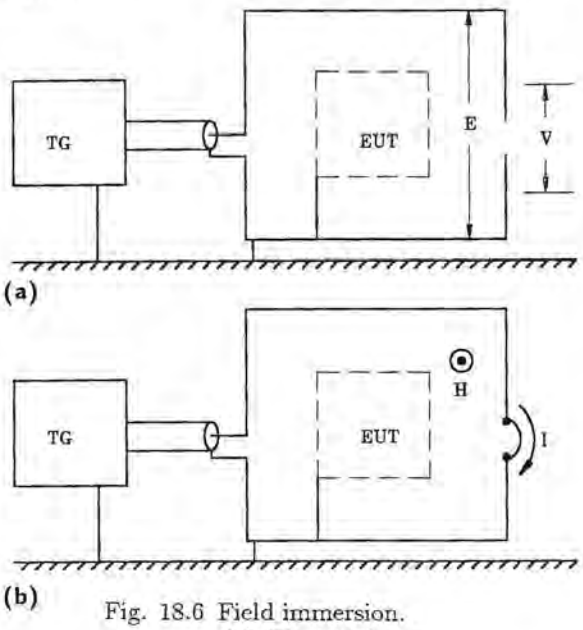

Fig. 18.6 Field immersion.
(a) Electric fields
(b) Magnetic fields

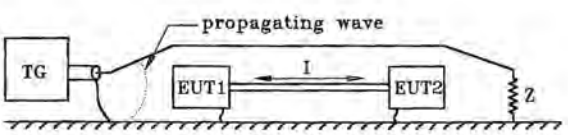

Fig. 18.7 Combined electric and magnetic fields.

18.2.6 Tests on Circuit Elements

Tests are sometimes necessary to evaluate breakdown voltages and currents of individual circuit elements, such as resistors, capacitors, and electromechanical components, or to evaluate interface protection for more complex circuits. Test connections are sketched in Fig. 18.8, but test techniques are beyond the scope of this material. Such tests can also be used to study how active circuits respond to various transients. Examples of such studies are given in [18.1] and [18.2].

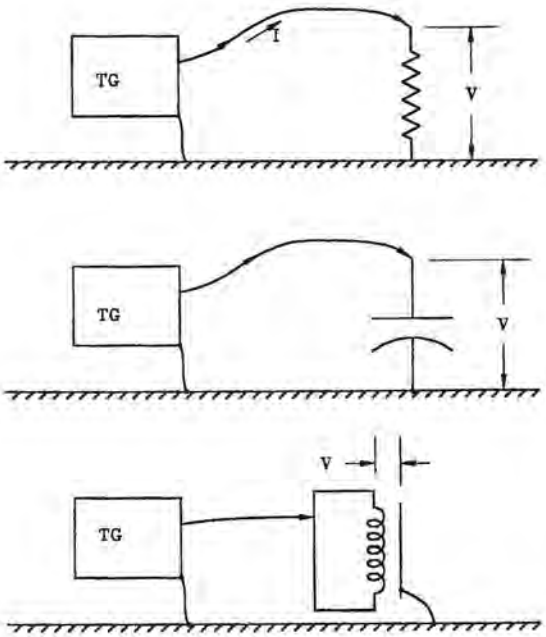

Fig. 18.8 Tests on circuit elements.

Results from such upset studies are generally used during circuit development. They cannot be used in lieu of tests on full systems since there may be interactions among the interconnected circuits that cannot be revealed by tests on individual protoype circuit elements.

18.3 Transient Generators

Most transient generators used for evaluation of indirect effects employ charged capacitors which are discharged into waveshaping circuits. Much of the technology is basically similar to that used in the 1940s and 1950s for radar modulators and described in [18.3]. Some generators for complex waveforms use waveform synthesizers and power amplifiers. Some generators are designed for only single shot operation, though some are designed to produce a series of similar pulses. Very few operate continuously. Almost all generators operate at power levels greatly exceeding those of normal laboratory signal generators.

18.3.1 Capacitor Discharge Generators

Generators may be designed for either unidirectional output with a waveshape approximating

$$E = E_0\left(\epsilon^{-\alpha t} - \epsilon^{-\beta t}\right) \qquad (18.1)$$

or for oscillatory output, with a waveshape approximating

$$E = E_0\left(\epsilon^{-\alpha t}\right)\sin(2\pi f t) \qquad (18.2)$$

Specifications for oscillatory waves sometimes express the waveshape as

$$E = E_0\left[\epsilon^{-(\pi f t/Q)}\right]\sin(2\pi f t) \qquad (18.3)$$

with Q governing the rate of decay of the oscillations. Specifications commonly cite values of $Q = 6$ to $Q = 24$.

Unidirectional transients: Basic unidirectional circuits are shown in Fig. 18.9. That of Fig. 18.9(a) uses series R and C to shape the front of the wave and has an output impedance that is largely capacitive. That of Fig. 18.9(b) uses series L and R to shape the front and has an output impedance that is largely resistive. The component values are approximately those required to produce the long duration voltage wave discussed in §16.6.2. Additional factors governing waveshape were discussed in §6.8.

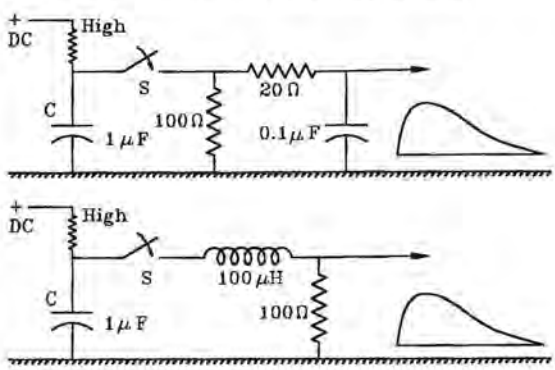

Fig. 18.9 Generators for unidirectional transients.
(a) RC waveshaping
(b) LR waveshaping

Both circuits assume the energy storage capacitor C to be connected to a charging supply through a resistance sufficiently high that the characteristics of the charging supply do not affect the waveshape. They also use a series switch S to connect the energy storage capacitor C to the waveshaping circuit and produce a positive output for a positive charging voltage. Reversing the positions of C and S, Fig. 18.10, results in a negative output for a positive input.

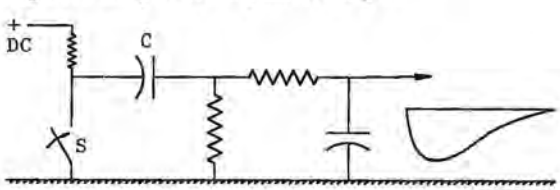

Fig. 18.10 Grounded switch configuration.

Oscillatory transients: Basic oscillatory circuits are shown in Fig. 18.11. The frequency of oscillation is

$$f = \frac{1}{2\pi\sqrt{LC}} \tag{18.4}$$

The decrement of the wave may be controlled either by adding series or parallel resistance or by the residual losses of the circuit and the load to which the generator is connected. Most commonly the intrinsic losses are enough to give $Q \approx 6$ and high enough to make it difficult to achieve $Q = 24$. Taking the output from only a portion of L results in a lower output impedance and makes the effect of load resistance less noticeable, but is achieved at the cost of reduced output magnitude.

The intrinsic output of Fig. 18.11(a) is a cosine wave, not the sine wave commonly cited in specifications. A sinusoidal outout can be obtained by taking the output from the energy storage capacitor, Fig. 18.11(b), using a blocking capacitor C_b, to avoid coupling the dc charging voltage to the output circuit.

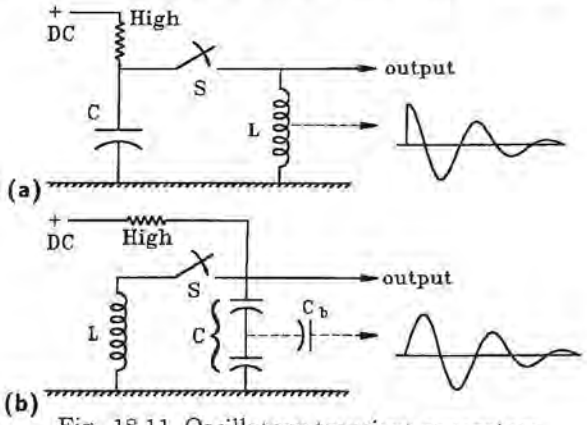

Fig. 18.11 Oscillatory transient generators
(a) Cosine front
(b) Sine front

Questions regarding waveshape: Specifications on oscillatory waveshapes commonly call for damped sine waves (Eqs. 18.2 or 18.3), but actually obtaining a true sinusoidal front is sometimes difficult. Sometimes second order effects come into play, particularly with high frequency generators and result in waveforms in which the highest amplitude of the transient occurs not on the initial half cycle, but on a subsequent half cycle.

A common deficiency in specifications is that they do not give tolerances on allowable waveform distortion. While specifications usually cite Eq. 18.3, that may only represent convention and not be a real engineering requirement. A better specification, from the standpoint of those making tests, would often be

$$E = E_0\left[\epsilon^{-(\pi ft/Q)}\right]\cos(2\pi ft) \tag{18.5}$$

From an engineering viewpoint the important points are probably:

1. Correct maximum amplitude in order to stress the components under test.

2. Correct decrement of the wave, over the first few cycles, in order to maintain stress for sufficient time.

3. Correct frequency, in order to excite internal resonances.

Questions for those preparing specifications or requiring tests are:

1. Does the exact shape of the first quarter cycle make any practical engineering difference?

2. Does the exact shape of the first few cycles make any practical engineering difference?

3. Does a test wave with a front that approximates a cosine wave suffice to satisfy a test requirement that calls for a sine wave defined by Eq. 18.3?

4. Does the fact that a test wave achieves its maximum amplitude later than the first half cycle make any practical engineering difference?

18.3.2 Switches for Generators

Several types of switch can be used for capacitor discharge generators. The best discussions of various types of switche are apt to be found in the older literature, such as [18.1]. In oscillatory circuits, losses associated with switches are one of the major factors governing the Q of the circuit.

Spark gaps: Higher power generators, those operating at voltages greater than $\approx 3 - 5$ kV, commonly use spark gaps as switches. They may be triggered gaps fired by applying a pulse to a trigger electrode, gaps that self-fire when the voltage across the energy storage capacitor exceeds the breakdown voltage or by mechanically closing the electrodes until sparkover takes place.

Gaps in air are the simplest to build, but with high power generators may cause enough audible noise to be disturbing to those nearby. Commercially available triggered gaps are generally enclosed.

Mechanically closed switches: The easiest method of switching is simply to bring two contacts together mechanically until they are close enough for an arc to

form between the contacts. With high power generators the contacts may burn and become ragged, but since operation is quite intermittent, cleaning from time to time with sandpaper or a file is sufficient to restore the switch. Rotating contacts can be used to produce multiple pulses. Immersing the contacts in insulating oil can reduce the arcing that takes place as the contacts close.

Mercury switches: Switches with mercury wetted contacts are useful for low power generators operating at a few hundred volts, largely because the contacts switch cleanly and do not bounce.

Thyratrons: Hydrogen thyratrons, such as the 5C22, are suitable for operation at up to about $10 - 15$ kV and peak currents of several hundred amperes. The miniature 2D21 is suitable up to about 1000 V and peak currents of several tens of amperes. Both will switch in about 20 ns. For operation in oscillatory generators a free–wheeling diode, Fig. 18.12, is necessary.

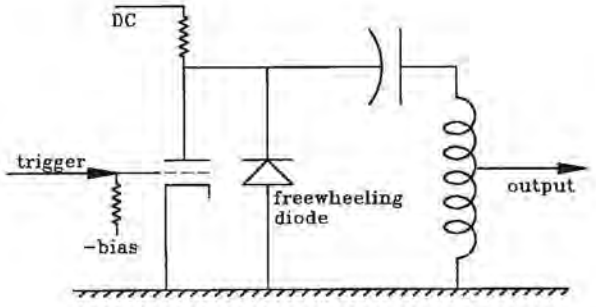

Fig. 18.12 Thyratron switch with free wheeling diode.

Thyristors: Low power, sensitive gate thyristors are suitable for charging voltages up to about 1000 V and discharge currents of several tens of amperes. They may also be operated in series for higher voltages. Switching time can be on the order of 100 ns, though care must be taken to give sufficient gate drive. Freewheeling diodes are necessary for use in oscillatory circuits.

18.3.3 Generators Using Power Amplifiers

Some waveforms are difficult to produce using capacitor discharge circuits, particularly the higher frequency oscillatory waveforms. Capacitors must be small to obtain the high frequency and consequently store little energy. Switches may not change state fast enough and circuit losses may be high, precluding the generation of transients with little damping, high Q.

Some of these problems can be overcome by generating the waveforms at low levels and using power amplifiers to couple the signal to the circuit under test. Amplifier aided circuits are also useful if the intent is to generate square waves or complex waves other than double exponential or damped oscillatory.

Waveform generation: Two basic approaches are possible. One, Fig. 18.13(a), involves direct generation of the desired waveform, followed by linear amplification. The other, Fig. 18.13(b), involves modulation of a sinusoidal input, followed by amplification. Waveforms for (a) may be generated by switching of R, L and C circuits or by digital synthesis with arbitrary waveform generators. Modulation may be either by direct amplitude modulation or by multiplication of a sinusoidal wave by the desired modulating pulse.

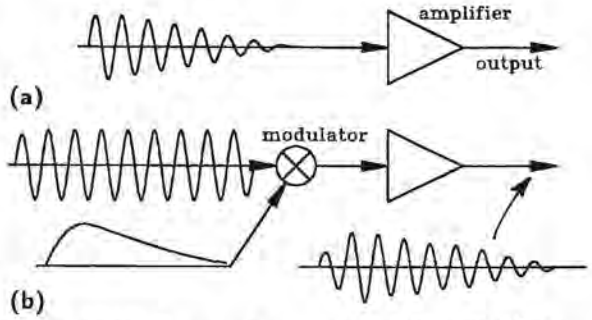

Fig. 18.13 Transient generation with amplifiers.
(a) Direct amplification
(b) Modulation of a sine wave

Amplifiers: Most indirect effects testing calls for high voltage and high current output from the amplifier. While average power levels may be low, peak power levels may be several tens of kilowatts. Amplifiers generally use high voltage vacuum tubes of the type used for broadcast transmitters. Vacuum tube amplifiers are well adapted to delivering high voltages, but many designs are not capable of delivering high short circuit currents. Size, complexity and cost of high power amplifiers are, in any case, great.

18.3.4 Multiple Pulse Generators

Some tests require injection of a group of pulses, most commonly to simulate the effects of the multiple stroke and multiple burst portions of the standardized lightning environment discussed in §5.5.6. If equipment is to be subjected to multiple pulses there may be little point in requiring single pulses as well.

Reasons for multiple pulses: Reasons for injecting multiple pulses, rather than just single pulses or single

pulses repeated slowly, include the following:

1. Multiple test pulses better evaluate the thermal duty on objects under test. Multiple pulses of actual lightning occur sufficiently fast that objects do not cool off between pulses.

2. Some types of system, analog systems in particular, respond to the cumulative effect of rapidly applied disturbances.

3. Some types of device are more susceptible to physical damage at certain points in a cycle. Semiconductors in particular are most susceptible to damage when they are changing from one state to another.

4. Some types of device are more susceptible to momentary upset at certain points in a cycle. Digital devices in particular are most susceptible to upset when they are changing state.

5. Some types of system are more susceptible to upset at certain points in a cycle when interface circuits are sampled or refreshed at periodic intervals.

Sometimes the multiple pulses can be generated by using low impedance charging networks so that a single energy storage capacitor can be charged and discharged rapidly. This may be difficult to do, particularly at high power levels, since instantaneous charging currents of hundreds or thousands of amperes may be drawn from the power mains feeding the laboratory.

An alternative technique is to use many energy storage capacitors, charge them slowly, and then discharge them one by one into the circuit under test.

Random pulsing: Questions regarding total number of pulses and repetition rate are still being resolved. The most common practice for multiple stroke tests presently requires injecting 24 pulses into the circuit, with the pulses spaced over a period not to exceed two seconds. Some suggestions have been made that the pulses be irregularly distributed to avoid any problems of synchronization with computer clock cycles. The term random has been used, but *random* implies a certain mathematical distribution, and raises the question of how often the tests must be repeated to obtain a truly random distribution.

Most commonly the concern is really only that the pulses not be precisely spaced in time, or precisely synchronized to any particular digital clock frequency. It is best to avoid the term *random* and require only that the pulses be *distributed* over a certain period of time.

The matter may not be of critical importance since spark gaps in generators may, without any special attention, jitter, or switch irregularly, on the scale of microseconds, even though the basic switch timing is fixed on a scale of milliseconds.

Standards do not presently deal with the question of spacing between pulses or the degree of randomness. If the matter is of actual importance, it should be discussed in the test plan.

18.3.5 Source Impedance of Generators

Present standards specify certain open circuit voltages and short circuit currents, but do not explicitly deal with the required source impedance of transient generators. Taking Table 16.2 as an example, the *implied* generator impedances are as follows.

1. For Waveform 1 (Fig. 16.12), which is representative of coupling by IR voltages and apertures, the impedance should be in the range 0.1 - 0.3 ohms.

2. For Waveform 2, which has a shape proportional to the derivative of Waveform 1 and is representative of voltages induced magnetically into unshielded circuits, the impedance should be 5 ohms.

3. For Waveform 3, which is somewhat typical of voltages and currents actually induced into aircraft wiring (perhaps superimposed on a waveform like 1 or 2), the impedance should be 25 ohms.

4. For Waveform 4, which is somewhat typical of voltages and currents induced onto shielded wiring, the impedance should be 5 ohms.

5. For Waveform 5, which is intended to represent the effects of current diffusing and redistributing through a resistive aircraft structure, the impedance should be on the order of 0.5 ohms.

6. The specifications given in Table 16.3 for oscillatory burst waveforms imply a source impedance of 100 ohms, an impedance different from the 25 ohms implied in Table 16.2.

The impedances so defined represent only the ratio of open circuit voltage to short circuit current and should not be taken as implying that the impedance must be resistive. Most commonly, the impedance of

practical generators will be inductive and short circuit current will have longer front and decay times than open circuit voltage.

Present standards discuss generator impedance, or *implied* generator impedance, in terms of the type of *waveshape* to be applied, with certain waveforms having been chosen in an attempt to address the type of *coupling mechanism* involved. As examples, Waveform 2 is primarily intended to address magnetic field coupling while Waveform 5 is intended to address voltage rises in the structure of the aircraft.

Linking generator impedance to waveforms is only an indirect method of addressing the generator impedance needed to evaluate the effects of different coupling mechanisms. As the art of indirect effects testing evolves, it might be better practice to discuss impedance directly in terms of the type of coupling mechanism being evaluated.

18.4 Injection Transformers

The most common method of performing indirect effects tests involves the use of injection transformers. Two basic modes of operation are shown in Fig. 18.14. One (a) involves injection of current into a shorted conductor and the other (b) involves injection of voltage into an open circuited wire. Most commonly the shorted conductor is provided by an overall cable shield grounded at each end.

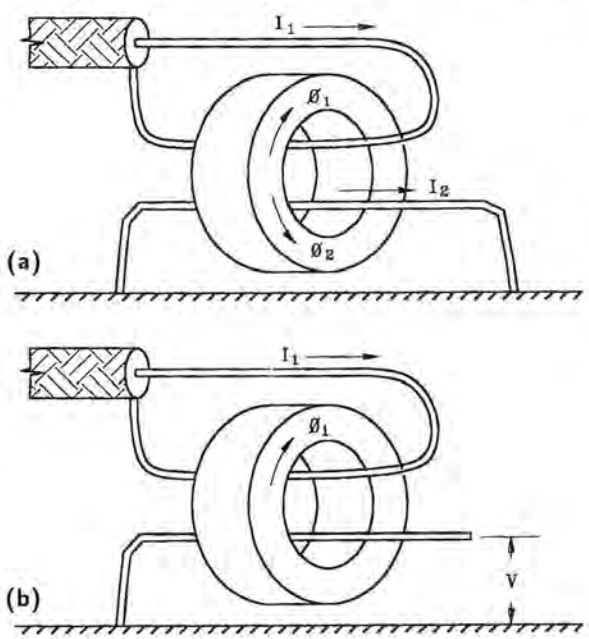

Fig. 18.14 Transformer injection of transients.
(a) Injection of current
(b) Injection of voltage

Operation follows the same physical laws governing any magnetic circuit, but the mode of operation is different in two respects from that normally involved in transformers. First, since the purpose is to inject transients into interconnecting wire bundles, there is a practical limit to the number of turns that can be placed on the core of the injection transformer. Most operation involves passing the bundle through the core only once, or at most a very few times, unlike conventional transformers which employ windings of many turns. Second, the transformer is generally energized with a driving current, unlike conventional transformers which are usually energized by voltage sources.

Each current carrying conductor passing through the magnetic core sets up a magnetic flux. When injecting current into a shorted conductor the induced current tends to have the same waveshape as the driving current and the two components of flux tend to cancel, leaving a small net magnetic flux in the core. When injecting voltage into an open circuited conductor there is no cancelling flux. The amount of voltage that can be induced is limited by the amount of flux that can be supported by the core.

18.4.1 Basic Principles of Magnetic Circuits

An elementary magnetic circuit is shown in Fig. 18.15. Quantities that define the core include the length of the magnetic path, l, and the cross sectional area, A, of the core. If the core has a large cross section, the average length measured around the center of the core is the quantity of interest. Scientific usage generally uses rationalized units with dimensions in meters. Specifications relating to magnetic material commonly use unrationalized units with dimensions in centimeters. Inches are frequently used in engineering design.

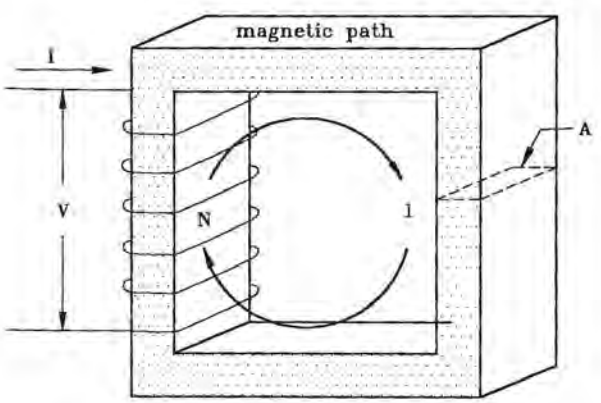

Fig. 18.15 Factors governing magnetic circuits.

Total magnetizing force: The total magnetizing force around the length of the core, MMF, may be given in ampere–turns, NI or in gilberts, $0.4\pi NI$. If there is an air gap in the magnetizing circuit, a large portion of the total magnetizing force may be needed to force magnetic flux across the air gap, even though the length of the air gap is very small compared to the total distance around the length of the core.

Magnetizing force per unit length: The magnetizing force acting on the magnetic material is

$$H = \frac{NI}{l} \tag{18.6}$$

and may be measured in ampere–turns per meter, ampere–turns per centimeter or in ampere–turns per inch. In material specifications it is commonly measured in oersteds or gilberts per centimeter.

$$H_{\text{gilberts/cm}} = \frac{0.4\pi NI}{l} \tag{18.7}$$

Total magnetic flux: Total magnetic flux may be measured in webers, lines (or maxwells) or in kilolines.

$$1 \text{ weber} = 10^8 \text{ lines} = 10^5 \text{ kilolines} \tag{18.8}$$

Flux density: Flux density may be measured in teslas (webers per square meter), gauss (or lines per square centimeter) or in lines (or kilolines) per square inch. In round numbers, a core made of grain oriented silicon steel can support a maximum flux density of about 100 kilolines per square inch or 16 000 gauss. A ferrite core can sustain a maximum flux density of about 4000 gauss.

Relations between units:

$$\begin{aligned}
1 \text{ gilbert} &= 1.257 \text{ ampere–turns} \\
1 \text{ oersted} &= 1 \text{ gilbert/cm} \\
1 \text{ oersted} &= 0.495 \text{ ampere–turns/in} \\
1 \text{ oersted} &= 1.257 \times 10^{-2} \text{ ampere–turns/m} \\
1 \text{ tesla} &= 1 \text{ weber per meter}^2 \\
1 \text{ tesla} &= 10^4 \text{ gauss} \\
1 \text{ tesla} &= 1.550 \times 10^{-5} \text{ lines/in}^2 \\
1 \text{ tesla} &= 1.550 \times 10^{-2} \text{ kilolines/in}^2 \\
1 \text{ kiloline/in}^2 &= 155 \text{ gauss}
\end{aligned}$$

Voltage vs. flux: The relations between voltage, V, and flux, ϕ, are

$$V = N\frac{d\phi}{dt} \tag{18.9}$$

$$\Delta\phi = \frac{1}{N}\int V dt \text{ webers} \tag{18.10}$$

$$\Delta\phi = \frac{10^8}{N}\int V dt \text{ lines} \tag{18.11}$$

Developing a transient voltage of given volt–second product in a transformer thus *absolutely* requires a given net change in magnetic flux. If the core cannot sustain the requisite flux, the voltage cannot be generated. As an example, a rectangular pulse of voltage, Fig. 18.16(a) with an amplitude of 100 volts and a duration of 10 μs, would have a volt–second product of 10^{-3}. Developing this voltage on a wire passing through an injection transformer one time would require the flux in the core to change by 10^5 lines, or 100 kilolines. If the core were of a ferrite material, one in which the residual flux from previous pulses is small, the cross sectional area would have to be about 25 square centimeters.

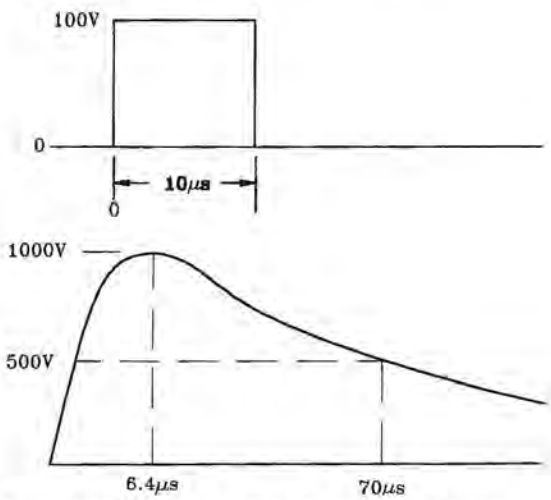

Fig. 18.16 Representative transient voltages.
(a) $V \cdot t = 10^{-3}$ volt-seconds
(b) $V \cdot t = 9.47 \times 10^{-2}$ volt-seconds

For a double exponential wave defined as

$$V = V_0\left[\epsilon^{-\alpha t} - \epsilon^{-\beta t}\right] \tag{18.12}$$

the total volt–second product is

$$\int_0^\infty V = V_0\left[1/\alpha - 1/\beta\right] \tag{18.13}$$

Developing on a single turn a voltage with a peak amplitude of 1000 volts, a front time of 6.4 μs and a time to half–value of 70 μs ($V_0 = 1093$, $\alpha = 11\ 354$, $\beta = 647\ 265$, volt–second product of 0.0947)

would require the flux to change by 9466 kilolines. A ferrite core would need a cross sectional area of about 2400 square centimeters, or about 350 square inches, a large core indeed!

Voltage vs current: A given magnetic flux in a transformer core is associated with a given magnetizing force or, for a fixed number of turns, a given magnetizing current. It follows that developing a pulse of voltage, Fig. 18.17(a), having a certain volt–second product, requires the current to change from an initial value, zero in Fig. 18.17(b), to a final value. Which comes first, voltage or current is somewhat a matter of semantics. One can say that a magnetic core has been carried to saturation by excessive magnetizing current, but it is generally most helpful to consider that a core has been carried to saturation by an excessive product of voltage and time.

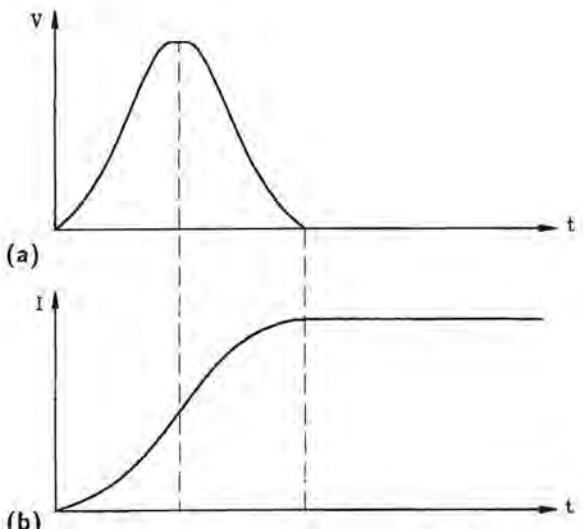

Fig. 18.17 Current as the integral of voltage.
(a) Voltage
(b) Current

Since most exciting current pulses applied to injection transformers eventually decay back to zero, it follows that a collapsing current will be associated with a voltage of polarity opposite to that which was associated with the rise of current. Fig. 18.18 illustrates the point. The voltage pulse will be underdamped with the positive (A_1) and negative (A_2) lobes having equal volt–second products.

Phrased another way, a double exponential current pulse passed through the primary of a pulse injection transformer *cannot* induce a unidirectional voltage pulse of the same waveshape in a secondary winding.

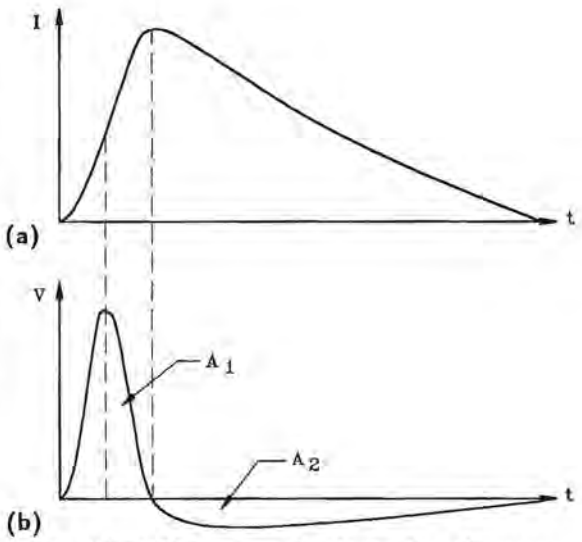

Fig. 18.18 Voltage as the derivative of current.
(a) Current
(b) Voltage

B–H loops: The magnetic characteristics of a magnetic material can be defined by its $B - H$ loop, Fig. 18.19. B and H are, respectively, flux per unit cross-sectional area and magnetizing force per unit length of path. For a transformer core of specific dimensions the loop could be defined in terms of ϕ and NI.

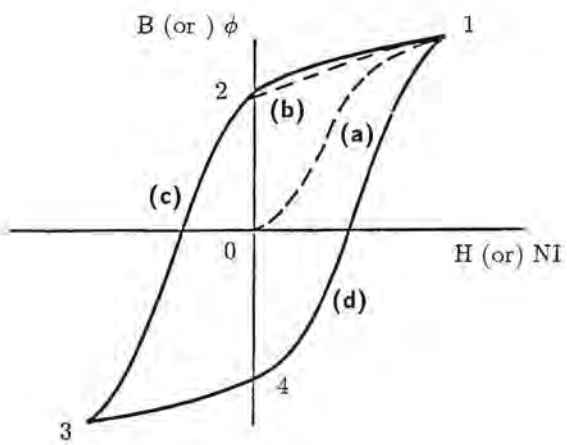

Fig. 18.19 $B - H$ loop.

For an initially unmagnetized core a current pulse might carry the magnetic state along path (a) from point 0 to point 1. Removing the current would allow the magnetic state to follow path (b) to point 2. Assuming that point 1 represents a flux density of 16 kilolines per square centimeter (16 000 gauss), a

core cross-sectional area of 592 cm^2 (92 in^2) would be needed to support the aforementioned 1000 volt double exponential pulse. In the context of indirect effects testing, that represents a *very* large transformer core and explains why it is difficult to use transformer coupling techniques to develop high amplitude, long duration voltages on open-circuited wires.

Multiple pulses: The problems of core size are compounded when multiple pulses are involved. If the first pulse carried the core along path (a) to point 1, a second pulse of the same magnitude and polarity would have to carry the flux along path (b) to a point far higher than point 1. The core would become saturated, the magnetizing current would become limited by the characteristics of the pulse generator and the desired voltage pulse would not be developed.

Full use of a transformer core for injection of multiple pulses would require pulses of opposite polarity and volt-second product, though not necessarily of equal magnitude or waveshape. The first pulse in a series would carry the flux to point 1, the second would carry it to point 3 and the third would again carry it to point 1.

Measurement of B–H loops: $B-H$ loops may be measured by exciting N_1 turns on a primary winding and allowing voltage to be induced in a second winding of N_2 turns, as shown in Fig. 18.20. A signal proportional to I (and hence to $N_1 I$ is applied to the horizontal input of an oscilloscope and a signal proportional to the integral of e_1 applied to the vertical input.

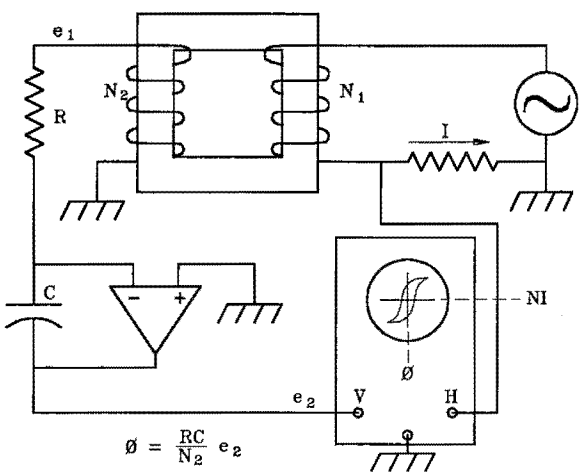

Fig. 18.20 Measurement of $B-H$ loop.

Examples of B–H loops: Figs. 18.21 and 18.22 show examples of $B-H$ loops as measured with the above technique. Fig. 18.21 refers to a ungapped toroidal core wound from grain oriented silicon steel of 0.36 mm (0.014 in) thickness. Fig. 18.22 refers to a core made from U–shaped ferrite blocks joined with no intentional air gap. The ferrite core provides a more linear $B-H$ characteristic than the steel core and has lower residual flux at zero magnetizing force. Other things being equal, it would be better than the steel core at transforming multiple pulses.

Ungapped steel cores will generally have a large $B-H$ loop and a large remnant flux. A gap in the core would reduce the remnant flux and make the $B-H$ loop more like that of Fig. 18.22. Some ferrite cores have a large remnant flux and some do not; it depends on the type of core material. Powdered iron cores would have a small remnant flux.

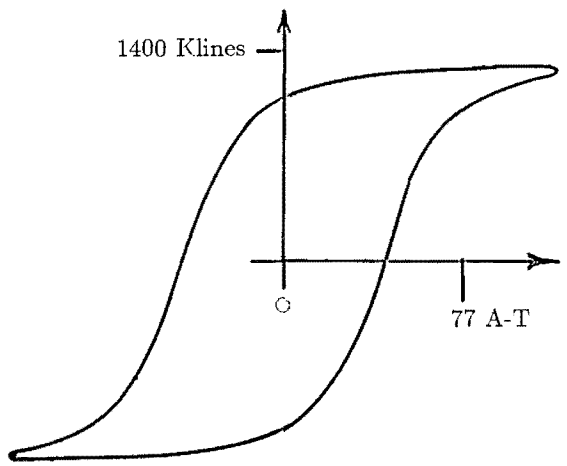

Fig. 18.21 $B-H$ loop of an ungapped steel core.

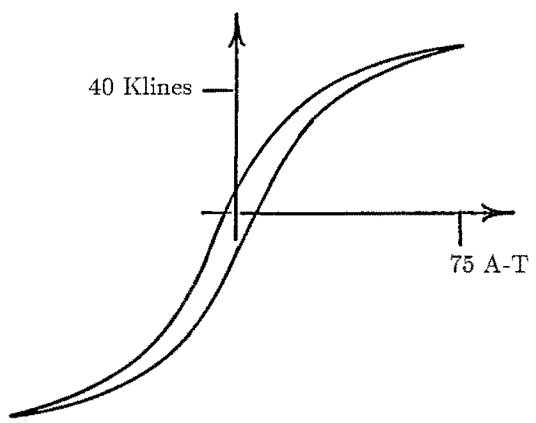

Fig. 18.22 $B-H$ loop of a gapped ferrite core.

Saturation effects when injecting current: In an *ideal* situation, Fig. 18.14(a) the induced current would be equal to the injected current (equal turns assumed)

and have the same waveshape. Under these *ideal* conditions there would be no limit to the amount of *current* that could be injected by a core.

In practice, two factors, shown in Fig. 18.23, act to limit the amount of current that may be transformed. One is brought about by the resistance of the conductor upon which current is induced. Current through that resistance develops a voltage which leads to an increase in core flux, even though the induced voltage may be distributed along the conductor and not measurable. The other is that the magnitude of the induced current will be less, by virtue of leakage inductance, than the inducing current, irrespective of the resistance of the conductor. The net result is that ϕ_2 will always be less than ϕ_1 and will eventually decay to zero. For sufficient I_1 the net flux in the core can increase until the core is saturated, at which point transformer action ceases.

Since long conductors have more resistance than short conductors, it follows that it is harder to induce current on long conductors than short ones.

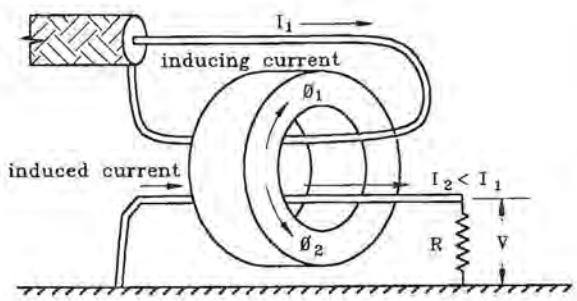

Fig. 18.23 Effect of conductor resistance on core flux.

18.4.2 Equivalent Circuits of Injection Transformers

Some of the parameters affecting the response of a complete current injection system are shown in Fig. 18.24. These include the capacitance of the storage capacitor; the inductance of the leads connecting the storage capacitor to the transformer; the primary, secondary, and leakage inductances of the transformer; and the inductance and resistance of the conductor under test.

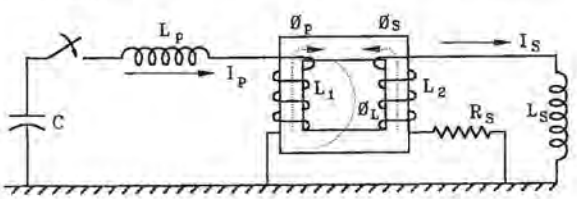

Fig. 18.24 Factors affecting performance of an injection transformer.

The characteristics of the injection transformer are among the most important properties. These parameters relate to the primary and secondary inductances, the flux in the transformer core, and the proportion of flux produced by current in the primary that links the secondary winding. The difference in these two fluxes is the leakage flux, and it is the leakage flux that prevents the secondary current from being as large as the primary current.

Determining inductance: For a given transformer, the primary and secondary magnetizing inductances may either be measured on an inductance bridge or be determined by discharging a known capacitor through the winding and observing the frequency of oscillation. The magnetizing inductance can also be determined from the average slope of the $B - H$ curve:

$$L = N\frac{d\phi}{dI} \tag{18.14}$$

Mutual inductance, which is related to the degree of coupling between windings, can be determined by connecting the primary and secondary windings in series, first so that the two magnetic fields set up are in the same direction (series aiding) and then so the magnetic fields are in opposite directions (series bucking), as shown in Fig. 18.25(a).

Equivalent circuit of transformer: Knowing the primary, secondary, and mutual inductances, one can produce an equivalent circuit of an injection transformer. One such circuit is the Pi circuit of Fig. 18.25(b). If the number of turns on the primary winding is equal to the number on the secondary winding (the usual case), the circuit reduces to that of Fig. 18.25(c). The basic factor governing the current that can be induced is the ratio of the series leakage inductance to the shunt magnetizing inductance. Leakage inductance is not particularly affected by saturation of the transformer, but saturation does affect the magnetizing inductance. When the core saturates, the shunt impedance drops to a low value and diverts current from the conductor under test.

Complete equivalent circuit: A complete equivalent circuit, Fig. 18.26, includes the parameters of the transient generator and the conductor under test, and possibly the stray capacitance of the injection transformer.

For a typical small injection transformer, Fig. 18.27(a), the measured parameters were as shown in Fig.18.27(b), indicating that an equivalent circuit would be as shown in Fig. 18.27(c).

Effects of multiple turns: The transformers are not constrained to be operated with only one turn on each

winding or, for that matter, with the same number of turns on the two windings. Figs. 18.28 and 18.29 show qualitatively some of the ways in which turns on one winding or the other affect the results if the number of turns on the two windings are not equal. For instance, if the conductor under test is looped through the core several times, a given excitation on the transformer will produce less short circuit current, more open circuit voltage, and a decrease in the frequency of the natural oscillatory mode of the cable under test. If there are more turns on the primary, there will be more short circuit current, less open circuit voltage, and a decrease in the frequency of the natural oscillatory mode of the pulse generator. There will also be a longer rise time of the current and voltage pulses.

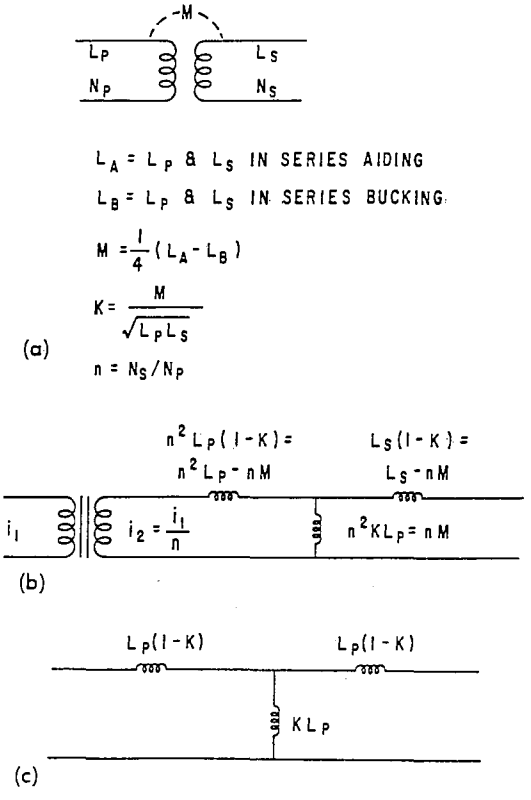

Fig. 18.25 Development of equivalent circuits.
(a) Basic transformer equations
(b) Equivalent circuit referred to secondary
(c) Circuit if $N_p = N_s$ and $L_p = L_s$

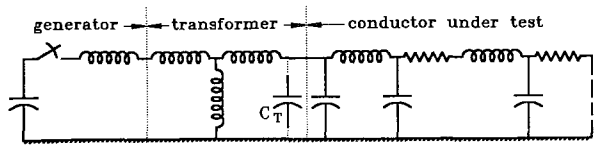

Fig. 18.26 Complete equivalent circuit of a conductor under test.

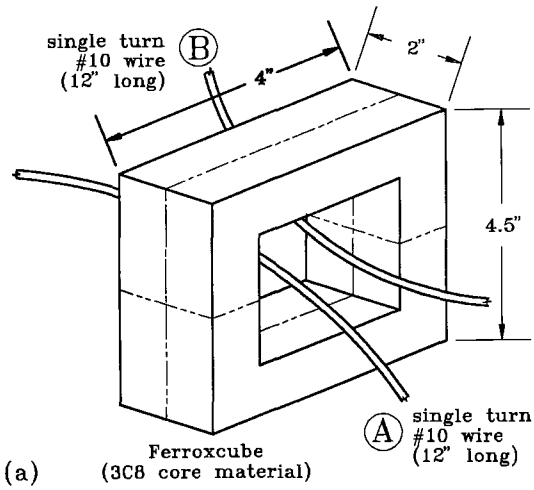

$L_P = L_S = 8.3\,\mu H$
$L_A = 28\,\mu H$
$L_B = 0.3\,\mu H$
$M = 6.93\,\mu H$
$K = 0.83$
$L_P(1-K) = L_{P_S}(1-K) = 1.38\,\mu H$
(b) $KL_P = 6.93\,\mu H$

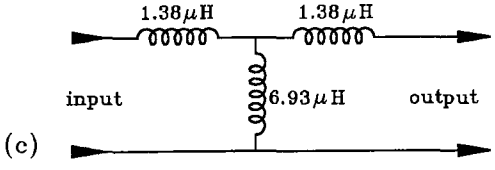

Fig. 18.27 Equivalent circuit of a typical transformer.
(a) Core dimensions
(b) Measured and derived quantities
(c) Equivalent circuit

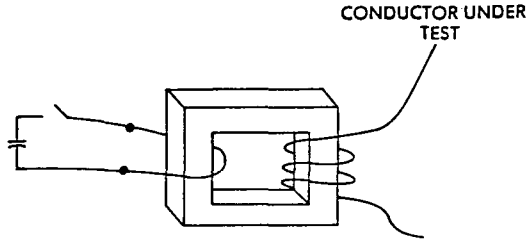

Fig. 18.28 Effect of more turns on secondary.
- Less short circuit current
- More open circuit voltage
- A decrease in the frequency of the natural oscillatory mode of the cable under test

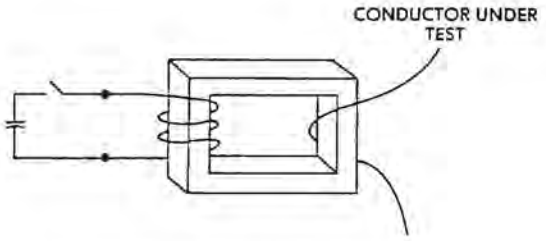

Fig. 18.29 Effect of more turns on primary.
- More short circuit current
- Less open circuit voltage
- A decrease in the frequency of the natural oscillatory mode of the cable under test
- A longer rise time of the current pulse

18.5 Measurements

Indirect effects testing involves high frequencies, high voltage and high current. A few notes on measurement techniques follow. Additional notes on measurement techniques are given in [18.4].

Oscilloscopes: Measuring oscilloscopes should have sufficient bandwidth, on the order of 100 MHz or greater. They should also be well shielded against interference from the surge generators and the circuit under test. Frequently this requires that they be housed in a shielding enclosure and physically as far from the test setup as possible. Techniques were previously discussed in §13.4.3 and Fig. 13.20.

Voltage probes: Conventional high impedance voltage probes are limited to input voltages of about 1000 volts and are somewhat susceptible to pickup of noise voltages. Since impedances of the circuits under test are generally low, suitable voltage probes can be made from carbon resistors, as sketched in Fig. 18.30. Wire wound resistors should be avoided because of excessive inductance. Total resistances of several thousands of ohms are satisfactory, distributed among several resistors, with voltage on individual 1/2 watt carbon resistors limited to about 1000 volts. Instantaneous power dissipated in the resistors may be high, but the average power is low.

Current transformers: Most measurements of current are made using current transformers. Transformers that are well shielded and that have wide bandwidths are commercially available, but transformers sufficiently suitable for many purposes can also be custom wound on toroidal magnetic cores, as shown in Fig. 18.31. The secondary winding should be uniformly wound around the core and the conductor upon which measurements are made should be kept near the center of the core. Transformers can also be made using split cores. These simplify insertion onto conductors, but have poorer low frequency response. A good discussion of the factors affecting the response of current transformers appears in [18.5].

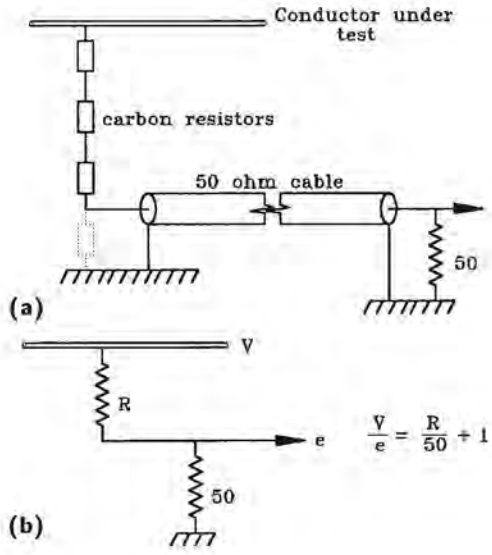

Fig. 18.30 Resistive divider for measurement of voltage.
(a) Circuit
(b) Evaluation of ratio

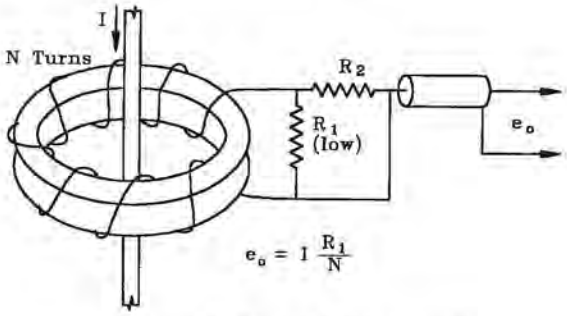

Fig. 18.31 Current transformer.

Low frequency response: An equivalent circuit of a current transformer is shown in Fig. 18.32(a). Primary current induces a voltage in the windings proportional to the derivative of the current. Because of the inductance, L, of the transformer windings the current applied to the viewing resistor, R, is initially proportional to the integral of the voltage and thus to the input current. The resistance, however prevents perfect integration and the result is that the output voltage gradually departs from the true waveshape of

the input current. Transformer specifications generally give this departure as the rated *droop*, Fig. 18.32(b). Care must be taken that the droop is not excessive for the pulse waveshape being observed. Split core transformers, particularly the small clamp–on transformers illustrated in Chapter 13, Fig. 13.18(a), are prone to have excessive droop.

Rogowski coils: If pulse length and amplitude are such that conventional current tranformers are unsuitable, Rogowski coils are an alternative. A Rogowski coil, Fig. 18.33, consists of a helical coil of wire surrounding the current to be measured.

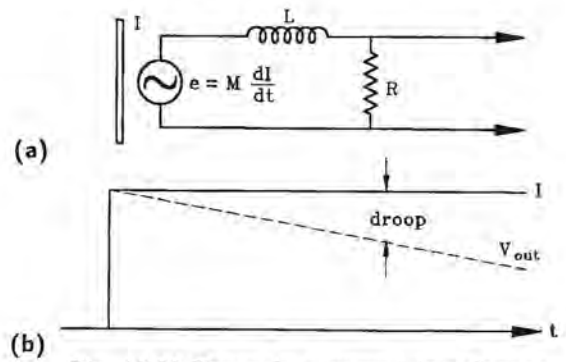

Fig. 18.32 Droop in a current transformer.

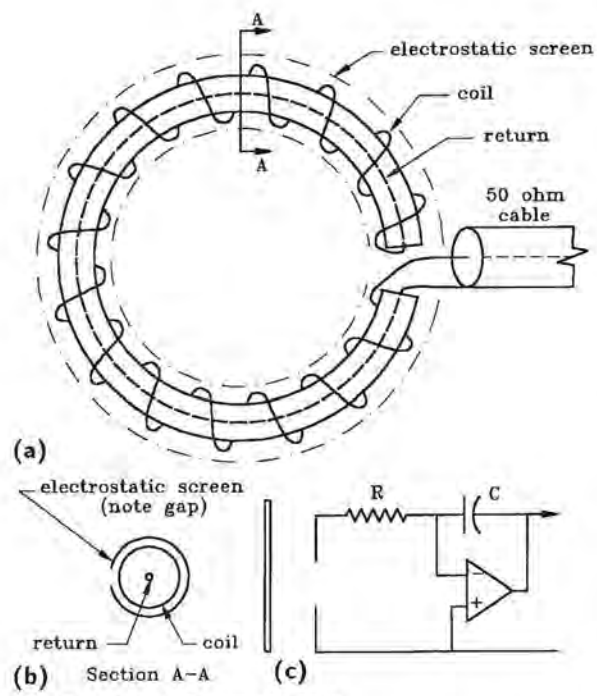

Fig. 18.33 Rogowski coil.
(a) Configuration of windings
(b) Configuration of shield
(c) Active integrator

The output from a Rogowski coil is proportional to the derivative of current and must be integrated to yield the true waveshape. Passive *RC* integrators are sometimes suitable, particularly for rapidly changing transients, but in general, active integrators, Fig. 18.33(c), are better.

Rogowski coils are characterized by a mutual inductance, M, related to the dimensions of the coil.

$$M = n\left(\frac{\pi d}{a}\right)^2 \text{ H} \qquad (18.15)$$

where

n = turns per unit length
a = radius of coil
d = diameter of coil form

For a given coil, and an integrator time constant of RC, the output is

$$e_o = \frac{M}{RC} I \qquad (18.16)$$

Resistive shunts: Resistive shunts, particular those having a coaxial construction, are useful for measuring the short circuit current from a generator and for calibrating current transformers and Rogowski coils. They can seldom be used for measuring current induced into conductors under test because they must be operated with one terminal connected to ground.

18.6 Procedures for Pin Injection Tests

Pin injection tests are performed primarily to check for damage tolerance. Checking for circuit upset is difficult, principally because a direct connection of a generator to a wire drastically changes the topology of the circuit. How the tests stress internal components depends on several factors, but two generic configurations predominate; ungrounded and grounded systems.

Whether or not the types of voltage applied to the pins duplicate the types of voltage observed in service is a question that may be beyond the scope of this discussion. Most commonly the tests are made with standardized waveforms and should be viewed only as an *evaluation* of the effects of lightning, not as a *duplication* of the effects.

18.6.1 Ungrounded systems

This situation is illustrated in Fig. 18.34. The case of the equipment under test, EUT, is grounded, but internal circuits are left ungrounded, including ground planes or ground buses if they are such that there is not a permanent connection between them

and the equipment case. If internal ground circuits are, in fact, permanently connected to the case, then the configuration is not applicable.

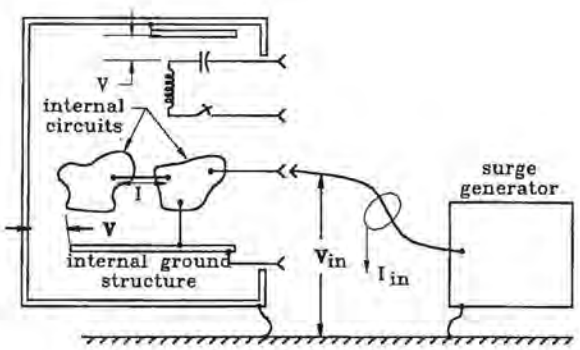

Fig. 18.34 Pin injection on an ungrounded system.

The test procedure is:

1. Ground the case of the EUT to the local ground system.

2. Remove all cables connecting the EUT to other equipment, except possibly those supplying power to the unit.

   Questions regarding the input power leads, and whether the EUT should be powered, deserve special attention. If the voltage of the system power is greater than about 10% of the applied voltage, or if the unit includes solid state devices, it is best to make tests with the EUT powered since the power connections can change the way that test current distributes in the EUT. A full discussion is, however, beyond the scope of this chapter.

3. Adjust the power level of the surge generator and verify that open circuit voltage is of the correct magnitude and waveshape. Once set, the power level of the generator should remain fixed for all tests at that nominal level.

4. Verify that the generator has the correct source impedance.

   This may be done by connecting to the output a resistor equal to the specified generator impedance and observing that the voltage under load drops to half the open circuit voltage. It may also be done by shorting the output and observing that the specified short circuit current flows.

5. If applicable, close switches or relays to connect internal circuit components to the pins of the connector under test. Temporary wiring across relays and switches is allowable.

6. Apply the specified surge to each pin, one pin at a time.

   Internal connections between pins may make some of the tests redundant, but connecting all pins together and applying the surge to all pins simultaneously is not generally permissible, except for very simple circuits.

7. Monitor and record applied voltage and current.

   Current should be small unless breakdown of insulation takes place and voltage should not be greatly different from the open circuit voltage. This observation does not apply to circuits fitted with protective devices or filters. These are discussed in §18.5.3.

   Permanent records should be made of the initial magnitude and waveshape, but making permanent records to document each and every applied pulse would probably be superfluous, unless breakdown is observed.

8. After the test has been completed, energize the equipment, observe whether operation is normal and, if not, record any abnormalities.

Number and polarity of applied surges: These should be discussed in a test plan, but testing practice is still evolving and there is not yet a consensus of opinion among laboratories and organizations as to best practice. Suggestions have been made that each pin should receive 10 pulses of each polarity for each of the specified test waves.

Care should be taken in specifications that the test does not become unwieldy. The product of two polarities, X pulses per pin, Y pins and Z waveforms can become excessive.

Type of stress applied: This type of test is most commonly done by applying common mode voltages and primarily stresses insulation between components and case, V as shown in Fig. 18.34. Some current, I in the figure, may flow through internal circuit components, but it will be small because there is no direct metal connection to the return side of the generator.

Application of common mode voltage most nearly duplicates the condition where all wires entering the EUT originate at a common point.

DC and low frequency hipot testing: An evaluation should be made of the type of device under test and the possible failure modes. In many cases, conducting a series of tests with all the various surge waveshapes specified in the standardized lightning environment may represent unnecessary work and expense. Conventional DC and low frequency high potential tests may be all that is actually needed, particularly if only electromechanical devices are involved.

18.6.2 Grounded systems

This situation is illustrated in Fig. 18.35(a). The case of the EUT is grounded and internal ground circuits as well. The ground connection may either be made internally, path *A*, if that is the normal mode of connection, or externally, path *B*. If path *A* is normally the only mode of grounding, then the tests should include injection onto the ground pin in order to determine whether the internal ground path can carry the surge current. An external ground path should be applied only after making the tests on the ground pin.

An external ground connection should normally be made to the local ground system and not, as in Fig. 18.35(b) through impedance to a remote ground point. If a remote ground is actually used on the EUT, then the matter deserves special study.

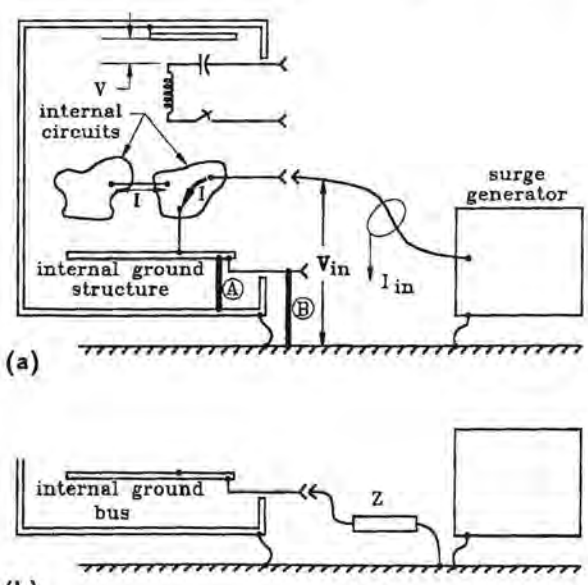

Fig. 18.35 Pin injection on a grounded system.

The test procedure is basically the same as in §18.5.1. Tests should be applied to each pin, one pin at a time, with the possible exception of any pin connecting the internal ground bus to an external local ground. If the ground bus is grounded internally, pulses should still be applied to grounded pins, in order to verify that ground wiring is capable of carrying surge currents.

Type of stress applied: This type of test stresses insulation between components and case, but also allows current to flow through components to the ground bus, *I* as shown in Fig. 18.35, and thus may provide a thermal stress to components as well. Whether or not such current does flow depends on the type of circuit and may depend on whether the system is powered or not.

For some types of circuit element it may make little difference whether or not the internal ground buses are grounded. Such may be the case with the inductive device shown at the top of Fig. 18.34. If a EUT is to be tested under both conditions, §18.5.1 and §18.5.2, it is probably better to repeat the tests on such components, rather than trying to analyze whether the tests might be redundant. There may be internal circuit paths not readily revealed by inspection.

Effects of circuit loading: Circuit loading may result in the voltage actually developed on a pin being lower in magnitude than observed under open circuit conditions. This is a normal response and the power level of the surge generator should not be adjusted to compensate. It is because the circuit may load the generator that impedance of generators is controlled.

18.6.3 Protected Circuits

Some circuits, as in Fig. 18.36, may be fitted with filters and others may be fitted with circuit protective devices, such as spark gaps, metal oxide varistors or protective diodes. As a general practice, these should be left connected during the test since one of the reasons for making tests is to verify that the protective devices can withstand the surge currents that flow when the devices operate.

Status of protective devices: Even if the EUT appears to function normally after the test, some type of inspection should be made to verify that the protective devices have not been damaged. A visual inspection may be sufficient, but if the test currents are known to have approached the limits of the protective device a more detailed inspection may be appropriate.

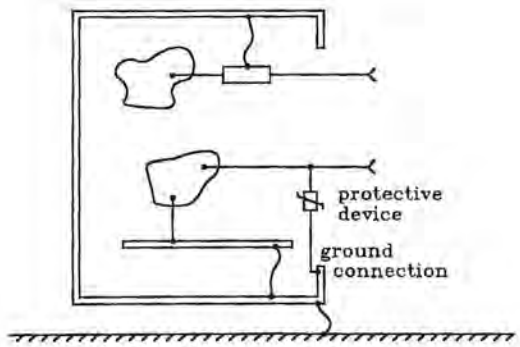

Fig. 18.36 Protected circuit.

Protective margin: If the EUT functions normally after the test it is *probably* safe to assume the protection was adequate, but there may still remain a question about how much protective margin the protective devices offer. Possibly the circuit was just on the edge of failure and a slightly less effective protector would have allowed failure. During engineering development it might be appropriate to determine whether the protective margin is satisfactory.

If an assessment of protective margin is desired, a suitable test procedure might be as follows.

1. Apply the normal test to the lead and measure the *voltage* developed on the circuit.

2. Reduce the power level of the surge generator to zero.

3. Disconnect the protective device.

   Filters are not involved in questions of protective margin and should not be disconnected.

4. Apply surges to the unprotected lead, starting at a low power level and increasing the level until the peak voltage developed is greater than it was in step 1 by an appropriate margin. The waveshape of the voltage will most likely be different from that developed in step 1.

   What constitutes an appropriate margin should be spelled out in the test plan. A margin of 30% may be appropriate.

5. Reconnect the protective device and test the circuit for proper operation.

It is **not** appropriate to disconnect the protective devices and then apply full level surges. The purpose of the protective devices is to relieve the circuit of having to withstand full amplitude surges.

18.7 Procedures for Transformer Injection Tests

Procedures depend somewhat on the objectives of the test and how the induced lightning threat is developed for the equipment under test. Test procedures are still evolving and there is not as yet uniformity among the various testing groups and agencies. Test practices may involve ambiguities that have not yet been resolved.

18.7.1 Adjustment of Power Level

The most prominent of these involves some rational method of adjusting the power level of the surge generator to the impedance characteristics of the equipment and cable system under test. Several fundamentally different approaches are possible.

1. Adjust the generator circuit and power level to deliver specified waves to an agreed upon dummy circuit. Then apply the circuit to the EUT and let I and V be what they may.

2. Adjust the circuit and power level to deliver specified I (or V) to the EUT, using whatever generator may be required.

3. Determine what power setting gives a specified V (or I). Treat this as a maximum power level for the test. Then adjust the power level to give a specified I (or V) without exceeding the maximum power level.

For the following discussions these three different approaches will be referred to as the "dummy circuit," the "Yellow Book," and the "Modified" approaches, although these are not names in widespread use.

18.7.2 Procedures for Waveforms 1 and 2.

The transformer and pulse generator must be adjusted together to deliver the required short circuit current or the appropriate open circuit voltage waveforms. Generally the tests involve generating either (but not both) the specified short circuit current (Waveform 1) or the specified open circuit voltage (Waveform 2), whichever is appropriate to the impedance of the circuit under test.

Calibration on a dummy circuit: Original proposals

[18.6, 18.7] regarding TCL tests were based on the premise that the test was intended to simulate the effects of a given amount of magnetic flux and not to circulate a specified current through the cable actually under test or to develop a specified voltage at the terminals of the device under test. The current through the actual cable under test, or the actual voltages developed at the terminal of the EUT, would then be different by an amount depending on how much the actual impedance of the interconnecting cable differed from that of the dummy cable.

The calibration procedure proposed, Fig. 18.37, was to place the injection transformer onto a dummy cable of specified size and length, and hence specified impedance, and then to adjust the power level of the surge generator until the desired short circuit current was obtained. The dummy cable was then open circuited and a check made to see that the desired open circuit voltage could be developed.

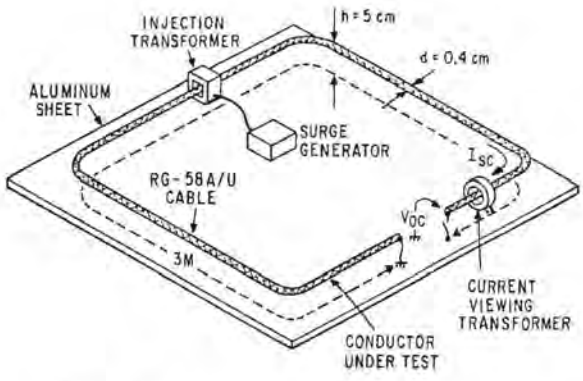

Fig. 18.37 Calibration on a dummy circuit.

The transformer was then to be placed on the cable under test. The magnitudes of the current and voltage induced on the cable were to be recorded, but the power level of the surge generator was not to be changed from that determined during the calibration.

The practice that has come to be most common is a variant of the originally suggested practice. Open circuit voltage is measured on a single turn winding threaded through the core, often made a permanent part of the injection transformer. Short circuit current is measured on a wire of minimum length threaded through the core, generally of # 10 to #14 AWG diameter.

"Yellow book" approach No. 1: This approach, not specifically labeled as No. 1 in [18.8], involves calibrating the transformer with the actual cable that would be used during the test, or a close replica thereof. The actual calibration procedure depends on the objective of the test.

The basic approach is to develop the specified voltage amplitude and waveshape on a cable. The generator is adjusted to deliver that voltage on the cable, as measured by a voltage probe connected to one of the cable wires open at one end and grounded at the other end. The cable is then shorted and the short circuit current noted to verify generator source impedance. The cable is then connected to the EUT and the appropriate number of tests applied.

For a low impedance cable, generally low by virtue of an overall shield grounded at each end, tests involve delivering a specified short circuit current. The output of the surge generator is adjusted to deliver that current, as measured by a measuring current transformer placed over the shorted cable. The appropriate number of pulses are then applied to the system.

"Yellow book" approach No. 2: This approach, not specifically labeled as No. 2 in [18.8], is applicable if the cable under test does not duplicate the actual vehicle cable. The recommended procedure is as follows.

1. Clamp the injection transformer over the open circuited test cable.

2. Adjust the generator until the desired open circuit voltage is obtained. Record the setting, S_v of the generator.

   If the cable cannot be readily open circuited, then the open circuit voltage can be measured on a single turn measuring loop on the injection transformer.

3. Short the cable and adjust the generator until the desired short circuit current is obtained. Record the setting, S_i of the generator.

4. Connect the cable to the EUT.

5. Reduce the power level of the generator to zero.

6. If $S_v < S_i$, adjust the power level of the generator until either the desired current is obtained or the setting reaches S_v. Apply the appropriate number of pulses.

7. If $S_i < S_v$, adjust the power level of the generator until either the desired circuit voltage is obtained or the setting reaches S_i. Apply the appropriate number of pulses.

Modified approach: This procedure calls only for adjusting the induced voltage magnitude to a specified maximum value. A separate adjustment is not made for short circuit current since the current would be related to the voltage by the specifications of generator impedance.

The open circuit voltage is measured on a single turn calibration winding on the injection transformer and the surge generator power setting is increased until the specified voltage is obtained, at which point the generator setting S_v is noted. The waveshape of the open circuit voltage should also be noted. The impedance characteristics of the injection transformer and surge generator are assumed to be basically sound if the requisite voltage waveshape is obtained.

The test procedure is as follows:

1. Connect the various pieces of equipment under test with suitable cables.

   Present drafts [18.9] of test procedures do not clearly address the question of what is suitable, but evolving practice suggests using the actual cable configuration if possible. If the length or construction of the actual cables is not known then the tests should be made using the best estimate of the actual lengths or construction. If the actual cables are too long for a practical test program, then test cables of shorter length may be used, but the method of shielding and termination of shields should replicate the actual cables as far as it is practical. Specially fabricated test cables should be a minimum of two meters long, this being a reflection of EMI/EMC test practices.

2. Position the injection and monitoring transformers as shown in Fig. 18.38.

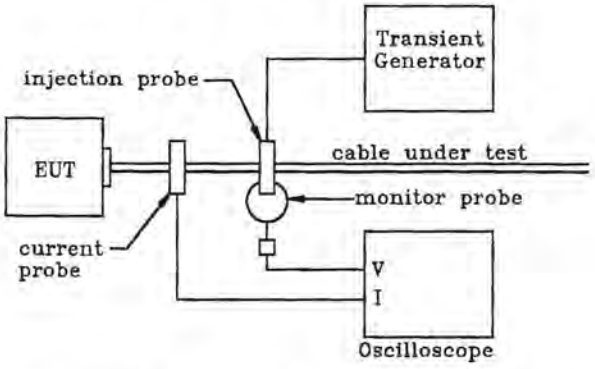

Fig. 18.38 Test setup for injection of waveforms 1 and 2.

3. Increase the power level of the surge generator until either (a) the specified current is obtained or (b) the setting S_v is reached.

4. Apply the requisite number of pulses.

18.7.3 Procedures for Oscillatory Waveforms

Procedures for injecting oscillatory currents are basically the same as for waveforms 1 and 2, but test practices differ as to the number of frequencies at which tests must be made.

"Yellow book" approach: Early guidelines [18.8] recommended making tests for assessment of damage at two frequencies, 1 MHz and 10 MHz. More recent proposals [18.9, 18.10] call for assessment of upset at multiple frequencies between 1 and 50 MHz of systems that might be susceptible to upset or damage at other frequencies.

The waveforms that can be developed, and the ratio of voltage to current, are more strongly influenced by impedances of the test circuit than in the case of waveforms 1 and 2. Cable impedance and the impedance of the test generator are both important. The SAE AE–4L requirements on the source impedance of the surge generator and injection transformer are that together they be capable of delivering into an open circuit a specified voltage and deliver into a short circuit a specified current. The ratio of voltage to current (peak values) is to be 25, but there are no specific frequency characteristics specified. Many generators have a resistive frequency characteristic, but the source impedance is not constrained to be resistive.

The test procedure would be as follows:

1. Remove the injection transformer from the test cable.

2. Adjust the generator until the desired open circuit voltage is obtained, as measured on a single turn calibration winding. Record the setting, S_v of the generator.

3. Clamp the injection transformer to a short circuited loop of wire and measure the short circuit current. The ratio of voltage to current should be 25, within an agreed upon tolerance.

4. If the short circuit current is not correct, or if the

test specifications call for voltages and currents other than those specified by [18.8], adjust the generator until the desired short circuit current is obtained. Record the setting, S_i of the generator.

5. Insert the injection transformer over the cable under test.

6. Reduce the power level of the generator to zero.

7. If $S_v < S_i$, adjust the power level of the generator until either the desired current is obtained on the cable or the setting reaches S_v. Apply the appropriate number of pulses.

8. If $S_i < S_v$, adjust the power level of the generator until either the desired circuit voltage is obtained or the setting reaches S_i. Apply the appropriate number of pulses.

Alternative verification of impedance: An alternative means of verifying the correct functioning of the surge generator and transformer, is to measure open circuit voltage, and then verify that the voltage falls by 50% when a 25 ohm resistive load is connected to the transformer. This method is most appropriate when the impedance of the generator and transformer is known to be predominantly resistive.

Modified multiple frequency approach: The approach starts by measuring the impedance of the cable under test using an impedance analyzer or a calibrated RF receiver. The recommended measuring setup is shown in Fig. 18.39, and a typical plot of cable impedance shown in Fig. 18.40. Points of impedance maxima and minima should be noted as they may indicate frequencies at which the system is particularly susceptible to interference.

Tests are made at the above frequencies, plus 50 frequencies logarithmically distributed between 1 and 50 MHz, the frequencies being given by

$$F_{\text{Mhz}} = 10^{0.0346729\times(n-1)} \qquad (18.16)$$

where $n = 1,\ 2,\ 3\ \ldots 50$.

The test procedure is as follows:

1. Position the injection transformer in a 100 ohm test jig, described in [18.9], and adjust the power setting of the surge generator to achieve the voltage level called for in Table 18.1. Record the setting as S_v.

2. Position the pieces of equipment under test and connect them with the appropriate cables.

3. At each of the above frequencies, start with the surge generator adjusted for a low power level and then raise the surge generator level until either the current level specified in Table 18.1 is reached or until it reaches S_v.

4. Apply the requisite number of pulses.

5. Upon completion of the test series verify that the operation of the EUT is within specifications.

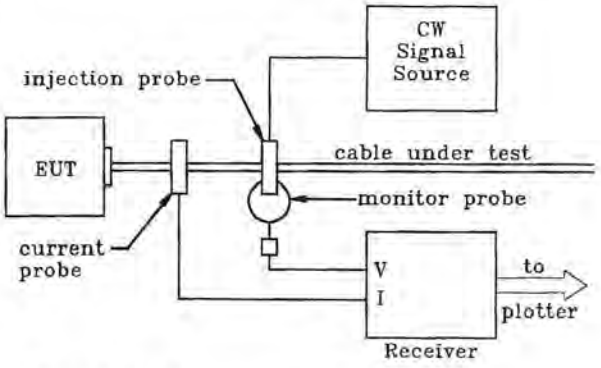

Fig. 18.39 Measurement of cable impedance.

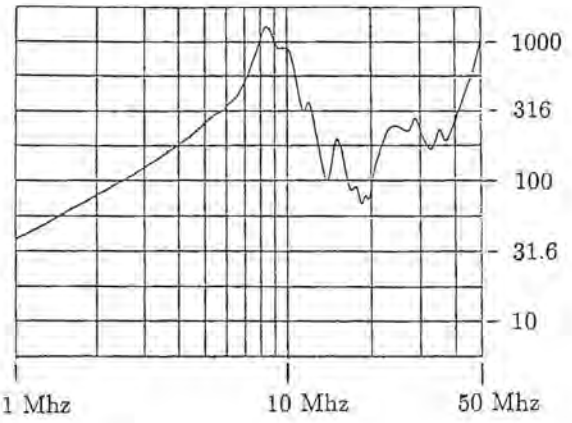

Fig. 18.40 Typical cable impedance.

18.8 Procedures for Ground Circuit Injection

Direct injection of surges into equipment ground points is an appropriate way to test for the effects of structural ground circuit rises. The basic test setup is shown in Fig. 18.41. Any lead from an internal ground point is connected to the ground stud of the equipment case. Cables connecting the case of the EUT to other pieces of equipment should be installed

as they would be in the actual installation. The EUT should be powered in its normal mode.

The test procedure would be as follows:

1. Disconnect the surge generator from the EUT and adjust the power level until the specified open circuit voltage is obtained. Record the level as S_v. Also, observe that the voltage waveshape is correct.

2. Ground the output of the surge generator and observe that the current is of the correct amplitude and waveshape. Note that the current waveshape does not need to be the same as that of the voltage to be "correct."

3. Reduce the power setting of the generator to zero.

4. Connect the surge generator to the ground terminal of the EUT and increase the output until either the specified current flows or S_v is reached.

5. Apply the requisite number of pulses.

6. Check the EUT for proper operation.

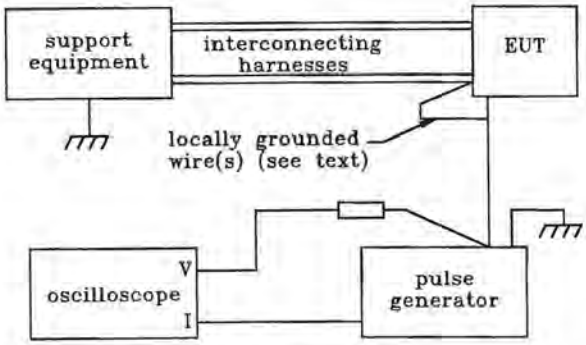

Fig. 18.41 Test setup for ground injection.

18.8.1 Procedures for Ground Injection of Waveform 5

Injection of Waveform 5 requires special attention because of its amplitude and duration. The current may impose severe duty on filters, surge suppression devices and shields of cables. Fusing, heating to a temperature damaging to cable insulation and sparking with resultant interference are all possible.

Where the test is to be applied to a system composed of several interconnected pieces of equipment, it may be necessary to insert resistors into various ground paths to force the injected current to flow in the desired paths. Determination of the required resistors is beyond the scope of this material, but is described in [18.9].

18.9 Electric and Magnetic Field Tests

Electric and magnetic field tests, particularly those performed with the aid of constant impedance strip line simulators, have mostly been performed to check for NEMP effects, but have been used for specialized purposes in studies of lightning indirect effects. Principally those have had to do with evaluating the shielding properties of equipment enclosures.

FAA, SAE AE4L, and the developing DO 160C specifications do not specifically call for tests using strip lines, but allow them when circumstances warrant. The SAE "Yellow book" [18.8] provides some discussion of methods of making strip line tests, but neither that document nor the SAE "Orange book" [18.10] make any specific recommendations as to field levels.

Further discussion of strip line test techniques is beyond the scope of this material.

18.10 Levels for Tests

Levels at which to conduct tests, and the waveforms to be used, depend somewhat on the type of test. Broadly speaking, tests in which voltages and currents are coupled to the pins of a device under test should be done at one of the levels given in Tables 16.2 and 16.3. Tests in which currents are injected into the shields of cables should be done at the levels expected to be produced by lightning.

Levels and waveshapes should be specified in a test plan prepared prior to the test. Some guidance as to what might be appropriate levels is given in the following sections.

18.10.1 Pin Injection Tests

The most common reason for making pin injection tests is to establish that the EUT will survive certain arbitrarily chosen voltages and currents. Unless there are specific reasons to the contrary, it is recommended that levels be chosen from those of Tables 16.2 and 16.3. Waveforms 2 and 3 of Fig. 16.12 are probably the ones most representative of what will be coupled to pins as a result of lightning attachment to metallic airframes. These *imply* that the transient generator should have an impedance of $5 - 25$ ohms.

Waveforms 4 and 5 are prominant in composite structures with Waveform 5 dominant on low impedance circuits. To evaluate their effects, generator impedances of 0.1 to 5 ohms are appropriate.

Some combination of all these waveforms will generally be present at some amplitude. Since these tests are intended to evaluate damage, only the most severe patterns of amplitude and energy content need to be applied to equipment.

18.10.2 Transformer Injection Tests

Injection into unshielded circuits: Injection into unshielded circuits is most commonly done to evaluate whether upset will occur with certain arbitrarily chosen voltages and currents. Unless there are specific reasons to the contrary the levels of Tables 16.2 and 16.3 should be used, just as with pin injection tests. Impedance of the source, transient generator and coupling transformer is a valid consideration since the coupled transients may manifest themselves either as voltage or current, according to the impedance of the circuit under test. Effective impedances of 5 – 25 ohms are appropriate.

Injection into shielded circuits: Injection into overall shields of cables (shields grounded at both ends) is most commonly done to evaluate the effectiveness of the shields and to see if the EUT will be affected by the residual signals coupled through the shield to the conductors in the shield. Current levels should approximate those expected to be produced by lightning, but estimating the required currents is a task totally separate from the conduct of the verification tests.

Source impedance is of little concern as long as the overall shield is continuous, grounded at each end and able to carry current. Under such conditions the important consideration is the amount and waveshape of the induced current. Source impedance is only of concern for tests on shielded cables when an attempt is made to observe the effects if the continuity of the overall shield is broken or degraded. Otherwise there is little reason to be concerned with what the open circuit voltage might be on an unshielded circuit if the circuit is, in fact, always going to be shielded.

18.10.3 Ground Injection Tests

Ground injection tests are generally made to evaluate the effects of airframe IR voltage on circuits with references to different points on the airframe. Most commonly, such circuits will be fitted with protective devices or contained in cables with overall shields.

Tests should be done at current levels determined by the techniques discussed in Chapters 10 - 14. Generator source impedance is an important consideration since structural voltage rises imply very low source impedance. Ideally, test generators should have impedances of a fraction of an ohm. If higher impedance generators are used, care must be taken to ensure that the requisite current is obtained.

18.11 Precautions Regarding Support Equipment

Most tests require the EUT to be supported and monitored by equipment that is not normally installed in the aircraft. Experience has shown that many of the problems involved in performance of lightning indirect tests involve the support equipment. It has also shown that some supposed "failures" of the equipment under test have really been caused by the support equipment. Problems can occur either because of malfunction of the support and monitoring equipment or because the leads to that equipment provide extraneous coupling paths into the EUT.

Care should be taken that this equipment and the connecting leads are well protected against lightning indirect effects since the test, of necessity, subjects the support equipment to as severe a test as it does the equipment being monitored. As a minimum, all leads connecting the monitoring equipment to the EUT should be shielded. Often it is appropriate to use copper tubing for the shields. If monitoring equipment is connected to the internal circuits of the EUT, optical isolation devices are appropriate. Also, the monitoring equipment should be as far from the EUT as possible in order to minimize direct radiation from the test circuit and EUT into the monitoring equipment.

18.12 Safety

Indirect effects testing, particularly at high power levels, involves the use of test equipment operating at voltage levels high enough to be lethal. Safety precautions are essential and must be addressed in test plans or laboratory procedures. Some minimal precautions are as follows.

1. Limit access to the test area to those operating the test equipment.

2. Provide all capacitor banks with a grounding stick or switch. Never touch a capacitor until it has been verified that the grounding stick or switch is in place.

3. Consider placing all high voltage equipment into a test cage fitted with interlocks that prevent energizing high voltage power supplies until all access

doors are closed.

4. Thoroughly ground all measuring leads and leads to support equipment as they leave the test area.

5. If the test might cause fragmentation of an item under test, use barriers to prevent fragments from leaving the test area.

REFERENCES

18.1 K. G. Wiles and R. T. Zeitler, "Component Lightning Test for the AFTI/F–16 Digital Fly–by–Wire System," *International Aerospace and Ground Conference on Lightning and Static Electricity*, June 21 - 23 1983, Fort Worth, TX., 1983, pp. 67-1 – 67-7 in *Addendum, Lightning Technolgy Roundup.*

18.2 K. G. Wiles and R. T. Zeitler, "AFTI/F–16 Lightning Analysis Report (CDRL 1016)," *Report 20PR090*, Contract No. F33615-78-C-3022, Project 2061, General Dynamics, Fort Worth, TX. 10 Jan. 1983.

18.3 *Pulse Generators*, E. D. Glasoe and J. V. Lebacqz, McGraw–Hill, New York, 1948.

18.4 *High–Voltage Measurement Techniques*, A. J. Schwab, The M.I.T. Press, Cambridge, MA. and London, England, 1972.

18.5 J. M. Anderson, "Wide Frequency Range Curent Transformers," *Review of Scientific Instruments*, Vol. 42, No. 7, July 1971, pp. 915-926.

18.6 F. A. Fisher and F. D. Martzloff, "Transient Control Levels, a Proposal for Insulation Coordination in Low–Voltage systems," *IEEE Transactions on Power Apparatus and Systems*, Vol. PAS-95, no. 1, Jan./Feb. 1976, pp. 120-129.

18.7 F. D. Martzloff and F. A. Fisher, "Transient Control Philosophy and Implementation, 1. The Reasoning Behind the Philosophy, 2. Techniques and Equipment for Making Tests," *2nd EMC Symposium on Electromagnetic Compatibility*, Montreux, June 28 - 30, 1977., Papers 73-M4 and 74-M5, pp. 383-394.

18.8 *Test Waveforms and Techniques for Assessing the Effects of Lightning–Induced Transients*, Report of SAE Committee AE4L, AE4L-81-2, 15 December 1981.

18.9 *Proposal for RTCA DO 160C, Environmental Conditions and Test Procedures for Airborne Equipment*, 1989.

18.10 *Recommended Draft Advisory Circular, Protection of Aircraft Electrical/Electronic Systems Against the Indirect Effects of Lightning*, Report of SAE Committee AE4L, Revision A, October 1988.

*U.S. GOVERNMENT PRINTING OFFICE: 1990—704-763/0702